β-Lactam Inhibitors Targeting Nucleophilic Cysteine and Serine Enzymes for Antiviral and Antibacterial Applications



Dorian-Gabriel Muntean

New College

Trinity Term 2025

A thesis presented to the Board of the Faculty of Mathematical, Physical and Life Sciences in partial fulfilment of the requirements for the degree of Doctor of Philosophy at the University of Oxford

Dedicated to my parents, Liliana and Vasile,

and

to my love, Emma

“In the midst of winter, I found there was, within me, an invincible summer.

And that makes me happy. For it says that no matter how hard the world pushes against me, within me, there’s something stronger – something better, pushing right back.”

Albert Camus

Abstract

β-Lactam antibiotics, which include penicillins, cephalosporins, carbapenems, and monobactams, are the most widely used class of antibacterial agents, and their clinical introduction revolutionised modern medicine. Their therapeutic efficacy stems from the ability to target penicillin-binding proteins (PBPs) by acylating the catalytic nucleophilic serine residue, thereby disrupting bacterial cell wall biosynthesis. The versatility of β-lactams, however, extends well beyond their traditional antibacterial role. The strained β-lactam ring is a reactive, covalent warhead that can be tailored for diverse therapeutic targets. More recently, during the coronavirus disease 2019 (COVID-19) pandemic, β-lactam derivatives were identified as potential inhibitors of the severe acute respiratory syndrome coronavirus 2 (SARS-CoV-2) main protease (M^{pro}). M^{pro} is a cysteine protease that plays a pivotal role in viral replication and is a validated therapeutic target. Crystallographic and mass spectrometric (MS) studies have shown that penicillin derivatives can react covalently with M^{pro} selectively at the active site, resulting in the *S*-acylation of the catalytic nucleophilic cysteine residue (Cys145). The work presented in this thesis describes the development of β-lactam derivatives for the potent inhibition of SARS-CoV-2 M^{pro}. Additionally, several inhibitors designed for antiviral studies emerged as compounds of interest due to their structural similarity with clinically used β-lactam antibiotics, thus prompting complementary studies into their antibacterial properties.

Chapter 1 provides a comprehensive literature review of β-lactam antibiotics from an antibacterial perspective, outlining their historical development across the different classes. The discussion then shifts to the non-antibacterial applications of β-lactams, highlighting their reported uses as antihypercholesterolemic, anticancer, anti-inflammatory, antifungal, and antiviral agents. **Chapter 2** describes a structure-activity relationship (SAR) study on C6-alkoxy penam derivatives as inhibitors of SARS-CoV-2 M^{pro}. Synthetic efforts were primarily directed at improving methodologies for the introduction of an alkoxy group at the C6 position of the penam scaffold. MS studies showed that most C6-alkoxy penam derivatives inhibited M^{pro} via a non-covalent mechanism, whereas modelling studies indicated that the presence of a C6-alkoxy group interferes with the positioning of the β-lactam carbonyl in proximity of the Cys145 thiolate, thereby hindering productive covalent reaction. **Chapter 3** describes the development of potent cephalosporin-based M^{pro} inhibitors. SAR studies revealed that key functional group modifications to the cephalosporin scaffold influence potency and the mechanism of inhibition, with both covalent and non-covalent modes being observed. Importantly, some cephalosporin derivatives were also found to suppress SARS-CoV-2 replication in infected cells, thus highlighting their potential as antiviral agents against SARS-CoV-2. **Chapter 4** describes the synthesis of C6-alkoxy penam derivatives for the inhibition of serine β-lactamases (SBLs). SBLs are hydrolytic enzymes that inactivate β-lactam antibiotics. SAR studies showed that the introduction of an alkoxy group at the C6 position of sulbactam alters its SBL inhibition profile, with crystallographic and MS investigations revealing that bulky C6-alkoxy group may improve the stability of acyl-enzyme complexes formed with SBLs by obstructing the access pathway of the hydrolytic water to the SBL active site. **Chapter 5** describes the synthesis of C6-methoxy penicillins derived from clinically used antibiotics, with the goal of examining the impact that the C6-methoxy group has on PBP inhibition. The results revealed that the introduction of a C6-methoxy group on the penicillin scaffold is not necessarily associated with a marked decrease in antimicrobial properties, thus highlighting the potential of C6-methoxy penicillins to be developed as next-generation

narrow-spectrum antibiotics. **Chapter 6** describes a streamlined synthetic route to C2-carboxypenam antibiotics, a non-classical subclass of β-lactam antibiotics where the carboxylic acid is shifted from the C3 to the C2 position of the penam scaffold. MS and crystallographic studies on C2-carboxypenam sulfones revealed that such derivatives reacted with PBP targets via an unusual mechanism that led to SO_2 extrusion. Additionally, C2-carboxypenam thioethers were found to inhibit SBLs, highlighting their potential to be developed not only as antibiotics but also as β-lactamase inhibitors. **Chapter 7** presents an overview of the work done in this thesis and offers futures directions regarding the development of key compounds of interest that emerged from the investigations conducted here.

Overall, the work presented in this thesis demonstrates the utility of β-lactams for the inhibition of nucleophilic cysteine and serine enzymes. Importantly, insights gained from developing β-lactams for antiviral purposes can equally inform the design of novel antibiotics, thus illustrating how mechanism-based inhibitors can be adapted for a wide range of therapeutic uses.

Declaration

I, Dorian-Gabriel Muntean, declare that the Thesis I am submitting is entirely my own work except where indicated in text, caption, footnote, or bibliography. This Thesis has not been submitted in whole or in part for any other academic degree or professional qualification.



09/10/2025

Signature ***Date***

Acknowledgements

Firstly, I would like to thank Prof. Christopher Schofield for his guidance, supervision, and support. I am deeply grateful to have been part of the Schofield group over the past five years, during both my MChem research year and my DPhil. Working on β-lactam chemistry has been a challenging and intellectually rewarding journey, and I have greatly valued Chris's mentorship, encouragement to pursue my scientific interests, and the many inspiring discussions we had over the years.

I am also very grateful for the generosity of Juliet and Paul Mason, whose contributions helped co-fund my DPhil studentship.

I am very thankful to Dr. Lennart Brewitz for his invaluable mentorship and support during my DPhil. His passion and dedication have been an inspiration throughout my studies. I have learnt so much from Lennart, and working together with him on so many different projects truly was a pleasure. I wish to express my gratitude also to colleagues of the Schofield group. A special thanks to Dr. Edmond Toma, a truly inspirational experimentalist, who never ceases to amaze me with his chemistry – it's always a pleasure talking about research with Eddie, and I am grateful for his advice and help in and out of the lab. I am delighted to have formed friendships also with Dr Damon Wen, Dr Lewis Ibbotson, and Dr Tom Corner during my time in the group – doing chemistry is always far more enjoyable with good humour and camaraderie. The work done in this thesis is the result of many fruitful collaborations, and it goes without saying that I am thankful for the help and assistance of Dr. Helen Smith, Dr. Liam Wilson, Dr. Karina Calvopina, Dr. Eidarus Salah, Dr. Linda Kinena, Dr. Ignacio Tobal Salcedo, Gurleen Kaur, Dóra Laczi, Wojtek Treyde, and Emily Freeman.

I also want to thank my parents, Liliana and Vasile, for believing in my dream and always supporting me. A special mention to my best friend, Dan, as his friendship matters a great deal to me. Lastly, and most importantly, an enormous thank you to Emma, you are my love and my anchor. There aren't enough words to express my gratitude, and this DPhil would not have been the same without your love and support.

Table of Contents

Chapter 1. Introduction **1**
1.1 β-Lactam antibiotics 1
1.2 Mechanism of action of β-lactam antibiotics 1
1.3 Antimicrobial resistance mechanisms 5
1.4 Penicillins 6
1.5 Cephalosporins 9
1.6 Carbapenems and penems 14
1.7 Monobactams 15
1.8 β-Lactamase-resistant β-lactams 16
1.9 β-Lactamases and β-lactamase inhibitors 18
1.9.1 β-Lactamase classification 18
1.9.2 β-Lactamase inhibitors 20
1.10 Investigational β-lactam antibiotics 24
1.11 Non-bacterial applications of β-lactams 27
1.11.1 Antihypercholesterolemic applications of β-lactams 28
1.11.2 Anticancer applications of β-lactams 30
1.11.3 Anti-inflammatory applications of β-lactams 40
1.11.4 Antifungal applications of β-lactams 45
1.11.5 Antiviral applications of β-lactams 47
1.12 SARS-CoV-2 52
1.12.1 Function and structure of SARS-CoV-2 M^{pro} 54
1.12.2 M^{pro} mechanism of action 55
1.12.3 Covalent and non-covalent inhibitors of M^{pro} 57
1.12.4 β-Lactam inhibitors of SARS-CoV-2 M^{pro} 60
1.13 Thesis objectives 62
1.14 References 64
Chapter 2. C6-Alkoxy substituted penicillins inhibit SARS-CoV-2 M^{pro} via a non-covalent mechanism **84**
2.1 Chapter overview 84

2.2 Manuscript I: C6-Alkoxy substituted penicillins are potent non-covalently binding inhibitors of the SARS-CoV-2 main protease 86
2.2.1 Abstract 86
2.2.2 Introduction 87
2.2.3 Results 89
2.2.4 Discussion 106
2.2.5 Conclusion 110
2.2.6 Supporting Figures 112
2.2.7 Computational methods 126
2.2.7.1 Docking 126
2.2.7.2 Parametrisation 126
2.2.7.3 Molecular dynamics simulations 127
2.2.8 References 130
2.3 Declaration of Authorship 140
Chapter 3. Development of cephalosporins as potent inhibitors of SARS-CoV-2 M^{pro} 141
3.1 Chapter overview 141
3.2 Manuscript II: Cephalosporin derivatives are potent inhibitors of the SARS-CoV-2 main protease 143
3.2.1 Abstract 143
3.2.2 Introduction 144
3.2.3 Results 146
3.2.4 Discussion 161
3.2.5 Conclusion 164
3.2.6 Supporting Figures 165
3.2.7 References 178
3.3 Declaration of Authorship 185
Chapter 4. Investigations into C6-alkoxy sulbactam derivatives 186
4.1 Chapter overview 186
4.2 Manuscript III: C6-Alkoxy substituents alter the reactivity profile of sulbactam with SBLs and PBPs 188
4.2.1 Abstract 188
4.2.2 Introduction 189
4.2.3 Results 192

4.2.4 Discussion....201
4.2.5 Conclusion....205
4.2.6 Supporting Figures....206
4.2.7 Methods....214
4.2.7.1 SBL inhibition assays....214
4.2.7.2 SBL POMS assays....214
4.2.7.3 MBL testing....214
4.2.7.4 PBP inhibition assays....215
4.2.7.5 Susceptibility assays....215
4.2.7.6 Crystallisation....216
4.2.7.7 Single-crystal X-ray structure....219
4.2.8 References....221
4.3 Declaration of Authorship....227
Chapter 5. Investigations into C6-methoxypenicillins....228
5.1 Chapter overview....228
5.2 Manuscript IV: Piperacillin is a promising scaffold for the development of C6-methoxypenicillins....230
5.2.1 Abstract....230
5.2.2 Introduction....231
5.2.3 Results and discussion....233
5.2.4 Conclusion....239
5.2.5 Supporting Figures....241
5.2.6 Methods....242
5.2.6.1 PBP expression....242
5.2.6.2 PBP inhibition assays....242
5.2.6.3 Susceptibility assays....243
5.2.7 References....244
5.3 Declaration of Authorship....250
Chapter 6. Synthesis of C2-carboxypenams and their mechanism of action....251
6.1 Chapter overview....251
6.2 Manuscript V: Reaction of C2-carboxypenams with penicillin-binding proteins proceeds via unusual SO_2 release mechanism....253
6.2.1 Abstract....253

6.2.2 Introduction 254
6.2.3 Results 256
6.2.4 Discussion....265
6.2.5 Conclusion....269
6.2.6 Supporting Figures 269
6.2.7 Methods 273
6.2.7.1 PBP expression 273
6.2.7.2 PBP inhibition assays....273
6.2.7.3 Susceptibility assays 273
6.2.7.4 SBL inhibition assays 273
6.2.7.5 Protein-observed MS assays 274
6.2.7.6 Crystallography....274
6.2.8 References 276
6.3 Declaration of Authorship....281
Chapter 7. Summary conclusions....**282**
8. Appendix....**296**
8.1 Appendix to Chapter 2 (Manuscript I) 296
8.1.1 General synthesis information....296
8.1.2 General synthetic procedures 296
8.1.3 Experimental procedures and compound characterisations 299
8.1.4 References 323
8.1.5 ^{1}H and ^{13}C NMR spectra of the compounds prepared for this study 324
8.2 Appendix to Chapter 3 (Manuscript II)....349
8.2.1 General synthesis information....349
8.2.2 General synthetic procedures 350
8.2.3 Experimental procedures and compound characterisations 353
8.2.4 References 406
8.2.5 ^{1}H and ^{13}C NMR spectra of the compounds prepared for this study 408
8.3 Appendix to Chapter 4 (Manuscript III) 457
8.3.1 General synthesis information....458
8.3.2 General synthetic procedures 458
8.3.3 Experimental procedures and compound characterisations 459

8.3.4 References 470
8.3.5 ^{1}H and ^{13}C NMR spectra of the compounds prepared for this study 471
8.4 Appendix to Chapter 5 (Manuscript IV) 485
8.4.1 General synthesis information 485
8.4.2 General synthetic procedures 486
8.4.3 Experimental procedures and compound characterisations 487
8.4.4 References 491
8.4.5 ^{1}H and ^{13}C NMR spectra of the compounds prepared for this study 492
8.5 Appendix to Chapter 6 (Manuscript V) 497
8.5.1 General synthetic procedures 497
8.5.2 Experimental procedures and compound characterisations 587
8.5.3 References 521
8.5.4 ^{1}H and ^{13}C NMR spectra of the compounds prepared for this study 522

Abbreviations

δ	Chemical shift
Δ	Heat
Abq	AB quartet
br	Broad
COVID-19	Coronavirus disease 2019
CPMG	Carr-Purcell-Meiboom-Gill
D-Ala	D-Alanine
d	Doublet
Da	Dalton
DAP	Diaminopimelic acid
DBO	Diazabicyclooctane
DHP-I	Dehydropeptidase I
DMSO	Dimethylsulfoxide
DMSO-d_6	Deuterated dimethylsulfoxide
DTT	Dithiothreitol
equiv.	Equivalent
ESI	Electrospray ionisation
FGI	Functional Group Interconversion
FP	Fluorescence polarisation
FRET	Fluorescence resonance energy transfer
HEPES	(4-(2-hydroxyethyl)-1-piperazineethanesulfonic acid)
His	Histidine
HIV	Human immunodeficiency virus
HLE	Human leukocyte elastase
HRMS	High resolution mass spectrometry
IC_{50}	Half-maximal inhibitory concentration
IR	Infra-red
Ldt	L,D-transpeptidases

J	Coupling constant
M	Molar
MBL	Metallo-β-lactamase
mCPBA	3-Chloroperoxybenzoic acid
MHz	Megahertz
MIC	Minimum inhibitory concentration
M^{pro}	main protease
MS	Mass spectrometry
MSSA	Methicillin-susceptible *S. aureus*
MRSA	Methicillin-resistant *S. aureus*
m	multiplet
m/z	Mass-to-charge ratio
mBBr	monobromobimane
mRNA	Messenger RNA
n.i.	No inhibition
nsps	Non-structural proteins
NAM	*N*-Acetyl-muramic acid
NAG	*N*-Acetyl-glucosamine
NMR	Nuclear magnetic resonance
PBP	Penicillin-binding protein
PDB	Protein data bank
Pd/C	Palladium on carbon
pNB	4-Nitrobenzyl
POMS	Protein-observed MS
PTSA	4-Toluenesulfonic acid
q	Quartet
RT	Room temperature
RMSD	Route mean square deviation
RNA	Ribonucleic acid
s	singlet

SARS-CoV-2	severe acute respiratory syndrome coronavirus-2
SBL	Serine β-lactamase
S_N2	Bimolecular nucleophilic substitution
S2d	2-((benzoyl-D-alanyl)thio)acetic acid
SPS-MS	Solid-phase extraction – mass spectrometry
t	Triplet
THF	Tetrahydrofuran
TLC	Thin-layer chromatography
$\tilde{\nu}$	Frequency (cm^{-1})

Standard three-letter abbreviations for amino acids, standard SI unit abbreviations and chemical element symbols are used throughout this thesis.

1 Introduction

1.1 β-Lactam antibiotics

The discovery of penicillin by Alexander Fleming in 1929,[1] followed by the development of fermentation and extraction procedures by Howard Florey and Ernst Chain in the early 1940s,[2] is one of the greatest achievements in modern medicine, as it enabled the treatment of bacterial infections in a safe, efficacious and affordable manner.[3] β-Lactam drugs are the most widely used class of antibiotics, and can be classified in five main subgroups (**Figure 1.1**): (i) penicillins, (ii) cephalosporins, (iii) carbapenems, (iv) penems, and (v) monobactams.[4-6] The defining characteristic of β-lactam antibiotics is the reactive β-lactam ring,[7] which interferes with bacterial cell wall biosynthesis.[8]

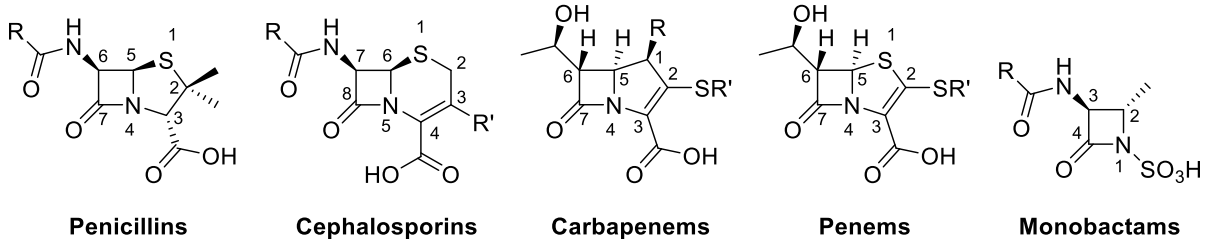

Figure 1.1: Schematic structures of the clinically used classes of β-lactam antibiotics: penicillins, cephalosporins, penems, carbapenems, and monobactams.

1.2 Mechanism of action of β-lactam antibiotics

The bacterial cell wall is an integral component of bacteria, providing structural support and acting as a permeable barrier that regulates the flux of molecules and ions in and out of cells.[9-11] Loss of cell wall integrity renders cells vulnerable to osmotic stress, often resulting in cell death via lysis.[12]

Bacteria can broadly be divided into two categories, Gram-positive[9] and Gram-negative[10], classified accordingly based on their response to the Gram staining test. Gram-positive species retain a characteristic purple stain, whereas Gram-negative bacteria do not, due to the presence of an outer cell membrane.[13]

A major component of the bacterial cell wall is peptidoglycan,[14, 15] typically a thick, rigid layer that consists of a repeating disaccharide backbone cross-linked by polypeptide chains. Although its nature is species-specific, peptidoglycan units generally contain *N*-acetyl-glucosamine (NAG), *N*-acetyl-muramic acid (NAM), and a short cross-linking peptide sequence (**Figure 1.2A**).[16] During bacterial growth, the peptidoglycan polymer is expanded via the cross-linking of the third amino acid in the sidechain sequence of the original unit with the fourth amino acid of the following glycan pentapeptide (**Figure 1.2B**). This cross-linking reaction, also known as 4,3-transpeptidation, is crucial for the cell wall synthesis, and is catalysed by penicillin-binding proteins (PBPs).[17] PBPs are a class of serine transpeptidases that recognise the D-Ala-D-Ala *C*-terminus sequence of the incoming glycan unit.[18] There are several classes of PBPs: PBP1-3 are responsible for most of the peptidoglycan biosynthesis and expansion, whereas PBP4 and PBP5 act mainly in cell wall maintenance and repair.[17]

The first step of the 4,3-transpeptidation reaction involves the attack of the active-site serine at the carbonyl group of the D-Ala-D-Ala peptide bond, resulting in the formation of an acyl-enzyme intermediate and the release of the terminal D-Ala. Subsequently, the amino group of *meso*-DAP from an adjacent peptide chain attacks the acyl-enzyme intermediate to form the 4,3-cross-link.[17, 18]

Although PBP-catalysed 4,3-transpeptidation is the predominant crosslinking process in most bacterial species, it only plays a minor role in mycobacteria such as *Mycobacterium abscessus* and *Mycobacterium tuberculosis*.[19, 20] Instead, peptidoglycan biosynthesis in *M. tuberculosis* involves 3,3-crosslinking reactions between *meso*-DAP amino acids from adjacent peptide chains,[20] which are catalysed by L,D-transpeptidase (Ldt) enzymes;[21] unlike PBPs, Ldts employ a nucleophilic cysteine residue at the active site to catalyse the transpeptidation reaction.[22, 23]

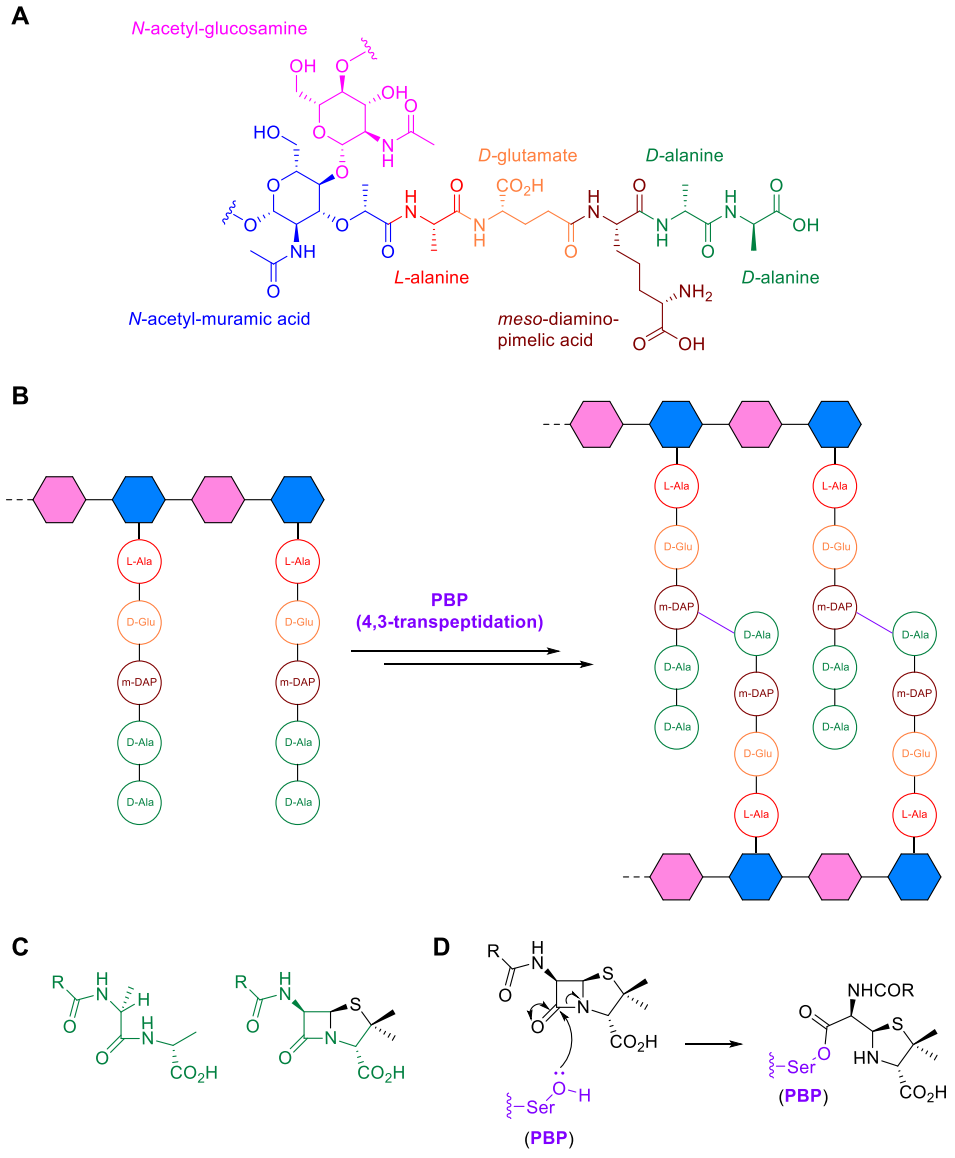

Figure 1.2: **A**. Structure of a peptidoglycan subunit consisting of a disaccharide backbone (*i.e.*, NAG and NAM) linked to a pentapeptide chain (L-Ala-L-Glu-*meso*-DAP-D-Ala-D-Ala), commonly found in Gram-negative bacteria.[16]

B. Outline mechanism of 4,3-transpeptidation catalysed by penicillin-binding proteins (PBPs), in which the ε-amino group of *meso*-diaminopimelic acid (m-DAP, position 3) from one peptide chain forms a peptide bond with the D-Ala (position 4) of an adjacent peptide chain, releasing the terminal D-Ala residue.[17, 18] **C**. Structural similarities between the PBP natural substrate, D-Ala-D-Ala, and penicillin.[24] **D**. Mechanism of inhibition of PBPs by penicillin.[8]

Strominger and Tipper[24] proposed that β-lactam antibiotics mimic the D-Ala-D-Ala substrate of PBPs (**Figure 1.2C**). Structural studies showed that β-lactams behave as transition-state analogues that are already preorganised for acylation at the active site (**Figure 1.3**).[25] The β-lactam ring displays a similarly strained, ~ 45° out-of-plane amide geometry that D-Ala-D-Ala is also forced to adopt in the enzyme active site.[26] After formation of the initial non-covalent PBP-inhibitor adduct, the strained, electrophilic β-lactam ring undergoes reaction with the nucleophilic active-site serine, resulting in a stable acyl-enzyme complex (AEC) that covalently inactivates the transpeptidase (**Figure 1.2D**).[8] As PBPs play a crucial role in critical bacterial processes such as cell wall growth, maintenance, and repair, disrupting their activity leads to cell lysis.[12]

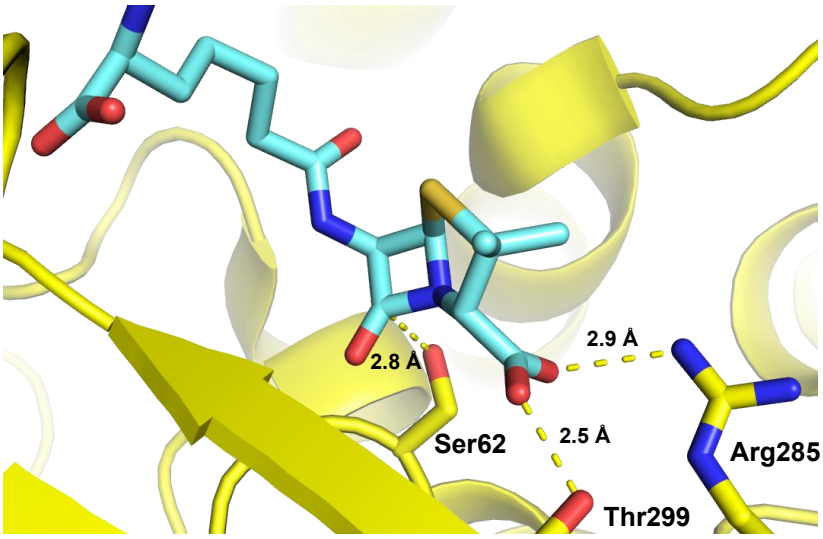

Figure 1.3: View from a crystal structure showing a non-covalent complex of a penicillin derivative with *Streptomyces* R61 D,D-peptidase (PDB ID: 1PW1).[25] The β-lactam carbonyl is poised for covalent reaction with Ser62 (O(Ser62)–C(O)(β-lactam) ~ 2.8 Å), while the C3-carboxylate is anchored via hydrogen bonding to Arg285 (2.9 Å) and Thr299 (2.5 Å).

1.3 Antimicrobial resistance mechanisms

The rapid spread of β-lactam antibiotic-resistant bacteria poses a serious threat to the efficient use of β-lactam antibiotics. Contributing factors to the problem include antibiotic overprescription, clinical mismanagement, lack of surveillance and regulation, and routine use of human antibiotics in livestock. Under selective pressure, bacteria have evolved to develop several resistance mechanisms:

1) Alteration of PBPs – amino acid residue modification in transpeptidases can lead to reduced antibiotic binding affinities, thus enabling the cell wall synthesis to continue (*e.g.*, PBP2a in methicillin-resistant *S. aureus* strains).[27-30]

2) Reduced membrane permeability – in Gram-negative bacteria, modifications in transporter proteins or outer membrane porins result in reduced cellular uptake of antibiotics.[31-33]

3) Efflux pumps – some bacteria possess active transport systems that remove antibiotics from the cytoplasm before they can reach their therapeutic targets.[34-36]

4) Enzymatic inactivation – bacteria can produce hydrolytic enzymes (β-lactamases) that catalyse the inactivation of β-lactam antibiotics to render them ineffective against PBPs.[37-40]

Given the ever-evolving threat posed by bacterial resistance, β-lactam antibiotics have undergone continuous development.[5] The following sections describe the successive generations of β-lactam antibiotics, examining how structural changes can impact antibacterial spectra.

1.4 Penicillins

Penicillin G (**I**) was the first discovered penicillin antibiotic, being isolated from *Penicillinium* spp..[1] Subsequent process development led to large-scale biosynthesis using engineered *Penicillinium chrysogenum* strains,[41] where fermentation in the presence of various hydrophobic acids (*e.g.*, phenoxyacetic acid) would yield other analogues, most notably **penicillin V** (**II**).[42] These pioneering advances allowed the isolation of 6-(+)-aminopenicillanic acid (**6-APA**), which is a valuable intermediate that is commonly used as a scaffold for the production of semi-synthetic penicillins.[43] **Penicillins G** (**I**) and **V** (**II**) are narrow spectrum antibiotics, primarily active against some Gram-positive pathogens such as streptococci and staphylococci.[44] However, due to their susceptibility to hydrolytic degradation by β-lactamases, their clinical scope is largely limited.[45]

Building on these 1st generation antibiotics, subsequent penicillins (and by extension, cephalosporins) featured increasingly more complex acylamido sidechains. Structure-activity relationship (SAR) studies showed that these sidechains proved crucial not only for improving PBP inhibition, but also for potentially increasing the hydrolytic stability of the β-lactam ring against β-lactamases. **Methicillin** (**III**), a 2nd generation penicillin, was once employed in the treatment of *Staphylococcus aureus* infections, thanks to its hydrolytic stability towards staphylococcal β-lactamases,[46] a property imparted by the bulky aromatic acyl sidechain, which sterically shields the β-lactam ring from β-lactamases.[47] Similarly, the bulky sidechain approach was also successfully applied in the development of both **nafcillin** (**IV**) and isoxazolyl penicillins (*i.e.*, **oxacillin**, **cloxacillin**, **dicloxacillin**, and **flucloxacillin**), all showing good activity against methicillin-susceptible *S. aureus* (MSSA).[48] However, the horizontal acquisition of the mecA gene

by *S. aureus* strains led to the global emergence of methicillin-resistant *S. aureus* (MRSA), wherein the encoded PBP2a displayed drastically reduced binding affinity for most β-lactam antibiotics.[49]

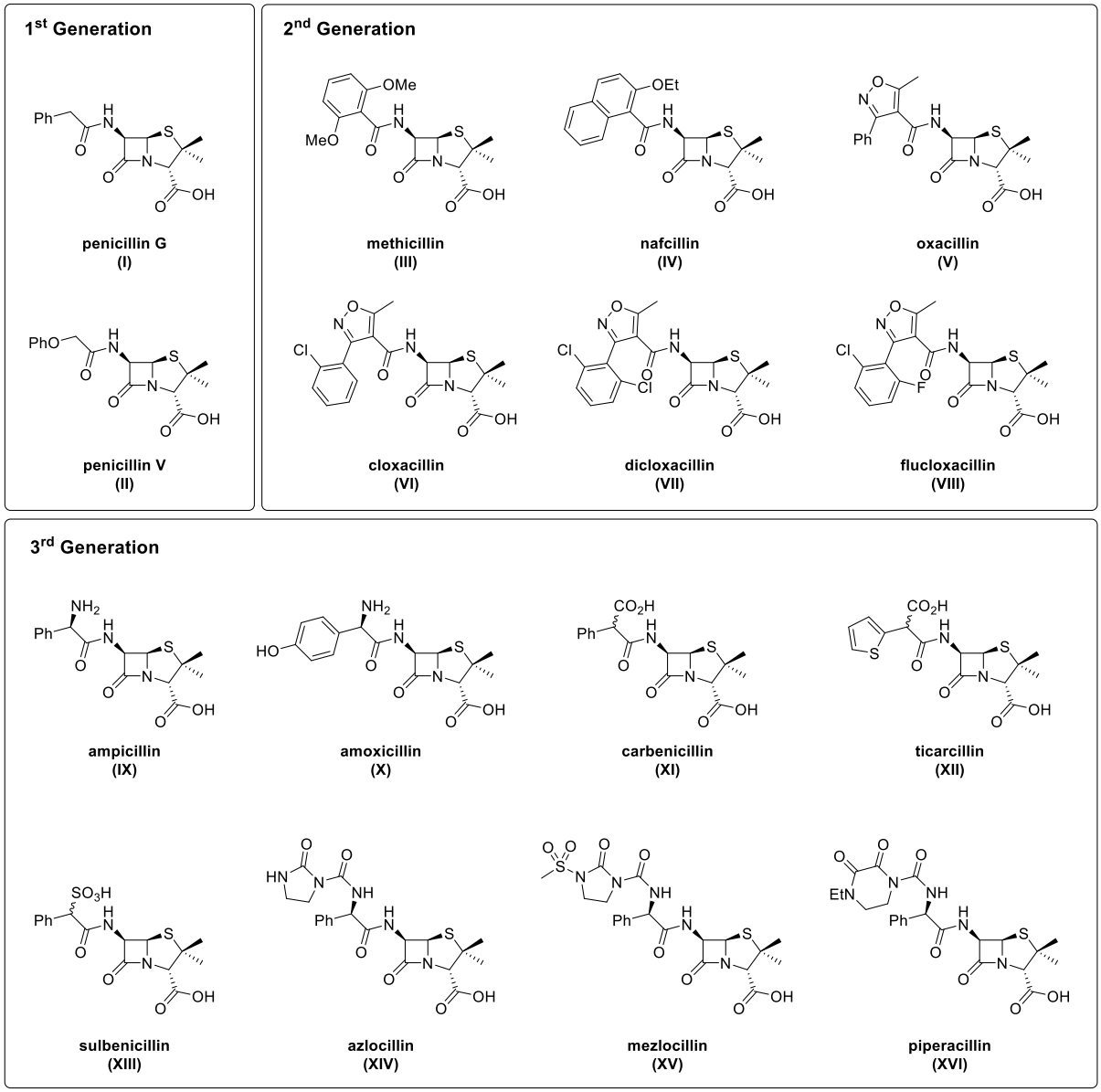

Figure 1.4: Structures of selected clinically important penicillin antibiotics.

Work on third-generation penicillins involved substitutions of the C6-phenylacetamido sidechain of **penicillin G** (**I**), wherein the introduction of strategic functional groups resulted in broader antimicrobial spectra than that of **penicillin G** (**I**). **Ampicillin** (**IX**) features an α-amino sidechain

which increases hydrophilicity and facilitates diffusion through porin channels situated on the outer membrane surface of Gram-negative pathogens, thus extending the spectra of penicillin activity to *E. coli*, *P. mirabilis*, *H. influenzae*, and *Salmonella* spp..[50-52] **Amoxicillin** (**X**), also an aminopenicillin, displays a similar profile to **ampicillin**, but offers improved oral availability thanks to the *p*-hydroxy group on the aromatic ring.[53-55] Another class of 3rd generation penicillins is represented by the carboxypenicillins, which feature an α-carboxy sidechain. Representative clinically used antibiotics include **carbenicillin** (**XI**)[56] and **ticarcillin** (**XII**),[57] which extend the spectra of activity beyond those of aminopenicillins, showing good efficacy against additional Gram-negative species, particularly *Pseudomonas aeruginosa*, *Proteus* spp., and *Acinetobacter* spp..[58, 59] A similar profile is also displayed by **sulbenicillin** (**XIII**), an analogue of **carbenicillin** (**XI**), wherein the carboxylate sidechain is replaced by its bioisostere sulfonate.[60] The last major subclass of third-generation penicillins is represented by ureidopenicillins, which share a structural backbone with **ampicillin** (**IX**). The key distinction between the two is the additional functionalisation of the α-amino group to ureido sidechains. These sidechains are able to improve binding by engaging additional PBP residues proximal to the active site (**Figure 1.5**).[61, 62] Representative members of this subclass include **azlocillin** (**XIV**), **mezlocillin** (**XV**), and **piperacillin** (**XVI**), which exhibit superior antimicrobial properties compared to either aminopenicillins or carboxypenicillins against certain Gram-negative pathogens, such as *Pseudomonas aeruginosa* and *Neisseria gonorrhoeae*.[61, 62] Despite the broader spectra of third-generation penicillins, their main clinical limitation is their susceptibility to β-lactamase-mediated hydrolysis. To restore activity and expand the clinical utility of these agents, third-generation penicillins are typically co-administered with β-lactamase inhibitors, which will be explored in **Section 1.9.2**.

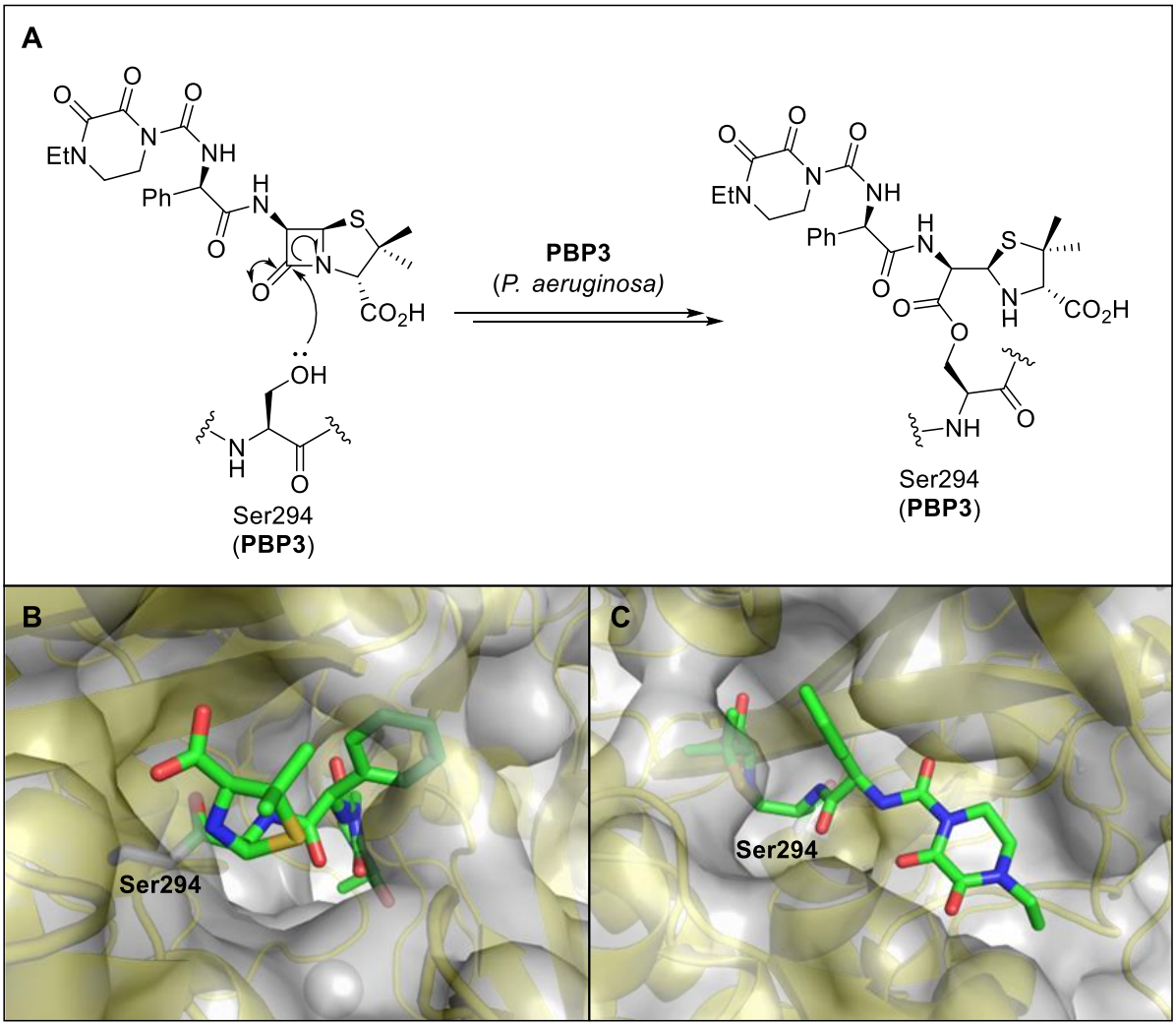

Figure 1.5: A. Outline mechanism for the reaction of **piperacillin** with the active-site nucleophilic serine residue Ser294 of *P. aeruginosa* PBP3.[63] **B**. Crystal structure view of the complex formed following covalent reaction of **piperacillin** with *P. aeruginosa* PBP3 (PDB ID: 4KQO).[63] **C**. Alternative crystal structure view of the complex formed following covalent reaction of **piperacillin** with *P. aeruginosa* PBP3 (PDB ID: 4KQO),[63] showing how the ureido sidechain engages the β3-β4 loop.

1.5 Cephalosporins

Despite their revolutionary medicinal impact on the treatment of bacterial infections, penicillins suffer from several shortcomings which limit their overall scope. Not only are penicillins susceptible to hydrolysis by β-lactamases,[64] but their metabolites can also trigger allergic reactions in certain population groups.[65, 66] In this context, cephalosporins represent a safer therapeutic alternative for patients with penicillin allergy.[67] The cephalosporin scaffold also presents unique

opportunities for expanding antimicrobial properties.[68] Over the five generations of cephalosporins developed to date (**Figure 1.6**),[68-73] the focus has been on optimising the C3 and C7 sidechains. These have been shown to influence both the physicochemical properties and the pharmacokinetic/pharmacodynamic profiles.[74-76]

First-generation cephalosporin antibiotics typically display C7 amido sidechains that resemble those encountered among penicillins.[75] **Cephalexin** (**XVII**)[77] and **cephadroxil** (**XVIII**)[78] both possess α-amino sidechains also found in **ampicillin** (**IX**) and **amoxicillin** (**X**), respectively, which account for their oral availability. **Cephalothin** (**XIX**)[79] and **cephaloridine** (**XX**)[80] carry a 2-thiophenylacetamide sidechain, analogous to the phenylacetamide sidechain of **penicillin G** (**I**); further mirroring **penicillin G** (**I**), the oral availabilities of **cephalothin** (**XIX**) and **cephaloridine** (**XX**) are poor, hence they are administered parenterally. In terms of C3 substituents, first-generation cephalosporins display either a simple methyl group at C3, as exemplified by **cephalexin** (**XVII**) and **cephadroxil** (**XVIII**), or can carry C3' leaving groups, such as acetate for **cephalothin** (**XIX**) or pyridine for **cephaloridine** (**XX**), which are released upon reacting with their PBP targets.[81] First-generation cephalosporins usually display strong activity against Gram-positive pathogens (*e.g.*, *Streptococcus pneumoniae*), but suffer from limited Gram-negative coverage and susceptibility to β-lactamase-mediated hydrolysis.[77-80]

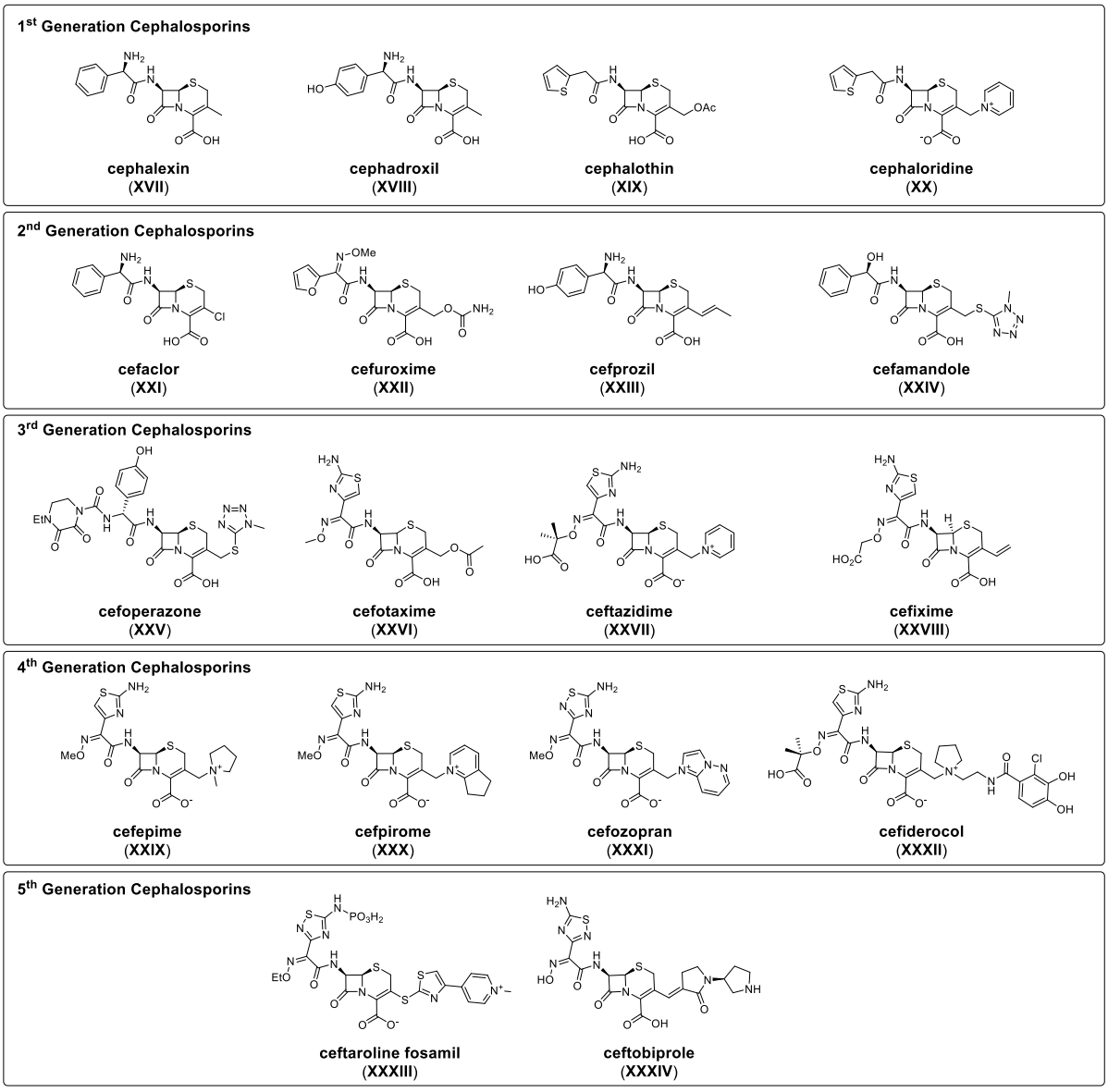

Figure 1.6: Structures of cephalosporin antibiotics.

Second-generation cephalosporins explore other C3 functional groups,[48, 68, 69] such as chloride in **cefaclor** (**XXI**), carbamoylmethyl in **cefuroxime** (**XXII**), propenyl in **cefprozil** (**XXIII**), or methylene-*N*-methylthiotetrazole in **cefamandole** (**XXIV**). These advances in polar and hydrophilic C3 substituents led to improved Gram-negative antimicrobial activity by assisting with crossing the outer membrane of Gram-negative pathogens.[5]

A significant leap in cephalosporin antibiotic design arrived with third-generation agents,[48, 71] which saw the introduction of C7 aminothiazole methoxime (ATMO) motifs, as exemplified by **cefotaxime** (**XXVI**),[82] **ceftazidime** (**XXVII**)[83] or **cefixime** (**XXVIII**).[84] The carboxylate extension on the ATMO sidechains of **ceftazidime** (**XXVII**) and **cefixime** (**XXVIII**) helps with improving Gram-negative outer membrane permeability.[85] In the case of **ceftazidime** (**XXVII**), this is further compounded by the zwitterionic nature of the pyridinium C3' substituent. This effect led to even further improvement in antibacterial activity against Gram-negative pathogens for third-generation cephalosporins, although, at times, this came at the expense of Gram-positive coverage. When introduced into clinical use, third-generation agents were resistant to β-lactamase degradation; in time, however, bacteria developed and/or acquired extended-spectrum β-lactamases capable of targeting these antibiotics as well.[86]

In fourth-generation cephalosporins, the design focus shifted to quaternary ammonium groups at the C3' position, which increase polarity and improve Gram-negative outer membrane permeability.[72] As a consequence, cephalosporins such as **cefepime** (**XXIX**),[87] **cefpirome** (**XXX**),[88] and **cefozopran** (**XXXI**)[89] not only show the same Gram-negative coverage as third-generation cephalosporins but also display activity against some Gram-positive pathogens (*e.g.*, MSSA);[48, 72] additionally, the quaternary ammonium cephalosporins are less susceptible to hydrolysis by β-lactamases in comparison to third-generation agents.[90] A noteworthy fourth-generation cephalosporin is **cefiderocol** (**XXXII**),[91] a potent antipseudomonal antibiotic that features a siderophoric catechol moiety connected to the C3' position via a linker. The siderophoric catechol moiety facilitates antibiotic uptake into bacteria by hijacking iron-transporters. An important mechanistic detail for quaternary ammonium cephalosporins is, that upon reaction with

their PBP target, β-lactam ring opening triggers further fragmentation that releases the C3' substituent.[81]

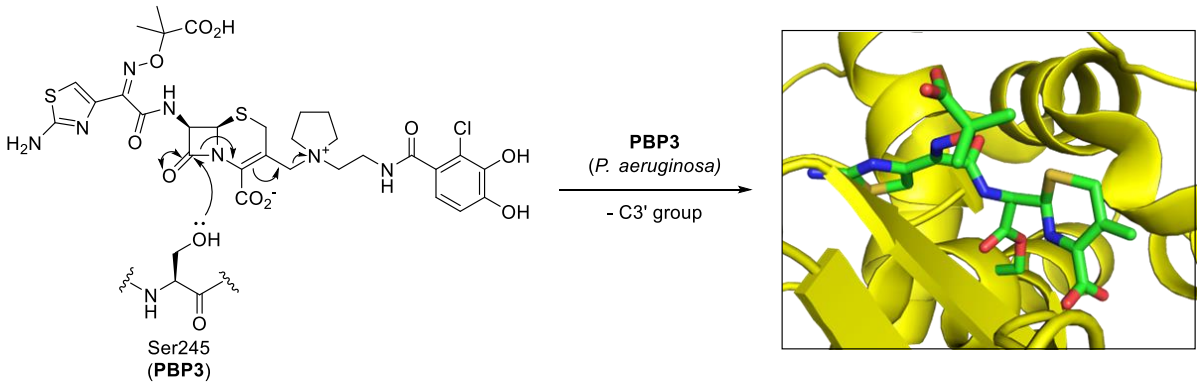

Figure 1.7: Outline mechanism for the reaction of **cefiderocol** with the active-site serine residue of *P. aeruginosa* PBP3, with crystallographic evidence showing the acyl-enzyme adduct lacking the C3' substituent (PDB ID: 6R3X).[81]

Lastly, fifth-generation cephalosporins include **ceftaroline fosamil** (**XXXIII**), an *N*-phosphono prodrug,[92] and **ceftobiprole** (**XXXIV**).[93] Beyond their coverage of Gram-negative pathogens,[92, 94] the two also display exceptional activity against MRSA by efficiently targeting PBP2a. Following allosteric site binding, which is facilitated by the C3 substituent of **ceftaroline**, conformational changes in PBP2a are triggered. Subsequently, the PBP2a active site is opened, thus allowing access to a second **ceftaroline** molecule to enter and acylate the catalytic serine residue.[95] **Ceftobiprole** (**XXXIV**) possess the ability to access the active site directly. The C3 substituent extends into a narrow cleft near the PBP2a active site and directs the molecule towards the active site.[30, 96] The C3 substituents of fifth-generation cephalosporins play a crucial role in the inhibition of multidrug-resistant pathogens, such as MRSA, highlighting once more their versatility and importance in β-lactam drug design.

1.6 Carbapenems and penems

The discovery of **thienamycin** (**XXXV**; **Figure 1.8**), a carbapenem natural product of *Streptomyces cattleya*, marked the beginning of carbapenem antibiotic research. **Thienamycin** (**XXXV**) exhibits broad activity against both Gram-positive and Gram-negative bacteria, and displays good hydrolytic stability against β-lactamases.[97] However, the limited stability of **thienamycin** (**XXXV**) at physiological pH prompted the development of improved semisynthetic carbapenem analogues,[98, 99] starting with its *N*-formimidoyl derivative, **imipenem** (**XXXVI**), and followed up by **panipenem** (**XXXVII**). Renal deactivation by dehydropeptidase I (DHP-I) of **imipenem** (**XXXVI**) and **panipenem** (**XXXVII**) drove further optimisation,[100, 101] leading to the introduction of the C1-β-methyl substituent in **meropenem** (**XXXVIII**), **ertapenem** (**XXXIX**), **biapenem** (**XL**), **doripenem** (**XLI**), and **tebipenem** (**XLII**).[99] Currently, carbapenems are employed as antibiotics of last resort, as they possess the broadest spectrum of activity against resistant bacterial strains.[99] Depending on the nature of the C2 sidechain, activity can be potentiated against specific species (*e.g.*, **tebipenem** for the treatment of MRSA infections).[102] Nonetheless, their successful clinical use is increasingly at risk, primarily due to the emergence of multidrug-resistant (MDR) pathogens possessing carbapenemase-encoding genes.[103-106]

Structurally related to the carbapenems are the penems, wherein the C1 atom has been replaced back with an S atom, as found in penicillins.[107, 108] This difference, albeit small, confers resistance to mammalian degradation by DHP-I.[109] **Faropenem** (**XLIII**) displays good activity against most Gram-positive and Gram-negative bacteria, but lacks potency against *P. aeruginosa*.[109, 110] **Sulopenem** (**XLIV**) is another representative penem, with an interesting history from a development perspective: first described in the late 1980s, its development was shortly paused,

only to re-enter clinical trials recently, due to the urgent need of potent antibiotic active against resistant Gram-negative pathogens.[111, 112] **Sulopenem** (**XLIV**) shows good activity against MDR Enterobacterales, displays excellent stability towards many β-lactamases, and is currently evaluated for the treatment of urinary tract infections,[113, 114] thus highlighting the value of repurposing old antibiotics for new uses.[115, 116]

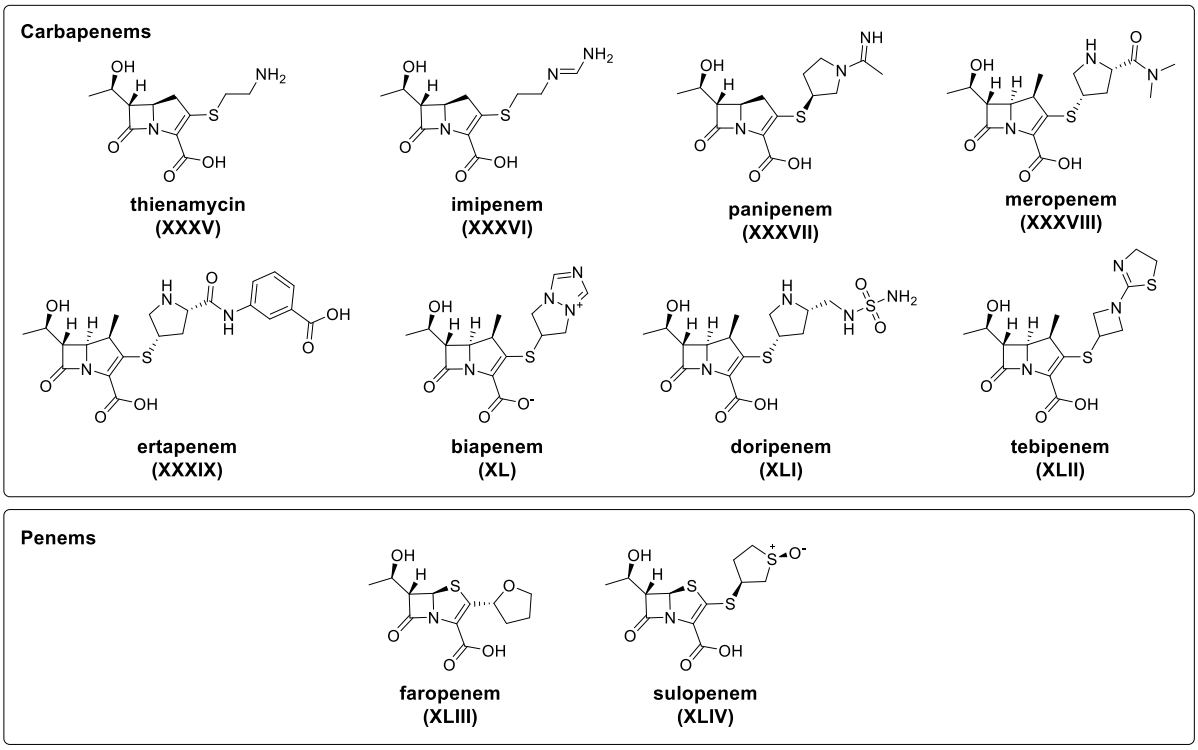

Figure 1.8: Structures of carbapenems and penems.

1.7 Monobactams

The monobactams (**Figure 1.9**) are another major class of clinically used β-lactam antibiotics that have drawn interest thanks to their unusual stability to β-lactamase hydrolysis. The monobactams are monocyclic β-lactams, which, unlike penicillins, cephalosporins and carbapenems, lack the secondary fused ring. **Sulfazecin** (**XLV**),[117] isolated from *Pseudomonas acidophila*, and **nocardicin A** (**XLVI**),[118] obtained from the fermentation broth of *Nocardia uniformis*, are amongst

the first monobactams discovered that displayed improved stability to hydrolysis catalysed by both plasmid-mediated and chromosomal β-lactamases.[119] Targeted optimisation of monobactam derivatives to increase binding affinity to PBPs led to the development of **aztreonam** (**XLVII**), the first (and only) synthetic monocyclic β-lactam that has been clinically used.[120] **Aztreonam**,[120] and its analogue **tigemonam** (**XLVIII**),[121] incorporate the ATMO sidechain, which grants them good coverage against Gram-negative pathogens; furthermore, unlike penicillins, cephalosporins, carbapenems and penems, which all possess a carboxylic acid, **aztreonam** displays a bioisosteric sulfonate group attached to the β-lactam nitrogen. Despite showing good hydrolytic stability to certain β-lactamases (*e.g.*, metallo-β-lactamases; see **Section 1.9.1**),[122] **aztreonam**'s efficacy is compromised by extended-spectrum β-lactamases (ESBLs).[123, 124]

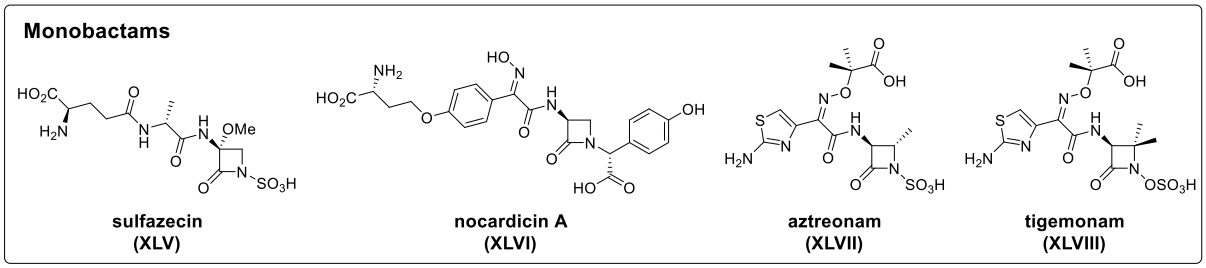

Figure 1.9: Structures of selected monobactams.

1.8 β-Lactamase-resistant β-lactams

Although many classes of β-lactam antibiotics have been developed, their efficient use is increasingly compromised by mutating resistant strains that produce novel β-lactamases.[4, 40, 125] In principle, this risk could be minimized, if β-lactam antibiotics could developed to be poor substrates of β-lactamases. One strategy to improve β-lactam antibiotic stability with respect to enzymatic degradation by β-lactamases entails structural modifications of the β-lactam core. In the case of cephalosporins, this effect was achieved by the introduction of a C7-methoxy group (*e.g.*,

cefoxitin; **Figure 1.10**).[70] This subclass of cephalosporins, known as cephamycins,[70] exhibits enhanced resistance to various β-lactamases,[126] while retaining a similar antimicrobial profile to that of their non-C7-methoxylated analogues.[127] A similar approach was applied to the penicillin scaffold, as exemplified by **temocillin** (**L**),[128, 129] the C6-methoxy derivative of **ticarcillin** (**XII**),[57] where the introduction of the C6-methoxy substituent broadened the antibacterial spectrum of activity against *Enterobacteriaceae* spp..[128, 129]

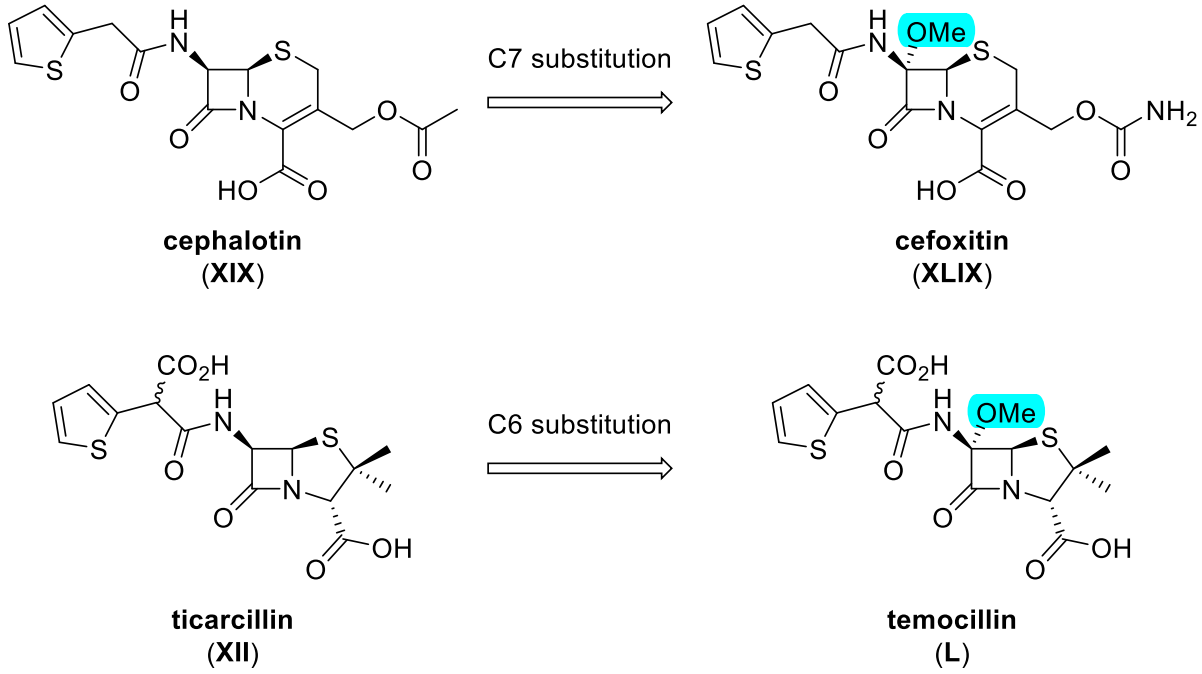

Figure 1.10: Structural modification of cephalosporins and penicillins to improve β-lactamase stability by the introduction of a C6/7-methoxy group.[126, 128]

However, C6/7-methoxy substitution also has several significant limitations:

i) the selective pressure exerted by β-lactam use can still drive the emergence of alternative resistance mechanisms – *e.g.*, PBP modifications can reduce the binding affinity of cephamycins, as seen with cefoxitin-resistant strains;[130, 131]

ii) with the penicillin scaffold, the introduction of a C6-methoxy group has a double-edged effect – while it enhances stability against degradation by β-lactamases, it ablates antibacterial activity against Gram-positive bacteria.[128, 129] This could possibly be due to increased sterics induced by -OMe, thus hindering productive covalent reaction with certain PBPs.[132] Furthermore, crystallographic evidence has shown that, when bound to *P. aeruginosa* PBP3, the increased steric repulsions induce conformational changes that render the acyl-enzyme complex less hydrolytically stable.[133]

Given these constraints, efforts have been made to directly target β-lactamases by employing tailored inhibitors co-administered with β-lactam antibiotics.[4]

1.9 β-Lactamases and β-lactamase inhibitors

1.9.1 β-Lactamase classification

In many pathogenic bacteria, β-lactamase production poses the greatest threat to the clinical efficacy of β-lactam antibiotics.[4, 40, 125] There are more than 2800 β-lactamases known to date,[40] which according to the Ambler classification system can be grouped into 4 classes (A-D).[134] Furthermore, based on their mechanism of action, β-lactamases are commonly divided into two major categories:[37, 40]

(i) Serine β-lactamases (SBLs) – by employing an active-site serine residue, SBLs bind to β-lactams via β-lactam ring opening to form a covalent acyl-enzyme intermediate (in a manner similar to the mechanism of PBP), which is subsequently hydrolysed to yield a ring-opened, non-bactericidal product (**Figure 1.11A**).[135] Ambler class A, C, and D enzymes are serine β-lactamases.

(ii) Metallo-β-lactamases (MBLs) – the hydrolysis of the β-lactam antibiotic is catalysed by Zn(II) ions present at the active site, without the formation of an acyl-enzyme covalent complex (**Figure 1.11B**).[136] Ambler class B enzymes are Zn(II) metalloenzymes.

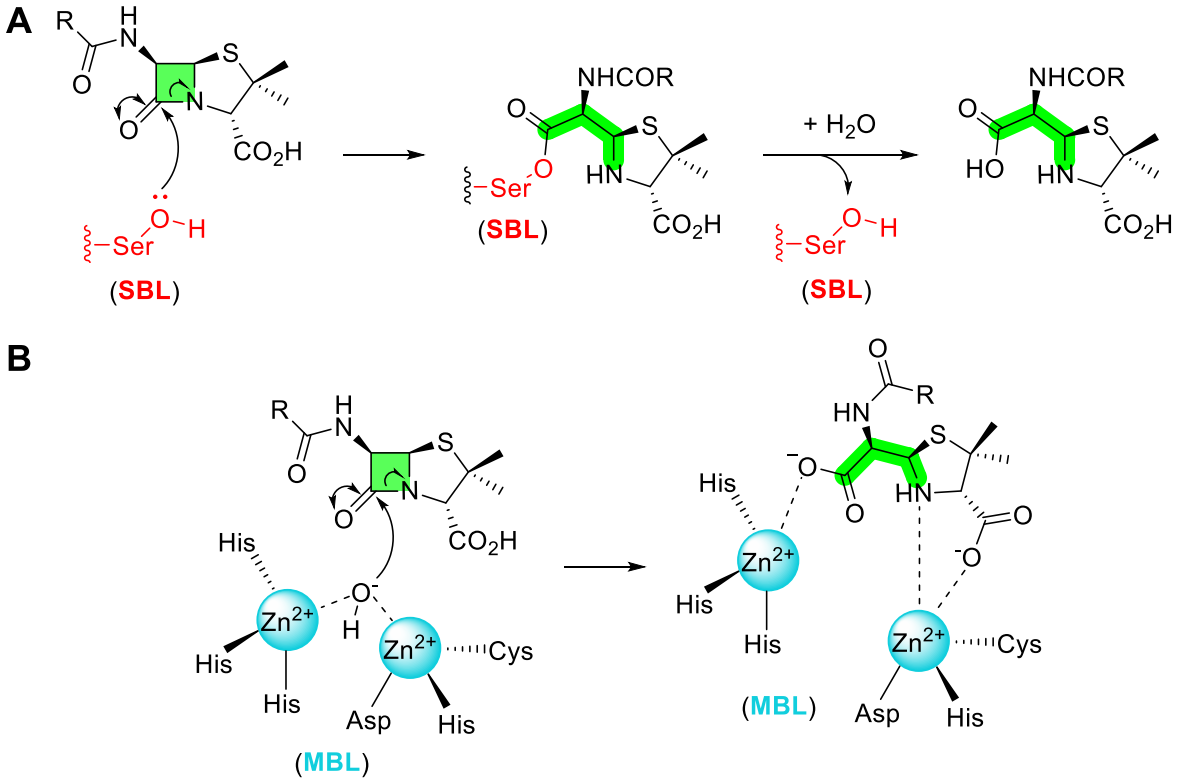

Figure 1.11: Outline hydrolysis mechanism of β-lactam antibiotics catalysed by (**A**) serine β-lactamases (SBLs), and (**B**) metallo-β-lactamases (MBLs).[40]

β-Lactamases of all four classes are widely distributed in both environmental bacteria and clinically-relevant pathogens. Among these, there are several, well-characterized β-lactamase families, in particular from Gram-negative pathogens, known to promote significant resistance even against last-resort antibiotics: i) class A: TEM, SHV, CTX-M, and KPC;[137] ii) class B: NDM, VIM, and IMP;[138] iii) class C: AmpC;[139] and iv) class D: OXA.[140]

1.9.2 β-Lactamase inhibitors

To date, there are three classes of clinically-approved SBL inhibitors: i) β-lactams (**Figure 1.12**); ii) diazabicyclooctanes (DBOs); and iii) boronic acids. Amongst these, β-lactam-based SBL inhibitors are the most widely used in clinical settings, thanks to their proven efficacies, well-established safety profiles, and broad utility in combination therapies with β-lactam antibiotic partners.[4]

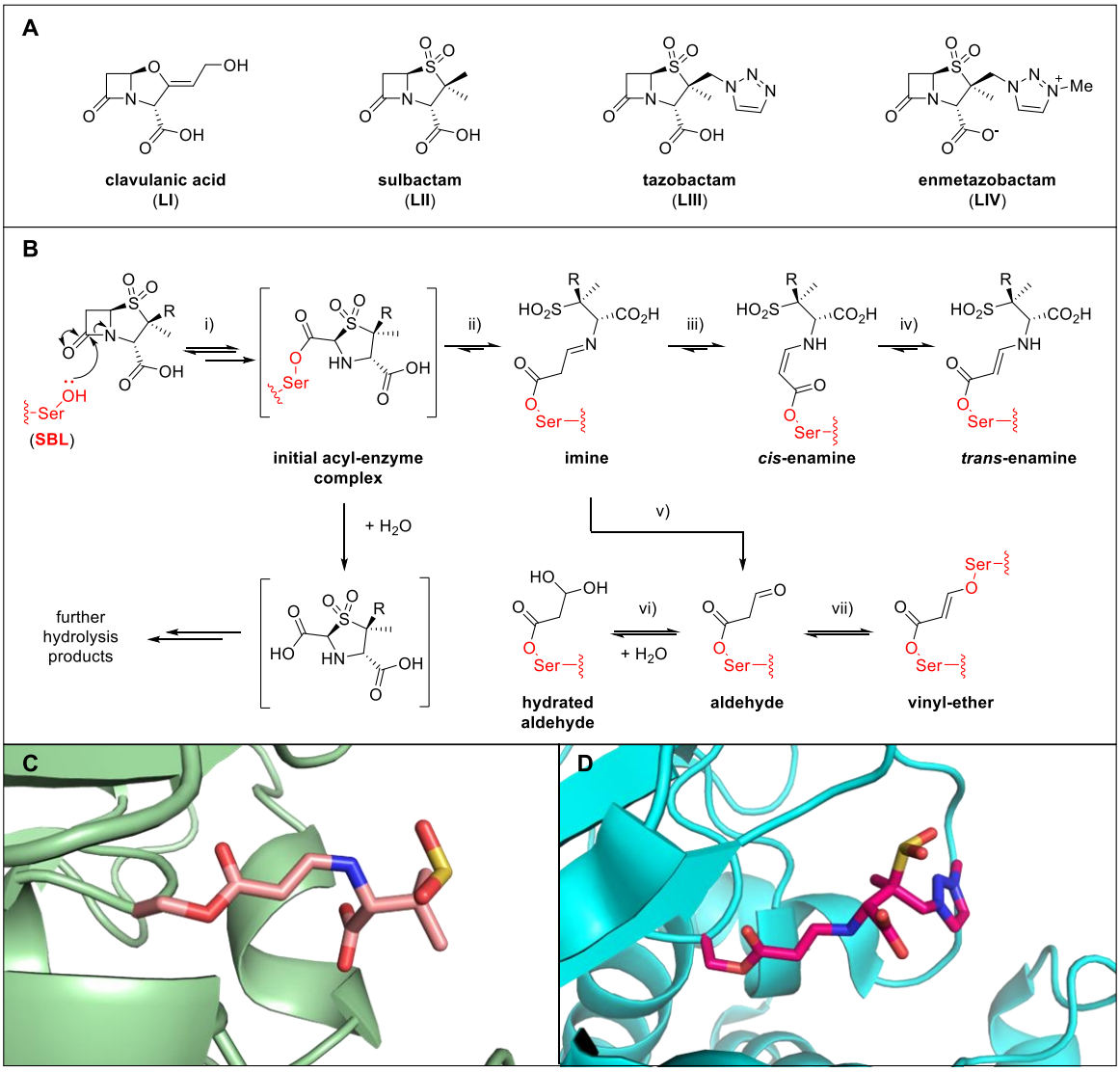

Figure 1.12: (**A**) Clinically approved β-lactam SBL inhibitors. (**B**) Outline mechanism for the reaction of penam sulfone inhibitors with SBLs. (**C**) Crystal structure view of the *trans*-enamine complex formed following covalent

reaction of **sulbactam** with SHV-1 variant (PDB ID: 2A3U).[141] (**D**) Crystal structure view of the *trans*-enamine complex formed following covalent reaction of **tazobactam** with AmpC (PDB ID: 6T35).[142]

Clavulanic acid (**LI**) was the first β-lactamase inhibitor introduced into clinical use, being initially isolated from *Streptomyces clavuligerus* and later produced at scale via fermentation.[143, 144] Its discovery prompted efforts into structurally-related semi-synthetic analogues, leading to the development of **sulbactam** (**LII**)[145] and its penam sulfone derivatives **tazobactam** (**LIII**) and **enmetazobactam** (**LIV**), each designed to broaden their spectrum of β-lactamase inhibition.[146, 147] Several β-lactam/β-lactamase inhibitor combinations have been approved to date, including **amoxicillin/clavulanic acid**,[53] **cefotaxime/sulbactam**,[148] **piperacillin/tazobactam**,[149] and **cefepime/enmetazobactam**.[150]

A common feature among the abovementioned β-lactam-based inhibitors is the fused [4.5] bicyclic skeleton, which resembles that of the penicillin scaffold, with the key distinction that the C6-amido sidechain is missing. The β-lactam-based SBL inhibitors generally exhibit moderate to weak antimicrobial properties with a limited spectrum of activity,[151, 152] likely reflecting the absence of the C6-amido sidechain, which is essential for enhancing active-site PBP binding, but not required for interactions with SBLs.[4]

The general mechanism via which β-lactam-based inhibitors inactive SBLs involves a multistep, irreversible covalent process (**Figure 1.12B**).[5, 40, 134] For instance, **sulbactam** (**LII**) undergoes nucleophilic attack by the SBL active-site serine, resulting in β-lactam ring opening and formation of a covalent acyl-enzyme intermediate. This species then undergoes thiazolidine ring fragmentation, yielding a transient imine species that can tautomerize to either the *cis*- or *trans*-enamines; these intermediates are particularly relevant for inhibition, as they stabilize the acyl-enzyme complexes and prevent enzymatic turnover. The transient imine may also undergo acid-

promoted fragmentation to the corresponding aldehyde, which can either hydrate or covalently react with another serine residue to form a vinyl-ether adduct.[5, 142, 153] This array of inhibition pathways highlights the therapeutic potential and mechanistic versatility of β-lactam-based inhibitors.

Although β-lactam-based inhibitors have proven their efficacy against many SBLs, a major limitation for their use is the lack of inhibitory activity against MBLs.[136] To address this therapeutic gap, other non-β-lactam-based classes of β-lactamase inhibitors were developed.[4, 154, 155] **Avibactam** (**LV**), the first clinically approved DBO, is a broad-spectrum SBL inhibitor, inhibiting class A, class C, and some class D enzymes.[156] The mechanism of action involves covalent modification by **avibactam** (**LV**) of the active site catalytic serine of SBLs. However, unlike β-lactam suicide inhibitors (*e.g.*, **sulbactam**), **avibactam** (**LV**) inhibits enzymatic target in a reversible manner, meaning that upon release it can recyclise, thus preserving its inhibitory properties.[157] The clinical success of **avibactam** (**LV**), as exemplified by the approved combinations with **ceftazidime** (**XXVII**) or **aztreonam** (**XLVII**),[158, 159] inspired the design of other DBOs such as **durlobactam** (used in combination with **sulbactam** for *A. baumanii* infections)[160] or **relebactam** (in combination with **imipenem** for Gram-negative infections),[161] validating the potential of this class to generate next-generation β-lactamase inhibitors.

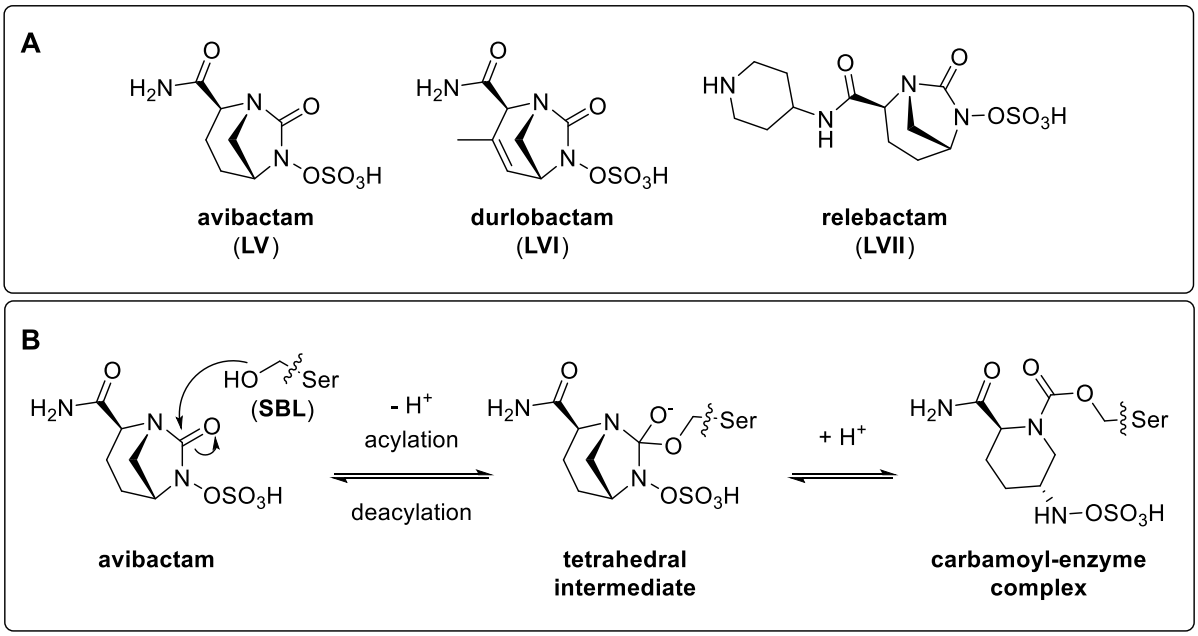

Figure 1.13: (**A**) Clinically approved DBO SBL inhibitors.[162] (**B**) Outline mechanism for the reaction of avibactam with SBLs.[157]

The last major class of SBL inhibitors is represented by the cyclic boronates (**Figure 1.14A**), which employ a boronate core as the reactive warhead. Boronates form reversible, covalent adducts with a tetrahedral geometry, thereby mimicking the high-energy tetrahedral intermediates formed during the hydrolysis of β-lactams by SBLs (**Figure 1.14B**).[163] A representative member is clinically-approved **vaborbactam** (in combination with **meropenem**),[164, 165] a potent inhibitor of class A and C SBLs, but not of class B (*i.e.*, MBLs) or D (*i.e.*, OXA enzymes).[164] Other boronates currently in clinical development include **QPX7728** (**LIX**)[166] and **taniborbactam** (**LX**),[167] which, in addition to SBL inhibition, are also able to target MBLs.

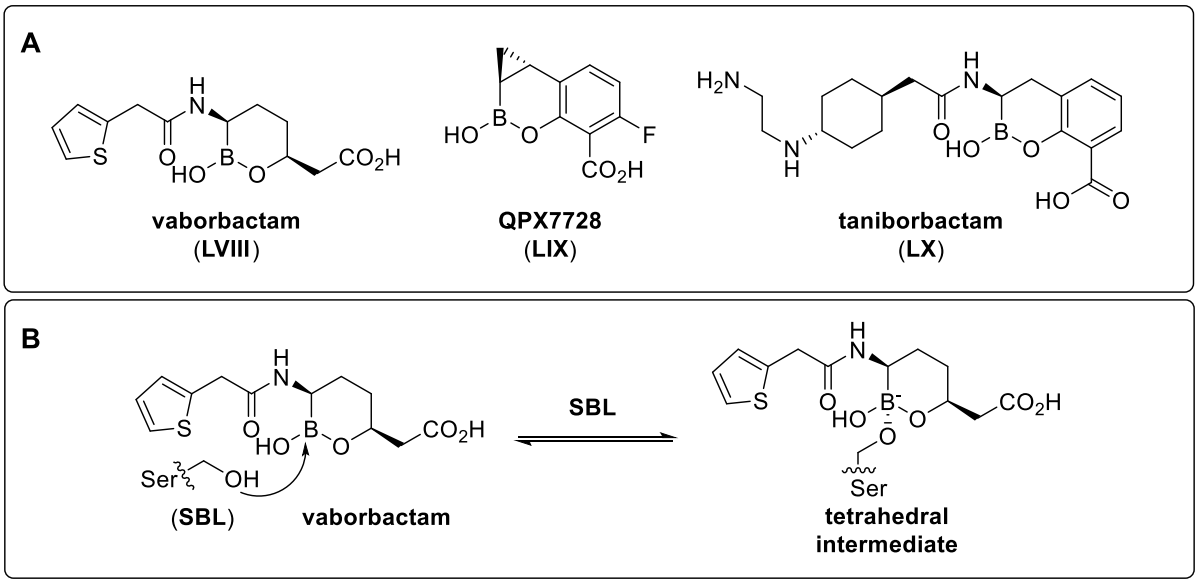

Figure 1.14: (**A**) Representative cyclic boronate inhibitors of β-lactamases.[164, 166, 167] (**B**) Outline mechanism for the reaction of vaborbactam with SBLs.[164]

β-Lactam/β-lactamase inhibitor combinations are a validated therapeutic strategy that extends the clinical scope of β-lactam antibiotics that otherwise would be rendered inactive by β-lactamases.[4] Although significant progress has been made in inhibiting SBLs clinically, to date, there are no clinically approved MBL inhibitors. This highlights once more the pressing need for improved agents that either are not susceptible to β-lactamase-mediated degradation or are themselves β-lactamase inhibitors.

1.10 Investigational β-lactam antibiotics

Beyond their use in clinically approved antibiotics, β-lactam scaffolds have demonstrated their versatility across many clinical candidates and experimental inhibitors. At times, β-lactams are employed in unconventional approaches against microbial targets. For example, cephalosporins have previously been designed as dual-action antibiotics in β-lactamase-producing bacteria, relying precisely on β-lactamase activity to further potentiate antimicrobial properties. β-Lactam ring hydrolysis of cephalosporin-based prodrugs by β-lactamases triggers fragmentation of the

dihydrothiazine ring and elimination of a C3' antimicrobial agent (**Figure 1.15A**).[168, 169] Reported C3′ payloads (**Figure 1.15B**) include broad-spectrum antibiotics (*e.g.*, **ciprofloxacin** – **LXI**)[170], antiseptics (*e.g.*, pyrothione – **LXII**; phenols – **LXIII**)[168, 171], biofilm-dispersion signalling agents (*e.g.*, nitric oxide – **LXIV**)[172], and β-lactamase inhibitors (*e.g.*, 8-thioquinoline – **LXV**).[173]

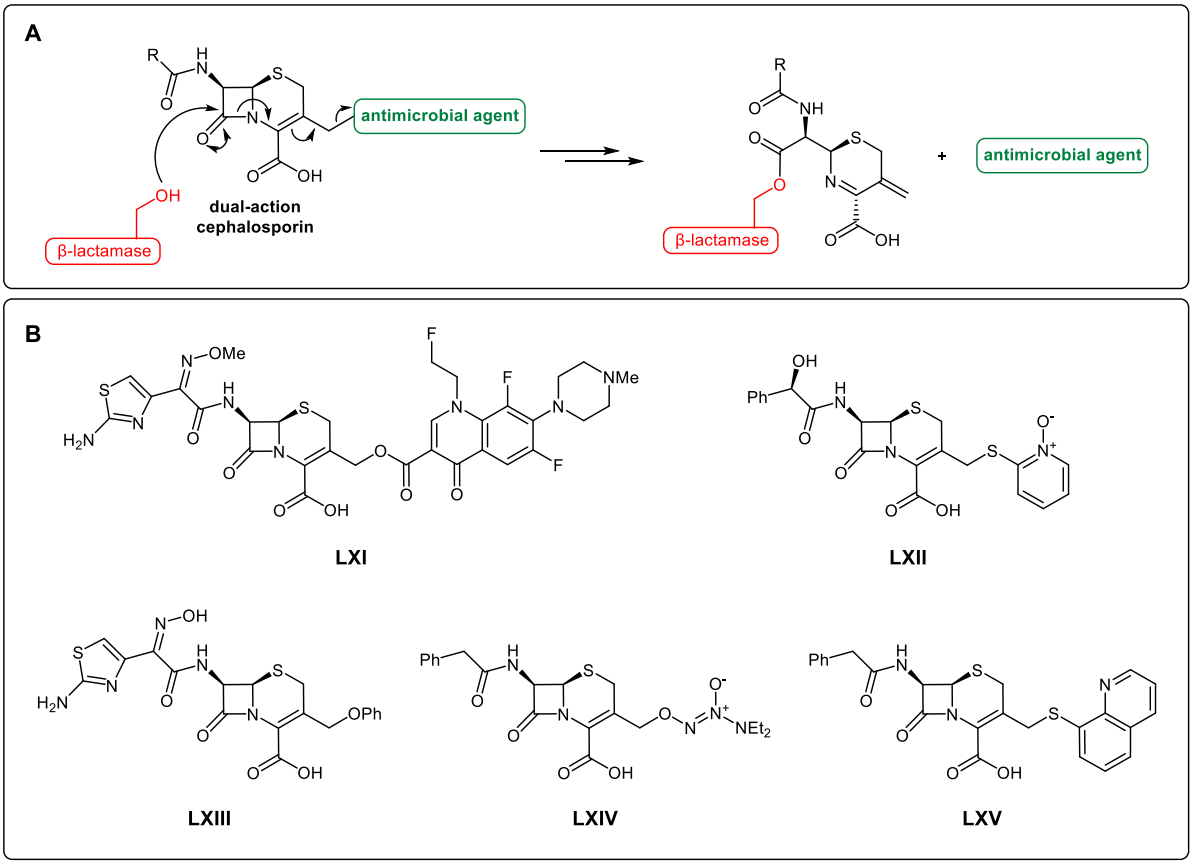

Figure 1.15: (**A**) Outline mechanism for the reaction of dual-action cephalosporins with β-lactamases.[169] (**B**) Structures of reported dual-action cephalosporin antibiotics.[168, 170-173]

Although most clinically-used β-lactams are mono- or bicyclic, tricyclic β-lactams with a fused [4.6.5] skeleton have also been explored.[174, 175] Tricyclic β-lactam **LXVI** (**Figure 1.16**), whose core is essentially a hybrid cephem-γ-lactone scaffold, was designed as a proof-of-concept antibiotic that combines potent PBP inhibition with reduced susceptibility to β-lactamase hydrolysis.[175] Indeed, **LXVI** displayed potent antimicrobial properties against class A, B, and D

β-lactamase producers, but not against class C β-lactamase producers. The first major optimisation consisted of altering the sulfur oxidation state, with the (*S*)-sulfoxide **LXVII** exhibiting reduced susceptibility to class C β-lactamases. Consequently, **LXVII** is a potent β-lactam antibiotic that can be used in the treatment of carbapenem-resistant Enterobacterales (CRE), demonstrating that single β-lactam antibiotics that do not require co-administration with β-lactamase inhibitors can be successfully developed.[175] Furthermore, to combat infections caused by bacteria that possess resistance mechanisms other than β-lactamase production, **LXVIII** was developed. The C7 sidechain was optimised (from sidechain carboxylate to hydroxyl groups) to improve outer membrane permeability in porin-deficient pathogens.[174]

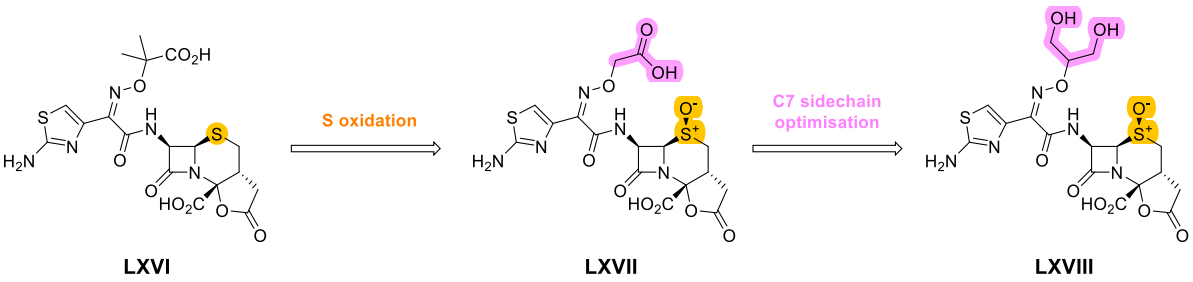

Figure 1.16: Structures of tricyclic β-lactam antibiotics.[174, 175]

It should also be noted that one of the more radical approaches employed during the design of β-lactamase-resistant β-lactam antibiotics challenged the long-standing dogma that β-lactam antibiotics must closely mimic the natural D-Ala-D-Ala substrate of PBPs.[24, 176] The C3-carboxylate group of penicillins plays a crucial role for PBP binding,[177-179] but it is also engaged by active site residues of β-lactamases.[180-182] In principle, if antimicrobial activity is maintained after removal of the C3-carboxylate group from the penicillin scaffold, then it would be possible to develop a β-lactam antibiotic that is not susceptible to β-lactamase-mediated hydrolysis. C2-Carboxypenams successfully employ this strategy, wherein the C3-carboxylate is shifted to the C2 position (**Figure 1.17**).[183, 184] C2-Carboxypenam **LXIX** was reported to display potent

antimicrobial properties against Gram-negative pathogens, including against strains that developed resistance towards **aztreonam** (**XLVII**) or **ceftazidime** (**XXVII**); the nature of this antimicrobial activity for C2-carboxypenams stems precisely from their ability to evade β-lactamase-mediated hydrolysis.[183, 185, 186] Furthermore, **LXIX** and **LXX** are potent antipseudomonal agents, exhibiting more potent inhibition of *P. aeruginosa* PBP3 than either **aztreonam** (**XLVII**) or **ceftazidime** (**XXVII**).[183] Subsequent development of C2-carboxypenams led to **LXXI**, which includes a siderophoric catechol moiety (similar to the one present in **cefiderocol**), thus further potentiating the antipseudomonal properties of this subclass of β-lactam antibiotics.[184]

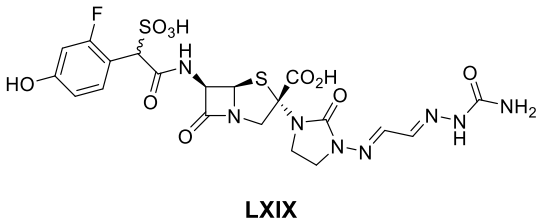

LXIX

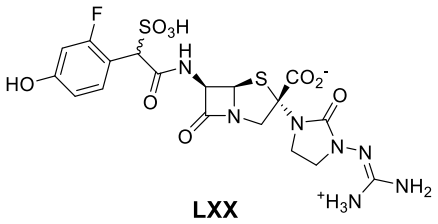

LXX

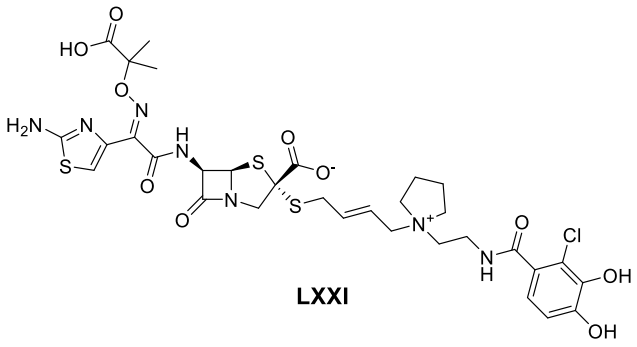

LXXI

Figure 1.17: Structures of C2-carboxypenams.[183, 184]

1.11 Non-bacterial applications of β-lactams

β-Lactam antibiotics represent the most widely used class of antibacterial agents, accounting for nearly two-thirds of all prescriptions worldwide.[4] Their clinical introduction revolutionised

modern medicine, transforming once lethal conditions such as tuberculosis, pneumonia, sepsis, and bacterial meningitis into treatable and often curable diseases.

The versatility of β-lactams, however, extends well beyond their traditional antibacterial role. The strained β-lactam ring is a reactive, covalent warhead that can, in principle, be tailored for diverse therapeutic targets. Reported non-antibacterial applications include antihypercholesterolemic,[187, 188] anticancer,[189-211] anti-inflammatory,[212-228] antifungal,[229-235] and antiviral uses,[236-245] thus highlighting the potential of the β-lactam scaffold as a broadly adaptable motif in drug discovery; of these, antihypercholesterolemic β-lactam agents are clinically used, whereas the remaining indications are currently investigational in nature.

1.11.1 Antihypercholesterolemic applications of β-lactams

Hypercholesterolemia is defined as elevated levels of cholesterol in the bloodstream, and it is a well-known risk factor responsible for the development of atherosclerosis and coronary artery disease.[246] Excess low-density lipoprotein (LDL) cholesterol promotes atherosclerotic plaque formation, which can cause arteries to narrow or rupture, leading to cardiovascular events such as thrombosis or myocardial infarction.[247] Cholesterol homeostasis is regulated through multiple complex processes, such as endogenous synthesis, intestinal absorption, and biliary clearance.[248] Crucially, the cholesterol levels present in plasma is determined by metabolic processes happening within and between the intestines and liver.[249]

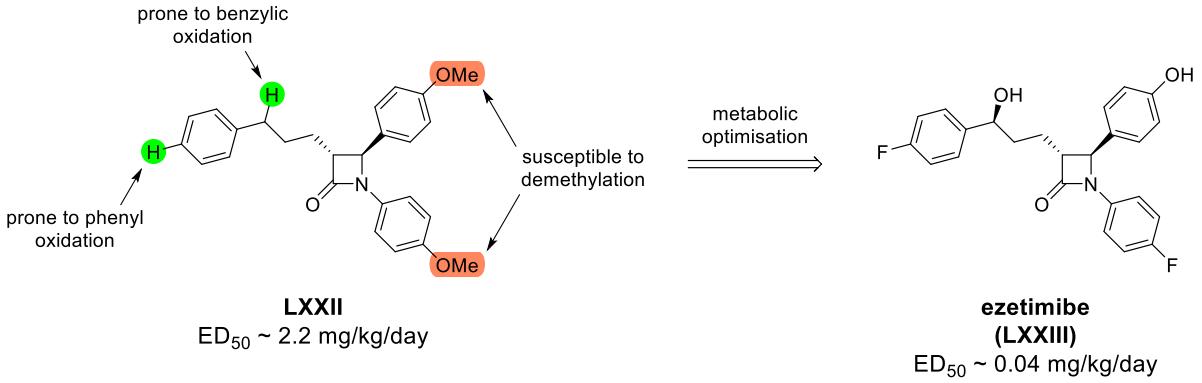

Figure 1.18: Structures of monocyclic β-lactams with antihypercholesterolemic properties. The shown ED_{50} values correspond to the reduction of liver cholesterol esters in hamsters.

Monocyclic-β-lactam **LXXII** is an orally active antihypercholesterolemic agent that promotes reduction in plasma cholesterol and liver cholesteryl ester concentrations in mammals fed a chloresterol-rich diet, operating via inhibition of the luminal cholesterol absorption.[188, 250] In order to improve metabolic stability and increase activity in humans, structural improvements of **LXXII** led to the development of **ezetimibe** (**LXXIII**). **Ezetimibe** is a clinically used orally available agent that targets the intestinal cholesterol transporter Niemann-Pick C1-like 1 (NPC1L1).[251] NPC1L1 is a transporter protein present in the small intestines on the surface of enterocytes, which are absorptive epithelial cells; NPC1L1 plays a crucial role in cholesterol homeostasis, facilitating the formation of transport complexes with cholesterol that subsequently undergo endocytosis. Although **ezetimibe** contains a β-lactam ring, its mechanism of action does not involve covalent acylation of NPC1L1, but rather non-covalent binding with the sterol-sensing domain of NPC1L1, thereby preventing the formation of the NPC1L1-cholesterol complex and blocking the downstream cholesterol uptake.[251]

1.11.2 Anticancer applications of β-lactams

Cancer is one of the leading causes of mortality worldwide, and its burden on the healthcare systems is projected to rise, being driven not only by aging populations but also by lifestyle and environmental risk factors.[252, 253] Despite significant advances in chemotherapy and immunotherapy,[254-256] factors such as tumour heterogeneity,[257] drug resistance,[258] or drug cytotoxicity[259] can sometimes limit the effectiveness of anticancer treatments. These challenges highlight the need for anticancer agents with improved safety profiles that can engage novel therapeutic targets and overcome resistance mechanisms.[260] In this context, β-lactams have been extensively investigated in cancer therapy, at times displaying antiproliferative properties via unexpected modes of action.[261-263]

One of the most promising anticancer applications of cephalosporins has been in the design of anticancer agents used in antibody-directed enzyme prodrug therapy (ADEPT).[189-193, 203, 205] ADEPT employs monoclonal antibody (mAb)-enzyme conjugates to selectively activate cytotoxic drugs at tumour sites: i) the mAb-enzyme conjugate is administered systemically, accumulating in tumour tissues by specifically-binding to malignancy-associated antigens; ii) the subsequent administration of a non-toxic prodrug, which releases the cytotoxic agent following enzymatic reaction with the mAb-enzyme conjugate at the tumour site.[264] Due to the catalytic nature of the mAb-enzyme conjugate, higher doses of prodrug and lower doses of conjugate can be administered, thus reducing side effects and improving the therapeutic index.

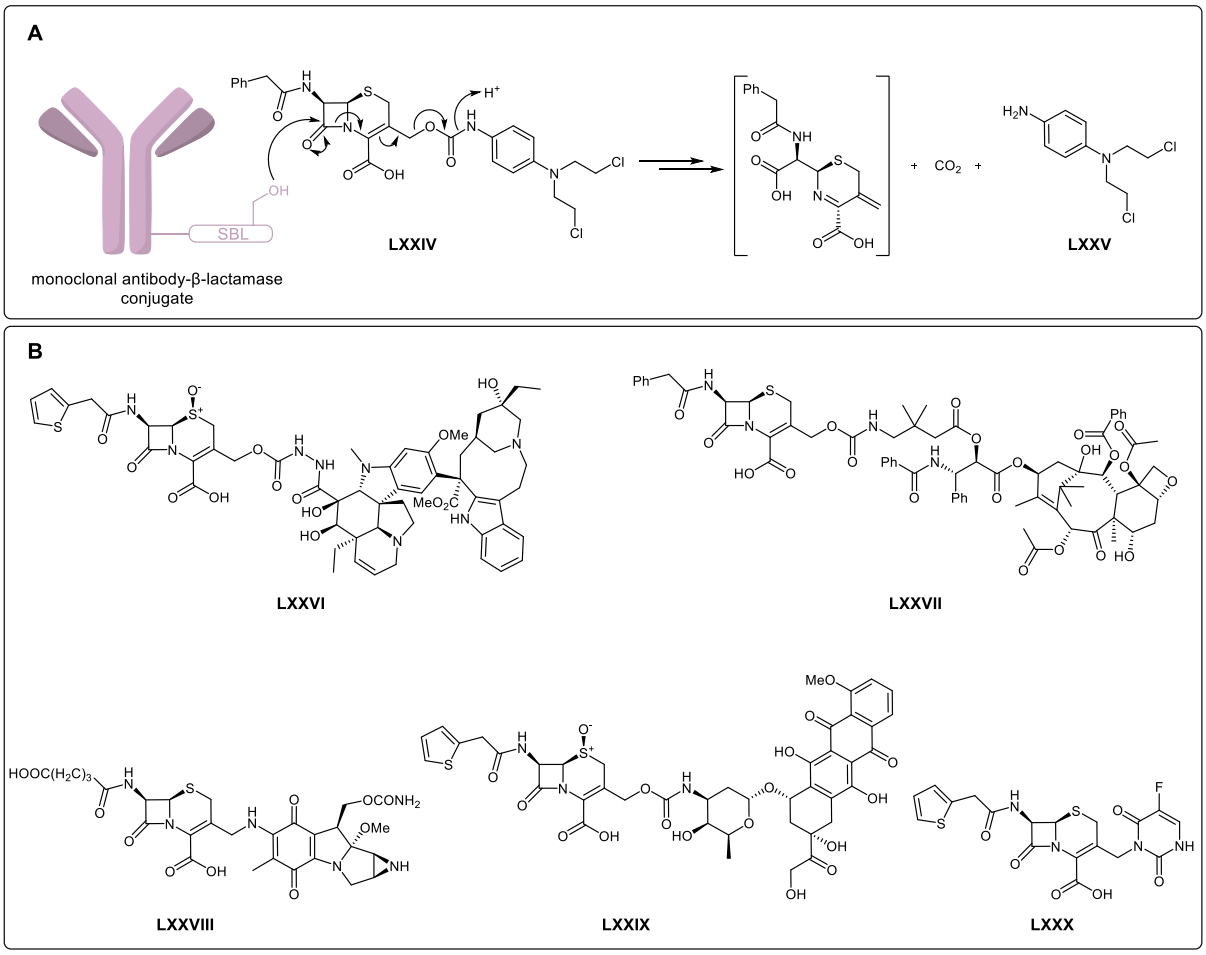

Figure 1.19: A. Reaction of mAb–β-lactamase conjugates with cephalosporin mustard prodrug **LXXIV** to release the cytotoxic agent **LXXV**.[189] **B**. Structures of reported cephalosporin prodrugs used in ADEPT.

β-Lactamases are non-endogenous to mammalian cells and display high specificity for β-lactam substrates such as penicillins and cephalosporins,[4, 40] making them suitable for use in ADEPT (the same strategy is also used in the design of dual-action cephalosporin antibiotics; see **Section 1.10**). Within this framework, mAb-β-lactamase conjugates function as molecular switches that selectively hydrolyse cephalosporin prodrugs for targeted release of cytotoxic agents (**Figure 1.19**). Reported cytotoxic payloads released following cephalosporin prodrug fragmentation include:

i) Nitrogen mustards[265] – potent alkylating agents that cross-link DNA; the cephalosporin-nitrogen mustard prodrug **LXXIV** showed ~50-fold reduction of *in vitro* cytotoxicity compared to phenylenediamine mustard **LXXV** in human adenocarninoma cells,[193] yet upon enzymatic activation by mAb-β-lactamase **LXXIV** exhibited similar potency to **LXXV**.[189]

ii) Vinca alkaloids[266] – oncolytic agents that target and destabilise microtubules, triggering mitotic arrest and apoptosis; *in vivo* mouse model studies in human colorectal carcinoma tumours showed that co-administration of prodrug **LXXVI** with a mAb-β-lactamase promotes long-term tumour regression.[202, 267]

iii) Paclitaxel[268] – a widely used chemotherapeutic agent that triggers mitotic arrest and apoptosis by binding to and stabilising the β-subunit of tubulin in assembled microtubules; *in vitro*, prodrug **LXXVII** was ~12-fold less toxic than paclitaxel in human melanoma cells, but recovered comparable potency to paclitaxel when activated by mAb-β-lactamase conjugates.[191]

iv) Mitomycin C[269] – a prodrug that is enzymatically reduced to an alkylating agent targeting DNA, thus inhibiting mitosis and causing apoptosis; mitomycin C prodrug **LXXVIII** showed ~16-fold reduced toxicity compared to mitomycin C in human lung adenocarcinoma cells, yet retaining similar potency to mitomycin C in the presence of mAb-β-lactamase conjugates.[192]

v) Doxorubicin[270] – a DNA-intercalating agent and topoisomerase II inhibitor that disrupts DNA replication and transcription; cephalosporin-doxorubicin prodrug **LXXIX** in conjunction with a mAb-β-lactamase conjugate facilitated the selective

delivery of doxorubicin to breast, ovarian and colon carcinoma cells, but despite showing comparable efficacy and lower cytotoxicity it did not promote tumour regression.[271]

vi) 5-Fluorouracil[272] – an oncolytic prodrug agent used in colorectal cancer therapy whose metabolites not only inhibit thymidylate synthase but are also incorporated into RNA and DNA; although efficiently cleaved by mAb-β-lactamases, prodrug **LXXX** showed similar cytotoxicity to 5-fluorouracil itself.[204, 273, 274]

Apart from their application as prodrug scaffolds in ADEPT strategies, certain clinically used cephalosporin antibiotics are also reported to display intrinsic anticancer properties (**Figure 1.20**). **Ceftriaxone** (**LXXXI**),[275] a third-generation antibiotic, inhibited the growth of gefitinib-resistant[276] lung adenocarcinoma cells, having as its therapeutic target Aurora B kinase.[194] Aurora B kinase plays an important role in regulating cell division, and its over-expression can lead to unchecked cell proliferation. **Ceftriaxone** (**LXXXI**) targets the ATP-binding site of Aurora B, thus suppressing cancerous lung cell growth. Since Aurora B kinase is also highly expressed in ovarian, colon, and prostate cancers,[277-279] these findings suggest that **ceftriaxone** could potentially target a broader spectrum of malignancies.

Cephalosporin antibiotics have also been investigated in cancer therapy as radiosensitizers.[195] **Cephalexin** (**XVII**) was shown to enhance the efficacy of ionizing radiation by promoting DNA damage in human breast cancer cells, presumably through increased production of reactive oxygen species (ROS).[195] Notably, β-lactam antibiotics (*e.g.*, **ampicillin**; **IX**) have been previously reported to induce mitochondrial dysfunction and ROS overproduction in mammalian cells.[280-282] Furthermore, increased ROS levels induced by certain cephalosporins have been used to promote

cytotoxicity in nasopharyngeal carcinoma.[196] For example, **cefotaxime** (**XXVI**) upregulates heme oxygenase-1 (HMOX1) expression, whose elevated activation increases the cellular concentration of Fe(II). This leads to the excessive generation of ROS, ultimately triggering ferroptosis (*i.e.*, iron-dependent cell death).[196] Together, these findings illustrate the oncological potential of cephalosporin antibiotics in radio- and chemotherapy, while also highlighting the need to minimize undesired ROS generation when designing new, safer β-lactams antibiotics for the treatment of bacterial infections.

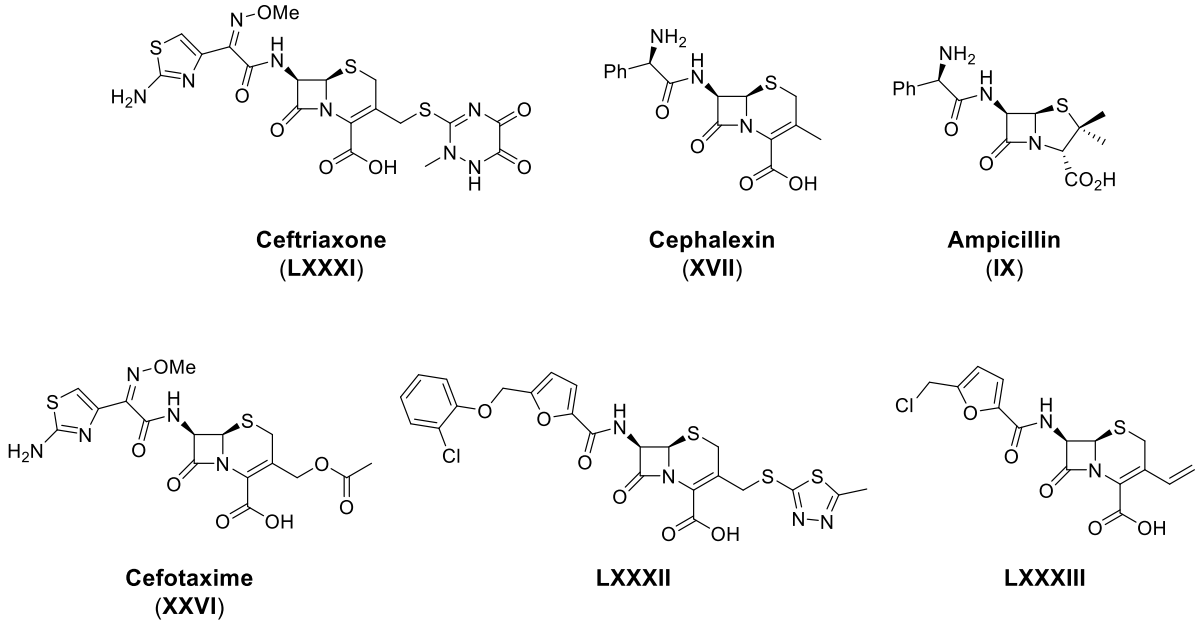

Figure 1.20: Structures of cephalosporin and penicillin derivatives with anticancer applications.

The cephalosporin scaffold was also employed to develop inhibitors of the Speckle-type POZ protein (SPOP).[197, 198] SPOP is an E3 ubiquitin ligase adaptor protein that mediates substrate protein recognition and ubiquitination;[283] SPOP dysregulation contributes to oncogenic signalling, particularly in clear cell renal cell carcinoma (ccRCC), where SPOP was discovered to be overexpressed.[284] Virtual screening and subsequent fluorescence polarization assays revealed that **LXXXII** inhibited SPOP ($IC_{50} \sim 4.5$ μM), with CPMG NMR assays suggesting that **LXXXII** binds

to SPOP in a non-covalent manner.[197] Inhibitor optimisation following a structure-activity relationship (SAR) analysis yielded **LXXXIII**, a potent SPOP inhibitor (IC_{50} ~ 0.6 μM) that not only disrupts SPOP-substrate interactions *in vitro*, but also suppresses the proliferation of ccRCC cells.[198]

Penicillin derivatives have also attracted attention as potential anticancer agents (**Figure 1.21**). Among these, C6-dihalopenicillins, in particular C6-dibromopenam derivatives such as **LXXXIV**, displayed potent cytotoxic activity against cancer cells, but their poor selectivity also resulted in toxicity towards normal cell lines.[207] To improve selectivity, scaffold modifications have been pursued to enhance target-specific interactions and minimize off-target effects. One emerging strategy is molecular hybridization,[285] in which pharmacophoric units and bioactive fragments are combined within a single scaffold to yield new hybrid compounds with optimized properties. For example, conjugation of the penicillin core at the C3 position with a peptide chain via a 1,2,3-triazole linker produced derivative **LXXXV**, which inhibited the growth of human cervix adenocarcinoma and murine melanoma cells while demonstrating ~34-fold reduced toxicity toward non-malignant cells.[207, 208] Other molecular hybrids such as penicillin-oxadiazoles have also been investigated (*e.g.*, **LXXXVI**);[209] although the achieved selectivity was reduced (only ~4-fold with respect to non-malignant cells), the results do show molecular hybridization is a versatile technique that can be employed to develop penicillin-based anticancer agents.

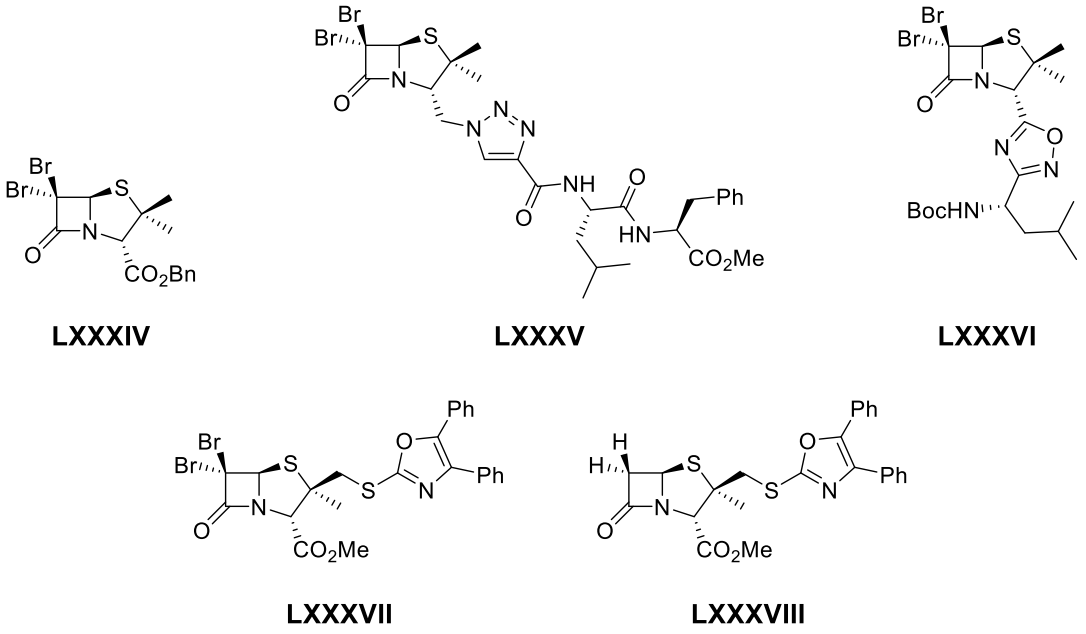

Figure 1.21: Structures of penicillin derivatives with anticancer applications.

Notably, the cytotoxic selectivity of C6-dibromopenicillin derivatives can also be improved by introducing key substituents at the C2-β-position.[206] For example, derivative **LXXXVII**, bearing a 2-(methylthio)-4,5-diphenyloxazole group, showed potent antiproliferative activity against cervix and breast cancer cells while demonstrating a selectivity index of ~4-fold relative to non-malignant cells. Interestingly, the corresponding dihydro analogue **LXXXVIII** also retained both cytotoxicity and selectivity, suggesting that the presence of C6-bromo substituents may not be essential for anticancer activity. Taken together, these results highlight the potential of penicillin scaffold optimisation for developing cytotoxic agents with improved selectivity and efficacy against malignant cells.

Although promising, both penicillin- and cephalosporin-based anticancer agents present limitations. The rigid bicyclic frameworks pose synthetic challenges when systematic structural modifications are required. By contrast, monocyclic β-lactams are synthetically more amenable to functionalisation, making them an attractive scaffold for structure-activity relationship (SAR)

studies. Thanks to the plethora of synthetic methodologies available,[286-288] monocyclic β-lactams (**Figure 1.22**) have been developed to cover a wide range of therapeutic targets:

i) Apoptosis induction – *N*-thiolated monocyclic β-lactams can trigger programmed cell death.[199] β-Lactam **LXXXIX**, which was identified as a potent anticancer agent against Jurkat T, breast, head-and-neck, and prostate cancer cells, had been found to cause DNA damage, which triggers a caspase enzyme cascade, the effect of caspase activity being apoptosis initiation.[289] While the exact mechanism by which *N*-thiolated β-lactams damage DNA is unclear, it is known that such compounds have dual covalent modalities, being able to react via either β-lactam ring opening or N-S bond cleavage.[290]

ii) Tubulin polymerisation – microtubules are cytoskeletal structures that play a critical role in mitosis and cell division, and they are a validated oncological therapeutic target.[291] β-Lactam **XC** inhibited tubulin polymerisation *in vitro*, disrupted microtubular structures in breast cancer cells, and suppressed tumour proliferation, while displaying minimal cytotoxicity towards non-malignant cells.[292]

iii) Poly(ADP-ribose)polymerase-1 (PARP1) – PARPs are a family of nuclear enzymes involved in DNA repair, gene transcription, telomere integrity and cell division, their primary role being polymerizing poly(ADP-ribose) on critical signalling proteins; thus, suppression of PARP-mediated DNA repair synergistically enhances the efficacy of traditional cancer therapies, resulting in cell death.[293] β-Lactam **XCI**, a *N*-derivative of tetrahydropyridopyridazinone, was reported to be a potent inhibitor of PARP1.[294] Given that non-β-lactam analogues of **XCI** also displayed PARP1 inhibition, the β-lactam ring itself is unlikely to act in a covalent manner but instead appears to

contribute to binding via non-covalent interactions. More importantly, **XCI** showed superior cellular activity compared to its N-succinimide analogue, indicating that the β-lactam moiety may modulate the metabolic stability and pharmacokinetic properties of the inhibitor.

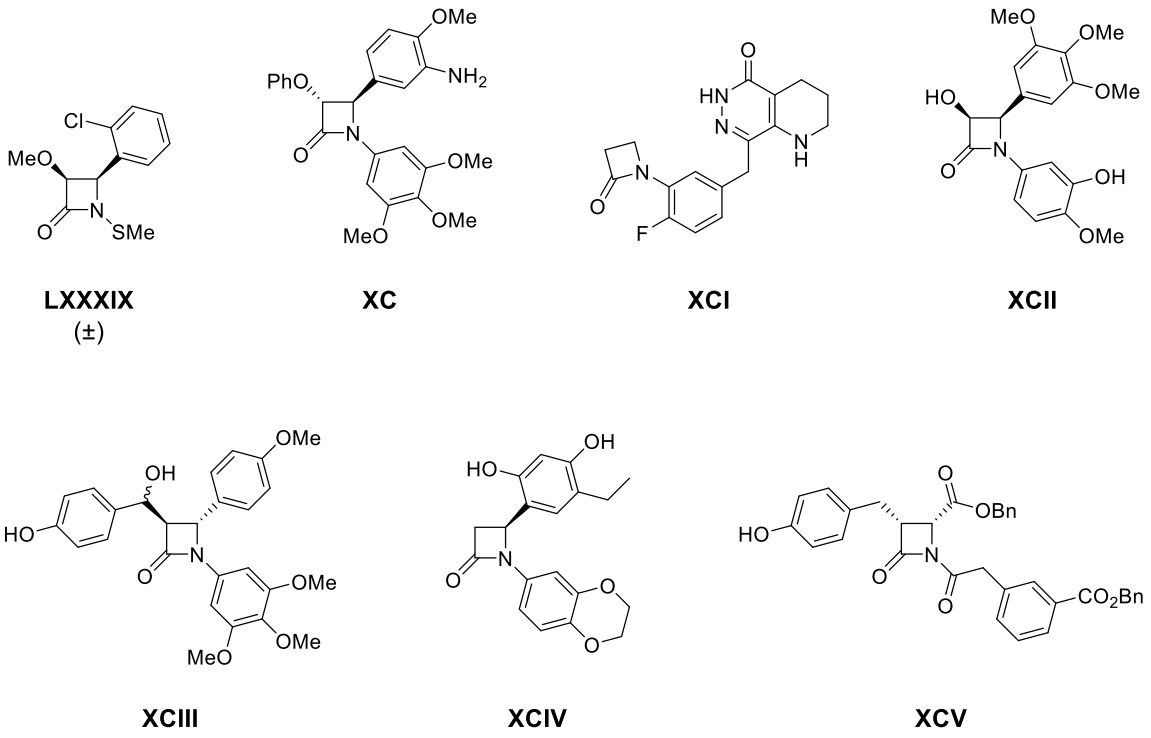

Figure 1.22: Structures of monocyclic β-lactams with anticancer applications.

iv) Adenosine monophosphate activated protein kinase (AMPK) – AMPK regulates cell cycle progression, and its activation can inhibit tumour growth.[295] β-Lactam **XCII** manifested cytotoxicity in duodenal adenocarcinoma cells, operating via inhibition of tubulin polymerisation, cleavage of caspase-3 and PARP, and activation of AMPK. **XCII** also exhibited a high selectivity index for malignant cell (~1000-fold higher than for normal cells).[296]

v) Estrogen receptors (ER) – ER regulate gene expression and cell proliferation in hormone-responsive tissues, particularly in breast tissues, and their overexpression contribute to the development of hormone-dependent cancers.[297] β-Lactam **XCIII** is a dual-action inhibitor that targets both ER and tubulin, thus inducing apoptosis in breast cancer cells. Furthermore, computational modelling studies indicated that **XCIII** is predicted to form stable non-covalent interactions with the binding-site resides of both ER and tubulin.[298]

vi) Heat shock protein 90 (Hsp90) - Hsp90 is a molecular chaperone involved in the maturation and stabilisation of multiple oncogenic proteins.[299] β-Lactam **XCIV** was reported to inhibit Hsp90 by blocking the ATP-binding site; however, the antiproliferation properties of **XCIV** in breast cancer cells were moderate, indicating future optimisation is required.[300]

vii) Prostate-specific antigen (PSA) – PSA is a serine protease used as a diagnostic biomarker in prostate carcinoma, with evidence indicating that it contributes to prostate malignant growth.[301, 302] Enzymatic assays showed that β-lactam **XCV** is a potent inhibitor of PSA (IC_{50} ~ 340 nM), with MS assays confirming that **XCV** forms a covalent adduct with PSA, following the nucleophilic attack of PSA Ser189 at the β-lactam ring, resulting in β-lactam ring opening.[211, 303]

All in all, β-lactams spanning multiple classes, from monocyclic derivatives to penicillins and cephalosporins, have proven their potential as promising anticancer agents. Considering the structural versatility of β-lactam derivatives, coupled with their diverse mechanisms of action, the

β-lactam scaffold clearly represents a valuable therapeutic platform in the ongoing development of improved anticancer agents.

1.11.3 Anti-inflammatory applications of β-lactams

Chronic inflammation is an underlying condition that contributes to the onset and progression of serious diseases, including but not limited to cardiovascular disease, diabetes, cancer, and neurodegeneration.[304] Given that more than 50% of all deaths can be linked to inflammation-related diseases, there is a pressing need to develop innovative strategies to tackle pathological inflammation.[305] In this context, β-lactams have been investigated as potential anti-inflammatory agents, with significant researched efforts being directed towards the development of human leukocyte elastase (HLE) inhibitors (**Figure 1.23**).[212-220, 224]

HLE is a serine protease released from polymorphonuclear leukocytes (PMNs) during inflammation, which under pathological conditions promotes the uncontrolled proteolytic degradation of structural tissues, in particular in the lungs and joints. Unchecked HLE activity has been linked to degenerative diseases such as cystic fibrosis, chronic bronchitis and rheumatoid arthritis, making it a relevant therapeutic target.[306-309]

C7-α-Methoxy cephem sulfone *tert*-butyl ester **XCVI** (**Figure 1.9**) emerged as a potent, time-dependent covalent inhibitor of HLE ($IC_{50} \sim 1$ μM), with SAR studies revealing critical insights into the stereoelectronic requirements for HLE inhibition.[212] Unlike cephalosporin antibiotics, where the C7 substituent is on the β-face, the C7-OMe group in **XCVI** is positioned on the α-face, likely reflecting the biological differences between bacterial and mammalian serine protease targets; since HLE cleaves L-L amino-acid peptide bonds, a C7-α orientation appears necessary for optimal active-site recognition. Increasing the steric bulk of the C7-alkyl ether substituent or

reducing the sulfur oxidation state diminished inhibition; moreover, SAR at the C4 position showed that carboxylic acids were poorly tolerated (*e.g.*, **XCVII**; IC_{50} >50 μM), whereas esters and amides (*e.g.*, **XCVIII** and **XCIX**; IC_{50} ~ 0.07 and 0.1 μM, respectively) improved inhibitory properties.[213] The latter observation likely reflects that HLE is an endopeptidase cleaving peptide linkages between non-ionic residues, highlighting the preference for neutrally-charged functional groups in the vicinity of the active site. Although cephem derivatives with C4 lipophilic ester substituents showed superior *in vitro* properties, the more polar amide analogues proved to be more efficacious *in vivo*. This observation led to the development of **C**, a potent HLE inhibitor suitable for formulation as a topical aerosol.[216] Further SAR studies showed that other β-lactam scaffolds can also serve as templates for HLE inhibition, as exemplified by penicillin sulfone ester **CI**, penem ester **CII**, and the orally active monocyclic β-lactam **CIII**.[214, 217, 218]

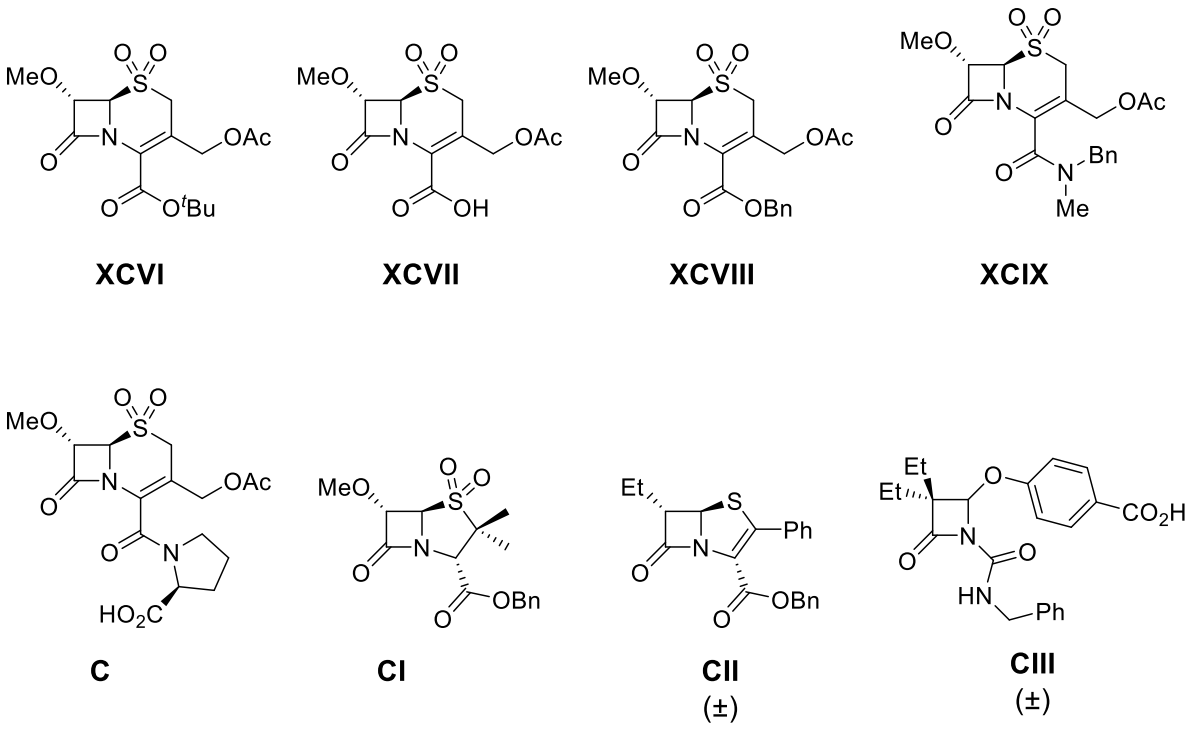

Figure 1.23: Structures of reported β-lactam inhibitors of HLE.

Notably, in addition to inhibiting serine proteases involved in inflammation, β-lactams are also known to target cysteine proteases, specifically lipid-metabolising enzymes such as *N*-acylethanolamine acid amidase (NAAA).[226-228] Among the innate inflammation regulatory mechanisms, fatty acid ethanolamides (FAEs), such as palmitoylethanolamide (PEA) and oleoylethanolamide (OEA), act as endogenous ligands for peroxisome proliferator-activated receptor-α (PPAR-α), thereby exerting anti-inflammatory and analgesic effects by inhibiting mast cell degranulation and supressing peripheral inflammation.[310] However, a key modulator of this pathway is NAAA,[311] a cysteine amidase localized in macrophages and lymphocytes, which degrades PEA. Therefore, it was envisioned that by inhibiting NAAA, PEA levels could be increased, thus reducing inflammation. β-Lactone **CIV** was identified as an NAAA inhibitor (IC_{50} ~ 0.42 μM), but despite its promising immunomodulatory properties, it suffered from limited chemical and plasma stabilities (**Figure 1.24**). To overcome stability issues, the β-lactone moiety was replaced by a β-lactam, as seen in **CV**. **CV** not only showed excellent inhibitory properties against NAAA (IC_{50} ~ 0.08 μM) but also displayed favourable physicochemical properties suitable for systemic administration. Further SAR exploration revealed that *N*-substitutions are not only well-tolerated but also led to a marked increase in inhibitory properties. **CVI** showed both *in vitro* (IC_{50} ~ 0.006 μM) and *in vivo* activities, while reducing heat hyperalgesia and paw edema in an inflammation mouse model. This class of immunomodulatory β-lactams are also of great mechanistic interest, as MS evidence showed that the active site cysteine residue of NAAA (Cys126) reacts covalently with the β-lactam ring, resulting in the formation of a *S*-acylation adduct.[227, 228]

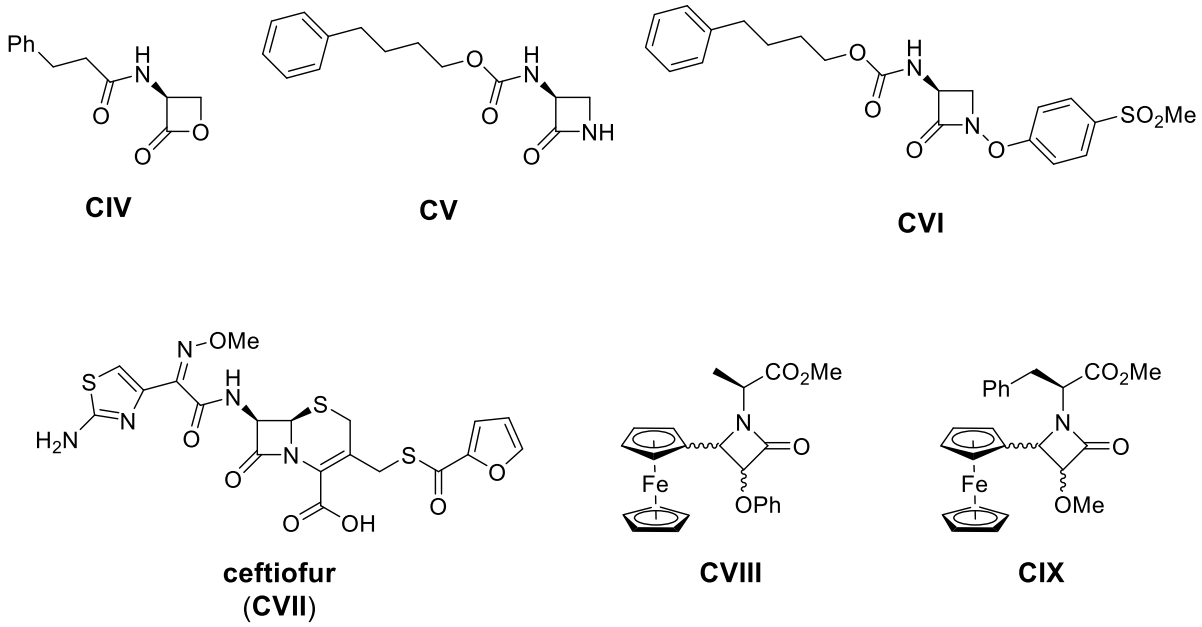

Figure 1.24: Structures of β-lactams with immunomodulatory properties.

Pathological inflammation can also be driven by bacterial infection, where an overactive immune response can trigger sepsis.[312, 313] In Gram-negative bacteria, lipopolysaccharides, an integral component of the bacterial outer membrane, induce the Toll-like receptor-4 (TLR4) complex activation on monocytes and macrophages, thus triggering the release of pro-inflammatory cytokines such as tumor necrosis factor-α (TNF-α), interleukin-1β (IL-1β), and interleukin-6 (IL-6). Although antibiotics treat sepsis by targeting the underlying bacterial infection, their effect on downregulating the innate inflammatory response is minimal. Therefore, dual-action antibiotic capable of eliciting an anti-inflammatory response are of great therapeutic interest. Ceftiofur (**CVII**), a third-generation cephalosporin antibiotic approved for veterinary use, displayed immunomodulatory properties and modulates cytokine production *in vitro*.[223] In the presence of microbial stimuli, mitogen-activated protein (MAP) kinases mediate cytokine production, while the nuclear factor-κB (NF-κB) regulates the transcription of key inflammatory genes; by inhibiting the activation of both pathways in the presence of lipopolysaccharides, ceftiofur downregulates

the production of TNF-α, IL-1β, and IL-6. Although the mechanism of inhibition by ceftiofur of these signalling is unclear, these findings do warrant further investigation, especially since there are other structurally related cephalosporin antibiotics that may also possess anti-inflammatory properties.

Another promising class of dual-action antibiotics with anti-inflammatory properties is represented by ferrocene-monocyclic-β-lactam hybrids (**Figure 1.24**).[225] Ferrocene, an organometallic complex comprising a Fe(II) ion coordinated by two cyclopentadienyl rings, is a versatile benzene bioisostere that shows high stability, low mammalian toxicity, and reversible redox behaviour.[314] Ferrocene has previously been incorporated into penicillin, cephalosporin, and penem derivatives, revealing that such hybrids manifest both high antibacterial properties and antiproliferative effects against breast and colon carcinoma cells.[315-317] Hybrids **CVIII** and **CIX** were reported not only to be active against both Gram-positive and Gram-negative bacteria, but also to possess anti-inflammatory properties by inhibiting inducible nitric oxide synthase (iNOS) and arginase activity.[225] During inflammation, iNOS catalyses the oxidative deamination of L-arginine to L-citrulline,[318] thus producing NO in macrophages, which becomes released into tissues. Although NO is known to possess antibacterial properties by dispersing the bacterial biofilm,[319] its excessive production can cause tissue damage. Similarly, by converting L-arginine to L-ornithine and urea, arginase modulates NO production and regulates inflammatory responses.[320] Considering that both iNOS- and arginase-catalysed processes involve redox reactions, it is plausible that the hybrids **CVIII** and **CIX** owe their inhibitory properties to the ferrocene moiety. Altogether, these findings highlight once again the versatility of the β-lactam scaffold, which can be tailored to combat bacterial pathogens while manifesting immunomodulatory activity.

1.11.4 Antifungal applications of β-lactams

Human fungal infections are a relatively neglected area of research.[321, 322] Although many fungi are harmless and/or symbiotic in the mammalian gut flora,[323] certain fungi can exhibit opportunistic behaviour and infect hosts with disrupted mucosal barriers or compromised immune systems. Among fungi of serious concern are *Candida* spp.,[324] the most common cause of fungal infections, ranging from superficial mycosis to invasive candidiasis, as well as pathogenic moulds associated with pulmonary disease, such as *Aspergillus fumigatus*.[325]

β-Lactam antibiotics generally lack antimycotic properties, which reflects the fundamental differences between the bacterial and fungal cell walls, and the enzymes catalysing their biosynthesis.[326, 327] The fungal cell wall primarily consists of chitin and β-glucans, the biosynthesis of the latter being facilitated by β-1,3-glucan synthases, a class of enzymes that catalyse the transfer of saccharide moieties from an activated nucleotide sugar to a nucleophilic glycosyl acceptor molecule. Nonetheless, several reports indicate that strategic scaffold and functional group modifications can impart antifungal properties to β-lactam derivatives.[229-235]

Beyond the reported anticancer and antibiotic properties of *N*-thiolated β-lactam **CX**, antifungal activity in *Candida* spp. has also been observed.[328] Interestingly, the primary cellular target of *N*-thiolated β-lactams in *Candida* spp. is coenzyme A (CoA), whose purpose is to regulate catalytic redox reactions (**Figure 1.25**). In species with high cytoplasmic concentrations of CoA, *N*-thiolated β-lactams deplete CoA and disrupt processes reliant on CoA.[234] Minimum inhibitory concentration (MIC) assays confirmed that **CX** inhibited fungal growth across a range of *Candida* spp. (MICs in the range of 5-15 μg/mL).

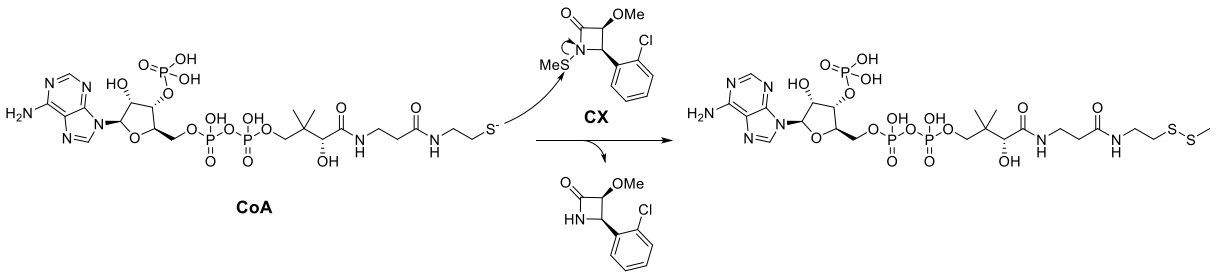

Figure 1.25: Outline mechanism for the reaction of CoA with *N*-thiolated β-lactam **CX**.[328]

Another interesting class of β-lactam antimycotic agents unexpectedly emerged from studies on β-lactam antibiotics biosynthesised by fungi. *S. clavuligerus,* most notably known for producing **clavulanic acid** (**LI**; **Figure 1.12**),[143] is also responsible for the biosynthesis of clavam **CXI** (**Figure 1.26**), which manifested moderate to weak antifungal properties.[329] On the other hand, the related **clavamycins A** (**CXII**) and **D** (**CXIII**), obtained from *S. hygroscopicus*, exhibited potent anti-*Candida* activities, inducing morphological changes consistent with disruptions in the cell wall biosynthesis.[230] Although inhibition of either chitin synthase or sterol biosynthesis is not observed, clavamycins appear to hijack the fungal peptide transport system. Clavamycins can then access the cell, where upon enzymatic degradation clavam **CXIV** is obtained. The antifungal activities of both **CXII** and **CXIII** are antagonised by methionine, indicating that their antifungal properties likely result from their ability to interfere with methionine biosynthesis.[230, 329] Furthermore, valclavam (**CXV**) and hydroxyethylclavam (**CXVI**), natural products of *S. antibioticus*, also displayed strong fungistatic properties across a wide range of species.[330] Interestingly, **CXV** and **CXVI** do not inhibit *Saccharomyces cerevisiae* by disrupting methionine biosynthesis, but rather by interfering with eukaryotic RNA synthesis.[330]

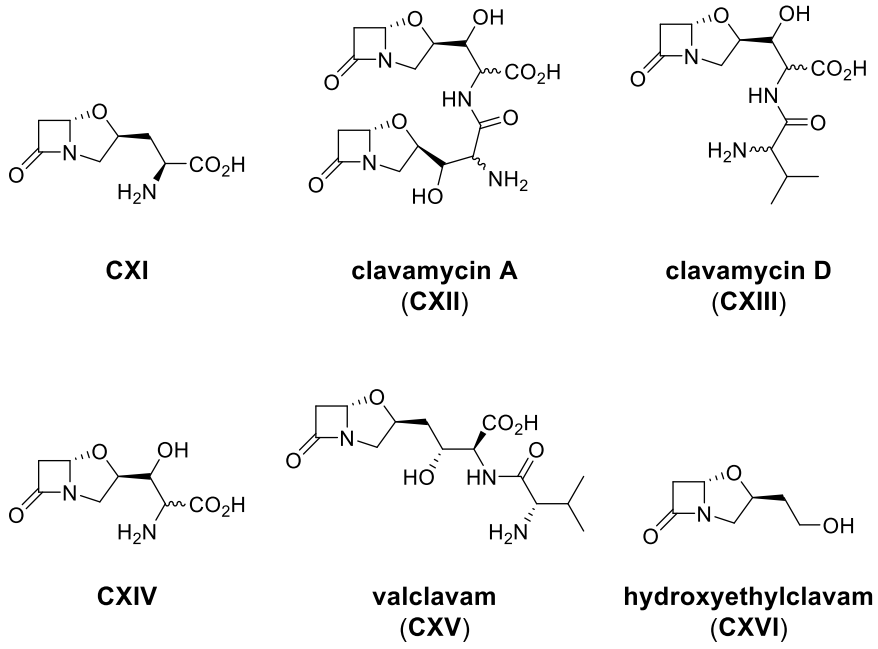

Figure 1.26: Structures of β-lactams with antifungal properties.

1.11.5 Antiviral applications of β-lactams

Viruses are infectious pathogens that, unlike bacteria or fungi, can only replicate within living organisms by hijacking the host cellular machinery.[331] Viral infections cause both acute illnesses such as influenza or dengue fever, and chronic, life-altering conditions such as hepatitis or HIV/AIDS.[332, 333] Throughout history, viruses have been responsible for triggering epidemics and pandemics marked by high mortality, such as smallpox, the Spanish flu pandemic (~50-100 million deaths), the HIV/AIDS epidemic (>33 million deaths since 1981), and, more recently, the COVID-19 pandemic (>27 million excess deaths).[334-336] Vaccination represents the first line of defence against viral infections, proving its efficacy time and time again, from Edward Jenner's pioneering smallpox vaccine[337] to the recent mRNA therapeutic platforms developed during the COVID-19 pandemic.[338, 339] However, vaccines are not an universal solution to viral diseases for a variety of reasons, ranging from reduced efficacy in rapidly mutating strains to limited availability and/or access in developing countries.[340, 341] In this context, antiviral drugs offer a complementary

therapeutic option to vaccines by targeting viral replication pathways and/or interfering with host-virus interactions, thus limiting viral transmission, slowing disease progression, and improving patient outcomes.[342, 343]

Given the well-established reactivity of the β-lactam ring towards serine and cysteine proteases, β-lactams have also been investigated as antiviral agents, being designed to target host or viral proteases that either facilitate entry to human cells or play a central role in viral replication.[236-245] Among the host proteases of therapeutic interest are cysteine cathepsins, a family of lysosomal proteases that mediate protein degradation.[344] Cathepsins are ubiquitously expressed in the body and are involved in essential physiological processes such as cell signalling, hormone secretion, and immune responses. However, cathepsin dysregulation has been associated with a range of human diseases, including cancer, diabetes, inflammation diseases, and viral infections.[345, 346] In the case of the latter, cathepsin promote viral entry not only for enveloped viruses, where cathepsin-catalysed cleavage of the viral glycoproteins enables membrane fusion and cellular viral genome release, but also for non-enveloped viruses, where cathepsins facilitate outer capsid disassembly and membrane penetration.[346]

Oxapenam **CXVII** (**Figure 1.27**) is a reported inhibitor of cathepsins B, L, K, and S, with IC_{50} values in the micromolar to nanomolar range.[347] **CXVII** bears a peptide-like substituent at the C6 position of the oxapenam scaffold, designed to engage the S2 and S3 subsites of cathepsins. Of particular importance is the phenylalanine fragment of the C6 substituent, which was deemed essential for binding to the S2 subsite and overall inhibition, as replacement of the aromatic group with an alkyl substituent ablates anti-cathepsin activity. Additionally, the 5*S* configuration of the oxazolidine ring in the oxapenam core was shown to play a critical role, as this particular spatial orientation enables hydrogen-bonding between the oxapenam O atom and the catalytic histidine

residue (His159). Further SAR studies revealed that penam sulfone **CXVIII** demonstrated even higher levels of cathepsin inhibition; O to SO_2 replacement enhanced key hydrogen-bond interactions involved in both the initial non-covalent binding states and the stabilisation of the formed acyl-enzyme adduct required for covalent inhibition.[236]

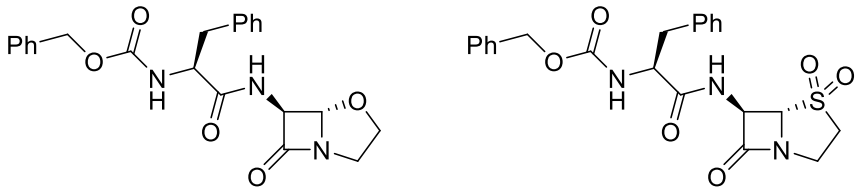

Figure 1.27: Structures of β-lactams with inhibitory properties against cathepsin enzymes.

β-Lactams incorporating a peptide sidechain have also been investigated as inhibitors of flaviviral NS2B-NS3 proteases.[237] Flaviviruses such as Dengue (DENV) or West Nile virus are pathogens most commonly spread by arthropods; although the symptoms are in most cases self-limiting, complications can lead to encephalitis, meningitis, and even death.[348, 349] Considering that there is a significant unmet need for vaccines against flaviviruses,[350] small-molecule inhibitors represent a critical therapeutic option in the management and treatment of flavivirus infections. An attractive therapeutic target is NS2B-NS3, a serine protease that catalyses the cleavage of flaviviral polyproteins, thereby enabling replication complex assembly and driving the progression of the viral replication cycle.

Tripeptide-β-lactam hybrid **CXIX** (**Figure 1.28**) displayed good inhibitory properties against DENV NS2B-NS3 both *in vitro* (IC_{50} ~ 3 μM) and *in vivo* (EC_{50} ~ 12 μM), while displaying minimal off-target effects against endogenous serine enzymes such as thrombin and trypsin.[351] MS assays revealed that **CXIX** operates in a mechanistically complex manner, displaying two distinct binding modes: i) Ser135 attacks the carbonyl group on the lysine residue, cleaving the tripeptide

into the corresponding dipeptide **CXX** and β-lactam **CXXI**; ii) NS2B-NS3 Ser135 attacks the β-lactam ring of **CXIX**, resulting in the formation of an acyl-enzyme complex that further gets hydrolysed to the ring-opened product **CXXII**.

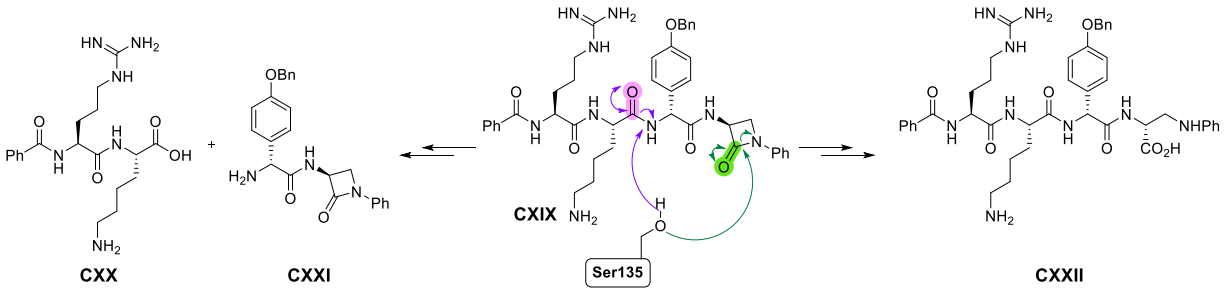

Figure 1.28: Outline mechanism for the reaction of tripeptide-β-lactam hybrid **CXIX** with DENV NS2B-NS3.[237]

Another promising antiviral application of β-lactams is their use as inhibitors of human cytomegalovirus (HCMV) protease.[238, 240, 244] HCMV is a β-herpesvirus that causes opportunistic infections in immunocompromised patients (*e.g.*, AIDS patients).[352] Given that the currently available treatment for HCMV infections are suboptimal from an efficacy and safety standpoint, there is an urgent need for developing improved anti-HCMV agents.[353, 354] A promising therapeutic target is the HCMV protease, a serine protease that is crucial for the viral replication cycle due to its role in capsid assembly and viral maturation.[355]

Following a screening programme for antiviral agents, β-lactams **CXXIII** and **CXXIV**, initially developed for HLE inhibition, exhibited inhibitory properties against HCMV protease (**Figure 1.29**).[238, 244] MS assays showed that **CXXIII** (IC_{50} >100 μM) induces covalent modification of the active site serine residue (Ser132) of HCMV protease, consistent with the formation of an acyl-enzyme complex (*i.e.*, **CXXVIII**); note that the observed adduct indicates that the collapse of the tetrahedral intermediate is accompanied by elimination of AcO^- (**Figure 1.15B**).[238] On the other hand, **CXXIV** (IC_{50} ~ 20 μM) did not promote the formation of an acyl-enzyme complex,

inhibiting HCMV protease via a non-covalent mechanism, presumably due to the increased steric bulk of 4-phenoxy-*tert*-butyl substituent. Furthermore, time course studies revealed that over a 24 h period **CXXIII** is completely turned over, highlighting the limited hydrolytic stability of adduct **CXXVIII**.

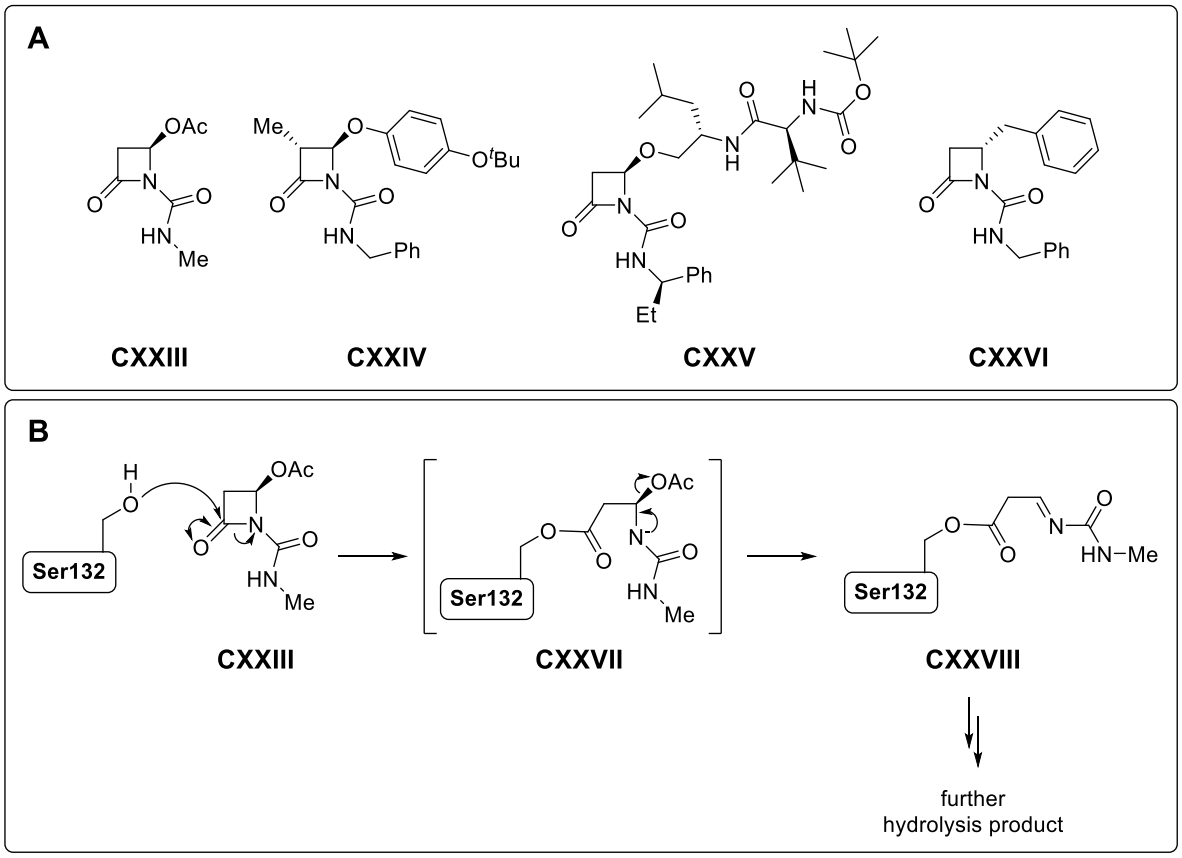

Figure 1.29: **A**. β-Lactam inhibitors of HCMV protease. **B**. Outline mechanism for the reaction of **CVIII** with the active site serine residue (Ser132) of HCMV protease.

Monocyclic β-lactams were further optimized to increase potency against HCMV protease; molecular hybridization was successfully applied to give **CXXV**, where the peptidomimetic sidechain was tailored to enhance binding to the active site ($IC_{50} \sim 0.07$ μM).[240] However, despite demonstrating excelling *in vitro* properties, viral replication inhibition failed *in vivo*. Poor antiviral activity is likely the consequence of the poor pharmacokinetic properties imparted by the peptidic

nature of **CXXV**. Attempts at improving *in vivo* activity led to the development of **CXXVI**, which, unlike **CXXV,** does not possess a cleavable leaving group, indicating that the nature of the C4 substituent is important for stabilising the acyl-enzyme complex; nonetheless, **CXXVI** only displayed moderate inhibitory properties both *in vitro* ($IC_{50} \sim 10$ μM) and *in vivo* assays ($EC_{50} \sim 53$ μM).[239]

More recently, at the height of the COVID-19 pandemic, drug repurposing screening efforts helped identify β-lactam derivatives as potential antiviral agents against SARS-CoV-2,[241] which will also represent one of the central objectives of the present thesis.

1.12 SARS-CoV-2

Severe acute respiratory syndrome coronavirus 2 (SARS-CoV-2), the causative agent responsible for the Coronavirus disease 2019 (COVID-19) pandemic, can trigger infections that result in a spectrum of clinical outcomes, from asymptomatic manifestation to severe respiratory disease that may results in complications and death.[356] SARS-CoV-2 is a positive-sense single-stranded RNA virus whose genome is encapsulated by the nucleocapsid protein (N) and enveloped by a lipid structure that incorporates the membrane-bound spike protein (S), the envelope protein (E), and the membrane glycoprotein (M).[357]

The viral life cycle begins with the viral invasion of host cells (**Figure 1.30**),[358] which can occur via two distinct mechanisms: i) the virus binds to the angiotensin-converting enzyme 2 (ACE2) receptor on the host cell surface, followed by endosomal internalisation, where within the endosome the spike protein is cleaved by cathepsin L, which enables downstream release of the viral RNA into the cytoplasm; ii) following the binding to ACE2, the spike protein may also be directly cleaved by the host transmembrane protease, serine 2 (TMPRSS2), which triggers plasma

membrane fusion and direct entry of the RNA genome to the cytoplasm.[359] Within the cytoplasm, the viral RNA hijacks the host ribosomes and is translated into viral polyproteins pp1a/1ab. The polyproteins comprise two proteases, namely the main protease (M^{pro}) and the papain-like protease (PL^{pro}), which are responsible for catalysing cleavage of pp1a/1ab into non-structural proteins (nsps) crucial for the viral replication cycle.[360] Among the nsps released, RNA-dependent RNA polymerase (RdRp) promotes viral genome replication and subgenomic RNAs transcription.[361] Lastly, the newly synthesized structural proteins assemble into an envelope around the genome, thus creating new virions that exit the cytoplasm via exocytosis to propagate viral infection.[357, 358]

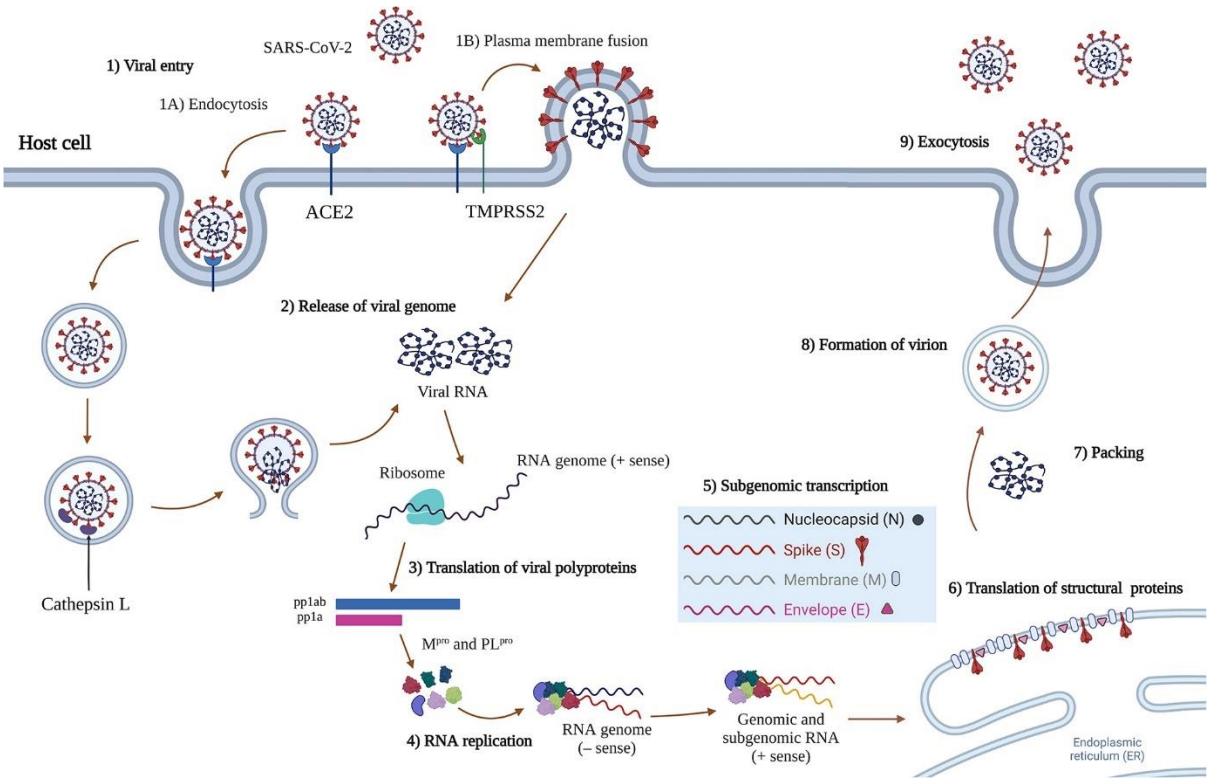

Figure 1.30: SARS-CoV-2 viral entry and replication cycle. Figure reprinted from B. Tan, R. Joyce, H. Tan, Y. Hu, and J. Wang, *Acc. Chem. Res.*, 2023, 56 (2), 157-168, doi: 10.1021/acs.accounts.2c00735, with permission from American Chemical Society, License No.: 6101860472008.

1.12.1 Function and structure of SARS-CoV-2 M^{pro}

M^{pro} (nsp5) is a nucleophilic cysteine protease that cleaves itself from the viral polyprotein and subsequently promotes the cleavage of pp1a/1ab at 11 different sites. M^{pro} is structurally divided into three distinct domains (**Figure 1.31**). Domains I (residues 8–101) and II (residues 102–184) are comprised of six-stranded antiparallel β-sheets, while domain III (residues 201–303) is predominantly α-helical in nature and serves as the interface where protomers interact to dimerise, thus forming a catalytically active M^{pro}. The N-terminal seven residues, termed N-finger, delineate the beginning of domain I, while the C-terminal tail constitute the terminus of domain III. Residues 185-200 form a loop region that connect domains II and III, which is critical not only for dimer formation but also for positioning the N-finger in proximity to the active site of the partner protomer. Although M^{pro} is known to exist in both monomeric and dimeric forms in solution, only the dimer displays enzymatic activity.[362]

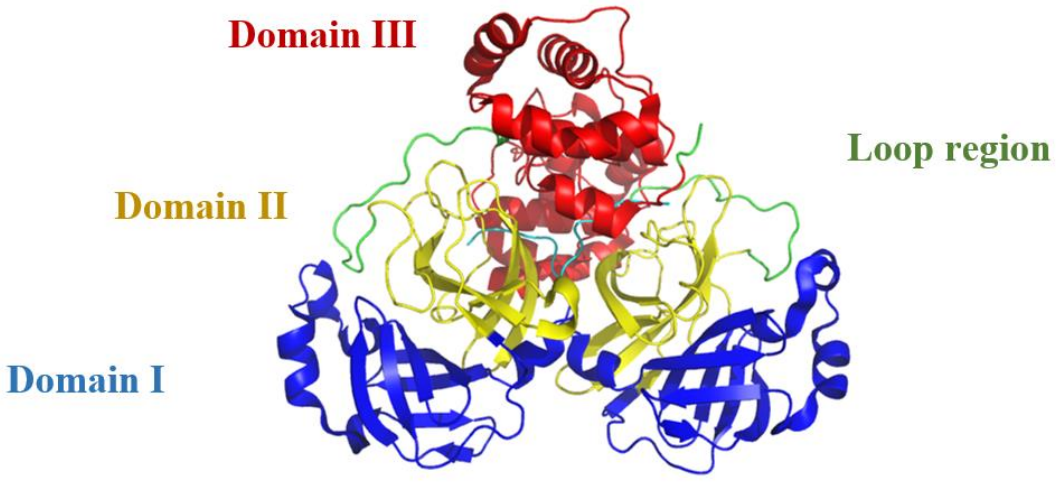

Figure 1.31: Crystal structure of SARS-CoV-2 M^{pro} (PDB ID: 7BB2).[363]

1.12.2 M^{pro} mechanism of action

M^{pro} features a catalytic dyad comprised of residues Cys145 and His41, wherein Cys145 is a nucleophilic cysteine residue that covalently reacts with substrates, while His41 is a basic histidine residue that deprotonates Cys145 and the hydrolytic water (**Figure 1.32**).[364] Following deprotonation by His41, the formed Cys145 thiolate attacks a scissile amide bond, generating a high-energy tetrahedral complex whose negatively charged oxyanion is stabilised in the oxyanion hole formed by the backbones of Gly143, Ser144, and Cys145. Collapse of the tetrahedral complex yields the C-terminal peptide product, resulting in the formation of an acyl-enzyme complex with Cys145, namely a thioester. The thioester is then attacked by an activated water molecule, forming a secondary tetrahedral complex, whose collapse results in the formation of the N-terminal peptide product while returning the enzyme to its ground state.

According to standard nomenclature rules for proteases, a peptide substrate is denoted P4-P3-P2-P1↓P1′, where ↓ designates the cleavage site. Residues on the N-terminal and C-terminal sides are labelled Pn and Pn', respectively, wherein n indicates the position of the residues relative to the scissile amide bond cleaved by the protease.[365] The corresponding binding pockets are designated Sn and Sn′, wherein residue Pn fits into subsite Sn and residue Pn' fits into subsite Sn'.

M^{pro} catalyses the self-cleavage from the polyprotein at the nsp4/5 and nsp5/6 sites, then it cleaves the part of the remaining polyprotein at 9 more sites (*i.e.*, nsp6-16). Analysis of the nsp4-16 substrates reveals that substrate specificity is strongly conserved for M^{pro}. A key determinant in substrate recognition is the presence of a glutamine residue at the P1 position; histidine was also identified as a tolerated residue in at least one M^{pro} substrate of human origin.[366, 367] Further

substrate specificity analysis reveals that there is a strong preference for serine or alanine at P1', while the most conserved residue at P2 is leucine.[368]

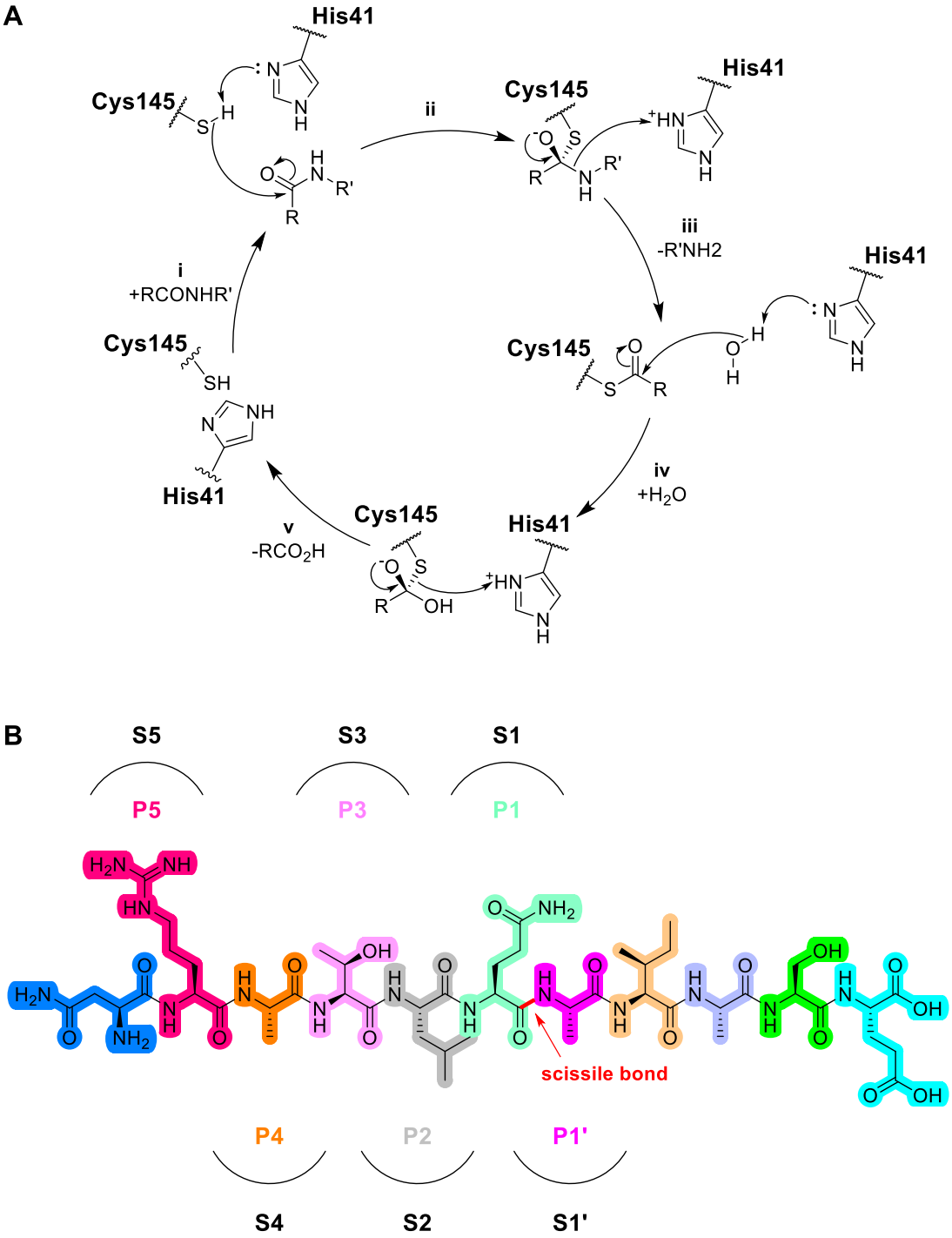

Figure 1.32: **A**. Outline mechanism for substrate proteolysis catalysed by M^{pro}. **B**. Example of peptide substrate of M^{pro} – NRATLQ/AIASE, the peptide sequence at the nsp7/8 cleavage site.

1.12.3 Covalent and non-covalent inhibitors of M^{pro}

M^{pro} has emerged as an attractive therapeutic target for several reasons: i) M^{pro} is responsible for most of the maturation proteolytic processes, so its inhibition disrupts the viral replication cycle;[369] ii) M^{pro} is highly conserved among coronaviruses,[370] including clinical SARS-CoV-2 variants of concern;[371] iii) SARS-CoV-2 M^{pro} shares 96% sequence similarity with SARS-CoV-1 M^{pro}, highlighting the potential for developing broad-spectrum antiviral agents against a spectrum of coronaviruses;[372] iv) there are no homologous enzymes of M^{pro} known in humans,[369, 373] thus minimizing the risk of off-target effects.

Multiple scaffolds have been investigated during the development of M^{pro} inhibitors, which can inhibit via covalent or non-covalent binding.[374-377] Given the plethora of electrophilic warheads available in the pharmacophore arsenal, covalent inhibitors had attracted considerable attention. Covalent inhibition of M^{pro} can be irreversible, with warheads such as Michael acceptors, terminal alkynes, and haloacetyl groups being designed to permanently inactivate enzymatic activity by blocking the catalytic cysteine residue (*i.e.*, Cys145).[378-382] By contrast, reversible covalent inhibitors form labile adducts, such as thiohemiketals, following the reaction of Cys145 with an electrophilic carbonyl group like aldehyde, α-ketoamides, or hydroxymethyl ketones.[383, 384] Reversible covalent inhibitors are designed to improve selectivity and reduce off-target effects, while scaffold modifications modulate reactivity to enhance potency.

One class of reversible covalent inhibitor that achieved clinical success is represented by peptidomimetic nitriles, as exemplified by **nirmatrelvir** (**CXXIX**; **Figure 1.33A**), the first clinically approved M^{pro} inhibitor and the active ingredient of Paxlovid.[385] Crystallographic studies revealed that the nitrile group of nirmatrelvir reacts covalently with Cys145 to give a thioimidate

adduct, while the peptidomimetic scaffold engages the S4-S1 subsites at the M^{pro} active site (**Figure 1.33B**). The γ-lactam ring at P1 mimics glutamine, the conserved natural substrate residue, forming hydrogen bonds with His163 and Glu166 in the S1 pocket, while the dimethyl-bicyclo[3.1.0]hexane-based proline derivative at P2 occupies S2 as a rigid mimic of P2 leucine. P3 and P4 further enhance inhibitor binding: the valine residue promotes hydrophobic interactions at S3, while the trifluoroacetamide group not only forms H-bonding between its amidic proton and Glu166, but also exhibits via the CF_3-group strong van der Waals and hydrophobic interactions within the S4 subsite.

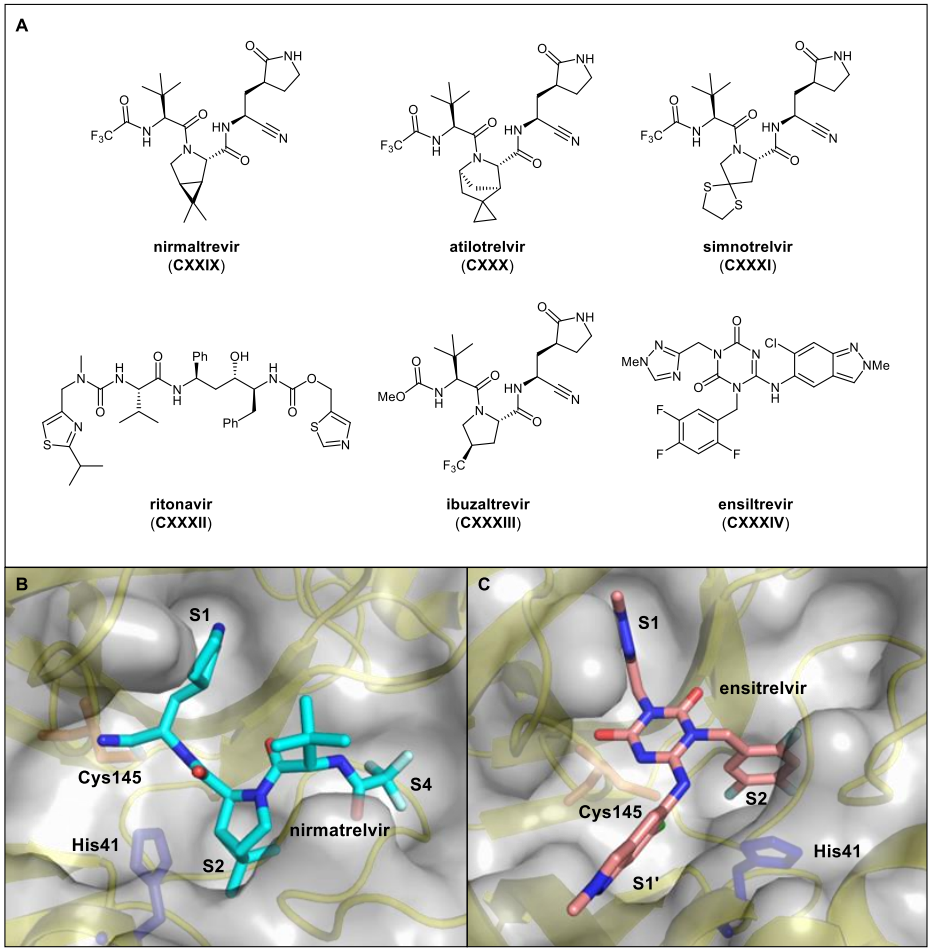

Figure 1.33: **A**. Reported clinically approved inhibitors of SARS-CoV-2 M^{pro}.[385-389] **B**. Crystal structure view of the complex formed following covalent reaction of **nirmatrelvir** with M^{pro} (PDB ID: 8DZ2).[385] **C**. Crystal structure view of the non-covalent complex of **ensitrelvir** with M^{pro} (PDB ID: 8HUR).[388]

Given that **nirmatrelvir** displays excellent *in vitro* (K_i ~ 4 nM) and *in vivo* (EC_{50} ~ 82 nM) activities against M^{pro}, it is no surprise that it inspired the development of related peptidomimetic nitrile inhibitors of M^{pro}, such as clinically used **atilotrelvir** (**CXXX**)[389] and **simnotrelvir** (**CXXXI**)[387]. However, the main drawback of **nirmatrelvir** and related analogues lies in their limited metabolic stability, requiring co-administration with **ritonavir** (**CXXXII**), an inhibitor of the cytochrome P450 oxygenase CYP3A4, to reduce metabolic degradation and maintain efficacious therapeutic levels. Consequently, the presence of **ritonavir** in the Paxlovid combination therapy limits its therapeutic scope, due to the side-effects associated with **ritonavir** and its potential to interfere with other commonly prescribed medications. To overcome these limitations and preclude the need of ritonavir co-administration, **ibuzatrelvir** (**CXXXIII**) was developed, with two key differences with respect to **nirmatrelvir**: i) the trifluoroacetamide group was replaced with a methylcarbamate; ii) the bicyclic (1*R*,5*S*)-3-azabicyclo[3.1.0]hexane proline was exchanged with a (4*R*)-4-trifluoromethylproline group.[386, 390] Crystallographic studies revealed that **ibuzatrelvir** and **nirmatrelvir** adopt similar conformations at the M^{pro} active site. Furthermore, the functional group substitutions are well tolerated, as **ibuzatrelvir** displayed similarly potent *in vitro* (K_i ~ 3 nM) and *in vivo* (EC_{50} ~ 180 nM) inhibitory properties against M^{pro}. Lastly, **ibuzatrelvir** exhibited a superior pharmacokinetic profile to **nirmatrelvir**, manifesting enhanced oral bioavailability and metabolic stability.

Non-covalent M^{pro} inhibitors were also extensively investigated, ranging from non-peptidic small-molecules to macrocyclic oligopeptides.[377, 391-398] In principle, non-covalent inhibitors can offer advantages over covalent inhibitors, as they do not induce permanent protein modifications, thereby reducing the likelihood of off-target interactions while potentially improving safety profiles.[399] Nonetheless, only one non-covalent small-molecule inhibitor of M^{pro} progressed to

clinical approval, **ensitrelvir** (**CXXXIV**).[388] Crystallographic studies revealed that **ensitrelvir** targets the S1, S2, and S1′ subsites of the M^{pro} active site (**Figure 1.33C**). The 1-methyl-1*H*-1,2,4-triazole group binds to the S1 pocket, mimicking the natural substrates P1 glutamine residue and engaging in H-bonding with imidazole N-H of His163. The 2,4,5-trifluorobenzyl moiety resides in the hydrophobic S2 subsite, where it engages in π–π stacking with His41. Lastly, the 6-chloro-2-methyl-2*H*-indazole unit resides in the S1′ subsite, where it forms a stabilising hydrogen bond with Thr26. **Ensitrelvir** not only displayed excellent *in vitro* (EC_{50} ~ 13 nM) and *in vivo* (EC_{50} ~ 370 nM) inhibitory properties against M^{pro}, but it also displayed pharmacokinetic/ pharmacodynamic profiles favourable for oral formulations.

Despite the successful development of clinically used M^{pro} inhibitors such as **nirmatrelvir** and **ensitrelvir**, rapidly mutating viral strains pose a serious threat to the therapeutical efficacy of currently available treatments, as active-site substitutions can compromise drug potency, thus leading to viral resistance. [400-402] Therefore, it is critical that next-generation M^{pro} inhibitors are investigated and developed to ensure preparedness against future coronavirus outbreaks.

1.12.4 β-Lactam inhibitors of SARS-CoV-2 M^{pro}

Following the development of a MS-based high-throughput *in vitro* inhibition assay using recombinant viral M^{pro}, β-lactams including penicillins, cephalosporins, and monocyclic β-lactam antibiotics were screened for inhibition against M^{pro}.[241] The results revealed that two penicillin-based derivatives (**Figure 1.34A**), penicillin V sulfone benzyl ester **CXXXV** and C6-methoxy penicillin G (*R*)-sulfoxide 4-nitrobenzyl ester **CXXXVI,** displayed potent inhibitory properties (IC_{50} ~ 1.5 and 3.5 μM, respectively). Protein-observed MS assays further revealed that **CXXXV** promoted covalent modification of M^{pro}, whereas **CXXXVI** apparently inhibited via a non-

covalent mechanism. The screen also revealed that certain cephalosporin acids such as **cefoxitin** (**XLIX**) promoted incomplete covalent modifications of M^{pro} but manifested only weak to no inhibition against M^{pro}.

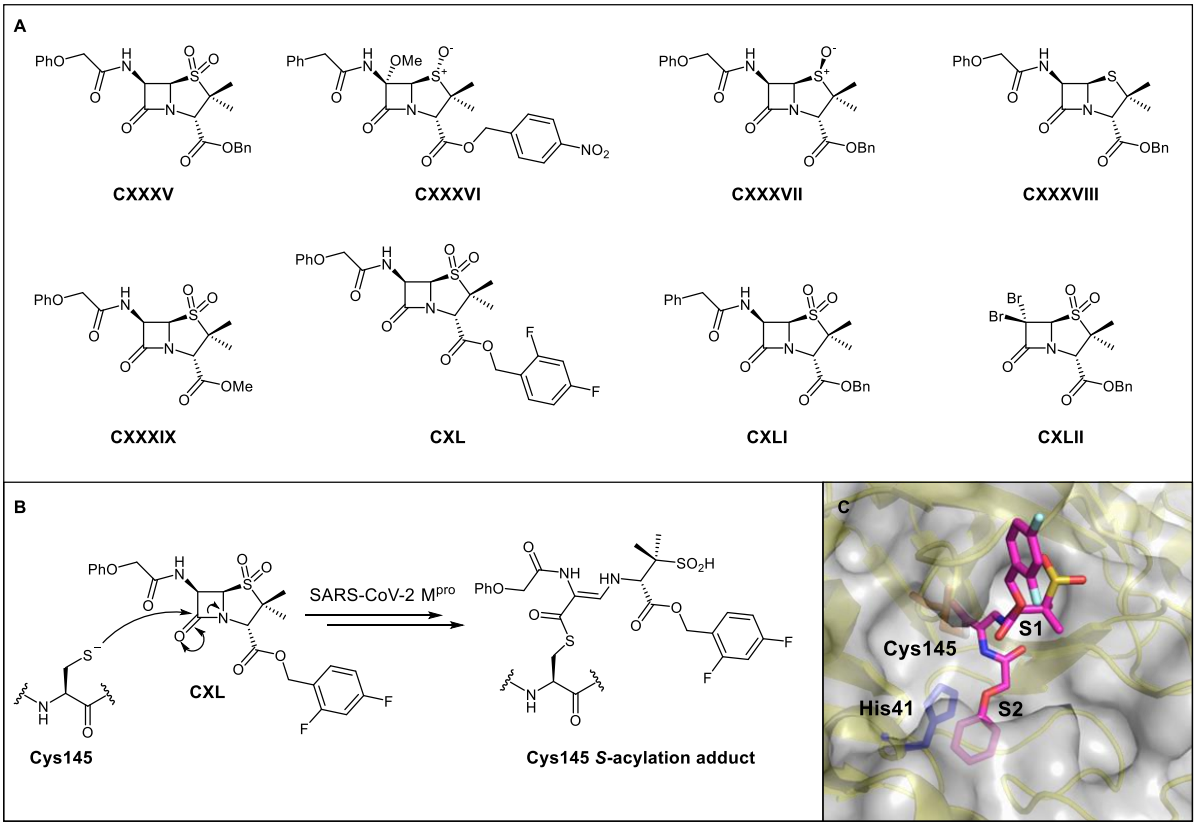

Figure 1.34: **A**. β-Lactam derivatives previously investigated as M^{pro} inhibitors.[241, 242] **B**. Outline mechanism for the covalent reaction of SARS-CoV-2 M^{pro} with penicillin V derivative **CXL**.[242] **C**. Crystal structure view of the complex formed following covalent reaction of **CXL** with M^{pro} (PDB ID: 7Z59).[242]

Subsequent SAR studies centered on penicillin V derivatives revealed that the sulfur oxidation state is a key factor that affects M^{pro} inhibition, with potency drastically decreasing from sulfone **CXXXV** to (*S*)-sulfoxide **CXXXVII** (IC_{50} ~ 23 μM) to sulfide **CXXXVIII** (IC_{50} > 50 μM).[242] C3-ester group substitutions were generally well tolerated, with a range of alkyl (*e.g.,* **CXXXIX**; IC_{50} ~ 8 μM) and aryl substituent (*e.g.,* **CXL**; IC_{50} ~ 3.6 μM) showing good inhibitory properties. SAR

analysis at the C6 position highlighted that the identity of the acylamido sidechain appears to be critical, as removal of the phenoxy ether oxygen (*e.g.,* **CXLI**; $IC_{50} > 50$ μM) or alteration of side-chain length abolished M^{pro} inhibition. Notably, C6-dibromo penam sulfone benzyl ester **CXLII** also emerged as a potent M^{pro} inhibitor ($IC_{50} \sim 0.6$ μM), while crystallographic studies confirmed that penicillin V sulfone **CXL** covalently modifies Cys145 through β-lactam ring opening and *S*-acylation (**Figure 1.34B-C**).

Taken together, these reports highlight the vast potential of β-lactam derivatives for developing potent M^{pro} inhibitors. The wide range of applications, from the traditional role as antibiotics to anticancer agents, reflect the high adaptability of the β-lactam scaffold, which can be tailored to bind therapeutic targets via either covalent or non-covalent modes. Therefore, the β-lactam warhead represents a versatile foundation for the development of improved antiviral agents active against not only SARS-CoV-2 but potentially also future coronaviruses.

1.13 Thesis objectives

The work presented in this thesis is focused on the synthesis and development of small-molecule β-lactam inhibitors of cysteine and serine proteases for viral and antibacterial applications. **Chapter 2** describes a structure-activity relationship (SAR) study on C6-alkoxy penam derivatives as inhibitors of the SARS-CoV-2 main protease (M^{pro}). Synthetic efforts were directed toward streamlined routes for introducing alkoxy groups at the C6 position of the penam scaffold, as well as improving methodologies for penicillin (*R*)-sulfoxides. Results from enzymatic assays and computational studies are reported, revealing non-covalent inhibition modalities against M^{pro}. **Chapter 3** shifts the focus to cephalosporin-based M^{pro} inhibitors operating via either covalent or non-covalent mechanisms, leading to the development of potent *in vitro* antivirals that also

suppress viral replication in cell-based assays. **Chapter 4** describes investigations on C6-alkoxy penam derivatives as inhibitors of serine- and metallo-β-lactamases (SBLs and MBLs). **Chapter 5** describes the effects of C6-methoxy substitutions on PBP inhibition for clinically used β-lactam antibiotics. **Chapter 6** presents the development of an improved synthetic route toward C2-carboxypenicillins, which may serve as templates for future penam-based antimicrobial agents. Lastly, **Chapter 7** summarises the key findings of this thesis and outlines potential directions for future research.

1.14 References

1. A. Fleming, THE DISCOVERY OF PENICILLIN, *Br. Med. Bull.*, 1944, **2**, 4–5.
2. B. L. Ligon, Penicillin: its discovery and early development, *Semin. Pediatr. Infect. Dis.*, 2004, **15**, 52–57.
3. M. I. Hutchings, et al., Antibiotics: past, present and future, *Curr. Opin. Microbiol.*, 2019, **51**, 72–80.
4. K. Bush, et al., β-Lactams and β-Lactamase Inhibitors: An Overview, *Cold Spring Harb. Perspect. Med.*, 2016, **6**, a025247.
5. L. M. Lima, et al., β-lactam antibiotics: An overview from a medicinal chemistry perspective, *Eur. J. Med. Chem.*, 2020, **208**, 112829.
6. A. Dalhoff, et al., Redefining penems, *Biochem. Pharmacol.*, 2006, **71**, 1085–1095.
7. V. S. R. Rao, et al., Conformation and Activity of β-Lactam Antibiotics, *Crit. Rev. Biochem.*, 1983, **14**, 173–206.
8. P. M. Blumberg, et al., Interaction of penicillin with the bacterial cell: penicillin-binding proteins and penicillin-sensitive enzymes, *Bacteriol. Rev.*, 1974, **38**, 291–335.
9. M. Rohde, The Gram-Positive Bacterial Cell Wall, *Microbiol. Spectr.*, 2019, **7**, 10.1128/microbiolspec.gpp1123–0044–2018.
10. J. Beveridge Terry, Structures of Gram-Negative Cell Walls and Their Derived Membrane Vesicles, *J. Bacteriol.*, 1999, **181**, 4725–4733.
11. B. Dmitriev, et al., Towards a comprehensive view of the bacterial cell wall, *Trends Microbiol.*, 2005, **13**, 569–574.
12. T. J. Franklin, et al., in *Biochemistry of Antimicrobial Action*, eds. T. J. Franklin and G. A. Snow, Springer Netherlands, Dordrecht, 1989, pp. 20–54.
13. R. Coico, Gram Staining, *Curr. Protoc. Microbiol.*, 2006, **00**, A.3C.1–A.3C.2.
14. S. Garde, et al., Peptidoglycan: Structure, Synthesis, and Regulation, *EcoSal Plus*, 2021, **9**.
15. W. Vollmer, et al., Peptidoglycan structure and architecture, *FEMS Microbiol. Rev.*, 2008, **32**, 149–167.
16. A. L. Lovering, et al., Structural Perspective of Peptidoglycan Biosynthesis and Assembly, *Annual Review of Biochemistry*, 2012, **81**, 451–478.
17. E. Sauvage, et al., The penicillin-binding proteins: structure and role in peptidoglycan biosynthesis, *FEMS Microbiol. Rev.*, 2008, **32**, 234–258.
18. J. M. Frère, et al., Penicillin-sensitive enzymes in peptidoglycan biosynthesis, *Crit. Rev. Microbiol.*, 1984, **11**, 299–396.
19. M. Lavollay, et al., The peptidoglycan of Mycobacterium abscessus is predominantly cross-linked by L,D-transpeptidases, *J. Bacteriol.*, 2011, **193**, 778–782.
20. M. Lavollay, et al., The Peptidoglycan of Stationary-Phase Mycobacterium tuberculosis Predominantly Contains Cross-Links Generated by l,d-Transpeptidation, *J. Bacteriol.*, 2008, **190**, 4360–4366.
21. A. Aliashkevich, et al., LD-transpeptidases: the great unknown among the peptidoglycan cross-linkers, *FEBS J.*, 2022, **289**, 4718–4730.
22. D. Both, et al., Structure of LdtMt2, an l,d-transpeptidase from Mycobacterium tuberculosis, *Acta Crystallogr. D.*, 2013, **69**, 432–441.

23. M. de Munnik, et al., Biochemical and crystallographic studies of l,d-transpeptidase 2 from Mycobacterium tuberculosis with its natural monomer substrate, *Commun. Bio.*, 2024, **7**, 1173.
24. D. J. Tipper, et al., Mechanism of action of penicillins: a proposal based on their structural similarity to acyl-D-alanyl-D-alanine, *Proc. Natl. Acad. Sci.*, 1965, **54**, 1133–1141.
25. N. R. Silvaggi, et al., Crystal Structures of Complexes between the R61 DD-peptidase and Peptidoglycan-mimetic β-Lactams: A Non-covalent Complex with a "Perfect Penicillin"††This article is dedicated to the memory of Professor Jean-Marie Ghuysen of the Université de Liège, Belgium, in recognition of his decades of contributions towards our understanding of and ability to combat bacterial infections, *J. Mol. Biol.*, 2005, **345**, 521–533.
26. B. Lee, Conformation of penicillin as a transition-state analog of the substrate of peptidoglycan transpeptidase, *J. Mol. Biol.*, 1971, **61**, 463–469.
27. A. Zapun, et al., Penicillin-binding proteins and β-lactam resistance, *FEMS Microbiol. Rev.*, 2008, **32**, 361–385.
28. D. P. M. Sethuvel, et al., β-Lactam Resistance in ESKAPE Pathogens Mediated Through Modifications in Penicillin-Binding Proteins: An Overview, *Infect. Dis. Ther.*, 2023, **12**, 829–841.
29. H. F. Chambers, Penicillin-Binding Protein-Mediated Resistance in Pneumococci and Staphylococci, *J. Infect. Dis.*, 1999, **179**, S353–S359.
30. J. Fishovitz, et al., Penicillin-binding protein 2a of methicillin-resistant Staphylococcus aureus, *IUBMB Life*, 2014, **66**, 572–577.
31. H. Nikaido, Molecular Basis of Bacterial Outer Membrane Permeability Revisited, *Microbiol. Mol. Biol. Rev.*, 2003, **67**, 593–656.
32. A. H. Delcour, Outer membrane permeability and antibiotic resistance, *Biochim. Biophys. Acta*, 2009, **1794**, 808–816.
33. J.-M. Pagès, et al., The porin and the permeating antibiotic: a selective diffusion barrier in Gram-negative bacteria, *Nat. Rev. Microbiol.*, 2008, **6**, 893–903.
34. X. Z. Li, et al., Efflux-mediated drug resistance in bacteria: An update, *Drugs*, 2009, **69**, 1555–1623.
35. X.-Z. Li, et al., The Challenge of Efflux-Mediated Antibiotic Resistance in Gram-Negative Bacteria, *Clin. Microbiol. Rev.*, 2015, **28**, 337–418.
36. A. Dulanto Chiang, et al., Efflux pump-mediated resistance to new beta lactam antibiotics in multidrug-resistant gram-negative bacteria, *Commun. Med.*, 2024, **4**, 170.
37. A. A. Medeiros, β-Lactamases: quality and resistance, *Clin. Microbiol. Infect.*, 1997, **3**, 4S2–4S9.
38. K. Bush, in *Antimicrobial Drug Resistance: Mechanisms of Drug Resistance, Volume 1*, eds. D. L. Mayers, J. D. Sobel, M. Ouellette, K. S. Kaye and D. Marchaim, Springer International Publishing, Cham, 2017, pp. 165–175.
39. K. Bush, New β-lactamases in gram-negative bacteria: Diversity and impact on the selection of antimicrobial therapy, *Clin. Infect. Dis.*, 2001, **32**, 1085–1089.
40. K. Bush, Past and Present Perspectives on β-Lactamases, *Antimicrob. Agents Chemother.*, 2018, **62**, 10.1128/aac.01076–01018.
41. C. Barreiro, et al., in *Adv. Appl. Microbiol.*, eds. G. M. Gadd and S. Sariaslani, Academic Press, 2024, vol. 127, pp. 143–221.

42. M. A. Peñalva, et al., The optimization of penicillin biosynthesis in fungi, *Trends Biotechnol.*, 1998, **16**, 483–489.
43. M. Cole, Formation of 6-Aminopenicillanic Acid, Penicillins, and Penicillin Acylase by Various Fungi, *Appl. Microbiol.*, 1966, **14**, 98–104.
44. D. Schlossberg, et al., in *Antibiotics Manual*, 2017, pp. 47–50.
45. W. M. M. Kirby, Extraction of a Highly Potent Penicillin Inactivator from Penicillin Resistant Staphylococci, *Science*, 1944, **99**, 452–453.
46. J. O. Jarlev, et al., In-vitro activity and β-lactamase stability of methicillin, isoxazolyl penicillins and cephalothin against coagulase-negative staphylococci, *J. Antimicrob. Chemother.*, 1988, **22**, 119–125.
47. R. Knox, A New Penicillin (BRL 1241) Active Against Penicillin-resistant Staphylococci, *Br. Med. J.*, 1960, **2**, 690–693.
48. R. S. Vardanyan, et al., in *Synthesis of Essential Drugs*, eds. R. S. Vardanyan and V. J. Hruby, Elsevier, Amsterdam, 2006, pp. 425–498.
49. C. Fuda, et al., The Basis for Resistance to β-Lactam Antibiotics by Penicillin-binding Protein 2a of Methicillin-resistant Staphylococcus aureus*, *J. Biol. Chem.*, 2004, **279**, 40802–40806.
50. B. D. Raynor, Penicillin and ampicillin, *Prim Care Update OB/GYNS*, 1997, **4**, 147–152.
51. R. E. W. Hancock, et al., Antibiotic uptake into gram-negative bacteria, *Eur. J. Clin. Microbiol. Infect. Dis.*, 1988, **7**, 713–720.
52. D. Kaushik, et al., Ampicillin: Rise fall & resurgence, *J. Clin. Diagn. Res.*, 2014, **8**.
53. A. Huttner, et al., Oral amoxicillin and amoxicillin–clavulanic acid: properties, indications and usage, *Clin. Microbiol. Infect.*, 2020, **26**, 871–879.
54. R. N. Brogden, et al., Amoxycillin:A Review of its Antibacterial and Pharmacokinetic Properties and Therapeutic Use, *Drugs*, 1975, **9**, 88–140.
55. A. Hunter Pamela, et al., Comparative Activity of Amoxycillin and Ampicillin in an Experimental Bacterial Infection in Mice, *Antimicrob. Agents Chemother.*, 1973, **4**, 285–293.
56. K. Butler, et al., Carbenicillin: Chemistry and Mode of Action, *J. Infect. Dis.*, 1970, **122**, S1–S8.
57. R. N. Brogden, et al., Ticarcillin: A Review of its Pharmacological Properties and Therapeutic Efficacy, *Drugs*, 1980, **20**, 325–352.
58. H. C. Neu, Carbenicillin and Ticarcillin, *Med. Clin. North Am.*, 1982, **66**, 61–77.
59. A. Notarrigo, et al., Disodium α carboxybenzylpenicillin (carbenicillin): the antimicrobic activity against strains of Pseudomonas aeruginosa, *Ann. Ist. Super. Sanità*, 1974, **10**, 26–34.
60. J. Kjellander, et al., Bacteriological and Clinical Studies of Sulbenicillin, *Scand. J. Infect. Dis.*, 1978, **10**, 235–241.
61. L. Verbist, Comparison of the Activities of the New Ureidopenicillins Piperacillin, Mezlocillin, Azlocillin, and Bay k 4999 Against Gram-Negative Organisms, *Antimicrob. Agents Chemother.*, 1979, **16**, 115–119.
62. J. M. Turner, et al., Ureidopenicillins Are Potent Inhibitors of Penicillin-Binding Protein 2 from Multidrug-Resistant Neisseria gonorrhoeae H041, *ACS Infect. Dis.*, 2024, **10**, 1298–1311.
63. S. S. van Berkel, et al., Binding of (5S)-Penicilloic Acid to Penicillin Binding Protein 3, *ACS Chem. Biol.*, 2013, **8**, 2112–2116.

64. K. Bush, Bench-to-bedside review: The role of β-lactamases in antibiotic-resistant Gram-negative infections, *Crit. Care*, 2010, **14**, 224.
65. M. Castells, et al., Penicillin Allergy, *New Engl. J. Med.*, 2019, **381**, 2338–2351.
66. A. Luintel, et al., The global prevalence of reported penicillin allergy: A systematic review and meta-analysis, *J. Infect.*, 2025, **90**.
67. J. D. Campagna, et al., The Use of Cephalosporins in Penicillin-allergic Patients: A Literature Review, *J. Emerg. Med.*, 2012, **42**, 612–620.
68. X. Lin, et al., Cephalosporins as key lead generation beta-lactam antibiotics, *Appl. Microbiol. Biotechnol.*, 2022, **106**, 8007–8020.
69. T. A. Tartaglione, et al., Review of the New Second-Generation Cephalosporins: Cefonicid, Ceforanide, and Cefuroxime, *Drug. Intell. Clin. Pharm.*, 1985, **19**, 188–198.
70. J. Hamilton-Miller, et al., Cephamycins: A review, prospects and some original observations, *Infection*, 1975, **3**, 183–188.
71. G. R. Donowitz, Third Generation Cephalosporins, *Infect. Dis. Clin. North Am.*, 1989, **3**, 595–612.
72. J. Garau, et al., Fourth-generation cephalosporins: a review of in vitro activity, pharmacokinetics, pharmacodynamics and clinical utility, *Clin. Microbiol. Infect.*, 1997, **3**, s87–s101.
73. I. W. Fong, in *New Antimicrobials: For the Present and the Future*, ed. I. W. Fong, Springer International Publishing, Cham, 2023, pp. 25–38.
74. J. Turner, et al., The Chemical Relationship Among Beta-Lactam Antibiotics and Potential Impacts on Reactivity and Decomposition, *Front. Microbiol.*, 2022, **Volume 13 - 2022**.
75. E. Kanis, et al., Structural Analysis and Protein Binding of Cephalosporins, *ACS Pharmacol. Transl. Sci.*, 2023, **6**, 88–91.
76. W. Christ, Pharmacological properties of cephalosporins, *Infection*, 1991, **19**, S244–S252.
77. S. Thornhill Thomas, et al., In Vitro Antimicrobial Activity and Human Pharmacology of Cephalexin, a New Orally Absorbed Cephalosporin C Antibiotic, *Appl. Microbiol.*, 1969, **17**, 457–461.
78. R. E. Buck, et al., Cefadroxil, a New Broad-Spectrum Cephalosporin, *Antimicrob. Agents Chemother.*, 1977, **11**, 324–330.
79. C. W. Godzeski, et al., Cephalothin, a New Cephalosporin with a Broad Antibacterial Spectrum, *Appl. Microbiol.*, 1963, **11**, 122–127.
80. M. TURCK, et al., New Cephalosporin Antibiotic— Cephaloridine: Clinical and Laboratory Evaluation, *Arch. Intern. Med.*, 1967, **119**, 50–59.
81. H. G. Smith, et al., Structural basis of Pseudomonas aeruginosa penicillin binding protein 3 inhibition by the siderophore-antibiotic cefiderocol, *Chem. Sci.*, 2024, **15**, 16928–16937.
82. A. A. Carmine, et al., Cefotaxime, *Drugs*, 1983, **25**, 223–289.
83. D. M. Richards, et al., Ceftazidime, *Drugs*, 1985, **29**, 105–161.
84. R. N. Brogden, et al., Cefixime, *Drugs*, 1989, **38**, 524–550.
85. D. Saxena, et al., Tackling the outer membrane: facilitating compound entry into Gram-negative bacterial pathogens, *npj Antimicrob. Resist.*, 2023, **1**, 17.
86. S. Kaye Keith, et al., Third-Generation Cephalosporin-Resistant Enterobacterales Are Critical Priority Pathogens, Too!, *Antimicrob. Agents Chemother.*, 2022, **66**, e00213–00222.
87. L. B. Barradell, et al., Cefepime, *Drugs*, 1994, **47**, 471–505.
88. L. R. Wiseman, et al., Cefpirome, *Drugs*, 1997, **54**, 117–140.

89. Y. Iizawa, et al., Therapeutic effect of cefozopran (SCE-2787), a new parenteral cephalosporin, against experimental infections in mice, *Antimicrob. Agents Chemother.*, 1993, **37**, 100–105.
90. W. R. Wilson, The Role of Fourth-Generation Cephalosporins in the Treatment of Serious Infectious Diseases in Hospitalized Patients, *Diagn. Microbiol. Infect. Dis.*, 1998, **31**, 473–477.
91. T. Aoki, et al., Cefiderocol (S-649266), A new siderophore cephalosporin exhibiting potent activities against Pseudomonas aeruginosa and other gram-negative pathogens including multi-drug resistant bacteria: Structure activity relationship, *Eur. J. Med. Chem.*, 2018, **155**, 847–868.
92. T. Ishikawa, et al., TAK-599, a novel N-Phosphono type prodrug of anti-MRSA cephalosporin T-91825: synthesis, physicochemical and pharmacological properties, *Bioorg. Med. Chem.*, 2003, **11**, 2427–2437.
93. J. M. Entenza, et al., BAL9141, a Novel Extended-Spectrum Cephalosporin Active against Methicillin-Resistant Staphylococcus aureus in Treatment of Experimental Endocarditis, *Antimicrob. Agents Chemother.*, 2002, **46**, 171–177.
94. C. M. Pillar, et al., In vitro activity profile of ceftobiprole, an anti-MRSA cephalosporin, against recent Gram-positive and Gram-negative isolates of European origin, *J. Antimicrob. Chemother.*, 2008, **61**, 595–602.
95. F. Jiao, et al., Unraveling the mechanism of ceftaroline-induced allosteric regulation in penicillin-binding protein 2a: insights for novel antibiotic development against methicillin-resistant Staphylococcus aureus, *Antimicrob. Agents Chemother.*, 2023, **67**, e00895–00823.
96. A. L. Lovering, et al., Structural Insights into the Anti-methicillin-resistant Staphylococcus aureus (MRSA) Activity of Ceftobiprole*, *J. Biol. Chem.*, 2012, **287**, 32096–32102.
97. J. S. Kahan, et al., Thienamycin, a new β-lactam antibiotic i. discovery, taxonomy, isolation and physical properties, *J. Antibiot.*, 1979, **32**, 1–12.
98. F. M. Kahan, et al., Thienamycin: development of imipenem-cilastatin, *J. Antimicrob. Chemother.*, 1983, **12**, 1–35.
99. M. Papp-Wallace Krisztina, et al., Carbapenems: Past, Present, and Future, *Antimicrob. Agents Chemother.*, 2011, **55**, 4943–4960.
100. M. Hikida, et al., Inactivation of new carbapenem antibiotics by dehydropeptidase-I from porcine and human renal cortex, *J. Antimicrob. Chemother.*, 1992, **30**, 129–134.
101. H. Kropp, et al., Metabolism of Thienamycin and Related Carbapenem Antibiotics by the Renal Dipeptidase, Dehydropeptidase-I, *Antimicrob. Agents Chemother.*, 1982, **22**, 62–70.
102. N. Cotroneo, et al., In Vitro and In Vivo Characterization of Tebipenem, an Oral Carbapenem, *Antimicrob. Agents Chemother.*, 2020, **64**, 10.1128/aac.02240–02219.
103. F. S. Codjoe, et al., Carbapenem Resistance: A Review.*Journal*, 2018, **6**.
104. A. A. Elshamy, et al., A Review on Bacterial Resistance to Carbapenems: epidemiology, Detection and Treatment Options, *Future Science OA*, 2020, **6**, FSO438.
105. D. M. Livermore, et al., Carbapenemases: a problem in waiting?, *Curr. Opin. Microbiol.*, 2000, **3**, 489–495.
106. B. A. Rasmussen, et al., Carbapenem-hydrolyzing beta-lactamases, *Antimicrob. Agents Chemother.*, 1997, **41**, 223–232.
107. S. Sayood, et al., The oral penems and carbapenems, *Clin. Microbiol. Rev.*, 2025, **0**, e00042–00024.

108. A. Rusu, et al., Recent Developments in Penem Antibiotics: Structural and Therapeutic Perspectives, *Molecules*, 2025, **30**, 2126.
109. J. M. T. Hamilton-Miller, Chemical and Microbiologic Aspects of Penems, a Distinct Class of β-Lactams: Focus on Faropenem, *Pharmacotherapy*, 2003, **23**, 1497–1507.
110. K. N. Schurek, et al., Faropenem: review of a new oral penem, *Expert Rev. Anti. Infect. Ther.*, 2007, **5**, 185–198.
111. T. Gootz, et al., In vitro activity of CP-65,207, a new penem antimicrobial agent, in comparison with those of other agents, *Antimicrob. Agents Chemother.*, 1989, **33**, 1160–1166.
112. M. Ednie Lois, et al., Antianaerobic Activity of Sulopenem Compared to Six Other Agents, *Antimicrob. Agents Chemother.*, 2009, **53**, 2163–2170.
113. M. W. Dunne, et al., Sulopenem for the Treatment of Complicated Urinary Tract Infections Including Pyelonephritis: A Phase 3, Randomized Trial, *Clin. Infect. Dis.*, 2023, **76**, 78–88.
114. G. G. Zhanel, et al., Sulopenem: An Intravenous and Oral Penem for the Treatment of Urinary Tract Infections Due to Multidrug-Resistant Bacteria, *Drugs*, 2022, **82**, 533–557.
115. R. Aloni-Grinstein, et al., New Frontiers for Old Medications: Repurposing Approved Drugs Against Gram-Negative Bacterial Infections, *Microorganisms*, 2025, **13**, 2115.
116. J. Jampilek, Drug repurposing to overcome microbial resistance, *Drug Discov. Today*, 2022, **27**, 2028–2041.
117. A. Imada, et al., Sulfazecin and isosulfazecin, novel β-lactam antibiotics of bacterial origin, *Nature*, 1981, **289**, 590–591.
118. H. Aoki, et al., Nocardicin a, a new monocyclic β-lactam antibiotic I. Discovery, isolation and characterization, *J. Antibiot.*, 1976, **29**, 492–500.
119. L. Decuyper, et al., Antibacterial and β-Lactamase Inhibitory Activity of Monocyclic β-Lactams, *Med. Res. Rev.*, 2018, **38**, 426–503.
120. R. B. Sykes, et al., Aztreonam: The first monobactam, *Am. J. Med.*, 1985, **78**, 2–10.
121. N. X. Chin, et al., Tigemonam, an oral monobactam, *Antimicrob. Agents Chemother.*, 1988, **32**, 84–91.
122. A. A. Poeylaut-Palena, et al., A minimalistic approach to identify substrate binding features in B1 Metallo-β-lactamases, *Bioorg. Med. Chem. Lett.*, 2007, **17**, 5171–5174.
123. M. Castanheira, et al., Extended-spectrum β-lactamases: an update on their characteristics, epidemiology and detection, *JAC-Antimicrob. Resist.*, 2021, **3**, dlab092.
124. M. Al Musawa, et al., Aztreonam–avibactam: The dynamic duo against multidrug-resistant gram-negative pathogens, *Pharmacotherapy*, 2024, **44**, 927–938.
125. R. A. Bonomo, β-Lactamases: A Focus on Current Challenges, *Cold Spring Harbor Perspectives in Medicine*, 2017, **7**.
126. H. R. Onishi, et al., Cefoxitin, a Semisynthetic Cephamycin Antibiotic: Resistance to Beta-Lactamase Inactivation, *Antimicrob. Agents Chemother.*, 1974, **5**, 38–48.
127. R. Daoust Donald, et al., Cephamycins, a New Family of β-Lactam Antibiotics: Antibacterial Activity and Resistance to β-Lactamase Degradation, *Antimicrob. Agents Chemother.*, 1973, **3**, 254–261.
128. K. Jules, et al., Antibacterial activity and beta-lactamase stability of temocillin, *Antimicrob. Agents Chemother.*, 1982, **22**, 453–460.
129. L. Verbist, In vitro activity of temocillin (BRL 17421), a novel beta-lactamase-stable penicillin, *Antimicrob. Agents Chemother.*, 1982, **22**, 157–161.

130. A. Philippon, et al., Plasmid-Determined AmpC-Type β-Lactamases, *Antimicrob. Agents Chemother.*, 2002, **46**, 1–11.
131. C. J. Fernandes, et al., Cefoxitin resistance as a surrogate marker for the detection of methicillin-resistant Staphylococcus aureus, *J. Antimicrob. Chemother.*, 2005, **55**, 506–510.
132. J. M. Indelicato, et al., Effect of 6-.alpha. substitution in penicillins and 7-.alpha. substitution in cephalosporins upon .beta.-lactam reactivity, *J. Med. Chem.*, 1974, **17**, 528–529.
133. M. Sacco, D., et al., Influence of the α-Methoxy Group on the Reaction of Temocillin with Pseudomonas aeruginosa PBP3 and CTX-M-14 β-Lactamase, *Antimicrob. Agents Chemother.*, 2019, **64**, 10.1128/aac.01473–01419.
134. K. Bush, et al., Updated functional classification of β-lactamases, *Antimicrob. Agents Chemother.*, 2010, **54**, 969–976.
135. M. Mora-Ochomogo, et al., β-Lactam antibiotic targets and resistance mechanisms: from covalent inhibitors to substrates, *RSC Med. Chem.*, 2021, **12**, 1623–1639.
136. E. Boyd Sara, et al., Metallo-β-Lactamases: Structure, Function, Epidemiology, Treatment Options, and the Development Pipeline, *Antimicrob. Agents Chemother.*, 2020, **64**, 10.1128/aac.00397–00320.
137. A. Philippon, et al., A Structure-Based Classification of Class A β-Lactamases, a Broadly Diverse Family of Enzymes, *Clin. Microbiol. Rev.*, 2015, **29**, 29–57.
138. F. Sobia, et al., in *Beta-Lactam Resistance in Gram-Negative Bacteria: Threats and Challenges*, eds. M. Shahid, A. Singh and H. Sami, Springer Nature Singapore, Singapore, 2022, pp. 81–92.
139. A. Philippon, et al., Class C β-Lactamases: Molecular Characteristics, *Clin. Microbiol. Rev.*, 2022, **35**, e00150–00121.
140. E.-J. Yoon, et al., Class D β-lactamases, *J. Antimicrob. Chemother.*, 2021, **76**, 836–864.
141. P. S. Padayatti, et al., High Resolution Crystal Structures of the trans-Enamine Intermediates Formed by Sulbactam and Clavulanic Acid and E166A SHV-1 β-Lactamase*, *J. Biol. Chem.*, 2005, **280**, 34900–34907.
142. P. A. Lang, et al., Studies on enmetazobactam clarify mechanisms of widely used β-lactamase inhibitors, *Proc. Natl. Acad. Sci.*, 2022, **119**, e2117310119.
143. S. E. Jensen, et al., Biosynthesis and Molecular Genetics of Clavulanic Acid, *Antonie Van Leeuwenhoek*, 1999, **75**, 125–133.
144. P. S. Saudagar, et al., Clavulanic acid: A review, *Biotechnol. Adv.*, 2008, **26**, 335–351.
145. R. English Arthur, et al., CP-45,899, a Beta-Lactamase Inhibitor That Extends the Antibacterial Spectrum of Beta-Lactams: Initial Bacteriological Characterization, *Antimicrob. Agents Chemother.*, 1978, **14**, 414–419.
146. S. C. Aronoff, et al., Comparative activities of the beta-lactamase inhibitors YTR 830, sodium clavulanate, and sulbactam combined with amoxicillin or ampicillin, *Antimicrob. Agents Chemother.*, 1984, **26**, 580–582.
147. M. Paul-Satyaseela, Invention of Enmetazobactam: An Indian Triumph in Antimicrobial Drug Discovery, *ACS Infect. Dis.*, 2025, **11**, 1–3.
148. K. Manncke, et al., Sulbactam in combination with mezlocillin, piperacillin or cefotaxime: clinical and bacteriological findings in the treatment of serious bacterial infections, *Int. J. Antimicrob. Agents*, 1996, **6**, S47–S54.
149. C. M. Perry, et al., Piperacillin/Tazobactam, *Drugs*, 1999, **57**, 805–843.

150. T. Bhowmick, et al., Cefepime-enmetazobactam: first approved cefepime-β- lactamase inhibitor combination for multi-drug resistant Enterobacterales, *Future Microbiol.*, 2025, **20**, 277–286.
151. J. Finlay, et al., A review of the antimicrobial activity of clavulanate, *J. Antimicrob. Chemother.*, 2003, **52**, 18–23.
152. S. M. McLeod, et al., Sulbactam–durlobactam: a β-lactam/β-lactamase inhibitor combination targeting Acinetobacter baumannii, *Future Microbiol.*, 2024, **19**, 563–576.
153. P. A. Lang, et al., How Clavulanic Acid Inhibits Serine β-Lactamases, *ChemBioChem*, 2024, **25**, e202400280.
154. V. Arer, et al., Biochemical exploration of β-lactamase inhibitors, *Front. Genet.*, 2023, **Volume 13 - 2022**.
155. D. Yahav, et al., New β-Lactam–β-Lactamase Inhibitor Combinations, *Clin. Microbiol. Rev.*, 2020, **34**, 10.1128/cmr.00115–00120.
156. D. Y. Wang, et al., The Road to Avibactam: The First Clinically Useful Non-β-Lactam Working Somewhat Like a β-Lactam, *Future Med. Chem.*, 2016, **8**, 1063–1084.
157. H. Choi, et al., Investigations on recyclisation and hydrolysis in avibactam mediated serine β-lactamase inhibition, *Org. Biomol. Chem.*, 2016, **14**, 4116–4128.
158. M. Shirley, Ceftazidime-Avibactam: A Review in the Treatment of Serious Gram-Negative Bacterial Infections, *Drugs*, 2018, **78**, 675–692.
159. G. Sangiorgio, et al., Aztreonam and avibactam combination therapy for metallo-β-lactamase-producing gram-negative bacteria: A Narrative Review, *Clin. Microbiol. Infect.*, 2025, **31**, 971–978.
160. A. B. Shapiro, et al., Durlobactam, a New Diazabicyclooctane β-Lactamase Inhibitor for the Treatment of Acinetobacter Infections in Combination With Sulbactam, *Front. Microbiol.*, 2021, **Volume 12 - 2021**.
161. Y.-A. Heo, Imipenem/Cilastatin/Relebactam: A Review in Gram-Negative Bacterial Infections, *Drugs*, 2021, **81**, 377–388.
162. F. de Sousa Coelho, et al., The multiple benefits of second-generation β-lactamase inhibitors in treatment of multidrug-resistant bacteria, *Infect. Dis. Now*, 2021, **51**, 510–517.
163. T. Cahill Samuel, et al., Cyclic Boronates Inhibit All Classes of β-Lactamases, *Antimicrob. Agents Chemother.*, 2017, **61**, 10.1128/aac.02260–02216.
164. R. Tsivkovski, et al., Biochemical Activity of Vaborbactam, *Antimicrob. Agents Chemother.*, 2020, **64**, 10.1128/aac.01935–01919.
165. A. Novelli, et al., Meropenem/vaborbactam: a next generation β-lactam β-lactamase inhibitor combination, *Expert Rev. Anti. Infect. Ther.*, 2020, **18**, 643–655.
166. S. J. Hecker, et al., Discovery of Cyclic Boronic Acid QPX7728, an Ultrabroad-Spectrum Inhibitor of Serine and Metallo-β-lactamases, *J. Med. Chem.*, 2020, **63**, 7491–7507.
167. B. Liu, et al., Discovery of Taniborbactam (VNRX-5133): A Broad-Spectrum Serine- and Metallo-β-lactamase Inhibitor for Carbapenem-Resistant Bacterial Infections, *J. Med. Chem.*, 2020, **63**, 2789–2801.
168. H. O'Callaghan Cynthia, et al., A New Cephalosporin with a Dual Mode of Action, *Antimicrob. Agents Chemother.*, 1976, **10**, 245–248.
169. D. Greenwood, et al., Dual-Action Cephalosporin Utilizing a Novel Therapeutic Principle, *Antimicrob. Agents Chemother.*, 1976, **10**, 249–252.
170. N. H. Georgopapadakou, et al., Mode of action of the dual-action cephalosporin Ro 23-9424, *Antimicrob. Agents Chemother.*, 1989, **33**, 1067–1071.

171. *US Pat.,* US 5389626 A, 1995.
172. N. R. Yepuri, et al., Synthesis of cephalosporin-3′-diazeniumdiolates: biofilm dispersing NO-donor prodrugs activated by β-lactamase, *Chem. Commun.*, 2013, **49**, 4791–4793.
173. M. J. van Haren, et al., Cephalosporin Prodrug Inhibitors Overcome Metallo-β-Lactamase Driven Antibiotic Resistance, *Chem. Eur. J.*, 2021, **27**, 3806–3811.
174. J. Sato, et al., Discovery of a Tricyclic β-Lactam as a Potent Antimicrobial Agent against Carbapenem-Resistant Enterobacterales, Including Strains with Reduced Membrane Permeability and Four-Amino Acid Insertion into Penicillin-Binding Protein 3: Structure–Activity-Relationships and In Vitro and In Vivo Activities, *ACS Infect. Dis.*, 2022, **8**, 400–410.
175. J. Sato, et al., A novel tricyclic β-lactam exhibiting potent antibacterial activities against carbapenem-resistant Enterobacterales: Synthesis and structure-activity-relationships, *Bioorg. Med. Chem.*, 2021, **46**, 116343.
176. N. C. Cohen, .beta.-Lactam antibiotics: geometrical requirements for antibacterial activities, *J. Med. Chem.*, 1983, **26**, 259–264.
177. US4031077A, 1977.
178. J. M. T. Hamilton-Miller, Chemical Manipulations of the Penicillin Nucleus: A Review, *Chemotherapia*, 2009, **12**, 73–88.
179. E. H. Flynn, *Cephalosporins and penicillins: chemistry and biology*, Academic Press, New York, 1972.
180. M.-R. Meini, et al., Overcoming differences: The catalytic mechanism of metallo-β-lactamases, *FEBS Lett.*, 2015, **589**, 3419–3432.
181. H. Feng, et al., Structural and Mechanistic Insights into NDM-1 Catalyzed Hydrolysis of Cephalosporins, *J. Am. Chem. Soc.*, 2014, **136**, 14694–14697.
182. S. M. Drawz, et al., Exploring sequence requirements for C3/C4 carboxylate recognition in the Pseudomonas aeruginosa cephalosporinase: Insights into plasticity of the AmpC β-lactamase, *Protein Sci.*, 2011, **20**, 941–958.
183. Y. Watanabe, et al., In vitro antibacterial properties of T-5575 and T-5578 novel parenteral 2-carboxypenams, *Antimicrob. Agents Chemother.*, 1995, **39**, 2787–2791.
184. *US Pat.,* US 11208421 B2, 2021.
185. N. Matsumura, et al., Antibacterial activity of T-5575, a novel 2-carboxypenam, and its stability to beta-lactamase, *J. Antimicrob. Chemother.*, 1997, **39**, 31–34.
186. N. Matsumura, et al., A beta-lactamase from Serratia marcescens hydrolyzing the 2-carboxypenam T-5575, *Antimicrob. Agents Chemother.*, 1995, **39**, 2132–2134.
187. S. B. Rosenblum, et al., Discovery of 1-(4-Fluorophenyl)-(3R)-[3-(4-fluorophenyl)-(3S)-hydroxypropyl]-(4S)-(4-hydroxyphenyl)-2-azetidinone (SCH 58235): A Designed, Potent, Orally Active Inhibitor of Cholesterol Absorption, *J. Med. Chem.*, 1998, **41**, 973–980.
188. D. A. Burnett, et al., 2-Azetidinones as Inhibitors of Cholesterol Absorption, *J. Med. Chem.*, 1994, **37**, 1733–1736.
189. V. M. Vrudhula, et al., Antitumor activities of a cephalosporin prodrug in combination with monoclonal antibody-.beta.-lactamase conjugates, *Bioconj. Chem.*, 1993, **4**, 334–340.
190. V. M. Vrudhula, et al., Cephalosporin Derivatives of Doxorubicin as Prodrugs for Activation by Monoclonal Antibody-.beta.-Lactamase Conjugates, *J. Med. Chem.*, 1995, **38**, 1380–1385.

191. V. M. Vrudhula, et al., Cephalosporin prodrugs of paclitaxel for immunologically specific activation by L-49-sFv-β-Lactamase fusion protein, *Bioorg. Med. Chem. Lett.*, 2003, **13**, 539–542.
192. V. M. Vrudhula, et al., Immunologically Specific Activation of a Cephalosporin Derivative of Mitomycin C by Monoclonal Antibody β-Lactamase Conjugates, *J. Med. Chem.*, 1997, **40**, 2788–2792.
193. H. P. Svensson, et al., Monoclonal antibody-.beta.-lactamase conjugates for the activation of a cephalosporin mustard prodrug, *Bioconj. Chem.*, 1992, **3**, 176–181.
194. X. Li, et al., Ceftriaxone, an FDA-approved cephalosporin antibiotic, suppresses lung cancer growth by targeting Aurora B, *Carcinogenesis*, 2012, **33**, 2548–2557.
195. E. Labay, et al., Repurposing cephalosporin antibiotics as pro-senescent radiosensitizers, *Oncotarget*, 2016, **7**.
196. X. He, et al., Cephalosporin antibiotics specifically and selectively target nasopharyngeal carcinoma through HMOX1-induced ferroptosis, *Life Sci.*, 2021, **277**, 119457.
197. L. Chen, et al., Sequence-based drug design as a concept in computational drug design, *Nat. Commun.*, 2023, **14**, 4217.
198. C. Zhou, et al., Synthesis and Biological Evaluation of β-Lactam Derivatives Targeting Speckle-Type POZ Protein (SPOP), *ACS Med. Chem. Lett.*, 2024, **15**, 270–279.
199. D. M. Smith, et al., A Novel Beta-Lactam Antibiotic Activates Tumor Cell Apoptotic Program by Inducing DNA Damage, *Mol. Pharmacol.*, 2002, **61**, 1348–1358.
200. I. Banik, et al., Stereoselective Synthesis of β-Lactams with Polyaromatic Imines: Entry to New and Novel Anticancer Agents, *J. Med. Chem.*, 2003, **46**, 12–15.
201. L. N. Jungheim, et al., Design of Antitumor Prodrugs: Substrates for Antibody Targeted Enzymes, *Chem. Rev.*, 1994, **94**, 1553–1566.
202. T. A. Shepherd, et al., A novel targeted delivery system utilizing a cephalosporin-oncolytic prodrug activated by an antibody β-lactamase conjugate for the treatment of cancer, *Bioorg. Med. Chem. Lett.*, 1991, **1**, 21–26.
203. R. P. Alexander, et al., AN-nitrosochloroethyl-cephalosporin carbamate prodrug for antibody-directed enzyme prodrug therapy (ADEPT), *Tetrahedron*, 1996, **52**, 5983–5988.
204. R. M. Phelan, et al., Design and synthesis of a β-lactamase activated 5-fluorouracil prodrug, *Bioorg. Med. Chem. Lett.*, 2009, **19**, 1261–1263.
205. R. P. Alexander, et al., Cephalosporin Nitrogen Mustard Carbamate prodrugs for "ADEPT", *Tetrahedron Lett.*, 1991, **32**, 3269–3272.
206. D. B. Boggián, et al., A solid- and solution-phase-based library of 2β-methyl substituted penicillin derivatives and their effects on growth inhibition of tumor cell lines, *MedChemComm*, 2015, **6**, 619–625.
207. P. G. Cornier, et al., In vitro anticancer activity and SAR studies of triazolyl aminoacyl(peptidyl) penicillins, *MedChemComm*, 2014, **5**, 214–218.
208. N. L. Martiren, et al., Synthetic Strategies Towards the Generation of Penicillin-Containing Hybrids in the Search for Anticancer Activity, *Chem. Biodivers.*, 2025, **22**, e202402198.
209. C. M. Camacho, et al., Design, synthesis and cytotoxic evaluation of a library of oxadiazole-containing hybrids, *RSC Adv.*, 2021, **11**, 29741–29751.
210. T. W. Hudyma, et al., Synthesis and release of doxorubicin from a cephalosporin based prodrug by a β-lactamase-immunoconjugate, *Bioorg. Med. Chem. Lett.*, 1993, **3**, 323–328.
211. R. M. Adlington, et al., Design and synthesis of novel monocyclic β-lactam inhibitors of prostate specific antigen, *Bioorg. Med. Chem. Lett.*, 1997, **7**, 1689–1694.

212. J. B. Doherty, et al., Cephalosporin antibiotics can be modified to inhibit human leukocyte elastase, *Nature*, 1986, **322**, 192–194.
213. P. E. Finke, et al., Inhibition of human leukocyte elastase. 2. Inhibition by substituted cephalosporin esters and amides, *J. Med. Chem.*, 1990, **33**, 2522–2528.
214. K. R. Thompson, et al., Inhibition of human leukocyte elastase. 6. Inhibition by 6-substituted penicillin esters, *Bioorg. Med. Chem. Lett.*, 1993, **3**, 2283–2288.
215. J. D. Buynak, et al., 7-Alkylidenecephalosporin Esters as Inhibitors of Human Leukocyte Elastase, *J. Med. Chem.*, 1997, **40**, 3423–3433.
216. P. E. Finke, et al., Inhibition of human leukocyte elastase. 4. Selection of a substituted cephalosporin (L-658,758) as a topical aerosol, *J. Med. Chem.*, 1992, **35**, 3731–3744.
217. P. E. Finke, et al., Inhibition of human leukocyte elastase. 5. Inhibition by 6-alkyl substituted penem benzyl esters, *Bioorg. Med. Chem. Lett.*, 1993, **3**, 2277–2282.
218. S. K. Shah, et al., Orally active .beta.-lactam inhibitors of human leukocyte elastase-1. Activity of 3,3-diethyl-2-azetidinones, *J. Med. Chem.*, 1992, **35**, 3745–3754.
219. R. Firestone, et al., Monocyclic β-lactam inhibitors of human leukocyte elastase, *Tetrahedron*, 1990, **46**, 2255–2262.
220. S. K. Shah, et al., Inhibition of human leukocyte elastase. 3. Synthesis and activity of 3'-substituted cephalosporins, *J. Med. Chem.*, 1990, **33**, 2529–2535.
221. J. R. Burke, et al., A β-Lactam Inhibitor of Cytosolic Phospholipase A2 which Acts in a Competitive, Reversible Manner at the Lipid/Water Interface, *J. Enzym Inhib.*, 1998, **13**, 195–206.
222. J. Sugatani, et al., In vitro actions of some antibiotics on phospholipases, *J. Antibiot.*, 1979, **32**, 734–739.
223. X. Ci, et al., Ceftiofur impairs pro-inflammatory cytokine secretion through the inhibition of the activation of NF-κB and MAPK, *Biochem. Biophys. Res. Commun.*, 2008, **372**, 73–77.
224. G. Cainelli, et al., 4-Alkylidene-azetidin-2-ones: novel inhibitors of leukocyte elastase and gelatinase, *Bioorg. Med. Chem.*, 2003, **11**, 5391–5399.
225. M. S. Genčić, et al., Repurposing of monocyclic β-lactams as anti-inflammatory agents – The case of new ferrocene-azetidin-2-one hybrids, *Eur. J. Med. Chem.*, 2024, **280**, 116910.
226. A. Fiasella, et al., 3-Aminoazetidin-2-one Derivatives as N-Acylethanolamine Acid Amidase (NAAA) Inhibitors Suitable for Systemic Administration, *ChemMedChem*, 2014, **9**, 1602–1614.
227. A. Nuzzi, et al., Potent α-amino-β-lactam carbamic acid ester as NAAA inhibitors. Synthesis and structure–activity relationship (SAR) studies, *Eur. J. Med. Chem.*, 2016, **111**, 138–159.
228. R. Petracca, et al., Progress in the development of β-lactams as N-Acylethanolamine Acid Amidase (NAAA) inhibitors: Synthesis and SAR study of new, potent N-O-substituted derivatives, *Eur. J. Med. Chem.*, 2017, **126**, 561–575.
229. L. C. Cheney, et al., β-Lactam antimicrobial agents which possess antifungal activity, *J. Med. Chem.*, 1971, **14**, 770–772.
230. H. D. King, et al., Clavamycins, new clavam antibiotics from two variants of streptomyces hygroscop1cus I. Taxonomy of the producing organisms, fermentation, and biological activities, *J. Antibiot.*, 1986, **39**, 510–515.
231. A. Arnoldi, et al., Synthesis and anti-fungal activity of simple β-lactams, *Eur. J. Med. Chem.*, 1988, **23**, 149–154.

232. D. Brown, et al., Structures of three novel β-lactams isolated from Streptomyces clavuligerus, *J. Chem. Soc., Chem. Commun.*, 1979, 282–283.
233. J. C. Müller, et al., A new clavam antibiotic from streptomyces clavuligerus: III. Absolute stereochemistry, *J. Antibiot.*, 1983, **36**, 217–225.
234. M. O'Driscoll, et al., Studies on the antifungal properties of N-thiolated β-lactams, *Bioorg. Med. Chem.*, 2008, **16**, 7832–7837.
235. A. Arnoldi, et al., Activity of a series of .beta.-lactams against some phytopathogenic fungi, *J. Agric. Food Chem.*, 1990, **38**, 2197–2199.
236. N. E. Zhou, et al., 6-Acylamino-penam derivatives: synthesis and inhibition of cathepsins B, L, K, and S, *Bioorg. Med. Chem. Lett.*, 2002, **12**, 3417–3419.
237. T. Dražić, et al., Peptide-β-lactam Inhibitors of Dengue and West Nile Virus NS2B-NS3 Protease Display Two Distinct Binding Modes, *J. Med. Chem.*, 2020, **63**, 140–156.
238. T. M. Haley, et al., Investigation of the covalent modification of the catalytic triad of human cytomegalovirus protease by pseudo-reversible β-lactam inhibitors and a peptide chloromethylketone, *J. Mass Spectrom.*, 1998, **33**, 1246–1255.
239. C. Yoakim, et al., β-Lactam Derivatives as Inhibitors of Human Cytomegalovirus Protease, *J. Med. Chem.*, 1998, **41**, 2882–2891.
240. R. Déziel, et al., Inhibition of human cytomegalovirus protease No with monocyclic β-lactams, *Bioorg. Med. Chem. Lett.*, 1998, **8**, 1437–1442.
241. T. R. Malla, et al., Mass spectrometry reveals potential of β-lactams as SARS-CoV-2 Mpro inhibitors, *Chem. Commun.*, 2021, **57**, 1430–1433.
242. T. R. Malla, et al., Penicillin Derivatives Inhibit the SARS-CoV-2 Main Protease by Reaction with Its Nucleophilic Cysteine, *J. Med. Chem.*, 2022, **65**, 7682–7696.
243. F. A. Ambrosio, et al., Targeting SARS-CoV-2 Main Protease: A Successful Story Guided by an In Silico Drug Repurposing Approach, *J. Chem. Inf. Model.*, 2023, **63**, 3601–3613.
244. A. D. Borthwick, et al., Design and synthesis of monocyclic β-lactams as mechanism-based inhibitors of human cytomegalovirus protease, *Bioorg. Med. Chem. Lett.*, 1998, **8**, 365–370.
245. E. L. Setti, et al., 3,4-Disubstituted azetidinones as selective inhibitors of the cysteine protease cathepsin K. Exploring P2 elements for selectivity, *Bioorg. Med. Chem. Lett.*, 2003, **13**, 2051–2053.
246. S. A. E. Peters, et al., Total cholesterol as a risk factor for coronary heart disease and stroke in women compared with men: A systematic review and meta-analysis, *Atherosclerosis*, 2016, **248**, 123–131.
247. B. A. Ference, et al., Low-density lipoproteins cause atherosclerotic cardiovascular disease. 1. Evidence from genetic, epidemiologic, and clinical studies. A consensus statement from the European Atherosclerosis Society Consensus Panel, *Eur. Heart J.*, 2017, **38**, 2459–2472.
248. Y. Duan, et al., Regulation of cholesterol homeostasis in health and diseases: from mechanisms to targeted therapeutics, *Signal Transduct. Target. Ther.*, 2022, **7**, 265.
249. J. Luo, et al., Mechanisms and regulation of cholesterol homeostasis, *Nature Reviews: Molecular Cell Biology*, 2020, **21**, 225–245.
250. B. G. Salisbury, et al., Hypocholesterolemic activity of a novel inhibitor of cholesterol absorption, SCH 48461, *Atherosclerosis*, 1995, **115**, 45–63.
251. M. Garcia-Calvo, et al., The target of ezetimibe is Niemann-Pick C1-Like 1 (NPC1L1), *Proc. Natl. Acad. Sci.*, 2005, **102**, 8132–8137.

252. L. M. Force, et al., The global, regional, and national burden of cancer, 1990-2023, with forecasts to 2050: a systematic analysis for the Global Burden of Disease Study 2023, *The Lancet*.
253. Z. Wu, et al., Global burden of cancer and associated risk factors in 204 countries and territories, 1980–2021: a systematic analysis for the GBD 2021, *J. Hematol. Oncol.*, 2024, **17**, 119.
254. U. Anand, et al., Cancer chemotherapy and beyond: Current status, drug candidates, associated risks and progress in targeted therapeutics, *Genes Dis.*, 2023, **10**, 1367–1401.
255. B. Liu, et al., Exploring treatment options in cancer: tumor treatment strategies, *Signal Transduct. Target. Ther.*, 2024, **9**, 175.
256. A. Zafar, et al., Advancements and limitations in traditional anti-cancer therapies: a comprehensive review of surgery, chemotherapy, radiation therapy, and hormonal therapy, *Discov. Oncol.*, 2025, **16**, 607.
257. A. Marusyk, et al., Intratumor Heterogeneity: The Rosetta Stone of Therapy Resistance, *Cancer Cell*, 2020, **37**, 471–484.
258. S. U. Khan, et al., Unveiling the mechanisms and challenges of cancer drug resistance, *Cell Commun. Signal.*, 2024, **22**, 109.
259. G. F. V. Ismael, et al., Novel cytotoxic drugs: Old challenges, new solutions, *Cancer Treat. Rev.*, 2008, **34**, 81–91.
260. R. A. Ward, et al., Challenges and Opportunities in Cancer Drug Resistance, *Chem. Rev.*, 2021, **121**, 3297–3351.
261. J. M. T. Hamilton-Miller, β-Lactams: variations on a chemical theme, with some surprising biological results, *J. Antimicrob. Chemother.*, 1999, **44**, 729–734.
262. D. Kuhn, et al., Beta-lactams and their potential use as novel anticancer chemotherapeutics drugs, *FBL*, 2004, **9**, 2605–2617.
263. P. D. Mehta, et al., 2-Azetidinone – A new profile of various pharmacological activities, *Eur. J. Med. Chem.*, 2010, **45**, 5541–5560.
264. I. Niculescu-Duvaz, et al., Antibody-directed enzyme prodrug therapy (ADEPT): a review, *Adv. Drug Del. Rev.*, 1997, **26**, 151–172.
265. R. K. Singh, et al., Therapeutic journery of nitrogen mustard as alkylating anticancer agents: Historic to future perspectives, *Eur. J. Med. Chem.*, 2018, **151**, 401–433.
266. E. Martino, et al., Vinca alkaloids and analogues as anti-cancer agents: Looking back, peering ahead, *Bioorg. Med. Chem. Lett.*, 2018, **28**, 2816–2826.
267. D. L. Meyer, et al., Site-specific Prodrug Activation by Antibody-β-Lactamase Conjugates: Regression and Long-Term Growth Inhibition of Human Colon Carcinoma Xenograft Models, *Cancer Res.*, 1993, **53**, 3956–3963.
268. B. A. Weaver, How Taxol/paclitaxel kills cancer cells, *Mol. Biol. Cell*, 2014, **25**, 2677–2681.
269. W. T. Bradner, Mitomycin C: a clinical update, *Cancer Treat. Rev.*, 2001, **27**, 35–50.
270. S. Y. van der Zanden, et al., New insights into the activities and toxicities of the old anticancer drug doxorubicin, *FEBS J.*, 2021, **288**, 6095–6111.
271. D. L. Meyer, et al., Site-Specific Prodrug Activation by Antibody-β-Lactamase Conjugates: Preclinical Investigation of the Efficacy and Toxicity of Doxorubicin Delivered by Antibody Directed Catalysis, *Bioconj. Chem.*, 1995, **6**, 440–446.
272. D. B. Longley, et al., 5-Fluorouracil: mechanisms of action and clinical strategies, *Nature Reviews Cancer*, 2003, **3**, 330–338.

273. C. S. Nervig, et al., Complementation Dependent Enzyme Prodrug Therapy Enables Targeted Activation of Prodrug on HER2-Positive Cancer Cells, *ACS Med. Chem. Lett.*, 2022, **13**, 1769–1775.
274. *EP Pat.,* EP 0382411 A3, 1992.
275. D. M. Richards, et al., Ceftriaxone, *Drugs*, 1984, **27**, 469–527.
276. T. Kosaka, et al., Mechanisms of Resistance to EGFR TKIs and Development of a New Generation of Drugs in Non-Small-Cell Lung Cancer, *BioMed Res. Int.*, 2011, **2011**, 165214.
277. R. Sorrentino, et al., Aurora B Overexpression Associates with the Thyroid Carcinoma Undifferentiated Phenotype and Is Required for Thyroid Carcinoma Cell Proliferation, *J. Clin. Endocrinol. Metab.*, 2005, **90**, 928–935.
278. Y.-J. Chen, et al., Overexpression of Aurora B is associated with poor prognosis in epithelial ovarian cancer patients, *Virchows Arch.*, 2009, **455**, 431–440.
279. M. Tatsuka, et al., Multinuclearity and increased ploidy caused by overexpression of the Aurora- and Ipl1-like midbody-associated protein mitotic kinase in human cancer cells, *Cancer Res.*, 1998, **58**, 4811–4816.
280. S. Kalghatgi, et al., Bactericidal Antibiotics Induce Mitochondrial Dysfunction and Oxidative Damage in Mammalian Cells, *Science Translational Medicine*, 2013, **5**, 192ra185–192ra185.
281. B. M. Tune, et al., The mitochondrial respiratory toxicity of cephalosporin antibiotics. An inhibitory effect on substrate uptake, *J. Pharmacol. Exp. Ther.*, 1988, **245**, 1054–1059.
282. B. M. Tune, Nephrotoxicity of beta-lactam antibiotics: mechanisms and strategies for prevention, *Pediatr. Nephrol.*, 1997, **11**, 768–772.
283. R.-S. Mani, The emerging role of speckle-type POZ protein (SPOP) in cancer development, *Drug Discov. Today*, 2014, **19**, 1498–1502.
284. A. Chauhan, et al., Speckle-type POZ protein as a diagnostic biomarker in renal cell carcinoma, *J. Cancer. Res. Ther.*, 2018, **14**.
285. V.-J. Claudio, et al., Molecular Hybridization: A Useful Tool in the Design of New Drug Prototypes, *Curr. Med. Chem.*, 2007, **14**, 1829–1852.
286. A. Saura-Sanmartin, et al., Stereoselective synthesis of β-lactams: recent examples, *Org. Biomol. Chem.*, 2023, **21**, 3296–3306.
287. H. O. L. Taíse, et al., Monocyclic beta-Lactam: A Review on Synthesis and Potential Biological Activities of a Multitarget Core, *Mini-Reviews in Medicinal Chemistry*, 2020, **20**, 1653–1682.
288. R. Sarkar, et al., Recent advances in the syntheses and reactions of biologically promising β-lactam derivatives, *Tetrahedron*, 2025, **177**, 134565.
289. N. Van Opdenbosch, et al., Caspases in Cell Death, Inflammation, and Disease, *Immunity*, 2019, **50**, 1352–1364.
290. G. Martelli, et al., N-Thio-β-lactams targeting L,D-transpeptidase-2, with activity against drug-resistant strains of Mycobacterium tuberculosis, *Cell Chem. Biol.*, 2021, **28**, 1321–1332.e1325.
291. R. Kaur, et al., Recent developments in tubulin polymerization inhibitors: An overview, *Eur. J. Med. Chem.*, 2014, **87**, 89–124.
292. T. F. Greene, et al., Synthesis and Biochemical Evaluation of 3-Phenoxy-1,4-diarylazetidin-2-ones as Tubulin-Targeting Antitumor Agents, *J. Med. Chem.*, 2016, **59**, 90–113.

293. A. Peralta-Leal, et al., PARP inhibitors: New partners in the therapy of cancer and inflammatory diseases, *Free Radical Biol. Med.*, 2009, **47**, 13–26.
294. G.-D. Zhu, et al., Discovery and SAR of orally efficacious tetrahydropyridopyridazinone PARP inhibitors for the treatment of cancer, *Bioorg. Med. Chem.*, 2012, **20**, 4635–4645.
295. J. R. Fay, et al., Energy homeostasis and cancer prevention: The AMP-activated protein kinase, *Cancer Prev. Res.*, 2009, **2**, 301–309.
296. F. Tripodi, et al., Synthesis and Biological Evaluation of 1,4-Diaryl-2-azetidinones as Specific Anticancer Agents: Activation of Adenosine Monophosphate Activated Protein Kinase and Induction of Apoptosis, *J. Med. Chem.*, 2012, **55**, 2112–2124.
297. J.-M. Renoir, et al., Estrogen receptor signaling as a target for novel breast cancer therapeutics, *Biochem. Pharmacol.*, 2013, **85**, 449–465.
298. N. M. O'Boyle, et al., β-Lactam Estrogen Receptor Antagonists and a Dual-Targeting Estrogen Receptor/Tubulin Ligand, *J. Med. Chem.*, 2014, **57**, 9370–9382.
299. S. Rastogi, et al., An update on the status of HSP90 inhibitors in cancer clinical trials, *Cell Stress and Chaperones*, 2024, **29**, 519–539.
300. N. M. O'Boyle, et al., Lead identification of β-lactam and related imine inhibitors of the molecular chaperone heat shock protein 90, *Bioorg. Med. Chem.*, 2011, **19**, 6055–6068.
301. A. Stamey Thomas, et al., Prostate-Specific Antigen as a Serum Marker for Adenocarcinoma of the Prostate, *New Engl. J. Med.*, 1987, **317**, 909–916.
302. J. E. Oesterling, Prostate Specific Antigen: A Critical Assessment of the Most Useful Tumor Marker for Adenocarcinoma of the Prostate, *J. Urol.*, 1991, **145**, 907–923.
303. P. Singh, et al., Mechanistic insights into the inhibition of prostate specific antigen by β-lactam class compounds, *Proteins: Structure, Function and Genetics*, 2008, **70**, 1416–1428.
304. D. Furman, et al., Chronic inflammation in the etiology of disease across the life span, *Nat. Med.*, 2019, **25**, 1822–1832.
305. G. A. Roth, et al., Global, regional, and national age-sex-specific mortality for 282 causes of death in 195 countries and territories, 1980–2017: a systematic analysis for the Global Burden of Disease Study 2017, *The Lancet*, 2018, **392**, 1736–1788.
306. L. Ekerot, et al., in *Proteases: Potential Role in Health and Disease*, eds. W. H. Hörl and A. Heidland, Springer US, Boston, MA, 1984, pp. 335–344.
307. G. L. Snider, Protease-antiprotease imbalance in the pathogensis of emphysema and chronic bronchial injury: A potential target for drug development, *Drug Dev. Res.*, 1987, **10**, 235–253.
308. S. Suter, et al., Granulocyte Neutral Proteases and Pseudomonas Elastase as Possible Causes of Airway Damage in Patients with Cystic Fibrosis, *J. Infect. Dis.*, 1984, **149**, 523–531.
309. D. A. Trainor, Synthetic inhibitors of human neutrophil elastase, *Trends Pharmacol. Sci.*, 1987, **8**, 303–307.
310. A. Calignano, et al., Antinociceptive activity of the endogenous fatty acid amide, palmitylethanolamide, *Eur. J. Pharmacol.*, 2001, **419**, 191–198.
311. K. Tsuboi, et al., The N-acylethanolamine-hydrolyzing acid amidase (NAAA), *Chem. Biodivers.*, 2007, **4**, 1914–1925.
312. H. Minasyan, Sepsis: mechanisms of bacterial injury to the patient, *cand. J. Trauma Resusc. Emerg. Med*, 2019, **27**, 19.

313. S. Gatica, et al., Novel evidence on sepsis-inducing pathogens: from laboratory to bedside, *Front. Microbiol.*, 2023, **Volume 14 - 2023**.
314. M. Patra, et al., The medicinal chemistry of ferrocene and its derivatives, *Nat. Rev. Chem.*, 2017, **1**, 0066.
315. J. Skiba, et al., Ferrocenyl bioconjugates of ampicillin and 6-aminopenicillinic acid – Synthesis, electrochemistry and biological activity, *Eur. J. Med. Chem.*, 2012, **57**, 234–239.
316. E. I. Edwards, et al., A new class of semi-synthetic antibiotics: ferrocenyl-penicillins and -cephalosporins, *J. Organomet. Chem.*, 1976, **107**, 351–357.
317. B. Long, et al., Synthesis, characterization and antibacterial activities of some new ferrocene-containing penems, *Eur. J. Med. Chem.*, 2010, **45**, 1181–1188.
318. M. A. Cinelli, et al., Inducible nitric oxide synthase: Regulation, structure, and inhibition, *Med. Res. Rev.*, 2020, **40**, 158–189.
319. N. Barraud, et al., Nitric oxide: A key mediator of biofilm dispersal with applications in infectious diseases, *Curr. Pharm. Des.*, 2015, **21**, 31–42.
320. F. Niu, et al., Arginase: An emerging and promising therapeutic target for cancer treatment, *Biomed. Pharmacother.*, 2022, **149**, 112840.
321. G. D. Brown, et al., The pathobiology of human fungal infections, *Nat. Rev. Microbiol.*, 2024, **22**, 687–704.
322. G. K. K. Reddy, et al., Fungal infections: Pathogenesis, antifungals and alternate treatment approaches, *Curr. Res. Microb. Sci.*, 2022, **3**, 100137.
323. J. C. Pérez, Fungi of the human gut microbiota: Roles and significance, *Int. J. Med. Microbiol.*, 2021, **311**, 151490.
324. P. G. Pappas, et al., Invasive candidiasis, *Nat. Rev. Dis. Primers*, 2018, **4**, 18026.
325. C. O. Morrissey, et al., Aspergillus fumigatus—a systematic review to inform the World Health Organization priority list of fungal pathogens, *Med. Mycol.*, 2024, **62**, myad129.
326. R. Garcia-Rubio, et al., The Fungal Cell Wall: Candida, Cryptococcus, and Aspergillus Species, *Front. Microbiol.*, 2020, **Volume 10 - 2019**.
327. N. A. R. Gow, Fungal cell wall biogenesis: structural complexity, regulation and inhibition, *Fungal Genet. Biol.*, 2025, **179**, 103991.
328. K. D. Revell, et al., N-thiolated β-lactams: Studies on the mode of action and identification of a primary cellular target in Staphylococcus aureus, *Bioorg. Med. Chem.*, 2007, **15**, 2453–2467.
329. D. L. Pruess, et al., A new clavam antibiotic from streptomyces clavuligerus: I. Discovery and biological activity, *J. Antibiot.*, 1983, **36**, 208–212.
330. F. Röhl, et al., Biological properties and mode of action of clavams, *Arch. Microbiol.*, 1987, **147**, 315–320.
331. J. Louten, in *Essential Human Virology*, ed. J. Louten, Academic Press, Boston, 2016, pp. 49–70.
332. N. Nathanson, in *Viral Pathogenesis (Third Edition)*, eds. M. G. Katze, M. J. Korth, G. L. Law and N. Nathanson, Academic Press, Boston, 2016, pp. 3–16.
333. C. Saraceni, et al., A Review of Hepatitis B Virus and Hepatitis C Virus Immunopathogenesis, *J. Clin. Transl. Hepatol.*, 2021, **9**, 409–418.
334. P. Berche, The Spanish flu, *Presse Med.*, 2022, **51**, 104127.
335. W. Msemburi, et al., The WHO estimates of excess mortality associated with the COVID-19 pandemic, *Nature*, 2023, **613**, 130–137.

336. C. Beyrer, A pandemic anniversary: 40 years of HIV/AIDS, *The Lancet*, 2021, **397**, 2142–2143.
337. S. Riedel, Edward Jenner and the History of Smallpox and Vaccination, *Bayl. Univ. Med. Cent. Proc.*, 2005, **18**, 21–25.
338. N. Chaudhary, et al., mRNA vaccines for infectious diseases: principles, delivery and clinical translation, *Nat. Rev. Drug Discov.*, 2021, **20**, 817–838.
339. G. Zhang, et al., mRNA vaccines in disease prevention and treatment, *Signal Transduct. Target. Ther.*, 2023, **8**, 365.
340. A. J. Pollard, et al., A guide to vaccinology: from basic principles to new developments, *Nat. Rev. Immunol.*, 2021, **21**, 83–100.
341. M. Dagovetz, et al., Global COVID-19 vaccination challenges: Inequity of access and vaccine hesitancy, *J. Med. Surg. Public Health*, 2025, **6**, 100197.
342. S. Kausar, et al., A review: Mechanism of action of antiviral drugs, *Int. J. Immunopathol. Pharmacol.*, 2021, **35**, 20587384211002621.
343. E. De Clercq, et al., Approved Antiviral Drugs over the Past 50 Years, *Clin. Microbiol. Rev.*, 2016, **29**, 695–747.
344. V. Turk, et al., Cysteine cathepsins: From structure, function and regulation to new frontiers, *Biochim. Biophys. Acta*, 2012, **1824**, 68–88.
345. K. Zhao, et al., The multifaceted roles of cathepsins in immune and inflammatory responses: implications for cancer therapy, autoimmune diseases, and infectious diseases, *Biomark. Res.*, 2024, **12**, 165.
346. T. Pathak, et al., Cathepsins in cellular entry of human pathogenic viruses, *J. Virol.*, 2025, **99**, e01642–01624.
347. N. E. Zhou, et al., Design and synthesis of 6-substituted amino-4-oxa-1-azabicyclo[3,2,0]heptan-7-one derivatives as cysteine proteases inhibitors, *Bioorg. Med. Chem. Lett.*, 2002, **12**, 3413–3415.
348. M. B. Khan, et al., Dengue overview: An updated systemic review, *J. Infect. Public Health*, 2023, **16**, 1625–1642.
349. J. Sejvar James, West Nile Virus Infection, *Microbiol. Spectr.*, 2016, **4**, 10.1128/microbiolspec.ei1110–0021–2016.
350. M. H. Collins, et al., Progress and Works in Progress: Update on Flavivirus Vaccine Development, *Clin. Ther.*, 2017, **39**, 1519–1536.
351. W. T. Han, et al., Azetidin-2-one derivatives as inhibitors of thrombin, *Bioorg. Med. Chem.*, 1995, **3**, 1123–1143.
352. P. Griffiths, et al., Pathogenesis of human cytomegalovirus in the immunocompromised host, *Nat. Rev. Microbiol.*, 2021, **19**, 759–773.
353. C. Gilbert, et al., Human Cytomegalovirus Resistance to Antiviral Drugs, *Antimicrob. Agents Chemother.*, 2005, **49**, 873–883.
354. S. Lurain Nell, et al., Antiviral Drug Resistance of Human Cytomegalovirus, *Clin. Microbiol. Rev.*, 2010, **23**, 689–712.
355. P. Chen, et al., Structure of the Human Cytomegalovirus Protease Catalytic Domain Reveals a Novel Serine Protease Fold and Catalytic Triad, *Cell*, 1996, **86**, 835–843.
356. M. M. Lamers, et al., SARS-CoV-2 pathogenesis, *Nat. Rev. Microbiol.*, 2022, **20**, 270–284.
357. S. Steiner, et al., SARS-CoV-2 biology and host interactions, *Nat. Rev. Microbiol.*, 2024, **22**, 206–225.

358. P. V'kovski, et al., Coronavirus biology and replication: implications for SARS-CoV-2, *Nat. Rev. Microbiol.*, 2021, **19**, 155–170.
359. T. Duan, et al., ACE2-dependent and -independent SARS-CoV-2 entries dictate viral replication and inflammatory response during infection, *Nat. Cell Biol.*, 2024, **26**, 628–644.
360. F. Nazir, et al., SARS-CoV-2 replication and drug discovery, *Mol. Cell. Probes*, 2024, **77**, 101973.
361. B. Malone, et al., Structures and functions of coronavirus replication–transcription complexes and their relevance for SARS-CoV-2 drug design, *Nat. Rev. Mol. Cell Biol.*, 2022, **23**, 21–39.
362. L. Silvestrini, et al., The dimer-monomer equilibrium of SARS-CoV-2 main protease is affected by small molecule inhibitors, *Sci. Rep.*, 2021, **11**, 9283.
363. E. Costanzi, et al., Structural and Biochemical Analysis of the Dual Inhibition of MG-132 against SARS-CoV-2 Main Protease (Mpro/3CLpro) and Human Cathepsin-L, *Int. J. Mol. Sci.*, 2021, **22**, 11779.
364. Q. Hu, et al., The SARS-CoV-2 main protease (Mpro): Structure, function, and emerging therapies for COVID-19, *MedComm*, 2022, **3**, e151.
365. I. Schechter, et al., On the size of the active site in proteases. I. Papain, *Biochem. Biophys. Res. Commun.*, 1967, **27**, 157–162.
366. T. Koudelka, et al., N-Terminomics for the Identification of In Vitro Substrates and Cleavage Site Specificity of the SARS-CoV-2 Main Protease, *Proteomics*, 2021, **21**, 2000246.
367. Q. Zhao, et al., Structure of the Main Protease from a Global Infectious Human Coronavirus, HCoV-HKU1, *J. Virol.*, 2008, **82**, 8647–8655.
368. A. M. Shaqra, et al., Defining the substrate envelope of SARS-CoV-2 main protease to predict and avoid drug resistance, *Nat. Commun.*, 2022, **13**, 3556.
369. Z. Jin, et al., Structure of Mpro from SARS-CoV-2 and discovery of its inhibitors, *Nature*, 2020, **582**, 289–293.
370. A. Hegyi, et al., Conservation of substrate specificities among coronavirus main proteases, *Journal of General Virology*, 2002, **83**, 595–599.
371. T. Lee Jonathan, et al., Genetic Surveillance of SARS-CoV-2 Mpro Reveals High Sequence and Structural Conservation Prior to the Introduction of Protease Inhibitor Paxlovid, *mBio*, 2022, **13**, e00869–00822.
372. K. Anand, et al., Coronavirus Main Proteinase (3CLpro) Structure: Basis for Design of Anti-SARS Drugs, *Science*, 2003, **300**, 1763–1767.
373. T. Pillaiyar, et al., An Overview of Severe Acute Respiratory Syndrome–Coronavirus (SARS-CoV) 3CL Protease Inhibitors: Peptidomimetics and Small Molecule Chemotherapy, *Journal of Medicinal Chemistry*, 2016, **59**, 6595–6628.
374. Y. L. Janin, On the origins of SARS-CoV-2 main protease inhibitors, *RSC Med. Chem.*, 2024, **15**, 81–118.
375. G. Li, et al., Therapeutic strategies for COVID-19: progress and lessons learned, *Nat. Rev. Drug Discov.*, 2023, **22**, 449–475.
376. A. M. Shawky, et al., Covalent small-molecule inhibitors of SARS-CoV-2 Mpro: Insights into their design, classification, biological activity, and binding interactions, *Eur. J. Med. Chem.*, 2024, **277**, 116704.

377. L. Song, et al., Medicinal chemistry strategies towards the development of non-covalent SARS-CoV-2 Mpro inhibitors, *Acta Pharm. Sin. B*, 2024, **14**, 87–109.
378. L. Brewitz, et al., Alkyne Derivatives of SARS-CoV-2 Main Protease Inhibitors Including Nirmatrelvir Inhibit by Reacting Covalently with the Nucleophilic Cysteine, *J. Med. Chem.*, 2023, **66**, 2663–2680.
379. C. Ma, et al., Discovery of Di- and Trihaloacetamides as Covalent SARS-CoV-2 Main Protease Inhibitors with High Target Specificity, *J. Am. Chem. Soc.*, 2021, **143**, 20697–20709.
380. B. Boras, et al., Preclinical characterization of an intravenous coronavirus 3CL protease inhibitor for the potential treatment of COVID19, *Nat. Commun.*, 2021, **12**, 6055.
381. J. K. Stille, et al., Design, synthesis and in vitro evaluation of novel SARS-CoV-2 3CLpro covalent inhibitors, *Eur. J. Med. Chem.*, 2022, **229**, 114046.
382. D. Laczi, et al., Silaproline-bearing nirmatrelvir derivatives are potent inhibitors of the SARS-CoV-2 main protease highlighting the value of silicon-derivatives in structure-activity-relationship studies, *Eur. J. Med. Chem.*, 2025, **291**, 117603.
383. Faridoon, et al., An update on the discovery and development of reversible covalent inhibitors, *Medicinal Chemistry Research*, 2023, **32**, 1039–1062.
384. N. Atatreh, et al., Exploring covalent inhibitors of SARS-CoV-2 main protease: from peptidomimetics to novel scaffolds, *J. Enzyme Inhib. Med. Chem.*, 2025, **40**, 2460045.
385. D. R. Owen, et al., An oral SARS-CoV-2 Mpro inhibitor clinical candidate for the treatment of COVID-19, *Science*, 2021, **374**, 1586–1593.
386. C. M. N. Allerton, et al., A Second-Generation Oral SARS-CoV-2 Main Protease Inhibitor Clinical Candidate for the Treatment of COVID-19, *J. Med. Chem.*, 2024, **67**, 13550–13571.
387. X. Jiang, et al., Structure-based development and preclinical evaluation of the SARS-CoV-2 3C-like protease inhibitor simnotrelvir, *Nat. Commun.*, 2023, **14**.
388. Y. Unoh, et al., Discovery of S-217622, a Noncovalent Oral SARS-CoV-2 3CL Protease Inhibitor Clinical Candidate for Treating COVID-19, *J. Med. Chem.*, 2022, **65**, 6499–6512.
389. H. Zhang, et al., Phase I study, and dosing regimen selection for a pivotal COVID-19 trial of GST-HG171, *Antimicrob. Agents Chemother.*, 2024, **68**.
390. L. Brewitz, et al., Fixing the Achilles Heel of Pfizer's Paxlovid for COVID-19 Treatment, *J. Med. Chem.*, 2024, **67**, 11656–11661.
391. R. Jimmidi, et al., DNA-encoded chemical libraries yield non-covalent and non-peptidic SARS-CoV-2 main protease inhibitors, *Commun. Chem.*, 2023, **6**, 164.
392. M. L. Boby, et al., Open science discovery of potent noncovalent SARS-CoV-2 main protease inhibitors, *Science*, **382**, eabo7201.
393. N. E. Zhou, et al., An oral non-covalent non-peptidic inhibitor of SARS-CoV-2 Mpro ameliorates viral replication and pathogenesis in vivo, *Cell Rep.*, 2024, **43**, 114929.
394. T. Miura, et al., In vitro selection of macrocyclic peptide inhibitors containing cyclic γ2,4-amino acids targeting the SARS-CoV-2 main protease, *Nat. Chem.*, 2023, **15**, 998–1005.
395. T. Miura, et al., Cyclic β2,3-amino acids improve the serum stability of macrocyclic peptide inhibitors targeting the SARS-CoV-2 main protease, *Bull. Chem. Soc. Jpn.*, 2024, **97**, uoae018.
396. Y. Tan, et al., De Novo Discovery of a Noncovalent Cell-Penetrating Bicyclic Peptide Inhibitor Targeting SARS-CoV-2 Main Protease, *J. Med. Chem.*, 2024, **67**, 20258–20274.

397. K. Harrison, et al., Exploiting Hydrophobic Amino Acid Scanning to Develop Cyclic Peptide Inhibitors of the SARS-CoV-2 Main Protease with Antiviral Activity, *Chem. Eur. J*, 2024, **30**, e202401606.
398. J. Johansen-Leete, et al., Antiviral cyclic peptides targeting the main protease of SARS-CoV-2, *Chem. Sci.*, 2022, **13**, 3826–3836.
399. A. Aljoundi, et al., Covalent Versus Non-covalent Enzyme Inhibition: Which Route Should We Take? A Justification of the Good and Bad from Molecular Modelling Perspective, *Protein J.*, 2020, **39**, 97–105.
400. S. Iketani, et al., Multiple pathways for SARS-CoV-2 resistance to nirmatrelvir, *Nature*, 2023, **613**, 558–564.
401. M. Kiso, et al., In vitro and in vivo characterization of SARS-CoV-2 resistance to ensitrelvir, *Nat. Commun.*, 2023, **14**, 4231.
402. J. D. Ip, et al., Global prevalence of SARS-CoV-2 3CL protease mutations associated with nirmatrelvir or ensitrelvir resistance, *eBioMedicine*, 2023, **91**, 104559.

Chapter 2. C6-Alkoxy substituted penicillins inhibit SARS-CoV-2 M^{pro} via a non-covalent mechanism

2.1 Chapter overview

Chapter 2 describes the synthesis of C6-alkoxy substituted penicillins and their evaluation as SARS-CoV-2 main protease (M^{pro}) inhibitors. Penicillin V derivatives have been previously reported to inhibit M^{pro} by reacting covalently with the active site Cys145 to give stable acyl-enzyme complexes. By contrast, the work presented in this Chapter shows that the introduction of a C6-alkoxy group on the penam scaffold alters the mechanism of inhibition. Combined mass spectrometric (MS) and computational analyses indicate that most C6-alkoxy penicillin derivatives bind non-covalently at the M^{pro} active site, resulting in potent, substrate-competitive inhibition. Modelling studies revealed that C6-alkoxy substitution increases the distance between the electrophilic β-lactam carbonyl and the Cys145 thiolate, thus disfavouring covalent adduct formation. Additionally, a C6-methoxypenicillin G derivative emerged as a compound of interest, not only because of its potency, but also because protein-observed MS assay results indicated that inhibition might occur via a mechanism other than β-lactam ring opening and formation of a stable acyl-enzyme complex.

Manuscript I

At the time of writing this thesis, Manuscript I was accepted for publication in *RSC Medicinal Chemistry*. A Statement of Authorship is appended at the end of the chapter. The synthetic experimental details and spectra of the compounds prepared can be found in the **Appendix**.

Muntean, **D.-G.**; Treyde, W.; Kinena, L.; Salah, E.; Choudhry, H.; Duarte, F.; Brewitz, L.; Schofield, C.J.: **C6-Alkoxy substituted penicillins are potent non-covalently binding inhibitors of the SARS-CoV-2 main protease**

2.2 Manuscript I: C6-Alkoxy substituted penicillins are potent non-covalently binding inhibitors of the SARS-CoV-2 main protease

2.2.1 Abstract

Inhibition of the SARS-CoV-2 main protease (M^{pro}) by small-molecules is a validated strategy for COVID-19 treatment. There is a need for improved M^{pro} inhibitors, including because M^{pro} mutations can confer resistance to clinically used M^{pro} inhibitors. Previous work has revealed the potential of penicillin derivatives as covalently reacting M^{pro} inhibitors. Here we report studies on M^{pro} inhibition by C6-alkoxy substituted penicillin derivatives. The combined mass spectrometric and computational evidence imply most of the tested penicillin C6-alkoxy derivatives bind via non-covalent interactions at the M^{pro} active site, resulting in potent substrate-competitive inhibition. Some penicillin C6-alkoxy derivatives ((*R*)-, but not (*S*)- sulfoxides) manifest covalent reaction to different extents. Penicillins and related drugs are widely used antibiotics, acting via covalent reaction of their β-lactam with a nucleophilic serine in their transpeptidase targets to give an acyl-enzyme complex. The results imply penicillin derivatives can be developed to inhibit enzymes via mechanisms other than formation of stable acyl-enzyme complexes.

Key words: SARS-CoV-2 main protease; M^{pro}; $3CL^{pro}$; nucleophilic cysteine / serine protease inhibition; covalent / non-covalent enzyme inhibition; β-lactam; transition state analogue; penicillin antibiotics; COVID-19.

2.2.2 Introduction

Small-molecule inhibitors of the severe acute respiratory syndrome coronavirus-2 (SARS-CoV-2) main protease (M^{pro}) have helped to overcome the coronavirus disease 2019 (COVID-19) pandemic.[1-3] M^{pro} is a nucleophilic cysteine protease that catalyses hydrolysis of the viral polyproteins 1a and 1ab (pp1a/1ab) to give non-structural proteins; inhibiting M^{pro} catalysis disrupts viral replication.[2-5] Nirmatrelvir[6] (**Figure 1A**) was the first M^{pro} inhibitor to be widely used in the clinic – it inhibits M^{pro} through reversible covalent reaction of its nitrile group with the nucleophilic cysteine (Cys145). Several derivatives of nirmatrelvir are also clinically used,[7, 8] but to date only one non-covalently binding M^{pro} inhibitor, ensitrelvir[9] (**Figure 1B**), has been developed for clinical use. Multiple other M^{pro} inhibitor scaffolds have also been investigated,[2, 3, 10, 11] including for inhibiting by irreversible covalent reaction,[12-16] and tight, non-covalent binding to M^{pro}.[11, 17-24]

There is growing interest in the development of improved M^{pro} inhibitors[25-29] in part because evidence suggests that variations in the M^{pro} active site can confer resistance against clinically used M^{pro} inhibitors.[30-35] Also, the clinical scope of nirmatrelvir is limited, as it requires co-administration with ritonavir in order to limit metabolic degradation.[6] The second-generation investigational M^{pro} inhibitor ibuzatrelvir (PF-07817883; **Figure 1C**) has improved metabolic stability compared to nirmatrelvir and does not require co-administration with ritonavir.[28, 29] Other factors to consider in the development of improved M^{pro} inhibitors that may be used on a large scale in a future pandemic include the cost of production (in part to facilitate global use), the need for sustainable synthesis, and environmental impacts.

Since their clinical introduction, penicillins and subsequent generations of β-lactam antibiotics became and, despite the emergence of widespread resistance, continue to be the most extensively

used class of antibacterials.[36, 37] Their effectiveness, proven safety profiles, affordable manufacturing,[38] and rapid environmental degradation due to the reactive nature of the β-lactam ring,[39, 40] foster their continued use. Considering the distinctive reactivity profile of the β-lactam drugs from an antimicrobial perspective, we developed a mass spectrometry (MS)-based screen for M^{pro} inhibitors at the onset of the COVID-19 pandemic, investigating β-lactams and related antimicrobial compounds.[41-44]

MS and crystallographic analyses showed that M^{pro} Cys145 covalently reacts with the β-lactam group of some penicillin V derivatives (*e.g.*, **1**; **Figure 1D-E**) to give stable acyl-enzyme complexes resulting in M^{pro} inhibition.[41, 42] By contrast, the results of these studies also suggested that a penicillin G derivative with a methoxy substituent at the C6 position (**2**, **Figure 1F**) apparently inhibited via non-covalent binding to M^{pro}.[41] This was an interesting observation, as it is known that the introduction of a C6-methoxy group onto the penicillin scaffold or of a C7-methoxy group onto the cephalosporin scaffold can alter the stability and conformations of the acyl-enzyme adducts formed when reacting with their transpeptidase targets and nucleophilic serine β-lactamases (**Supporting Figure S1**).[45, 46, 47]

Here we report a structure-activity relationship (SAR) analysis and computational studies on C6-alkoxy penicillins, which provide insights into their mechanism of SARS-CoV-2 M^{pro} inhibition. The results imply that most C6-alkoxy penicillins inhibit M^{pro} through non-covalent binding at the active site, suggesting that this inhibition mode should also be considered when investigating the effects of related β-lactams on other nucleophilic enzymes beyond M^{pro}.

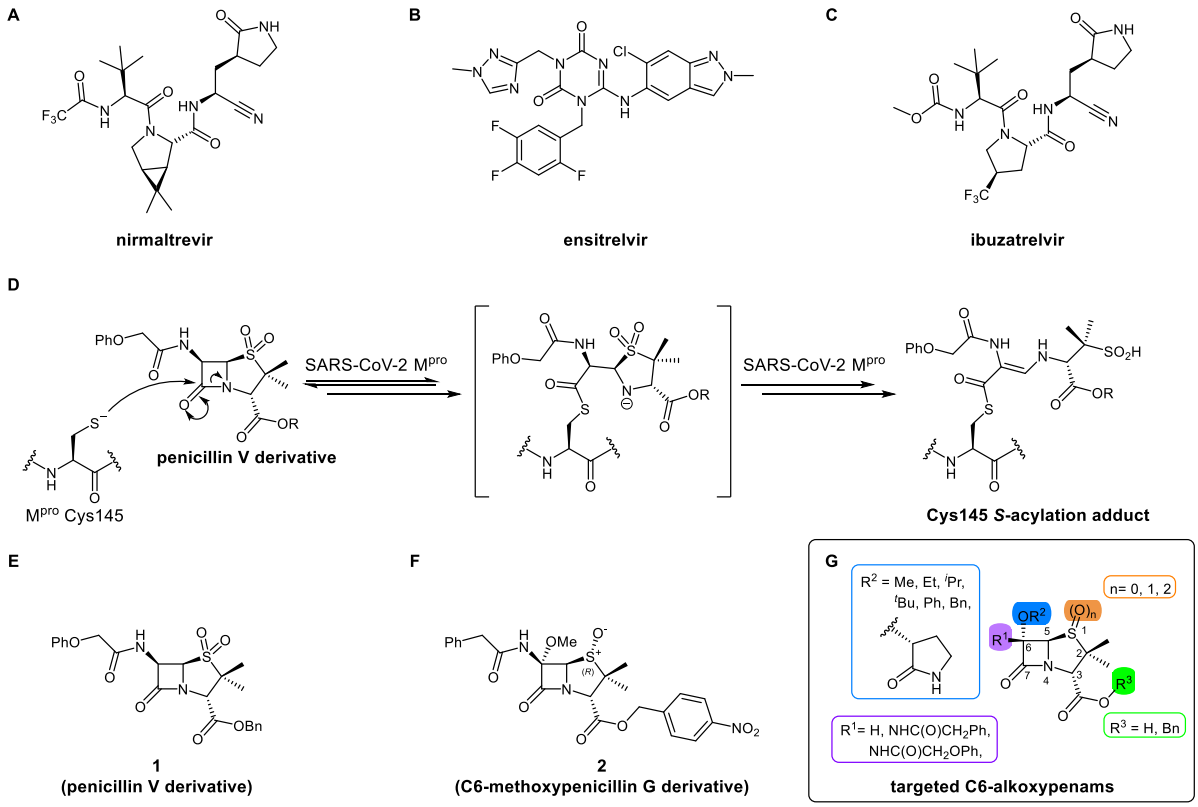

Figure 1. SARS-CoV-2 M^{pro} inhibitors. (**A**) Nirmatrelvir;[6] (**B**) ensiltrevir;[9] (**C**) ibuzaltrevir;[28] (**D**) mechanism of covalent modification of M^{pro} Cys145 by penicillin V sulfone esters;[41, 42] (**E**) penicillin V sulfone derivative (**1**);[41, 42] (**F**) C6-methoxy penicillin G (*R*)-sulfoxide derivative (**2**);[41] (**G**) penicillin C6-alkoxy derivatives investigated for M^{pro} inhibition in this work.

2.2.3 Results

Computational studies suggest stable non-covalent binding of C6-methoxy penicillins to the M^{pro} active site.

To explore how C6-alkoxy substitutions influence penicillin binding at the M^{pro} active site, we initially conducted docking studies and molecular dynamics (MD) simulations. Specifically, we compared the binding of C6 unsubstituted penicillin V sulfone benzyl ester **1** with the C6-methoxy penicillin G (*R*)-sulfoxide derivative **3**, which is the benzyl ester analogue of the initial hit **2** (**Figure 2C**). This comparison maintains consistency in terms of C3 substitution, as previous

structure-activity relationship studies indicate that C3 modifications have minimal impact on inhibition potency.[42]

The MD simulations show a distinct binding mode for **1** within the active site. The C6-phenoxyacetamido substituent positions itself in the S1 pocket, and the benzyl ester group occupies the S2 pocket (**Figure 2A**). This binding mode differs from that of nirmatrelvir, for which crystal structures show that it interacts with the S1, S2, S3 and S4 pockets (**Supporting Figure S2A**). It also differs from the crystallographically observed structure of the covalently bound product of **4** (**Figure 2D**), a derivative of **1**, where the C6-phenoxyacetamido substituent binds to the S2 pocket (**Supporting Figure S2B**). Despite these differences, MD simulations indicate that **1** is well positioned for covalent reaction with Cys145 (**Figure 2A**), as evidenced by a S(Cys145)-C(O)(β-lactam) distance of 4.8 Å ± 1.5 Å and a Bürgi-Dunitz angle of 97° ± 24° (mean ± standard deviation (SD); across three replicates; **Supporting Figure S5A**), consistent with MS evidence.[41, 42 42] The simulations also show hydrogen bond interactions between the C6 amido NH group of **1** and the *pro-S* sulfone oxygen, potentially promoting a conformation conductive to M^{pro} binding.

Modelling of **3,** which contains a C6-methoxy group, suggests a binding mode similar to **1**, with the C6-methoxy group occupying the S1 pocket (**Figure 2B**, **Supporting Figure S3)**. While additional hydrogen interactions with Ser144 and Glu166 are observed, the interaction with His163 is lost and the average S(Cys145)-C(O)(β-lactam) distance increases to 6.9 Å ± 1.7 Å, suggesting a binding mode that is not productive for covalent reaction (**Supporting Figure S5B**). Overall, these results suggest that C6-alkoxy substitution may hinder proximity of Cys145 to the β-lactam ring in a manner that is not suitable for nucleophilic attack by Cys145 but allows for a stable, non-covalent binding mode involving hydrogen bonding interactions.

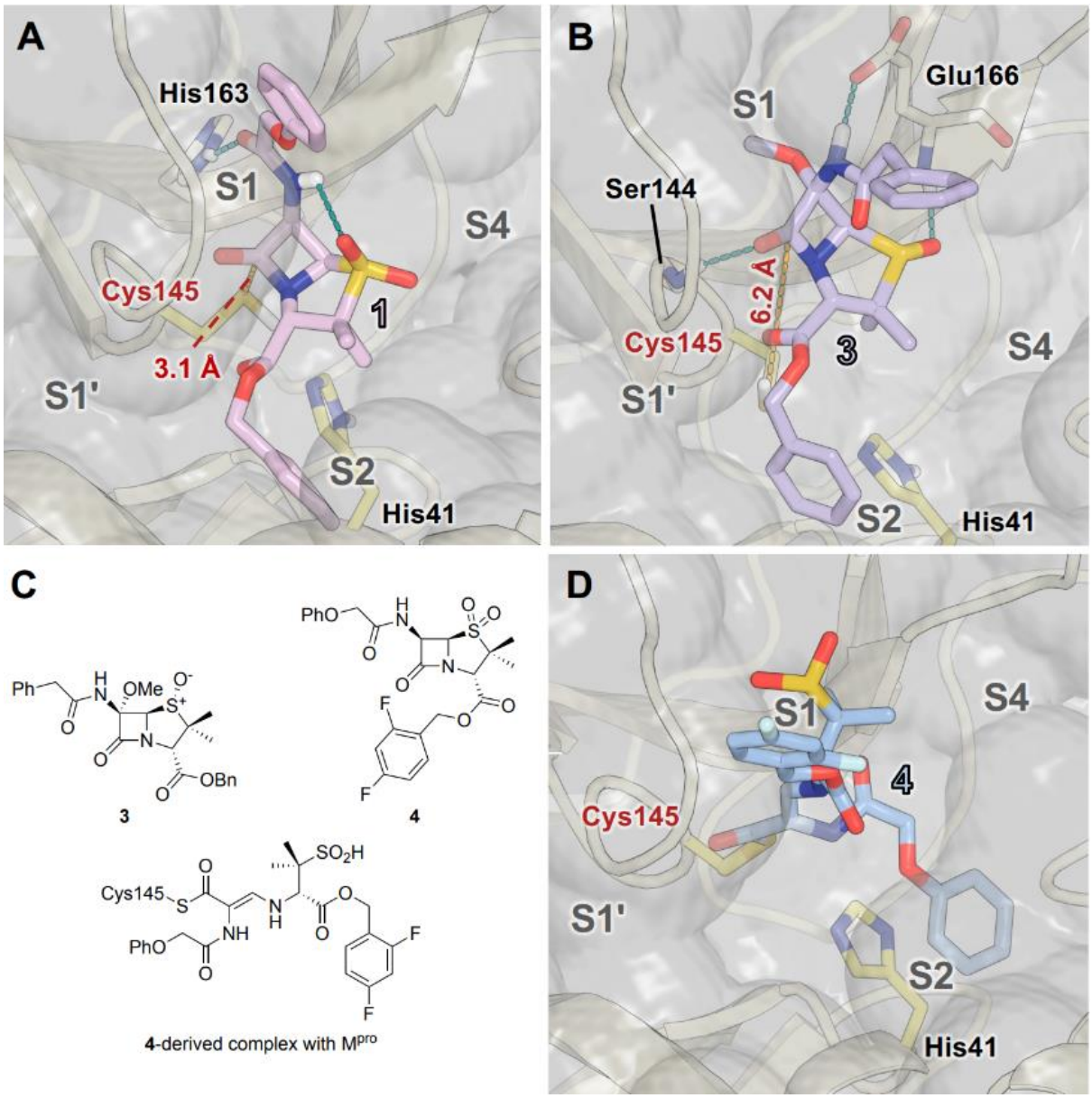

Figure 2: Modelling studies predict the penicillin C6-methoxy group may impair covalent reaction with M^{pro}. (**A** and **B**) Representative structures of (**A**) M^{pro}:**1** and (**B**) M^{pro}:**3** complexes from cluster analysis of 3x100 ns MD simulations. The C6-amido and C3-ester groups of **1** occupy the M^{pro} S1 and S2 pockets, respectively. **1** is predicted to interact with His163 and to form an intramolecular hydrogen bond involving its C6 amide NH and the *pro*-R sulfone O. The C6-methoxy group of **3** is predicted to bind in the S1 pocket. **3** is predicted to interact with Ser144 and Glu166. (**C**) Penicillin G derivative **3**, penicillin V derivative **4**, and the structure of **4** following covalent reaction with M^{pro}. (**D**) Crystal structure view of the complex formed following covalent reaction of **4** with M^{pro} (PDB ID: 7Z59).[42] The S(Cys145)-C(O)(β-lactam) distance for this representative snapshot is in red (dashed yellow lines), with average values from MD simulations provided in **Supporting Figure S5**. Atoms are coloured by element (N: blue, O: red, S:

yellow, F: cyan, H: white), with carbon atoms coloured differently for each penicillin derivative. Active site His41 and Cys145 side chain C atoms are in bright yellow; C atoms of other residues are in pale yellow.

C6-Methoxy penicillin V derivatives inhibit M^{pro} via non-covalent binding

Building on these results, a set of penicillin V C6-methoxy derivatives were synthesised in 3-4 steps from penicillin V to investigate whether the presence of a C6-methoxy group affects the mechanism of M^{pro} inhibition as predicted by the modelling studies (**Figure 3**). Thus, penicillin V was alkylated using benzyl bromide to give the reported ester **5**,[42] which was oxidized using *meta*-chloroperbenzoic acid (mCPBA) to give the corresponding (*S*)-sulfoxide **6** or sulfone **1**, depending on the stoichiometry of the reaction. Conversion of the (*S*)-sulfoxide **6** to the C6-methoxy derivative **7** was achieved in 45% yield employing a variation of a reported protocol that used *tert*-butyl hypochlorite (^{t}BuOCl) and LiOMe solution in methanol (1 M) at -30 °C.[48] The (*S*)-sulfoxide **7** was efficiently reduced to the thioether **8** using KI/AcCl (99% yield)[49] or oxidized to the sulfone **9** using mCPBA (65% yield).

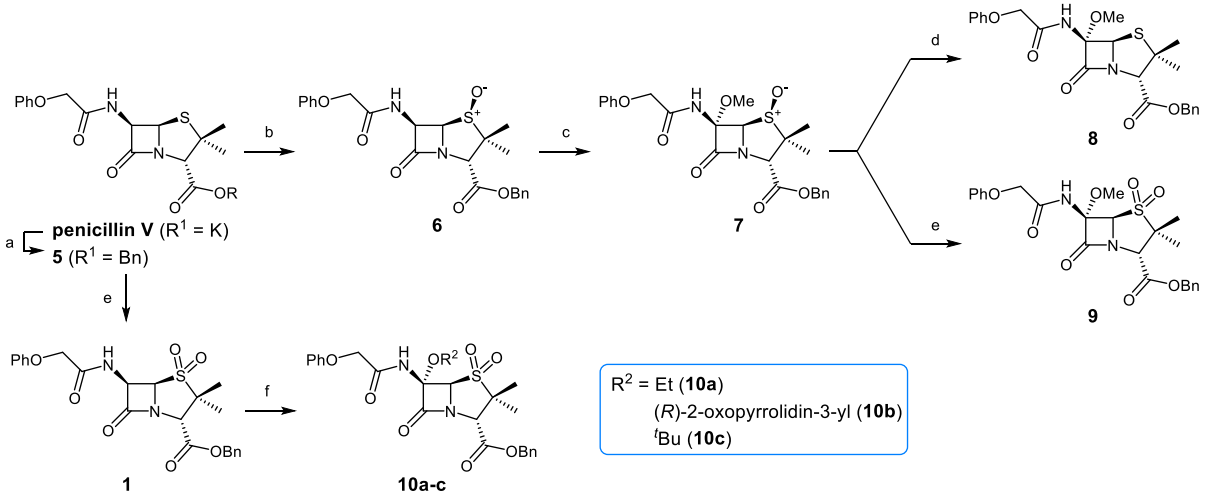

Figure 3. Synthesis of C6-methoxypenicillin V derivatives. Reagents and conditions: a) BnBr (1.1 equiv.), *N,N*-dimethylformamide, rt, 18 h, 82%; b) mCPBA (1.1 equiv.), CH_2Cl_2, 0°C to rt, 4 h, 72%; c) ^{t}BuOCl (1.5 equiv.), LiOMe solution in MeOH (1 M; 1.1 equiv.), CH_2Cl_2, -30 °C, 1 h, 54%; d) KI (18 equiv.), AcCl (7 equiv.), *N.N*-dimethylformamide, 0°C, 1 h, 99%; e) mCPBA (2-2.5 equiv.), CH_2Cl_2, rt, 16 h, 39-65%; f) ^{t}BuOCl (1.5 equiv.), base

(EtONa or Et_3N; 1.1 equiv.), ROH (EtOH or (*R*)-3-hydroxypyrrolidin-2-one; 6-10 equiv.), CH_2Cl_2, - 30 °C, 1 h, 7-35%.

Table 1. Effects of penicillin V derivatives on SARS-CoV-2 M^{pro} catalysis.

	Penicillin derivative	[(a)]IC_{50} [μM]		Penicillin derivative	[(a)]IC_{50} [μM]
i	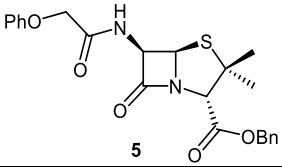 **5**	>50 (reported[42]: >50)	vi	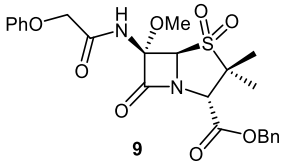 **9**	>50
ii	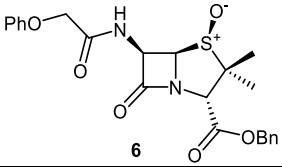 **6**	6.3 ± 1.0 (reported[42]: ~23)	vii	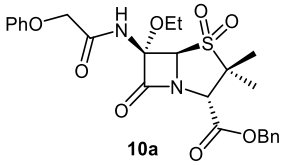 **10a**	5.8 ± 1.9
iii	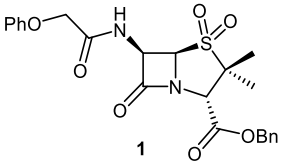 **1**	2.9 ± 0.4 (reported[42]: ~6.6)	vii i	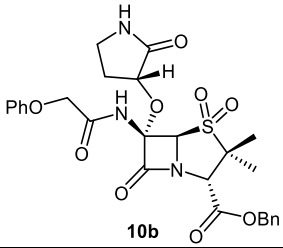 **10b**	5.3 ±1.6
iv	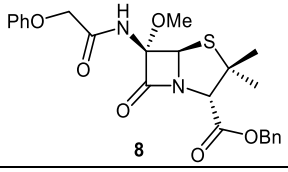 **8**	>50	ix	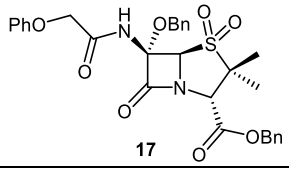 **17**	8.3 ± 2.6
v	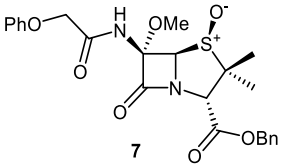 **7**	2.3 ± 0.3	x	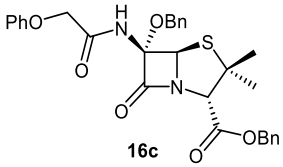 **16c**	>50

[(a)] M^{pro} inhibition assays were performed using SPE-MS as reported,[12, 41] utilizing SARS-CoV-2 M^{pro} (0.05 μM) and substrate (2.0 μM). Results are means of three independent experiments (n = 3; mean ± SD), each in technical duplicates. Representative dose-response curves are shown in **Supporting Figure S8**. Bn: $–CH_2Ph$.

The effects of the C6-methoxy penicillin V derivatives **7**-**9** on M^{pro} catalysis were investigated using reported solid phase extraction coupled to mass spectrometry (SPE-MS) assays,[41] and compared to those of the corresponding penicillin V derivatives lacking the C6-methoxy substituent (**Table 1**). Analysis of the half-maximal inhibitory concentrations (IC_{50} values) reveals that increasing the thiazolidine sulfur oxidation state of the penicillin V derivatives from the sulfide **5** via the (*S*)-sulfoxide **6** to the sulfone **1** correlated with increased inhibition potency (Table 1,

entries i-iii), in accord with reported results.[42] Note that the IC_{50} for **6** differs from that reported, an observation which may reflect differences in assay conditions.[12, 41]

C6-Methoxy substitution substantially affected the inhibition profiles of the penicillin V derivatives (**Table 1**, entries iv-vi): addition of a C6-methoxy substituent to the penicillin V sulfone benzyl ester **1** ablated M^{pro} inhibition in the tested concentration range (**9**; $IC_{50} > 50$ μM; Table 1, entry vi), whereas its addition to the corresponding (*S*)-sulfoxide **6** did not alter potency within experimental error (**7**; $IC_{50} \sim 2.3$ μM; Table 1, entry v). Note that variable IC_{50} values were observed for the C6-methoxy penicillin V derivative **8**, the C6-methoxy analogue of **5**. Like **5**, **8** showed no inhibition in the tested concentration range in independent triplicates using freshly prepared DMSO stock solutions. However, additional replicates using premade DMSO stock solutions indicated moderate inhibition by **8** ($IC_{50} \sim 5.0$ μM), perhaps reflecting the limited stability of **8** in DMSO, with partial oxidation of **8** to the corresponding more potent (*S*)-sulfoxide inhibitor **7** possibly accounting for the observed discrepancies. This proposal is in accord with observations that penicillin derivatives degrade gradually in DMSO, potentially compromising the reproducibility. Alternatively, the mode of inhibition (see below) may influence reproducibility for penicillin derivatives with relatively low inhibitory potency ($IC_{50} > 10$ μM).

Protein-observed MS studies were performed to test for covalent reaction of the penicillin V derivatives investigated in this study with M^{pro} under denaturing conditions.[41] The penicillin V derivatives were incubated with M^{pro} (5:1 ratio) for >15 h prior to analysis by MS (**Figure 4**). The results reveal that, in accord with the predicted binding modes of β-lactams **1** and **3** (**Figure 2**) and reported results on their reactivity with SARS-CoV-2 M^{pro},[41, 42] the introduction of a C6-methoxy

substituent onto the penicillin V scaffold prevents efficient covalent reaction with M^{pro} (**Figures 4A** and **4B**).

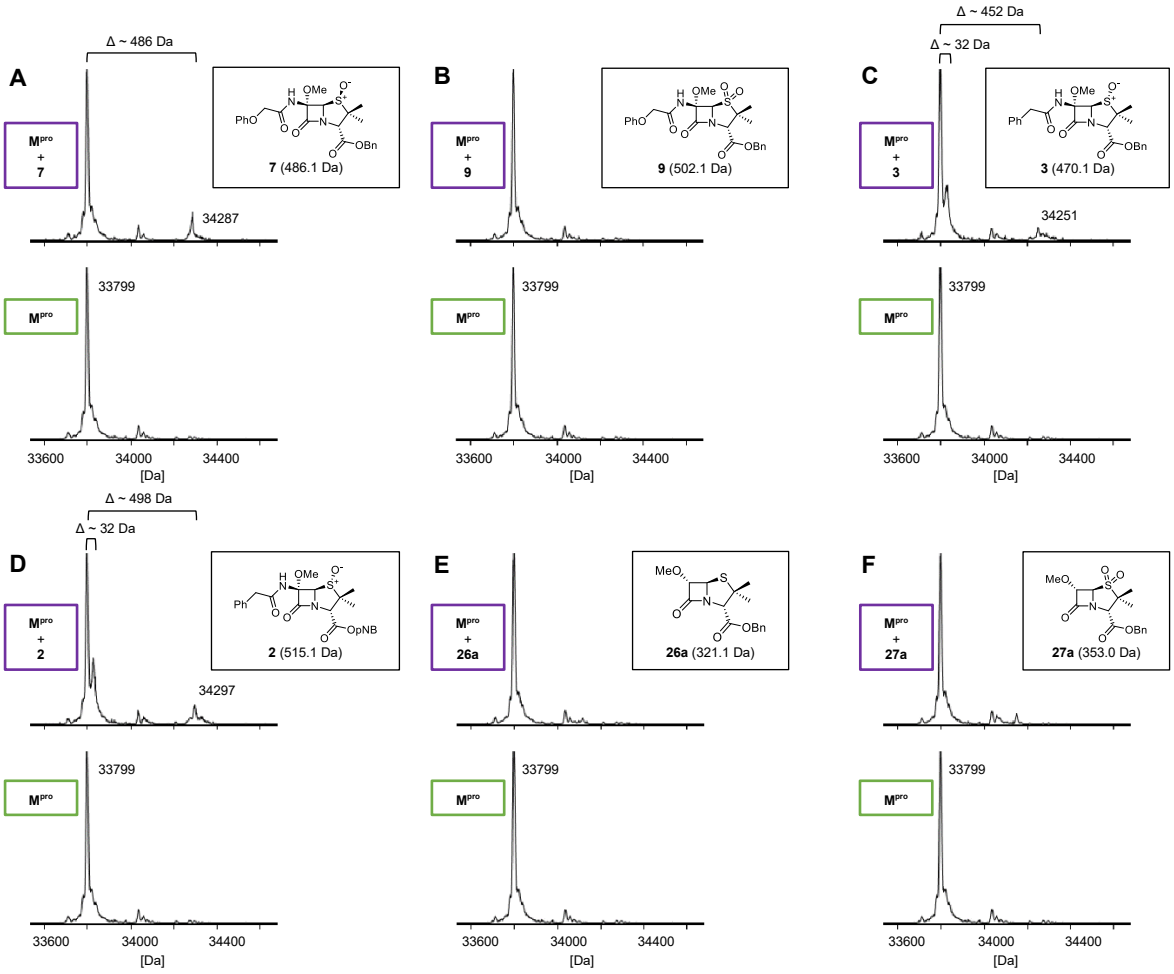

Figure 4: Reaction of C6-methoxy penams with isolated recombinant M^{pro}. Analysis of M^{pro} reactions with C6-methoxy penam derivatives: (**A**) **7**, (**B**) **9**, (**C**) **3**, (**D**) **2**, (**E**) **26a**, (**F**) **27a** prior (bottom) and after >15 h of incubation (top) with the respective β-lactam. Assays were performed using SPE-MS as reported,[41] employing SARS-CoV-2 M^{pro} (3.0 μM) and, if appropriate, a β-lactam (15 μM) in buffer (20 mM HEPES, pH 7.5). Representative spectra of technical duplicates are shown. Protein-observed mass spectra for other tested β-lactams are in **Supporting Figure S9**. Note that in no case were substantial amounts of species corresponding to covalent modification observed, suggesting inhibition by these compounds is (at least, principally) via non-covalent binding; in the cases of **2** and **3** low levels of species with mass shifts corresponding to potential acyl-enzyme species were observed.

The nature of the penam C6-alkoxy substituent affects inhibition potency

C6-Alkoxy derivatives of penicillin V were synthesised to investigate the effects of C6 substituents other than methoxy groups on M^{pro} inhibition potency and mechanism. The synthesis of the C6-ethoxy penicillin V sulfone derivative **10a** was achieved from **1** in 35% yield by substituting LiOMe/MeOH for NaOEt/EtOH (**Figure 3**). Notably, this route simplifies reported syntheses of **10a** that employed more steps and/or undesirable, potentially toxic reagents.[50, 51] Similarly, the secondary alcohol (*R*)-3-hydroxypyrrolidin-2-one was employed to synthesize **10b** in 6% yield from **1** under slightly modified conditions, with triethylamine as the base; the γ-lactam group was introduced to possibly mimic the interactions of the nirmatrelvir γ-lactam group with the M^{pro} S1 pocket.[6]

Attempts to convert **1** to the corresponding C6-*tert*-butoxy derivative **10c** using LiO^{t}Bu/^{t}BuOH failed, perhaps reflecting the increased steric bulk of *tert*-butoxide, an observation which reveals the limitation of this method for preparation of C6-alkoxy penicillins. An alternative route to C6-*tert*-butoxy penicillin derivatives via imine **13** was trialled (**Figure 5**); **13** is a reported intermediate in the synthesis of related C6-alkoxy and C6-formamido penicillins.[52, 53] However, imine **13** and related reaction intermediates were unstable/challenging to purify, resulting in poor reproducibility. Although the C6-benzyloxy penicillin **16c** was obtained (12% yield from **12** over 4 steps) via this route, the corresponding C6-ethoxy and C6-*iso*-propoxy derivatives **16a** and **16b** were obtained in <1% yield, while the C6-*tert*-butoxy derivative **16d** could not be obtained; **16c** was converted to the corresponding C6-benzyloxy penicillin V sulfone benzyl ester **17** using mCPBA.

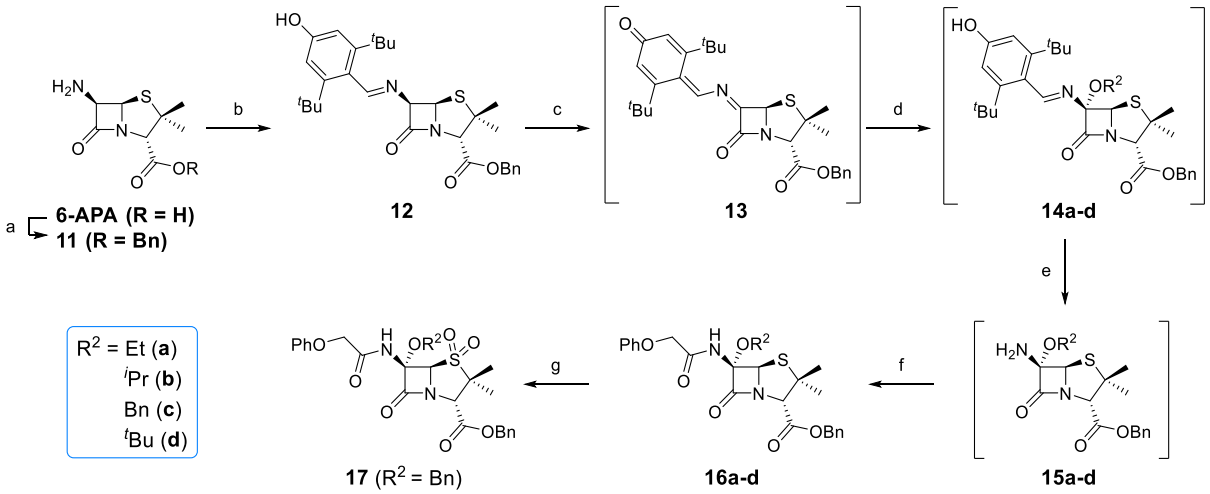

Figure 5. Synthesis of C6-alkoxy penicillin V derivatives. Reagents and conditions: a) BnBr (1.1 equiv.), Et_3N (1.1 equiv.), acetone, 0°C, 4 h, 33%; b) 3,5-di-*tert*-butyl-4-hydroxy-benzaldehyde,[52] benzene, reflux, 1 h; c) 2,3-dichloro-5,6-dicyano-1,4-benzoquinone[52] (0.9 equiv.), CH_2Cl_2, rt, 1 h; d) ROH (10 equiv.), CH_2Cl_2, rt, 21 h; e) trimethylacetohydrazideammonium chloride (0.8 equiv.),[52] MeOH, CH_2Cl_2, rt, 3 h; f) $PhOCH_2Cl_2$ (5 equiv.), Et_3N (7 equiv.), CH_2Cl_2, rt, 16 h, 1-12% (4 steps); g) mCPBA (2.2 equiv.), CH_2Cl_2, 0-10 °C, 1 h, 21%.

SPE-MS assay results revealed that C6-alkoxy penicillin substituents which were sterically bulkier than a methoxy group restored M^{pro} inhibition compared to the inactive C6-methoxy penicillin sulfone derivative **17** (**Table 1**, entries vii-ix). The C6-ethoxy (**10a**), C6-benzyloxy (**17**), and C6-alkoxy **10b** penicillin sulfones manifested similar levels of M^{pro} inhibition (**Table 1**, entries vii-ix), whereas the C6-benzyloxy penicillin V sulfide **16c**, like **9**, was inactive. SPE-MS assays revealed that none of the penicillin V derivatives bearing C6-alkoxy substituents covalently reacted, at least efficiently, with M^{pro} (**Supporting Figure S9**). The low levels of reaction observed in some cases (*e.g.*, **7**; **Figure 4A**) may reflect non-selective reaction with one or more of the 12 cysteine residues in M^{pro}.[41, 43]

MD simulations showed that changing the S-oxidation state, *e.g.*, to a sulfoxide (**7**), or increasing the steric bulk of the C6-alkoxy substituent beyond methoxide, *e.g.*, to the ethoxy (**10a**), benzyloxy (**17**), and γ-lactam bearing C6-ether (**10b**) alters the binding mode at the M^{pro} active site (**Figure**

6A-D), which helps explain differences in the observed IC_{50} values. While for **3**, the C6-methoxy group binds to the S1 pocket, the C6-methoxy group of **7** and the C6-ethoxy group of **10a** bind to the S1' pocket, whereas the C6-benzyloxy group of **17** binds to the S1 pocket. Importantly, however, none of these compounds are predicted to be oriented for productive covalent reaction with Cys145 (**Supporting Figure S6**), in accord with the MS assay results (**Figure 5**). Note that the modelled pose of **10b** involves binding of its γ-lactam moiety in the S1 pocket, in an analogous manner to the γ-lactam of nirmatrelvir (**Supporting Figure S4**).[6]

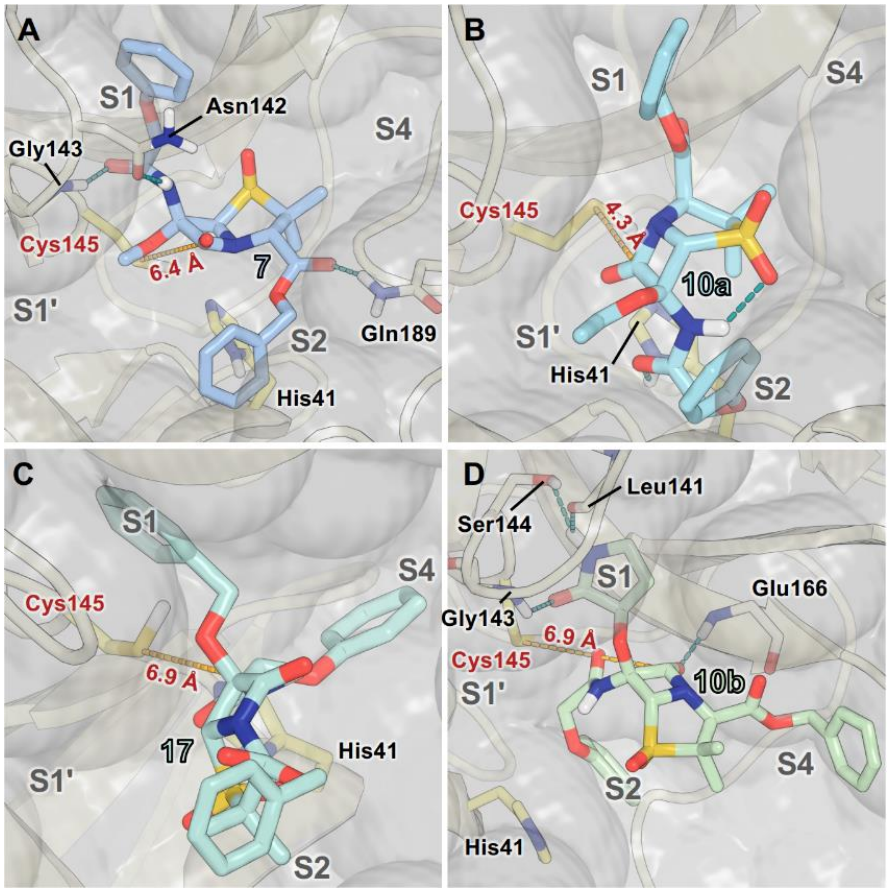

Figure 6: Representative M^{pro} binding modes of selected penicillin V derivatives from cluster analysis of 3x100 ns MD simulations. (**A**) The C6-amide and the C6-methoxy groups of penicillin V derivative **7** is predicted to occupy the S1 and S1′ pockets, respectively, with the C3-ester in the S2 pocket. **7** is predicted to hydrogen bonds with Asn142, Gly143, and Gln189. (**B**) The C6-amide group of penicillin V derivative **10a** is predicted to occupy the S2 pocket, while its C6-ethoxy and C3-ester groups might occupy the S1′ and S1 sites, respectively. **10a** is predicted to interact with His41 and to form an intramolecular hydrogen bond between its C6-amido N-H and the *pro-R*-sulfone O. (**C**)

The C6-benzyloxy group of penicillin V derivative **17** is predicted to occupy the S1 site and its C6-amide the S4 site. (**D**) The C6-γ-lactam group of penicillin V derivative **10b** is predicted to occupy the S1 pocket, its C6-amide the S2 pocket, and its C3 ester the S4 pocket. **10b** is predicted to hydrogen bond with Leu141, Gly143, Ser144, and Glu166. The S(Cys145)-C(O)(β-lactam) distance for this representative snapshot is in red (dashed yellow lines), with average values from MD simulations provided in **Supporting Figure S6**. Atoms are coloured by element (N: blue, O: red, S: yellow, F: cyan, H: white), with carbon atoms coloured differently for each penicillin derivative. Active site His41 and Cys145 side chain C atoms are in bright yellow; C atoms of other residues are in pale yellow.

C6-Methoxy penicillin G (*R*)-sulfoxide ester derivatives are potent M^{pro} inhibitors.

A set of C6-methoxy penicillin G derivatives was then synthesised to investigate the effects of the C6-phenylacetamido ether oxygen on M^{pro} inhibition, because previous studies have shown that both the position and the presence/absence of the C6 side chain oxygen can influence potency.[42] Modelling studies and reported work on penicillin V derivatives imply that the ester group does not substantially affect inhibition potency (**Figures 2A** and **2D**);[41, 42] therefore, penicillin G benzyl ester derivatives were synthesized for comparison with the penicillin V benzyl esters, following the synthesis of the corresponding C6-methoxy penicillin V derivatives (**Figure 7**). Penicillin G was alkylated to give the reported benzyl ester **18**,[54] which was oxidized using mCPBA to give sulfone **19** or (*S*)-sulfoxide **21**. The isomeric (*R*)-sulfoxide **23** was obtained from **18** in 22% yield by oxidation using ^{t}BuOCl[55] in the presence of 2,6-lutidine. C6-Methoxylation of penicillin G derivatives **19**, **21**, and **23** yielded penams **20**, **22**, and **3**, respectively, using ^{t}BuOCl and LiOMe in methanol (1 M) at -30 °C (36–54%). A related protocol enabled the direct conversion of penicillin G to the C6-methoxypenicillin G acid **24**, though in lower yield (18%). Subsequent alkylation of **24** gave ester **25** (49%).

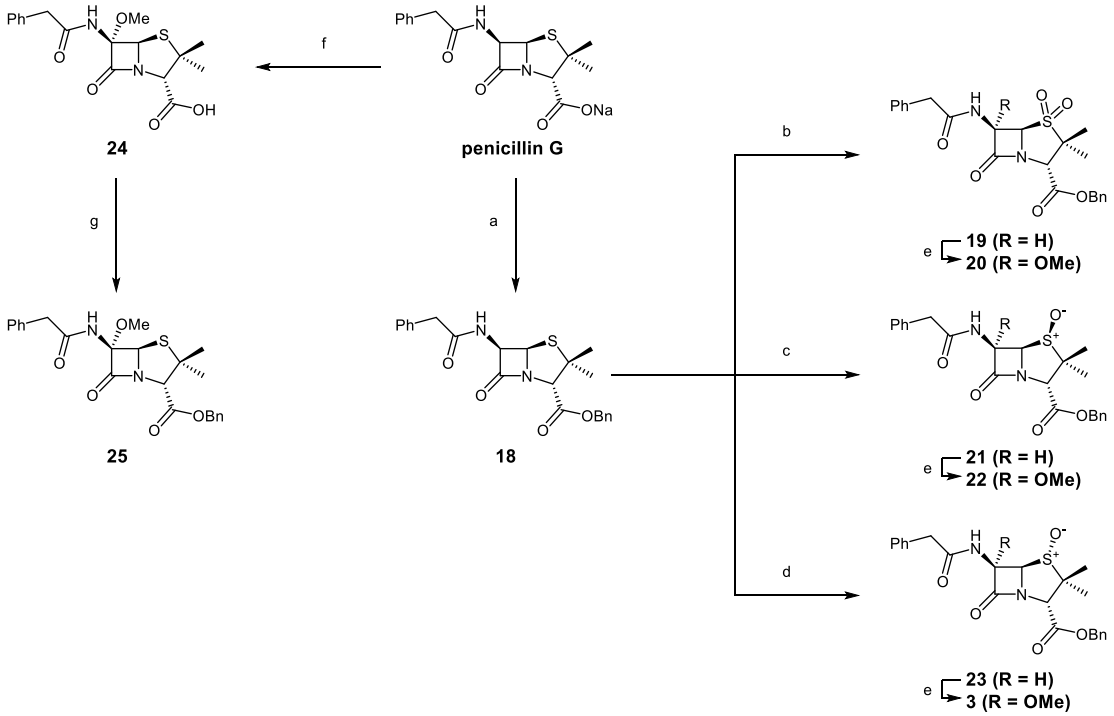

Figure 7. Synthesis of C6-methoxy penicillin G derivatives. Reagents and conditions: a) BnBr (1.2 equiv.), *N,N*-dimethylformamide, rt, 16 h, 84%; b) mCPBA (2.5 equiv.), CH_2Cl_2, 0 °C to rt, 16 h, 55%; c) mCPBA (1.1 equiv.), CH_2Cl_2, 0 °C, 1 h, 83%; d) 2,6-lutidine (2.4 equiv.), ^{t}BuOCl (1.1 equiv.), THF:H_2O (10:1), - 5 °C, 5 min, 22%; e) ^{t}BuOCl (1.5 equiv.), LiOMe (1 M in MeOH; 1.1 equiv.), CH_2Cl_2, -30 °C, 1 h, 36-54%; f) ^{t}BuOCl (1.5 equiv.), LiOMe (1 M in MeOH; 1.1 equiv.), *N,N*-dimethylformamide:MeOH (7:1), -78 °C, 15 min, 18%; g) BnBr (1.4 equiv.), $NaHCO_3$ (1.5 equiv.), *N,N*-dimethylformamide, rt, 16 h, 49%.

SPE-MS assays reveal that penicillin G derivatives without a C6-alkoxy group do not inhibit M^{pro} (**Table 2**, entries i-v), as reported,[41, 42] likely reflecting knowledge that the phenoxy oxygen atom is important in inhibition (**Figure 2**). By contrast, the corresponding penicillin G derivatives bearing a methoxy group at the C6 position inhibited M^{pro} (**Table 2**, entries vii-xi).

Table 2. Effects of penicillin G derivatives on SARS-CoV-2 M^{pro} catalysis.

	Penicillin G derivative	[(a)]IC_{50} [μM]		C6-Methoxy penicillin G derivative	[(a)]IC_{50} [μM]
i	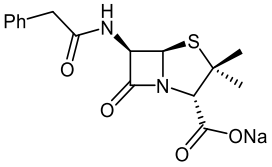 **penicillin G**	>50 (reported[41]: >50)	vii	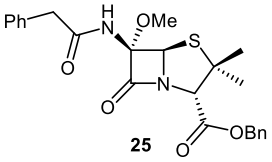 **25**	11 ± 6
ii	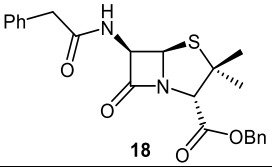 **18**	>50	viii	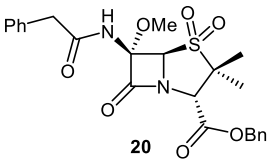 **20**	11 ± 4
iii	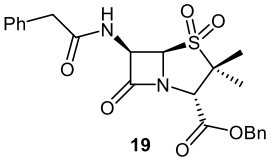 **19**	>50	ix	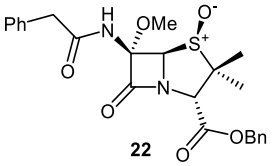 **22**	7.3 ± 6.5
iv	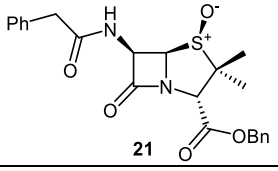 **21**	>50	x	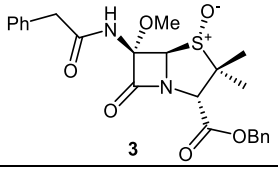 **3**	0.8 ± 0.1
v	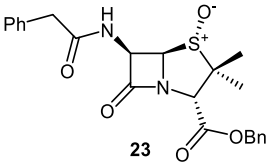 **23**	>50	xi	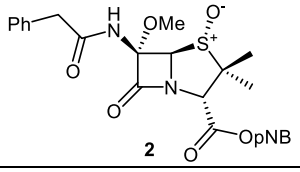 **2**	0.5 ± 0.1 (reported[41]: ~3.5)
vi	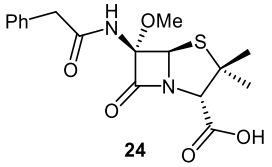 **24**	>50[(b)]			

[(a)] M^{pro} inhibition assays were performed using SPE-MS as reported,[12, 41] utilizing SARS-CoV-2 M^{pro} (0.05 μM) and substrate (2.0 μM). Results are means of three independent experiments (n = 3; mean ± SD), each in technical duplicates. [(b)] Representative dose-response curves are shown in **Supporting Figure S7**. Bn: $–CH_2Ph$; pNB: $–CH_2C_6H_4(4\text{-}NO_2)$.

The penam sulfide **25**, (*S*)-sulfoxide **22**, and sulfone **20** inhibited M^{pro} with similar potencies (**Table 2**, entries vii-ix), whereas the C6-methoxy (*R*)-sulfoxide penicillin G benzyl ester **3** inhibited M^{pro} ~9-fold more efficiently than its (*S*)-sulfoxide isomer **22** (IC_{50} ~ 0.8 and 7.3 μM, respectively; **Table 2**, entries x and ix). Note that variations in the IC_{50} values for the C6-methoxy penicillin G derivative **24** were observed (**Table 2**; entry vi), with moderate inhibition potency

being observed in some cases (IC_{50} = 15 ± 8 μM), possibly due to instability of **24** in DMSO, as also noted with **8** (see above).

Protein-observed MS studies showed that the tested penicillin G derivatives **2**, **3**, and **18-25** did not covalently modify M^{pro}, even after relatively long incubation times of >15 h (**Supporting Figure S9E-G**), consistent with the MD simulations indicating that penicillin C6-methoxy substituents increased the average distances between the β-lactam carbonyl and the Cys145 thiol (**Figure 2B**; **Supporting Figure S5B**).

Interestingly, the penicillin G (*R*)-sulfoxides **2** and **3** were both observed to covalently react with M^{pro} by SPE-MS; however, +515 Da and +470 Da mass shifts corresponding to acyl-enzyme complex formation were not observed with high intensity, even after >15 h incubation (**Figure 4C-D**). By contrast, concentration-dependent formation of a +32 Da M^{pro} adduct was observed with both **2** and **3** (**Supporting Figure S10**). The combined results indicate that the formation of the +32 Da M^{pro} adduct depended on the sulfoxide configuration, but apparently not (or at least to a lesser extent) on the nature of the penicillin ester. Note that re-analysis of the reported MS spectrum of the M^{pro} reaction with **2** also evidences for formation of a +32 Da adduct after >60 min, albeit at relatively low levels.[41]

To investigate the relevance of the +32 Da M^{pro} adduct to inhibition, we monitored the covalent reaction of the penicillin derivative **2** with M^{pro} over ~45 min using SPE-MS (**Figure 8**), because IC_{50} values were determined following 45 min incubations of M^{pro} with penicillin derivatives (**Tables 1** and **2**). A +515 Da mass shift of consistently weak intensity was observed (t = 0 min), corresponding to the mass of **2**. A +498 Da adduct of increasing intensity was formed within 15 min, likely corresponding to dehydrated **2** covalently attached to M^{pro}. After 45 min, low levels of a +32 Da adduct were visible. If the enhanced inhibition with the (*R*)-sulfoxides corresponds to

covalent reaction, it is likely not a result of the +32 Da species, but of the dehydrated +498 Da species which may, over time, convert to the +32 Da species (**Figures 8**, **Supporting Figure S10**). Note that the ~9-fold increases in M^{pro} inhibition potency for the (*R*)-sulfoxides **2** and **3** compared to the (*S*)-sulfoxide **22** apparently manifested in no evidence for covalent M^{pro} modification with the latter (**Supporting Figure S9F**).

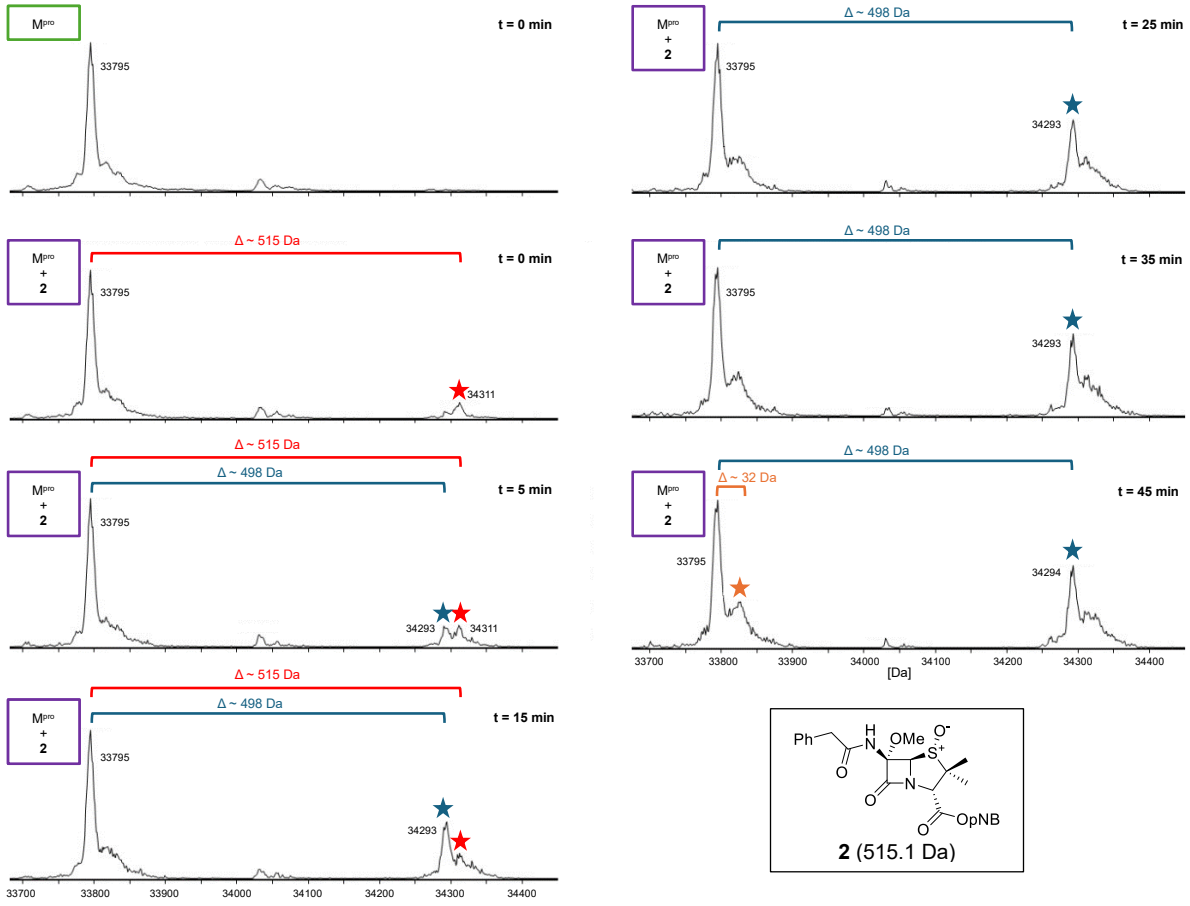

Figure 8: **Evidence for covalent reaction of M^{pro} with the C6-methoxy penicillin G (*R*)-sulfoxide derivative 2.** SPE-MS analysis showed initial formation of a +515 Da adduct (★) at low levels, followed by the time-dependant formation of a +498 Da adduct (★) (5:1 inhibitor:**M^{pro}** ratio; data obtained using a 10:1 inhibitor:**M^{pro}** ratio conditions is available in the Supporting Information (**Supporting Figure S11**). A possible low intensity +32 Da adduct (★) was also detected after 45 min incubation. pNB: $–CH_2C_6H_4(4\text{-}NO_2)$.

Effects of C6-alkoxy penam and sulbactam derivatives on M^{pro} inhibition

The effects of removing the C6-acetamido substituent of the C6-alkoxy penicillin sulfone derivatives on M^{pro} inhibition potency and reactivity were investigated. The mono-substituted C6-alkoxy penam sulfides **26a-f** were synthesized in two steps from penam **11** (15-37%), via stereospecific reactions of a C6-diazo penicillin intermediate with different alcohols in the presence of BF_3 etherate complex.[56, 57] Sulfides **26a-f** were oxidized to sulfones **27a-f** using mCPBA (**Figure 9**). The (*S*)-sulfoxides were not synthesized due to a lack of reported stereoselective methods to oxidize penams in the absence of a directing C6-amido substituent.

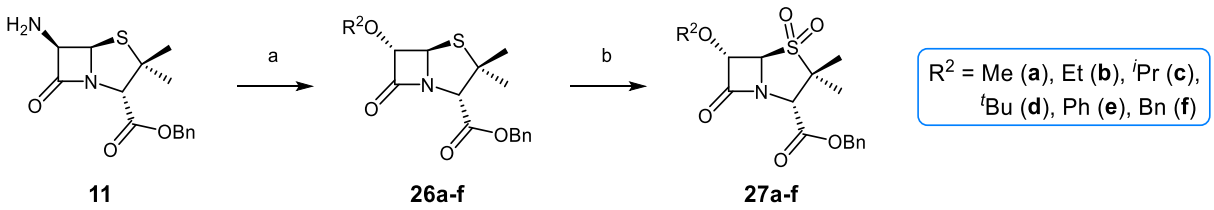

11 **26a-f** **27a-f**

Figure 9. Synthesis of monosubstituted C6-alkoxy penam derivatives. Reagents and conditions: a) i) $NaNO_2$ (2.6 equiv.), *para*-toluenesulfonic acid monohydrate (0.6 equiv.), CH_2Cl_2:H_2O (4:1), 0 ºC, 20 min; ii) ROH (1.6-110 equiv.), $BF_3{\cdot}O(C_2H_5)_2$ (0.1 equiv.), CH_2Cl_2, 20 ºC, 15 min, 15-37% (two steps); b) mCPBA (2.2 equiv.), CH_2Cl_2, 0 ºC to rt, 16 h, 28-77%.

SPE-MS assays indicate that C6-alkoxy substituted penams in the sulfide oxidation state (*i.e.*, **26a-f**) typically inhibited M^{pro} with higher potency than those in the sulfone oxidation state (**27a-f**) (**Table 3**). Penicillins bearing sterically less bulky and/or conformationally relatively flexible C6-alkoxy substituents, such as the C6-methoxy (**26a**), -ethoxy (**26b**), and -benzyloxy (**26f**) derivatives, showed higher inhibition (**Table 3**, entries i, ii, and vi, respectively) than those bearing bulky and rigid substituents (*i.e.*, derivatives **26c-e**; **Table 3**, entries iii-v).

Table 3. Effects of penicillin V derivatives without a C6 amido group on SARS-CoV-2 M^{pro} catalysis.

	C6-Alkoxy penam derivative	[(a)]IC_{50} [μM]		C6-alkoxy sulbactam derivative	[(a)]IC_{50} [μM]
i	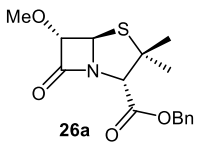 **26a**	1.2 ± 0.1	vii	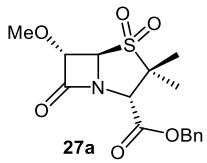 **27a**	7.7 ± 4.9
ii	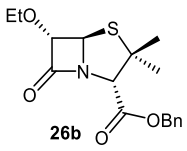 **26b**	0.8 ± 0.1	viii	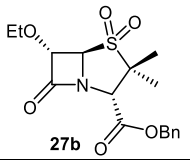 **27b**	44 ± 4
iii	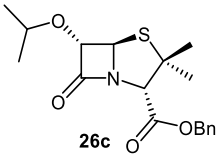 **26c**	47 ± 13	ix	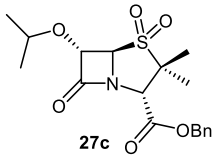 **27c**	19 ± 14
iv	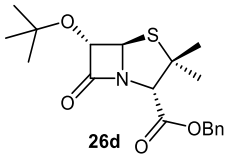 **26d**	39 ± 9	x	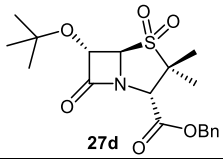 **27d**	21 ± 3
v	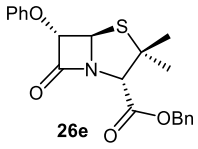 **26e**	>50	xi	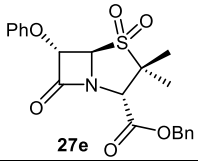 **27e**	>50
vi	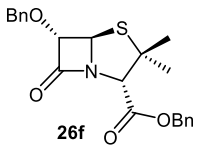 **26f**	7.3 ± 1.4	xii	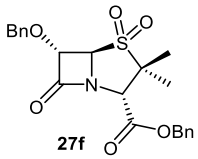 **27f**	35 ± 2

M^{pro} inhibition assays were performed using SPE-MS as reported,[12, 41] utilizing SARS-CoV-2 M^{pro} (0.05 μM) and substrate (2.0 μM). Results are means of three independent experiments (n = 3; mean ± SD), each in technical duplicates. Representative dose-response curves are shown in **Supporting Figure S7**. Bn: $–CH_2Ph$.

Modelling of **27a** at the M^{pro} active site predicted stable binding poses (**Figure 10A**), but with an average S(Cys145)-C(O)(β-lactam) distance of 9.0 Å (**Supporting Figure S7**), likely hindering covalent reaction with M^{pro}. In accord with the modelling predictions, SPE-MS analyses did not provide evidence for covalent reaction of the penam sulfides **26a-f** and sulfones **27a-f** with isolated M^{pro} (**Figures 4E-F** and **Supporting Figure S9H-O**). While the C6-methoxy and the C3-ester of **27a** are predicted to bind to the S1 and S2 pockets, respectively, the sulfone oxygens are predicted not to directly interact with M^{pro}, in agreement with the higher potency of the sulfide oxidation

state. Notably, the predicted pose of the C6-methoxy penam sulfide **26a** (**Figure 10B**) substantially differed from that of **27a**, suggesting that the observed lower potency of the sulfones **27a-f** relative to sulfides **26a-f** may arise from the adoption of distinct active site binding modes.

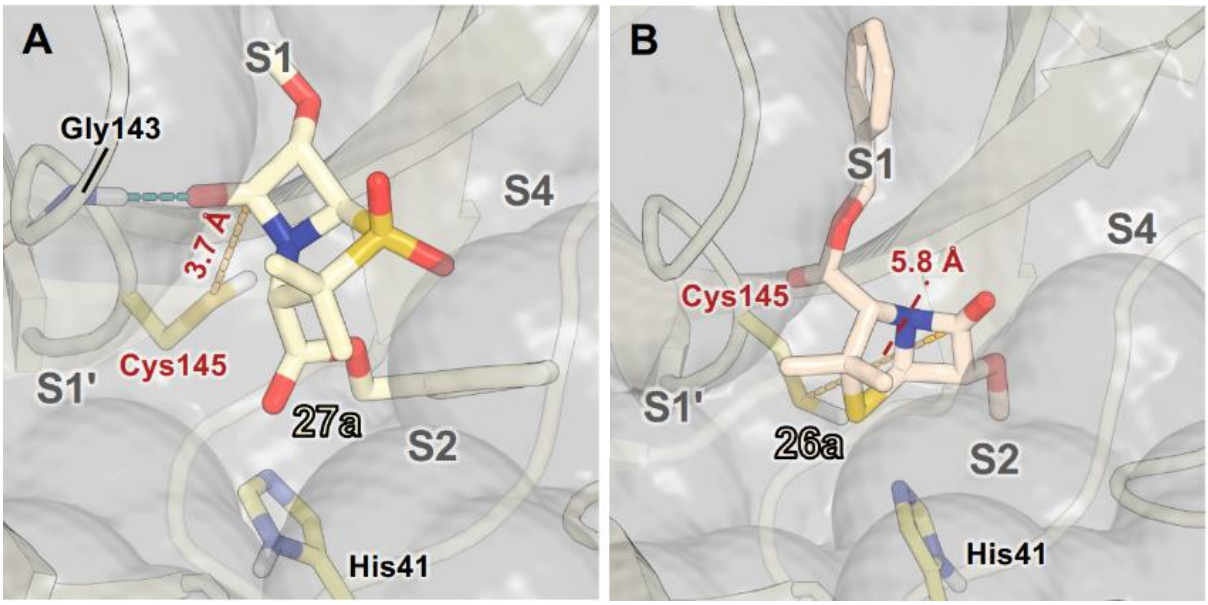

Figure 10: Representative poses of C6-methoxy penam sulfones with M^{pro} from cluster analysis of 3x100 ns MD simulations. (**A**) The C6-methoxy and the C3-ester groups of sulfone **27a** are predicted to occupy the M^{pro} S1 and S2 pockets, respectively, (**B**) while they are predicted to occupy the M^{pro} S2 and S1 pockets for sulfide **26a**. **27a** is predicted to interact with Gly143, whereas **26a** did not appear to form stable hydrogen bonds. The S(Cys145)-C(O)(β-lactam) distance for this representative snapshot is in red (dashed yellow lines), with average values from MD simulations provided in **Supporting Figure S7**. Atoms are coloured by element (N: blue, O: red, S: yellow, F: cyan, H: white), with carbon atoms coloured differently for each penicillin derivative. Active site His41 and Cys145 side chain C atoms are in bright yellow; C atoms of other residues are in pale yellow.

2.2.4 Discussion

β-Lactam antibiotics are widely used for treatment of bacterial infections.[40] There is extensive evidence with isolated enzymes and with cells that their antibacterial activity is a result of covalent reaction with a nucleophilic serine residue in bacterial transpeptidases, leading to formation of stable acyl–enzyme complexes via β-lactam ring opening with consequent inhibition of bacterial cell wall biosynthesis.[40, 58] The continued widespread use of β-lactam antibiotics is *inter alia*

threatened by resistance mediated by serine β-lactamases (SBLs), which are nucleophilic serine enzymes related to transpeptidases, but which catalyse β-lactam degradation via hydrolytically labile acyl-enzyme complexes.[37, 59]

Penicillins bearing a C6-methoxy substituent have been developed with the aim of countering antibiotic resistance by SBLs:[60-62] temocillin,[45] the clinically used C6-methoxy derivative of ticarcillin,[63] shows increased resistance towards SBL-catalysed β-lactam ring opening.[46, 64] The same strategy to provide β-lactam stabilization is also used with cephalosporin antibiotics (*i.e.*, cephamycins; **Supporting Figure S1**), which bear a C7-methoxy group (the penicillin C6-equivalent position).[40, 47, 65, 66] The precise reasons for the decreased SBL reactivity with penicillins/cephalosporins bearing a C6/C7-methoxy group are unclear, but may reflect that the increased steric hindrance adjacent to the β-lactam carbonyl group slows the rate of hydrolysis of the acyl-enzyme complex, possibly by blocking the access of the hydrolytic water to the acyl-enzyme carbonyl group.[46]

Although β-lactam antibiotics are best known for their covalent inhibition of bacterial transpeptidases, their inhibitory activity is not solely dictated by ring strain and electrophilicity. Their ability to mimic transition-state conformations during amide hydrolysis may also contribute to target binding and specificity.[58, 67, 68] In this light, appropriately substituted β-lactams have potential to act as competitive, non-covalent inhibitors of serine and cysteine proteases. Indeed, it cannot be entirely ruled out that some of the antibiotic activity of penicillins and other β-lactams results from non-covalent inhibition. Indeed, intact penicillins have been observed in complex with a bacterial transpeptidases when the enzymes were inactivated at the active site either by cross-linking or mutation.[69, 70] The proposal is precedented by the development of substituted

monocyclic β-lactams which engage with protein targets through non-covalent interactions, including *e.g.*, ezetimibe (**Supporting Figure S12A**).[71, 72] Furthermore, penicillins and cephalosporins with appropriately-substituted C6-amido sidechains (**Supporting Figure S12B**) are reported to inhibit the Speckle-type POZ protein (SPOP)[73] potentially via non-covalent binding that disrupts SPOP-substrate interactions.[74, 75]

As part of a wider search for potent SARS-CoV-2 antiviral agents, we and others have reported on the utility of β-lactams and related electrophiles for SARS-CoV-2 M^{pro} inhibition.[41, 42, 44, 76-78] Although our previous work focused on development of covalently reacting β-lactam M^{pro} inhibitors, we obtained preliminary evidence showing the potential of penicillin derivatives to inhibit M^{pro} via non-covalent binding at the active site.[41] The combined results described here indicate that apparently minor structural modification to the penicillin substitution pattern and sulfur oxidation state can affect not only M^{pro} inhibition potency, but also the mechanism by which penicillins inhibit M^{pro} (**Figures 2**, **4**, **6**, **8**, **10**).

Modelling and MS analyses reveal that, at least in most cases, C6-alkoxy substituted penicillin V and G derivatives do not directly react with isolated M^{pro} to give covalent adducts via β-lactam ring opening, but efficiently bind to the M^{pro} active site to inhibit catalysis via competing with the substrate for binding (**Figure 4** and **Supporting Figure S9**). The modelling studies predicted that the penicillin C6-alkoxy substitution increased the distance between the electrophilic β-lactam carbonyl C-atom and the nucleophilic thiolate S-atom of Cys145, thus impairing efficient covalent reaction (**Figures 2**, **6** and **10**).

Interestingly, our results reveal that penicillin C6-alkoxy derivatives have capacity to covalently react with M^{pro}, if apparently stringent requirements on penicillin substitution pattern, penicillin

sulfur oxidation state, and configuration of penicillin stereocentres are matched (**Figure 8** and **9**). Monitoring the reaction of isolated M^{pro} with penicillin derivative **2** using SPE-MS revealed formation of a covalent M^{pro} adduct corresponding to penicillin dehydration within 45 min in a concentration dependent manner (**Figure 8**), which apparently slowly reacted (within >15) h to a +32 Da M^{pro} species (**Supporting Figure S10**). Furthermore, covalent adduct formation apparently correlated with ~9-fold increase in inhibition potency compared to isomeric penicillin derivatives which did not promote covalent adduct formation (**Table 2, entries x and xi**).

The observed +32 Da mass shift could be the result of cysteine thiol oxidation to give either a sulfinic acid (+2 O) or a persulfide (+ S); these modifications cannot be distinguished using SPE-MS due to insufficient resolution. Nonetheless, cysteinyl thiol oxidation to sulfinic acids and persulfides are known post-translational modifications,[79, 80] and the formation of persulfidated M^{pro} is precedented by crystallographically observed M^{pro} disulfide adducts derived from thiocyanate-based inhibitors,[81] and further supported by reactions of Cys145 (and other cysteine residues[43]) with ebselen derivatives to give sulfur–selenium (S–Se) adducts.[82, 83]

A possible mechanism for the reaction of M^{pro} with C6-methoxy penicillin G (*R*)-sulfoxide esters **2** and **3** involves C3 deprotonation of **2** at the M^{pro} active site, followed by thiazolidine ring opening to form a sulfenic acid[84] (**Supporting Figure 13, I**); note that the base-catalysed thiazolidine ring opening of related penicillin sulfone ester derivatives via C3 deprotonation is known.[85] The reaction of penicillin sulfenic acid intermediates with thiols to give mixed disulfides is also documented;[86-88] the sulfenic acid intermediate **I** may further react with a cysteine thiol to generate a mixed disulfide (+498 Da; **Supporting Figure 13**, **II**), which may slowly eliminate to the persulfidated M^{pro} adduct (+32 Da; **Supporting Figure 13**, **III**). Note that we did not accrue

evidence for reaction of Cys145, and that the nature of this +32 Da adduct is subject to ongoing investigations.

Beyond their applications as antibiotics, C6-alkoxy substituted penicillin derivatives have been reported to target non-bacterial enzymes: the C6-alkoxy penam sulfones **27a**, **27b**, and **27f** are known covalent inhibitors of human leukocyte elastase (HLE),[89] a serine protease implicated in inflammatory conditions.[90] Interestingly, in contrast to their reported reactivity with HLE, C6-alkoxy penams (*e.g.*, **26a** and **27a**) did not evidence covalent modification of M^{pro}, exhibiting a similar pattern to the C6-alkoxy penicillin V and G derivatives investigated in this study.

2.2.5 Conclusion

Almost a century following Fleming's observation of the activity of penicillins,[91] β-lactam containing antibacterials remain amongst the most important medicines.[40] Our combined results further demonstrate the largely untapped potential of penicillin scaffolds for targeting enzymes other than those involved in bacterial cell wall biosynthesis, as first evidenced by work on elastase inhibition[89, 92, 93] and more recently in work on M^{pro} inhibition.[41, 42] There is strong evidence that clinically used β-lactam antibiotics inhibit transpeptidases via mechanisms involving covalent reactions to form stable acyl-enzyme complexes (though it cannot be ruled out that some of the antibiotic activity of β-lactams results from non-covalent inhibition). In some cases, the initially formed complexes can undergo further reaction that increase stability of the acyl-enzyme complexes, as reported with SBL inhibitors, including clavulanic acid and related compounds.[94, 95] The work presented here highlights the potential of non-covalent, non-acylating enzyme inhibition mechanisms for penicillins and other bicyclic β-lactams. One potential application of these mechanisms is to enable inhibition of bacterial cell wall biosynthesis in a manner that is not

prone to current mechanisms of resistance, in particular β-lactamase production or transpeptidase mutation.

2.2.6 Supporting Figures

Supporting Figure S1. Representative β-lactam antibiotics bearing a methoxy (MeO) group α to the β-lactam carbonyl group. A. C6-Methoxy penicillin: temocillin.[45] **B.** C7-methoxy cephalosporins: cephamycin C,[47] cefoxitin,[96] cefmetazole,[65] cefbuperazone,[97] cefotetan.[98] **C.** C7-methoxy oxacephalosporin: moxalactam.[99] **D.** C3-methoxy monobactam: sulfazecin.[100]

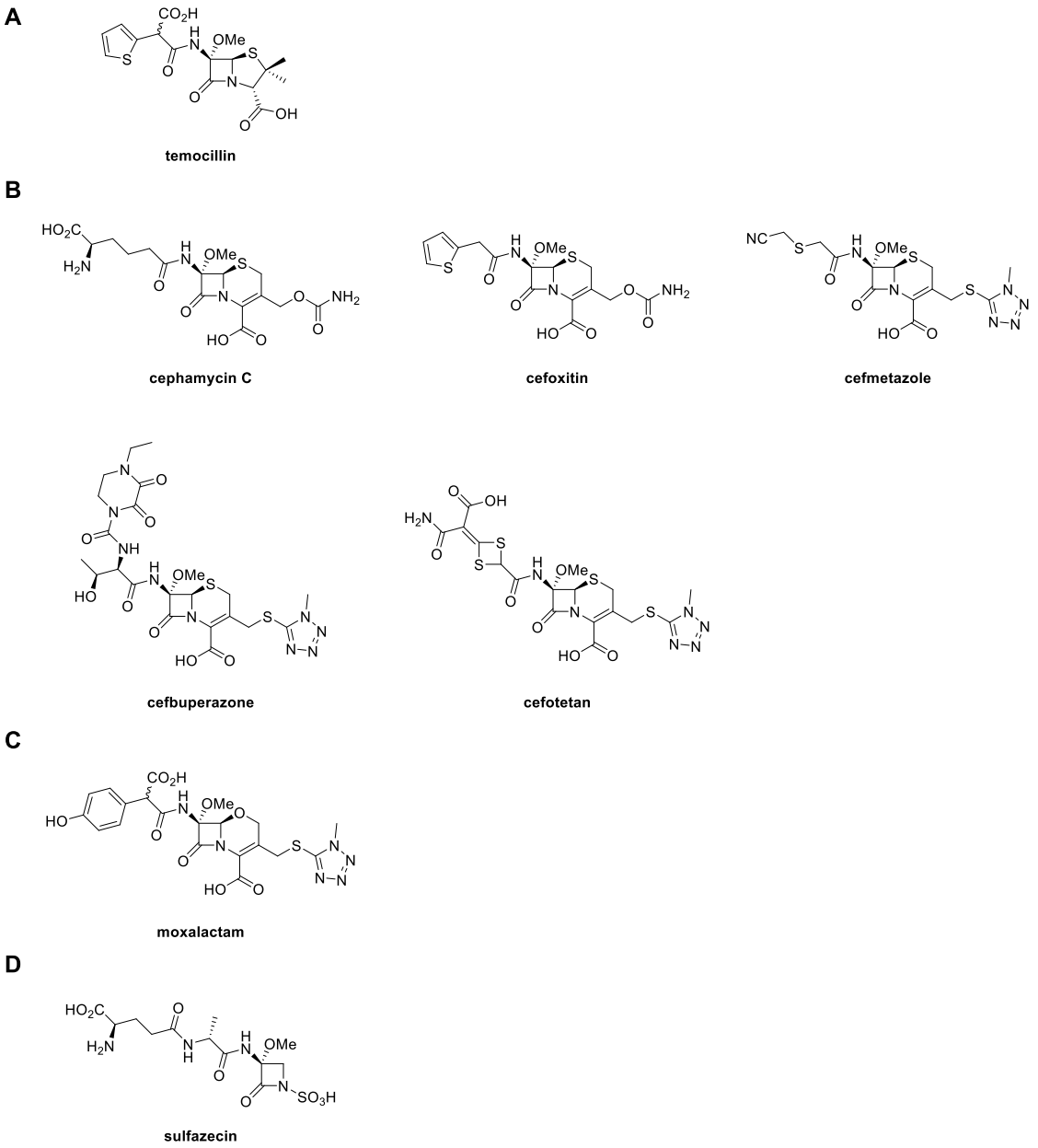

Supporting Figure S2. Comparison of predicted M^{pro}:penicillin derivatives complexes with reported M^{pro} complex structures. A. Superimposition of the MD-predicted M^{pro}:penicillin V derivative **1** (pink) complex and the crystallographically observed covalent M^{pro}:nirmatrelvir (cyan blue) adduct (PDB ID: **7VH8**[6]). **B.** Superimposition of the MD-predicted M^{pro}:penicillin V derivative **1** (pink) complex and the crystallographically observed covalent M^{pro}:penicillin V derivative **4** (blue) adduct (PDB ID: **7Z59**[42]). S1', S1, S2, and S4 indicate the respective M^{pro} binding pockets.

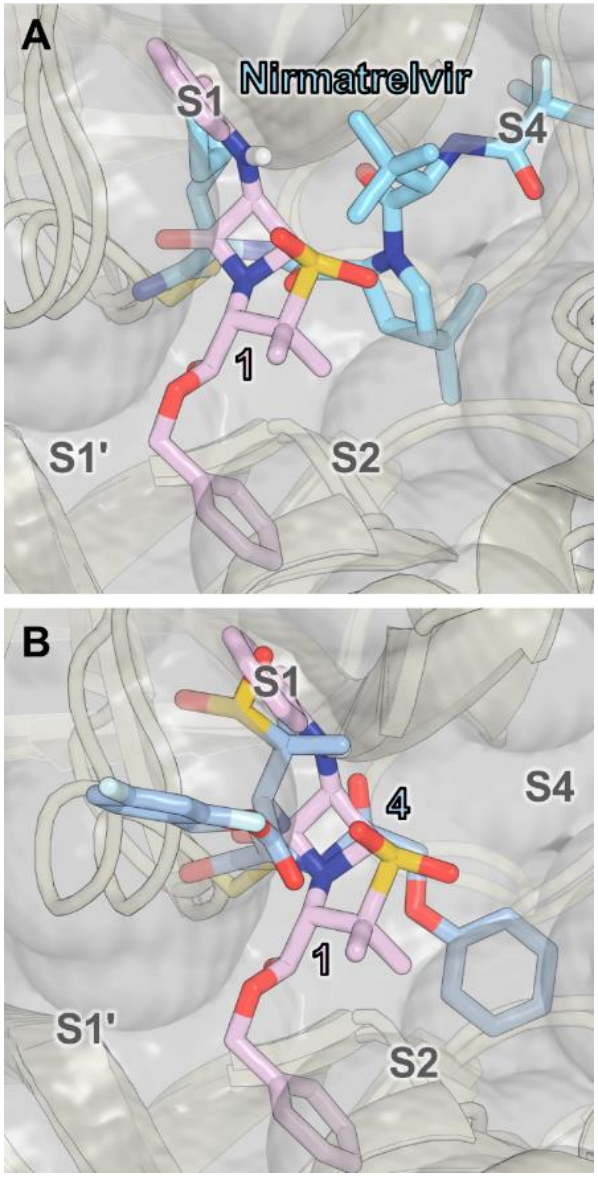

Supporting Figure S3. Comparison of predicted M^{pro}:penicillin derivative complex structures. Superimposition of the MD-predicted M^{pro}:penicillin V derivative **1** and M^{pro}:C6-methoxypenicillin G derivative **3** (purple) complex structures. S1', S1, S2, and S4 indicate the respective M^{pro} substrate residue binding pockets.

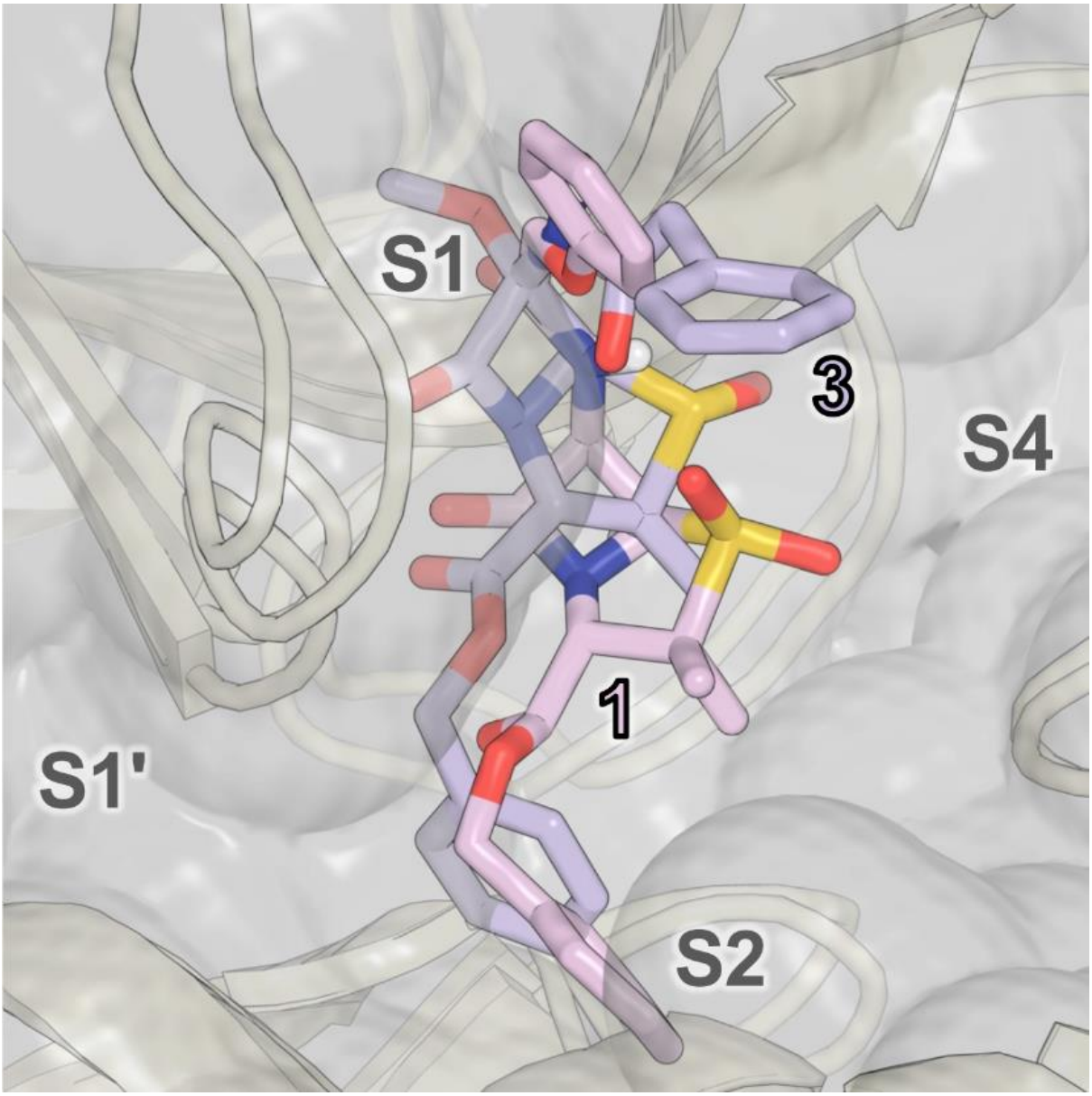

Supporting Figure S4. Comparison of predicted M^{pro}:penicillin derivative complex structures with reported M^{pro} complex structures. Superimposition of the MD-predicted M^{pro}:penicillin V derivative **10b** complex structure (green) and the crystallographically-observed covalent adduct of nirmatrelvir (cyan blue) with M^{pro} (PDB ID: **7VH8**[42]). S1', S1, S2, and S4 indicate the respective M^{pro} substrate residue binding pockets.

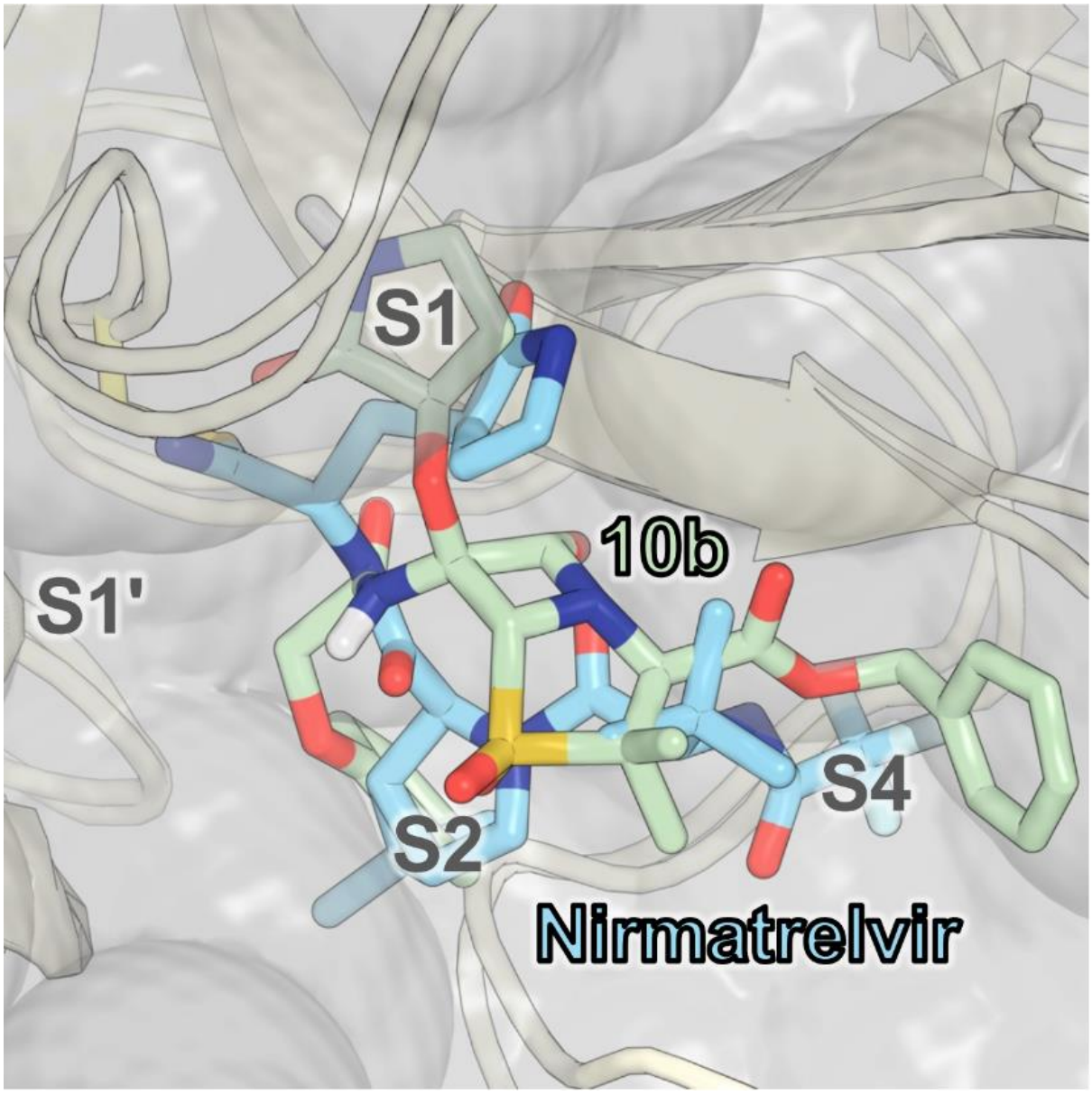

Supporting Figure S5. Molecular dynamics analysis predicts that β-lactam 1 may be better poised than β-lactam 3 for covalent reaction with M^{pro} via β-lactam ring opening. Ligand root-mean-square deviation (RMSD) values relative to the cluster representative of the largest cluster, and distances between the sulfur of Cys145 and the carbonyl carbon of the β-lactam ring (S(Cys145)-C(O)(β-lactam)) and Bürgi-Dunitz angles for S(Cys145) and the C(O)(β-lactam) for: (**A**) β-lactam **1** and (**B**) β-lactam **3**, over three independent replicas of 100 ns MD simulations. Only frames in which the S–C distance was less than 5 Å were included in the angle analyses (59% and 19% of frames for **1** and **3**, respectively). The RMSD was used to assess the stability of the ligand pose.

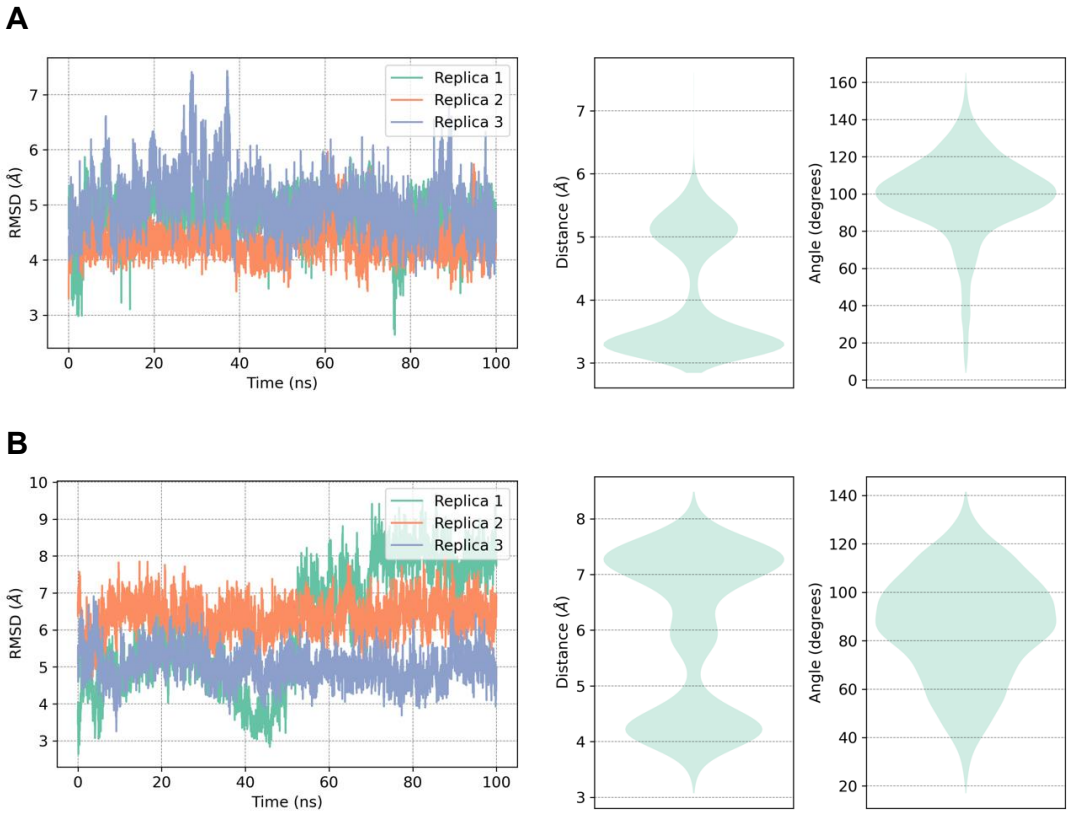

Supporting Figure S6. Modelled C6-alkoxy penicillin V derivatives show no sustained proximity or geometry favouring covalent reaction with M^{pro} Cys145. Ligand RMSD values relative to the cluster representative of the largest cluster, as well as S(Cys145)-C(O)(β-lactam) distances and Bürgi-Dunitz angles for S(Cys145) and the C(O)(β-lactam) for: **7** (**A**), **10a** (**B**), **17** (**C**), and **10b** (**D**; continues on the following page), over three independent replicas of 100 ns MD simulations. Only frames in which the S–C distance was less than 5 Å were included in the angle analyses (2%, 49%, < 1%, and 3% of frames for **7**, **10a**, **17**, and **10b**, respectively). The RMSD was used to assess the stability of the ligand pose.

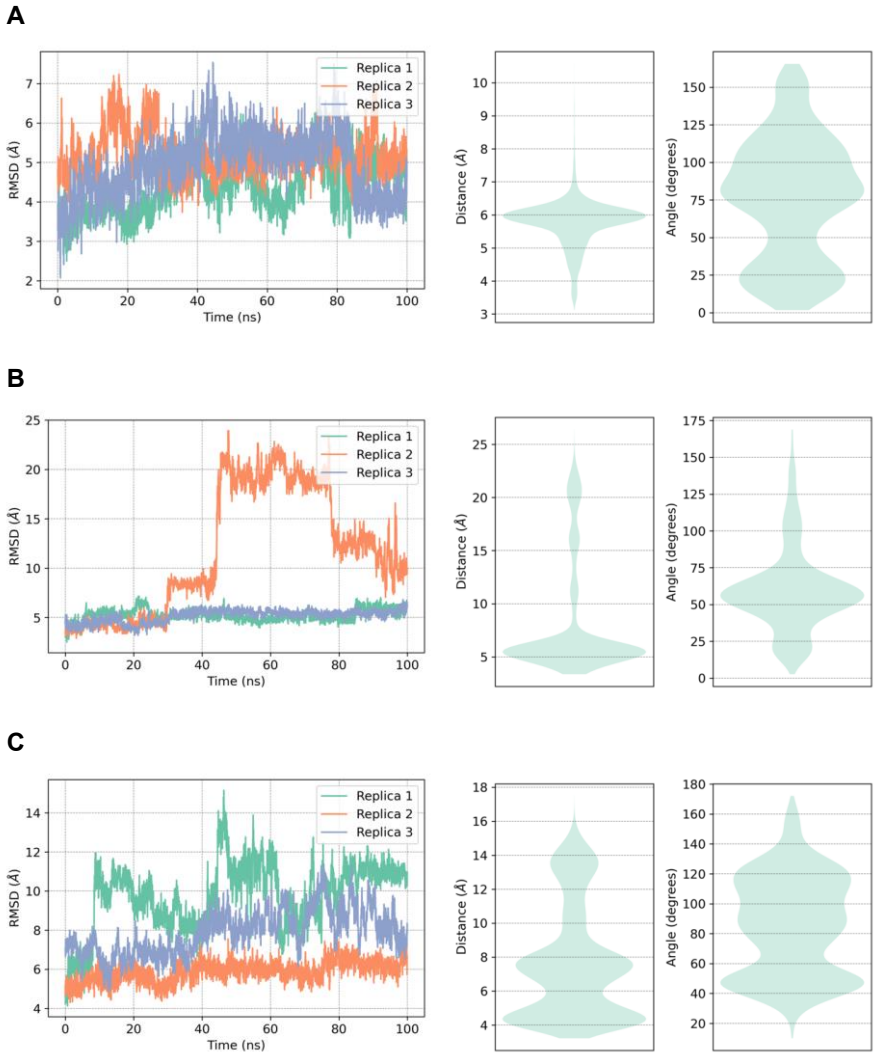

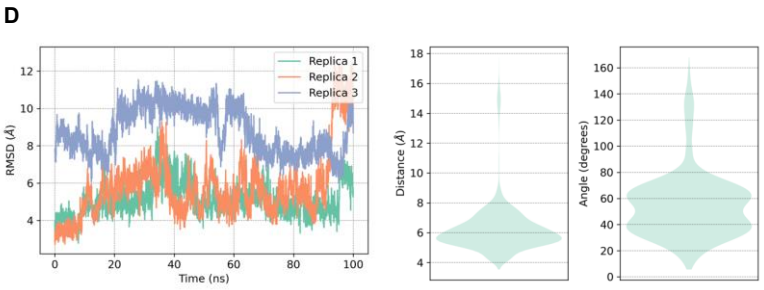

Supporting Figure S7. Modelled C6-methoxy penam derivatives show no sustained proximity or geometry favouring covalent reaction with M^{pro} Cys145. Ligand RMSD values relative to the cluster representative of the largest cluster, as well as S(Cys145)-C(O)(β-lactam) distances and Bürgi-Dunitz angles for S(Cys145) and the C(O)(β-lactam) for **27a** (**A**) and **26a** (**B**) over three independent replicas of 100 ns MD simulations. Only frames in which the S–C distance was less than 5 Å were included in the angle analyses (53% and 2% of frames for **27a** and **26a**, respectively). The RMSD was used to assess the stability of the ligand pose. Note that, interestingly, **27a** dissociated from M^{pro} in replica 2.

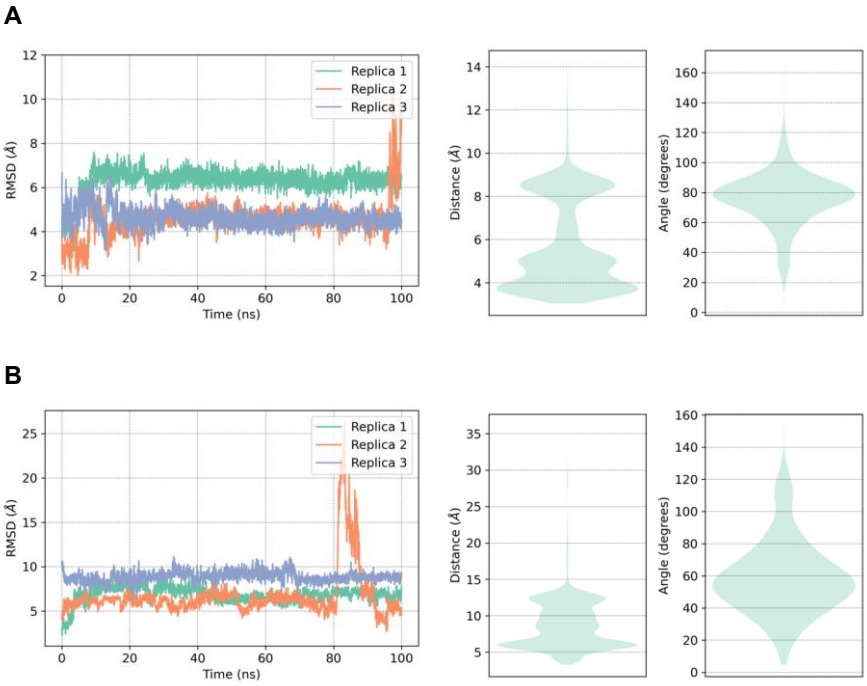

Supporting Figure S8. Representative dose response curves. Representative dose response curves for M^{pro} inhibition by C6-alkoxy penicillin: (**a**) **2** (black triangles), **3** (orange circles), **7** (blue squares), **10a** (green diamonds), **10b** (red inverse triangles), **17** (mustard green hexagons), and (**b**) **20** (black triangles), **22** (orange circles), **25** (blue squares), **26a** (green diamonds), **26b** (red inverse triangles), **26f** (mustard green hexagons), **27** (purple dots). Dose response curves are means of technical duplicates. IC_{50} values in **Tables 1-3** are means of three independent repeats (n = 3, mean ± SD), each composed of technical duplicates. Conditions: SPE-MS M^{pro} inhibition assays were performed using SPE-MS as reported,[12] employing SARS-CoV-2 M^{pro} (0.05 µM) and substrate (2.0 µM).

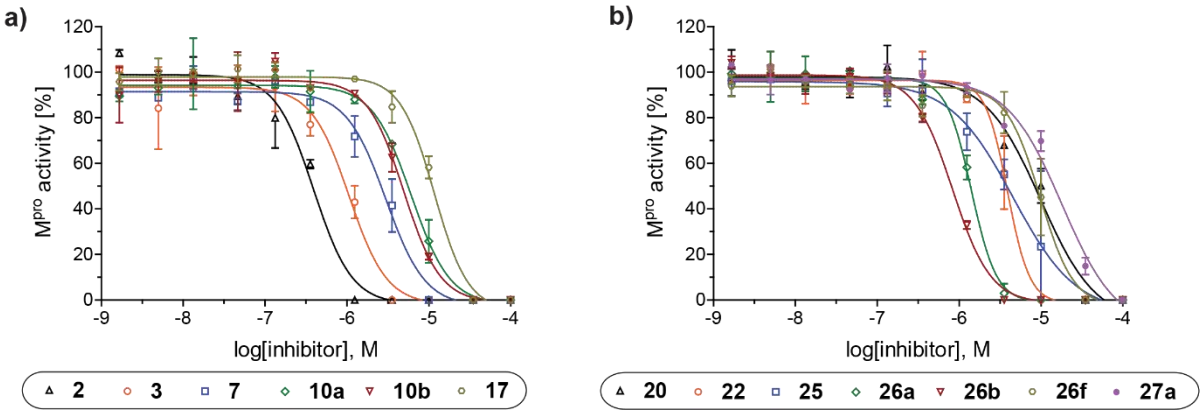

Supporting Figure S9. Most C6-alkoxy penam derivatives do not efficiently covalently react with isolated recombinant M^{pro} (continues on the following page). Analysis of reaction mixtures of M^{pro} and β-lactams: (**A**) **8**, (**B**) **10a**, (**C**) **10b**, (**D**) **16c**, (**E**) **20**, (**F**) **22**, (**G**) **24**, (**H**) **26b**, (**I**) **26d**, (**J**) **26e**, (**K**) **26f**, (**L**) **27c**, (**M**) **27d**, (**N**) **27e**, and (**O**) **27f**, prior (bottom) and >15 h post incubation (top) with the respective β-lactam. Assays were performed using SPE-MS, employing SARS-CoV-2 M^{pro} (3.0 µM) and, if appropriate, a β-lactam (15 µM) in buffer (20 mM HEPES, pH 7.5). Representative spectra of technical duplicates are shown.

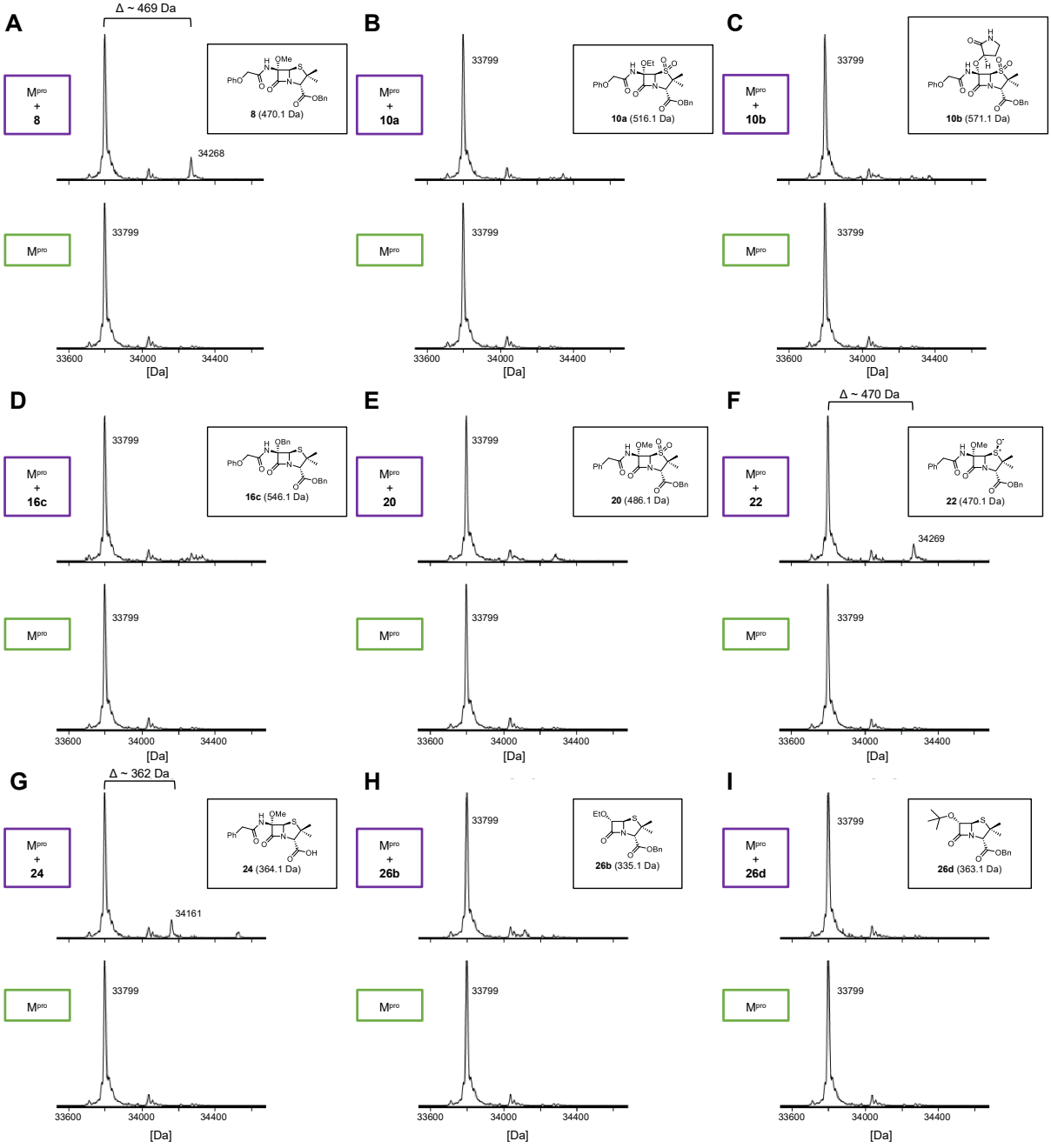

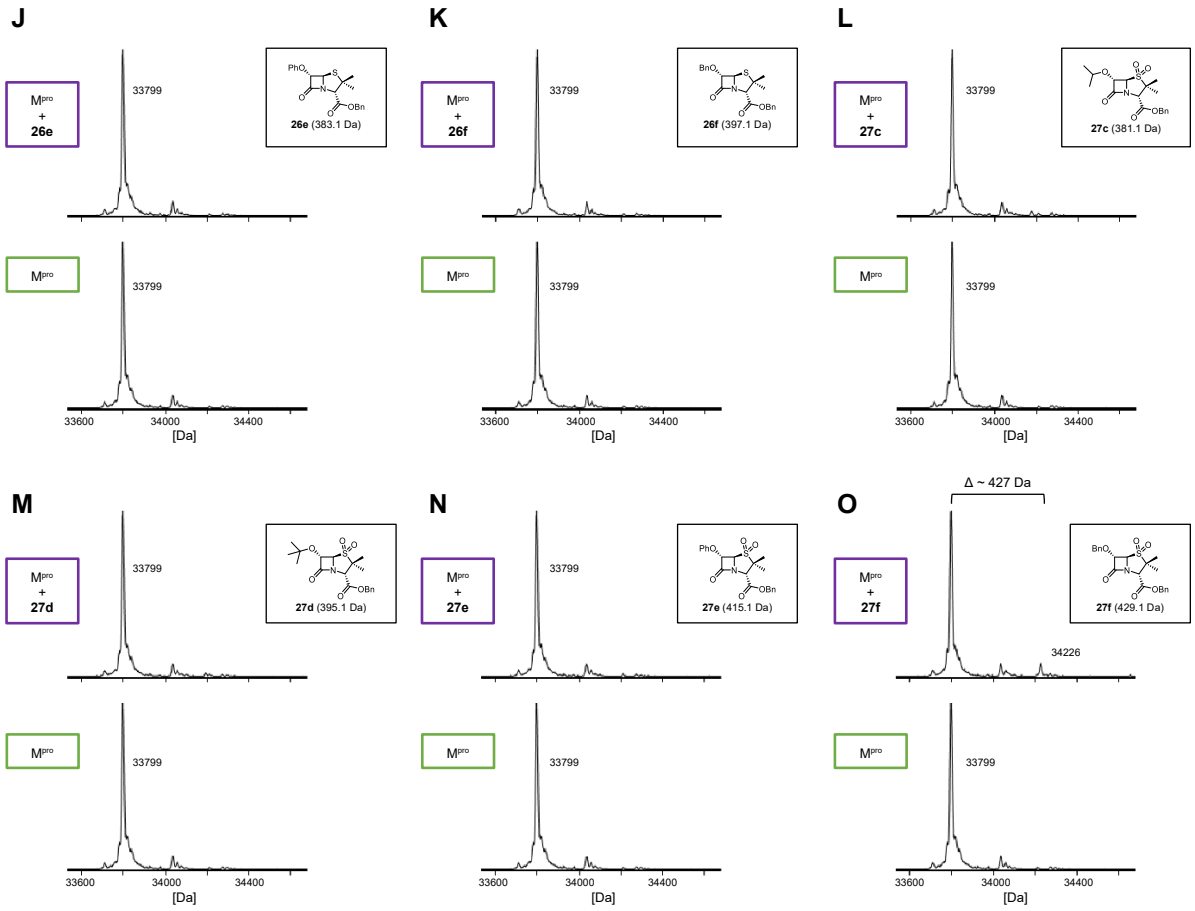
J
Mpro + 26e
33799
26e (383.1 Da)
Mpro
33799
33600
34000
34400
[Da]
K
Mpro + 26f
33799
26f (397.1 Da)
Mpro
33799
33600
34000
34400
[Da]
L
Mpro + 27c
33799
27c (381.1 Da)
Mpro
33799
33600
34000
34400
[Da]
M
Mpro + 27d
33799
27d (395.1 Da)
Mpro
33799
33600
34000
34400
[Da]
N
Mpro + 27e
33799
27e (415.1 Da)
Mpro
33799
33600
34000
34400
[Da]
O
Δ ~ 427 Da
Mpro + 27f
34226
27f (429.1 Da)
Mpro
33799
33600
34000
34400
[Da]

Supporting Figure S10. Levels of M^{pro} adduct formation depend on β-lactam concentration. SPE-MS analysis indicates that an increased penicillin derivative:M^{pro} ratio correlates with higher intensity of the +32 Da M^{pro} mass shift (annotated with ★) observed with both **2** (**A**) and **3** (**B**) (denaturing conditions; 20 mM HEPES, pH 7.5). Penicillin derivative:M^{pro} ratios were: 1:5 (top spectra) or 1:10 (bottom spectra). Bn: $–CH_2Ph$; pNB: $–CH_2C_6H_4(4\text{-}NO_2)$.

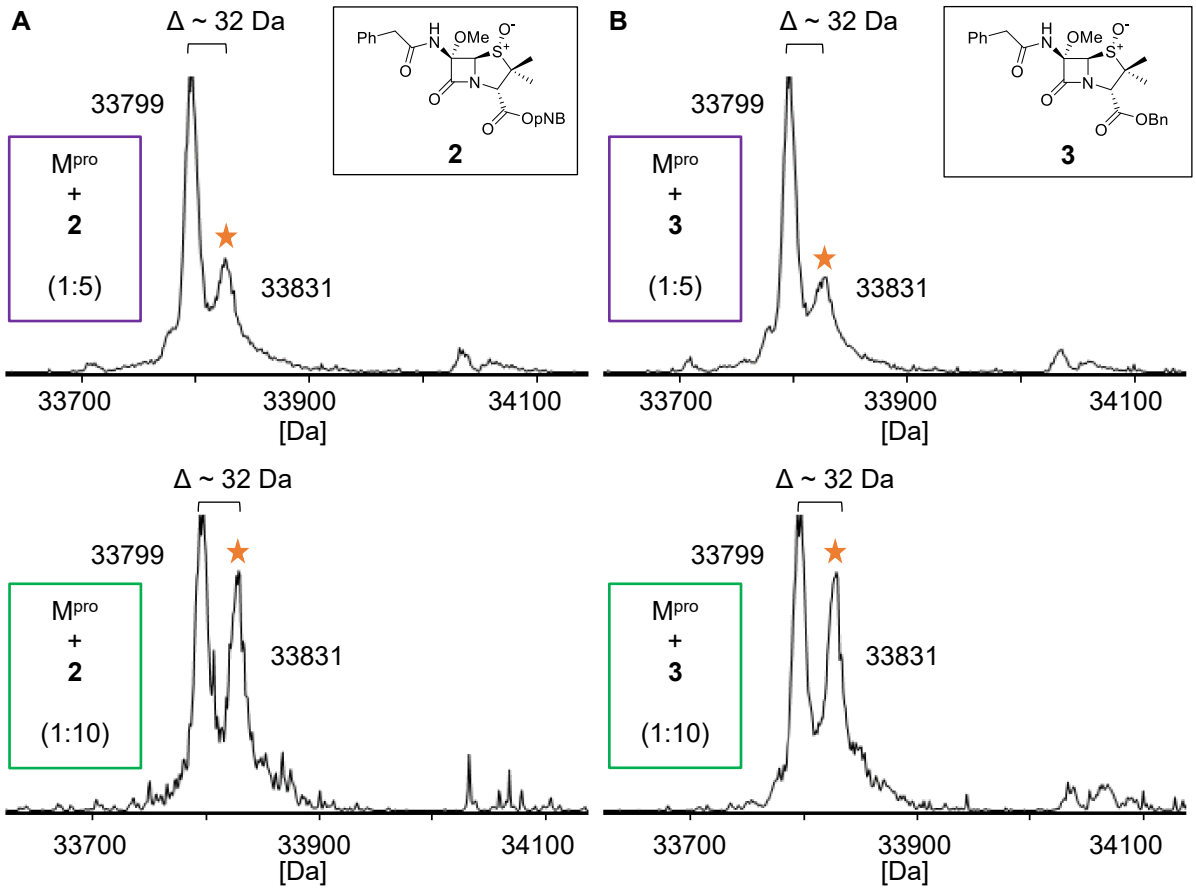

Supporting Figure S11: **The outcome of the covalent reaction between M^{pro} and C6-methoxy penicillin derivative 2 is time dependent.** SPE-MS analysis showed initial formation of a +515 Da M^{pro} adduct (★), followed by the appearance of a +498 Da M^{pro} adduct (★) with increasing intensity over 45 min (denaturing conditions; **2**:M^{pro} ratio: 10:1; 20 mM HEPES, pH 7.5). A +32 Da M^{pro} adduct (★) of low intensity was also detected after 45 min incubation. pNB: $–CH_2C_6H_4(4\text{-}NO_2)$.

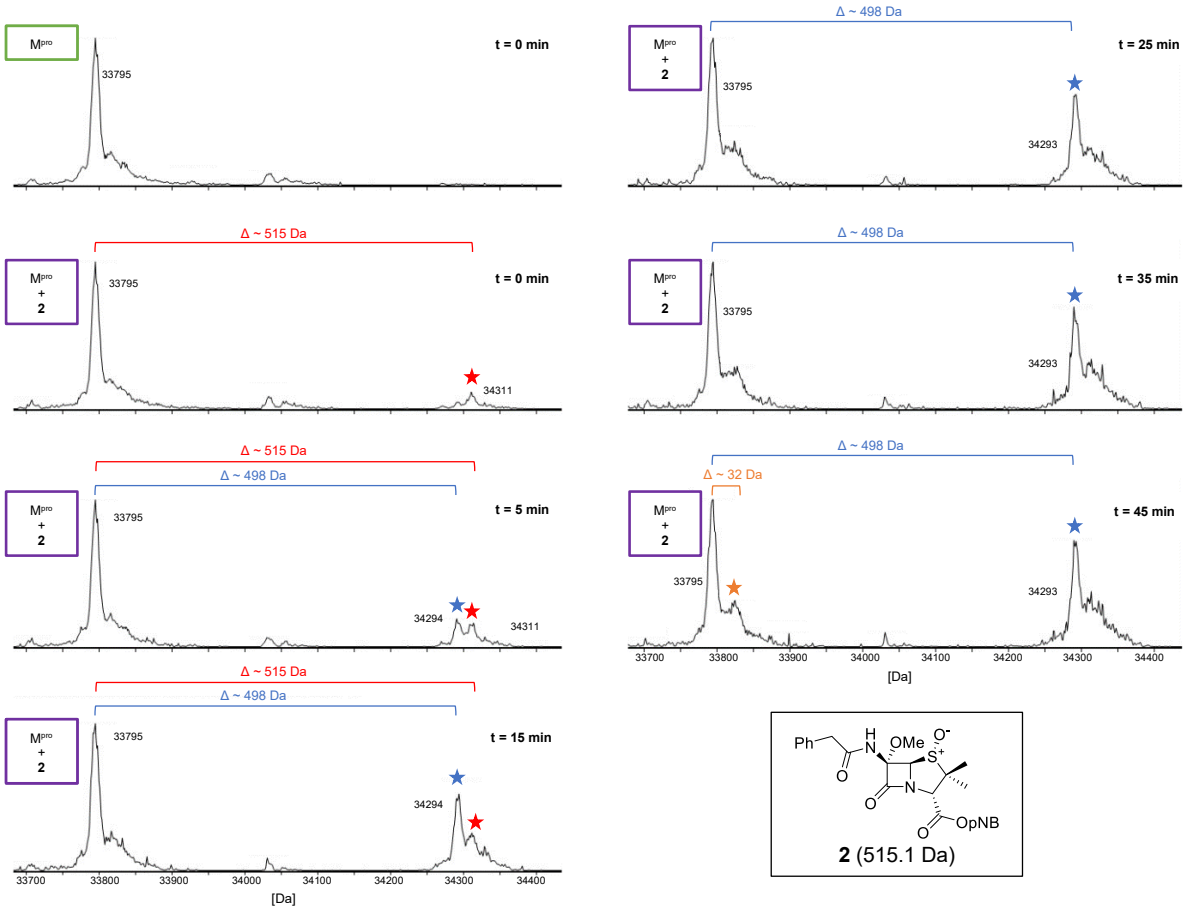

Supporting Figure S12. β-Lactams have potential for protein inhibition via non-covalent mechanisms. Structures of reported β-lactams that inhibit proteins via non-covalent binding: (**A**) Ezetimibe[71] is an anticholesteremic drug that competitively inhibits the NPC1L1 transporter. (**B**) Penicillin A11 and cephalosporin E1 are likely non-covalent inhibitors of SPOP (reported IC_{50} ~ 20 and 0.58 μM, respectively).[75]

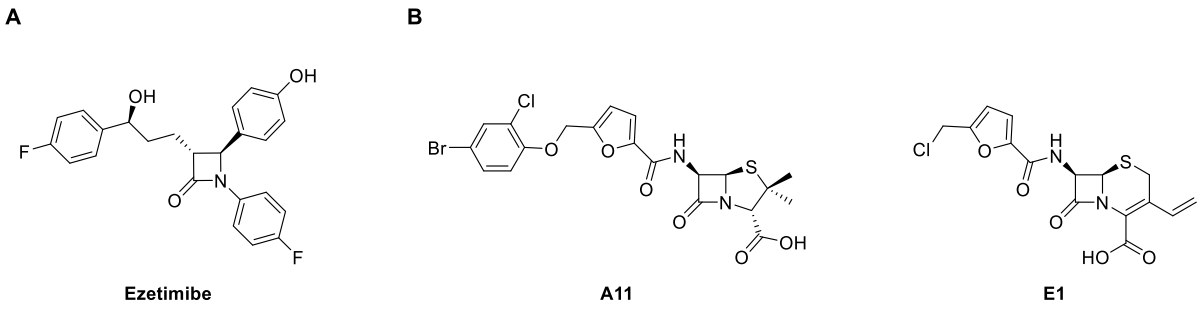

Supporting Figure S13. Possible outline mechanism for covalent reaction of M^{pro} with C6-methoxy penicillin G (*R*)-sulfoxide esters. Reaction of M^{pro} with **2** may involve: a) active-site mediated deprotonation of the relatively acidic C3 proton of **2**, giving sulfenic acid (**I**); b) S-S bond formation via reaction with a M^{pro} cysteine thiol (+498 Da; **II**); c) elimination of the M^{pro} persulfide **II** (+32 Da; see **Figure 8** and **Supporting Figure S11** for relevant MS details), likely followed by: d) hydration of the intermediate β-lactam **IV**. pNB: $–CH_2C_6H_4(4\text{-}NO_2)$.

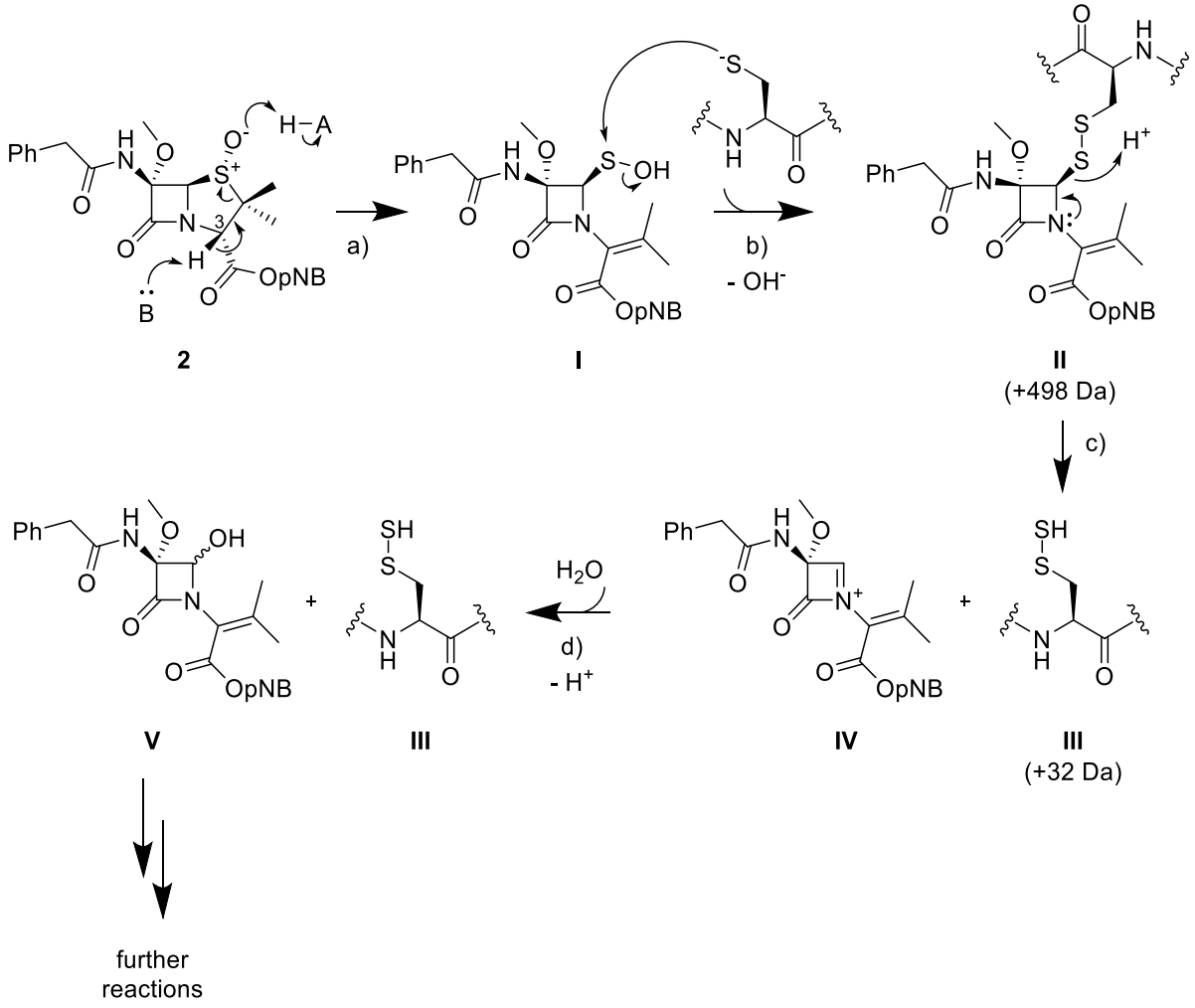

2.2.7 Computational methods

2.2.7.1 Docking

Docking was performed using an *apo* SARS-CoV-2 M^{pro} crystal structure (PDB ID 6YB7, 1.25 Å resolution). Small-molecule input conformations were generated using Schrödinger's LigPrep tool, the protein was prepared using Schrödinger's Protein Preparation Workflow,[101, 102] both with default settings. Solvent molecules were removed. δ-Nitrogens of His41 and His80 were protonated. ε-Nitrogens of His64, His163, His164, His172, and His246 were protonated.

Docking calculations were performed using Glide XP[103] with a bounding box (inner and outer edge length: 10 Å and 30 Å, respectively) centred on the Cys145 sulphur atom and a flexible Cys145 thiol group, keeping at most 30 poses per ligand. Output poses were clustered based on interaction fingerprints using default settings. Structures closest to the centroid of each cluster were rescored using molecular mechanics with generalised Born and surface area continuum solvation (MM-GBSA) calculations, minimising all protein atoms within 5 Å of the ligand, and the top three structures were kept for further analysis. For penams **1**, **7**, and **10b** cluster representatives were highly similar (RMSD < 3 Å), and thus only cluster the representative with the lowest MM-GBSA score was kept. MM-GBSA scores substantially altered the ranking of cluster representatives; in some cases, the lowest-ranking pose according to docking scores was ranked the highest according to MM-GBSA scores.

2.2.7.2 Parametrisation

Parameters for the inhibitors were generated using Antechamber[104, 105]. Partial charges were computed using the optimised geometry of the highest-ranking conformer using the Restrained Electrostatic Potential (RESP) procedure.[106] QM calculations used to derive ESP were performed

at the HF/6-31G(d) level of theory using the Gaussian16 software package[107]. Docked protein-ligand complexes were prepared using LEaP[108, 109]. The ff14SB[110] force field was used for the protein and GAFF[104, 105] for the small molecules.

2.2.7.3 Molecular dynamics simulations

The protein-ligand complexes obtained from docking were used as starting points for MD simulations. The system was placed in a truncated octahedral box with a 12 Å buffer, solvated with the TIP3P water model[111], and neutralised with 4 sodium ions. To ensure the planarity of the β-lactam carbonyl, the barrier height for the corresponding improper torsion was set to 10.5 kcal/mol.

Molecular dynamics (MD) simulations were performed using Amber24[104, 105, 108, 110]. The system was subjected to energy minimisation in two stages, first with positional restraints on protein and ligand atoms at 500 kcal/mol $Å^{-2}$, followed by unrestrained minimisation. The system was then heated from 0 to 300 K in 50 K increments under constant volume using Langevin dynamics with a time step of 2 fs, gradually releasing positional restraints on the protein and ligand (starting at 210 kcal/mol $Å^{-2}$ and decreasing to 10 kcal/mol $Å^{-2}$). Equilibration was performed for 2 ns using a 2 fs time step in the NPT ensemble at 1 bar and 300 K. Temperature and pressure were maintained using a Langevin thermostat (collision frequency: 1.0 ps^{-1}) and a Berendsen barostat (relaxation time: 2.0 ps)[110], respectively.

Production MD simulations were conducted for 100 ns using the NPT ensemble at 1 bar and 300 K. A 10 Å cut-off was applied for non-bonded interactions. Covalent bonds involving hydrogen atoms were constrained using the SHAKE algorithm[112], and periodic boundary conditions were

employed with particle mesh Ewald (PME)[113] for long-range electrostatics. Three independent replicas of minimisation, heating, and equilibration, and production simulations were performed.

CPPTRAJ[108, 114] was used to analyse trajectories. The pose stability was determined by ligand root-mean-square deviation (RMSD) compared to the initial, docked pose after aligning the protein backbone, and validated by visual inspection. To identify representative ligand binding modes, the trajectories from the independent replicas were concatenated and aligned to the protein backbone atoms. Water molecules and ions were removed, and hierarchical agglomerative clustering based on ligand heavy atom RMSD was performed using the average linkage method with an epsilon cut-off of 1.0 Å. Cluster populations and representative structures were extracted, with the largest cluster considered to represent the most probable binding mode. H bonds were required to have a donor-acceptor distance < 3.0 Å and an angle between the H bond donor, the H atom, and the H bond acceptor > 135°. The fraction of simulation time that each hydrogen bond was observed is given in **Supporting Table S1**. A H bond was considered relevant if it was present for at least 10% of the simulation time. Visualisations were generated using PyMOL. Asn142 was excluded from the protein surface for visual clarity. Simulation input files, scripts, and final poses are available in a GitHub repository (https://github.com/duartegroup/C6-alkoxy-penicillins).

Supporting Table S1: Fractions of simulation time across the concatenated three independent replicas that the indicated hydrogen bonds were present.

Hydrogen bond	Fraction of simulation time
1 : His163 sidechain	22%
1 sulfone O : 1 amide NH	10%
3 : Ser144 backbone	11%
3 ; Glu166 backbone	33%
3, Glu166 sidechain	20%/15% (for each sidechain O)
7 : Asn142 sidechain	40%
7 : Gly143 backbone	35%
7 : Gln189 sidechain	12%
10a : His41 sidechain	22%
10a : sulfone O : 10a amide NH	11%
10b : Leu141 backbone	13%
10b : Gly143 backbone	18%
10b : Ser144 sidechain	15%
10b : Glu166 backbone	13%
27a : Gly143 backbone	28%

2.2.8 References

1. T. Kronenberger, S. A. Laufer and T. Pillaiyar, COVID-19 therapeutics: Small-molecule drug development targeting SARS-CoV-2 main protease, *Drug Discov. Today*, 2023, **28**, 103579.
2. G. Li, R. Hilgenfeld, R. Whitley and E. De Clercq, Therapeutic strategies for COVID-19: progress and lessons learned, *Nature Reviews Drug Discovery*, 2023, **22**, 449–475.
3. Y. L. Janin, On the origins of SARS-CoV-2 main protease inhibitors, *RSC Medicinal Chemistry*, 2024, **15**, 81–118.
4. J. Breidenbach, C. Lemke, T. Pillaiyar, L. Schäkel, G. Al Hamwi, M. Diett, R. Gedschold, N. Geiger, V. Lopez, S. Mirza, V. Namasivayam, A. C. Schiedel, K. Sylvester, D. Thimm, C. Vielmuth, L. Phuong Vu, M. Zyulina, J. Bodem, M. Gütschow and C. E. Müller, Targeting the Main Protease of SARS-CoV-2: From the Establishment of High Throughput Screening to the Design of Tailored Inhibitors, *Angewandte Chemie International Edition*, 2021, **60**, 10423–10429.
5. Z. Jin, X. Du, Y. Xu, Y. Deng, M. Liu, Y. Zhao, B. Zhang, X. Li, L. Zhang, C. Peng, Y. Duan, J. Yu, L. Wang, K. Yang, F. Liu, R. Jiang, X. Yang, T. You, X. Liu, X. Yang, F. Bai, H. Liu, X. Liu, L. W. Guddat, W. Xu, G. Xiao, C. Qin, Z. Shi, H. Jiang, Z. Rao and H. Yang, Structure of Mpro from SARS-CoV-2 and discovery of its inhibitors, *Nature*, 2020, **582**, 289–293.
6. D. R. Owen, C. M. N. Allerton, A. S. Anderson, L. Aschenbrenner, M. Avery, S. Berritt, B. Boras, R. D. Cardin, A. Carlo, K. J. Coffman, A. Dantonio, L. Di, H. Eng, R. Ferre, K. S. Gajiwala, S. A. Gibson, S. E. Greasley, B. L. Hurst, E. P. Kadar, A. S. Kalgutkar, J. C. Lee, J. Lee, W. Liu, S. W. Mason, S. Noell, J. J. Novak, R. S. Obach, K. Ogilvie, N. C. Patel, M. Pettersson, D. K. Rai, M. R. Reese, M. F. Sammons, J. G. Sathish, R. S. P. Singh, C. M. Steppan, A. E. Stewart, J. B. Tuttle, L. Updyke, P. R. Verhoest, L. Wei, Q. Yang and Y. Zhu, An oral SARS-CoV-2 Mpro inhibitor clinical candidate for the treatment of COVID-19, *Science*, 2021, **374**, 1586–1593.
7. X. Chen, X. Huang, Q. Ma, P. Kuzmič, B. Zhou, S. Zhang, J. Chen, J. Xu, B. Liu, H. Jiang, W. Zhang, C. Yang, S. Wu, J. Huang, H. Li, C. Long, X. Zhao, H. Xu, Y. Sheng, Y. Guo, C. Niu, L. Xue, Y. Xu, J. Liu, T. Zhang, J. Spencer, Z. Zhu, W. Deng, X. Chen, S.-H. Chen, N. Zhong, X. Xiong and Z. Yang, Preclinical evaluation of the SARS-CoV-2 Mpro inhibitor RAY1216 shows improved pharmacokinetics compared with nirmatrelvir, *Nat. Microbiol.*, 2024, **9**, 1075–1088.
8. X. Jiang, H. Su, W. Shang, F. Zhou, Y. Zhang, W. Zhao, Q. Zhang, H. Xie, L. Jiang, T. Nie, F. Yang, M. Xiong, X. Huang, M. Li, P. Chen, S. Peng, G. Xiao, H. Jiang, R. Tang, L. Zhang, J. Shen and Y. Xu, Structure-based development and preclinical evaluation of the SARS-CoV-2 3C-like protease inhibitor simnotrelvir, *Nat. Commun.*, 2023, **14**, 6463.
9. Y. Unoh, S. Uehara, K. Nakahara, H. Nobori, Y. Yamatsu, S. Yamamoto, Y. Maruyama, Y. Taoda, K. Kasamatsu, T. Suto, K. Kouki, A. Nakahashi, S. Kawashima, T. Sanaki, S. Toba, K. Uemura, T. Mizutare, S. Ando, M. Sasaki, Y. Orba, H. Sawa, A. Sato, T. Sato, T. Kato and Y. Tachibana, Discovery of S-217622, a Noncovalent Oral SARS-CoV-2 3CL Protease Inhibitor Clinical Candidate for Treating COVID-19, *J. Med. Chem.*, 2022, **65**, 6499–6512.
10. A. M. Shawky, F. A. Almalki, H. A. Alzahrani, A. N. Abdalla, B. G. M. Youssif, N. A. Ibrahim, M. Gamal, H. A. M. El-Sherief, M. M. Abdel-Fattah, A. A. Hefny, A. H.

Abdelazeem and A. M. Gouda, Covalent small-molecule inhibitors of SARS-CoV-2 Mpro: Insights into their design, classification, biological activity, and binding interactions, *Eur. J. Med. Chem.*, 2024, **277**, 116704.

11. L. Song, S. Gao, B. Ye, M. Yang, Y. Cheng, D. Kang, F. Yi, J.-P. Sun, L. Menéndez-Arias, J. Neyts, X. Liu and P. Zhan, Medicinal chemistry strategies towards the development of non-covalent SARS-CoV-2 Mpro inhibitors, *Acta Pharm. Sin. B*, 2024, **14**, 87–109.
12. L. Brewitz, L. Dumjahn, Y. Zhao, C. D. Owen, S. M. Laidlaw, T. R. Malla, D. Nguyen, P. Lukacik, E. Salah, A. D. Crawshaw, A. J. Warren, J. Trincao, C. Strain-Damerell, M. W. Carroll, M. A. Walsh and C. J. Schofield, Alkyne Derivatives of SARS-CoV-2 Main Protease Inhibitors Including Nirmatrelvir Inhibit by Reacting Covalently with the Nucleophilic Cysteine, *J. Med. Chem.*, 2023, **66**, 2663–2680.
13. C. Ma, Z. Xia, M. D. Sacco, Y. Hu, J. A. Townsend, X. Meng, J. Choza, H. Tan, J. Jang, M. V. Gongora, X. Zhang, F. Zhang, Y. Xiang, M. T. Marty, Y. Chen and J. Wang, Discovery of Di- and Trihaloacetamides as Covalent SARS-CoV-2 Main Protease Inhibitors with High Target Specificity, *J. Am. Chem. Soc.*, 2021, **143**, 20697–20709.
14. B. Boras, R. M. Jones, B. J. Anson, D. Arenson, L. Aschenbrenner, M. A. Bakowski, N. Beutler, J. Binder, E. Chen, H. Eng, H. Hammond, J. Hammond, R. E. Haupt, R. Hoffman, E. P. Kadar, R. Kania, E. Kimoto, M. G. Kirkpatrick, L. Lanyon, E. K. Lendy, J. R. Lillis, J. Logue, S. A. Luthra, C. Ma, S. W. Mason, M. E. McGrath, S. Noell, R. S. Obach, M. N. O'Brien, R. O'Connor, K. Ogilvie, D. R. Owen, M. Pettersson, M. R. Reese, T. F. Rogers, R. Rosales, M. I. Rossulek, J. G. Sathish, N. Shirai, C. M. Steppan, M. Ticehurst, L. Updyke, S. Weston, Y. Zhu, K. M. White, A. García-Sastre, J. Wang, A. K. Chatterjee, A. D. Mesecar, M. B. Frieman, A. S. Anderson and C. Allerton, Preclinical characterization of an intravenous coronavirus 3CL protease inhibitor for the potential treatment of COVID19, *Nat. Commun.*, 2021, **12**, 6055.
15. J. K. Stille, J. Tjutrins, G. Wang, F. A. Venegas, C. Hennecker, A. M. Rueda, I. Sharon, N. Blaine, C. E. Miron, S. Pinus, A. Labarre, J. Plescia, M. Burai Patrascu, X. Zhang, A. S. Wahba, D. Vlaho, M. J. Huot, T. M. Schmeing, A. K. Mittermaier and N. Moitessier, Design, synthesis and in vitro evaluation of novel SARS-CoV-2 3CLpro covalent inhibitors, *Eur. J. Med. Chem.*, 2022, **229**, 114046.
16. D. Laczi, S. S. Huamán, T. Andrews-Clark, S. M. Laidlaw, E. Salah, L. Dumjahn, P. Lukacik, H. Choudhry, M. A. Walsh, M. W. Carroll, C. J. Schofield and L. Brewitz, Silaproline-bearing nirmatrelvir derivatives are potent inhibitors of the SARS-CoV-2 main protease highlighting the value of silicon-derivatives in structure-activity-relationship studies, *Eur. J. Med. Chem.*, 2025, **291**, 117603.
17. R. Jimmidi, S. Chamakuri, S. Lu, M. N. Ucisik, P.-J. Chen, K. M. Bohren, S. A. Moghadasi, L. Versteeg, C. Nnabuife, J.-Y. Li, X. Qin, Y.-C. Chen, J. C. Faver, P. Nyshadham, K. L. Sharma, B. Sankaran, A. Judge, Z. Yu, F. Li, J. Pollet, R. S. Harris, M. M. Matzuk, T. Palzkill and D. W. Young, DNA-encoded chemical libraries yield non-covalent and non-peptidic SARS-CoV-2 main protease inhibitors, *Commun. Chem.*, 2023, **6**, 164.
18. M. L. Boby, D. Fearon, M. Ferla, M. Filep, L. Koekemoer, M. C. Robinson, C. M. C. The, J. D. Chodera, A. A. Lee, N. London, A. von Delft and F. von Delft, Open science discovery of potent noncovalent SARS-CoV-2 main protease inhibitors, *Science*, **382**, eabo7201.

19. N. E. Zhou, S. Tang, X. Bian, M. K. Parai, I. V. Krieger, A. Flores, P. K. Jaiswal, R. Bam, J. L. Wood, Z. Shi, L. J. Stevens, T. Scobey, M. V. Diefenbacher, F. R. Moreira, T. J. Baric, A. Acharya, J. Shin, M. M. Rathi, K. C. Wolff, L. Riva, M. A. Bakowski, C. W. McNamara, N. J. Catanzaro, R. L. Graham, D. C. Schultz, S. Cherry, Y. Kawaoka, P. J. Halfmann, R. S. Baric, M. R. Denison, T. P. Sheahan and J. C. Sacchettini, An oral non-covalent non-peptidic inhibitor of SARS-CoV-2 Mpro ameliorates viral replication and pathogenesis in vivo, *Cell Rep.*, 2024, **43**, 114929.
20. T. Miura, T. R. Malla, C. D. Owen, A. Tumber, L. Brewitz, M. A. McDonough, E. Salah, N. Terasaka, T. Katoh, P. Lukacik, C. Strain-Damerell, H. Mikolajek, M. A. Walsh, A. Kawamura, C. J. Schofield and H. Suga, In vitro selection of macrocyclic peptide inhibitors containing cyclic γ2,4-amino acids targeting the SARS-CoV-2 main protease, *Nat. Chem.*, 2023, **15**, 998–1005.
21. T. Miura, T. R. Malla, L. Brewitz, A. Tumber, E. Salah, K. J. Lee, N. Terasaka, C. D. Owen, C. Strain-Damerell, P. Lukacik, M. A. Walsh, A. Kawamura, C. J. Schofield, T. Katoh and H. Suga, Cyclic β2,3-amino acids improve the serum stability of macrocyclic peptide inhibitors targeting the SARS-CoV-2 main protease, *Bull. Chem. Soc. Jpn.*, 2024, **97**, uoae018.
22. Y. Tan, J. Yang, M. Wang, Q. Peng, Y. Li, L. Fu, M. Zhang, J. Wu, G. Yang, C. J. Hipolito, Y. Zhang, J. Qi, Y. Shi and Y. Yin, De Novo Discovery of a Noncovalent Cell-Penetrating Bicyclic Peptide Inhibitor Targeting SARS-CoV-2 Main Protease, *J. Med. Chem.*, 2024, **67**, 20258–20274.
23. K. Harrison, P. W. Carlos, S. Ullrich, A. Aggarwal, J. Johansen-Leete, V. M. Sasi, I. Barter, J. W. C. Maxwell, M. J. Bedding, M. Larance, S. Turville, A. Norman, C. J. Jackson, C. Nitsche and R. J. Payne, Exploiting Hydrophobic Amino Acid Scanning to Develop Cyclic Peptide Inhibitors of the SARS-CoV-2 Main Protease with Antiviral Activity, *Chem. Eur. J*, 2024, **30**, e202401606.
24. J. Johansen-Leete, S. Ullrich, S. E. Fry, R. Frkic, M. J. Bedding, A. Aggarwal, A. S. Ashhurst, K. B. Ekanayake, M. C. Mahawaththa, V. M. Sasi, S. Luedtke, D. J. Ford, A. J. O'Donoghue, T. Passioura, M. Larance, G. Otting, S. Turville, C. J. Jackson, C. Nitsche and R. J. Payne, Antiviral cyclic peptides targeting the main protease of SARS-CoV-2, *Chem. Sci.*, 2022, **13**, 3826–3836.
25. M. Westberg, Y. Su, X. Zou, P. Huang, A. Rustagi, J. Garhyan, P. B. Patel, D. Fernandez, Y. Wu, C. Hao, C.-W. Lo, M. Karim, L. Ning, A. Beck, P. Saenkham-Huntsinger, V. Tat, A. Drelich, B.-H. Peng, S. Einav, C.-T. K. Tseng, C. Blish and M. Z. Lin, An orally bioavailable SARS-CoV-2 main protease inhibitor exhibits improved affinity and reduced sensitivity to mutations, *Sci. Transl. Med.*, **16**, eadi0979.
26. J. Breidenbach, R. Voget, Y. Si, A. Hingst, T. Claff, K. Sylvester, V. Wolf, V. Krasniqi, A. Useini, N. Sträter, Y. Ogura, A. Kawaguchi, C. E. Müller and M. Gütschow, Macrocyclic Azapeptide Nitriles: Structure-Based Discovery of Potent SARS-CoV-2 Main Protease Inhibitors as Antiviral Drugs, *J. Med. Chem.*, 2024, **67**, 8757–8790.
27. M. H. J. Rhodin, A. C. Reyes, A. Balakrishnan, N. Bisht, N. M. Kelly, J. S. Gibbons, J. Lloyd, M. Vaine, T. Cressey, M. Crepeau, R. Shen, N. Manalo, J. Castillo, R. E. Levene, D. Leonard, T. Zang, L. Jiang, K. Daniels, R. M. Cox, C. M. Lieber, J. D. Wolf, R. K. Plemper, S. R. Leist, T. Scobey, R. S. Baric, G. Wang, B. Goodwin and Y. S. Or, The small molecule inhibitor of SARS-CoV-2 3CLpro EDP-235 prevents viral replication and transmission in vivo, *Nat. Commun.*, 2024, **15**, 6503.

28. C. M. N. Allerton, J. T. Arcari, L. M. Aschenbrenner, M. Avery, B. M. Bechle, M. A. Behzadi, B. Boras, L. M. Buzon, R. D. Cardin, N. R. Catlin, A. A. Carlo, K. J. Coffman, A. Dantonio, L. Di, H. Eng, K. A. Farley, R. A. Ferre, S. S. Gernhardt, S. A. Gibson, S. E. Greasley, S. R. Greenfield, B. L. Hurst, A. S. Kalgutkar, E. Kimoto, L. Lanyon, G. H. Lovett, Y. Lian, W. Liu, L. A. Martínez Alsina, S. Noell, R. S. Obach, D. R. Owen, N. C. Patel, D. K. Rai, M. R. Reese, H. A. Rothan, S. Sakata, M. F. Sammons, J. G. Sathish, R. Sharma, C. M. Steppan, J. B. Tuttle, P. R. Verhoest, L. Wei, Q. Yang, I. Yurgelonis and Y. Zhu, A Second-Generation Oral SARS-CoV-2 Main Protease Inhibitor Clinical Candidate for the Treatment of COVID-19, *J. Med. Chem.*, 2024, **67**, 13550–13571.
29. L. Brewitz and C. J. Schofield, Fixing the Achilles Heel of Pfizer's Paxlovid for COVID-19 Treatment, *J. Med. Chem.*, 2024, **67**, 11656–11661.
30. S. Iketani, H. Mohri, B. Culbertson, S. J. Hong, Y. Duan, M. I. Luck, M. K. Annavajhala, Y. Guo, Z. Sheng, A.-C. Uhlemann, S. P. Goff, Y. Sabo, H. Yang, A. Chavez and D. D. Ho, Multiple pathways for SARS-CoV-2 resistance to nirmatrelvir, *Nature*, 2023, **613**, 558–564.
31. N. S. Zuckerman, E. Bucris, D. Keidar-Friedman, M. Amsalem and T. Brosh-Nissimov, Nirmatrelvir Resistance—de Novo E166V/L50V Mutations in an Immunocompromised Patient Treated With Prolonged Nirmatrelvir/Ritonavir Monotherapy Leading to Clinical and Virological Treatment Failure—a Case Report, *Clinical Infectious Diseases*, 2024, **78**, 352–355.
32. Y. Zhou, K. A. Gammeltoft, L. A. Ryberg, L. V. Pham, H. D. Tjørnelund, A. Binderup, C. R. Duarte Hernandez, C. Fernandez-Antunez, A. Offersgaard, U. Fahnøe, G. H. J. Peters, S. Ramirez, J. Bukh and J. M. Gottwein, Nirmatrelvir-resistant SARS-CoV-2 variants with high fitness in an infectious cell culture system, *Sci. Adv.*, **8**, eadd7197.
33. E. Heilmann, F. Costacurta, S. A. Moghadasi, C. Ye, M. Pavan, D. Bassani, A. Volland, C. Ascher, A. K. H. Weiss, D. Bante, R. S. Harris, S. Moro, B. Rupp, L. Martinez-Sobrido and D. von Laer, SARS-CoV-2 3CLpro mutations selected in a VSV-based system confer resistance to nirmatrelvir, ensitrelvir, and GC376, *Sci. Transl. Med.*, **15**, eabq7360.
34. N. Petrišič, M. Adamek, A. Kežar, S. B. Hočevar, E. Žagar, G. Anderluh and M. Podobnik, Structural basis for the unique molecular properties of broad-range phospholipase C from Listeria monocytogenes, *Nature Communications*, 2023, **14**, 6474.
35. J. D. Ip, A. Wing-Ho Chu, W.-M. Chan, R. Cheuk-Ying Leung, S. M. Umer Abdullah, Y. Sun and K. K.-W. To, Global prevalence of SARS-CoV-2 3CL protease mutations associated with nirmatrelvir or ensitrelvir resistance, *eBioMedicine*, 2023, **91**.
36. U. Theuretzbacher, K. Bush, S. Harbarth, M. Paul, J. H. Rex, E. Tacconelli and G. E. Thwaites, Critical analysis of antibacterial agents in clinical development, *Nat. Rev. Microbiol.*, 2020, **18**, 286–298.
37. K. Bush and P. A. Bradford, β-Lactams and β-Lactamase Inhibitors: An Overview, *Cold Spring Harb. Perspect. Med.*, 2016, **6**, a025247.
38. G. Ozcengiz and A. L. Demain, Recent advances in the biosynthesis of penicillins, cephalosporins and clavams and its regulation, *Biotechnol. Adv.*, 2013, **31**, 287–311.
39. D. Y. Wang, M. I. Abboud, M. S. Markoulides, J. Brem and C. J. Schofield, The Road to Avibactam: The First Clinically Useful Non-β-Lactam Working Somewhat Like a β-Lactam, *Future Medicinal Chemistry*, 2016, **8**, 1063–1084.

40. L. M. Lima, B. N. M. da Silva, G. Barbosa and E. J. Barreiro, β-lactam antibiotics: An overview from a medicinal chemistry perspective, *European Journal of Medicinal Chemistry*, 2020, **208**, 112829.
41. T. R. Malla, A. Tumber, T. John, L. Brewitz, C. Strain-Damerell, C. D. Owen, P. Lukacik, H. T. H. Chan, P. Maheswaran, E. Salah, F. Duarte, H. Yang, Z. Rao, M. A. Walsh and C. J. Schofield, Mass spectrometry reveals potential of β-lactams as SARS-CoV-2 Mpro inhibitors, *Chem. Commun.*, 2021, **57**, 1430–1433.
42. T. R. Malla, L. Brewitz, D.-G. Muntean, H. Aslam, C. D. Owen, E. Salah, A. Tumber, P. Lukacik, C. Strain-Damerell, H. Mikolajek, M. A. Walsh and C. J. Schofield, Penicillin Derivatives Inhibit the SARS-CoV-2 Main Protease by Reaction with Its Nucleophilic Cysteine, *J. Med. Chem.*, 2022, **65**, 7682–7696.
43. S. T. D. Thun-Hohenstein, T. F. Suits, T. R. Malla, A. Tumber, L. Brewitz, H. Choudhry, E. Salah and C. J. Schofield, Structure-Activity Studies Reveal Scope for Optimisation of Ebselen-Type Inhibition of SARS-CoV-2 Main Protease, *ChemMedChem*, 2022, **17**, e202100582.
44. Gayatri, L. Brewitz, L. Ibbotson, E. Salah, S. Basak, H. Choudhry and C. J. Schofield, Thiophene-fused γ-lactams inhibit the SARS-CoV-2 main protease via reversible covalent acylation, *Chem. Sci.*, 2024, **15**, 7667–7678.
45. L. Verbist, In vitro activity of temocillin (BRL 17421), a novel beta-lactamase-stable penicillin, *Antimicrob. Agents Chemother.*, 1982, **22**, 157–161.
46. M. Sacco, D., K. G. Kroeck, M. T. Kemp, X. Zhang, L. D. Andrews and Y. Chen, Influence of the α-Methoxy Group on the Reaction of Temocillin with Pseudomonas aeruginosa PBP3 and CTX-M-14 β-Lactamase, *Antimicrob. Agents Chemother.*, 2019, **64**, 10.1128/aac.01473–01419.
47. J. Hamilton-Miller and W. Brumfitt, Cephamycins: A review, prospects and some original observations, *Infection*, 1975, **3**, 183–188.
48. J. E. Baldwin, F. J. Urban, R. D. G. Cooper and F. L. Jose, Direct 6-methoxylation of penicillin derivatives. Convenient pathway to substituted .beta.-lactam antibiotics, *J. Am. Chem. Soc.*, 1973, **95**, 2401–2403.
49. J. Cooper, D. C. Humber, B. Laundon, A. G. Long and A. L. Lynd, Synthesis of functionalized penicillins and cephalosporins by photo-initiated bromination a novel route to ampicillin and cephalexin from penicillin g, *Tetrahedron*, 1984, **40**, 4153–4157.
50. P. H. Bentley, J. P. Clayton, M. O. Boles and R. J. Girven, Transformations using benzyl 6-isocyanopenicillanate, *J. Chem. Soc., Perkin Trans. 1*, 1979, 2455–2467.
51. W. A. Spitzer and T. Goodson, The synthesis of s-methyl and o-methyl β-lactam antibiotics, *Tetrahedron Lett.*, 1973, **14**, 273–276.
52. H. Kamachi, T. Okita, T. Yamasaki and T. Naito, Direct introduction of a formamido group into the 7α(6α)-position of cephalosporins (pencillins), *J. Antibiot.*, 1990, **43**, 820–829.
53. H. Yanagisawa, M. Fukushima, A. Ando and H. Nakao, SYNTHESIS OF 7α-SUBSTITUTED CEPHALOSPORINS. V, *J. Antibiot.*, 1976, **29**, 969–972.
54. A. W. Chow, N. M. Hall and J. R. E. Hoover, Penicillin Sulfoxides and Sulfones, *J. Org. Chem.*, 1962, **27**, 1381–1383.
55. D. H. R. Barton, F. Comer, D. G. T. Greig, P. G. Sammes, C. M. Cooper, G. Hewitt and W. G. E. Underwood, Transformations of penicillin. Part I. Preparation and rearrangements of 6β-phenylacetamidopenicillanic sulphoxides, *J. Chem. Soc. C Org.*, 1971, 3540–3550.

56. P. J. Giddings, D. I. John, E. J. Thomas and D. J. Williams, Preparation of 6α-monosubstituted and 6,6-disubstituted penicillanates from 6-diazopenicillanates: Reactions of 6-diazopenicillanates with alcohols, thiols, phenylseleninyl compounds, and allylic sulphides, and their analogues, *J. Chem. Soc., Perkin Trans. 1*, 1982, 2757–2766.
57. P. J. Giddings, D. I. John and E. J. Thomas, Some lewis acid catalysed reactions of 2,2,2-trichloroethyl 6-diazopenicillanate, *Tetrahedron Lett.*, 1978, **19**, 995–998.
58. P. M. Blumberg and J. L. Strominger, Interaction of penicillin with the bacterial cell: penicillin-binding proteins and penicillin-sensitive enzymes, *Bacteriol. Rev.*, 1974, **38**, 291–335.
59. M. Mora-Ochomogo and C. T. Lohans, β-Lactam antibiotic targets and resistance mechanisms: from covalent inhibitors to substrates, *RSC Medicinal Chemistry*, 2021, **12**, 1623–1639.
60. G. Burton, M. J. Basker, D. J. Best, F. P. Harrington and A. W. Taylor, Preparation and structure-activity relationships of some 6α-substituted penicillins, *The Journal of Antibiotics*, 1985, **38**, 721–739.
61. J. M. Indelicato and W. L. Wilham, Effect of 6-.alpha. substitution in penicillins and 7-.alpha. substitution in cephalosporins upon .beta.-lactam reactivity, *J. Med. Chem.*, 1974, **17**, 528–529.
62. D. M. Livermore and P. M. Tulkens, Temocillin revived, *J. Antimicrob. Chemother.*, 2009, **63**, 243–245.
63. R. N. Brogden, R. C. Heel, T. M. Speight and G. S. Avery, Ticarcillin: A Review of its Pharmacological Properties and Therapeutic Efficacy, *Drugs*, 1980, **20**, 325–352.
64. K. Jules and H. C. Neu, Antibacterial activity and beta-lactamase stability of temocillin, *Antimicrob. Agents Chemother.*, 1982, **22**, 453–460.
65. R. N. Jones, Cefmetazole (CS-1170), a "new" cephamycin with a decade of clinical experience, *Diagn. Microbiol. Infect. Dis.*, 1989, **12**, 367–379.
66. A. K. Miller, E. Celozzi, A. Pelak Barbara, O. Stapley Edward and D. Hendlin, Cephamycins, a New Family of β-Lactam Antibiotics. III. In Vitro Studies, *Antimicrob. Agents Chemother.*, 1972, **2**, 281–286.
67. B. Lee, Conformation of penicillin as a transition-state analog of the substrate of peptidoglycan transpeptidase, *J. Mol. Biol.*, 1971, **61**, 463–469.
68. H. R. Josephine, I. Kumar and R. F. Pratt, The Perfect Penicillin? Inhibition of a Bacterial DD-Peptidase by Peptidoglycan-Mimetic β-Lactams, *J. Am. Chem. Soc.*, 2004, **126**, 8122–8123.
69. N. R. Silvaggi, H. R. Josephine, A. P. Kuzin, R. Nagarajan, R. F. Pratt and J. A. Kelly, Crystal Structures of Complexes between the R61 DD-peptidase and Peptidoglycan-mimetic β-Lactams: A Non-covalent Complex with a "Perfect Penicillin"††This article is dedicated to the memory of Professor Jean-Marie Ghuysen of the Université de Liège, Belgium, in recognition of his decades of contributions towards our understanding of and ability to combat bacterial infections, *J. Mol. Biol.*, 2005, **345**, 521–533.
70. M. A. McDonough, J. W. Anderson, N. R. Silvaggi, R. F. Pratt, J. R. Knox and J. A. Kelly, Structures of Two Kinetic Intermediates Reveal Species Specificity of Penicillin-binding Proteins, *J. Mol. Biol.*, 2002, **322**, 111–122.
71. S. B. Rosenblum, T. Huynh, A. Afonso, H. R. Davis, N. Yumibe, J. W. Clader and D. A. Burnett, Discovery of 1-(4-Fluorophenyl)-(3R)-[3-(4-fluorophenyl)-(3S)- hydroxypropyl]-

(4S)-(4-hydroxyphenyl)-2-azetidinone (SCH 58235): A Designed, Potent, Orally Active Inhibitor of Cholesterol Absorption, *J. Med. Chem.*, 1998, **41**, 973–980.
72. H. R. Davis, L.-j. Zhu, L. M. Hoos, G. Tetzloff, M. Maguire, J. Liu, X. Yao, S. P. N. Iyer, M.-H. Lam, E. G. Lund, P. A. Detmers, M. P. Graziano and S. W. Altmann, Niemann-Pick C1 Like 1 (NPC1L1) Is the Intestinal Phytosterol and Cholesterol Transporter and a Key Modulator of Whole-body Cholesterol Homeostasis*, *J. Biol. Chem.*, 2004, **279**, 33586–33592.
73. R.-S. Mani, The emerging role of speckle-type POZ protein (SPOP) in cancer development, *Drug Discovery Today*, 2014, **19**, 1498–1502.
74. L. Chen, Z. Fan, J. Chang, R. Yang, H. Hou, H. Guo, Y. Zhang, T. Yang, C. Zhou, Q. Sui, Z. Chen, C. Zheng, X. Hao, K. Zhang, R. Cui, Z. Zhang, H. Ma, Y. Ding, N. Zhang, X. Lu, X. Luo, H. Jiang, S. Zhang and M. Zheng, Sequence-based drug design as a concept in computational drug design, *Nat. Commun.*, 2023, **14**, 4217.
75. C. Zhou, X. Hao, Z. Chen, R. Zhang, Q. Zhou, Z. Fan, M. Zheng, H. Hou, S. Zhang and H. Guo, Synthesis and Biological Evaluation of β-Lactam Derivatives Targeting Speckle-Type POZ Protein (SPOP), *ACS Medicinal Chemistry Letters*, 2024, **15**, 270–279.
76. D. Jelisejevs, A. L. Bula and L. Kinena, Pyrazolidinone-based peptidomimetic SARS-CoV-2 Mpro inhibitors, *Bioorg. Med. Chem. Lett.*, 2023, **96**, 129530.
77. R. A. Eid, M. O. Elgendy, A. O. El-Gendy, S. O. Elgendy, L. Belbahri, A. M. Sayed and M. E. Rateb, *Antibiotics*, 2021, **10**.
78. F. A. Ambrosio, G. Costa, I. Romeo, F. Esposito, M. Alkhatib, R. Salpini, V. Svicher, A. Corona, P. Malune, E. Tramontano, F. Ceccherini-Silberstein, S. Alcaro and A. Artese, Targeting SARS-CoV-2 Main Protease: A Successful Story Guided by an In Silico Drug Repurposing Approach, *Journal of Chemical Information and Modeling*, 2023, **63**, 3601–3613.
79. C.-t. Yang, N. O. Devarie-Baez, A. Hamsath, X.-d. Fu and M. Xian, S-Persulfidation: Chemistry, Chemical Biology, and Significance in Health and Disease, *Antioxid. Redox. Signal.*, 2019, **33**, 1092–1114.
80. K. Borbényi-Galambos, Á. Czikora, K. Erdélyi and P. Nagy, Versatile roles of cysteine persulfides in tumor biology, *Curr. Opin. Chem. Biol.*, 2024, **79**, 102440.
81. P. Ren, H. Li, T. Nie, X. Jian, C. Yu, J. Li, H. Su, X. Zhang, S. Li, X. Yang, C. Peng, Y. Yin, L. Zhang, Y. Xu, H. Liu and F. Bai, Discovery and Mechanism Study of SARS-CoV-2 3C-like Protease Inhibitors with a New Reactive Group, *J. Med. Chem.*, 2023, **66**, 12266–12283.
82. P. Sahoo, D. R. Lenka, M. Batabyal, P. K. Pain, S. Kumar, D. Manna and A. Kumar, Detailed Insights into the Inhibitory Mechanism of New Ebselen Derivatives against Main Protease (Mpro) of Severe Acute Respiratory Syndrome Coronavirus-2 (SARS-CoV-2), *ACS Pharmacol. Transl. Sci.*, 2023, **6**, 171–180.
83. K. Amporndanai, X. Meng, W. Shang, Z. Jin, M. Rogers, Y. Zhao, Z. Rao, Z.-J. Liu, H. Yang, L. Zhang, P. M. O'Neill and S. Samar Hasnain, Inhibition mechanism of SARS-CoV-2 main protease by ebselen and its derivatives, *Nat. Commun.*, 2021, **12**, 3061.
84. V. Gupta and K. S. Carroll, Sulfenic acid chemistry, detection and cellular lifetime, *Biochim. Biophys. Acta - Gen. Subj.*, 2014, **1840**, 847–875.
85. C. M. Pant, J. Steele and R. J. Stoodley, Studies related to penicillins. Part 21. β-Elimination reactions of S,S-dioxides of penicillanic esters, *J. Chem. Soc., Perkin Trans. 1*, 1982, 595–602.

86. R. D. Allan, D. H. R. Barton, M. Girijavallabhan, P. G. Sammes and M. V. Taylor, Transformations of penicillins. Part IV. On the trapping of sulphenic acids from penicillins with thiols, *J. Chem. Soc., Perkin Trans. 1*, 1973, 1182–1187.
87. R. J. Stoodley, Rearrangements of penicillanic acid derivatives, *Tetrahedron*, 1975, **31**, 2321–2345.
88. R. G. Micetich, S. N. Maiti, M. P. Singh, M. Tanaka, T. Yamazaki and K. Ogawa, The trapping of sulfenic acids from penicillin sulfoxides - use of 2,5-dimercapto-1,3,4-thiadiazole and 2,4-dimercaptopyrimidine as trapping agents, *Tetrahedron Lett.*, 1985, **26**, 5611–5614.
89. K. R. Thompson, P. E. Finke, S. K. Shah, B. M. Ashe, M. E. Dahlgren, A. L. Maycock and J. B. Doherty, Inhibition of human leukocyte elastase. 6. Inhibition by 6-substituted penicillin esters, *Bioorganic & Medicinal Chemistry Letters*, 1993, **3**, 2283–2288.
90. W. Bode, E. Meyer, Jr. and J. C. Powers, Human leukocyte and porcine pancreatic elastase: x-ray crystal structures, mechanism, substrate specificity, and mechanism-based inhibitors, *Biochemistry*, 1989, **28**, 1951–1963.
91. A. Fleming, THE DISCOVERY OF PENICILLIN, *British Medical Bulletin*, 1944, **2**, 4–5.
92. J. B. Doherty, B. M. Ashe, L. W. Argenbright, P. L. Barker, R. J. Bonney, G. O. Chandler, M. E. Dahlgren, C. P. Dorn, P. E. Finke, R. A. Firestone, D. Fletcher, W. K. Hagmann, R. Mumford, L. O'Grady, A. L. Maycock, J. M. Pisano, S. K. Shah, K. R. Thompson and M. Zimmerman, Cephalosporin antibiotics can be modified to inhibit human leukocyte elastase, *Nature*, 1986, **322**, 192–194.
93. S. K. Shah, C. P. Dorn, Jr., P. E. Finke, J. J. Hale, W. K. Hagmann, K. A. Brause, G. O. Chandler, A. L. Kissinger and B. M. Ashe, Orally active .beta.-lactam inhibitors of human leukocyte elastase-1. Activity of 3,3-diethyl-2-azetidinones, *J. Med. Chem.*, 1992, **35**, 3745–3754.
94. P. A. Lang, M. de Munnik, A. O. Oluwole, T. D. W. Claridge, C. V. Robinson, J. Brem and C. J. Schofield, How Clavulanic Acid Inhibits Serine β-Lactamases, *ChemBioChem*, 2024, **25**, e202400280.
95. P. A. Lang, R. Raj, A. Tumber, C. T. Lohans, P. Rabe, C. V. Robinson, J. Brem and C. J. Schofield, Studies on enmetazobactam clarify mechanisms of widely used β-lactamase inhibitors, *Proc. Natl. Acad. Sci.*, 2022, **119**, e2117310119.
96. R. N. Brogden, R. C. Heel, T. M. Speight and G. S. Avery, Cefoxitin: A Review of its Antibacterial Activity, Pharmacological Properties and Therapeutic Use, *Drugs*, 1979, **17**, 1–37.
97. R. H. Prabhala, H. Thadepalli, B. Rao, M. B. Bansal and R. Marshall, In vitro activity of cefbuperazone, a new cephamycin, against anaerobic bacteria, *Antimicrob. Agents Chemother.*, 1985, **27**, 640–642.
98. R. Wise, J. M. Andrews and J. Hancox, In vitro activity of cefotetan, a new cephamycin derivative, compared with that of other beta-lactam compounds, *Antimicrob. Agents Chemother.*, 1982, **21**, 486–491.
99. A. A. Carmine, R. N. Brogden, R. C. Heel, J. A. Romankiewicz, T. M. Speight and G. S. Avery, Moxalactam (Latamoxef), *Drugs*, 1983, **26**, 279–333.
100. A. Imada, K. Kitano, K. Kintaka, M. Muroi and M. Asai, Sulfazecin and isosulfazecin, novel β-lactam antibiotics of bacterial origin, *Nature*, 1981, **289**, 590–591.

101. G. Madhavi Sastry, M. Adzhigirey, T. Day, R. Annabhimoju and W. Sherman, Protein and ligand preparation: parameters, protocols, and influence on virtual screening enrichments, *J. Comput. Aided Mol. Des.*, 2013, **27**, 221–234.
102. L. Schrödinger, Maestro.*Journal*, 2023.
103. R. A. Friesner, R. B. Murphy, M. P. Repasky, L. L. Frye, J. R. Greenwood, T. A. Halgren, P. C. Sanschagrin and D. T. Mainz, Extra Precision Glide: Docking and Scoring Incorporating a Model of Hydrophobic Enclosure for Protein−Ligand Complexes, *J. Med. Chem.*, 2006, **49**, 6177–6196.
104. J. Wang, R. M. Wolf, J. W. Caldwell, P. A. Kollman and D. A. Case, Development and testing of a general amber force field, *J. Comput. Chem.*, 2004, **25**, 1157–1174.
105. J. Wang, W. Wang, P. A. Kollman and D. A. Case, Automatic atom type and bond type perception in molecular mechanical calculations, *J. Mol. Graphics Modell.*, 2006, **25**, 247–260.
106. C. I. Bayly, P. Cieplak, W. Cornell and P. A. Kollman, A well-behaved electrostatic potential based method using charge restraints for deriving atomic charges: the RESP model, *J. Phys. Chem.*, 1993, **97**, 10269–10280.
107. M. J. Frisch, G. W. Trucks, H. B. Schlegel, G. E. Scuseria, M. A. Robb, J. R. Cheeseman, G. Scalmani, V. Barone, G. A. Petersson, H. Nakatsuji, X. Li, M. Caricato, A. V. Marenich, J. Bloino, B. G. Janesko, R. Gomperts, B. Mennucci, H. P. Hratchian, J. V. Ortiz, A. F. Izmaylov, J. L. Sonnenberg, Williams, F. Ding, F. Lipparini, F. Egidi, J. Goings, B. Peng, A. Petrone, T. Henderson, D. Ranasinghe, V. G. Zakrzewski, J. Gao, N. Rega, G. Zheng, W. Liang, M. Hada, M. Ehara, K. Toyota, R. Fukuda, J. Hasegawa, M. Ishida, T. Nakajima, Y. Honda, O. Kitao, H. Nakai, T. Vreven, K. Throssell, J. A. Montgomery Jr., J. E. Peralta, F. Ogliaro, M. J. Bearpark, J. J. Heyd, E. N. Brothers, K. N. Kudin, V. N. Staroverov, T. A. Keith, R. Kobayashi, J. Normand, K. Raghavachari, A. P. Rendell, J. C. Burant, S. S. Iyengar, J. Tomasi, M. Cossi, J. M. Millam, M. Klene, C. Adamo, R. Cammi, J. W. Ochterski, R. L. Martin, K. Morokuma, O. Farkas, J. B. Foresman and D. J. Fox, Gaussian 16 Rev. C.01.*Journal*, 2016.
108. H. M. A. D.A. Case, K. Belfon, I.Y. Ben-Shalom, J.T. Berryman, S.R. Brozell, D.S. Cerutti, T.E. Cheatham, III, G.A. Cisneros, V.W.D. Cruzeiro, T.A. Darden, N. Forouzesh, M. Ghazimirsaeed, G. Giambaşu, T. Giese, M.K. Gilson, H. Gohlke, A.W. Goetz, J. Harris, Z. Huang, S. Izadi, S.A. Izmailov, K. Kasavajhala, M.C. Kaymak, A. Kovalenko, T. Kurtzman, T.S. Lee, P. Li, Z. Li, C. Lin, J. Liu, T. Luchko, R. Luo, M. Machado, M. Manathunga, K.M. Merz, Y. Miao, O. Mikhailovskii, G. Monard, H. Nguyen, K.A. O'Hearn, A. Onufriev, F. Pan, S. Pantano, A. Rahnamoun, D.R. Roe, A. Roitberg, C. Sagui, S. Schott-Verdugo, A. Shajan, J. Shen, C.L. Simmerling, N.R. Skrynnikov, J. Smith, J. Swails, R.C. Walker, J. Wang, J. Wang, X. Wu, Y. Wu, Y. Xiong, Y. Xue, D.M. York, C. Zhao, Q. Zhu, and P.A. Kollman, Amber 2024.*Journal*, 2024.
109. D. A. Case, H. M. Aktulga, K. Belfon, D. S. Cerutti, G. A. Cisneros, V. W. D. Cruzeiro, N. Forouzesh, T. J. Giese, A. W. Götz, H. Gohlke, S. Izadi, K. Kasavajhala, M. C. Kaymak, E. King, T. Kurtzman, T.-S. Lee, P. Li, J. Liu, T. Luchko, R. Luo, M. Manathunga, M. R. Machado, H. M. Nguyen, K. A. O'Hearn, A. V. Onufriev, F. Pan, S. Pantano, R. Qi, A. Rahnamoun, A. Risheh, S. Schott-Verdugo, A. Shajan, J. Swails, J. Wang, H. Wei, X. Wu, Y. Wu, S. Zhang, S. Zhao, Q. Zhu, T. E. Cheatham, III, D. R. Roe, A. Roitberg, C. Simmerling, D. M. York, M. C. Nagan and K. M. Merz, Jr., AmberTools, *J. Chem. Inf. Model.*, 2023, **63**, 6183–6191.

110. H. J. C. Berendsen, J. P. M. Postma, W. F. van Gunsteren, A. DiNola and J. R. Haak, Molecular dynamics with coupling to an external bath, *J. Chem. Phys.*, 1984, **81**, 3684–3690.
111. W. L. Jorgensen, J. Chandrasekhar, J. D. Madura, R. W. Impey and M. L. Klein, Comparison of simple potential functions for simulating liquid water, *J. Chem. Phys.*, 1983, **79**, 926–935.
112. J.-P. Ryckaert, G. Ciccotti and H. J. C. Berendsen, Numerical integration of the cartesian equations of motion of a system with constraints: molecular dynamics of n-alkanes, *J. Comput. Phys.*, 1977, **23**, 327–341.
113. J. A. Maier, C. Martinez, K. Kasavajhala, L. Wickstrom, K. E. Hauser and C. Simmerling, ff14SB: Improving the Accuracy of Protein Side Chain and Backbone Parameters from ff99SB, *J. Chem. Theory Comput.*, 2015, **11**, 3696–3713.
114. D. R. Roe and T. E. Cheatham, III, PTRAJ and CPPTRAJ: Software for Processing and Analysis of Molecular Dynamics Trajectory Data, *J. Chem. Theory Comput.*, 2013, **9**, 3084–3095.

2.3 Statement of Authorship

Title of Paper	C6-Alkoxy substituted penicillins are potent non-covalently binding inhibitors of the SARS-CoV-2 main protease
Publication Status	□Published ☒Accepted for Publication □Submitted for Publication □Unpublished and unsubmitted work written in a manuscript style
Publication Details	**Muntean, D.-G.**; Treyde, W.; Kinena, L.; Salah, E.; Choudhry, H.; Duarte, F.; Brewitz, L.; Schofield, C.J.: **C6-Alkoxy substituted penicillins are potent non-covalently binding inhibitors of the SARS-CoV-2 main protease**

Student Confirmation

Student Name:	Dorian-Gabriel Muntean		
Contribution to the Paper	D.-G.M. conducted the SAR study on C6-alkoxypenicillin M^{pro} inhibitors, designed the synthetic routes, and carried out most of the synthesis. D.-G.M. conceptualised and prepared the first draft of the manuscript. W.T. conducted the modelling studies. L.K. synthesised C6-ethoxy penicillin V sulfone benzyl ester and C6-benzyloxy penicillin V benzyl ester. E.S. produced M^{pro} enzyme. F.D. provided supervision of the modelling studies. H.C. provided resources. L.B. provided supervision of the synthetic work, obtained the IC_{50} data, conducted protein-observed MS experiments with M^{pro}, and assisted with manuscript reviewing/editing. C.J.S. is the principal investigator/supervisor of the research described in the manuscript, contributed extensively to project/data conceptualization and visualization, and manuscript reviewing/editing.		
Signature 		Date	09/10/2025

Supervisor Confirmation

By signing the Statement of Authorship, you are certifying that the candidate made a substantial contribution to the publication, and that the description described above is accurate

Supervisor name and title: Prof. Christopher J. Schofield		
Supervisor comments:		
Signature 	Date	09/10/2025

Chapter 3. Development of cephalosporins as potent inhibitors of SARS-CoV-2 M^{pro}

3.1 Chapter overview

Chapter 3 describes structure-activity relationship (SAR) studies on cephalosporin derivatives for SARS-CoV-2 main protease (M^{pro}) inhibition. A screen of commercially sourced cephalosporins led to the identification of cephalosporin G 3-chloromethyl *p*-methoxybenzyl ester (**GCLE**) as a potent inhibitor of M^{pro} ($IC_{50} \sim 30$ nM). Protein-observed mass-spectrometric (MS) assays revealed that **GCLE** is a covalent inhibitor that selectively *S*-acylates the nucleophilic cysteine residue, Cys145. SAR investigations revealed that variations at the C3 position of the cephalosporin scaffold are critical for both tuning potency and modulating the mechanism by which cephalosporin derivatives inhibit M^{pro}, with a clear preference for C3 electron-withdrawing groups being observed. While C3-chloromethyl cephalosporins displayed the most potent inhibition of M^{pro}, good activity was also observed for both C3-formyl cephalosporins, which promote covalent modification of M^{pro}, and C3' quaternary ammonium cephalosporins, which inhibited M^{pro} via a non-covalent mechanism. Preliminary cellular studies show that cephalosporin derivatives suppress SARS-CoV-2 replication in infected cells, highlighting the potential of developing cephalosporin-based M^{pro} inhibitors as antiviral agents.

Manuscript II

At the time of writing this thesis, Manuscript II is in preparation for publication. A Statement of Authorship is appended at the end of the chapter. The synthetic experimental details and spectra of the compounds prepared can be found in the **Appendix**.

Muntean, **D.-G.**; Brewitz, L.; Laczi, D.; Salah, E.; Laidlaw, S.; Carol, M.; Schofield, C.J.: **Cephalosporin derivatives are potent inhibitors of the SARS-CoV-2 main protease**

3.2 Manuscript II: Cephalosporin derivatives are potent inhibitors of the SARS-CoV-2 main protease

3.2.1 Abstract

The SARS-CoV-2 main protease (M^{pro}), which contains a cysteine-histidine catalytic dyad, plays a pivotal role in viral replication and is a validated therapeutic target. Building on the known efficacy of β-lactams as inhibitors of nucleophilic serine enzymes, we have previously shown that derivatives of clinically used antibiotics can inhibit M^{pro} through formation of stable acyl-enzyme complexes, as supported by mass spectrometric (MS) and crystallographic studies. Here we report the development of a novel cephalosporin derivative that displays exceptional inhibition of SARS-CoV-2 M^{pro} (IC_{50} ~ 30 nM). Structure-activity relationship (SAR) studies on the cephalosporin scaffold revealed that the identity of the C3 substituent influences both potency and the mechanism of inhibition, with covalent and non-covalent modes of action being observed. Some cephalosporin-based M^{pro} inhibitors were also found to suppress SARS-CoV-2 replication in infected cells. The results imply that cephalosporin derivatives can be developed as potent antiviral agents against SARS-CoV-2.

Key words: SARS-CoV-2 main protease; M^{pro}; nucleophilic cysteine inhibition; β-lactam; cephalosporin; covalent inhibitors; non-covalent inhibitors; COVID-19.

3.2.2 Introduction

The β-lactam ring is an important structural motifs in medicinal chemistry, with its intrinsic ring strain conferring reactivity that, in part, enables efficient covalent modification of nucleophilic residues.[1-5] The β-lactam ring is the defining feature of β-lactam antibiotics, which include penicillins, cephalosporins, carbapenems, and monobactams;[1] although their substitution patterns and fused ring systems differ, the primary targets of β-lactam antibiotics are penicillin-binding proteins (PBPs), the transpeptidases responsible for bacterial cell wall biosynthesis.[6-8] β-Lactam antibiotics compete with the natural D-Ala-D-Ala containing substrate of penicillin-binding proteins (PBPs);[6-8] they selectively acylate the nucleophilic serine residues of PBPs, thereby preventing the cross-linking of peptidoglycan and ultimately resulting in cell lysis and death.[9]

Beyond their traditional antibacterial role, β-lactams have also been explored in alternative therapeutic areas,[10-14] including clinical applications such as antihypercholesterolemic agents,[15, 16] as well as investigational uses in oncology,[17-39] inflammation,[40-56] fungal infections,[57-61] and viral diseases.[62-71] β-Lactams have emerged as a promising scaffold for the development of SARS-CoV-2 main protease (M^{pro}) inhibitors.[67, 68] M^{pro} is a cysteine protease with a crucial role in the viral cycle of SARS-CoV-2, where it catalyses hydrolysis of the viral polyproteins 1a and 1ab (pp1a/1ab) to give non-structural proteins.[72-75] Therefore, inhibition of M^{pro} catalysis leads to the disruption of viral replication,[74, 75] and M^{pro} inhibition is a validated therapeutic strategy.

Penicillin V derivative **1** (**Figure 1**) was identified as a covalent inhibitor of M^{pro},[67] with mass spectrometry (MS)-based assays and crystallographic studies showing that penicillin V sulfone esters selectively *S*-acylate the nucleophilic cysteine residue Cys145 of M^{pro}.[68] Reported modelling studies predicted that cephalosporin derivatives, including clinically used agents, might display favourable binding poses at the M^{pro} active site;[69, 76] subsequently, **cefaclor**, **cefoperazone** and

ceftaroline fosamil were tested in fluorescence resonance energy transfer (FRET)-based assays, reportedly inhibiting M^{pro} in the micromolar range.[69] By contrast, our MS assays revealed that **cefaclor**, **cefepime**, and **cephalosporin C** exhibited modest or weak M^{pro} inhibitory properties (*i.e.*, 9-80% inhibition at 20 μM concentration) and that **cefotetan**, **cefbuperazone** and **cefoxitin** covalently reacted with M^{pro}, albeit not with 1:1 stoichiometry, suggesting non-specific reactions.[67]

Given that the structural versatility of cephalosporin antibiotics is greater than that of penicillin antibiotics, it was of interest to explore whether informed substituent modifications on the cephalosporin core, coupled with strategic functional group changes (as inspired by penicillin ester derivatives), could results in the optimisation of cephalosporin derivatives for enhanced M^{pro} inhibition. Here, we report MS studies with isolated SARS-CoV-2 M^{pro} and a representative set of ~40 clinically used cephalosporins, showing that only **ceftaroline**, the metabolite of prodrug **ceftaroline fosamil**,[77, 78] inhibited M^{pro} catalysis efficiently. Importantly, it was also observed that the cephalosporin G 3-chloromethyl *p*-methoxybenzyl ester (**GCLE**; **Figure 1**), an intermediate commonly used in the synthesis of cephalosporin antibiotics, possesses exceptional inhibitory properties against M^{pro}, displaying >200-fold potency improvement over penicillin V sulfone **1**. Subsequent structure-activity relationship (SAR) studies on **GCLE** afforded highly efficient M^{pro} inhibitors that suppressed SARS-CoV-2 replication in infected cells, thereby demonstrating that scaffold hopping from the penicillin to the cephalosporin core can confer a marked improvement in potency.

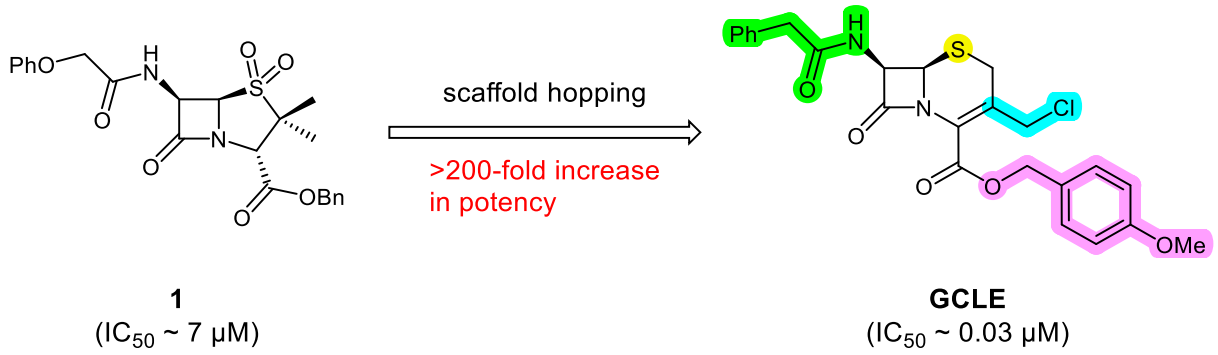

1
(IC_{50} ~ 7 μM)

GCLE
(IC_{50} ~ 0.03 μM)

Figure 1. Development of M^{pro} β-lactam-based inhibitors.

3.2.3 Results

GCLE is a potent M^{pro} inhibitor

The effects of 40 representative commercially sourced cephalosporins on the activity of isolated recombinant SARS-CoV-2 M^{pro} were investigated using reported SPE-MS assays[67] to inform on their potential for inhibitor development (**Table 1** and **Supporting Table S1**). The results reveal that most of the cephalosporins did not inhibit, including the reported[69] M^{pro} inhibitors **cefaclor**, **cefoperazone**, and **ceftaroline fosamil** (IC_{50} > 50 μM; **Table 1**, entries i-iii). By contrast, **ceftaroline**, without the *N*-phosphono group of prodrug **ceftaroline fosamil**,[77] inhibited M^{pro} (IC_{50} ~ 3.0 μM; **Table 1**, entry iv). Notably, the screen identified the cephalosporin G 3-chloromethyl *p*-methoxybenzyl ester (**GCLE**) as a very efficient M^{pro} inhibitor (IC_{50} ~ 0.03 μM; **Table 1**, entry v). Protein-observed MS studies were conducted under denaturing conditions to test for the covalent reaction of M^{pro} with **ceftaroline** and **GCLE**. While **ceftaroline** did not promote the formation of a covalent adduct with M^{pro}, suggesting that inhibition is non-covalent in nature, incubation of M^{pro} with **GCLE** (486.1 Da) for >15 h manifested an M^{pro} mass shift of ~451 Da, indicating that loss of chloride from **GCLE** occurs upon covalent reaction with M^{pro} (**Supporting Figure S2**).

Table 1. Inhibition of SARS-CoV-2 M^{pro} by selected cephalosporin antibiotics.

	Cephalosporin	[(a)]IC_{50} [μM]
i	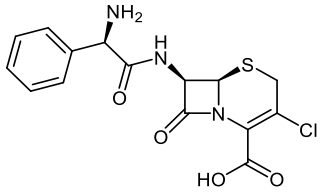 **Cefaclor**	>50 (reported[69]: ~ 24)
ii	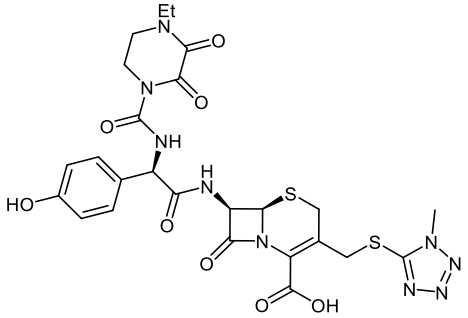 **Cefoperazone**	>50 (reported[69]: ~ 5)
iii	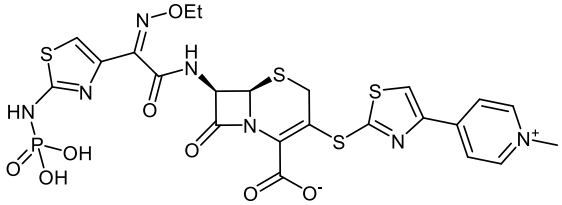 **Ceftaroline fosamil**	>50 (reported[69]: ~ 19)
iv	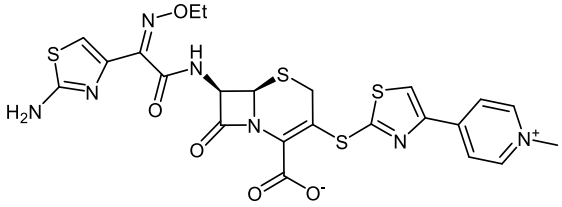 **Ceftaroline**	3.0 ± 0.4
v	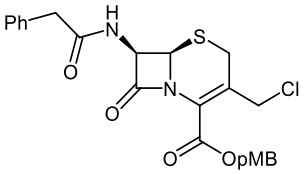 **GCLE**	0.03 ± 0.01

[(a)] M^{pro} inhibition assays were performed using SPE-MS as reported,[67, 79] utilizing SARS-CoV-2 M^{pro} (0.05 μM) and substrate (2.0 μM). Results are means of three independent biological experiments, each in technical duplicates (n = 3; mean ± SD). Additional IC_{50} data are available in **Supporting Table S1**. pMB: $–CH_2C_6H_4$(4-OMe).

GCLE selectively acylates M^{pro} Cys145

To further investigate the mechanism via which **GCLE** inhibits M^{pro}, the reaction was monitored for ~ 60 min using SPE-MS.[68, 79] The results showed that **GCLE** led to the initial formation of two covalent adducts corresponding to +486 Da and +451 Da mass shifts (**Figure 2A**); after 10 min, M^{pro} was completely converted to the +451 Da covalent adduct, and the +486 Da species was no longer observed. Based on these observations, it was proposed that that **GCLE** acylates a nucleophile residue of M^{pro} (**Figure 2B**), likely Cys145, to initially give acyl-enzyme complex **I** (+486 Da), which then further fragments to eliminate the C3' chloride (+451 Da).

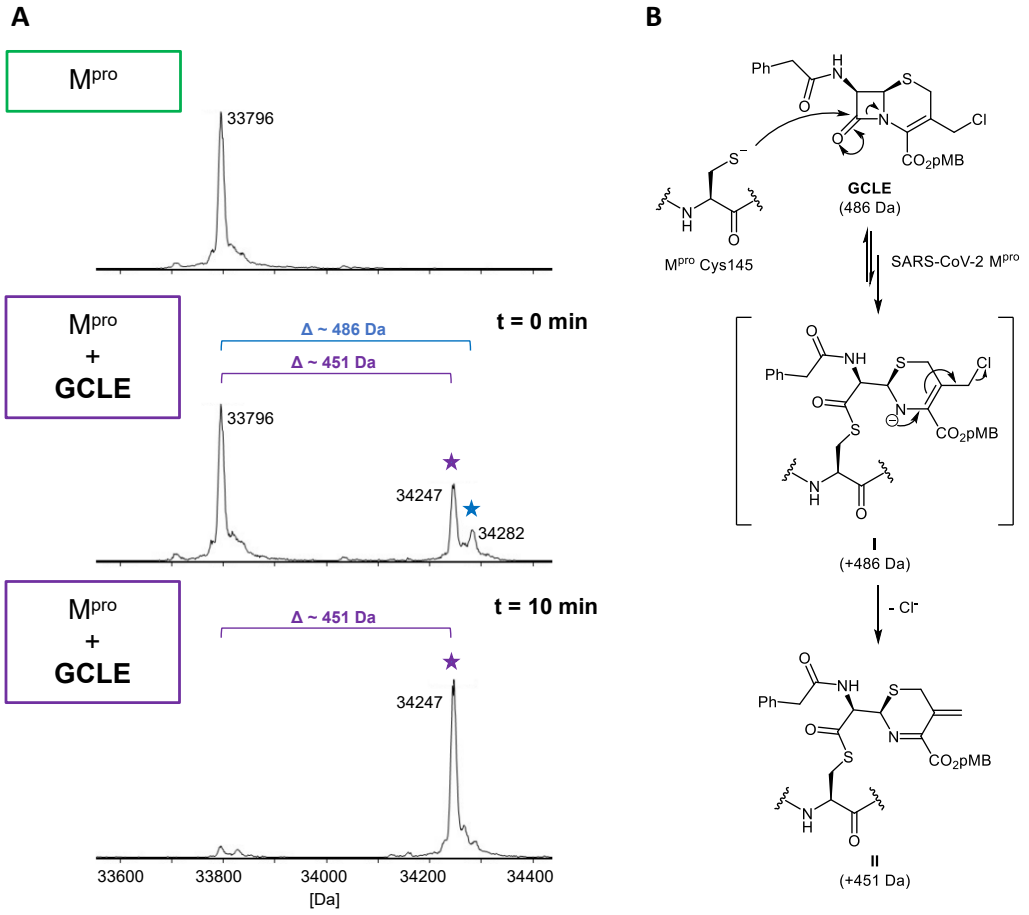

Figure 2: **A.** Evidence for covalent reaction of M^{pro} with **GCLE**. SPE-MS analysis showed initial formation of +486 Da (★) and +451 Da adducts (★); after 10 min, complete covalent modification of M^{pro} to the +451 Da adduct was observed (10:3 inhibitor:M^{pro} ratio). **B**. Proposed outline mechanism for the reaction of **GCLE** with M^{pro}.

To validate that **GCLE** reacts at the active site of M^{pro} with Cys145, isolated recombinant Mpro was first incubated with a ~16-fold excess of the small-molecule alkyne inhibitor **2**,[79] which selectively and irreversibly modifies Cys145 via stoichiometric thioenol-ether formation (**Figure 3**; **Supporting Figure S3**). After removal of excess **2**, the resulting covalent M^{pro}:**2** complex was incubated with **GCLE**. Under these conditions, **GCLE** did not form a covalent adduct with the M^{pro}:**2** complex within 4 h, indicating that **GCLE** reacts selectively with Cys145 and does not covalently modify (at least not substantially) other M^{pro} surface-exposed cysteine residues.

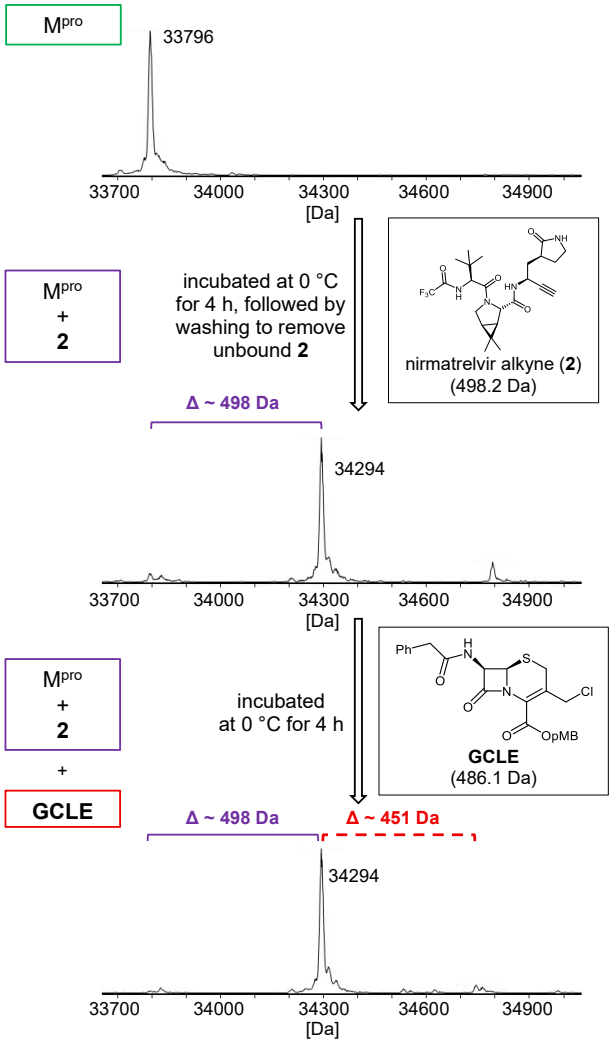

Figure 3: Evidence that **GCLE** inhibits M^{pro} by selective covalent reaction with Cys145. Assays were performed using reported SPE-MS conditions[79, 80] employing SARS-CoV-2 M^{pro} (3.0 μM) and, if appropriate, a β-lactam (10 μM) in buffer (20 mM HEPES, pH 7.5).

GCLE sulfur oxidation decreases M^{pro} inhibition potency

Given the exceptional potency of **GCLE** relative to reported penicillin V sulfone **1**, SAR studies on the **GCLE** scaffold were conducted to examine how systematic functional group modifications affect M^{pro} inhibition.

Initially, we investigated the effects of the **GCLE** sulfur oxidation state on M^{pro} inhibition potency, because our reported SAR studies on penicilin derivative **1** have shown that the penicillin sulfoxide and sulfide analogues of **1** were less potent M^{pro} inhibitors than **1**.[68] Thus, commercially-sourced **GCLE** was oxidized as reported[81] using *meta*-chloroperbenzoic acid (mCPBA) to give either (*S*)-sulfoxide **3**[81] (76%) or sulfone **4** (28%), depending on the mCPBA stoichiometry (**Figure 4**). Note that (*S*)-sulfoxide **3** was poorly soluble in dichloromethane and that the oxidation of **GCLE** to sulfone **4** required the use of *N*,*N*-dimethylformamide.

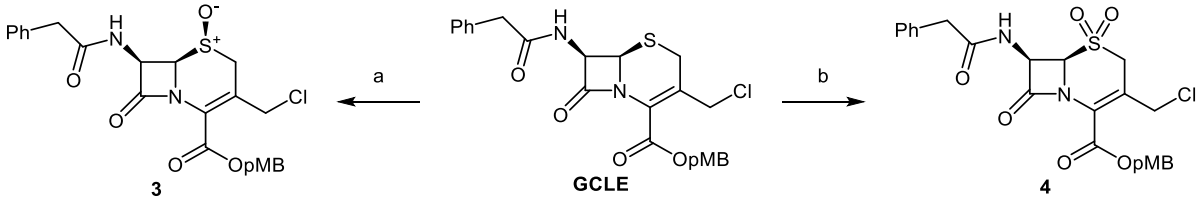

Figure 4. Synthesis of the sulfoxide and sulfone derivatives of GCLE. Reagents and conditions: a) mCPBA (1.02 equiv.), CH_2Cl_2, 0 °C, 1.5 h, 76%; b) mCPBA (3 equiv.), *N*,*N*-dimethylformamide, 0 °C to room temperature, 48 h, 28%.

The SPE-MS[67] assay results reveal that the **GCLE** (*S*)-sulfoxide and sulfone derivatives **3** and **4** were ~40-fold and ~150-fold less potent in inhibiting M^{pro} than **GCLE** (**Table 2**, entries i and ii), respectively, suggesting that the mode of M^{pro} inhibition of **GCLE** differs from that reported for penicillin sulfone **1**.[68] Protein-observed MS studies reveal that the **GCLE** derivatives **4** and **5** did not covalently react with M^{pro} (**Supporting Figure S4**), in accord with their reduced inhibition potency.

Table 2. Inhibition of SARS-CoV-2 M^{pro} by **GCLE** analogues.

	Cephalosporin	[(a)]IC_{50} [μM]		Cephalosporin	[(a)]IC_{50} [μM]
i	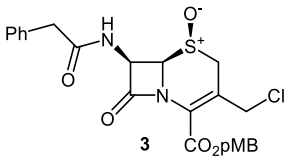 **3**	1.3 ± 0.1	viii	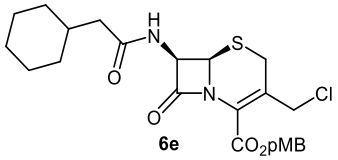 **6e**	0.08 ± 0.02
ii	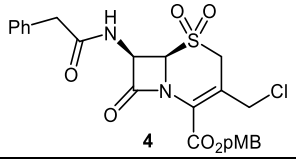 **4**	4.7 ± 1.2	viii	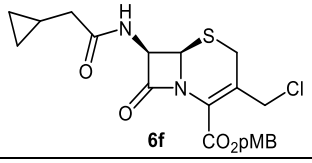 **6f**	0.1 ± 0.05
iii	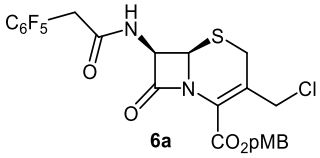 **6a**	0.05 ± 0.02	ix	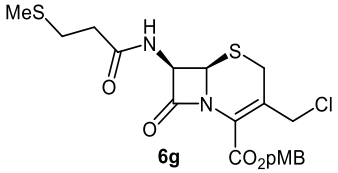 **6g**	0.08 ± 0.01
iv	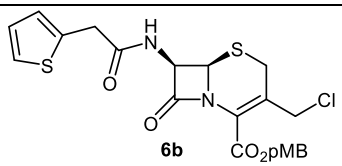 **6b**	0.02 ± 0.01	x	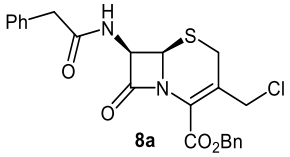 **8a**	0.02 ± 0.01
v	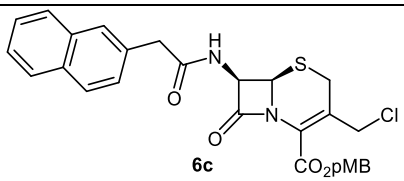 **6c**	0.02 ± 0.01	xi	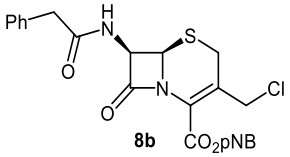 **8b**	0.03 ± 0.01
vi	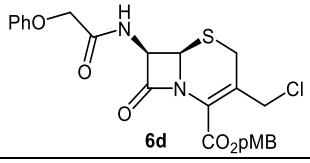 **6d**	0.06 ± 0.01	xii	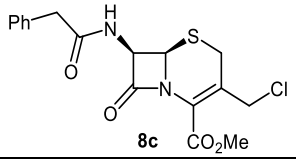 **8c**	0.05 ± 0.02

[(a)] M^{pro} inhibition assays were performed using SPE-MS as reported,[67, 79] utilizing SARS-CoV-2 M^{pro} (0.05 μM) and substrate (2.0 μM). Results are means of three independent biological experiments, each in technical duplicates (n = 3; mean ± SD). pMB: $–CH_2C_6H_4$(4-OMe); Bn: $–CH_2C_6H_5$; pNB: $–CH_2C_6H_4$(4-NO_2).

C7 Amide and C4 ester analogues of GCLE display similar M^{pro} inhibition

Prior work on penicillin-based M^{pro} inhibitors has shown that while ester group substitutions are generally well tolerated, changes in the identity of the amido sidechain can drastically alter reactivity.[68] Thus, we synthesised a set of **GCLE** derivatives with either altered C7 amido or C4 ester substituents (**Figure 5**). The C7 amide derivatives **6a-g** were synthesised from commercially sourced 7-amino-3-chloromethyl-3-cephem-4-carboxylic acid *p*-methoxybenzyl ester

hydrochloride (**5**) using phenyl dichlorophosphate, *N*-methylmorpholine and the required carboxylic acid (7-43%).[82] Additionally, acid-catalysed ester deprotection of **GCLE** afforded, as an intermediate with limited stability, cephalosporin G 3-chloromethyl acid **7** (~37%), which was directly coupled with either benzyl alcohol, 4-nitrobenzyl alcohol, or methanol using either *N*,*N*'-dicyclohexylcarbodiimide (DCC) or 1-ethyl-3-(3-dimethylaminopropyl)carbodiimide hydrochloride (EDCI) to give the corresponding esters **8a-c** (13-27%).

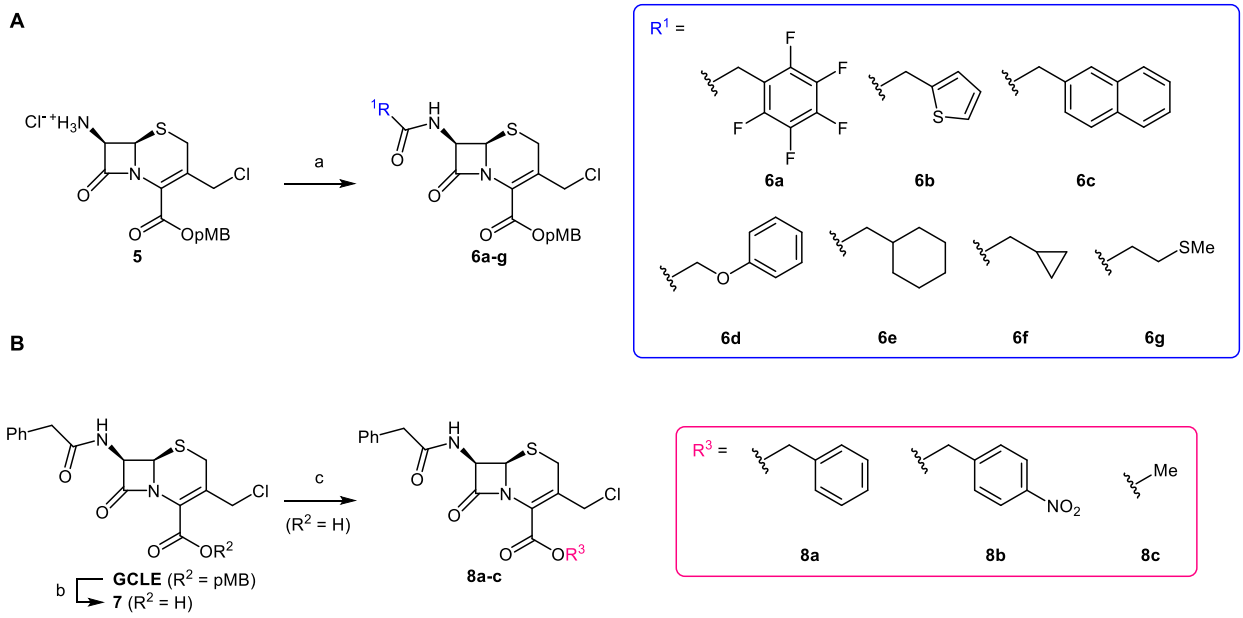

Figure 5. Synthesis of C7 amide and C4 ester analogues of GCLE. Reagents and conditions: (a) R^1COOH (1 equiv.), phenyl dichlorophosphate (1.2 equiv.), *N*-methylmorpholine (4 equiv.), EtOAc, -20 °C, 1.5-3 h, 7-43%; (b) trifluoroacetic acid, CH_2Cl_2, 0 °C, 30 min, ~37%; (c) R^3OH (4 equiv.), 4-(dimethylamino)pyridine (0.15 equiv.), *N*,*N*'-dicyclohexylcarbodiimide or 1-ethyl-3-(3-dimethylaminopropyl)carbodiimide hydrochloride (1.1 equiv.), CH_2Cl_2, 0 °C, 2-3 h, 13-27%.

The SPE-MS[67] assays revealed that variations in both the C7 amide and C4 ester groups of **GCLE** are well tolerated (**Table 2**, entries iii-xii), with amides **6a-g** and esters **8a-c** inhibiting M^{pro} with similar potency to **GCLE**. Furthermore, protein-observed MS assays showed that both C7 amide and C4 ester **GCLE** analogues bind covalently to M^{pro} Cys145 (**Supporting Figures S5-7**), with the corresponding adducts indicating loss of chloride upon binding, similarly to **GCLE**.

Cephalosporin C3 substituents modulate M^{pro} inhibition

The effect of the C3 substituent on M^{pro} inhibition potency and covalent reaction was also investigated. Commercially-sourced cephems **9a-h** were converted to the corresponding C7-phenylacetamides **10a-h** (**Figure 6A**) following reaction with $PhCH_2COCl$ (26-73%). The C7-phenylacetamides **10a-f** were then reacted with 4-methoxybenzyl bromide and $NaHCO_3$ in a mixture of 1,4-dioxane and *N*,*N*-dimethylformamide to afford esters **11a-f** as single Δ3 alkene isomers (19-45%).[82] By contrast, acids **10g** and **10h** afforded inseparable mixtures of Δ3/Δ2 regioisomers **11g**/**11'g** (5:1 ratio; 58%) and **11h**/**11'h** (10:1 ratio; 23%), respectively, as previously reported in the synthesis of related cephalosporin esters.[82-85] Cephalosporin G acid (**10a**) was subjected to aqueous HCl solution (37% (w/w)) to give lactone **12** (81%).[86] Additionally, **GCLE** itself served as a functionalisation platform for C3 derivatives (**Figure 6B**); reaction of **GCLE** with NaI in acetone yielded iodide **13**, which was then subjected to a series of nucleophilic substitutions. Reaction of **13** with NaSCN or PhSNa gave the thiocyanate **14** (66%) or the reported thioether[87] **15** (14%), respectively. Carboxylates **16a**/**16'a** (10:1 ratio; 70%) and **17b**/**17'b** (10:4 ratio; 60%) were also obtained from **13** following reaction with CF_2HCO_2Na and $PhCO_2Na$, respectively. Lastly, nucleophilic substitutions of **13** in the presence of CH_3SO_2Na, CF_3SO_2Na, or *para*-toluenesulfinate sodium salt were also successful, affording sulfone derivatives **18a**/**18'a** (10:1 ratio; 13%), **18b** (17%) and **18c** (23%), accordingly.

The SPE-MS[67] assay results revealed that while acids **10a-h** showed weak to negligible M^{pro} inhibitory properties (**Table 4**, entries i-viii), the corresponding esters **11a-h** showed improved M^{pro} inhibition (**Table 4**, entries x-xvii), highlighting the role played by the C4 ester group in M^{pro} binding and inhibition. Nonetheless, esters **11a-h** were >50-fold less potent M^{pro} inhibitors than

GCLE. Moreover, protein-observed MS showed that in this series only the C3 vinyl cephem **11d** promoted covalent adduct formation with M^{pro} (**Supporting Figure S8**).

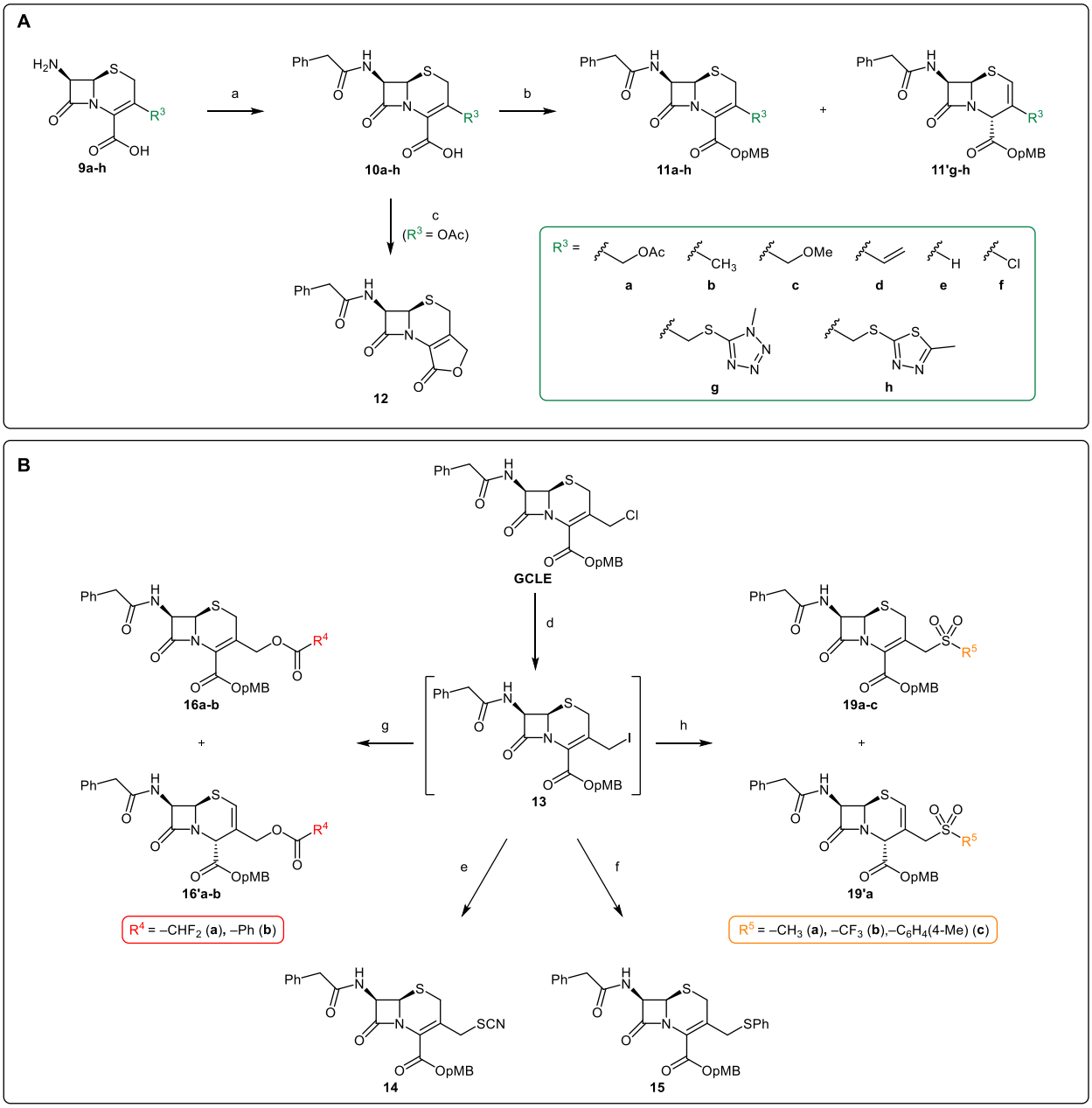

Figure 6. Synthetic routes to C3 analogues of GCLE. Reagents and conditions: a) $PhCH_2COCl$ (1.1 equiv.), Na_2CO_3 (1.1 equiv.), H_2O:acetone (1:1), -5 to 0 °C, 3 h, 26-73%; b) 4-methoxybenzyl chloride (1.35 equiv.), NaBr (7.6 equiv.), $NaHCO_3$ (1.1 equiv.), *N*,*N*-dimethylformamide:1,4-dioxane (5:3), room temperature, 16-18 h, 19-58%;[82] c) aqueous HCl solution (37% (w/w)), 1,4-dioxane, room temperature, 18 h, 81%;[86] d)) NaI (1.25 equiv.), acetone, room temperature, 2 h, 87%; e) NaSCN (1.7 equiv.), acetone, 0 °C, 2 h, 66%; f) PhSNa (1 equiv.), *N*,*N*-dimethylformamide,

room temperature, 18 h, 14%; g) R^4CO_2Na (1 equiv.), *N*,*N*-dimethylformamide, room temperature, 18 h, 60-70%; h) R^5SO_2Na (1.14 equiv.), *N*,*N*-dimethylformamide, room temperature, 18 h, 13-23%.

Table 3. Effects of cephalosporin C3 functional group modification on SARS-CoV-2 M^{pro} catalysis.

	Cephalosporin	[(a)]IC_{50} [μM]		Cephalosporin	[(a)]IC_{50} [μM]
i	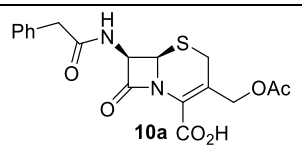 **10a**	30 ± 18	x	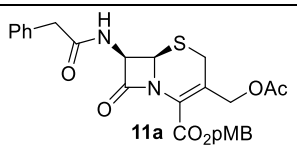 **11a**	3.9 ± 1.4
ii	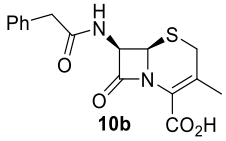 **10b**	>50	xi	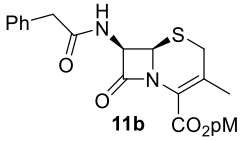 **11b**	6.1 ± 2.8
iii	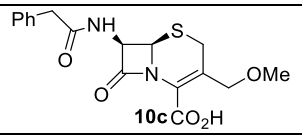 **10c**	>50	xii	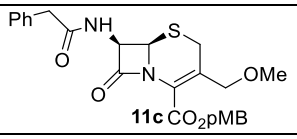 **11c**	3.0 ± 0.6
iv	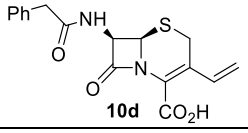 **10d**	15 ± 9	xiii	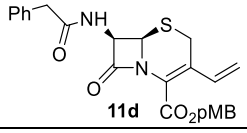 **11d**	2.4 ± 1.2
v	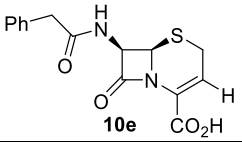 **10e**	>50	xiv	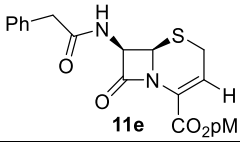 **11e**	25 ± 12
vi	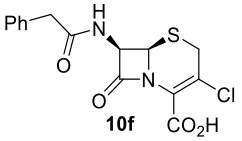 **10f**	>50	xv	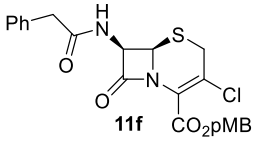 **11f**	3.0 ± 0.5
vii	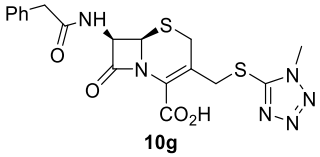 **10g**	31 ± 9	xvi	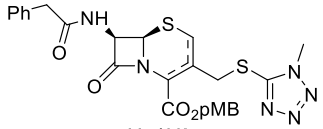 **11g/11'g** (5:1)	1.5 ± 0.1
viii	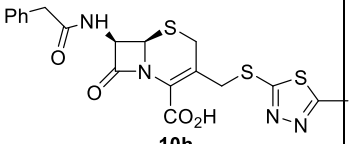 **10h**	>50	xvii	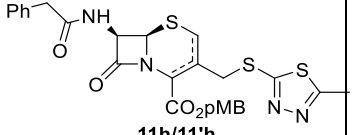 **11h/11'h** (10:1)	1.5 ± 0.3
ix	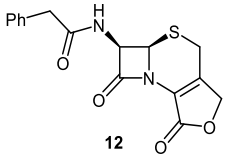 **12**	15 ± 5			

[(a)] M^{pro} inhibition assays were performed using SPE-MS as reported,[67, 79] utilizing SARS-CoV-2 M^{pro} (0.05 μM) and substrate (2.0 μM). Results are means of three independent biological experiments, each in technical duplicates (n = 3; mean ± SD). pMB: – $CH_2C_6H_4$(4-OMe).

Among the C3 analogues obtained following nucleophilic substitutions with **GCLE** iodide **13**, thiocyanate **14** was the most active compound (IC_{50} ~ 0.63 μM; **Table 4**, entry i), displaying only a ~21-fold loss in potency relative to **GCLE**, whereas **15-17** inhibited M^{pro} catalysis >30-fold less efficiently than **GCLE**. Additionally, protein-observed MS assays revealed that **14** promoted partial covalent modification of M^{pro}, whereas **15-17** did not (**Supporting Figure S9**).

Table 4. Inhibition of SARS-CoV-2 M^{pro} catalysis by C3 cephem analogues of **GCLE**.

	Cephalosporin	[(a)]IC_{50} [μM]		Cephalosporin	[(a)]IC_{50} [μM]
i	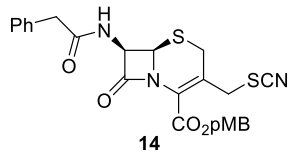 **14**	0.63 ± 0.11	v	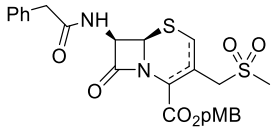 **17a/17'a** (10:1)	1.8 ± 0.2
ii	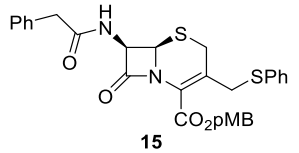 **15**	1.3 ± 0.4	vi	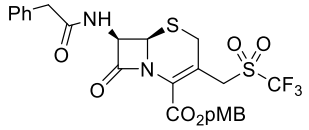 **17b**	0.9 ± 0.2
iii	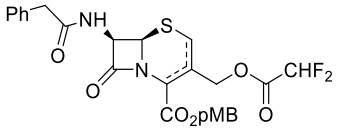 **16a/16'a** (10:1)	2.9 ± 0.9	vii	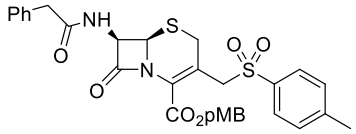 **17c**	5.1 ± 1.5
iv	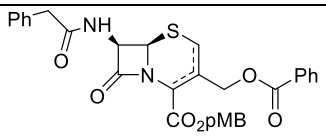 **16b/16'b** (10:4)	4.8 ± 1.0			

[(a)] M^{pro} inhibition assays were performed using SPE-MS as reported,[67, 79] utilizing SARS-CoV-2 M^{pro} (0.05 μM) and substrate (2.0 μM). Results are means of three independent biological experiments, each in technical duplicates (n = 3; mean ± SD). pMB: – $CH_2C_6H_4$(4-OMe).

C3 Formyl and aldoxime cephalosporins are potent M^{pro} inhibitors

Reported oxidation[88] of iodide **13** in the presence of O_2 and catalytic phosphomolybdic acid afforded C3-formyl cephem **18** (32%), which was condensed with hydroxylamine or *O*-alkoxyhydroxylamines to give aldoximes **19a-d** (11-71%).

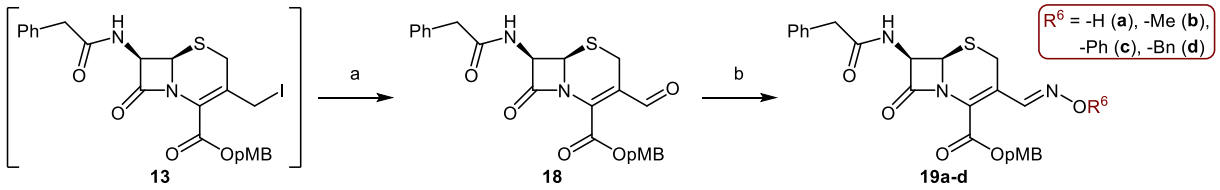

Figure 7. Synthesis of C3 cephem derivatives. Reagents and conditions: a) O_2, phosphomolybdic acid (0.07 equiv.), *N*-methyl-2-pyrrolidone, 35 °C, 4 h, 32%; b) $NH_2OR^6 \cdot HCl$ (1 equiv.), AcONa (1 equiv.), tetrahydrofuran-H_2O or MeOH-$CHCl_3$, room temperature, 1-18 h, 11-71%.

The SPE-MS[67] assay results reveal that both cephems **18** and **19a** inhibited M^{pro} only ~5-fold less efficiently than **GCLE** (IC_{50} ~ 0.16 and 0.18 μM, respectively; **Table 5**, entries i and ii), suggesting that electron-withdrawing groups at C3 are required for efficient M^{pro} inhibition. Consistent with this proposal, the more electron rich aldoxime ethers **19b**, **19c**, and **19d** displayed substantially poorer inhibition than aldoxime **19a** (**Table 5**, entries iii-v). Protein-observed MS assays[80] showed that M^{pro} covalently reacted with **18** and **19a**, albeit less efficiently than with **GCLE**, whereas no covalent adduct formation was observed with **19b-d** (**Supporting Figure S10-11**). Interestingly, for both **18** and **19a** a +450 Da mass shift was observed, which may correspond to the loss of the formyl O/aldoxime NOH, suggesting **18** and **19a** form an identical adduct with M^{pro}. To elucidate how these adducts may arise, additional protein-observed MS assays were conducted: i) incubation experiments where the M^{pro} active site was blocked with alkyne **2** showed that both **18** and **19a** react covalently with Cys145 (**Supporting Figure S12**); ii) time-course assays with **18** (**Figure 8**) revealed that Cys145 reacts with **18** to form an initial covalent adduct corresponding to a +466 Da mass shift (indicative of *S*-acylation following β-lactam ring opening), which over time gives rise to the +450 Da adduct (time-course assays with **19** revealed a similar behaviour; **Supporting Figure S13**).

Table 5. Inhibition of SARS-CoV-2 M^{pro} by C3 formyl and aldoxime cephem derivatives.

	Cephalosporin	[(a)]IC_{50} [μM]		Cephalosporin	[(a)]IC_{50} [μM]
i	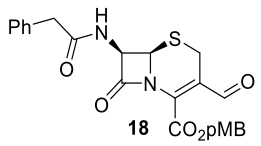 **18**	0.16 ± 0.04	iv	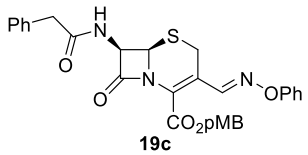 **19c**	3.5 ± 0.6
ii	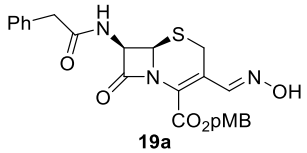 **19a**	0.18 ± 0.05	v	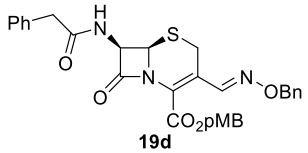 **19d**	2.0 ± 0.4
iii	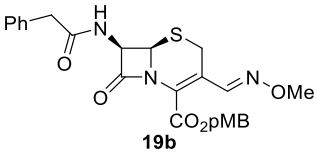 **19b**	1.3 ± 0.2			

[(a)] M^{pro} inhibition assays were performed using SPE-MS as reported,[67, 79] utilizing SARS-CoV-2 M^{pro} (0.05 μM) and substrate (2.0 μM). Results are means of three independent biological experiments, each in technical duplicates (n = 3; mean ± SD). pMB: – $CH_2C_6H_4$(4-OMe).

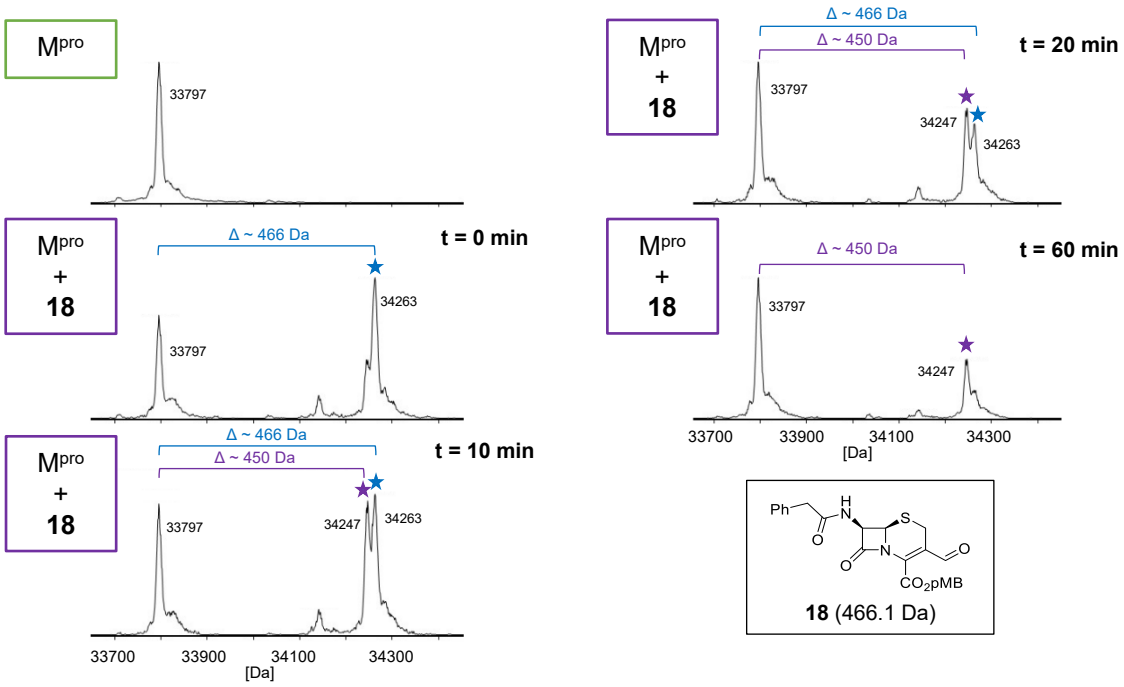

Figure 8: Evidence for covalent reaction of M^{pro} with **18**. SPE-MS analysis showed initial formation of a +466 Da adduct (★), which after ~ 60 min is mostly converted to a secondary +450 Da adduct (★) (10:3 inhibitor:M^{pro} ratio).

C3' Quaternary ammonium cephalosporins are potent, non-covalently binding M^{pro} inhibitors

Given that cephalosporin derivatives possessing electron-withdrawing groups at C3 displayed excellent inhibitory properties (*e.g.*, **18**), it was envisioned that cephems with positively charged C3 substituents may also be potent M^{pro} inhibitors. C3' Quaternary ammonium cephalosporins (**Figure 9**) were synthesised from iodide **13** following nucleophilic reactions with a range of aromatic nitrogen heterocycles to afford **20a-h** (19-57%).

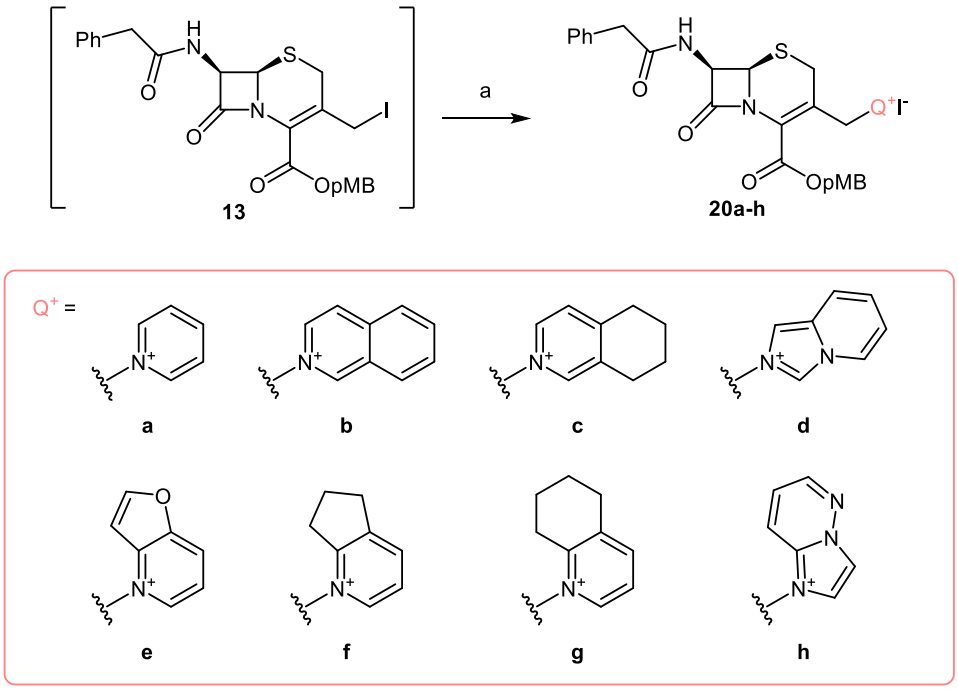

Figure 9. Synthesis of cephem quaternary ammonium iodide salts**.** Reagents and conditions: a) nitrogen aromatic heterocycle (1-4 equiv.), EtOAc, 0 °C to room temperature, 18 h, 19-57%.

SPE-MS assay[67] revealed that C3' quaternary ammonium cephems with bicyclic heteroaromatic (*i.e.*, **20b-h**) were more potent than the monocyclic pyridinium analogue **20a** (**Table 6**). Furthermore, cephem **20e** was the most potent M^{pro} inhibitor (IC_{50} ~ 0.12 μM; **Table 6**, entry v) amongst the quaternary ammonium salts **20a-h**, exhibiting a ~3-7-fold more efficient inhibition than **20a-d** and **20f-h**, and only ~4-fold less efficient inhibition than **GCLE**. The results also

indicate that variations in the electronics of the heteroaryl group and, importantly, the orientation of the bicyclic system modulate activity: i) the *ortho*,*meta*-substitution pattern on the pyridine ring (*i.e.*, **20e-g**) was associated with greater potency than the *meta,para*- arrangement (*i.e.*, **20b-c**); ii) fully aromatic heterocyclic substituents also favoured stronger M^{pro} inhibition (*e.g.*, **20e** versus **20f**). Lastly, protein-observed MS assays[68] revealed that **20a-h** did not promote covalent adduct formation with M^{pro} (**Supporting Figure S14**), suggesting that the inhibition of M^{pro} catalysis by **20a-h** is non-covalent in nature.

Table 6. Inhibition of SARS-CoV-2 M^{pro} by C3-substituted cephem derivatives.

	Cephalosporin	[(a)]IC_{50} [μM]		Cephalosporin	[(a)]IC_{50} [μM]
i	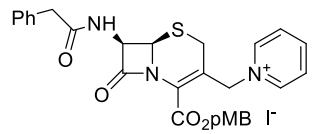 **20a**	1.1 ± 0.6	v	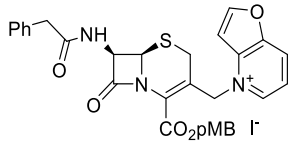 **20e**	0.12 ± 0.04
ii	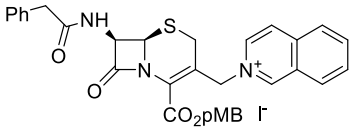 **20b**	0.68 ± 0.04	vi	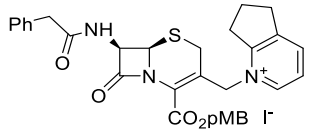 **20f**	0.41 ± 0.03
iii	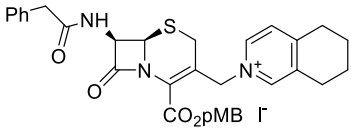 **20c**	0.88 ± 0.21	vii	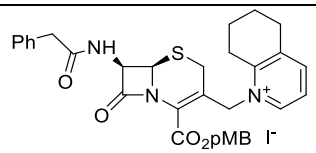 **20g**	0.58 ± 0.01
iv	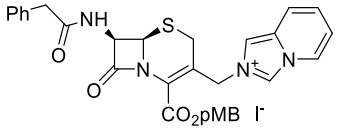 **20d**	0.53 ± 0.21	viii	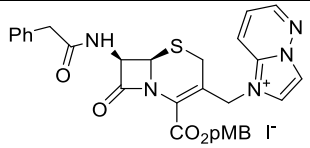 **20h**	0.47 ± 0.02

[(a)] M^{pro} inhibition assays were performed using SPE-MS as reported,[67, 79] utilizing SARS-CoV-2 M^{pro} (0.05 μM) and substrate (2.0 μM). Results are means of at least two independent biological experiments, each in technical duplicates ($n \geq 2$; mean ± SD). pMB: – $CH_2C_6H_4$(4-OMe).

Cephalosporin M^{pro} inhibitors suppress SARS-CoV-2 replication in infected cells

The antiviral activity of selected cephalosporin M^{pro} inhibitors was assessed in SARS-CoV-2 infected VeroE6 cells at a fixed concentration of 20 μM. At this dose, the compounds reduced

infected foci by ~10–31% (**Table 7**), with the C3 formyl cephem **18** showing the greatest effect (**Table 7**, entry v). While these preliminary results confirm cellular activity, the magnitude of inhibition is lower than what would be expected from the IC_{50} values against isolated recombinant M^{pro}, suggesting that the inhibitors are not yet optimized for cellular activity.

Table 7. Effects of cephalosporin M^{pro} inhibitors on SARS-CoV-2 infection in VeroE6 cells.

	Cephalosporin	Relative reduction of infected foci (%) at 20 μM inhibitor concentration[(a)]
i	**GCLE**	16 ± 2
ii	**6b**	14 ± 1
iii	**6g**	20 ± 3
iv	**8c**	30 ± 7
v	**18**	31 ± 3
vi	**19a**	14 ± 1
vii	**20d**	24 ± 2
viii	**20h**	10 ± 1

[(a)]The potency of the cephalosporin SARS-CoV-2 M^{pro} inhibitors in cells was tested using SARS-CoV-2 (Victoria strain[89] MT007544.1) infected VeroE6 cells as reported[79] (fixed inhibitor concentration: 20 μM). Relative reduction (%) reflects decrease in infected foci compared to the DMSO controls (mean ± SD; n = 2).

3.2.4 Discussion

Cephalosporins are a major class of β-lactam antibiotics, first identified in the 1940s as natural products from the marine fungus *Acremonium chrysogenum*.[90, 91] Later development of semi-synthetic derivatives led to the clinical introduction of cephalothin in the 1960s,[92] which marked the beginning of subsequent antibiotic "generations" with progressively broader antibacterial spectra.[1, 90, 93-97] These advances in antimicrobial therapy are most recently exemplified by ceftobiprole medocaril[98] and ceftaroline fosamil[77], as these antibiotics are able to target multidrug-resistant pathogens such as methicillin-resistant *Staphylococcus aureus* (MRSA).[99-101]

Beyond their traditional antibacterial use, cephalosporins have attracted considerable attention for other potential therapeutic applications, most notably in oncology and inflammation.[13, 14] Not only do certain cephalosporin antibiotics reportedly display intrinsic anticancer properties (*e.g.*,

ceftriaxone inhibits Aurora B kinase activity,[22] thereby suppressing cancer cell proliferation), but the cephalosporin scaffold can also be developed as a prodrug that carries cytotoxic agents at the C3′ position.[17, 30] Moreover, cephalosporin ester derivatives have been reported as potent covalent inhibitors of the human leukocyte elastase (HLE), a serine protease implicated in inflammatory diseases such rheumatoid arthritis.[40, 41, 44] In the present work, we have shown that cephalosporin derivatives can be developed for antiviral applications, in particular as potent inhibitors of SARS-CoV-2 M^{pro}.

SAR studies on **GCLE**, the most potent β-lactam-based M^{pro} inhibitor identified to date, provided key insights into how future inhibitors may be further optimised. The C7 amide (**6a-g**) and C4 ester (**8a-c**) analogues of **GCLE** displayed comparable M^{pro} inhibitory potencies, indicating that structural variations at these positions are generally well tolerated. In contrast, a marked reduction in activity was observed upon changing the oxidation state of the cephem thioether of **GCLE**. This behaviour differs from that observed previously for penicillin-derived M^{pro} inhibitors,[68] where penicillin sulfone derivatives were the most potent inhibitors and modifications at the C6 amide position were poorly tolerated, suggesting that the cephalosporin and penicillin scaffolds might initially engage M^{pro} via distinct binding interactions.

SAR studies further revealed that substitution at the C3′ position had a pronounced effect on both the potency and the mechanism via which cephalosporin derivatives inhibit M^{pro}. Empirically, for C3'-substituted cephalosporins, potent inhibition was broadly associated with leaving-group ability at C3'. Cephalosporins bearing C3' moieties with poor leaving-group ability, such as sulfones, carboxylates, thioethers and ethers (*e.g.*, **11a**, **11c**, **15**, and **17c**), displayed markedly weaker inhibition than **GCLE**, inhibiting through a non-covalent mechanism. In contrast, thiocyanate **14**, a pseudohalide[102, 103] with leaving-group ability closer to that of chloride, promoted partial

covalent modification of M^{pro} and was more potent than other C3′-substituted derivatives, although still ~20-fold less active than **GCLE**.

Notably, C3′ quaternary ammonium cephalosporin derivatives (*e.g.*, **20a-h**), which inhibit M^{pro} non-covalently and whose C3' substituents are also poorer leaving groups than chloride, show that inhibition can be modulated by varying the heteroaryl ring. Optimisation of the aromatic framework and its electronics can enhance activity, with **20e** being only ~4-fold less potent than **GCLE**. These results indicate that, even in the absence of covalent modification, favourable electrostatic and π–π interactions between C3′ substituents and the M^{pro} active site residues can substantially improve M^{pro} binding affinity and inhibition.

SAR investigations also revealed that cephalosporins lacking a C3′ substituent can still inhibit M^{pro}, provided that the C3 group maintains the electron-withdrawing properties typically associated with reactive cephem scaffolds. In particular, the C3′ formyl (**18a**) and C3′ aldoxime (**19a**) derivatives displayed potent inhibition of M^{pro} and inhibited via a covalent mechanism. Protein-observed MS assays (**Figure 8**, **Supporting Figure S13**) revealed that both compounds produced an adduct of identical mass (+450 Da), suggesting a common reaction pathway. Based on these observations, we propose the following mechanism (**Figure 10**): (i) nucleophilic attack of Cys145 on the β-lactam carbonyl leading to β-lactam ring opening and formation of an initial acyl-enzyme complex (+466 Da); (ii) tautomerisation of the aldehyde intermediate (adduct **I**) to the corresponding enol form (adduct **II**); (iii) subsequent attack of a secondary active-site residue (possibly His41) to form a bridged species (adduct **III**); and (iv) elimination of the C3′ alcohol via an addition-elimination sequence, affording the final covalent adduct (**IV**; +450 Da). Crystallographic studies to confirm the structure of this adduct are currently ongoing.

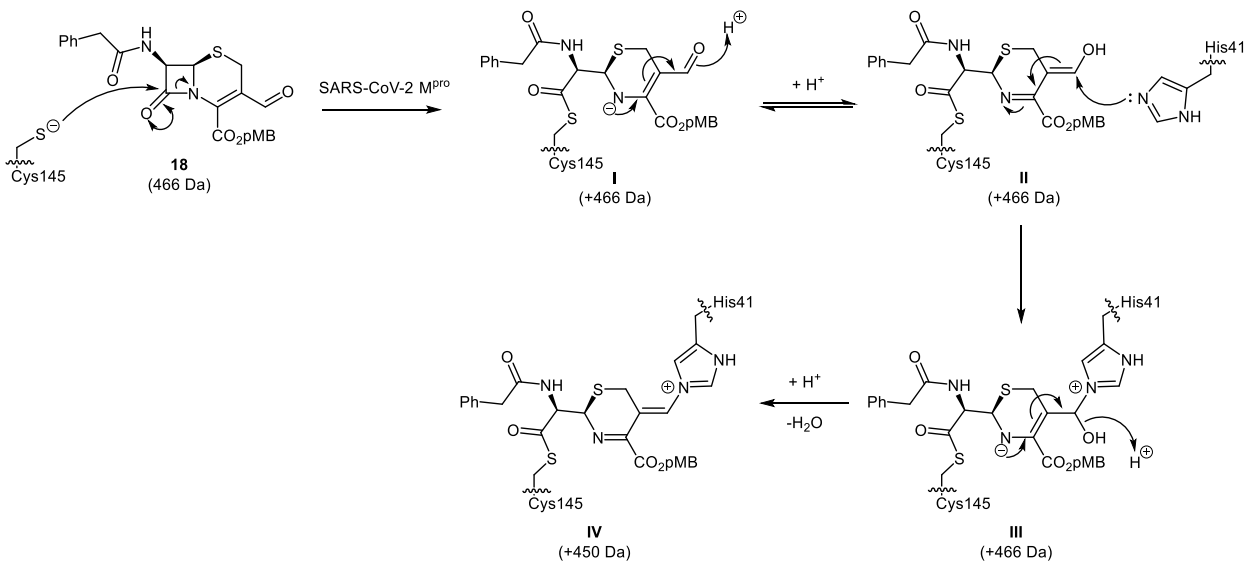

Figure 10. Possible outline mechanism for the covalent reaction of M^{pro} with **18**.

Lastly, preliminary cell-based studies showed that cephalosporin-based M^{pro} inhibitors suppress viral replication in SARS-CoV-2 infected cells, although the extent of this effect was significantly less pronounced than against the isolated recombinant enzyme (**Table 7**). This discrepancy indicates that the tested cephalosporin ester derivatives are yet to be optimised for cellular activity, possibly reflecting insufficient cellular stability and/or limited cellular uptake.

3.2.5 Conclusions

The combined results demonstrate that cephalosporin-based derivatives can be developed as potent M^{pro} inhibitors. It was shown that key substitutions at the C3 position of the cephalosporin scaffold not only tune potency but also modulate the mechanism of action, with cephem derivatives displaying both covalent and non-covalent modes of inhibition. Given the well-established clinical use of cephalosporins, we suggest that cephem-based inhibitors warrant further investigation as antiviral agents, particularly toward improving cellular activity.

3.2.6 Supporting Figures

Supporting Figure S1: Structures of the commercially sourced cephalosporins screened in this study.

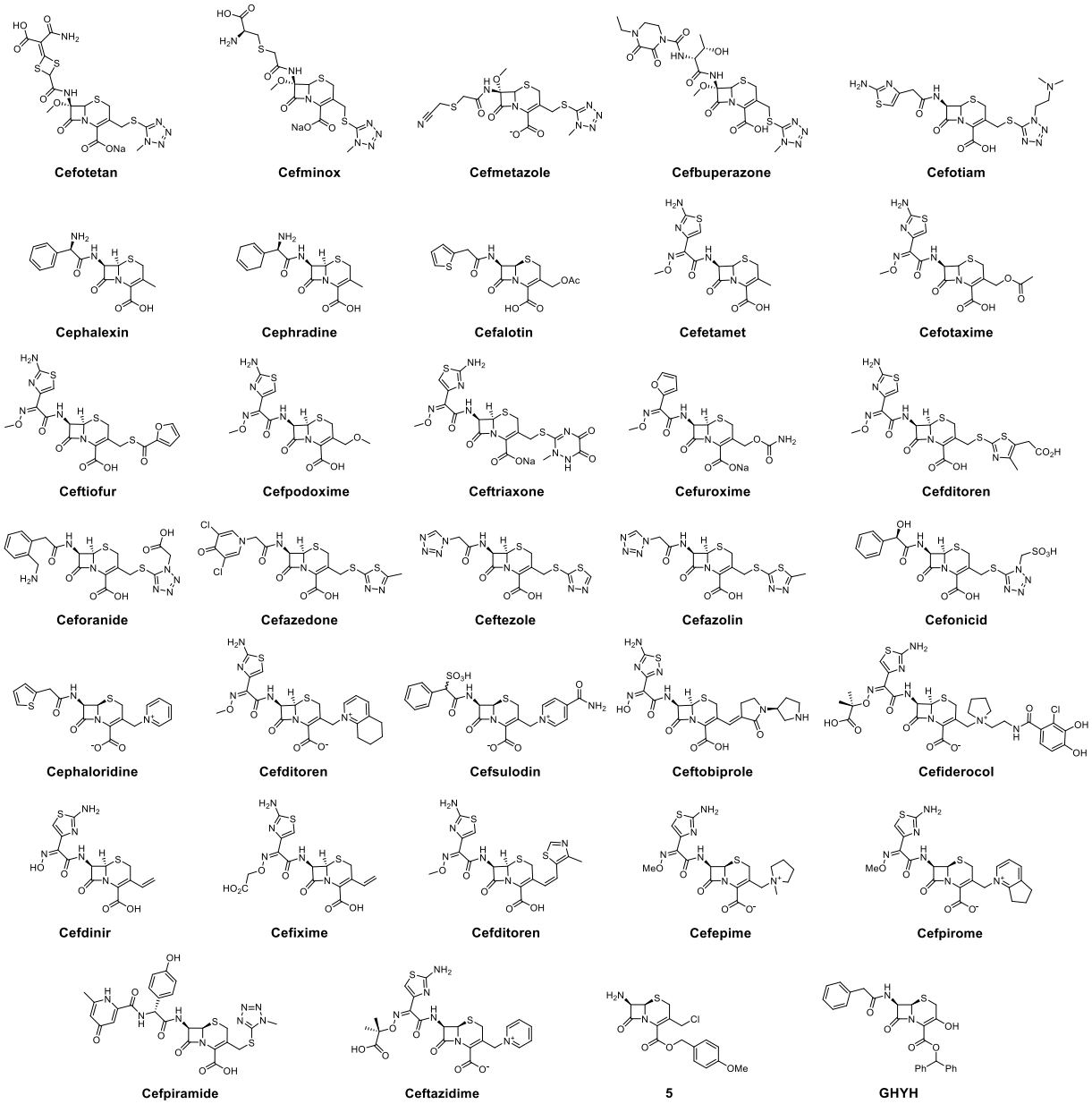

Supporting Table S1: Inhibition of SARS-CoV-2 M^{pro} by cephalosporin antibiotics.

	Cephalosporin	[(a)]IC_{50} [μM]		Cephalosporin	[(a)]IC_{50} [μM]
i	Cefotetan	32 ± 4	xviii	Ceftezole	>50
ii	Cefminox	>50	xix	Cefazolin	>50
iii	Cefmetazole	>50	xx	Cefonicid	>50
iv	Cefbuperazone	>50	xxi	Cephaloridine	>50
v	Cefotiam	>50	xxii	Cefditoren	>50
vi	Cephalexin	>50	xxiii	Cefsulodin	>50
vii	Cephradine	>50	xxiv	Ceftobiprole	>50
viii	Cephalothin	>50	xxv	Cefiderocol	>50
ix	Cefetamet	>50	xxvi	Cefdinir	>50
x	Cefotaxime	>50	xxvii	Cefixime	>50
xi	Ceftiofur	>50	xxviii	Cefditoren	>50
xii	Cefpoxodime	>50	xxix	Cefpiramide	>50 (reported[69]: ~30)
xiii	Ceftriaxone	>50	xxx	Ceftazidime	>50
xiv	Cefuroxime	>50	xxxi	Cefepime	>50
xv	Cefditoren	>50	xxxii	Cefpirome	>50
xvi	Ceforanide	>50 (reported[69]: ~14.9)	xxxiii	**5**	>50
xvii	Cefazedone	>50	xxxiv	**GHYH**	>50

[(a)] M^{pro} inhibition assays were performed using SPE-MS as reported,[67, 79] utilizing SARS-CoV-2 M^{pro} (0.05 μM) and substrate (2.0 μM). Results are means of three independent biological experiments, each in technical duplicates (n = 3; mean ± SD).

Supporting Figure S2: Reaction of cephalosporins with isolated recombinant M^{pro}. Analysis of M^{pro} reactions with (**A**) **ceftaroline**, and (**B**) **GCLE**, prior (bottom) and after >15 h of incubation (top) with the respective β-lactam. Assays were performed using SPE-MS as reported,[67] employing SARS-CoV-2 M^{pro} (3.0 µM) and, if appropriate, a β-lactam (15 µM) in buffer (20 mM HEPES, pH 7.5). Representative spectra of technical duplicates are shown.

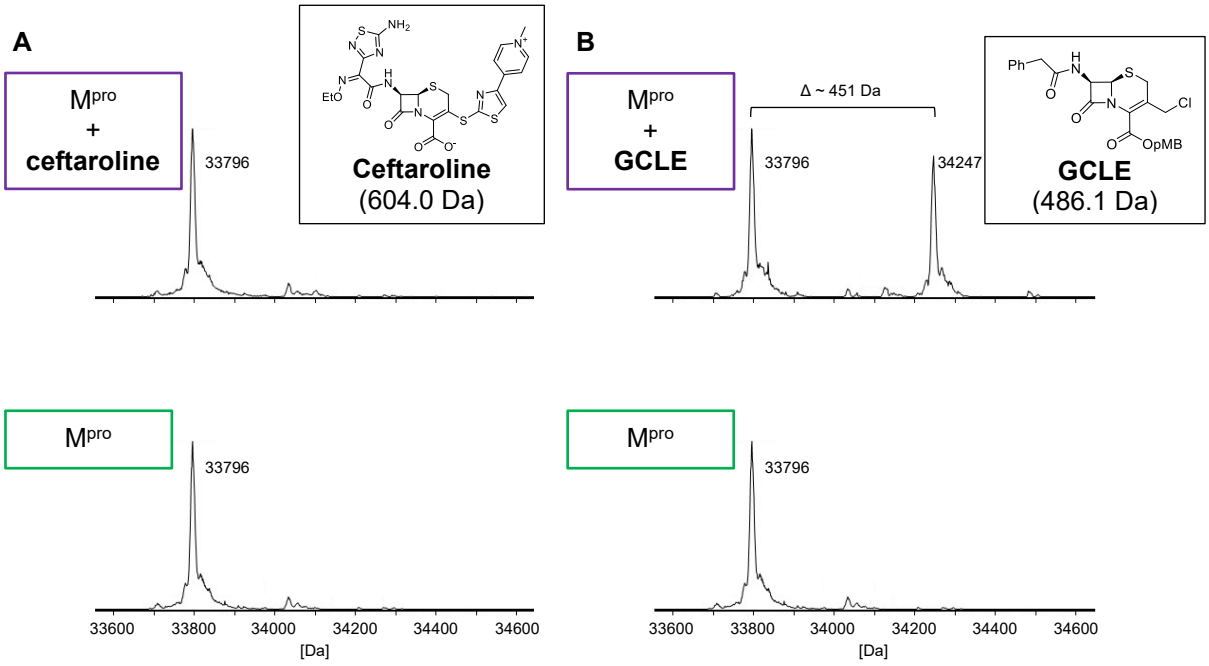

Supporting Figure S3: Outline mechanism for the irreversible, covalent reaction of alkyne **2** with M^{pro} Cys145.[79]

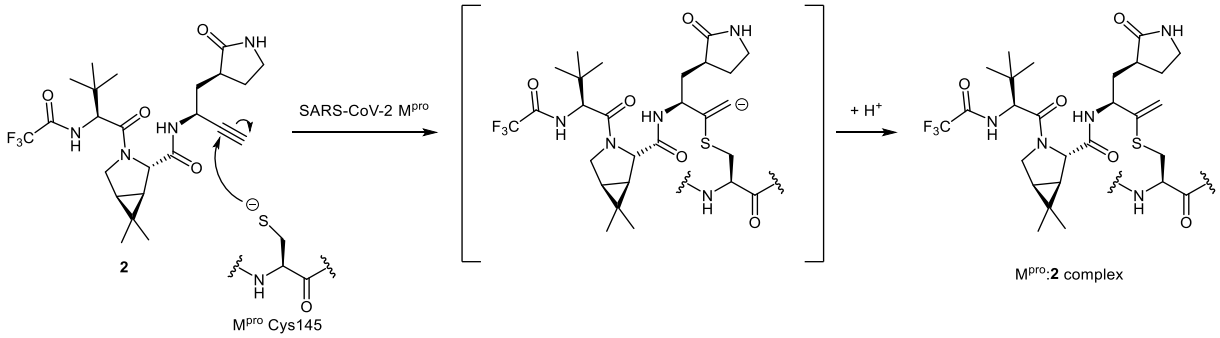

Supporting Figure S4: Reaction of cephalosporins with isolated recombinant M^{pro}. Analysis of M^{pro} reactions with (**A**) **3**, and (**B**) **4**, prior (top) and after >15 h of incubation (bottom) with the respective β-lactam. Assays were performed using SPE-MS as reported,[67] employing SARS-CoV-2 M^{pro} (3.0 µM) and, if appropriate, a β-lactam (15 µM) in buffer (20 mM HEPES, pH 7.5). Representative spectra of technical duplicates are shown.

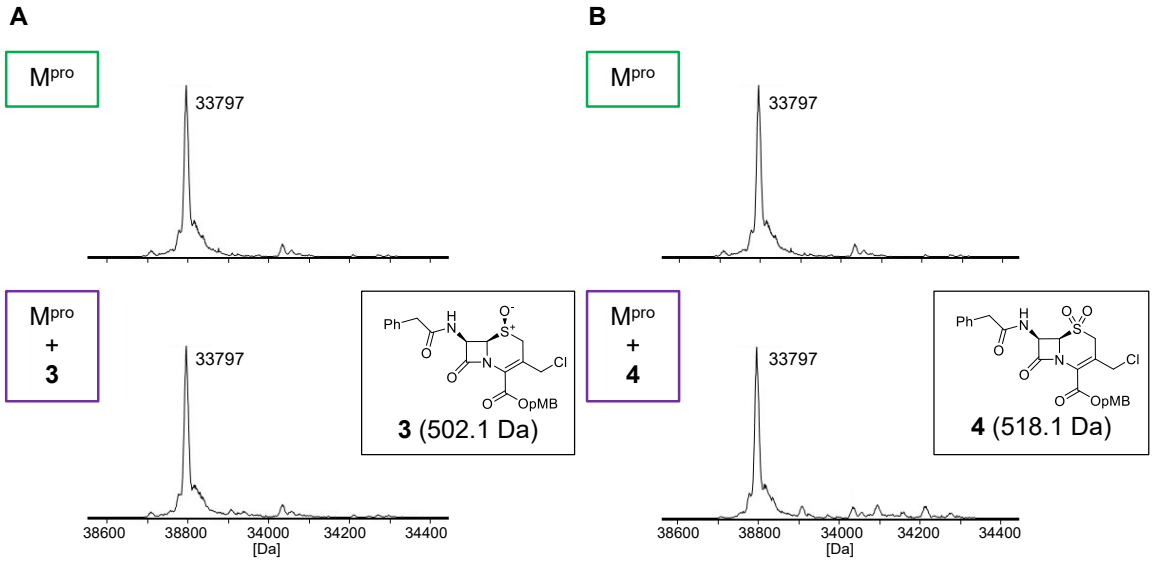

Supporting Figure S5: Reaction of C7 amide and C4 ester analogues of GCLE with isolated recombinant M^{pro}. Analysis of M^{pro} reactions with cephalosporin derivatives: (**A**) **6b**, (**B**) **6f**, (**C**) **6g**, (**D**) **8a**, (**E**) **8b**, (**F**) **8c** prior (bottom) and after >15 h of incubation (top) with the respective β-lactam. Assays were performed using SPE-MS as reported,[67] employing SARS-CoV-2 M^{pro} (3.0 µM) and, if appropriate, a β-lactam (15 µM) in buffer (20 mM HEPES, pH 7.5). Representative spectra of technical duplicates are shown.

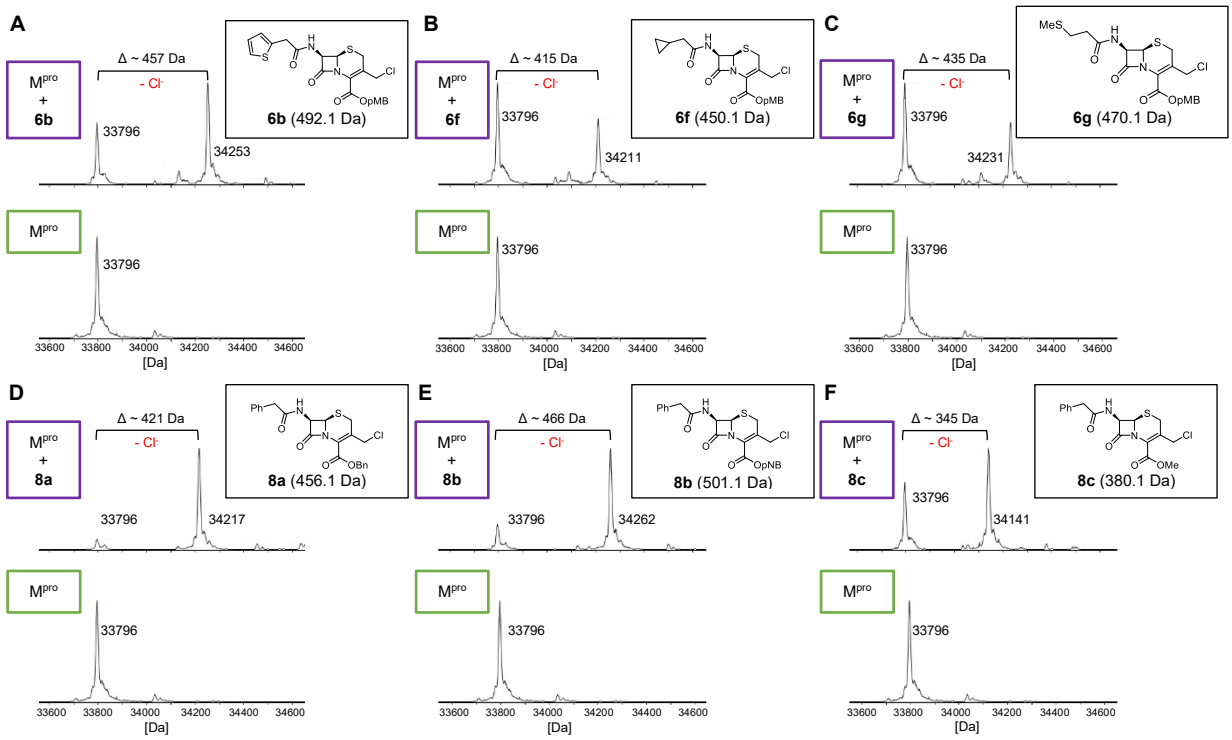

Supporting Figure S6: Evidence that C7 amide analogues of **GCLE** inhibit M^{pro} by selective covalent reaction with Cys145. Assays were performed using reported SPE-MS conditions[79, 80] employing SARS-CoV-2 M^{pro} (3.0 μM) and, if appropriate, a β-lactam (10 μM) in buffer (20 mM HEPES, pH 7.5).

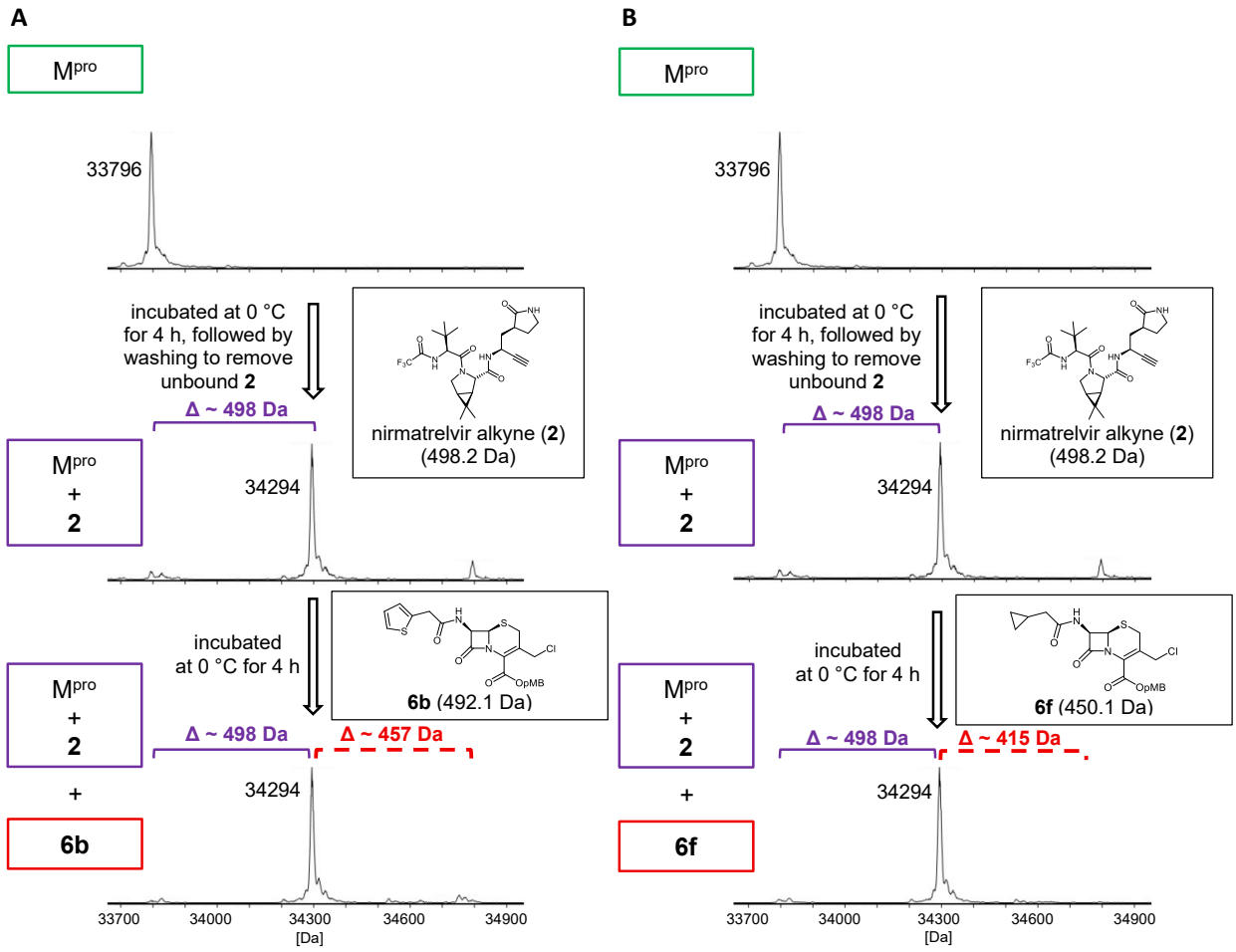

Supporting Figure S7: Evidence that C4 ester analogues of **GCLE** inhibit M^{pro} by selective covalent reaction with Cys145. Assays were performed using reported SPE-MS conditions[79, 80] employing SARS-CoV-2 M^{pro} (3.0 μM) and, if appropriate, a β-lactam (10 μM) in buffer (20 mM HEPES, pH 7.5).

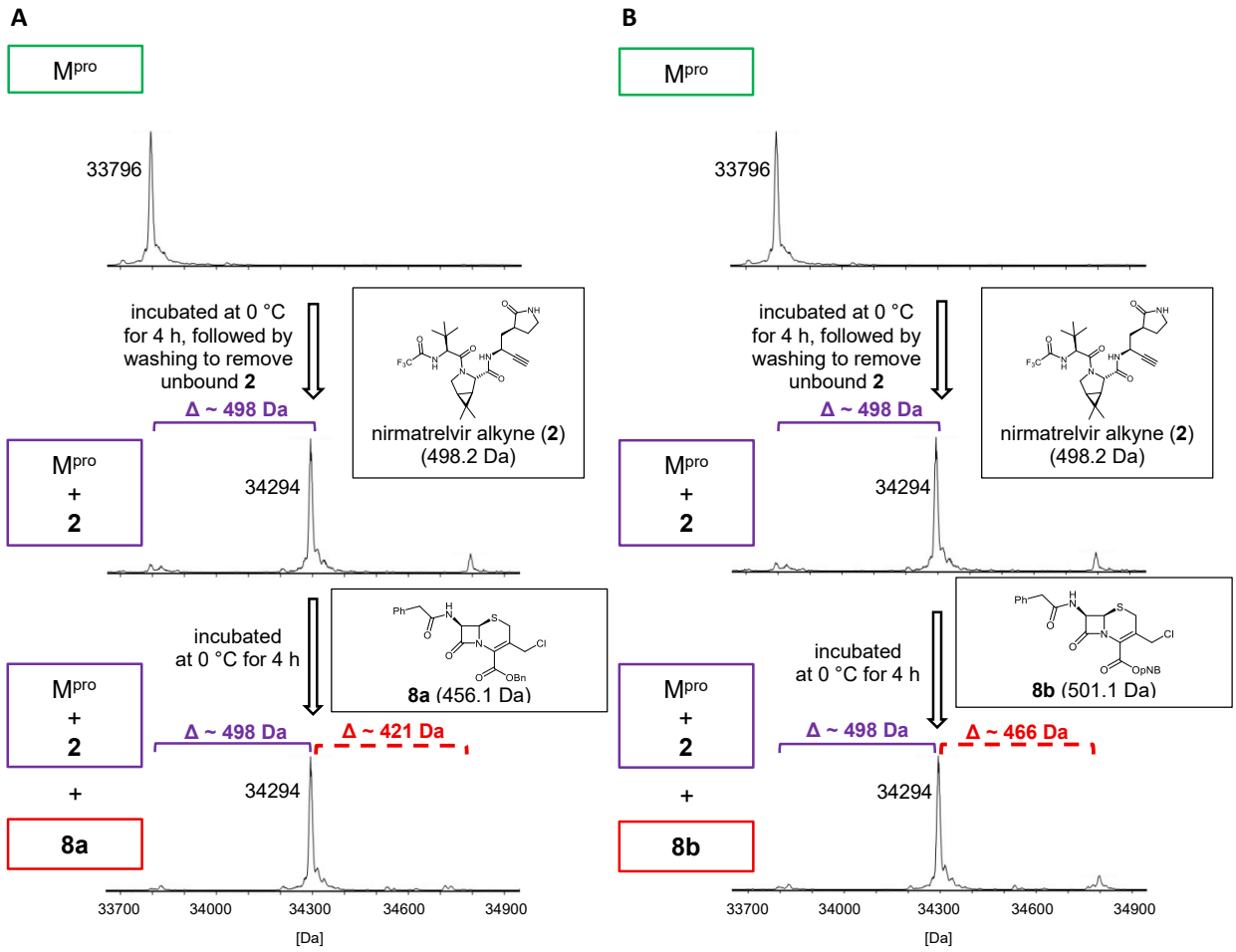

Supporting Figure S8: Reaction of C3 cephem analogues of GCLE with isolated recombinant M^{pro}. Analysis of M^{pro} reactions with cephalosporin derivatives: (**A**) **11a**, (**B**) **11b**, (**C**) **11c**, (**D**) **11d**, (**E**) **11f**, (**F**) **11h** prior (bottom) and after >15 h of incubation (top) with the respective β-lactam. Assays were performed using SPE-MS as reported,[67] employing SARS-CoV-2 M^{pro} (3.0 μM) and, if appropriate, a β-lactam (15 μM) in buffer (20 mM HEPES, pH 7.5). Representative spectra of technical duplicates are shown.

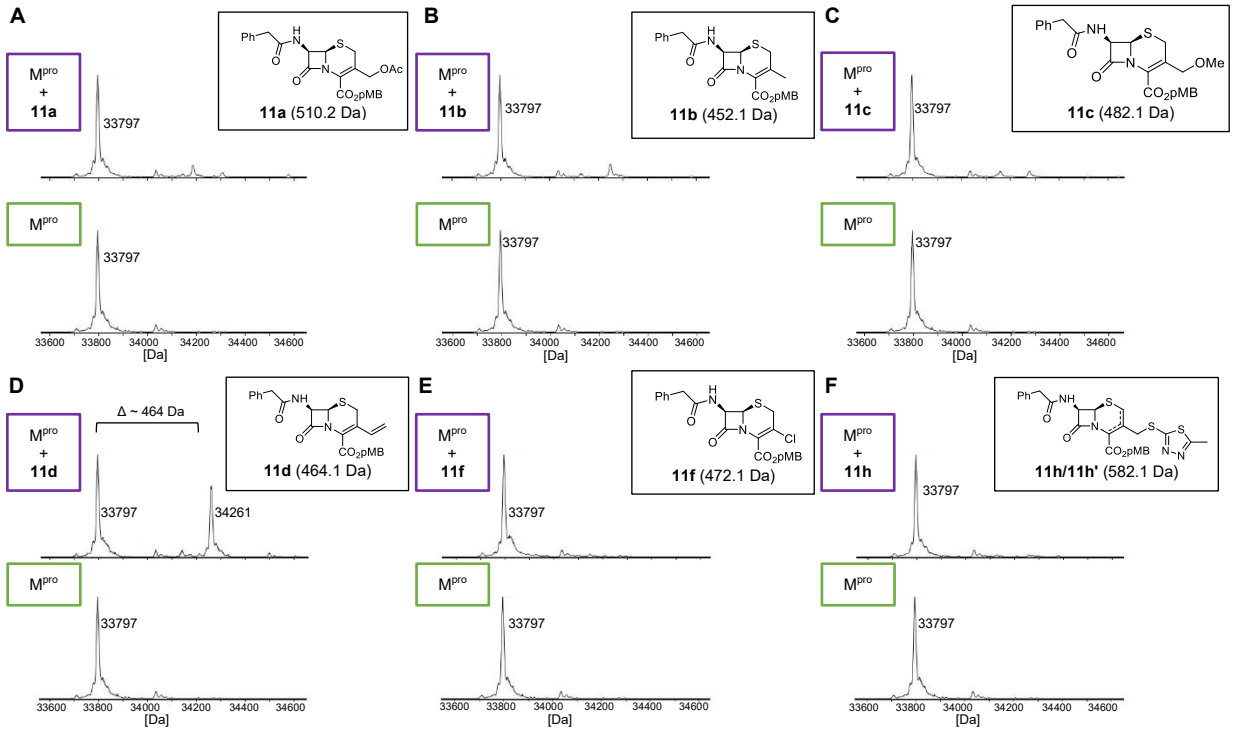

Supporting Figure S9: Analysis of M^{pro} reactions with C3 cephalosporin derivatives: (**A**) **14**, (**B**) **15**, (**C**) **16**, (**D**) **11d**, (**E**) **11f**, (**F**) **11h** prior (bottom) and after >15 h of incubation (top) with the respective β-lactam. Assays were performed using SPE-MS as reported,[67] employing SARS-CoV-2 M^{pro} (3.0 μM) and, if appropriate, a β-lactam (15 μM) in buffer (20 mM HEPES, pH 7.5). Representative spectra of technical duplicates are shown. **G**. Proposed mechanism for the formation of the observed M^{pro} adducts following reaction with **14**.

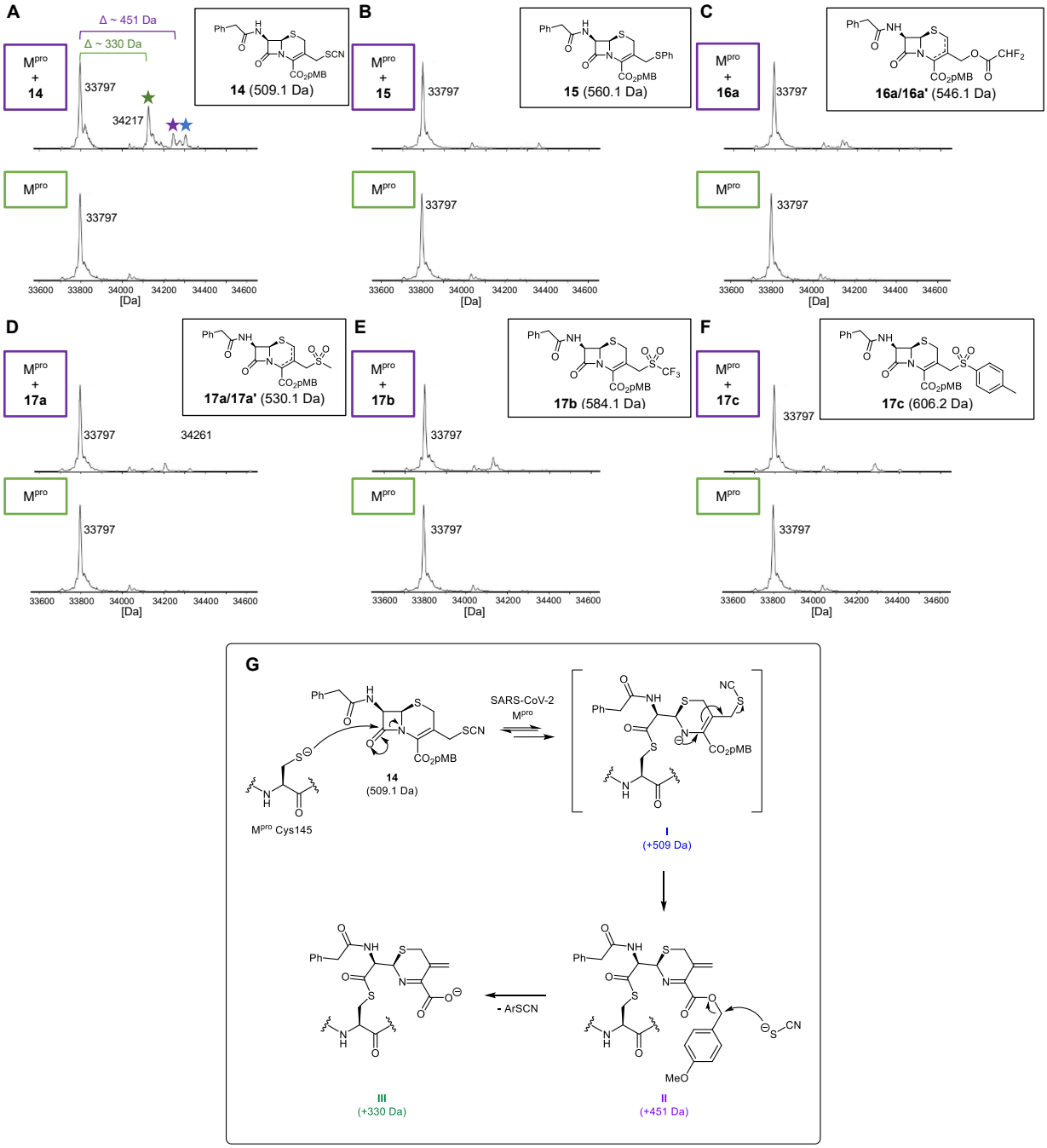

Supporting Figure S10: Analysis of M^{pro} reactions with C3 formyl and aldoxime cephalosporin derivatives: (**A**) **18**, and (**B**) **19a**, prior (bottom) and after >15 h of incubation (top) with the respective β-lactam. Assays were performed using SPE-MS as reported,[67] employing SARS-CoV-2 M^{pro} (3.0 μM) and, if appropriate, a β-lactam (15 μM) in buffer (20 mM HEPES, pH 7.5). Representative spectra of technical duplicates are shown.

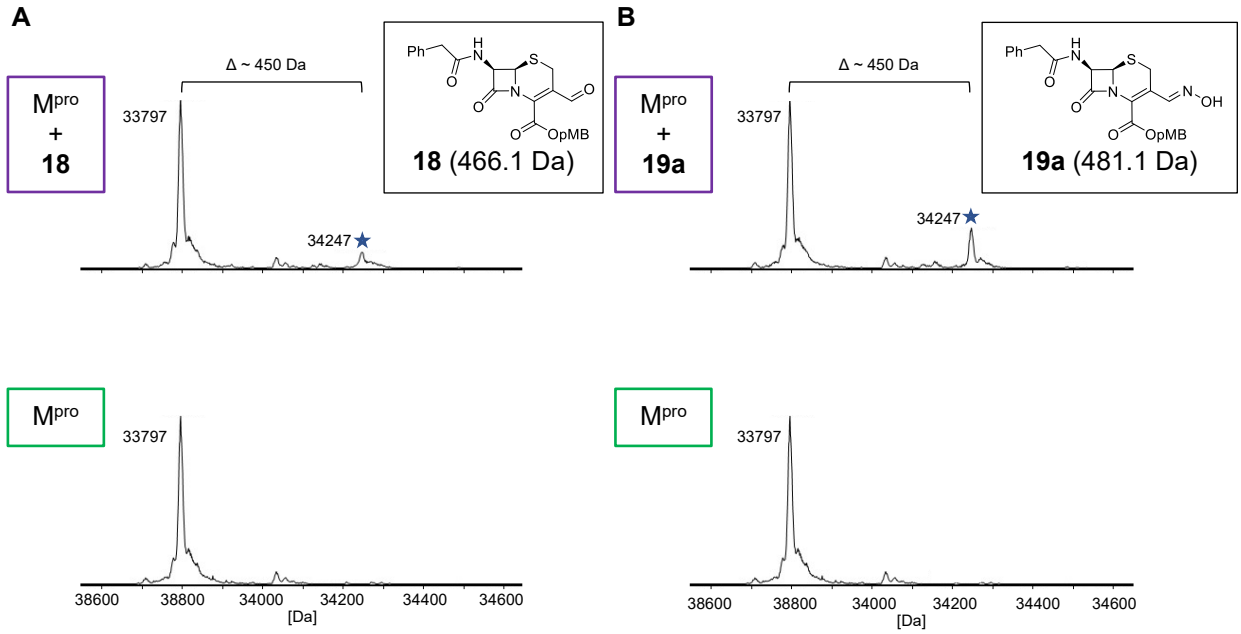

Supporting Figure S11: Analysis of M^{pro} reactions with C3 aldoxime ether cephalosporin derivatives: (**A**) **19b**, (**B**) **19c**, and (**C**) **19d**, prior (bottom) and after >15 h of incubation (top) with the respective β-lactam. Assays were performed using SPE-MS as reported,[67] employing SARS-CoV-2 M^{pro} (3.0 μM) and, if appropriate, a β-lactam (15 μM) in buffer (20 mM HEPES, pH 7.5). Representative spectra of technical duplicates are shown.

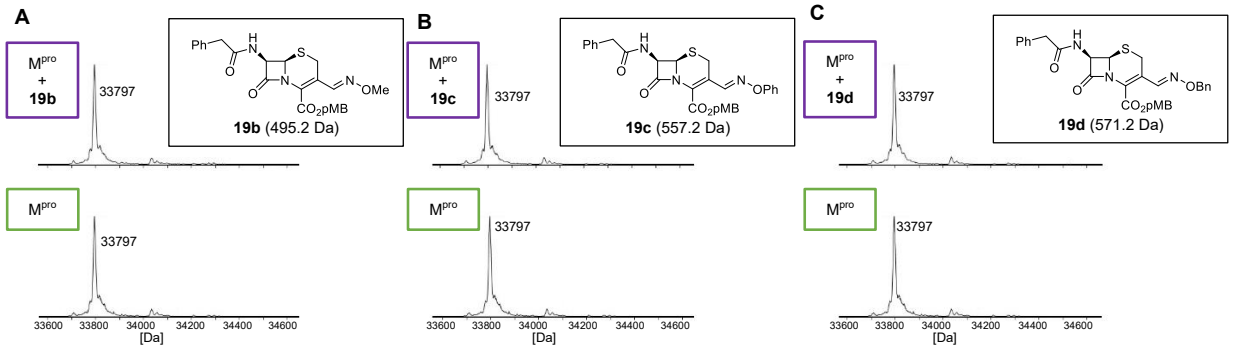

Supporting Figure S12: Evidence that **18** and **19a** inhibit M^{pro} by selective covalent reaction with Cys145. Assays were performed using reported SPE-MS conditions[79, 80] employing SARS-CoV-2 M^{pro} (3.0 μM) and, if appropriate, a β-lactam (10 μM) in buffer (20 mM HEPES, pH 7.5). Representative spectra of technical duplicates are shown.

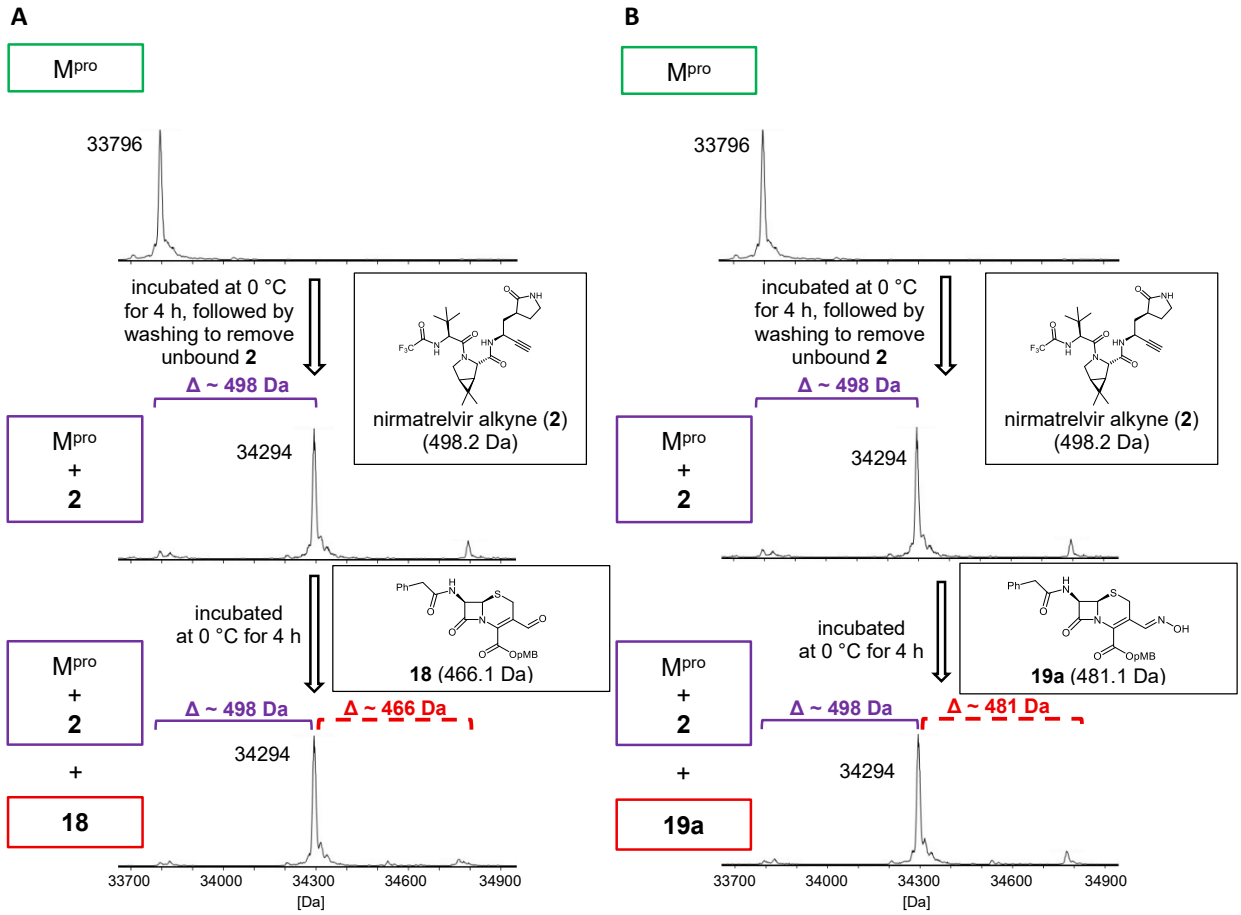

Supporting Figure S13: Evidence for covalent reaction of M^{pro} with **19a**. SPE-MS analysis showed initial formation of a +481 Da adduct (★), which after ~ 10 min gives rise to a secondary +450 Da adduct (★) (10:3 inhibitor:M^{pro} ratio).

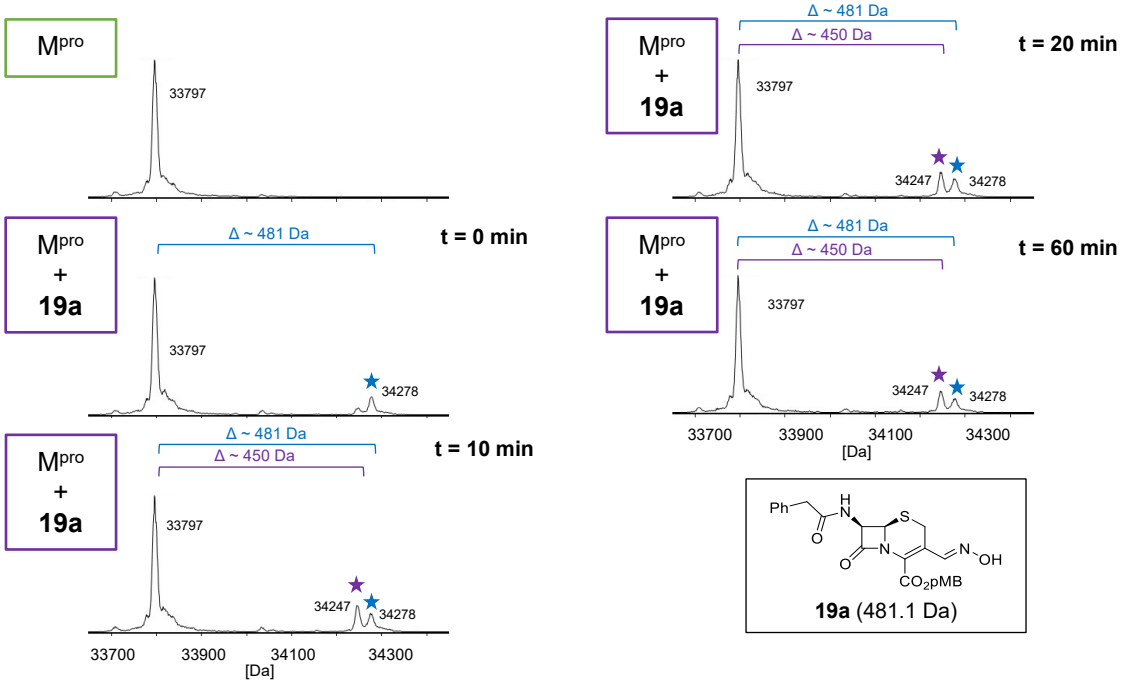

Supporting Figure S14: Reaction of C3' quaternary ammonium cephalosporins with isolated recombinant M^{pro}. Analysis of M^{pro} reactions with cephalosporin derivatives: (**A**) **20a**, (**B**) **20b**, (**C**) **20c**, (**D**) **20e**, (**E**) **20f**, (**F**) **20h** prior (bottom) and after >15 h of incubation (top) with the respective β-lactam. Assays were performed using SPE-MS as reported,[67] employing SARS-CoV-2 M^{pro} (3.0 µM) and, if appropriate, a β-lactam (15 µM) in buffer (20 mM HEPES, pH 7.5). Representative spectra of technical duplicates are shown.

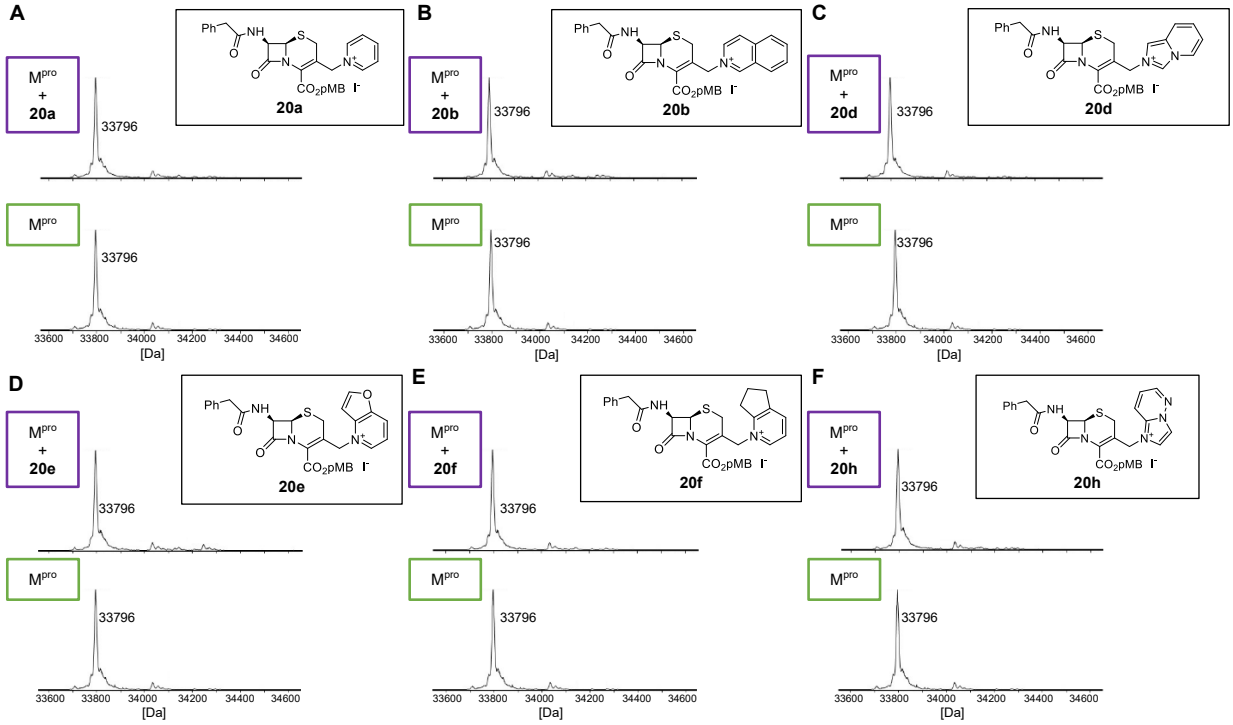

3.2.7 References

1. L. M. Lima, B. N. M. da Silva, G. Barbosa and E. J. Barreiro, β-lactam antibiotics: An overview from a medicinal chemistry perspective, *Eur. J. Med. Chem.*, 2020, **208**, 112829.
2. M. Mora-Ochomogo and C. T. Lohans, β-Lactam antibiotic targets and resistance mechanisms: from covalent inhibitors to substrates, *RSC Med. Chem.*, 2021, **12**, 1623–1639.
3. K. Bush and P. A. Bradford, β-Lactams and β-Lactamase Inhibitors: An Overview, *Cold Spring Harb. Perspect. Med.*, 2016, **6**, a025247.
4. M. I. Page, in *The Chemistry of β-Lactams*, ed. M. I. Page, Springer Netherlands, Dordrecht, 1992, pp. 129–147.
5. L. I. Llarrull, S. A. Testero, J. F. Fisher and S. Mobashery, The future of the β-lactams, *Curr. Opin. Microbiol.*, 2010, **13**, 551–557.
6. P. M. Blumberg and J. L. Strominger, Interaction of penicillin with the bacterial cell: penicillin-binding proteins and penicillin-sensitive enzymes, *Bacteriol. Rev.*, 1974, **38**, 291–335.
7. B. Lee, Conformation of penicillin as a transition-state analog of the substrate of peptidoglycan transpeptidase, *J. Mol. Biol.*, 1971, **61**, 463–469.
8. D. J. Tipper and J. L. Strominger, Mechanism of action of penicillins: a proposal based on their structural similarity to acyl-D-alanyl-D-alanine, *Proc. Natl. Acad. Sci.*, 1965, **54**, 1133–1141.
9. T. J. Franklin and G. A. Snow, in *Biochemistry of Antimicrobial Action*, eds. T. J. Franklin and G. A. Snow, Springer Netherlands, Dordrecht, 1989, pp. 20–54.
10. A. Kamath and I. Ojima, Advances in the chemistry of β-lactam and its medicinal applications, *Tetrahedron*, 2012, **68**, 10640–10664.
11. P. D. Mehta, N. P. S. Sengar and A. K. Pathak, 2-Azetidinone – A new profile of various pharmacological activities, *Eur. J. Med. Chem.*, 2010, **45**, 5541–5560.
12. D.-J. Fu, Y.-F. Zhang, A.-Q. Chang and J. Li, β-Lactams as promising anticancer agents: Molecular hybrids, structure activity relationships and potential targets, *Eur. J. Med. Chem.*, 2020, **201**, 112510.
13. D. Kuhn, C. Coates, K. Daniel, D. Chen, M. Bhuiyan, A. Kazi, E. Turos and Q. P. Dou, Beta-lactams and their potential use as novel anticancer chemotherapeutics drugs, *FBL*, 2004, **9**, 2605–2617.
14. J. M. T. Hamilton-Miller, β-Lactams: variations on a chemical theme, with some surprising biological results, *J. Antimicrob. Chemother.*, 1999, **44**, 729–734.
15. S. B. Rosenblum, T. Huynh, A. Afonso, H. R. Davis, N. Yumibe, J. W. Clader and D. A. Burnett, Discovery of 1-(4-Fluorophenyl)-(3R)-[3-(4-fluorophenyl)-(3S)- hydroxypropyl]-(4S)-(4-hydroxyphenyl)-2-azetidinone (SCH 58235): A Designed, Potent, Orally Active Inhibitor of Cholesterol Absorption, *J. Med. Chem.*, 1998, **41**, 973–980.
16. D. A. Burnett, M. A. Caplen, H. R. Davis, Jr., R. E. Burrier and J. W. Clader, 2-Azetidinones as Inhibitors of Cholesterol Absorption, *J. Med. Chem.*, 1994, **37**, 1733–1736.
17. V. M. Vrudhula, H. P. Svensson, K. A. Kennedy, P. D. Senter and P. M. Wallace, Antitumor activities of a cephalosporin prodrug in combination with monoclonal antibody-.beta.-lactamase conjugates, *Bioconj. Chem.*, 1993, **4**, 334–340.

18. V. M. Vrudhula, H. P. Svensson and P. D. Senter, Cephalosporin Derivatives of Doxorubicin as Prodrugs for Activation by Monoclonal Antibody-.beta.-Lactamase Conjugates, *J. Med. Chem.*, 1995, **38**, 1380–1385.
19. V. M. Vrudhula, D. E. Kerr, N. O. Siemers, G. M. Dubowchik and P. D. Senter, Cephalosporin prodrugs of paclitaxel for immunologically specific activation by L-49-sFv-β-Lactamase fusion protein, *Bioorg. Med. Chem. Lett.*, 2003, **13**, 539–542.
20. V. M. Vrudhula, H. P. Svensson and P. D. Senter, Immunologically Specific Activation of a Cephalosporin Derivative of Mitomycin C by Monoclonal Antibody β-Lactamase Conjugates, *J. Med. Chem.*, 1997, **40**, 2788–2792.
21. H. P. Svensson, J. F. Kadow, V. M. Vrudhula, P. M. Wallace and P. D. Senter, Monoclonal antibody-.beta.-lactamase conjugates for the activation of a cephalosporin mustard prodrug, *Bioconj. Chem.*, 1992, **3**, 176–181.
22. X. Li, H. Li, S. Li, F. Zhu, D. J. Kim, H. Xie, Y. Li, J. Nadas, N. Oi, T. A. Zykova, D. H. Yu, M.-H. Lee, M. O. Kim, L. Wang, W. Ma, R. A. Lubet, A. M. Bode, Z. Dong and Z. Dong, Ceftriaxone, an FDA-approved cephalosporin antibiotic, suppresses lung cancer growth by targeting Aurora B, *Carcinogenesis*, 2012, **33**, 2548–2557.
23. E. Labay, H. J. Mauceri, E. V. Efimova, A. C. Flor, H. G. Sutton, S. J. Kron and R. R. Weichselbaum, Repurposing cephalosporin antibiotics as pro-senescent radiosensitizers, *Oncotarget*, 2016, **7**.
24. X. He, Q. Yao, D. Fan, L. Duan, Y. You, W. Liang, Z. Zhou, S. Teng, Z. Liang, D. D. Hall, L.-S. Song and B. Chen, Cephalosporin antibiotics specifically and selectively target nasopharyngeal carcinoma through HMOX1-induced ferroptosis, *Life Sci.*, 2021, **277**, 119457.
25. L. Chen, Z. Fan, J. Chang, R. Yang, H. Hou, H. Guo, Y. Zhang, T. Yang, C. Zhou, Q. Sui, Z. Chen, C. Zheng, X. Hao, K. Zhang, R. Cui, Z. Zhang, H. Ma, Y. Ding, N. Zhang, X. Lu, X. Luo, H. Jiang, S. Zhang and M. Zheng, Sequence-based drug design as a concept in computational drug design, *Nat. Commun.*, 2023, **14**, 4217.
26. C. Zhou, X. Hao, Z. Chen, R. Zhang, Q. Zhou, Z. Fan, M. Zheng, H. Hou, S. Zhang and H. Guo, Synthesis and Biological Evaluation of β-Lactam Derivatives Targeting Speckle-Type POZ Protein (SPOP), *ACS Med. Chem. Lett.*, 2024, **15**, 270–279.
27. D. M. Smith, A. Kazi, L. Smith, T. E. Long, B. Heldreth, E. Turos and Q. P. Dou, A Novel Beta-Lactam Antibiotic Activates Tumor Cell Apoptotic Program by Inducing DNA Damage, *Mol. Pharmacol.*, 2002, **61**, 1348–1358.
28. I. Banik, F. F. Becker and B. K. Banik, Stereoselective Synthesis of β-Lactams with Polyaromatic Imines: Entry to New and Novel Anticancer Agents, *J. Med. Chem.*, 2003, **46**, 12–15.
29. L. N. Jungheim and T. A. Shepherd, Design of Antitumor Prodrugs: Substrates for Antibody Targeted Enzymes, *Chem. Rev.*, 1994, **94**, 1553–1566.
30. T. A. Shepherd, L. N. Jungheim, D. L. Meyer and J. J. Starling, A novel targeted delivery system utilizing a cephalosporin-oncolytic prodrug activated by an antibody β-lactamase conjugate for the treatment of cancer, *Bioorg. Med. Chem. Lett.*, 1991, **1**, 21–26.
31. R. P. Alexander, R. W. Bates, A. J. Pratt and J. A. E. Kraunsoe, AN-nitrosochloroethyl-cephalosporin carbamate prodrug for antibody-directed enzyme prodrug therapy (ADEPT), *Tetrahedron*, 1996, **52**, 5983–5988.
32. R. M. Phelan, M. Ostermeier and C. A. Townsend, Design and synthesis of a β-lactamase activated 5-fluorouracil prodrug, *Bioorg. Med. Chem. Lett.*, 2009, **19**, 1261–1263.

33. R. P. Alexander, N. R. A. Beeley, M. O'Driscoll, F. P. O'Neill, T. A. Millican, A. J. Pratt and F. W. Willenbrock, Cephalosporin Nitrogen Mustard Carbamate prodrugs for "ADEPT", *Tetrahedron Lett.*, 1991, **32**, 3269–3272.
34. D. B. Boggián, P. G. Cornier, E. G. Mata, V. C. Blank, M. G. Cárdenas and L. P. Roguin, A solid- and solution-phase-based library of 2β-methyl substituted penicillin derivatives and their effects on growth inhibition of tumor cell lines, *MedChemComm*, 2015, **6**, 619–625.
35. P. G. Cornier, C. M. L. Delpiccolo, F. C. Mascali, D. B. Boggián, E. G. Mata, M. G. Cárdenas, V. C. Blank and L. P. Roguin, In vitro anticancer activity and SAR studies of triazolyl aminoacyl(peptidyl) penicillins, *MedChemComm*, 2014, **5**, 214–218.
36. N. L. Martiren, S. Bajicoff, Y. Bellizzi, V. C. Blank, L. P. Roguin, P. G. Cornier, E. G. Mata and C. M. L. Delpiccolo, Synthetic Strategies Towards the Generation of Penicillin-Containing Hybrids in the Search for Anticancer Activity, *Chem. Biodivers.*, 2025, **22**, e202402198.
37. C. M. Camacho, M. G. Pizzio, D. L. Roces, D. B. Boggián, E. G. Mata, Y. Bellizzi, E. Barrionuevo, V. C. Blank and L. P. Roguin, Design, synthesis and cytotoxic evaluation of a library of oxadiazole-containing hybrids, *RSC Adv.*, 2021, **11**, 29741–29751.
38. T. W. Hudyma, K. Bush, K. L. Colson, R. A. Firestone and H. D. King, Synthesis and release of doxorubicin from a cephalosporin based prodrug by a β-lactamase-immunoconjugate, *Bioorg. Med. Chem. Lett.*, 1993, **3**, 323–328.
39. R. M. Adlington, J. E. Baldwin, B. Chen, S. L. Cooper, W. McCoull, G. J. Pritchard, T. J. Howe, G. W. Becker, R. B. Hermann, A. M. McNulty and B. L. Neubauer, Design and synthesis of novel monocyclic β-lactam inhibitors of prostate specific antigen, *Bioorg. Med. Chem. Lett.*, 1997, **7**, 1689–1694.
40. J. B. Doherty, B. M. Ashe, L. W. Argenbright, P. L. Barker, R. J. Bonney, G. O. Chandler, M. E. Dahlgren, C. P. Dorn, P. E. Finke, R. A. Firestone, D. Fletcher, W. K. Hagmann, R. Mumford, L. O'Grady, A. L. Maycock, J. M. Pisano, S. K. Shah, K. R. Thompson and M. Zimmerman, Cephalosporin antibiotics can be modified to inhibit human leukocyte elastase, *Nature*, 1986, **322**, 192–194.
41. P. E. Finke, B. M. Ashe, W. B. Knight, A. L. Maycock, M. A. Navia, S. K. Shah, K. R. Thompson, D. J. Underwood and H. Weston, Inhibition of human leukocyte elastase. 2. Inhibition by substituted cephalosporin esters and amides, *J. Med. Chem.*, 1990, **33**, 2522–2528.
42. K. R. Thompson, P. E. Finke, S. K. Shah, B. M. Ashe, M. E. Dahlgren, A. L. Maycock and J. B. Doherty, Inhibition of human leukocyte elastase. 6. Inhibition by 6-substituted penicillin esters, *Bioorg. Med. Chem. Lett.*, 1993, **3**, 2283–2288.
43. J. D. Buynak, A. S. Rao, G. P. Ford, C. Carver, G. Adam, B. Geng, B. Bachmann, S. Shobassy and S. Lackey, 7-Alkylidenecephalosporin Esters as Inhibitors of Human Leukocyte Elastase, *J. Med. Chem.*, 1997, **40**, 3423–3433.
44. P. E. Finke, S. K. Shah, B. M. Ashe, R. G. Ball, T. J. Blacklock, R. J. Bonney, K. A. Brause, G. O. Chandler and M. Cotton, Inhibition of human leukocyte elastase. 4. Selection of a substituted cephalosporin (L-658,758) as a topical aerosol, *J. Med. Chem.*, 1992, **35**, 3731–3744.
45. P. E. Finke, M. E. Dahlgren, H. Weston, A. L. Maycock and J. B. Doherty, Inhibition of human leukocyte elastase. 5. Inhibition by 6-alkyl substituted penem benzyl esters, *Bioorg. Med. Chem. Lett.*, 1993, **3**, 2277–2282.

46. S. K. Shah, C. P. Dorn, Jr., P. E. Finke, J. J. Hale, W. K. Hagmann, K. A. Brause, G. O. Chandler, A. L. Kissinger and B. M. Ashe, Orally active .beta.-lactam inhibitors of human leukocyte elastase-1. Activity of 3,3-diethyl-2-azetidinones, *J. Med. Chem.*, 1992, **35**, 3745–3754.
47. R. Firestone, P. L. Parker, J. M. Pisano, B. M. Ashe and M. E. Dahlgren, Monocyclic β-lactam inhibitors of human leukocyte elastase, *Tetrahedron*, 1990, **46**, 2255–2262.
48. S. K. Shah, K. A. Brause, G. O. Chandler, P. E. Finke, B. M. Ashe, H. Weston, W. B. Knight, A. L. Maycock and J. B. Doherty, Inhibition of human leukocyte elastase. 3. Synthesis and activity of 3'-substituted cephalosporins, *J. Med. Chem.*, 1990, **33**, 2529–2535.
49. J. R. Burke, K. R. Gregor, R. Padmanabha, J. Banville, M. R. Witmer, L. B. Davern, S. P. Manly and K. M. Tramposch, A β-Lactam Inhibitor of Cytosolic Phospholipase A2 which Acts in a Competitive, Reversible Manner at the Lipid/Water Interface, *J. Enzym Inhib.*, 1998, **13**, 195–206.
50. J. Sugatani, K. Saito and I. Honjo, In vitro actions of some antibiotics on phospholipases, *J. Antibiot.*, 1979, **32**, 734–739.
51. X. Ci, Y. Song, F. Zeng, X. Zhang, H. Li, X. Wang, J. Cui and X. Deng, Ceftiofur impairs pro-inflammatory cytokine secretion through the inhibition of the activation of NF-κB and MAPK, *Biochem. Biophys. Res. Commun.*, 2008, **372**, 73–77.
52. G. Cainelli, P. Galletti, S. Garbisa, D. Giacomini, L. Sartor and A. Quintavalla, 4-Alkylidene-azetidin-2-ones: novel inhibitors of leukocyte elastase and gelatinase, *Bioorganic & Medicinal Chemistry*, 2003, **11**, 5391–5399.
53. M. S. Genčić, N. M. Stojanović, J. M. Denić, Z. Z. Stojanović-Radić, P. Stojanović, K. Van Hecke, L. S. Jovanović, M. V. Nikolić, T. Jevtović-Stoimenov, N. S. Radulović and M. D'Hooghe, Repurposing of monocyclic β-lactams as anti-inflammatory agents – The case of new ferrocene-azetidin-2-one hybrids, *Eur. J. Med. Chem.*, 2024, **280**, 116910.
54. A. Fiasella, A. Nuzzi, M. Summa, A. Armirotti, G. Tarozzo, G. Tarzia, M. Mor, F. Bertozzi, T. Bandiera and D. Piomelli, 3-Aminoazetidin-2-one Derivatives as N-Acylethanolamine Acid Amidase (NAAA) Inhibitors Suitable for Systemic Administration, *ChemMedChem*, 2014, **9**, 1602–1614.
55. A. Nuzzi, A. Fiasella, J. A. Ortega, C. Pagliuca, S. Ponzano, D. Pizzirani, S. M. Bertozzi, G. Ottonello, G. Tarozzo, A. Reggiani, T. Bandiera, F. Bertozzi and D. Piomelli, Potent α-amino-β-lactam carbamic acid ester as NAAA inhibitors. Synthesis and structure–activity relationship (SAR) studies, *Eur. J. Med. Chem.*, 2016, **111**, 138–159.
56. R. Petracca, S. Ponzano, S. M. Bertozzi, O. Sasso, D. Piomelli, T. Bandiera and F. Bertozzi, Progress in the development of β-lactams as N-Acylethanolamine Acid Amidase (NAAA) inhibitors: Synthesis and SAR study of new, potent N-O-substituted derivatives, *Eur. J. Med. Chem.*, 2017, **126**, 561–575.
57. L. C. Cheney, W. J. Gottstein, A. H. Eachus, P. F. Misco, M. Misiek and K. E. Price, β-Lactam antimicrobial agents which possess antifungal activity, *J. Med. Chem.*, 1971, **14**, 770–772.
58. H. D. King, J. Langharig and J. J. Sanglier, Clavamycins, new clavam antibiotics from two variants of streptomyces hygroscop1cus I. Taxonomy of the producing organisms, fermentation, and biological activities, *J. Antibiot.*, 1986, **39**, 510–515.
59. A. Arnoldi, S. Grasso, G. Meinardi and L. Merlini, Synthesis and anti-fungal activity of simple β-lactams, *Eur. J. Med. Chem.*, 1988, **23**, 149–154.

60. D. Brown, J. R. Evans and R. A. Fletton, Structures of three novel β-lactams isolated from Streptomyces clavuligerus, *J. Chem. Soc., Chem. Commun.*, 1979, 282–283.
61. J. C. Müller, V. Toome, D. L. Pruess, J. F. Blount and M. Weigele, A new clavam antibiotic from streptomyces clavuligerus: III. Absolute stereochemistry, *J. Antibiot.*, 1983, **36**, 217–225.
62. N. E. Zhou, J. Kaleta, E. Purisima, R. Menard, R. G. Micetich and R. Singh, 6-Acylamino-penam derivatives: synthesis and inhibition of cathepsins B, L, K, and S, *Bioorg. Med. Chem. Lett.*, 2002, **12**, 3417–3419.
63. T. Dražić, S. Kopf, J. Corridan, M. M. Leuthold, B. Bertoša and C. D. Klein, Peptide-β-lactam Inhibitors of Dengue and West Nile Virus NS2B-NS3 Protease Display Two Distinct Binding Modes, *J. Med. Chem.*, 2020, **63**, 140–156.
64. T. M. Haley, S. J. Angier, A. D. Borthwick, D. S. Montgomery, I. J. Purvis, D. H. Smart, C. Bessant, C. Van Wely and G. J. Hart, Investigation of the covalent modification of the catalytic triad of human cytomegalovirus protease by pseudo-reversible β-lactam inhibitors and a peptide chloromethylketone, *J. Mass Spectrom.*, 1998, **33**, 1246–1255.
65. C. Yoakim, W. W. Ogilvie, D. R. Cameron, C. Chabot, I. Guse, B. Haché, J. Naud, J. A. O'Meara, R. Plante and R. Déziel, β-Lactam Derivatives as Inhibitors of Human Cytomegalovirus Protease, *J. Med. Chem.*, 1998, **41**, 2882–2891.
66. R. Déziel and E. Malenfant, Inhibition of human cytomegalovirus protease No with monocyclic β-lactams, *Bioorg. Med. Chem. Lett.*, 1998, **8**, 1437–1442.
67. T. R. Malla, A. Tumber, T. John, L. Brewitz, C. Strain-Damerell, C. D. Owen, P. Lukacik, H. T. H. Chan, P. Maheswaran, E. Salah, F. Duarte, H. Yang, Z. Rao, M. A. Walsh and C. J. Schofield, Mass spectrometry reveals potential of β-lactams as SARS-CoV-2 Mpro inhibitors, *Chem. Commun.*, 2021, **57**, 1430–1433.
68. T. R. Malla, L. Brewitz, D.-G. Muntean, H. Aslam, C. D. Owen, E. Salah, A. Tumber, P. Lukacik, C. Strain-Damerell, H. Mikolajek, M. A. Walsh and C. J. Schofield, Penicillin Derivatives Inhibit the SARS-CoV-2 Main Protease by Reaction with Its Nucleophilic Cysteine, *J. Med. Chem.*, 2022, **65**, 7682–7696.
69. F. A. Ambrosio, G. Costa, I. Romeo, F. Esposito, M. Alkhatib, R. Salpini, V. Svicher, A. Corona, P. Malune, E. Tramontano, F. Ceccherini-Silberstein, S. Alcaro and A. Artese, Targeting SARS-CoV-2 Main Protease: A Successful Story Guided by an In Silico Drug Repurposing Approach, *J. Chem. Inf. Model.*, 2023, **63**, 3601–3613.
70. A. D. Borthwick, G. Weingarten, T. M. Haley, M. Tomaszewski, W. Wang, Z. Hu, J. Bedard, H. Jin, L. Yuen and T. S. Mansour, Design and synthesis of monocyclic β-lactams as mechanism-based inhibitors of human cytomegalovirus protease, *Bioorg. Med. Chem. Lett.*, 1998, **8**, 365–370.
71. E. L. Setti, D. Davis, T. Chung and J. McCarter, 3,4-Disubstituted azetidinones as selective inhibitors of the cysteine protease cathepsin K. Exploring P2 elements for selectivity, *Bioorg. Med. Chem. Lett.*, 2003, **13**, 2051–2053.
72. F. Nazir, A. John Kombe Kombe, Z. Khalid, S. Bibi, H. Zhang, S. Wu and T. Jin, SARS-CoV-2 replication and drug discovery, *Mol. Cell. Probes*, 2024, **77**, 101973.
73. Y. Duan, H. Wang, Z. Yuan and H. Yang, Structural biology of SARS-CoV-2 Mpro and drug discovery, *Curr. Opin. Struct. Biol.*, 2023, **82**, 102667.
74. Y. Yang, Y.-D. Luo, C.-B. Zhang, Y. Xiang, X.-Y. Bai, D. Zhang, Z.-Y. Fu, R.-B. Hao and X.-L. Liu, Progress in Research on Inhibitors Targeting SARS-CoV-2 Main Protease (Mpro), *ACS Omega*, 2024, **9**, 34196–34219.

75. Q. Hu, Y. Xiong, G.-H. Zhu, Y.-N. Zhang, Y.-W. Zhang, P. Huang and G.-B. Ge, The SARS-CoV-2 main protease (Mpro): Structure, function, and emerging therapies for COVID-19, *MedComm*, 2022, **3**, e151.
76. A. Mubarik, M. A. Khan, S. Mutahir, A. A. Almehizia and X.-H. Ju, Novel Cephalosporins Against the Main Protease of SARS CoV (Mpro O, Mpro WT): Molecular Docking and DFT Study, *ChemistrySelect*, 2024, **9**, e202403176.
77. T. Ishikawa, N. Matsunaga, H. Tawada, N. Kuroda, Y. Nakayama, Y. Ishibashi, M. Tomimoto, Y. Ikeda, Y. Tagawa, Y. Iizawa, K. Okonogi, S. Hashiguchi and A. Miyake, TAK-599, a novel N-Phosphono type prodrug of anti-MRSA cephalosporin T-91825: synthesis, physicochemical and pharmacological properties, *Bioorganic & Medicinal Chemistry*, 2003, **11**, 2427–2437.
78. H. Poon, M. H. Chang and H. B. Fung, Ceftaroline Fosamil: A Cephalosporin With Activity Against Methicillin-Resistant Staphylococcus Aureus, *Clin. Ther.*, 2012, **34**, 743–765.
79. L. Brewitz, L. Dumjahn, Y. Zhao, C. D. Owen, S. M. Laidlaw, T. R. Malla, D. Nguyen, P. Lukacik, E. Salah, A. D. Crawshaw, A. J. Warren, J. Trincao, C. Strain-Damerell, M. W. Carroll, M. A. Walsh and C. J. Schofield, Alkyne Derivatives of SARS-CoV-2 Main Protease Inhibitors Including Nirmatrelvir Inhibit by Reacting Covalently with the Nucleophilic Cysteine, *J. Med. Chem.*, 2023, **66**, 2663–2680.
80. Gayatri, L. Brewitz, L. Ibbotson, E. Salah, S. Basak, H. Choudhry and C. J. Schofield, Thiophene-fused γ-lactams inhibit the SARS-CoV-2 main protease via reversible covalent acylation, *Chem. Sci.*, 2024, **15**, 7667–7678.
81. S. S. van Berkel, J. Brem, A. M. Rydzik, R. Salimraj, R. Cain, A. Verma, R. J. Owens, C. W. G. Fishwick, J. Spencer and C. J. Schofield, Assay Platform for Clinically Relevant Metallo-β-lactamases, *J. Med. Chem.*, 2013, **56**, 6945–6953.
82. S. Mobashery and M. Johnston, Preparation of ceph-3-em esters unaccompanied by Δ3/Δ2 isomerization of the cephalosporin, *J. Org. Chem.*, 1986, **51**, 4723–4726.
83. R. B. Morin, B. G. Jackson, R. A. Mueller, E. R. Lavagnino, W. B. Scanlon and S. L. Andrews, Chemistry of cephalosporin antibiotics. XV. Transformations of penicillin sulfoxide. Synthesis of cephalosporin compounds, *J. Am. Chem. Soc.*, 1969, **91**, 1401–1407.
84. R. B. Woodward, K. Heusler, J. Gosteli, P. Naegeli, W. Oppolzer, R. Ramage, S. Ranganathan and H. Vorbrüggen, The Total Synthesis of Cephalosporin C1, *J. Am. Chem. Soc.*, 1966, **88**, 852–853.
85. E. Pop, M. E. Brewster, N. Bodor and J. J. Kaminski, Theoretical aspects of cephalosporin isomerism, *Int. J. Quantum Chem*, 1989, **36**, 291–300.
86. J. D. Cocker, S. Eardley, G. I. Gregory, M. E. Hall and A. G. Long, Cephalosporanic acids. Part IV. 7-Acylamidoceph-2-em-4-carboxylic acids, *J. Chem. Soc. C Org.*, 1966, 1142–1151.
87. H. Tanaka, Y. Tokumaru, K.-i. Fukui, M. Kuroboshi, S. Torii, A. Jutand and C. Amatore, Chemo- and Product-selective Electrooxidation of 3-(Arylthiomethyl)-Δ^3-cephems, *Synthesis*, 2009, **2009**, 3449–3459.
88. H. Tanaka, R. Kikuchi and S. Torii, Aerobic Oxidation of 3-Iodomethyl-Δ3-cephem-4-carboxylate to 3-Formyl-Δ3-cephem-4-carboxylate through 3-Hydroperoxymethyl-Δ3-cephem-4-carboxylate, *Bull. Chem. Soc. Jpn.*, 1996, **69**, 229–233.

89. L. Caly, J. Druce, J. Roberts, K. Bond, T. Tran, R. Kostecki, Y. Yoga, W. Naughton, G. Taiaroa, T. Seemann, M. B. Schultz, B. P. Howden, T. M. Korman, S. R. Lewin, D. A. Williamson and M. G. Catton, Isolation and rapid sharing of the 2019 novel coronavirus (SARS-CoV-2) from the first patient diagnosed with COVID-19 in Australia, *Med. J. Aust.*, 2020, **212**, 459–462.
90. X. Lin and U. Kück, Cephalosporins as key lead generation beta-lactam antibiotics, *Appl. Microbiol. Biotechnol.*, 2022, **106**, 8007–8020.
91. J. M. T. Hamilton-Miller, Sir Edward Abraham's contribution to the development of the cephalosporins: a reassessment, *Int. J. Antimicrob. Agents*, 2000, **15**, 179–184.
92. R. S. Griffith and H. R. Black, Cephalothin—A New Antibiotic: Preliminary Clinical and Laboratory Studies, *JAMA*, 1964, **189**, 823–828.
93. T. A. Tartaglione and R. E. Polk, Review of the New Second-Generation Cephalosporins: Cefonicid, Ceforanide, and Cefuroxime, *Drug. Intell. Clin. Pharm.*, 1985, **19**, 188–198.
94. J. Hamilton-Miller and W. Brumfitt, Cephamycins: A review, prospects and some original observations, *Infection*, 1975, **3**, 183–188.
95. G. R. Donowitz, Third Generation Cephalosporins, *Infect. Dis. Clin. North Am.*, 1989, **3**, 595–612.
96. J. Garau, W. W. Wilson, M. Wood and J. Carlet, Fourth-generation cephalosporins: a review of in vitro activity, pharmacokinetics, pharmacodynamics and clinical utility, *Clinical Microbiology and Infection*, 1997, **3**, s87–s101.
97. I. W. Fong, in *New Antimicrobials: For the Present and the Future*, ed. I. W. Fong, Springer International Publishing, Cham, 2023, pp. 25–38.
98. P. Hebeisen, I. Heinze-Krauss, P. Angehrn, P. Hohl, G. P. Page Malcolm and L. Then Rudolf, In Vitro and In Vivo Properties of Ro 63-9141, a Novel Broad-Spectrum Cephalosporin with Activity against Methicillin-Resistant Staphylococci, *Antimicrob. Agents Chemother.*, 2001, **45**, 825–836.
99. D. F. Bavaro, A. Belati, L. Bussini, V. Cento, L. Diella, M. Gatti, A. Saracino, F. Pea, P. Viale and M. Bartoletti, Safety and effectiveness of fifth generation cephalosporins for the treatment of methicillin-resistant staphylococcus aureus bloodstream infections: a narrative review exploring past, present, and future, *Expert Opin. Drug Saf.*, 2024, **23**, 9–36.
100. D. Kaushik, S. Rathi and A. Jain, Ceftaroline: a comprehensive update, *Int. J. Antimicrob. Agents*, 2011, **37**, 389–395.
101. I. Gentile, S. Giuliano, S. Corcione, F. G. De Rosa, M. Falcone, D. R. Giacobbe, A. E. Maraolo, C. M. Mastroianni, A. Oliva, R. Pascale, C. Tascini, G. Tiseo, P. Viale and M. Bassetti, Current role of ceftobiprole in the treatment of hospital-acquired and community-acquired pneumonia: expert opinion based on literature and real-life experiences, *Expert Rev. Anti. Infect. Ther.*, 2025, **23**, 217–225.
102. J. D. Chandler and B. J. Day, Biochemical mechanisms and therapeutic potential of pseudohalide thiocyanate in human health, *Free Radical Res.*, 2015, **49**, 695–710.
103. J. D. Chandler and B. J. Day, THIOCYANATE: A potentially useful therapeutic agent with host defense and antioxidant properties, *Biochem. Pharmacol.*, 2012, **84**, 1381–1387.

3.3 Statement of Authorship

Title of Paper	Cephalosporin derivatives are potent inhibitors of SARS-CoV-2 main protease
Publication Status	□Published □ Accepted for Publication □Submitted for Publication ☒Unpublished and unsubmitted work written in a manuscript style
Publication Details	**Muntean, D.-G.;** Brewitz, L.; Laczi, D.; Salah, E.; Laidlaw, S.; Carol, M.; Schofield, C.J.: **Cephalosporin derivatives are potent inhibitors of the SARS-CoV-2 main protease**

Student Confirmation

Student Name:	Dorian-Gabriel Muntean		
Contribution to the Paper	D.-G.M. conducted the SAR study on cephalosporin-based M^{pro} inhibitors and carried out all the organic synthesis. D.-G.M. conceptualised and prepared the first draft of the manuscript. L.B. provided supervision of the synthetic work, obtained the IC_{50} data, conducted protein-observed MS experiments with $M^{pro,}$ and assisted with manuscript reviewing/editing. D.L. also conducted protein-observed MS experiments with M^{pro}. S.L. and M.C. conducted the cell assays. C.J.S. is the principal investigator/supervisor of the research described in the manuscript, contributed extensively to project/data conceptualization and visualization, and manuscript reviewing/editing.		
Signature		Date	09/10/2025

Supervisor Confirmation

By signing the Statement of Authorship, you are certifying that the candidate made a substantial contribution to the publication, and that the description described above is accurate.

Supervisor name and title: Prof. Christopher J. Schofield		
Supervisor comments:		
Signature 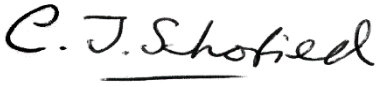	Date	09/10/2025

Chapter 4. Investigations into C6-alkoxy sulbactam derivatives

4.1 Chapter overview

Chapter 4 describes the synthesis of C6-alkoxy sulbactam derivatives and their evaluation as inhibitors of β-lactamases and penicillin-binding proteins (PBPs). **Sulbactam** is a clinically used β-lactamase inhibitor that displays good coverage of Ambler class A serine-β-lactamases (SBLs), but it also exhibits intrinsic antibacterial activity in *A. baumannii* through inhibition of PBP3. However, **sulbactam** has limited efficacy against class C and D SBLs, and no activity against class B metallo-β-lactamases (MBLs). To address these limitations, structure-activity relationship (SAR) studies were conducted at the C6 position of the penam sulfone and thioether scaffolds. The results of this Chapter show that the introduction of a C6-alkoxy group on the sulbactam scaffold generally diminished both class A SBL and PBP3 inhibition. In contrast, the presence of a bulky alkoxide conferred inhibitory properties against class D SBLs, with crystallographic studies showing that in the C6-*tert*-butoxy derivative of sulbactam, the *tert*-butoxy substituent likely stabilises the acyl-enzyme complex (AEC) formed with OXA-48 (class D SBL) by preventing the access of the hydrolytic water to the active site. Additionally, non-covalent inhibition of class A and C SBLs was observed for the C6-*tert*-butoxy penam thioether derivative, which parallels findings from **Chapter 2**, where the presence of C6-alkoxy groups in penam esters also led to non-covalent inhibition of SARS-CoV-2 M^{pro}. Overall, these results suggest that C6-alkoxy penam substitution is a promising strategy for designing β-lactam-based β-lactamase inhibitors, thanks to the potential for increased AEC stability and/or reversible binding profiles.

Manuscript III

At the time of writing this thesis, Manuscript III is in preparation for publication. A Statement of Authorship is appended at the end of the chapter. The synthetic experimental details and spectra of the compounds prepared can be found in the **Appendix**.

Muntean, **D.-G.**; Freeman, E.; Kaur, G.; Smith, H.G., Wilson, L.; Calvopiña, K.; Crumpton, A.; Brewitz, L.; Schofield, C.J.: **C6-Alkoxy substituents alter the reactivity profile of sulbactam with SBLs and PBPs.**

4.2 Manuscript III: C6-Alkoxy substituents alter the reactivity profile of sulbactam with SBLs and PBPs.

4.2.1 Abstract

Sulbactam is a clinically used β-lactamase inhibitor with activity against class A serine-β-lactamases (SBLs) but lacks good coverage with class C/D SBLs and does not inhibit class B metallo-β-lactamases (MBLs). Sulbactam also inhibits penicillin-binding protein 3 (PBP3) of *A. baumanii*, thereby exerting antibacterial properties. In the present work, we investigate how C6-alkoxy substitution on the penam sulfone and thioether scaffolds affects β-lactamase and PBP inhibition. While C6-alkoxy substitution generally decreases potency against class A SBLs and PBP3, it was noted that the C6-*tert*-butoxy derivative of sulbactam was more potent than sulbactam against class D SBLs, with crystallographic studies showing that the C6-*tert*-butoxy group may play a role in stabilising the acyl-enzyme complex (AEC). Protein-observed mass-spectrometric assays showed that the analogous C6-*tert*-butoxy penam thioether inhibited class A and C SBLs unexpectedly via a non-covalent mechanism. The combined results suggest that steric tuning at the C6 position of penam inhibitors can alter their reactivity and inhibitory spectra, potentially informing on the design of β-lactamase inhibitors with broadened spectra and mixed covalent/non-covalent mechanisms of action.

Key words: sulbactam; C6-alkoxy; β-lactamases; β-lactam-based β-lactamase inhibitors; penicillin-binding proteins.

4.2.2 Introduction

β-Lactam antibiotics, including penicillins, cephalosporins, carbapenems, and monobactams, are the most important class of antibiotics. They disrupt bacterial cell wall biosynthesis by inhibiting penicillin-binding proteins (PBPs), which catalyse peptidoglycan cross-linking during cell wall biosynthesis, via formation of stable acyl-enzyme complexes;[1-3] PBP inhibition results in loss of cell wall integrity triggering lysis.[4]

The clinical efficacy of β-lactam antibiotics is threatened by β-lactamases, which catalyse hydrolysis of the β-lactam ring of β-lactam antibiotics, rendering them inactive.[2, 5, 6] Serine β-lactamases (SBLs) employ a nucleophilic serine residue that covalently reacts with the β-lactam rings of antibiotics to form a covalent acyl-enzyme complex (AEC) that is subsequently hydrolysed. By contrast, metallo-β-lactamases (MBLs) employ Zn(II) ions to catalyse β-lactam ring hydrolysis, a reaction which does not involve formation of an acyl-enzyme complex.[2, 6, 7]

Three classes of SBL inhibitors are currently in clinical use to rescue the activity of β-lactam antibiotics, *i.e.*, β-lactams, diazabicyclooctanes (DBOs), and boronic acids (**Figure 1A**).[2, 8-10] Clavulanic acid was the first β-lactam-based SBL inhibitor to be widely used clinically,[11, 12] being followed by other penam-based β-lactam SBL inhibitors, *i.e.*, sulbactam, tazobactam, and, more recently, enmetazobactam.[2] Sulbactam shares the penam core structure with penicillin antibiotics, with the notable difference that its sulfur is in the sulfone oxidation state and that it lacks the C6 amido substituent of penicillin antibiotics. β-Lactam-based SBL inhibitors work as suicide inhibitors by acylating the active site serine residue of SBLs to generate stable covalent acyl-enzyme complexes (**Figure 1B**).[11, 13]

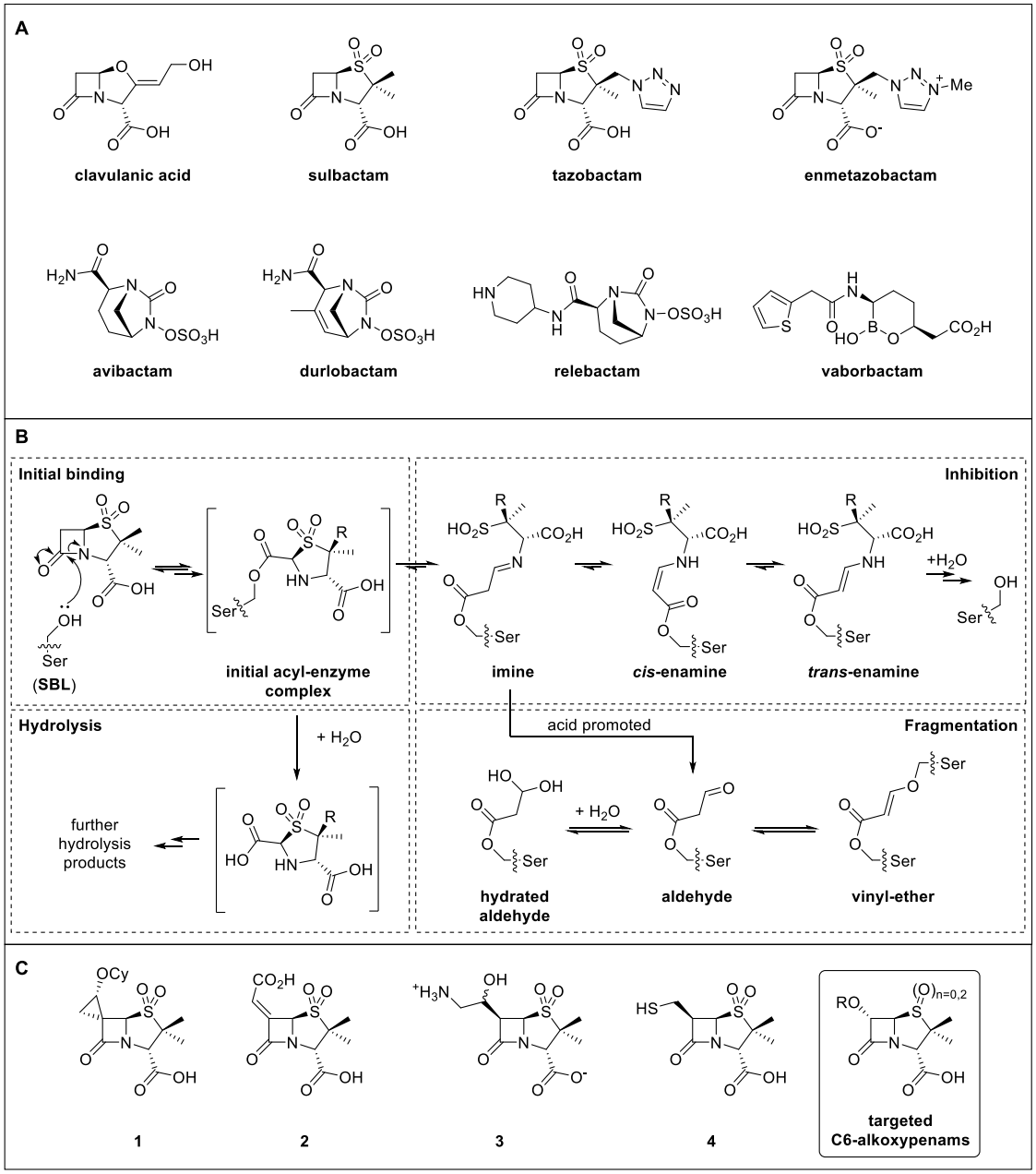

Figure 1: A. Structures of clinically β-lactamase inhibitors.[2, 10] **B**. Possible reaction pathways for the reaction of **sulbactam** with SBLs.[13] **C**. Structures of reported C6-substituted penam sulfone β-lactamase inhibitors (**1**-**4**),[21-24] and the targets of this study, C6-alkoxypenam acids. Cy: –cyclohexyl.

The non-β-lactam-containing DBO class of SBL inhibitors inhibit SBLs via reversible covalent acylation, but typically show efficacy for a broader panel of SBLs, including SBLs from Ambler classes A, C, and D.[14-18] By contrast, the cyclic boronates react with the catalytic serine residue of

SBLs to form stable covalent adducts which mimic the tetrahedral intermediate generated during β-lactam hydrolysis.[19, 20]

Sulbactam also displays intrinsic antibacterial properties, notably against *Acinetobacter baumannii*, where sulbactam inhibits PBP1 and PBP3.[25] However, because sulbactam is active primarily against Ambler class A SBLs (*e.g.*, TEM), its weak activity against class C (AmpC) and class D (OXA) enzymes, which are prevalent in *A. baumannii*, leads to hydrolytic degradation, thereby preventing sulbactam from inhibiting *A. baumannii* PBPs.[25, 26] To restore its antibacterial properties, sulbactam is clinically used in combination with durlobactam, a broad-spectrum DBO that inhibits β-lactamases from Ambler classes A, C, and D in *A. baumannii*.[27, 28]

Despite recent advances, there is a pressing need to develop improved, broad-spectrum β-lactamase inhibitors.[29, 30] Although clinically available β-lactamase inhibitors can provide activity against class A enzymes and subsets of class C and D SBLs, no inhibitors of MBL have yet been approved.[30, 31] This therapeutic gap is concerning not only because of the expanding prevalence of MBLs among Enterobacterales, but also because the frequent co-production of SBLs and MBLs within isolates of clinical interest compromises the efficacy of available treatments.[32-35]

To address these limitations, extensive efforts have been made to optimise the sulbactam scaffold, with structure-activity relationship (SAR) studies revealing that C6 substitution can enhance AEC stability, thereby improving both inhibitory potency and β-lactamase coverage (**Figure 1C**).[21-24, 36-42] For example, the C6-spirocyclopropyl penam sulfone **1** acylates the active-site serine of SBLs and subsequently undergoes spiro-fragmentation to form an oxycarbenium intermediate that can cross-link secondary nucleophilic residues, resulting in potent, irreversible inactivation of class A and class C enzymes.[41] The C6-(carboxymethylene) penam sulfone **2** is also reported to potently inactivate class A (TEM-2) and class C (AmpC) β-lactamases by forming stable acyl-enzyme

complexes; after β-lactam ring opening and thiazolidine ring fragmentation, intramolecular reaction of the C6-methylenecarboxylate with the imine intermediate gives a β-amino-β-acyloxyacrylate intermediate that slows the deacylation step.[23] Penam sulfone **3** employs a C6′ hydroxyl substituent to further stabilise the AEC formed with SBLs, wherein the hydroxyl group interferes with the hydrolytic pathway and biases the active-site base to deprotonate the C6 proton of the imine AEC to give the more stable enamine AEC.[21] The C6-mercaptomethyl penam sulfone **4** is reported to inhibit both SBLs and MBLs: it forms stabilised AECs with class A and C SBLs, and its thiol can also coordinate Zn(II) at metallo-β-lactamase active sites, thus enabling inhibition of MBLs (Ambler class B).[22]

The addition of a C6/7-methoxy group to the scaffold of penicillin and cephalosporin antibiotics is proposed to reduce susceptibility to β-lactamase-mediated hydrolysis, with crystallographic evidence suggesting that the methoxy group may prevent the access of the hydrolytic water to AEC.[43-45] It was envisioned that a similar strategy may be employed to design improved β-lactamase inhibitors that produce stabilised AECs. Here, we report the synthesis of C6-alkoxypenam sulfones and thioethers and their evaluation as β-lactamase inhibitors (**Figure 1C**), showing that C6-alkoxy substitution is a valid approach that may be effective in the development of class D SBL inhibitors.

4.2.3 Results

Synthesis of C6-alkoxy sulbactam derivatives

C6-Alkoxypenam esters were synthesized in 3-4 steps starting from commercially sourced (+)-**6-aminopenicillanic acid** (**6-APA**) using reported procedures.[46] Thus, **6-APA** was treated with Et_3N and either BnBr or *para*-nitrobenzyl bromide, which after treatment with *para*-toluenesulfonic

acid (PTSA) gave the corresponding benzyl (**5**) and *para*-nitrobenzyl (**6**) 6-aminopenicillate *para*-toluenesulfonate salts, respectively (**Figure 2**). Treatment of **5** with $NaNO_2$ under acidic conditions afforded the corresponding diazopenicillate (**Supporting Figure S1**), which was converted in a stereospecific manner into C6-α-alkoxypenam benzyl esters (**7a-d**) using BF_3 etherate complex as catalyst (35-37%). **7a-d** were oxidised to the corresponding sulfones **8a-d** using *meta*-chloroperbenzoic acid (mCPBA), which were then converted into C6-α-alkoxypenam sulfone acids **9a-d** using Pd/C mediated hydrogenation (31-69%). C6-α-Alkoxypenam *p*-nitrobenzyl esters **10a-d** were also obtained in 2 steps from **6**, to give after Pd/C mediated hydrogenation the desired C6-alkoxypenam thioethers **11a-d** (27-59%). Note that the direct hydrogenation of **7a-d** to **11a-d** using Pd/C under ambient conditions (room temperature, 1 atm) was not successful, possibly due to catalyst poisoning by the penam thioether.[47]

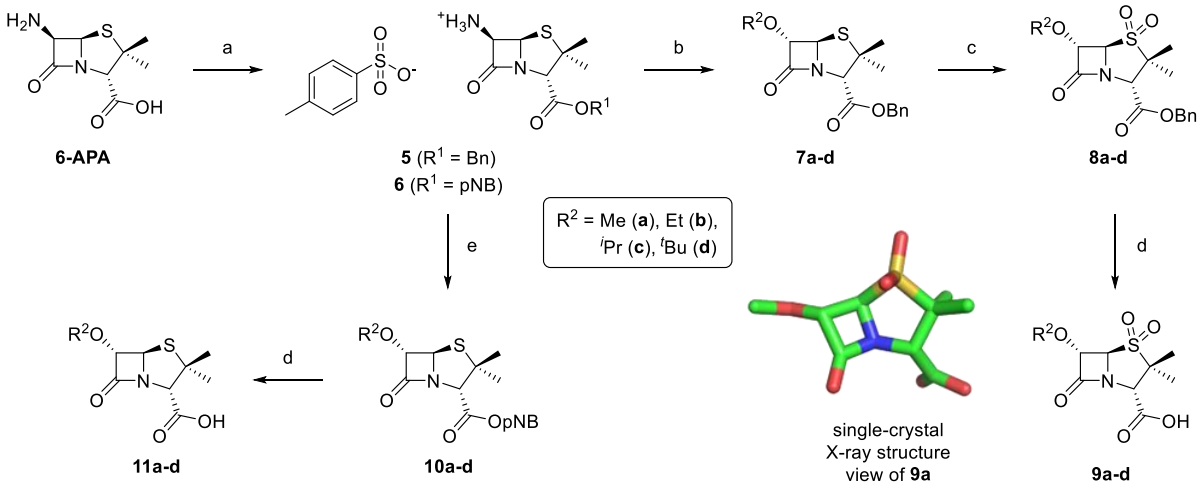

Figure 2. Synthesis of C6-alkoxypenam acids. Reagents and conditions: a) i) Et_3N (1.1 equiv.), $ArCH_2Br$ (1.1 equiv.), acetone (0.05 M), 0 ºC, 4.5 h; ii) *para*-toluenesulfonic acid monohydrate (1.1 equiv.), 44-63% (two steps); b) i) $NaNO_2$ (2.6 equiv.), *para*-toluenesulfonic acid monohydrate (0.6 equiv.), CH_2Cl_2:H_2O (4:1), 0 ºC, 20 min; ii) ROH (48-110 equiv.), $BF_3{\cdot}O(C_2H_5)_2$ (0.1 equiv.), CH_2Cl_2, 20 ºC, 15 min, 35-37% (two steps); c) mCPBA (2.2 equiv.), CH_2Cl_2, 0 ºC to rt, 16 h, 38-77%; d) H_2, Pd/C (0.55-0.75 equiv.), EtOAc, room temperature, 4 h, 19-69%; e)) i) $NaNO_2$ (2.6 equiv.), *para*-toluenesulfonic acid monohydrate (0.6 equiv.), CH_2Cl_2:H_2O (4:1), 0 ºC, 20 min; ii) ROH (40-120 equiv.), *para*-toluenesulfonic acid monohydrate (0.1 equiv.), CH_2Cl_2, 0 ºC to room temperature, 1-18 h, 9-29% (two steps). pNB: $–CH_2C_6H_4(4\text{-}NO_2)$.

C6-Alkoxy sulbactam derivatives can inhibit SBLs

The effects of the C6-alkoxy penams **9a-d** and **11a-d** on catalysis of representative isolated SBLs from Ambler classes A (TEM-116), C (AmpC), and D (OXA-10 and OXA-48) were investigated using reported fluorescence-based assays.[48] Sulbactam (**Table 1**, entry i), used as a positive inhibition control, inhibited TEM-116 (pIC_{50} ~ 6.5) ~2 orders of magnitude more efficiently than either AmpC (pIC_{50} ~ 4.4) or OXA-10 (pIC_{50} ~ 4.5), but it did not inhibit OXA-48. By contrast, most of the tested C6-alkoxy penams displayed little to no activity against the tested SBLs, with the notable exceptions of the C6-*tert*-butoxy sulfone **9d** and the C6-*tert*-butoxy penam sulfide **11d** (**Table 1**).

Table 1. Effects of C6-alkoxypenam derivatives on catalysis of isolated SBLs and PBP3 (*A. baumanii*).

	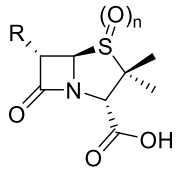			pIC_{50}[(a)]				
	Compound	R	n	TEM-116	AmpC	OXA-10	OXA-48	PBP3 (*A. baumanii*)
i	**sulbactam**	H	2	6.5 ± 0.1	4.4 ± 0.1	4.5 ± 0.1	*n.i.*	6.2 ± 0.1
ii	**9a**	OMe	2	*n.i.*	<4.0	*n.i.*	*n.i.*	5.2 ± 0.1
iii	**9b**	OEt	2	<4.0	4.5 ± 0.1	<4.0	*n.i.*	5.1 ± 0.1
iv	**9c**	O^{i}Pr	2	<4.0	4.2 ± 0.1	<4.0	4.0 ± 0.1	5.0 ± 0.1
v	**9d**	O^{t}Bu	2	<4.0	<4.0	4.3 ± 0.1	5.4 ± 0.1	4.0 ± 0.1
vi	**11a**	OMe	0	<4.0	<4.0	<4.0	<4.0	4.7 ± 0.1
vii	**11b**	OEt	0	<4.0	<4.0	<4.0	<4.0	<4.0
viii	**11c**	O^{i}Pr	0	<4.0	<4.0	<4.0	<4.0	<4.0
ix	**11d**	O^{t}Bu	0	4.5 ± 0.1	5.3 ± 0.1	<4.0	<4.0	<4.0

[(a)] Experimental details can be found in the Methods section. *n.i.* – no inhibition. Representative dose-response curves are shown in **Supporting Figure S2** and **Supporting Figure S4**.

Penam **9d** inhibited OXA-48 (pIC_{50} ~ 5.4; **Table 1**, entry v), but not SBLs from classes A or C, while penam **11d** demonstrated moderate inhibition of AmpC (pIC_{50} ~ 5.3; **Table 1**, entry ix). Notably, penam **11d** inhibited AmpC an order of magnitude more efficiently than sulbactam, but was ~2 orders of magnitude less efficient than **sulbactam** in inhibiting TEM-116. Additionally, note that penams **9a-d** and **11a-d** did not affect catalysis of selected isolated MBLs (*i.e.*, NDM-1, VIM-1, VIM-2, and IMP-1) (**Supplementary Table S1**).

C6-Alkoxy substituents reduce sulbactam's ability to inhibit PBP3

The effects of the C6-alkoxy penams **9a-d** and **11a-d** on catalysis of isolated *A. baumannii* PBP3 were investigated using reported fluorescence intensity assays[49] (**Table 1**), because **sulbactam** is a reported inhibitor of some PBPs.[25] The results reveal that penams **9a-c** inhibited PBP3 an order of magnitude less efficiently than **sulbactam** (pIC_{50} ~ 6.2), which was used as a positive inhibition control (**Table 1**, entries i-iv). By contrast, C6 *tert*-butoxy penam **9d** inhibited ~2 orders of magnitude less efficiently than sulbactam (**Table 1**, entry v). The penam sulfide **11a** inhibited PBP3 ~2 orders of magnitude less efficiently than sulbactam (**Table 1**, entry vi), whereas penams with sterically bulkier C6 substituents such as **11b-d** did not inhibit.

Protein-observed MS assays with SBLs

The reaction of SBLs with selected C6-alkoxypenams was investigated using reported MS assays to probe their mechanism.[11, 13] The results reveal that AmpC reacted less efficiently with the C6-ethoxy penam sulfone **9b**, to give only relatively low levels of acylated AmpC (+277 Da), than with **sulbactam**, which promotes the formation of an acyl-enzyme complex (+233 Da) over 30 min (**Figure 3A-B**); this was an interesting observations, as both **9b** and **sulbactam** manifest similar levels of AmpC inhibition (**Table 1**, entries i and iii). By contrast, OXA-48 reacted with

the C6-*tert*-butoxy penam **9d** more efficiently than with **sulbactam**, which did not form covalent adducts with OXA-48 within 15 min (**Figure 3C-D**). The observed mass shifts with **9d** (+143 Da, +161 Da, +305 Da) indicate the formation of multiple acyl-enzyme complexes.

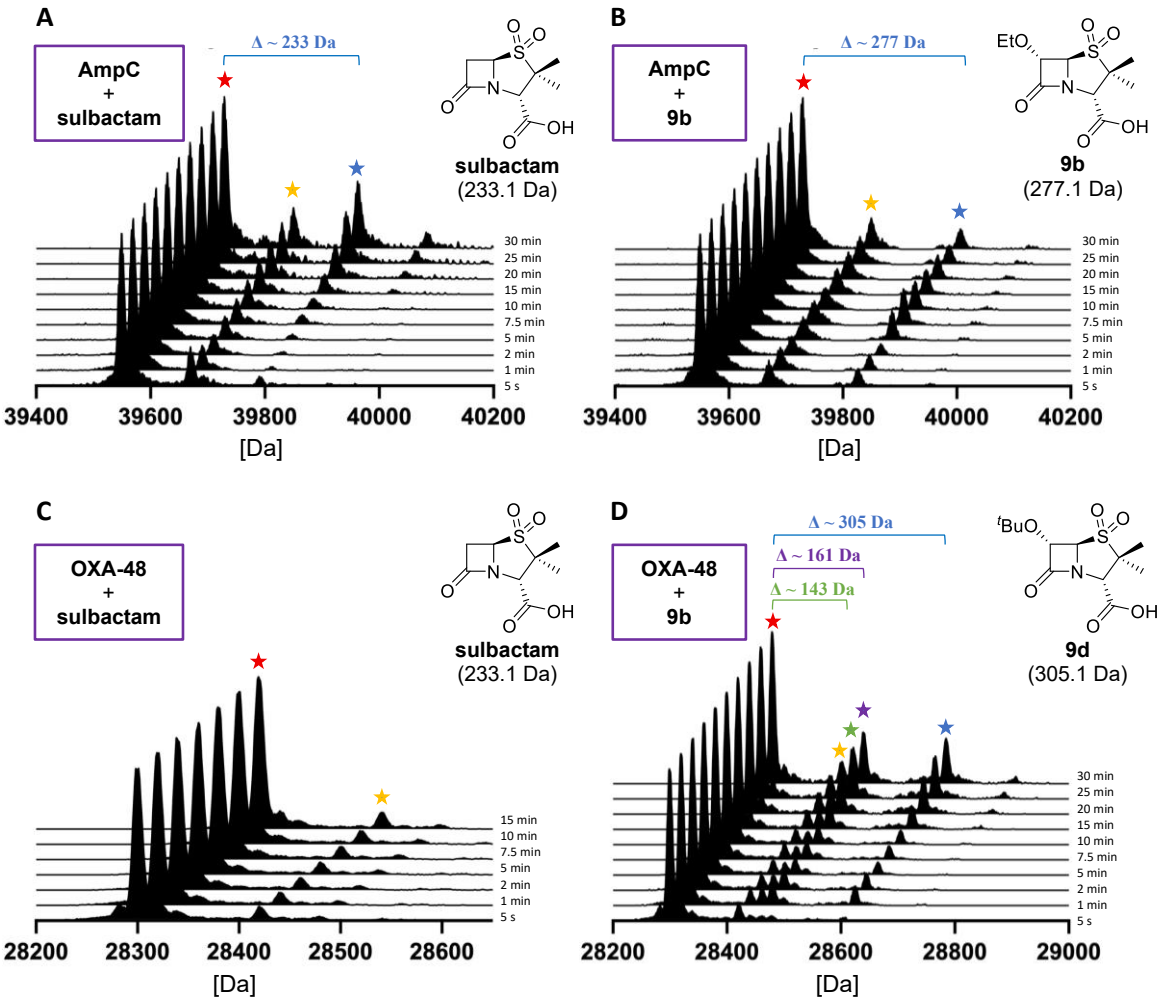

Figure 3. Comparative protein-observed MS time-course analyses of the reaction mixtures of SBLs with **sulbactam** and selected C6-alkoxypenam derivatives. For reactions with AmpC, SPE-MS analysis revealed the time-dependent formation of a +233 Da adduct with sulbactam (**A**) and a +277 Da adduct with **9b** (**B**). In the case of OXA-48, **sulbactam** did not promote any covalent adducts of appreciable intensity (**C**), whereas **9d** gave rise to multiple covalent adducts (**D**). The +120 Da mass shift (★) corresponds to a tris(hydroxymethyl)aminomethane (Tris) adduct. Reaction progression was monitored over a 15–30 min period. For **A-D**, assays were performed as previously reported[50] using a 10:1 inhibitor-to-SBL ratio.

MS studies with penam **11d** showed a distinct behaviour (**Figure 4**): against AmpC and TEM-116, which **11d** inhibits, no covalent adduct formation was observed, indicating that the inhibition is

non-covalent in nature. Interestingly, although no inhibition of OXA-10 and OXA-48 was detected, both enzymes formed covalent adducts upon reaction with **11d**.

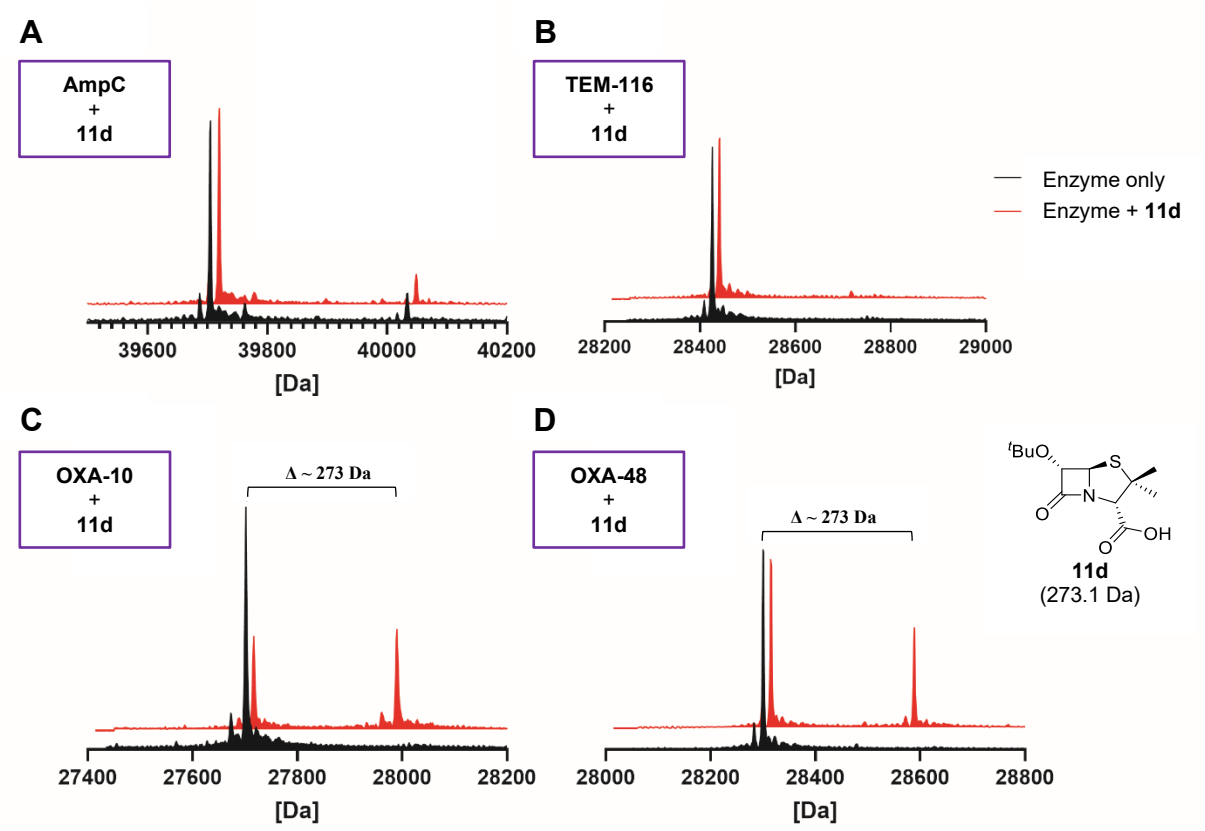

Figure 4. Protein-observed MS assay results for AmpC (**A**), TEM-116 (**B**), OXA-10 (**C**), and OXA-48 (**D**) after incubation with **11d**. The enzyme only control spectra are shown in black, while the spectra after the addition of **11d** are shown in red. Experimental details can be found in the Methods section.

Crystallography

A crystal structure of OXA-48 in complex with the C6-*tert*-butoxy penam **9d** (**Figure 5**) was obtained via co-crystallisation in the $P2_12_12_1$ space group with two molecules per dimer in the asymmetric unit and diffracted to a resolution of 2.03 Å. The initial structure was solved using molecular replacement (MR) in Phenix.[51] The reported structure of OXA-48 (PDB ID: 3HBR) was used as the search model.[52] Model building comprised of iterative rounds of refinement using phenix.refine with manual model building and visualisation using COOT.[53] Restraints for the acyl-

enzyme complex formed with **9d** were generated using eLBOW.[54] Analysis of electron density maps reveals that the nucleophilic alcohol of the catalytic OXA-48 serine residue (Ser70) reacted covalently with the β-lactam ring of **9d** to form an acyl-enzyme complex (**Figure 3**, **Supporting Figure S5**), in accord with the +305 Da mass shift observed during protein-observed MS assays (**Figure 2**). The carboxylate group on the **9d**-derived thiazolidine sulfone ring is positioned to interact with the sidechains of Thr209 and Arg250 (2.8 and 3.0 Å, respectively), possibly stabilising binding at the active site. A single water molecule was observed in proximity of Ser70. Notably, the hydrophobic C6-*tert*-butoxy group is positioned in proximity of the Val120/Leu158 hydrophobic tunnel,[52, 55] possibly restricting the access of the hydrolytic water to the carbonyl of the acyl-enzyme complex.

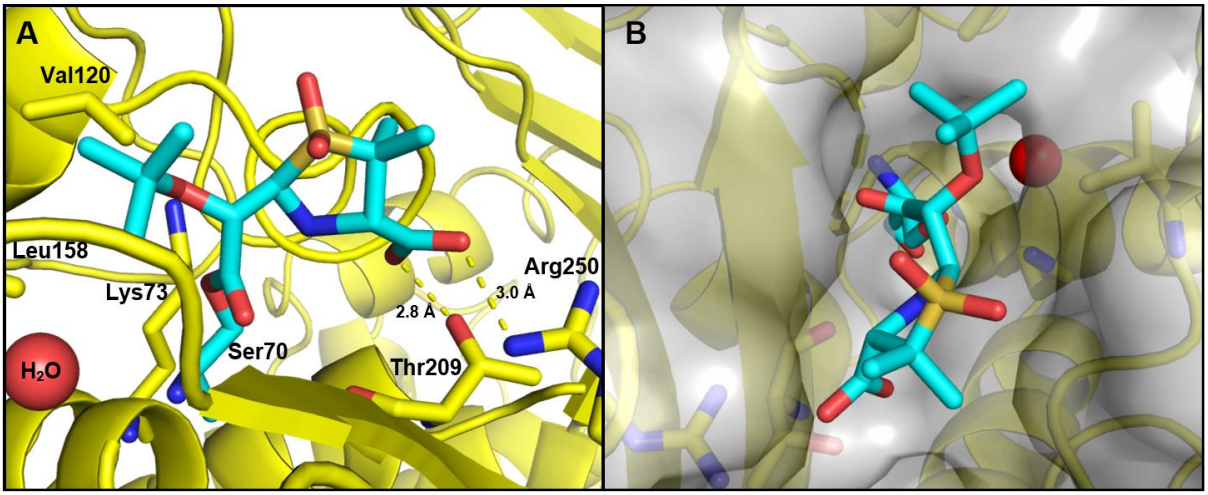

Figure 5. Crystal structure view of the complex formed following covalent reaction of **9d** with OXA-48. **A**. Stick view of the OXA-48 active site showing the acylation of Ser70 by **9d** (cyan). **B**. Alternative surface view highlighting the water channel between Val120 and Leu158, capped by the C6-*tert*-butoxy substituent, which effectively traps the hydrolytic water molecule within the channel.

Given that C6-methoxy penam **9a** inhibited *A. baumannii* PBP3 ~10-fold less efficiently than **sulbactam**, the effect of the C6-methoxy group on the binding of the sulbactam scaffold to PBP3 was investigated using crystallography. A crystal structure of *A. baumannii* PBP3 in complex with the **9a** (**Figure 6**) was obtained via co-crystallisation in the $P2_12_12_1$ space group with a single

molecule per asymmetric unit and diffracted to a resolution of 1.8 Å. Structures were determined by molecular replacement in Phaser,[56] using an AlphaFold2 model of *Pseudomonas aeruginosa* PBP3 as the search template.[57] Iterative refinement was carried out in Phenix with manual rebuilding in COOT between cycles, continuing until R_{work} and R_{free} converged.[51, 53] Analysis of electron density maps reveals that **9a** covalently crosslinked the Ser300 with the Lys435 sidechain; this was an interesting observations, as β-lactam antibiotics typically acylate the catalytic Ser294 of PBP3 to form stable acyl-enzyme complexes (AECs), not Ser300.[58]

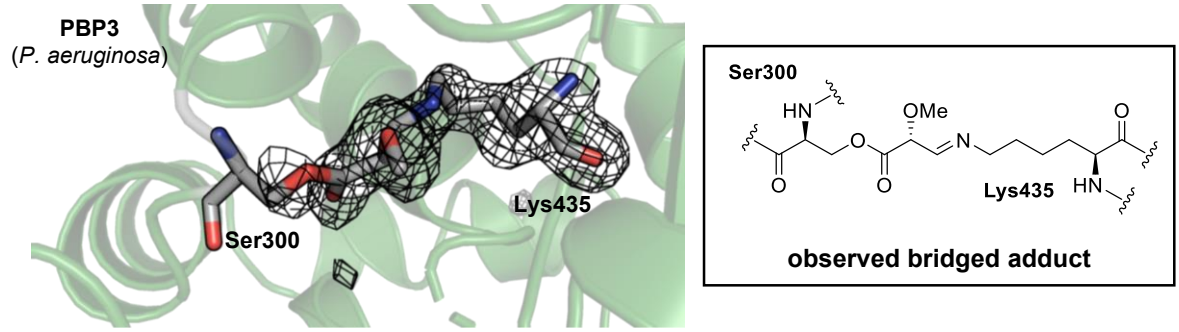

Figure 6. Crystal structure view of the complex formed following covalent reaction of **9a** with PBP3 (*P. aeruginosa*). The polder map is carved at 5*σ*. Numbering of residues was done relative to a previously reported structure (PDB ID: 6UN1).[43]

Combinations with C6-alkoxy penam derivatives have a limited microbiological impact

Given that some of the C6-alkoxy sulbactam derivatives inhibited SBL and/or PBP3 activity *in vitro*, their effects on selected Gram-negative (*A. baumannii*, *C. freundii*, *E. coli*, *K. pneumoniae*, *P. mirabilis*) and Gram-positive (*S. aureus*) strains were investigated using the clinically approved **ampicillin/sulbactam** combination as a control (**Table 2**). Analysis of minimum inhibitory concentrations (MICs) reveals that the **ampicillin/sulbactam** combination was particularly effective against *K. pneumoniae*, manifesting a 16-fold reduction in MICs compared to **ampicillin** alone (MIC ~ 2 and 32 μg/mL, respectively; **Table 2**, entries i and ii). By contrast, combinations

of **ampicillin** with C6-alkoxy sulbactam derivatives **9a-d** and **11a-d** showed no meaningful improvement in growth inhibition over **ampicillin** alone (**Table 1**).

Table 2. Antibacterial activity of ampicillins combinations with C6-alkoxy penam derivatives.

		MIC (μg/mL)[(a)]					
		A. baumanii 13304	*C. freundii* 09750	*E. coli* 25922	*K. pneumoniae 9663*	*P. mirabilis* 11938	*S. aureus* 12981
i	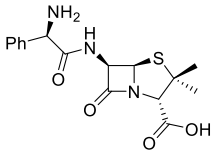 **ampicillin**	>64	4	4	32	0.125	0.0625
ii	**ampicillin + sulbactam**	>64	8	*n.d.*	2	0.125	0.0625
iii	**ampicillin + 9a**	>64	4	*n.d.*	32	0.125	0.0625
iv	**ampicillin + 9b**	>64	16	*n.d.*	32	0.125	0.0625
v	**ampicillin + 9c**	>64	8	*n.d.*	32	0.125	0.0625
vi	**ampicillin + 9d**	>64	4	*n.d.*	32	0.125	0.0625
vii	**ampicillin + 11a**	>256	32	2	>256	0.125	<0.25
viii	**ampicillin + 11b**	>256	32	2	>256	0.125	<0.25
ix	**ampicillin + 11c**	>256	32	2	>256	0.125	<0.25
x	**ampicillin + 11d**	>256	32	2	>256	0.125	<0.25

[(a)]Experimental details can be found in the Methods section.

The effects of C6-alkoxy sulbactam derivatives on *A. baumannii* strains was investigated both in the presence and absence of **durlobactam**, because the **sulbactam**/**durlobactam** combination is clinically used to treat *A. baumannii* infections (**Table 3**). Like **sulbactam**, the tested sulbactam derivatives **9a** and **11a-d** did not efficiently inhibit *A. baumannii* growth (MICs > 32-256 μg/mL). Interestingly, unlike the **sulbactam**/**durlobactam** combination (MIC < 0.5 μg/mL),[28] the C6-alkoxy sulbactam derivatives **9a-d** and **11a-d** in combination with **durlobactam** did not inhibit the bacterial growth of *A. baumannii* (MICs > 32-64 μg/mL).

Table 3. Antibacterial activity of C6-alkoxy penams in combination with durlobactam against *A. baumanii*.

	Compound	MIC (μg/mL)[(a)]		Combination	MIC (μg/mL)[(a)]
		A. baumanii 13304			*A. baumanii* 13304
i	**sulbactam**	32	xi	**sulbactam + durlobactam**	<0.5
ii	**9a**	>256	xii	**9a + durlobactam**	>64
iii	**9b**	*n.d*	xiii	**9b + durlobactam**	>64
iv	**9c**	*n.d*	xiv	**9c + durlobactam**	>64
v	**9d**	*n.d*	xv	**9d + durlobactam**	>64
vi	**11a**	>32	xvi	**11a + durlobactam**	>32
vii	**11b**	>32	xvii	**11b + durlobactam**	>32
viii	**11c**	>32	xviii	**11c + durlobactam**	>32
ix	**11d**	>32	xix	**11d + durlobactam**	>32
x	**durlobactam**	128			

[(a)]Experimental details can be found in the Methods section.

4.2.4 Discussion

β-Lactamase inhibitors are crucial therapeutic agents designed to counteract one of the most widespread resistance mechanisms in antibiotic-resistant bacteria.[2] **Sulbactam**, developed by researchers at Pfizer, was shown to display dual activity, not only extending the antibacterial spectrum of β-lactam antibiotics such as **ampicillin** against class A enzyme producing bacterial pathogens but also displaying intrinsic antibacterial properties against certain Gram-negative bacteria such as *N. gonorrhoeae* and *A. baumanii*.[28, 59, 60] Beyond the clinically approved combinations, **sulbactam** has been evaluated in a variety of investigational regimens further comprising other antibiotics, including but not limited to polymyxins,[61] amikacin,[62] carbapenems,[63] and tetracyclines.[64] Nonetheless, given that the activity of **sulbactam** is largely limited to class A SBLs, it is of therapeutic interest to expand its coverage, and SAR explorations

have shown that key substitutions on the **sulbactam** scaffold can alter its inhibitory properties.[22, 65-69]

Our work on C6-alkoxypenam derivatives revealed that introducing an α-alkoxy substituent reduced inhibition of class A enzymes like TEM-116, which are clinically relevant targets of **sulbactam**. While some C6-alkoxypenam derivatives (**9b**, **9c**, and **11d**) maintained moderate inhibition of AmpC in a similar manner to **sulbactam**, a surprising finding of this study was that C6-*tert*-butoxy penam sulfone **9d** inhibited OXA-48 (a class D enzyme), whereas **sulbactam** did not (**Table 1**). Structural insights from crystallographic studies (**Figure 5**) indicated that the inhibition of OXA-48 by **9d** might be due to the presence of the C6-*tert*-butoxy group, which is proposed to stabilise the acyl-enzyme complex by preventing the access pathway of the hydrolytic water. This behaviour was also observed with **temocillin** (**Supporting Figure S6**), a C6-methoxy penicillin antibiotic, which upon binding with CTX-M-14, a class A enzyme, the C6-methoxy group also impeded the access of the catalytic water to the acyl-enzyme complex.[43] Furthermore, time-course MS studies with **9d** and OXA-48 indicated the presence of multiple acyl-enzyme adducts (**Figure 3**). We propose that, following β-lactam ring opening by the nucleophilic Ser70 (**Figure 7**), the crystallographically observed adduct **I** (+305 Da) undergoes further fragmentation of the thiazolidine ring to yield **II** (+305 Da). Hydrolysis of the imine moiety would then lead to the release of aldehyde **III** (+143 Da), which can equilibrate with its hydrate form **IV** (+161 Da).

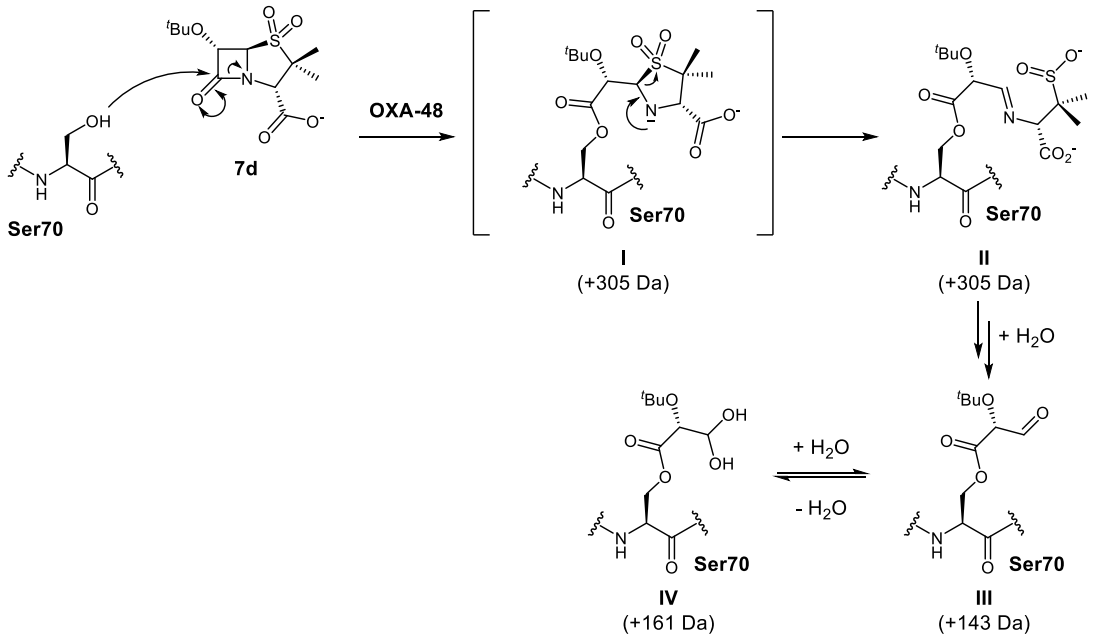

Figure 7. Proposed outline mechanism for the reaction of **9d** with OXA-48.

Interestingly, the C6-*tert*-butoxypenam sulfide **11d**, the only C6-alkoxypenam sulfide investigated that showed any inhibition again SBLs (**Table 1**, entries vi-ix), did not manifest covalent adduct formation with either TEM-116 or AmpC (**Figure 4**). This observation is precedented by the behaviour of the related C6-methoxypenam benzyl ester **12** (**Figure 8A**), which is a potent inhibitor of cysteine protease SARS-CoV-2 M^{pro}; time-course MS data with M^{pro} did not evidence the formation of an acyl-enzyme complex with **12**, while modelling studies indicated that the presence of the C6-methoxy group interferes with the positioning of the β-lactam ring in proximity of the active site cysteine residue (*i.e.*, Cys145), thus hindering productive covalent reaction and preventing the formation of a covalent adduct.

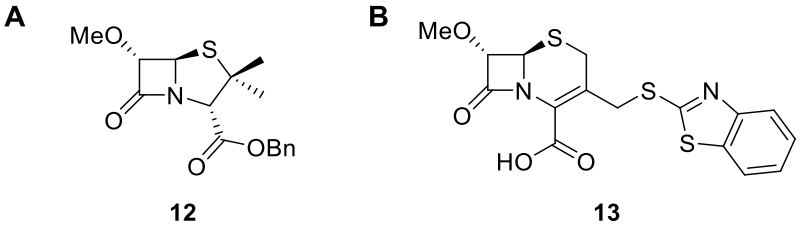

Figure 8. A. C6-Methoxypenam benzyl ester (**12**), a potent SARS-CoV-2 M^{pro} non-covalent inhibitor. **B**. Structure of **13**, a reported C7-methoxycephalosporin inhibitor of NDM-1.[70]

None of the C6-alkoxypenam derivatives investigated in this study displayed inhibition of MBLs (**Supporting Table S1**), in contrast to the recently reported C7-methoxy cephalosporin **13** (**Figure 8B**), which inhibits NDM-1 by forming a stable, hydrolysed product-enzyme complex (**Supporting Figure S7**). The basis for this divergence in MBL inhibitory properties is not understood and warrants investigation. Possible contributing factors include: i) the different conformational requirements imposed by the penam and cephem bicyclic scaffolds may influence the stability of the initial non-covalent inhibitor-enzyme complex; ii) the presence of a leaving group at the C3′ position of cephalosporin **13** may facilitate non-covalent interactions within the NDM-1 active site, while driving the formation of the crystallographically observed α,β-unsaturated imine **13'** (**Supporting Figure S7**); and iii) the overall stability of the hydrolysed product-enzyme complex, where the α,β-unsaturated imine N of **13'** coordinates one of the NDM-1 active site Zn(II) ions.

Lastly, C6-alkoxypenam derivatives (**9a-d** and **11a-d**) showed reduced inhibition of PBP3 relative to **sulbactam**, which is consistent with the MIC data (**Tables 1** and **3**). A clear trend was observed in which increasing the steric bulk of the C6-alkoxy group led to a progressive loss of potency. Unexpectedly, crystallographic studies with PBP3 from *P. aeruginosa* revealed that **9a** did not acylate the catalytically active Ser294, but instead reacted with a proximal serine residue, Ser300, to form a bridged adduct with Lys435. A plausible mechanism via which the bridged adduct might arise from entails the following steps (**Figure 9**): (i) β-lactam ring opening by Ser300; (ii) fragmentation of the thiazolidine ring of intermediate **I**; (iii) hydrolysis of the imine intermediate **II** to generate aldehyde **III**; (iv) condensation of aldehyde **III** with Lys435, resulting in the bridged species **IV**. Note, however, that adduct **IV** may also be a crystallographic artefact, and its existence is currently investigated using MS assays. Interestingly, with respect to PBP inhibition, the

behaviour of the C6-alkoxy penam derivatives investigated here is similar to that of **temocillin**, for which reported PBP structural studies have shown that its C6-methoxy group destabilises the acyl-enzyme complex with Ser294 of *P. aeruginosa* PBP3 (**Supporting Figure S6**).[43]

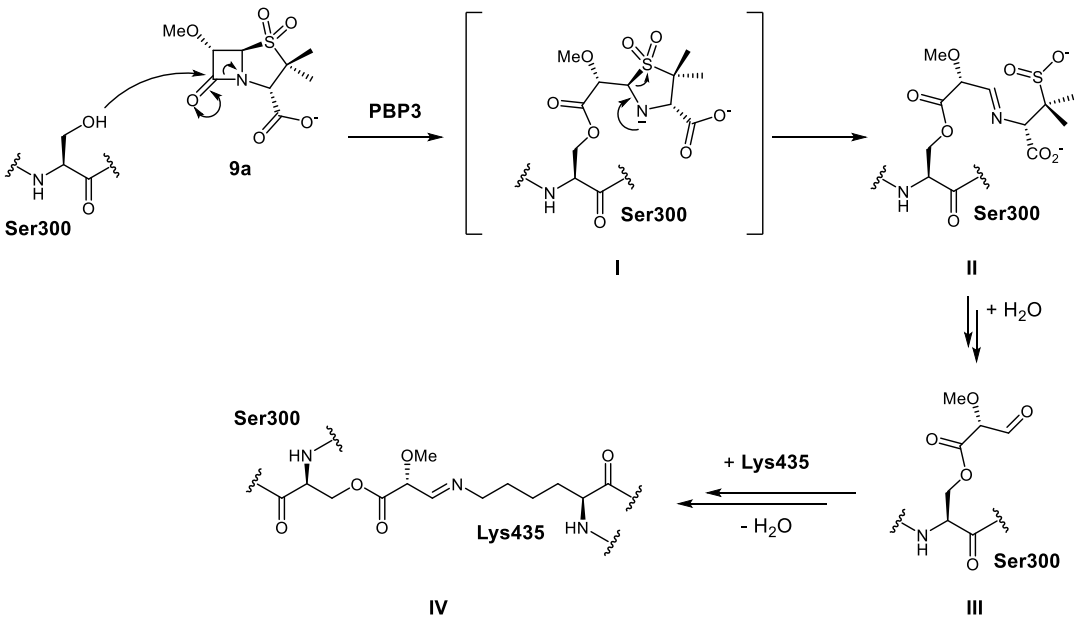

Figure 9. Proposed outline mechanism for the reaction of **9a** with PBP3 (*P. aeruginosa*).

4.2.5 Conclusions

The combined results further clarify the impact of C6-alkoxy groups on modulating the inhibitory properties of penam derivatives bearing this moiety against SBLs, MBLs and PBPs. While some C6-alkoxypenams were more potent against certain SBLs than **sulbactam**, none of the combinations with **ampicillin** proved to be more efficacious at inhibiting microbial growth than **ampicillin-sulbactam**. Nonetheless, the MS and crystallographic studies described here offer mechanistic insights, not only revealing new modes of binding to enzyme targets, but also potentially paving the way for optimising sulbactam-based inhibitors for class D enzymes.

4.2.6 Supporting figures

Supporting Figure S1. Outline mechanism for the stereospecific synthesis of C6-α-alkoxypenam derivatives.[46] Following the formation of C6-diazopenicillate benzyl ester **5'**, stereospecific protonation from the sterically less hindered convex face gives intermediate **I**; subsequently, a selected alcohol reacts with intermediate **I** in a S_N2 manner to eliminate N_2, resulting in inversion of configuration at the C6 position. Representative reagents and conditions: a) i) $NaNO_2$ (2.6 equiv.), *para*-toluenesulfonic acid monohydrate (0.6 equiv.), CH_2Cl_2:H_2O (4:1), 0 ºC, 20 min; ii) ROH (48-110 equiv.), $BF_3{\cdot}O(C_2H_5)_2$ (0.1 equiv.), CH_2Cl_2, 20 ºC, 15 min.[46]

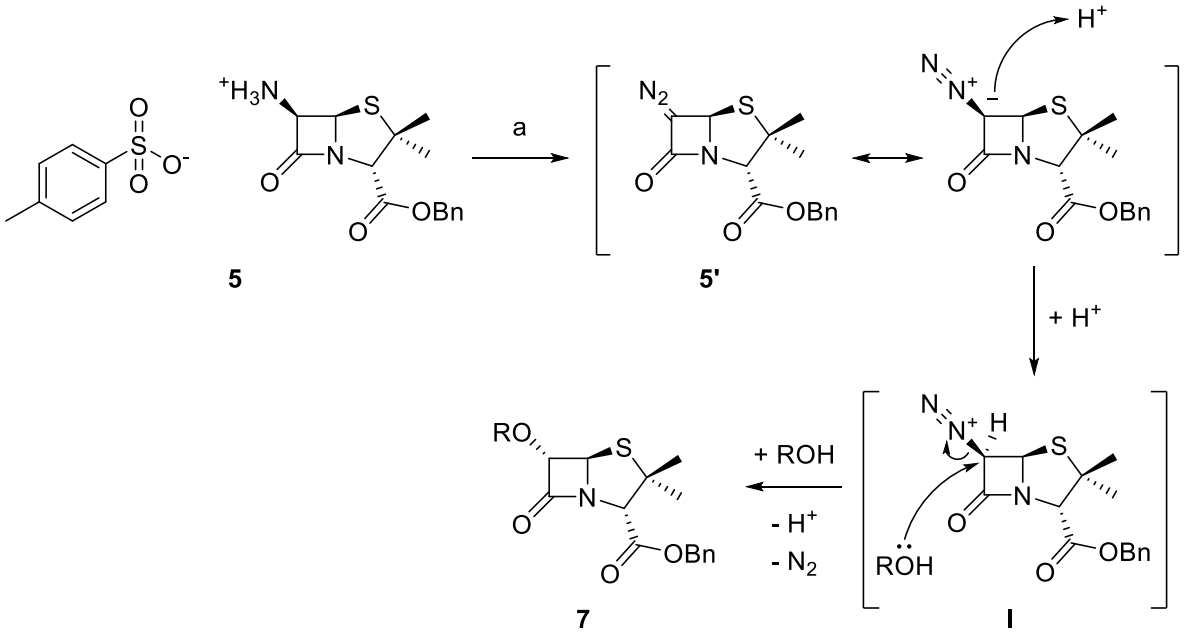

Supporting Figure S2. Representative dose response curves. Representative dose response curves for inhibition of TEM-116 (**A**), AmpC (**B**), OXA-10 (**C**), OXA-48 (**D**) by **avibactam** (circles), **sulbactam** (squares), **7a** (triangles), **7b** (inverse triangles), **7c** (diamonds), **7d** (hollow circles). **Avibactam** was also used as a positive control against TEM-116 (pIC_{50} ~ 8.0), AmpC (pIC_{50} ~ 7.0), OXA-10 (pIC_{50} ~ 4.6) and OXA-48 (pIC_{50} ~ 5.8).

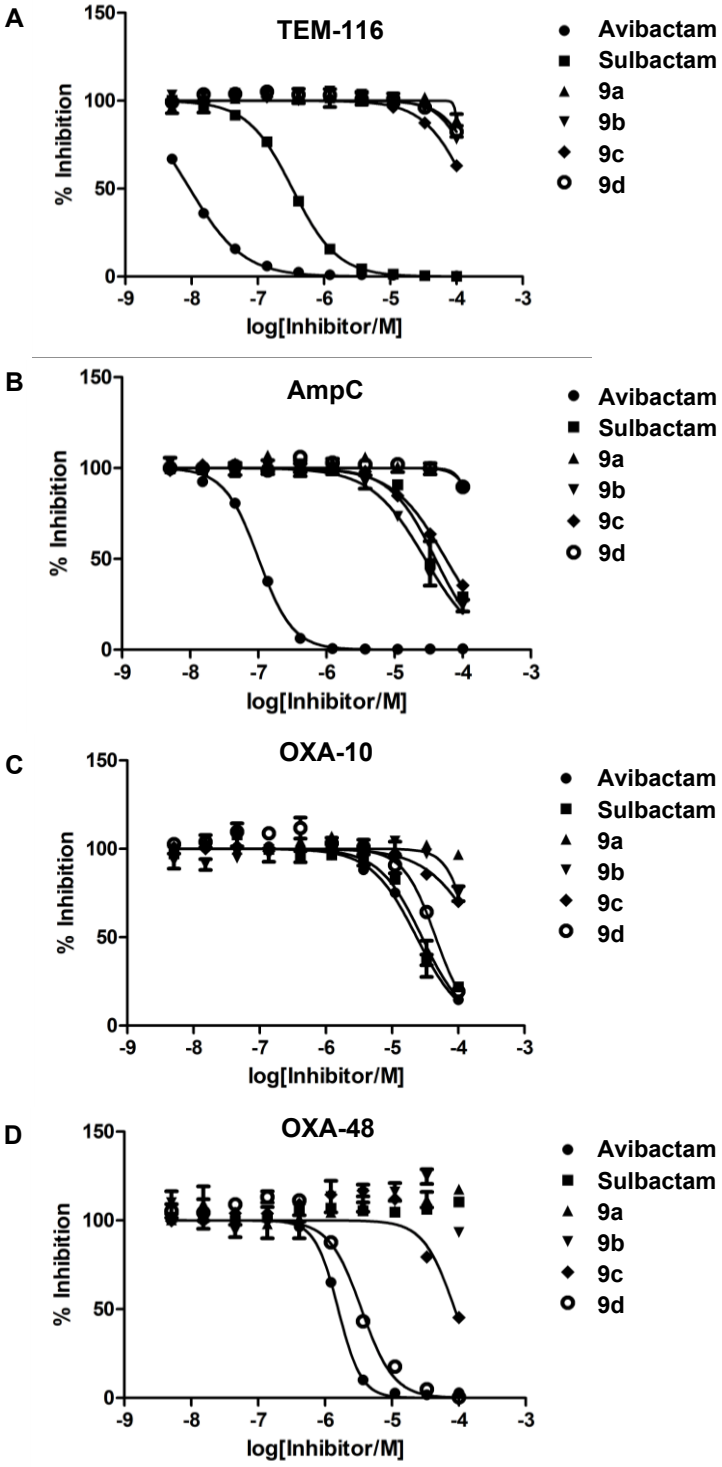

Supporting Figure S3. Representative dose response curves for inhibition of VIM-1 (**A**), VIM-2 (**B**), NDM-1 (**C**), IMP-1 (**D**) by **sulbactam** (red circles), **9a** (orange squares), **9b** (green triangles), **9c** (blue inverse triangles), **9d** (purple diamonds). **Captopril** (green hollow circles) was employed as a positive control against VIM-1 ($pIC_{50} \sim 4.5$) and VIM-2 ($pIC_{50} \sim 5.6$). Dose response curves are means of technical duplicates. IC_{50} values in **Supporting Table 1** are means of at least two independent repeats ($n \geq 2$, mean ± SD), each composed of technical duplicates.

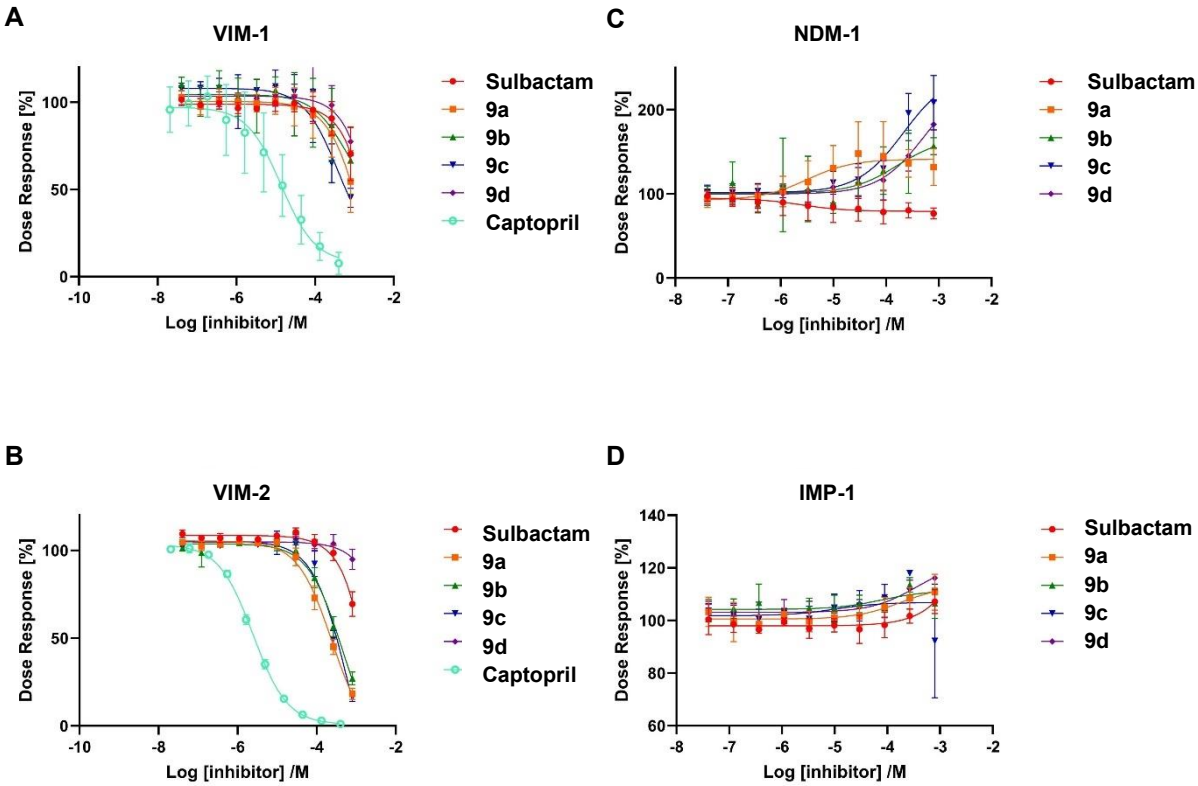

Supplementary Table S1. Inhibition of MBL activity by C6-alkoxypenam derivatives.

	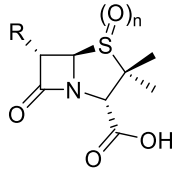			pIC_{50}[(a)]			
	Compound	R	n	NDM-1 (class B)	VIM-1 (class B)	VIM-2 (class B)	IMP-1 (class B)
i	**sulbactam**	H	2	-	<4.0	<4.0	<4.0
ii	**9a**	OMe	2	-	<4.0	<4.0	<4.0
iii	**9b**	OEt	2	-	<4.0	<4.0	<4.0
iv	**9c**	O^{i}Pr	2	-	<4.0	<4.0	<4.0
v	**9d**	O^{t}Bu	2	-	<4.0	<4.0	<4.0
vi	**11a**	OMe	0	<4.0	<4.0	<4.0	<4.0
vii	**11b**	OEt	0	<4.0	<4.0	<4.0	<4.0
viii	**11c**	O^{i}Pr	0	<4.0	<4.0	<4.0	<4.0
ix	**11d**	O^{t}Bu	0	<4.0	<4.0	<4.0	<4.0

[(a)]Experimental details can be found in the Methods section. *n.i.* – no inhibition. Representative dose-response curves are shown in **Supporting Figure S3**.

Supporting Figure S4. A. Representative dose response curves for inhibition of PBP3 (*P. aeruginosa*) by **9a** (orange circles), **9b** (red squares), **9c** (brown triangle), **9d** (purple inverse triangles), and **sulbactam** (blue diamonds). **B.** Representative dose response curves for inhibition of PBP3 (*P. aeruginosa*) by **11a** (orange circles), **11b** (red squares), **11c** (brown triangle), **11d** (purple inverse triangles), and **sulbactam** (blue diamonds). Dose response curves are means of technical duplicates. IC_{50} values in **Table 1** are means of at least two independent repeats ($n \geq 2$, mean ± SD), each composed of technical duplicates.

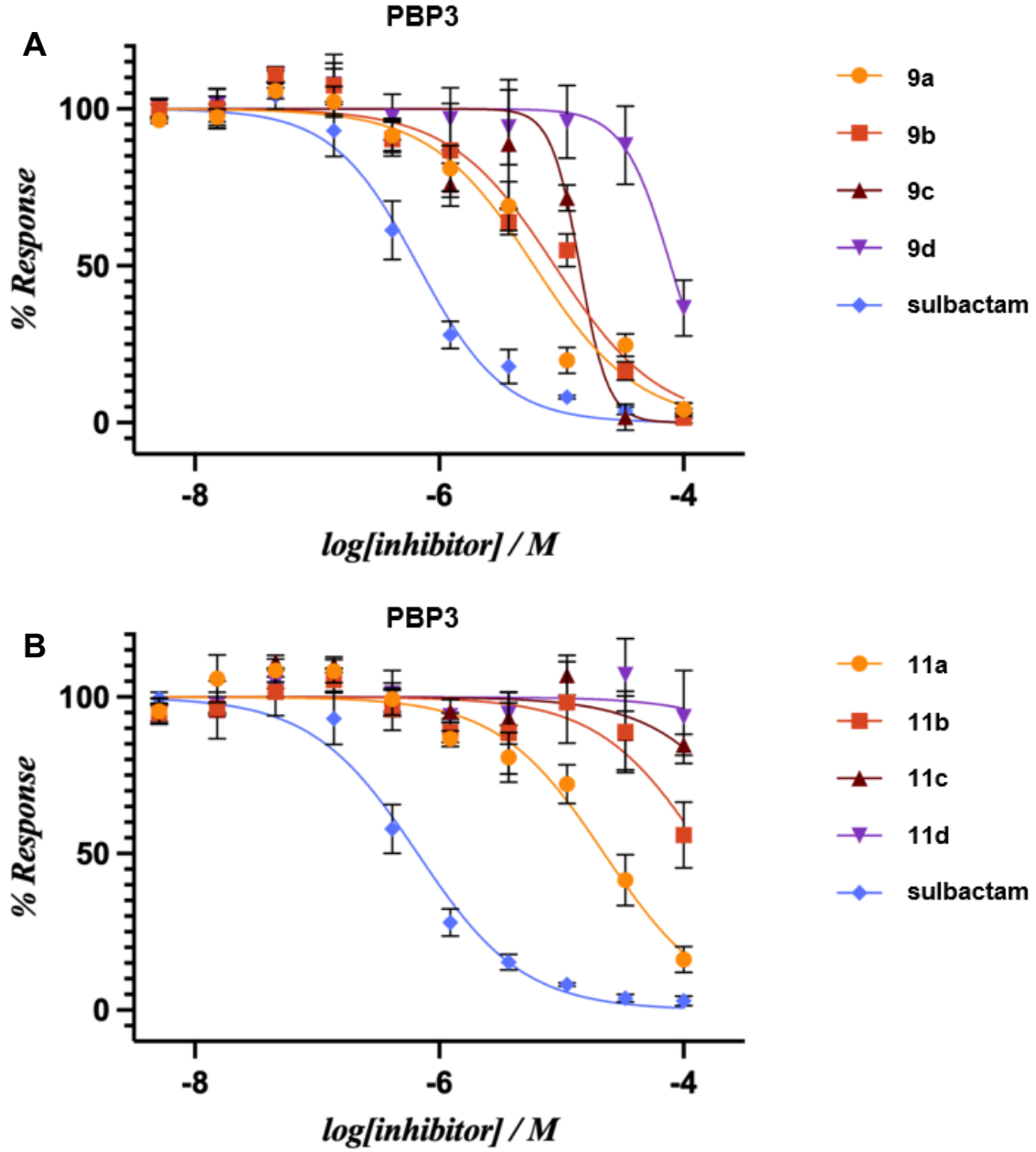

Supporting Figure S5: Crystal structure view of the complex formed following covalent reaction of **9d** with OXA-48. The polder map is carved at 4.5σ.

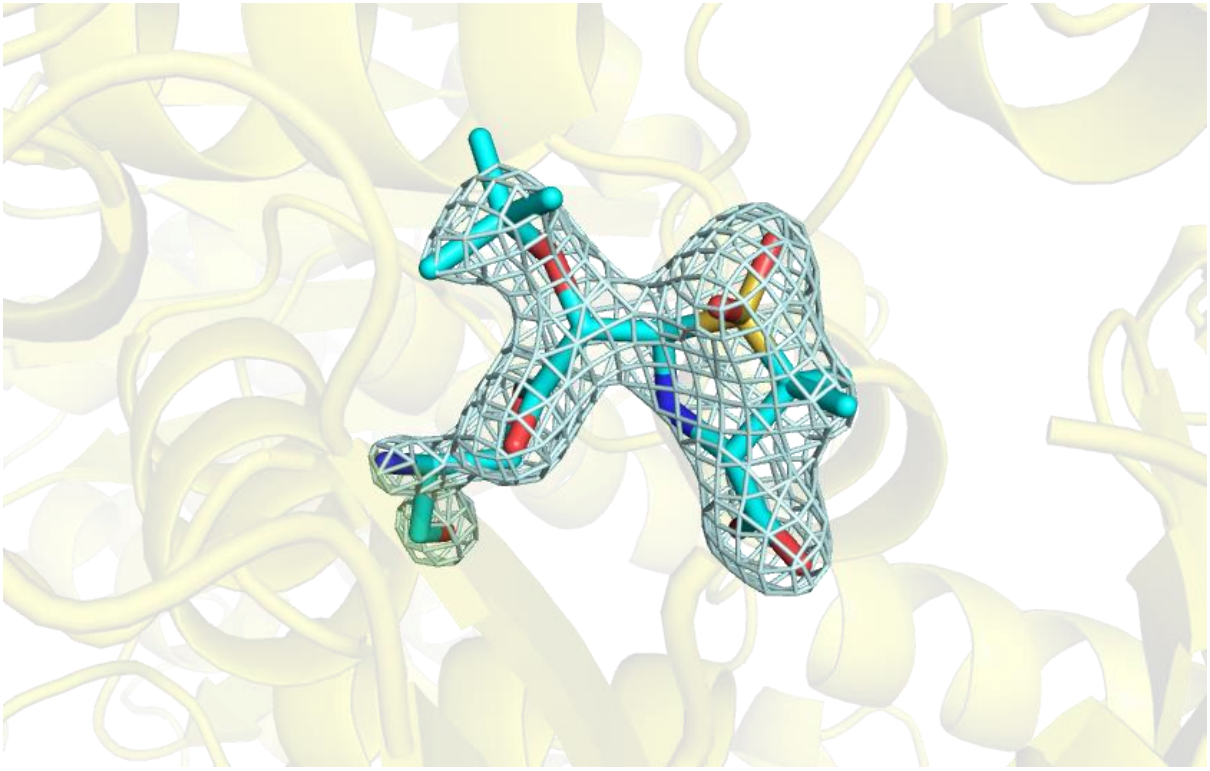

Supporting Figure S6. A. Temocillin, a clinically used C6-methoxy penicillin antibiotic.[44] **B**. Crystal structure view of the complex formed following covalent reaction of **temocillin** (cyan) with PBP3 from *P. aeruginosa* (PDB ID: 6UN1).[43] The C6-methoxy group interferes with the hydrogen bonding between the amide carbonyl of the C6 sidechain with Asn351, thus affecting the stability the acyl-enzyme complex. **C**. Crystal structure view of the complex formed following covalent reaction of **temocillin** (cyan) with CTX-M-14 (PDB ID: 6UNB).[43] The C6-methoxy group of temocillin contributes to the stability of the acyl–enzyme complex in CTX-M-14 by rotating outward to avoid steric clashes, while the repositioned amide carbonyl stabilizes the catalytic water, thus preventing hydrolytic attack on the acyl-enzyme complex.

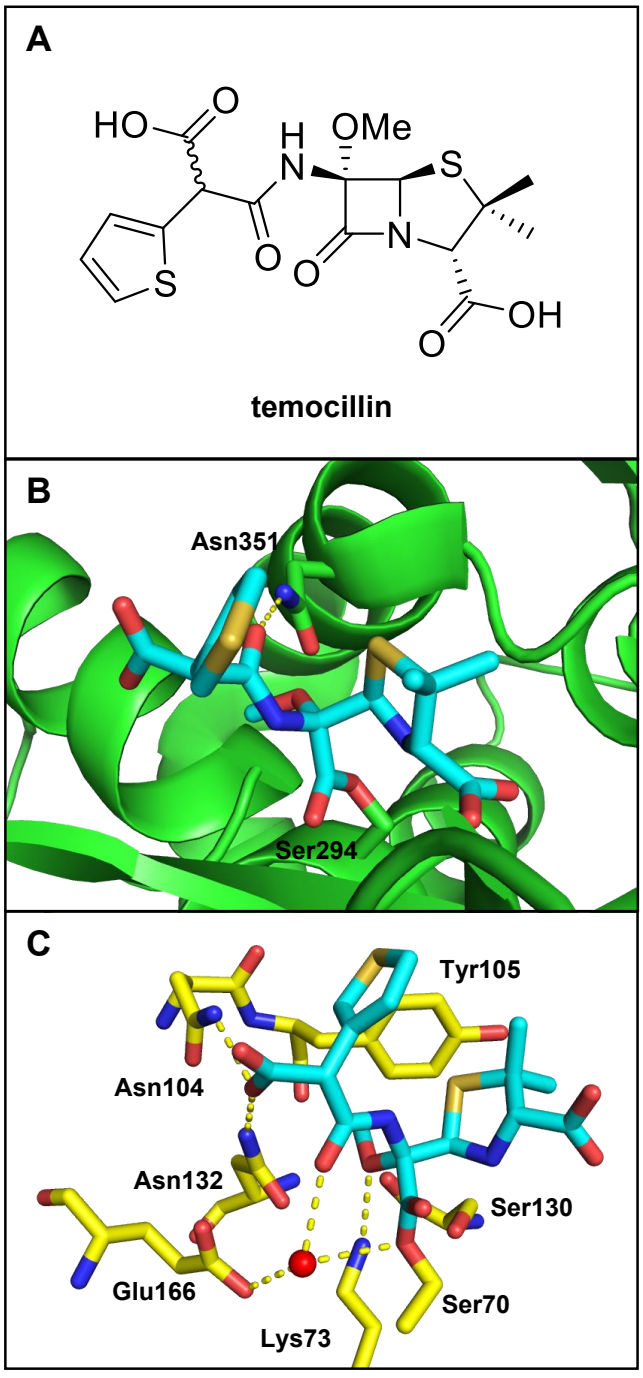

Supporting Figure S7. Proposed outline mechanism for the reaction of C7-methoxy cephalosporin 1**3** with NDM-1 to give imine **13'**, which is the crystallographically observed adduct with NDM-1 (PDB ID: 7VQJ).[70] ArSH denotes 2-mercaptobenzothiazole.

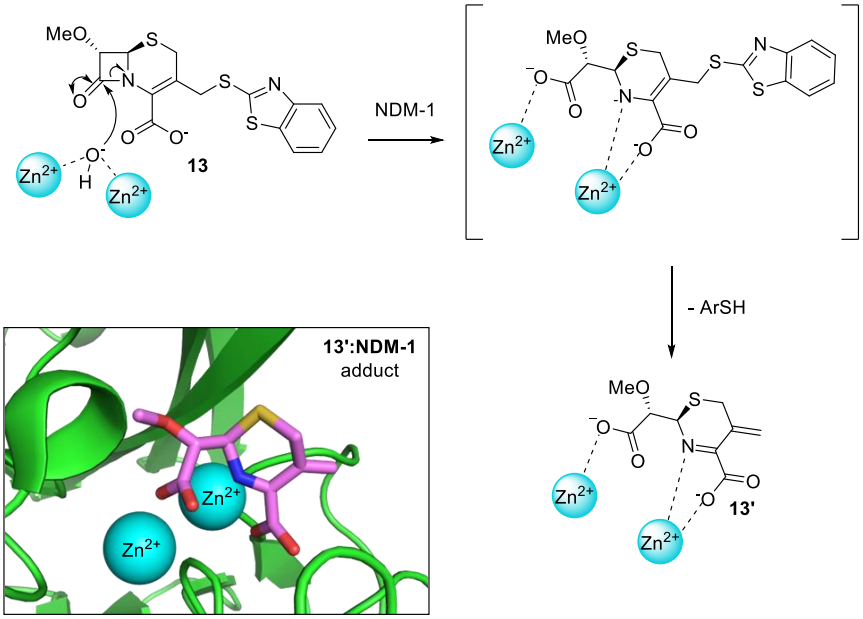

4.2.7 Methods

4.2.7.1 SBL inhibition assays

pIC_{50} values were determined as reported[71], using the fluorogenic cephalosporin FC-5[72] as a substrate in steady-state competition assays monitoring hydrolysis. Assays were performed in quadruplicate in the assay buffer (phosphate buffer (50 mM, pH 7.5), Triton X-100 (0.01% v/v)), with OXA assays also carried out with additional 50 mM sodium bicarbonate supplementation where noted. TEM-116 (1 nM), $AmpC_{EC}$ (500 pM), OXA-10 (250 pM), OXA-48 (12.5 nM) were incubated at room temperature with the various inhibitor concentrations for 10 minutes prior to reaction initiation by FC-5 addition (5 μM, in DMSO). Fluorescence intensity was measured in plate-mode every 2.5 minutes using a CLARIOstar plate reader (BMG Labtech), recording emission spectra at λ_{ex} = 380 nm and λ_{em} = 460 nm. Initial reaction velocities were determined by linear regression of the initial slopes and normalised to positive and negative controls. Nonlinear regression analyses and logarithmic translation were performed by Prism 10 (GraphPad Software).

4.2.7.2 SBL POMS assays

The protein samples were transferred into 100mM ammonium acetate pH 7.4 and the concentration adjusted to 1μM. 50uM 8d was then added to the protein solution which was then incubated at room temperature for 30 minutes. After incubation the covalent product was observed via denaturing protein LC-MS using a ProSwift RP-4H column (Thermo Scientific) and a Xevo G2-S QTOF mass spectrometer (Waters). Mass deconvolution was calculated using MassLynx (v.4.2).

4.2.7.3 MBL testing[48]

Compounds of interest serially diluted 3-fold with a top concentration of 200 μM. Relevant enzyme, buffers and substrate stocks dispensed using CyBi and Integra WellJet dispenser to a

final concentration of 25 µl per well. Assays performed in the Greiner 384-well black assay plate in accordance with the excitation and emission spectra of FC5 (ex: 380 nm em: 460 nm). Fluorescence intensity was monitored using the CLARIOstar Plus for 10 cycles, 50 flashes and 170s cycle time. The initial slopes were calculated, normalised against the controls and expressed as % inhibition of the respective MBL.

Average slopes from technical quadruplicate repeats were plotted against the logarithmic substrate concentrations on Graphpad. pIC_{50} values were obtained using the dose response three-parameter fit. Captopril pIC_{50} values were used as a reference compound with a top concentration of 400 µM.[73]

4.2.7.4 PBP inhibition assays

PBP inhibition assays were performed using fluorescence polarisation (FP) as reported,[49] utilizing recombinant isolated PBP3 from *A. baumanii*[74] (300 nM) in S2d assay buffer (25 mM HEPES, 100 mM NaCl, pH 7.4), inhibitor (100 µM to 5 nM, ten concentrations total, 3-fold dilution series), S2d probe[75] (1.5 mM) and monobromobimane (mBBr, 0.5 mM).

4.2.7.5 Susceptibility assay

Minimum inhibitory concentrations (MICs) were determined using the broth microdilution method, according to the guidelines of the Clinical and Laboratory Standards Institute (CLSI, USA).[76] Measurements were obtained in triplicates, with compounds being tested alone (0.25-256 µg/mL) against selected strains. Compounds were tested at a fixed concentration (4 µg/mL) in combination with ampicillin (0.25-64 µg/mL) against the following isolates: NCTC 13304, NCTC 09750, ATCC 25922, NCTC 9663, NCTC 11938, and NCTC 12981. Alternatively, compounds were tested alone at a fixed concentration (0.25-256 µg/mL) or in combination with durlobactam at a fixed concentration (4 µg/mL) against the isolate NCTC 13304.

4.2.7.6 Crystallisation

Apo OXA-48 crystals were obtained using 13 mg/ml OXA-48 using the vapour diffusion method.[52, 77] Protein was mixed with the precipitant and seed stock at varying protein:precipitant ratios using the liquid handling robot Mosquito (STP Labtech) into a 96-well Swiss Sci plate. Crystals formed in; 0.1 M BES/TEA, 10-25% 1,5- pentanediol, 4-14.5% PEG 8000, adapted from Morpheus II condition E7.[78] Crystals of OXA-48- ligand complexes were obtained through soaking a 20 mM solution of **9d** with apo crystals for one hour (20% final DMSO concentration with crystal well solution). Crystals were cryoprotected with a final concentration of 20% glycerol, fished with nylon loops and flash frozen in liquid nitrogen.

For **9a**, a variation of a crystallisation protocol was followed.[49] Crystals of the PBP3-inhibitor complex were obtained by pre-incubating PBP3 with inhibitor (0.5 mM) for 10 min before setting up crystallization trays. Crystals with **9a** were obtained in Morpheus condition B4: the crystallization well contained 0.09 M Halogens (0.3 M each NaF, NaBr, NaI), 0.1 M Buffer System 1 (1.0 M imidazole–MES) at pH 6.5, and 37.5% Precipitant Mix 4 (25 % v/v MPD, 25 % PEG 1000, 25 % w/v PEG 3350).

X-ray diffraction data were collected using beamline I03 at the Diamond Light Source (Harwell, UK), and images were indexed and integrated with DIALS.

Supporting Table S2: Data collection and refinement statistics for OXA-48 in complex with **9d**.

	OXA-48 in complex with 9d[(a)]
Wavelength (Å)	0.97626
Resolution range (Å)	59.53 - 2.098 (2.13 - 2.1)
Space group	$P2_12_12_1$
Unit cell	64.052, 108.507, 161.35, 90, 90, 90
Total reflections	1219524 (43605)
Unique reflections	88091 (3373)
Multiplicity	13.8 (12.9)
Completeness (%)	99.44 (93.28)
Mean I/sigma(I)	5.50 (0.29)
Wilson B-factor	35.69
R-merge	0.2929 (4.656)
R-meas	0.3041 (4.847)
R-pim	0.08146 (1.343)
CC1/2	0.997 (0.723)
CC*	0.999 (0.703)
Reflections used in refinement	66245 (2569)
Reflections used for R-free	3322 (132)
R-work	0.2159 (0.3340)
R-free	0.2465 (0.3755)
Number of non-hydrogen atoms	8375
macromolecules	7897
ligands	104
solvent	366
Protein residues	965
RMS(bonds)	0.008
RMS(angles)	1.04
Ramachandran favored (%)	97.68
Ramachandran allowed (%)	2.22
Ramachandran outliers (%)	0.11
Rotamer outliers (%)	0.60
Clashscore	4.26
Average B-factor	45.78
macromolecules	45.80
ligands	42.79
solvent	46.38

[(a)]Statistics for the highest-resolution shell are shown in parentheses.

Supporting Table S3: Data collection and refinement statistics for *P. aeruginosa* PBP3 in complex with **9a**.

	***P. aeruginosa* PBP3 in complex with 9a**[(a)]
Wavelength (Å)	0.97626
Resolution range (Å)	44.8 - 1.8 (1.85 - 1.8)
Space group	$P2_12_12_1$
Unit cell	68.119, 80.02, 88.865, 90, 90, 90
Total reflections	617278 (44334)
Unique reflections	45660 (3193)
Multiplicity	13.5 (13.9)
Completeness (%)	99.87 (98.49)
Mean I/sigma(I)	9.16 (0.87)
Wilson B-factor	29.28
R-merge	0.1265 (1.649)
R-meas	0.1316 (1.712)
R-pim	0.03565 (0.4563)
CC1/2	0.999 (0.75)
CC*	1 (0.926)
Reflections used in refinement	45644 (3190)
Reflections used for R-free	1964 (141)
R-work	0.1898 (0.3294)
R-free	0.2264 (0.3605)
Number of non-hydrogen atoms	4117
macromolecules	3815
ligands	15
solvent	287
Protein residues	497
RMS(bonds)	0.006
RMS(angles)	0.83
Ramachandran favored (%)	97.96
Ramachandran allowed (%)	2.04
Ramachandran outliers (%)	0.00
Rotamer outliers (%)	0.25
Clashscore	3.38
Average B-factor	36.94
macromolecules	36.71
ligands	30.57
solvent	40.36

[(a)]Statistics for the highest-resolution shell are shown in parentheses.

4.2.7.7 Single-crystal X-ray structure

The single-crystal X-ray structure of **9a** was obtained by the Chemical Crystallography Service of the Chemistry Research Laboratory at Department of Chemistry, University of Oxford. The asymmetric unit contains two molecules, with the Flack parameter clearly indicative of a single enantiomer. Crystal data and structure refinement for **9a** is available in **Supporting Table S4**.

Supporting Table S4: Crystal data and structure refinement for **9a**

Empirical formula	$C_9H_{13}NO_6S$
Formula weight	263.27
Temperature	100 K
Wavelength	1.54184 Å
Crystal system	Triclinic
Space group	*P*1
Unit cell dimensions	a = 7.78430(10) Å α= 90.271(2)°. b = 8.5987(2) Å β= 110.955(2)°. c = 9.1038(2) Å γ = 92.449(2)°.
Volume	568.41(2) $Å^3$
Z	2
Density (calculated)	1.538 Mg/m^3
Absorption coefficient	2.739 mm^{-1}
F(000)	275.999
Crystal size	0.114 x 0.043 x 0.020 mm^3
Theta range for data collection	5.150 to 74.128°.
Index ranges	-9<=h<=8, -10<=k<=10, -11<=l<=11
Reflections collected	4289
Independent reflections	4289 [R(int) = 0.000]
Completeness to theta = 72.645°	99.7 %
Absorption correction	Semi-empirical from equivalents
Max. and min. transmission	0.95 and 0.81
Refinement method	Full-matrix least-squares on F^2
Data / restraints / parameters	4285 / 3 / 308
Goodness-of-fit on F^2	1.0040

Final R indices [I>2sigma(I)]	R1 = 0.0340, wR2 = 0.0922
R indices (all data)	R1 = 0.0358, wR2 = 0.0937
Absolute structure parameter	0.007(9)
Largest diff. peak and hole	0.24 and -0.34 e.$Å^{-3}$

4.2.8 References

1. P. M. Blumberg and J. L. Strominger, Interaction of penicillin with the bacterial cell: penicillin-binding proteins and penicillin-sensitive enzymes, *Bacteriol. Rev.*, 1974, **38**, 291–335.
2. K. Bush and P. A. Bradford, β-Lactams and β-Lactamase Inhibitors: An Overview, *Cold Spring Harb. Perspect. Med.*, 2016, **6**, a025247.
3. L. M. Lima, B. N. M. da Silva, G. Barbosa and E. J. Barreiro, β-lactam antibiotics: An overview from a medicinal chemistry perspective, *Eur. J. Med. Chem.*, 2020, **208**, 112829.
4. E. Sauvage, F. Kerff, M. Terrak, J. A. Ayala and P. Charlier, The penicillin-binding proteins: structure and role in peptidoglycan biosynthesis, *FEMS Microbiol. Rev.*, 2008, **32**, 234–258.
5. K. Bush, in *Antimicrobial Drug Resistance: Mechanisms of Drug Resistance, Volume 1*, eds. D. L. Mayers, J. D. Sobel, M. Ouellette, K. S. Kaye and D. Marchaim, Springer International Publishing, Cham, 2017, pp. 165–175.
6. K. Bush, Past and Present Perspectives on β-Lactamases, *Antimicrob. Agents Chemother.*, 2018, **62**, 10.1128/aac.01076–01018.
7. K. Bush and G. A. Jacoby, Updated functional classification of β-lactamases, *Antimicrob. Agents Chemother.*, 2010, **54**, 969–976.
8. K. H. M. E. Tehrani and N. I. Martin, β-lactam/β-lactamase inhibitor combinations: an update, *MedChemComm*, 2018, **9**, 1439–1456.
9. A. Alarcia-Lacalle, A. Canut-Blasco, M. Á. Solinís, A. Isla and A. Rodríguez-Gascón, Clinical efficacy, safety and pharmacokinetics of novel β-lactam/β-lactamase inhibitor combinations: a systematic review, *JAC-Antimicrob. Resist.*, 2025, **7**, dlaf096.
10. K. M. Papp-Wallace, The latest advances in β-lactam/β-lactamase inhibitor combinations for the treatment of Gram-negative bacterial infections, *Expert Opin. Pharmacother.*, 2019, **20**, 2169–2184.
11. P. A. Lang, M. de Munnik, A. O. Oluwole, T. D. W. Claridge, C. V. Robinson, J. Brem and C. J. Schofield, How Clavulanic Acid Inhibits Serine β-Lactamases, *ChemBioChem*, 2024, **25**, e202400280.
12. D. Monnaie and J.-M. Frere, Interaction of clavulanate with class C β-lactamases, *FEBS Lett.*, 1993, **334**, 269–271.
13. P. A. Lang, R. Raj, A. Tumber, C. T. Lohans, P. Rabe, C. V. Robinson, J. Brem and C. J. Schofield, Studies on enmetazobactam clarify mechanisms of widely used β-lactamase inhibitors, *Proc. Natl. Acad. Sci.*, 2022, **119**, e2117310119.
14. F. de Sousa Coelho and J. L. Mainardi, The multiple benefits of second-generation β-lactamase inhibitors in treatment of multidrug-resistant bacteria, *Infect. Dis. Now*, 2021, **51**, 510–517.
15. H. Choi, R. S. Paton, H. Park and C. J. Schofield, Investigations on recyclisation and hydrolysis in avibactam mediated serine β-lactamase inhibition, *Org. Biomol. Chem.*, 2016, **14**, 4116–4128.
16. D. Y. Wang, M. I. Abboud, M. S. Markoulides, J. Brem and C. J. Schofield, The Road to Avibactam: The First Clinically Useful Non-β-Lactam Working Somewhat Like a β-Lactam, *Future Med. Chem.*, 2016, **8**, 1063–1084.

17. G. Sangiorgio, M. Calvo and S. Stefani, Aztreonam and avibactam combination therapy for metallo-β-lactamase-producing gram-negative bacteria: A Narrative Review, *Clin. Microbiol. Infect.*, 2025, **31**, 971–978.
18. H. Mansour, A. E. L. Ouweini, E. B. Chahine and L. R. Karaoui, Imipenem/cilastatin/relebactam: A new carbapenem β-lactamase inhibitor combination, *Am. J. Health Syst. Pharm.*, 2021, **78**, 674–683.
19. C. L. Tooke, P. Hinchliffe, A. Krajnc, A. J. Mulholland, J. Brem, C. J. Schofield and J. Spencer, Cyclic boronates as versatile scaffolds for KPC-2 β-lactamase inhibition, *RSC Med. Chem.*, 2020, **11**, 491–496.
20. T. S. Patel, J. M. Pogue, J. P. Mills and K. S. Kaye, Meropenem–Vaborbactam: A New Weapon in the War Against Infections Due to Resistant Gram-Negative Bacteria, *Future Microbiol.*, 2018, **13**, 971–983.
21. M. Nottingham, C. R. Bethel, S. R. R. Pagadala, E. Harry, A. Pinto, Z. A. Lemons, S. M. Drawz, F. v. d. Akker, P. R. Carey, R. A. Bonomo and J. D. Buynak, Modifications of the C6-substituent of penicillin sulfones with the goal of improving inhibitor recognition and efficacy, *Bioorg. Med. Chem. Lett.*, 2011, **21**, 387–393.
22. J. D. Buynak, H. Chen, L. Vogeti, V. R. Gadhachanda, C. A. Buchanan, T. Palzkill, R. W. Shaw, J. Spencer and T. R. Walsh, Penicillin-derived inhibitors that simultaneously target both metallo- and serine-β-lactamases, *Bioorg. Med. Chem. Lett.*, 2004, **14**, 1299–1304.
23. J. D. Buynak, B. Geng, B. Bachmann and H. Ling, The synthesis and lactamase inhibitory activity of 6-(carboxymethylene)penicillins and 7-(carboxymethylene)cephalosporins, *Bioorg. Med. Chem. Lett.*, 1995, **5**, 1513–1518.
24. V. P. Sandanayaka, A. S. Prashad, Y. Yang, R. T. Williamson, Y. I. Lin and T. S. Mansour, Spirocyclopropyl β-Lactams as Mechanism-Based Inhibitors of Serine β-Lactamases. Synthesis by Rhodium-Catalyzed Cyclopropanation of 6-Diazopenicillanate Sulfone, *J. Med. Chem.*, 2003, **46**, 2569–2571.
25. F. Penwell William, B. Shapiro Adam, A. Giacobbe Robert, R.-F. Gu, N. Gao, J. Thresher, E. McLaughlin Robert, D. Huband Michael, L. M. DeJonge Boudewijn, E. Ehmann David and A. Miller Alita, Molecular Mechanisms of Sulbactam Antibacterial Activity and Resistance Determinants in Acinetobacter baumannii, *Antimicrob. Agents Chemother.*, 2015, **59**, 1680–1689.
26. B. Shapiro Adam, Kinetics of Sulbactam Hydrolysis by β-Lactamases, and Kinetics of β-Lactamase Inhibition by Sulbactam, *Antimicrob. Agents Chemother.*, 2017, **61**, 10.1128/aac.01612–01617.
27. A. B. Shapiro, S. H. Moussa, S. M. McLeod, T. Durand-Réville and A. A. Miller, Durlobactam, a New Diazabicyclooctane β-Lactamase Inhibitor for the Treatment of Acinetobacter Infections in Combination With Sulbactam, *Front. Microbiol.*, 2021, **Volume 12 - 2021**.
28. A. El-Ghali, A. J. Kunz Coyne, K. Caniff, C. Bleick and M. J. Rybak, Sulbactam-durlobactam: A novel β-lactam-β-lactamase inhibitor combination targeting carbapenem-resistant Acinetobacter baumannii infections, *Pharmacotherapy*, 2023, **43**, 502–513.
29. X. Li, J. Zhao, B. Zhang, X. Duan, J. Jiao, W. Wu, Y. Zhou and H. Wang, Drug development concerning metallo-β-lactamases in gram-negative bacteria, *Front. Microbiol.*, 2022, **Volume 13 - 2022**.

30. M. F. Mojica, M.-A. Rossi, A. J. Vila and R. A. Bonomo, The urgent need for metallo-β-lactamase inhibitors: an unattended global threat, *Lancet Infect. Dis.*, 2022, **22**, e28–e34.
31. C. L. Tooke, P. Hinchliffe, E. C. Bragginton, C. K. Colenso, V. H. A. Hirvonen, Y. Takebayashi and J. Spencer, β-Lactamases and β-Lactamase Inhibitors in the 21st Century, *J. Mol. Biol.*, 2019, **431**, 3472–3500.
32. Y. Yang, Y.-H. Yan, C. J. Schofield, A. McNally, Z. Zong and G.-B. Li, Metallo-β-lactamase-mediated antimicrobial resistance and progress in inhibitor discovery, *Trends Microbiol.*, 2023, **31**, 735–748.
33. M. Falcone, C. Giordano, A. Leonildi, V. Galfo, A. Lepore, L. R. Suardi, N. Riccardi, S. Barnini and G. Tiseo, Clinical Features and Outcomes of Infections Caused by Metallo-β-Lactamase–Producing Enterobacterales: A 3-Year Prospective Study From an Endemic Area, *Clin. Infect. Dis.*, 2024, **78**, 1111–1119.
34. M. Kazmierczak Krystyna, S. Rabine, M. Hackel, E. McLaughlin Robert, J. Biedenbach Douglas, K. Bouchillon Samuel, F. Sahm Daniel and A. Bradford Patricia, Multiyear, Multinational Survey of the Incidence and Global Distribution of Metallo-β-Lactamase-Producing Enterobacteriaceae and Pseudomonas aeruginosa, *Antimicrob. Agents Chemother.*, 2016, **60**, 1067–1078.
35. T. Salvia, K. G. Dolma, O. P. Dhakal, B. Khandelwal and L. S. Singh, Phenotypic Detection of ESBL, AmpC, MBL, and Their Co-occurrence among MDR Enterobacteriaceae Isolates, *J. Lab. Phys.*, **14**.
36. T. S. Mansour, P. A. Bradford and A. M. Venkatesan, in *Annu. Rep. Med. Chem.*, ed. J. E. Macor, Academic Press, 2008, vol. 43, pp. 247–267.
37. P. S. Vincent and S. P. Amar, Resistance to Beta-Lactam Antibiotics: Structure and Mechanism Based Design of Beta-Lactamase Inhibitors, *Curr. Med. Chem.*, 2002, **9**, 1145–1165.
38. K. M. Papp-Wallace, C. R. Bethel, T. D. Gootz, W. Shang, J. Stroh, W. Lau, D. McLeod, L. Price, A. Marfat, A. Distler, S. M. Drawz, H. Chen, E. Harry, M. Nottingham, P. R. Carey, J. D. Buynak and R. A. Bonomo, Inactivation of a class A and a class C β-lactamase by 6β-(hydroxymethyl)penicillanic acid sulfone, *Biochem. Pharmacol.*, 2012, **83**, 462–471.
39. S. Hanessian and M. Alpegiani, Highly stereoselective free radical C-6-allylation of penams - synthesis of a noval β-lactamase inhibitor, *Tetrahedron*, 1989, **45**, 941–950.
40. S. Vanwetswinkel, J. Fastrez and J. Marchand-Brynaert, Synthesis of new sulfonylamido-penicillanic acid sulfones inhibitors of β-lactamases, *J. Antibiot.*, 1994, **47**, 1041–1051.
41. V. P. Sandanayaka and Y. Yang, Dipolar Cycloaddition of Novel 6-(Nitrileoxidomethyl) Penam Sulfone: An Efficient Route to a New Class of β-Lactamase Inhibitors, *Org. Lett.*, 2000, **2**, 3087–3090.
42. J. D. Buynak, A. S. Rao, G. P. Ford, C. Carver, G. Adam, B. Geng, B. Bachmann, S. Shobassy and S. Lackey, 7-Alkylidenecephalosporin Esters as Inhibitors of Human Leukocyte Elastase, *J. Med. Chem.*, 1997, **40**, 3423–3433.
43. M. Sacco, D., K. G. Kroeck, M. T. Kemp, X. Zhang, L. D. Andrews and Y. Chen, Influence of the α-Methoxy Group on the Reaction of Temocillin with Pseudomonas aeruginosa PBP3 and CTX-M-14 β-Lactamase, *Antimicrob. Agents Chemother.*, 2019, **64**, 10.1128/aac.01473–01419.
44. L. Verbist, In vitro activity of temocillin (BRL 17421), a novel beta-lactamase-stable penicillin, *Antimicrob. Agents Chemother.*, 1982, **22**, 157–161.

45. J. Hamilton-Miller and W. Brumfitt, Cephamycins: A review, prospects and some original observations, *Infection*, 1975, **3**, 183–188.
46. P. J. Giddings, D. I. John, E. J. Thomas and D. J. Williams, Preparation of 6α-monosubstituted and 6,6-disubstituted penicillanates from 6-diazopenicillanates: reactions of 6-diazopenicillanates with alcohols, thiols, phenylseleninyl compounds, and allylic sulphides, and their analogues, *J. Chem. Soc., Perkin Trans. 1*, 1982, 2757–2766.
47. A. Mori, T. Mizusaki, Y. Miyakawa, E. Ohashi, T. Haga, T. Maegawa, Y. Monguchi and H. Sajiki, Chemoselective hydrogenation method catalyzed by Pd/C using diphenylsulfide as a reasonable catalyst poison, *Tetrahedron*, 2006, **62**, 11925–11932.
48. S. S. van Berkel, J. Brem, A. M. Rydzik, R. Salimraj, R. Cain, A. Verma, R. J. Owens, C. W. G. Fishwick, J. Spencer and C. J. Schofield, Assay Platform for Clinically Relevant Metallo-β-lactamases, *J. Med. Chem.*, 2013, **56**, 6945–6953.
49. H. G. Smith, S. Basak, V. Aniebok, M. J. Beech, F. M. Alshref, M. D. Allen, A. J. M. Farley and C. J. Schofield, Structural basis of Pseudomonas aeruginosa penicillin binding protein 3 inhibition by the siderophore-antibiotic cefiderocol, *Chem. Sci.*, 2024, **15**, 16928–16937.
50. P. A. Lang, R. Raj, A. Tumber, C. T. Lohans, P. Rabe, C. V. Robinson, J. Brem and C. J. Schofield, Studies on enmetazobactam clarify mechanisms of widely used β-lactamase inhibitors, *Proc. Natl. Acad. Sci. U. S. A.*, 2022, **119**, e2117310119.
51. D. Liebschner, P. V. Afonine, M. L. Baker, G. Bunkoczi, V. B. Chen, T. I. Croll, B. Hintze, L.-W. Hung, S. Jain, A. J. McCoy, N. W. Moriarty, R. D. Oeffner, B. K. Poon, M. G. Prisant, R. J. Read, J. S. Richardson, D. C. Richardson, M. D. Sammito, O. V. Sobolev, D. H. Stockwell, T. C. Terwilliger, A. G. Urzhumtsev, L. L. Videau, C. J. Williams and P. D. Adams, Macromolecular structure determination using X-rays, neutrons and electrons: recent developments in Phenix, *Acta Crystallogr. D.*, 2019, **75**, 861–877.
52. J.-D. Docquier, V. Calderone, F. De Luca, M. Benvenuti, F. Giuliani, L. Bellucci, A. Tafi, P. Nordmann, M. Botta, G. M. Rossolini and S. Mangani, Crystal Structure of the OXA-48 β-Lactamase Reveals Mechanistic Diversity among Class D Carbapenemases, *Chem. Biol.*, 2009, **16**, 540–547.
53. P. Emsley, B. Lohkamp, W. G. Scott and K. Cowtan, Features and development of Coot, *Acta Crystallogr. D.*, 2010, **66**, 486–501.
54. N. W. Moriarty, R. W. Grosse-Kunstleve and P. D. Adams, electronic Ligand Builder and Optimization Workbench (eLBOW): a tool for ligand coordinate and restraint generation, *Acta Crystallogr. D.*, 2009, **65**, 1074–1080.
55. A. Smith Clyde, K. Stewart Nichole, M. Toth and B. Vakulenko Sergei, Structural Insights into the Mechanism of Carbapenemase Activity of the OXA-48 β-Lactamase, *Antimicrob. Agents Chemother.*, 2019, **63**, 10.1128/aac.01202–01219.
56. A. J. McCoy, R. W. Grosse-Kunstleve, P. D. Adams, M. D. Winn, L. C. Storoni and R. J. Read, Phaser crystallographic software, *J. Appl. Crystallogr.*, 2007, **40**, 658–674.
57. J. Jumper, R. Evans, A. Pritzel, T. Green, M. Figurnov, O. Ronneberger, K. Tunyasuvunakool, R. Bates, A. Žídek, A. Potapenko, A. Bridgland, C. Meyer, S. A. A. Kohl, A. J. Ballard, A. Cowie, B. Romera-Paredes, S. Nikolov, R. Jain, J. Adler, T. Back, S. Petersen, D. Reiman, E. Clancy, M. Zielinski, M. Steinegger, M. Pacholska, T. Berghammer, S. Bodenstein, D. Silver, O. Vinyals, A. W. Senior, K. Kavukcuoglu, P.

Kohli and D. Hassabis, Highly accurate protein structure prediction with AlphaFold, *Nature*, 2021, **596**, 583–589.
58. S. Sainsbury, L. Bird, V. Rao, S. M. Shepherd, D. I. Stuart, W. N. Hunter, R. J. Owens and J. Ren, Crystal Structures of Penicillin-Binding Protein 3 from Pseudomonas aeruginosa: Comparison of Native and Antibiotic-Bound Forms, *J. Mol. Biol.*, 2011, **405**, 173–184.
59. R. English Arthur, A. Retsema James, E. Girard Arthur, E. Lynch John and E. Barth Wayne, CP-45,899, a Beta-Lactamase Inhibitor That Extends the Antibacterial Spectrum of Beta-Lactams: Initial Bacteriological Characterization, *Antimicrob. Agents Chemother.*, 1978, **14**, 414–419.
60. S. M. McLeod, J. P. O'Donnell, N. Narayanan, J. P. Mills and K. S. Kaye, Sulbactam–durlobactam: a β-lactam/β-lactamase inhibitor combination targeting Acinetobacter baumannii, *Future Microbiol.*, 2024, **19**, 563–576.
61. J. Zhang, S. Diao, Y. Liu, H. Wang, Y. Liu, S. Zhu, K. Feng, X. Tang, C. Oo, P. Zhu, Z. Lv, M. Yu, S. K. B. Sy and Y. Zhu, The combination effect of meropenem/sulbactam/polymyxin-B on the pharmacodynamic parameters for mutant selection windows against carbapenem-resistant Acinetobacter baumannii, *Front. Microbiol.*, 2022, **Volume 13 - 2022**.
62. S. Zhu, C. Song, J. Zhang, S. Diao, T. M. Heinrichs, F. S. Martins, Z. Lv, Y. Zhu, M. Yu and S. K. B. Sy, Effects of amikacin, polymyxin-B, and sulbactam combination on the pharmacodynamic indices of mutant selection against multi-drug resistant Acinetobacter baumannii, *Front. Microbiol.*, 2022, **Volume 13 - 2022**.
63. N.-Y. Lee, C.-L. Wang, Y.-C. Chuang, W.-L. Yu, H.-C. Lee, C.-M. Chang, L.-R. Wang and W.-C. Ko, Combination Carbapenem-Sulbactam Therapy for Critically Ill Patients with Multidrug-Resistant Acinetobacter baumannii Bacteremia: Four Case Reports and an In Vitro Combination Synergy Study, *Pharmacotherapy*, 2007, **27**, 1506–1511.
64. A. Jitmuang, S. Tiengrim, V. Thamlikitkul and P. Koomanachai, In vitro activity of sulbactam in combination with other antimicrobial agents against extensively drug-resistant Acinetobacter baumannii, *Microbiol. Spectr.*, 2025, **13**, e01379–01325.
65. R. A. Bonomo, S. A. Rudin and D. M. Shlaes, Tazobactam is a potent inactivator of selected inhibitor-resistant class A β-lactamases, *FEMS Microbiol. Lett.*, 1997, **148**, 59–62.
66. M. Paul-Satyaseela, Invention of Enmetazobactam: An Indian Triumph in Antimicrobial Drug Discovery, *ACS Infect. Dis.*, 2025, **11**, 1–3.
67. C. Vázquez-Ucha Juan, M. Maneiro, M. Martínez-Guitián, J. Buynak, R. Bethel Christopher, A. Bonomo Robert, G. Bou, M. Poza, C. González-Bello and A. Beceiro, Activity of the β-Lactamase Inhibitor LN-1-255 against Carbapenem-Hydrolyzing Class D β-Lactamases from Acinetobacter baumannii, *Antimicrob. Agents Chemother.*, 2017, **61**, 10.1128/aac.01172–01117.
68. G. Bou, E. Santillana, A. Sheri, A. Beceiro, J. M. Sampson, M. Kalp, C. R. Bethel, A. M. Distler, S. M. Drawz, S. R. R. Pagadala, F. van den Akker, R. A. Bonomo, A. Romero and J. D. Buynak, Design, Synthesis, and Crystal Structures of 6-Alkylidene-2′-Substituted Penicillanic Acid Sulfones as Potent Inhibitors of Acinetobacter baumannii OXA-24 Carbapenemase, *J. Am. Chem. Soc.*, 2010, **132**, 13320–13331.
69. P. Pattanaik, C. R. Bethel, A. M. Hujer, K. M. Hujer, A. M. Distler, M. Taracila, V. E. Anderson, T. R. Fritsche, R. N. Jones, S. R. R. Pagadala, F. van den Akker, J. D. Buynak

and R. A. Bonomo, Strategic Design of an Effective β-Lactamase Inhibitor: LN-1-255, A 6-ALKYLIDENE-2′-SUBSTITUTED PENICILLIN SULFONE, *J. Biol. Chem.*, 2009, **284**, 945–953.
70. L. Hu, H. Yang, T. Yu, F. Chen, R. Liu, S. Xue, S. Zhang, W. Mao, C. Ji, H. Wang and H. Xie, Stereochemically altered cephalosporins as potent inhibitors of New Delhi metallo-β-lactamases, *Eur. J. Med. Chem.*, 2022, **232**, 114174.
71. P. A. Lang, A. Parkova, T. M. Leissing, K. Calvopiña, R. Cain, A. Krajnc, T. D. Panduwawala, J. Philippe, C. W. G. Fishwick, P. Trapencieris, M. G. P. Page, C. J. Schofield and J. Brem, Bicyclic Boronates as Potent Inhibitors of AmpC, the Class C β-Lactamase from Escherichia coli, *Biomolecules*, 2020, **10**.
72. S. S. van Berkel, J. Brem, A. M. Rydzik, R. Salimraj, R. Cain, A. Verma, R. J. Owens, C. W. Fishwick, J. Spencer and C. J. Schofield, Assay platform for clinically relevant metallo-β-lactamases, *J. Med. Chem.*, 2013, **56**, 6945–6953.
73. J. Brem, S. van Berkel Sander, D. Zollman, Y. Lee Sook, O. Gileadi, J. McHugh Peter, R. Walsh Timothy, A. McDonough Michael and J. Schofield Christopher, Structural Basis of Metallo-β-Lactamase Inhibition by Captopril Stereoisomers, *Antimicrob. Agents Chemother.*, 2015, **60**, 142–150.
74. S. Han, N. Caspers, R. P. Zaniewski, B. M. Lacey, A. P. Tomaras, X. Feng, K. F. Geoghegan and V. Shanmugasundaram, Distinctive Attributes of β-Lactam Target Proteins in Acinetobacter baumannii Relevant to Development of New Antibiotics, *J. Am. Chem. Soc.*, 2011, **133**, 20536–20545.
75. J. F. Simon, A. Bouillez, J.-M. Frère, A. Luxen and A. Zervosen, Synthesis of an enantiopure thioester as key substrate for screening the sensitivity of penicillin binding proteins to inhibitors, *ARKIVOC*, 2016, **2016**, 22–31.
76. B. Geibel, J. Dowell, D. Dickerson and T. Henkel, 1401. A Randomized, Double-Blind, Placebo-Controlled Study of the Safety and Pharmacokinetics of Single and Repeat Doses of VNRX-5133 in Healthy Subjects, *Open Forum Infect. Dis.*, 2018, **5**, S431–S431.
77. D. M. Taylor, J. Anglin, L. Hu, L. Wang, B. Sankaran, J. Wang, M. M. Matzuk, B. V. V. Prasad and T. Palzkill, Unique Diacidic Fragments Inhibit the OXA-48 Carbapenemase and Enhance the Killing of Escherichia coli Producing OXA-48, *ACS Infect. Dis.*, 2021, **7**, 3345–3354.
78. F. Gorrec, The MORPHEUS II protein crystallization screen, *Acta Crystallogr. Sect. F*, 2015, **71**, 831–837.
79. T. R. Malla, L. Brewitz, D.-G. Muntean, H. Aslam, C. D. Owen, E. Salah, A. Tumber, P. Lukacik, C. Strain-Damerell, H. Mikolajek, M. A. Walsh and C. J. Schofield, Penicillin Derivatives Inhibit the SARS-CoV-2 Main Protease by Reaction with Its Nucleophilic Cysteine, *J. Med. Chem.*, 2022, **65**, 7682–7696.

4.3 Statement of Authorship

Title of Paper	C6-Alkoxy substituents alter the reactivity profile of sulbactam with SBLs and PBPs.
Publication Status	□Published □ Accepted for Publication □Submitted for Publication ☒Unpublished and unsubmitted work written in a manuscript style
Publication Details	**Muntean, D.-G.;** Freeman, E.; Kaur, G.; Smith, H.G., Wilson, L.; Calvopiña, K.; Crumpton, A.; Brewitz, L.; Schofield, C.J.: **C6-Alkoxy substituents alter the reactivity profile of sulbactam with SBLs and PBPs.**

Student Confirmation

Student Name:	Dorian-Gabriel Muntean		
Contribution to the Paper	D.-G.M. designed the synthetic routes towards C6-alkoxy penams and carried out all the organic synthesis. D.-G.M. conceptualised and prepared the first draft of the manuscript. E.F and L.W. obtained the IC_{50} data for SBLs and conducted the POMS experiments. G.K. conducted the MBL inhibition assays, obtained the crystal structure with OXA-48 and refined it. H.G.S. obtained the inhibition data for PBP3 and obtained the crystal structure with *P. aeruginosa* PBP3 and refined the structure. K.C. conducted the MIC assays. A.C. obtained the single-crystal X-ray structure of C6-methoxy sulbactam. L.B. provided supervision of the synthetic work and assisted with manuscript reviewing/editing. C.J.S. is the principal investigator/supervisor of the research described in the manuscript, contributed extensively to project/data conceptualization and visualization, and manuscript reviewing/editing.		
Signature 		Date	09/10/2025

Supervisor Confirmation

By signing the Statement of Authorship, you are certifying that the candidate made a substantial contribution to the publication, and that the description described above is accurate.

Supervisor name and title: Prof. Christopher J. Schofield		
Supervisor comments:		
Signature 	Date	09/10/2025

Chapter 5. Investigations into C6-methoxypenicillins

5.1 Chapter overview

Chapter 5 describes the synthesis of C6-methoxypenicillins and the assessment of their inhibitory and antimicrobial properties. Temocillin, a C6-methoxypenicillin, is a narrow-spectrum antibiotic with exceptional stability towards certain serine β-lactamases, thanks to the presence of its C6-methoxy group, which is believed to block access of the hydrolytic water to the catalytic active site. The C6-methoxy group of temocillin, however, also destabilises the acyl-enzyme complexes formed via reaction with penicillin-binding proteins (PBPs). Given the recent interest in repurposing temocillin for novel uses, the work described in this Chapter aims to re-examine the effect of introducing a C6-methoxy group onto the scaffold of clinically used penicillin antibiotics, with the goal of identifying other C6-methoxypenicillins that may also be employed as narrow-spectrum antibiotics. Pleasingly, the C6-methoxy derivative of piperacillin was identified as a potent inhibitor of recombinant isolated PBP3s from Gram-negative pathogens, showing a superior profile to temocillin in both enzymatic and cell-based assays. Considering the rapid rise of antibiotic-resistant bacteria possessing β-lactamase-encoding genes, this finding is of interest, as it could inform the design of next-generation C6-methoxy penicillin antibiotics that are potent PBP inhibitors.

Manuscript IV

At the time of writing this thesis, Manuscript IV is in preparation for publication. A Statement of Authorship is appended at the end of the chapter. The synthetic experimental details and spectra of the compounds prepared can be found in the **Appendix**.

Muntean, **D.-G.**; Smith, H.G.; Calvopiña, K.; Brewitz, L.; Schofield, C.J.: **Piperacillin is a promising scaffold for the development of C6-methoxypenicillins.**

5.2 Manuscript IV: Piperacillin is a promising scaffold for the development of C6-methoxypenicillins.

5.2.1 Abstract

One of the most critical bacterial resistance mechanisms is the production of β-lactamases, hydrolytic enzymes that inactivate β-lactam antibiotics. Developing β-lactamase-resistant β-lactams is a priority in antibiotic research. Temocillin, a narrow-spectrum C6-methoxypenicillin antibiotic, has recently been investigated for clinical repurposing, thanks to its excellent stability toward certain serine β-lactamases. However, the presence of the C6-methoxy group, while conferring resistance to β-lactamase-mediated hydrolysis, also interferes with the stability of the acyl-enzyme complexes formed following the reaction with penicillin-binding proteins (PBPs), thus limiting its antibacterial potency.

In the present work, we investigated the C6-methoxy derivatives of several clinically used penicillins and evaluated both their PBP inhibitory properties and antibacterial activities. Piperacillin emerged as an interesting molecule, as its C6-methoxy analogue retained high PBP3 potency and exhibited an antibacterial profile superior to that of temocillin in both enzymatic and cell-based assays. These findings demonstrate that the C6-methoxylation of penicillins does not necessarily compromise antimicrobial activity, highlighting the potential of C6-methoxypiperacillin, and, by extension, related C6-methoxypenicillins, as β-lactam antibiotic candidates that warrant further investigation.

Key words: C6-methoxypenicillins; temocillin; piperacillin; penicillin-binding proteins; β-lactamases.

5.2.2 Introduction

Broad-spectrum antibiotics are essential for reducing infection-related mortality, but their indiscriminate use in healthcare and agriculture drives antibiotic resistance.[1-3] Incomplete treatment courses further favour survival of partially suppressed pathogens, thus intensifying evolutionary pressure for resistance.[4] Antibiotic resistance is now a major global health threat.[4-9]

Narrow-spectrum antibiotics are a valuable therapeutic option for infections with a known pathogen, offering potential benefits including because: (i) they reduce the risk of antibiotic resistance by minimising collateral selective pressure associated with broad-spectrum agents;[10] (ii) they cause minimal disruption of the human microbiota, thereby reducing side effects;[11-14] (iii) their use lowers the risk of secondary infections caused by opportunistic gastrointestinal pathogens (*e.g.*, *Clostridioides difficile*);[15, 16] and (iv) narrow-spectrum antibiotics may be more effective against targeted species than broad-spectrum antibiotics.[17-20]

In recent years, growing attention has been directed to the potential use of early-generation antibiotics, that, despite their favourable profiles against bacterial resistance mechanisms, have been shelved due to limited spectra of activity.[21-23] One such example is **temocillin**,[24, 25] the C6-methoxy penicillin derivative of **ticarcillin**, which is active against multidrug-resistant (MDR) Enterobacterales,[26] displaying exceptional stability towards classical and extended-spectrum serine β-lactamases (SBLs), including but not limited to TEM, SHV, CTX-M, and AmpC. However, **temocillin** lacks any useful activity against Gram-positives, anaerobes, or non-fermenting Gram-negative pathogens such as *A. baumanii* or *P. aeruginosa.*[27-31]

Crystallographic studies have led to the proposal that the C6-methoxy group of **temocillin** prevents productive access of the hydrolytic water molecule to the intermediate SBL acyl-enzyme complex,

thus accounting for the inhibitory properties of **temocillin** against certain SBLs (*e.g.*, CTX-M).[32] However, the C6-methoxy group imparts a double-edged effect, as it can also interfere with the stability of the acyl-enzyme complexes formed with the penicillin-binding proteins (PBPs) of some species (*e.g.*, *P. aeruginosa* PBP3).[32] Because PBPs are a primary target of β-lactam antibiotics,[33, 34] diminished inhibition of certain PBPs represents a major clinical limitation of **temocillin** and accounts for its narrow-spectrum antibacterial profile.[32, 35]

Recent reports indicate that **temocillin** might be successfully repurposed, including for the treatment of infections caused by *Burkholderia* spp.;[23] such repurposing may help spare the use of last-resort, broad-spectrum antibiotics (*e.g.*, carbapenems)[36] in situations where these are not absolutely necessary.[36, 37] Given the renewed clinical interest in **temocillin**,[37] we investigated how C6-methoxy substitution affects the PBP inhibitory properties of penicillin antibiotics other than **ticarcillin**. Here, we report the synthesis of C6-methoxy derivatives of clinically used penicillin antibiotics and reassess the influence of C6-methoxy substitution on PBP inhibition and antibacterial activity.

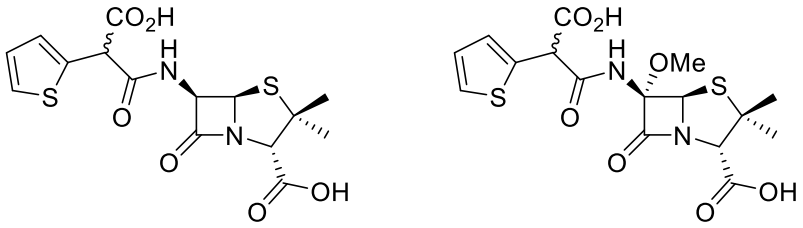

Figure 1: Structures of **ticarcillin** and its C6-methoxy analogue, **temocillin**.

5.2.3 Results and Discussion

Synthesis of C6-methoxypenicillin

Several protocols for preparing C6-methoxypenicillins are reported in the academic and patent literature, some involving multistep sequences (such as protection steps to stabilise reactive β-lactam intermediates).[38-42] A single-step direct modification of commercially sourced penicillins was deemed preferable over optimal yields in order to provide facile access to compounds for biological screening. Therefore, the reported C6-methoxylation reaction of **ticarcillin** with *tert*-BuOCl in the presence of LiOMe in MeOH to directly give **temocillin** was assessed for generality (**Supplementary Figure S1**);[38] this method was also useful to afford the C6-methoxy derivatives of **penicillin G**, **oxacillin**, **cloxacillin**, **dicloxacillin**, **carbenicillin**, and **piperacillin** (**Figure 2**), *i.e.*, C6-methoxy penicillins **1a-f** (yields: 3-18%).

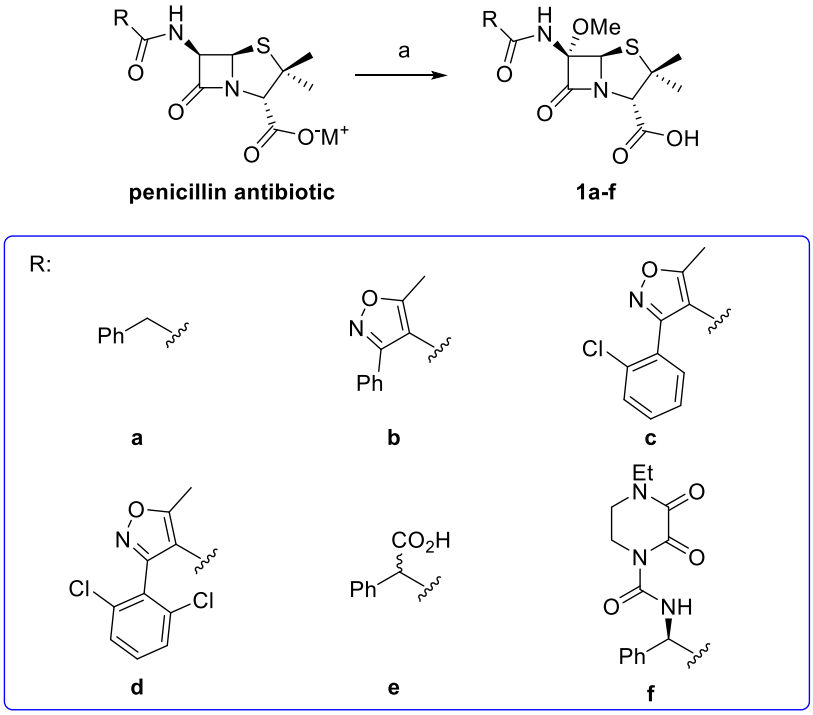

Figure 1: Synthesis of C6-methoxypenicillin. Reaction conditions: a) ^{t}BuOCl (1.7 equiv.), LiOMe (1.5 equiv.), MeOH, *N*,*N*-dimethylformamide, -75 °C, 5 min, 3-18%.

PBP inhibition studies

Given **temocillin**'s reported activity against Gram-negative pathogens,[25] inhibitory properties of clinically used penicillins and their C6-methoxy derivatives were assessed against recombinant PBP3s from Gram-negative bacteria (**Tables 1**), *i.e*., *A. baumannii, E. coli, K. pneumoniae,* and *P. aeruginosa*. Although **penicillin G**, **oxacillin**, **cloxacillin**, and **dicloxacillin** are primarily used for the treatment of Gram-positive infections, all of them inhibited Gram-negative PBP3s with low-micromolar to sub-micromolar potencies (**Table 1**, entries i, iii, v, and vii). Notably, **penicillin G** was consistently the most potent PBP3 inhibitor across species (pIC_{50} ~ 6.2-7.0), whereas the isoxazolyl penicillins (**oxacillin**, **cloxacillin**, **dicloxacillin**) showed lower potencies (pIC_{50} ~ 5.6-6.5), corresponding to ~3-10-fold weaker PBP3 inhibition relative to penicillin G. The corresponding C6-methoxy derivatives **1a-f** were consistently less efficient in inhibiting PBP3 than the unmodified penicillins (**Table 1**, entries ii, iv, vi, and viii), with the most pronounced decrease in activity being observed for C6-methoxypenicillin G **1a** (~ 30-400 times less potent than **penicillin G**). By contrast, **1b-d** displayed ~10-100-fold reduced inhibition potency relative to their isoxazolyl penicillin counterparts. Interestingly, C6-methoxypenicillin G **1a** and C6-methoxy isoxazoyl penicillins **1b-d** manifested similar levels of inhibitions (pIC_{50} ~ 4.1-4.7).

Ticarcillin showed slightly higher PBP3 inhibition than **carbenicillin**, with the highest potency observed against the PBP3 from *P. aeruginosa* (pIC_{50} ~ 6.7, **Table 1**, entry ix and xi). **Piperacillin** displayed the strongest PBP3 inhibition overall, with pIC_{50} values >7.4 against all four PBP3s. Introduction of a C6-methoxy group led to a ~10-100-fold reduction in inhibition potency for both **carbenicillin** (*i.e*., **1e**) and **ticarcillin** (*i.e*., **temocillin**), with **temocillin** being ~10-fold less potent than **1e** (**Table 1**, entries x and xii). Interestingly, **1f**, the C6-methoxy derivative of **piperacillin**,

retained excellent high potency against all the tested PBP3s (pIC_{50} ~ 7-7.4), thus standing out as the clear exception among all C6-methoxypenicillins tested (*i.e.*, **1a-e** and **temocillin**).

Table 1. Inhibition of PBP3 by narrow-spectrum penicillins and their C6-methoxy derivatives.

	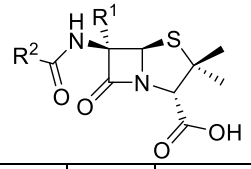			pIC_{50}[(a)] (PBP3)			
	Compound	R^1	R^2	*A. baumanii*	*E. coli*	*K. pneumoniae*	*P. aeruginosa*
i	**Penicillin G**	H	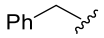	7.0 ± 0.1	6.2 ± 0.1	6.2 ± 0.1	6.5 ± 0.1
ii	**1a**	OMe	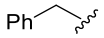	4.4 ± 0.1	4.2 ± 0.1	4.3 ± 0.1	4.7 ± 0.1
iii	**Oxacillin**	H	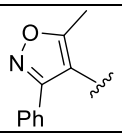	6.0 ± 0.1	6.0 ± 0.1	5.8 ± 0.1	6.0 ± 0.1
iv	**1b**	OMe	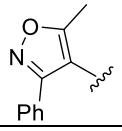	4.1 ± 0.1	4.5 ± 0.1	4.6 ± 0.1	4.6 ± 0.1
v	**Cloxacillin**	H	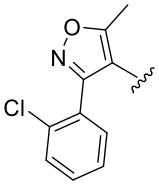	6.0 ± 0.1	6.5 ± 0.1	6.4 ± 0.1	5.6 ± 0.1
vi	**1c**	OMe	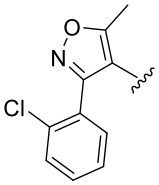	4.7 ± 0.1	4.5 ± 0.1	4.6 ± 0.1	4.7 ± 0.1
vii	**Dicloxacillin**	H	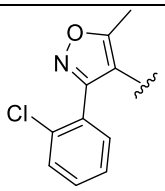	6.0 ± 0.1	6.0 ± 0.1	5.9 ± 0.1	5.6 ± 0.1
viii	**1d**	OMe	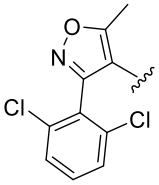	4.7 ± 0.1	4.4 ± 0.1	4.4 ± 0.1	4.5 ± 0.1
ix	**Carbenicillin**	H	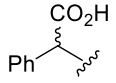	6.1 ± 0.1	5.7 ± 0.1	5.8 ± 0.1	6.3 ± 0.1

x	**1e**	OMe	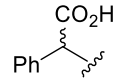	5.5 ± 0.1	5.0 ± 0.1	4.8 ± 0.1	6.1 ± 0.1
xi	**Ticarcillin**	H	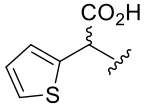	6.5 ± 0.1	5.7 ± 0.1	5.7 ± 0.1	6.7 ± 0.1
xii	**Temocillin**	OMe	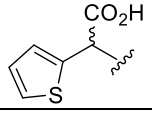	4.5 ± 0.1	4.2 ± 0.1	4.2 ± 0.1	5.2 ± 0.1
xiii	**Piperacillin**	H	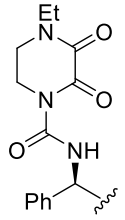	> 7.4	> 7.4	> 7.4	> 7.4
xiv	**1f**	OMe	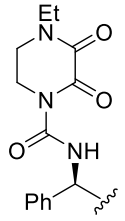	7.0 ± 0.1	7.2 ± 0.1	7.3 ± 0.1	> 7.4
xv	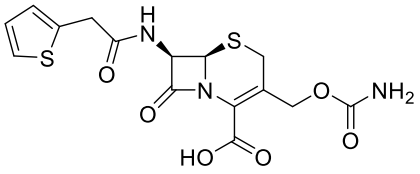 **2**			6.1 ± 0.1	5.6 ± 0.1	5.6 ± 0.1	5.3 ± 0.1
xvi	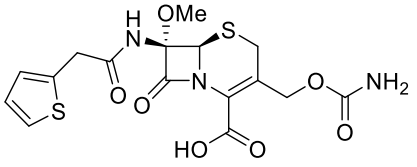 **Cefoxitin**			5.9 ± 0.1	5.3 ± 0.1	5.2 ± 0.1	5.8 ± 0.1

[(a)] Experimental details can be found in the Methods section.

Finally, the PBP3 inhibition activities of C6-methoxypenicillins **1a-f** were compared with a representative cephamycin (*i.e.*, **cefoxitin**). Unlike the pronounced losses in potency seen following the introduction of a C6-methoxy group onto the penicillin core, C7-methoxylation of the cephalosporin scaffold did not cause a significant impact on PBP3 inhibition. Interestingly, **cefoxitin** was marginally more potent than its non-C7-methoxylated analogue **2** against *P. aeruginosa* PBP3 (**Table 1**, entries xv and xvi). Nonetheless, C6-methoxypiperacillin **1f**

maintained significantly more potent inhibition than cefoxitin across all the tested PBP3s (**Table 1**, entries xiii and xvi).

Antibacterial effects of C6-methoxy penicillin derivatives

Minimum inhibitory concentrations (MICs) were determined for **1a-f**, **2**, and their non-C6/7-methoxylated analogues against *A. baumannii, C. freundii, E. coli, K. pneumoniae, P. mirabilis,* and *S. aureus* (**Table 2**). C6-Methoxypenicillin G **1a** and C6-methoxy isoxazolyl penicillins **1b-d** did not exhibit any antimicrobial activity against the tested strains, mirroring their non-C6-methoxy counterparts (**Table 2**, entries i-viii), with the only exception being **penicillin G**, which showed some activity only against *P. mirabilis* and *S. aureus* (MICs ~ 2 and 4 μg/mL, respectively).

Carbenicillin also showed activity only against *P. mirabilis* and *S. aureus* (MIC ~ 8 and 4 μg/mL, respectively; **Table 2**, entry ix). By contrast, its C6-methoxy analogue **1e** not only retained activity against *P. mirabilis* and *S. aureus* (MICs ~ 8 and 16 μg/mL, respectively; **Table 2**, entry x) but also showed moderate activity against *C. freundii* (MIC ~ 8 μg/mL). **Ticarcillin** exhibited an improved PBP3 profile relative to **carbenicillin**, with moderate activity against *C. freundii* and *E. coli* (MIC ~ 16 μg/mL; **Table 2**, entry xi), but its C6-methoxy derivative, **temocillin**, performed worse than either **ticarcillin** or **1e**, displaying no antibacterial activity within the tested range against any of the strains (MIC >32 μg/mL; **Table 2**, entry xii).

Compared with the other penicillins tested, **piperacillin** displayed the strongest antibacterial activity (**Table 2**, entry xiii), inhibiting *C. freundii* (MIC ~ 16 μg/mL), *E. coli* (MIC ~ 8 μg/mL), *P. mirabilis* (MIC ~ 1 μg/mL), and *S. aureus* (MIC ~ 4 μg/mL). Notably, its C6-methoxy analogue **1f** showed a similar profile (**Table 2**, entry xiv), also displaying activity against *C. freundii* (MIC

~ 16 μg/mL), *E. coli* (MIC ~ 16 μg/mL), *P. mirabilis* (MIC ~ 2 μg/mL), and *S. aureus* (MIC ~ 8 μg/mL). Lastly, the antibacterial profile of **cefoxitin** mirrored that of its non-C7-methoxylated analogue **2**, with the notable exception of *E. coli*, for which **cefoxitin** strongly inhibited growth (MIC ~ 2 μg/mL; **Table 2**, entry xvi), whereas **2** did not (MIC ~ 32 μg/mL; **Table 2**, entry xv).

Table 3. Antibacterial properties of penicillins and their C6-methoxy derivatives.

		MIC (μg/mL)[(a)]					
		A. baumanii 13304	*C. freundii* 09750	*E. coli* 25922	*K. pneumoniae 9663*	*P. mirabilis* 11938	*S. aureus* 6571
i	**Penicillin G**	>32	>32	>32	>32	4	2
ii	**1a**	>32	>32	>32	>32	>32	>32
iii	**Oxacillin**	>32	>32	>32	>32	>32	*n.d.*
iv	**1b**	>32	>32	>32	>32	>32	>32
v	**Cloxacillin**	>32	>32	>32	>32	>32	*n.d.*
vi	**1c**	>32	>32	>32	>32	>32	>32
vii	**Dicloxacillin**	>32	>32	>32	>32	>32	*n.d.*
viii	**1d**	>32	>32	>32	>32	>32	>32
ix	**Carbenicillin**	>32	>32	>32	>32	8	4
x	**1e**	>32	8	>32	>32	8	16
xi	**Ticarcillin**	>32	16	16	>32	4	1
xii	**Temocillin**	>32	>32	>32	>32	>32	>32
xiii	**Piperacillin**	>32	16	8	>32	1	4
xiv	**1f**	>32	16	16	>32	2	8
xv	**2**	>32	>32	32	16	4	2
xvi	**Cefoxitin**	>32	32	2	16	4	4

[(a)] Experimental detail can be found in the Methods section.

Taken together, these results indicate that C6-methoxylation across the penicillin series does not necessarily lead to markedly poorer antimicrobial properties. Although the C6-methoxypenicillins generally showed reduced PBP3 inhibition relative to their non-methoxylated counterparts, the extent of this reduction varied considerably. Some penicillin derivatives (e.g., **penicillin G**) exhibited large losses in potency following C6-methoxylation, whereas others were only modestly affected, suggesting that the C6-acylamido side chain plays a key role in compensating for the binding penalty imposed by the C6-methoxy group. Notably, C6-methoxypiperacillin **1f** retained high potency despite its C6-methoxy substituent, displaying stronger inhibition than either temocillin or cefoxitin against the tested PBP3 enzymes. This finding provides proof of concept that, as with the cephamycins (*i.e.*, C7-methoxycephalosporins), C6-methoxypenicillins can also achieve strong target engagement when sidechain substituents are properly optimised. Furthermore, C6-methoxypiperacillin **1f** displayed an antibacterial profile closely matching that of **piperacillin**, inhibiting the same spectrum of organisms with only minor shifts in MIC values, in contrast to the loss of activity observed on C6-methoxylating **ticarcillin** to **temocillin**. Overall, C6-methoxylation does not inevitably compromise antimicrobial potency, as exemplified by **1f**, indicating that piperacillin is a particularly attractive scaffold for the development of next-generation C6-methoxypenicillins.

5.2.4 Conclusions

β-Lactam antibiotics are invaluable antibacterial agents whose efficacy is increasingly threatened by the spread of antibiotic-resistant bacteria.[5, 43] There is growing interest in reviving old and shelved narrow-spectrum antibiotics for targeted, precision therapy.[21, 37, 44] C6-Methoxypenicillins show promise thanks to their exceptional hydrolytic stability to β-lactamases.[25, 27-29, 45] We have shown that the extent of reduction in PBP inhibition associated with C6-methoxylation is

dependent on the identity of the C6-amide sidechain, indicating that functional group optimisation at C6 (and elsewhere) can, in principle, minimise the penalty in binding and inhibition of PBPs incurred by the addition of the C6-methoxy group. Lastly, focused microbiological screenings may also reveal novel narrow-spectrum indications for C6-methoxypenicillins.

5.2.5 Supporting figures

Supporting Figure S1: Proposed outline mechanism for the conversion of **ticarcillin** to **temocillin**. Reported reaction conditions[38]: a) ^{t}BuOCl (1.7 equiv.), LiOMe (1.5 equiv.), MeOH, *N*,*N*-dimethylformamide, -75 °C, 5 min, 58%.

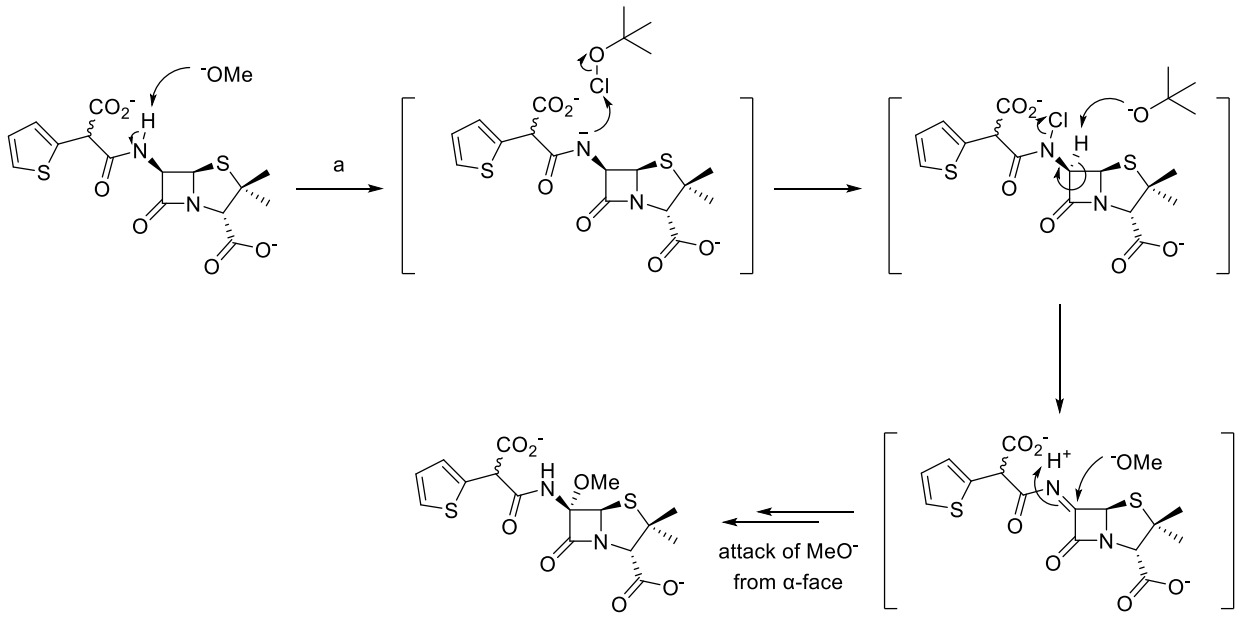

5.2.6 Methods

5.2.6.1 PBP expression

Overproductions and purifications of *P. aeruginosa* PBP3 and *A. baumanii* PBP3 were carried out as described previously.[46, 47] *E. coli* PBP3 and *K. pneumoniae* PBP3 were purified following procedures similar to those for *P. aeruginosa* PBP3 and *A. baumanii* PBP3.[46, 47]

5.2.6.2 PBP inhibition assays

PBP inhibition assays were performed using fluorescence polarisation (FP) as reported,[46] utilizing recombinant isolated PBP3s (300 nM) in S2d assay buffer (25 mM HEPES, 100 mM NaCl, pH 7.4), inhibitor (100 μM to 5 nM, ten concentrations total, 3-fold dilution series), S2d probe[48] (1.5 mM) and monobromobimane (mBBr, 0.5 mM).

Supporting Figure S2: Outline mechanism for the reaction between the S2d probe and carboxypeptidases. Following the hydrolysis of the thioester bond in S2d, 2-mercaptoacetic acid is released, which reacts with monobromobimane to give a fluorescence active probe that is used to investigate PBPs kinetics.

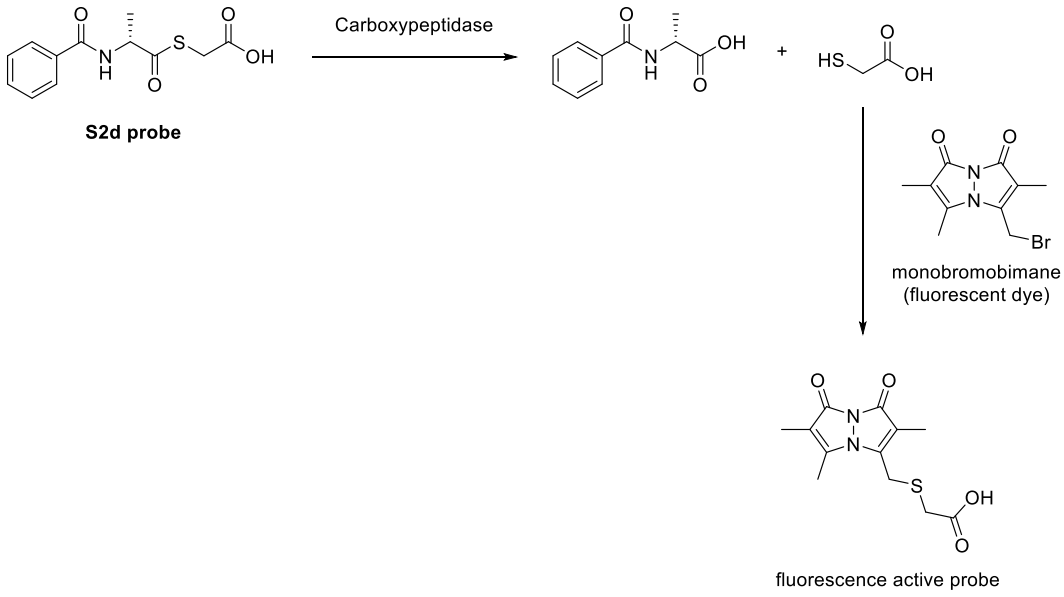

5.2.6.3 Susceptibility assay

Minimum inhibitory concentrations (MICs) were determined using the broth microdilution method, according to the guidelines of the Clinical and Laboratory Standards Institute (CLSI, USA).[49] Measurements were obtained in triplicate, with compounds being tested alone (0.25-256 μg/mL) against selected strains.

5.2.7 References

1. A. H. Holmes, L. S. P. Moore, A. Sundsfjord, M. Steinbakk, S. Regmi, A. Karkey, P. J. Guerin and L. J. V. Piddock, Understanding the mechanisms and drivers of antimicrobial resistance, *The Lancet*, 2016, **387**, 176–187.
2. B. G. Bell, F. Schellevis, E. Stobberingh, H. Goossens and M. Pringle, A systematic review and meta-analysis of the effects of antibiotic consumption on antibiotic resistance, *BMC Infectious Diseases*, 2014, **14**, 13.
3. A. Andremont, C. Brun-Buisson and M. Struelens, Evaluating and predicting the ecologic impact of antibiotics, *Clin. Microbiol. Infect.*, 2001, **7**, 1–6.
4. S. K. Ahmed, S. Hussein, K. Qurbani, R. H. Ibrahim, A. Fareeq, K. A. Mahmood and M. G. Mohamed, Antimicrobial resistance: Impacts, challenges, and future prospects, *Journal of Medicine, Surgery, and Public Health*, 2024, **2**, 100081.
5. M. Naghavi, S. E. Vollset, K. S. Ikuta, L. R. Swetschinski, A. P. Gray, E. E. Wool, G. Robles Aguilar, T. Mestrovic, G. Smith, C. Han, R. L. Hsu, J. Chalek, D. T. Araki, E. Chung, C. Raggi, A. Gershberg Hayoon, N. Davis Weaver, P. A. Lindstedt, A. E. Smith, U. Altay, N. V. Bhattacharjee, K. Giannakis, F. Fell, B. McManigal, N. Ekapirat, J. A. Mendes, T. Runghien, O. Srimokla, A. Abdelkader, S. Abd-Elsalam, R. G. Aboagye, H. Abolhassani, H. Abualruz, U. Abubakar, H. J. Abukhadijah, S. Aburuz, A. Abu-Zaid, S. Achalapong, I. Y. Addo, V. Adekanmbi, T. E. Adeyeoluwa, Q. E. S. Adnani, L. A. Adzigbli, M. S. Afzal, S. Afzal, A. Agodi, A. J. Ahlstrom, A. Ahmad, S. Ahmad, T. Ahmad, A. Ahmadi, A. Ahmed, H. Ahmed, I. Ahmed, M. Ahmed, S. Ahmed, S. A. Ahmed, M. A. Akkaif, S. Al Awaidy, Y. Al Thaher, S. O. Alalalmeh, M. T. AlBataineh, W. A. Aldhaleei, A. A. S. Al-Gheethi, N. B. Alhaji, A. Ali, L. Ali, S. S. Ali, W. Ali, K. Allel, S. Al-Marwani, A. Alrawashdeh, A. Altaf, A. B. Al-Tammemi, J. A. Al-Tawfiq, K. H. Alzoubi, W. A. Al-Zyoud, B. Amos, J. H. Amuasi, R. Ancuceanu, J. R. Andrews, A. Anil, I. A. Anuoluwa, S. Anvari, A. E. Anyasodor, G. L. C. Apostol, J. Arabloo, M. Arafat, A. Y. Aravkin, D. Areda, A. Aremu, A. A. Artamonov, E. A. Ashley, M. O. Asika, S. S. Athari, M. M. d. W. Atout, T. Awoke, S. Azadnajafabad, J. M. Azam, S. Aziz, A. Y. Azzam, M. Babaei, F.-X. Babin, M. Badar, A. A. Baig, M. Bajcetic, S. Baker, M. Bardhan, H. J. Barqawi, Z. Basharat, A. Basiru, M. Bastard, S. Basu, N. S. Bayleyegn, M. A. Belete, O. O. Bello, A. Beloukas, J. A. Berkley, A. S. Bhagavathula, S. Bhaskar, S. S. Bhuyan, J. A. Bielicki, N. I. Briko, C. S. Brown, A. J. Browne, D. Buonsenso, Y. Bustanji, C. G. Carvalheiro, C. A. Castañeda-Orjuela, M. Cenderadewi, J. Chadwick, S. Chakraborty, R. M. Chandika, S. Chandy, V. Chansamouth, V. K. Chattu, A. A. Chaudhary, P. R. Ching, H. Chopra, F. R. Chowdhury, D.-T. Chu, M. Chutiyami, N. Cruz-Martins, A. G. da Silva, O. Dadras, X. Dai, S. D. Darcho, S. Das, F. P. De la Hoz, D. M. Dekker, K. Dhama, D. Diaz, B. F. R. Dickson, S. G. Djorie, M. Dodangeh, S. Dohare, K. G. Dokova, O. P. Doshi, R. K. Dowou, H. L. Dsouza, S. J. Dunachie, A. M. Dziedzic, T. Eckmanns, A. Ed-Dra, A. Eftekharimehrabad, T. C. Ekundayo, I. El Sayed, M. Elhadi, W. El-Huneidi, C. Elias, S. J. Ellis, R. Elsheikh, I. Elsohaby, C. Eltaha, B. Eshrati, M. Eslami, D. W. Eyre, A. O. Fadaka, A. F. Fagbamigbe, A. Fahim, A. Fakhri-Demeshghieh, F. O. Fasina, M. M. Fasina, A. Fatehizadeh, N. A. Feasey, A. Feizkhah, G. Fekadu, F. Fischer, I. Fitriana, K. M. Forrest, C. Fortuna Rodrigues, J. E. Fuller, M. A. Gadanya, M. Gajdács, A. P. Gandhi, E. E. Garcia-Gallo, D. O. Garrett, R. K. Gautam, M. W. Gebregergis, M. Gebrehiwot, T. G. Gebremeskel, C. Geffers, L. Georgalis, R. M. Ghazy, M. Golechha, D. Golinelli, M. Gordon, S. Gulati, R. D. Gupta, S. Gupta, V. K.

Gupta, A. D. Habteyohannes, S. Haller, H. Harapan, M. L. Harrison, A. I. Hasaballah, I. Hasan, R. S. Hasan, H. Hasani, A. H. Haselbeck, M. S. Hasnain, I. I. Hassan, S. Hassan, M. S. Hassan Zadeh Tabatabaei, K. Hayat, J. He, O. E. Hegazi, M. Heidari, K. Hezam, R. Holla, M. Holm, H. Hopkins, M. M. Hossain, M. Hosseinzadeh, S. Hostiuc, N. R. Hussein, L. D. Huy, E. D. Ibáñez-Prada, A. Ikiroma, I. M. Ilic, S. M. S. Islam, F. Ismail, N. E. Ismail, C. D. Iwu, C. J. Iwu-Jaja, A. Jafarzadeh, F. Jaiteh, R. Jalilzadeh Yengejeh, R. D. G. Jamora, J. Javidnia, T. Jawaid, A. W. J. Jenney, H. J. Jeon, M. Jokar, N. Jomehzadeh, T. Joo, N. Joseph, Z. Kamal, K. K. Kanmodi, R. S. Kantar, J. A. Kapisi, I. M. Karaye, Y. S. Khader, H. Khajuria, N. Khalid, F. Khamesipour, A. Khan, M. J. Khan, M. T. Khan, V. Khanal, F. F. Khidri, J. Khubchandani, S. Khusuwan, M. S. Kim, A. Kisa, V. A. Korshunov, F. Krapp, R. Krumkamp, M. Kuddus, M. Kulimbet, D. Kumar, E. A. P. Kumaran, A. Kuttikkattu, H. H. Kyu, I. Landires, B. K. Lawal, T. T. T. Le, I. M. Lederer, M. Lee, S. W. Lee, A. Lepape, T. L. Lerango, V. S. Ligade, C. Lim, S. S. Lim, L. W. Limenh, C. Liu, X. Liu, X. Liu, M. J. Loftus, H. I. M Amin, K. L. Maass, S. B. Maharaj, M. A. Mahmoud, P. Maikanti-Charalampous, O. M. Makram, K. Malhotra, A. A. Malik, G. D. Mandilara, F. Marks, B. A. Martinez-Guerra, M. Martorell, H. Masoumi-Asl, A. G. Mathioudakis, J. May, T. A. McHugh, J. Meiring, H. N. Meles, A. Melese, E. B. Melese, G. Minervini, N. S. Mohamed, S. Mohammed, S. Mohan, A. H. Mokdad, L. Monasta, A. Moodi Ghalibaf, C. E. Moore, Y. Moradi, E. Mossialos, V. Mougin, G. D. Mukoro, F. Mulita, B. Muller-Pebody, E. Murillo-Zamora, S. Musa, P. Musicha, L. A. Musila, S. Muthupandian, A. J. Nagarajan, P. Naghavi, F. Nainu, T. S. Nair, H. H. R. Najmuldeen, Z. S. Natto, J. Nauman, B. P. Nayak, G. T. Nchanji, P. Ndishimye, I. Negoi, R. I. Negoi, S. A. Nejadghaderi, Q. P. Nguyen, E. A. Noman, D. C. Nwakanma, S. O'Brien, T. J. Ochoa, I. A. Odetokun, O. A. Ogundijo, T. R. Ojo-Akosile, S. R. Okeke, O. C. Okonji, A. T. Olagunju, A. Olivas-Martinez, A. A. Olorukooba, P. Olwoch, K. I. Onyedibe, E. Ortiz-Brizuela, O. Osuolale, P. Ounchanum, O. T. Oyeyemi, M. P. P A, J. L. Paredes, R. R. Parikh, J. Patel, S. Patil, S. Pawar, A. Y. Peleg, P. Peprah, J. Perdigão, C. Perrone, I.-R. Petcu, K. Phommasone, Z. Z. Piracha, D. Poddighe, A. J. Pollard, R. Poluru, A. Ponce-De-Leon, J. Puvvula, F. N. Qamar, N. H. Qasim, C. D. Rafai, P. Raghav, L. Rahbarnia, F. Rahim, V. Rahimi-Movaghar, M. Rahman, M. A. Rahman, H. Ramadan, S. K. Ramasamy, P. S. Ramesh, P. W. Ramteke, R. K. Rana, U. Rani, M.-M. Rashidi, D. Rathish, S. Rattanavong, S. Rawaf, E. M. M. Redwan, L. F. Reyes, T. Roberts, J. V. Robotham, V. D. Rosenthal, A. G. Ross, N. Roy, K. E. Rudd, C. J. Sabet, B. A. Saddik, M. R. Saeb, U. Saeed, S. Saeedi Moghaddam, W. Saengchan, M. Safaei, A. Saghazadeh, N. Saheb Sharif-Askari, A. Sahebkar, S. S. Sahoo, M. Sahu, M. Saki, N. Salam, Z. Saleem, M. A. Saleh, Y. L. Samodra, A. M. Samy, A. Saravanan, M. Satpathy, A. E. Schumacher, M. Sedighi, S. Seekaew, M. Shafie, P. A. Shah, S. Shahid, M. J. Shahwan, S. Shakoor, N. Shalev, M. A. Shamim, M. A. Shamshirgaran, A. Shamsi, A. Sharifan, R. P. Shastry, M. Shetty, A. Shittu, S. Shrestha, E. E. Siddig, T. Sideroglou, J. Sifuentes-Osornio, L. M. L. R. Silva, E. A. F. Simões, A. J. H. Simpson, A. Singh, S. Singh, R. Sinto, S. S. M. Soliman, S. Soraneh, N. Stoesser, T. Z. Stoeva, C. K. Swain, L. Szarpak, S. S. T Y, S. Tabatabai, C. Tabche, Z. M.-A. Taha, K.-K. Tan, N. Tasak, N. Y. Tat, A. Thaiprakong, P. Thangaraju, C. C. Tigoi, K. Tiwari, M. R. Tovani-Palone, T. H. Tran, M. Tumurkhuu, P. Turner, A. J. Udoakang, A. Udoh, N. Ullah, S. Ullah, A. G. Vaithinathan, M. Valenti, T. Vos, H. T. L. Vu, Y. Waheed, A. S. Walker, J. L. Walson, T. Wangrangsimakul, K. G. Weerakoon, H. F. L. Wertheim, P. C. M. Williams, A. A. Wolde, T. M. Wozniak, F. Wu, Z. Wu, M. K. K. Yadav, S. Yaghoubi, Z. S. Yahaya, A. Yarahmadi, S. Yezli, Y. E. Yismaw, D.

K. Yon, C.-W. Yuan, H. Yusuf, F. Zakham, G. Zamagni, H. Zhang, Z.-J. Zhang, M. Zielińska, A. Zumla, S. e. H. H. Zyoud, S. H. Zyoud, S. I. Hay, A. Stergachis, B. Sartorius, B. S. Cooper, C. Dolecek and C. J. L. Murray, Global burden of bacterial antimicrobial resistance 1990–2021: a systematic analysis with forecasts to 2050, *The Lancet*, 2024, **404**, 1199–1226.

6. M. A. Salam, M. Y. Al-Amin, M. T. Salam, J. S. Pawar, N. Akhter, A. A. Rabaan and M. A. A. Alqumber, Antimicrobial Resistance: A Growing Serious Threat for Global Public Health.*Journal*, 2023, **11**.
7. I. Roca, M. Akova, F. Baquero, J. Carlet, M. Cavaleri, S. Coenen, J. Cohen, D. Findlay, I. Gyssens, O. E. Heure, G. Kahlmeter, H. Kruse, R. Laxminarayan, E. Liébana, L. López-Cerero, A. MacGowan, M. Martins, J. Rodríguez-Baño, J. M. Rolain, C. Segovia, B. Sigauque, E. Tacconelli, E. Wellington and J. Vila, The global threat of antimicrobial resistance: science for intervention, *New Microbes and New Infections*, 2015, **6**, 22–29.
8. C. S. Ho, C. T. H. Wong, T. T. Aung, R. Lakshminarayanan, J. S. Mehta, S. Rauz, A. McNally, B. Kintses, S. J. Peacock, C. de la Fuente-Nunez, R. E. W. Hancock and D. S. J. Ting, Antimicrobial resistance: a concise update, *The Lancet Microbe*, 2025, **6**.
9. F. Akram, M. Imtiaz and I. u. Haq, Emergent crisis of antibiotic resistance: A silent pandemic threat to 21st century, *Microbial Pathogenesis*, 2023, **174**, 105923.
10. G. Karam, J. Chastre, M. H. Wilcox and J.-L. Vincent, Antibiotic strategies in the era of multidrug resistance, *Critical Care*, 2016, **20**, 136.
11. C. A. Lozupone, J. I. Stombaugh, J. I. Gordon, J. K. Jansson and R. Knight, Diversity, stability and resilience of the human gut microbiota, *Nature*, 2012, **489**, 220–230.
12. A. Langdon, N. Crook and G. Dantas, The effects of antibiotics on the microbiome throughout development and alternative approaches for therapeutic modulation, *Genome Medicine*, 2016, **8**, 39.
13. K. Raymann, Z. Shaffer and N. A. Moran, Antibiotic exposure perturbs the gut microbiota and elevates mortality in honeybees, *PLOS Biology*, 2017, **15**, e2001861.
14. C. Jernberg, S. Löfmark, C. Edlund and J. K. Jansson, Long-term ecological impacts of antibiotic administration on the human intestinal microbiota, *The ISME Journal*, 2007, **1**, 56–66.
15. C. Ubeda and E. G. Pamer, Antibiotics, microbiota, and immune defense, *Trends in Immunology*, 2012, **33**, 459–466.
16. V. Stevens, G. Dumyati, L. S. Fine, S. G. Fisher and E. van Wijngaarden, Cumulative Antibiotic Exposures Over Time and the Risk of Clostridium difficile Infection, *Clin. Infect. Dis.*, 2011, **53**, 42–48.
17. C. A. Demeke, G. M. Adinew, T. B. Abebe, A. T. Gelaye, S. G. H. Gemeda and D. K. Yimenu, Comparative analysis of the effectiveness of narrow-spectrum versus broad-spectrum antibiotics for the treatment of childhood pneumonia, *SAGE Open Medicine*, 2021, **9**, 20503121211044379.
18. R. A. Alm and S. D. Lahiri, Narrow-Spectrum Antibacterial Agents—Benefits and Challenges, *Antibiotics*, 2020, **9**, 418.
19. J. S. Gerber, R. K. Ross, M. Bryan, A. R. Localio, J. E. Szymczak, R. Wasserman, D. Barkman, F. Odeniyi, K. Conaboy, L. Bell, T. E. Zaoutis and A. G. Fiks, Association of Broad- vs Narrow-Spectrum Antibiotics With Treatment Failure, Adverse Events, and Quality of Life in Children With Acute Respiratory Tract Infections, *JAMA*, 2017, **318**, 2325–2336.

20. J. L. Markham, A. Burns, M. Hall, M. J. Molloy, J. R. Stephens, E. McCoy, I. T. Ugalde, M. J. Steiner, J. M. Cotter, S. A. House, M. E. Collins, A. G. Yu, M. J. Tchou and S. S. Shah, Outcomes associated with initial narrow-spectrum versus broad-spectrum antibiotics in children hospitalized with urinary tract infections, *Journal of Hospital Medicine*, 2024, **19**, 777–786.
21. U. Theuretzbacher, F. Van Bambeke, R. Cantón, C. G. Giske, J. W. Mouton, R. L. Nation, M. Paul, J. D. Turnidge and G. Kahlmeter, Reviving old antibiotics, *J. Antimicrob. Chemother.*, 2015, **70**, 2177–2181.
22. R. J. Melander, D. V. Zurawski and C. Melander, Narrow-spectrum antibacterial agents, *MedChemComm*, 2018, **9**, 12–21.
23. T. Zeiser Elise, A. Becka Scott, D. Barnes Melissa, A. Taracila Magdalena, J. LiPuma John and M. Papp-Wallace Krisztina, Resurrecting Old β-Lactams: Potent Inhibitory Activity of Temocillin against Multidrug-Resistant Burkholderia Species Isolates from the United States, *Antimicrob. Agents Chemother.*, 2019, **63**, 10.1128/aac.02315–02318.
24. K. Jules and H. C. Neu, Antibacterial activity and beta-lactamase stability of temocillin, *Antimicrobial Agents and Chemotherapy*, 1982, **22**, 453–460.
25. L. Verbist, In vitro activity of temocillin (BRL 17421), a novel beta-lactamase-stable penicillin, *Antimicrob. Agents Chemother.*, 1982, **22**, 157–161.
26. K. L. Heard, K. Killington, N. Mughal, L. S. P. Moore and S. Hughes, Clinical outcomes of temocillin use for invasive Enterobacterales infections: a single-centre retrospective analysis, *JAC-Antimicrob. Resist.*, 2021, **3**, dlab005.
27. H. Rodriguez-Villalobos, V. Malaviolle, J. Frankard, R. d. Mendonça, C. Nonhoff and M. J. Struelens, In vitro activity of temocillin against extended spectrum β-lactamase-producing Escherichia coli, *J. Antimicrob. Chemother.*, 2006, **57**, 771–774.
28. Y. Glupczynski, T. D. Huang, C. Berhin, G. Claeys, M. Delmée, L. Ide, G. Ieven, D. Pierard, H. Rodriguez-Villalobos, M. Struelens and J. Vaneldere, In vitro activity of temocillin against prevalent extended-spectrum beta-lactamases producing Enterobacteriaceae from Belgian intensive care units, *European Journal of Clinical Microbiology & Infectious Diseases*, 2007, **26**, 777–783.
29. D. M. Livermore, R. Hope, E. J. Fagan, M. Warner, N. Woodford and N. Potz, Activity of temocillin against prevalent ESBL- and AmpC-producing Enterobacteriaceae from south-east England, *J. Antimicrob. Chemother.*, 2006, **57**, 1012–1014.
30. T. Lupia, I. De Benedetto, G. Stroffolini, S. Di Bella, S. Mornese Pinna, V. Zerbato, B. Rizzello, R. Bosio, N. Shbaklo, S. Corcione and F. G. De Rosa, Temocillin: Applications in Antimicrobial Stewardship as a Potential Carbapenem-Sparing Antibiotic, *Antibiotics*, 2022, **11**, 493.
31. L. Cosimi, V. Zerbato, N. Grasselli Kmet, A. Oliva, F. Cogliati Dezza, N. Geremia, D. Cattaneo, K. Nadrah, M. Pirs, R. Saletinger, A. Nunnari, F. Mearelli, F. G. Di Girolamo, G. Avena, R. Russo, C. Fabiani, S. Venturini, L. Principe, G. M. Nicolò and S. Di Bella, Temocillin: A Narrative Review of Its Clinical Reappraisal.*Journal*, 2025, **14**.
32. M. Sacco, D., K. G. Kroeck, M. T. Kemp, X. Zhang, L. D. Andrews and Y. Chen, Influence of the α-Methoxy Group on the Reaction of Temocillin with Pseudomonas aeruginosa PBP3 and CTX-M-14 β-Lactamase, *Antimicrob. Agents Chemother.*, 2019, **64**, 10.1128/aac.01473–01419.

33. D. J. Tipper and J. L. Strominger, Mechanism of action of penicillins: a proposal based on their structural similarity to acyl-D-alanyl-D-alanine, *Proc. Natl. Acad. Sci.*, 1965, **54**, 1133–1141.
34. P. M. Blumberg and J. L. Strominger, Interaction of penicillin with the bacterial cell: penicillin-binding proteins and penicillin-sensitive enzymes, *Bacteriol. Rev.*, 1974, **38**, 291–335.
35. R. Labia, P. Baron, J. M. Masson, G. Hill and M. Cole, Affinity of temocillin for Escherichia coli K-12 penicillin-binding proteins, *Antimicrob. Agents Chemother.*, 1984, **26**, 335–338.
36. D. A. Enoch, M. E. Murphy, T. Gouliouris, R. Santos and C. Micallef, Temocillin use as a carbapenem-sparing option in a UK teaching hospital for treating serious Gram-negative bacterial infections, *JAC-Antimicrob. Resist.*, 2022, **4**, dlac111.
37. D. M. Livermore and P. M. Tulkens, Temocillin revived, *J. Antimicrob. Chemother.*, 2009, **63**, 243–245.
38. *US Pat.,* US 5750684 A, 1998.
39. *GB Pat.,* GB 1339007 A, 1973.
40. P. H. Milner and A. V. Stachulski, Further synthetic studies in penicillin C(6)-substitution including the versatile 6α-succinimidooxy leaving group, *J. Chem. Soc., Perkin Trans. 1*, 1991, 2343–2352.
41. G. Burton, M. J. Basker, D. J. Best, F. P. Harrington and A. W. Taylor, Preparation and structure-activity relationships of some 6α-substituted penicillins, *J. Antibiot.*, 1985, **38**, 721–739.
42. P. H. Bentley, J. P. Clayton, M. O. Boles and R. J. Girven, Transformations using benzyl 6-isocyanopenicillanate, *J. Chem. Soc., Perkin Trans. 1*, 1979, 2455–2467.
43. T. M. Uddin, A. J. Chakraborty, A. Khusro, B. M. R. M. Zidan, S. Mitra, T. B. Emran, K. Dhama, M. K. H. Ripon, M. Gajdács, M. U. K. Sahibzada, M. J. Hossain and N. Koirala, Antibiotic resistance in microbes: History, mechanisms, therapeutic strategies and future prospects, *J. Infect. Public Health*, 2021, **14**, 1750–1766.
44. A. Howard, D. M. Hughes, P. L. Green, A. Velluva, A. Gerada, S. Maskell, I. E. Buchan and W. Hope, Personalised antimicrobial susceptibility testing with clinical prediction modelling informs appropriate antibiotic use, *Nat. Commun.*, 2024, **15**, 9924.
45. A. Matagne, J. Lamotte-Brasseur, G. Dive, J. R. Knox and J. M. Frère, Interactions between active-site-serine β-lactamases and compounds bearing a methoxy side chain on the α-face of the β-lactam ring: kinetic and molecular modelling studies, *Biochem. J.*, 1993, **293**, 607–611.
46. H. G. Smith, S. Basak, V. Aniebok, M. J. Beech, F. M. Alshref, M. D. Allen, A. J. M. Farley and C. J. Schofield, Structural basis of Pseudomonas aeruginosa penicillin binding protein 3 inhibition by the siderophore-antibiotic cefiderocol, *Chemical Science*, 2024, **15**, 16928–16937.
47. S. Han, N. Caspers, R. P. Zaniewski, B. M. Lacey, A. P. Tomaras, X. Feng, K. F. Geoghegan and V. Shanmugasundaram, Distinctive Attributes of β-Lactam Target Proteins in Acinetobacter baumannii Relevant to Development of New Antibiotics, *J. Am. Chem. Soc.*, 2011, **133**, 20536–20545.
48. J. F. Simon, A. Bouillez, J.-M. Frère, A. Luxen and A. Zervosen, Synthesis of an enantiopure thioester as key substrate for screening the sensitivity of penicillin binding proteins to inhibitors, *ARKIVOC*, 2016, **2016**, 22–31.

49. B. Geibel, J. Dowell, D. Dickerson and T. Henkel, 1401. A Randomized, Double-Blind, Placebo-Controlled Study of the Safety and Pharmacokinetics of Single and Repeat Doses of VNRX-5133 in Healthy Subjects, *Open Forum Infect. Dis.*, 2018, **5**, S431–S431.
50. M. Benz, T. M. Klapötke, J. Stierstorfer and M. Voggenreiter, Synthesis and Characterization of Binary, Highly Endothermic, and Extremely Sensitive 2,2′-Azobis(5-azidotetrazole), *J. Am. Chem. Soc.*, 2022, **144**, 6143–6147.
51. P. Feyen and W. Schröck, Stereospezifische, einstufige Einführung einer Methoxygruppe an C6 von Penicillinen und C7 von Cephalosporinen, *Angewandte Chemie*, 1981, **93**, 814–815.

5.3 Statement of Authorship

Title of Paper	Piperacillin is a promising scaffold for the development of C6-methoxypenicillins.
Publication Status	□Published □ Accepted for Publication □Submitted for Publication ☒Unpublished and unsubmitted work written in a manuscript style
Publication Details	**Muntean, D.-G.;** Smith, H.G.; Calvopiña, K.; Brewitz, L.; Schofield, C.J.: **Piperacillin is a promising scaffold for the development of C6-methoxypenicillins.**

Student Confirmation

Student Name:	Dorian-Gabriel Muntean		
Contribution to the Paper	D.-G.M conducted all the organic synthesis of C6-methoxypenicillins. D.-G.M. also conceptualised and prepared the first draft of the manuscript. H.G.S. obtained the inhibition data for PBPs. K.C. conducted the MIC assays. L.B. provided supervision of the synthetic work and assisted with manuscript reviewing/editing. C.J.S. is the principal investigator/supervisor of the research described in the manuscript, contributed extensively to project/data conceptualization and visualization, and manuscript reviewing/editing.		
Signature 		Date	09/10/2025

Supervisor Confirmation

By signing the Statement of Authorship, you are certifying that the candidate made a substantial contribution to the publication, and that the description described above is accurate.

Supervisor name and title: Prof. Christopher J. Schofield		
Supervisor comments:		
Signature 	Date	09/10/2025

Chapter 6. Synthesis of C2-carboxypenams and their mechanism of action

6.1 Chapter overview

Chapter 6 describes the synthesis of C2-carboxypenams, a noncanonical class of β-lactam antibiotics. The scarcity of peer-reviewed synthetic routes to C2-carboxypenams has hindered their development, despite reports detailing potent antimicrobial activity against Gram-negative pathogens and reduced susceptibility to β-lactamase-mediated hydrolysis. The work presented in this Chapter offers an optimised, scalable route to the C2-carboxypenam scaffold that enables late-stage diversification. Preliminary biochemical investigations showed that C2-carboxypenam sulfone acids react with penicillin-binding proteins (PBP) in an unexpected manner, with crystallographic and mass-spectrometric (MS) evidence demonstrating that, upon binding with the active-site serine residue, the β-lactam ring opening is accompanied by thiazolidine fragmentation and SO_2 extrusion. Lastly, C2-carboxypenam thioether acids were found to inhibit β-lactamases, displaying potent activity particularly against OXA-10. Taken together, these results highlight the largely untapped potential of C2-carboxypenams, which, in principle, can be developed into both antibiotics and β-lactamase inhibitors.

Manuscript V

At the time of writing this thesis, Manuscript V is in preparation for publication. A Statement of Authorship is appended at the end of the chapter. The synthetic experimental details and spectra of the compounds prepared can be found in the **Appendix**.

Muntean, **D.-G.**; Smith, H.G.; Wilson, L.; Calvopiña, K.; Brewitz, L.; Schofield, C.J.: **Reaction of C2-carboxypenams with penicillin-binding proteins proceeds via unusual SO_2 release mechanism.**

6.2 Manuscript V: Reaction of C2-carboxypenams with penicillin-binding proteins proceeds via unusual SO_2 release mechanism.

6.2.1 Abstract

β-Lactam antibiotics are the most widely used class of antibacterials, their defining characteristic being the strained β-lactam ring which reacts with the active-site serine residue of penicillin-binding proteins (PBPs), thereby disrupting cell wall biosynthesis. However, their efficient clinical use is threatened by the rapid spread of antibiotic-resistant bacteria that produce β-lactamases, enzymes which catalyse β-lactam ring hydrolysis, thereby rendering β-lactam antibiotics inactive. C2-Carboxypenams are reported potent antibiotics that display improved stability toward β-lactamases, but despite their promising antibacterial properties, their broader exploration has likely been limited by the scarcity of reported synthetic routes. Here, we report an improved, scalable synthesis of C2-carboxypenams in six steps and 12% overall yield from commercially sourced penicillin G. Notably, preliminary biochemical investigations indicate that C2-carboxypenam sulfones react with PBPs via an unusual mechanism involving SO_2 extrusion. These findings suggest that C2-carboxypenam sulfones can be developed as dual-action antibiotics, exerting antimicrobial activity via both PBP inhibition and *in situ* SO_2 generation.

Key words: β-Lactam antibiotics; C2-carboxypenams; penicillin-binding proteins; β-lactamases; SO_2 extrusion; mechanism-based inhibition.

6.2.2 Introduction

β-Lactams are the most clinically impactful class of antibiotics,[1] their therapeutic efficacy stemming from the ability to target penicillin-binding proteins (PBPs),[2] serine transpeptidases that catalyse peptidoglycan cross-linking.[3] By mimicking the D-Ala-D-Ala terminus of the PBP natural substrates,[2, 4, 5] β-lactams acylate the catalytic nucleophilic serine residue and disrupt bacterial cell wall biosynthesis, thus causing cell lysis and death.[6] However, the emergence of multidrug resistant bacteria compromises the successful clinical use of β-lactams antibiotics.[7, 8] A major bacterial resistance mechanism is represented by a group of hydrolytic enzymes known as β-lactamases, which include serine-β-lactamases (SBLs) and metallo-β-lactamases (MBLs).[1, 9] β-Lactamases catalyse β-lactam ring hydrolysis, thus rendering β-lactams antibiotics inactive against PBPs.[1] To mitigate this, β-lactamase inhibitors can be co-administered with β-lactam antibiotics, whereby the β-lactamase inhibitors inhibit β-lactamase activity.[10] This strategy has been clinically validated against SBL-producing pathogens (*e.g.*, ampicillin/sulbactam), but it should be noted that approved β-lactam/β-lactamase inhibitor combinations remain largely ineffective against MBL-producing strains, and may offer in the future only limited coverage against SBL producers should pathogens acquire new resistance mechanisms.[10-13]

It is of interest to develop β-lactam antibiotics that not only potently inhibit PBPs but also display high intrinsic stability to β-lactamase hydrolysis. However, achieving this effect is challenging, in part because evidence indicates that SBLs evolved from PBPs, which accounts for their structural and mechanistic similarities.[14, 15] Furthermore, structure-activity relationship (SAR) studies on penicillin derivatives have shown that structural changes that would improve β-lactamase stability can also lead to a decrease in PBP inhibition, as seen with *e.g.*, temocillin,[16] where its C6-methoxy group interferes with the stability of acyl-enzyme complexes with PBPs. SAR studies on the penam

core also confirmed that the C3-carboxylate plays a crucial role in binding to PBPs, as functional group modifications of this moiety generally led to a decrease in antimicrobial properties.[17-20] Nonetheless, if the loss in PBP binding affinity following C3-carboxylate modifications could be prevented, it can be envisioned, at least in principle, that this strategy would decrease susceptibility to β-lactamase hydrolysis, as β-lactamases also engage the penicillin C3-carboxylate during substrate binding.[21-23]

C2-Carboxypenams are an investigational class of β-lactam antibiotics, wherein the C3-α-carboxylate group of penicillin antibiotics is shifted to the C2 position of the penam scaffold. C2-carboxypenam **1** is a reported potent antibiotic against Gram-negative bacteria such as *Pseudomonas aeruginosa*; remarkably, **1** exhibited higher binding affinities to PBP3 than "classical" β-lactam antibiotics like ceftazidime or aztreonam, while displaying exceptional hydrolytic stability to both SBLs and MBLs.[24-26] Given their good inhibitory activity against *P. aeruginosa*, C2-carboxypenams were further developed into compounds such as **2**,[27] which include a siderophoric sidechain, in a manner reminiscent of cefiderocol,[28] in which the catechol moiety chelates Fe(III) and hijacks iron transporters to enter the bacterial periplasmic space.

C2-Carboxypenams show therapeutic potential, especially as antipseudomonal agents, but the structural complexity of derivatives such as **1** and **2** poses a substantial synthetic challenge. Peer-reviewed synthetic procedures for C2-carboxypenam antibiotics are scarce, most disclosures residing in the patent literature and describing relatively lengthy routes from advanced intermediates that are not readily available.[27, 29] C2-Carboxypenam esters of general formula **3** may serve as versatile intermediates to enable C2 functionalisation. To the best of our knowledge, only two synthetic procedures for **3** have been reported, both suffering from low overall yields and/or relying on unstable intermediates obtained using relatively hazardous reaction conditions.[30,

[31] To address this gap, here we report an improved, scalable six-step route to C2-carboxypenam esters of type **3** (12% overall yield).

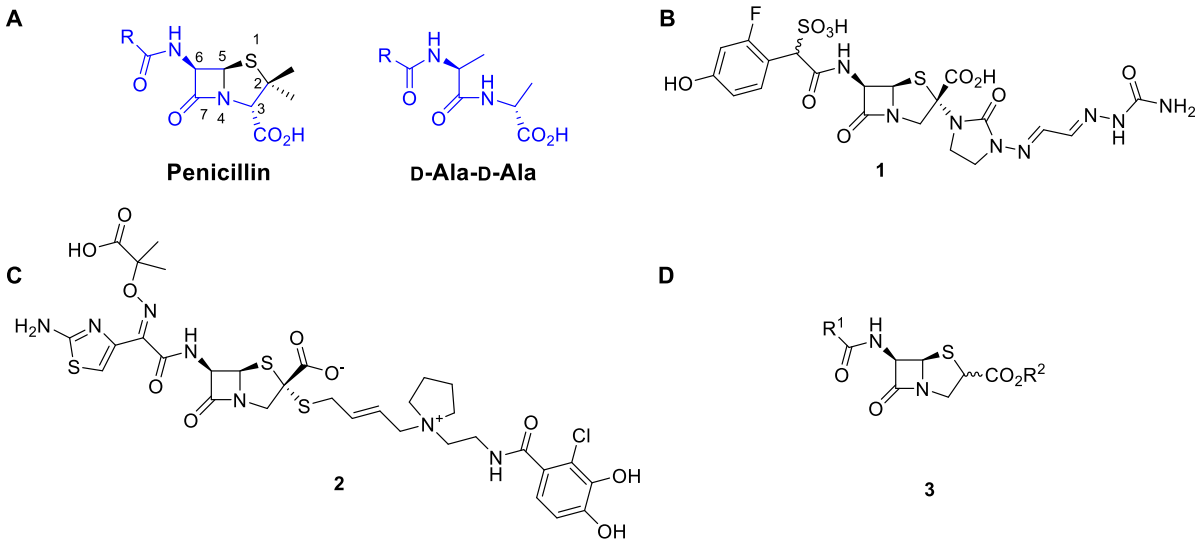

Figure 1: A. Structural similarities between the penicillin scaffold and the PBP natural substrate, D-Ala-D-Ala.[4] **B**. C2-Carboxypenam **1**, an antibiotic effective against Gram-negative bacteria.[25] **C**. **2**, a C2-carboxypenam further connected at C2 via a linker to a catechol siderophore.[27] **D**. **3**, the synthetic target of the present study.

6.2.3 Results

Synthesis of C2-carboxypenams

As demonstrated by previous syntheses of bicyclic β-lactams,[32, 33] an expedient route to **3** could involve the late-stage construction of the thiazolidine ring, as the β-lactam core can be derived from commercially sourced penicillins.[34] Retrosynthetic analysis suggests that a route employing a C2-C3 disconnection of **3** to **4**, subsequently followed by thioether and hemiaminal disconnections, would give the thiazoline azetidinone **6** (**Figure 2**), a commonly used intermediate in the semisynthesis of β-lactam derivatives.[34-38]

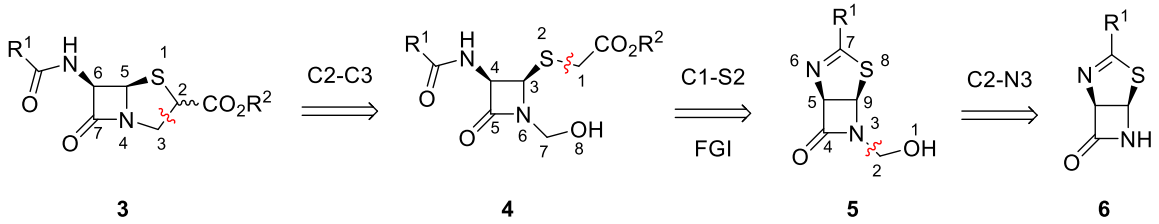

Figure 2: Retrosynthetic analysis of C2-carboxypenam **3** via a key C2-C3 disconnection.

Methylation of commercially sourced **penicillin G** potassium salt (**Figure 3**), followed by oxidation using *meta*-chloroperbenzoic acid (mCPBA) yielded penicillin G (*S*)-sulfoxide methyl ester **7**,[39] which underwent reductive rearrangement to **8** in the presence of $P(OMe)_3$ under reflux (**Supporting Figure S1**).[35] Base-catalysed isomerization of **8** yielded enamine **9**, which was converted to β-lactam **10** following oxidative cleavage of the α,β-unsaturated *N*-substituent in the presence of aqueous $KMnO_4$.[35, 36] An improved route to **9**, which required fewer steps and no column chromatography purifications, was subsequently developed. This route employed a one-pot conversion of **11** to **12**,[40] which was subsequently methylated to give the desired product **9** (46% over two steps).

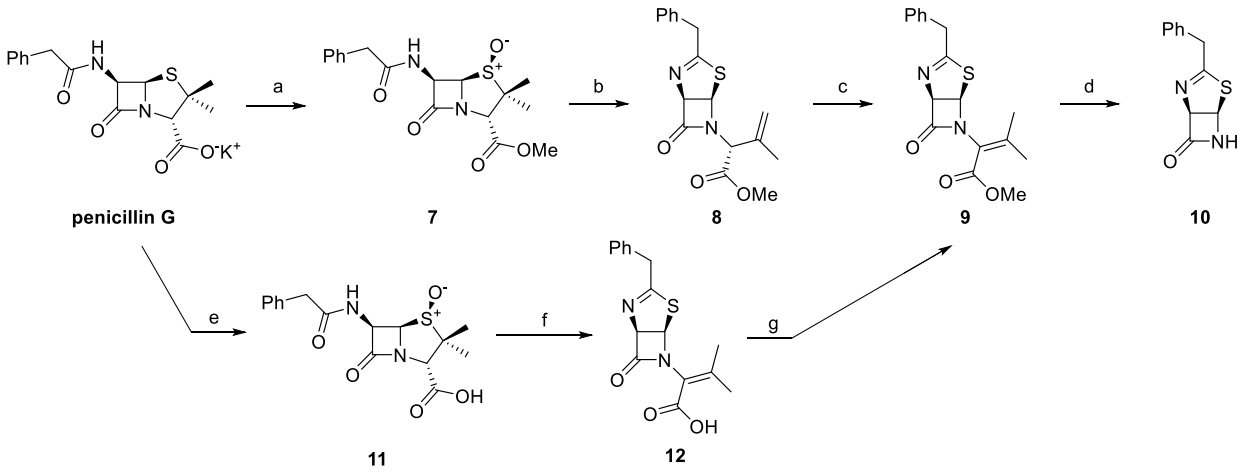

Figure 3: Reagents and conditions: a) i) MeI (1.1 equiv.), *N*,*N*-dimethylformamide, room temperature, 17 h, 94%; ii) mCPBA (1.05 equiv.), CH_2Cl_2, room temperature, 2.5 h, 84%; b) $P(OMe)_3$ (2.2 equiv.), $MgSO_4$, toluene, reflux, 24 h, 77%; c) Et_3N (0.5 equiv.), CH_2Cl_2, room temperature, 3 h, 91%; d) $KMnO_4$ (2.1 equiv.), EtOH, H_2O, 0 °C, 105 min, 54%; e) $NaIO_4$ (1.07 equiv.), H_2O, room temperature, 2 h, 93%; f) 1,3-bis(trimethylsilyl)urea (1.7 equiv.), $(BuO)_3P$

(1.1 equiv.), BuOAc, reflux, 90 min, then Et_3N (1.1 equiv.), 50%; g) MeI (1.1 equiv.), Cs_2CO_3 (1.1 equiv.), *N*,*N*-dimethylformamide, room temperature, 24 h, 78%.

Treatment of β-lactam **10** with paraformaldehyde yielded hemiaminal **13**, which upon acidic hydrolysis of its thiazoline ring afforded thiol **14**. Under basic conditions, **14** was converted to the corresponding thiolate (**14'**; **Supporting Figure S2**), which reacted with benzyl 2-bromoacetate, benzyl 2-bromopropionate, and dibenzyl 2-bromomalonate, to give thioethers **15a**, **15b**, and **15c** in 99%, 58%, and 4% yield, respectively. The decrease in yield from **15a** to **15b** may reflect the lower reactivity of secondary carbon electrophiles, while analysis of the **14→15c** transformation revealed the surprising formation of the byproduct dibenzyl malonate (**16**; **Supporting Figure S2**); this observation indicated that, rather than undergoing S_N2 substitution, the thiolate followed an alternative pathway involving debromination of dibenzyl 2-bromomalonate. The yield of **15c** was improved by employing a bulkier leaving group than bromide that would not permit this undesired reaction pathway; pleasingly, reaction of **14** with dibenzyl 2-(tosyloxy)malonate (**17**) produced only **15c** in 66% yield. Following the conversion of hemiaminals **15a-c** to the corresponding tosylates **18a-c**, *in situ* cyclization was attempted in the presence of 1,8-diazabicyclo[5.4.0]undec-7-ene (DBU); however, only **18c** underwent successful cyclisation under the tested conditions (25%), resulting in bicyclic β-lactam **19**.

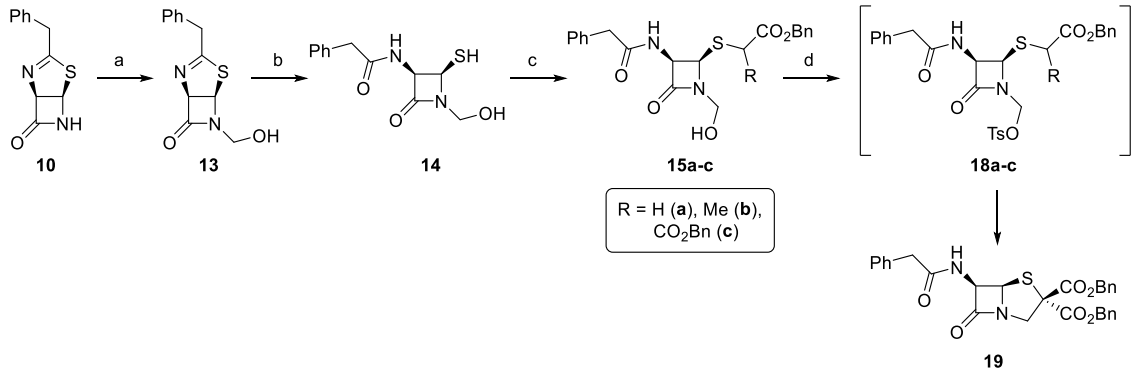

Figure 4: Reagents and conditions: a) CH_2O (1.5 equiv.), K_2CO_3 (0.05 equiv.), tetrahydrofuran, H_2O, room temperature, 6 h, 77%; b) aqueous HCl solution (1 M; 1.3 equiv.), MeOH, 0 °C, 30 min, 66%; c) $RCH(Br)CO_2Bn$ or

17 (1 equiv.), Et_3N (1 equiv.), *N*,*N*-dimethylformamide, 0 °C, 30 min; d) 4-toluenesulfonyl chloride (1 equiv.), 2,6-lutidine (1 equiv.), 0 °C, 90 min, then DBU (1 equiv.), -20 °C, 30 min, 25%. Ts: $–SO_2C_6H_4(4\text{-}Me)$.

As **19** does not allow further facile functionalisation at C2, an alternative synthetic route towards C2-carboxypenams was devised (**Figure 5**). Disconnection of the S1-C2 bond, followed by FGI (*i.e.*, hydrolysis of the thiazoline ring) gives intermediate **21**, which may be obtained as the aza-Michael addition product of **6** and **22**.

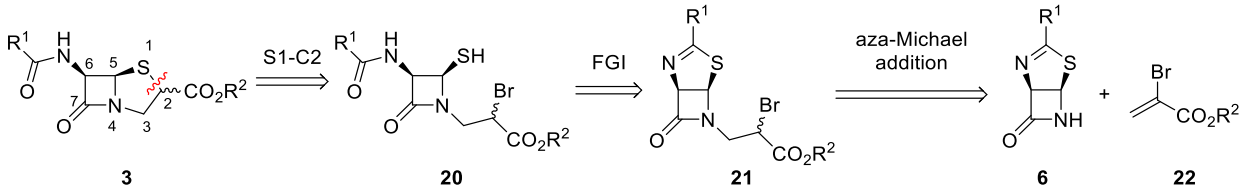

Figure 5: Alternative retrosynthesis of penam **3**.

The aza-Michael reaction of β-lactam **10** with benzyl 2-bromoacrylate (**22a**; R^2 = Bn) or *para*-nitrobenzyl bromide 2-bromoacrylate (**22b**; $R^2 = CH_2C_6H_4(4\text{-}NO_2)$) proceeded under mildly basic conditions to give diastereomeric mixture **23a/23a'** (**Figure 6**). Subsequent acidic hydrolysis of the thiazoline ring revealed thiols **24a/24a'**, which under basic conditions readily underwent cyclisation to C2-carboxypenam esters **25a/25a'** (90% over 2 steps; d.r. ~ 1:1).

Having achieved the synthesis of C2-carboxypenam esters **25a/25a'**, it was of interest to carry out preliminary investigations into the antimicrobial properties of C2-carboxypenam thioethers **26/26'** and C2-carboxypenam sulfones **28/28'**. Thus, hydrogenation of benzyl ester **25a/25a'** was attempted using Pd/C, but no product was observed, likely due to catalyst poisoning by the penam thioether sulfur. To circumvent this problem, the more reactive *p*-nitrobenzyl C2-carboxypenam esters **25b/25b'** (82%; d.r. ~ 1.25:1) were synthesized from **10** in an analogous manner to **25a/25a'**. Subsequent hydrogenation of **25b/25b'** yielded the C2-carboxypenam acids **26/26'** (17%). C2-Carboxypenam sulfide esters **25b/25b'** were also oxidized using mCPBA to the corresponding

sulfones **27/27'** (75%), which following deprotection using H_2 and Pd/C yielded the C2-carboxypenam sulfone acids **28/28'** (25%).

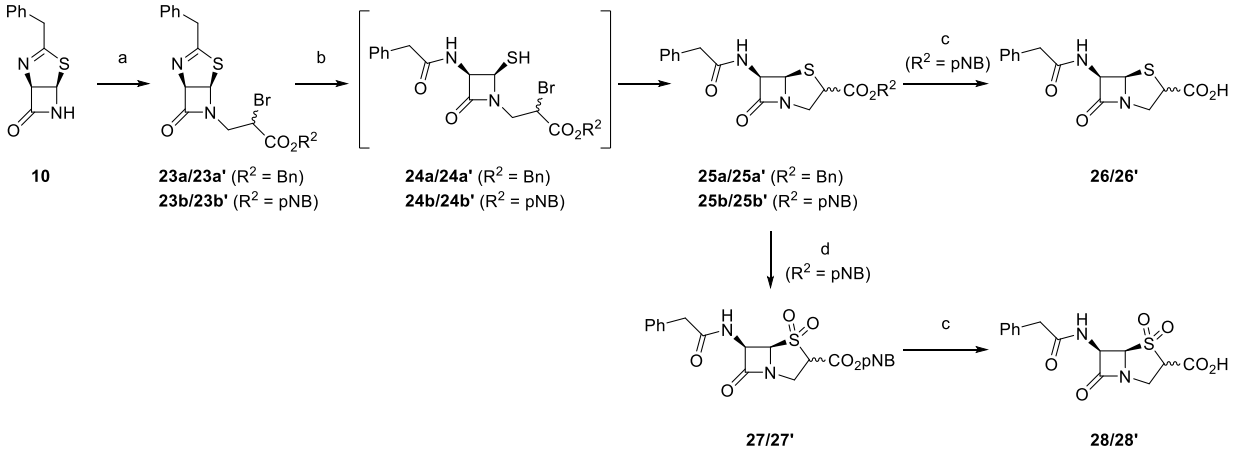

Figure 6: Reagents and conditions: a) CH_2=C(Br)CO_2R^2 (2 equiv.), K_2CO_3 (1 equiv.), room temperature, 48 h, 54-72%; b) i) aqueous HCl solution (1 M; 1.3 equiv.), acetone, 0 °C, 1 h; ii) K_2CO_3 (1 equiv.), tetrahydrofuran, room temperature, 5-15 h (82-90% over 2 steps); c) $KMnO_4$ (2.2 equiv.), AcOH, H_2O, tetrahydrofuran, 0 °C, 2.5 h, 75%; v) H_2, Pd/C (10 wt. %; 0.4 equiv.), tetrahydrofuran, room temperature, 3 h, 17-25%.

C2-carboxypenams can inhibit isolated PBPs

C2-Carboxypenam derivatives were evaluated for their ability to inhibit isolated recombinant *E. coli* PBP4-6 using reported fluorescence polarisation (FP)-based assays[41] (**Table 1**). At 100 μM concentration, both **26/26′** and **28/28′** displayed levels of PBP5 and PBP6 inhibition (in the range of 90-96%) comparable to penicillin G; at 10 μM inhibitor concentration, however, **26/26′** and **28/28′** displayed reduced potencies, eliciting ~2.5-3-fold lower inhibition than penicillin G. **26/26′** displayed modest levels of PBP4 inhibition at 100 μM inhibitor concentration, while **28/28′** did not inhibit.

Table 1. Inhibition of *E. coli* PBP activity by C2-carboxypenam derivatives.

	% inhibition[(a)]	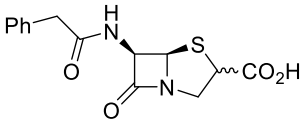 **26/26'**	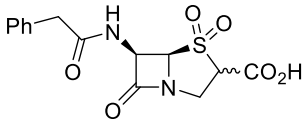 **28/28'**	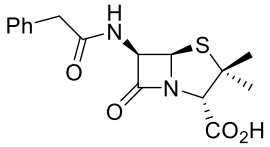 **Penicillin G**
i	*E. coli* PBP4 ([I] = 100 μM)	34.8 ± 2.9 %	< 0 %	98.4 ± 0.1 %
ii	*E. coli* PBP4 ([I] = 10 μM)	< 0 %	< 0 %	96.6 ± 2.9 %
iii	*E. coli* PBP5 ([I] = 100 μM)	90.0 ± 2.9 %	96.8 ± 1.3 %	99.8 ± 0.1 %
iv	*E. coli* PBP5 ([I] = 10 μM)	23.4 ± 4.3 %	28.3 ± 4.0 %	75.2 ± 2.0 %
v	*E. coli* PBP6 ([I] = 100 μM)	90.0 ± 1.9 %	92.0 ± 1.8 %	99.7 ± 0.2 %
vi	*E. coli* PBP6 ([I] = 10 μM)	33.9 ± 2.5 %	35.1 ± 3.3 %	90.3 ± 1.2 %

[(a)] Experimental details can be found in the Methods section.

Minimum inhibitory concentration (MIC) of C2-carboxypenam derivatives were obtained against a panel of Gram-negative (*K. pneumoniae* and *E. coli*) and Gram-positive (*S. aureus*) pathogens (**Table 2**). The results reveal that neither thioether **26/26′** nor sulfoxide **28/28′** displayed measurable inhibition of *K. pneumoniae* strains within the tested concentration range, mirroring penicillin G. Similarly, no activity was observed for the C2-carboxypenams against *E. coli*, while penicillin G showed moderate activity (MIC ~ 32 μg/mL). **26/26′** inhibited some *S. aureus* strains, most notably the NEWMAN strain (MIC ~ 8 μg/mL), with weaker effects on USA300 (MIC ~ 128 μg/mL) and no activity against the methicillin-susceptible strain (MIC > 256 μg/mL); the antimicrobial properties of **26/26′** were weaker than those of penicillin G. By contrast, the sulfones **28/28′** showed no detectable antimicrobial activity across the tested *S. aureus* strains (MIC > 256 μg/mL).

Table 2. Antibacterial activity of C2-carboxypenam derivatives against Gram-negative and Gram-positive species.

	MIC (μg/mL)[(a)]	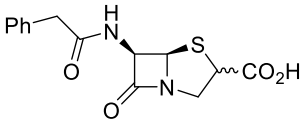 **26/26'**	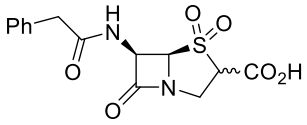 **28/28'**	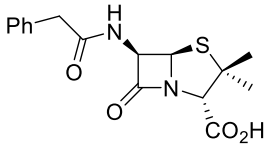 **Penicillin G**
i	*K. pneumoniae* NCTC13443	>256	>256	>256
ii	*K. pneumoniae* NCTC13442	>256	>256	>256
iii	*E. coli* ATCC25922	>256	>256	32
iv	*S. aureus* NEWMAN	8	>256	0.5
v	*S. aureus* USA300	128	>256	0.25
vi	*S. aureus* Methicillin S	>256	>256	32

[(a)] Experimental details can be found in the Methods section.

C2-Carboxypenams can inhibit isolated SBLs

The inhibitory properties of C2-carboxypenam acids against SBLs were investigated using a fluorescence-based assay,[42] with results showing a comparable or improved profile relative to penicillin G (**Table 3**). Notably, thioethers **26/26′** were ~100-fold more potent against OXA-10 (pIC_{50} ~ 6.7), showing superior inhibition than even avibactam. By contrast, **26/26′** and **28/28′** inhibited TEM-116 and OXA-48 with similar potency to penicillin G, but less potently than avibactam, while none of the tested C2-carboxypenam derivatives inhibited AmpC (as also observed with penicillin G).

Table 3. Inhibition of SBL activity by C2-carboxypenam derivatives.

	Compound	pIC_{50}[(a)]			
		TEM-116 (class A)	AmpC (class C)	OXA-10 (class D)	OXA-48 (class D)
i	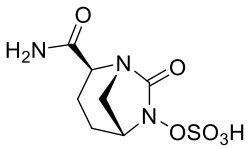 **Avibactam**	8.2 ± 0.1	6.8 ± 0.1	4.9 ± 0.1	6.1 ± 0.1
ii	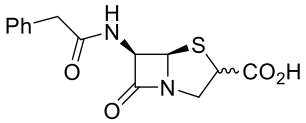 **26/26'**	<4.0	*n.i.*	6.7 ± 0.1	4.9 ± 0.1
iii	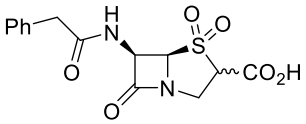 **28/28'**	4.5 ± 0.1	*n.i.*	4.8 ± 0.1	4.3 ± 0.1
iv	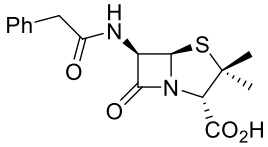 **Penicillin G**	<4.0	*n.i.*	4.6 ± 0.1	4.2 ± 0.1

[(a)] Experimental details can be found in the Methods Section. *n.i.* – no inhibition. Representative dose-response curves are shown in **Supporting Figure S3**.

Crystallographic and MS studies

A crystal structure of *E.coli* PBP5 in complex with the C2-carboxypenam sulfones **28/28'** (**Figure 7A**) was obtained via co-crystallisation ($P2_1$ space group, 2.03 Å resolution). The structure was solved via molecular replacement using Phaser,[43] wherein a previous structure of PBP5 (PDB ID: 5J8X) was employed as the starting model.[44] Multiple rounds of refinement were undertaken using Phenix with manual model building undertaken using Coot (**Supporting Table S1**).[45, 46]

Analysis of the electron density maps reveals that the active site nucleophilic serine residue of PBP5 (*i.e.*, Ser44) covalently reacted with the β-lactam ring of **28/28'**, which triggered fragmentation of the thiazolidine ring and extrusion of SO_2 (**Figure 7B**). Importantly, this

fragmentation pattern is also observed with **28**/**28'** in solution, as protein-observed MS studies revealed formation of the **28**:**PBP5** adduct (+ 273 Da). **26/26'** is also observed to promote a mass shift with PBP5 (+ 305 Da), consistent with the formation of an acyl-enzyme complex.

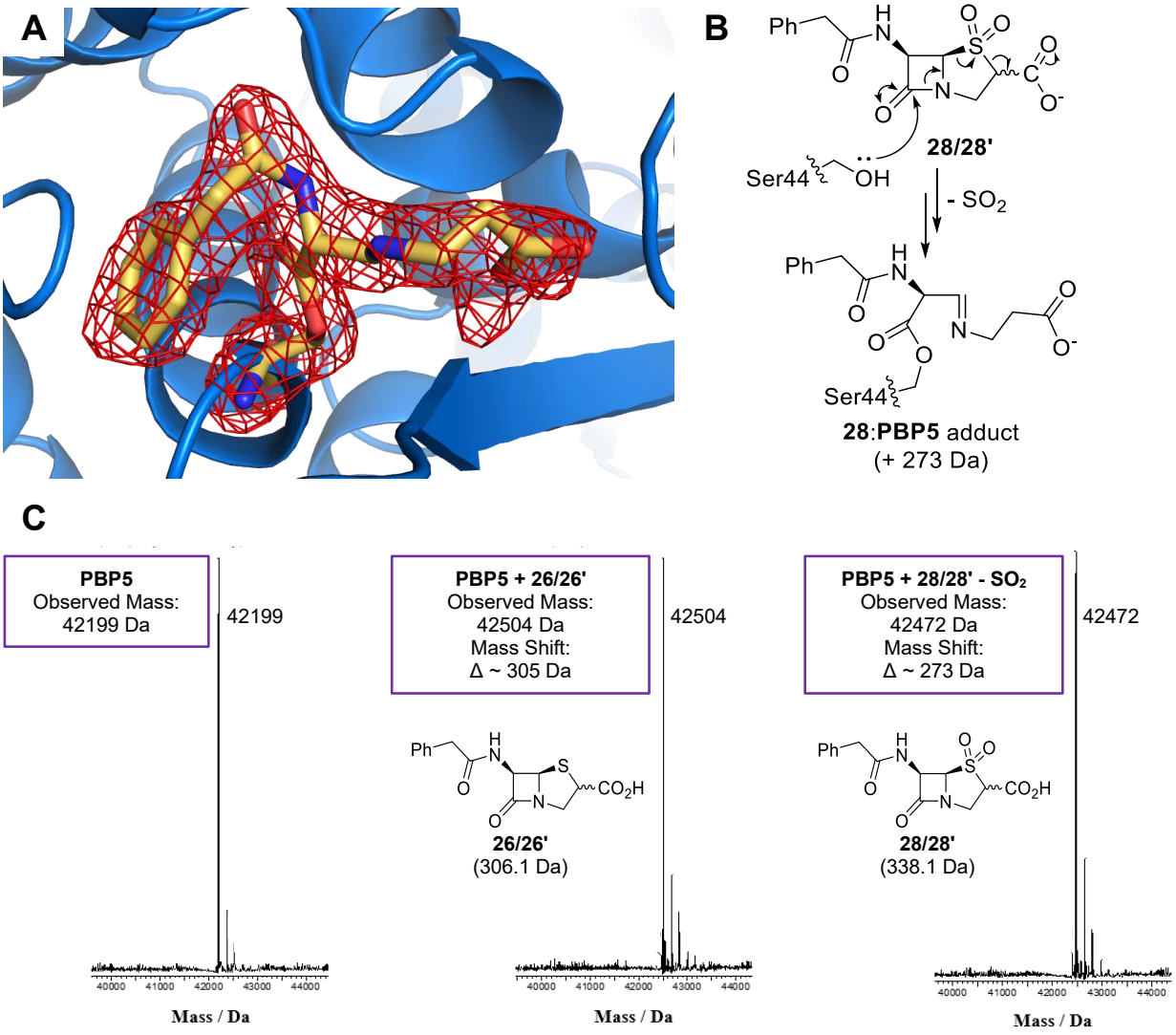

Figure 7: **A.** Active site view of the **28**:**PBP5** complex crystal structure (the polder map is carved at 5σ). **B.** Proposed outline mechanism for the reaction of **28/28'** with PBP5. **C**. Protein-observed MS spectra showing the formation of covalent adducts following the reaction of C2-carboxypenam acids with PBP5. Experimental details can be found in the Methods section.

6.2.4 Discussion

There is growing interest in non-classical β-lactam antibiotics that that combine potent PBP inhibition with reduced β-lactamase susceptibility. Tricyclic cephem derivatives (**Supporting Figure S4**) have demonstrated potent activity against carbapenem-resistant Enterobacterales (CRE), displaying hydrolytic stability to class A, B and D β-lactamases.[47, 48] Furthermore, sanfetrinem (**Supporting Figure S4**),[49-52] a tricyclic carbapenem that has entered clinical trials for the treatment of tuberculosis,[53] was also reported to show strong antibacterial properties against Gram-negative and Gram-positive bacteria, exhibiting high stability to many β-lactamases relative to bicyclic penams.[49-52] In this context, C2-carboxypenams are attractive for the development of potent antibiotics active against β-lactamase-producing pathogens. However, to facilitate development of such derivatives, improved synthetic routes are required.

The C2-carboxypenam ester scaffold **3** was considered an ideal precursor for functional group diversification, but previously reported syntheses presented practical limitations (**Figure 8**). Thiol **30**, obtained in 6 steps from penicillin V, reacted with benzyl 2-bromoacrylate **22a** in a thia-Michael addition manner to reportedly give bisnorpenicillin esters **31/31'** (36%), while C2-carboxypenam **32** was also isolated as a minor product (4%); although the mechanism via which **32** is produced was not defined, it is possible that **30** reacts in an aza-Michael reaction with benzyl 2-bromoacrylate, as seen in the **10→23a/23a'** conversion (**Figure 6**).[30] The other disclosed synthesis (**Figure 8**) of C2-carboxypenam esters started from penicillin G, which was converted in 5 steps to disulfide **33**. **33** reacted with benzyl 2-bromoacrylate to give **34/34'**; subsequent disulfide reduction of **34/34'** generated the corresponding reactive thiols, which undergo intramolecular cyclisation to **25/25'**.

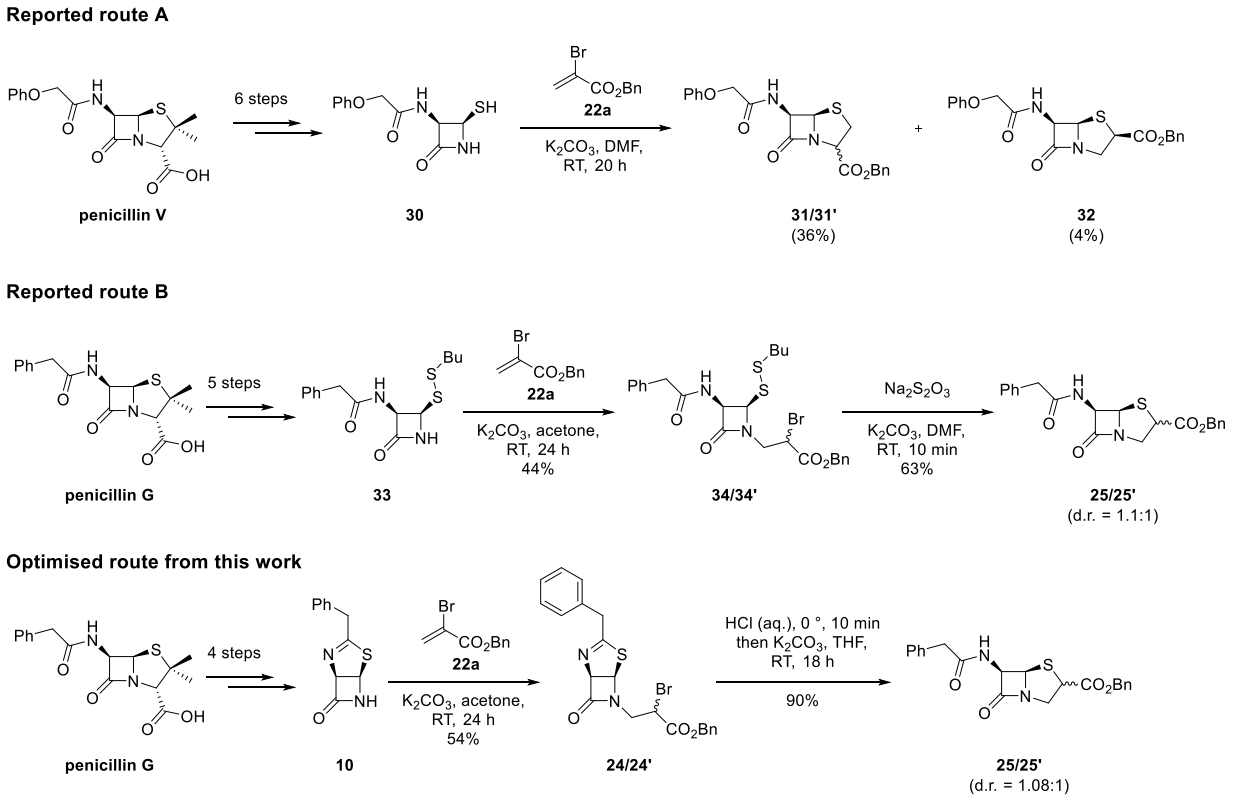

Figure 8: Synthetic routes towards C2-carboxypenam derivatives.[30, 31]

In both the reported routes[30, 31] and the optimized route described here (**Figure 8**), the crucial synthetic step is the late-stage reconstruction of the thiazolidine ring via intramolecular cyclisation. Conceptually, the addition of **10** to benzyl 2-bromoacrylate (**22a**) to provide **24/24′** parallels the reaction of disulfide **33** with **22a** to yield **34/34′**; in each case, subsequent deprotection affords the reactive thiols **25/25′** (**Figure 6**), which then cyclise by intramolecular attack of the thiolate on the bromide-bearing carbon. However, route B presents several shortcomings relative to the present route that complicate large-scale work: i) **33** is typically prepared by ozonolysis,[54] a step requiring stringent control for safety and to avoid overoxidation of the disulfide bridge; ii) β-lactam disulfide derivatives are unstable intermediates, making them problematic to purify (particularly by chromatography); and iii) the **34/34'→25/25'** conversion proceeds in 63% yield, whereas the corresponding **24/24'→25/25'** cyclisation in the optimised sequence occurs in 90% yield.

Beyond establishing an improved synthetic route, synthesis of **26/26'** and **28/28'** also enabled studies on the biological properties of C2-carboxypenams. Importantly, C2-carboxypenams **26/26'** and **28/28'** inhibited isolated *E. coli* PBP4-6, albeit to a lesser extent than penicillin G possibly reflecting that they were not optimized for PBP affinity. Notably, **26/26′** exhibited promising activity against a *S. aureus* strain (MIC ~ 8 μg/mL), whereas **26/26'** and **28/28'** did not display antibacterial activity against most of the other tested Gram-positive and Gram-negative bacteria. Given that the latest-generations of β-lactam antibiotics[55] typically bear a 2-amino-4-thiazolyl methoxyimino (ATMO) group (or related) as part of the C6/7-amido sidechain, it may be possible to optimise the antibacterial activity of **26/26'** and **28/28'**. Furthermore, the observation that **26/26'** inhibited recombinant isolated OXA-10 more potently than avibactam suggests that OXA-10-producing strains such as *P. aeruginosa*[56] may be preferred targets of C2-carboxypenam antibiotics and highlight the potential of the C2-carboxypenam scaffold for development not only as antibiotics but also as β-lactamase inhibitors.

Mechanistically, protein-observed MS assays confirmed covalent adduct formation with PBP5 for both **26/26'** and **28/28'**. Notably, **28/28'** undergoes thiazolidine fragmentation, followed by SO_2 extrusion, to give the crystallographically-observed **28**:**PBP5** adduct. It is plausible that the loss of SO_2 is facilitated by the presence of the C2-carboxylate, which may stabilise the formation of the corresponding anionic intermediate (**Figure 9A**). Interestingly, loss of SO_2 has previously been observed with C2-substituted penam sulfone β-lactamase inhibitors (**Figure 9B**); upon binding with SBLs, C2-β-alkenyl penam sulfone **35** undergoes β-lactam ring opening, fragmentation of the thiazolidine ring, and loss of SO_2, via either a pericyclic or anionic mechanism.[57] It should also be noted that, for both **28/28'** and **35**, the loss of SO_2 occurs due to the presence of an electron-withdrawing group at the C2 position.

From a medicinal chemistry perspective, the extrusion of SO_2 from C2-carboxypenam sulfones presents therapeutic potential, as the antimicrobial properties of SO_2 are well known: not only SO_2 is widely used in the wine-making industry,[58] but also SO_2-releasing prodrugs have recently been investigated as potential antibacterial agents.[59-63] Based on this, it should be possible, at least in principle, to design a dual-action C2-carboxypenam sulfone antibiotic that exerts antimicrobial properties via both inhibition of PBPs and *in situ* generation of SO_2.

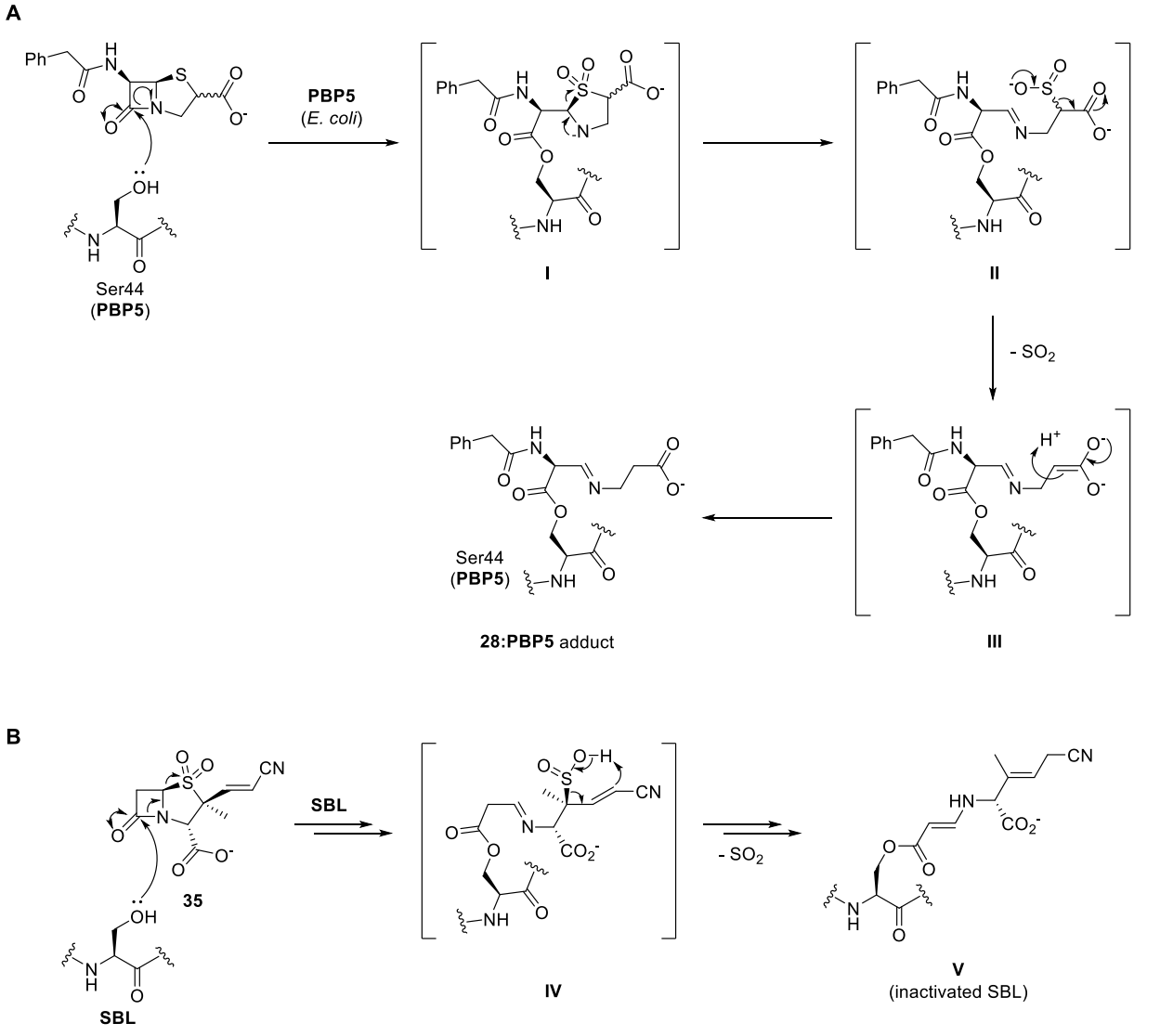

Figure 9: A. Proposed outline mechanism for the reaction of **28/28'** with PBP5 (*E. coli*). **B**. Proposed outline mechanism for the reaction of C2-β-alkenyl penam sulfone **35**.[57]

6.2.5 Conclusions

β-Lactam antibiotics are crucial therapeutic agents that treat bacterial infection. However, as bacteria evolve and acquire resistance mechanisms, novel β-lactams with increasingly complex scaffolds are being developed, which highlights the need of robust syntheses that are amenable to scale-up. In the present study, we established a streamlined six-step route (~12%) towards C2-carboxypenam esters, with future efforts being aimed at increasing the overall yield by further optimising the reaction conditions for each step. Furthermore, the preliminary biological studies provided structural and mechanistic insights that should guide the rational design of C2-carboxypenam antibiotics and, potentially, β-lactamase inhibitors.

6.2.6 Supporting figures

Supporting Figure S1: Outline mechanism for the conversion of **7** to **8**.[64] Thermal rearrangement of penam sulfoxide **2** leads to the formation of sulfenic acid **A**, which upon reduction by $P(OMe)_3$ reduction yields thiol **C**; subsequent intramolecular cyclization and dehydration of **D** produces thiazoline azetidinone **8**.

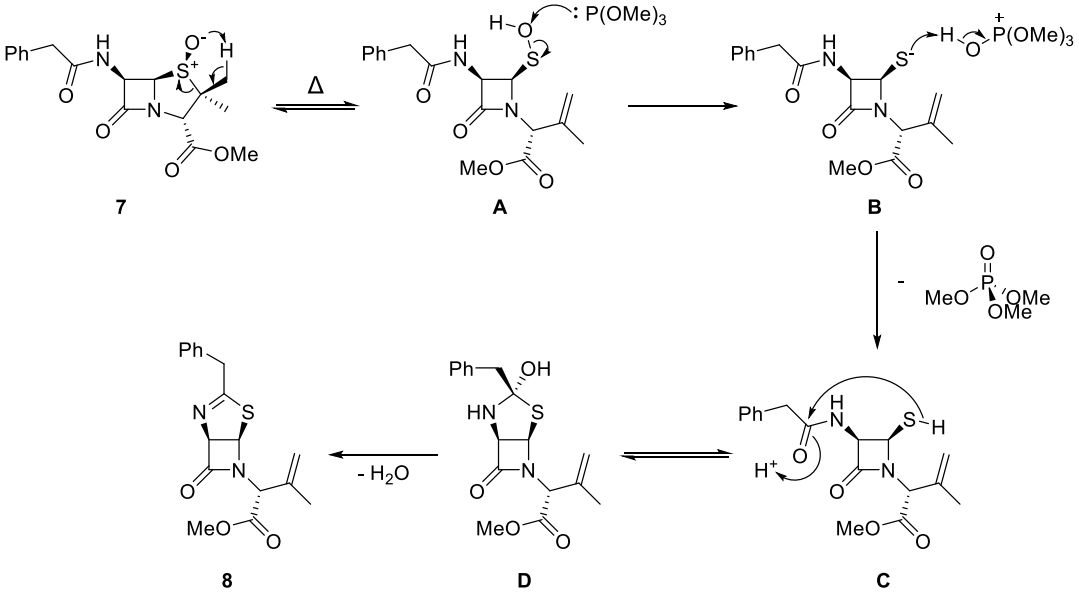

Supporting Figure S2: Proposed possible mechanisms for the reaction of **9** with dibenzyl 2-bromomalonate. The low yield of **15c** (4%) and isolation of dibenzyl malonate **16** suggest that debromination of dibenzyl 2-bromomalonate by thiolate **14c'** may be the preferred reaction pathway.

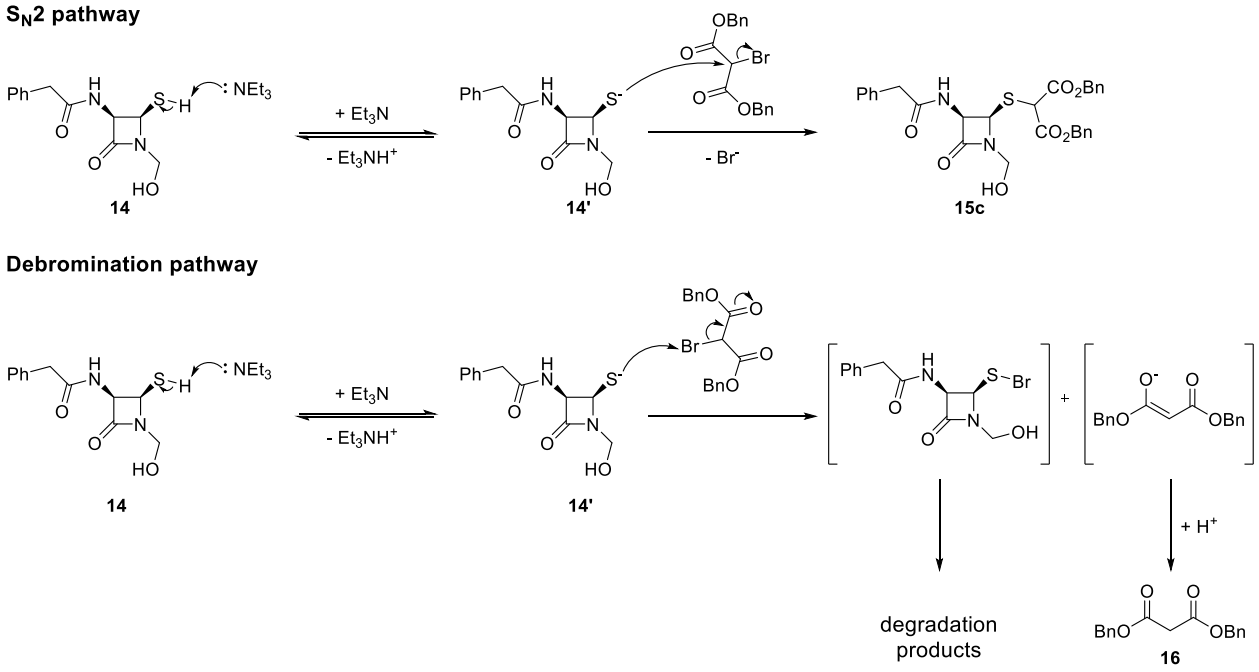

Supporting Figure S3: Representative dose response curves for inhibition of AmpC, TEM-116, OXA-10 and OXA-48 by **avibactam** (black circles), **28/28'** (blue squares), **26/26'** (red triangles), and **penicillin G** (green inverse triangles). Dose response curves are means of technical duplicates. IC_{50} values in **Table 2** are means of at least two independent repeats ($n \geq 2$, mean ± SD), each composed of technical duplicates. For more details see **Methods section**.

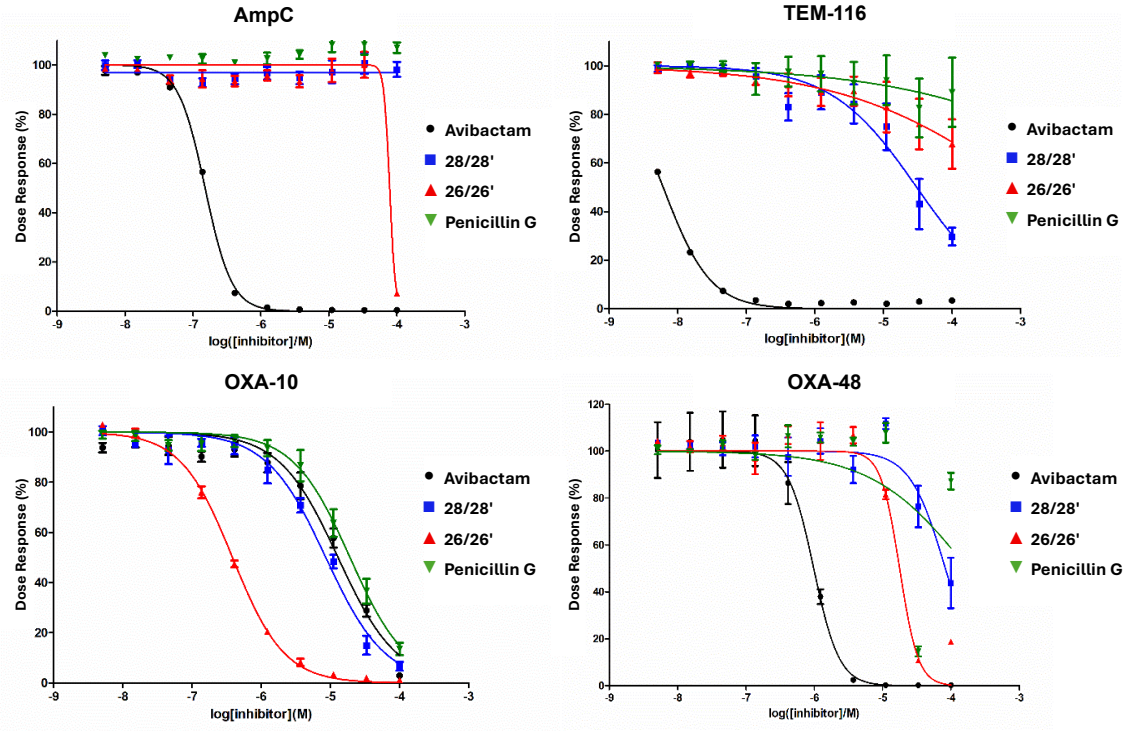

Supporting Figure S4: Structures of non-classical β-lactam antibiotics with intrinsic high stability to β-lactamases.[47, 49]

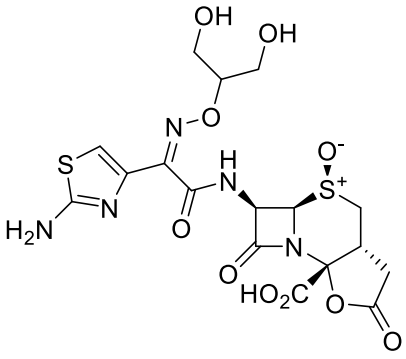

29

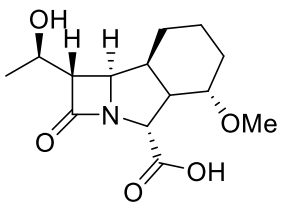

Sanfetrinem

6.2.7 Methods

6.2.7.1 PBP expression

Overproduction and purification of *E. coli* PBP5 (DacA) and *E. coli* PBP6 (DacC) were carried out as described previously.[65] *E. coli* PBP4 (DacB) was purified following an identical procedure.[65]

6.2.7.2 PBP inhibition assays

PBP inhibition assays were performed using fluorescence polarisation (FP) as reported,[41] utilising recombinant isolated PBP4-6 from *E. coli* (300 nM) in S2d assay buffer (25 mM HEPES, 100 mM NaCl, pH 7.4), substrate (two fixed concentrations, 100 μM and 10 μM), S2d probe (1.5 mM) and monobromobimane (mBBr, 0.5 mM).

6.2.7.3 Susceptibility assay

Minimum inhibitory concentrations (MICs) were determined using broth microdilution, according to the guidelines of the Clinical and Laboratory Standards Institute (CLSI, USA).[66] Measurements were obtained in triplicates, with compounds being tested alone (0.25-256 μg/mL) against selected strains.

6.2.7.4 SBL inhibition assays

SBL pIC_{50} values were determined using a fluorogenic cephalosporin analogue FC-5 (5 μM) as previously reported. [67, 68] Each recombinant SBL ($AmpC_{EC}$, 500 pM; TEM-116, 1 nM; OXA-10, 250 pM; OXA-48, 12.5 nM) was pre-incubated with each compound (various concentrations) for 10 minutes prior to the addition of the FC-5 substrate. Assay buffer: phosphate buffer (50 mM, pH 7.5), Triton X-100 (0.01% v/v).

6.2.7.5 Protein-observed MS assays

Assays were performed using UPLC-ESI-Q-TOF MS as reported,[41] employing *E. coli* PBP5 (84 μM) and, if appropriate, a β-lactam (1.68 mM) in buffer (25 mM HEPES pH 7.9, 100 mM NaCl) samples were diluted (5 μM PBP5) prior to analysis.

6.2.7.6 Crystallography

Crystals of *E. coli* PBP5 were obtained according to a previously published procedure.[69, 70] Briefly, crystals of PBP5 (5.5 mg/mL, 12.5 mM compound) were obtained in 8% PEG 400, 100 mM Tris pH 8.0. Crystals were cryoprotected using mother liquor containing glycerol (final concentration 25%). X-ray data were collected at beamline I03 at Diamond Light Source (Harwell, UK). Diffraction data were indexed and integrated using DIALS.

Supporting Table S1: Data collection and refinement statistics.

	***E. coli* PBP5 in complex with 28/28'**[(a)]
Wavelength (Å)	0.97626
Resolution range (Å)	44.12 - 2.032 (2.07 - 2.03)
Space group	$P2_1$
Unit cell	50.402, 116.123, 77.84, 90, 108.88, 90
Total reflections	352232 (17085)
Unique reflections	50027 (2527)
Multiplicity	7.0 (6.8)
Completeness (%)	99.85 (98.70)
Mean I/sigma(I)	9.41 (1.75)
Wilson B-factor	25.22
R-merge	0.1302 (0.9184)
R-meas	0.1406 (0.9952)
R-pim	0.05265 (0.3799)
CC1/2	0.997 (0.73)
CC*	0.999 (0.919)
Reflections used in	54399 (2801)

refinement	
Reflections used for R-free	2726 (143)
R-work	0.1691 (0.2446)
R-free	0.1945 (0.2664)
Number of non-hydrogen atoms	6500
macromolecules	5585
ligands	8
solvent	907
Protein residues	708
RMS(bonds)	0.004
RMS(angles)	0.68
Ramachandran favored (%)	98.57
Ramachandran allowed (%)	1.43
Ramachandran outliers (%)	0.00
Rotamer outliers (%)	1.01
Clashscore	3.87
Average B-factor	29.90
macromolecules	28.47
ligands	35.51
solvent	38.28

[a]Statistics for the highest-resolution shell are shown in parentheses.

6.2.8 References

1. K. Bush and P. A. Bradford, β-Lactams and β-Lactamase Inhibitors: An Overview, *Cold Spring Harb. Perspect. Med.*, 2016, **6**, a025247.
2. P. M. Blumberg and J. L. Strominger, Interaction of penicillin with the bacterial cell: penicillin-binding proteins and penicillin-sensitive enzymes, *Bacteriol. Rev.*, 1974, **38**, 291–335.
3. E. Sauvage, F. Kerff, M. Terrak, J. A. Ayala and P. Charlier, The penicillin-binding proteins: structure and role in peptidoglycan biosynthesis, *FEMS Microbiol. Rev.*, 2008, **32**, 234–258.
4. D. J. Tipper and J. L. Strominger, Mechanism of action of penicillins: a proposal based on their structural similarity to acyl-D-alanyl-D-alanine, *Proc. Natl. Acad. Sci.*, 1965, **54**, 1133–1141.
5. B. Lee, Conformation of penicillin as a transition-state analog of the substrate of peptidoglycan transpeptidase, *J. Mol. Biol.*, 1971, **61**, 463–469.
6. T. J. Franklin and G. A. Snow, in *Biochemistry of Antimicrobial Action*, eds. T. J. Franklin and G. A. Snow, Springer Netherlands, Dordrecht, 1989, pp. 20–54.
7. E. M. Halawa, M. Fadel, M. W. Al-Rabia, A. Behairy, N. A. Nouh, M. Abdo, R. Olga, L. Fericean, A. M. Atwa, M. El-Nablaway and A. Abdeen, Antibiotic action and resistance: updated review of mechanisms, spread, influencing factors, and alternative approaches for combating resistance, *Front. Pharmacol.*, 2024, **Volume 14 - 2023**.
8. T. M. Uddin, A. J. Chakraborty, A. Khusro, B. M. R. M. Zidan, S. Mitra, T. B. Emran, K. Dhama, M. K. H. Ripon, M. Gajdács, M. U. K. Sahibzada, M. J. Hossain and N. Koirala, Antibiotic resistance in microbes: History, mechanisms, therapeutic strategies and future prospects, *J. Infect. Public Health*, 2021, **14**, 1750–1766.
9. K. Bush, Past and Present Perspectives on β-Lactamases, *Antimicrob. Agents Chemother.*, 2018, **62**, 10.1128/aac.01076–01018.
10. K. H. M. E. Tehrani and N. I. Martin, β-lactam/β-lactamase inhibitor combinations: an update, *MedChemComm*, 2018, **9**, 1439–1456.
11. K. Nelson, P. Hemarajata, D. Sun, D. Rubio-Aparicio, R. Tsivkovski, S. Yang, R. Sebra, A. Kasarskis, H. Nguyen, M. Hanson Blake, S. Leopold, G. Weinstock, O. Lomovskaya and M. Humphries Romney, Resistance to Ceftazidime-Avibactam Is Due to Transposition of KPC in a Porin-Deficient Strain of Klebsiella pneumoniae with Increased Efflux Activity, *Antimicrob. Agents Chemother.*, 2017, **61**, 10.1128/aac.00989–00917.
12. K. E. Goodman, P. J. Simner, P. D. Tamma and A. M. Milstone, Infection control implications of heterogeneous resistance mechanisms in carbapenem-resistant Enterobacteriaceae (CRE), *Expert Rev. Anti. Infect. Ther.*, 2016, **14**, 95–108.
13. P. G. Ambrose, O. Lomovskaya, D. C. Griffith, M. N. Dudley and B. VanScoy, β-Lactamase inhibitors: what you really need to know, *Curr. Opin. Pharmacol.*, 2017, **36**, 86–93.
14. B. G. Hall and M. Barlow, Evolution of the serine β-lactamases: past, present and future, *Drug Res. Updat.*, 2004, **7**, 111–123.
15. I. Massova and S. Mobashery, Kinship and Diversification of Bacterial Penicillin-Binding Proteins and β-Lactamases, *Antimicrob. Agents Chemother.*, 1998, **42**, 1–17.
16. M. Sacco, D., K. G. Kroeck, M. T. Kemp, X. Zhang, L. D. Andrews and Y. Chen, Influence of the α-Methoxy Group on the Reaction of Temocillin with Pseudomonas aeruginosa

PBP3 and CTX-M-14 β-Lactamase, *Antimicrob. Agents Chemother.*, 2019, **64**, 10.1128/aac.01473–01419.
17. US4031077A, 1977.
18. J. M. T. Hamilton-Miller, Chemical Manipulations of the Penicillin Nucleus: A Review, *Chemotherapia*, 2009, **12**, 73–88.
19. E. H. Flynn, *Cephalosporins and penicillins: chemistry and biology*, Academic Press, New York, 1972.
20. N. C. Cohen, .beta.-Lactam antibiotics: geometrical requirements for antibacterial activities, *J. Med. Chem.*, 1983, **26**, 259–264.
21. M.-R. Meini, L. I. Llarrull and A. J. Vila, Overcoming differences: The catalytic mechanism of metallo-β-lactamases, *FEBS Lett.*, 2015, **589**, 3419–3432.
22. H. Feng, J. Ding, D. Zhu, X. Liu, X. Xu, Y. Zhang, S. Zang, D.-C. Wang and W. Liu, Structural and Mechanistic Insights into NDM-1 Catalyzed Hydrolysis of Cephalosporins, *J. Am. Chem. Soc.*, 2014, **136**, 14694–14697.
23. S. M. Drawz, M. Taracila, E. Caselli, F. Prati and R. A. Bonomo, Exploring sequence requirements for C3/C4 carboxylate recognition in the Pseudomonas aeruginosa cephalosporinase: Insights into plasticity of the AmpC β-lactamase, *Protein Sci.*, 2011, **20**, 941–958.
24. N. Matsumura, S. Minami and S. Mitsuhashi, Antibacterial activity of T-5575, a novel 2-carboxypenam, and its stability to beta-lactamase, *J. Antimicrob. Chemother.*, 1997, **39**, 31–34.
25. Y. Watanabe, S. Minami, T. Hayashi, H. Araki, R. Kitayama and H. Ochiai, In vitro antibacterial properties of T-5575 and T-5578 novel parenteral 2-carboxypenams, *Antimicrob. Agents Chemother.*, 1995, **39**, 2787–2791.
26. N. Matsumura and S. Mitsuhashi, A beta-lactamase from Serratia marcescens hydrolyzing the 2-carboxypenam T-5575, *Antimicrob. Agents Chemother.*, 1995, **39**, 2132–2134.
27. *US Pat.,* US 11208421 B2, 2021.
28. T. Aoki, H. Yoshizawa, K. Yamawaki, K. Yokoo, J. Sato, S. Hisakawa, Y. Hasegawa, H. Kusano, M. Sano, H. Sugimoto, Y. Nishitani, T. Sato, M. Tsuji, R. Nakamura, T. Nishikawa and Y. Yamano, Cefiderocol (S-649266), A new siderophore cephalosporin exhibiting potent activities against Pseudomonas aeruginosa and other gram-negative pathogens including multi-drug resistant bacteria: Structure activity relationship, *Eur. J. Med. Chem.*, 2018, **155**, 847–868.
29. *US Pat.,* US 2022/0241249 A1, 2022.
30. N. F. Osborne, The chemistry of 4-mercaptoazetidin-2-ones. Part 2. Synthesis of bisnorpenicillins, *J. Chem. Soc., Perkin Trans. 1*, 1980, 150–155.
31. *GB Pat.,* GB 1368234 A, 1974.
32. R. B. Woodward, K. Heusler, J. Gosteli, P. Naegeli, W. Oppolzer, R. Ramage, S. Ranganathan and H. Vorbrüggen, The Total Synthesis of Cephalosporin C1, *J. Am. Chem. Soc.*, 1966, **88**, 852–853.
33. J. E. Baldwin and M. A. Christie, Stereospecific synthesis of penicillins. Stereoelectronic control in the conversion of a peptide into a penicillin, *J. Am. Chem. Soc.*, 1978, **100**, 4597–4599.
34. L. Ghosez, J. Marchand-Brynaert, J. Vekemans, S. Bogdan and E. Cossement, Synthesis of 2-oxo-penams and penems from penicillin g, *Tetrahedron*, 1983, **39**, 2493–2503.

35. R. Busson, E. Roets and H. Vanderhaeghe, Circular dichroism of monocyclic .beta.-lactams, *J. Org. Chem.*, 1978, **43**, 4434–4437.
36. S. Wolfe, S. Ro, C.-K. Kim and Z. Shi, Synthesis and decarboxylation of Δ2-cephem-4,4-dicarboxylic acids, *Can. J. Chem.*, 2001, **79**, 1238–1258.
37. E. G. Brain, A. J. Eglington, J. H. C. Nayler, M. J. Pearson and R. Southgate, Syntheses based on 1,2-secopenicillins. Part I. Oxidation, *J. Chem. Soc., Perkin Trans. 1*, 1976, 447–451.
38. R. D. G. Cooper and F. L. Jose, Structural studies on penicillin derivatives. IX. Synthesis of thiazolidine-azetidinones, *J. Am. Chem. Soc.*, 1972, **94**, 1021–1022.
39. R. G. Micetich, S. N. Maiti, M. Tanaka, T. Yamazaki and K. Ogawa, Studies on 6-halo- and 6,6-dihalopenicillins: the rearrangement of methyl 6,6-dibromopenicillanate to 1,4-thiazepine, *J. Org. Chem.*, 1986, **51**, 853–858.
40. P. A. M. van der Klein, H. A. Witkamp and E. de Vroom, Reductive rearrangements of silylated penicillin G 1-oxide, *Tetrahedron Lett.*, 1994, **35**, 8691–8692.
41. H. G. Smith, S. Basak, V. Aniebok, M. J. Beech, F. M. Alshref, M. D. Allen, A. J. M. Farley and C. J. Schofield, Structural basis of Pseudomonas aeruginosa penicillin binding protein 3 inhibition by the siderophore-antibiotic cefiderocol, *Chem. Sci.*, 2024, **15**, 16928–16937.
42. S. S. van Berkel, J. Brem, A. M. Rydzik, R. Salimraj, R. Cain, A. Verma, R. J. Owens, C. W. G. Fishwick, J. Spencer and C. J. Schofield, Assay Platform for Clinically Relevant Metallo-β-lactamases, *J. Med. Chem.*, 2013, **56**, 6945–6953.
43. A. J. McCoy, R. W. Grosse-Kunstleve, P. D. Adams, M. D. Winn, L. C. Storoni and R. J. Read, Phaser crystallographic software, *J. Appl. Crystallogr.*, 2007, **40**, 658–674.
44. J. Brem, R. Cain, S. Cahill, M. A. McDonough, I. J. Clifton, J.-C. Jiménez-Castellanos, M. B. Avison, J. Spencer, C. W. G. Fishwick and C. J. Schofield, Structural basis of metallo-β-lactamase, serine-β-lactamase and penicillin-binding protein inhibition by cyclic boronates, *Nat. Commun.*, 2016, **7**, 12406.
45. D. Liebschner, P. V. Afonine, M. L. Baker, G. Bunkoczi, V. B. Chen, T. I. Croll, B. Hintze, L.-W. Hung, S. Jain, A. J. McCoy, N. W. Moriarty, R. D. Oeffner, B. K. Poon, M. G. Prisant, R. J. Read, J. S. Richardson, D. C. Richardson, M. D. Sammito, O. V. Sobolev, D. H. Stockwell, T. C. Terwilliger, A. G. Urzhumtsev, L. L. Videau, C. J. Williams and P. D. Adams, Macromolecular structure determination using X-rays, neutrons and electrons: recent developments in Phenix, *Acta Crystallogr. D.*, 2019, **75**, 861–877.
46. P. Emsley, B. Lohkamp, W. G. Scott and K. Cowtan, Features and development of Coot, *Acta Crystallogr. D.*, 2010, **66**, 486–501.
47. J. Sato, H. Kusano, T. Aoki, S. Shibuya, K. Yokoo, K. Komano, T. Oguma, S. Matsumoto, R. Nakamura, T. Sato and K. Yamawaki, Discovery of a Tricyclic β-Lactam as a Potent Antimicrobial Agent against Carbapenem-Resistant Enterobacterales, Including Strains with Reduced Membrane Permeability and Four-Amino Acid Insertion into Penicillin-Binding Protein 3: Structure–Activity-Relationships and In Vitro and In Vivo Activities, *ACS Infect. Dis.*, 2022, **8**, 400–410.
48. J. Sato, H. Kusano, T. Aoki, S. Shibuya, K. Yokoo, K. Komano, T. Oguma, S. Matsumoto, T. Sato, K. Yasuo and K. Yamawaki, A novel tricyclic β-lactam exhibiting potent antibacterial activities against carbapenem-resistant Enterobacterales: Synthesis and structure-activity-relationships, *Bioorg. Med. Chem.*, 2021, **46**, 116343.

49. S. Tamura, S. Miyazaki, K. Tateda, A. Ohno, Y. Ishii, T. Matsumoto, N. Furuya and K. Yamaguchi, In Vivo Antibacterial Activities of Sanfetrinem Cilexetil, a New Oral Tricyclic Antibiotic, *Antimicrob. Agents Chemother.*, 1998, **42**, 1858–1861.
50. K. V. Singh, T. M. Coque and B. E. Murray, In vitro activity of the trinem sanfetrinem (GV104326) against gram-positive organisms, *Antimicrob. Agents Chemother.*, 1996, **40**, 2142–2146.
51. S. K. Spangler, M. R. Jacobs and P. C. Appelbaum, MIC and time-kill studies of antipneumococcal activity of GV 118819X (sanfetrinem) compared with those of other agents, *Antimicrob. Agents Chemother.*, 1997, **41**, 148–155.
52. R. Wise, J. M. Andrews and N. Brenwald, In vitro activity of the tricyclic beta-lactam GV104326, *Antimicrob. Agents Chemother.*, 1996, **40**, 1248–1253.
53. S. Ramón-García, R. González del Río, M. P. Arenaz-Callao, H. I. Boshoff, J. Rullas, S. Anca, M. Cacho Izquierdo, E. Porras de Francisco, E. Pérez Herrán, A. Santos-Villarejo, A. Mendoza-Losana, S. Ferrer-Bazaga, C. J. Thompson, D. Barros Aguirre and R. H. Bates, Sanfetrinem, an oral β-lactam antibiotic repurposed for the treatment of tuberculosis, *Drug Res. Updat.*, 2025, **80**, 101213.
54. I. Ernest, J. Gosteli, C. W. Greengrass, W. Holick, H. R. Pfaendler and R. B. Woodward, The penems, a new class of .beta.-lactam antibiotics: 6-acylaminopenem-3-carboxylic acids, *J. Am. Chem. Soc.*, 1978, **100**, 8214–8222.
55. C. Hubschwerlen, in *Comprehensive Medicinal Chemistry II*, eds. J. B. Taylor and D. J. Triggle, Elsevier, Oxford, 2007, pp. 479–518.
56. R. F. Polse, H. M. Khalid and W. M. S. Mero, Distribution of blaOXA-10, blaPER-1, and blaSHV genes in ESBL-producing Pseudomonas aeruginosa strains isolated from burn patients, *Sci. Rep.*, 2023, **13**, 18402.
57. H. G. F. Richter, P. Angehrn, C. Hubschwerlen, M. Kania, M. G. P. Page, J.-L. Specklin and F. K. Winkler, Design, Synthesis, and Evaluation of 2β-Alkenyl Penam Sulfone Acids as Inhibitors of β-Lactamases, *J. Med. Chem.*, 1996, **39**, 3712–3722.
58. X. Feng, Y. Dong, Y. Feng, A. Zhang, Z. Huang, S. Wang and D. Niu, Recent advances in physical/chemical methods as alternatives to SO2 for winemaking: Principles, challenges and perspectives, *Innov. Food Sci. Emerg. Technol.*, 2024, **97**, 103839.
59. A. Mondal, T. Mondal, S. Jana, A. Banerjee and P. De, Structurally Engineered SO2–Releasing Polymeric Nanoassembly for Broad-Spectrum Antibacterial Activity, *Biomacromolecules*, 2025, **26**, 3200–3212.
60. W. Wang, X. Ji, Z. Du and B. Wang, Sulfur dioxide prodrugs: triggered release of SO2via a click reaction, *Chem. Commun.*, 2017, **53**, 1370–1373.
61. C. M. Black, A. J. Chu, G. H. Thomas, A. Routledge and A.-K. Duhme-Klair, Synthesis and antimicrobial activity of an SO2-releasing siderophore conjugate, *J. Inorg. Biochem.*, 2022, **234**, 111875.
62. S. R. Malwal, D. Sriram, P. Yogeeswari, V. B. Konkimalla and H. Chakrapani, Design, Synthesis, and Evaluation of Thiol-Activated Sources of Sulfur Dioxide (SO2) as Antimycobacterial Agents, *J. Med. Chem.*, 2012, **55**, 553–557.
63. S. R. Malwal, D. Sriram, P. Yogeeswari and H. Chakrapani, Synthesis and antimycobacterial activity of prodrugs of sulfur dioxide (SO2), *Bioorg. Med. Chem. Lett.*, 2012, **22**, 3603–3606.
64. R. D. G. Cooper and F. L. Jose, Structural studies on penicillin derivatives. IV. Novel rearrangement of penicillin V sulfoxide, *J. Am. Chem. Soc.*, 1970, **92**, 2575–2576.

65. S. R. Inglis, M. Strieker, A. M. Rydzik, A. Dessen and C. J. Schofield, A boronic-acid-based probe for fluorescence polarization assays with penicillin binding proteins and β-lactamases, *Anal. Biochem.*, 2012, **420**, 41–47.
66. B. Geibel, J. Dowell, D. Dickerson and T. Henkel, 1401. A Randomized, Double-Blind, Placebo-Controlled Study of the Safety and Pharmacokinetics of Single and Repeat Doses of VNRX-5133 in Healthy Subjects, *Open Forum Infect. Dis.*, 2018, **5**, S431–S431.
67. S. S. van Berkel, J. Brem, A. M. Rydzik, R. Salimraj, R. Cain, A. Verma, R. J. Owens, C. W. Fishwick, J. Spencer and C. J. Schofield, Assay platform for clinically relevant metallo-β-lactamases, *J. Med. Chem.*, 2013, **56**, 6945–6953.
68. P. A. Lang, A. Parkova, T. M. Leissing, K. Calvopiña, R. Cain, A. Krajnc, T. D. Panduwawala, J. Philippe, C. W. G. Fishwick, P. Trapencieris, M. G. P. Page, C. J. Schofield and J. Brem, Bicyclic Boronates as Potent Inhibitors of AmpC, the Class C β-Lactamase from Escherichia coli, *Biomolecules*, 2020, **10**.
69. G. Nicola, S. Peddi, M. Stefanova, R. A. Nicholas, W. G. Gutheil and C. Davies, Crystal Structure of Escherichia coli Penicillin-Binding Protein 5 Bound to a Tripeptide Boronic Acid Inhibitor: A Role for Ser-110 in Deacylation, *Biochemistry*, 2005, **44**, 8207–8217.
70. R. A. Nicholas, S. Krings, J. Tomberg, G. Nicola and C. Davies, Crystal Structure of Wild-type Penicillin-binding Protein 5 from Escherichia coli: IMPLICATIONS FOR DEACYLATION OF THE ACYL-ENZYME COMPLEX*, *J. Biol. Chem.*, 2003, **278**, 52826–52833.
71. M. R. Bell, J. A. Carlson and R. Oesterlin, Degradation of penicillin G methyl ester with trifluoroacetic acid, *J. Org. Chem.*, 1972, **37**, 2733–2735.
72. S. Wolfe, J.-B. Ducep and J. D. Greenhorn, A Novel Base-promoted Rearrangement of Penicillin G, *Can. J. Chem.*, 1975, **53**, 3435–3438.
73. D. H. R. Barton, F. Comer, D. G. T. Greig, P. G. Sammes, C. M. Cooper, G. Hewitt and W. G. E. Underwood, Transformations of penicillin. Part I. Preparation and rearrangements of 6β-phenylacetamidopenicillanic sulphoxides, *J. Chem. Soc. C Org.*, 1971, 3540–3550.
74. J. J. De Koning, H. J. Kooreman, H. S. Tan and J. Verweij, One-step, high yield conversion of penicillin sulfoxides to deacetoxycephalosporins, *J. Org. Chem.*, 1975, **40**, 1346–1347.
75. D. S. Pedersen and C. Rosenbohm, Dry Column Vacuum Chromatography, *Synthesis*, 2001, **2001**, 2431–2434.

6.3 Statement of Authorship

Title of Paper	Reaction of C2-carboxypenams with penicillin-binding proteins proceeds via unusual SO_2 release mechanism.
Publication Status	□Published □ Accepted for Publication □Submitted for Publication ☒Unpublished and unsubmitted work written in a manuscript style
Publication Details	**Muntean, D.-G.**; Smith, H.G.; Wilson, L.; Calvopiña, K.; Allen, M; Brewitz, L.; Schofield, C.J.: **Reaction of C2-carboxypenams with penicillin-binding proteins proceeds via unusual SO_2 release mechanism.**

Student Confirmation

Student Name:	Dorian-Gabriel Muntean		
Contribution to the Paper	D.-G.M. designed the synthetic routes towards C2-carboxypenams and carried out all the organic synthesis. D.-G.M. conceptualised and prepared the first draft of the manuscript. H.G.S. obtained the inhibition data for PBPs, conducted the protein-observed MS assays, obtained the crystal structure with *E. coli* PBP5 and refined the structure. L.W. obtained the inhibition data for SBLs. K.C. conducted the MIC assays. M.A. helped with processing the raw crystallographic data. L.B. provided supervision of the synthetic work and assisted with manuscript reviewing/editing. C.J.S. is the principal investigator/supervisor of the research described in the manuscript, contributed extensively to project/data conceptualization and visualization, and manuscript reviewing/editing.		
Signature 		Date	09/10/2025

Supervisor Confirmation

By signing the Statement of Authorship, you are certifying that the candidate made a substantial contribution to the publication, and that the description described above is accurate.

Supervisor name and title: Prof. Christopher J. Schofield		
Supervisor comments:		
Signature 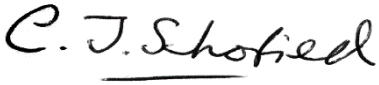	Date	09/10/2025

Chapter 7. Summary and conclusions

β-Lactam antibiotics are the most widely used class of antibiotics worldwide, owing their special antimicrobial properties to the reactive β-lactam ring.[1] β-Lactams acylate the active-site nucleophilic serine residue of penicillin-binding proteins (PBPs), thereby blocking transpeptidation steps in peptidoglycan assembly and thus disrupting bacterial cell-wall biosynthesis.[2, 3] β-Lactams can also be tailored to inhibit other families of serine enzymes, such as β-lactamases, which hydrolyse the β-lactam ring of β-lactam antibiotics, and represent one of the main resistance mechanisms in antibiotic-resistant bacteria.[1, 4] Beyond antibacterial applications, the chemical versatility of the strained β-lactam ring has enabled both clinical and/or investigational uses across many other therapeutic areas, leading to the development of antihypercholesterolemic, anticancer, antifungal, anti-inflammatory, and antiviral agents, thus highlighting its value in medicinal chemistry and drug discovery.[5-8]

At the height of the COVID-19 pandemic, screening efforts revealed penicillin-derived β-lactams as micromolar inhibitors of the SARS-CoV-2 main protease (M^{pro}), a nucleophilic cysteine protease essential for viral polyprotein processing and replication.[9-11] This was an important discovery, not only because M^{pro} is a validated antiviral target,[12] but also because β-lactams have a favourable clinical safety profile.[13] Although numerous M^{pro} inhibitors have emerged (via both repurposing and *de novo* design),[14-27] viral resistance is already posing a threat to the efficacy of some antiviral agents.[28-33] In this context, further development of chemically diverse scaffolds is not only desirable but needed, both to preserve therapeutic options against mutated SARS-CoV-2 strains and to build preparedness for future coronaviruses and related pathogens. The work described in this thesis aimed to further develop β-lactams for M^{pro} inhibition, with the extended objective of identifying cell-active β-lactam-based inhibitors. Moreover, it was noted that several

of the inhibitors designed for antiviral studies shared structural features with clinically used β-lactam antibiotics, thus prompting complementary investigations into their antibacterial properties and mechanisms of action. In this manner, the work described here comes full circle, from employing antibiotic scaffolds for antiviral applications back to investigating the potential of novel β-lactams to engage target bacterial enzymes.

Chapter 2 describes the synthesis of C6-alkoxypenicillins and their evaluation as SARS-CoV-2 M^{pro} inhibitors. Combined molecular modelling studies and protein-observed mass spectrometry (MS) indicated that most of the tested C6-alkoxypenicillins bind via non-covalent interactions at the M^{pro} active site, resulting in potent substrate-competitive inhibition (**Figure 1**). Among the investigated C6-methoxypenicillin G derivatives, the most potent were the (*R*)-sulfoxides **2** and **3** (IC_{50} ~ 0.5 and 0.8 μM, respectively), with structure-activity relationship (SAR) studies showing that altering their sulfur oxidation state leads to a significant loss in potency. Modelling of **3** indicated that the C6-methoxy group interferes with the positioning of the β-lactam ring relative to Cys145, reflected by an increased S(Cys145)–C(O)(β-lactam) distance (~ 6.2 Å), thereby precluding productive covalent reaction via β-lactam ring opening.

The penicillin V scaffold was also successfully employed to develop micromolar inhibitors of M^{pro}, with SAR studies revealing that activity is highly dependent on the interplay between the sulfur oxidation state and the identity of the C6-alkoxy substituent: while (*S*)-sulfoxide **7** displayed good activity (IC_{50} ~ 2.3 μM), its sulfone analogue was inactive. Furthermore, modelling of **10b** indicated that its C6-alkoxy substituent, a γ-lactam, might cause an increase in the S(Cys145)–C(O)(β-lactam) distance (~ 6.9 Å), thus also obstructing productive covalent reaction with Cys145; on the other hand, the C6-alkoxy group is predicted to form a network of stabilising hydrogen bonds with key S1 pocket residues (Leu141, Gly143, and Ser144), effectively mimicking the

natural P1 substrate. Lastly, it was shown that the C6-β-amido sidechain is not required for inhibition, as exemplified by C6-methoxypenam benzyl ester **26a**, with modelling studies indicating once more that the C6-methoxy group of **26a** is predicted to induce a binding pose with an increased S(Cys145)–C(O)(β-lactam) distance (~ 5.8 Å). Note that in this case the thioether oxidation state was required for more potent inhibition, unlike with the penicillin G and V derivatives for which the sulfoxide or sulfone oxidation state resulted in more potent inhibition (**Figure 1**).

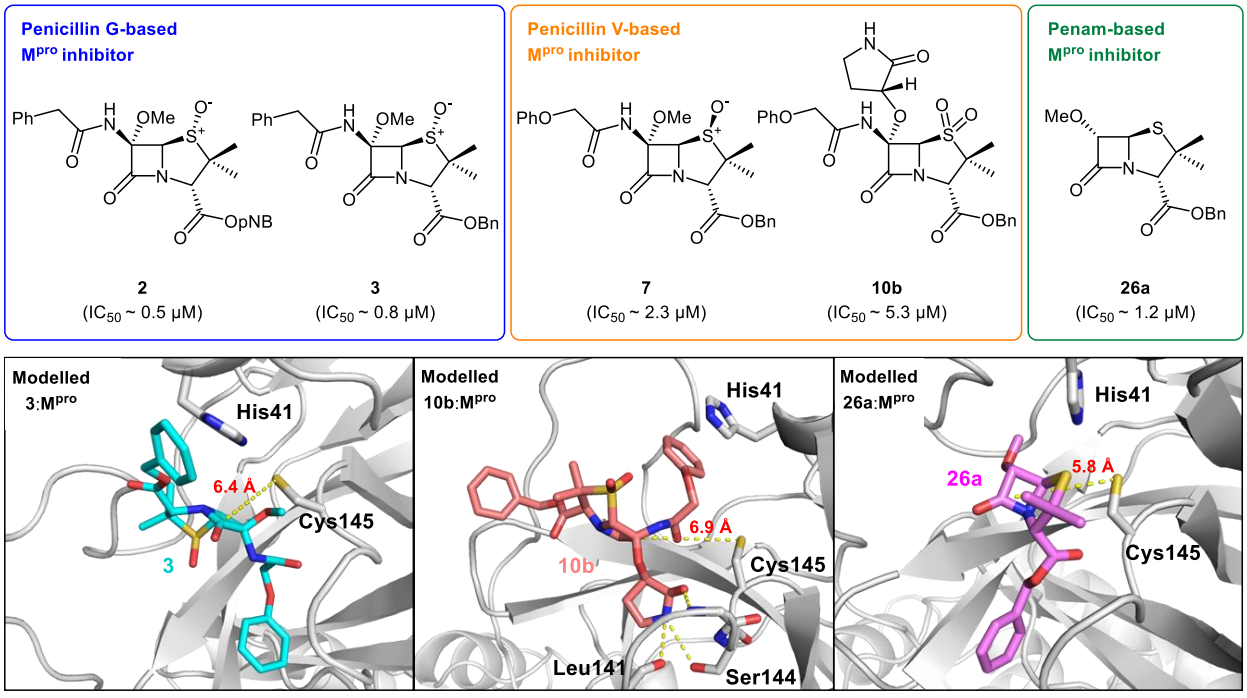

Figure 1: Overview of the key C6-alkoxypenicillin M^{pro} inhibitors developed in this thesis, and their predicted binding poses at the M^{pro} active site.

For C6-alkoxypenicillin V derivatives (*e.g.*, **7** and **10**) and C6-alkoxypenam derivatives (*e.g.*, **26a**) protein-observed MS did not show evidence for the formation of covalent adducts with M^{pro}, consistent with the modelling studies, indicating that inhibition occurs predominantly via non-covalent interactions. In contrast, C6-methoxypenicillin G (*R*)-sulfoxides (*e.g.*, **2** and **3**) displayed an unexpected behaviour (**Figure 2**): after 45 min incubation, **2** (515.1 Da) promoted partial

covalent modification of M^{pro}, with the dominant covalent adduct corresponding to a +498 Da mass shift, which is likely indicative of a dehydrated species derived from **2**. After 15 h, while the +498 Da adduct disappeared, a distinct +32 Da adduct was observed instead, which could correspond to a M^{pro} persulfide species. Given that the formation of the +32 Da adduct was unique to the C6-methoxypenicillin G (*R*)-sulfoxides investigated in this study, and supported by the modelling results for **3**, the evidence suggests that these derivatives react covalently with M^{pro} via a mechanism that does not involve β-lactam ring opening.

C6-Methoxypenicillin G (*R*)-sulfoxides **2** and **3** are potent M^{pro} inhibitors and merit further development as lead compounds. Unambiguous elucidation of their inhibitory mechanism has practical implications, as these findings could also inform the design of β-lactams that inhibit enzymes via modes other than stable acyl-enzyme complex formation. Future work should include time-resolved crystallography to define the structures of both the intermediates (*e.g.*, the +498 Da adduct) and the +32 Da adduct. To test whether the latter is a persulfide species, reductive quenching experiments (*e.g.*, with dithiothreitol or β-mercaptoethanol) could also be undertaken.

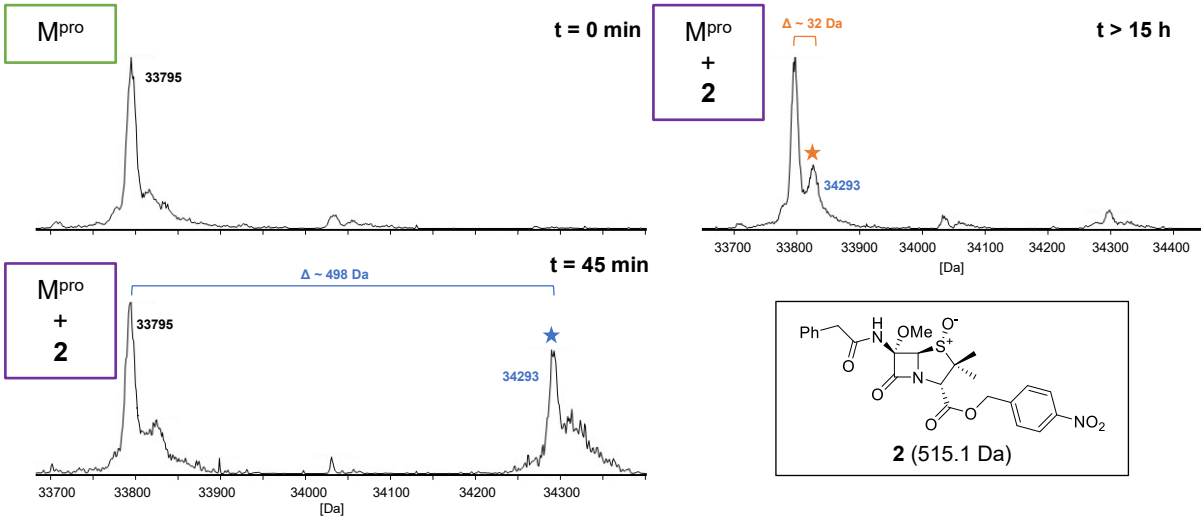

Figure 2: Evidence for the formation of covalent adducts with M^{pro} for C6-methoxypenicillin G (*R*)-sulfoxide derivative **2**. After 45 min, a +498 Da adduct (★) is detected, which largely disappears after 15 h, leaving a +32 Da adduct (★) as the principal covalently modified species.

Chapter 3 shifts the investigational focus from penam- to cephalosporin-based M^{pro} inhibitors. Following the screening of clinically used cephalosporins and related derivatives, two hits were identified: i) **ceftaroline** (IC_{50} ~ 3 μM), which inhibited M^{pro} via a non-covalent mechanism, and **GCLE** (IC_{50} ~ 30 nM), which promoted covalent adduct formation with M^{pro}, reacting with Cys145 via β-lactam ring opening. Given the exceptional potency of **GCLE**, unparalleled by any of the previously investigated β-lactam inhibitors, subsequent SAR studies were then centred on the **GCLE** core itself, with several key trends emerging: (i) C7-amide modifications were broadly tolerated, with many analogues maintaining nanomolar potency (IC_{50} ~ 20-100 nM); (ii) variations in the C4-ester group did not alter potency (IC_{50} ~ 20-50 nM); however, the cephalosporin acids investigated showed markedly poorer inhibition (IC_{50} > 15 μM); (iii) altering the sulfur oxidation state also reduced activity substantially, as sulfoxide and sulfone analogues of **GCLE** were considerably less active; and (iv) the identity of the C3 substituent proved critical for inhibition. Replacing the C3′-chloride of **GCLE** with acetates, thioethers, sulfones, or alkoxides led to >50-fold losses in potency (IC_{50} > 1.5 μM), irrespective of the leaving-group ability. On the other hand, C3'-quaternary ammonium salts were identified as acceptable substitutes for the C3'-chloride, albeit at the loss of some potency (<40-fold; IC_{50} ~ 0.12-1.1 μM); notably, these derivatives inhibited M^{pro} via a non-covalent mechanism, in contrast to **GCLE**.

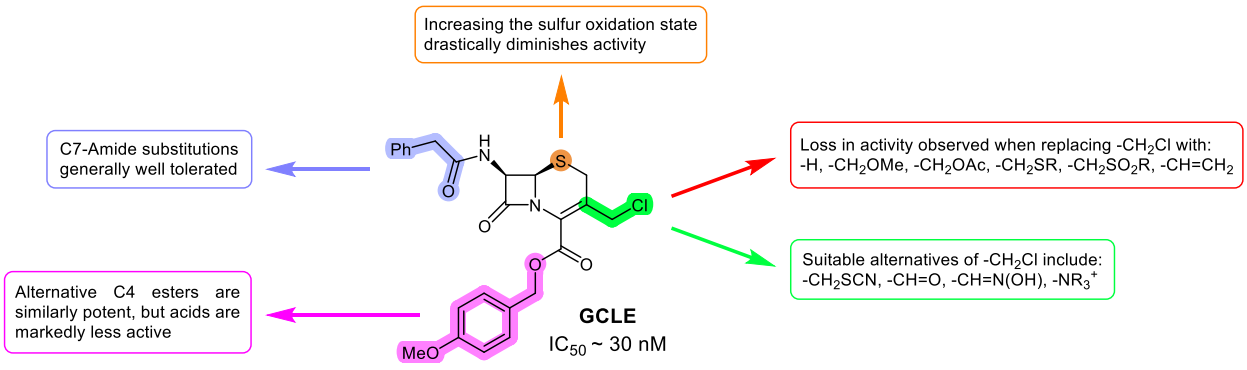

Figure 3: SAR analysis of **GCLE**, a newly identified potent inhibitor of SARS-CoV-2 M^{pro}.

Preliminary results demonstrated that selected **GCLE** derivatives inhibit SARS-CoV-2 replication in cells. Future work should prioritize determining effective cellular concentrations, thus enabling a quantitative comparison with biochemical potency and with clinically used benchmark inhibitors. Subsequent optimisation of **GCLE** should focus on improving cellular potency, addressing key challenges such as increasing compound solubility, assessing the susceptibility of the C4-ester to enzymatic hydrolysis, and improving cell permeability. Approaches may include replacing the C4-ester with C4-amides or neutral bioisosteres (*e.g.*, tetrazoles) to enhance metabolic stability, with further fine-tuning of the reactivity of the β-lactam ring by varying the C3 substituent also to be considered. In parallel, crystallographic studies should also be conducted to clarify the binding modes of the formed covalent adduct following the reaction of M^{pro} with **GCLE**, and to guide the design of future cephalosporin-based inhibitors.

Lastly, among the cephem inhibitors described in **Chapter 3**, the C3'-thiocyanate **14** and C3'-sulfone **17** show potential for development into antibacterial agents (**Figure 4**). Readily available from **GCLE** in good yields, **14** and **17** could serve as valuable synthetic intermediates that would give access to cephalosporin acids bearing optimised "ATMO"-type C7 sidechains. Notably, such cephalosporins bearing C3'-thiocyanate or C3'-sulfone substituents, to our knowledge, have not been explored as antibiotics. Under the pressure of rising antibiotic resistance, β-lactams with novel structural motifs should be investigated and extensively profiled for antibacterial activity.

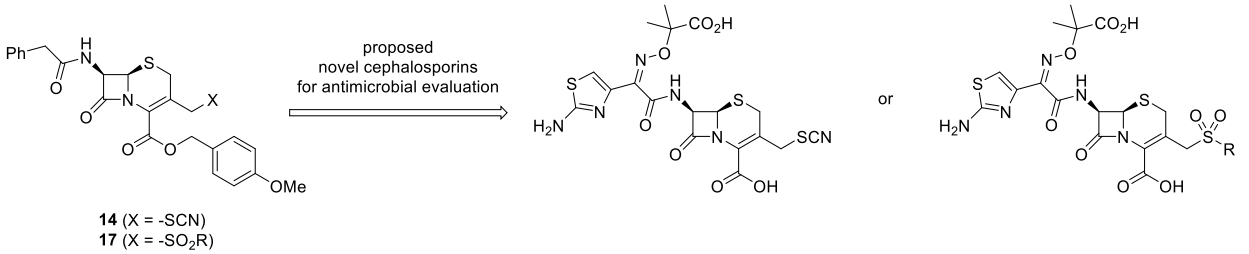

Figure 4: Proposed strategy for converting cephalosporin-based M^{pro} inhibitors into antibacterial leads.

Chapter 4 examines how C6-α-alkoxy substitution on the **sulbactam** core affects β-lactamase inhibition. Building on the results from **Chapter 2**, where C6-alkoxypenam esters were evaluated against M^{pro}, the work presented in this chapter describes the synthesis of C6-alkoxypenam acids from the corresponding esters, followed by an assessment of their inhibitory properties against serine-β-lactamases (SBLs) and metallo-β-lactamases (MBLs). Although introducing a C6-alkoxy group into the **sulbactam** scaffold generally diminished activity against class A enzymes (*e.g.*, TEM-116) relative to **sulbactam**, it did confer measurable inhibition of either class C or D β-lactamases. Notably, the C6-*tert*-butoxy sulfone **9d** inhibited class D enzyme OXA-48 (pIC_{50} ~ 5.4), whereas sulbactam was inactive (**Figure 5**), suggesting that C6-alkoxy sulbactam derivatives can be developed to outperform **sulbactam** in clinical settings.

Crystallographic evidence with OXA-48 and **9d** implied that the bulky *tert*-butoxy substituent sterically hindered access of the catalytic water to the active site, thus preventing hydrolysis of the acyl-enzyme complex. For AmpC (class C), the C6-*tert*-butoxy penam sulfide **11d** was ~10-fold more potent than sulbactam, with protein-observed MS revealing a non-covalent mode of inhibition, which mirrored the non-covalent behaviour observed for C6-alkoxypenam esters against M^{pro} (**Chapter 2**). Collectively, these results suggest that steric tuning at C6 can impart inhibitory properties against class C and D β-lactamases.

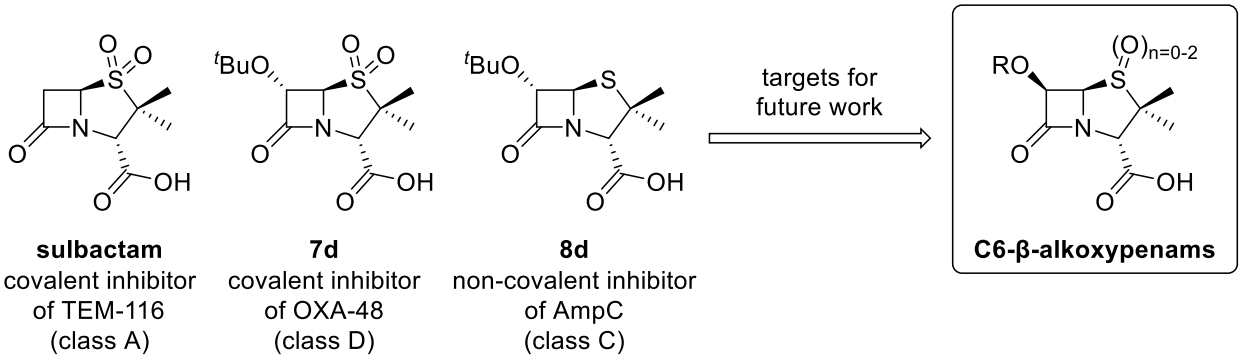

sulbactam
covalent inhibitor
of TEM-116
(class A)

7d
covalent inhibitor
of OXA-48
(class D)

8d
non-covalent inhibitor
of AmpC
(class C)

Figure 5: C6-Alkoxy substituents modulate the reactivity of sulbactam derivatives with SBLs.

Given that β-lactamases are one of the main drivers of antibiotic resistance,[1, 4] new β-lactamase inhibitors are urgently needed. In this context, C6-alkoxypenams merit further investigation: future work should explore not only penam derivatives with sterically bulky C6-α-alkoxy substituent (both aliphatic and aromatic in nature) but also the diastereomeric C6-β-alkoxypenams to determine whether altered spatial orientation improves potency against β-lactamases.

Chapter 5 explores, similarly to **Chapter 4**, the impact of C6-methoxy substitution on penicillin scaffolds, focusing on their antimicrobial properties. **Temocillin** (**Figure 6**),[34] a clinically used C6-methoxypenicillin, is known for its exceptional stability to β-lactamases, but its main drawback is its reduced PBP inhibition profile compared to its non-C6-methoxy analogue **ticarcillin**. To investigate whether penicillin scaffolds other than **ticarcillin** might display superior PBP inhibitory properties, several clinically used penicillins, including **oxacillin**, **carbenicillin**, and **piperacillin**, were converted to their corresponding C6-methoxy derivatives. Inhibition assays with isolated recombinant PBP3 from Gram-negative species revealed, as expected, that C6-methoxy substitution generally led to reduced inhibitory properties relative to the parent penicillins.

Nonetheless, the most notable finding was that C6-methoxypiperacillin **1f** still retained excellent potency ($pIC_{50} > 7.0$ against all PBPs tested), exceeding the inhibition profile of **temocillin** ($pIC_{50} \sim 4.2$-5.2). These results suggest that **1f** is a promising lead for the development of improved antibiotics. Accordingly, future work should include assessing the stability of **1f** to β-lactamases, as well as a broad screen against a panel of Gram-positive and Gram-negative pathogens to identify potential uses. To further improve PBP inhibition, SAR efforts should centre on optimising both the aromatic ring and the identity of the ureido substituent of **1f**.

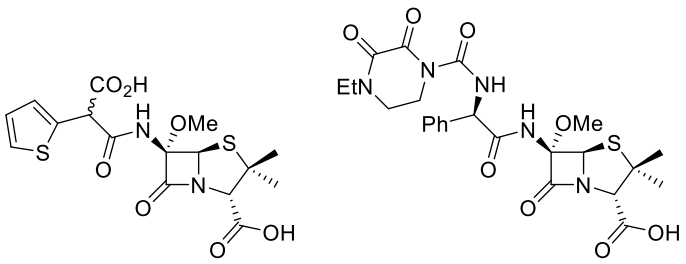

Figure 6: C6-Methoxypenicillins hold potential as narrow-spectrum antibiotics with improved β-lactamase stability.

Lastly, departing from the conventional penam scaffold utilised in the previous chapters, **Chapter 6** describes the development of an improved synthetic route toward C2-carboxypenams. C2-Carboxypenams are an investigational class of noncanonical β-lactam antibiotics that evade hydrolytic degradation by β-lactamases, wherein the C3-α-carboxylate group of penicillins is shifted to the C2 position of the penam scaffold.[35, 36]

Despite showing promising antibacterial profiles, reported syntheses of C2-carboxypenams have been low-yielding, thus limiting access to structurally diverse analogues.[37, 38] In this work, starting from **penicillin G**, the thiazolidine ring was deconstructed and subsequently rebuilt, delivering C2-carboxypenam esters **25/25'** in six steps (~12% overall yield). Preliminary biological studies with the corresponding penam acids **26/26'** revealed reduced PBP inhibition relative to **penicillin G**, yet unexpectedly good inhibition of OXA-10 (pIC_{50} ~ 6.7). These findings suggest that this scaffold holds promise both as a potential antibiotic and as a β-lactamase inhibitor. Future work should focus on improving PBP inhibition by optimising substituents, such as replacing the C6-phenylacetamido with an "ATMO" sidechain instead, and on evaluating C2-carboxysulbactam analogues to assess their potential as next-generation β-lactamase inhibitors. The work highlights the promise of semi-synthetic approaches to access novel penicillin-derived types of antibiotics.

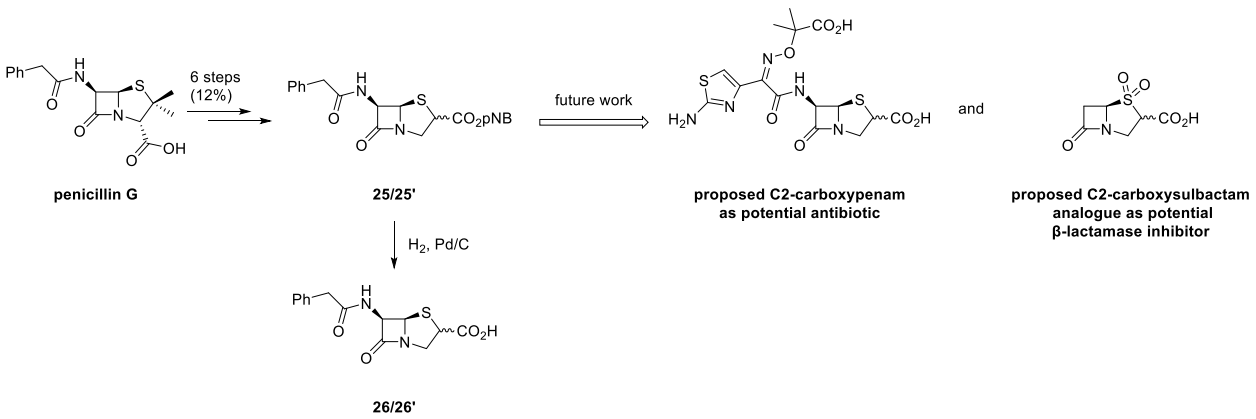

Figure 7: C2-Carboxypenams, non-canonical β-lactam derivatives with potential for development as both antibiotics and β-lactamase inhibitors.

Overall, the work presented in this thesis highlights the utility of β-lactams for the inhibition of nucleophilic cysteine and serine enzyme. β-Lactams are versatile warheads that can be tailored to target diverse targets through either covalent or non-covalent mechanisms. Notably, insights gained while designing β-lactam inhibitors of cysteine enzymes such as M^{pro} can inform the development of novel antibacterial agents (and *vice versa*), thus highlighting the value of integrating antiviral and antibacterial research. Furthermore, several molecules emerged as compounds of interest, either for their high potency or for their unusual modes of action. Further research efforts centred on these inhibitors, either for antiviral or antibiotic applications, could potentially yield clinically useful agents.

References

1. K. Bush and P. A. Bradford, β-Lactams and β-Lactamase Inhibitors: An Overview, *Cold Spring Harb. Perspect. Med.*, 2016, **6**, a025247.
2. D. J. Tipper and J. L. Strominger, Mechanism of action of penicillins: a proposal based on their structural similarity to acyl-D-alanyl-D-alanine, *Proc. Natl. Acad. Sci.*, 1965, **54**, 1133–1141.
3. P. M. Blumberg and J. L. Strominger, Interaction of penicillin with the bacterial cell: penicillin-binding proteins and penicillin-sensitive enzymes, *Bacteriol. Rev.*, 1974, **38**, 291–335.
4. K. Bush, Past and Present Perspectives on β-Lactamases, *Antimicrob. Agents Chemother.*, 2018, **62**, 10.1128/aac.01076–01018.
5. J. M. T. Hamilton-Miller, β-Lactams: variations on a chemical theme, with some surprising biological results, *J. Antimicrob. Chemother.*, 1999, **44**, 729–734.
6. D. Kuhn, C. Coates, K. Daniel, D. Chen, M. Bhuiyan, A. Kazi, E. Turos and Q. P. Dou, Beta-lactams and their potential use as novel anticancer chemotherapeutics drugs, *FBL*, 2004, **9**, 2605–2617.
7. P. D. Mehta, N. P. S. Sengar and A. K. Pathak, 2-Azetidinone – A new profile of various pharmacological activities, *Eur. J. Med. Chem.*, 2010, **45**, 5541–5560.
8. S. B. Rosenblum, T. Huynh, A. Afonso, H. R. Davis, N. Yumibe, J. W. Clader and D. A. Burnett, Discovery of 1-(4-Fluorophenyl)-(3R)-[3-(4-fluorophenyl)-(3S)- hydroxypropyl]-(4S)-(4-hydroxyphenyl)-2-azetidinone (SCH 58235): A Designed, Potent, Orally Active Inhibitor of Cholesterol Absorption, *J. Med. Chem.*, 1998, **41**, 973–980.
9. T. R. Malla, A. Tumber, T. John, L. Brewitz, C. Strain-Damerell, C. D. Owen, P. Lukacik, H. T. H. Chan, P. Maheswaran, E. Salah, F. Duarte, H. Yang, Z. Rao, M. A. Walsh and C. J. Schofield, Mass spectrometry reveals potential of β-lactams as SARS-CoV-2 Mpro inhibitors, *Chem. Commun.*, 2021, **57**, 1430–1433.
10. T. R. Malla, L. Brewitz, D.-G. Muntean, H. Aslam, C. D. Owen, E. Salah, A. Tumber, P. Lukacik, C. Strain-Damerell, H. Mikolajek, M. A. Walsh and C. J. Schofield, Penicillin Derivatives Inhibit the SARS-CoV-2 Main Protease by Reaction with Its Nucleophilic Cysteine, *J. Med. Chem.*, 2022, **65**, 7682–7696.
11. Y. Duan, H. Wang, Z. Yuan and H. Yang, Structural biology of SARS-CoV-2 Mpro and drug discovery, *Curr. Opin. Struct. Biol.*, 2023, **82**, 102667.
12. Y. Yang, Y.-D. Luo, C.-B. Zhang, Y. Xiang, X.-Y. Bai, D. Zhang, Z.-Y. Fu, R.-B. Hao and X.-L. Liu, Progress in Research on Inhibitors Targeting SARS-CoV-2 Main Protease (Mpro), *ACS Omega*, 2024, **9**, 34196–34219.
13. N. Pandey and M. Cascella, in *StatPearls [Internet]*, StatPearls Publishing, 2023.
14. L. Brewitz, L. Dumjahn, Y. Zhao, C. D. Owen, S. M. Laidlaw, T. R. Malla, D. Nguyen, P. Lukacik, E. Salah, A. D. Crawshaw, A. J. Warren, J. Trincao, C. Strain-Damerell, M. W. Carroll, M. A. Walsh and C. J. Schofield, Alkyne Derivatives of SARS-CoV-2 Main Protease Inhibitors Including Nirmatrelvir Inhibit by Reacting Covalently with the Nucleophilic Cysteine, *J. Med. Chem.*, 2023, **66**, 2663–2680.
15. C. Ma, Z. Xia, M. D. Sacco, Y. Hu, J. A. Townsend, X. Meng, J. Choza, H. Tan, J. Jang, M. V. Gongora, X. Zhang, F. Zhang, Y. Xiang, M. T. Marty, Y. Chen and J. Wang, Discovery of Di- and Trihaloacetamides as Covalent SARS-CoV-2 Main Protease Inhibitors with High Target Specificity, *J. Am. Chem. Soc.*, 2021, **143**, 20697–20709.

16. B. Boras, R. M. Jones, B. J. Anson, D. Arenson, L. Aschenbrenner, M. A. Bakowski, N. Beutler, J. Binder, E. Chen, H. Eng, H. Hammond, J. Hammond, R. E. Haupt, R. Hoffman, E. P. Kadar, R. Kania, E. Kimoto, M. G. Kirkpatrick, L. Lanyon, E. K. Lendy, J. R. Lillis, J. Logue, S. A. Luthra, C. Ma, S. W. Mason, M. E. McGrath, S. Noell, R. S. Obach, M. N. O'Brien, R. O'Connor, K. Ogilvie, D. R. Owen, M. Pettersson, M. R. Reese, T. F. Rogers, R. Rosales, M. I. Rossulek, J. G. Sathish, N. Shirai, C. M. Steppan, M. Ticehurst, L. Updyke, S. Weston, Y. Zhu, K. M. White, A. García-Sastre, J. Wang, A. K. Chatterjee, A. D. Mesecar, M. B. Frieman, A. S. Anderson and C. Allerton, Preclinical characterization of an intravenous coronavirus 3CL protease inhibitor for the potential treatment of COVID19, *Nat. Commun.*, 2021, **12**, 6055.
17. J. K. Stille, J. Tjutrins, G. Wang, F. A. Venegas, C. Hennecker, A. M. Rueda, I. Sharon, N. Blaine, C. E. Miron, S. Pinus, A. Labarre, J. Plescia, M. Burai Patrascu, X. Zhang, A. S. Wahba, D. Vlaho, M. J. Huot, T. M. Schmeing, A. K. Mittermaier and N. Moitessier, Design, synthesis and in vitro evaluation of novel SARS-CoV-2 3CLpro covalent inhibitors, *Eur. J. Med. Chem.*, 2022, **229**, 114046.
18. D. Laczi, S. S. Huamán, T. Andrews-Clark, S. M. Laidlaw, E. Salah, L. Dumjahn, P. Lukacik, H. Choudhry, M. A. Walsh, M. W. Carroll, C. J. Schofield and L. Brewitz, Silaproline-bearing nirmatrelvir derivatives are potent inhibitors of the SARS-CoV-2 main protease highlighting the value of silicon-derivatives in structure-activity-relationship studies, *Eur. J. Med. Chem.*, 2025, **291**, 117603.
19. R. Jimmidi, S. Chamakuri, S. Lu, M. N. Ucisik, P.-J. Chen, K. M. Bohren, S. A. Moghadasi, L. Versteeg, C. Nnabuife, J.-Y. Li, X. Qin, Y.-C. Chen, J. C. Faver, P. Nyshadham, K. L. Sharma, B. Sankaran, A. Judge, Z. Yu, F. Li, J. Pollet, R. S. Harris, M. M. Matzuk, T. Palzkill and D. W. Young, DNA-encoded chemical libraries yield non-covalent and non-peptidic SARS-CoV-2 main protease inhibitors, *Commun. Chem.*, 2023, **6**, 164.
20. L. Song, S. Gao, B. Ye, M. Yang, Y. Cheng, D. Kang, F. Yi, J.-P. Sun, L. Menéndez-Arias, J. Neyts, X. Liu and P. Zhan, Medicinal chemistry strategies towards the development of non-covalent SARS-CoV-2 Mpro inhibitors, *Acta Pharm. Sin. B*, 2024, **14**, 87–109.
21. M. L. Boby, D. Fearon, M. Ferla, M. Filep, L. Koekemoer, M. C. Robinson, C. M. C. The, J. D. Chodera, A. A. Lee, N. London, A. von Delft and F. von Delft, Open science discovery of potent noncovalent SARS-CoV-2 main protease inhibitors, *Science*, **382**, eabo7201.
22. N. E. Zhou, S. Tang, X. Bian, M. K. Parai, I. V. Krieger, A. Flores, P. K. Jaiswal, R. Bam, J. L. Wood, Z. Shi, L. J. Stevens, T. Scobey, M. V. Diefenbacher, F. R. Moreira, T. J. Baric, A. Acharya, J. Shin, M. M. Rathi, K. C. Wolff, L. Riva, M. A. Bakowski, C. W. McNamara, N. J. Catanzaro, R. L. Graham, D. C. Schultz, S. Cherry, Y. Kawaoka, P. J. Halfmann, R. S. Baric, M. R. Denison, T. P. Sheahan and J. C. Sacchettini, An oral non-covalent non-peptidic inhibitor of SARS-CoV-2 Mpro ameliorates viral replication and pathogenesis in vivo, *Cell Rep.*, 2024, **43**, 114929.
23. T. Miura, T. R. Malla, C. D. Owen, A. Tumber, L. Brewitz, M. A. McDonough, E. Salah, N. Terasaka, T. Katoh, P. Lukacik, C. Strain-Damerell, H. Mikolajek, M. A. Walsh, A. Kawamura, C. J. Schofield and H. Suga, In vitro selection of macrocyclic peptide inhibitors containing cyclic γ2,4-amino acids targeting the SARS-CoV-2 main protease, *Nat. Chem.*, 2023, **15**, 998–1005.
24. T. Miura, T. R. Malla, L. Brewitz, A. Tumber, E. Salah, K. J. Lee, N. Terasaka, C. D. Owen, C. Strain-Damerell, P. Lukacik, M. A. Walsh, A. Kawamura, C. J. Schofield, T. Katoh and H. Suga, Cyclic β2,3-amino acids improve the serum stability of macrocyclic peptide

inhibitors targeting the SARS-CoV-2 main protease, *Bull. Chem. Soc. Jpn.*, 2024, **97**, uoae018.
25. Y. Tan, J. Yang, M. Wang, Q. Peng, Y. Li, L. Fu, M. Zhang, J. Wu, G. Yang, C. J. Hipolito, Y. Zhang, J. Qi, Y. Shi and Y. Yin, De Novo Discovery of a Noncovalent Cell-Penetrating Bicyclic Peptide Inhibitor Targeting SARS-CoV-2 Main Protease, *J. Med. Chem.*, 2024, **67**, 20258–20274.
26. K. Harrison, P. W. Carlos, S. Ullrich, A. Aggarwal, J. Johansen-Leete, V. M. Sasi, I. Barter, J. W. C. Maxwell, M. J. Bedding, M. Larance, S. Turville, A. Norman, C. J. Jackson, C. Nitsche and R. J. Payne, Exploiting Hydrophobic Amino Acid Scanning to Develop Cyclic Peptide Inhibitors of the SARS-CoV-2 Main Protease with Antiviral Activity, *Chem. Eur. J*, 2024, **30**, e202401606.
27. J. Johansen-Leete, S. Ullrich, S. E. Fry, R. Frkic, M. J. Bedding, A. Aggarwal, A. S. Ashhurst, K. B. Ekanayake, M. C. Mahawaththa, V. M. Sasi, S. Luedtke, D. J. Ford, A. J. O'Donoghue, T. Passioura, M. Larance, G. Otting, S. Turville, C. J. Jackson, C. Nitsche and R. J. Payne, Antiviral cyclic peptides targeting the main protease of SARS-CoV-2, *Chem. Sci.*, 2022, **13**, 3826–3836.
28. S. Iketani, H. Mohri, B. Culbertson, S. J. Hong, Y. Duan, M. I. Luck, M. K. Annavajhala, Y. Guo, Z. Sheng, A.-C. Uhlemann, S. P. Goff, Y. Sabo, H. Yang, A. Chavez and D. D. Ho, Multiple pathways for SARS-CoV-2 resistance to nirmatrelvir, *Nature*, 2023, **613**, 558–564.
29. N. S. Zuckerman, E. Bucris, D. Keidar-Friedman, M. Amsalem and T. Brosh-Nissimov, Nirmatrelvir Resistance—de Novo E166V/L50V Mutations in an Immunocompromised Patient Treated With Prolonged Nirmatrelvir/Ritonavir Monotherapy Leading to Clinical and Virological Treatment Failure—a Case Report, *Clinical Infectious Diseases*, 2024, **78**, 352–355.
30. Y. Zhou, K. A. Gammeltoft, L. A. Ryberg, L. V. Pham, H. D. Tjørnelund, A. Binderup, C. R. Duarte Hernandez, C. Fernandez-Antunez, A. Offersgaard, U. Fahnøe, G. H. J. Peters, S. Ramirez, J. Bukh and J. M. Gottwein, Nirmatrelvir-resistant SARS-CoV-2 variants with high fitness in an infectious cell culture system, *Sci. Adv.*, **8**, eadd7197.
31. E. Heilmann, F. Costacurta, S. A. Moghadasi, C. Ye, M. Pavan, D. Bassani, A. Volland, C. Ascher, A. K. H. Weiss, D. Bante, R. S. Harris, S. Moro, B. Rupp, L. Martinez-Sobrido and D. von Laer, SARS-CoV-2 3CLpro mutations selected in a VSV-based system confer resistance to nirmatrelvir, ensitrelvir, and GC376, *Sci. Transl. Med.*, **15**, eabq7360.
32. N. Petrišič, M. Adamek, A. Kežar, S. B. Hočevar, E. Žagar, G. Anderluh and M. Podobnik, Structural basis for the unique molecular properties of broad-range phospholipase C from Listeria monocytogenes, *Nature Communications*, 2023, **14**, 6474.
33. J. D. Ip, A. Wing-Ho Chu, W.-M. Chan, R. Cheuk-Ying Leung, S. M. Umer Abdullah, Y. Sun and K. K.-W. To, Global prevalence of SARS-CoV-2 3CL protease mutations associated with nirmatrelvir or ensitrelvir resistance, *eBioMedicine*, 2023, **91**.
34. L. Verbist, In vitro activity of temocillin (BRL 17421), a novel beta-lactamase-stable penicillin, *Antimicrob. Agents Chemother.*, 1982, **22**, 157–161.
35. Y. Watanabe, S. Minami, T. Hayashi, H. Araki, R. Kitayama and H. Ochiai, In vitro antibacterial properties of T-5575 and T-5578 novel parenteral 2-carboxypenams, *Antimicrob. Agents Chemother.*, 1995, **39**, 2787–2791.

36. N. Matsumura, S. Minami and S. Mitsuhashi, Antibacterial activity of T-5575, a novel 2-carboxypenam, and its stability to beta-lactamase, *J. Antimicrob. Chemother.*, 1997, **39**, 31–34.
37. N. F. Osborne, The chemistry of 4-mercaptoazetidin-2-ones. Part 2. Synthesis of bisnorpenicillins, *J. Chem. Soc., Perkin Trans. 1*, 1980, 150–155.
38. *GB Pat.,* GB 1368234 A, 1974.

8. Appendix

8.1 Appendix to Chapter II (Manuscript I)

8.1.1 General synthesis information

All reagents were obtained from commercial sources (Sigma-Aldrich, Inc.; Fluorochem Ltd.; Manchester Organics; Tokyo Chemical Industry Ltd.) and were used without further purification. Benzyl (2*S*,5*R*,6*R*)-3,3-dimethyl-7-oxo-6-(2-phenoxyacetamido)-4-thia-1-azabicyclo[3.2.0]heptane-2-carboxylate 4,4-dioxide (**1**)[1], 4-nitrobenzyl (2*S*,4*R*,5*R*,6*S*)-6-methoxy-3,3-dimethyl-7-oxo-6-(2-phenylacetamido)-4-thia-1-azabicyclo[3.2.0]heptane-2-carboxylate 4-oxide (**2**)[2], benzyl (2*S*,5*R*,6*R*)-3,3-dimethyl-7-oxo-6-(2-phenoxyacetamido)-4-thia-1-azabicyclo[3.2.0]heptane-2-carboxylate (**5**)[1], benzyl (2*S*,4*S*,5*R*,6*R*)-3,3-dimethyl-7-oxo-6-(2-phenoxyacetamido)-4-thia-1-azabicyclo[3.2.0]heptane-2-carboxylate 4-oxide (**6**)[1], benzyl (2*S*,5*R*,6*R*)-6-amino-3,3-dimethyl-7-oxo-4-thia-1-azabicyclo[3.2.0]heptane-2-carboxylate toluene-*p*-sulfonic acid salt (**11**)[1], benzyl (2*S*,5*R*,6*R*)-6-(((*E*)-2,6-di-tert-butyl-4-hydroxybenzylidene)amino)-3,3-dimethyl-7-oxo-4-thia-1-azabicyclo[3.2.0]heptane-2-carboxylate (**12**)[3], benzyl (2*S*,5*R*,6*R*)-3,3-dimethyl-7-oxo-6-(2-phenylacetamido)-4-thia-1-azabicyclo[3.2.0]heptane-2-carboxylate (**18**)[4], benzyl (2*S*,5*R*,6*R*)-3,3-dimethyl-7-oxo-6-(2-phenylacetamido)-4-thia-1-azabicyclo[3.2.0]heptane-2-carboxylate 4,4-dioxide (**19**)[1], and benzyl (2*S*,4*S*,5*R*,6*R*)-3,3-dimethyl-7-oxo-6-(2-phenylacetamido)-4-thia-1-azabicyclo[3.2.0]heptane-2-carboxylate 4-oxide (**21**)[4] were synthesized as reported.

Anhydrous solvents (Sigma-Aldrich, Inc.) were kept under an atmosphere of argon. HPLC grade solvents (Sigma-Aldrich Inc.) were used for reaction work-ups, extractions, and purifications.

Flash column chromatography was performed using an automated Biotage Isolera One purification machine equipped with Biotage®Sfär flash chromatography cartridges. ^{1}H and ^{13}C NMR spectra were recorded using Bruker AVANCE AVIIIHD 400, 500 and 600 MHz machines. Chemical shifts for protons are reported in parts per million (ppm) downfield from tetramethylsilane and are referenced to residual protium in the NMR solvent (*i.e.*, $CDCl_3$: δ = 7.26 ppm; DMSO-d_6: δ = 2.50 ppm). For ^{13}C NMR, chemical shifts are reported in the scale relative to the NMR solvent (*i.e.*, $CDCl_3$: δ = 77.2 ppm; DMSO-d_6: δ = 39.5 ppm). NMR data are reported in the following manner: chemical shift, multiplicity, coupling constant (J, Hz; to nearest 0.1 Hz), and integration.

Infrared (IR) spectroscopy was performed using a Bruker Tensor-27 Fourier transform infrared (FT-IR) spectrometer. High-resolution mass spectrometry (HRMS) was performed using either electro-spray ionization (ESI) mass spectrometry (MS) in the positive or negative ionization modes employing a Thermo Scientific Exactive mass spectrometer (ThermoFisher Scientific), or atmospheric pressure chemical ionization (APCI) in the positive mode using an Agilent 7200 Accurate mass spectrometer; data are presented as a mass-to-charge ratio (m/z). Optical rotation ($[\alpha]_D^{25}$) measurements were performed using either a Unipol (Schmidt Haensch) or Bellingham + Stanley (ADP450) polarimeter.

8.1.2 General synthetic procedures

General procedure A:

A variation of a reported procedure was followed[5]. To a stirred solution of a penam in anhydrous CH_2Cl_2 (1 equiv.; 0.1-0.2 M) was added freshly prepared $^{t}BuOCl$[6] (1.5 equiv.), followed by a solution of LiOMe (1.1 equiv.) in MeOH (1 M) at -30 °C. The reaction mixture was stirred under nitrogen atmosphere for 1 h at -30 °C, before the addition of AcOH (1 equiv.). The mixture was

diluted with CH_2Cl_2 and was sequentially washed with saturated aqueous $NaHCO_3$ solution, aqueous $Na_2S_2O_3$ (5% (w/v)) solution, and brine. The organic layer was dried over Na_2SO_4, filtered, concentrated *in vacuo*, and purified by flash column chromatography.

General procedure B:

A variation of a reported procedure was followed[7]. To a stirred solution of a penam in CH_2Cl_2 (1 equiv.; 0.16 M) was added an ice-cold aqueous solution of $NaNO_2$ (2.6 equiv.; 0.9 M), followed by addition of *p*-toluenesulfonic acid monohydrate (0.3 equiv.). After stirring the reaction mixture for 20 min at 0 °C, the organic layer was separated, and the aqueous phase was then extracted with CH_2Cl_2. The combined extracts were sequentially washed with saturated aqueous $NaHCO_3$, H_2O, then dried over Na_2SO_4, filtered, and concentrated *in vacuo* at 30 °C to give crude benzyl (2*S*,5*R*)-6-diazo-3,3-dimethyl-7-oxo-4-thia-1-azabicyclo[3.2.0]heptane-2-carboxylate[8]. The crude residue was dissolved in anhydrous CH_2Cl_2 (0.2 M), to which an anhydrous alcohol (1-110 equiv.) and boron trifluoride diethyl etherate (0.1 equiv.) were added sequentially. The mixture was stirred at 20 °C for 15 min, before being diluted with CH_2Cl_2. The mixture was washed with saturated aqueous $NaHCO_3$ solution and H_2O. The organic layer was dried over Na_2SO_4, filtered, concentrated *in vacuo*, and purified by flash column chromatography.

General procedure C:

A variation of a reported procedure was followed[1]. To a stirred solution of a penam in anhydrous CH_2Cl_2 (1 equiv.; 0.1 M) was added *m*-chloroperbenzoic acid (<77% purity; 2.3 equiv.) in portions over 5 min at 0 °C. The reaction mixture was stirred for 1 h at 10 °C, and then at room temperature overnight (16-20 h), before being diluted with CH_2Cl_2. The mixture was sequentially washed with aqueous $Na_2S_2O_5$ (10% (w/v)) solution, saturated aqueous $NaHCO_3$ solution, water, and brine. The

organic layer was dried over Na_2SO_4, filtered, concentrated *in vacuo*, and purified by flash column chromatography.

8.1.3 Experimental procedures and compounds characterisations

Benzyl (2*S*,4*S*,5*R*,6*S*)-6-methoxy-3,3-dimethyl-7-oxo-6-(2-phenoxyacetamido)-4-thia-1-azabicyclo[3.2.0]heptane-2-carboxylate 4-oxide (7)

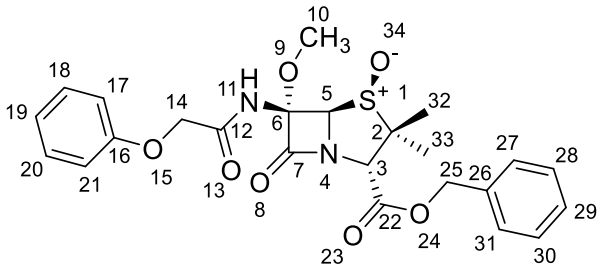

General procedure A[5] was used with penam **6** (1.17 g, 2.56 mmol). Purification by flash column chromatography (25 g Sfär, 100%$_{v/v}$ cyclohexane (2 CV), followed by a linear gradient (9 CV): 0%$_{v/v}$ →11%$_{v/v}$ ethyl acetate in cyclohexane, followed by 11%$_{v/v}$ ethyl acetate in cyclohexane (2 CV), followed by a linear gradient (14 CV): 11%$_{v/v}$ →28%$_{v/v}$ ethyl acetate in cyclohexane, followed by 28%$_{v/v}$ ethyl acetate in cyclohexane (2 CV), followed by a linear gradient (18 CV): 28%$_{v/v}$ →60%$_{v/v}$ ethyl acetate in cyclohexane) yielded **7** (570 mg, 45%).

Amorphous foam; ^{1}H NMR (500 MHz, 298 K, $CDCl_3$): δ = 7.53 (s, 1H, *N11H*), 7.40 – 7.36 (m, 5H, *C27H*, *C28H*, *C29H*, *C30H*, *C31H*), 7.32 – 7.28 (m, 2H, *C18H*, *C20H*), 7.02 (m, *J* = 7.5, 1.0 Hz, 1H, *C19H*), 6.96 – 6.92 (m, 2H, *C17H*, *C21H*), 5.32 (d, *J* = 12.0 Hz, 1H, *C25H*), 5.19 (d, *J* = 12.0 Hz, 1H, *C25H*), 4.99 (s, 1H, *C5H*), 4.62 – 4.50 (m, 3H, *C3H, C14H$_2$*), 3.49 (s, 3H, *C10H$_3$*), 1.58 (s, 3H, *C32H$_3$*), 1.08 ppm (s, 3H, *C33H$_3$*); ^{13}C NMR (126 MHz, 298 K, $CDCl_3$): δ = 170.3, 167.6, 166.8, 157.1, 134.8, 129.9, 129.05, 128.98, 128.9, 122.5, 115.0, 90.8, 79.4, 77.4, 71.7, 68.1, 67.2, 64.2, 53.5, 19.4, 18.5 ppm; IR (film): $\tilde{\nu}$ = 1792, 1753, 1696, 1599, 1496, 1438, 1215, 1172,

1060 cm^{-1}; HRMS (ESI): m/z calculated for $C_{24}H_{26}N_2O_7S$ $[M+Na]^+$: 509.1353, found: 509.1350; $[\alpha]_D^{25}$ = +224 (c =0.006 g/mL, $CHCl_3$).

Benzyl (2*S*,5*R*,6*S*)-6-methoxy-3,3-dimethyl-7-oxo-6-(2-phenoxyacetamido)-4-thia-1-azabicyclo[3.2.0]heptane-2-carboxylate (8)

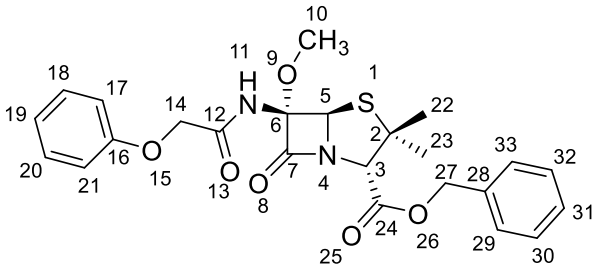

To a solution of **7** (300 mg, 0.615 mmol, 1 equiv.) in *N*,*N*-dimethylformamide (6.1 mL) cooled to 0°C were sequentially added KI (1.85 g, 11.1 mmol, 18 equiv.) then CH_3COCl (0.31 mL, 4.34 mmol, 7 equiv.). The reaction mixture was stirred for 1 h at 0°C, then it was diluted with EtOAc (50 mL). The organic layer was sequentially washed with an aqueous solution of $Na_2S_2O_3$ (5% (w/v)), saturated aqueous $NaHCO_3$ solution, and brine, before being dried over Na_2SO_4, filtered, concentrated *in vacuo*. Purification by flash column chromatography (25 g Sfär, 100%$_{v/v}$ cyclohexane (4 CV), followed by a linear gradient (14 CV): 0%$_{v/v}$ →21%$_{v/v}$ ethyl acetate in cyclohexane, followed by 21%$_{v/v}$ ethyl acetate in cyclohexane (8 CV)) yielded **8** (290 mg, 99%). The analytical data are consistent with those reported.[9]

Amorphous foam; ^{1}H NMR (400 MHz, 298 K, DMSO-d_6): δ = 9.64 (s, 1H, *N11H*), 7.45 – 7.35 (m, 5H, *C29*, *C30H*, *C31H*, *C32H*, *C33H*), 7.31 – 7.26 (m, 2H, *C18H*, *C20H*), 6.98 – 6.90 (m, 3H, *C17H*, *C19H*, *C21H*), 5.42 (s, 1H, *C5H*), 5.21 (m, 2H, *C27H$_2$*), 4.66 (d, *J* = 15.4 Hz, 1H, *C14H*), 4.61 – 4.55 (m, 2H, *C3H*, *C14H*), 3.38 (s, 3H, *C10H$_3$*), 1.45 (s, 3H, *C22H$_3$*), 1.31 ppm (s, 3H, *C23H$_3$*); ^{13}C NMR (101 MHz, 298 K, DMSO-d_6): δ = 168.5, 167.5, 166.9, 157.7, 135.2, 129.3, 128.4 (2C), 128.3, 121.0, 114.5, 94.8, 73.7, 68.0, 66.8, 66.1, 61.7, 52.9, 31.8, 25.4 ppm; IR (film):

$\tilde{\nu}$ = 1774, 1746, 1703, 1598, 1505, 1437, 1316, 1237, 1205, 1186, 1111 cm^{-1}; HRMS (ESI): m/z calculated for $C_{24}H_{26}N_2O_6S$ $[M+Na]^+$: 493.1404, found: 493.1409; $[\alpha]_D^{25}$ = +163 (c = 0.003 g/mL, $CHCl_3$).

Benzyl (2*S*,5*R*,6*S*)-6-methoxy-3,3-dimethyl-7-oxo-6-(2-phenoxyacetamido)-4-thia-1-azabicyclo[3.2.0]heptane-2-carboxylate 4,4-dioxide (9)

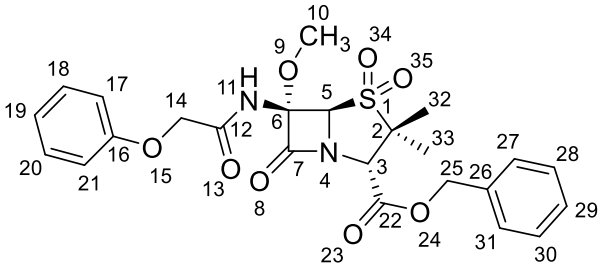

mCPBA (<77% purity; 1.5 equiv., 70 mg) was added at 0 °C to a stirred solution of **7** (100 mg, 0.205 mmol, 1 equiv.) in anhydrous $CHCl_3$ (4 mL). The reaction mixture was further stirred for another 4 h at room temperature, at which point an additional portion of m-CPBA (<77% purity; 23 mg) was added. The reaction mixture was stirred at room temperature for 16 h, before it was diluted with CH_2Cl_2, then sequentially washed with an aqueous solution of $Na_2S_2O_3$ (5% (w/v)), saturated aqueous $NaHCO_3$ solution, water, and brine. The organic layer was dried over Na_2SO_4, filtered, concentrated *in vacuo*. Purification by flash column chromatography (10 g Sfär, 100%$_{v/v}$ cyclohexane (2 CV), followed by a linear gradient (36 CV): 0%$_{v/v}$ →60%$_{v/v}$ ethyl acetate in cyclohexane) yielded **9** (67 mg, 65%).

Amorphous solid; ^{1}H NMR (600 MHz, 298 K, DMSO-*d*$_6$): δ = 7.40 (m, 5H, *C27H*, *C28H*, *C29H*, *C30H*, *C31H*), 7.33 – 7.29 (m, 2H, *C18H*, *C20H*), 7.02 – 6.97 (m, 4H, *N11H*, *C17H*, *C19H*, *C21H*), 5.25 (s, 2H, *C25H*$_2$), 5.02 (s, 1H, *C5H*), 4.32 (d, *J* = 9.7 Hz, 1H, *C14H*), 4.24 (d, *J* = 9.7 Hz, 1H, *C14H*), 3.71 (s, 3H, *C10H*$_3$), 1.52 (s, 3H, *C32H*$_3$), 1.31 ppm (s, 3H, *C33H*$_3$); ^{13}C NMR (151 MHz, 298 K, DMSO-*d*$_6$): δ = 166.1, 157.9, 155.9, 151.9, 135.0, 129.5, 128.51, 128.48, 128.4, 121.3,

115.0, 82.0, 71.6, 70.5, 67.4, 62.3, 60.3, 54.2, 20.6, 17.6, ppm; IR (film): $\tilde{\nu}$ = 1801, 1758, 1701, 1600, 1496, 1464, 1378, 1333, 1217, 1174, 1120, 1070 cm^{-1}; HRMS (ESI): m/z calculated for $C_{24}H_{26}N_2O_8S$ $[M+Na]^+$: 525.1302, found: 525.1297; $[\alpha]_D^{25}$ = +91 (c = 0.012 g/mL, $CHCl_3$).

Benzyl (2*S*,5*R*,6*S*)-6-ethoxy-3,3-dimethyl-7-oxo-6-(2-phenoxyacetamido)-4-thia-1-azabicyclo[3.2.0]heptane-2-carboxylate 4,4-dioxide (10a)

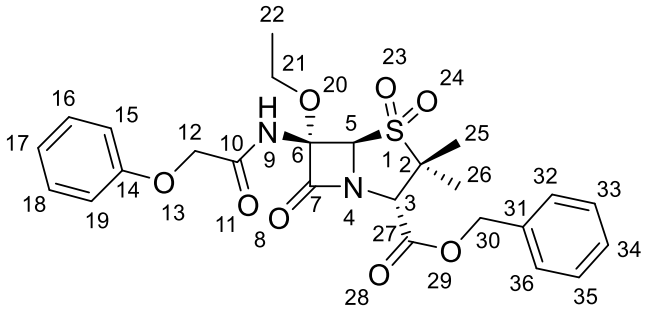

To a solution of **1** (249 mg, 0.53 mmol, 1 equiv.) in anhydrous CH_2Cl_2 (4 mL) cooled to -30 °C was added freshly prepared ^tBuOCl[6] (0.095 mL, 0.84 mmol, 1.6 equiv.), followed by a solution of NaOEt solution in EtOH (3M, 0.19 mL). The solution was stirred for 1 h at -30 °C, before the addition of AcOH (0.16 mL). The mixture was diluted with CH_2Cl_2, and sequentially washed with saturated aqueous $NaHCO_3$ solution, aqueous $Na_2S_2O_3$ (5% (w/v)) solution, and brine. The organic layer was dried over Na_2SO_4, filtered, and concentrated *in vacuo*. Purification by flash column chromatography (10 g Sfär, 100%$_{v/v}$ cyclohexane (2 CV), followed by a linear gradient (30 CV): 0%$_{v/v}$ →30%$_{v/v}$ ethyl acetate in cyclohexane) yielded **10a** (97 mg, 35%).

Amorphous foam; ^{1}H NMR (500 MHz, 298 K, DMSO-d_6): δ = 7.43 – 7.36 (m, 5H, *C32H*, *C33H*, *C34H*, *C35H*, *C36H*), 7.33 – 7.29 (m, 2H, *C16H*, *C18H*), 7.01 – 6.96 (m, 4H, *N9H*, *C15H*, *C17H*, *C19H*), 5.25 (s, 2H, *C30H$_2$*), 5.23 (s, 1H, *C5H*), 5.02 (s, 1H, *C3H*), 4.31 (d, *J* = 9.7 Hz, 1H, *C12H*), 4.21 (d, *J* = 9.7 Hz, 1H, *C12H*), 4.14 – 4.10 (m, 2H, *C21H$_2$*), 1.52 (s, 3H, *C25H$_3$*), 1.31 (s, 3H, *C26H$_3$*), 1.25 ppm (t, *J* = 7.0 Hz, 3H, *C22H$_3$*); ^{13}C NMR (126 MHz, 298 K, DMSO-d_6): δ = 166.1,

158.0, 155.3, 152.0, 135.0, 129.5, 128.5, 128.5, 128.4, 121.3, 114.9, 81.9, 71.6, 70.5, 67.4, 63.0, 62.3, 60.3, 20.6, 17.6, 13.6 ppm; IR (film): $\tilde{\nu}$ = 1797, 1757, 1708, 1693, 1600, 1496, 1454, 1331, 1237, 1215, 1119, 1057, 1010 cm^{-1}; HRMS (ESI): m/z calculated for $C_{25}H_{29}N_2O_8S$ $[M+H]^+$: 517.1639; found: 517.1649; $[\alpha]_D^{25}$ = +159 (c = 0.008 g/mL, $CHCl_3$).

Benzyl (2*S*,5*R*,6*S*)-3,3-dimethyl-7-oxo-6-(((*R*)-2-oxopyrrolidin-3-yl)oxy)-6-(2-phenoxyacetamido)-4-thia-1-azabicyclo[3.2.0]heptane-2-carboxylate 4,4-dioxide (10b)

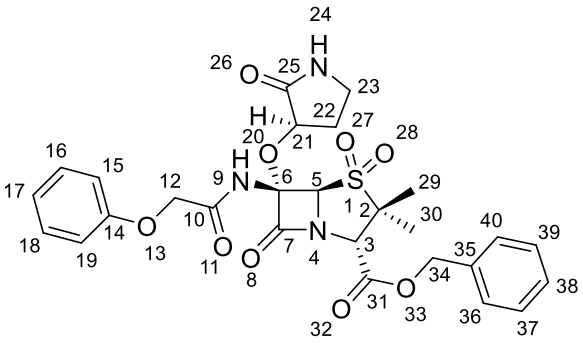

To a solution of **1** (466 mg, 0.99 mmol) in anhydrous tetrahydrofuran (10 mL was added freshly prepared ^{t}BuOCl[6] (0.17 mL, 1.47 mmol) at -30 °C, followed by Et_3N (0.15 mL, 1.08 mmol, 1.1 equiv.) and a solution of (*R*)-3-hydroxypyrrolidin-2-one (1 g, 9.9 mmol, 10 equiv.) in *N*,*N*-dimethylformamide (6 mL). The reaction mixture was stirred for 1 h at -30 °C, before AcOH (0.1 mL) was added. The mixture was diluted with CH_2Cl_2, before it was sequentially washed with saturated aqueous $NaHCO_3$ solution, aqueous $Na_2S_2O_3$ (5% (w/v)) solution, and brine. The organic layer was dried over Na_2SO_4, filtered, concentrated *in vacuo*. Purification by flash column chromatography (25 g Sfär, 100%$_{v/v}$ cyclohexane (3 CV), followed by a linear gradient (9 CV): 0%$_{v/v}$ →45%$_{v/v}$ ethyl acetate in cyclohexane, followed by 45%$_{v/v}$ ethyl acetate in cyclohexane (4 CV)) yielded **10b** (38 mg, 7%).

Amorphous solid; ^{1}H NMR (500 MHz, 298 K, DMSO-d_6): δ = 9.88 (s, 1H, *N9H*), 8.02 (s, 1H, *N24H*), 7.47 – 7.34 (m, 5H, *C36H*, *C37H*, *C38H*, *C39H*, *C40H*), 7.32 – 7.22 (m, 2H, *C16H*, *C18H*), 6.98 – 6.91 (m, 3H, *C15H*, *C17H*, *C19H*), 5.61 (s, 1H, *C5H*), 5.32 (d, *J* = 12.1 Hz, 1H, *C34H*),

5.24 (d, *J* = 12.1 Hz, 1H, *C34H*), 4.73 (s, 1H, *C3H*), 4.68 (d, *J* = 15.7 Hz, 1H, *C12H*), 4.57 (d, *J* = 15.7 Hz, 1H, *C12H*), 4.47 (t, *J* = 8.1 Hz, 1H, *C21H*), 3.22 – 3.18 (m, 1H, *C23H*), 3.10 (m, 1H, *C23H*), 2.32 (m, 1H, *C22H*), 1.90 (m, 1H, *C22H*), 1.40 (s, 3H, *C29H*), 1.25 ppm (s, 3H, *C30H*); ^{13}C NMR (126 MHz, 298 K, DMSO-d_6): δ = 172.9, 170.3, 167.2, 166.3, 157.8, 135.0, 129.4, 128.6, 128.5 (2C), 121.1, 114.6, 90.2, 72.9, 71.4, 67.5, 65.9, 63.4, 61.4, 37.8, 28.8, 19.5, 17.4 ppm; IR (film): $\tilde{\nu}$ = 1802, 1754, 1713, 1599, 1495, 1437, 1332, 1299, 1261, 1216, 1176, 1119, 1086 cm^{-1}; HRMS (ESI): m/z calculated for $C_{27}H_{30}N_3O_9S$ $[M+H]^+$: 572.1697; found: 572.1700; $[\alpha]_D^{25}$ = +79 (c = 0.008 g/mL, $CHCl_3$).

Benzyl (2*S*,5*R*,6*S*)-6-(benzyloxy)-3,3-dimethyl-7-oxo-6-(2-phenoxyacetamido)-4-thia-1-azabicyclo[3.2.0]heptane-2-carboxylate (16c)

To a solution of **12** (900 mg, 1.72 mmol, 1 equiv.) in anhydrous CH_2Cl_2 (0.1 M) was added 2,3-dichloro-5,6-dicyano-1,4-benzoquinone (352 mg, 1.55 mmol, 0.9 equiv.) at room temperature. After stirring the reaction mixture for 1 h, the formed precipitate was removed by filtration.

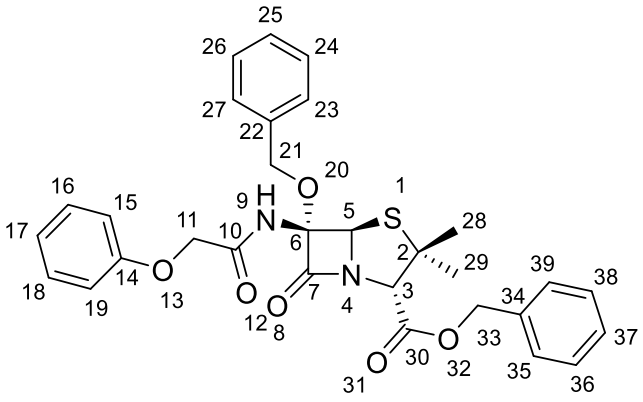

Then, benzyl alcohol (1.71 mL, 17.2 mmol, 10 equiv.) was added to the filtrate, and the solution was stirred at room temperature for 21 h, before the reaction mixture was evaporated *in vacuo*. The presence of intermediate **14c** (benzyl (2*S*,5*R*,6*S*)-6-(benzyloxy)-6-(((*E*)-2,6-di-*tert*-butyl-4-hydroxybenzylidene)amino)-3,3-dimethyl-7-oxo-4-thia-1-azabicyclo[3.2.0]heptane-2-carboxylate) was identified in the crude mixture by ^{1}H NMR analysis, alongside other components and excess benzyl alcohol. The crude mixture was partially purified by flash column

chromatography (25 g Sfär, 100%$_{v/v}$ cyclohexane (3 CV), followed by a linear gradient (33 CV): 0%$_{v/v}$ →10%$_{v/v}$ ethyl acetate in cyclohexane) to yield 350 mg of a mixture consisting of **14c**, benzyl alcohol and non-characterized impurities. This mixture was then dissolved in anhydrous CH_2Cl_2 (10 mL), to which trimethylacetohydrazideammonium chloride (233 mg, 1.39 mmol, 0.8 equiv.) in anhydrous MeOH (4 mL) was added dropwise. The reaction mixture was stirred at room temperature for 3 h, then evaporated *in vacuo*. The residue was redissolved in CH_2Cl_2, and the resulting mixture was washed with H_2O, dried over Na_2SO_4, and concentrated *in vacuo* to yield crude benzyl (2*S*,5*R*,6*S*)-6-amino-6-(benzyloxy)-3,3-dimethyl-7-oxo-4-thia-1-azabicyclo[3.2.0]heptane-2-carboxylate **15c** (312 mg), which was used directly in the next step without any further purification (attempted purification by either column chromatography or recrystallisation resulted in degradation).

The crude mixture of **15c** (312 mg) was dissolved in anhydrous CH_2Cl_2 (5 mL), before dropwise addition of Et_3N (0.74 mL, 5.32 mmol) and phenoxyacetyl chloride (0.52 mL, 3.8 mmol) at 0 °C. The reaction mixture was stirred room temperature for 16 h, after which it was diluted with CH_2Cl_2. The mixture was washed with saturated aqueous $NaHCO_3$ solution and H_2O. The organic layer was dried over Na_2SO_4, filtered, and concentrated *in vacuo*. Purification by flash column chromatography (25 g Sfär, 100%$_{v/v}$ cyclohexane (2 CV), followed by a linear gradient (22 CV): 0%$_{v/v}$ →22%$_{v/v}$ ethyl acetate in cyclohexane) yielded **16c** (120 mg, 12%).

Amorphous foam; ^{1}H NMR (600 MHz, 298 K, DMSO-*d*$_6$): δ = 9.83 (s, 1H, *N9H*), 7.44 – 7.25 (m, 12H, *C16H*, *C18H*, *C23H*, *C24H*, *C25H*, *C26H*, *C27H*, *C35H*, *C36H*, *C37H*, *C38H, C39H*), 6.95 (m, 1H, *C17H*), 6.93 – 6.89 (m, 2H, *C16H*, *C18H*), 5.50 (s, 1H, *C5H*), 5.21 (m, 2H, *C33H*$_2$), 4.73 – 4.65 (m, 2H, *C21H*$_2$), 4.65 – 4.57 (m, 3H, *C3H*, *C11H*$_2$), 1.47 (s, 3H, *C28H*$_3$), 1.32 ppm (s, 3H, *C29H*$_3$); ^{13}C NMR (151 MHz, 298 K, DMSO-*d*$_6$): δ = 168.6, 167.6, 167.0, 157.8, 137.1, 135.2,

129.4, 128.54, 128.51, 128.4, 128.3, 127.8, 127.77, 121.1, 114.6, 94.5, 74.0, 68.0, 67.4, 66.8, 66.1, 61.8, 31.9, 25.4 ppm; IR (film): $\tilde{\nu}$ = 1778, 1746, 1707, 1599, 1495, 1456, 1372, 1310, 1239, 1207, 1186, 1131, 1084, 1067, 1026 cm^{-1}; HRMS (ESI): m/z calculated for $C_{30}H_{31}N_2O_6S$ $[M+H]^+$: 547.1897; found: 547.1897; $[\alpha]_D^{25}$ = +164 (c = 0.007 g/mL, $CHCl_3$).

Benzyl (2*S*,5*R*,6*S*)-6-(benzyloxy)-3,3-dimethyl-7-oxo-6-(2-phenoxyacetamido)-4-thia-1-azabicyclo[3.2.0]heptane-2-carboxylate 4,4-dioxide (17)

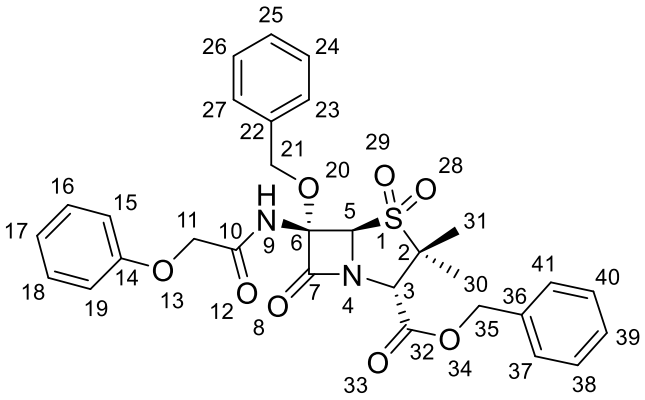

To a stirred solution of **16c** (101 mg, 0.36 mmol, 1 equiv.) in anhydrous CH_2Cl_2 (5 mL), m-CPBA (<77% purity; 116 mg, 0.78 mmol, 2.2 equiv.) was added at 0 °C in portions over 5 min. The reaction mixture was stirred for 1 h at 10 °C, before being stirred at room temperature overnight for 16 h. The reaction mixture was diluted with CH_2Cl_2, washed with aqueous $Na_2S_2O_5$ (10% (w/v)) solution, saturated aqueous $NaHCO_3$ solution, water, and brine. The organic layer was dried over Na_2SO_4, filtered, concentrated *in vacuo*. Purification by flash column chromatography (10 g Sfär, 100%$_{v/v}$ cyclohexane (2 CV), followed by a linear gradient (25 CV): 0%$_{v/v}$ →30%$_{v/v}$ ethyl acetate in cyclohexane) yielded **27** (45 mg, 21%).

Amorphous solid; ^{1}H NMR (500 MHz, 298 K, DMSO-*d*$_6$): δ = 7.42 – 7.33 (m, 12H, *C16H*, *C18H*, *C23H*, *C24H*, *C25H*, *C26H*, *C27H*), 7.09 (s, 1H, *N9H*), 7.03 – 6.97 (m, 3H, *C15H*, *C17H*, *C19H*), 5.29 (s, 1H, *C5H*), 5.24 (m, 2H, *C35H*$_2$), 5.16 – 5.10 (m, 2H, *C21H*$_2$), 5.03 (s, 1H, *C5H*), 4.35 (d, *J* = 9.7 Hz, 1H, *C11H*), 4.27 (d, *J* = 9.7 Hz, 1H, *C11H*), 1.53 (s, 3H, *C31H*$_3$), 1.32 ppm (s, 3H,

C30H₃); ^{13}C NMR (151 MHz, 298 K, DMSO-*d₆*): δ = 166.1, 158.0, 155.2, 151.9, 135.3, 135.0, 129.5, 128.6, 128.50, 128.45, 128.43, 128.4, 121.3, 115.0, 82.1, 71.5, 70.5, 68.4, 67.4, 62.4, 60.3, 20.6, 17.6 ppm; IR (film): ṽ = 1797, 1757, 1708, 1693, 1600, 1496, 1454, 1331, 1237, 1215, 1177, 1119, 1057, 1010 cm^{-1}; HRMS (ESI): m/z calculated for $C_{30}H_{31}N_2O_8S$ $[M+H]^+$: 579.1796, found: 579.1802; $[\alpha]_D^{25}$ = +66 (c = 0.01 g/mL, $CHCl_3$).

Benzyl (2*S*,5*R*,6*S*)-6-methoxy-3,3-dimethyl-7-oxo-6-(2-phenylacetamido)-4-thia-1-azabicyclo[3.2.0]heptane-2-carboxylate 4,4-dioxide (20)

General procedure A[5] was used with penam **19** (1.17 g, 2.56 mmol, 1 equiv.). Purification by flash column chromatography (25 g Sfär, 100%$_{v/v}$ cyclohexane (2 CV), followed by a linear gradient (30 CV): 0%$_{v/v}$ →50%$_{v/v}$ ethyl acetate in cyclohexane) afforded **20** (453 mg, 36%).

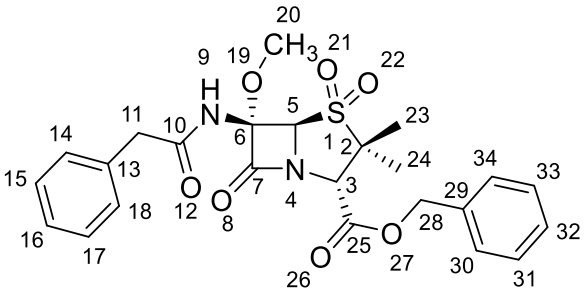

Amorphous solid; ^{1}H NMR (600 MHz, 298 K, DMSO-*d₆*): δ = 9.73 (s, 1H, *N9H*), 7.46 – 7.22 (m, 10H, *C14H*, *C15H*, *C16H*, *C17H*, *C18H*, *C30H*, *C31H*, *C32H*, *C33H*, *C34H*), 5.51 (s, 1H, *C5H*), 5.31 (d, *J* = 12.1 Hz, 1H, *C28H*), 5.24 (d, *J* = 12.1 Hz, 1H, *C28H*), 4.68 (s, 1H, *C3H*), 3.67 (d, *J* = 14.7 Hz, 1H, *C11H*), 3.49 (d, *J* = 14.7 Hz, 1H, *C11H*), 3.31 (s, 3H, *C20H₃*), 1.40 (s, 3H, *C23H₃*), 1.26 ppm (s, 3H, *C24H₃*); ^{13}C NMR (151 MHz, 298 K, DMSO-*d₆*): δ = 172.5, 167.8, 166.4, 135.2, 135.0, 129.3, 128.6, 128.5, 128.2, 126.5, 90.9, 70.3, 67.5, 63.3, 61.4, 52.5, 41.3, 40.1, 19.4, 17.4 ppm; IR (film): ṽ = 3353, 3029, 2938, 1798, 1757, 1698, 1498, 1456, 1334, 1261, 1217, 1174, 1121, 1001 cm^{-1}; HRMS (ESI): m/z calculated for $C_{24}H_{26}N_2O_7SK$ $[M+K]^+$: 525.1092, found: 525.1093; $[\alpha]_D^{25}$ = +107 (c = 0.01 g/mL, $CHCl_3$).

Benzyl (2*S*,*4S*,5*R*,6*S*)-6-methoxy-3,3-dimethyl-7-oxo-6-(2-phenylacetamido)-4-thia-1-azabicyclo[3.2.0]heptane-2-carboxylate 4-oxide (22)

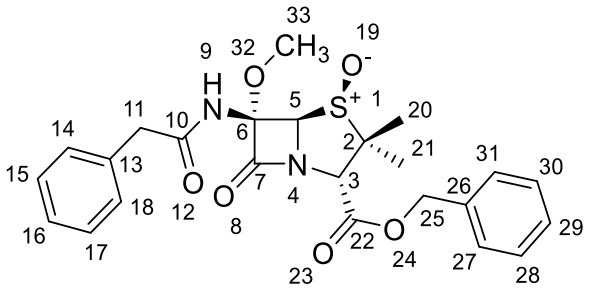

General procedure A[5] was used with penam **21** (750 mg, 1.7 mmol, 1 equiv.). Purification by flash column chromatography (25 g Sfär, 100%$_{v/v}$ cyclohexane (2 CV), followed by a linear gradient (30 CV): 0%$_{v/v}$ →30%$_{v/v}$ ethyl acetate in cyclohexane) afforded **22** (257 mg, 54%).

Amorphous foam; ^{1}H NMR (500 MHz, 298 K, DMSO-*d*$_6$): δ = 9.56 (s, 1H, *N9H*), 7.46 – 7.35 (m, 5H, *C27H*, *C28H*, *C29H*, *C30H*, *C31H*), 7.31 – 7.22 (m, 5H, *C14H*, *C15H*, *C16H*, *C17H*, *C18H*), 5.36 (s, 1H, *C5H*), 5.30 (d, *J* = 12.2 Hz, 1H, *C25H*), 5.22 (d, *J* = 12.2 Hz, 1H, *C25H*), 4.48 (s, 1H, *C3H*), 3.62 (d, *J* = 14.9 Hz, 1H, *C11H*), 3.45 (d, *J* = 14.9 Hz, 1H, *C11H*), 3.29 (s, 3H, *C33H*$_3$), 1.46 (s, 3H, *C20H*$_3$), 1.08 ppm (s, 3H, *C21H*$_3$); ^{13}C NMR (126 MHz, 298 K, DMSO-*d*$_6$): δ = 171.8, 167.7, 167.2, 135.5, 135.2, 129.4, 128.6, 128.6, 128.5, 128.1, 126.4, 90.6, 78.3, 70.4, 67.3, 63.4, 52.2, 41.3, 19.2, 17.7 ppm; IR (film): ṽ = 1789, 1751, 1684, 1522, 1497, 1457, 1377, 1318, 1261, 1215, 1165, 1077, 1057, 1003 cm^{-1}; HRMS (ESI): m/z calculated for $C_{24}H_{26}N_2O_6SNa$ $[M+Na]^+$: 493.1404, found: 493.1402; $[\alpha]_D^{25}$ = +163 (c = 0.02 g/mL, $CHCl_3$)

Benzyl (2*S*,*4R*,5*R*,6*R*)-3,3-dimethyl-7-oxo-6-(2-phenylacetamido)-4-thia-1-azabicyclo[3.2.0]heptane-2-carboxylate 4-oxide (23)

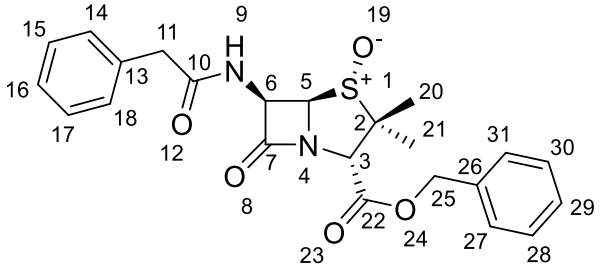

To a solution of penam **18** (1.55 g, 3.65 mmol, 1 equiv.) in tetrahydrofuran (10 mL) were sequentially added 2,6-lutidine (1 mL, 8.6 mmol, 2.4 equiv.), H_2O (1 mL), and freshly prepared ^{t}BuOCl[6] (4 mmol, 0.46 mL, 1.1 equiv.) at -5 °C. The reaction mixture was stirred at -5 °C for 5 min, before addition of an aqueous H_2SO_4 solution (4 mL; 2.5 M). The mixture was then poured into an aqueous HCl solution (100 mL; 1 M), and was extracted with EtOAc (100 mL). The organic layer was separated and washed with saturated aqueous $NaHCO_3$ solution, and brine. The organic layer was then dried over Na_2SO_4, filtered, and concentrated *in vacuo*. Purification by flash column chromatography (25 g Sfär, 100%$_{v/v}$ cyclohexane (2 CV), followed by a linear gradient (23 CV): 0%$_{v/v}$→43%$_{v/v}$ ethyl acetate in cyclohexane, followed by 43%$_{v/v}$ ethyl acetate in cyclohexane (7 CV), followed by a linear gradient (8 CV): 43%$_{v/v}$ →58%$_{v/v}$ ethyl acetate in cyclohexane, followed by 58% ethyl acetate in cyclohexane (10 CV), followed by a linear gradient (3 CV): 58%$_{v/v}$ →90%$_{v/v}$ ethyl acetate in cyclohexane; followed by 90%$_{v/v}$ ethyl acetate in cyclohexane (5 CV)) afforded penam **23** (360 mg, 22%).

Amorphous foam; ^{1}H NMR (500 MHz, 298 K, DMSO-*d*$_6$): δ = 9.26 (d, *J* = 7.4 Hz, 1H, *N9H*), 7.46 – 7.35 (m, 5H, *C27H*, *C28H*, *C29H*, *C30H*, *C31H*), 7.27 (m, 5H, *C14H*, *C15H*, *C16H*, *C17H*, *C18H*), 5.44 (dd, *J* = 7.3, 4.2 Hz, 1H, *C6H*), 5.24 (m, 2H, *C25H*$_2$), 4.77 (d, *J* = 4.3 Hz, 1H, *C5H*), 4.53 (s, 1H, *C3H*), 3.56 (s, 3H), 1.52 (s, 3H, *C20H*$_3$), 1.11 ppm (s, 3H, *C21H*$_3$); ^{13}C NMR (126 MHz, 298 K, DMSO-*d*$_6$): δ = 170.9, 170.8, 167.3, 135.4, 135.2, 129.0, 128.59, 128.55, 128.5, 128.3, 126.6, 78.8, 68.4, 67.2, 64.1, 57.3, 41.4, 23.7, 15.4 ppm; IR (film): $\tilde{\nu}$ = 1793, 1748, 1664,

1526, 1498, 1456, 1347, 1300, 1253, 1199, 1161, 1057 cm^{-1}; HRMS (ESI): m/z calculated for $C_{23}H_{24}N_2O_5SNa$ $[M+Na]^+$: 463.1298, found: 493.1402; $[\alpha]_D^{25}$ = +91 (c = 0.002 g/mL, $CHCl_3$).

Benzyl (2*S*,*4R*,5*R*,6*S*)-6-methoxy-3,3-dimethyl-7-oxo-6-(2-phenylacetamido)-4-thia-1-azabicyclo[3.2.0]heptane-2-carboxylate 4-oxide (3)

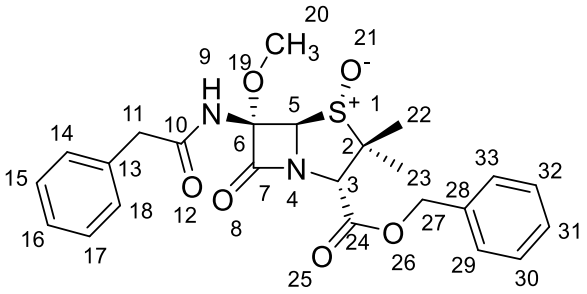

General procedure A^5 was used with penam **23** (190 mg, 0.43 mmol, 1 equiv.). Purification by flash column chromatography (10 g Sfär, 100% cyclohexane (2 CV), followed by a linear gradient (16 CV): $0\%_{v/v} \rightarrow 32\%_{v/v}$ ethyl acetate in cyclohexane, followed by $32\%_{v/v}$ ethyl acetate in cyclohexane (5 CV), followed by a linear gradient (10 CV): $32\%_{v/v} \rightarrow 52\%_{v/v}$ ethyl acetate in cyclohexane, followed by $52\%_{v/v}$ ethyl acetate in cyclohexane (3 CV)) afforded **3** (75 mg, 37%).

Amorphous foam; ^1H NMR (500 MHz, 298 K, DMSO-d_6): δ = 9.92 (s, 1H, *N9H*), 7.45 – 7.23 (m, 10H, *C14H*, *C15H*, *C16H*, *C17H*, *C18H*, *C29H*, *C30H*, *C31H*, *C32H*, *C33H*), 5.23 – 5.17 (m, 2H, $C27H_2$), 4.85 (s, 1H, *C5H*), 4.83 (s, 1H, *C3H*), 3.61 – 3.53 (m, 2H, $C11H_2$), 3.35 (s, 3H, $C20H_3$), 1.21 (s, 3H, $C22H_3$), 1.15 ppm (s, 3H, $C22H_3$); ^{13}C NMR (126 MHz, 298 K, DMSO-d_6): δ = 171.4, 166.9, 166.1, 135.1, 135.0, 129.2, 129.1, 128.5, 128.4, 128.2, 126.6, 93.2, 89.0, 69.1, 67.1, 65.1, 52.9, 41.7, 23.3, 16.4 ppm; IR (film): $\tilde{\nu}$ = 1787, 1737, 1687, 1550, 1523, 1455, 1327, 1159, 1044 cm^{-1}; HRMS (ESI): m/z calculated for $C_{24}H_{26}N_2O_6SK$ $[M+K]^+$: 509.1143, found: 509.1150; $[\alpha]_D^{25}$ = +75 (c = 0.003 g/mL, $CHCl_3$).

(2*S*,5*R*,6*S*)-6-Methoxy-3,3-dimethyl-7-oxo-6-(2-phenylacetamido)-4-thia-1-azabicyclo[3.2.0]heptane-2-carboxylic acid (24)

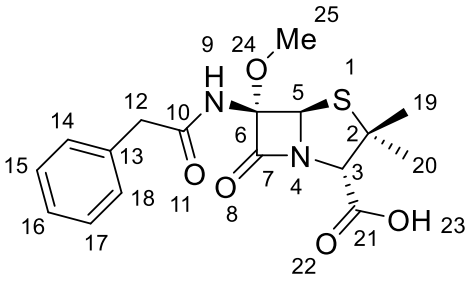

To a solution of commercially-sourced penicillin G sodium (1 g, 2.8 mmol, 1 equiv.) in *N*,*N*-dimethylformamide (14.4 mL) and methanol (2.2 mL) was added dropwise a solution of 1 M LiOMe in MeOH (4.8 mL) at -78 °C, followed by freshly prepared ^{t}BuOCl[6] (0.54 mL, 4.7 mmol, 1.7 equiv.). The reaction mixture was stirred for 15 min at -78°C, before the addition of concentrated H_2SO_4 (0.07 mL). The reaction mixture was warmed to room temperature, before it was diluted with water and acidified to pH 2 by addition of an aqueous H_2SO_4 solution (1 M). The mixture was extracted with $CHCl_3$, and the combined organic extracts were sequentially washed with saturated aqueous LiCl solution, H_2O, and brine. The organic extracts were dried over Na_2SO_4, concentrated *in vacuo*, and purified by reverse-phase flash column chromatography (30 g Sfär C18 D; 100%$_{v/v}$ aqueous formic acid solution (0.1%) in H_2O (10 CV), followed by a linear gradient (20 CV): 0%$_{v/v}$ → 100%$_{v/v}$ aqueous formic acid solution (0.1%) in CH_3CN). The fractions containing the purified **24** were collected and lyophilised to afford the desired product (247 mg, 18%). The analytical data are consistent with those reported.[10]

Amorphous solid; ^{1}H NMR (600 MHz, 298 K, DMSO-*d*$_6$): δ = 9.62 (s, 1H, *N9H*), 7.30 – 7.23 (m, 5H, *C14H*, *C15H*, *C16H*, *C17H*, *C18H*), 5.33 (s, 1H, *C5H*), 4.32 (s, 1H, *C3H*), 3.58 (d, *J* = 13.9 Hz, 1H, *C12H*), 3.50 (d, *J* = 13.9 Hz, 1H, *C12H*), 3.31 (s, 3H, *C25H*$_3$), 1.42 (s, 3H, *C19H*$_3$), 1.38 ppm (s, 3H, *C20H*$_3$); ^{13}C NMR (126 MHz, 298 K, DMSO-*d*$_6$): δ = 170.8, 168.7, 167.9, 135.5, 129.2, 128.1, 126.4, 94.7, 73.5, 68.3, 61.0, 52.7, 41.9, 40.4, 39.7, 31.7, 25.8 ppm; IR (film): $\tilde{\nu}$ = 1780, 1749, 1672, 1661, 1516, 1497, 1457, 1392, 1371, 1300, 1260, 1180, 1100, 1000 cm^{-1}; HRMS

(ESI): m/z calculated for $C_{17}H_{20}N_2O_5SNa$ $[M+Na]^+$: 387.0985; found: 387.0982; $[\alpha]_D^{25}$ = +435 (c = 0.001 g/mL, $CHCl_3$).

Benzyl (2*S*,5*R*,6*S*)-6-methoxy-3,3-dimethyl-7-oxo-6-(2-phenylacetamido)-4-thia-1-azabicyclo[3.2.0]heptane-2-carboxylate (25)

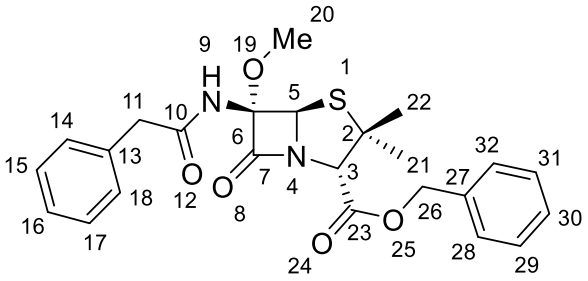

To a solution of **24** (172 mg, 0.47 mmol) in anhydrous *N*,*N*-dimethylformamide (5 mL) at room temperature were sequentially added $NaHCO_3$ (59 mg, 0.7 mmol, 1.5 equiv.), and BnBr (0.08 mL, 0.67 mmol, 1.42 equiv.), and the reaction mixture was stirred for 16 h, and after thin-layer chromatography analysis indicated complete conversion of the starting material, it was poured into ice water and extracted with EtOAc. The organic layer washed with saturated aqueous LiCl solution, saturated aqueous $NaHCO_3$ solution, and brine, then it was dried over Na_2SO_4, filtered, and concentrated *in vacuo*. Purification by flash column chromatography (10 g Sfär, 100%$_{v/v}$ cyclohexane (7 CV), followed by a linear gradient (20 CV): 0%$_{v/v}$ →30%$_{v/v}$ ethyl acetate in cyclohexane) yielded ester **25** (121 mg, 49%). The analytical data are consistent with those reported.[10]

Amorphous solid; ^{1}H NMR (600 MHz, 298 K, DMSO-*d*$_6$): δ = 9.65 (s, 1H, *N9H*), 7.44 – 7.33 (m, 5H, *C14H*, *C15H*, *C16H*, *C17H*, *C18H*), 7.32 – 7.20 (m, 5H, *C28H*, *C29H*, *C30H*, *C31H*, *C32H*), 5.36 (s, 1H, *C5H*), 5.20 (m, 2H, *C26H*$_2$), 4.55 (s, 1H, *C3H*), 3.58 (d, *J* = 14.1 Hz, 1H, *C11H*), 3.50 (d, *J* = 14.1 Hz, 1H, *C11H*), 3.31 (s, 3H, *C20H*$_3$), 1.40 (s, 3H, *C22H*$_3$), 1.27 ppm (s, 3H, *C21H*$_3$); ^{13}C NMR (151 MHz, 298 K, DMSO-*d*$_6$): δ = 170.8, 167.9, 167.0, 135.4, 135.2, 129.2, 128.5, 128.5, 128.4, 128.1, 126.5, 94.9, 73.7, 67.9, 66.8, 61.4, 52.7, 41.9, 31.8, 25.4 ppm; IR (film): ṽ = 1777,

1749, 1686, 1647, 1522, 1498, 1458, 1375, 1261, 1208, 1065 cm^{-1}; HRMS (ESI): m/z calculated for $C_{24}H_{27}N_2O_5S$ $[M+H]^+$: 455.1635, found: 455.1633; $[\alpha]_D^{25}$ = +165 (c = 0.002 g/mL, $CHCl_3$).

Benzyl (2*S*,5*R*,6*S*)-6-methoxy-3,3-dimethyl-7-oxo-4-thia-1-azabicyclo[3.2.0]heptane-2-carboxylate (26a)

General procedure B[7] was used with penam **11** (1.6 g, 3.34 mmol) and MeOH (14 mL) as the solvent. Purification by flash column chromatography (25 g Sfär, 100%$_{v/v}$ cyclohexane (2 CV), followed by a linear gradient (20 CV): 0%$_{v/v}$ →20%$_{v/v}$ ethyl acetate in cyclohexane) yielded **26a** (383 mg, 1.19 mmol, 37%). The analytical data are consistent with those reported.[11]

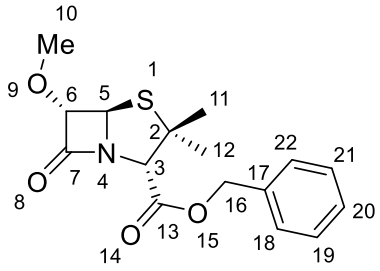

Yellow oil; ^{1}H NMR (400 MHz, 298 K, $CDCl_3$): δ = 7.38 – 7.36 (m, 5H, *C18H*, *C19H*, *C20H*, *C21H*, *C22H*), 5.31 (d, *J* = 1.4 Hz, 1H, *C6H*), 5.19 (m, 2H, *C16H$_2$*), 4.58 (d, *J* = 1.4 Hz, 1H, *C5H*), 4.52 (s, 1H, *C3H*), 3.53 (s, 3H, *C10H$_3$*), 1.54 (s, 3H, *C11H$_3$*), 1.39 ppm (s, 3H, *C12H$_3$*); ^{13}C NMR (101 MHz, 298 K, $CDCl_3$): δ = 169.5, 167.4, 134.9, 128.8, 128.8, 92.7, 77.4, 69.1, 68.6, 67.5, 64.5, 57.9, 33.9, 25.8 ppm; IR (film): $\tilde{\nu}$ = 2931, 2359, 1781, 1746, 1684, 1543, 1499, 1456, 1373, 1286, 1206, 1128, 1082, 1040 cm^{-1}; HRMS (ESI): m/z calculated for $C_{16}H_{19}NO_4S$ $[M+Na]^+$: 344.0927, found: 344.0932; $[\alpha]_D^{25}$ = +96 (0.012 g/mL, $CHCl_3$).

Benzyl (2*S*,5*R*,6*S*)-6-ethoxy-3,3-dimethyl-7-oxo-4-thia-1-azabicyclo[3.2.0]heptane-2-carboxylate (26b)

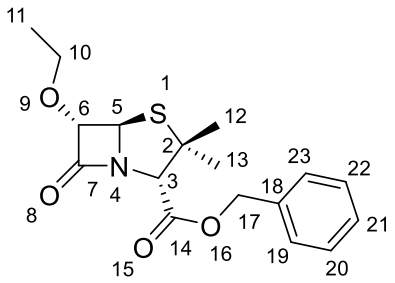

General procedure B[7] was used with penam **11** (1.6 g, 3.34 mmol) and EtOH (15 mL) as the solvent. Purification by flash column chromatography (25 g Sfär, 100%$_{v/v}$ cyclohexane (2 CV), followed by a linear gradient (20 CV): 0%$_{v/v}$ →20%$_{v/v}$ ethyl acetate in cyclohexane) yielded **26b** (323 mg, 0.96 mmol, 36%). The analytical data are consistent with those reported.[12]

Yellow oil; ^{1}H NMR (500 MHz, 298 K, DMSO-*d*$_6$): δ = 7.45 – 7.34 (m, 5H, *C19H*, *C20H*, *C21H*, *C22H*, *C23H*), 5.27 (d, *J* = 1.3 Hz, 1H, *C6H*), 5.20 (s, 2H, *C17H*$_2$), 4.73 (d, *J* = 1.4 Hz, 1H, *C5H*), 4.62 (s, 1H, *C3H*), 3.64 (q, *J* = 7.0 Hz, 2H, *C10H*$_2$), 1.49 (s, 3H, *C12H*$_3$), 1.33 (s, 3H, *C13H*$_3$), 1.15 ppm (t, *J* = 7.0 Hz, 3H, *C11H*$_3$); ^{13}C NMR (126 MHz, 298 K, DMSO-*d*$_6$): δ = 169.4, 167.1, 135.3, 128.6, 128.5, 128.4, 89.9, 68.4, 68.3, 66.8, 65.6, 64.1, 32.4, 25.2, 15.0 ppm; IR (film): $\tilde{\nu}$ = 1779, 1747, 1560, 1578, 1391, 1354, 1299, 1202 cm^{-1}; HRMS (ESI): m/z calculated for $C_{17}H_{22}NO_4S$ $[M+H]^+$: 336.1264, found: 336.1267; $[\alpha]_D^{25}$ = +110 (c = 0.013 g/mL, $CHCl_3$).

Benzyl (2*S*,5*R*,6*S*)-6-(*iso*-propoxy)-3,3-dimethyl-7-oxo-4-thia-1-azabicyclo[3.2.0]heptane-2-carboxylate (26c)

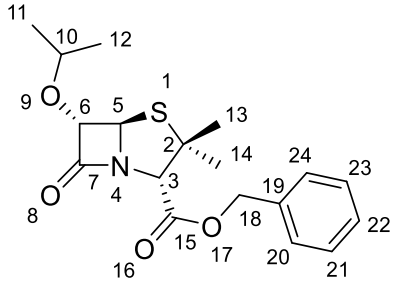

General procedure B[7] was used with penam **11** (1.6 g, 3.34 mmol) and ^{i}PrOH (15 mL) as the solvent. Purification by flash column chromatography (25 g Sfär, 100%$_{v/v}$ cyclohexane (2 CV), followed by a linear gradient (20 CV): 0%$_{v/v}$ →20%$_{v/v}$ ethyl acetate in cyclohexane) yielded **26c** (288 mg, 0.82 mmol, 36%).

Yellow oil; ^{1}H NMR (600 MHz, 298 K, DMSO-*d*$_6$): 7.44 – 7.33 (m, 5H, *C20H*, *C21H*, *C22H*, *C23H*, *C24H*), 5.20 (s, 2H, *C18H*$_2$), 5.17 (d, *J* = 1.4 Hz, 1H, *C6H*), 4.74 (d, *J* = 1.4 Hz, 1H, *C5H*), 4.62 (s, 1H, *C3H*), 3.84 (m, 1H, *C10H*), 1.49 (s, 3H, *C13H*$_3$), 1.34 (s, 3H, *C14H*$_3$), 1.15 (d, *J* = 6.1 Hz, 3H, *C11H*$_3$), 1.12 ppm (d, *J* = 6.1 Hz, 3H, *C12H*$_3$); ^{13}C NMR (151 MHz, 298 K, DMSO-*d*$_6$): δ = 169.7, 167.1, 135.3, 128.6, 128.5, 128.4, 88.7, 72.9, 69.7, 68.3, 66.8, 64.0, 32.4, 25.2, 22.3, 22.1 ppm; IR (film): $\tilde{\nu}$ = 1781, 1748, 1464, 1377, 1301, 1260, 1203, 1185, 1129, 1027 cm^{-1}; HRMS (ESI): m/z calculated for $C_{18}H_{23}NO_4SNa$ $[M+Na]^+$: 372.1240; found: 372.1246; $[\alpha]_D^{25}$ = +145 (c = 0.003 g/mL, $CHCl_3$).

Benzyl (2*S*,5*R*,6*S*)-6-(*tert*-butoxy)-3,3-dimethyl-7-oxo-4-thia-1-azabicyclo[3.2.0]heptane-2-carboxylate (26d)

General procedure B[7] was used with penam **11** (1.6 g, 3.34 mmol) and ^{t}BuOH (15 mL) as the solvent. Purification by flash column chromatography (25 g Sfär, 100%$_{v/v}$ cyclohexane (2 CV), followed by a linear gradient (20 CV): 0%$_{v/v}$ →20%$_{v/v}$ ethyl acetate in cyclohexane) yielded **26d** (285 mg, 0.78 mmol, 35%).

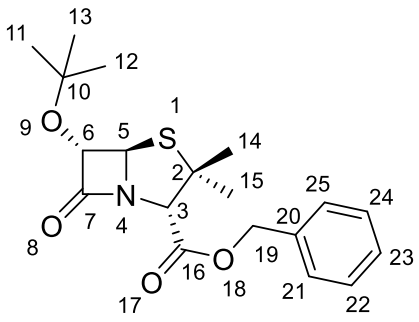

Yellow oil; ^{1}H NMR (500 MHz, 298 K, DMSO-*d*$_6$): δ = 7.44 – 7.33 (m, 5H, *C21H*, *C22H*, *C23H*, *C24H*, *C25H*), 5.20 (s, 2H, *C19H*$_2$), 5.12 (d, *J* = 1.4 Hz, 1H, *C6H*), 4.77 (d, *J* = 1.4 Hz, 1H, *C5H*), 4.62 (s, 1H, *C3H*), 1.51 (s, 3H, *C14H*$_3$), 1.34 (s, 3H, *C15H*$_3$), 1.18 ppm (s, 9H, *C11H*$_3$, *C12H*$_3$, *C13H*$_3$); ^{13}C NMR (126 MHz, 298 K, DMSO-*d*$_6$): δ = 170.2, 167.1, 135.3, 128.6, 128.5, 128.4, 84.5, 76.0, 70.9, 68.4, 66.8, 63.9, 32.5, 27.5, 25.3 ppm; IR (film): $\tilde{\nu}$ = 1782, 1749, 1458, 1392,

1370, 1301, 1262, 1238, 1181.33, 1119, 1090, 1025 cm^{-1}; HRMS (ESI): m/z calculated for $C_{19}H_{25}NO_4S$ $[M+Na]^+$: 386.1397, found: 386.1402; $[\alpha]_D^{25}$ = +42 (c = 0.008 g/mL, $CHCl_3$).

Benzyl (2*S*,5*R*,6*S*)-3,3-dimethyl-7-oxo-6-phenoxy-4-thia-1-azabicyclo[3.2.0]heptane-2-carboxylate (26e)

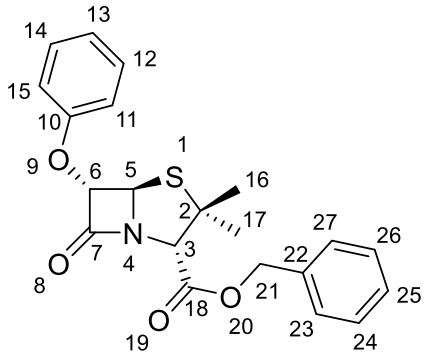

General procedure B[7] was applied using penam **11** (1.6 g, 3.34 mmol) and PhOH (470 mg, 5 mmol). Purification by flash column chromatography (25 g Sfär, 100%$_{v/v}$ cyclohexane (3 CV), followed by a linear gradient (25 CV): 0%$_{v/v}$ →20%$_{v/v}$ ethyl acetate in cyclohexane) resulted in partial purification. The fractions enriched in **26e** were combined and concentrated *in vacuo*, and the obtained oil was then purified a second time by flash column chromatography (25 g Sfär, 100%$_{v/v}$ cyclohexane (3 CV), followed by a linear gradient (13 CV): 0%$_{v/v}$ →3%$_{v/v}$ acetone in cyclohexane, followed by a linear gradient (7 CV): 3%$_{v/v}$ →10%$_{v/v}$ acetone in cyclohexane) to yield **26e** (178 mg, 15%).

Colourless oil; ^{1}H NMR (400 MHz, 298 K, $CDCl_3$): δ = 7.40 – 7.36 (m, 5H, *C23H*, *C24H*, *C25H*, *C26H*, *C27H*), 7.34 – 7.30 (m, 2H, *C12H*, *C14H*), 7.07 – 7.02 (m, 1H, *C13H*), 6.96 – 6.91 (m, 2H, *C11H*, *C15H*), 5.39 (d, *J* = 1.4 Hz, 1H, *C6H*), 5.24 – 5.16 (m, 3H, *C5H*, *C21H$_2$*), 4.60 (s, 1H, *C3H*), 1.61 (s, 3H, *C16H$_3$*), 1.43 ppm (s, 3H, *C17H$_3$*); ^{13}C NMR (126 MHz, 298 K, $CDCl_3$): δ = 167.9, 167.2, 157.0, 134.9, 130.0, 128.88, 128.87, 128.82, 122.7, 115.4, 88.6, 69.6, 69.4, 67.6, 64.5, 34.2, 25.7 ppm; IR (film): $\tilde{\nu}$ = 2360, 2341, 1800, 1757, 1630, 1579, 1501, 1464, 1423, 1383, 1320, 1286, 1194, 1159, 1118, 1089 cm^{-1}; HRMS (ESI): m/z calculated for $C_{21}H_{22}NO_4S$ $[M+H]^+$: 384.1264, found: 384.1259; $[\alpha]_D^{25}$ = +94 (0.004 g/mL, $CHCl_3$).

Benzyl (2*S*,5*R*,6*S*)-6-(benzyloxy)-3,3-dimethyl-7-oxo-4-thia-1-azabicyclo[3.2.0]heptane-2-carboxylate (26f)

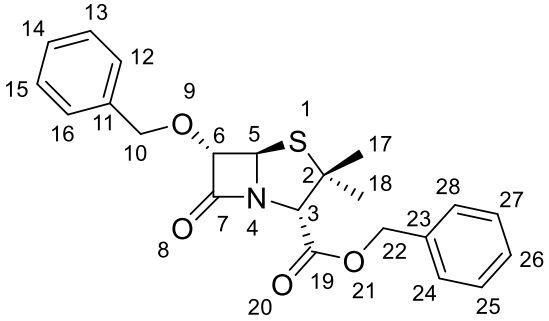

General procedure B[7] was used with penam **11** (1.6 g, 3.34 mmol) and BnOH (15 mL) as the solvent. Purification by flash column chromatography (25 g Sfär, 100%$_{v/v}$ cyclohexane (5 CV), followed by a linear gradient (40 CV): 0%$_{v/v}$ →10%$_{v/v}$ ethyl acetate in cyclohexane) yielded **26f** (221 mg, 0.55 mmol, 18%).

Colourless oil; ^{1}H NMR (400 MHz, 298 K, $CDCl_3$): δ = 7.39 – 7.33 (m, 10H, *C12H*, *C13H*, *C14H*, *C15H*, *C16H*, *C24H*, *C25H*, *C26H*, *C27H*, *C28H*), 5.17 (m, 2H, *C22H$_2$*), 5.15 (d, *J* = 1.4 Hz, 1H, *C6H*), 4.79 (d, *J* = 11.5 Hz, 1H, *C10H*), 4.67 (d, *J* = 1.4 Hz, 1H, *C5H*), 4.63 (d, *J* = 11.5 Hz, 1H, *C10H*), 4.50 (s, 1H, *C3H*), 1.52 (s, 3H, *C17H$_3$*), 1.36 ppm (s, 3H, *C18H$_3$*); ^{13}C NMR (126 MHz, 298 K, $CDCl_3$): δ = 169.5, 167.4, 136.4, 134.9, 128.83, 128.82 (2 C), 128.75, 128.6, 128.5, 91.1, 73.2, 69.4, 69.1, 67.5, 64.3, 34.0, 25.7 ppm; IR (film): ṽ = 2963, 1779, 1746, 1498, 1455, 1372, 1352, 1302, 1261, 1203, 1182, 1156, 1124, 1090, 1026 cm^{-1}; HRMS (ESI): m/z calculated for $C_{22}H_{23}NO_4S$ $[M+Na]^+$: 420.1240, found: 420.1244; $[\alpha]_D^{25}$ = +143 (c = 0.008 g/mL, $CHCl_3$);

Benzyl (2*S*,5*R*,6*S*)-6-methoxy-3,3-dimethyl-7-oxo-4-thia-1-azabicyclo[3.2.0]heptane-2-carboxylate 4,4-dioxide (27a)

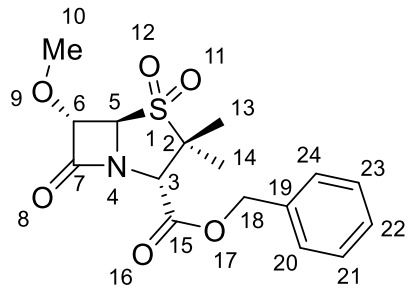

General procedure C[1] was used with penam **26a** (115 mg, 0.358 mmol), yielding after work-up crude **27a** (95 mg). A portion of **27a** (25 mg) was purified by reverse phase flash column chromatography (6 g Sfär C18 D; 100%$_{v/v}$ aqueous

formic acid solution (0.1%) in H_2O (3 CV), followed by a linear gradient (16 CV): 0%$_{v/v}$ → 100%$_{v/v}$ aqueous formic acid solution (0.1%) in CH_3CN). The collected fractions containing product were lyophilised to yield **27a** (16 mg).

Amorphous solid; ^{1}H NMR (500 MHz, 298 K, DMSO-*d*$_6$): δ = 7.45 – 7.36 (m, 5H, *C20H*, *C21H*, *C22H*, *C23H*, *C24H*), 5.49 (d, *J* = 1.3 Hz, 1H, *C6H*), 5.32 – 5.21 (m, 2H, *C18H*$_2$), 5.05 (d, *J* = 1.3 Hz, 1H, *C5H*), 4.73 (s, 1H, *C3H*), 3.47 (s, 3H, *C10H*$_3$), 1.43 (s, 3H, *C13H*$_3$), 1.28 ppm (s, 3H, *C14H*$_3$); ^{13}C NMR (126 MHz, 298 K, DMSO-*d*$_6$): δ = 169.0, 166.4, 135.0, 128.57, 128.56, 128.54 83.5, 67.5, 65.7, 62.9, 61.7, 57.6, 19.3, 17.4 ppm; IR (film): ṽ = 2358, 2335, 1802, 1753, 1458, 1324, 1284, 1217, 1191, 1118, 1087 cm^{-1}; HRMS (ESI): m/z calculated for $C_{16}H_{19}NO_6SNa$ $[M+Na]^+$: 376.0825, found: 376.0833; $[\alpha]_D^{25}$ = +157 (c = 0.009 g/mL, $CHCl_3$).

Benzyl (2*S*,5*R*,6*S*)-6-ethoxy-3,3-dimethyl-7-oxo-4-thia-1-azabicyclo[3.2.0]heptane-2-carboxylate 4,4-dioxide (27b)

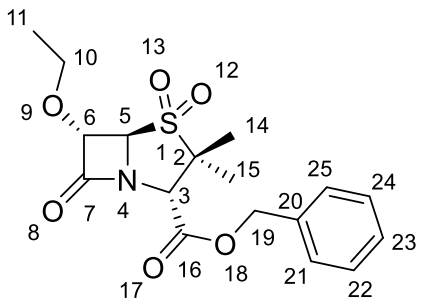

General procedure C[1] was used with penam **26b** (100 mg, 0.298 mmol), yielding after work-up crude **27b** (85 mg). A portion of **27b** (10 mg) was further purified by reverse phase flash column chromatography (6 g Sfär C18 D; 100%$_{v/v}$ aqueous formic acid solution (0.1%) in H_2O (3 CV), followed by a linear gradient (10 CV): 0%$_{v/v}$ → 100%$_{v/v}$ aqueous formic acid solution (0.1%) in CH_3CN). The collected fractions containing product were lyophilised to yield **27b** (4 mg). The analytical data are consistent with those reported.[12]

Amorphous solid; ^{1}H NMR (600 MHz, 298 K, DMSO-*d*$_6$): δ = 7.46 – 7.36 (m, 5H, *C21H*, *C22H*, *C23H*, *C24H*, *C25H*), 5.43 (d, *J* = 1.3 Hz, 1H, *C6H*), 5.29 (d, *J* = 12.2 Hz, 1H, *C19H*), 5.23 (d, *J*

= 12.2 Hz, 1H, *C19H*), 5.05 (d, *J* = 1.3 Hz, 1H, *C5H*), 4.72 (s, 1H, *C3H*), 3.75 (m, 1H, *C10H*), 3.64 (m, 1H, *C10H*), 1.43 (s, 3H, $C14H_3$), 1.27 (s, 3H, $C15H_3$), 1.18 ppm (t, *J* = 7.0 Hz, 3H, $C11H_3$); ^{13}C NMR (151 MHz, 298 K, DMSO-d_6): δ = 169.2, 166.4, 135.0, 128.6 (2 C), 128.5, 82.2, 67.5, 66.4, 66.3, 62.9, 61.7, 19.2, 17.4, 14.7 ppm; IR (film): ṽ = 1799, 1757, 1559, 1460, 1376, 1322, 1286, 1195, 1159, 1118, 1089, 1041 cm^{-1}; HRMS (ESI): m/z calculated for $C_{17}H_{21}NO_6SNa$ $[M+Na]^+$: 390.0982, found: 390.0976; $[\alpha]_D^{25}$ = +113 (c = 0.007 g/mL, $CHCl_3$).

Benzyl (2*S*,5*R*,6*S*)-6-(*iso*-propoxy)-3,3-dimethyl-7-oxo-4-thia-1-azabicyclo[3.2.0]heptane-2-carboxylate 4,4-dioxide (27c)

General procedure C[1] was used with penam **26c** (100 mg, 0.286 mmol). After work-up, no further purification was required, yielding the product **27c** (42 mg, 38%).

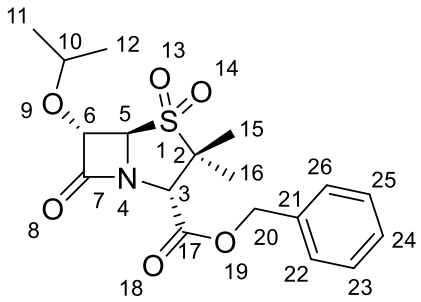

Amorphous solid; ^{1}H NMR (500 MHz, 298 K, $CDCl_3$): δ = 7.41 – 7.35 (m, 5H, *C22H*, *C23H*, *C24H*, *C25H*, *C26H*), 5.28 (d, *J* = 12.0 Hz, 1H, *C20H*), 5.19 (d, *J* = 12.0 Hz, 1H, *C20H*), 5.02 (d, *J* = 1.5 Hz, 1H, *C6H*), 4.53 (d, *J* = 1.5 Hz, 1H, *C5H*), 4.39 (s, 1H, *C3H*), 3.87 (m, 1H, *C10H*), 1.52 (s, 3H, $C15H_3$), 1.29 – 1.22 ppm (m, 9H, $C16H_3$, $C11H_3$, $C12H_3$); ^{13}C NMR (126 MHz, 298 K, $CDCl_3$): δ = 169.6, 166.5, 134.5, 129.2, 129.02, 128.98, 82.7, 75.4, 69.4, 68.4, 63.5, 62.8, 22.6, 22.1, 20.0, 18.8 ppm; IR (film): ṽ = 1799, 1757, 1458, 1381, 1320, 1285, 1193, 1159, 1117, 1088 cm^{-1}; HRMS (ESI): m/z calculated for $C_{18}H_{23}NO_6SNa$ $[M+Na]^+$: 404.1138, found: 404.1141; $[\alpha]_D^{25}$ = +133 (c = 0.007 g/mL, $CHCl_3$).

Benzyl (2*S*,5*R*,6*S*)-6-(*tert*-butoxy)-3,3-dimethyl-7-oxo-4-thia-1-azabicyclo[3.2.0]heptane-2-carboxylate 4,4-dioxide (27d)

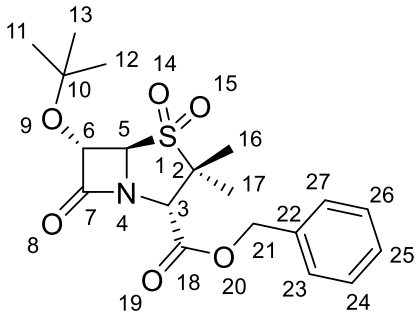

General procedure C[1] was used with penam **26d** (81 mg, 0.223 mmol). After work-up, no further purification was required, yielding the product **27d** (46 mg, 55%).

Amorphous solid; ^{1}H NMR (400 MHz, 298 K, $CDCl_3$): δ = 7.40 – 7.37 (m, 5H, *C23H*, *C24H*, *C25H*, *C26H*, *C27H*), 5.28 (d, *J* = 12.0 Hz, 1H, *C21H*), 5.19 (d, *J* = 12.0 Hz, 1H, *C21H*), 5.13 (d, *J* = 1.5 Hz, 1H, *C6H*), 4.49 (d, *J* = 1.5 Hz, 1H, *C5H*), 4.38 (s, 1H, *C3H*), 1.52 (s, 3H, *C16H$_3$*), 1.29 (s, 9H, *C11H$_3$*, *C12H$_3$*, *C13H$_3$*), 1.26 ppm (s, 3H, *C17H$_3$*); ^{13}C NMR (126 MHz, 298 K, $CDCl_3$): δ = 170.2, 166.5, 134.5, 129.2, 129.01, 128.97, 78.0, 77.6, 70.3, 68.3, 63.6, 62.8, 27.7, 20.0, 18.9 ppm; IR (film): $\tilde{\nu}$ = 1800, 1758, 1463, 1372, 1321, 1285, 1186, 1116, 1090 cm^{-1}; HRMS (ESI): m/z calculated for $C_{19}H_{25}NO_6SK$ $[M+K]^+$: 434.1034, found: 434.1043; $[\alpha]_D^{25}$ = +130 (c = 0.003 g/mL, $CHCl_3$).

Benzyl (2*S*,5*R*,6*S*)-3,3-dimethyl-7-oxo-6-phenoxy-4-thia-1-azabicyclo[3.2.0]heptane-2-carboxylate 4,4-dioxide (27e)

General procedure C[1] was used with penam **26e** (137 mg, 0.357 mmol). Purification by flash column chromatography (10 g Sfär, 100%$_{v/v}$ cyclohexane (0 CV), followed by a linear gradient (40 CV): 0%$_{v/v}$ →10%$_{v/v}$ ethyl acetate in cyclohexane) yielded **27e** (42 mg, 28%).

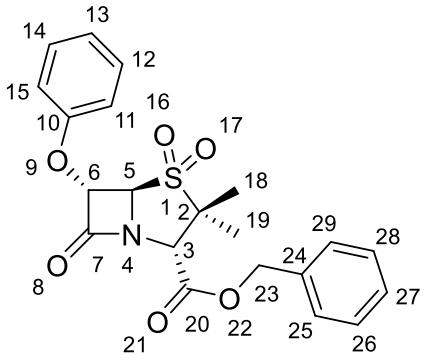

Colourless oil; ^{1}H NMR (500 MHz, 298 K, $CDCl_3$): δ = 7.42 – 7.37 (m, 5H, *C25H*, *C26H*, *C27H*, *C28H*, *C29H*), 7.37 – 7.32 (m, 2H, *C12H*, *C14H*), 7.09 (m, 1H, *C13H*), 7.03 – 6.98 (m, 2H, *C11H*, *C15H*), 5.60 (d, *J* = 1.5 Hz, 1H, *C6H*), 5.31 (d, *J* = 12.0 Hz, 1H, *C23H*), 5.21 (d, *J* = 12.0 Hz, 1H, *C23H*), 4.73 (d, *J* = 1.5 Hz, 1H, *C5H*), 4.49 (s, 1H, *C3H*), 1.57 (s, 3H, *C18H$_3$*), 1.29 ppm (s, 3H, *C19H$_3$*); ^{13}C NMR (126 MHz, 298 K, $CDCl_3$): δ = 167.5, 166.3, 156.5, 134.4, 130.2, 129.2, 129.04, 129.02, 123.5, 115.4, 81.1, 68.5, 68.3, 63.7, 63.1, 20.0, 18.8 ppm; IR (film): $\tilde{\nu}$ = 2361, 2340, 1805, 1758, 1599, 1496, 1458, 1324, 1290, 1236, 1192, 1119, 1088 cm^{-1}; HRMS (ESI): m/z calculated for $C_{21}H_{21}NO_6SNa$ $[M+Na]^+$: 438.0982, found: 438.0983; $[\alpha]_D^{25}$ = +106 (c = 0.008 g/mL, $CHCl_3$).

Benzyl (2*S*,5*R*,6*S*)-6-(benzyloxy)-3,3-dimethyl-7-oxo-4-thia-1-azabicyclo[3.2.0]heptane-2-carboxylate 4,4-dioxide (27f)

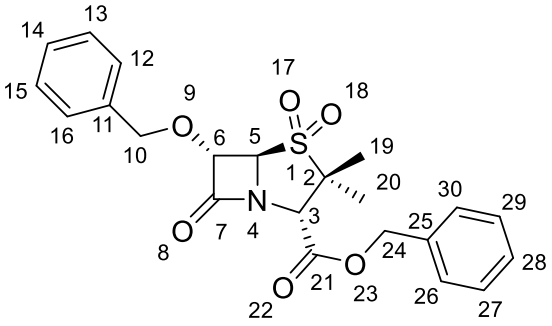

General procedure C[1] was used with penam **26f** (105 mg, 0.264 mmol), yielding after work-up crude **27f** (76 mg, 67%). A portion (20 mg) was purified by reverse phase flash column chromatography (6 g Sfär C18 D; 100%$_{v/v}$ aqueous formic acid solution (0.1%) (3 CV), followed by a linear gradient (10 CV): 0%$_{v/v}$ → 100%$_{v/v}$ aqueous formic acid solution (0.1%) in CH_3CN). The fractions containing product were lyophilised to yield **27f** (8 mg).

Amorphous solid; ^{1}H NMR (500 MHz, 298 K, DMSO-*d*$_6$): δ = 7.46 – 7.33 (m, 10H, *C12H*, *C13H*, *C14H*, *C15H*, *C16H*, *C26H*, *C27H*, *C28H*, *C29H*, *C30H*), 5.42 (d, *J* = 1.3 Hz, 1H, *C6H*), 5.30 (d, *J* = 12.1 Hz, 1H, *C24H*), 5.23 (d, *J* = 12.1 Hz, 1H, *C24H*), 5.15 (d, *J* = 1.3 Hz, 1H, *C5H*), 4.77 (d, *J* = 11.1 Hz, 1H, *C10H*), 4.74 (s, 1H, *C3H*), 4.69 (d, *J* = 11.1 Hz, 1H, *C10H*), 1.42 (s, 3H, *C19H*$_3$), 1.27 ppm (s, 3H, *C20H*$_3$); ^{13}C NMR (126 MHz, 298 K, DMSO-*d*$_6$): δ = 169.0, 166.4, 136.1, 135.0, 128.6, 128.55, 128.50, 128.35, 128.3, 82.0, 72.4, 67.5, 66.5, 62.9, 61.7, 19.2, 17.4; IR (film): ṽ = 2925, 1799, 1757, 1498, 1457, 1322, 1287, 1191, 1117, 1088 cm^{-1}; HRMS (ESI): m/z calculated for $C_{22}H_{23}NO_6SNa$ $[M+Na]^+$: 452.1138, found: 452.1143; $[\alpha]_D^{25}$ = +129 (c = 0.008 g/mL, $CHCl_3$).

8.1.4 References

1. T. R. Malla, et al., Penicillin Derivatives Inhibit the SARS-CoV-2 Main Protease by Reaction with Its Nucleophilic Cysteine, *J. Med. Chem.*, 2022, **65**, 7682–7696.
2. *CA Pat.,* CA 1040620 A, 1978.
3. H. Kamachi, et al., Direct introduction of a formamido group into the 7α(6α)-position of cephalosporins (pencillins), *J. Antibiot.*, 1990, **43**, 820–829.
4. A. W. Chow, et al., Penicillin Sulfoxides and Sulfones, *J. Org. Chem.*, 1962, **27**, 1381–1383.
5. J. E. Baldwin, et al., Direct 6-methoxylation of penicillin derivatives. Convenient pathway to substituted .beta.-lactam antibiotics, *J. Am. Chem. Soc.*, 1973, **95**, 2401–2403.
6. M. Benz, et al., Synthesis and Characterization of Binary, Highly Endothermic, and Extremely Sensitive 2,2′-Azobis(5-azidotetrazole), *J. Am. Chem. Soc.*, 2022, **144**, 6143–6147.
7. P. J. Giddings, et al., Preparation of 6α-monosubstituted and 6,6-disubstituted penicillanates from 6-diazopenicillanates: Reactions of 6-diazopenicillanates with alcohols, thiols, phenylseleninyl compounds, and allylic sulphides, and their analogues, *J. Chem. Soc., Perkin Trans. 1*, 1982, 2757–2766.
8. B. M. Sadeghpour, et al., Synthesis of 6β-methoxy-6α-hydroxymethylpenems, *Tetrahedron*, 1995, **51**, 10723–10730.
9. Y. S. Lo, et al., 6.alpha.-Substituted penicillins, *J. Org. Chem.*, 1975, **40**, 191–192.
10. T. Jen, et al., Stereospecific synthesis of C-6(7) methoxypenicillin and cephalosporin derivatives, *J. Org. Chem.*, 1973, **38**, 2857–2859.
11. J. A. Aimetti, et al., Stereoselective synthesis of 6β-substituted penicillanates, *Tetrahedron Lett.*, 1979, **20**, 4631–4634.
12. *US Pat.,* US 4847247 A, 1989.

8.1.5 ^{1}H and ^{13}C NMR spectra of the compounds prepared for this study

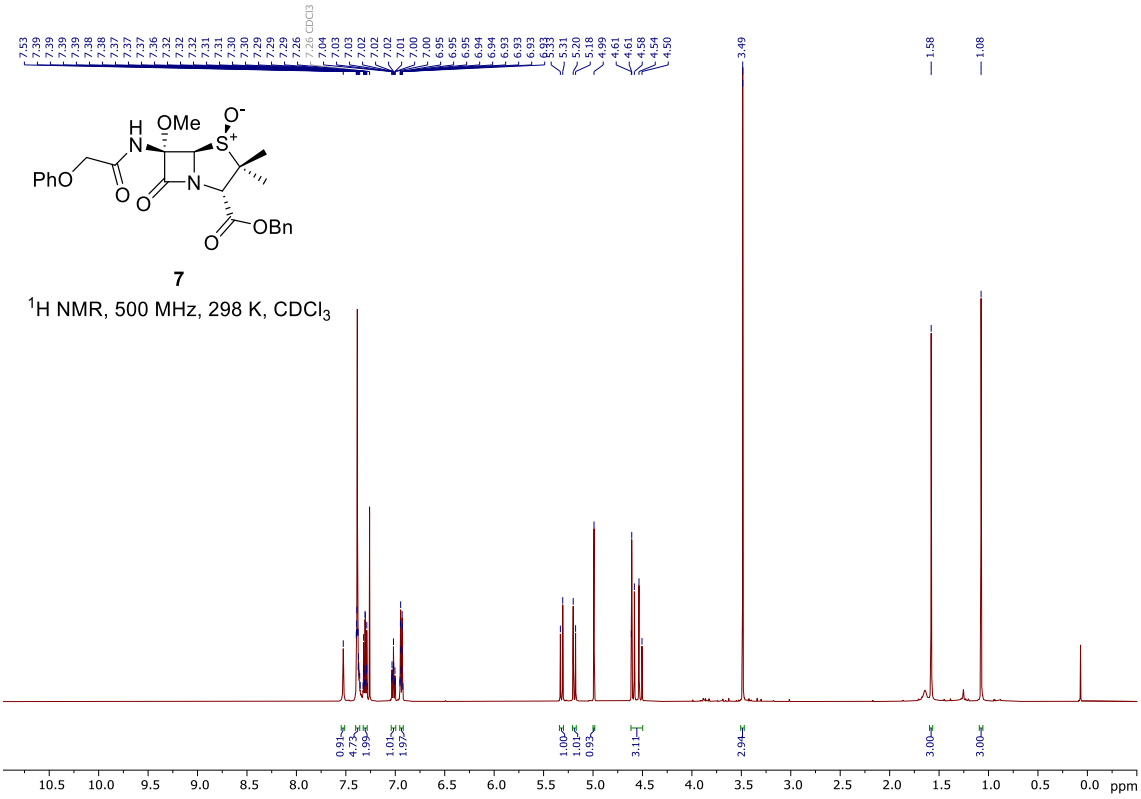

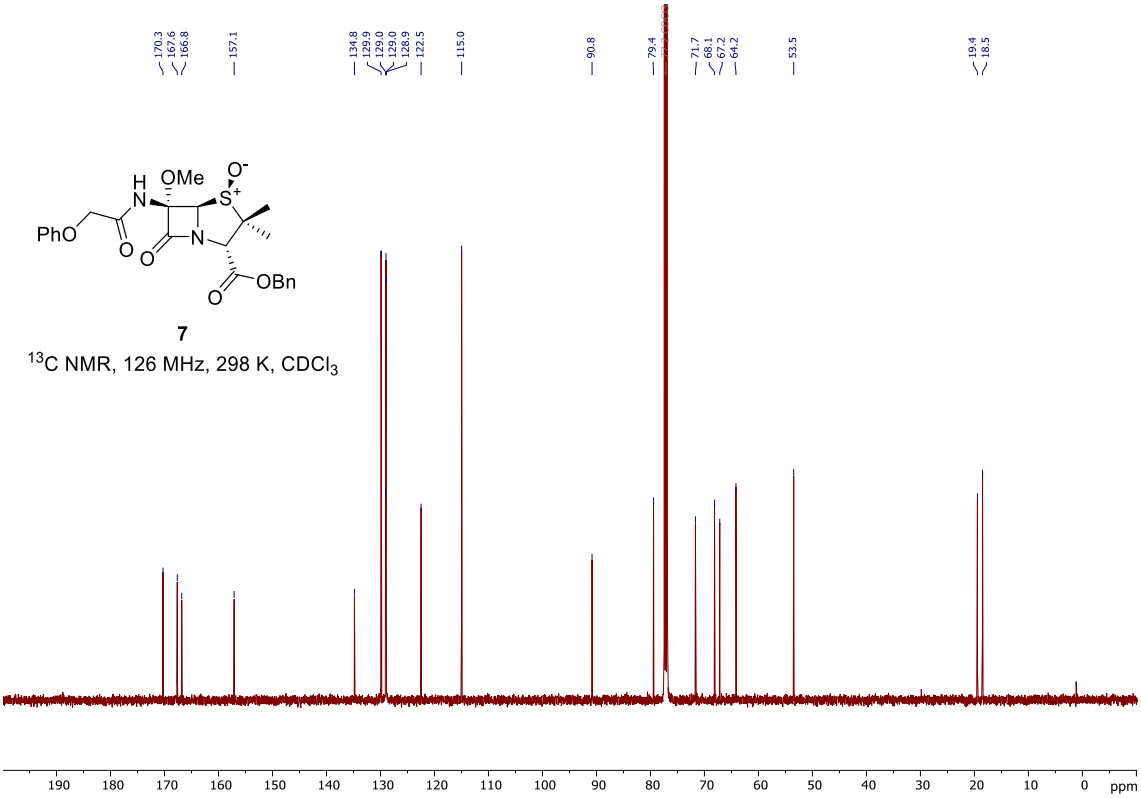

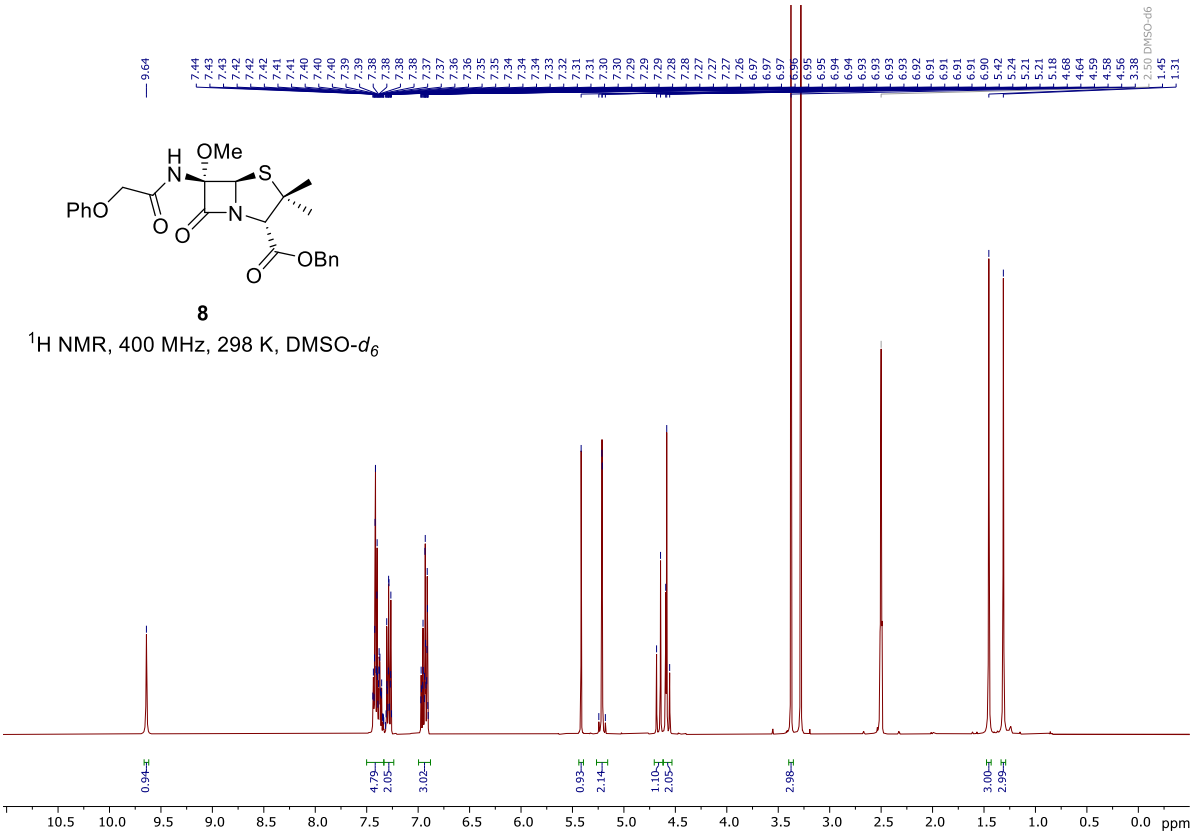

8

^{1}H NMR, 400 MHz, 298 K, DMSO-d_6

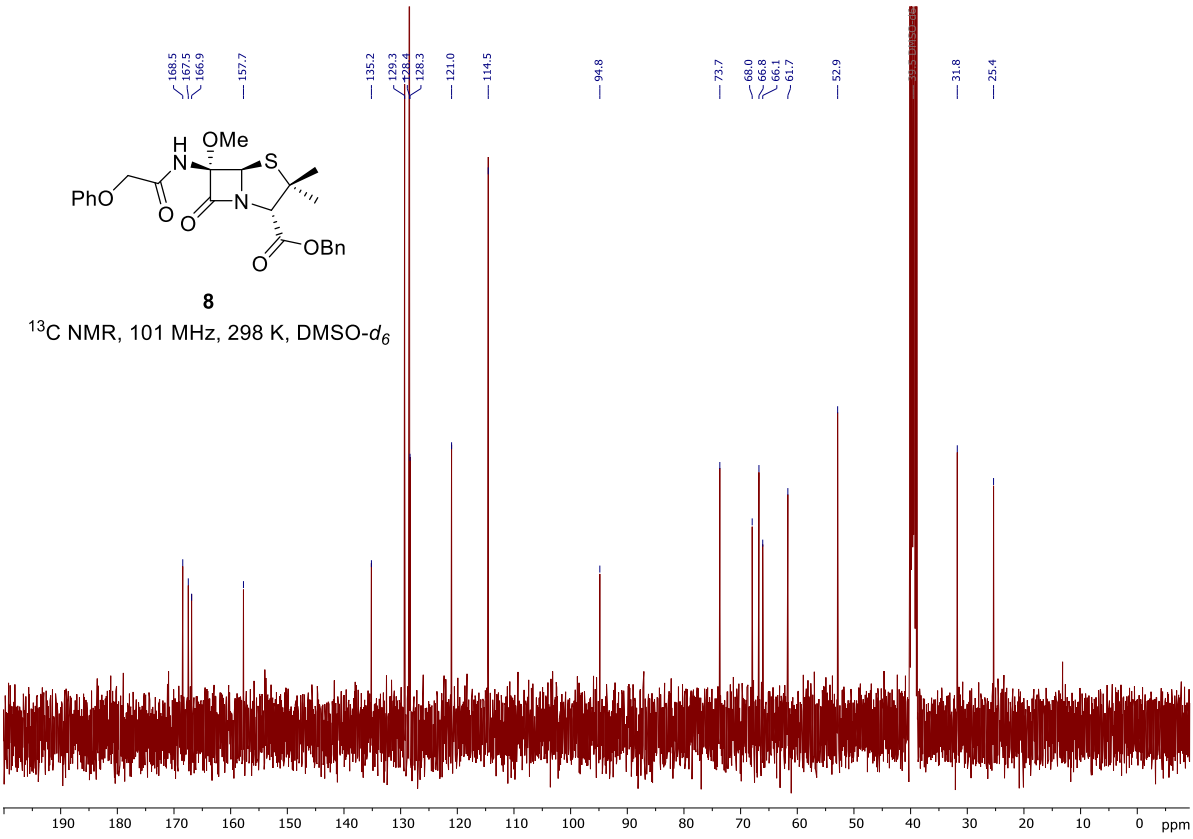

8

^{13}C NMR, 101 MHz, 298 K, DMSO-d_6

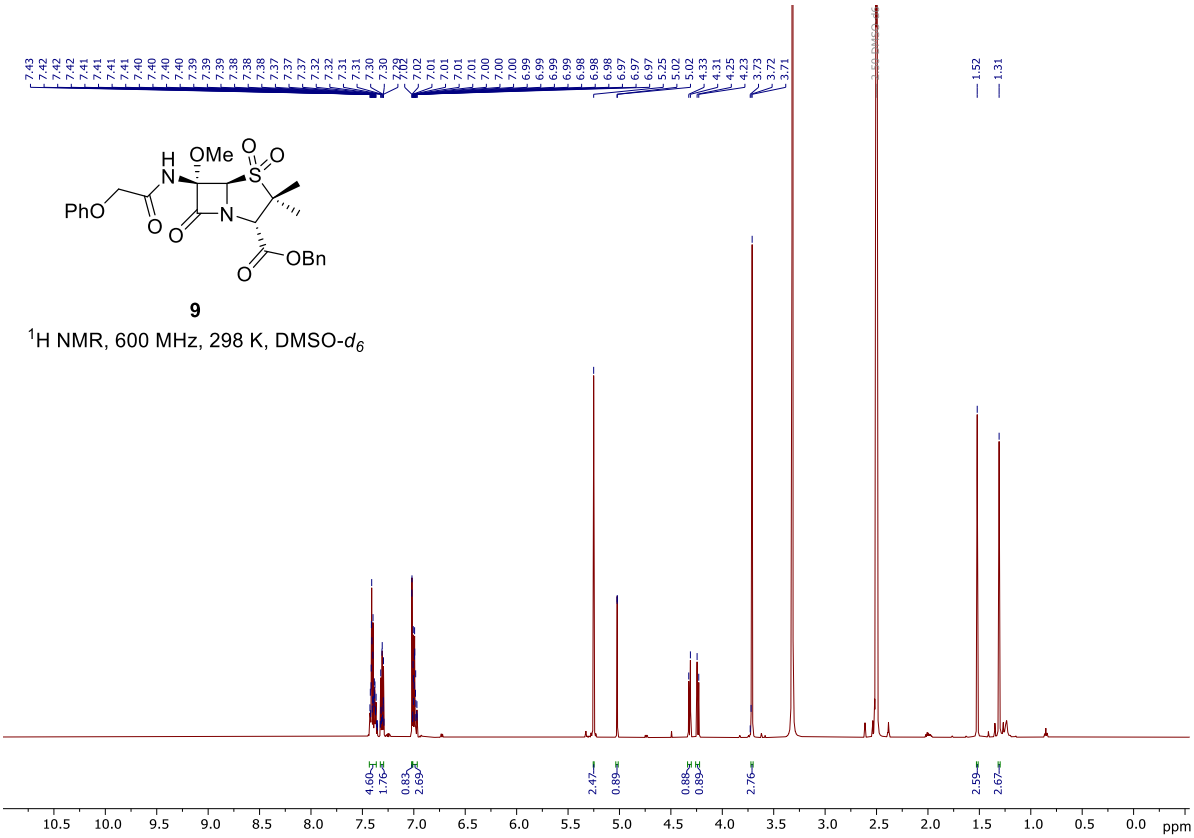

^{1}H NMR, 600 MHz, 298 K, DMSO-d_6

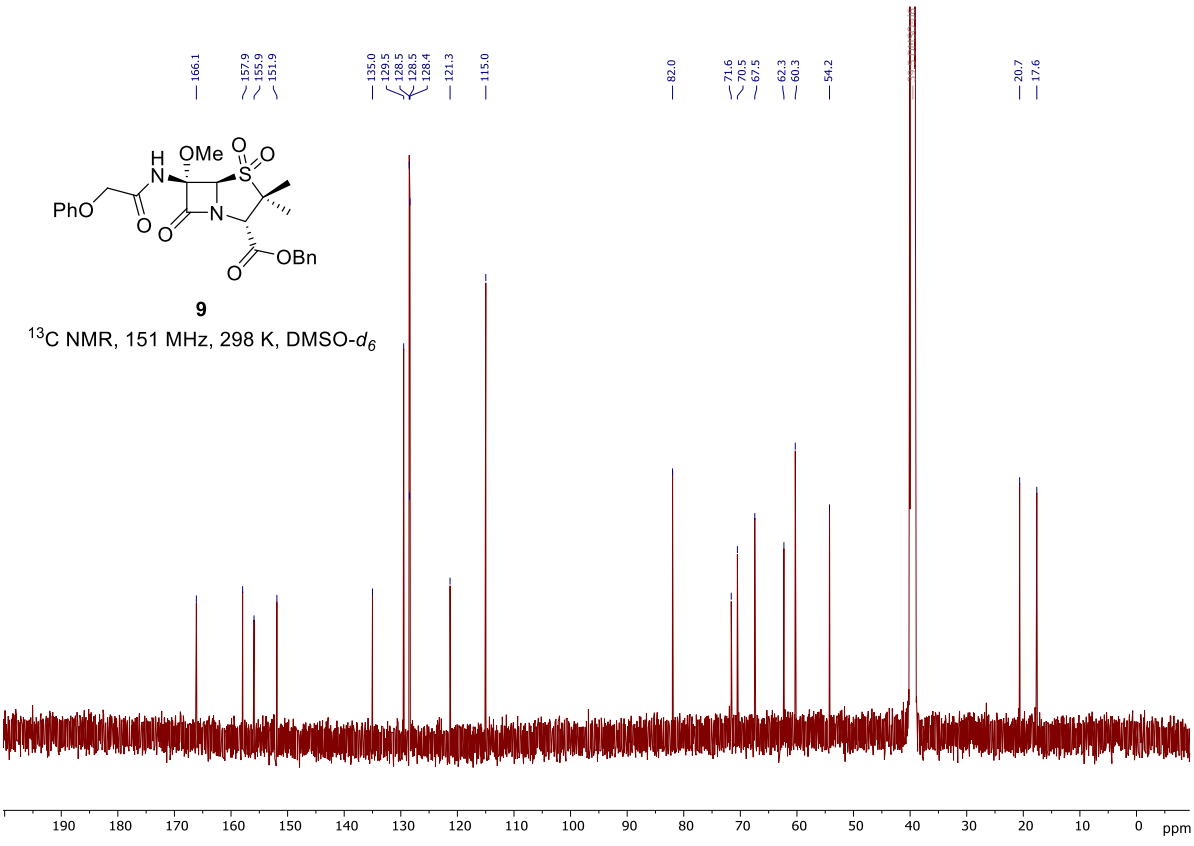

^{13}C NMR, 151 MHz, 298 K, DMSO-d_6

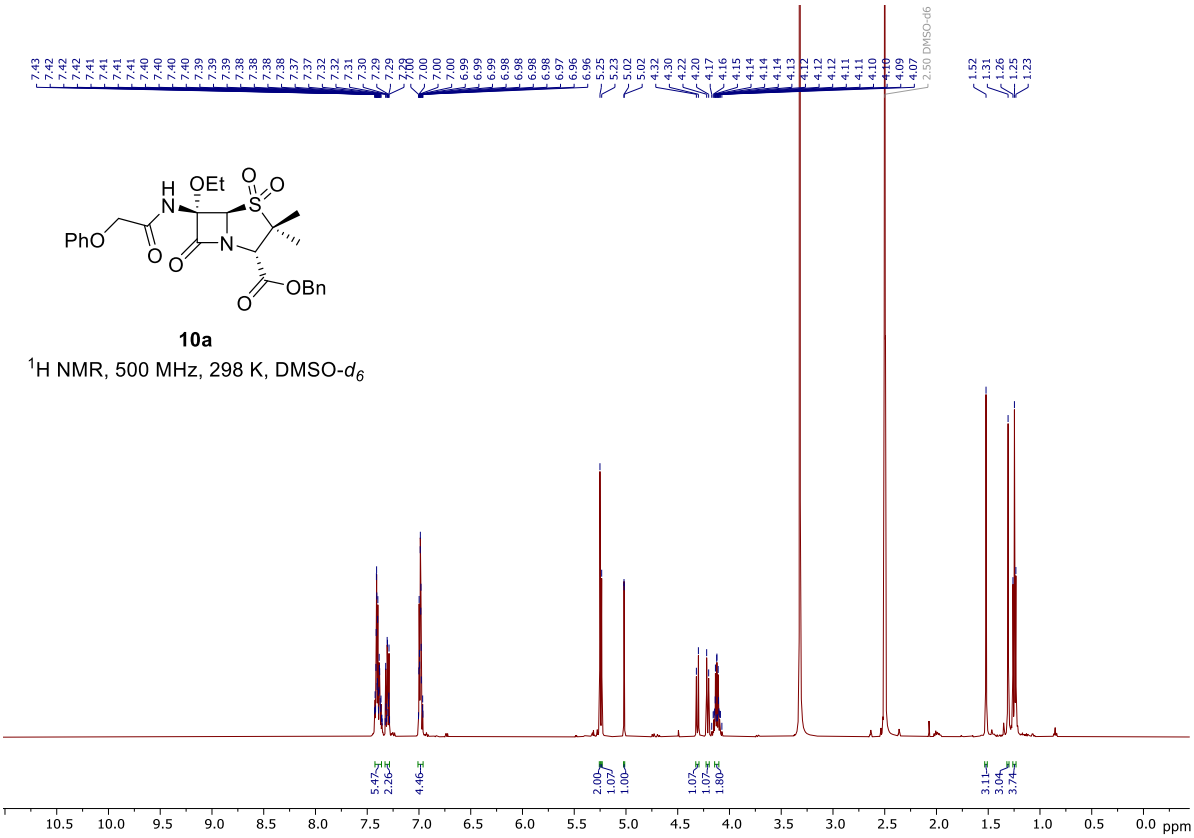

10a

^{1}H NMR, 500 MHz, 298 K, DMSO-d_6

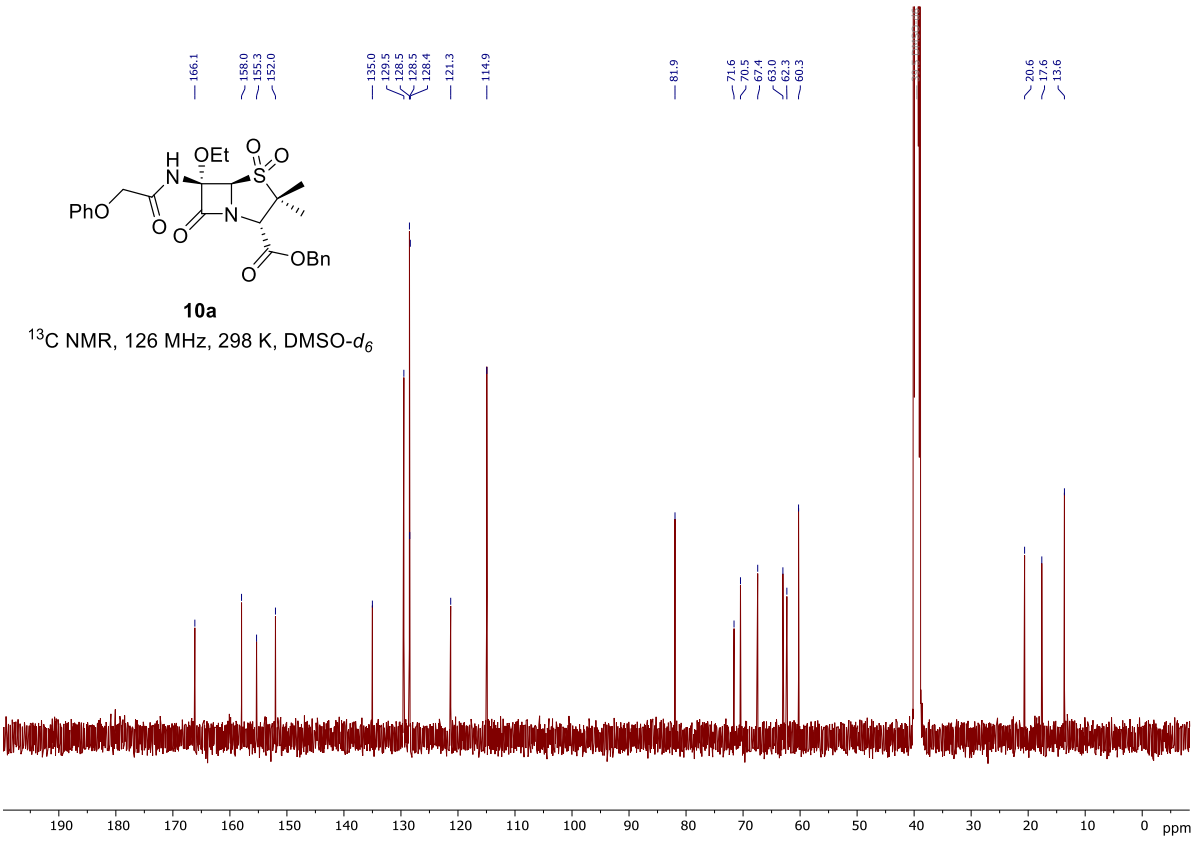

10a

^{13}C NMR, 126 MHz, 298 K, DMSO-d_6

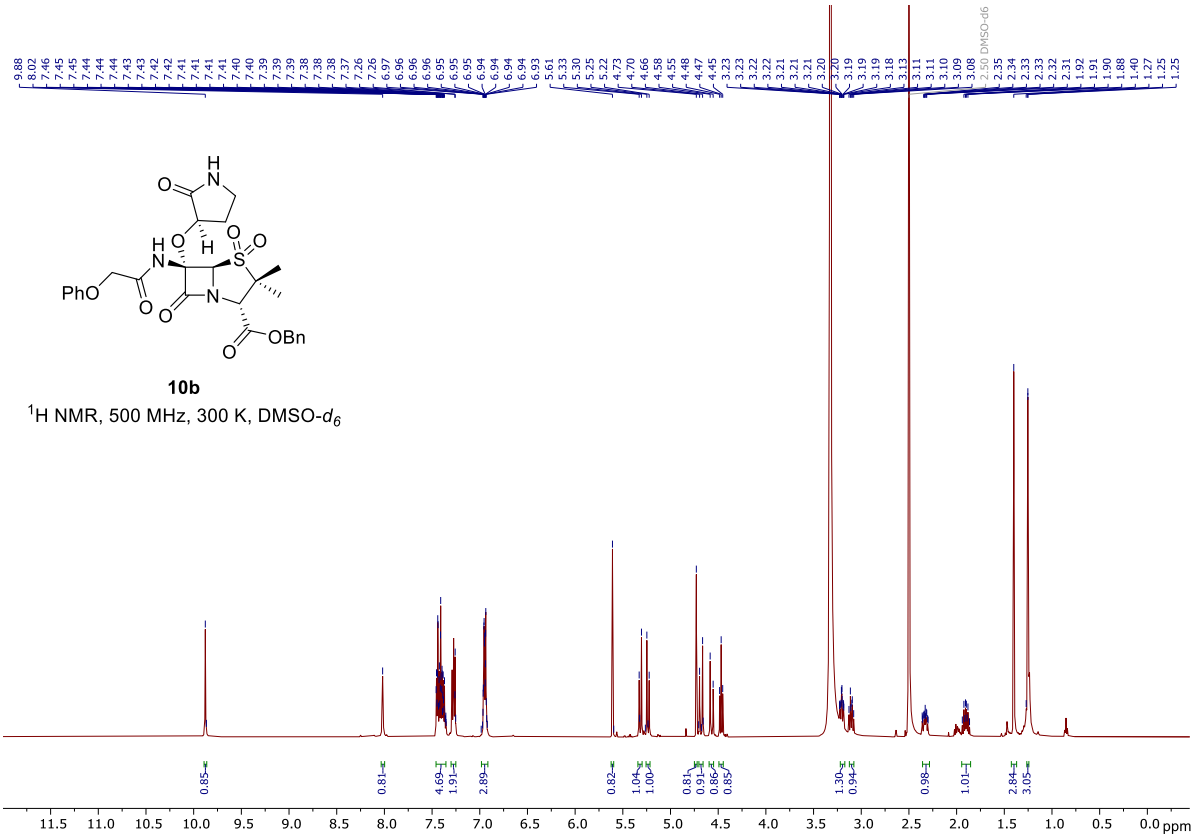

10b

^{1}H NMR, 500 MHz, 300 K, DMSO-d_6

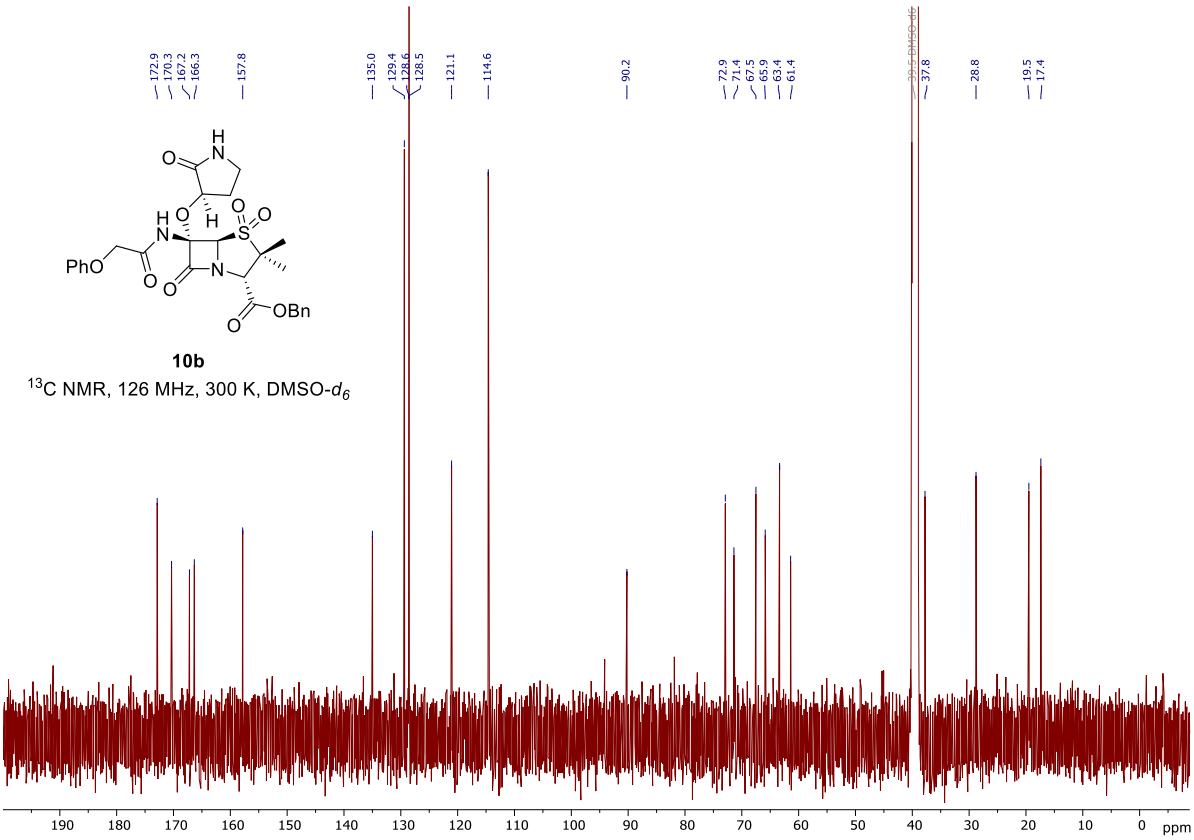

10b

^{13}C NMR, 126 MHz, 300 K, DMSO-d_6

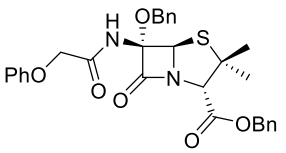

16c

^{1}H NMR, 600 MHz, 298 K, DMSO-d_6

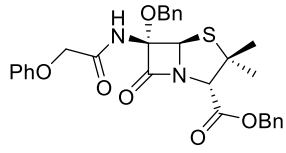

16c

^{13}C NMR, 151 MHz, 298 K, DMSO-d_6

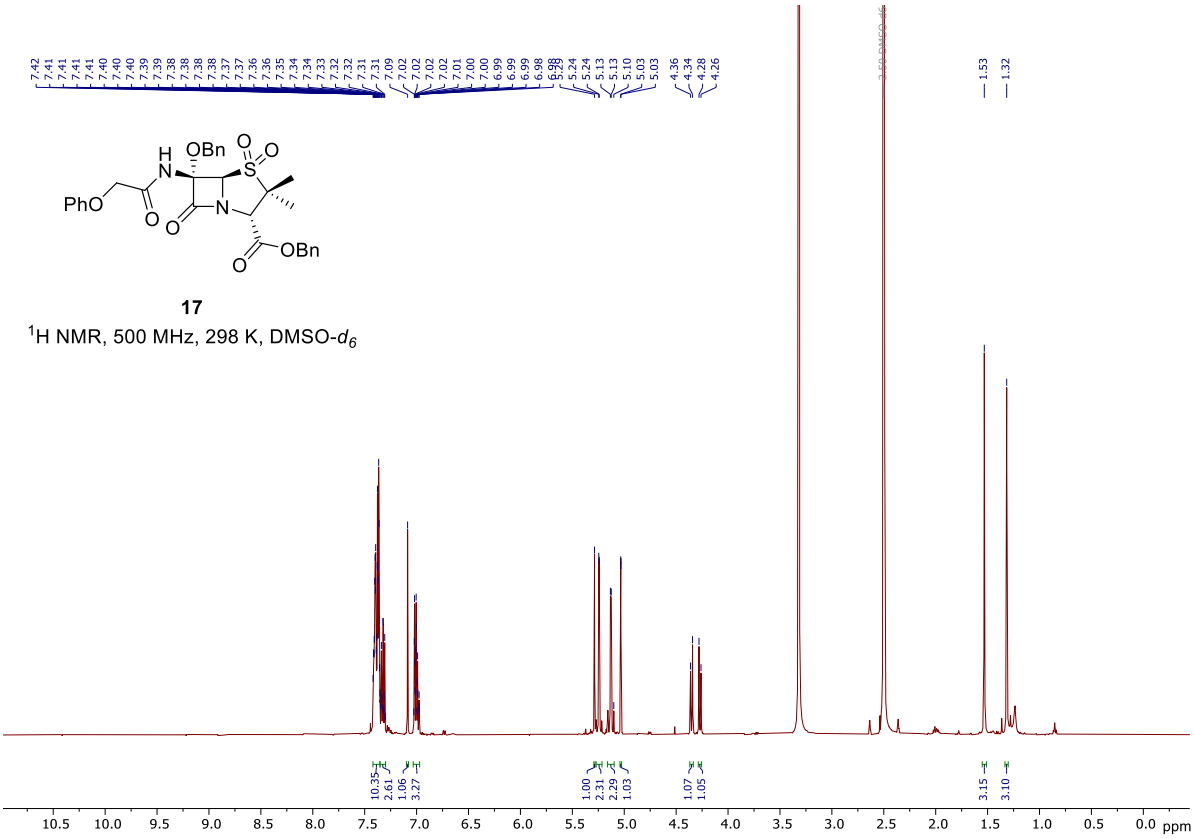

17

^{1}H NMR, 500 MHz, 298 K, DMSO-d_6

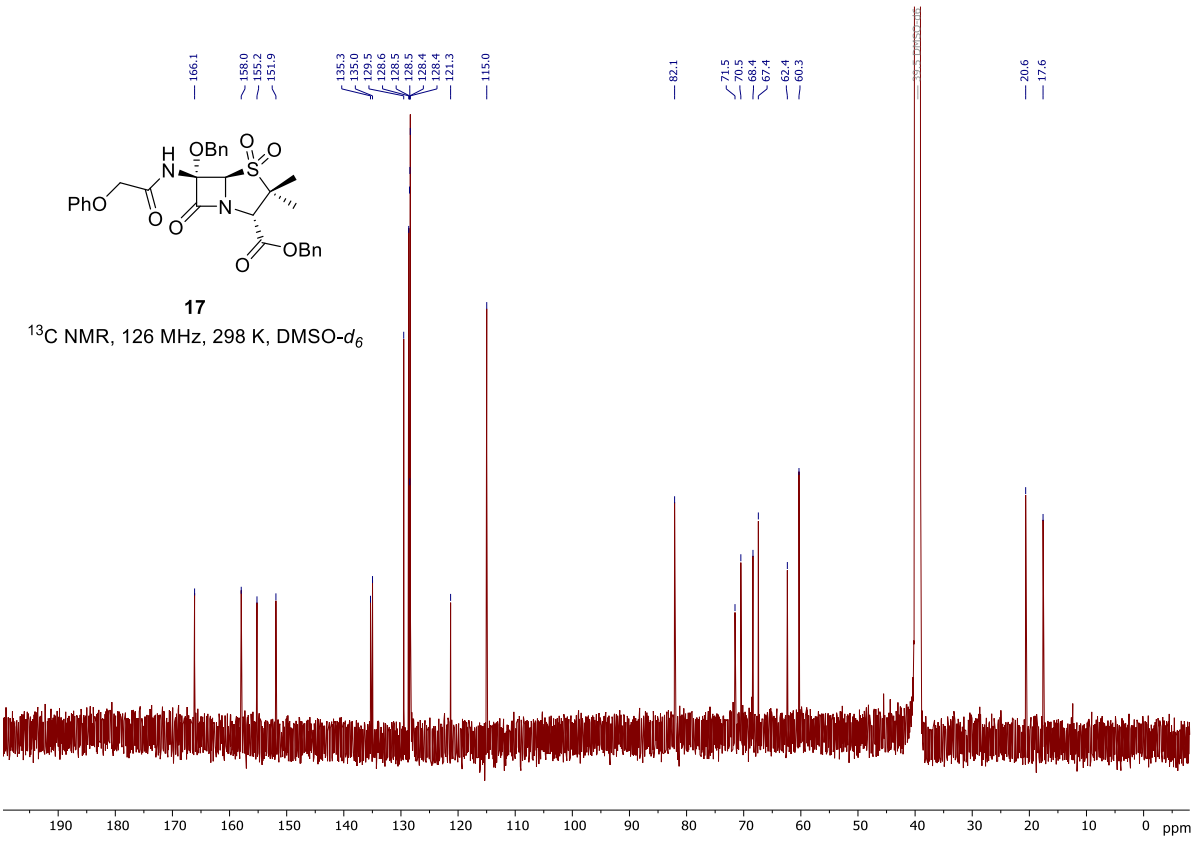

17

^{13}C NMR, 126 MHz, 298 K, DMSO-d_6

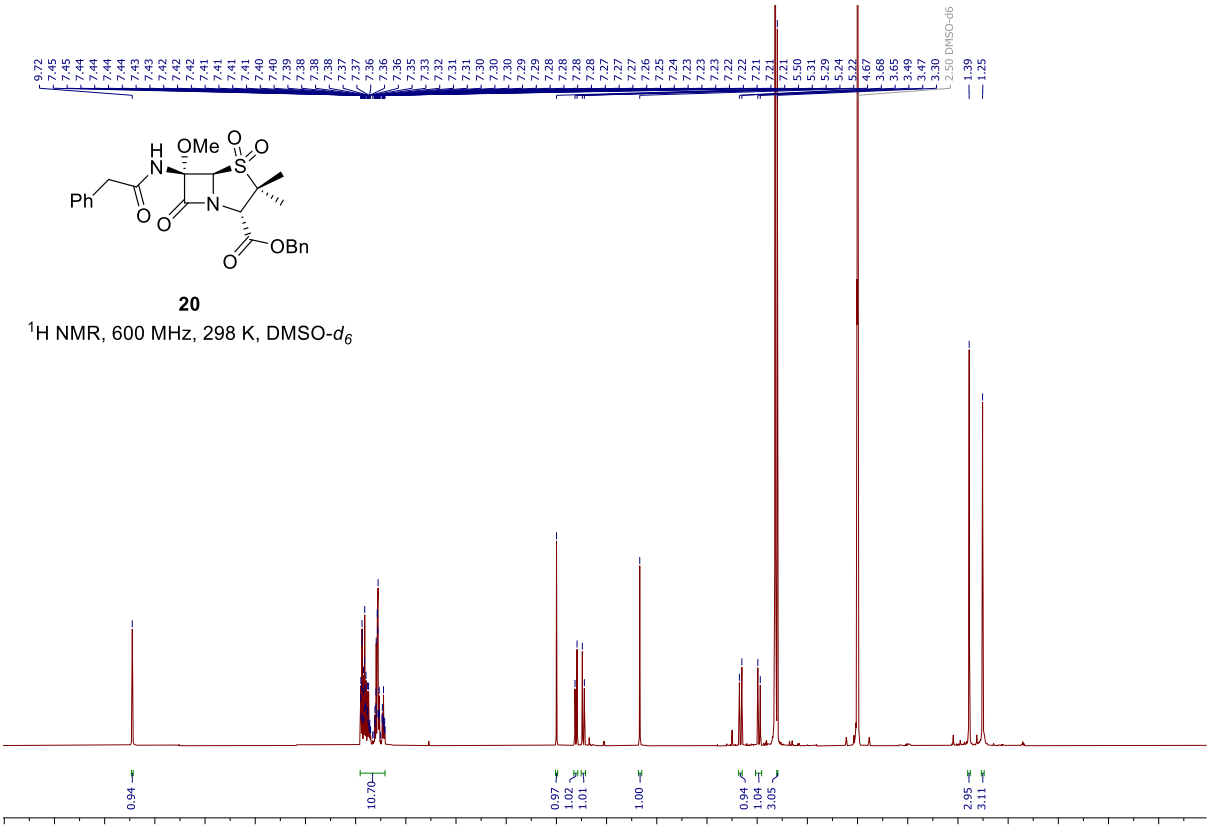

20

^{1}H NMR, 600 MHz, 298 K, DMSO-d_6

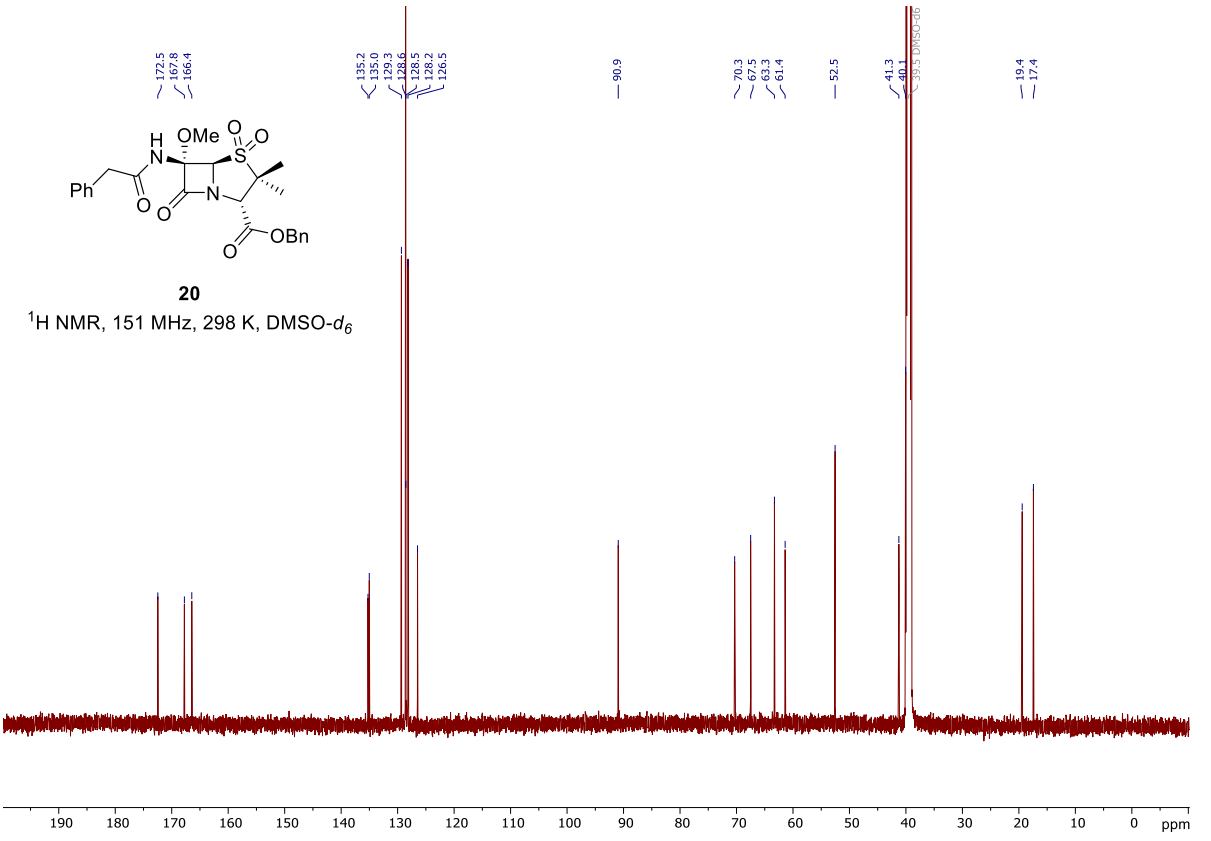

20

^{1}H NMR, 151 MHz, 298 K, DMSO-d_6

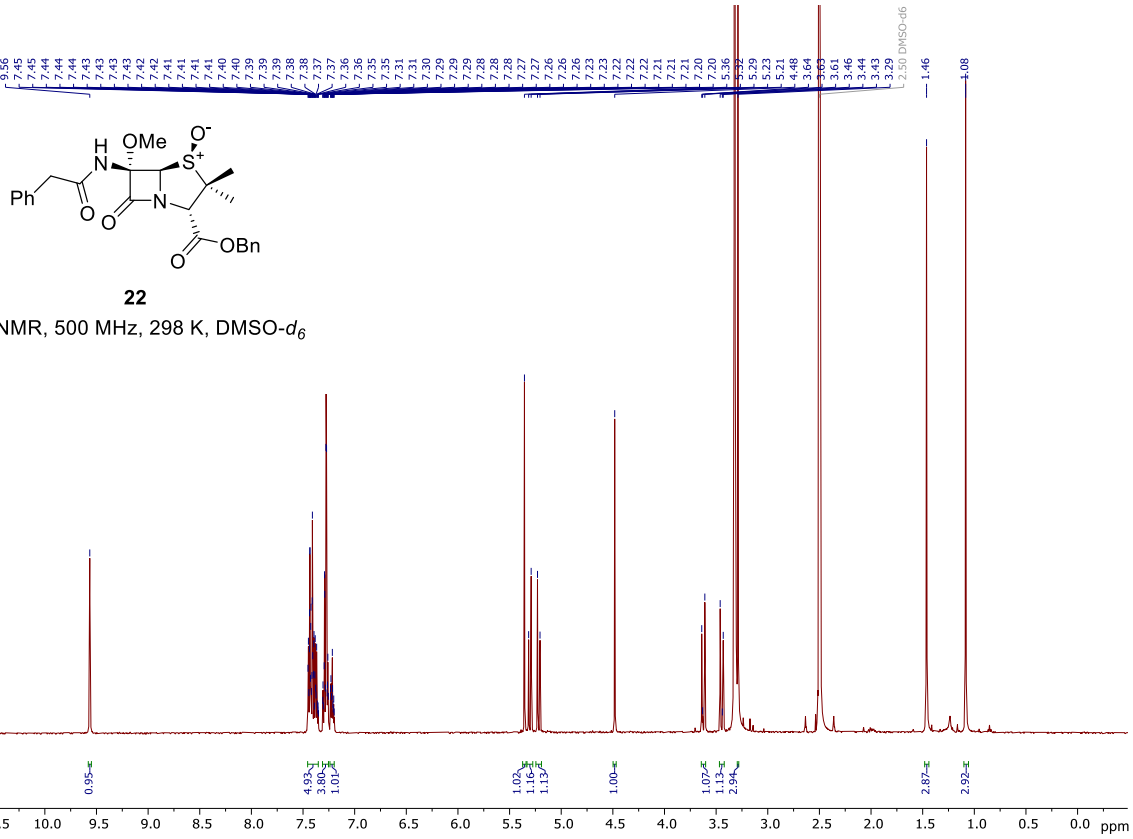

22

^{1}H NMR, 500 MHz, 298 K, DMSO-d_6

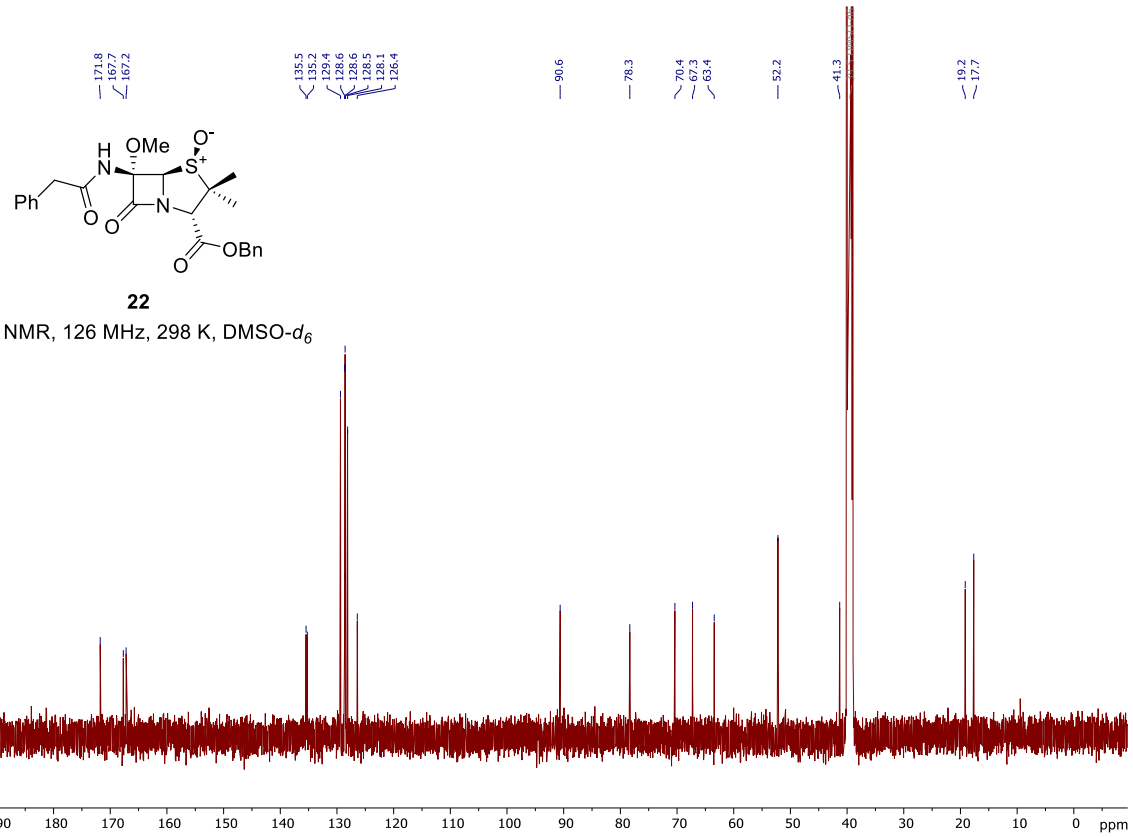

22

^{13}C NMR, 126 MHz, 298 K, DMSO-d_6

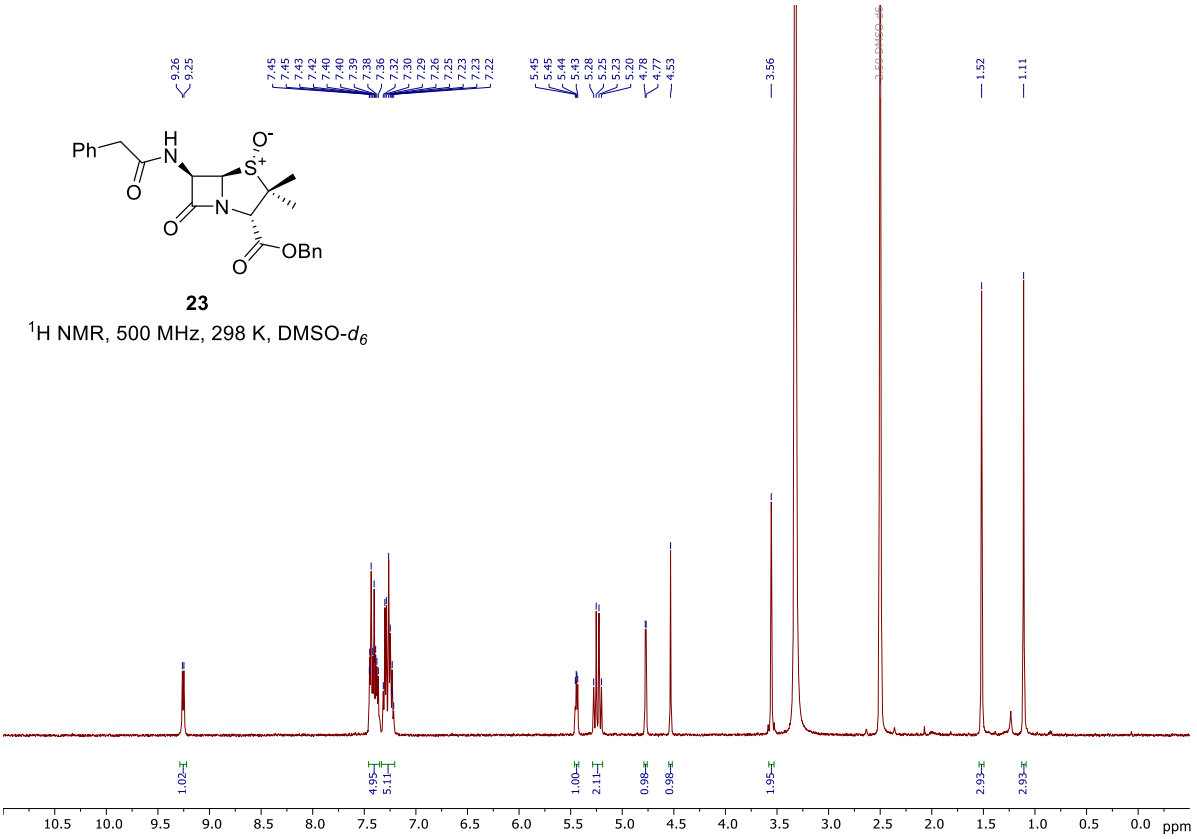

23

^{1}H NMR, 500 MHz, 298 K, DMSO-d_6

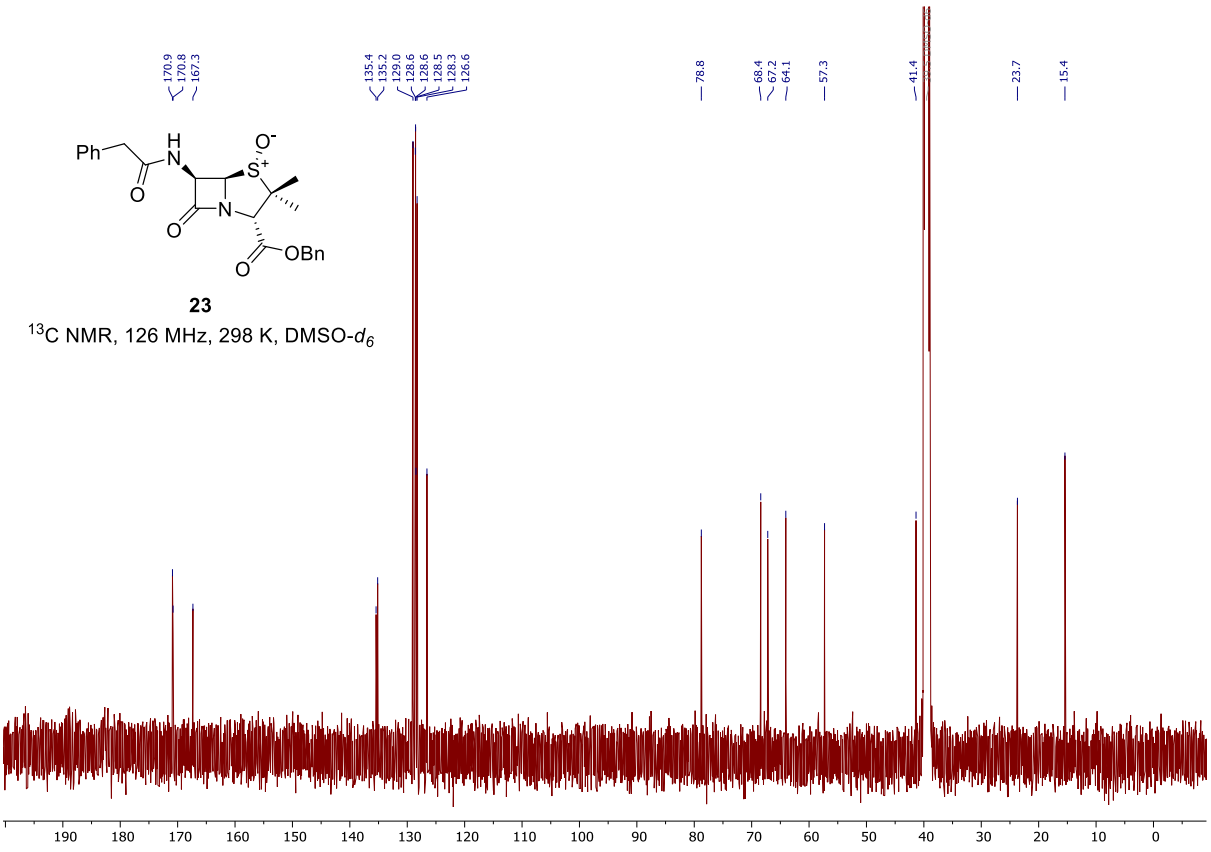

23

^{13}C NMR, 126 MHz, 298 K, DMSO-d_6

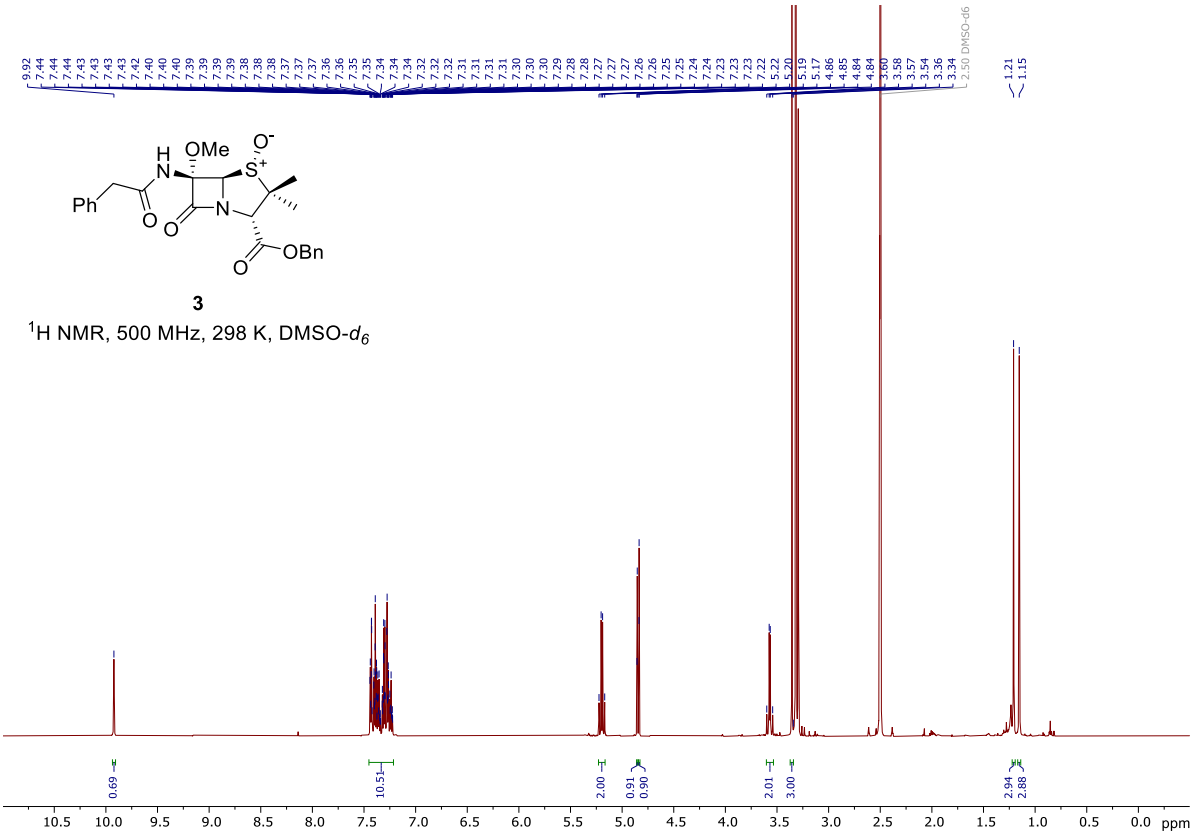

3

^{1}H NMR, 500 MHz, 298 K, DMSO-d_6

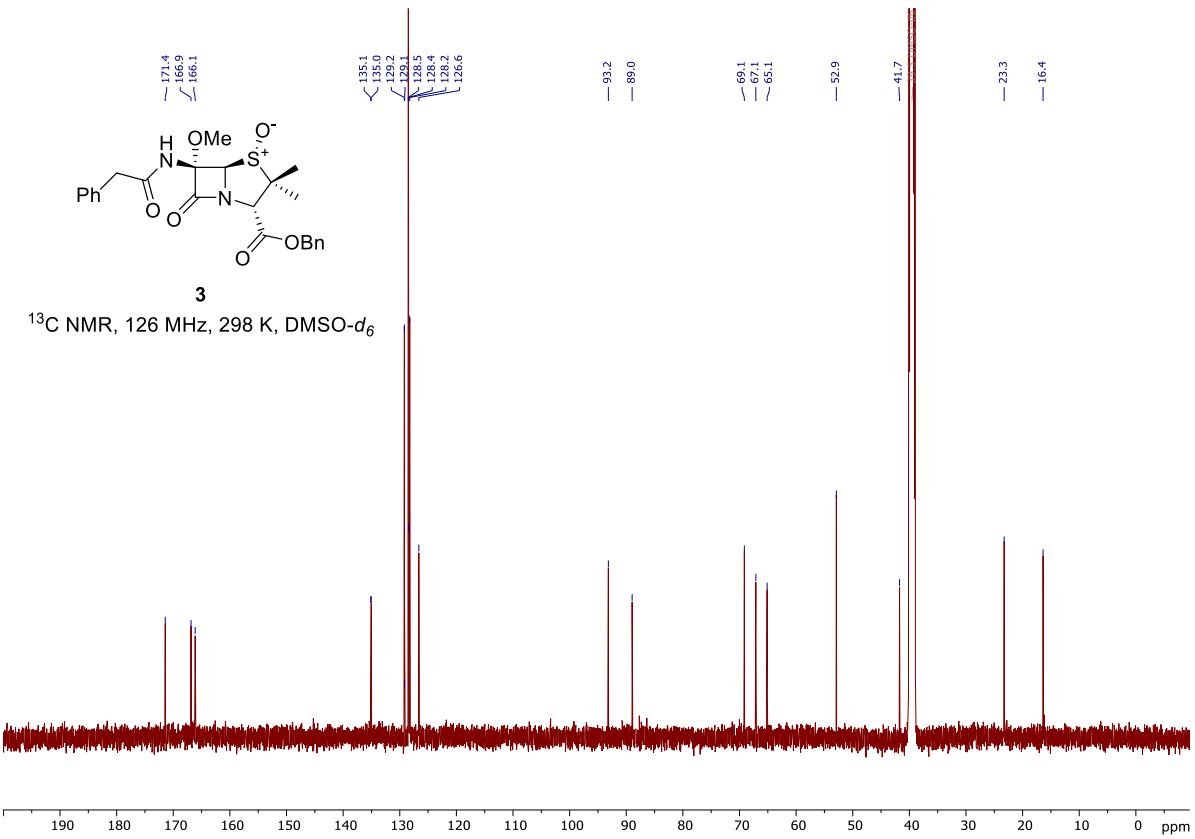

3

^{13}C NMR, 126 MHz, 298 K, DMSO-d_6

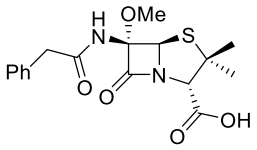

24

^{1}H NMR, 600 MHz, 298 K, DMSO-d_6

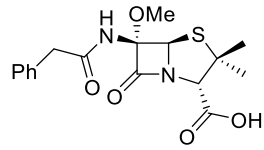

24

^{13}C NMR, 126 MHz, 298 K, DMSO-d_6

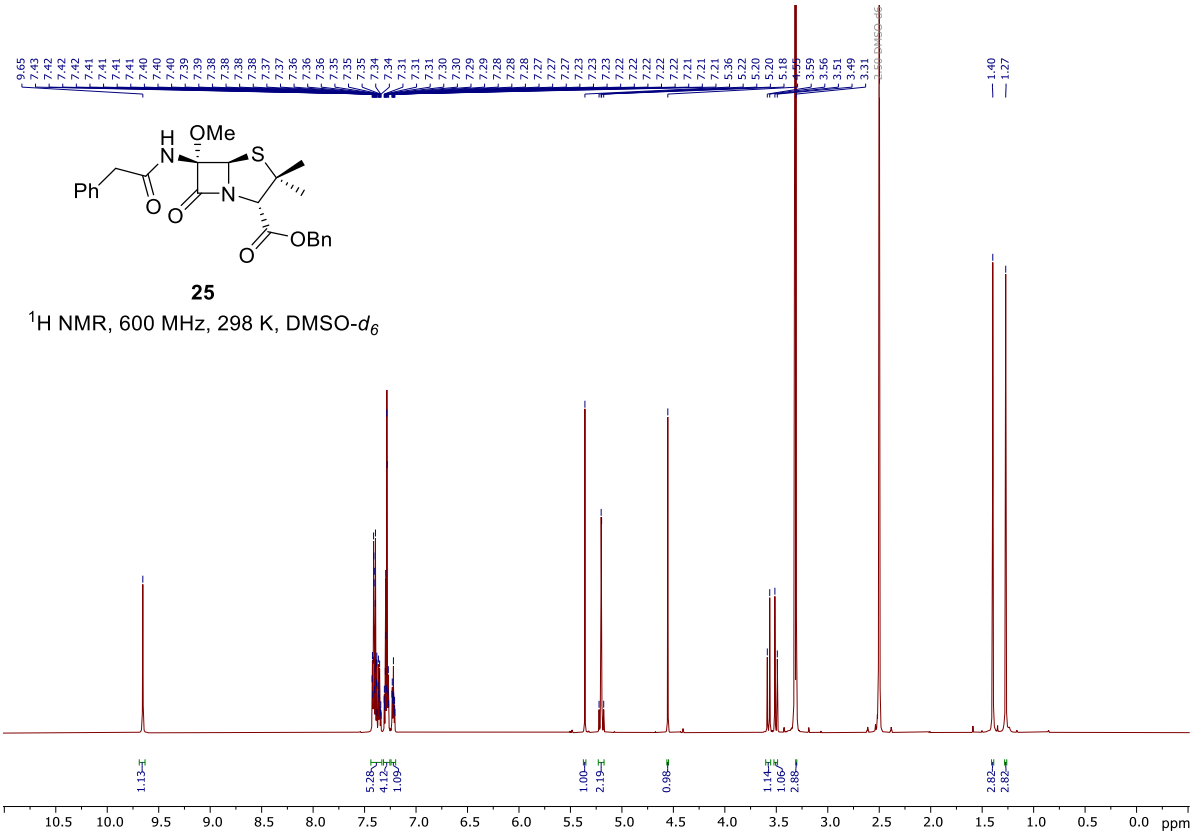

25

^{1}H NMR, 600 MHz, 298 K, DMSO-d_6

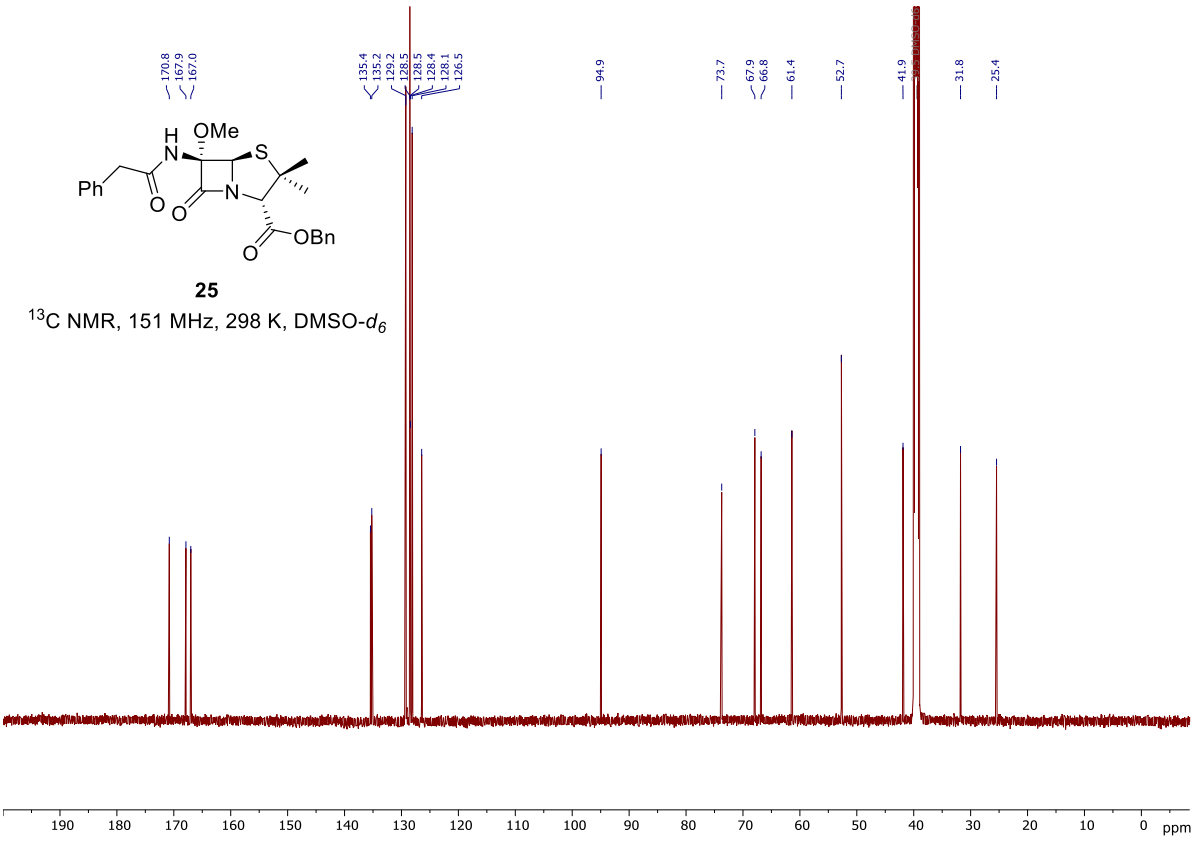

25

^{13}C NMR, 151 MHz, 298 K, DMSO-d_6

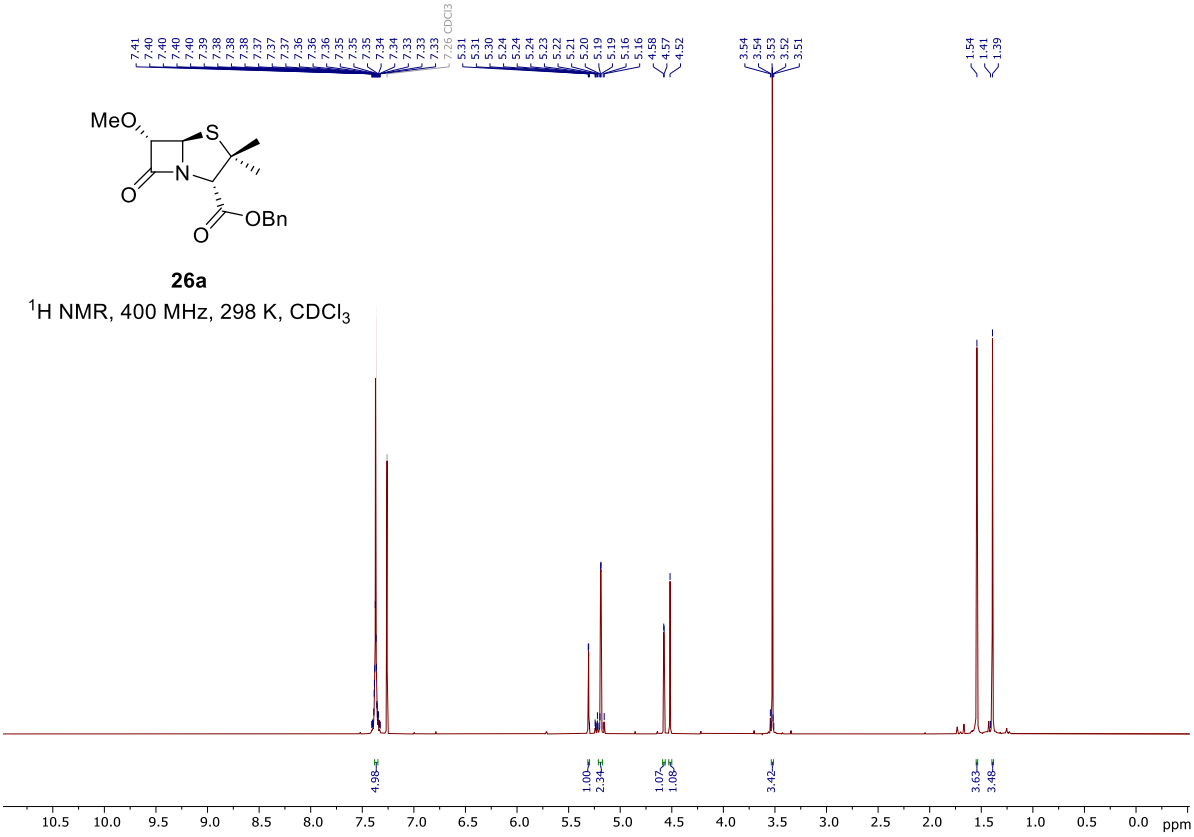

26a

^{1}H NMR, 400 MHz, 298 K, $CDCl_3$

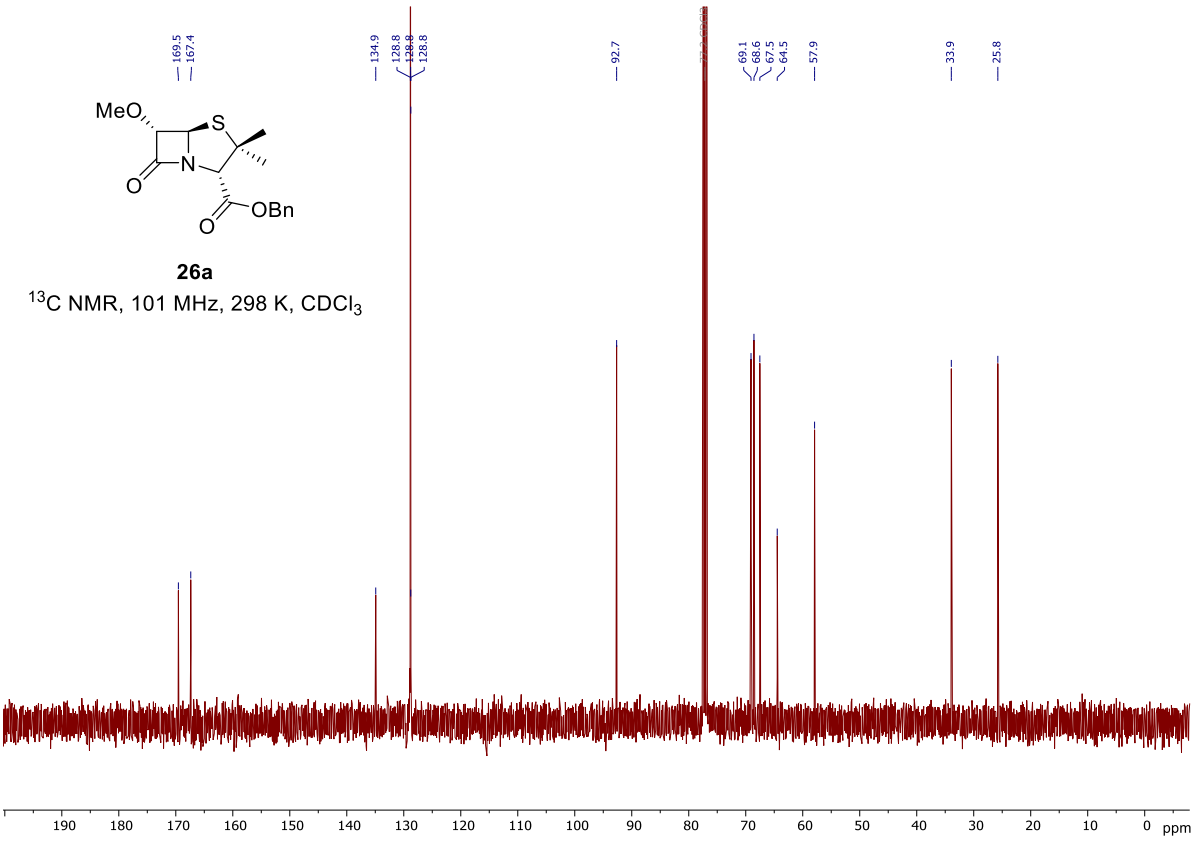

26a

^{13}C NMR, 101 MHz, 298 K, $CDCl_3$

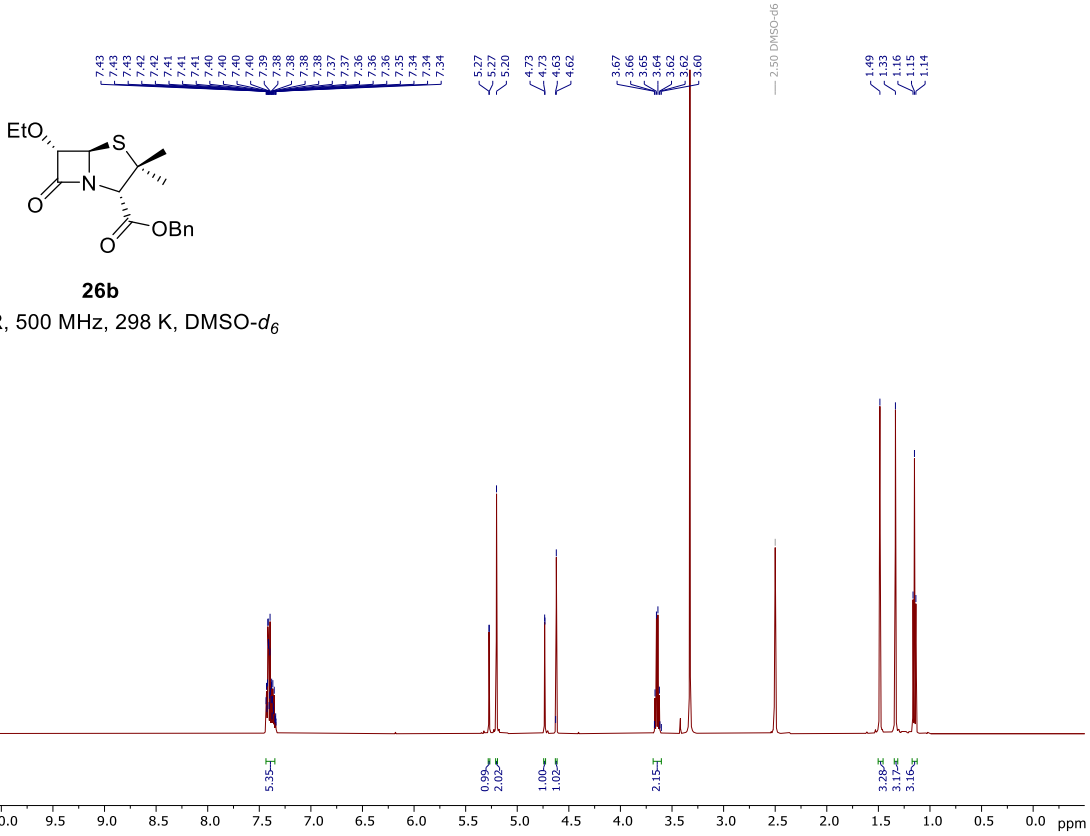

26b

^{1}H NMR, 500 MHz, 298 K, DMSO-d_6

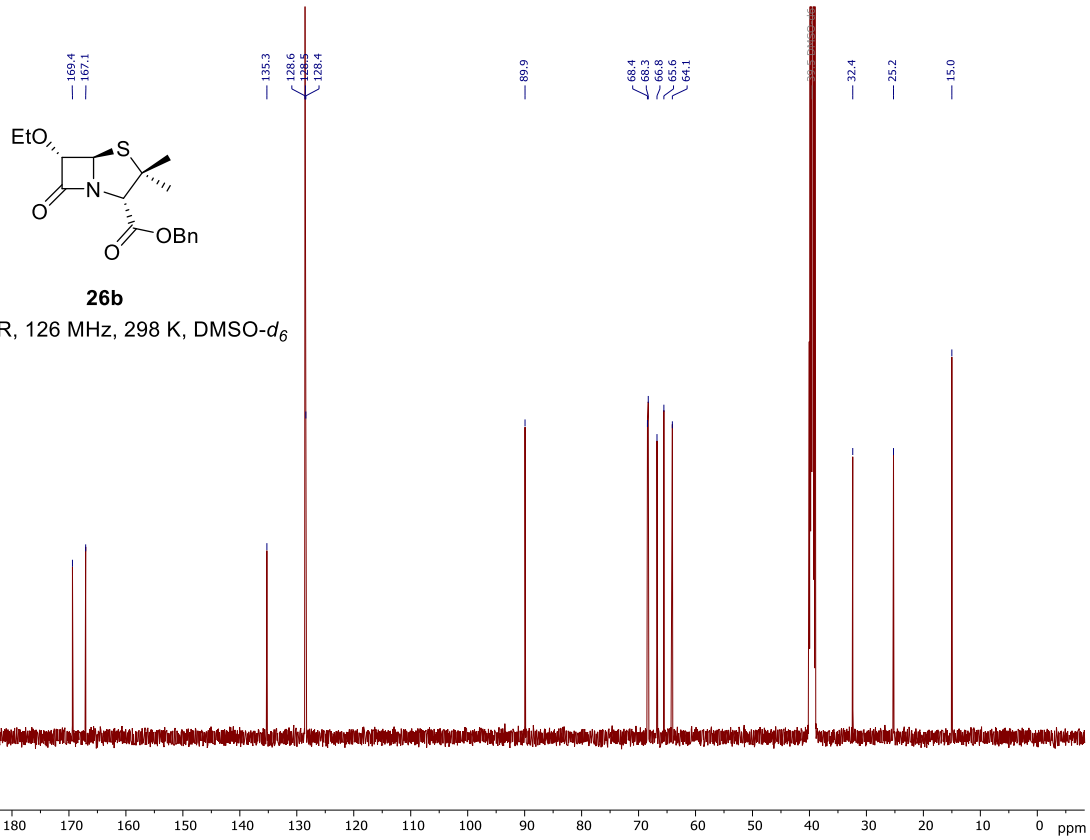

26b

^{13}C NMR, 126 MHz, 298 K, DMSO-d_6

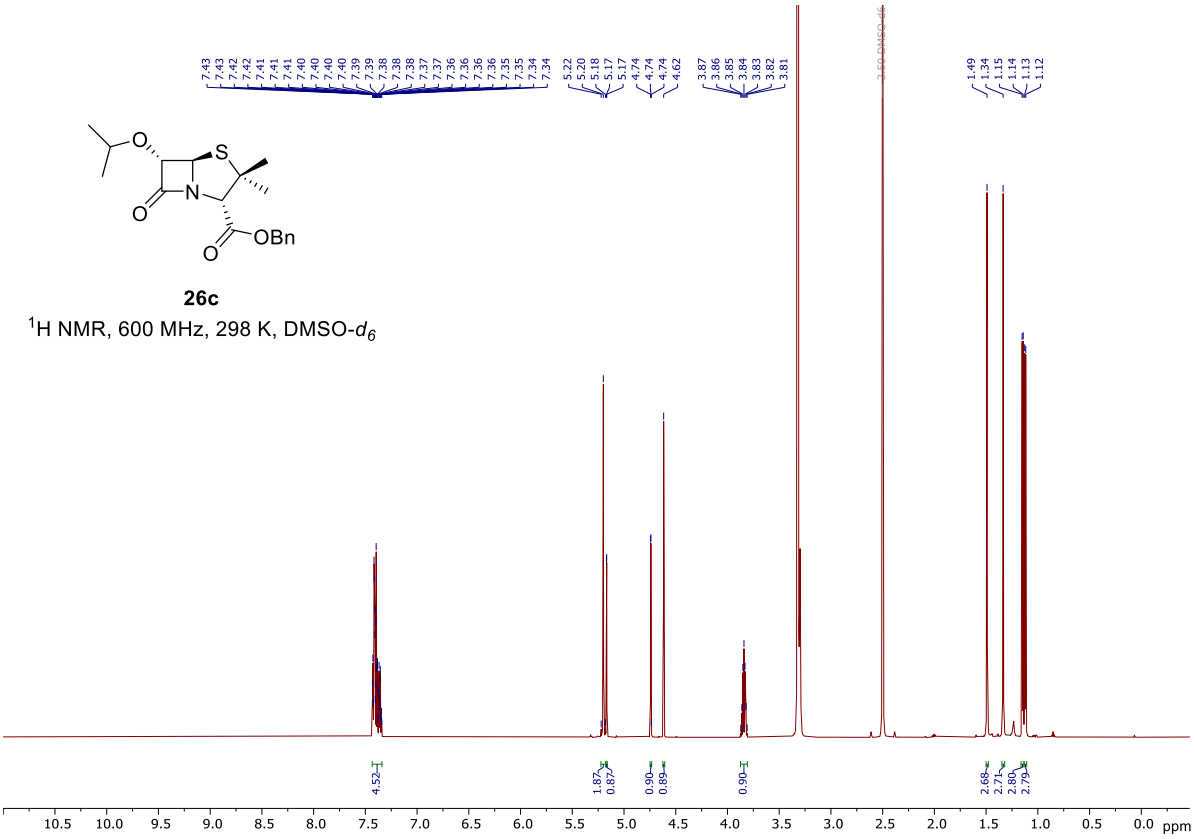

26c

^{1}H NMR, 600 MHz, 298 K, DMSO-d_6

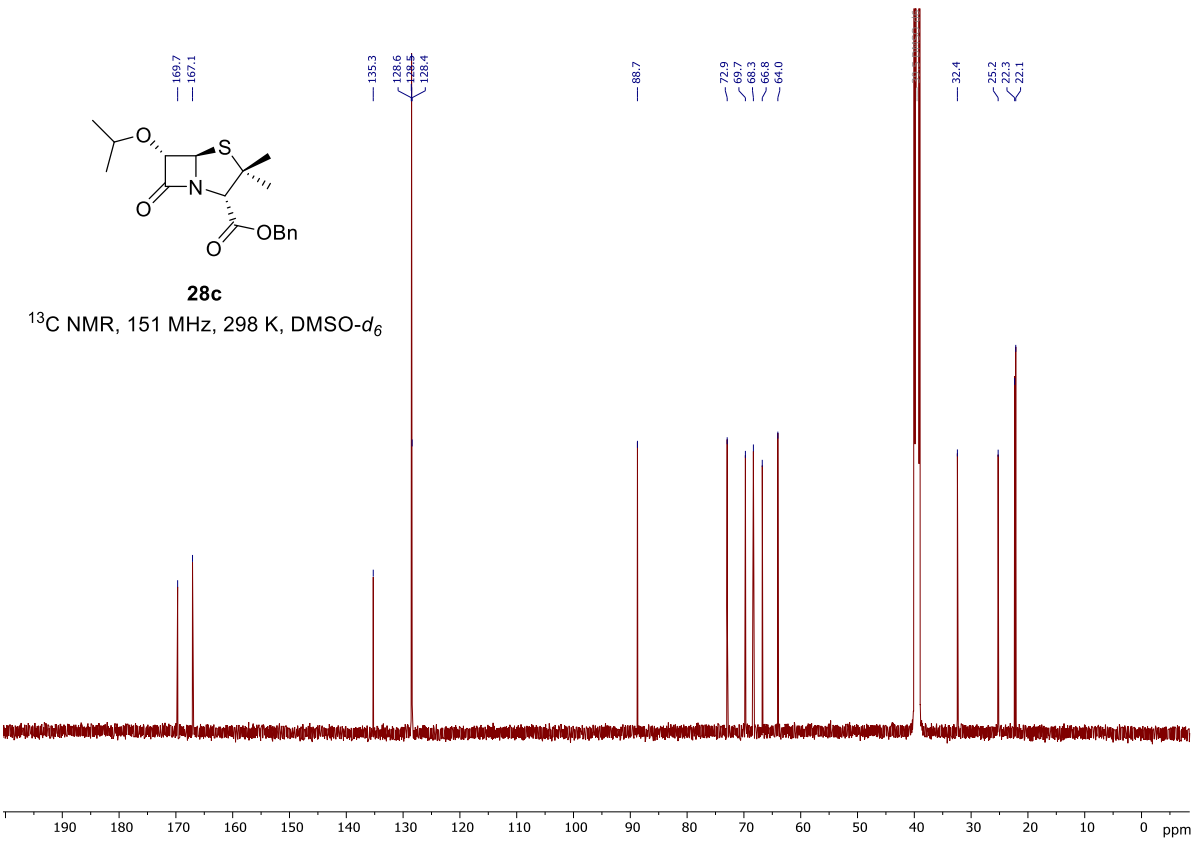

28c

^{13}C NMR, 151 MHz, 298 K, DMSO-d_6

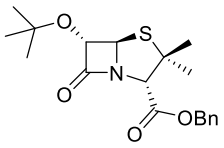

26d

^{1}H NMR, 500 MHz, 298 K, DMSO-d_6

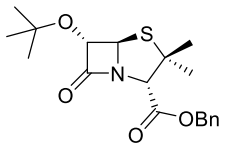

26d

^{13}C NMR, 126 MHz, 298 K, DMSO-d_6

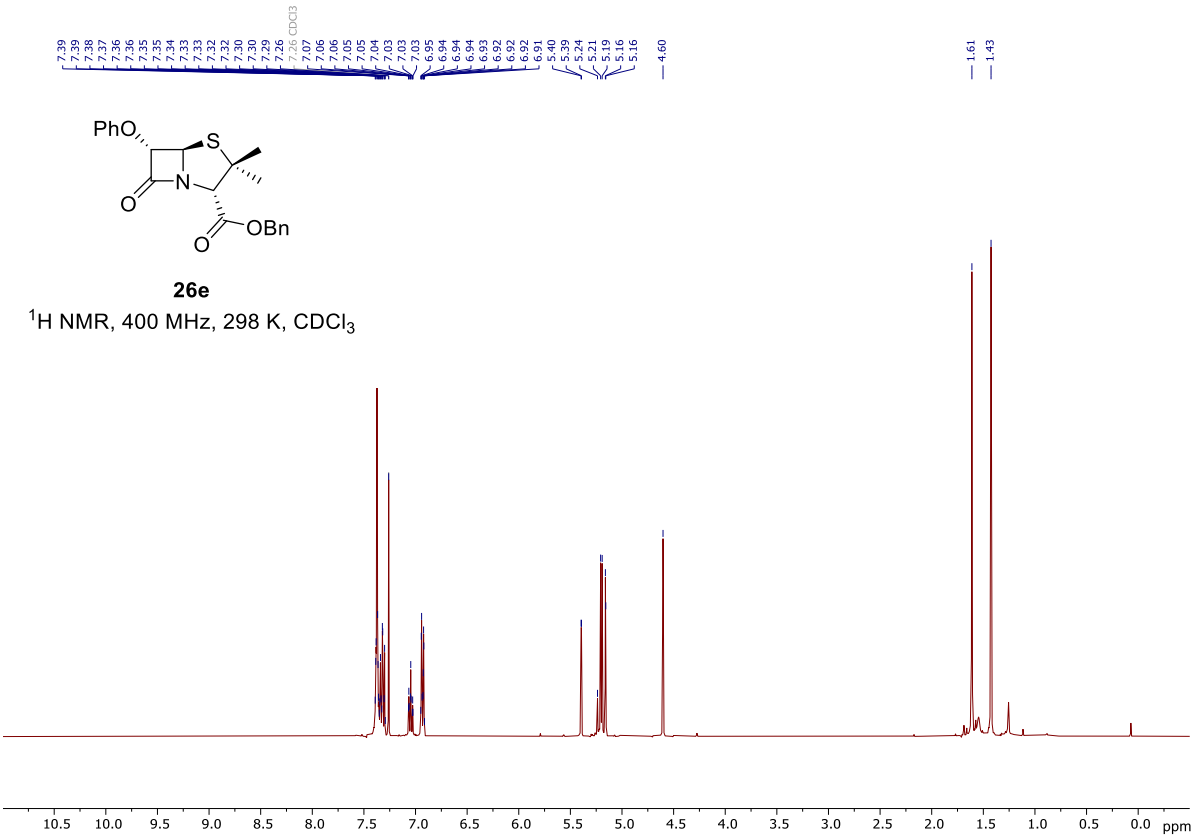

26e

^{1}H NMR, 400 MHz, 298 K, $CDCl_3$

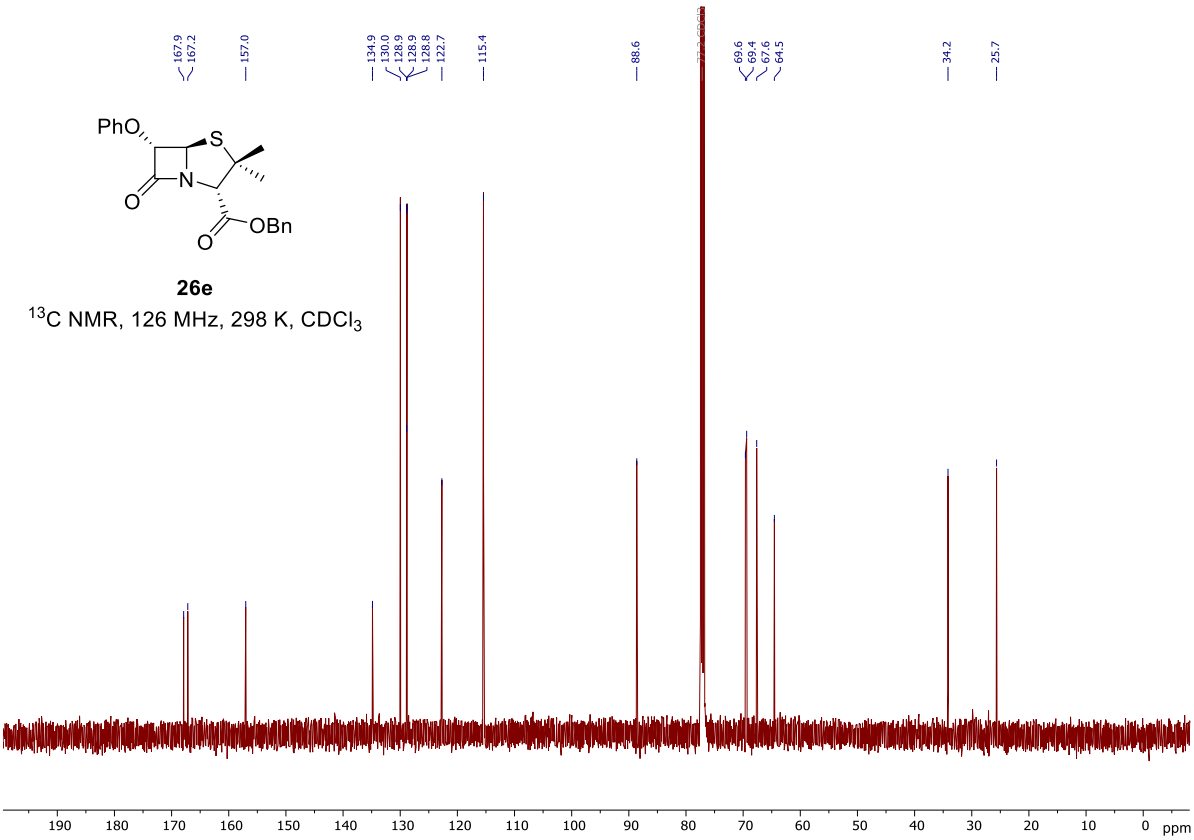

26e

^{13}C NMR, 126 MHz, 298 K, $CDCl_3$

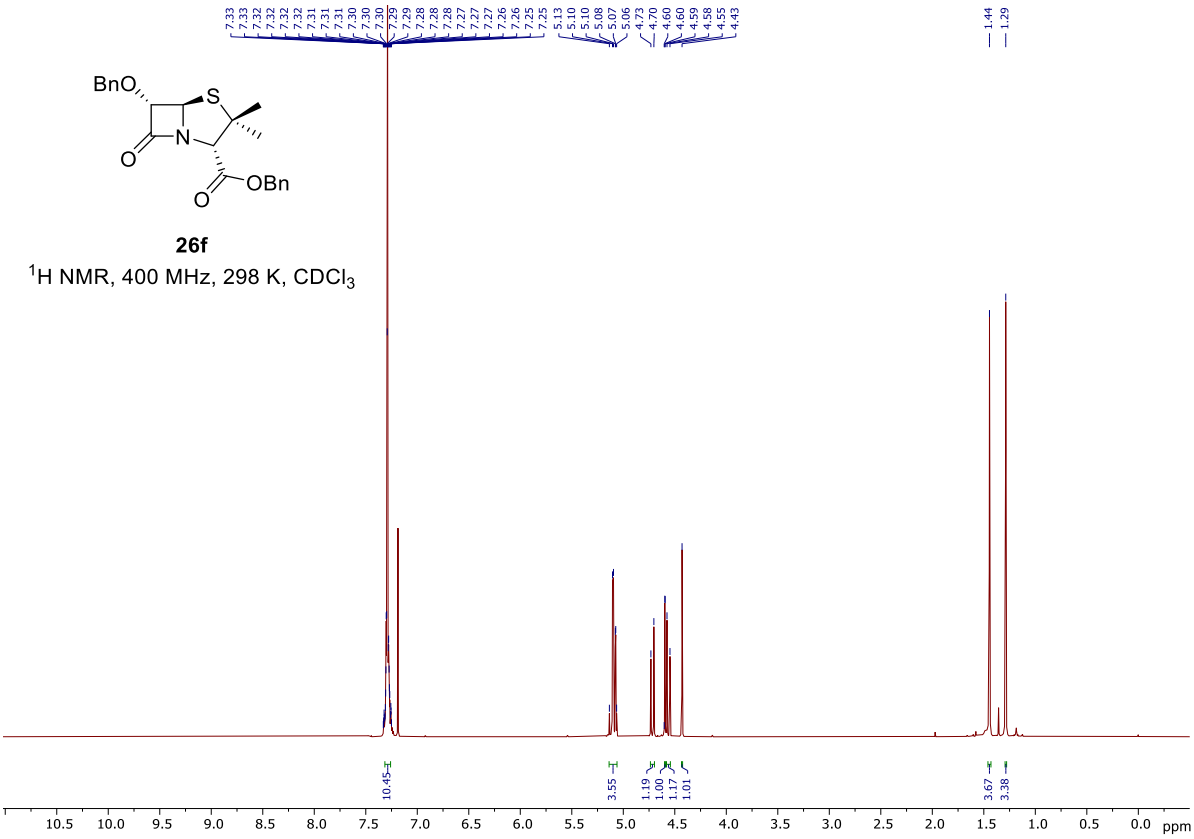

26f

^{1}H NMR, 400 MHz, 298 K, $CDCl_3$

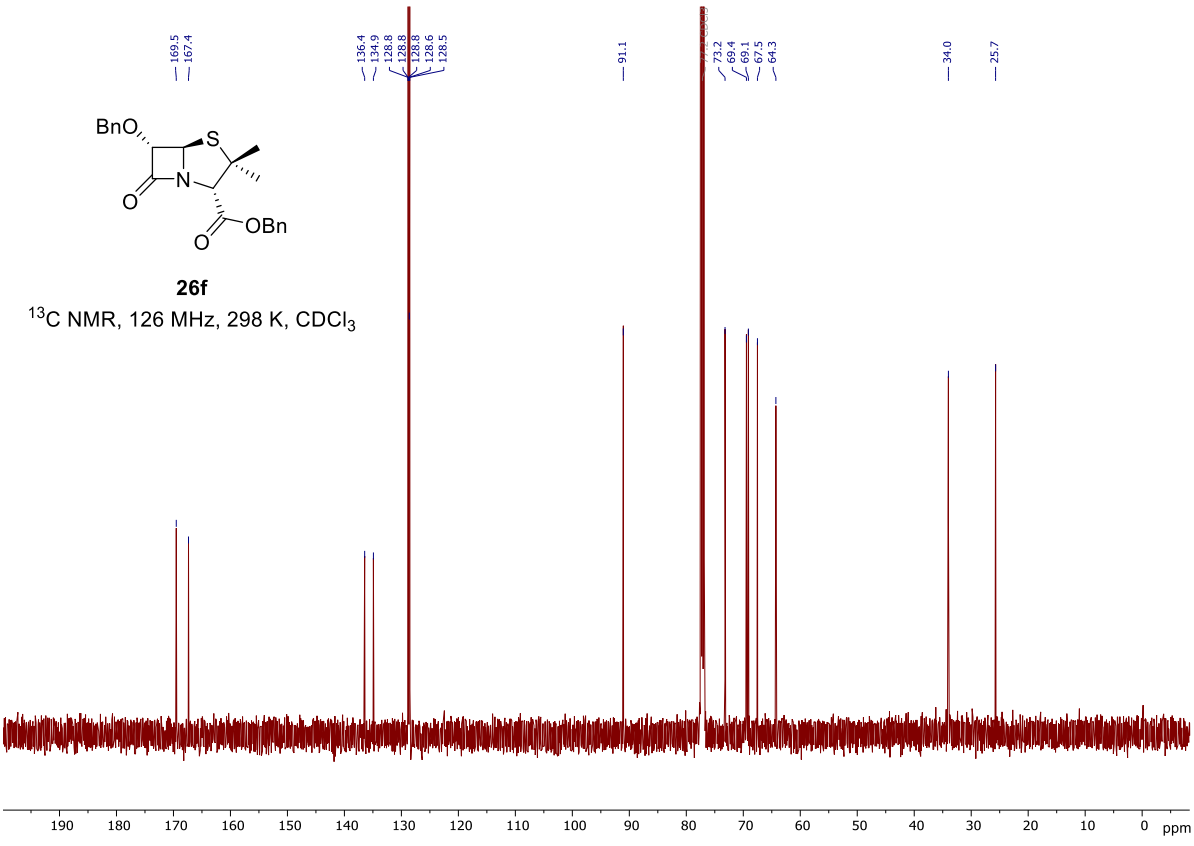

26f

^{13}C NMR, 126 MHz, 298 K, $CDCl_3$

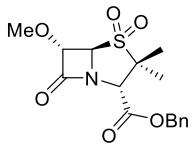

27a

^{1}H NMR, 500 MHz, 298 K, DMSO-d_6

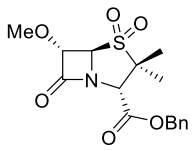

27a

^{13}C NMR, 126 MHz, 298 K, DMSO-d_6

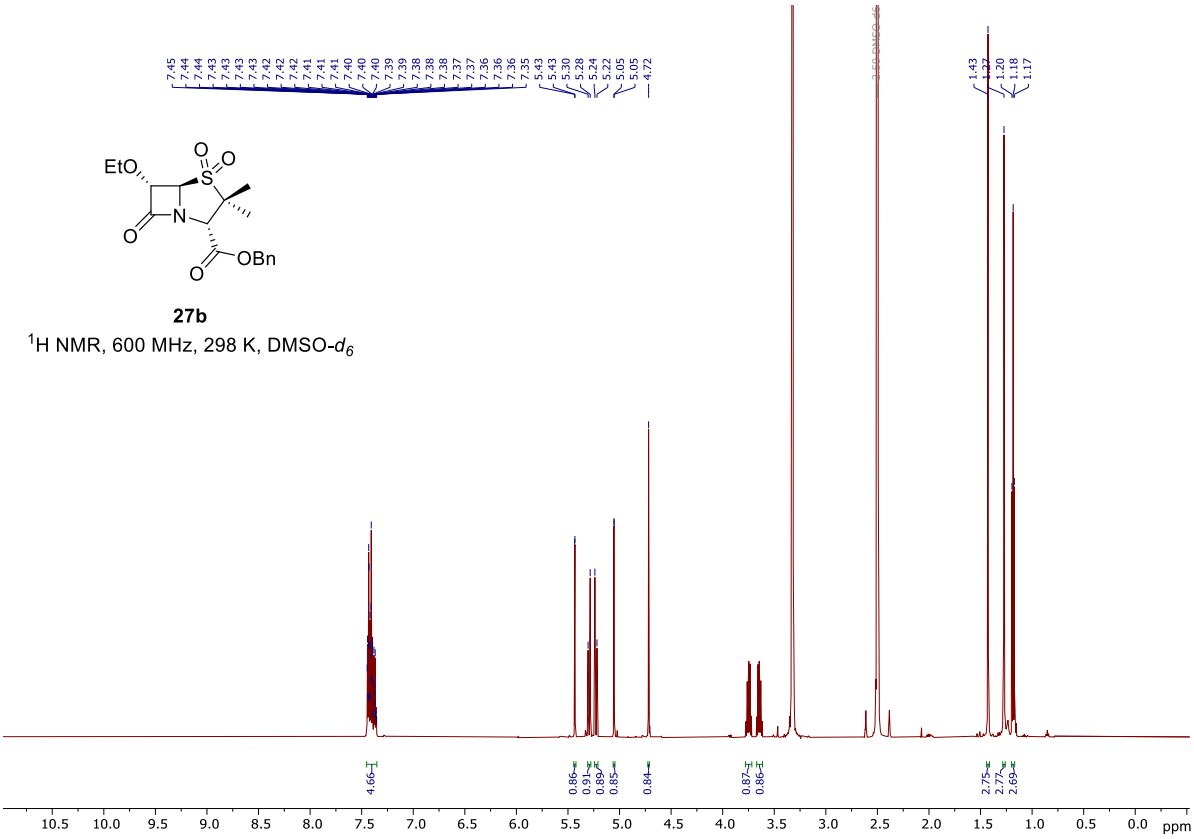

27b

^{1}H NMR, 600 MHz, 298 K, DMSO-d_6

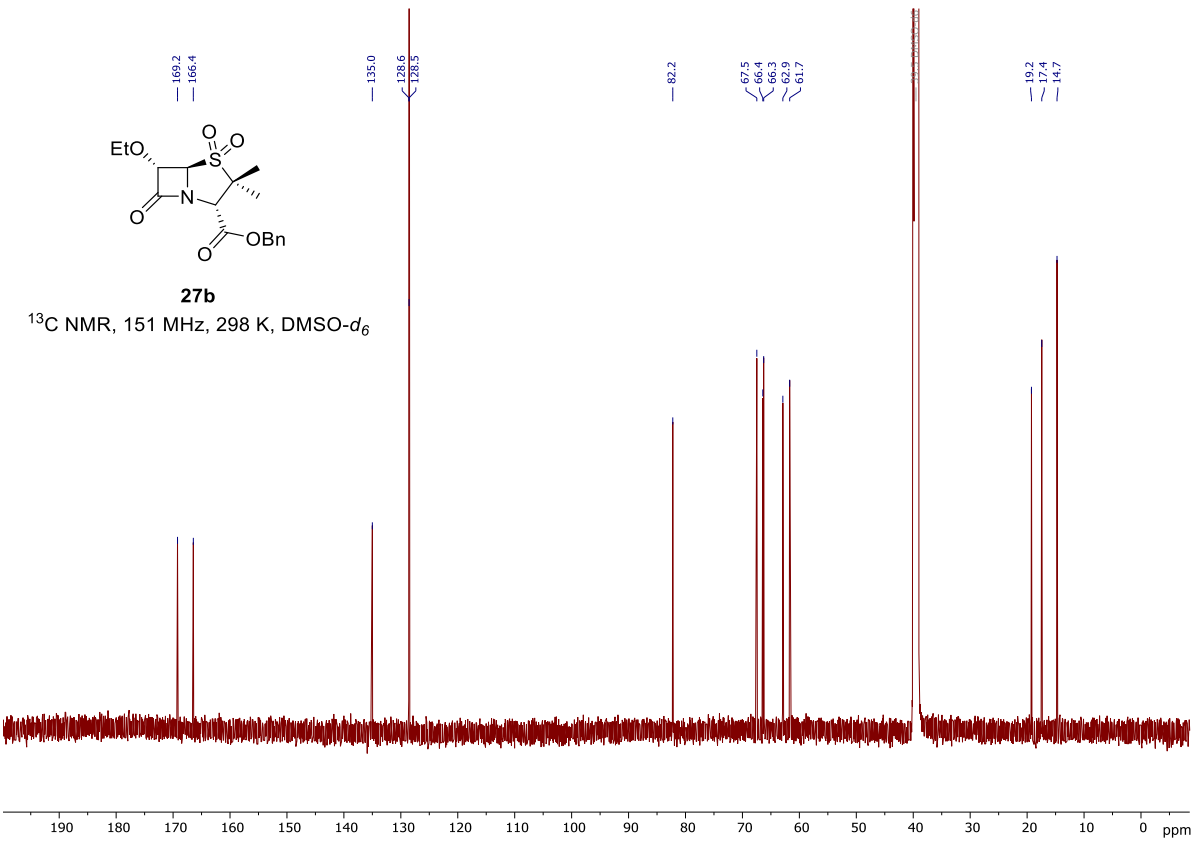

27b

^{13}C NMR, 151 MHz, 298 K, DMSO-d_6

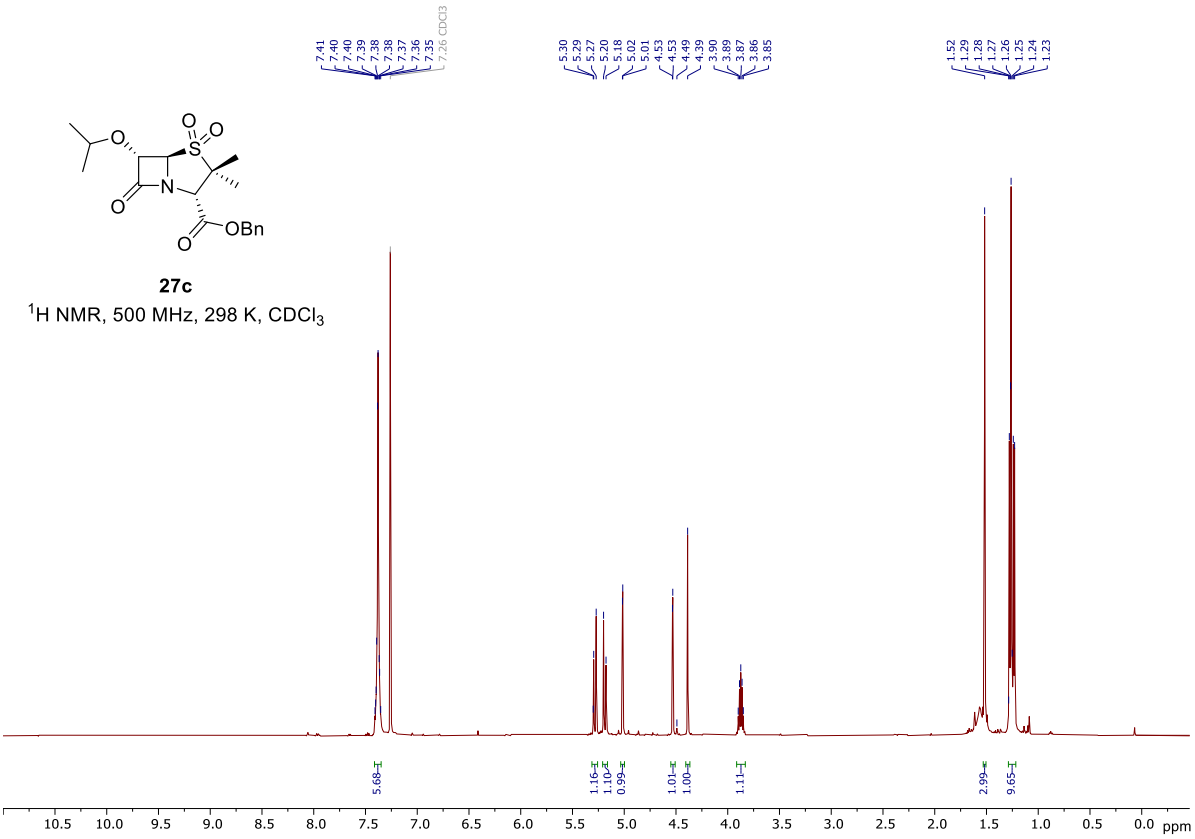

27c

^{1}H NMR, 500 MHz, 298 K, $CDCl_3$

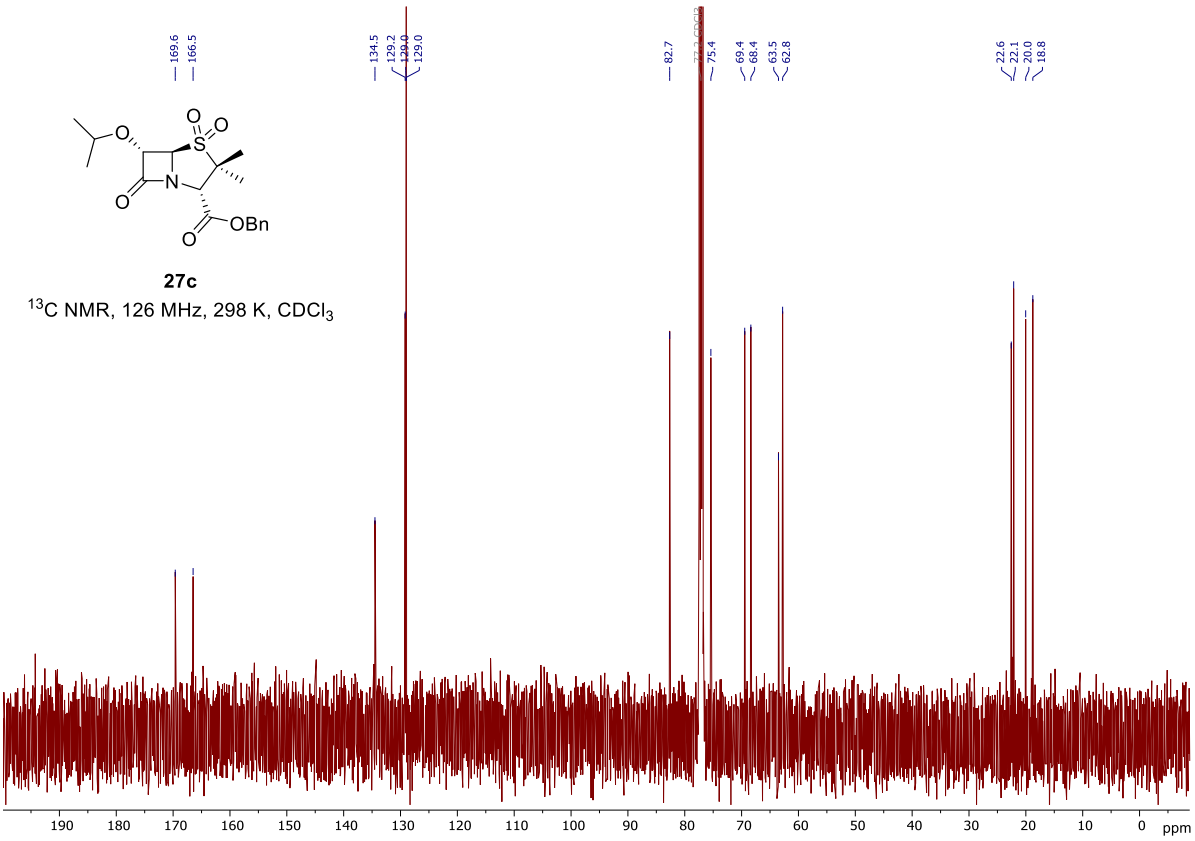

27c

^{13}C NMR, 126 MHz, 298 K, $CDCl_3$

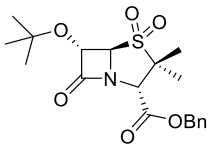

27d

^{1}H NMR, 500 MHz, 298 K, $CDCl_3$

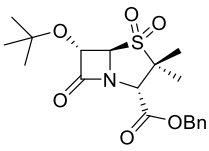

27d

^{13}C NMR, 126 MHz, 298 K, $CDCl_3$

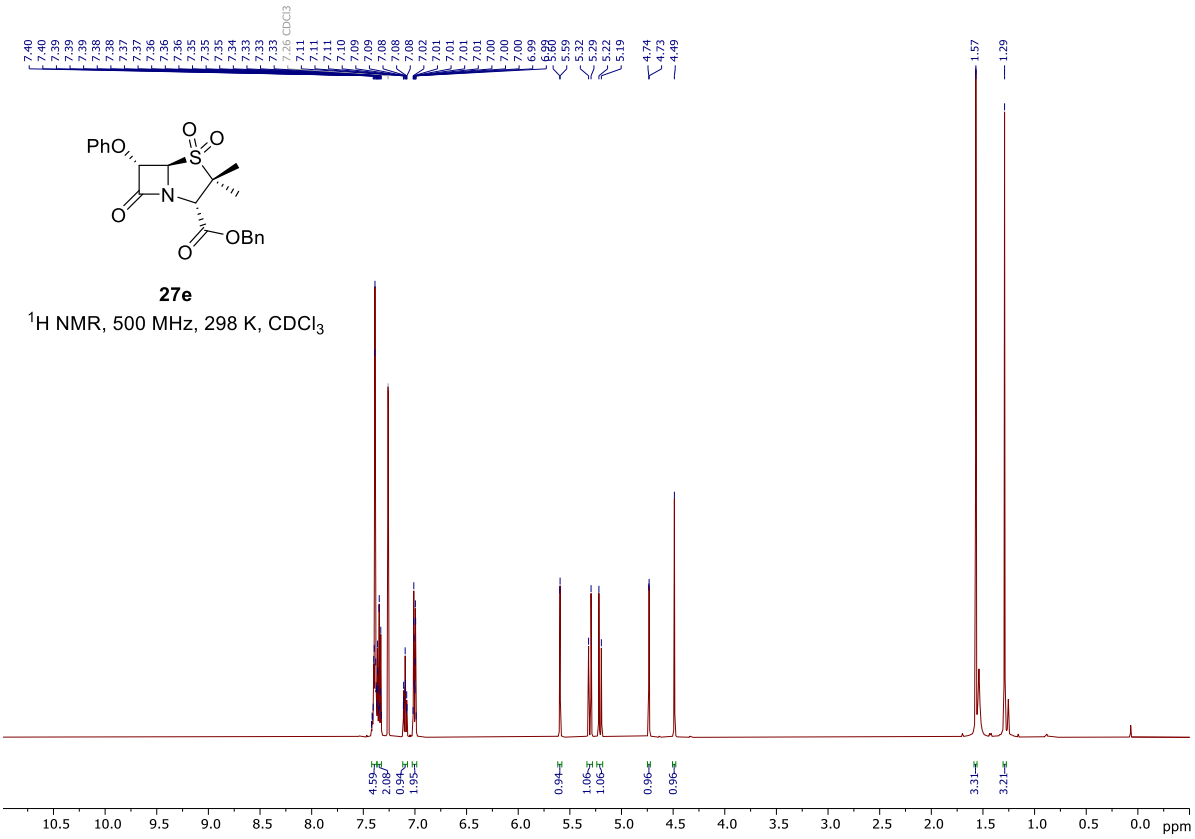
PhO
O
S
N
OBn
27e
1H NMR, 500 MHz, 298 K, CDCl3

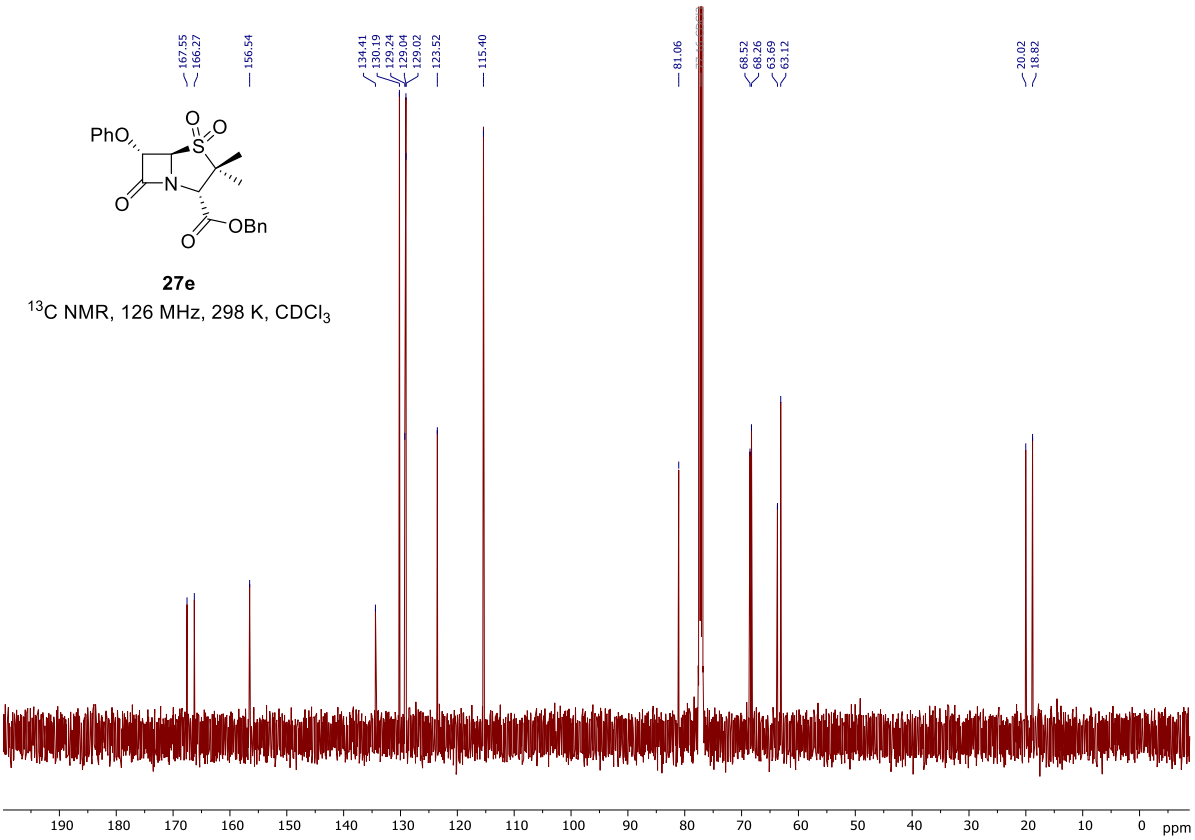
PhO
O
S
N
OBn
27e
13C NMR, 126 MHz, 298 K, CDCl3

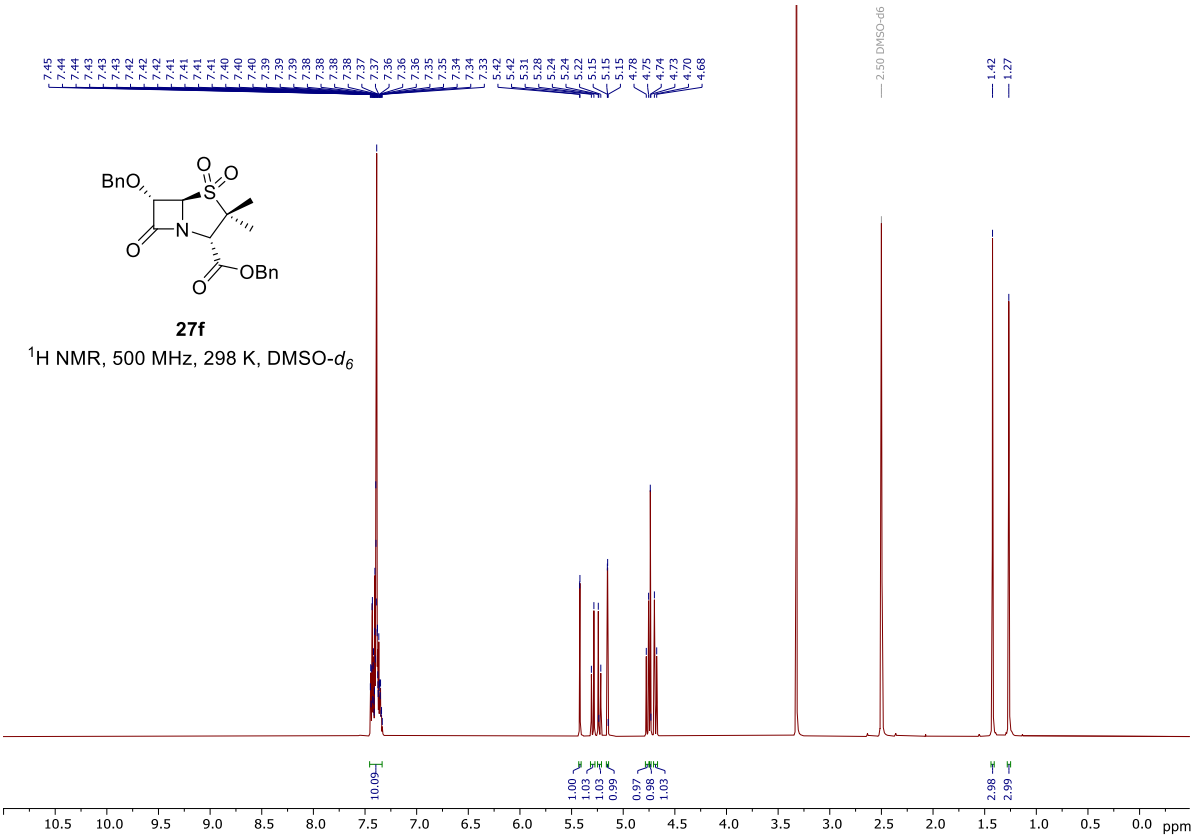

27f

^{1}H NMR, 500 MHz, 298 K, DMSO-d_6

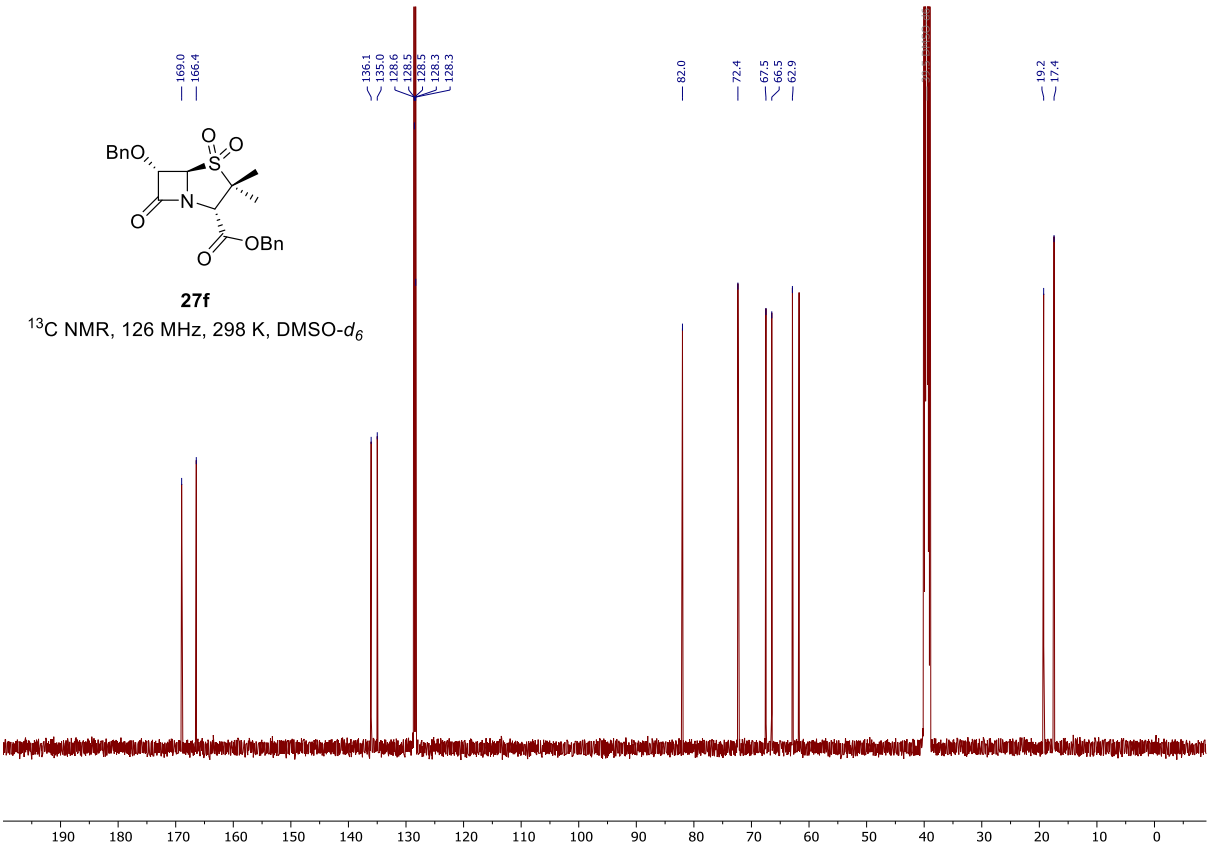

27f

^{13}C NMR, 126 MHz, 298 K, DMSO-d_6

8.2 Appendix to Chapter III (Manuscript II)

8.2.1 General synthesis information

All reagents and cephalosporin antibiotics were obtained from commercial sources (Sigma-Aldrich, Inc.; Flurochem Ltd.; Manchester Organics; Tokyo Chemical Industry Ltd.; Ambeed Inc.; MedChemExpress LLC; AstaTech Inc.; AK Scientific Inc.; Apollo Scientific Ltd.; Key Organics Ltd.; Aurum Pharmatech LLC; Biosynth Ltd.) and were used without further purification.

Ceftaroline,[1] 4-methoxybenzyl (5*S*,6*R*,7*R*)-3-(chloromethyl)-8-oxo-7-(2-phenylacetamido)-5-thia-1-azabicyclo[4.2.0]oct-2-ene-2-carboxylate 5-oxide (**3**),[2] (6*R*,7*R*)-3-(acetoxymethyl)-8-oxo-7-(2-phenylacetamido)-5-thia-1-azabicyclo[4.2.0]oct-2-ene-2-carboxylic acid (**10a**),[3] (6*R*,7*R*)-3-methyl-8-oxo-7-(2-phenylacetamido)-5-thia-1-azabicyclo[4.2.0]oct-2-ene-2-carboxylic acid (**10b**),[4] (6*R*,7*R*)-3-(((1-methyl-1*H*-tetrazol-5-yl)thio)methyl)-8-oxo-7-(2-phenylacetamido)-5-thia-1-azabicyclo[4.2.0]oct-2-ene-2-carboxylic acid (**10g**),[5] 4-methoxybenzyl (6*R*,7*R*)-3-(acetoxymethyl)-8-oxo-7-(2-phenylacetamido)-5-thia-1-azabicyclo[4.2.0]oct-2-ene-2-carboxylate (**11a**),[6] *N*-((5*aR*,6*R*)-1,7-dioxo-1,4,5a,6-tetrahydro-3H,7H-azeto[2,1-b]furo[3,4-d][1,3]thiazin-6-yl)-2-phenylacetamide (**12**),[7] 4-methoxybenzyl (6R,7R)-3-(iodomethyl)-8-oxo-7-(2-phenylacetamido)-5-thia-1-azabicyclo[4.2.0]oct-2-ene-2-carboxylate (**13**),[8] 4-methoxybenzyl (6R,7R)-3-formyl-8-oxo-7-(2-phenylacetamido)-5-thia-1-azabicyclo[4.2.0]oct-2-ene-2-carboxylate (**18**),[9] 1-(((6*R*,7*R*)-2-(((4-methoxybenzyl)oxy)carbonyl)-8-oxo-7-(2-phenylacetamido)-5-thia-1-azabicyclo[4.2.0]oct-2-en-3-yl)methyl)pyridin-1-ium iodide (**20a**),[10] 1-(((6*R*,7*R*)-2-(((4-methoxybenzyl)oxy)carbonyl)-8-oxo-7-(2-phenylacetamido)-5-thia-1-azabicyclo[4.2.0]oct-2-en-3-yl)methyl)-6,7-dihydro-5*H*-cyclopenta[*b*]pyridin-1-ium iodide (**20f**)[11] were synthesized as reported.

Anhydrous solvents (Sigma-Aldrich, Inc.) were kept under an atmosphere of argon. HPLC grade solvents (Sigma-Aldrich Inc.) were used for reaction work-ups, extractions, and purifications. Flash column chromatography was performed using an automated Biotage Isolera One purification machine equipped with Biotage®Sfär flash chromatography cartridges. ^{1}H and ^{13}C NMR spectra were recorded using Bruker AVANCE AVIIIHD 400, 500 and 600 MHz machines. Chemical shifts for protons are reported in parts per million (ppm) downfield from tetramethylsilane and are referenced to residual protium in the NMR solvent (*i.e.*, $CDCl_3$: $\delta = 7.26$ ppm; DMSO-d_6: $\delta = 2.50$ ppm). For ^{13}C NMR, chemical shifts are reported in the scale relative to the NMR solvent (*i.e.*, $CDCl_3$: $\delta = 77.2$ ppm; DMSO-d_6: $\delta = 39.5$ ppm). NMR data are reported in the following manner: chemical shift, multiplicity, coupling constant (J, Hz; to nearest 0.1 Hz), and integration.

Infrared (IR) spectroscopy was performed using a Bruker Tensor-27 Fourier transform infrared (FT-IR) spectrometer. High-resolution mass spectrometry (HRMS) was performed using either electro-spray ionization (ESI) mass spectrometry (MS) in the positive or negative ionization modes employing a Thermo Scientific Exactive mass spectrometer (ThermoFisher Scientific), or atmospheric pressure chemical ionization (APCI) in the positive mode using an Agilent 7200 Accurate mass spectrometer; data are presented as a mass-to-charge ratio (m/z). Optical rotation ($[\alpha]_D^{25}$) measurements were performed using a Bellingham + Stanley (ADP450) polarimeter.

8.2.2 General synthesis procedures

General procedure A:

A variation of a reported procedure was followed.[12] To a stirred solution of commercially sourced 7-amino-3-chloromethyl-3-cephem-4-carboxylic acid *p*-methoxybenzyl ester hydrochloride (1 equiv.) and carboxylic acid (1.2 equiv.) in anhydrous EtOAc (0.2 M) was added phenyl

dichlorophosphate (1.2 equiv.) at -20 °C, followed by dropwise addition over 5 min of *N*-methylmorpholine (4 equiv.). The reaction mixture was at -20 °C for 1.5-3 h, before being diluted with EtOAc. The mixture was sequentially washed with aqueous HCl solution (1 M), H_2O, saturated aqueous $NaHCO_3$ solution, and brine. The organic layer was then dried over Na_2SO_4, filtered, concentrated *in vacuo*, and purified by flash column chromatography.

General procedure B

To a solution of a cephem (1 equiv.) in CH_2Cl_2 (0.05 M) cooled to 0 °C were sequentially added a coupling reagent (1.1 equiv.), an alcohol (4 equiv.), and 4-(dimethylamino)pyridine (0.15 equiv.). After stirring for 2-3 h at 0 °C, the reaction mixture was filtered, then diluted with CH_2Cl_2. The organic layer was washed with aqueous HCl solution (1 M) and brine, then dried over Na_2SO_4, filtered, concentrated *in vacuo*, and purified by flash column chromatography.

General procedure C

A variation of a reported procedure was followed.[4] A cephem (1 equiv.) was added to a stirred solution of Na_2CO_3 (1.1 equiv.) in H_2O:acetone (1:1; 0.4 M) at -5 °C, then stirred for 5 min, before dropwise addition of phenylacetyl chloride (1.1 equiv.). The reaction mixture was stirred for 2 h at -5 °C, then diluted with an equal volume of H_2O and further stirred for 1 h at 0 °C, before being acidified to pH 3 by addition of an aqueous HCl solution (1 M). The mixture was extracted with EtOAc, and the combined organic extracts were washed with saturated brine. The organic layer was dried over Na_2SO_4, filtered, concentrated *in vacuo*. The solid residue was washed with Et_2O and then dried *in vacuo*, before being purified by reverse-phase flash column chromatography.

General procedure D

A variation of a reported procedure was followed.[13] To a solution of 4-methoxybenzyl chloride (1.35 equiv.) in *N*,*N*-dimethylformamide (0.9 M) was added NaBr (7.6 equiv.); the mixture was stirred for 2 h, then diluted with 1,4-dioxane (5:3 *N*,*N*-dimethylformamide:1,4-dioxane ratio; 0.6 M final solution concentration). To the resultant solution were sequentially added a cephem (1 equiv.), then $NaHCO_3$ (1.1 equiv.); the reaction mixture was then stirred for 16-18 h at room temperature, before being diluted with brine and EtOAc. The organic layer was separated, and the aqueous layer was further extracted twice with EtOAc. The combined organic extracts were washed with saturated aqueous LiCl solution, water, saturated aqueous $NaHCO_3$ solution and brine. The organic layer was dried over Na_2SO_4, filtered, concentrated *in vacuo*, and recrystallised from a mixture of EtOAc and cyclohexane. The obtained recrystallised solid was then purified by flash column chromatography.

General procedure E

A variation of a reported procedure was followed.[14] To a solution of a cephem (1 equiv.) in MeOH-$CHCl_3$ (1:1; 0.03 M) was added the HCl salt of an *O*-alkoxyhydroxylamine (1-1.1 equiv.) and AcONa (1 equiv.), and the reaction mixture was stirred for 1-18 h at room temperature, before dilution with $CHCl_3$. The organic layer was washed with aqueous phosphate buffer (NaH_2PO_4/Na_2HPO_4, 1:9 (w/w), 0.1 M, pH 8), then dried over Na_2SO_4, filtered, concentrated *in vacuo*, and purified by flash column chromatography.

General procedure F

To a solution of a cephem (1 equiv.) in *N*,*N*-dimethylformamide (0.3 M) was added RSO_2Na (1.14 equiv.), and the reaction mixture was stirred at room temperature for 18 h, before being diluted with brine and EtOAc. The organic layer was separated, and the aqueous layer was further extracted twice with EtOAc. The combined organic extracts were washed with saturated aqueous LiCl solution, water, and brine. The organic layer was dried over Na_2SO_4, filtered, concentrated *in vacuo*, and purified by flash column chromatography.

General procedure G

A variation of a reported procedure was followed.[10] To a solution of cephem (1 equiv.) in ethyl acetate (0.07-0.2 M) was added a base (1-4 equiv.), and the reaction mixture was stirred at 0 °C for 1 h, then at room temperature for 18 h; the formed precipitate was filtered, washed with Et_2O, and dried *in vacuo*. No further purification was performed.

8.2.3 Experimental procedures and compounds characterisations

4-Methoxybenzyl (5*S*,6*R*,7*R*)-3-(chloromethyl)-8-oxo-7-(2-phenylacetamido)-5-thia-1-azabicyclo[4.2.0]oct-2-ene-2-carboxylate 5-oxide (3)[2]

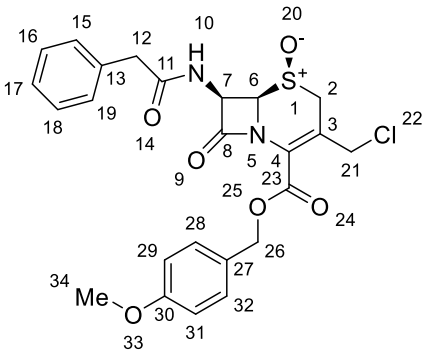

A variation of a reported procedure was followed.[2] To a stirred solution of 4-methoxybenzyl (6*R*,7*R*)-3-(chloromethyl)-8-oxo-7-(2-phenylacetamido)-5-thia-1-azabicyclo[4.2.0]oct-2-ene-2-carboxylate (200 mg, 0.411 mmol, 1 equiv.) in anhydrous CH_2Cl_2 (5 mL) was added *m*-chloroperbenzoic acid (<77% purity; 94 mg, 1.02 equiv.) in

portions over 5 min at 0 °C. The reaction mixture was stirred for 1.5 h at 0 °C, before being diluted with CH_2Cl_2. The mixture was sequentially washed with aqueous $NaHSO_3$ solution (10% (w/v)), H_2O, saturated aqueous $NaHCO_3$ solution, and brine. The organic layer was dried over Na_2SO_4, filtered, and concentrated *in vacuo*. After work-up, no further purifications were required, yielding the product **3** (156 mg, 76%). The analytical data are consistent with those reported.[2]

White solid; m.p.: 206 °C (decomposition); ^{1}H NMR (500 MHz, 298 K, DMSO-d_6): δ = 8.44 (d, *J* = 8.4 Hz, 1H, *N10H*), 7.39 – 7.35 (m, 2H, *C28H*, *C32H*), 7.30 (m, 4H, *C15H*, *C16H*, *C18H*, *C19H*), 7.23 (m, 1H, *C17H*), 6.97 – 6.90 (m, 2H, *C29H*, *C31H*), 5.85 (dd, *J* = 8.3, 4.8 Hz, 1H, *C7H*), 5.29 and 5.21 (ABq, *J* = 12.0 Hz, 2H, *C26H*$_2$), 4.92 (dd, *J* = 4.8, 1.6 Hz, 1H, *C5H*), 4.67 and 4.51 (ABq, *J* = 11.5 Hz, 2H, *C21H*$_2$), 3.92 (d, *J* = 18.3 Hz, 1H, *C2H*), 3.75 (s, 3H, *C34H*$_3$), 3.72 – 3.66 (m, 2H, *C2H*, *C12H*), 3.55 ppm (d, *J* = 14.0 Hz, 1H, *C12H*); ^{13}C NMR (126 MHz, 298 K, DMSO-d_6): δ = 171.0, 164.4, 160.4, 159.4, 135.8, 130.4, 129.1, 128.3, 126.8, 126.5, 124.9, 120.2, 113.8, 67.5, 66.5, 58.3, 55.1, 46.0, 44.1, 41.4 ppm; IR (film): $\tilde{\nu}$ = 1783, 1715, 1645, 1528, 1518, 1454, 1395, 1366, 1302, 1251, 1177, 1145, 1104, 1069, 1033 cm^{-1}; HRMS (ESI): m/z calculated for $C_{24}H_{24}ClN_2O_6S$ $[M+H]^+$: 503.1038, found: 503.1038; $[\alpha]_D^{25}$ could not be obtained due to limited solubility in suitable solvents even at low concentrations.

4-Methoxybenzyl (6*R*,7*R*)-3-(chloromethyl)-8-oxo-7-(2-phenylacetamido)-5-thia-1-azabicyclo[4.2.0]oct-2-ene-2-carboxylate 5,5-dioxide (**4**)

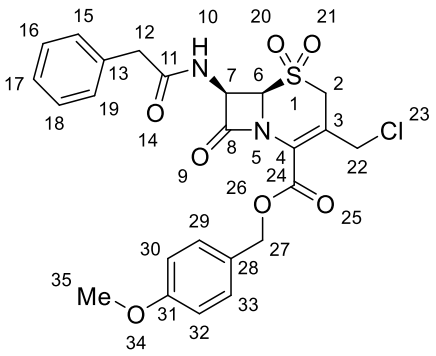

To a stirred solution of 4-methoxybenzyl (6*R*,7*R*)-3-(chloromethyl)-8-oxo-7-(2-phenylacetamido)-5-thia-1-azabicyclo[4.2.0]oct-2-ene-2-carboxylate (487 mg, 1 mmol, 1 equiv.) in anhydrous *N*,*N*-dimethylformamide (20 mL) was added *m*-chloroperbenzoic acid (<77% purity; 670 mg, 3 equiv.) at 0 °C. The reaction mixture was stirred for 48 h at room temperature, before being diluted with EtOAc. The mixture was sequentially washed with aqueous $NaHSO_3$ solution (10% (w/v)), H_2O, saturated aqueous $NaHCO_3$ solution, saturated aqueous LiCl solution, and brine. The organic layer was dried over Na_2SO_4, filtered, and concentrated *in vacuo*. Purification by flash column chromatography (10 g Sfär, $100\%_{v/v}$ cyclohexane (2 CV), followed by a linear gradient (36 CV): $0\%_{v/v} \rightarrow 60\%_{v/v}$ ethyl acetate in cyclohexane) afforded **4** (145 mg, 28%).

White solid; m.p.: 148-150 °C; ^{1}H NMR (500 MHz, 298 K, DMSO-*d*$_6$): δ = 8.92 (d, *J* = 8.7 Hz, 1H, *N10H*), 7.39 – 7.33 (m, 2H, *C29H*, *C33H*), 7.32 – 7.18 (m, 5H, *C15H*, *C16H*, *C17H*, *C18H*, *C19H*), 6.97 – 6.91 (m, 2H, *C30H*, *C32H*), 6.00 (dd, *J* = 8.7, 4.9 Hz, 1H, *C7H*), 5.44 (d, *J* = 4.8 Hz, 1H, *C6H*), 5.28 and 5.21 (ABq, *J* = 12.0 Hz, 2H, *C27H*$_2$), 4.55 – 4.43 (m, 3H, *C2H*, *C22H*$_2$), 4.12 (d, *J* = 17.9 Hz, 1H, *C2H*), 3.75 (s, 3H, *C35H*$_3$), 3.64 – 3.53 ppm (m, 2H, *C12H*$_2$); ^{13}C NMR (126 MHz, 298 K, DMSO-*d*$_6$): δ = 170.9, 164.5, 160.3, 159.4, 135.5, 130.4, 129.1, 128.2, 126.6, 126.5, 125.1, 124.1, 113.8, 67.8, 66.9, 58.4, 55.1, 51.1, 42.6, 41.2 ppm; IR (film): $\tilde{\nu}$ = 1770, 1733, 1701, 1646, 1614, 1516, 1455, 1439, 1328, 1234, 1178, 1134, 1123, 1095, 1062, 1020 cm^{-1}; HRMS

(ESI): m/z calculated for $C_{24}H_{23}ClN_2O_7SNa$ $[M+Na]^+$: 541.0807, found: 541.0809; $[\alpha]_D^{25}$ = -70 (c = 0.004 g/mL, $CHCl_3$).

4-Methoxybenzyl (6*R*,7*R*)-3-(chloromethyl)-8-oxo-7-(2-(perfluorophenyl)acetamido)-5-thia-1-azabicyclo[4.2.0]oct-2-ene-2-carboxylate (6a)

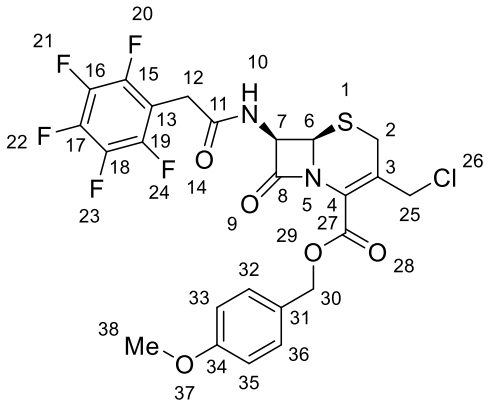

General procedure A was applied using 7-amino-3-chloromethyl-3-cephem-4-carboxylic acid *p*-methoxybenzyl ester hydrochloride (300 mg, 0.74 mmol, 1 equiv.) and 2,3,4,5,6-pentafluorophenylacetic acid (203 mg, 0.9 mmol, 1.2 equiv.). Purification by flash column chromatography (25 g Sfär, 100%$_{v/v}$ cyclohexane (2 CV), followed by a linear gradient (40 CV): 0%$_{v/v}$ →60%$_{v/v}$ ethyl acetate in cyclohexane) afforded **6a** (74 mg, 14%).

White solid; m.p.: 185 °C (decomposition); ^{1}H NMR (500 MHz, 298 K, DMSO-*d*$_6$): δ = 9.33 (d, *J* = 8.3 Hz, 1H, *N10H*), 7.38 – 7.34 (m, 2H, *C32H*, *C36H*), 6.95 – 6.92 (m, 2H, *C33H*, *C35H*), 5.74 (dd, *J* = 8.3, 4.9 Hz, 1H, *C7H*), 5.26 (d, *J* = 12.0 Hz, 1H, *C30H*), 5.19 – 5.16 (m, 2H, *C6H*, *C30H*), 4.54 and 4.46 (ABq, *J* = 11.3 Hz, 2H, *C25H*$_2$), 3.79 – 3.69 (m, 6H, *C2H*, *C12H*$_2$, *C38H*$_3$), 3.58 ppm (d, *J* = 18.0 Hz, 1H, *C2H*); ^{13}C NMR (126 MHz, 298 K, DMSO): δ = 167.7, 164.6, 161.1, 159.4, 130.3 (3 C), 126.9, 125.3, 125.0, 113.8 (3 C), 67.3, 59.3, 57.7, 55.1, 43.8, 28.3, 26.1; ^{19}F NMR (377 MHz, 298 K, DMSO-*d*$_6$): δ = -142.27 (dd, *J* = 23.9, 7.7 Hz, 2F, *C15F*, *C19F*), -156.56 (t, *J* = 22.3 Hz, 1F, *C17F*), -163.43 ppm (m, 2F, *C16F*, *C18F*); IR (film): $\tilde{\nu}$ = 1879, 1785, 1724, 1710, 1691, 1676, 1659, 1641, 1630, 1612, 1548, 1510, 1482, 1467, 1441, 1412, 1390, 1357,

1305, 1263, 1176, 1102, 1033 cm^{-1}; HRMS (ESI): m/z calculated for $C_{24}H_{22}ClF_5N_3O_5S$ $[M+NH_4]^+$: 594.0883, found: 594.0892; $[\alpha]_D^{25}$ = +61 (c = 0.003 g/mL, $CHCl_3$).

4-Methoxybenzyl (6*R*,7*R*)-3-(chloromethyl)-8-oxo-7-(2-(thiophen-2-yl)acetamido)-5-thia-1-azabicyclo[4.2.0]oct-2-ene-2-carboxylate (6b)[15]

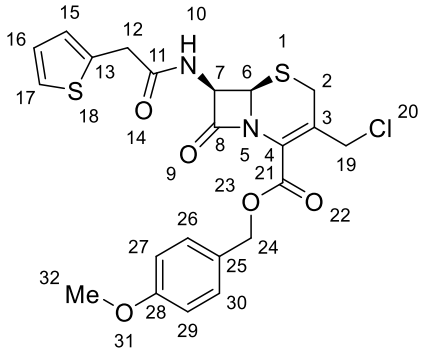

General procedure A was applied using 7-amino-3-chloromethyl-3-cephem-4-carboxylic acid *p*-methoxybenzyl ester hydrochloride (300 mg, 0.74 mmol, 1 equiv.) and 2-thiopheneacetic acid (128 mg, 0.9 mmol, 1.2 equiv.). Purification by flash column chromatography (25 g Sfär, 100%$_{v/v}$ cyclohexane (2 CV), followed by a linear gradient (36 CV): 0%$_{v/v}$ →60%$_{v/v}$ ethyl acetate in cyclohexane) afforded **6b** (72 mg, 26%). Synthesis of **6b** was achieved following an alternative experimental procedure to that reported.[15] The analytical data are consistent with those reported.[15]

White solid; m.p.: 164 °C; ^{1}H NMR (500 MHz, 298 K, DMSO-d_6): δ = 9.17 (d, *J* = 8.4 Hz, 1H, *N10H*), 7.39 – 7.34 (m, 3H, *C17H*, *C26H*, *C30H*), 6.97 – 6.91 (m, 4H, *C15H*, *C16H*, *C27H*, *C29H*), 5.74 (dd, *J* = 8.4, 4.9 Hz, 1H, *C7H*), 5.26 (d, *J* = 12.0 Hz, 1H, *C24H*), 5.19 – 5.15 (m, 2H, *C6H*, *C24H*), 4.54 and 4.45 (ABq, *J* = 11.3 Hz, 2H, $C19H_2$), 3.79 – 3.69 (m, 6H, *C2H*, $C12H_2$, $C32H_3$), 3.56 ppm (d, *J* = 18.0 Hz, *C2H*); ^{13}C NMR (126 MHz, 298 K, DMSO-d_6): δ = 169.9, 165.0, 161.1, 159.4, 136.8, 130.3, 126.9, 126.6, 126.3, 125.3, 125.0, 124.9, 113.8, 67.3, 59.2, 57.8, 55.1, 43.8, 35.8, 26.1 ppm; IR (film): $\tilde{\nu}$ = 1782, 1717, 1669, 1615, 1516, 1457, 1437, 1387, 1362, 1304, 1247, 1174, 1099, 1065, 1032 cm^{-1}; HRMS (ESI): m/z calculated for $C_{22}H_{25}ClN_3O_5S_2$ $[M+NH_4]^+$: 510.0919, found: 510.0927; $[\alpha]_D^{25}$ = -17 (c = 0.007 g/mL, $CHCl_3$).

4-Methoxybenzyl (6*R*,7*R*)-3-(chloromethyl)-7-(2-(naphthalen-2-yl)acetamido)-8-oxo-5-thia-1-azabicyclo[4.2.0]oct-2-ene-2-carboxylate (6c)

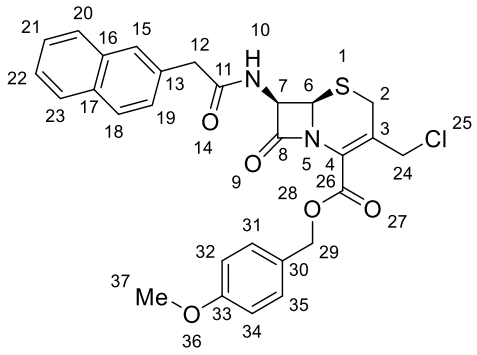

General procedure A was applied using 7-amino-3-chloromethyl-3-cephem-4-carboxylic acid *p*-methoxybenzyl ester hydrochloride (300 mg, 0.74 mmol, 1 equiv.) and 2-naphtaleneacetic acid (137 mg, 0.9 mmol, 1.2 equiv.). Purification by flash column chromatography (25 g Sfär, 100%$_{v/v}$ cyclohexane (2 CV), followed by a linear gradient (32 CV): 0%$_{v/v}$ →60%$_{v/v}$ ethyl acetate in cyclohexane) afforded **6c** (72 mg, 15%).

White solid; m.p.: 147 °C (decomposition); ^{1}H NMR (500 MHz, 298 K, $CDCl_3$): δ = 7.87 – 7.77 (m, 3H, *C18H*, *C20H*, *C23H*), 7.74 – 7.70 (m, 1H, *C15H*), 7.51 – 7.45 (m, 2H, *C21H*, *C22H*), 7.36 (dd, *J* = 8.5, 1.8 Hz, 1H, *C19H*), 7.33 – 7.29 (m, 2H, *C31H*, *C35H*), 6.92 – 6.84 (m, 2H, *C32H*, *C34H*), 6.18 (d, *J* = 9.1 Hz, 1H, *N10H*), 5.82 (dd, *J* = 9.1, 4.9 Hz, 1H, *C7H*), 5.18 (s, 2H, *C29H$_2$*), 4.91 (d, *J* = 4.9 Hz, 1H, *C6H*), 4.49 and 4.35 (ABq, *J* = 11.8 Hz, 2H, *C24H$_2$*), 3.82 and 3.77 (ABq, *J* = 16.2 Hz, 2H, *C12H$_2$*), 3.79 (s, 3H, *C37H$_3$*), 3.57 and 3.36 ppm (ABq, *J* = 18.2 Hz, 2H, *C2H$_2$*); ^{13}C NMR (126 MHz, 298 K, $CDCl_3$): δ = 171.2, 164.6, 161.2, 160.1, 133.7, 132.8, 131.1, 130.8, 129.2, 128.6, 127.92, 127.88, 127.2, 126.7, 126.7, 126.4, 126.1, 125.7, 114.1, 68.4, 59.4, 57.8, 55.4, 43.6, 43.4, 27.2 ppm; IR (film): $\tilde{\nu}$ = 1787, 1724, 1665, 1613, 1548, 1514, 1441, 1363, 1303, 1262, 1174, 1098, 1031 cm^{-1}; HRMS (ESI): m/z calculated for $C_{28}H_{26}ClN_2O_5S$ $[M+H]^+$: 537.1245, found: 535.1247; $[\alpha]_D^{25}$ = -6.6 (c = 0.003 g/mL, $CHCl_3$).

4-Methoxybenzyl (6*R*,7*R*)-3-(chloromethyl)-8-oxo-7-(2-phenoxyacetamido)-5-thia-1-azabicyclo[4.2.0]oct-2-ene-2-carboxylate (6d)

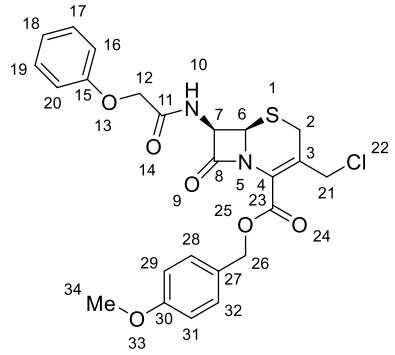

General procedure A was applied using 7-amino-3-chloromethyl-3-cephem-4-carboxylic acid *p*-methoxybenzyl ester hydrochloride (300 mg, 0.74 mmol, 1 equiv.) and phenoxyacetic acid (137 mg, 0.9 mmol, 1.2 equiv.). Purification by flash column chromatography (25 g Sfär, 100%$_{v/v}$ cyclohexane (2 CV), followed by a linear gradient (30 CV): 0%$_{v/v}$ →30%$_{v/v}$ ethyl acetate in cyclohexane) afforded **6d** (54 mg, 12%).

White solid; m.p.: 139-140 °C; ^{1}H NMR (600 MHz, 298 K, DMSO-*d*$_6$): δ = 9.16 (d, *J* = 8.4 Hz, 1H, *N10H*), 7.40 – 7.34 (m, 2H, *C28H*, *C32H*), 7.32 – 7.26 (m, 2H, *C17H*, *C19H*), 6.99 – 6.89 (m, 5H, *C16H*, *C18H*, *C20H*, *C29H, C31H*), 5.78 (dd, *J* = 8.4, 4.9 Hz, 1H, *C7H*), 5.26 (d, *J* = 12.0 Hz, 1H, *C26H*), 5.21 – 5.15 (m, 2H, *C6H*, *C26H*), 4.66 – 4.56 (m, 2H, *C12H*$_2$), 4.54 and 4.46 (ABq, *J* = 11.3 Hz, 2H, *C21H*$_2$), 3.75 (s, 3H, *C34H*$_3$), 3.72 and 3.57 ppm (ABq, *J* = 18.0 Hz, 2H, *C2H*$_2$); ^{13}C NMR (151 MHz, 298 K, DMSO-*d*$_6$): δ = 168.5, 164.4, 161.1, 159.4, 157.7, 130.4, 129.5, 126.9, 125.4, 124.9, 121.1, 114.5, 113.8, 67.3, 66.1, 58.9, 57.7, 55.1, 43.8, 26.2 ppm; IR (film): $\tilde{\nu}$ = 1786, 1722, 1691, 1613, 1517, 1494, 1441, 1361, 1304, 1260, 1174, 1100, 1022 cm^{-1}; HRMS (ESI): m/z calculated for $C_{24}H_{27}ClN_3O_6S$ $[M+NH_4]^+$: 520.1304, found: 520.1308; $[\alpha]_D^{25}$ = -6 (c = 0.004 g/mL, $CHCl_3$).

4-Methoxybenzyl (6*R*,7*R*)-3-(chloromethyl)-7-(2-cyclohexylacetamido)-8-oxo-5-thia-1-azabicyclo[4.2.0]oct-2-ene-2-carboxylate (6e)

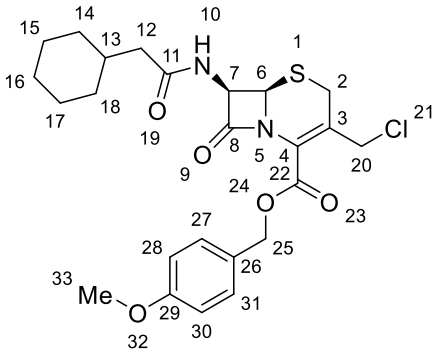

General procedure A was applied using 7-amino-3-chloromethyl-3-cephem-4-carboxylic acid *p*-methoxybenzyl ester hydrochloride (300 mg, 0.74 mmol, 1 equiv.) and cyclohexylacetic acid (130 mg, 0.9 mmol, 1.2 equiv.). Purification by flash column chromatography (25 g Sfär, 100%$_{v/v}$ cyclohexane (2 CV), followed by a linear gradient (30 CV): 0%$_{v/v}$ →60%$_{v/v}$ ethyl acetate in cyclohexane) afforded **6e** (33 mg, 7%).

White solid; m.p.: 165 °C (decomposition); ^{1}H NMR (500 MHz, 298 K, DMSO-*d*$_6$): δ = 8.82 (d, *J* = 8.3 Hz, 1H, *N10H*), 7.41 – 7.33 (m, 2H, *C27H*, *C31H*), 6.96 – 6.92 (m, 2H, *C28H*, *C30H*), 5.71 (dd, *J* = 8.3, 4.9 Hz, 1H, *C7H*), 5.25 (d, *J* = 12.0 Hz, 1H, *C25H*), 5.19 – 5.13 (m, 2H, *C6H*, *C25H*), 4.52 and 4.44 (d, *J* = 11.3 Hz, 1H, *C20H*$_2$), 3.75 (s, 3H, *C33H*$_3$), 3.71 and 3.55 (ABq, *J* = 18.0 Hz, 2H, *C2H*$_2$), 2.13 – 1.98 (m, 2H, *C12H*$_2$), 1.64 (m, 5H, *C13H, C14H*, *C15H*, *C17H*, *C18H*), 1.25 – 1.09 (m, 4H, *C15H*, *C16H*$_2$, *C17H*), 0.94 – 0.83 ppm (m, 2H, *C14H*, *C18H*); ^{13}C NMR (126 MHz, 298 K, DMSO-*d*$_6$): δ 172.2, 165.2, 161.1, 159.4, 130.3, 126.9, 125.4, 124.6, 113.8, 67.3, 59.1, 58.0, 55.1, 43.8, 42.5, 34.8, 32.5, 32.3, 26.1, 25.8, 25.6, 25.57 ppm; IR (film): ṽ = 1782, 1723, 1658, 1643, 1548, 1530, 1514, 1443, 1359, 1261, 1219, 1099 cm^{-1}; HRMS (ESI): m/z calculated for $C_{24}H_{30}ClN_2O_5S$ $[M+H]^+$: 493.1558, found: 493.1559; $[\alpha]_D^{25}$ = +55 (c = 0.003 g/mL, $CHCl_3$).

4-Methoxybenzyl (6*R*,7*R*)-3-(chloromethyl)-7-(2-cyclopropylacetamido)-8-oxo-5-thia-1-azabicyclo[4.2.0]oct-2-ene-2-carboxylate (6f)

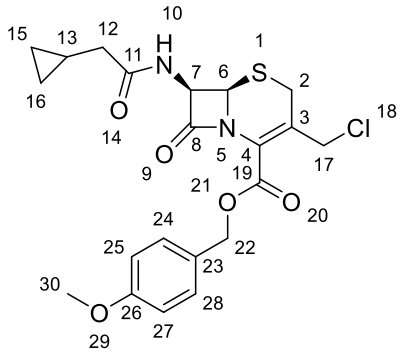

General procedure A was applied using 7-amino-3-chloromethyl-3-cephem-4-carboxylic acid *p*-methoxybenzyl ester hydrochloride (300 mg, 0.74 mmol, 1 equiv.) and cyclopropylacetic acid (90 mg, 0.9 mmol, 1.2 equiv.). Purification by flash column chromatography (25 g Sfär, 100%$_{v/v}$ cyclohexane (2 CV), followed by a linear gradient (32 CV): 0%$_{v/v}$ →60%$_{v/v}$ ethyl acetate in cyclohexane) afforded **6f** (58 mg, 14%).

White solid; m.p.: 154 °C (decomposition); ^{1}H NMR (500 MHz, 298 K, DMSO-*d*$_6$): δ = 8.76 (d, *J* = 8.5 Hz, 1H, *N10H*), 7.41 – 7.33 (m, 2H, *C24H*, *C28H*), 6.97 – 6.90 (m, 2H, *C25H*, *C27H*), 5.74 (dd, *J* = 8.5, 4.9 Hz, 1H, *C7H*), 5.25 (d, *J* = 11.9 Hz, 1H, *C22H*), 5.20 – 5.13 (m, 2H, *C6H*, *C22H*), 3.75 (s, 3H, *C30H*$_3$), 3.71 and 3.55 (ABq, *J* = 18.0 Hz, 2H, *C2H*$_2$), 2.13 – 2.01 (m, 2H, *C12H*$_2$), 0.95 (m, 1H, *C13H*), 0.47 – 0.38 (m, 2H, *C15H*, *C16H*), 0.18 – 0.09 ppm (m, 2H, *C15H*, *C16H*); ^{13}C NMR (126 MHz, 298 K, DMSO-*d*$_6$): δ = 172.4, 165.2, 161.1, 159.4, 130.3, 126.9, 125.4, 124.7, 113.8, 67.3, 59.1, 57.9, 55.1, 43.8, 26.1, 7.8, 4.2, 4.1 ppm; IR (film): $\tilde{\nu}$ = 1782, 1720, 1669, 1614, 1516, 1457, 1386, 1363, 1304, 1249, 1174, 1089, 1030 cm^{-1}; HRMS (ESI): m/z calculated for $C_{21}H_{23}ClN_2O_5SNa$ $[M+Na]^+$: 473.0908, found: 473.0912; $[\alpha]_D^{25}$ = +6 (c = 0.005 g/mL, $CHCl_3$).

4-Methoxybenzyl (6*R*,7*R*)-3-(chloromethyl)-7-(3-(methylthio)propanamido)-8-oxo-5-thia-1-azabicyclo[4.2.0]oct-2-ene-2-carboxylate (6g)

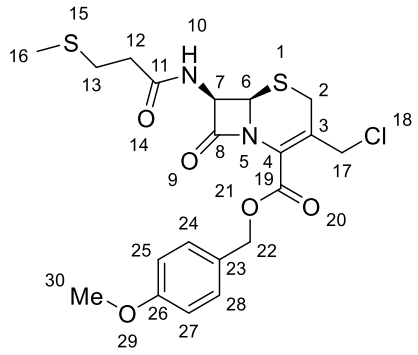

General procedure A was applied using 7-amino-3-chloromethyl-3-cephem-4-carboxylic acid *p*-methoxybenzyl ester hydrochloride (300 mg, 0.74 mmol, 1 equiv.) and 3-(methylthio)propionic acid (109 mg, 0.9 mmol, 1.2 equiv.). Purification by flash column chromatography (25 g Sfär, 100%$_{v/v}$ cyclohexane (2 CV), followed by a linear gradient (30 CV): 0%$_{v/v}$ →60%$_{v/v}$ ethyl acetate in cyclohexane) afforded **6g** (186 mg, 43%).

White solid; m.p.: 109-111 °C; ^{1}H NMR (400 MHz, 298 K, $CDCl_3$): δ = 7.39 – 7.30 (m, 2H, *C24H*, *C28H*), 6.94 – 6.86 (m, 2H, *C25H*, *C27H*), 6.47 (d, *J* = 9.0 Hz, 1H, *N10H*), 5.86 (dd, *J* = 9.0, 4.9 Hz, 1H, *C7H*), 5.23 (m, 2H, *C22H$_2$*), 4.98 (d, *J* = 4.9 Hz, 1H, *C6H*), 4.54 and 4.44 (ABq, *J* = 11.8 Hz, 2H, *C17H$_2$*), 3.81 (s, 3H, *C30H$_3$*), 3.66 and 3.49 (ABq, *J* = 18.3 Hz, 2H, *C2H$_2$*), 2.86 – 2.74 (m, 2H, *C12H$_2$*), 2.64 – 2.48 (m, 2H, *C13H$_2$*), 2.14 ppm (s, 3H, *C16H$_3$*); ^{13}C NMR (101 MHz, 298 K, $CDCl_3$): δ = 171.6, 164.9, 161.3, 160.1, 130.9, 126.7, 126.2, 125.8, 114.2, 68.4, 59.4, 57.8, 55.4, 43.4, 35.9, 29.6, 27.4, 15.8 ppm; IR (film): $\tilde{\nu}$ = 1784, 1719, 1670, 1614, 1540, 1517, 1457, 1386, 1361, 1304, 1260, 1174, 1098, 1065, 1030 cm^{-1}; HRMS (ESI): m/z calculated for $C_{20}H_{24}ClN_2O_5S_2$ $[M+H]^+$: 471.0810, found: 471.0807; $[\alpha]_D^{25}$ = +21 (c = 0.005 g/mL, $CHCl_3$).

(6*R*,7*R*)-3-(Chloromethyl)-8-oxo-7-(2-phenylacetamido)-5-thia-1-azabicyclo[4.2.0]oct-2-ene-2-carboxylic acid (**7**)

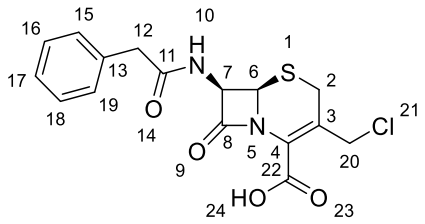

To a solution of (6*R*,7*R*)-4-methoxybenzyl 3-(chloromethyl)-8-oxo-7-(2-phenylacetamido)-5-thia-1-azabicyclo[4.2.0]oct-2-ene-2-carboxylate (5 g, 10.2 mmol, 1 equiv.) in anhydrous CH_2Cl_2 (25 mL) was added at 0 °C trifluoroacetic acid (45 mL), and the reaction mixture was stirred for 30 min at 0 °C, before being poured into a 1:1:1 solution of H_2O, Et_2O and CH_2Cl_2. After removing the aqueous layer, the organic layer was washed with H_2O and brine, dried over Na_2SO_4, filtered, concentrated *in vacuo*, before triturating with Et_2O. The obtained solid was filtered and dried *in vacuo* to yield crude **7** (1.38 g, <95% purity, ~37%). The crude product was used directly in the next steps (attempted purification by either recrystallisation or column chromatography resulted in degradation; reported related compounds are also known for their instability[16]).

Yellow amorphous solid; characteristic analytical data: ^{1}H NMR (500 MHz, 298 K, DMSO-d_6): δ = 9.14 (d, *J* = 8.4 Hz, 1H, *N10H*), 7.32 – 7.21 (m, 5H, *C15H*, *C16H*, *C17H*, *C18H*, *C19H*), 5.70 (dd, *J* = 8.5, 4.9 Hz, 1H, *C7H*), 5.13 (d, *J* = 4.9 Hz, 1H, *C6H*), 4.58 and 4.53 (ABq, *J* = 11.2 Hz, 2H, *C20H*$_2$), 3.70 (d, *J* = 18.0 Hz, 1H, *C2H*), 3.58 – 3.46 ppm (m, 3H, *C2H*, *C12H*$_2$).

Benzyl (6*R*,7*R*)-3-(chloromethyl)-8-oxo-7-(2-phenylacetamido)-5-thia-1-azabicyclo[4.2.0]oct-2-ene-2-carboxylate (8a)

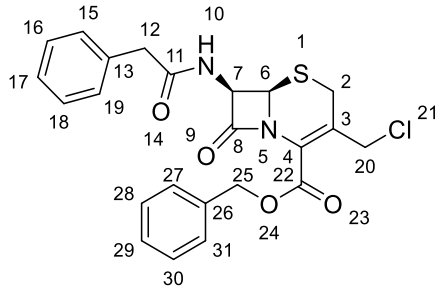

General procedure B was applied using cephem **7** (<95% purity; 210 mg, 0.546 mmol, 1 equiv.), coupling reagent *N*,*N*'-dicyclohexylcarbodiimide (124 mg, 0.6 mmol, 1.1 equiv.), benzyl alcohol (0.23 mL, 2.18 mmol, 4 equiv.) and 4-dimethylaminopyridine (9 mg, 0.082 mmol, 0.15 equiv.). Purification by flash column chromatography (25 g Sfär, 100%$_{v/v}$ cyclohexane (4 CV), followed by a linear gradient (45 CV): 0%$_{v/v}$ →45%$_{v/v}$ ethyl acetate in cyclohexane) afforded **8a** (69 mg, 27%).

Amorphous white solid; ^{1}H NMR (400 MHz, 298 K, DMSO-*d*$_6$): δ = 9.15 (d, *J* = 8.4 Hz, 1H, *N10H*), 7.46 – 7.18 (m, 10H, *C15H*, *C16H*, *C17H*, *C18H*, *C19H*, *C27H*, *C28H*, *C29H*, *C30H*, *C31H*), 5.74 (dd, *J* = 8.4, 4.9 Hz, 1H, *C7H*), 5.34 and 5.25 (ABq, *J* = 12.4 Hz, 2H, *C25H*$_2$), 5.16 (d, *J* = 4.9 Hz, 1H, *C6H*), 4.56 and 4.46 (ABq, *J* = 11.4 Hz, 2H, *C20H*$_2$), 3.72 (d, *J* = 18.1 Hz, 1H, *C2H*), 3.61 – 3.46 ppm (m, 3H, *C2H*, *C12H*$_2$); ^{13}C NMR (126 MHz, 298 K, DMSO-*d*$_6$): δ = 170.9, 165.2, 161.1, 135.8, 135.0, 129.0, 128.4, 128.3 (2C), 128.2, 126.5, 125.2, 125.1, 67.5, 59.2, 57.9, 43.8, 41.6, 26.1 ppm; IR (film): ṽ = 1787, 1725, 1670, 1528, 1453, 1387, 1364, 1262, 1165, 1099, 1064, 1032 cm^{-1}; HRMS (ESI): m/z calculated for $C_{23}H_{21}ClN_2O_4SNa$ $[M+Na]^+$: 479.0803, found: 479.0808; $[\alpha]_D^{25}$ = +40 (c = 0.003 g/mL, $CHCl_3$).

4-Nitrobenzyl (6*R*,7*R*)-3-(chloromethyl)-8-oxo-7-(2-phenylacetamido)-5-thia-1-azabicyclo[4.2.0]oct-2-ene-2-carboxylate (8b)

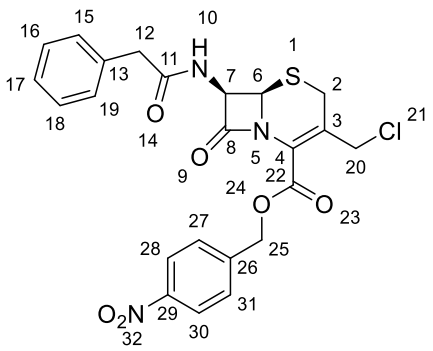

General procedure B was applied using cephem **7** (<95% purity; 210 mg, 0.546 mmol, 1 equiv.), coupling reagent 1-ethyl-3-(3-dimethylaminopropyl)carbodiimide hydrochloride (116 mg, 0.6 mmol, 1.1 equiv.), 4-nitrobenzyl alcohol (0.19 mL, 0.81 mmol, 1.5 equiv.) and 4-dimethylaminopyridine (9 mg, 0.082 mmol, 0.15 equiv.). Purification by flash column chromatography (25 g Sfär, 100%$_{v/v}$ cyclohexane (2 CV), followed by a linear gradient (23 CV): 0%$_{v/v}$ →23%$_{v/v}$ ethyl acetate in cyclohexane, followed by 23%$_{v/v}$ ethyl acetate in cyclohexane (6 CV), followed by a linear gradient (23 CV): 23%$_{v/v}$ →45%$_{v/v}$ ethyl acetate in cyclohexane) afforded **8b** (49 mg, 18%).

White solid; m.p.: 160 °C (decomposition); ^{1}H NMR (500 MHz, 298 K, DMSO-*d*$_6$): δ = 9.16 (d, *J* = 8.4 Hz, 1H, *N10H*), 8.28 – 8.22 (m, 2H, *C28H*, *C30H*), 7.71 (m, 2H, *C27H*, *C31H*), 7.32 – 7.20 (m, 5H, *C15H*, *C16H*, *C17H*, *C18H*, *C19H*), 5.78 (dd, *J* = 8.4, 4.9 Hz, 1H, *C7H*), 5.47 and 5.42 (ABq, *J* = 13.5 Hz, 2H, *C25H*$_2$), 5.18 (d, *J* = 4.9 Hz, 1H, *C6H*), 4.60 and 4.48 (ABq, *J* = 11.4 Hz, 2H, *C20H*$_2$), 3.74 (d, *J* = 18.1 Hz, 1H, *C2H*), 3.63 – 3.54 (m, 2H, *C2H*, *C12H*), 3.49 ppm (d, *J* = 13.8 Hz, 1H, *C12H*); ^{13}C NMR (126 MHz, 298 K, DMSO-*d*$_6$): δ 170.9, 165.4, 160.9, 147.3, 142.8, 135.7, 129.0 (2C), 128.2, 126.5, 126.0, 124.8, 123.6, 66.2, 59.2, 57.9, 43.7, 41.6, 26.2; IR (film): ṽ = 1784, 1726, 1665, 1641, 1631, 1605, 1547, 1526, 1494, 1482, 1468, 1442, 1348, 1262, 1099, 1028 cm^{-1}; HRMS (ESI): m/z calculated for $C_{23}H_{21}ClN_3O_6S$ $[M+H]^+$: 502.0834, found: 502.0836; $[\alpha]_D^{25}$ = -36 (c = 0.004 g/mL, $CHCl_3$).

Methyl (6*R*,7*R*)-3-(chloromethyl)-8-oxo-7-(2-phenylacetamido)-5-thia-1-azabicyclo[4.2.0]oct-2-ene-2-carboxylate (8c)

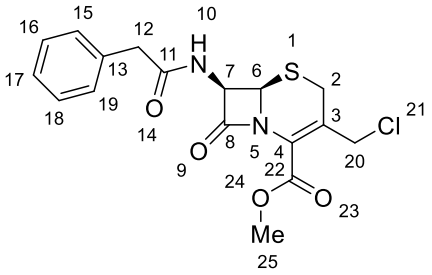

General procedure B was applied using cephem **7** (<95% purity; 210 mg, 0.546 mmol, 1 equiv.), coupling reagent 1-ethyl-3-(3-dimethylaminopropyl)carbodiimide hydrochloride (116 mg, 0.6 mmol, 1.1 equiv.*)*, methanol (0.2 mL, 4.36 mmol, 8 equiv.) and 4-dimethylaminopyridine (9 mg, 0.082 mmol, 0.15 equiv.). Purification by flash column chromatography (25 g Sfär, 100%$_{v/v}$ cyclohexane (2 CV), followed by a linear gradient (33 CV): 0%$_{v/v}$ →45%$_{v/v}$ ethyl acetate in cyclohexane) afforded **8c** (59 mg, 28%).

Amorphous grey solid; ^{1}H NMR (600 MHz, 298 K, DMSO-*d*$_6$): δ = 9.15 (d, *J* = 8.4 Hz, 1H, *N10H*), 7.33 – 7.19 (m, 5H, *C15H*, *C16H*, *C17H*, *C18H*, *C19H*), 5.73 (dd, *J* = 8.4, 4.9 Hz, 1H, *C7H*), 5.16 (d, *J* = 4.9 Hz, 1H, *C6H*), 4.55 and 4.47 (ABq, *J* = 11.4 Hz, 2H, *C20H*$_2$), 3.80 (s, 3H, *C25H*$_3$), 3.74 – 3.70 (m, 1H, *C2H*), 3.59 – 3.54 (m, 2H, *C2H*, *C12H*), 3.49 ppm (m, 1H, *C12H*); ^{13}C NMR (151 MHz, 298 K, DMSO-*d*$_6$): δ = 170.9, 165.1, 161.7, 135.8, 129.0, 128.2, 126.5, 125.1, 125.0, 59.3, 57.9, 52.8, 43.8, 41.6, 26.1; IR (film): $\tilde{\nu}$ = 1786, 1726, 1665, 1631, 1548, 1530, 1513, 1494, 1440, 1369, 1263, 1101, 1030 cm^{-1}; HRMS (ESI): m/z calculated for $C_{17}H_{17}ClN_2O_4SNa$ $[M+Na]^+$: 403.0490, found: 403.0492; $[\alpha]_D^{25}$ = +8.5 (c = 0.008 g/mL, acetonitrile).

(6*R*,7*R*)-3-(Acetoxymethyl)-8-oxo-7-(2-phenylacetamido)-5-thia-1-azabicyclo[4.2.0]oct-2-ene-2-carboxylic acid (10a)[3]

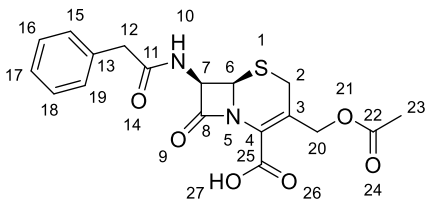

A variation of a reported procedure was followed.[3] **General procedure C** was applied using (6*R*,7*R*)-3-(acetoxymethyl)-7-amino-8-oxo-5-thia-1-azabicyclo[4.2.0]oct-2-ene-2-carboxylic acid (2 g, 7.38 mmol), yielding after work-up **10a** (2.12 g, 73%). A portion (50 mg) was further purified by reverse phase flash column chromatography (6 g Sfär C18 D; 100%$_{v/v}$ aqueous formic acid solution (0.1%) (3 CV), followed by a linear gradient (10 CV): 0%$_{v/v}$ → 100%$_{v/v}$ aqueous formic acid solution (0.1%) in CH_3CN). The fractions containing product were lyophilised to yield **10a** (42 mg). The analytical data are consistent with those reported.[3]

White solid; m.p.: 167 °C (decomposition); ^{1}H NMR (500 MHz, 298 K, DMSO-*d*$_6$): δ = 13.68 (s, 1H, *O27H*), 9.10 (d, *J* = 8.3 Hz, 1H, *N10H*), 7.34 – 7.19 (m, 5H, *C15H*, *C16H*, *C17H*, *C18H*, *C19H*), 5.68 (dd, *J* = 8.3, 4.8 Hz, 1H, *C7H*), 5.08 (d, *J* = 4.8 Hz, 1H, *C6H*), 5.00 and 4.69 (ABq, *J* = 12.8 Hz, 2H, *C20H*$_2$), 3.66 – 3.45 (m, 4H, *C2H*$_2$, *C12H*$_2$), 2.03 ppm (s, 3H, *C23H*$_3$); ^{13}C NMR (126 MHz, 298 K, DMSO-*d*$_6$): δ = 170.9, 170.2, 164.8, 162.8, 135.8, 129.0, 128.2, 126.5, 126.4, 123.3, 62.7, 59.1, 57.4, 41.6, 25.5, 20.6 ppm; IR (film): $\tilde{\nu}$ = 1782, 1749, 1712, 1660, 1538, 1345, 1228, 1190, 1070, 1030 cm^{-1}; HRMS (ESI): m/z calculated for $C_{18}H_{18}N_2O_6SNa$ $[M+Na]^+$: 413.0778, found: 413.0783; $[\alpha]_D^{25}$ = -8.6 (c = 0.002 g/mL, acetone).

(6*R*,7*R*)-3-Methyl-8-oxo-7-(2-phenylacetamido)-5-thia-1-azabicyclo[4.2.0]oct-2-ene-2-carboxylic acid (10b)[4]

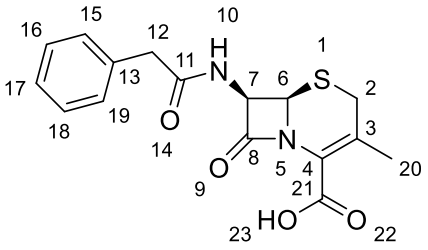

A variation of a reported procedure was followed.[4] **General procedure C** was applied using (6*R*,7*R*)-7-amino-3-methyl-8-oxo-5-thia-1-azabicyclo[4.2.0]oct-2-ene-2-carboxylic acid being the cephem (1 g, 4.67 mmol), yielding after work-up **10b** (425 mg, 27%). A portion (100 mg) was further purified by reverse phase flash column chromatography (6 g Sfär C18 D; 100%$_{v/v}$ aqueous formic acid solution (0.1%) (3 CV), followed by a linear gradient (10 CV): 0%$_{v/v}$ → 100%$_{v/v}$ aqueous formic acid solution (0.1%) in CH_3CN). The fractions containing product were lyophilised to yield **10b** (57 mg). The analytical data are consistent with those reported.[4]

White amorphous solid; ^{1}H NMR (400 MHz, 298 K, DMSO-*d*$_6$): δ = 13.19 (s, 1H, *O23H*), 9.06 (d, *J* = 8.2 Hz, 1H, *N10H*), 7.33 – 7.19 (m, 5H, *C15H*, *C16H*, *C17H*, *C18H*, *C19H*), 5.58 (dd, *J* = 8.2, 4.6 Hz, 1H, *C7H*), 5.02 (d, *J* = 4.6 Hz, 1H, *C6H*), 3.60 – 3.48 (m, 3H, *C2H*, *C12H*$_2$), 3.40 – 3.32 (m, 1H, *C2H*), 2.02 ppm (s, 3H, *C20H*$_3$); ^{13}C NMR (101 MHz, 298 K, DMSO-*d*$_6$): δ = 171.0, 164.4, 163.5, 135.9, 129.8, 129.0, 128.2, 126.5, 122.8, 58.9, 57.1, 41.6, 29.0, 19.4 ppm; IR (film): $\tilde{\nu}$ = 1763, 1702, 1657, 1550, 1418, 1366, 1341, 1234, 1179 cm^{-1}; HRMS (ESI): m/z calculated for $C_{16}H_{17}N_2O_4S$ $[M+H]^+$: 333.0904, found: 333.0908; $[\alpha]_D^{25}$ = +113 (c = 0.007 g/mL, acetonitrile).

(6*R*,7*R*)-3-(Methoxymethyl)-8-oxo-7-(2-phenylacetamido)-5-thia-1-azabicyclo[4.2.0]oct-2-ene-2-carboxylic acid (10c)

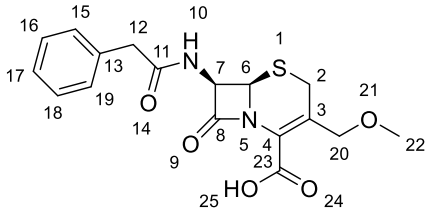

General procedure C was applied using (6*R*,7*R*)-7-amino-3-(methoxymethyl)-8-oxo-5-thia-1-azabicyclo[4.2.0]oct-2-ene-2-carboxylic acid (2 g, 8.19 mmol). After work-up, no further purifications were required, yielding **10c** (953 mg, 32%).

White solid; m.p.: 157-159 °C; ^{1}H NMR (500 MHz, 298 K, DMSO-d_6): δ = 13.56 (s, 1H, *O25H*), 9.11 (d, *J* = 8.3 Hz, 1H, *N10H*), 7.32 – 7.20 (m, 5H, *C15H*, *C16H*, *C17H*, *C18H*, *C19H*), 5.66 (dd, *J* = 8.3, 4.7 Hz, 1H, *C7H*), 5.08 (d, *J* = 4.7 Hz, 1H, *C6H*), 4.18 (m, 2H, *C20H*$_2$), 3.60 – 3.45 (m, 4H, *C2H*$_2$, *C12H*$_2$), 3.21 ppm (s, 3H, *C22H*$_3$); ^{13}C NMR (126 MHz, 298 K, DMSO-d_6): δ = 171.0, 164.7, 163.1, 135.8, 129.0, 128.2, 126.5, 125.9, 125.5, 69.9, 59.0, 57.6, 57.3, 41.6, 25.3 ppm; IR (film): $\tilde{\nu}$ = 1768, 1719, 1698, 1654, 1533, 1401, 1341, 1217, 1151, 1105, 1068, 1026 cm^{-1}; HRMS (ESI): m/z calculated for $C_{17}H_{18}N_2O_5SNa$ $[M+Na]^+$: 385.0829, found: 385.0835; $[\alpha]_D^{25}$ = +72 (c = 0.01 g/mL, acetonitrile).

(6*R*,7*R*)-8-Oxo-7-(2-phenylacetamido)-3-vinyl-5-thia-1-azabicyclo[4.2.0]oct-2-ene-2-carboxylic acid (10d)[17]

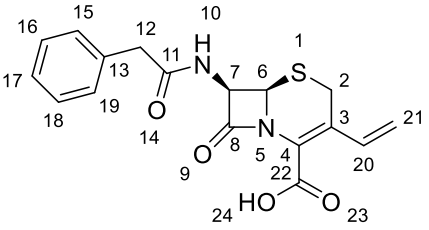

General procedure C was applied using (6*R*,7*R*)-7-amino-8-oxo-3-vinyl-5-thia-1-azabicyclo[4.2.0]oct-2-ene-2-carboxylic acid (1 g, 4.42 mmol), yielding after work-up **10d** (545 mg, 35%). A portion (60 mg) was further purified by reverse phase flash column chromatography (6 g Sfär C18 D; 100%$_{v/v}$ aqueous formic acid solution (0.1%) (3 CV), followed by a linear gradient (10 CV): 0%$_{v/v}$ → 100%$_{v/v}$ aqueous formic acid solution (0.1%) in CH_3CN).

The fractions containing product were lyophilised to yield **10d** (44 mg). Synthesis of **10d** was achieved following an alternative experimental procedure to that reported.[17] The analytical data are consistent with those reported.[17]

Amorphous white solid; ^{1}H NMR (500 MHz, 298 K, DMSO-d_6): δ = 13.62 (s, 1H, *O24H*), 9.14 (d, *J* = 8.3 Hz, 1H, *N10H*), 7.34 – 7.19 (m, 5H, *C15H*, *C16H*, *C17H*, *C18H*, *C19H*), 6.91 (dd, *J* = 17.5, 11.2 Hz, 1H, *C20H*), 5.67 (dd, *J* = 8.3, 4.8 Hz, 1H, *C7H*), 5.59 and 5.31 (ABq, *J* = 17.5 Hz, 2H, *C21H*$_2$), 5.12 (d, *J* = 4.8 Hz, 1H, *C6H*), 3.87 (d, *J* = 17.7 Hz, 1H, *C2H*), 3.60 – 3.47 ppm (m, 3H, *C2H*, *C12H*$_2$); ^{13}C NMR (126 MHz, 298 K, DMSO-d_6): δ = 171.0, 164.6, 163.2, 135.8, 132.0, 129.0, 128.2, 126.5, 125.5, 124.1, 117.2, 59.2, 57.7, 41.6, 23.1 ppm; IR (film): ṽ = 1773, 1687, 1655, 1537, 1496, 1426, 1348, 1240, 1180, 1111, 1029 cm^{-1}; HRMS (ESI): m/z calculated for $C_{17}H_{16}N_2O_4SNa$ $[M+Na]^+$: 367.0723, found: 367.0728; $[\alpha]_D^{25}$ = -67 (c = 0.007 g/mL, acetonitrile).

(6*R*,7*R*)-8-Oxo-7-(2-phenylacetamido)-5-thia-1-azabicyclo[4.2.0]oct-2-ene-2-carboxylic acid (10e)[17]

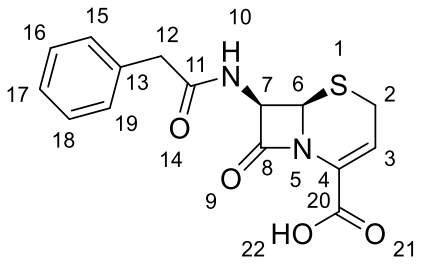

General procedure C was applied using (6*R*,7*R*)-7-amino-8-oxo-5-thia-1-azabicyclo[4.2.0]oct-2-ene-2-carboxylic acid (1.64 g, 8.19 mmol), yielding after work-up **10e** (1.2 g, 45%). A portion (80 mg) was further purified by reverse phase flash column chromatography (6 g Sfär C18 D; 100%$_{v/v}$ aqueous formic acid solution (0.1%) (3 CV), followed by a linear gradient (10 CV): 0%$_{v/v}$ → 100%$_{v/v}$ aqueous formic acid solution (0.1%) in CH_3CN). The fractions containing product were lyophilised to yield **10e** (57 mg). Synthesis of **10e** was achieved following an alternative experimental procedure to that reported.[17] The analytical data are consistent with those reported.[17]

White solid; m.p.: 190 °C (decomposition); ^{1}H NMR (500 MHz, 298 K, DMSO-*d*$_6$): δ = 13.22 (s, 1H, *O22H*), 9.09 (d, *J* = 8.4 Hz, 1H, *N10H*), 7.34 – 7.19 (m, 5H, *C15H*, *C16H*, *C17H*, *C18H*, *C19H*), 6.49 (dd, *J* = 6.2, 2.7 Hz, 1H, *C3H*), 5.71 (dd, *J* = 8.4, 4.9 Hz, 1H, *C7H*), 5.03 (d, *J* = 4.9 Hz, 1H, *C6H*), 3.66 – 3.48 ppm (m, 4H, *C2H*$_2$, *C12H*$_2$); ^{13}C NMR (126 MHz, 298 K, DMSO-*d*$_6$) δ 171.0, 164.5, 162.7, 135.9, 129.0, 128.2, 127.9, 126.5, 120.3, 59.4, 56.9, 41.5, 23.5 ppm; IR (film): $\tilde{\nu}$ = 1767, 1688, 1626, 1522, 1449, 1397, 1346, 1297, 1243, 1166, 1056 cm^{-1}; HRMS (ESI): m/z calculated for $C_{15}H_{14}N_2O_4SNa$ $[M+Na]^+$: 341.0567, found: 341.0568; $[\alpha]_D^{25}$ = +134 (c = 0.008 g/mL, acetone).

(6*R*,7*R*)-3-Chloro-8-oxo-7-(2-phenylacetamido)-5-thia-1-azabicyclo[4.2.0]oct-2-ene-2-carboxylic acid (10f)[17]

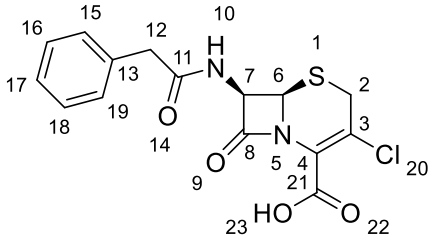

General procedure C was applied using (6*R*,7*R*)-7-amino-3-chloro-8-oxo-5-thia-1-azabicyclo[4.2.0]oct-2-ene-2-carboxylic acid (1.42 g, 6 mmol), yielding after work-up **10f** (584 mg, 27%). A portion (50 mg) was further purified by reverse phase flash column chromatography (6 g Sfär C18 D; 100%$_{v/v}$ aqueous formic acid solution (0.1%) (3 CV), followed by a linear gradient (10 CV): 0%$_{v/v}$ → 100%$_{v/v}$ aqueous formic acid solution (0.1%) in CH_3CN). The fractions containing product were lyophilised to yield **10f** (27 mg). The analytical data are consistent with those reported.[17]

White amorphous solid; ^{1}H NMR (400 MHz, 298 K, DMSO-*d*$_6$): δ = 13.93 (s, 1H, *O23H*), 9.18 (d, *J* = 8.2 Hz, 1H, *N10H*), 7.34 – 7.18 (m, 5H, *C15H*, *C16H*, *C17H*, *C18H*, *C19H*), 5.69 (dd, *J* = 8.2, 4.8 Hz, 1H, *C7H*), 5.17 (d, *J* = 4.8 Hz, 1H, *C6H*), 3.97 and 3.69 (ABq, *J* = 18.1 Hz, 2H, *C2H*$_2$), 3.56 and 3.49 ppm (ABq, *J* = 13.9 Hz, 1H, *C12H*$_2$); ^{13}C NMR (126 MHz, 298 K, DMSO-*d*$_6$): δ =

170.9, 164.1, 161.6, 135.7, 129.0 (2C), 128.2 (2C), 126.5, 59.0, 57.3, 41.5, 29.9 ppm; IR (film): $\tilde{\nu}$ = 1781, 1736, 1695, 1655, 1532, 1351, 1244, 1203, 1179, 1115, 1004 cm^{-1}; HRMS (ESI): m/z calculated for $C_{15}H_{13}ClN_2O_4SNa$ $[M+Na]^+$: 370.0177, found: 370.0181; $[\alpha]_D^{25}$ = +77 (c = 0.007 g/mL, acetonitrile).

(6*R*,7*R*)-3-(((1-Methyl-1*H*-tetrazol-5-yl)thio)methyl)-8-oxo-7-(2-phenylacetamido)-5-thia-1-azabicyclo[4.2.0]oct-2-ene-2-carboxylic acid (10g)[5]

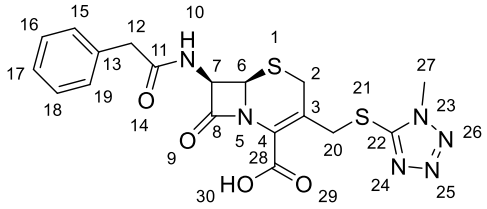

A variation of a reported procedure was followed.[5] **General procedure C** was applied using (6*R*,7*R*)-7-amino-3-(((1-methyl-1*H*-tetrazol-5-yl)thio)methyl)-8-oxo-5-thia-1-azabicyclo[4.2.0]oct-2-ene-2-carboxylic acid (2 g, 6.09 mmol), yielding after work-up **10g** (730 mg, 26%). A portion (50 mg) was further purified by reverse phase flash column chromatography (6 g Sfär C18 D; 100%$_{v/v}$ aqueous formic acid solution (0.1%) (3 CV), followed by a linear gradient (10 CV): 0%$_{v/v}$ → 100%$_{v/v}$ aqueous formic acid solution (0.1%) in CH_3CN). The fractions containing product were lyophilised to yield **10g** (33 mg). The analytical data are consistent with those reported.[5]

White amorphous solid; ^{1}H NMR (500 MHz, 298 K, DMSO-*d*$_6$): δ = 13.68 (s, 1H, *O30H*), 9.11 (d, *J* = 8.3 Hz, 1H, *N10H*), 7.33 – 7.18 (m, 5H, *C15H*, *C16H*, *C17H*, *C18H*, *C19H*), 5.66 (dd, *J* = 8.3, 4.8 Hz, 1H, *C7H*), 5.05 (d, *J* = 4.8 Hz, 1H, *C6H*), 4.35 and 4.24 (ABq, *J* = 13.3 Hz, 2H, *C20H*$_2$), 3.94 (s, 3H, *C27H*$_3$), 3.75 and 3.62 (ABq, *J* = 18.0 Hz, 2H, *C2H*$_2$), 3.56 and 3.48 ppm (ABq, *J* = 13.8 Hz, 2H, *C12H*$_2$); ^{13}C NMR (126 MHz, 298 K, DMSO-*d*$_6$): δ = 170.9, 164.7, 162.8, 153.1, 135.8, 129.0, 128.2, 126.5, 126.0, 125.3, 59.0, 57.5, 41.6, 35.5, 33.8, 26.8 ppm; IR (film):

$\tilde{\nu}$ = 1779, 1717, 1664, 1532, 1360, 1238, 1173, 1096, 1002 cm^{-1}; HRMS (ESI): m/z calculated for $C_{18}H_{18}N_6O_4S_2K$ $[M+K]^+$: 485.0463, found: 485.0455; $[\alpha]_D^{25}$ = -71 (c = 0.005 g/mL, acetonitrile).

(6*R*,7*R*)-3-(((5-Methyl-1,3,4-thiadiazol-2-yl)thio)methyl)-8-oxo-7-(2-phenylacetamido)-5-thia-1-azabicyclo[4.2.0]oct-2-ene-2-carboxylic acid (10f)[18]

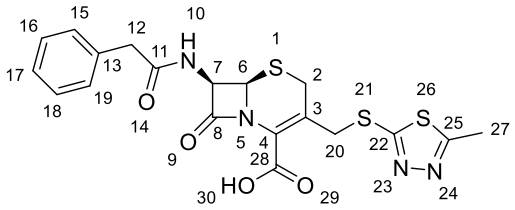

A variation of a reported procedure was followed.[19] **General procedure C** was applied using (6*R*,7*R*)-7-amino-3-(((5-methyl-1,3,4-thiadiazol-2-yl)thio)methyl)-8-oxo-5-thia-1-azabicyclo[4.2.0]oct-2-ene-2-carboxylic acid (2.1 g, 6.1 mmol), yielding after work-up **10f** (920 mg, 32%). A portion (60 mg) was further purified by reverse phase flash column chromatography (6 g Sfär C18 D; 100%$_{v/v}$ aqueous formic acid solution (0.1%) (3 CV), followed by a linear gradient (10 CV): 0%$_{v/v}$ → 100%$_{v/v}$ aqueous formic acid solution (0.1%) in CH_3CN). The fractions containing product were lyophilised to yield **10f** (47 mg). The analytical data are consistent with those reported.[18]

White solid; m.p.: 176 °C; ^{1}H NMR (500 MHz, 298 K, DMSO-*d*$_6$): δ = 13.68 (s, 1H, *O30H*), 9.10 (d, *J* = 8.4 Hz, 1H, *N10H*), 7.33 – 7.19 (m, 5H, *C15H*, *C16H*, *C17H*, *C18H*, *C19H*), 5.66 (dd, *J* = 8.4, 4.8 Hz, 1H, *C7H*), 5.07 (d, *J* = 4.8 Hz, 1H, *C6H*), 4.50 and 4.22 (ABq, *J* = 13.3 Hz, 2H, *C20H*$_2$), 3.75 (d, *J* = 18.0 Hz, 1H, *C2H*), 3.61 – 3.46 (m, 3H, *C2H*, *C12H*$_2$), 2.68 ppm (s, 3H, *C27H*$_3$); ^{13}C NMR (126 MHz, 298 K, DMSO-*d*$_6$): δ = 170.9, 166.2, 164.7, 164.1, 162.9, 135.8, 129.0, 128.2, 126.5, 126.2, 125.3, 59.0, 57.6, 41.6, 35.9, 27.0, 15.3 ppm; IR (film): $\tilde{\nu}$ = 1770, 1708, 1654, 1531, 1397, 1303, 1226, 1183, 1053, 1003 cm^{-1}; HRMS (ESI): m/z calculated for $C_{19}H_{19}N_4O_4S_3$ $[M+H]^+$: 463.0563, found: 463.0560; $[\alpha]_D^{25}$ = -117 (c = 0.003 g/mL, acetone).

4-Methoxybenzyl (6*R*,7*R*)-3-(acetoxymethyl)-8-oxo-7-(2-phenylacetamido)-5-thia-1-azabicyclo[4.2.0]oct-2-ene-2-carboxylate (11a)[6]

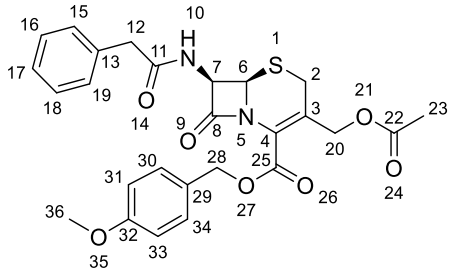

A variation of a reported procedure was followed.[6] **General procedure D** was applied using **10a** (200 mg, 0.512 mmol, 1 equiv.), yielding after recrystallisation **11a** (79 mg, 30%). A portion (30 mg) was further purified by reverse phase flash column chromatography (6 g Sfär C18 D; 100%$_{v/v}$ aqueous formic acid solution (0.1%) (3 CV), followed by a linear gradient (10 CV): 0%$_{v/v}$ → 100%$_{v/v}$ aqueous formic acid solution (0.1%) in CH_3CN). The fractions containing product were lyophilised to yield **11a** (19 mg). The analytical data are consistent with those reported.[6]

White amorphous solid; ^{1}H NMR (600 MHz, 298 K, DMSO-*d*$_6$): δ = 9.11 (d, *J* = 8.3 Hz, 1H, *N10H*), 7.36 – 7.18 (m, 7H, *C15H*, *C16H*, *C17H*, *C18H*, *C19H*, *C30H*, *C34H*), 6.96 – 6.90 (m, 2H, *C31H*, *C33H*), 5.71 (dd, *J* = 8.4, 4.8 Hz, 1H, *C7H*), 5.23 and 5.13 (ABq, *J* = 12.0 Hz, 2H, *C28H*$_2$), 5.11 (d, *J* = 4.8 Hz, 1H, *C6H*), 4.92 and 4.67 (ABq, *J* = 12.8 Hz, 2H, *C20H*$_2$), 3.75 (s, 3H, *C36H*$_3$), 3.64 (d, *J* = 18.2 Hz, 1H, *C2H*), 3.58 – 3.47 (m, 3H, *C2H*, *C12H*$_2$), 2.00 ppm (s, 3H, *C23H*$_3$); ^{13}C NMR (151 MHz, 298 K, DMSO-*d*$_6$): δ = 170.9, 170.1, 165.0, 161.4, 159.3, 135.8, 130.3, 129.0, 128.2, 126.9, 126.5, 125.2, 124.5, 113.8, 67.2, 62.5, 59.2, 57.6, 55.1, 41.6, 25.7, 20.5 ppm; IR (film): $\tilde{\nu}$ = 1783, 1739, 1726, 1666, 1613, 1516, 1384, 1353, 1303, 1221, 1177, 1104, 1068, 1031 cm^{-1}; HRMS (ESI): m/z calculated for $C_{26}H_{30}N_3O_7S$ $[M+NH_4]^+$: 528.1799, found: 528.1786; $[\alpha]_D^{25}$ = +25 (c = 0.006 g/mL, $CHCl_3$).

4-Methoxybenzyl (6*R*,7*R*)-3-methyl-8-oxo-7-(2-phenylacetamido)-5-thia-1-azabicyclo[4.2.0]oct-2-ene-2-carboxylate (11b)

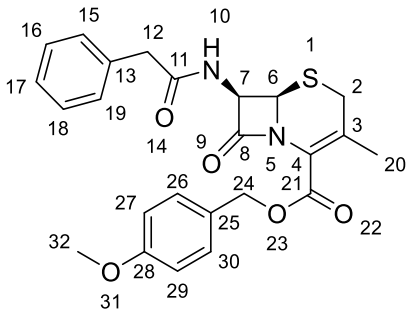

General procedure D was applied using **10b** (340 mg, 1.02 mmol, 1 equiv.), yielding after recrystallisation **11b** (89 mg, 19%). A portion (30 mg) was further purified by reverse phase flash column chromatography (6 g Sfär C18 D; $100\%_{v/v}$ aqueous formic acid solution (0.1%) (3 CV), followed by a linear gradient (10 CV): $0\%_{v/v} \rightarrow 100\%_{v/v}$ aqueous formic acid solution (0.1%) in CH_3CN). The fractions containing product were lyophilised to yield **11b** (24 mg).

White amorphous solid; ^{1}H NMR (600 MHz, 298 K, DMSO-*d*$_6$): δ = 9.07 (d, *J* = 8.3 Hz, 1H, *N10H*), 7.37 – 7.32 (m, 2H, *C26H*, *C30H*), 7.31 – 7.19 (m, 5H, *C15H*, *C16H*, *C17H*, *C18H*, *C19H*), 6.96 – 6.90 (m, 2H, *C27H*, *C29H*), 5.61 (dd, *J* = 8.3, 4.6 Hz, 1H, *C7H*), 5.19 and 5.12 (ABq, *J* = 12.0 Hz, 2H, *C24H*$_2$), 5.05 (d, *J* = 4.6 Hz, 1H, *C6H*), 3.75 (s, 3H, *C32H*$_3$), 3.61 – 3.54 (m, 2H, *C2H*, *C12H*), 3.50 (d, *J* = 13.9 Hz, 1H, *C12H*), 3.40 (d, *J* = 18.2 Hz, 1H, *C2H*), 2.00 ppm (s, 3H, *C20H*$_3$); ^{13}C NMR (151 MHz, 298 K, DMSO-*d*$_6$): δ = 170.9, 164.6, 162.0, 159.2, 135.8, 131.0, 130.1, 129.0, 128.2, 127.4, 126.5, 121.7, 113.8, 66.5, 58.9, 57.2, 55.1, 41.6, 29.0, 19.4 ppm; IR (film): $\tilde{\nu}$ = 1764, 1714, 1655, 1614, 1537, 1517, 1388, 1358, 1303, 1260, 1177, 1157, 1106, 1031 cm^{-1}; HRMS (ESI): m/z calculated for $C_{24}H_{25}N_2O_5S$ $[M+H]^+$: 453.1479, found: 453.1480; $[\alpha]_D^{25}$ = +56 (c = 0.005 g/mL, $CHCl_3$).

4-Methoxybenzyl (6*R*,7*R*)-3-(methoxymethyl)-8-oxo-7-(2-phenylacetamido)-5-thia-1-azabicyclo[4.2.0]oct-2-ene-2-carboxylate (11c)[20]

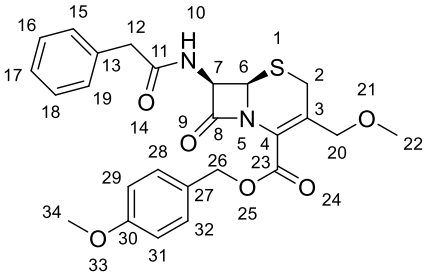

General procedure D was applied using **10c** (200 mg, 0.552 mmol, 1 equiv.), yielding after recrystallisation **10c** (68 mg, 25%). A portion (50 mg) was further purified by reverse phase flash column chromatography (6 g Sfär C18 D; 100%$_{v/v}$ aqueous formic acid solution (0.1%) (3 CV), followed by a linear gradient (10 CV): 0%$_{v/v}$ → 100%$_{v/v}$ aqueous formic acid solution (0.1%) in CH_3CN). The fractions containing product were lyophilised to yield **11c** (17 mg). Synthesis of **11c** was achieved following an alternative experimental procedure to that reported.[20] The analytical data are consistent with those reported.[20]

White solid; m.p.: 169 °C; ^{1}H NMR (600 MHz, 298 K, DMSO-*d*$_6$): δ = 9.12 (d, *J* = 8.4 Hz, 1H, *N10H*), 7.37 – 7.33 (m, 2H, *C28H*, *C32H*), 7.33 – 7.19 (m, 5H, *C15H*, *C16H*, *C17H*, *C18H*, *C19H*), 6.96 – 6.91 (m, 2H, *C29H*, *C31H*), 5.69 (dd, *J* = 8.4, 4.8 Hz, 1H, *C7H*), 5.22 and 5.15 (ABq, *J* = 11.9 Hz, 2H, *C26H*$_2$), 5.11 (d, *J* = 4.8 Hz, 1H, *C6H*), 4.14 – 4.07 (m, 2H, *C20H*$_2$), 3.75 (s, 3H, *C34H*$_3$), 3.62 – 3.53 (m, 2H, *C2H*, *C12H*), 3.52 – 3.46 (m, 2H, *C2H*, *C12H*), 3.14 ppm (s, 3H, *C22H*$_3$); ^{13}C NMR (151 MHz, 298 K, DMSO-*d*$_6$): δ = 170.9, 165.0, 161.6, 159.4, 135.8, 130.4, 129.0, 128.2, 127.1, 126.8, 126.5, 124.3, 113.8, 69.8, 67.0, 59.1, 57.7, 57.3, 55.1, 41.6, 25.4 ppm; IR (film): $\tilde{\nu}$ = 1789, 1759, 1666, 1629, 1541, 1491, 1410, 1374, 1351, 1290, 1217, 1145, 1094, 1057, 1001 cm^{-1}; HRMS (ESI): m/z calculated for $C_{25}H_{27}N_2O_6S$ $[M+H]^+$: 483.1584, found: 483.1584; $[\alpha]_D^{25}$ = +33 (c = 0.005 g/mL, $CHCl_3$).

4-Methoxybenzyl (6*R*,7*R*)-8-oxo-7-(2-phenylacetamido)-3-vinyl-5-thia-1-azabicyclo[4.2.0]oct-2-ene-2-carboxylate (11d)[21]

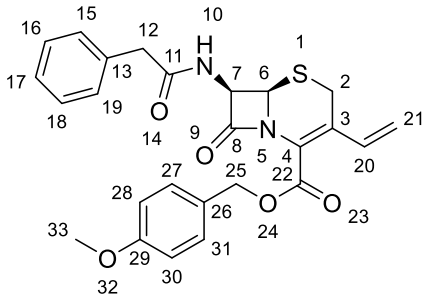

General procedure D was applied using **10d** (200 mg, 0.581 mmol, 1 equiv.), yielding after recrystallisation **11d** (124 mg, 45%). No further purification by column chromatography was performed. Synthesis of **11d** was achieved following an alternative experimental procedure to that reported.[21] The analytical data are consistent with those reported.[21]

White solid; m.p.: 159 °C (decomposition); ^{1}H NMR (500 MHz, 298 K, $CDCl_3$): δ = 7.40 – 7.27 (m, 7H, *C15H*, *C16H*, *C17H*, *C18H*, *C19H*, *C27H*, *C31H*), 7.05 (dd, *J* = 17.6, 11.2 Hz, 1H, *C20H*), 6.92 – 6.85 (m, 2H, *C28H*, *C30H*), 6.00 (d, *J* = 9.5 Hz, 1H, *N10H*), 5.80 (d, *J* = 9.5, 4.9 Hz, 1H, *C7H*), 5.44 (d, *J* = 17.6 Hz, 1H, *C21H*), 5.32 (d, *J* = 11.2 Hz, 1H, *C21H*), 5.24 – 5.16 (m, 2H, $C25H_2$), 4.95 (d, *J* = 4.9 Hz, 1H, *C6H*), 3.80 (s, 3H, $C33H_3$), 3.71 – 3.59 (m, 3H, *C2H*, $C12H_2$), 3.46 ppm (d, *J* = 17.8 Hz, 1H, *C2H*); ^{13}C NMR (126 MHz, 298 K, $CDCl_3$): δ = 171.2, 164.6, 161.8, 160.0, 133.7, 132.0, 130.8, 129.6, 129.4, 128.0, 127.0, 126.3, 124.4, 117.8, 114.1, 68.1, 59.4, 57.6, 55.4, 43.5, 24.1 ppm; HRMS (ESI): m/z calculated for $C_{25}H_{24}N_2O_5SK$ $[M+K]^+$: 503.1038, found: 503.1047; IR (film): $\tilde{\nu}$ = 1770, 1712, 1657, 1613, 1585, 1536, 1516, 1425, 1385, 1357, 1303, 1250, 1230, 1176, 1161, 1109, 1031 cm^{-1}; $[\alpha]_D^{25}$ = -146 (c = 0.005 g/mL, $CHCl_3$).

4-Methoxybenzyl (6*R*,7*R*)-8-oxo-7-(2-phenylacetamido)-5-thia-1-azabicyclo[4.2.0]oct-2-ene-2-carboxylate (11e)[22]

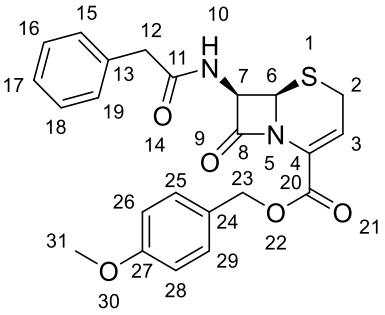

General procedure D was applied using **10e** (288 mg, 1.104 mmol, 1 equiv.), yielding after recrystallisation **11e** (92 mg, 27%). No further purification by column chromatography was required. Synthesis of **11e** was achieved following an alternative experimental procedure to that reported.[22] The analytical data are consistent with those reported.[22]

White solid; m.p.: 196-198 °C; ^{1}H NMR (400 MHz, 298 K, $CDCl_3$): δ = 7.40 – 7.24 (m, 7H, *C15H*, *C16H*, *C17H*, *C18H*, *C19H*, *C25H*, *C29H*), 6.88 (m, 2H, *C26H*, *C28H*), 6.50 (dd, *J* = 6.4, 2.5 Hz, 1H, *C3H*), 6.09 (d, *J* = 9.1 Hz, 1H, *N10H*), 5.86 (dd, *J* = 9.1, 5.0 Hz, 1H, *C7H*), 5.19 (m, 2H, $C23H_2$), 4.90 (d, *J* = 5.0 Hz, 1H, *C6H*), 3.80 (s, 3H, $C31H_3$), 3.70 – 3.58 (m, 2H, $C12H_2$), 3.53 (dd, *J* = 19.2, 2.5 Hz, 1H, *C2H*), 3.33 ppm (dd, *J* = 19.2, 6.4 Hz, 1H, *C2H*). ^{13}C NMR (126 MHz, 298 K, $CDCl_3$): δ = 171.2, 164.5, 161.5, 160.0, 133.8, 130.6, 129.6, 129.3, 128.2, 127.9, 127.2, 119.9, 114.1, 67.7, 59.8, 59.7, 57.0, 55.4, 43.5, 43.5, 24.2 ppm; IR (film): $\tilde{\nu}$ = 1789, 1731, 1655, 1626, 1613, 1584, 1539, 1516, 1454, 1400, 1365, 1327, 1304, 1278, 1258, 1244, 1214, 1187, 1172, 1100, 1054, 1020, 1001 cm^{-1}; HRMS (ESI): m/z calculated for $C_{23}H_{22}N_2O_5SNa$ $[M+Na]^+$: 461.1142, found: 461.1137; $[\alpha]_D^{25}$ = +78 (c = 0.007 g/mL, $CHCl_3$).

4-Methoxybenzyl (6*R*,7*R*)-3-chloro-8-oxo-7-(2-phenylacetamido)-5-thia-1-azabicyclo[4.2.0]oct-2-ene-2-carboxylate (11f)[22]

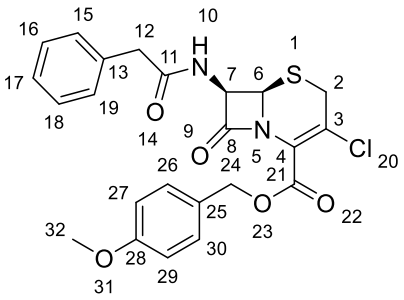

General procedure D was applied using **10f** (200 mg, 0.568 mmol, 1 equiv.). Purification by flash column chromatography (10 g Sfär, 100%$_{v/v}$ cyclohexane (2 CV), followed by a linear gradient (40 CV): 0%$_{v/v}$ →60%$_{v/v}$ ethyl acetate in cyclohexane) afforded **11f** (54 mg, 20%). Synthesis of **11f** was achieved following an alternative experimental procedure to that reported.[22] The analytical data are consistent with those reported.[22]

White solid: m.p.: 171-172 °C; ^{1}H NMR (500 MHz, 298 K, $CDCl_3$): δ = 7.39 – 7.29 (m, 5H, *C15H*, *C16H*, *C17H*, *C18H*, *C19H*), 7.27 – 7.24 (m, 2H, *C26H*, *C30H*), 6.90 – 6.85 (m, 2H, *C27H*, *C29H*), 6.01 (d, *J* = 9.1 Hz, 1H, *N10H*), 5.80 (dd, *J* = 9.1, 4.8 Hz, 1H, *C7H*), 5.25 – 5.19 (m, 2H, *C24H$_2$*), 4.98 (d, *J* = 4.8 Hz, 1H, *C6H*), 3.80 (s, 3H, *C32H$_3$*), 3.74 and 3.42 (ABq, *J* = 18.5 Hz, 2H, *C2H$_2$*), 3.67 and 3.61 ppm (ABq, *J* = 16.1 Hz, 2H, *C12H$_2$*); ^{13}C NMR (126 MHz, 298 K, $CDCl_3$): δ = 171.2, 164.0, 160.2, 160.1, 133.6, 130.8, 129.6, 129.4, 128.0, 126.8, 124.6, 124.3, 114.1, 68.3, 59.3, 59.2, 57.4, 55.4, 43.5, 31.1 ppm; HRMS (ESI): m/z calculated for $C_{23}H_{25}ClN_3O_5S$ $[M+NH_4]^+$: 490.1198, found: 490.1204; IR (film): $\tilde{\nu}$ = 1776, 1727, 1655, 1518, 1263, 1177, 1111, 1033 cm^{-1}; $[\alpha]_D^{25}$ = +38 (c = 0.004 g/mL, $CHCl_3$).

4-Methoxybenzyl (6R,7R)-3-(((1-methyl-1*H*-tetrazol-5-yl)thio)methyl)-8-oxo-7-(2-phenylacetamido)-5-thia-1-azabicyclo[4.2.0]oct-2-ene-2-carboxylate (11g) and **4-methoxybenzyl (2R,6R,7R)-3-(((1-methyl-1*H*-tetrazol-5-yl)thio)methyl)-8-oxo-7-(2-phenylacetamido)-5-thia-1-azabicyclo[4.2.0]oct-3-ene-2-carboxylate (11'g)**

General procedure D was applied using **10g** (200 mg, 0.448 mmol, 1 equiv.). Purification by flash column chromatography (10 g Sfär, 100%$_{v/v}$ cyclohexane (2 CV), followed by a linear gradient (30 CV): 0%$_{v/v}$ →60%$_{v/v}$ ethyl acetate in cyclohexane) afforded an inseparable mixture of Δ3 regioisomer **11g** and Δ2 regioisomer **11'g** (Δ3:Δ2 = 5:1 ratio; 149 mg, 58%) as a yellow wax.

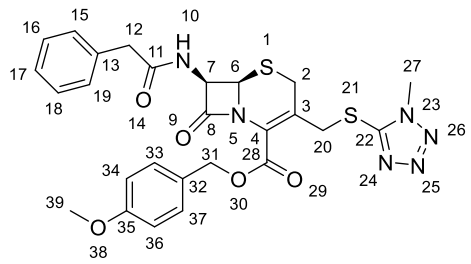

11g: ^{1}H NMR (500 MHz, 298 K, DMSO-*d*$_6$): δ = 9.11 (d, *J* = 8.4 Hz, 1H, *N10H*), 7.39 – 7.32 (m, 2H, *C33H*, *C37H*), 7.31 – 7.19 (m, 5H, *C15H*, *C16H*, *C17H*, *C18H*, *C19H*), 6.95 – 6.89 (m, 2H, *C34H*, *C36H*), 5.68 (dd, *J* = 8.4, 4.8 Hz, 1H, *C7H*), 5.20 – 5.12 (m, 2H, *C31H*$_2$), 5.07 (d, *J* = 4.8 Hz, 1H, *C6H*), 4.43 and 4.18 (ABq, *J* = 13.5 Hz, 2H, *C20H*$_2$), 3.92 (s, 3H, *C39H*$_3$), 3.78 and 3.63 (ABq, *J* = 18.0 Hz, 2H, *C2H*$_2$), 3.75 (s, 3H, *C27H*$_3$), 3.55 and 3.48 ppm (ABq, *J* = 13.9 Hz, 2H, *C12H*$_2$); ^{13}C NMR (151 MHz, 298 K, DMSO-*d*$_6$): δ = 170.9, 164.9, 161.4, 159.3, 153.1, 135.8, 130.4, 129.0, 128.2, 126.9, 126.5, 125.9, 124.9, 113.8, 67.3, 59.1, 57.7, 55.1, 41.6, 35.2, 33.7, 26.9 ppm;

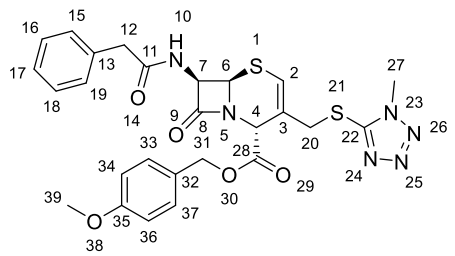

11'g: ^{1}H NMR (500 MHz, 298 K, DMSO-*d*$_6$): δ = 9.17 (d, *J* = 7.7 Hz, 1H, *N10H*), 7.39 – 7.32 (m, 2H, *C33H*, *C37H*), 7.31 – 7.19 (m, 5H, *C15H*, *C16H*, *C17H*, *C18H*, *C19H*), 6.95 – 6.91 (m, 2H, *C34H*, *C36H*), 6.70 (s, 1H, *C2H*), 5.42 (dd, *J* = 7.7, 3.9 Hz, 1H, *C7H*), 5.24 (d, *J* = 1.7 Hz, 1H, *C4H*), 5.20 – 5.12 (m, 2H, *C31H*$_2$), 5.09 (d, *J* = 3.9 Hz, 1H, *C6H*), 4.23 – 4.19 (m, 1H, *C20H*), 4.07 – 4.03 (m, 1H, *C20H*), 3.91 (s, 3H, *C39H*$_3$), 3.75 (s, 3H, *C27H*$_3$), 3.55 – 3.47 ppm (m, 2H, *C12H*$_2$); ^{13}C NMR (151 MHz, 298 K, DMSO-*d*$_6$): δ = 170.9, 166.9, 163.7, 159.4, 152.9, 135.7, 130.1, 129.1, 128.2, 128.2, 127.0, 121.8, 118.4, 113.9, 67.3, 60.7, 55.1, 52.6, 49.9, 41.5, 37.5, 33.7 ppm;

HRMS (ESI): m/z calculated for $C_{26}H_{27}N_6O_5S_2$ $[M+H]^+$: 567.1479, found: 567.1488.

4-Methoxybenzyl (6*R*,7*R*)-3-(((5-methyl-1,3,4-thiadiazol-2-yl)thio)methyl)-8-oxo-7-(2-phenylacetamido)-5-thia-1-azabicyclo[4.2.0]oct-2-ene-2-carboxylate (**11h**) and **4-methoxybenzyl (2R,6R,7R)-3-(((5-methyl-1,3,4-thiadiazol-2-yl)thio)methyl)-8-oxo-7-(2-phenylacetamido)-5-thia-1-azabicyclo[4.2.0]oct-3-ene-2-carboxylate** (**11'h**)

General procedure D was applied using **10h** (200 mg, 0.448 mmol, 1 equiv.). Purification by flash column chromatography (10 g Sfär, 100%$_{v/v}$ cyclohexane (2 CV), followed by a linear gradient (30 CV): 0%$_{v/v}$ →60%$_{v/v}$ ethyl acetate in cyclohexane) afforded an inseparable mixture of Δ3 regioisomer **11h** and Δ2 regioisomer **11'h** (Δ3:Δ2 = 10:1 ratio; 62 mg, 23%) as a yellow amorphous solid.

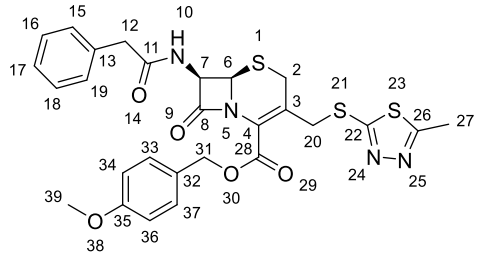

11h: ^{1}H NMR (600 MHz, 298 K, DMSO-*d*$_6$): δ = 9.11 (d, *J* = 8.5 Hz, 1H, *N10H*), 7.40 – 7.34 (m, 2H, *C33H*, *C37H*), 7.33 – 7.20 (m, 5H, *C15H*, *C16H*, *C17H*, *C18H*, *C19H*), 6.95 – 6.89 (m, 2H, *C34H*, *C36H*), 5.68 (dd, *J* = 8.4, 4.8 Hz, 1H, *C7H*), 5.22 and 5.15 (ABq, *J* = 12.0 Hz, 2H, *C31H*$_2$), 5.09 (d, *J* = 4.8 Hz, 1H, *C6H*), 4.55 and 4.14 (d, *J* = 13.4 Hz, 1H, *C20H*$_2$), 3.77 and 3.60 (ABq, *J* = 17.9 Hz, 2H, *C2H*$_2$), 3.75 (s, 3H, *C39H*$_3$), 3.55 and 3.48 (ABq, *J* = 13.9 Hz, 2H, *C12H*$_2$), 2.66 ppm (s, 3H, *C27H*$_3$); ^{13}C NMR (151 MHz, 298 K, DMSO-*d*$_6$): δ = 170.9, 166.1, 164.9, 163.7, 161.4, 159.3, 135.8, 130.4, 129.0, 128.2, 127.0, 126.5, 125.9, 125.0, 113.8, 67.2, 59.1, 57.8, 55.1, 41.6, 35.7, 27.1, 15.2 ppm;

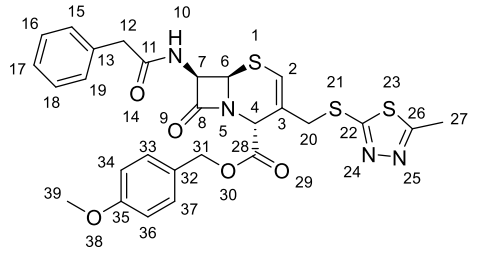

11'h: ^{1}H NMR (600 MHz, 298 K, DMSO-*d*$_6$): δ = 9.19 (d, *J* = 7.7 Hz, 1H, *N10H*), 7.40 – 7.34 (m, 2H, *C33H*, *C37H*), 7.33 – 7.20 (m, 5H, *C15H*, *C16H*, *C17H*, *C18H*, *C19H*), 6.95 – 6.91 (m, 2H, *C34H*, *C36H*), 6.73 (d, *J* = 1.6 Hz, 1H, *C2H*), 5.43 (dd, *J* = 7.7, 3.9 Hz, 1H, *C7H*), 5.19 (d, *J* = 1.6 Hz, 1H, *C4H*), 5.12 (m, 2H, *C31H*$_2$), 5.11 (d, *J* = 3.9 Hz, 1H, *C6H*), 4.21 (d, *J* = 14.0 Hz, 1H, *C20H*), 4.05 (d, *J* = 14.0 Hz, 1H, *C20H*), 3.75 (s, 3H, *C39H*$_3$), 3.54 – 3.48 (m, 2H, *C12H*$_2$), 2.68 ppm (s, 3H, *C27H*$_3$); ^{13}C NMR (151 MHz, 298 K, DMSO-*d*$_6$): δ = 167.4, 166.5, 164.3, 164.1, 161.9, 159.8, 159.8, 136.2, 130.6, 129.5, 128.7, 127.5, 122.2, 118.8, 114.3, 67.8, 61.2, 55.6, 53.1, 50.4, 42.0, 38.7, 15.2 ppm;

HRMS (ESI): m/z calculated for $C_{27}H_{27}N_4O_5S_3$ $[M+H]^+$: 583.1138, found: 583.1146.

***N*-((5*aR*,6*R*)-1,7-Dioxo-1,4,5a,6-tetrahydro-3H,7H-azeto[2,1-b]furo[3,4-d][1,3]thiazin-6-yl)-2-phenylacetamide (12)**[7, 23]

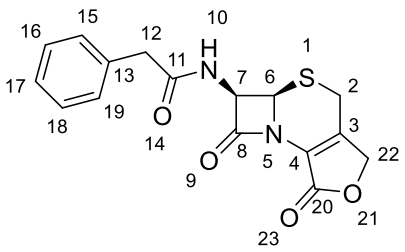

A variation of a reported procedure was followed.[7] To a solution of (6*R*,7*R*)-3-(acetoxymethyl)-8-oxo-7-(2-phenylacetamido)-5-thia-1-azabicyclo[4.2.0]oct-2-ene-2-carboxylic acid (581 mg, 1.49 mmol) in 1,4-dioxane (4 mL) was added dropwise at room temperature an aqueous HCl solution (37% (w/w)), and the reaction mixture was stirred for 18 h. The precipitate solid was filtered, washed with an aqueous 1,4-dioxane solution (50% (v/v)) cooled to 0 °C, and dried *in vacuo*, yielding product **12** (400 mg, 81%). No further purification was required. The analytical data are consistent with those reported, apart from the observed difference in the melting point.[7, 23]

White solid; m.p.: 178 °C (decomposition; reported m.p.[7, 23]: 210 °C); ^{1}H NMR (400 MHz, 298 K, $CDCl_3$): δ = 9.17 (d, *J* = 8.4 Hz, 1H, *N10H*), 7.35 – 7.18 (m, 5H, *C15H*, *C16H*, *C17H*, *C18H*, *C19H*), 5.83 (dd, *J* = 8.4, 5.0 Hz, 1H, *C7H*), 5.09 (d, *J* = 5.0 Hz, 1H, *C6H*), 5.04 (s, 2H, $C22H_2$), 3.79 (m, 2H, $C12H_2$), 3.58 and 3.50 ppm (ABq, *J* = 13.9 Hz, 2H, $C2H_2$); ^{13}C NMR (101 MHz, 298 K, $CDCl_3$): δ = 171.0, 166.6, 164.2, 142.6, 135.8, 129.0, 128.3, 126.5, 122.7, 71.4, 59.7, 57.4, 41.6, 22.4 ppm; IR (film): $\tilde{\nu}$ = 1775, 1736, 1678, 1660, 1612, 1549, 1442, 1416, 1313, 1203, 1144, 1098, 1023 cm^{-1}; HRMS (ESI): m/z calculated for $C_{16}H_{14}N_2O_4SNa$ $[M+Na]^+$: 353.0567, found: 353.0569; $[\alpha]_D^{25}$ = +120 (c = 0.006 g/mL, acetonitrile).

4-Methoxybenzyl (6*R*,7*R*)-3-(iodomethyl)-8-oxo-7-(2-phenylacetamido)-5-thia-1-azabicyclo[4.2.0]oct-2-ene-2-carboxylate (13)[8]

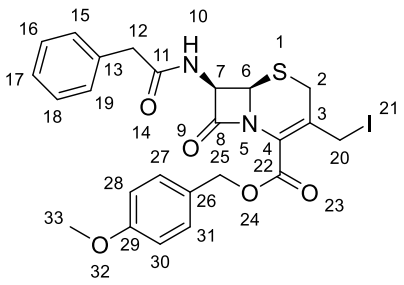

A variation of a reported procedure was followed.[8] To a solution of (6*R*,7*R*)-4-methoxybenzyl 3-(chloromethyl)-8-oxo-7-(2-phenylacetamido)-5-thia-1-azabicyclo[4.2.0]oct-2-ene-2-carboxylate (600 mg, 1.23 mmol, 1 equiv.) in acetone (12 mL; 0.1 M) was added NaI (231 mg, 1.55 mmol, 1.25 equiv.), and the reaction mixture was stirred at room temperature for 2 h, before addition of H_2O (18 mL). The aqueous layer was extracted thrice with CH_2Cl_2, and the combined organic extracts were washed with aqueous $Na_2S_2O_5$ (10% (w/v)) solution and brine. The organic layer was then dried over Na_2SO_4, filtered, and concentrated *in vacuo* to yield crude **13** (623 mg, 87%) as an amorphous yellow foam, which was directly used in the next step. (Attempted purification of this intermediate by either column chromatography or recrystallisation resulted in degradation). The analytical data are consistent with those reported.[8]

Yellow amorphous solid; characteristic analytical data: ^{1}H NMR (500 MHz, 298 K, $CDCl_3$): δ = 7.39 – 7.29 (m, 5H, *C15H*, *C16H*, *C17H*, *C18H*, *C19H*), 7.27 – 7.24 (m, 2H, *C27H*, *C31H*), 6.91 – 6.86 (m, 2H, *C28H*, *C30H*), 6.07 (d, *J* = 9.0 Hz, 1H, *N10H*), 5.77 (dd, *J* = 9.0, 4.9 Hz, 1H, *C7H*), 5.21 (s, 2H, *C25H*$_2$), 4.90 (d, *J* = 4.9 Hz, 1H, *C6H*), 4.36 and 4.29 (ABq, *J* = 9.3 Hz, 2H, *C20H*$_2$), 3.80 (s, 3H, *C33H*$_3$), 3.71 and 3.44 (ABq, *J* = 18.1 Hz, 2H, *C2H*$_2$), 3.68 – 3.59 ppm (m, 2H, *C12H*$_2$).

4-Methoxybenzyl (6R,7R)-8-oxo-7-(2-phenylacetamido)-3-(thiocyanatomethyl)-5-thia-1-azabicyclo[4.2.0]oct-2-ene-2-carboxylate (14)

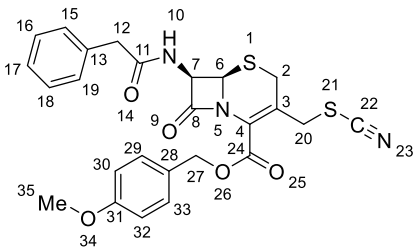

To a solution of cephem **14** (320 mg, 0.55 mmol, 1 equiv.) in acetone (20 mL) was added NaSCN (75 mg, 0.92 mmol, 1.7 equiv.) at 0 °C. After stirring for 2 h at 0 °C, the reaction mixture was diluted with H_2O, then extracted thrice with EtOAc. The organic layer was then washed with H_2O, and brine, then it was dried over Na_2SO_4, filtered, and concentrated *in vacuo*. Purification by flash column chromatography (10 g Sfär, 100%$_{v/v}$ cyclohexane (2 CV), followed by a linear gradient (30 CV): 0%$_{v/v}$ →60%$_{v/v}$ ethyl acetate in cyclohexane) yielded **14** (186 mg, 66%).

Pale yellow solid; m.p.: 121-122 °C; ^{1}H NMR (500 MHz, 298 K, DMSO-*d*$_6$): δ = 9.17 (d, *J* = 8.5 Hz, 1H, *N10H*), 7.38 – 7.19 (m, 7H, *C15H*, *C16H*, *C17H*, *C18H*, *C19H*, *C29H*, *C33H*), 6.96 – 6.89 (m, 2H), 5.74 (dd, *J* = 8.4, 4.8 Hz, 1H), 5.22 – 5.13 (m, 3H), 4.18 (m, 2H), 3.79 (d, *J* = 18.1 Hz, 1H), 3.75 (s, 3H), 3.60 – 3.47 ppm (m, 3H); ^{13}C NMR (126 MHz, 298 K, DMSO-*d*$_6$): δ = 170.9, 165.0, 161.1, 159.3, 135.8, 130.3, 129.0, 128.2, 126.8, 126.5, 125.6, 125.5, 113.8, 112.4, 67.3, 59.1, 58.0, 55.1, 41.6, 35.6, 26.9 ppm; HRMS (ESI): m/z calculated for $C_{25}H_{23}N_3O_5S_2K$ $[M+K]^+$: 548.0711, found: 548.0720; IR (film): $\tilde{\nu}$ = 1792, 1719, 1699, 1664, 1558, 1540, 1520, 1456, 1304, 1261, 1245, 1171, 1110, 1032 cm^{-1}; $[\alpha]_D^{25}$ = -132 (c = 0.004 g/mL, $CHCl_3$).

4-Methoxybenzyl (6*R*,7*R*)-8-oxo-7-(2-phenylacetamido)-3-((phenylthio)methyl)-5-thia-1-azabicyclo[4.2.0]oct-2-ene-2-carboxylate (15)[20]

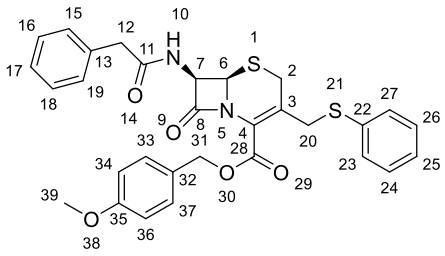

To a solution of cephem **13** (578 mg, 1 mmol, 1 equiv.) in *N*,*N*-dimethylformamide (0.1 M) was added PhSNa (132 mg, 1 mmol, 1 equiv.), and the reaction mixture was stirred at room temperature for 18 h, before being diluted with brine and EtOAc. The organic layer was separated, and the aqueous layer was further extracted twice with EtOAc. The combined organic extracts were washed with saturated aqueous LiCl solution, water, and brine. The organic layer was dried over Na_2SO_4, filtered, and concentrated *in vacuo*. Purification by flash column chromatography (25 g Sfär, 100%$_{v/v}$ cyclohexane (2 CV), followed by a linear gradient (26 CV): 0%$_{v/v}$ →26%$_{v/v}$ ethyl acetate in cyclohexane, followed by 26%$_{v/v}$ ethyl acetate in cyclohexane (12 CV)) yielded **15** (80 mg, 14%). Synthesis of **15** was achieved following an alternative experimental procedure to that reported.[20] The analytical data are consistent with those reported.[20]

Yellow wax; ^{1}H NMR (500 MHz, 298 K, DMSO-d_6): δ = 9.09 (d, *J* = 8.4 Hz, 1H, *N10H*), 7.27 (m, 12H, *C15H*, *C16H*, *C17H*, *C18H*, *C19H*, *C23H*, *C24H*, *C25H*, *C26H*, *C27H*, *C33H*, *C37H*), 6.91 (m, 2H, *C34H*, *C36H*), 5.63 (dd, *J* = 8.4, 4.7 Hz, 1H, *C7H*), 5.06 – 5.00 (m, 2H, *C31H*$_2$), 5.05 (d, *J* = 4.7 Hz, 2H, *C6H*), 4.15 and 3.90 (ABq, *J* = 13.2 Hz, 2H, *C20H*$_2$), 3.75 – 3.70 (m, 1H, *C2H*), 3.74 (s, 3H, *C39H*$_3$), 3.58 – 3.45 ppm (m, 3H, *C2H*, *C12H*$_2$); ^{13}C NMR (126 MHz, 298 K, DMSO-d_6): δ = 170.9, 164.8, 161.4, 159.3, 135.8, 134.4, 131.0, 130.3, 129.1, 129.0, 128.2, 128.1, 127.2, 127.0, 126.5, 123.9, 113.8, 66.9, 59.0, 57.9, 55.1, 41.6, 36.3, 27.4 ppm; HRMS (ESI): m/z calculated for $C_{30}H_{29}N_2O_5S_2$ $[M+H]^+$: 561.1512, found: 561.1505; IR (film): $\tilde{\nu}$ = 1783, 1764, 1723,

1665, 1612, 1547, 1514, 1439, 1357, 1246, 1219, 1164, 1093, 1023 cm^{-1}; $[\alpha]_D^{25}$ = 0.6 (c = 0.003 g/mL, $CHCl_3$).

4-Methoxybenzyl (6*R*,7*R*)-3-((2,2-difluoroacetoxy)methyl)-8-oxo-7-(2-phenylacetamido)-5-thia-1-azabicyclo[4.2.0]oct-2-ene-2-carboxylate (**16a**) and **4-methoxybenzyl (2*R*,6*R*,7*R*)-3-((2,2-difluoroacetoxy)methyl)-8-oxo-7-(2-phenylacetamido)-5-thia-1-azabicyclo[4.2.0]oct-3-ene-2-carboxylate** (**16'a**)

To a solution of cephem **13** (578 mg, 1 mmol, 1 equiv.) in *N*,*N*-dimethylformamide (0.1 M) was added sodium difluoroacetate (118 mg, 1 mmol, 1 equiv.), and the reaction mixture was stirred at room temperature for 18 h, before being diluted with brine and EtOAc. The organic layer was separated, and the aqueous layer was further extracted twice with EtOAc. The combined organic extracts were washed with saturated aqueous LiCl solution, water, and brine. The organic layer was dried over Na_2SO_4, filtered, and concentrated *in vacuo*. Purification by flash column chromatography (25 g Sfär, 100%$_{v/v}$ cyclohexane (3 CV), followed by a linear gradient (27 CV): 0%$_{v/v}$ →45%$_{v/v}$ ethyl acetate in cyclohexane) yielded an inseparable mixture of Δ3 regioisomer **16a** and Δ2 regioisomer **16'a** (10:1 ratio; 381 mg, 70%) as a yellow wax.

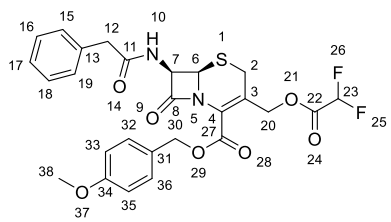

16a: ^{1}H NMR (600 MHz, 298 K, DMSO-d_6): δ = 9.12 (d, *J* = 8.4 Hz, 1H, *N10H*), 7.37 – 7.21 (m, 7H, *C15H*, *C16H*, *C17H*, *C18H*, *C19H*, *C32H*, *C36H*), 6.96 – 6.90 (m, 2H, *C33H*, *C35H*), 6.44 (t, *J* = 52.6 Hz, 1H, *C23H*), 5.74 (dd, *J* = 8.4, 4.9 Hz, 1H, *C7H*), 5.23 (d, *J* = 12.0 Hz, 1H, *C30H*), 5.16 – 5.12 (m, 2H, *C20H*, *C30H*), 4.94 (d, *J* = 12.6 Hz, 1H, *C20H*), 3.75 (s, 3H, *C38H$_3$*), 3.66 (d, *J* = 18.2 Hz, 1H, *C2H*), 3.60 – 3.54 (m, 2H, *C2H*, *C12H*), 3.49 ppm (d, *J* = 13.9 Hz, 1H, *C12H*); ^{13}C NMR (151 MHz, 298 K, DMSO-d_6): δ =

170.9, 165.1, 162.2, 161.2, 159.4, 135.8, 130.3, 129.0, 128.2, 126.8, 126.5, 126.2, 122.7, 113.8, 107.0 (t, J = 246 Hz), 67.4, 64.7, 59.3, 57.7, 55.1, 41.6, 25.6 ppm; ^{19}F NMR (377 MHz, 298 K, DMSO-d_6): δ = -127.4 ppm (d, J = 52.9 Hz, 2F, *C23F*$_2$);

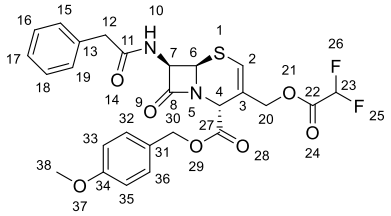

16'a: ^{1}H NMR (600 MHz, 298 K, DMSO-d_6): δ = 9.21 (d, J = 7.7 Hz, 1H, *N10H*), 7.37 – 7.21 (m, 7H, *C15H*, *C16H*, *C17H*, *C18H*, *C19H*, *C32H*, *C36H*), 6.96 – 6.90 (m, 3H, *C2H*, *C33H*, *C35H*), 6.42 (t, J = 52.6 Hz, 1H, *C23F*), 5.43 (dd, J = 7.7, 3.9 Hz, 1H, *C7H*), 5.14 (m, 1H, *C4H*), 5.11 (d, J = 3.9 Hz, 1Hz, *C6H*), 4.88 (d, J = 12.2 Hz, 1H, *C30H*), 4.83 (d, J = 12.2 Hz, 1H, *C30H*), 3.86 (d, J = 8.7 Hz, 1H, *C20H*), 3.75 (s, 3H, *C38H*$_3$), 3.60 – 3.55 (m, 1H, *C20H*), 3.52 ppm (m, 2H, *C12H*$_2$); ^{13}C NMR (151 MHz, 298 K, DMSO-d_6): δ = 166.9, 163.6, 162.4, 162.1, 162.0, 135.7, 130.1, 129.1, 128.4, 128.2, 127.1, 124.9, 117.4, 113.9, 107.0, 67.2, 60.8, 56.2, 55.6, 52.7, 49.6, 41.6 ppm; ^{19}F NMR (377 MHz, 298 K, DMSO-d_6): δ = -127.3 ppm (d, J = 52.7, 1.8 Hz, 2F, *C23F*$_2$);

HRMS (ESI): m/z calculated for $C_{26}H_{24}F_2N_2O_7SNa$ $[M+Na]^+$: 569.1165, found: 569.1163.

4-Methoxybenzyl (6*R*,7*R*)-3-((benzoyloxy)methyl)-8-oxo-7-(2-phenylacetamido)-5-thia-1-azabicyclo[4.2.0]oct-2-ene-2-carboxylate (**16b**) and **4-methoxybenzyl (2*R*,6*R*,7*R*)-3-((benzoyloxy)methyl)-8-oxo-7-(2-phenylacetamido)-5-thia-1-azabicyclo[4.2.0]oct-3-ene-2-carboxylate** (**16'b**)

To a solution of cephem **13** (578 mg, 1 mmol, 1 equiv.) in *N*,*N*-dimethylformamide (0.1 M) was added sodium benzoate (144 mg, 1 mmol, 1 equiv.), and the reaction mixture was stirred at room temperature for 18 h, before being diluted with brine and EtOAc. The organic layer was separated, and the aqueous layer was further extracted twice with EtOAc. The combined organic extracts

were washed with saturated aqueous LiCl solution, water, and brine. The organic layer was dried over Na_2SO_4, filtered, and concentrated *in vacuo*. Purification by flash column chromatography (25 g Sfär, 100%$_{v/v}$ cyclohexane (2 CV), followed by a linear gradient (24 CV): 0%$_{v/v}$ →30%$_{v/v}$ ethyl acetate in cyclohexane, followed by 30%$_{v/v}$ ethyl acetate in cyclohexane (18 CV)) yielded an inseparable mixture of Δ3 regioisomer **16b** and Δ2 regioisomer **16'b** (10:4 ratio, 344 mg, 60%) as a white amorphous solid.

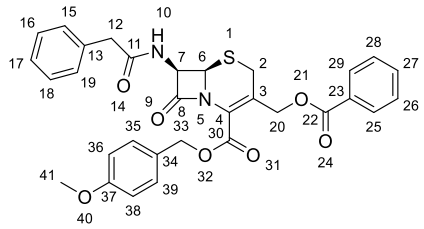

16b: ^{1}H NMR (500 MHz, 298 K, DMSO-d_6): δ = 9.14 (d, *J* = 8.4 Hz, 1H, *N10H*), 7.98 – 7.92 (m, 2H, *C25H*, *C29H*), 7.69 (m, 1H, *C27H*), 7.55 (m, 2H, *C26H*, *C28H*), 7.34 – 7.21 (m, 7H, *C15H*, *C16H*, *C17H*, *C18H*, *C19H*, *C35H*, *C39H*), 6.91 – 6.86 (m, 2H, *C36H*, *C38H*), 5.75 (dd, *J* = 8.4, 4.8 Hz, 1H, *C7H*), 5.24 (d, *J* = 12.0 Hz, 1H, *C33H*), 5.22 – 5.18 (m, 1H, *C33H*), 5.16 – 5.13 (m, 2H, *C6H*, *C20H*), 4.95 (d, *J* = 12.9 Hz, 1H, *C20H*), 3.79 and 3.70 (ABq, *J* = 18.2 Hz, 2H, $C2H_2$), 3.73 (s, 3H, $C41H_3$), 3.57 and 3.50 ppm (ABq, *J* = 13.8 Hz, 2H, $C12H_2$); ^{13}C NMR (126 MHz, 298 K, DMSO-d_6): δ = 170.9, 165.4, 165.1, 161.4, 159.3, 135.8, 133.5, 130.2, 129.3, 129.0, 128.8, 128.2 (2), 126.9, 126.5, 125.4, 124.4, 113.8, 67.3, 63.5, 59.2, 57.6, 55.1, 41.6, 25.9 ppm;

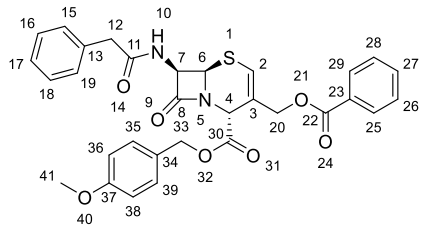

16'b: ^{1}H NMR (500 MHz, 298 K, DMSO-d_6): δ = 9.21 (d, *J* = 7.8 Hz, 1H, *N10H*), 7.98 – 7.92 (m, 2H, *C25H*, *C29H*), 7.69 (m, 1H, *C27H*), 7.55 (m, 2H, *C26H*, *C28H*), 7.34 – 7.21 (m, 7H, *C15H*, *C16H*, *C17H*, *C18H*, *C19H*, *C35H*, *C39H*), 6.92 (d, *J* = 1.7 Hz, 1H, *C2H*), 6.91 – 6.86 (m, 2H, *C36H*, *C38H*), 5.45 (dd, *J* = 7.8, 3.9 Hz, 1H, *C7H*), 5.20 (d, *J* = 1.7 Hz, 1H, *C4H*), 5.15 (m, 1H, *C6H*), 5.09 – 5.01 (m, 2H, $C33H_2$), 4.93 – 4.85 (m, 2H, $C20H_2$), 3.73 (s, 3H, $C41H_3$), 3.56 – 3.48 ppm (m, 2H, $C12H_2$); ^{13}C NMR (126 MHz, 298

K, DMSO-d_6): δ = 170.9, 165.2, 163.9, 159.3, 135.7, 133.5, 129.3, 129.2, 129.1, 128.8, 128.2 (2C), 126.9, 126.5, 123.0, 118.8, 113.8, 67.2, 66.1, 60.7, 52.8, 50.0, 41.6, 25.9 ppm;

HRMS (ESI): m/z calculated for $C_{31}H_{28}N_2O_7SNa$ $[M+Na]^+$: 595.1509, found: 595.1508;

4-Methoxybenzyl (6*R*,7*R*)-3-((methylsulfonyl)methyl)-8-oxo-7-(2-phenylacetamido)-5-thia-1-azabicyclo[4.2.0]oct-2-ene-2-carboxylate (**17a**) and **4-methoxybenzyl (2*R*,6*R*,7*R*)-3-((methylsulfonyl)methyl)-8-oxo-7-(2-phenylacetamido)-5-thia-1-azabicyclo[4.2.0]oct-3-ene-2-carboxylate** (**17'a**)

General procedure F was applied using cephem **13** (1.3 g, 2.24 mmol, 1 equiv.) and sodium p-methanesulfinate (260 mg, 2.55 mmol, 1.14 equiv.). Purification by flash column chromatography (50 g Sfär, 100%$_{v/v}$ cyclohexane (4 CV), followed by a linear gradient (50 CV): 0%$_{v/v}$ →100%$_{v/v}$ ethyl acetate in cyclohexane) yielded an inseparable mixture of Δ3 regiosiomer **17a** and Δ2 regioisomer **17'a** (10:1 ratio, 160 mg, 13%) as a yellow amorphous solid.

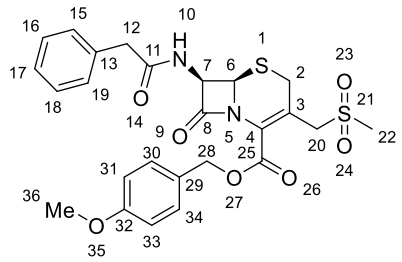

17a: ^{1}H NMR (600 MHz, 298 K, DMSO-d_6): δ = 9.14 (d, *J* = 8.4 Hz, 1H, *N10H*), 7.37 – 7.32 (m, 2H, *C30H*, *C34H*), 7.33 – 7.20 (m, 5H, *C15H*, *C16H*, *C17H*, *C18H*, *C19H*), 6.94 – 6.91 (m, 2H, *C31H*, *C33H*), 5.73 (dd, *J* = 8.4, 4.9 Hz, 1H, *C7H*), 5.23 and 5.13 (ABq, *J* = 12.0 Hz, 2H, $C28H_2$), 5.20 (d, *J* = 4.9 Hz, 1H, *C6H*), 4.51 and 4.32 (ABq, *J* = 13.9 Hz, 1H, $C20H_2$), 3.79 and 3.65 (ABq, *J* = 18.1 Hz, 2H, $C2H_2$), 3.75 (s, 3H, $C36H_3$), 3.56 and 3.49 (ABq, *J* = 13.9 Hz, 2H, $C12H_2$), 2.97 ppm (s, 3H, $C22H_3$); ^{13}C NMR (151 MHz, 298 K, DMSO-d_6): 170.9, 165.0, 161.4, 159.4, 135.8, 130.3, 129.0, 128.2, 127.4, 126.8, 126.5, 118.3, 113.8, 67.3, 59.2, 57.9, 56.9, 55.1, 41.6, 40.6, 28.2 ppm;

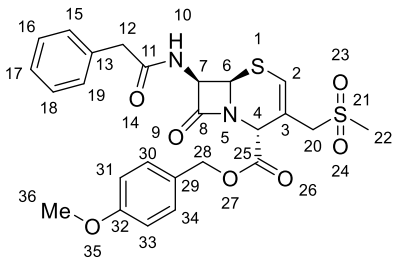

17'a: ^{1}H NMR (600 MHz, 298 K, DMSO-d_6): δ = 9.26 (d, J = 7.8 Hz, 1H, *N10H*), 7.37 – 7.32 (m, 2H, *C30H*, *C34H*), 7.33 – 7.20 (m, 5H, *C15H*, *C16H*, *C17H*, *C18H*, *C19H*), 6.94 – 6.91 (m, 2H, *C31H*, *C33H*), 6.79 (d, J = 1.6 Hz, 1H, *C2H*), 5.41 (dd, J = 7.8, 3.9 Hz, 1H, *C7H*), 5.29 (d, J = 1.6 Hz, 1H, *C4H*), 5.13 (s, 2H, $C28H_2$), 5.10 (d, J = 3.9 Hz, 1H, *C6H*), 4.18 and 3.90 (ABq, J = 14.3 Hz, 2H, $C20H_2$), 3.75 (s, 3H, $C36H_3$), 3.55 – 3.49 (m, 2H, $C12H_2$), 2.96 ppm (s, 3H, $C22H_3$); ^{13}C NMR (151 MHz, DMSO-d_6): δ = 170.9, 166.7, 163.5, 159.4, 135.7, 130.1, 129.1, 128.2, 127.9, 127.1, 125.7, 113.9, 112.2, 67.3, 60.8, 58.0, 55.1, 52.3, 50.5, 41.6, 40.6 ppm;

HRMS (ESI): m/z calculated for $C_{25}H_{26}N_2O_7S_2Na$ $[M+Na]^+$: 553.1074, found: 553.1078.

4-Methoxybenzyl (6*R*,7*R*)-8-oxo-7-(2-phenylacetamido)-3-(((trifluoromethyl)sulfonyl)methyl)-5-thia-1-azabicyclo[4.2.0]oct-2-ene-2-carboxylate (17b)

General procedure F was applied using cephem **13** (1.3 g, 2.24 mmol, 1 equiv.) and sodium trifluoromethanesulfinate (398 mg, 2.55 mmol, 1.14 equiv.). Purification by flash column chromatography (50 g Sfär, 100%$_{v/v}$ cyclohexane (3 CV), followed by a linear gradient (36 CV): 0%$_{v/v}$ →100%$_{v/v}$ ethyl acetate in cyclohexane) yielded **17b** (255 mg, 17%).

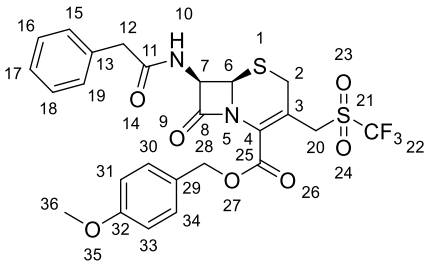

Cream yellow solid; m.p.: 159 °C; ^{1}H NMR (600 MHz, 298 K, DMSO-d_6): δ = 9.17 (d, J = 8.4 Hz, 1H, *N10H*), 7.36 – 7.20 (m, 7H, *C15H*, *C16H*, *C17H*, *C18H*, *C19H*, *C30H*, *C34H*), 6.96 – 6.90 (m, 2H, *C31H*, *C33H*), 5.78 (dd, J = 8.4, 5.0 Hz, 1H, *C7H*), 5.28 – 5.22 (m, 2H, *C6H*, *C28H*), 5.21 – 5.12 (m, 2H, *C20H*, *C28H*), 5.05 (d, J = 14.4 Hz, 1H, *C20H*), 3.79 and 3.66 (ABq, J = 18.1 Hz,

2H, *C2H₂*), 3.75 (s, 3H, *C36H*), 3.55 and 3.49 ppm (ABq, *J* = 13.9 Hz, 2H, *C12H₂*); ^{13}C NMR (151 MHz, 298 K, DMSO-*d₆*): δ = 171.4, 165.6, 161.5, 159.9, 136.2, 130.9, 129.8, 129.5, 128.7, 119.6 (q, *J* = 329 Hz) 120.7, 118.5, 114.3, 114.2, 68.1, 59.8, 58.7, 55.6, 53.0, 42.0, 28.6 ppm; ^{19}F NMR (565 MHz, 298K, DMSO-*d₆*): δ = -77.44 ppm (s, 3F, *C22F₃*); IR (film): ṽ = 1792, 1724, 1671, 1614, 1517, 1456, 1365, 1303, 1248, 1218, 1120, 1017 cm^{-1}; HRMS (ESI): m/z calculated for $C_{25}H_{23}F_3N_2O_7S_2Na$ $[M+Na]^+$: 607.0791, found: 607.0792; $[\alpha]_D^{25}$ = +83 (c = 0.002 g/mL, $CHCl_3$).

4-Methoxybenzyl (6*R*,7*R*)-8-oxo-7-(2-phenylacetamido)-3-(tosylmethyl)-5-thia-1-azabicyclo[4.2.0]oct-2-ene-2-carboxylate (**17c**)

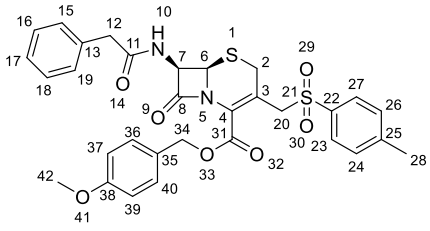

General procedure F was applied using cephem **13** (1.3 g, 2.24 mmol, 1 equiv.) and sodium p-toluenesulfinate (453 mg, 2.55 mmol, 1.14 equiv.). Purification by flash column chromatography (50 g Sfär, 100%$_{v/v}$ cyclohexane (2 CV), followed by a linear gradient (40 CV): 0%$_{v/v}$ →100%$_{v/v}$ ethyl acetate in cyclohexane) yielded **17c** (311 mg, 23%).

Amorphous yellow solid; ^{1}H NMR (500 MHz, 298 K, $CDCl_3$): δ = 7.68 – 7.62 (m, 2H, *C23H*, *C27H*), 7.40 – 7.23 (m, 9H, *C15H*, *C16H*, *C17H*, *C18H*, *C19H*, *C24H*, *C26H*, *C36H*, *C40H*), 6.91 – 6.84 (m, 2H, *C37H*, *C39H*), 5.97 (d, *J* = 9.2 Hz, 1H, *N10H*), 5.79 (dd, *J* = 9.2, 4.9 Hz, 1H, *C7H*), 5.06 – 4.98 (m, 2H, *C20H*, *C34H*), 4.94 (d, *J* = 4.9 Hz, 1H, *C6H*), 4.90 (d, *J* = 11.8 Hz, 1H, *C34H*), 3.93 (d, *J* = 13.8 Hz, 1H, *C20H*), 3.81 and 3.39 (ABq, *J* = 18.5 Hz, 2H, *C2H₂*), 3.80 (s, 3H, *C42H₃*), 3.70 – 3.57 (m, 2H, *C12H₂*), 2.41 ppm (s, 3H, *C28H₃*); ^{13}C NMR (126 MHz, 298 K, $CDCl_3$): δ = 171.1, 164.6, 161.1, 160.1, 145.4, 135.2, 133.7, 130.7, 130.0, 129.6, 129.4, 128.6, 128.2, 128.0, 126.6, 118.9, 114.1, 68.2, 59.5, 59.3, 57.8, 55.4, 43.5, 29.6, 21.9 ppm; IR (film): ṽ = 1781, 1719,

1673, 1613, 1516, 1361, 1303, 1247, 1147, 1121, 1085, 1031 cm^{-1}; HRMS (ESI): m/z calculated for $C_{31}H_{34}N_3O_7S_2$ $[M+NH_4]^+$: 624.1833, found: 624.1838; $[\alpha]_D^{25}$ = +10 (c = 0.01 g/mL, $CHCl_3$).

4-Methoxybenzyl (6R,7R)-3-formyl-8-oxo-7-(2-phenylacetamido)-5-thia-1-azabicyclo[4.2.0]oct-2-ene-2-carboxylate (18)[9]

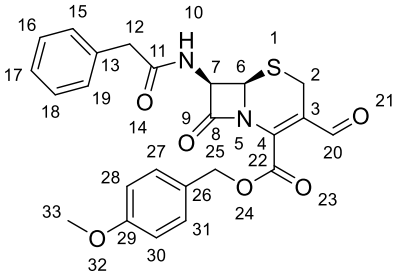

A variation of a reported procedure was followed.[9] To a solution of cephem **13** (2.7 g, 4.7 mmol, 1 equiv.) in *N*-methyl-2-pyrrolidone (47 ml; 0.1 M) was added phosphomolybdic acid (628 mg, 0.34 mmol, 0.07 equiv.), and the reaction mixture was stirred under bubbling O_2 at 35 °C for 4 h, before dilution with EtOAc (200 mL). The organic layer was washed with H_2O, aqueous $Na_2S_2O_3$ (5% (w/v)) solution, and brine, before being dried over Na_2SO_4, filtered, and concentrated *in vacuo*. Purification by flash column chromatography (25 g Sfär, 100%$_{v/v}$ cyclohexane (2 CV), followed by a linear gradient (20 CV): 0%$_{v/v}$ →60%$_{v/v}$ ethyl acetate in cyclohexane) yielded **18** (709 mg, 32%) as an amorphous foam. The analytical data are consistent with those reported.[9]

Yellow solid; m.p.: 143 °C; ^{1}H NMR (500 MHz, 298 K, DMSO-*d*$_6$): δ = 9.65 (s, 1H, *C20H*), 9.22 (d, *J* = 8.4 Hz, 1H, *N10H*), 7.41 – 7.36 (m, 2H, *C27H*, *C31H*), 7.33 – 7.19 (m, 5H, *C15H*, *C16H*, *C17H*, *C18H*, *C19H*), 6.98 – 6.93 (m, 2H, *C28H*, *C30H*), 5.89 (dd, *J* = 8.5, 5.3 Hz, 1H, *C7H*), 5.34 and 5.28 (ABq, *J* = 11.8 Hz, 2H, *C25H*$_2$), 5.25 (d, *J* = 5.3 Hz, 1H, *C6H*), 3.91 and 3.46 (ABq, *J* = 17.8, 2H, *C2H*$_2$), 3.76 (s, 3H, *C33H*$_3$), 3.54 and 3.49 ppm (ABq, *J* = 14.0 Hz, 2H, *C12H*$_2$); ^{13}C NMR (126 MHz, 298 K, DMSO-*d*$_6$): δ = 188.3, 170.9, 165.7, 160.4, 159.6, 138.6, 135.6, 130.7, 129.0, 128.3, 126.5, 126.4, 122.0, 113.9, 68.4, 60.1, 59.5, 55.1, 41.6, 21.5 ppm; HRMS (ESI): m/z

calculated for $C_{24}H_{23}N_2O_6S$ $[M+H]^+$: 467.1271, found: 467.1281; IR (film): $\tilde{\nu}$ = 1797, 1726, 1666, 1611, 1515, 1357, 1260, 1177, 1095, 1027 cm^{-1}; $[\alpha]_D^{25}$ = -140 (c = 0.007 g/mL, $CHCl_3$).

4-Methoxybenzyl (6*R*,7*R*)-3-((*E*)-(hydroxyimino)methyl)-8-oxo-7-(2-phenylacetamido)-5-thia-1-azabicyclo[4.2.0]oct-2-ene-2-carboxylate (19a)

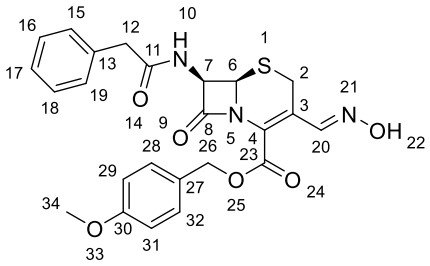

To a solution of cephem **18** (500 mg, 1.07 mmol, 1 equiv.) in tetrahydrofuran-H_2O (12:1 (v/v); 0.13 M) was added hydroxylamine hydrochloride (74.5 mg, 1.07 mmol, 1 equiv.), and the reaction mixture was stirred for 4 h at 60 °C, before cooling down to room temperature. The reaction mixture was diluted with EtOAc, then washed with H_2O and brine, dried over Na_2SO_4, filtered, and concentrated *in vacuo*. Purification by flash column chromatography (25 g Sfär, 100%$_{v/v}$ cyclohexane (2 CV), followed by a linear gradient (30 CV): 0%$_{v/v}$ →50%$_{v/v}$ tetrahydrofuran in cyclohexane) yielded **19a** (368 mg, 71%).

Amorphous solid; ^{1}H NMR (500 MHz, 298 K, DMSO-*d*$_6$): δ = 11.68 (s, 1H, *O22H*), 9.17 (d, *J* = 8.4 Hz, 1H, *N10H*), 8.12 (s, 1H, *C20H*), 7.39 – 7.33 (m, 2H, *C26H*, *C32H*), 7.32 – 7.19 (m, 5H, *C15H*, *C16H*, *C17H*, *C18H*, *C19H*), 6.97 – 6.90 (m, 2H, *C29H*, *C31H*), 5.76 (dd, *J* = 8.4, 4.9 Hz, 1H, *C7H*), 5.27 and 5.16 (ABq, *J* = 12.0 Hz, 2H, *C26H*$_2$), 5.18 (d, *J* = 4.9 Hz, 1H, *C6H*), 4.00 and 3.64 (ABq, *J* = 18.0 Hz, 2H, *C2H*$_2$), 3.75 (s, 3H, *C34H*$_3$), 3.59 – 3.47 ppm (m, 2H, *C12H*$_2$); ^{13}C NMR (126 MHz, 298 K, DMSO-*d*$_6$): δ = 171.4, 165.6, 161.7, 159.9, 146.2, 136.2, 133.7, 130.9, 129.5, 128.7, 127.4, 127.0, 126.6, 114.3, 67.9, 60.0, 58.7, 55.6, 42.0, 23.4 ppm; HRMS (ESI): m/z calculated for $C_{24}H_{24}N_3O_6S$ $[M+H]^+$: 482.1380, found: 482.1388; IR (film): $\tilde{\nu}$ = 1771, 1717, 1646,

1613, 1515, 1455, 1385, 1363, 1302, 1260, 1227, 1175, 1154, 1108, 1069, 1031 cm^{-1}; $[\alpha]_D^{25}$ = -74 (c = 0.004 g/mL, acetonitrile).

4-Methoxybenzyl (6*R*,7*R*)-3-((*E*)-(methoxyimino)methyl)-8-oxo-7-(2-phenylacetamido)-5-thia-1-azabicyclo[4.2.0]oct-2-ene-2-carboxylate (19b)

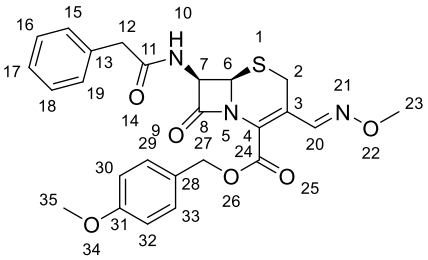

General procedure E was applied using cephem **18** (156.8 mg, 0.336 mmol, 1 equiv.) and *O*-methylhydroxylamine hydrochloride (28.1 mg, 0.338 mmol, 1.1 equiv.). Purification by flash column chromatography (25 g Sfär, 100%$_{v/v}$ cyclohexane (2 CV), followed by a linear gradient (20 CV): 0%$_{v/v}$ →25%$_{v/v}$ ethyl acetate in cyclohexane, followed by 25%$_{v/v}$ ethyl acetate in cyclohexane (10 CV)) yielded **19b** (19 mg, 11%).

Amorphous solid; ^{1}H NMR (600 MHz, 298 K, DMSO-d_6): δ = 9.18 (d, *J* = 8.4 Hz, 1H, *N10H*), 8.16 (s, 1H, *C20H*), 7.37 – 7.33 (m, 2H, *C29H*, *C33H*), 7.32 – 7.20 (m, 5H, *C15H*, *C16H*, *C17H*, *C18H*, *C19H*), 6.96 – 6.91 (m, 2H, *C30H*, *C32H*), 5.78 (dd, *J* = 8.4, 5.0 Hz, 1H, *C7H*), 5.26 and 5.16 (ABq, *J* = 11.9 Hz, 2H, *C27H$_2$*), 5.19 (d, *J* = 5.0 Hz, 1H, *C6H*), 3.96 and 3.62 (ABq, *J* = 18.0 Hz, 2H, *C2H$_2$*), 3.87 (s, 3H, *C23H$_3$*), 3.75 (s, 3H, *C35H$_3$*), 3.55 and 3.50 ppm (ABq, *J* = 13.9 Hz, 2H, *C12H$_2$*); ^{13}C NMR (151 MHz, 298 K, DMSO-d_6): δ = 170.9, 165.1, 161.0, 159.4, 146.1, 135.7, 130.5, 129.0, 128.2, 127.5, 126.8, 126.5, 120.3, 113.8, 67.6, 62.1, 59.6, 58.3, 55.1, 41.5, 22.8 ppm; IR (film): $\tilde{\nu}$ = 1781, 1709, 1656, 1613, 1538, 1517, 1455, 1388, 1354, 1318, 1248, 1178, 1156, 1102, 1072, 1050 cm^{-1}; HRMS (ESI): m/z calculated for $C_{25}H_{26}N_3O_6S$ $[M+H]^+$: 496.1537, found: 496.1533; $[\alpha]_D^{25}$ = -235 (c = 0.01 g/mL, $CHCl_3$).

4-Methoxybenzyl (6*R*,7*R*)-8-oxo-3-((*E*)-(phenoxyimino)methyl)-7-(2-phenylacetamido)-5-thia-1-azabicyclo[4.2.0]oct-2-ene-2-carboxylate (19c)

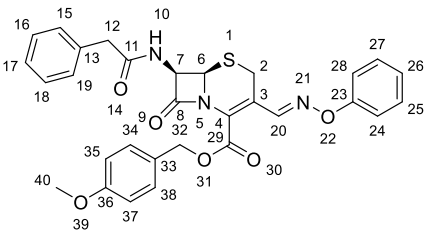

General procedure E was applied using cephem **18** (120 mg, 0.257 mmol, 1 equiv.) and *O*-phenylhydroxylamine hydrochloride (42 mg, 0.289 mmol, 1.1 equiv.). Purification by flash column chromatography (25 g Sfär, 100%$_{v/v}$ cyclohexane (2 CV), followed by a linear gradient (17 CV): 0%$_{v/v}$ →23%$_{v/v}$ ethyl acetate in cyclohexane, followed by 23%$_{v/v}$ ethyl acetate in cyclohexane (5 CV)) yielded **19c** (33 mg, 23%).

Yellow solid; m.p.: 164 °C; ^{1}H NMR (600 MHz, 298 K, DMSO-*d*$_6$): δ = 9.21 (d, *J* = 8.3 Hz, 1H, *N10H*), 8.56 (s, 1H, *C20H*), 7.42 – 7.20 (m, 11H, *C15H*, *C16H*, *C17H*, *C18H*, *C19H, C24H*, *C25H*, *C27H*, *C28H*, *C34H*, *C38H*), 7.07 (m, 1H, *C26H*), 6.97 – 6.92 (m, 2H, *C35H*, *C37H*), 5.83 (dd, *J* = 8.3, 5.0 Hz, 1H, *C7H*), 5.30 and 5.22 (ABq, *J* = 11.8 Hz, 2H, *C32H*$_2$), 5.25 (d, *J* = 5.0 Hz, 1H, *C6H*), 4.20 and 3.73 (ABq, *J* = 18.0 Hz, 2H, *C2H*$_2$), 3.75 (s, 3H, *C40H*$_3$), 3.56 and 3.51 ppm (ABq, *J* = 13.9 Hz, 2H, *C12H*$_2$); ^{13}C NMR (151 MHz, 298 K, DMSO-*d*$_6$): δ = 170.9, 165.1, 160.9, 159.5, 158.6, 149.7, 135.7, 130.5, 129.6, 129.4, 129.0, 128.2, 126.7, 126.5, 122.7, 119.2, 114.2, 113.9, 67.9, 59.8, 58.4, 55.1, 41.6, 22.8 ppm; HRMS (ESI): m/z calculated for $C_{30}H_{28}N_3O_6S$ $[M+H]^+$: 558.1693, found: 558.1704; IR (film): $\tilde{\nu}$ = 1780, 1718, 1651, 1592, 1540, 1517, 1490, 1457, 1436, 1385, 1354, 1291, 1251, 1233, 1215, 1177, 1162, 1103, 1073, 1040, 1022 cm^{-1}; $[\alpha]_D^{25}$ = -295 (c = 0.004 g/mL, $CHCl_3$).

4-Methoxybenzyl (6*R*,7*R*)-3-((*E*)-((benzyloxy)imino)methyl)-8-oxo-7-(2-phenylacetamido)-5-thia-1-azabicyclo[4.2.0]oct-2-ene-2-carboxylate (19d)

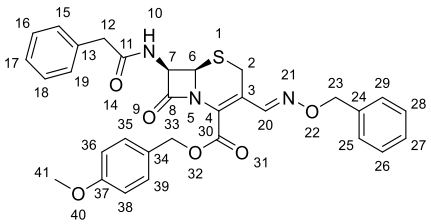

General procedure E was applied using cephem **18** (120 mg, 0.257 mmol, 1 equiv.) and *O*-benzylhydroxylamine hydrochloride (41 mg, 0.257 mmol, 1 equiv.). Purification by flash column chromatography (25 g Sfär, 100%$_{v/v}$ cyclohexane (2 CV), followed by a linear gradient (20 CV): 0%$_{v/v}$ →23%$_{v/v}$ ethyl acetate in cyclohexane, followed by 23%$_{v/v}$ ethyl acetate in cyclohexane (10 CV)) yielded **19d** (32 mg, 22%).

White solid; m.p.: 188 °C; ^{1}H NMR (500 MHz, 298 K, $CDCl_3$): δ = 8.42 (s, 1H, *C20H*), 7.42 – 7.31 (m, 10H, *C15H*, *C16H*, *C17H*, *C18H*, *C19H*, *C26H*, *C27H*, *C28H*, *C35H*, *C39H*), 7.30-7.27 (m, 2H, *C36H*, *C38H*), 6.93 – 6.86 (m, 2H, *C36H*, *C38H*), 5.99 (d, *J* = 9.2 Hz, 1H, *N10H*), 5.87 (dd, *J* = 9.3, 4.9 Hz, 1H, *C7H*), 5.24 and 5.18 (ABq, *J* = 11.8 Hz, 2H, $C33H_2$), 5.15 (s, 2H, $C23H_2$), 4.98 (d, *J* = 4.9 Hz, 1H, *C6H*), 4.03 and 3.45 (ABq, *J* = 18.5 Hz, 2H, $C2H_2$), 3.82 (s, 3H, $C41H_3$), 3.70 and 3.64 ppm (ABq, *J* = 16.2 Hz, 2H, $C12H_2$); ^{13}C NMR (126 MHz, 298 K, $CDCl_3$): δ = 171.1, 164.7, 161.1, 160.1, 146.5, 137.2, 133.6, 130.9, 129.6, 129.4, 128.6, 128.5, 128.3, 128.0, 127.2, 126.8, 122.5, 114.2, 77.0, 68.4, 59.7, 58.1, 55.4, 43.5, 23.6 ppm; HRMS (ESI): m/z calculated for $C_{31}H_{30}N_3O_6S$ $[M+H]^+$: 572.1850, found: 572.1856; IR (film): $\tilde{\nu}$ = 1785, 1721, 1664, 1612, 1547, 1536, 1515, 1495, 1452, 1358, 1303, 1248, 1221, 1176, 1157, 1104, 1023 cm^{-1}; $[\alpha]_D^{25}$ = -195 (c = 0.004 g/mL, $CHCl_3$).

1-(((6*R*,7*R*)-2-(((4-Methoxybenzyl)oxy)carbonyl)-8-oxo-7-(2-phenylacetamido)-5-thia-1-azabicyclo[4.2.0]oct-2-en-3-yl)methyl)pyridin-1-ium iodide (20a)

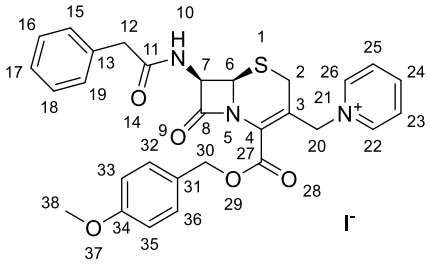

A variation of a reported procedure was followed.[10] **General procedure G** was applied using cephem **13** (1 g, 1.72 mmol, 1 equiv.) and pyridine (0.56 mL, 6.88 mmol, 4 equiv.) to yield **20a** (620 mg, 55%). The analytical data are consistent with those reported.[10]

Cream solid; m.p.: 145 °C; ^{1}H NMR (500 MHz, 298 K, DMSO-d_6): δ = 9.13 (d, J = 8.3 Hz, 1H, *N10H*), 9.00 – 8.95 (m, 2H, *C22H*, *C26H*), 8.66 (m, 1H, *C24H*), 8.23 – 8.17 (m, 2H, *C23H*, *C25H*), 7.38 – 7.31 (m, 2H, *C32H*, *C36H*), 7.31 – 7.18 (m, 5H, *C15H*, *C16H*, *C17H*, *C18H*, *C19H*), 6.96 – 6.89 (m, 2H, *C33H*, *C35H*), 5.81 (dd, J = 8.4, 4.9 Hz, 1H, *C7H*), 5.63 – 5.51 (m, 2H, *C20H*$_2$), 5.27 and 5.20 (ABq, J = 11.9 Hz, 2H, *C30H*$_2$), 5.15 (d, J = 4.9 Hz, 1H, *C6H*), 3.76 (s, 3H, *C38H*), 3.57 – 3.45 ppm (m, 4H, *C2H*$_2$, *C12H*$_2$); ^{13}C NMR (126 MHz, 298 K, DMSO-d_6): δ = 170.9, 165.3, 161.3, 159.4, 146.3, 144.8, 135.7, 130.4, 129.0, 128.4, 128.2, 128.0, 126.5, 126.5, 120.8, 113.8, 67.9, 60.5, 59.4, 57.8, 55.2, 41.6, 25.4 ppm; IR (film): $\tilde{\nu}$ = 1787, 1700, 1650, 1518, 1496, 1481, 1388, 1360, 1301, 1244, 1177, 1148, 1106, 1031 cm^{-1}; HRMS (ESI): m/z calculated for $C_{29}H_{28}N_3O_5S$ $[M\text{-}I]^+$: 530.1744, found: 530.1745; $[\alpha]_D^{25}$ = -57 (c = 0.006 g/mL, acetonitrile).

2-(((6*R*,7*R*)-2-(((4-Methoxybenzyl)oxy)carbonyl)-8-oxo-7-(2-phenylacetamido)-5-thia-1-azabicyclo[4.2.0]oct-2-en-3-yl)methyl)isoquinolin-2-ium iodide (20b)

General procedure G was applied using cephem **13** (1 g, 1.72 mmol, 1 equiv.) and isoquinoline (0.81 mL, 6.88 mmol, 4 equiv.) to yield **20b** (697 mg, 57%).

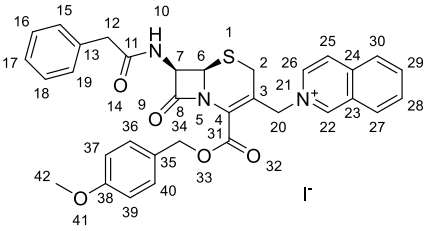

Brown solid; m.p.: 155-156 °C; ^{1}H NMR (400 MHz, 298 K, DMSO-d_6): δ = 9.98 (s, 1H, *C22H*), 9.13 (d, *J* = 8.3 Hz, 1H, *N10H*), 8.67 – 8.58 (m, 2H, *C25H*, *C26H*), 8.49 (d, *J* = 8.3 Hz, 1H, *C27H*), 8.37 (d, *J* = 8.3 Hz, 1H, *C30H*), 8.30 (ddd, *J* = 8.3, 6.9, 1.3 Hz, 1H, *C29H*), 8.10 (ddd, *J* = 8.3, 6.9, 1.3 Hz, 1H, *C28H*), 7.37 – 7.31 (m, 2H, *C36H*, *C40H*), 7.29 – 7.18 (m, 5H, *C15H*, *C16H*, *C17H*, *C18H*, *C19H*), 6.91 – 6.83 (m, 2H, *C37H*, *C39H*), 5.81 (dd, *J* = 8.3, 4.9 Hz, 1H, *C7H*), 5.73 and 5.65 (ABq, *J* = 14.9 Hz, 2H, *C20H*$_2$), 5.29 and 5.22 (ABq, *J* = 11.9 Hz, 2H, *C34H*$_2$), 5.16 (d, *J* = 4.9 Hz, 1H, *C6H*), 3.73 (s, 3H, *C42H*$_3$), 3.59 – 3.45 ppm (m, 4H,*C2H*$_2$, *C12H*$_2$); ^{13}C NMR (151 MHz, 298 K, DMSO-d_6): δ = 170.9, 165.3, 161.4, 159.4, 150.8, 137.31, 137.28, 135.7, 134.1, 131.3, 130.8, 130.4, 129.0, 128.2, 127.9, 127.30, 127.27, 126.51, 126.47, 126.2, 121.1, 113.8, 68.0, 60.5, 59.4, 57.8, 55.1, 41.6, 25.4 ppm; ; HRMS (ESI): m/z calculated for $C_{33}H_{30}N_3O_5S^+$ $[M-I]^+$: 580.1901, found: 580.1920; IR (film): ṽ = 1774, 1705, 1651, 1518, 1455, 1394, 1372, 1351, 1305, 1278, 1255, 1228, 1195, 1178, 1157, 1114, 1071, 1038 cm^{-1}; $[\alpha]_D^{25}$ = -101 (c = 0.01 g/mL, acetonitrile).

2-(((6*R*,7*R*)-2-(((4-Methoxybenzyl)oxy)carbonyl)-8-oxo-7-(2-phenylacetamido)-5-thia-1-azabicyclo[4.2.0]oct-2-en-3-yl)methyl)-5,6,7,8-tetrahydroisoquinolin-2-ium iodide (**20c**)

General procedure G was applied using cephem **13** (578 mg, 1 mmol, 1 equiv.) and 5,6,7,8-tetrahydroisoquinoline (134 mg, 1 mmol, 1 equiv.) to yield **20c** (376 mg, 52%).

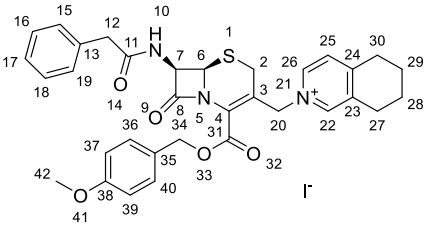

Amorphous light green solid; ^{1}H NMR (400 MHz, 298 K, DMSO-d_6): δ = 9.14 (d, J = 8.3 Hz, 1H, *N10H*), 8.68 (s, 1H, *C22H*), 8.58 (d, J = 6.4, 1H, *C26H*), 7.87 (d, J = 6.4 Hz, 1H, *C25H*), 7.37 – 7.33 (m, 2H, *C36H*, *C40H*), 7.32 – 7.17 (m, 5H, *C15H*, *C16H*, *C17H*, *C18H*, *C19H*), 6.98 – 6.88 (m, 2H, *C37H*, *C39H*), 5.79 (dd, J = 8.3, 4.9 Hz, 1H, *C7H*), 5.53 – 5.39 (m, 2H, $C20H_2$), 5.27 and 5.21 (ABq, J = 11.9 Hz, 2H, $C34H_2$), 5.15 (d, J = 4.9 Hz, 1H, *C6H*), 3.75 (s, 3H, $C42H_3$), 3.59 – 3.44 (m, 4H, $C2H_2$, $C12H_2$), 2.98 (m, 2H, $C27H_2$), 2.81 (m, 2H, $C30H_2$), 1.79 ppm (m, 4H, $C28H_2$, $C29H_2$); ^{13}C NMR (101 MHz, 298 K, DMSO-d_6): δ = 170.9, 165.2, 161.3, 159.4, 158.4, 143.9, 140.2, 137.9, 135.7, 130.5, 129.0, 128.2, 127.8, 127.7, 126.5 (2C), 120.9, 113.8, 67.9, 59.6, 59.4, 57.8, 55.2, 41.6, 28.9, 25.8, 25.4, 20.63, 20.60 ppm; HRMS (ESI): m/z calculated for $C_{33}H_{34}N_3O_5S^+$ $[M\text{-}I]^+$: 584.2214, found: 584.2224; IR (film): $\tilde{\nu}$ = 1782, 1709, 1659, 1515, 1454, 1360, 1302, 1248, 1221, 1176, 1104, 1030 cm^{-1}; $[\alpha]_D^{25}$ = -58 (c = 0.006 g/mL, acetonitrile).

2-(((6*R*,7*R*)-2-(((4-Methoxybenzyl)oxy)carbonyl)-8-oxo-7-(2-phenylacetamido)-5-thia-1-azabicyclo[4.2.0]oct-2-en-3-yl)methyl)imidazo[1,5-*a*]pyridin-2-ium iodide (**20d**)

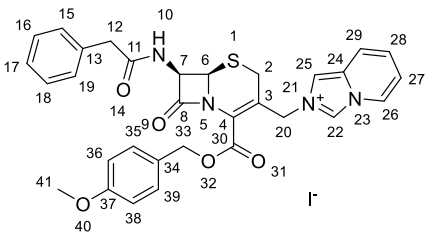

General procedure G was applied using cephem **13** (578 mg, 1 mmol, 1 equiv.) and imidazolo[1,5-a]pyridine (178 mg, 1.5 mmol, 1.5 equiv.) to yield **20d** (306 mg, 43%).

Amorphous violet solid; ^{1}H NMR (600 MHz, 298 K, DMSO-d_6): δ = 9.71 (s, 1H, *C22H*), 9.10 (d, *J* = 8.2 Hz, 1H, *N10H*), 8.62 (d, *J* = 7.1 Hz, 1H, *C26H*), 8.10 (s, 1H, *C25H*), 7.87 (d, *J* = 9.3 Hz, 1H, *C29H*), 7.39 – 7.34 (m, 2H, *C35H*, *C39H*), 7.33 – 7.18 (m, 7H, *C15H*, *C16H*, *C17H*, *C18H*, *C19H*, *C27H*, *C28H*), 6.95 – 6.88 (m, 2H, *C36H*, *C38H*), 5.80 (dd, *J* = 8.2, 4.9 Hz, 1H, *C7H*), 5.44 and 5.35 (ABq, *J* = 14.6 Hz, 2H, *C20H*$_2$), 5.30 and 5.24 (ABq, *J* = 12.0 Hz, 2H, *C33H*$_2$), 5.14 (d, *J* = 4.9 Hz, 1H, *C6H*), 3.74 (s, 3H, *C41H*$_3$), 3.61 (d, *J* = 18.4 Hz, 1H, *C2H*), 3.57 – 3.46 ppm (m, 3H, *C2H*, *C12H*$_2$); ^{13}C NMR (151 MHz, 298 K, DMSO-d_6): δ = 170.9, 165.3, 161.5, 159.4, 135.7, 130.5, 129.6, 129.0, 128.2, 127.2, 127.0, 126.6, 126.5, 124.8, 124.4, 122.4, 118.2, 117.5, 113.8, 113.1, 67.9, 59.4, 57.6, 55.1, 50.2, 41.5, 25.5 ppm; HRMS (ESI): m/z calculated for $C_{31}H_{29}N_4O_5S^+$ $[M\text{-}I]^+$: 569.1853, found: 569.1860; IR (film): $\tilde{\nu}$ = 1799, 1710, 1655, 1516, 1454, 1356, 1301, 1249, 1175, 1146, 1104, 1069, 1029 cm^{-1}; $[\alpha]_D^{25}$ = -81 (c = 0.01 g/mL, acetonitrile).

5-(((6*R*,7*R*)-2-(((4-Methoxybenzyl)oxy)carbonyl)-8-oxo-7-(2-phenylacetamido)-5-thia-1-azabicyclo[4.2.0]oct-2-en-3-yl)methyl)furo[3,2-*c*]pyridin-5-ium iodide (**20e**)

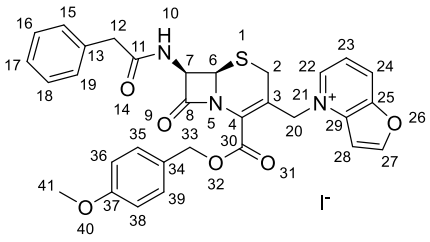

General procedure G was applied using cephem **13** (578 mg, 1 mmol, 1 equiv.) and furo[3,2-*b*]pyridine (119 mg, 1 mmol, 1 equiv.) to yield **20e** (136 mg, 19%).

Amorphous pale brown solid; ^{1}H NMR (500 MHz, 298 K, DMSO-d_6): δ = 9.14 (d, J = 8.3 Hz, 1H, *N10H*), 8.97 (d, J = 8.4 Hz, 1H, *C22H*), 8.94 (d, J = 2.4 Hz, 1H, *C27H*), 8.77 (d, J = 6.1 Hz, 1H, *C24H*), 8.05 (dd, J = 8.4, 6.1 Hz, 1H, *C23H*), 7.69 (d, J = 2.4 Hz, 1H, *C28H*), 7.31 – 7.20 (m, 7H, *C15H*, *C16H*, *C17H*, *C18H*, *C19H*, *C35H*, *C39H*), 6.91 – 6.85 (m, 2H, *C36H*, *C38H*), 5.80 (dd, J = 8.3, 5.0 Hz, 1H, *C7H*), 5.77 and 5.69 (ABq, J = 15.2 Hz, 2H, *C20H*$_2$), 5.27 and 5.21 (ABq, J = 11.8 Hz, 2H, *C33H*$_2$), 5.14 (d, J = 5.0 Hz, 1H, *C6H*), 3.76 (s, 3H, *C41H*$_3$), 3.57 – 3.46 (m, 2H, *C12H*$_2$), 3.46 – 3.41 ppm (m, 2H, *C2H*$_2$); ^{13}C NMR (151 MHz, 298 K, DMSO-d_6): δ = 170.9, 165.2, 161.4, 159.5, 156.6, 150.4, 141.9, 139.9, 135.7, 130.5, 129.0, 128.2, 128.1, 127.9, 126.5, 126.4, 121.7, 120.4, 113.8, 103.0, 68.0, 59.5, 57.8, 57.4, 55.1, 41.6, 25.3 ppm; HRMS (ESI): m/z calculated for $C_{31}H_{28}N_3O_6S^+$ $[M-I]^+$: 570.1693, found: 570.1696; IR (film): $\tilde{\nu}$ = 1783, 1770, 1712, 1675, 1612, 1515, 1453, 1390, 1245, 1218, 1175, 1137, 1101, 1029 cm^{-1}; $[\alpha]_D^{25}$ = -17 (c = 0.006 g/mL, acetonitrile).

1-(((6*R*,7*R*)-2-(((4-Methoxybenzyl)oxy)carbonyl)-8-oxo-7-(2-phenylacetamido)-5-thia-1-azabicyclo[4.2.0]oct-2-en-3-yl)methyl)-6,7-dihydro-5*H*-cyclopenta[*b*]pyridin-1-ium iodide (20f)

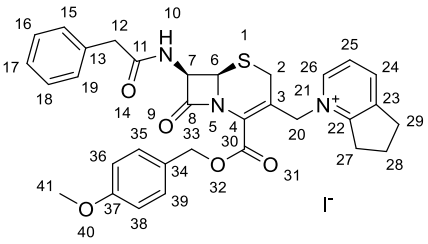

A variation of a reported procedure was followed.[11] **General procedure G** was applied using cephem **13** (578 mg, 1 mmol, 1 equiv.) and 6,7-dihydro-5*H*-cyclopenta[b]pyridine (0.14 mL, 1.2 mmol, 1.2 equiv.) to yield **20f** (330 mg, 47%). The analytical data are consistent with those reported.[11]

Amorphous brown solid; ^{1}H NMR (400 MHz, 298 K, DMSO-d_6): δ = 9.15 (d, *J* = 8.3 Hz, 1H, *N10H*), 8.54 (d, *J* = 6.2 Hz, 1H, *C26H*), 8.40 (d, *J* = 7.7 Hz, 1H, *C24H*), 7.89 (dd, *J* = 7.7, 6.2 Hz, 1H, *C25H*), 7.34 – 7.19 (m, 7H, *C15H*, *C16H*, *C17H*, *C18H*, *C19H*, *C35H*, *C39H*), 6.98 – 6.88 (m, 2H, *C36H*, *C38H*), 5.80 (dd, *J* = 8.3, 4.9 Hz, 1H, *C7H*), 5.47 (s, 2H, $C20H_2$), 5.30 (d, *J* = 11.8 Hz, 1H, *C33H*), 5.19 – 5.13 (m, 2H, *C6H*, *C33H*), 3.76 (s, 3H, $C41H_3$), 3.60 – 3.44 (m, 4H, $C2H_2$, $C12H_2$), 3.24 – 3.01 (m, 4H, $C27H_2$, $C29H_2$), 2.23 – 2.04 ppm (m, 2H, $C28H_2$); ^{13}C NMR (101 MHz, DMSO) δ 171.0, 165.1, 161.7, 161.2, 159.5, 145.4, 141.2, 141.1, 135.7, 130.6, 129.0, 128.2, 127.9, 126.54, 126.50, 125.6, 119.5, 113.8, 67.9, 59.4, 58.2, 57.7, 55.2, 41.6, 31.3, 30.5, 25.3, 21.9 ppm; HRMS (ESI): m/z calculated for $C_{32}H_{32}N_3O_5S^+$ $[M-I]^+$: 570.2057, found: 570.2075; IR (film): $\tilde{\nu}$ = 1785, 1722, 1675, 1613, 1515, 1388, 1246, 1176, 1101, 1027 cm^{-1}; $[\alpha]_D^{25}$ = -7.6 (c = 0.01 g/mL, acetonitrile).

1-(((6*R*,7*R*)-2-(((4-Methoxybenzyl)oxy)carbonyl)-8-oxo-7-(2-phenylacetamido)-5-thia-1-azabicyclo[4.2.0]oct-2-en-3-yl)methyl)-5,6,7,8-tetrahydroquinolin-1-ium iodide (20g)

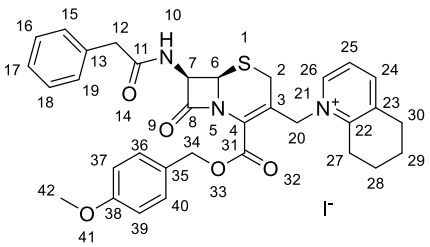

General procedure G was applied using cephem **13** (578 mg, 1 mmol, 1 equiv.) and 5,6,7,8-tetrahydroquinoline (0.12 mL, 1 mmol, 1; equiv.) to yield **20g** (389 mg, 54%). Amorphous green solid; ^{1}H NMR (400 MHz, 298 K, DMSO-d_6): δ = 9.15 (d, *J* = 8.2 Hz, 1H, *N10H*), 8.58 (d, *J* = 6.2 Hz, 1H, *C26H*), 8.32 (d, *J* = 7.8 Hz, 1H, *C24H*), 7.89 (dd, *J* = 7.8, 6.2 Hz, 1H, *C25H*), 7.32 – 7.21 (m, 7H, *C15H*, *C16H*, *C17H*, *C18H*, *C19H*, *C36H*, *C40H*), 6.93 – 6.87 (m, 2H, *C37H*, *C39H*), 5.80 (dd, *J* = 8.2, 4.9 Hz, 1H, *C7H*), 5.54 – 5.42 (m, 2H, $C20H_2$), 5.26 (d, *J* = 11.8 Hz, 1H, *C34H*), 5.17 – 5.13 (m, 2H, *C6H*, *C34H*), 3.76 (s, 3H, $C42H_3$), 3.56 and 3.50 (ABq, *J* = 13.8 Hz, 2H, $C12H_2$), 3.44 (s, 2H, $C2H_2$), 2.94 – 2.84 (m, 4H, $C27H_2$, $C30H_2$), 1.84 – 1.69 ppm (m, 4H, $C28H_2$, $C29H_2$); ^{13}C NMR (101 MHz, 298 K, DMSO-d_6): δ = 170.9, 165.1, 161.1, 159.5, 154.4, 145.9, 142.8, 139.2, 135.7, 130.6, 129.0, 128.2, 127.9, 126.5, 126.5, 124.3, 119.7, 113.8, 67.8, 59.4, 57.7, 57.4, 55.2, 41.6, 28.1, 26.2, 25.3, 20.9, 19.9 ppm; HRMS (ESI): m/z calculated for $C_{33}H_{34}N_3O_5S^+$ $[M\text{-}I]^+$: 584.2214, found: 584.2203; IR (film): $\tilde{\nu}$ = 1784, 1723, 1675, 1613, 1515, 1453, 1389, 1302, 1246, 1175, 1104, 1028 cm^{-1}; $[\alpha]_D^{25}$ = +18 (c = 0.007 g/mL, acetonitrile).

1-(((6*R*,7*R*)-2-(((4-Methoxybenzyl)oxy)carbonyl)-8-oxo-7-(2-phenylacetamido)-5-thia-1-azabicyclo[4.2.0]oct-2-en-3-yl)methyl)imidazo[1,2-*b*]pyridazin-1-ium iodide (**20h**)

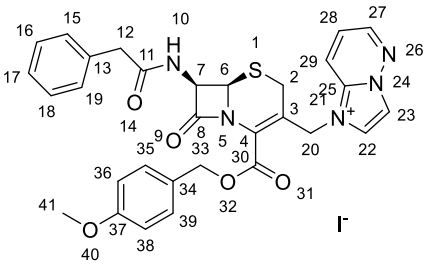

General procedure G was applied using cephem **13** (578 mg, 1 mmol, 1 equiv.) and imidazo[1,2-b]pyridazine (120 mg, 1 mmol, 1 equiv.) to yield **20h** (154 mg, 22%).

Amorphous brown solid; ^{1}H NMR (400 MHz, 298 K, DMSO-d_6): δ = 9.13 (m, 2H, *N10H*, *C27H*), 8.86 (d, *J* = 2.2 Hz, 1H, *C22H*), 8.83 – 8.78 (m, 1H, *C29H*), 8.28 (d, *J* = 2.3 Hz, 1H, *C23H*), 8.03 (dd, *J* = 9.5, 4.6 Hz, 1H, *C28H*), 7.38 – 7.35 (m, 2H, *C35H*, *C39H*), 7.28 – 7.19 (m, 5H, *C15H*, *C16H*, *C17H*, *C18H*, *C19H*), 6.94 – 6.89 (m, 2H, *C36H*, *C38H*), 5.77 (dd, *J* = 8.3, 4.9 Hz, 1H, *C7H*), 5.52 – 5.38 (m, 2H, *C20H*$_2$), 5.31 and 5.23 (ABq, *J* = 11.9 Hz, 2H, *C33H*$_2$), 5.13 (d, *J* = 4.9 Hz, 1H, *C6H*), 3.75 (s, 3H, *C41H*$_3$), 3.56 – 3.35 ppm (m, 4H, *C2H*$_2$, *C12H*$_2$); ^{13}C NMR (101 MHz, 298 K, DMSO-d_6): δ = 171.0, 165.3, 161.6, 159.5, 148.3, 136.4, 135.7, 130.5, 129.0, 128.2, 126.8, 126.6, 126.5, 125.6, 125.1, 122.2, 121.0, 119.2, 113.9, 67.9, 59.4, 57.7, 55.2, 47.7, 41.6, 25.2 ppm; HRMS (ESI): m/z calculated for $C_{30}H_{28}N_5O_5S^+$ [M-I]$^+$: 570.1806, found: 570.1809; IR (film): $\tilde{\nu}$ = 1783, 1721, 1671, 1613, 1515, 1453, 1385, 1302, 1246, 1176, 1102, 1027 cm^{-1}; $[\alpha]_D^{25}$ = -48 (c = 0.003 g/mL, acetonitrile).

8.2.4 References

1. V. Srisuknimit, et al., Peptidoglycan Cross-Linking Preferences of Staphylococcus aureus Penicillin-Binding Proteins Have Implications for Treating MRSA Infections, *J. Am. Chem. Soc.*, 2017, **139**, 9791–9794.
2. S. S. van Berkel, et al., Assay Platform for Clinically Relevant Metallo-β-lactamases, *J. Med. Chem.*, 2013, **56**, 6945–6953.
3. R. Keltjens, et al., A New Convenient Synthesis of 3-Carboxycephems Starting from 7-Aminocephalosporanic Acid (7-ACA), *European Journal of Organic Chemistry*, 2001, **2001**, 2529–2534.
4. K. H. M. E. Tehrani, et al., Novel Cephalosporin Conjugates Display Potent and Selective Inhibition of Imipenemase-Type Metallo-β-Lactamases, *Journal of Medicinal Chemistry*, 2021, **64**, 9141–9151.
5. F. Xiong, et al., A novel synthetic route to 7-MAC from 7-ACA, *Journal of the Iranian Chemical Society*, 2016, **13**, 1019–1025.
6. L. D. Patterson, et al., Enzymatic Deprotection of the Cephalosporin 3′-Acetoxy Group Using Candida antarctica Lipase B, *The Journal of Organic Chemistry*, 2010, **75**, 1289–1292.
7. J. D. Cocker, et al., Cephalosporanic acids. Part IV. 7-Acylamidoceph-2-em-4-carboxylic acids, *J. Chem. Soc. C Org.*, 1966, 1142–1151.
8. G. Zhao, et al., Syntheses and studies of quinolone-cephalosporins as potential anti-tuberculosis agents, *Bioorg. Med. Chem. Lett.*, 2006, **16**, 5534–5537.
9. H. Tanaka, et al., Aerobic Oxidation of 3-Iodomethyl-Δ3-cephem-4-carboxylate to 3-Formyl-Δ3-cephem-4-carboxylate through 3-Hydroperoxymethyl-Δ3-cephem-4-carboxylate, *Bull. Chem. Soc. Jpn.*, 1996, **69**, 229–233.
10. S. Chen, et al., Exploration of membrane-active cephalosporin derivatives as potent antibacterial agents against Staphylococcus aureus biofilms and persisters, *European Journal of Medicinal Chemistry*, 2025, **289**, 117484.
11. X. Duan, et al., One-Pot Synthesis of Cefpirome Sulfate from GCLE, *Synthetic Communications*, 2011, **41**, 629–636.
12. T. Aoki, et al., Cefiderocol (S-649266), A new siderophore cephalosporin exhibiting potent activities against Pseudomonas aeruginosa and other gram-negative pathogens including multi-drug resistant bacteria: Structure activity relationship, *European Journal of Medicinal Chemistry*, 2018, **155**, 847–868.
13. S. Mobashery, et al., Preparation of ceph-3-em esters unaccompanied by Δ3/Δ2 isomerization of the cephalosporin, *J. Org. Chem.*, 1986, **51**, 4723–4726.
14. J. L. Fahey, et al., 3-Cyanocephems and carbon-13 heterocyclic-substituted cephems via 1,3-dipolar cycloadditions, *Journal of Medicinal Chemistry*, 1976, **19**, 562–565.
15. M. Lee, et al., A Practical Synthesis of Nitrocefin, *The Journal of Organic Chemistry*, 2005, **70**, 367–369.
16. J. Singh, et al., A Practical Synthesis of an Anti-Methicillin Resistant Staphylococcus aureus Cephalosporin BMS-247243, *Organic Process Research & Development*, 2000, **4**, 488–497.
17. K. H. Cha, et al., A Facile Removal of P-Methoxybenzyl and Diphenylmethyl Ester with Iodotrimethyl-Silane-Triphenylphosphine, *Synthetic Communications*, 1999, **29**, 3533–3540.

18. S. Torii, et al., Deprotection of carboxylic esters of .beta.-lactam homologs. Cleavage of p-methoxybenzyl, diphenylmethyl, and tert-butyl esters effected by a phenolic matrix, *The Journal of Organic Chemistry*, 1991, **56**, 3633–3637.
19. Y. Yoshida, et al., studies on anti-helicobacter pylori agents. part 2: new cephem derivatives, *Biorg. Med. Chem.*, 2000, **8**, 2317–2335.
20. H. Tanaka, et al., Chemo- and Product-selective Electrooxidation of 3-(Arylthiomethyl)-Δ^3-cephems, *Synthesis*, 2009, **2009**, 3449–3459.
21. M. Chao, et al., An Improved and Scaleable Preparation of 7-Amino-3-vinylcephem-4-carboxylic acid, *Organic Process Research & Development*, 2009, **13**, 924–927.
22. H. Tanaka, et al., Synthesis of 2-exo-Methylenepenam and 3-Chloro-Δ3-cephem through a Sequential Reductive 1,2-Elimination/S−S Bond Fission or Chloride Ion-Addition/Cyclization of 3,4-Disubstituted 2-Butenoates in Metal Salt/Metal Combinations, *The Journal of Organic Chemistry*, 1997, **62**, 3610–3617.
23. K. K. Prasad, et al., Conversion of Penicillin to Cephalosporin Lactones. Preliminary Communication, *Helv. Chim. Acta*, 1976, **59**, 2298–2300.

8.2.5 ^{1}H and ^{13}C NMR spectra of the compounds prepared for this study

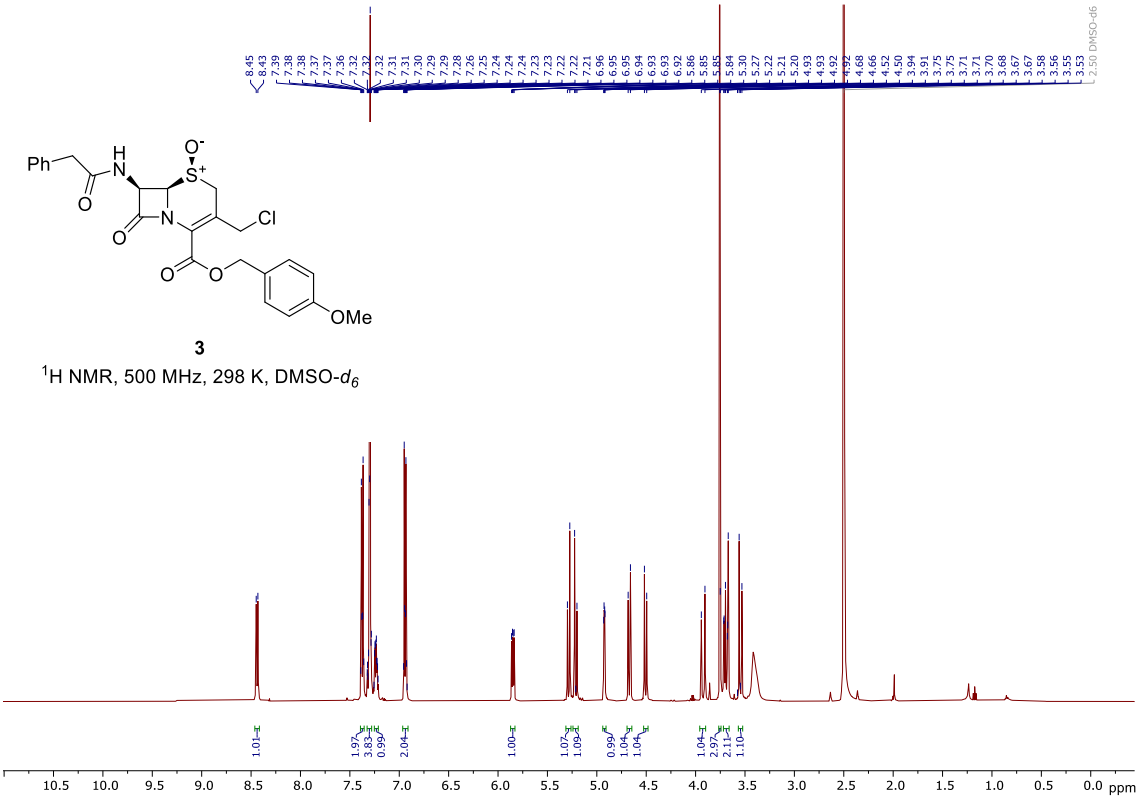

3

^{1}H NMR, 500 MHz, 298 K, DMSO-d_6

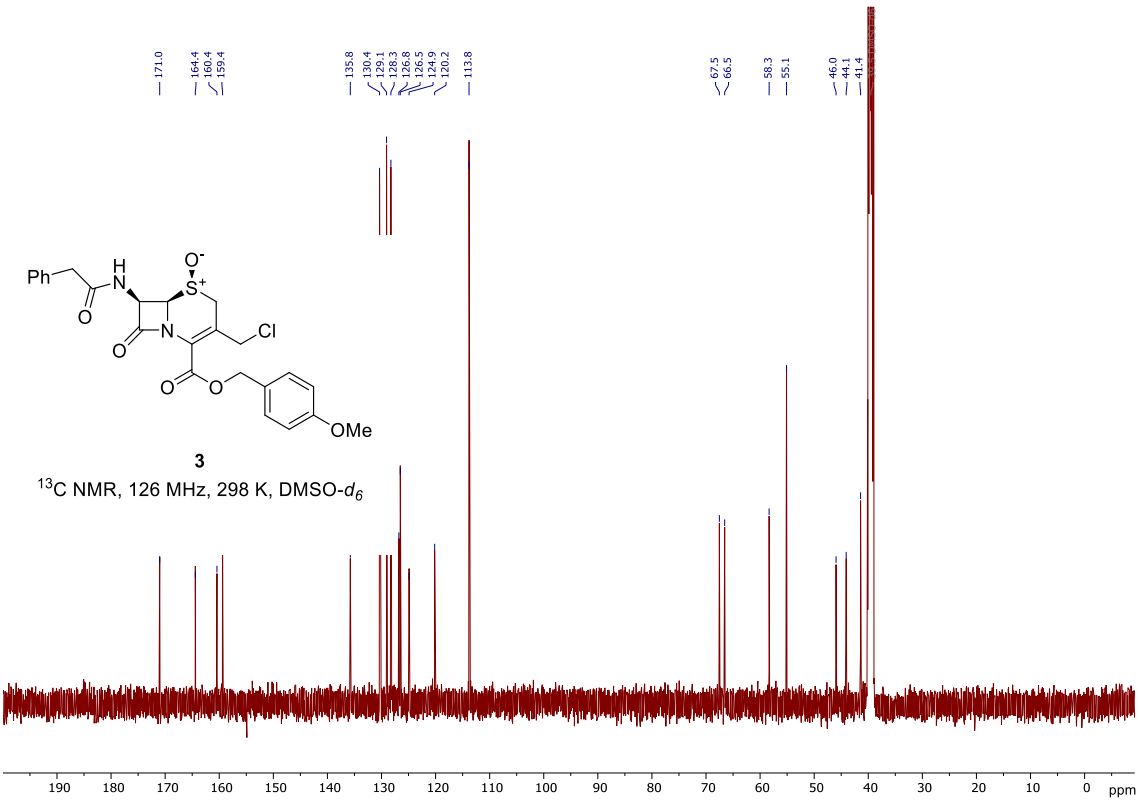

3

^{13}C NMR, 126 MHz, 298 K, DMSO-d_6

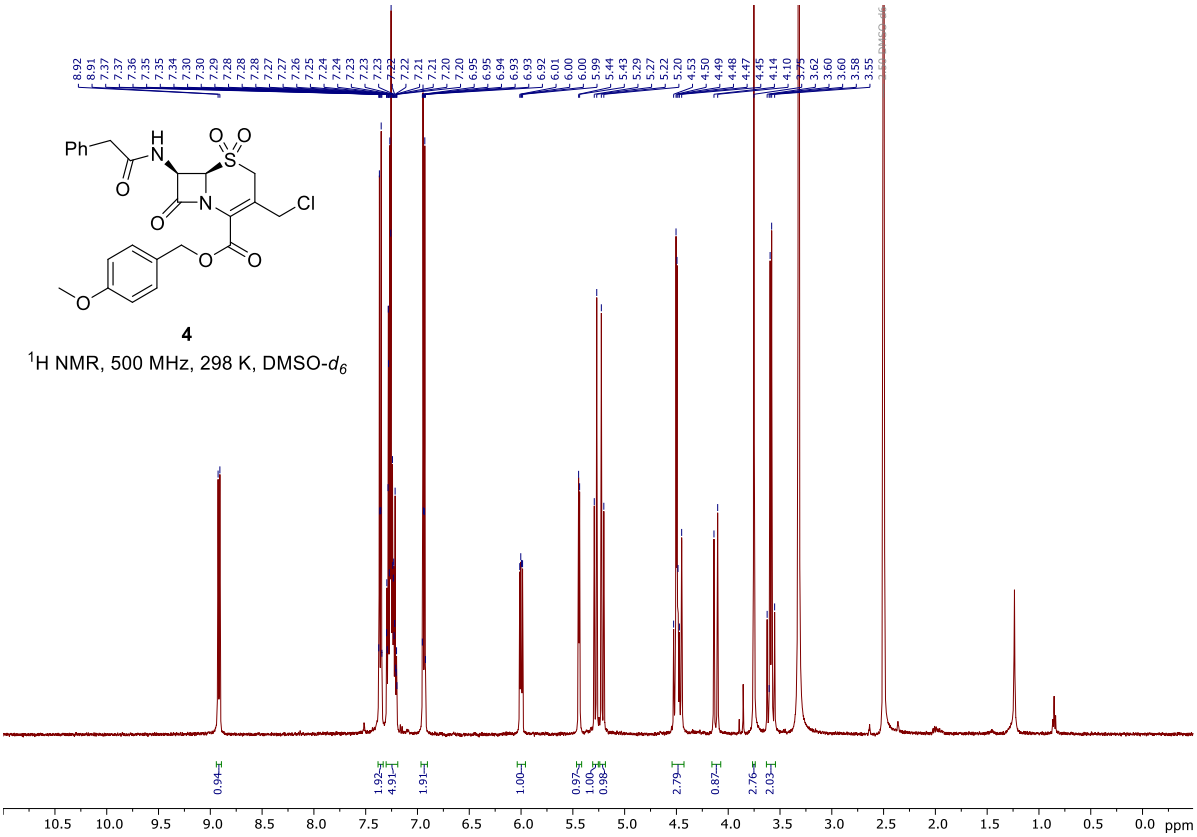

4

^{1}H NMR, 500 MHz, 298 K, DMSO-d_6

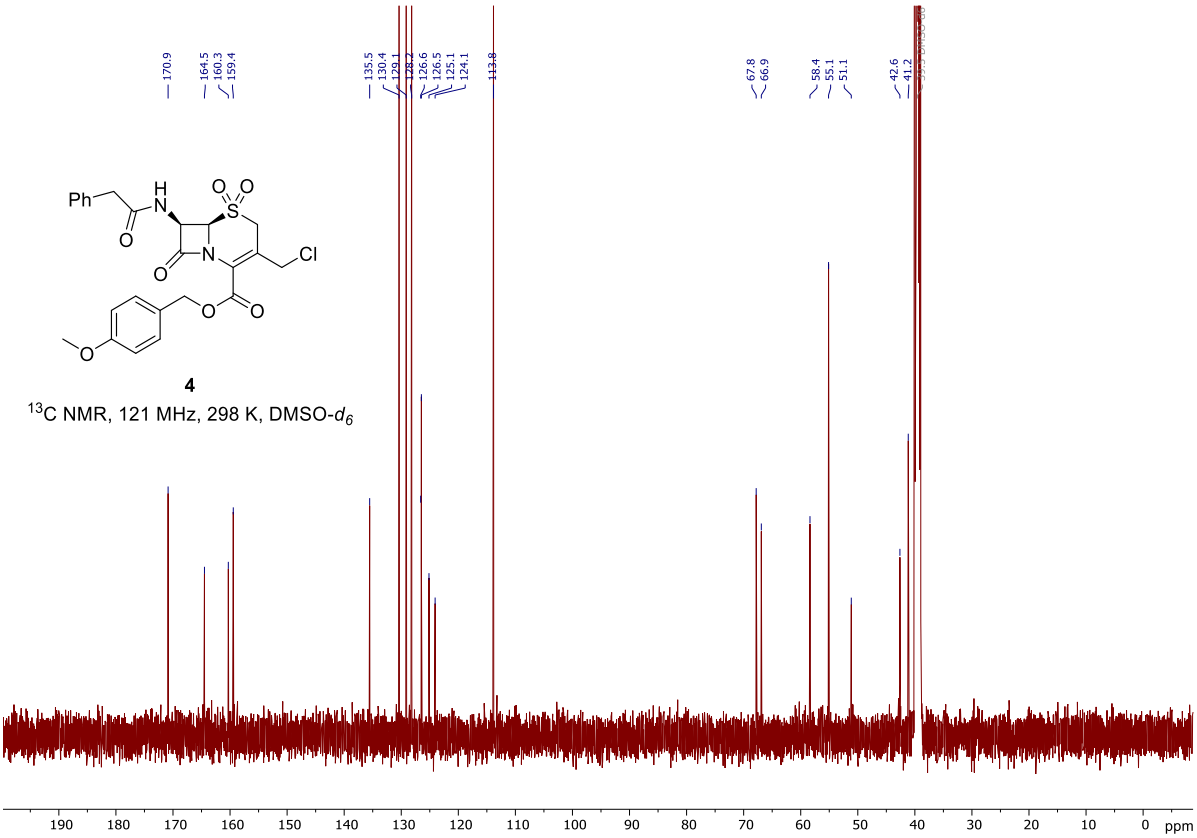

4

^{13}C NMR, 121 MHz, 298 K, DMSO-d_6

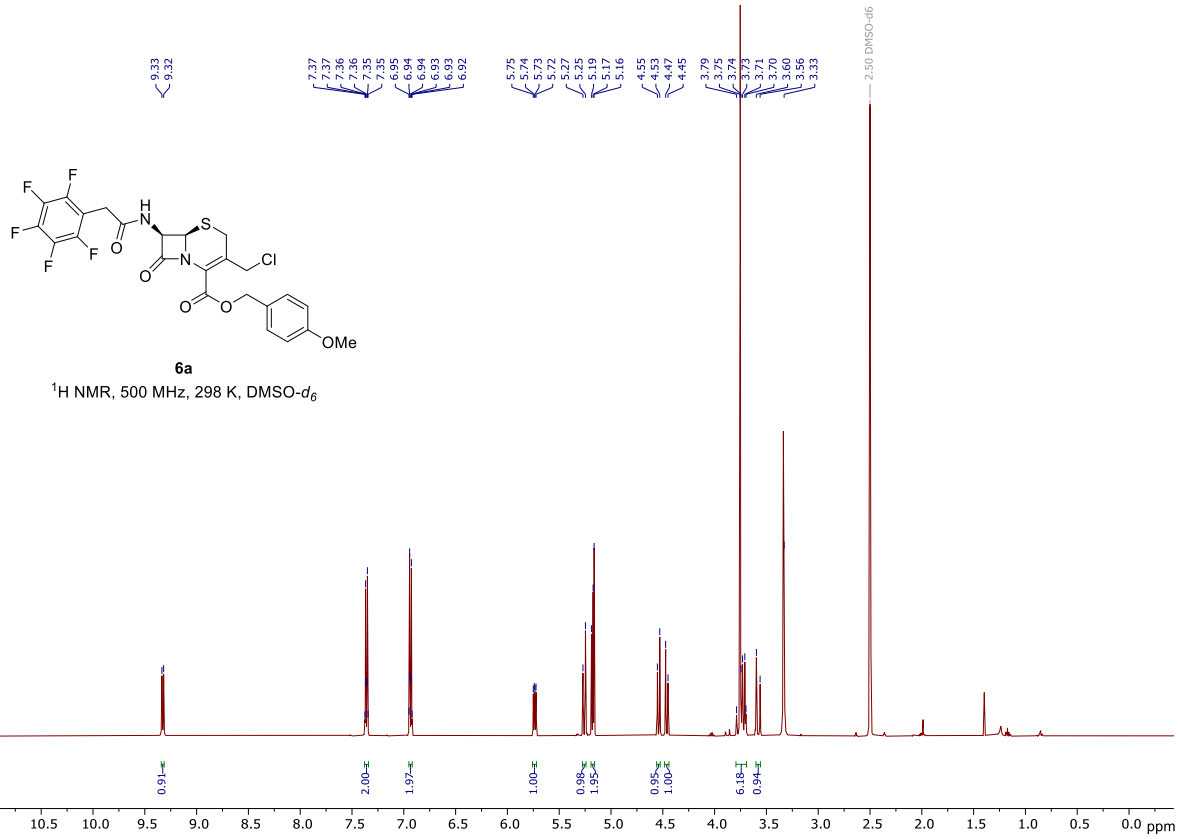

6a

^{1}H NMR, 500 MHz, 298 K, DMSO-d_6

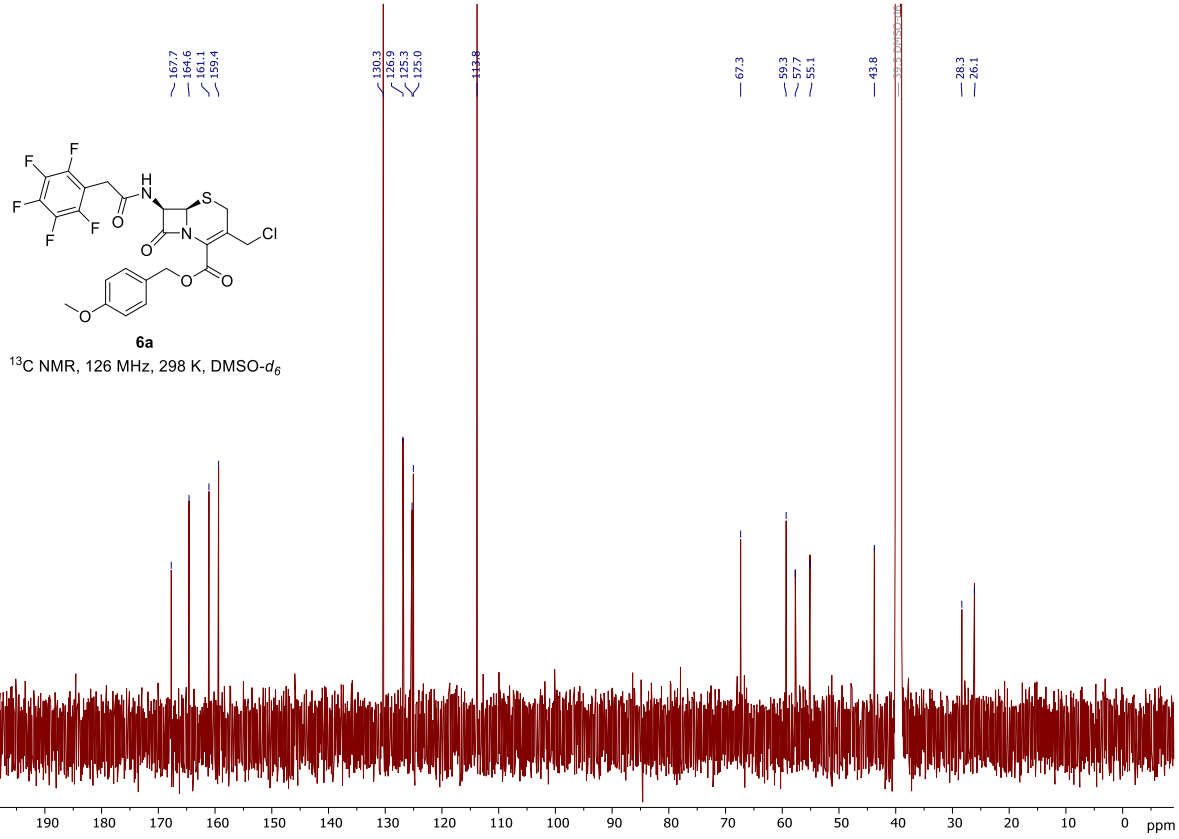

6a

^{13}C NMR, 126 MHz, 298 K, DMSO-d_6

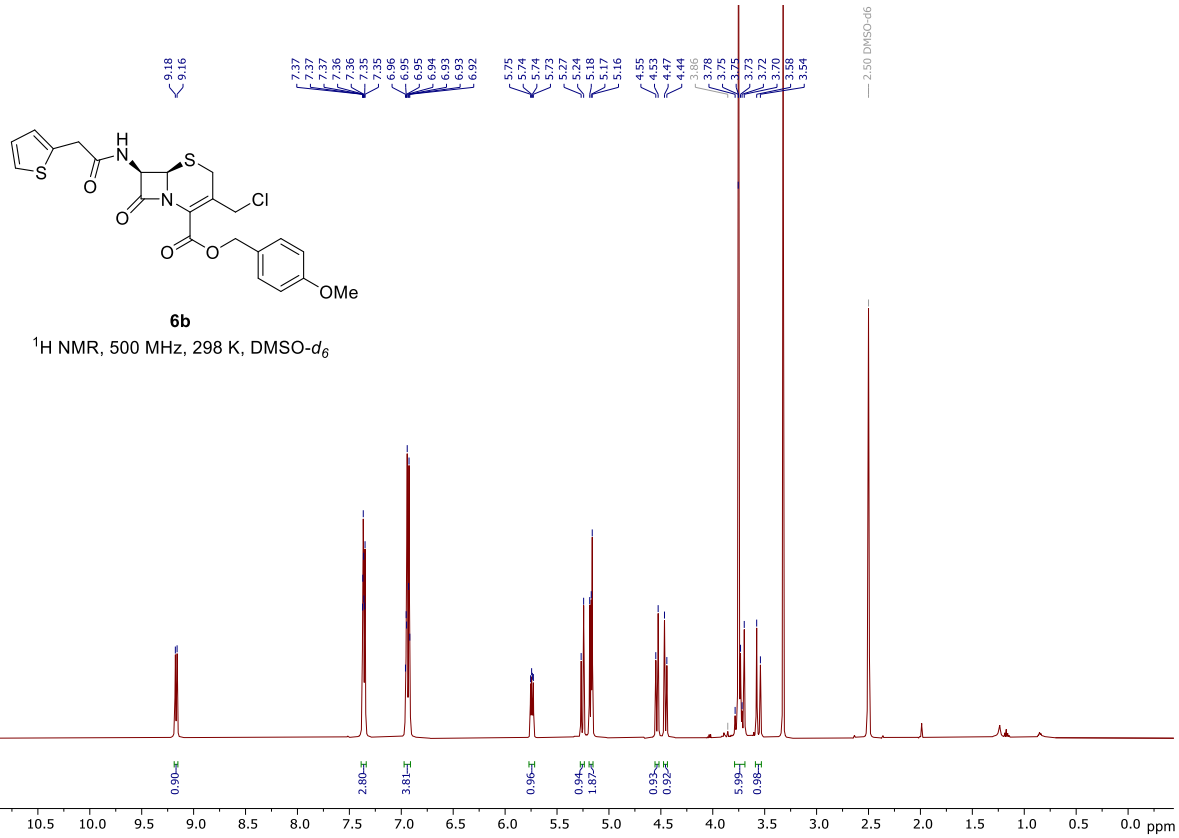

6b

^{1}H NMR, 500 MHz, 298 K, DMSO-d_6

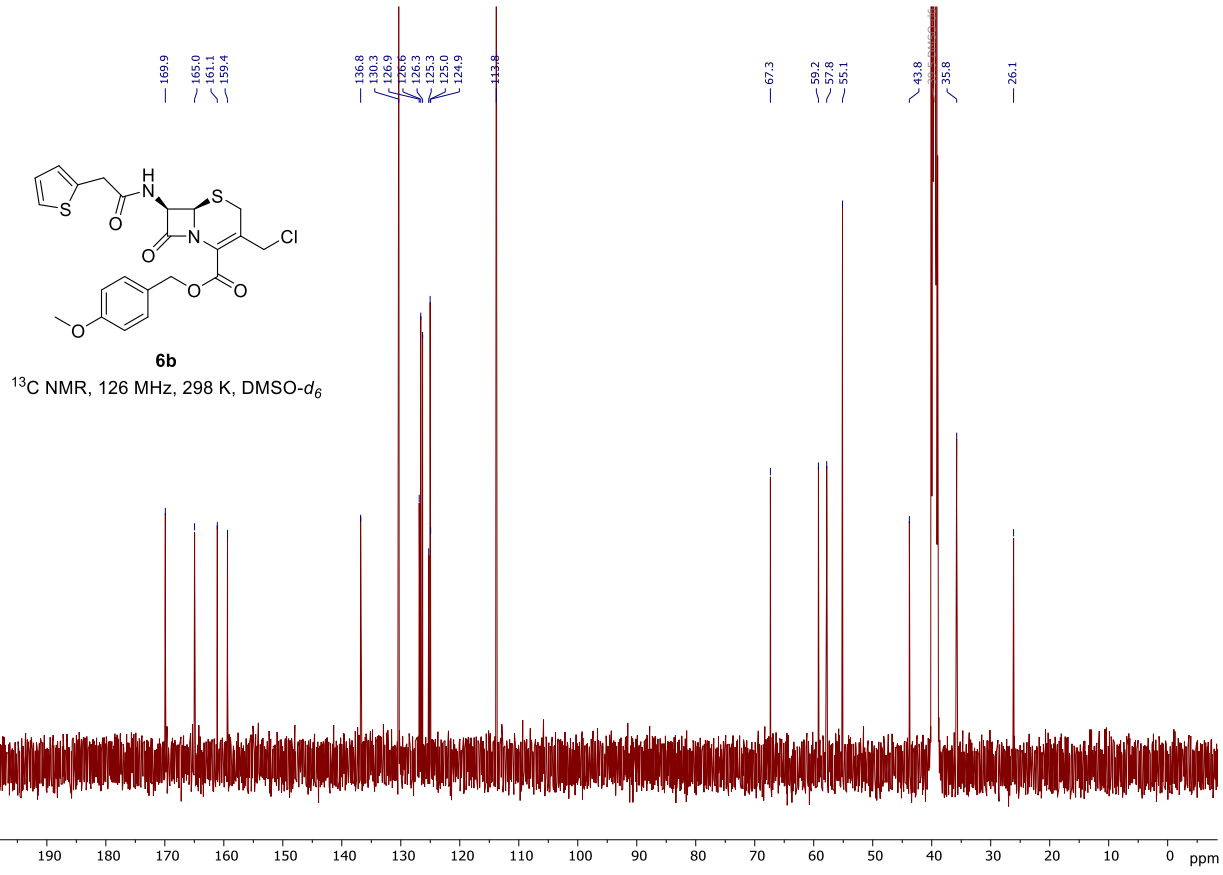

6b

^{13}C NMR, 126 MHz, 298 K, DMSO-d_6

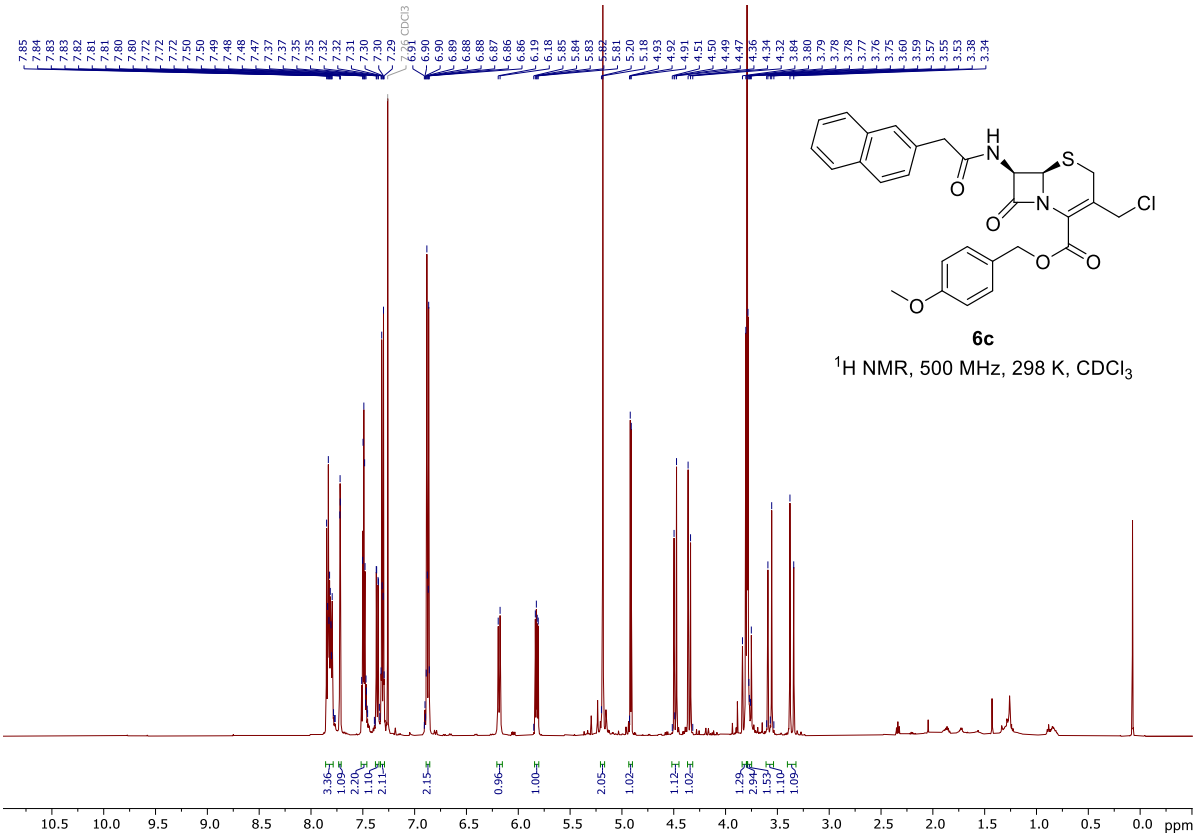

6c

^{1}H NMR, 500 MHz, 298 K, $CDCl_3$

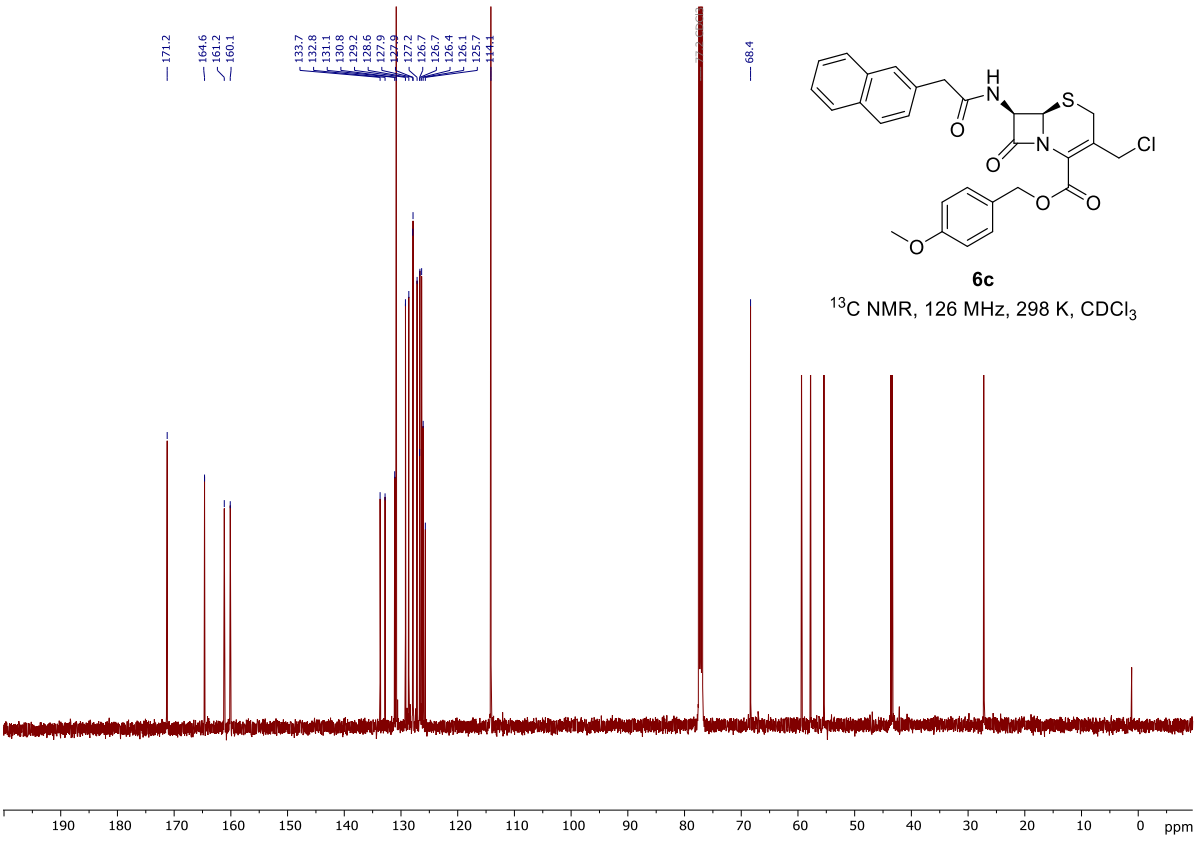

6c

^{13}C NMR, 126 MHz, 298 K, $CDCl_3$

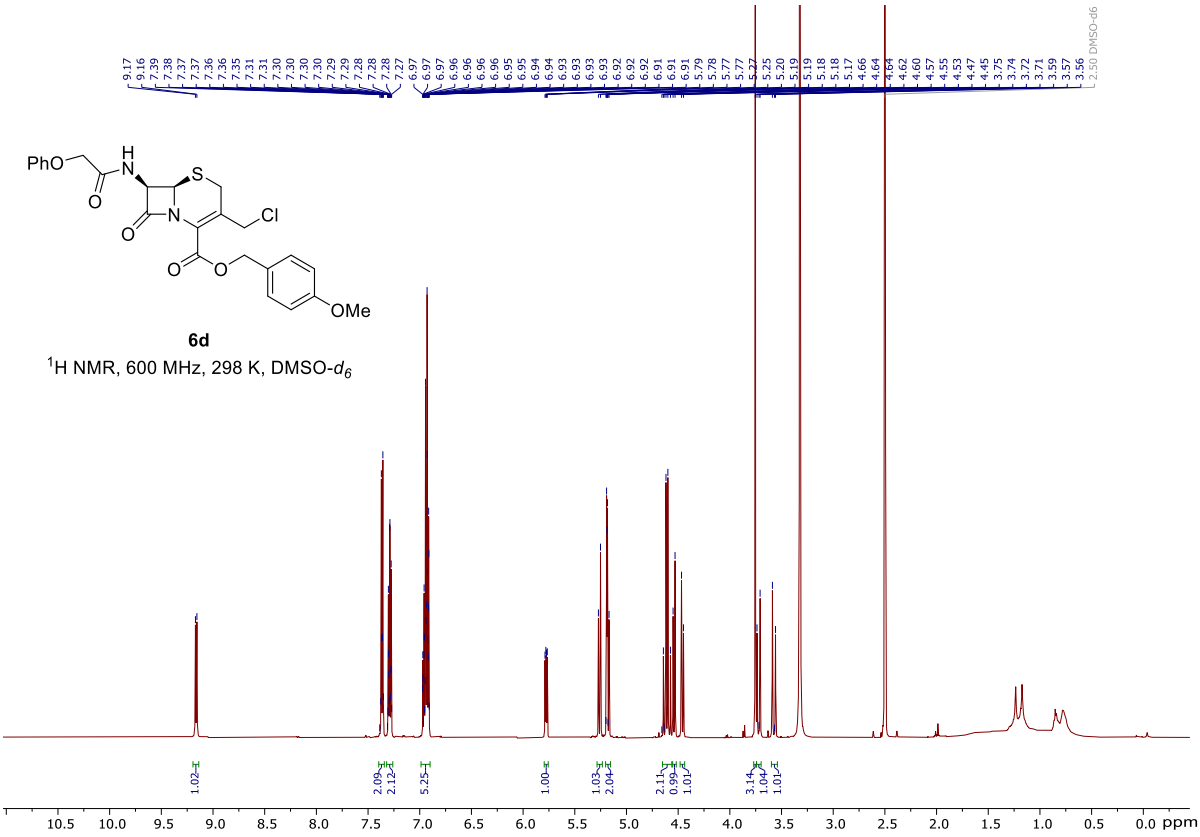

6d

^{1}H NMR, 600 MHz, 298 K, DMSO-d_6

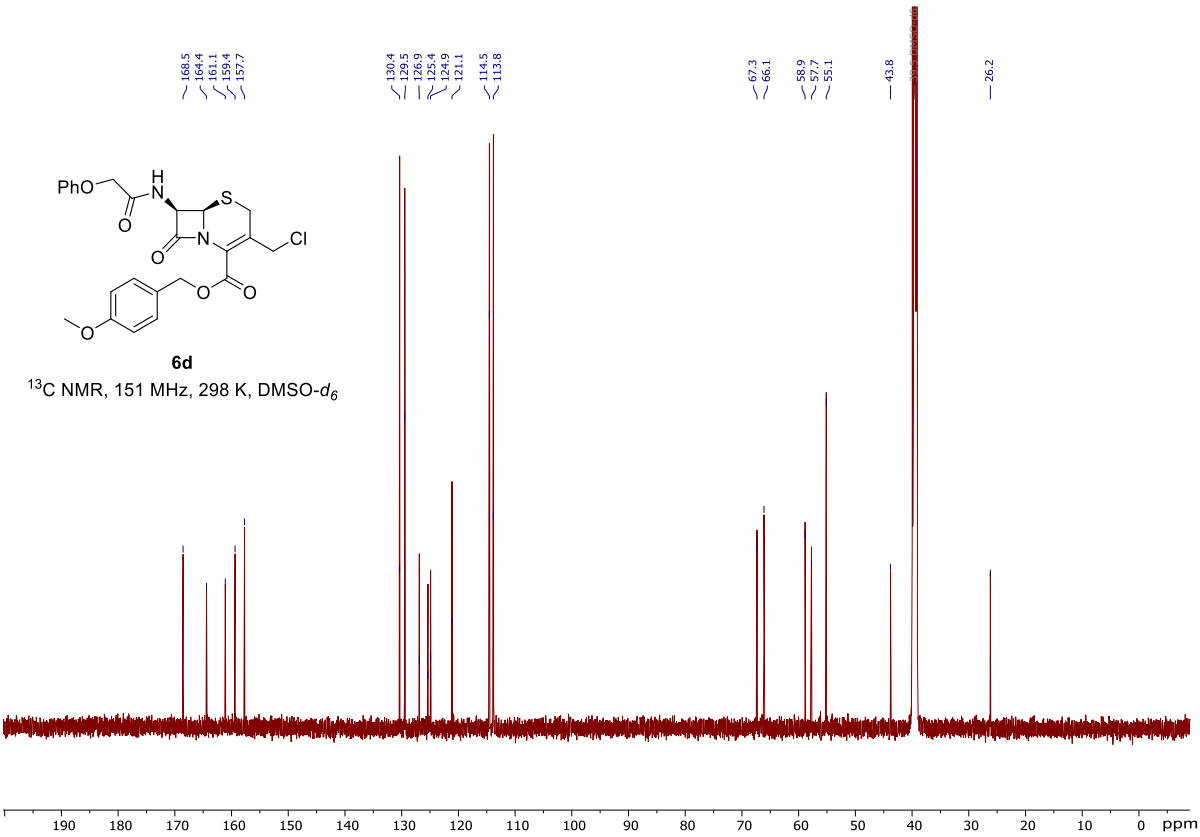

6d

^{13}C NMR, 151 MHz, 298 K, DMSO-d_6

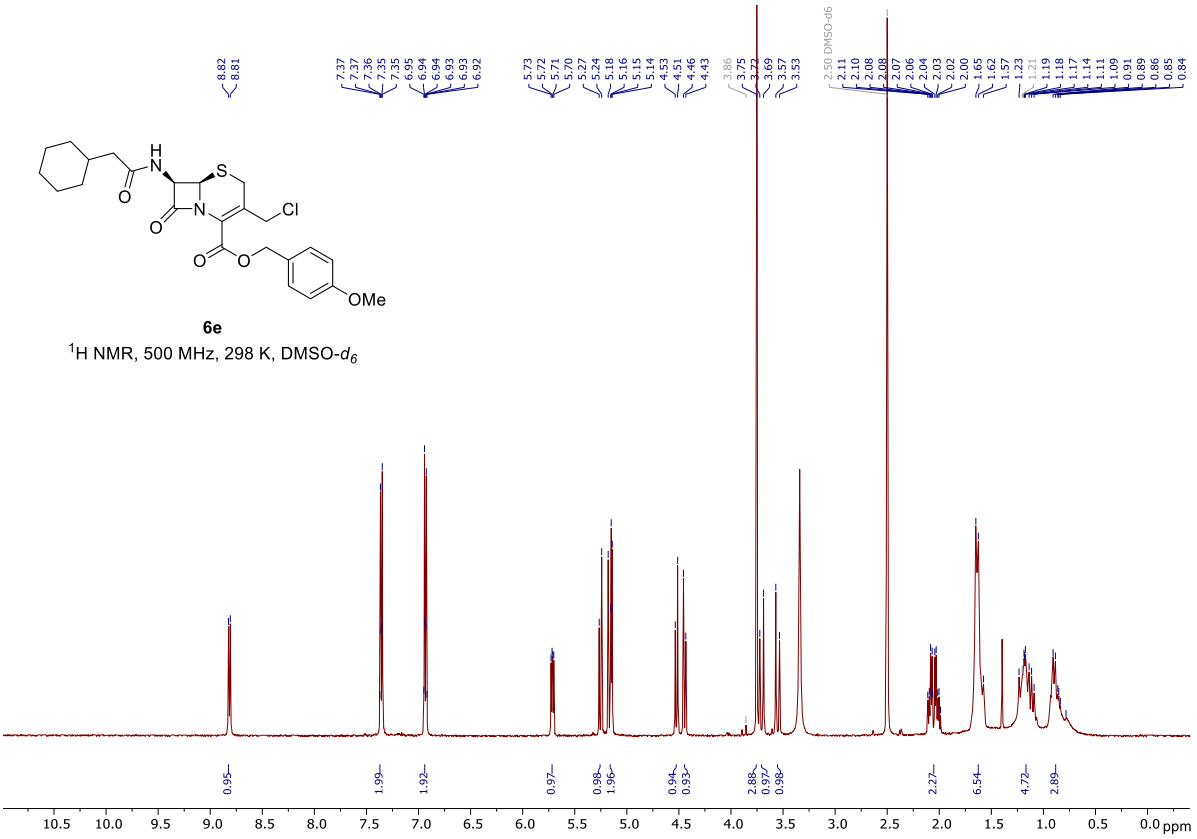

6e

^{1}H NMR, 500 MHz, 298 K, DMSO-d_6

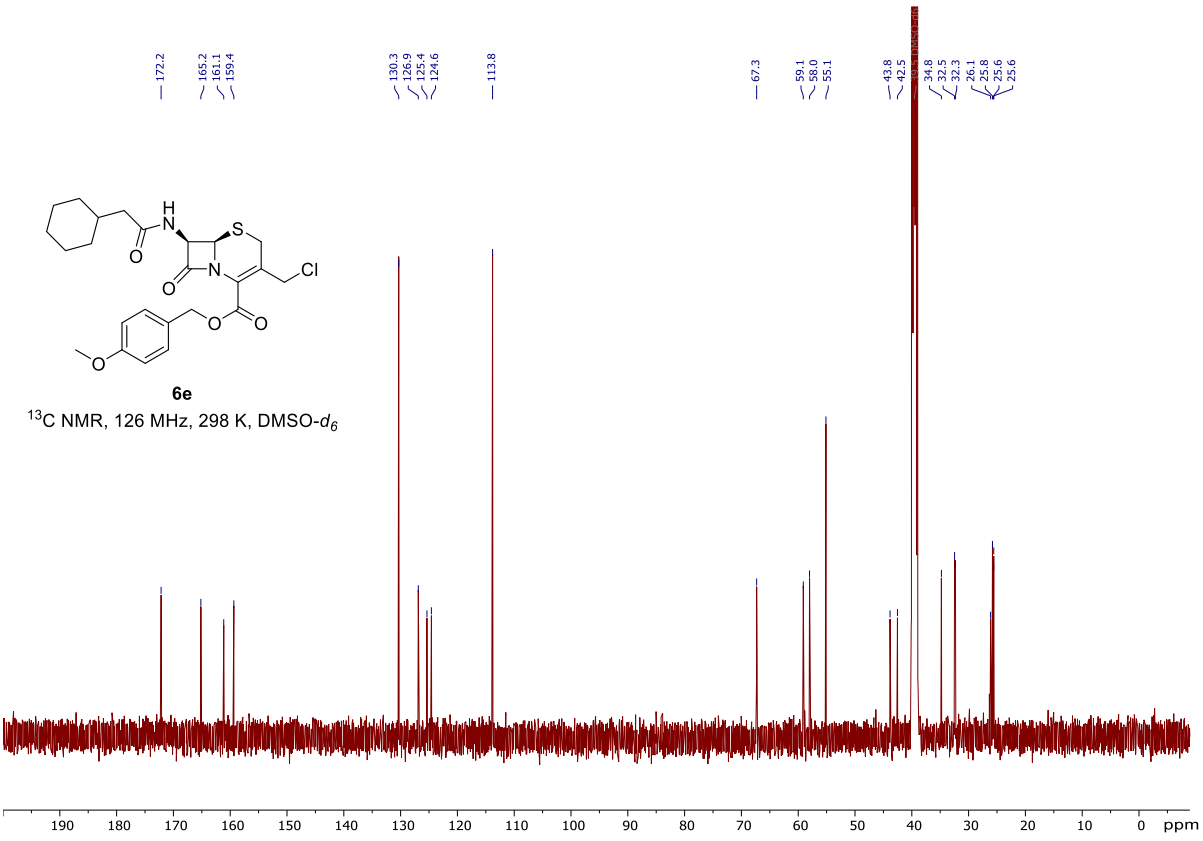

6e

^{13}C NMR, 126 MHz, 298 K, DMSO-d_6

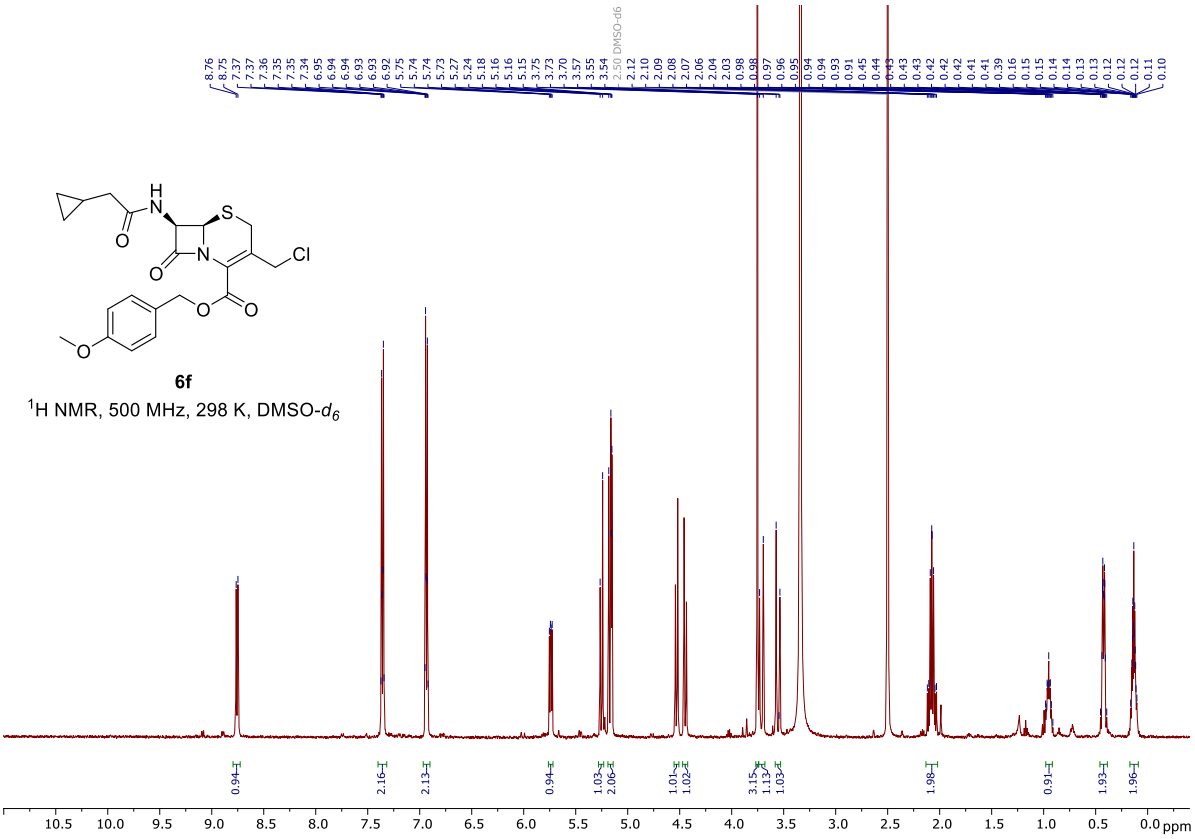

6f

^{1}H NMR, 500 MHz, 298 K, DMSO-d_6

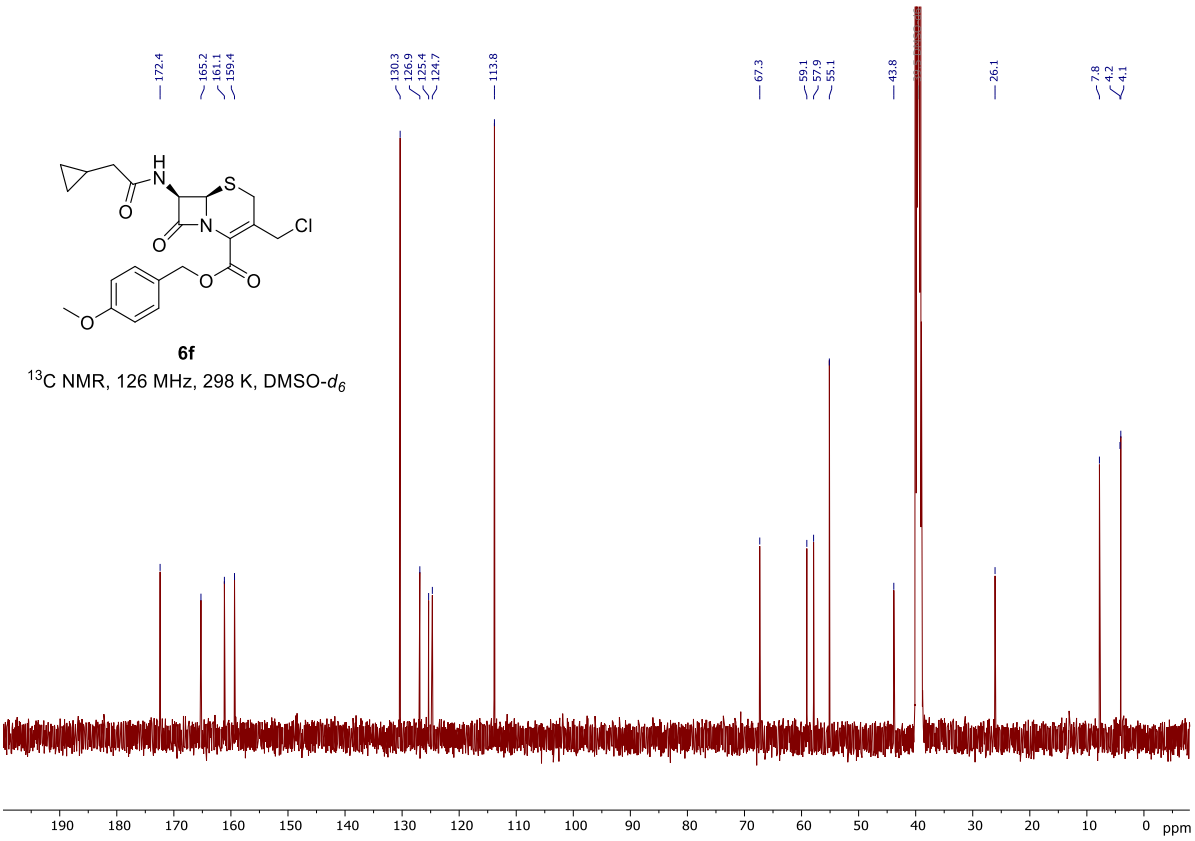

6f

^{13}C NMR, 126 MHz, 298 K, DMSO-d_6

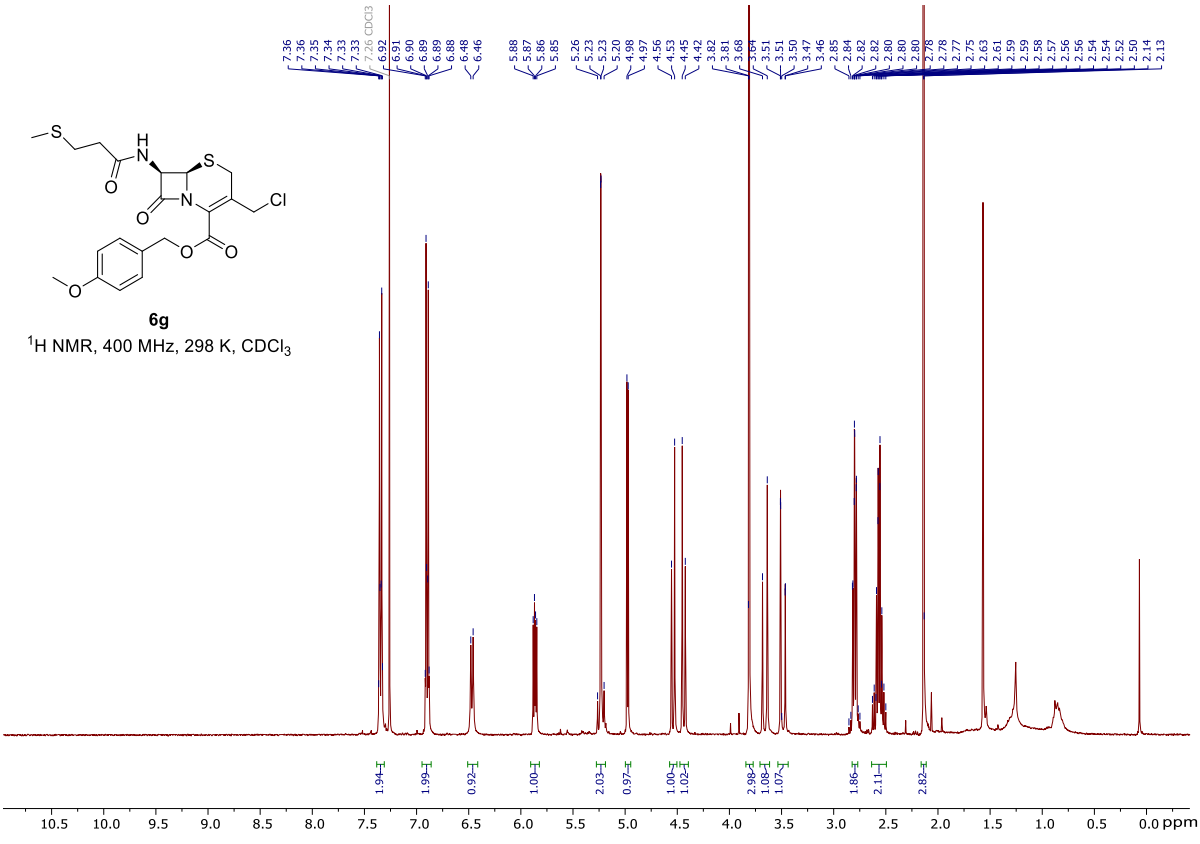

6g

^{1}H NMR, 400 MHz, 298 K, $CDCl_3$

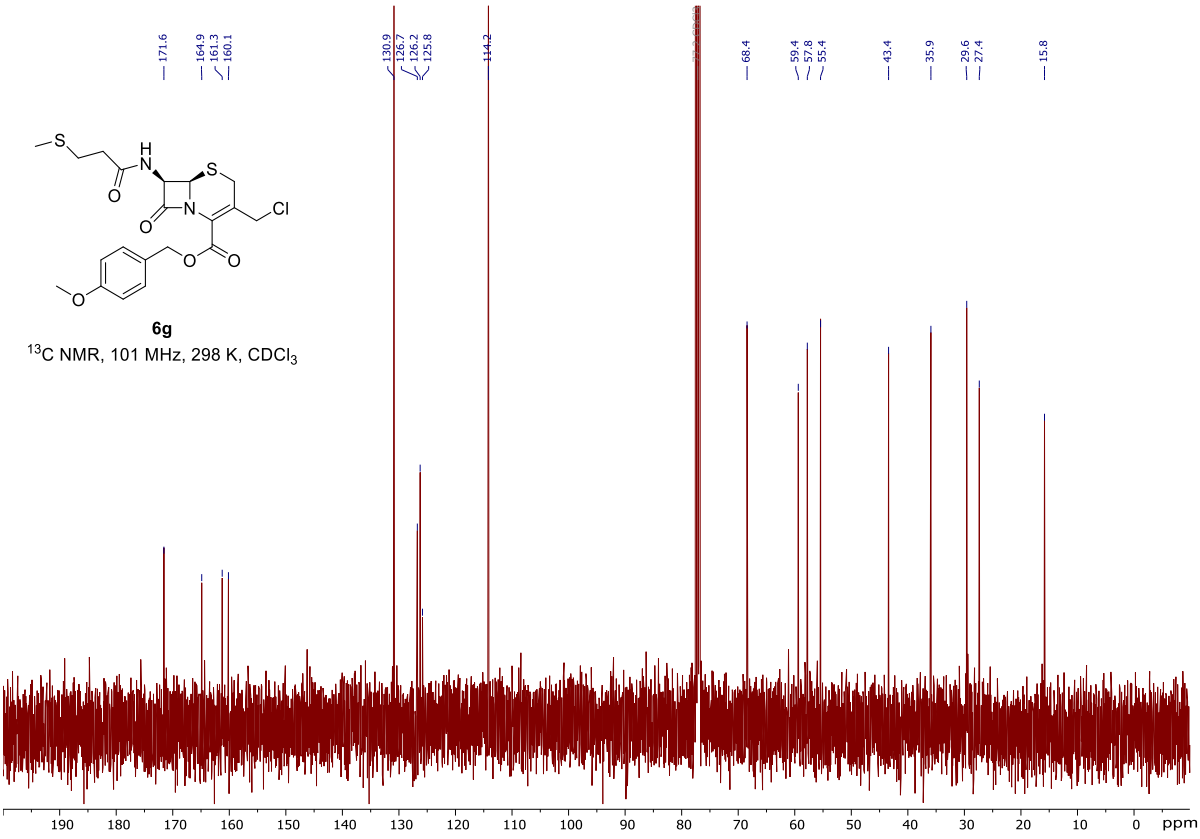

6g

^{13}C NMR, 101 MHz, 298 K, $CDCl_3$

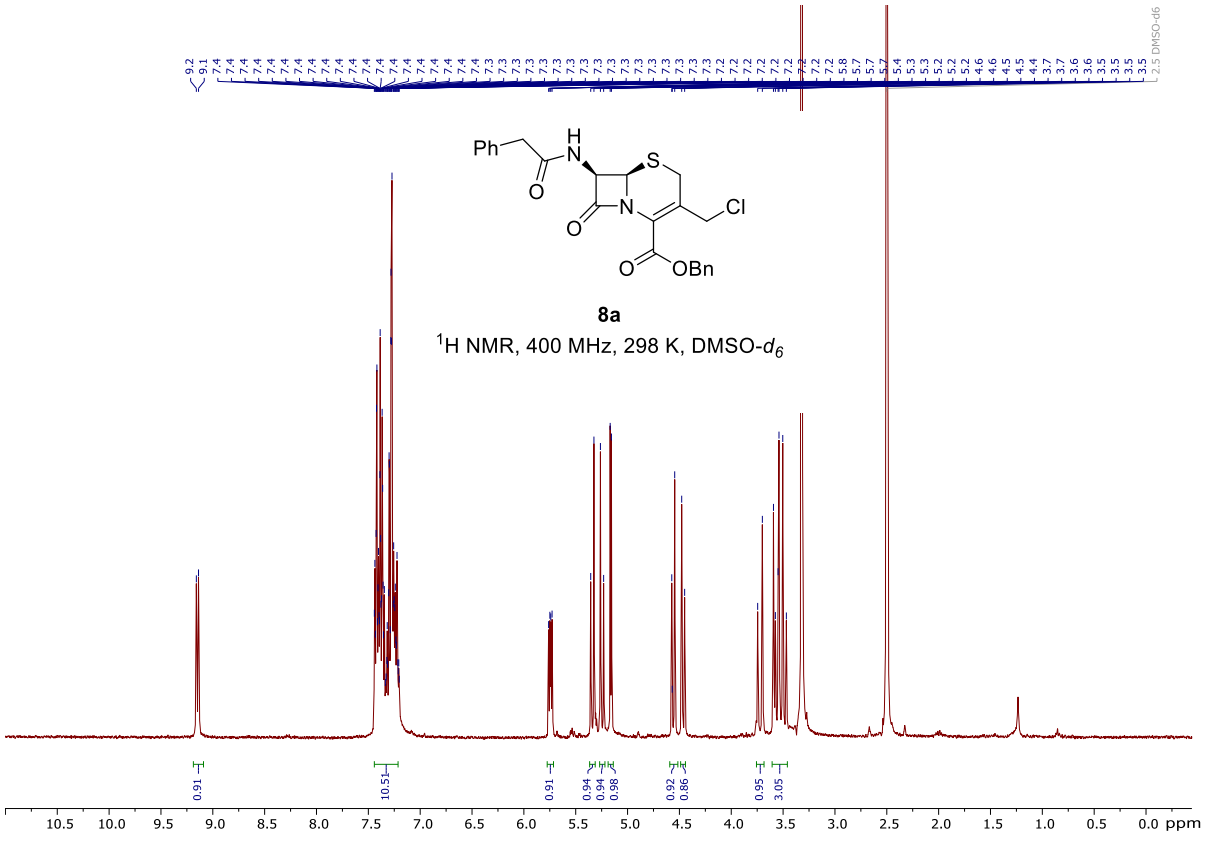

8a

^{1}H NMR, 400 MHz, 298 K, DMSO-d_6

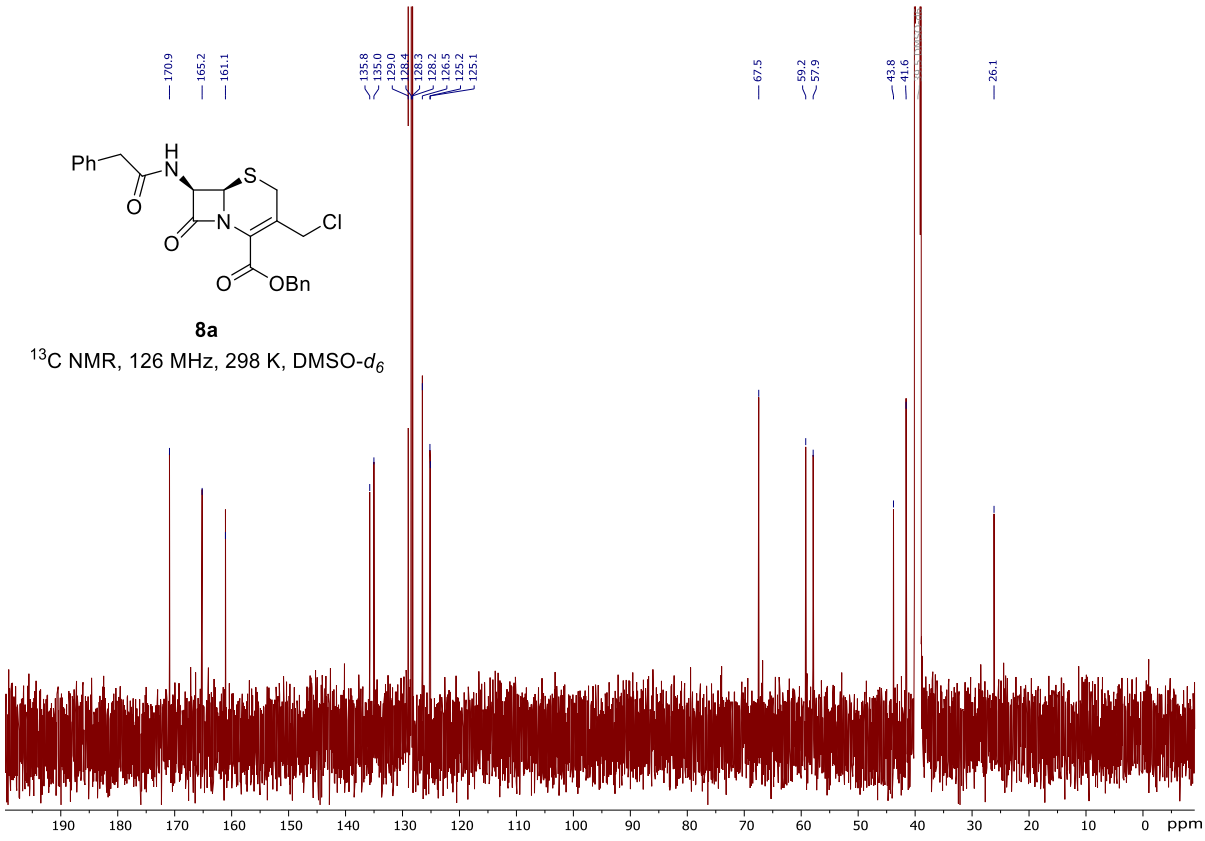

8a

^{13}C NMR, 126 MHz, 298 K, DMSO-d_6

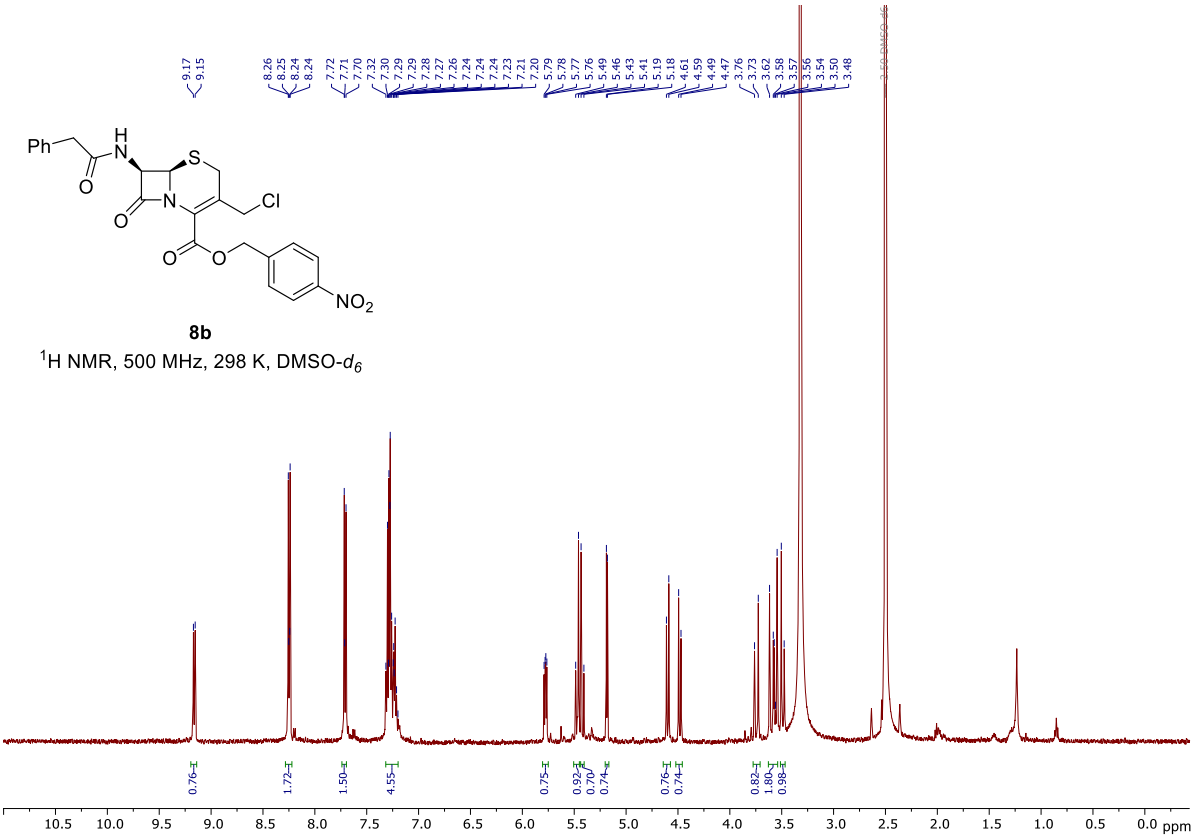

8b

^{1}H NMR, 500 MHz, 298 K, DMSO-d_6

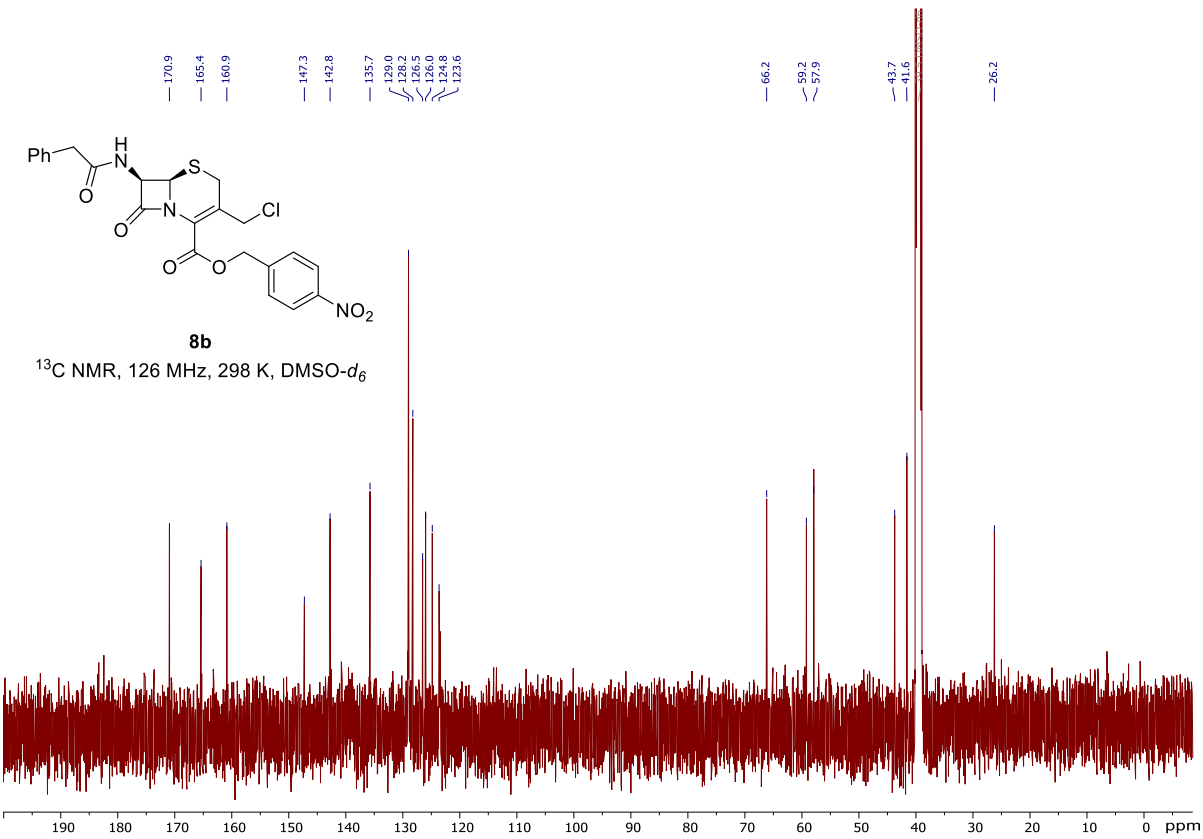

8b

^{13}C NMR, 126 MHz, 298 K, DMSO-d_6

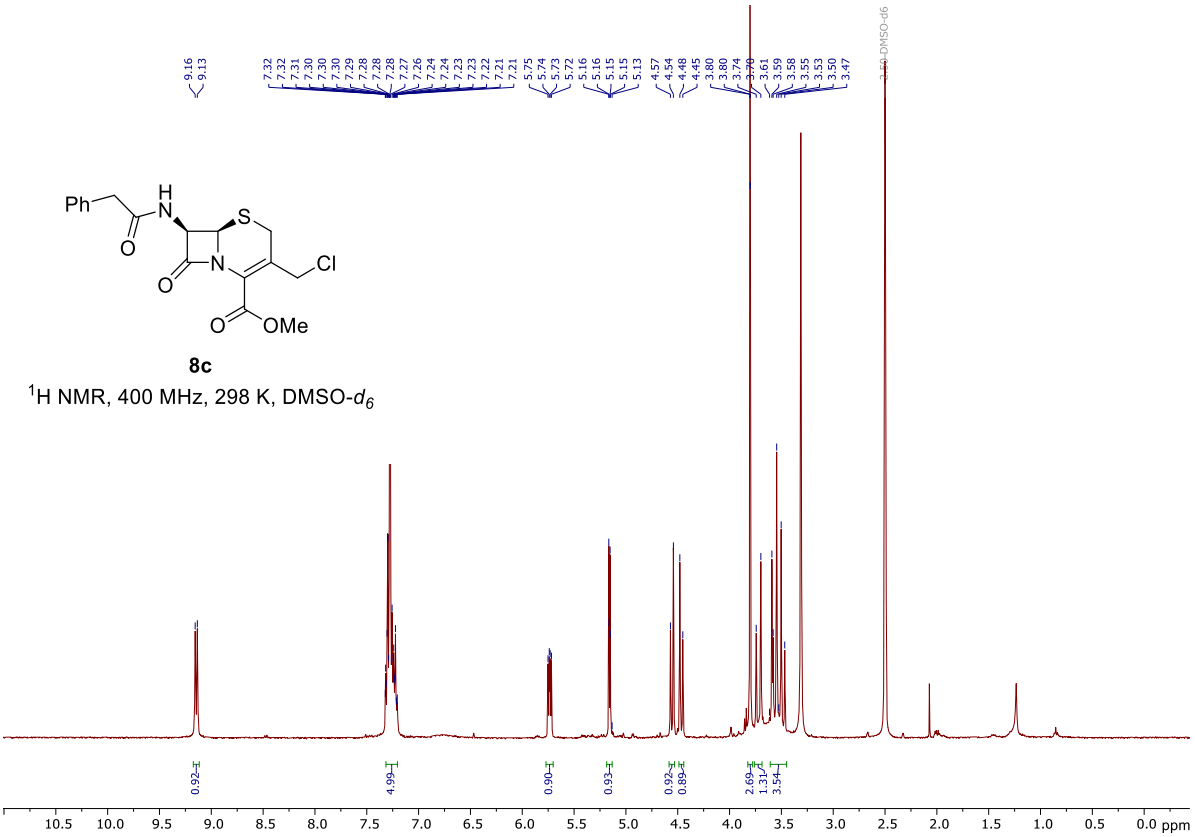

8c

^{1}H NMR, 400 MHz, 298 K, DMSO-d_6

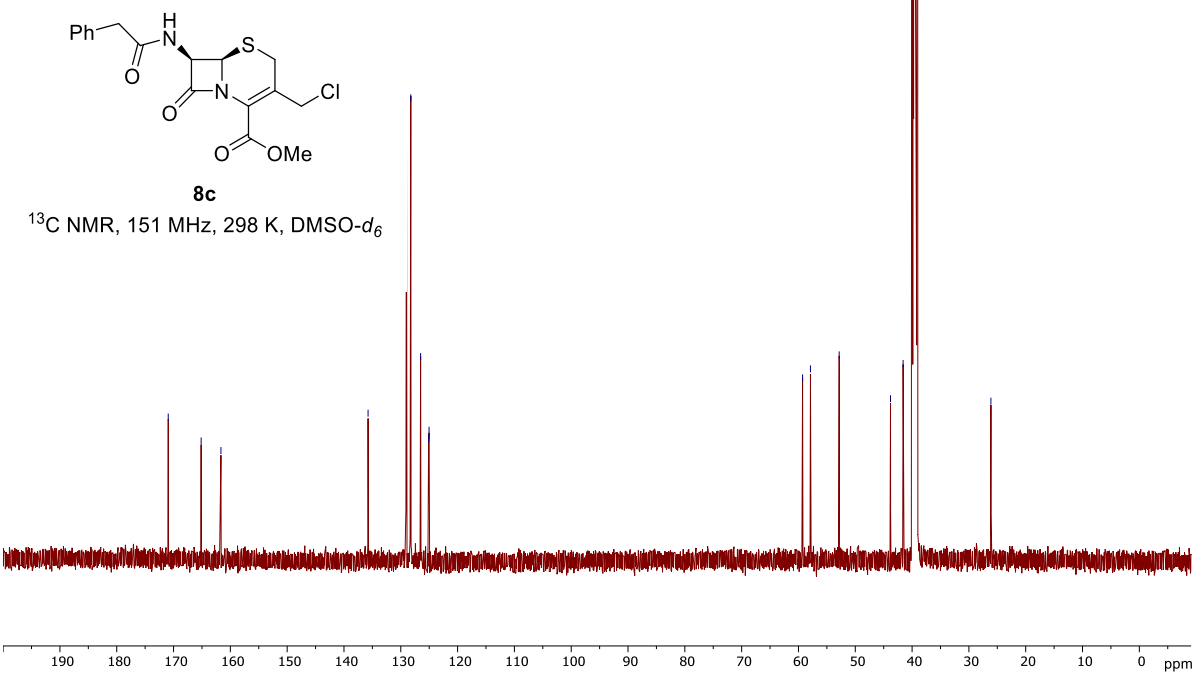

8c

^{13}C NMR, 151 MHz, 298 K, DMSO-d_6

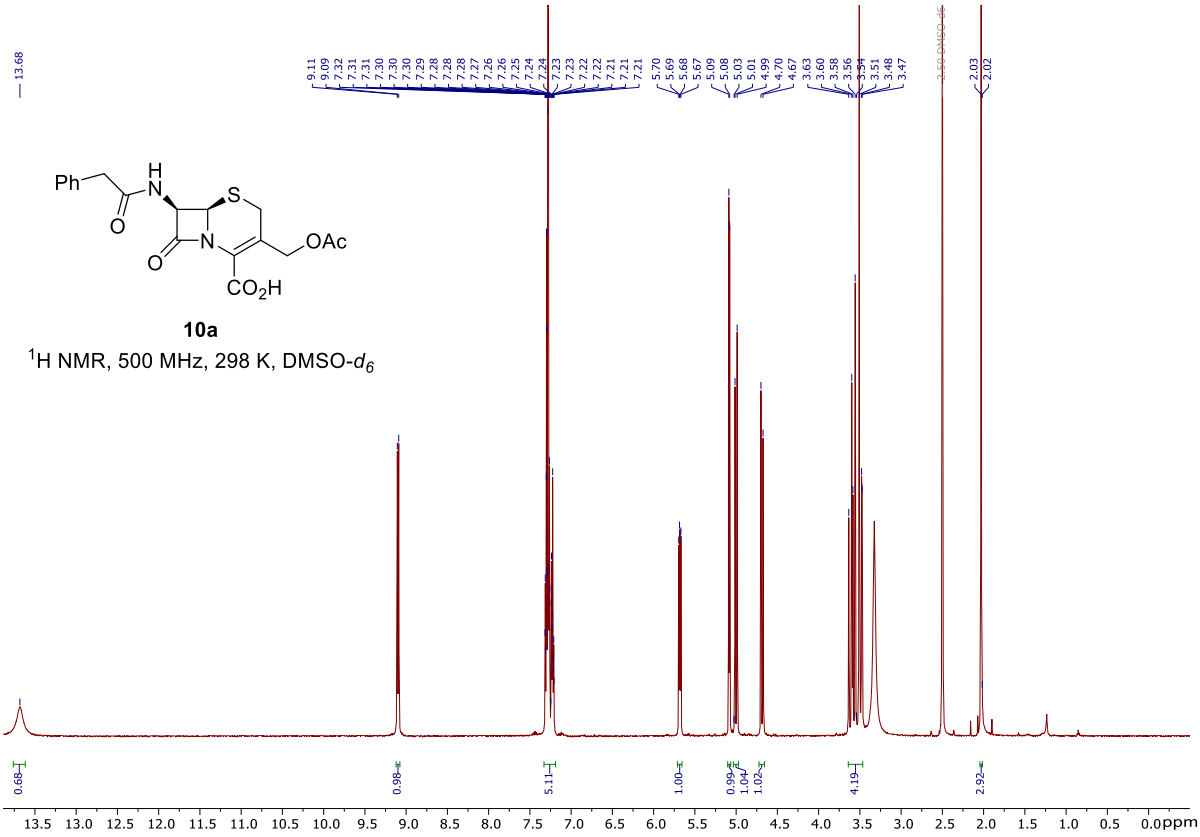

10a

^{1}H NMR, 500 MHz, 298 K, DMSO-d_6

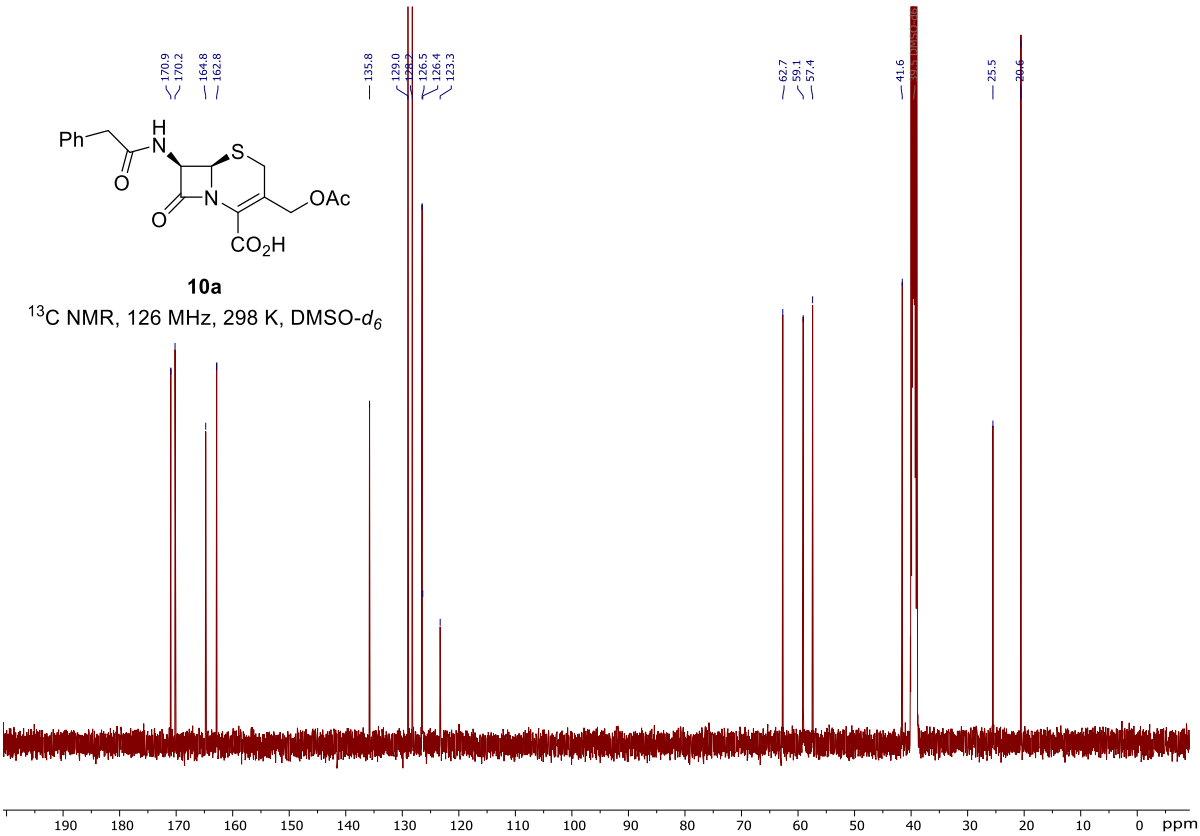

10a

^{13}C NMR, 126 MHz, 298 K, DMSO-d_6

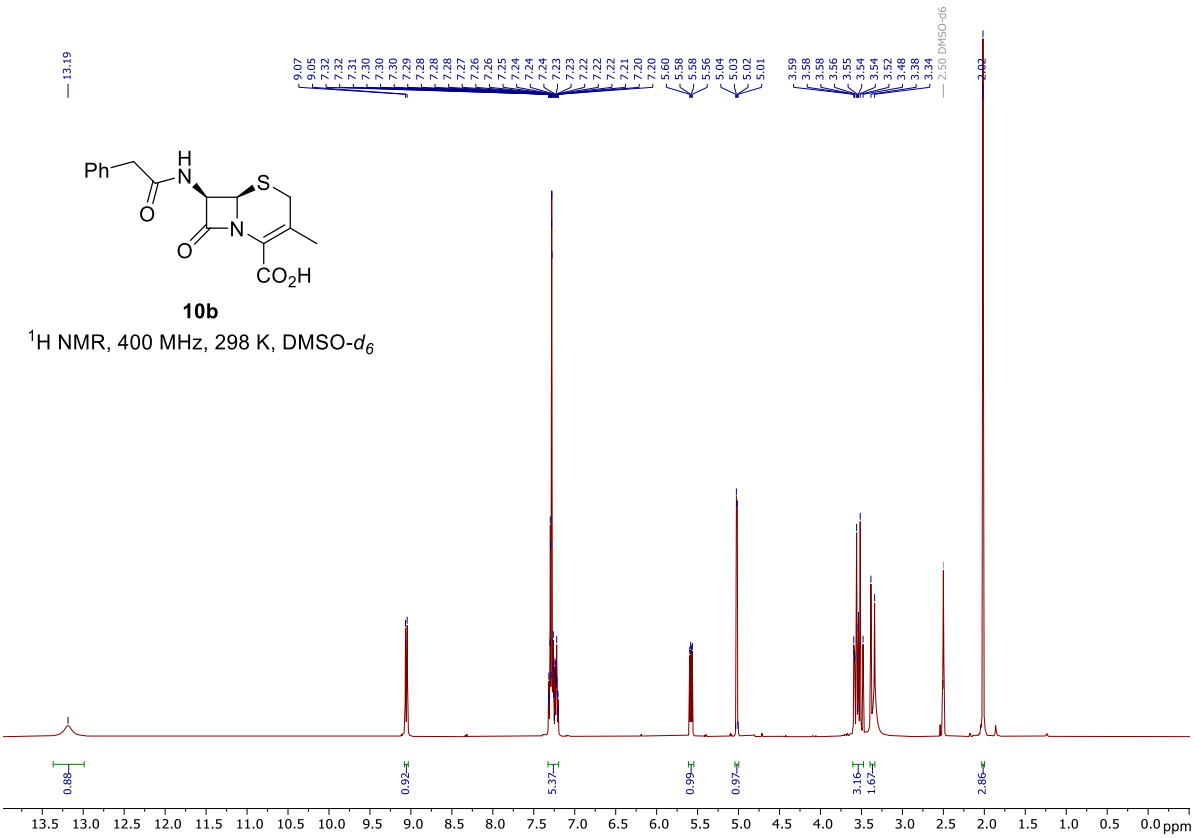

10b

^{1}H NMR, 400 MHz, 298 K, DMSO-d_6

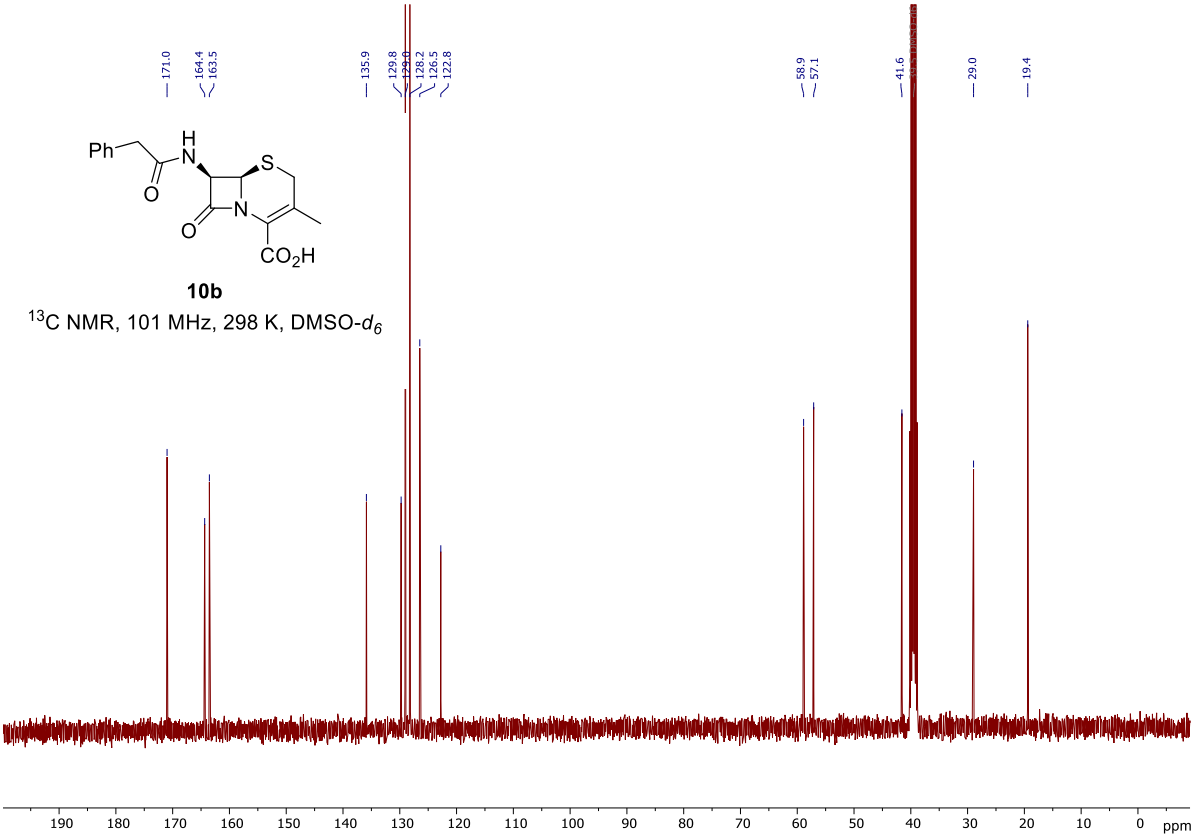

10b

^{13}C NMR, 101 MHz, 298 K, DMSO-d_6

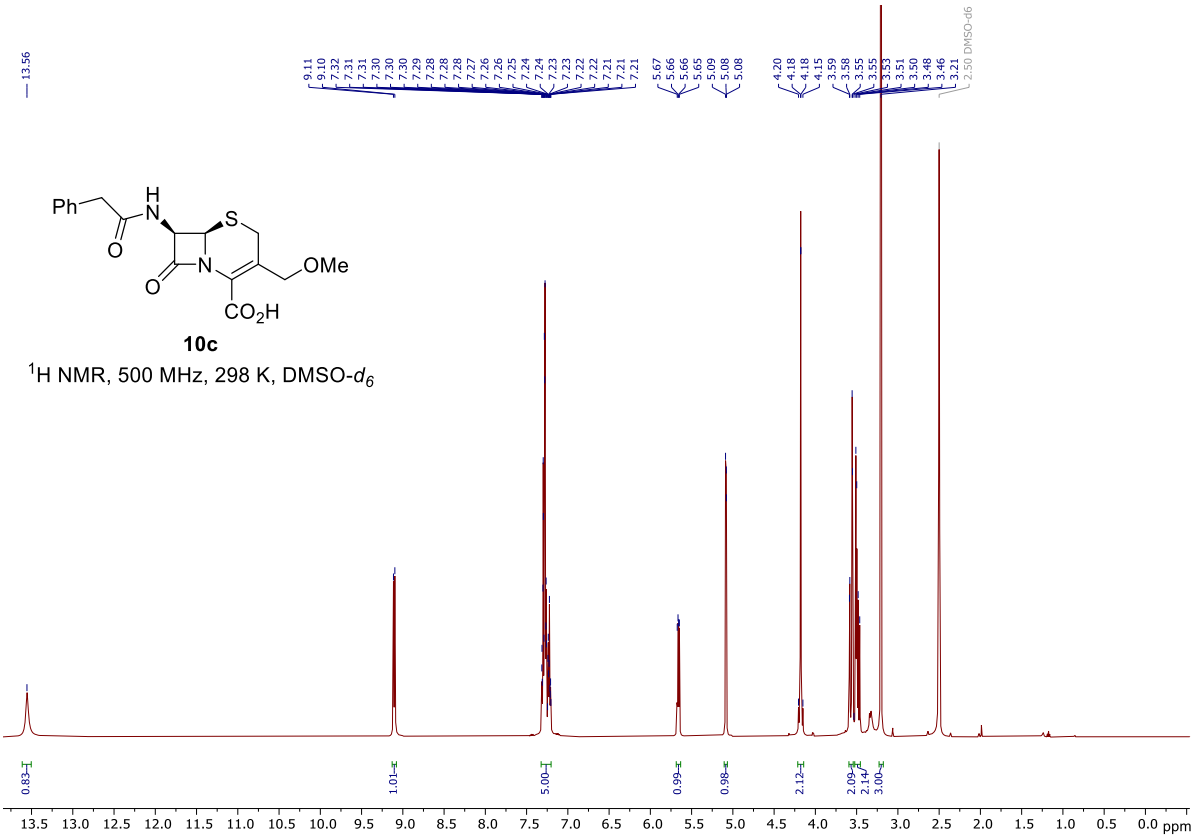

10c

^{1}H NMR, 500 MHz, 298 K, DMSO-d_6

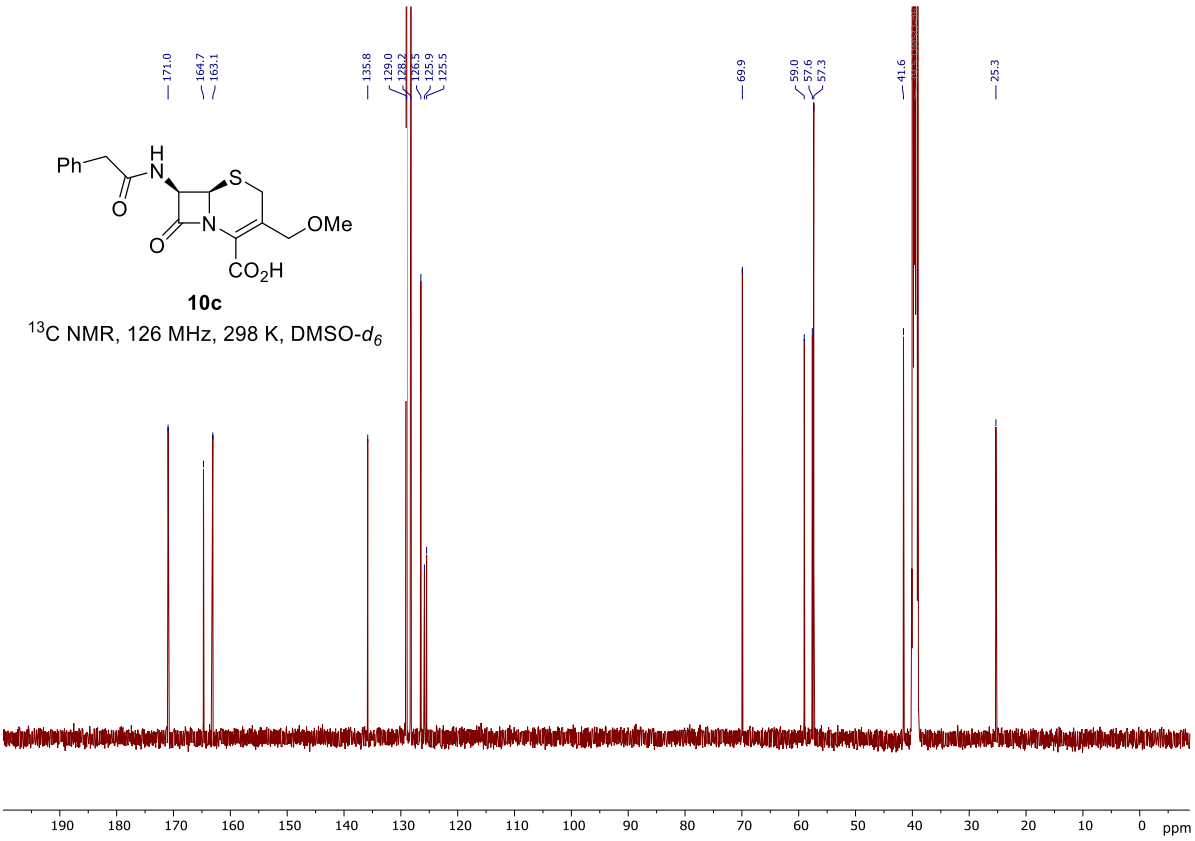

10c

^{13}C NMR, 126 MHz, 298 K, DMSO-d_6

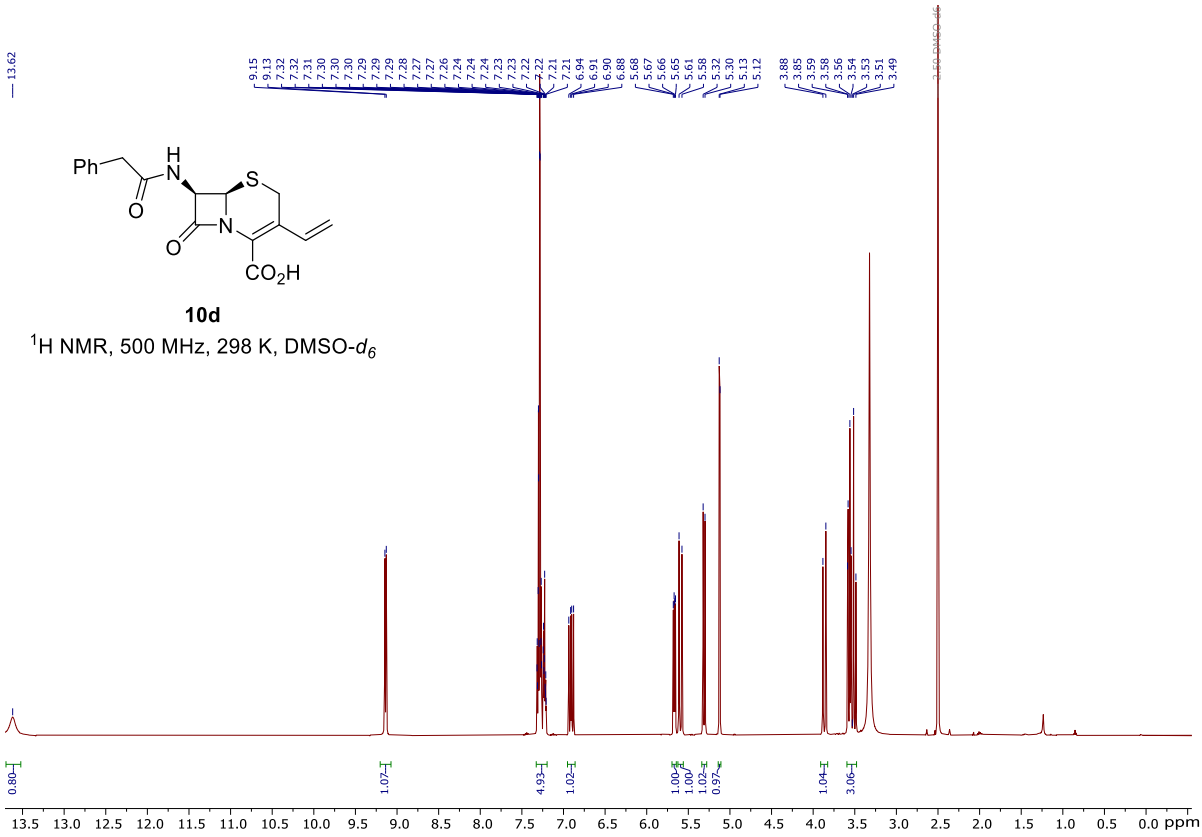

10d

^{1}H NMR, 500 MHz, 298 K, DMSO-d_6

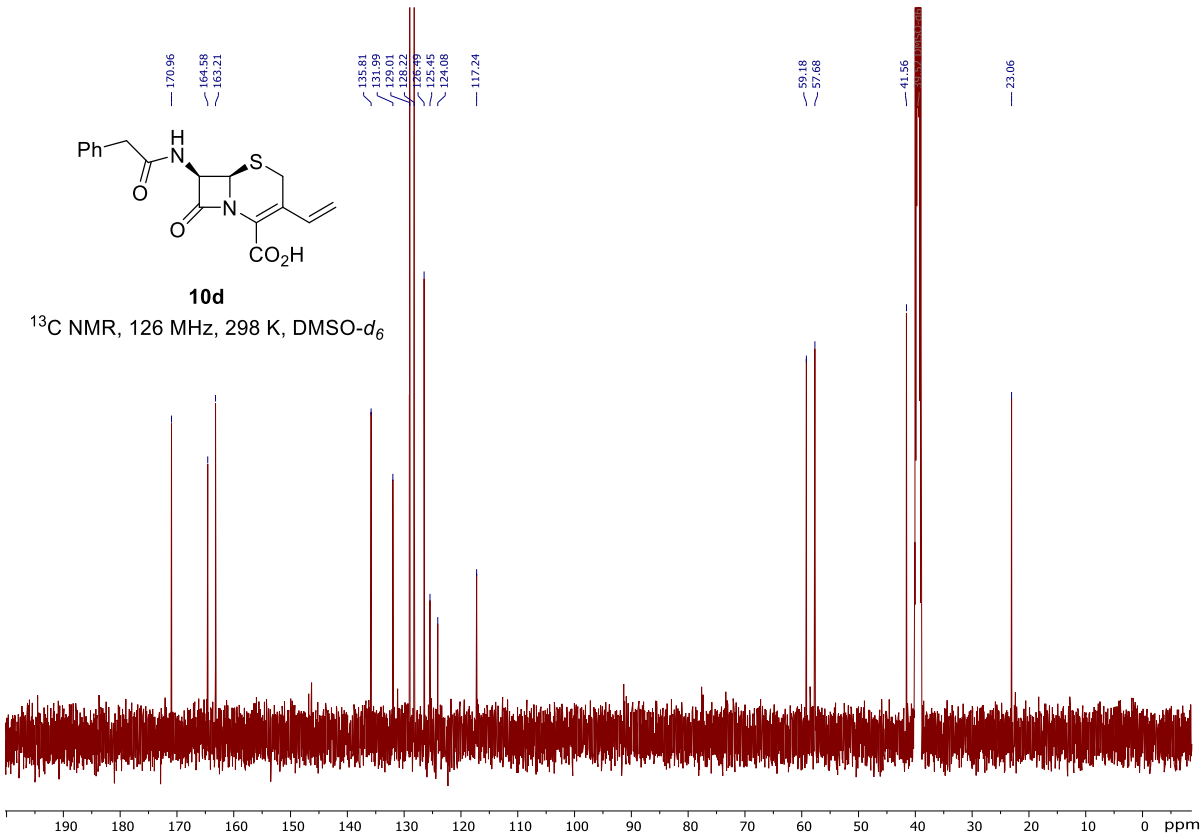

10d

^{13}C NMR, 126 MHz, 298 K, DMSO-d_6

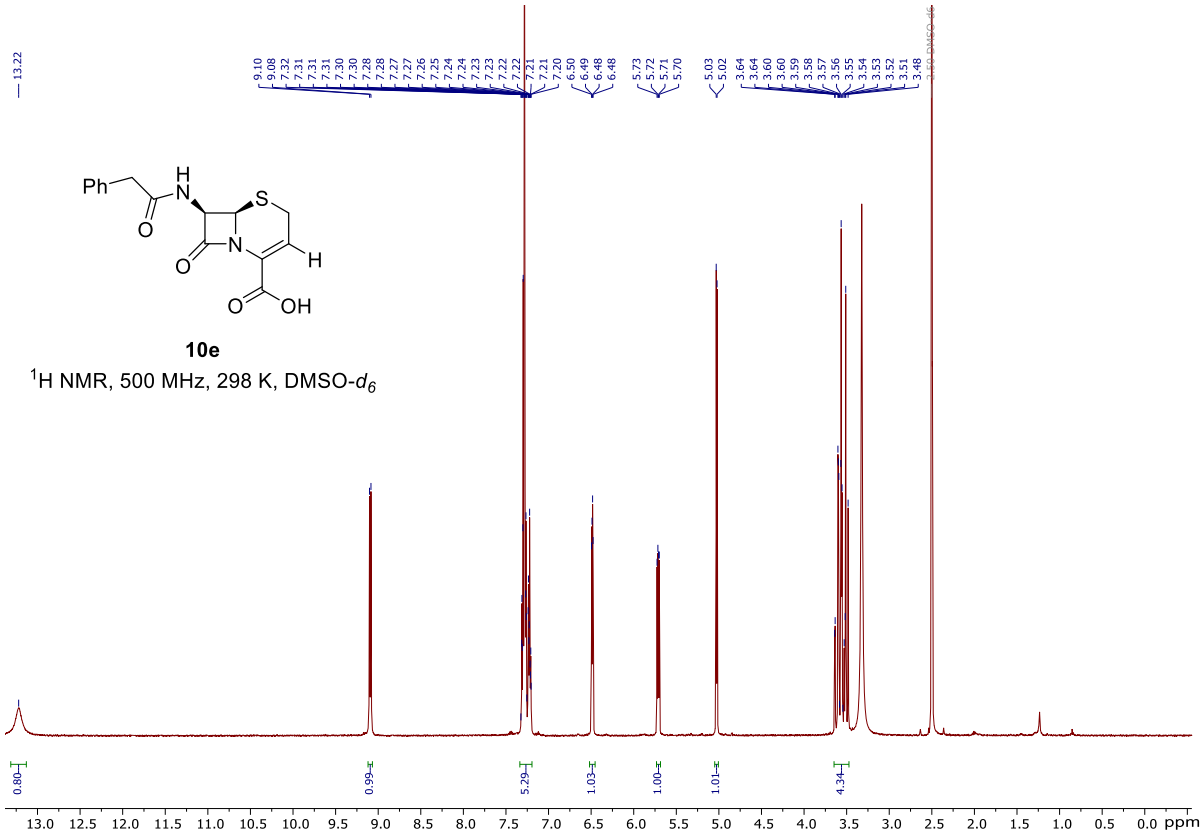

10e

^{1}H NMR, 500 MHz, 298 K, DMSO-d_6

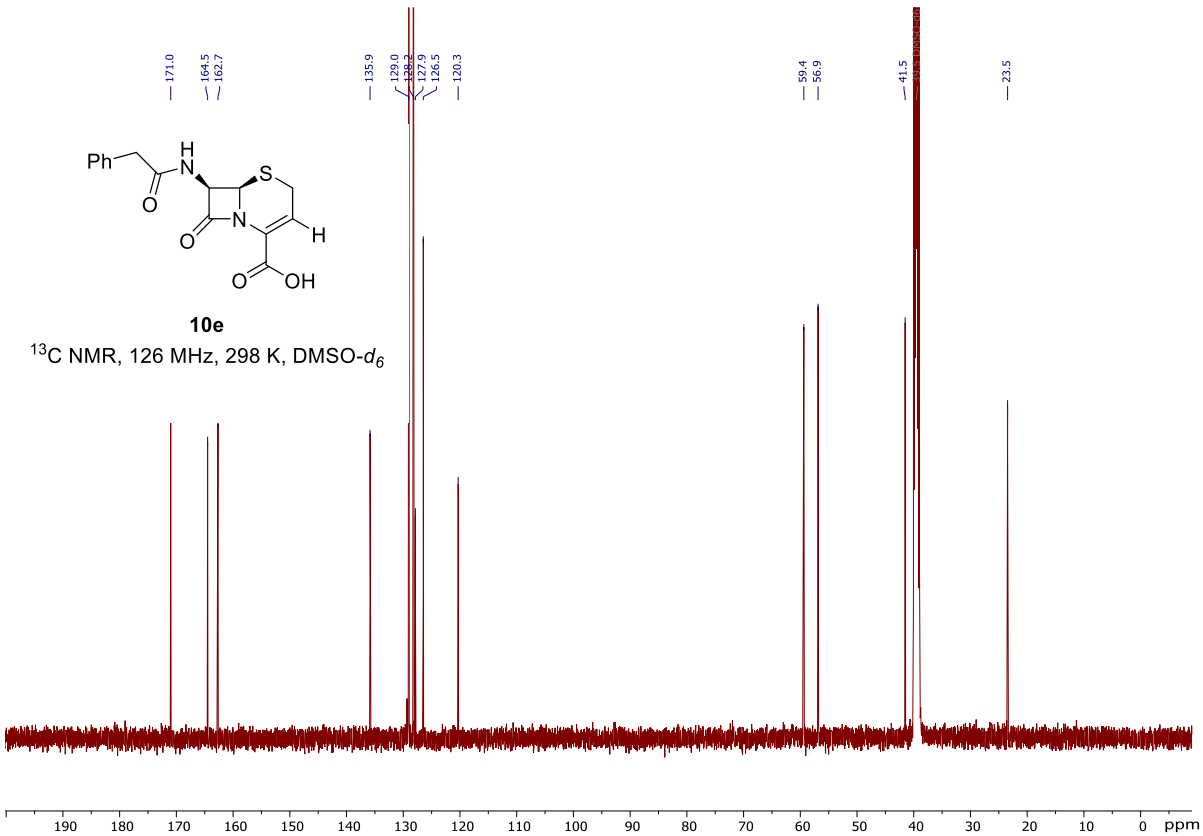

10e

^{13}C NMR, 126 MHz, 298 K, DMSO-d_6

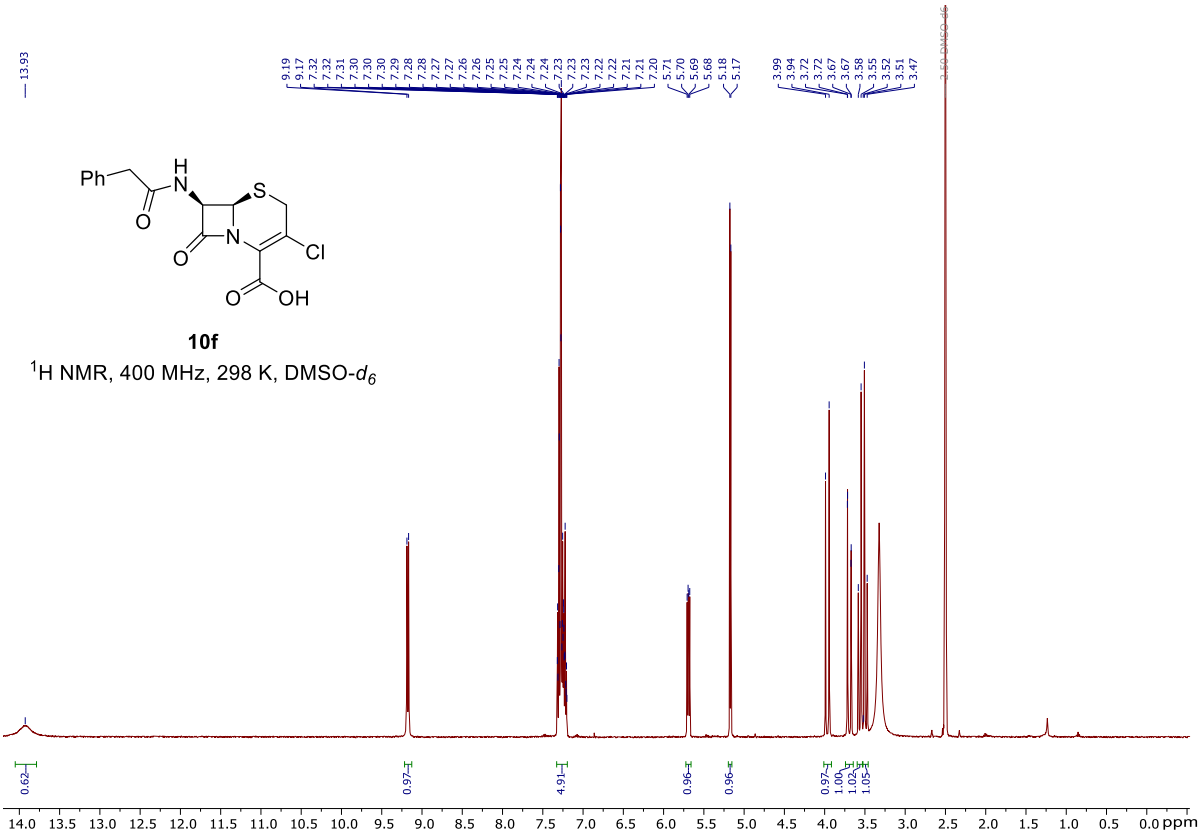
13.93
9.19
9.17
7.32
7.31
7.30
7.29
7.28
7.27
7.26
7.25
7.24
7.23
7.22
7.21
7.20
5.71
5.70
5.69
5.68
5.18
5.17
3.99
3.94
3.72
3.67
3.58
3.55
3.52
3.51
3.47
2.50 DMSO-d6
0.62
0.97
4.91
0.96
0.96
0.97
1.00
1.02
1.05
14.0 13.5 13.0 12.5 12.0 11.5 11.0 10.5 10.0 9.5 9.0 8.5 8.0 7.5 7.0 6.5 6.0 5.5 5.0 4.5 4.0 3.5 3.0 2.5 2.0 1.5 1.0 0.5 0.0 ppm

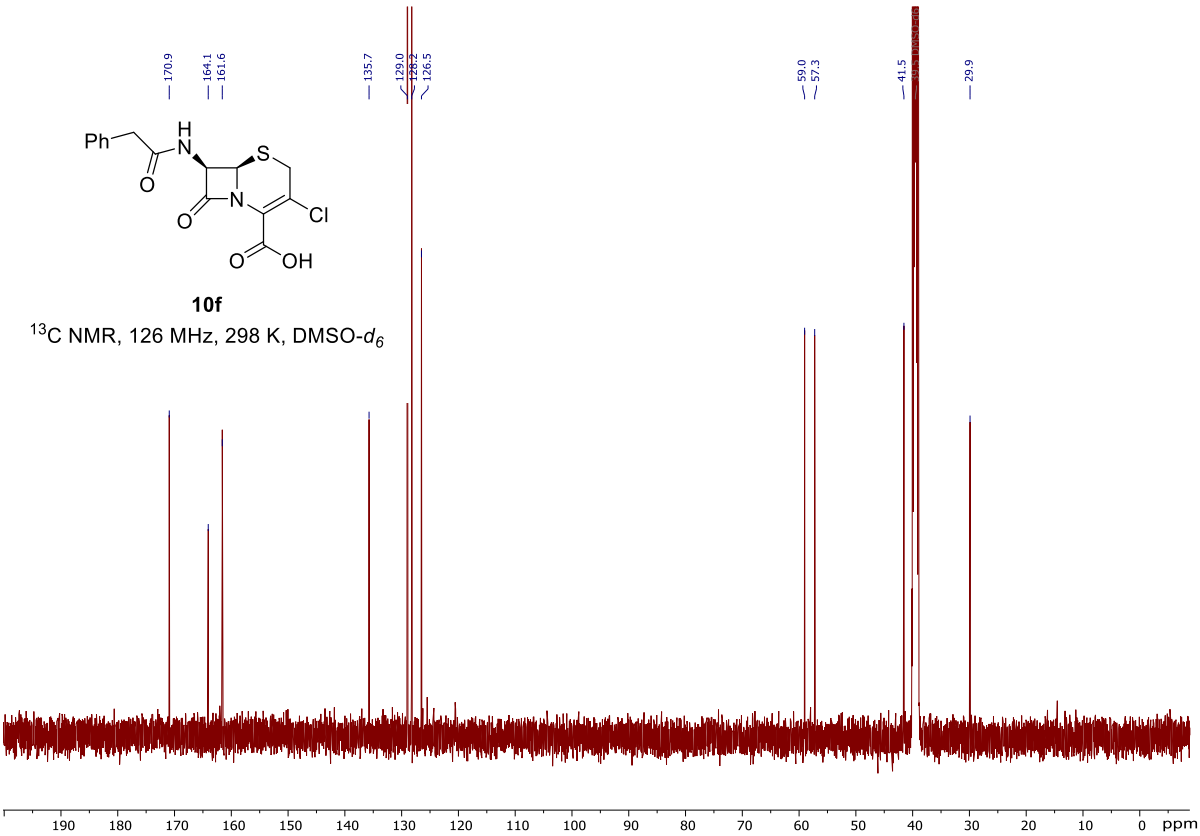
170.9
164.1
161.6
135.7
129.0
128.2
126.5
59.0
57.3
41.5
29.9
190 180 170 160 150 140 130 120 110 100 90 80 70 60 50 40 30 20 10 0 ppm

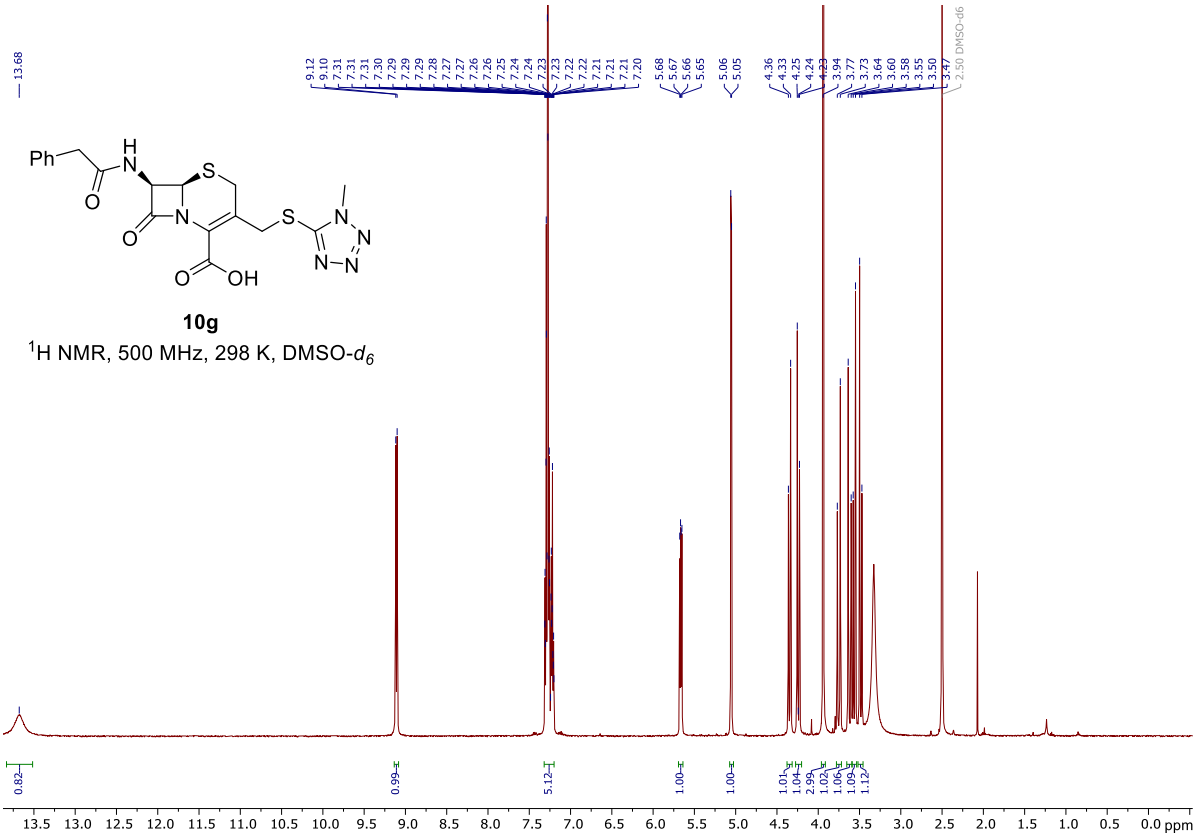

10g

^{1}H NMR, 500 MHz, 298 K, DMSO-d_6

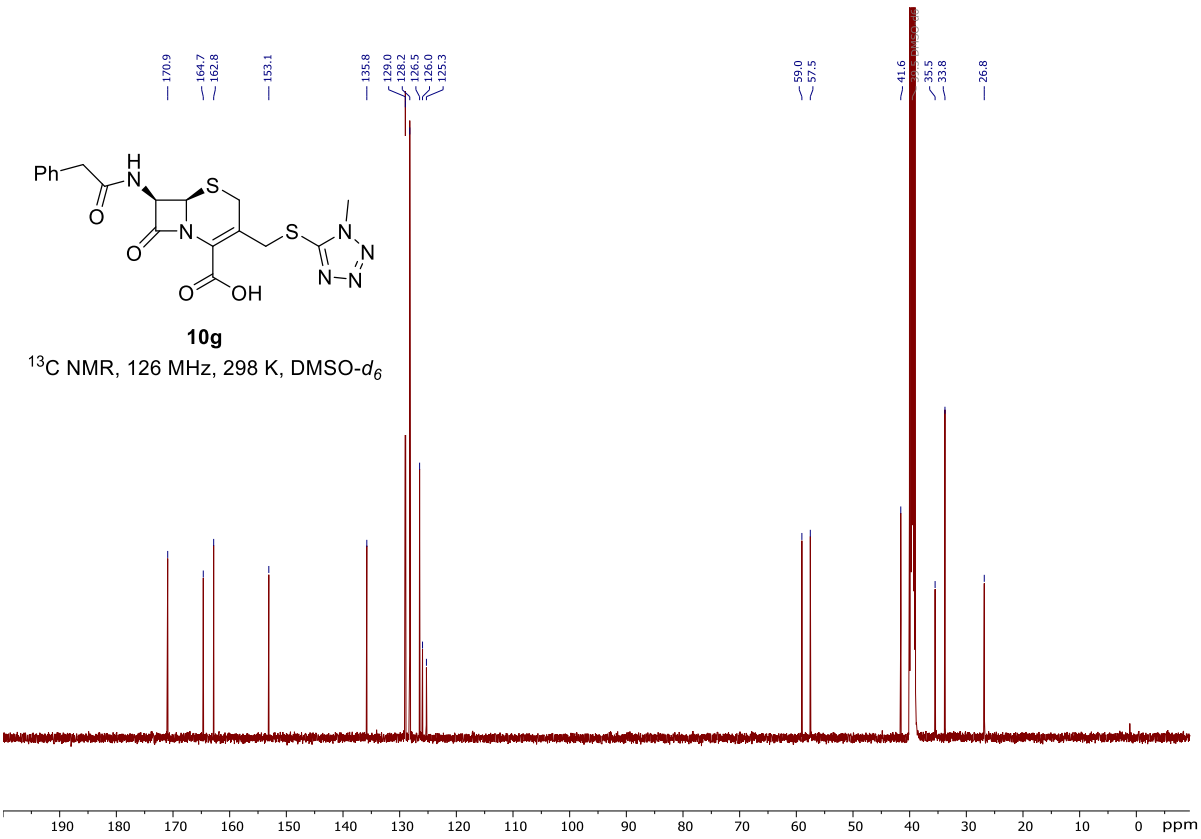

10g

^{13}C NMR, 126 MHz, 298 K, DMSO-d_6

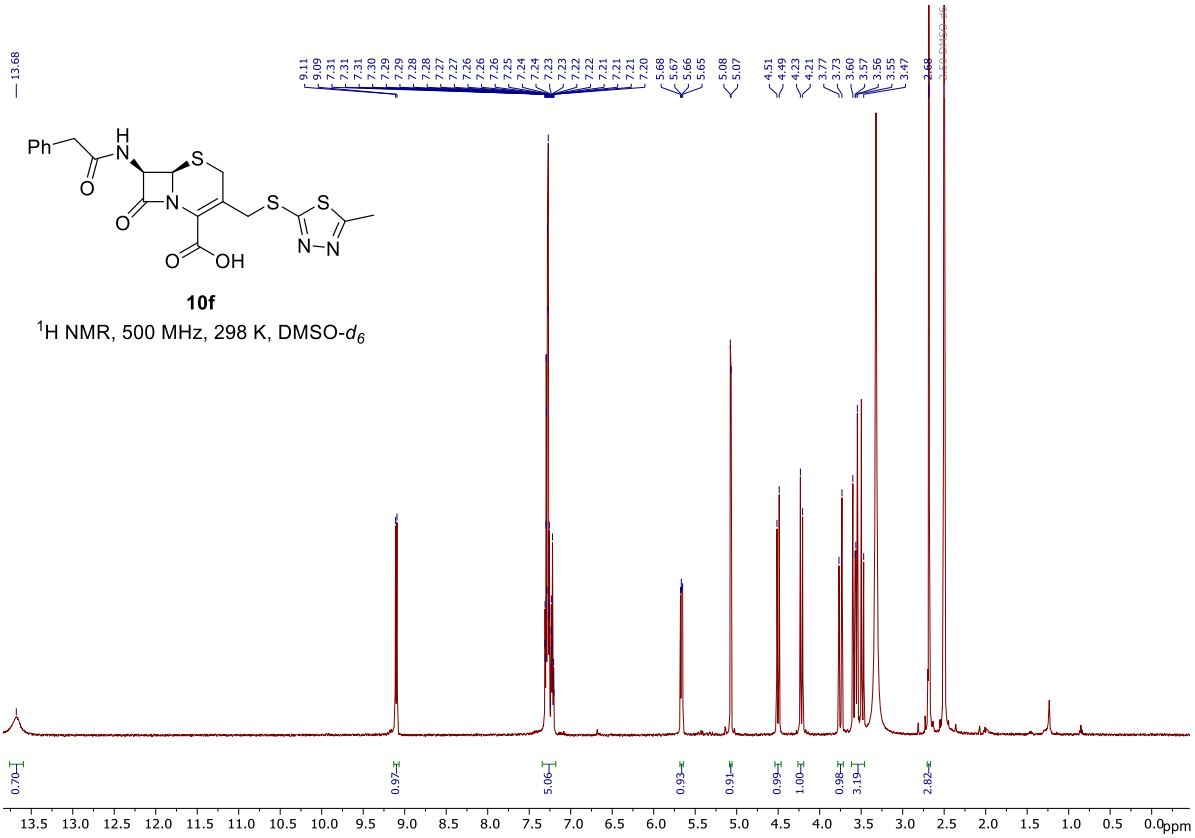

10f

^{1}H NMR, 500 MHz, 298 K, DMSO-d_6

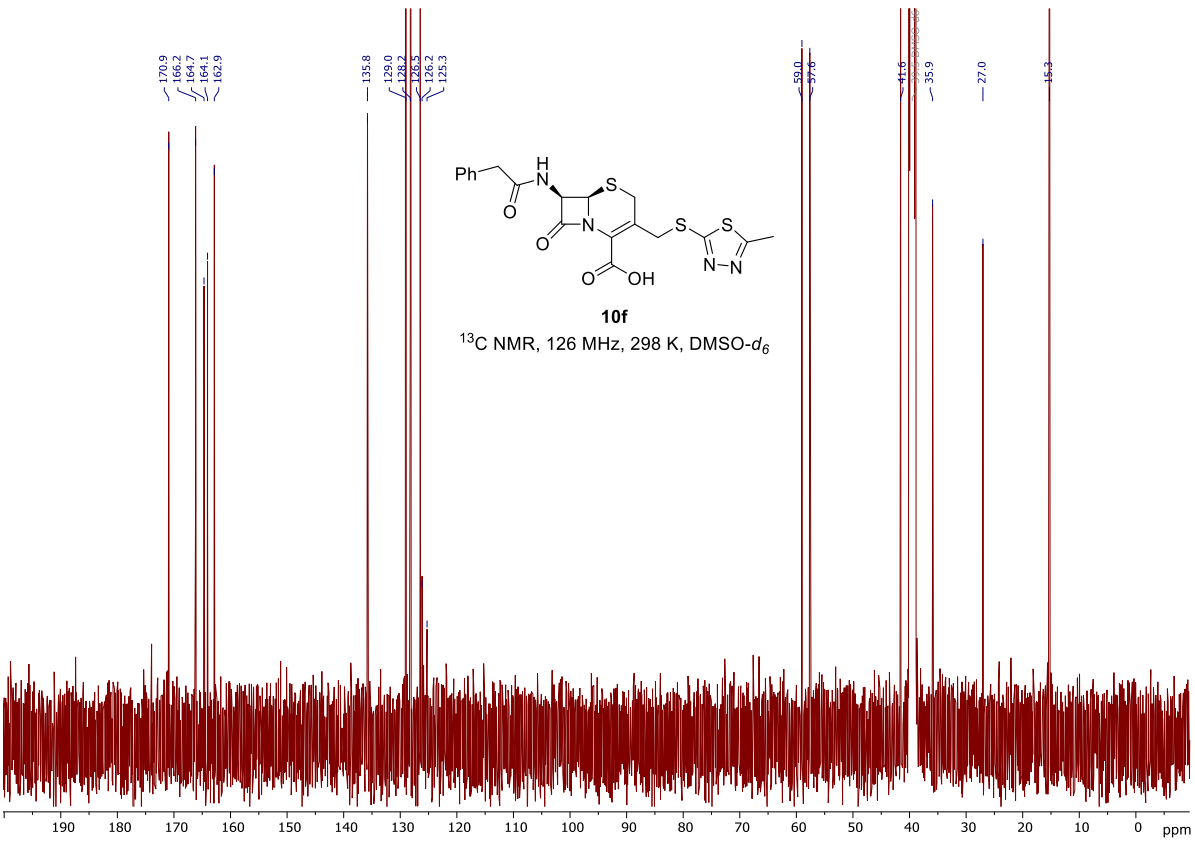

10f

^{13}C NMR, 126 MHz, 298 K, DMSO-d_6

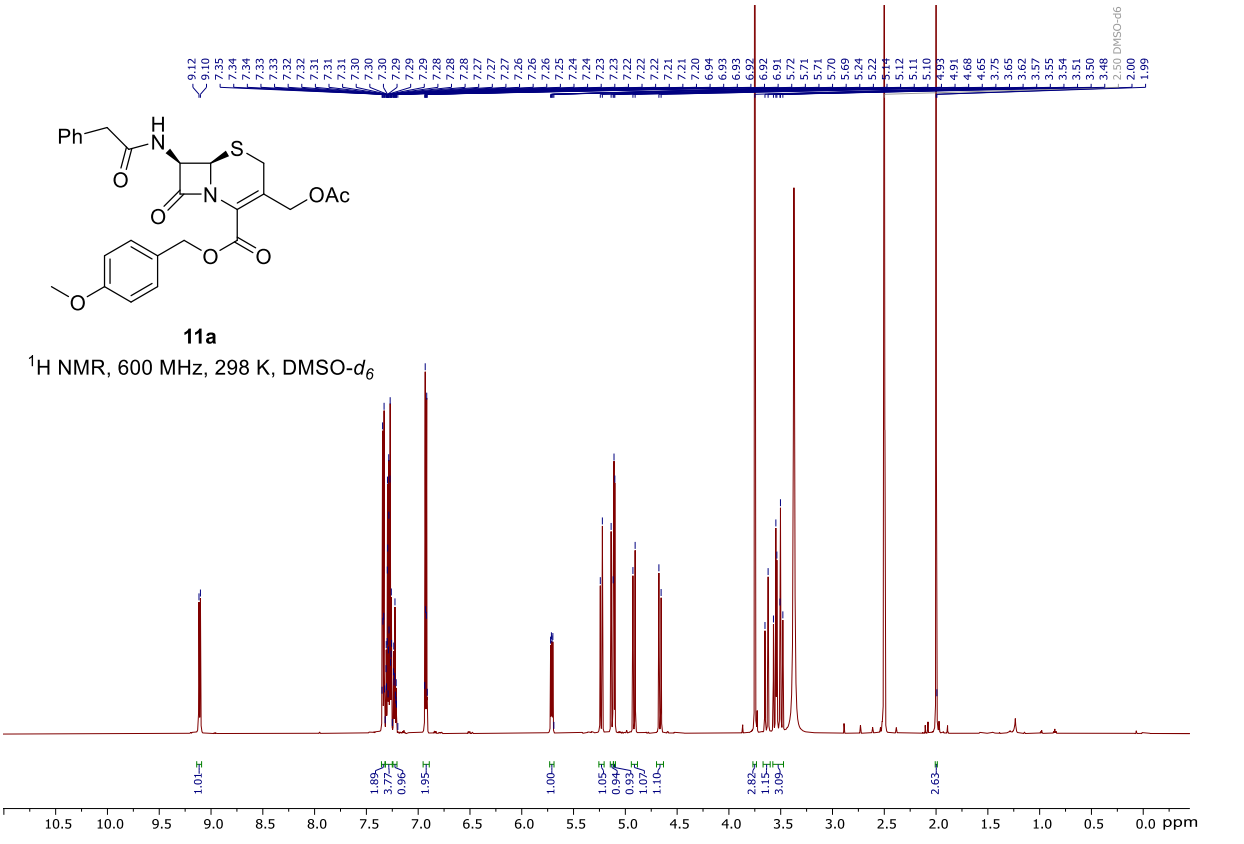

11a

^{1}H NMR, 600 MHz, 298 K, DMSO-d_6

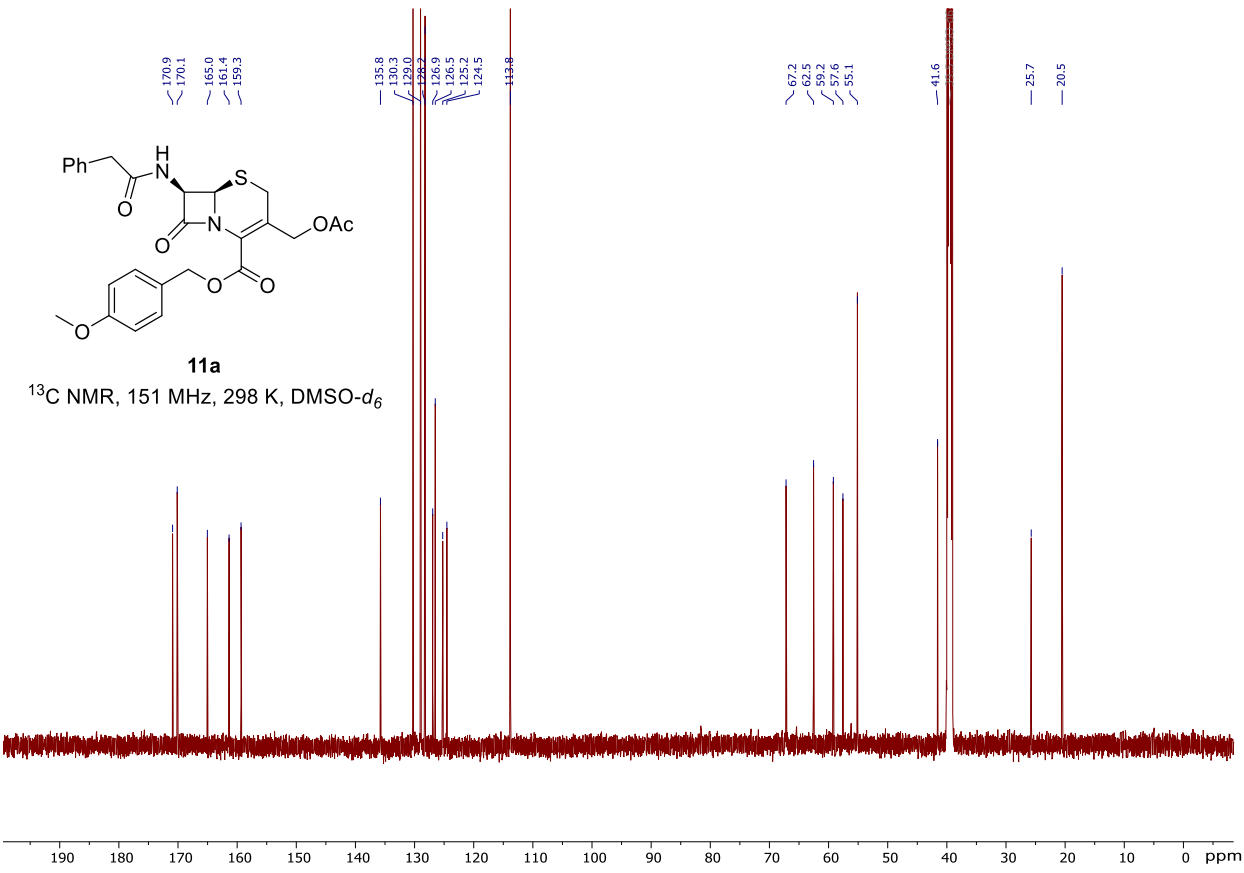

11a

^{13}C NMR, 151 MHz, 298 K, DMSO-d_6

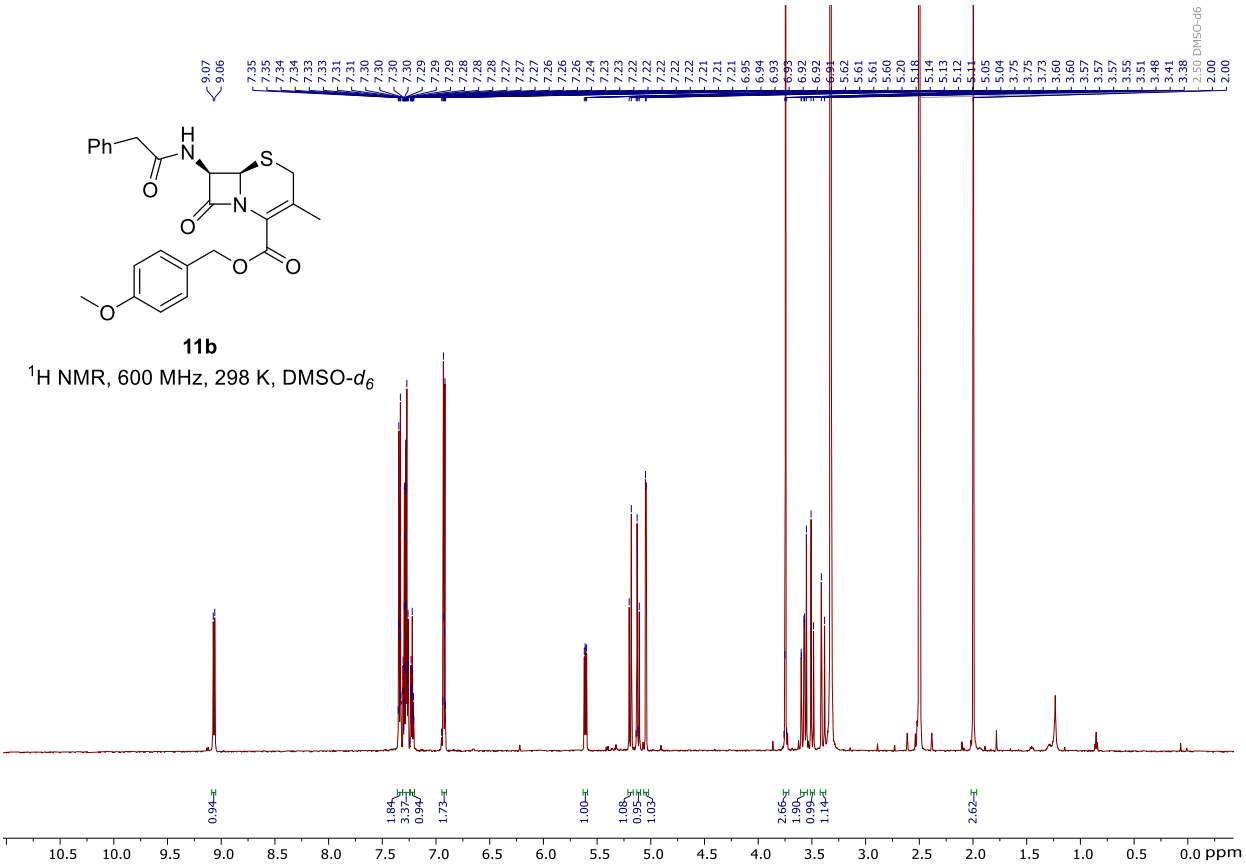
Ph
H
N
S
O
O
N
O
O
O
O
11b
1H NMR, 600 MHz, 298 K, DMSO-d6
9.07
9.06
7.35
7.34
7.33
7.31
7.30
7.29
7.28
7.27
7.26
7.24
7.23
7.22
6.95
6.94
6.93
6.92
6.91
5.62
5.61
5.60
5.20
5.18
5.14
5.13
5.12
5.11
5.05
5.04
3.75
3.73
3.60
3.57
3.55
3.51
3.48
3.41
3.38
2.50 DMSO-d6
2.00
0.94
1.84
3.37
0.94
1.73
1.00
1.08
0.95
1.03
2.66
1.90
0.99
1.14
2.62
10.5 10.0 9.5 9.0 8.5 8.0 7.5 7.0 6.5 6.0 5.5 5.0 4.5 4.0 3.5 3.0 2.5 2.0 1.5 1.0 0.5 0.0 ppm

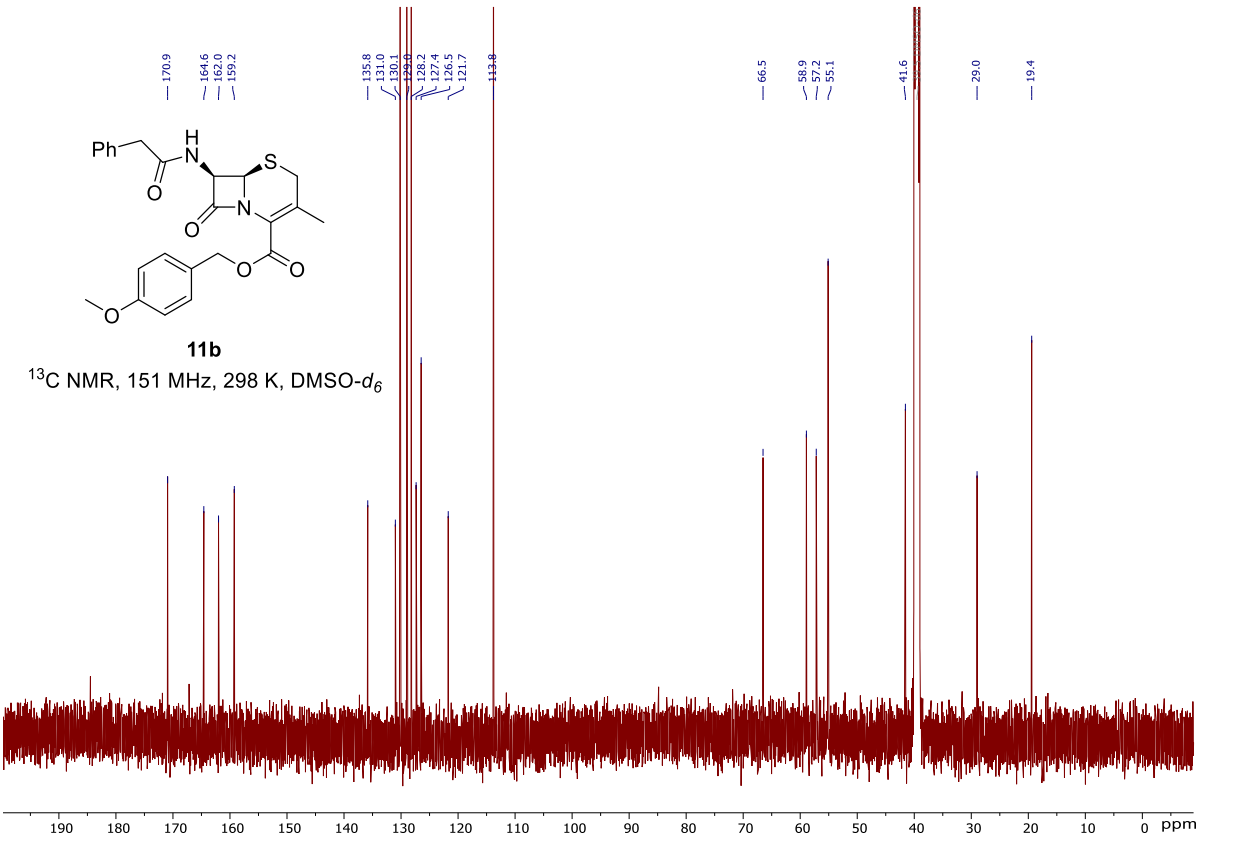
Ph
H
N
S
O
O
N
O
O
O
O
11b
13C NMR, 151 MHz, 298 K, DMSO-d6
170.9
164.6
162.0
159.2
135.8
131.0
130.1
129.0
128.2
127.4
126.5
121.7
113.8
66.5
58.9
57.2
55.1
41.6
29.0
19.4
190 180 170 160 150 140 130 120 110 100 90 80 70 60 50 40 30 20 10 0 ppm

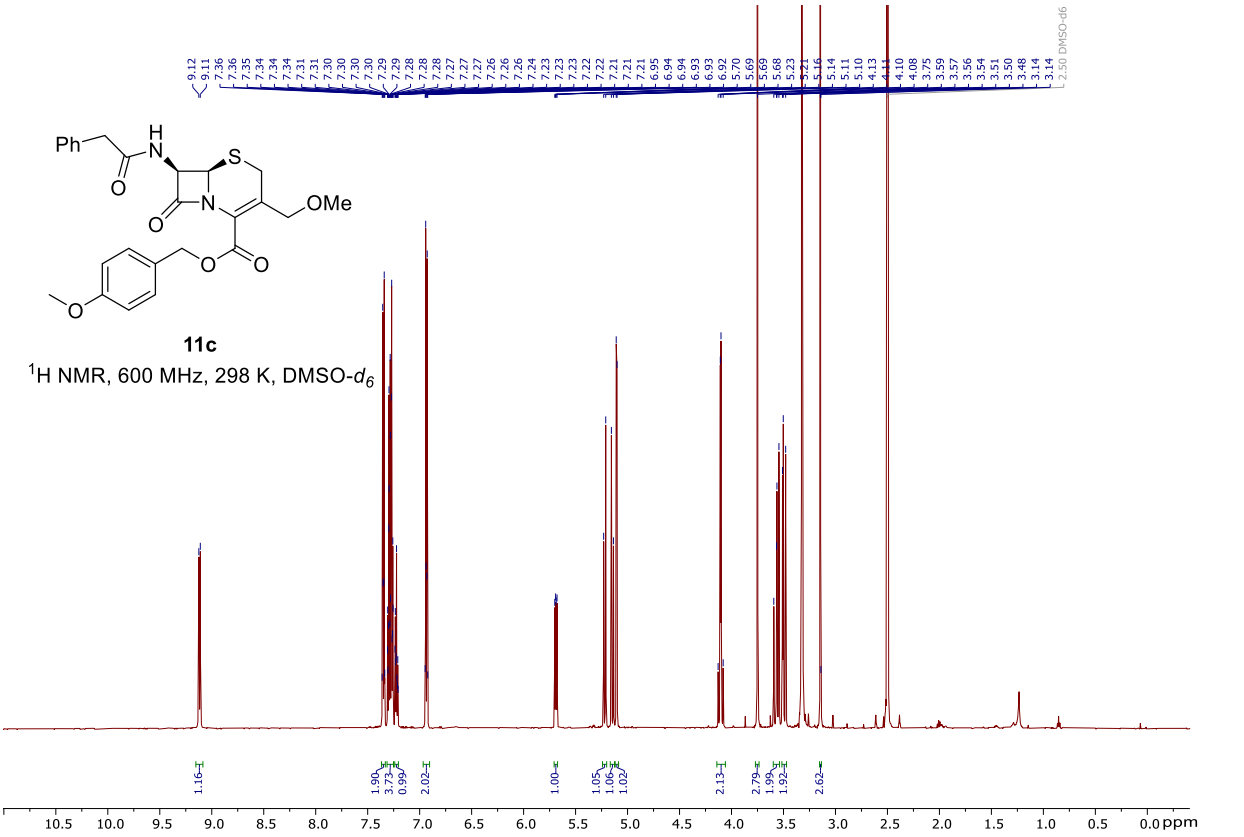
Ph
H
N
O
S
N
O
OMe
O
O
O
O
11c
^{1}H NMR, 600 MHz, 298 K, DMSO-d_6

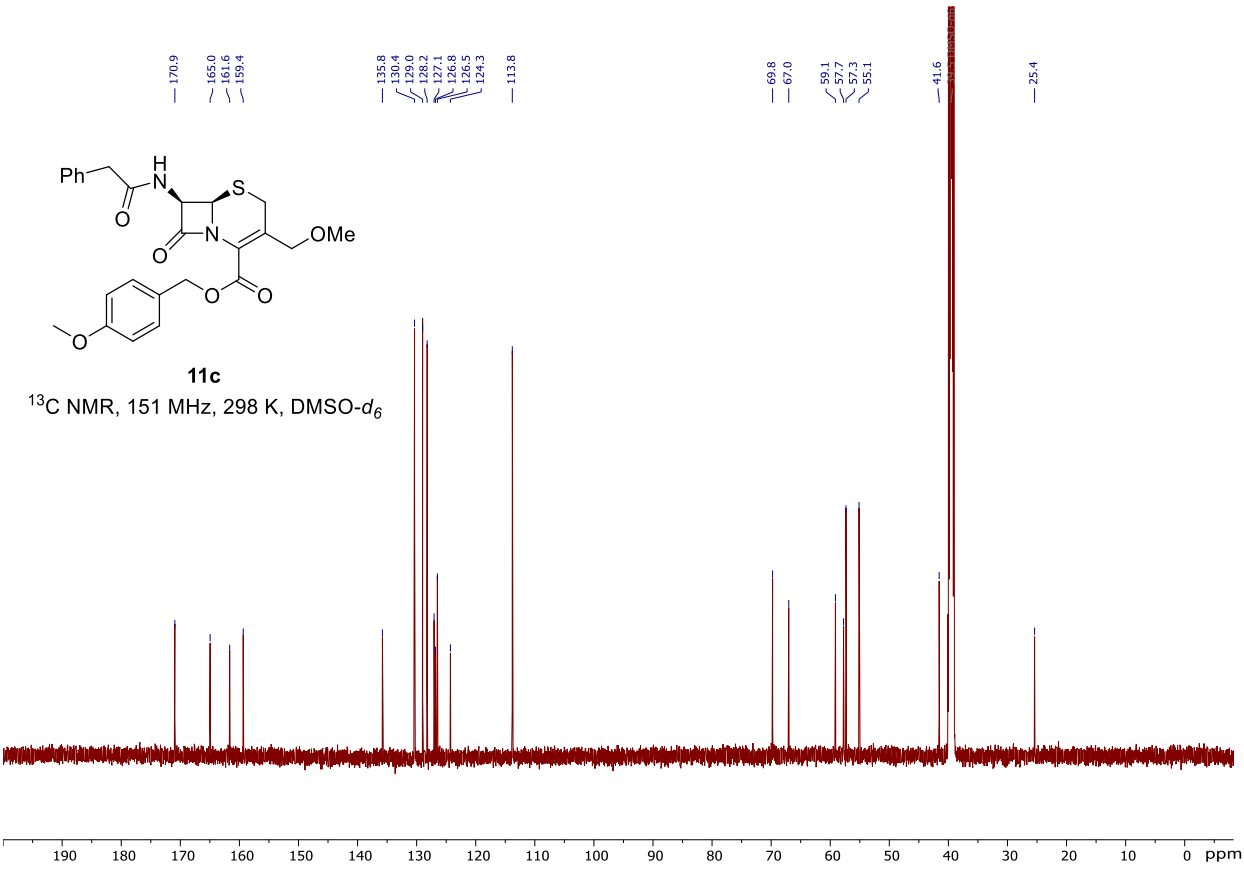
Ph
H
N
O
S
N
O
OMe
O
O
O
O
11c
^{13}C NMR, 151 MHz, 298 K, DMSO-d_6

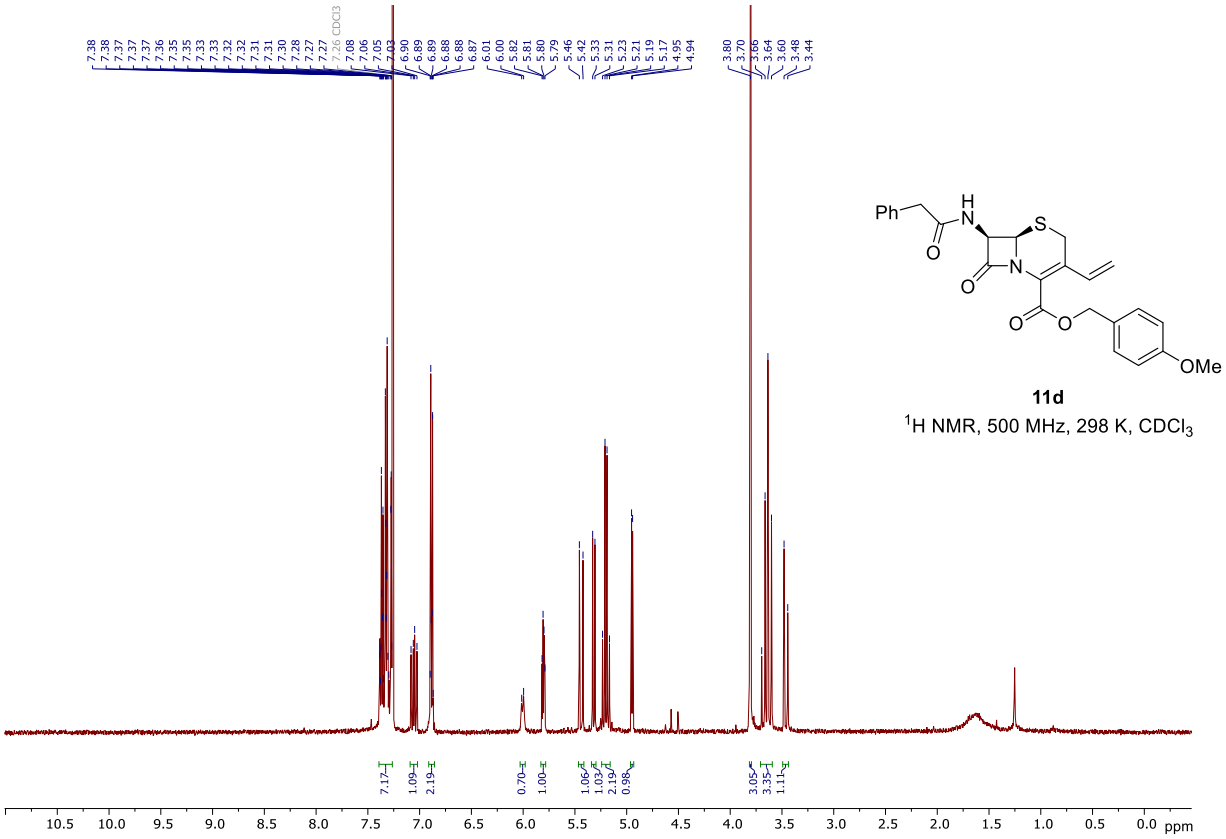

11d

^{1}H NMR, 500 MHz, 298 K, $CDCl_3$

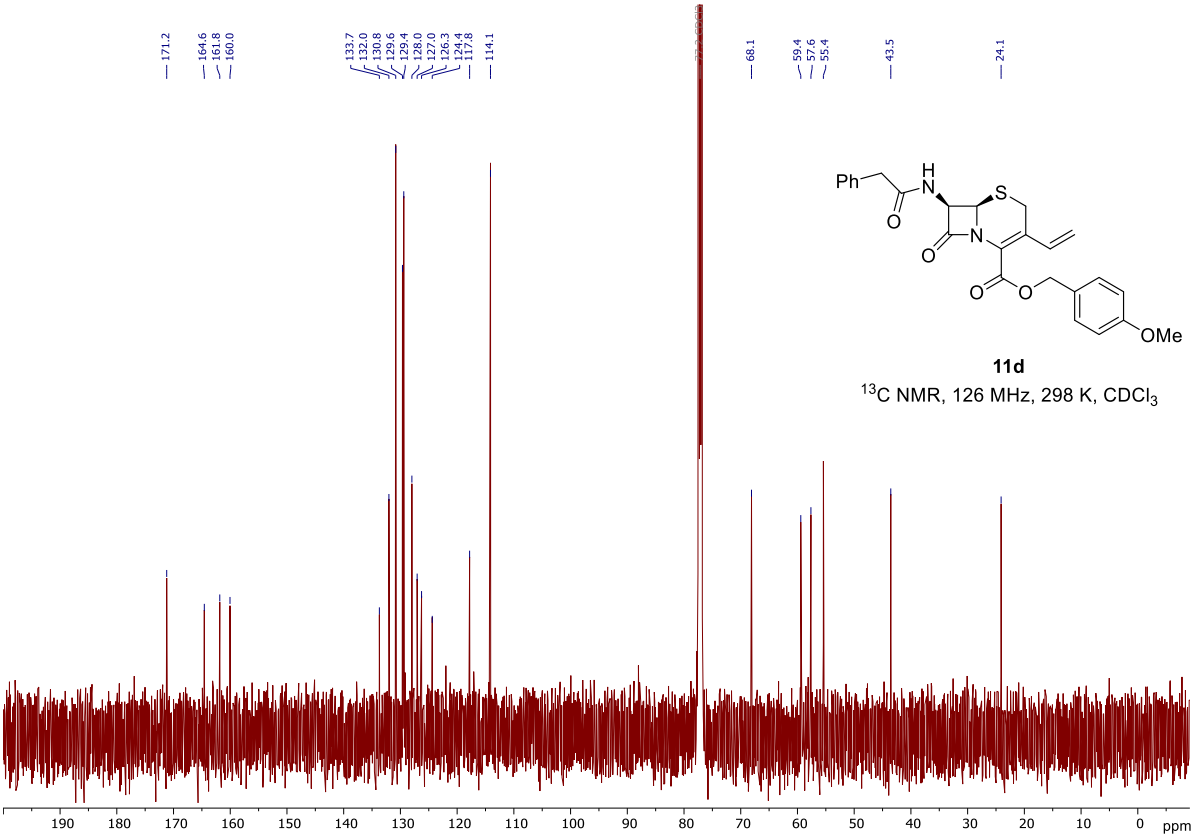

11d

^{13}C NMR, 126 MHz, 298 K, $CDCl_3$

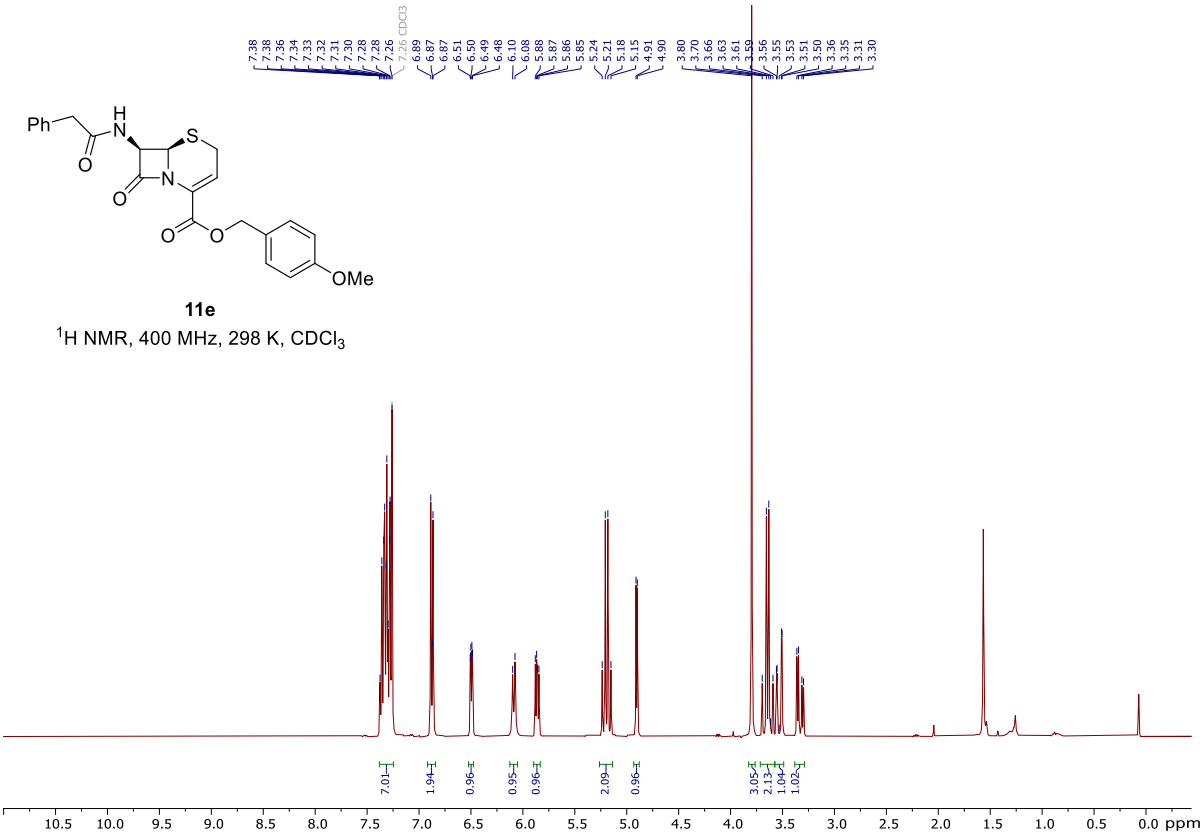

11e

^{1}H NMR, 400 MHz, 298 K, $CDCl_3$

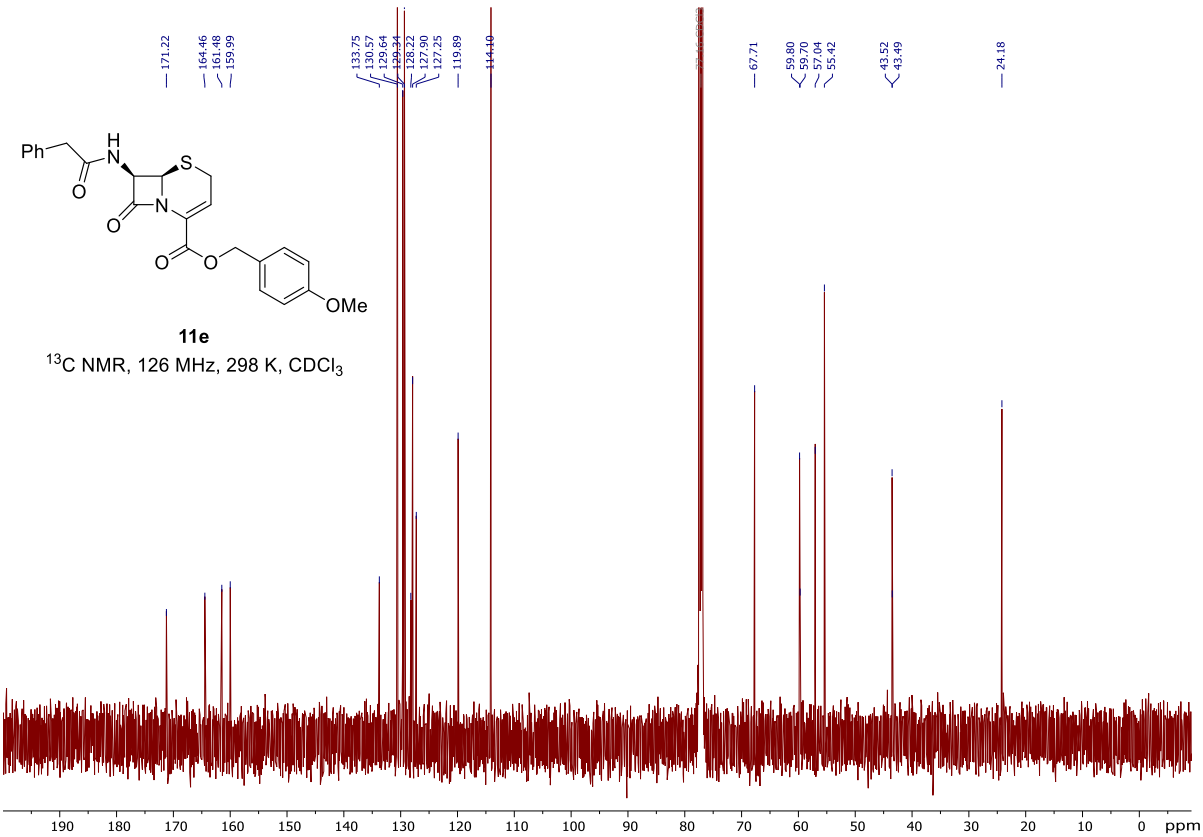

11e

^{13}C NMR, 126 MHz, 298 K, $CDCl_3$

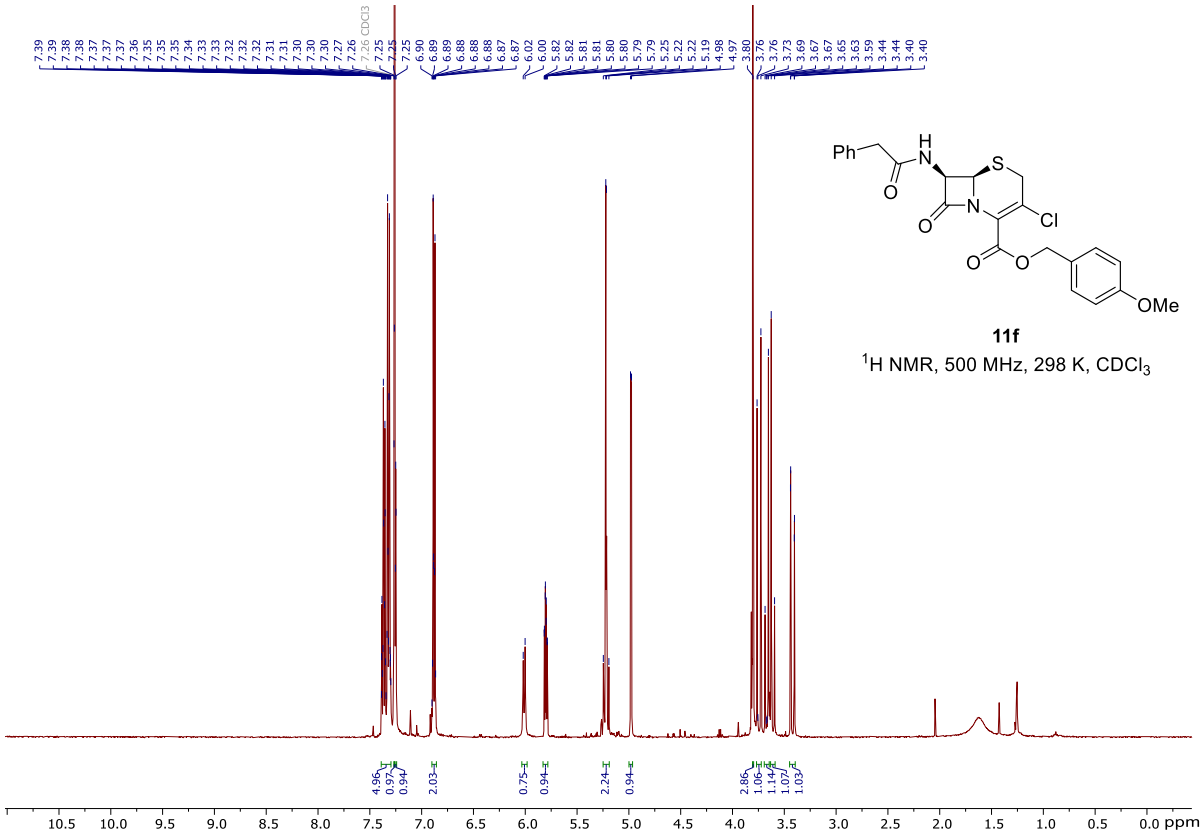

11f

^{1}H NMR, 500 MHz, 298 K, $CDCl_3$

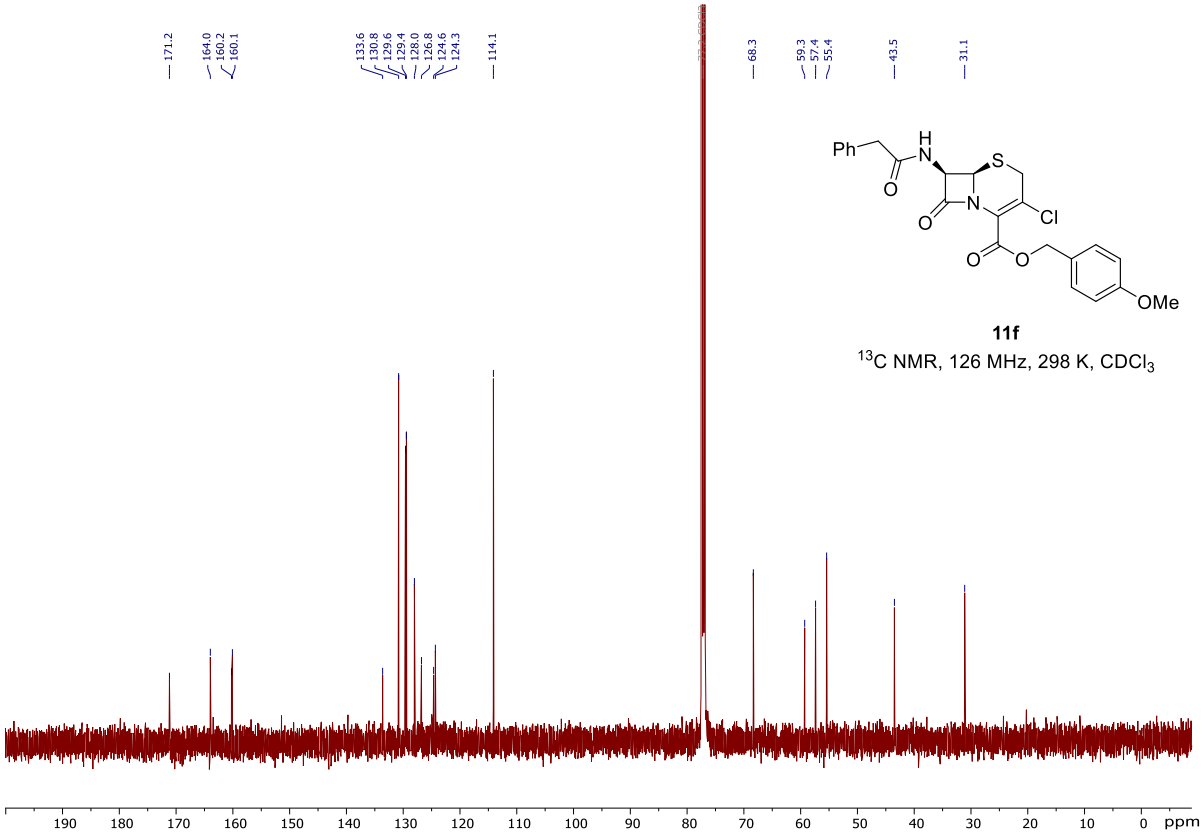

11f

^{13}C NMR, 126 MHz, 298 K, $CDCl_3$

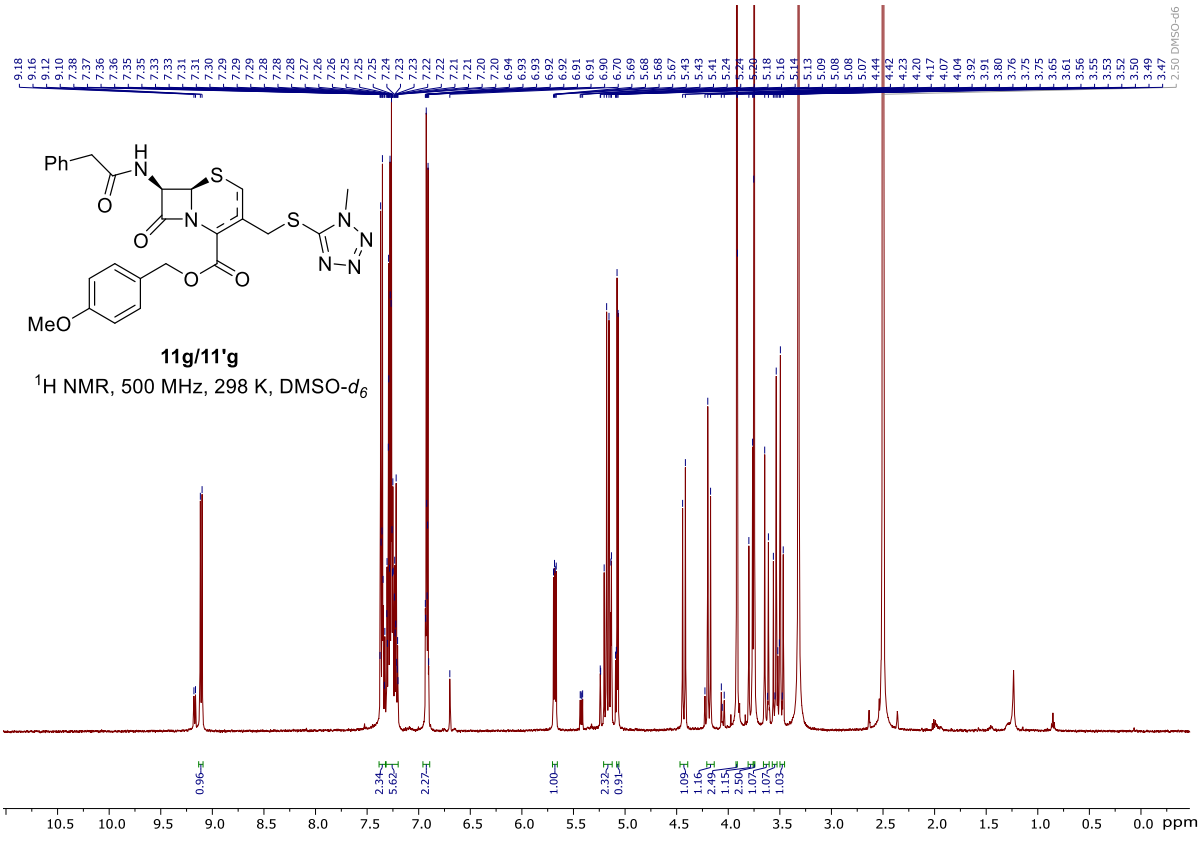
11g/11'g
1H NMR, 500 MHz, 298 K, DMSO-d6
10.5 10.0 9.5 9.0 8.5 8.0 7.5 7.0 6.5 6.0 5.5 5.0 4.5 4.0 3.5 3.0 2.5 2.0 1.5 1.0 0.5 0.0 ppm

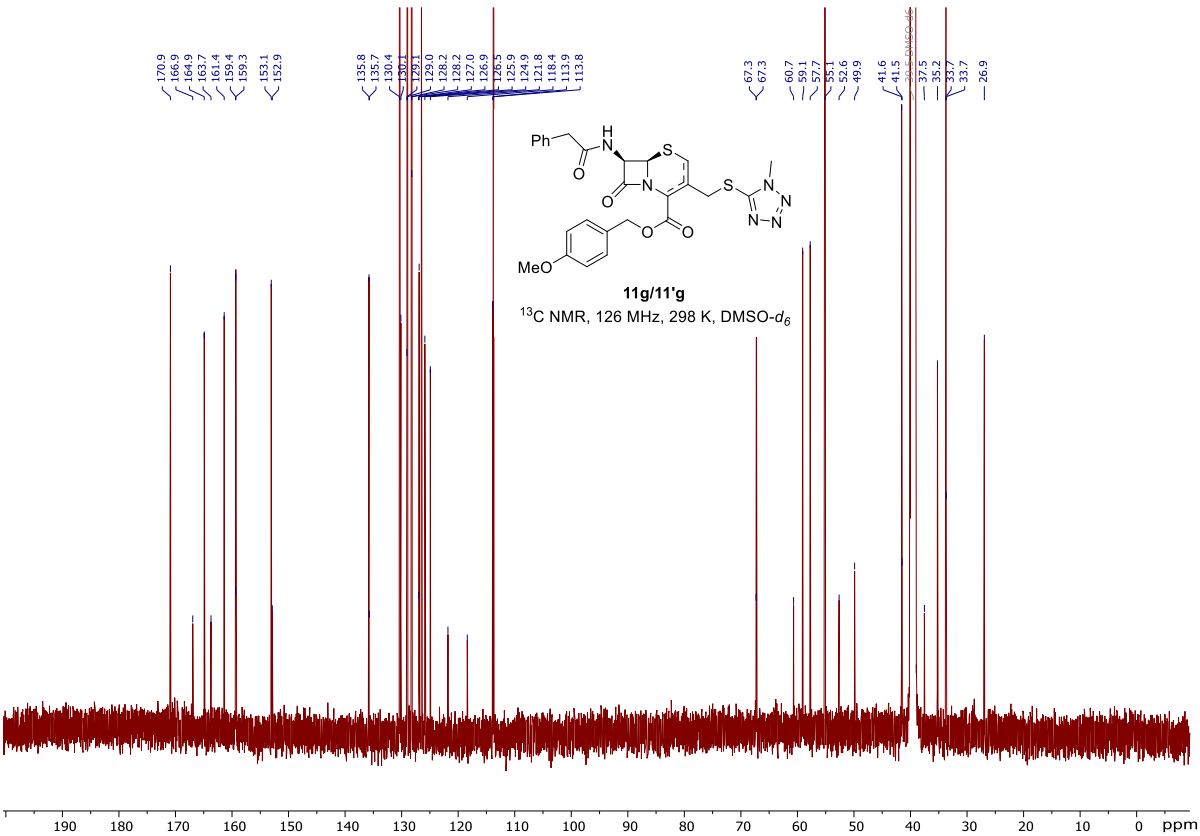
11g/11'g
13C NMR, 126 MHz, 298 K, DMSO-d6
190 180 170 160 150 140 130 120 110 100 90 80 70 60 50 40 30 20 10 0 ppm

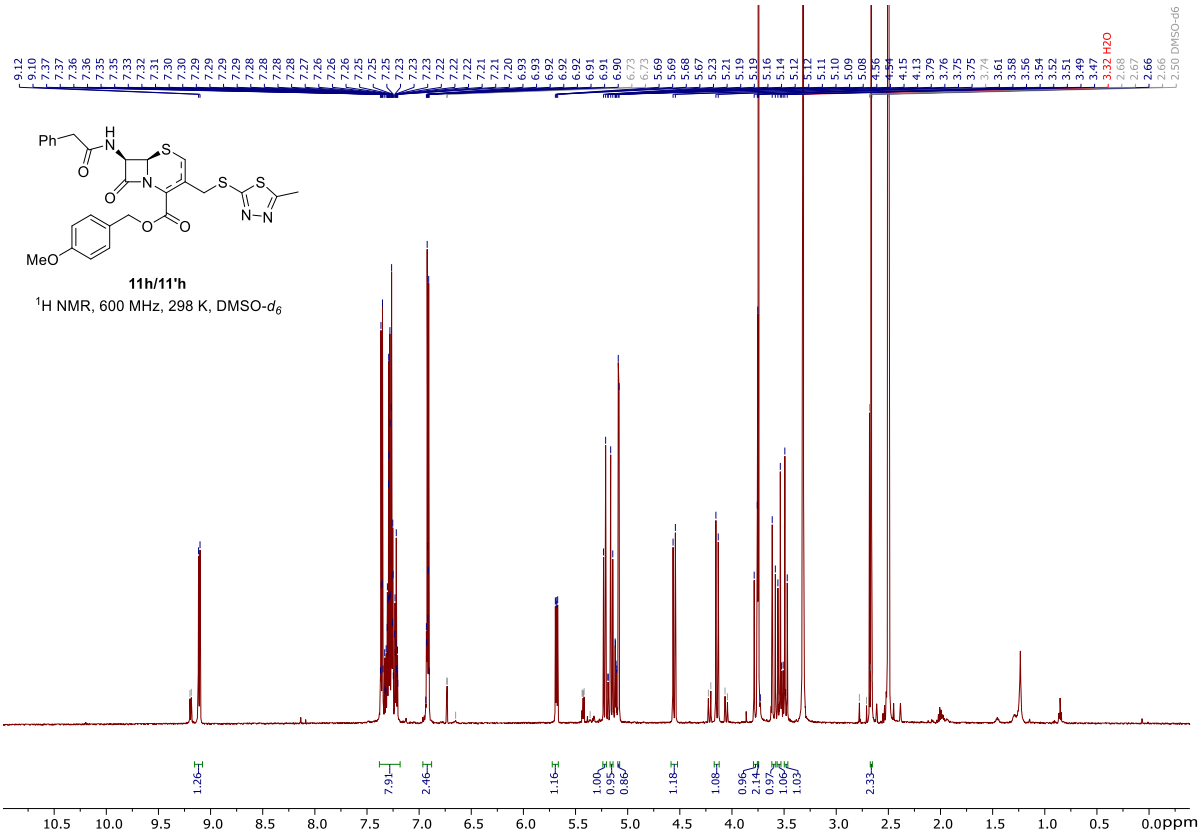
Ph
H
N
O
S
O
N
S
S
N
N
O
O
O
MeO
11h/11'h
1H NMR, 600 MHz, 298 K, DMSO-d6
3.32 H2O
2.50 DMSO-d6
1.26
7.91
2.46
1.16
1.00
0.95
0.86
1.18
1.08
0.96
2.14
0.97
1.06
1.03
2.33
ppm

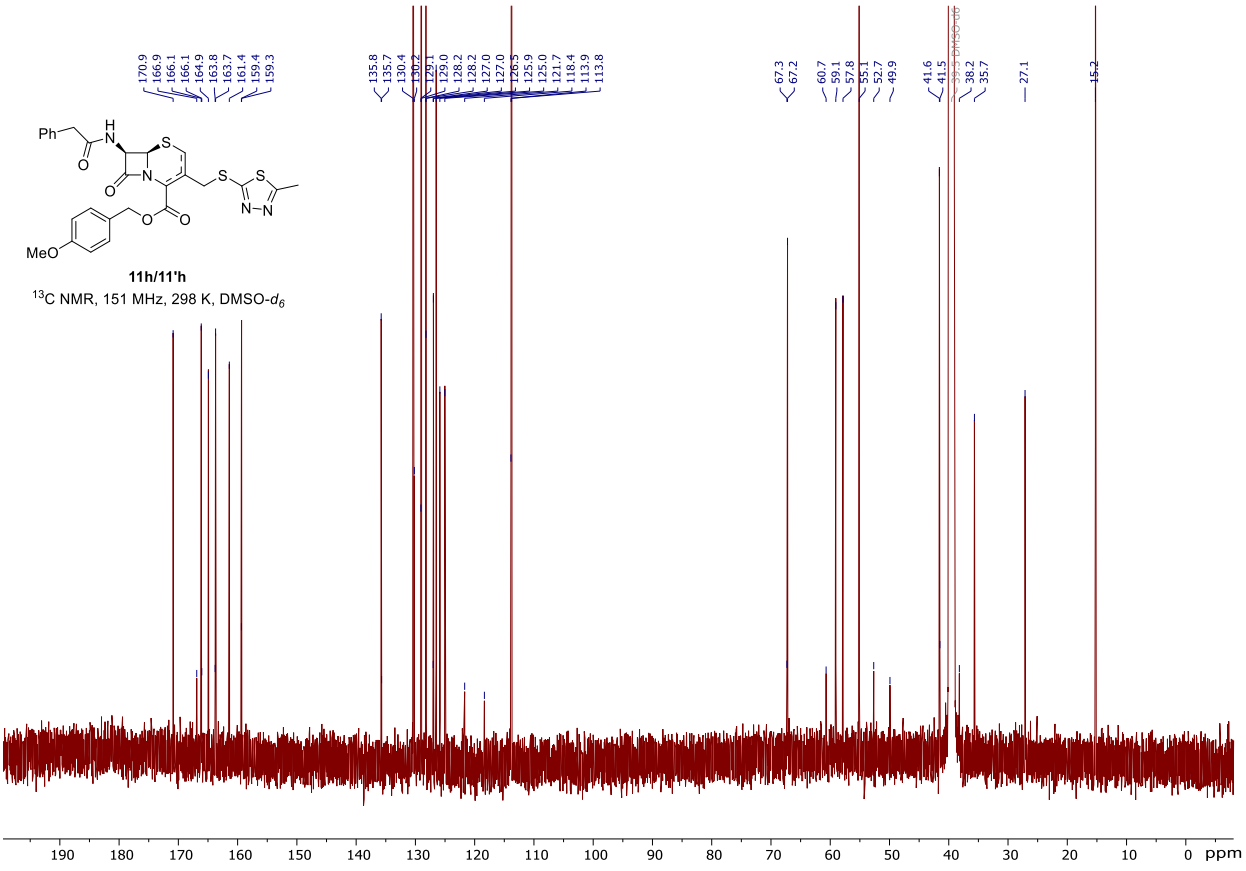
Ph
H
N
O
S
O
N
S
S
N
N
O
O
O
MeO
11h/11'h
13C NMR, 151 MHz, 298 K, DMSO-d6
170.9
166.9
166.1
166.1
164.9
163.8
163.7
161.4
159.4
159.3
135.8
135.7
130.4
130.2
129.1
129.0
128.2
128.2
127.0
127.0
126.5
125.9
125.0
121.7
118.4
113.9
113.8
67.3
67.2
60.7
59.1
57.8
55.1
52.7
49.9
41.6
41.5
39.5 DMSO-d6
38.2
35.7
27.1
15.2
ppm

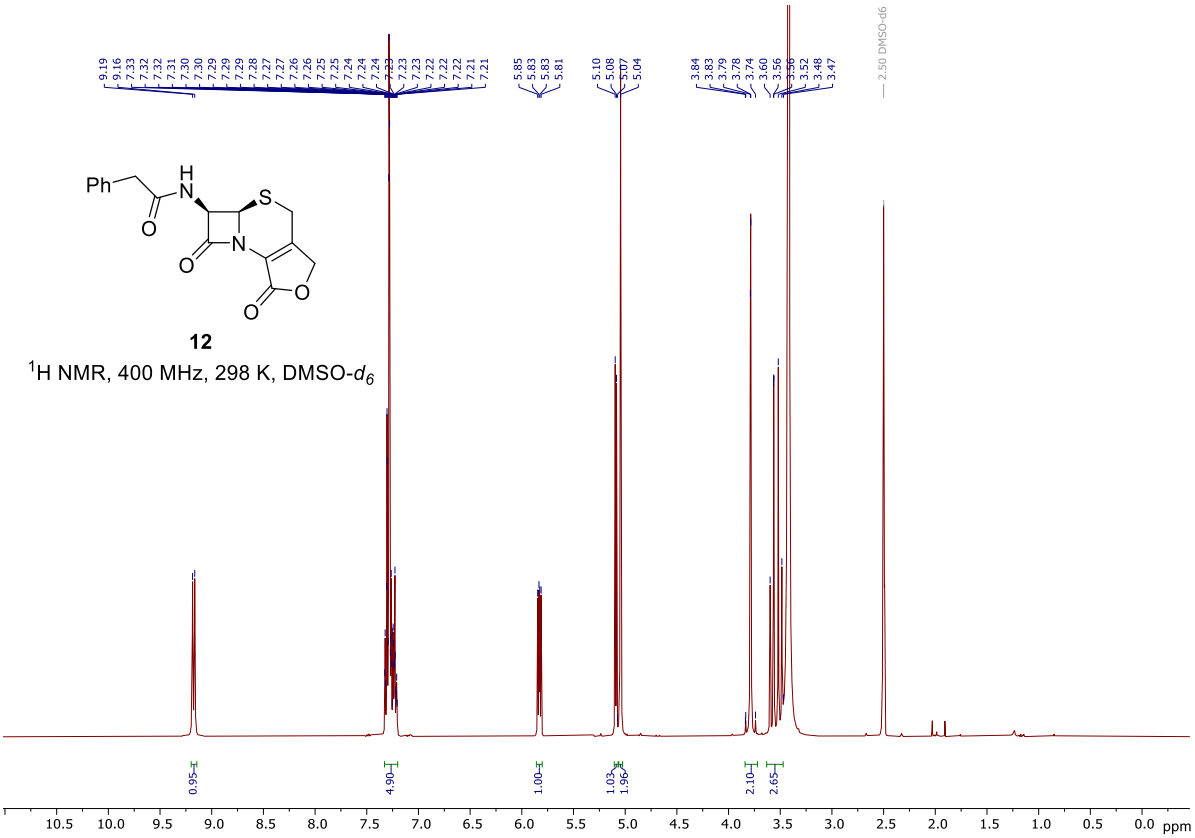

12

^{1}H NMR, 400 MHz, 298 K, DMSO-d_6

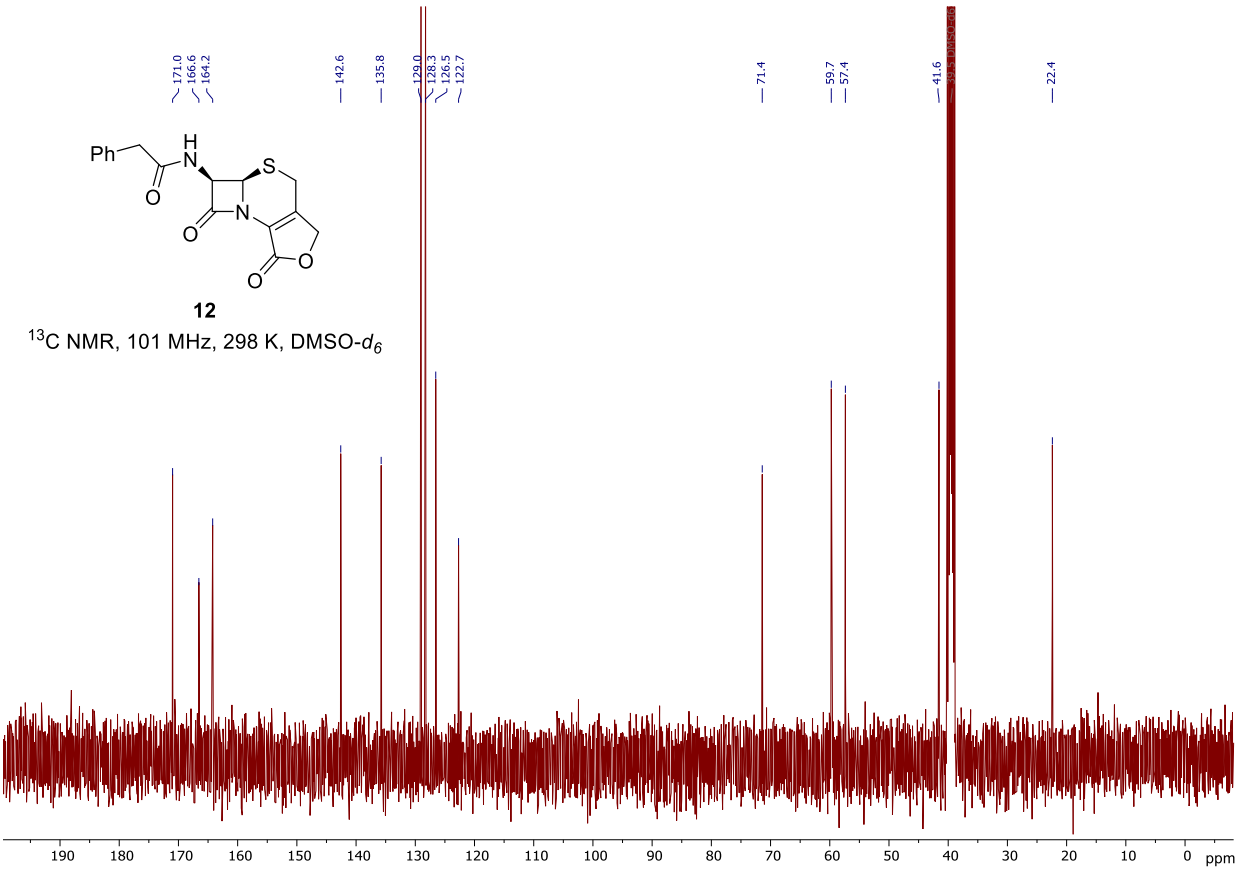

12

^{13}C NMR, 101 MHz, 298 K, DMSO-d_6

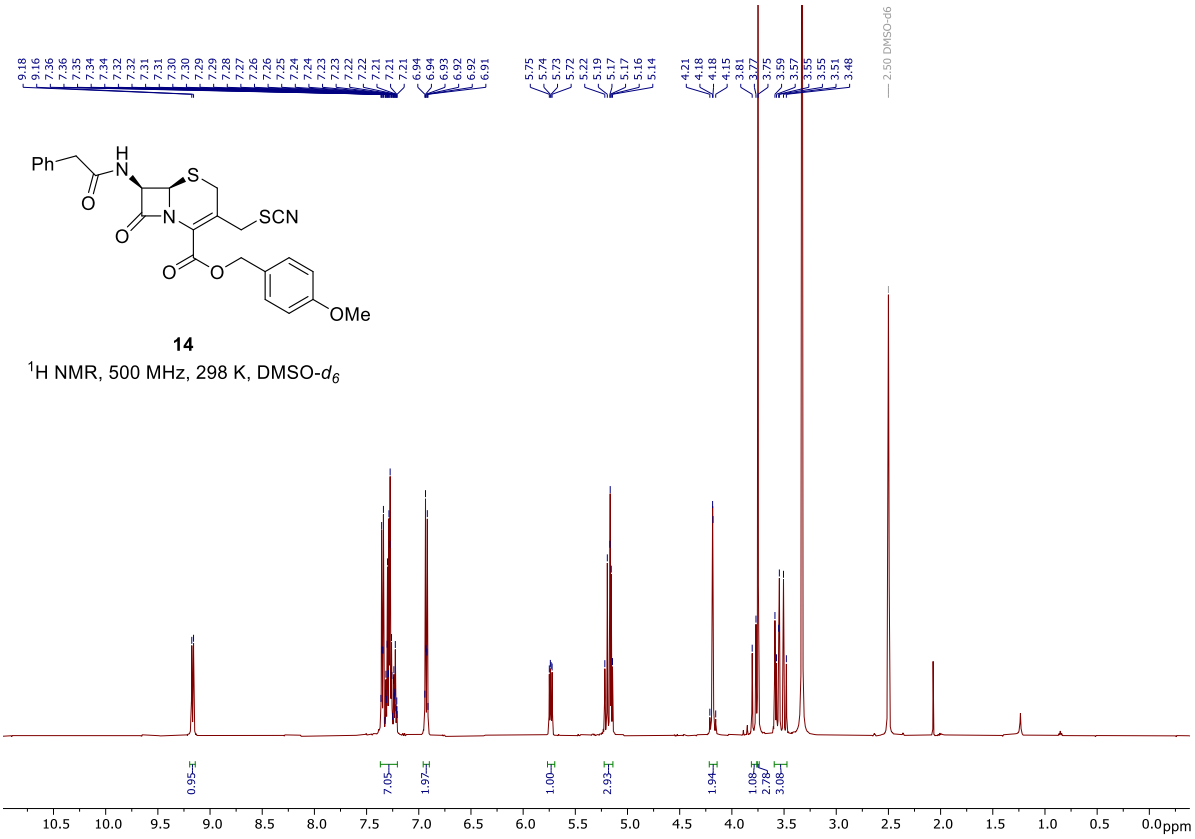

14

^{1}H NMR, 500 MHz, 298 K, DMSO-d_6

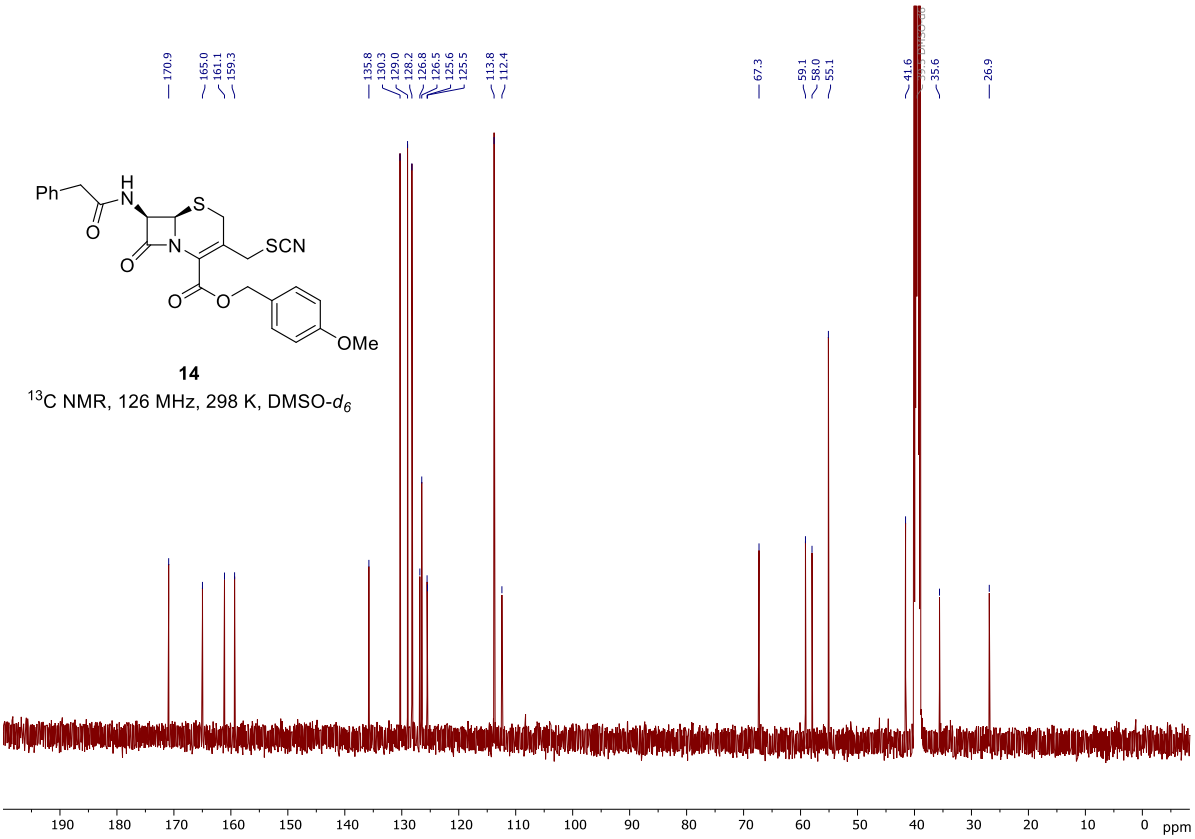

14

^{13}C NMR, 126 MHz, 298 K, DMSO-d_6

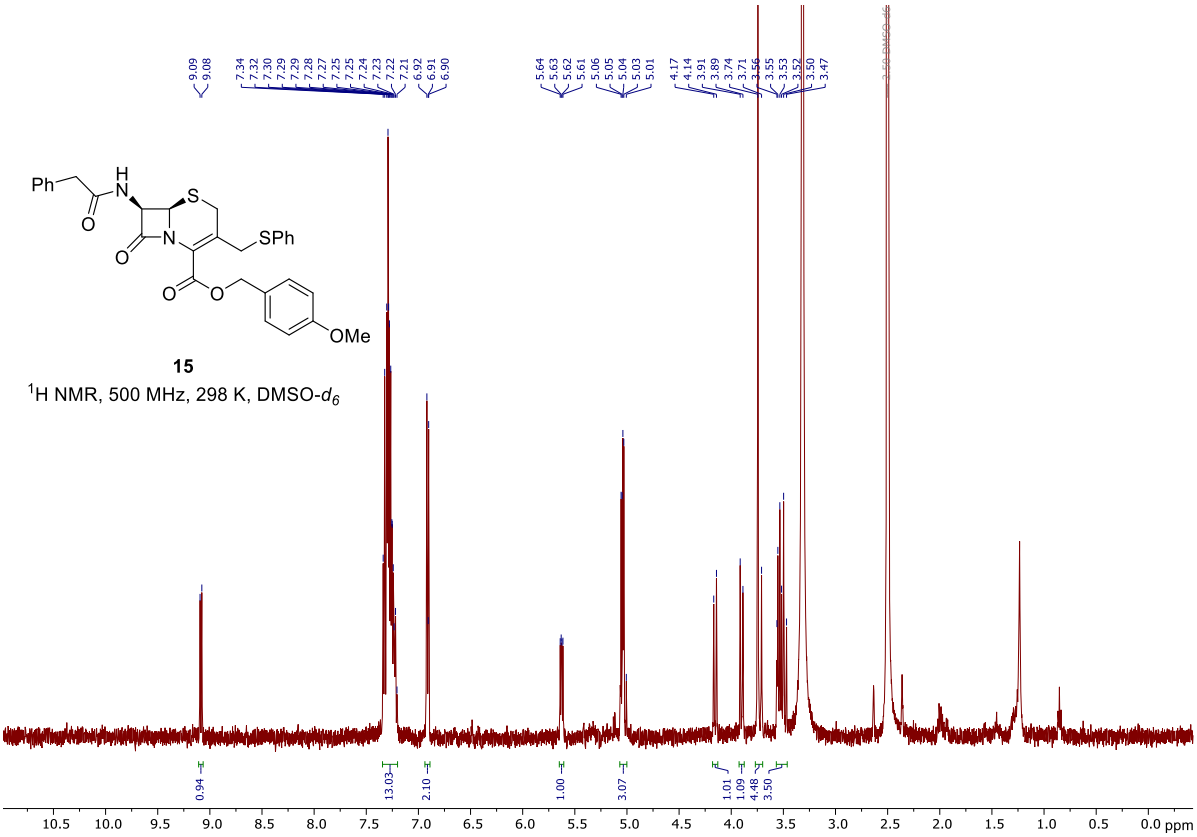

15

^{1}H NMR, 500 MHz, 298 K, DMSO-d_6

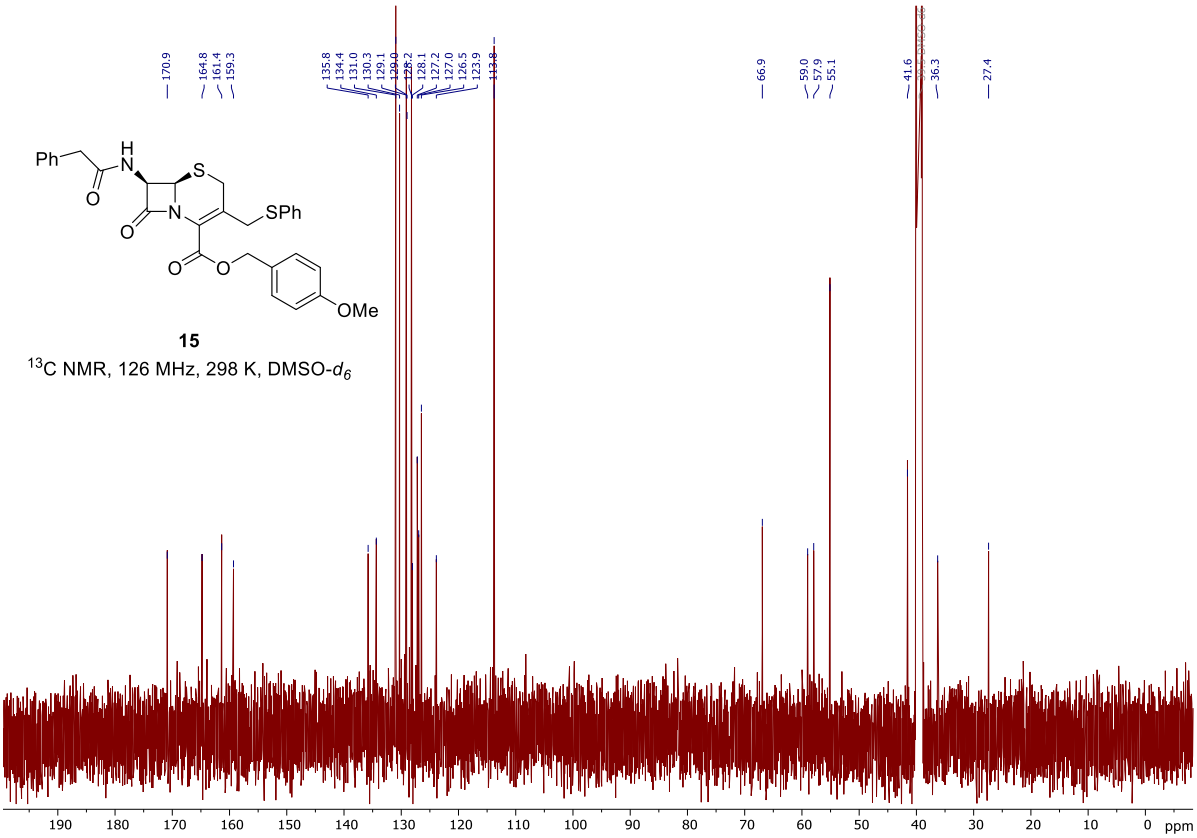

15

^{13}C NMR, 126 MHz, 298 K, DMSO-d_6

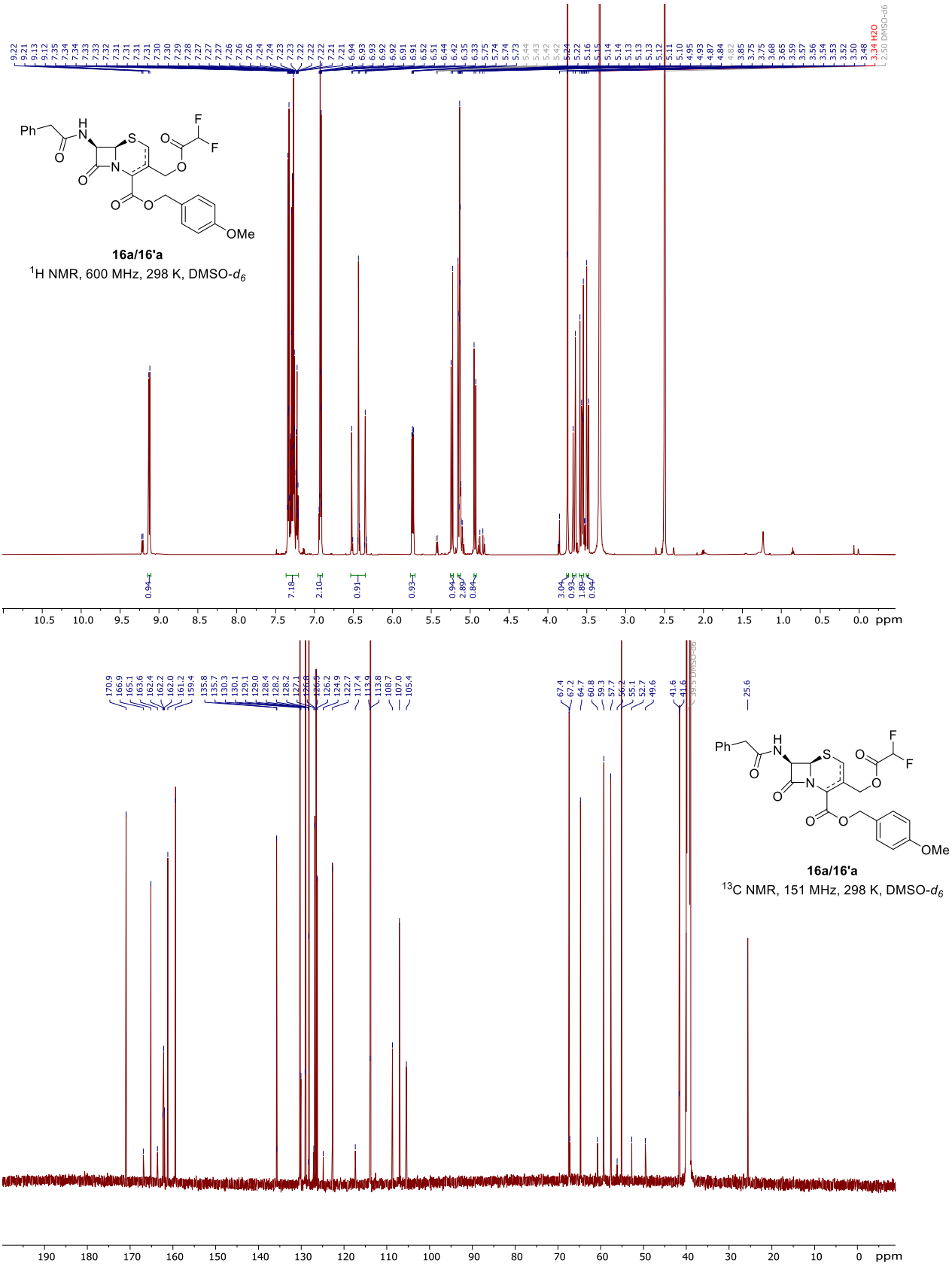
16a/16'a
1H NMR, 600 MHz, 298 K, DMSO-d6
16a/16'a
13C NMR, 151 MHz, 298 K, DMSO-d6

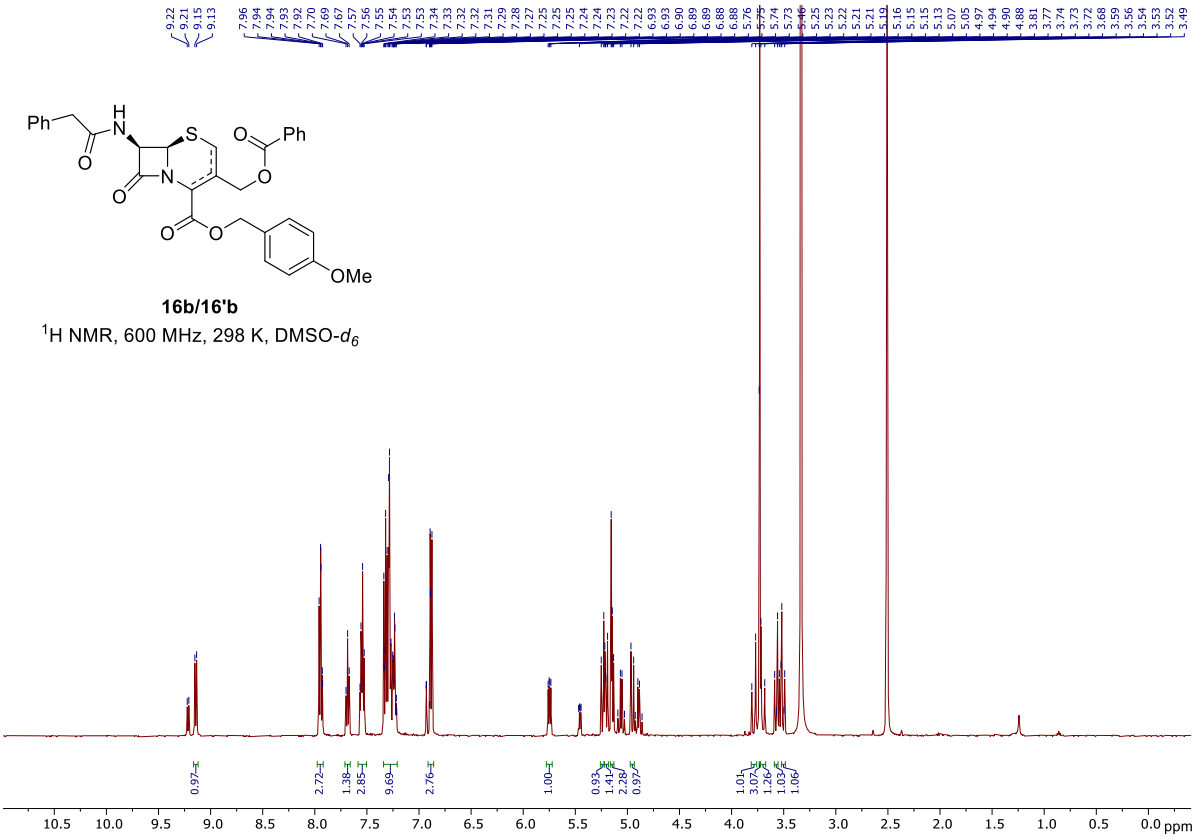

16b/16'b

^{1}H NMR, 600 MHz, 298 K, DMSO-d_6

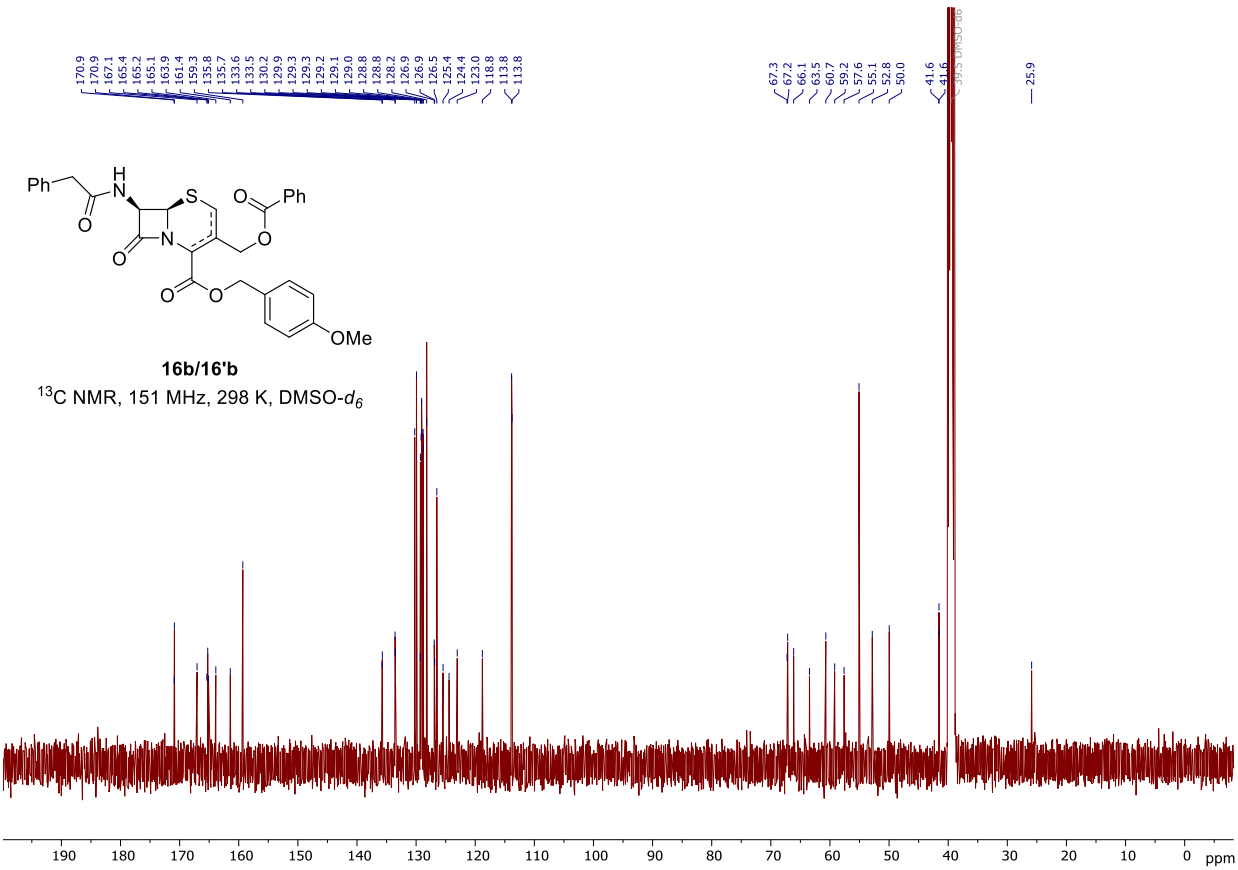

16b/16'b

^{13}C NMR, 151 MHz, 298 K, DMSO-d_6

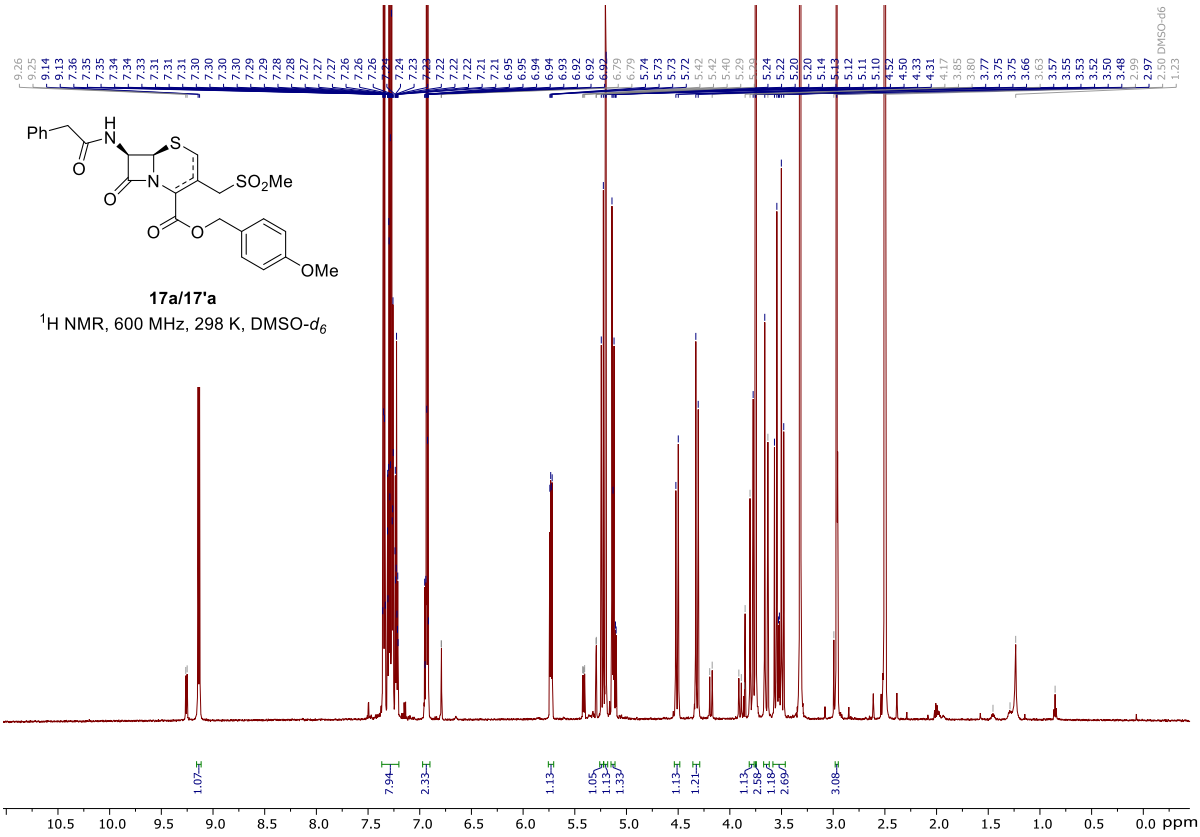

17a/17'a

^{1}H NMR, 600 MHz, 298 K, DMSO-d_6

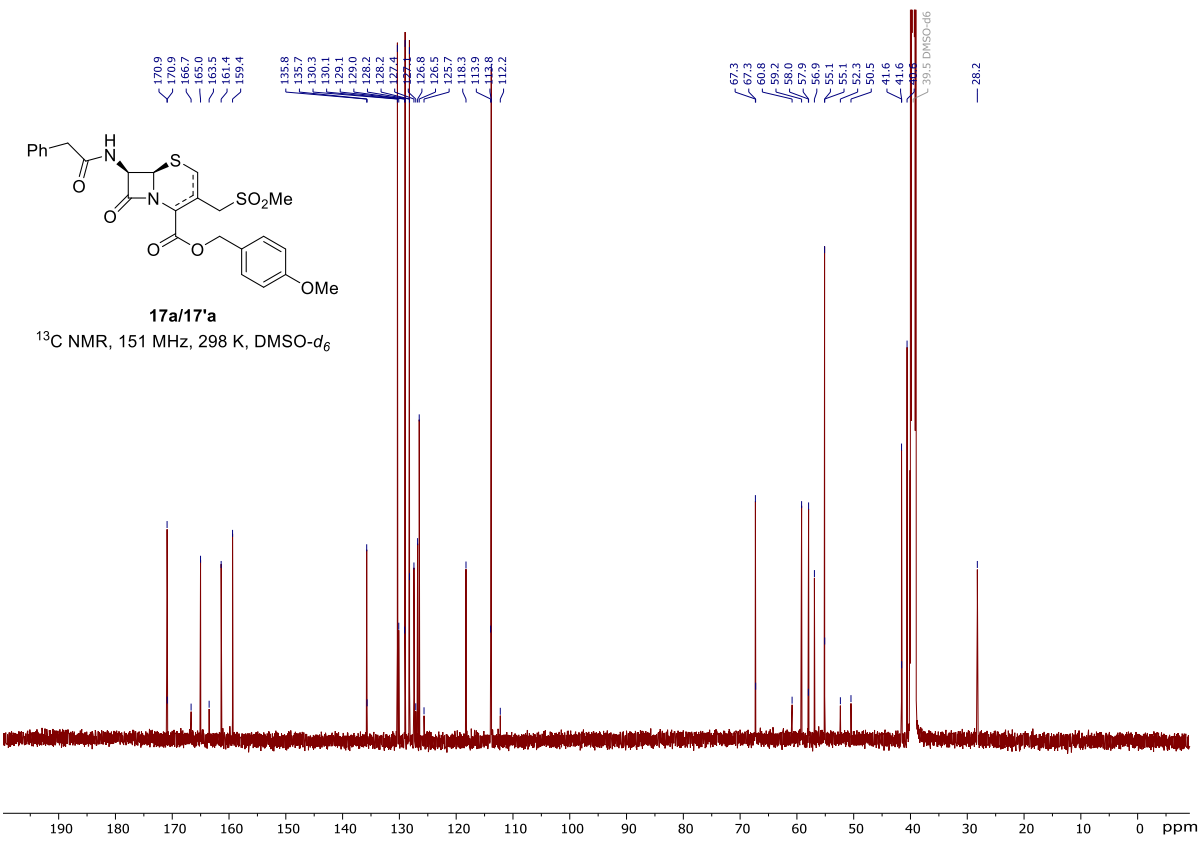

17a/17'a

^{13}C NMR, 151 MHz, 298 K, DMSO-d_6

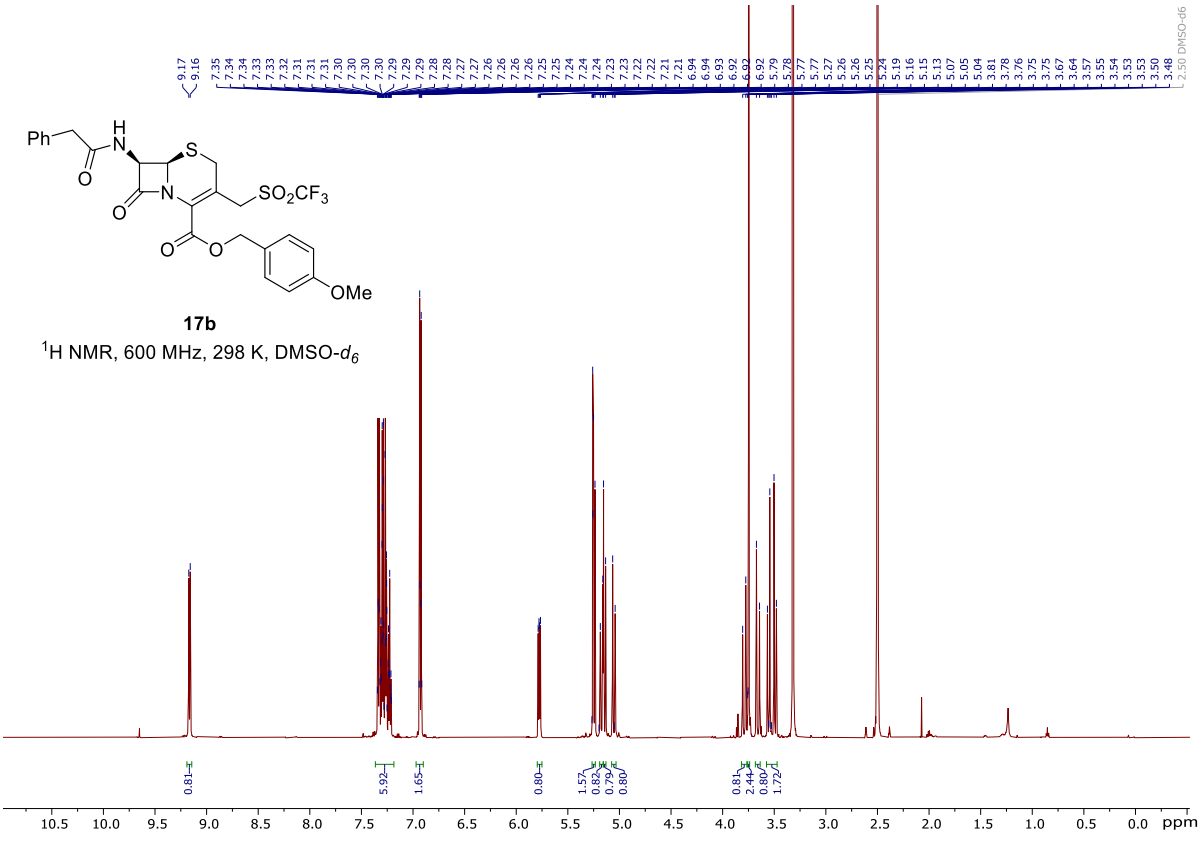

17b

^{1}H NMR, 600 MHz, 298 K, DMSO-d_6

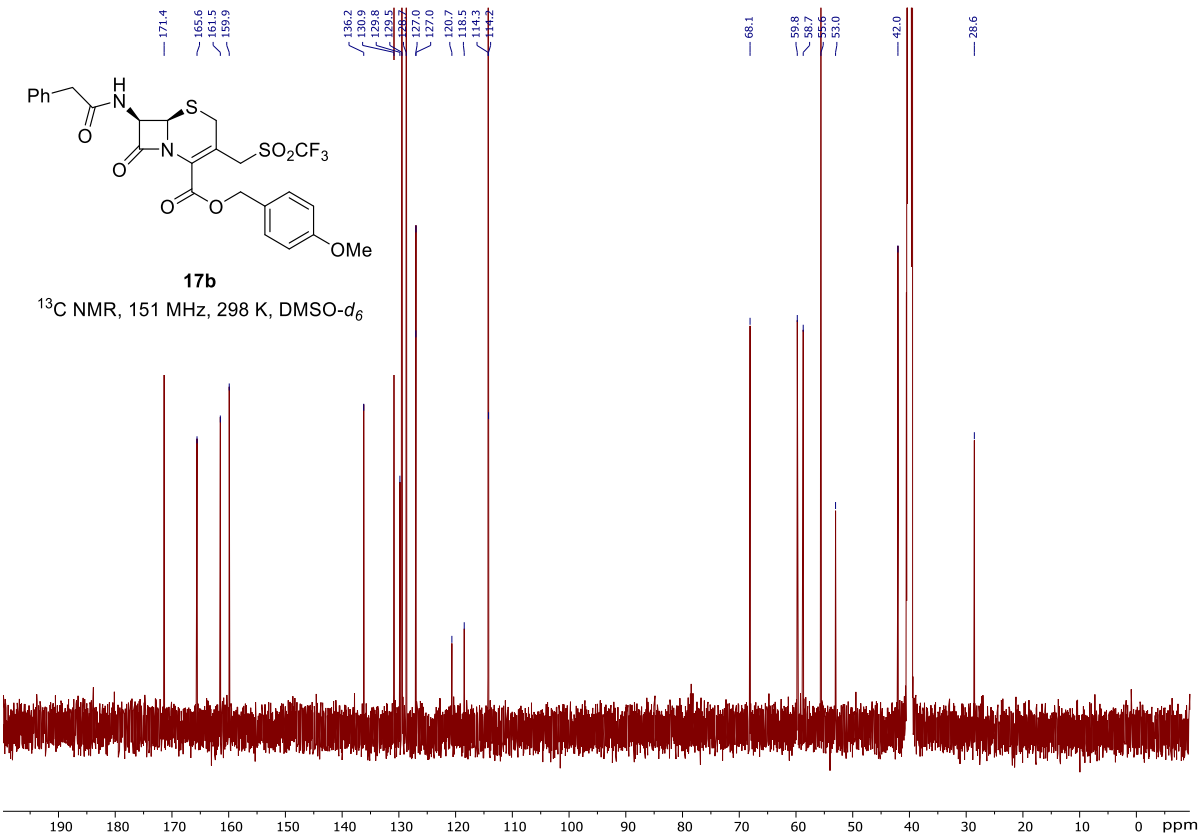

17b

^{13}C NMR, 151 MHz, 298 K, DMSO-d_6

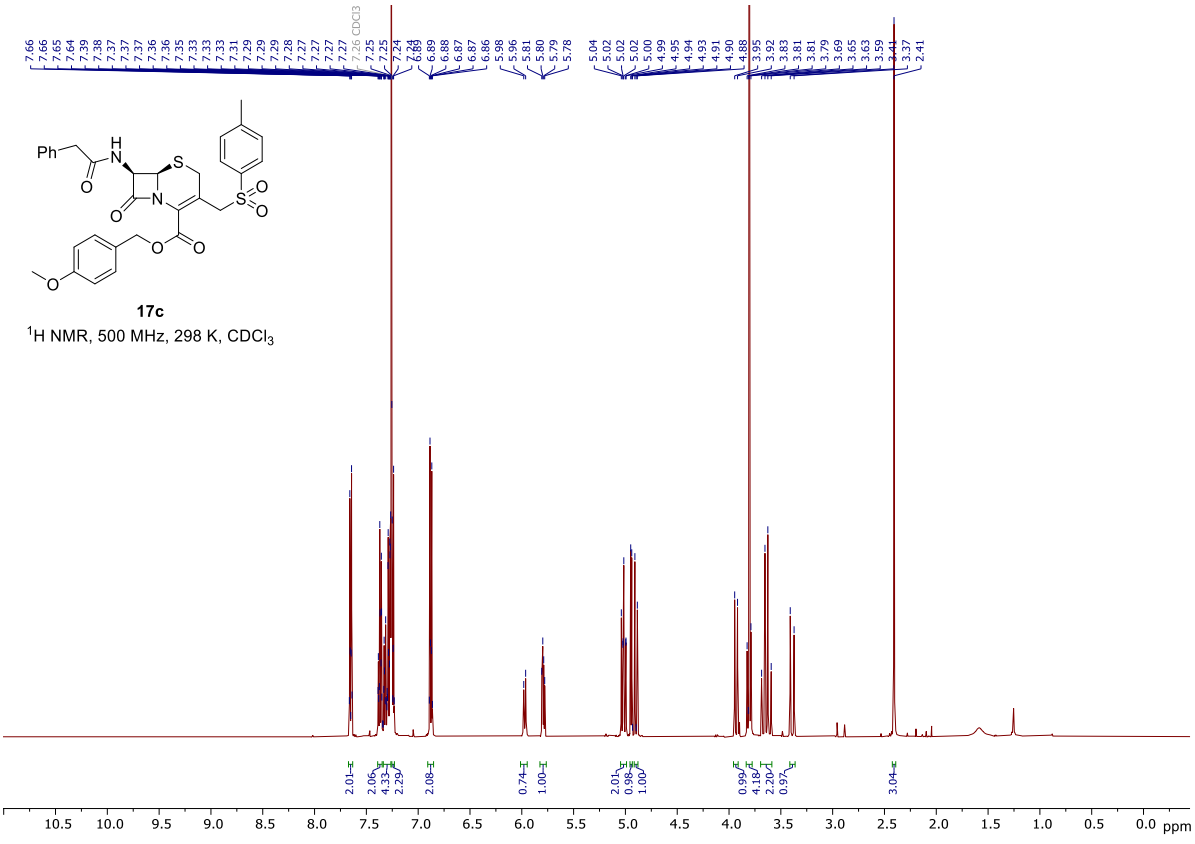
Ph
H
N
S
O
O
N
O
S
O
O
O
O
O
17c
^{1}H NMR, 500 MHz, 298 K, $CDCl_3$

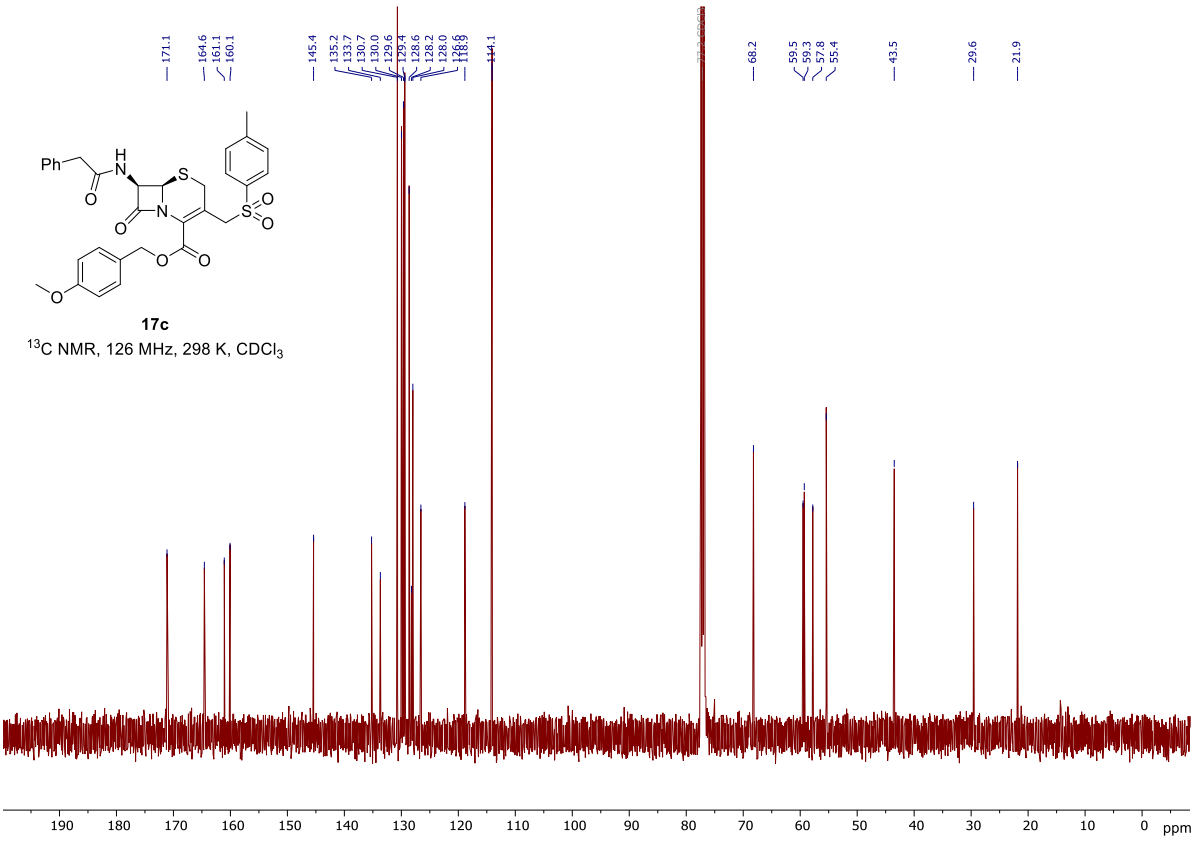
Ph
H
N
S
O
O
N
O
S
O
O
O
O
O
17c
^{13}C NMR, 126 MHz, 298 K, $CDCl_3$
ppm

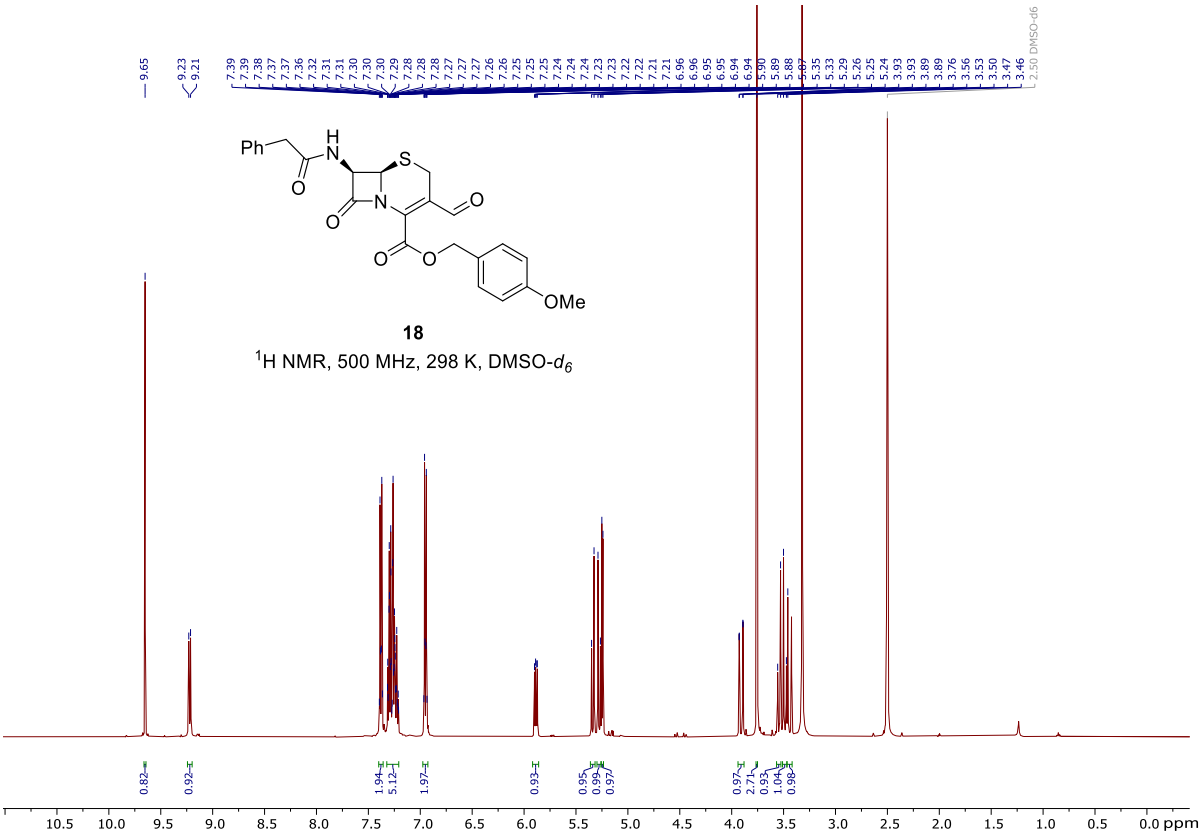

18

^{1}H NMR, 500 MHz, 298 K, DMSO-d_6

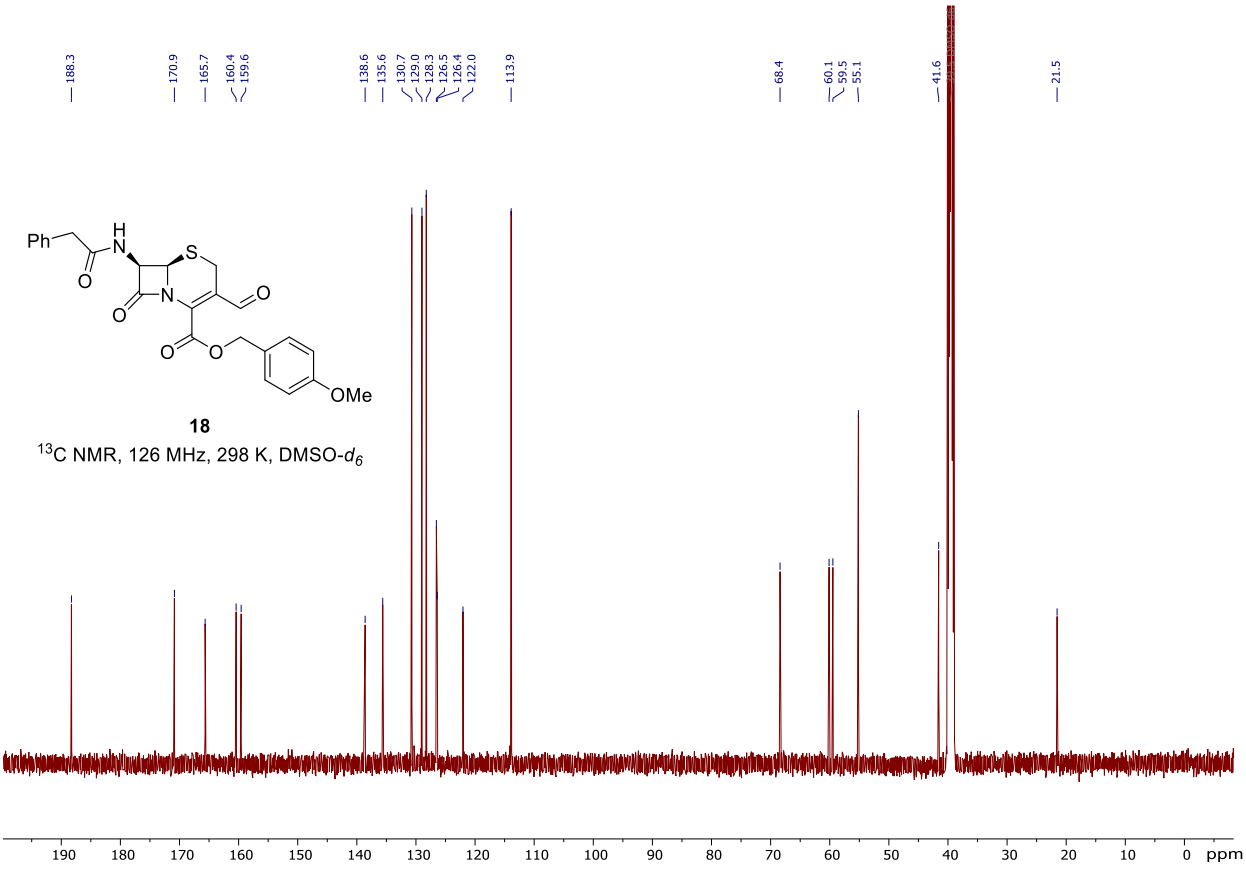

18

^{13}C NMR, 126 MHz, 298 K, DMSO-d_6

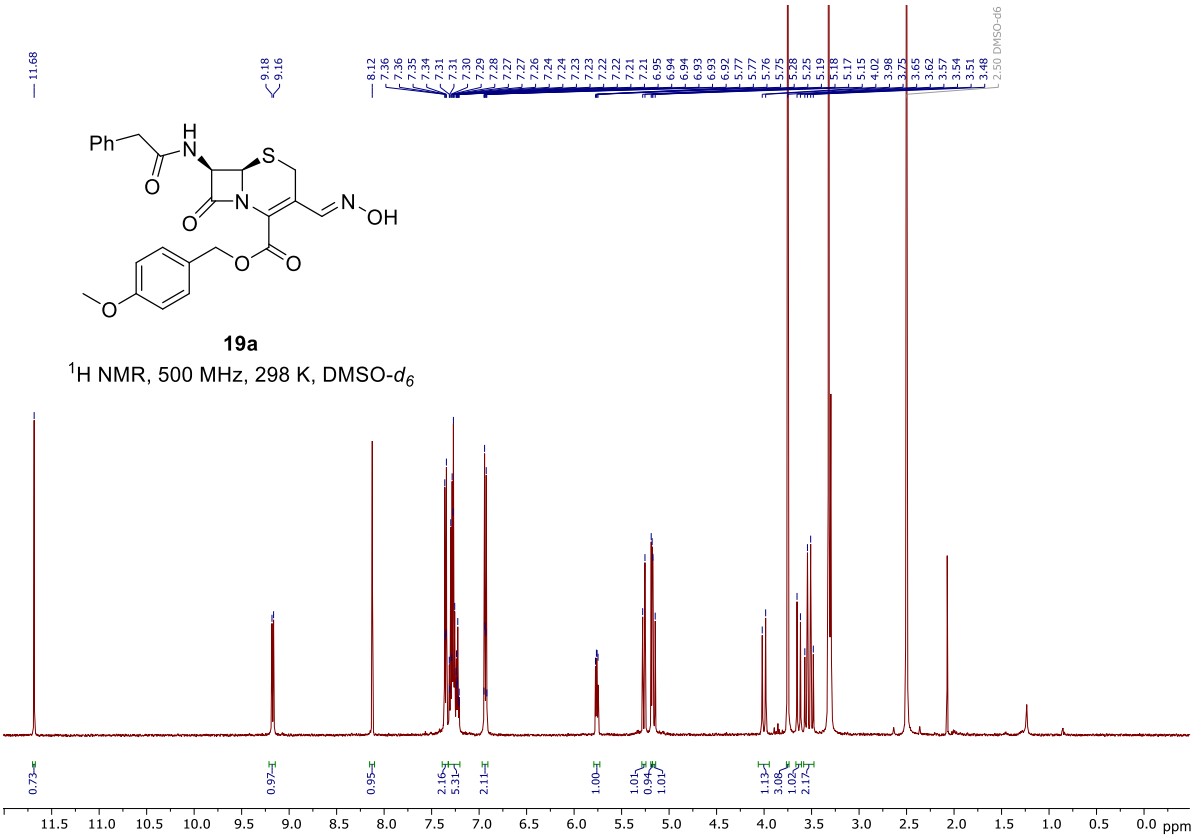

19a

^{1}H NMR, 500 MHz, 298 K, DMSO-d_6

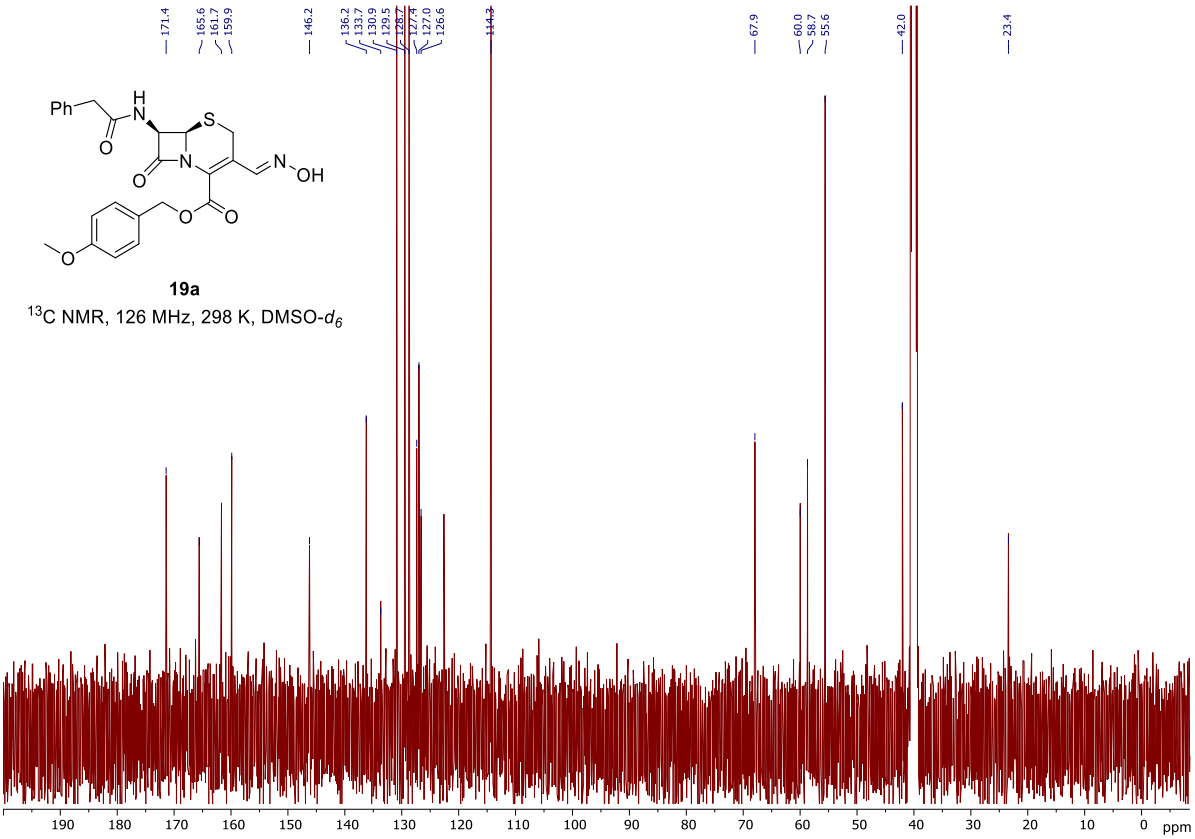

19a

^{13}C NMR, 126 MHz, 298 K, DMSO-d_6

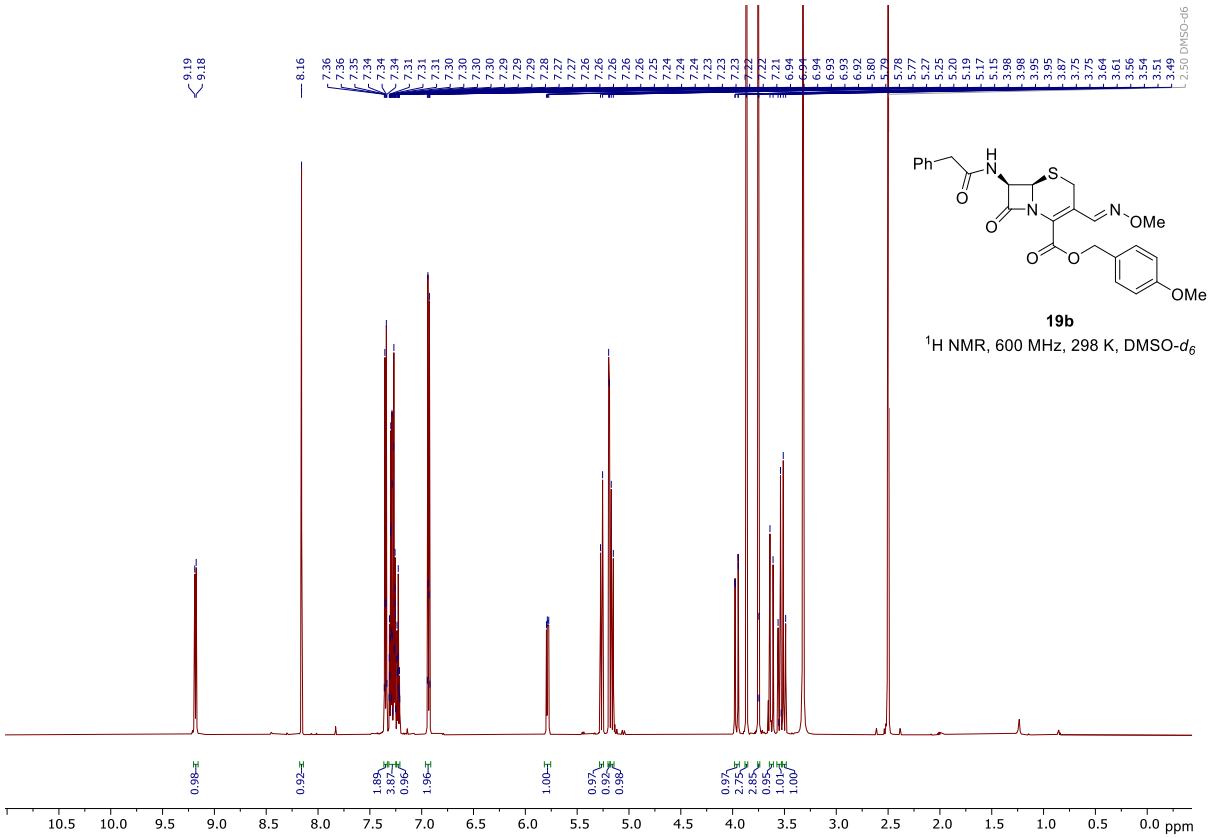
Ph
H
N
S
O
N
N
OMe
O
O
O
OMe
19b
^{1}H NMR, 600 MHz, 298 K, DMSO-d_6

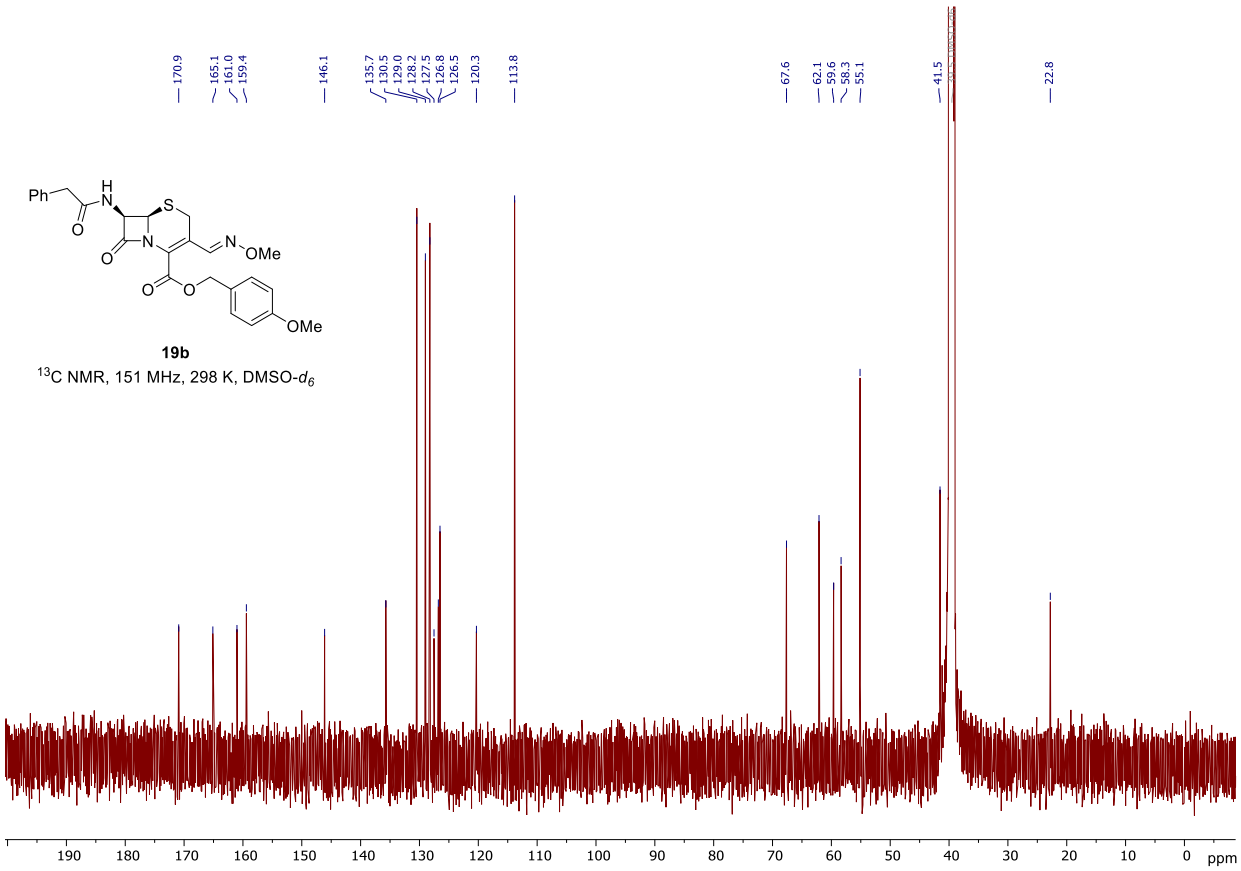
Ph
H
N
S
O
N
N
OMe
O
O
O
OMe
19b
^{13}C NMR, 151 MHz, 298 K, DMSO-d_6

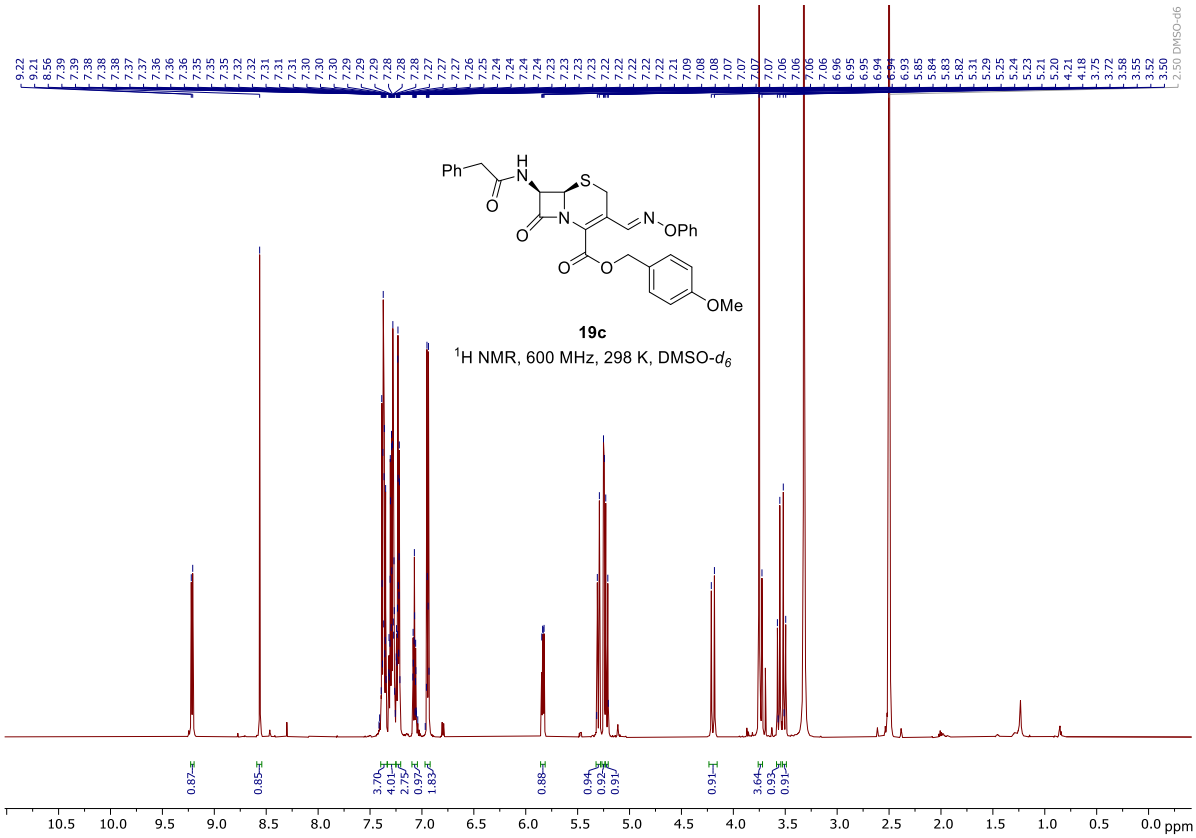
Ph
H
N
O
S
N
O
N
OPh
O
O
OMe
19c
^{1}H NMR, 600 MHz, 298 K, DMSO-d_6
DMSO-d6
0.87
0.85
3.70
4.01
2.75
0.97
1.83
0.88
0.94
0.92
0.91
0.91
3.64
0.93
0.91
ppm

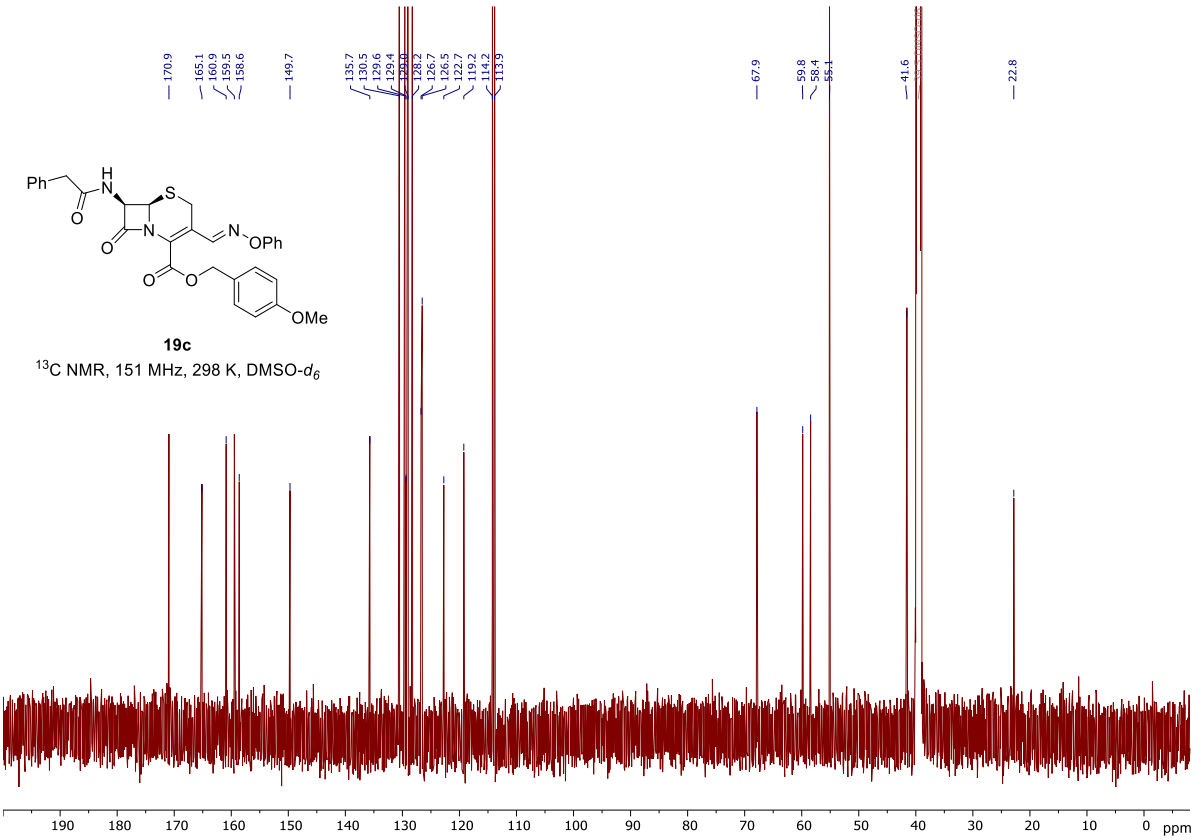
170.9
165.1
160.9
159.5
158.6
149.7
135.7
130.5
129.6
129.4
128.2
126.7
126.5
122.7
119.2
114.2
113.9
67.9
59.8
58.4
55.1
41.6
22.8
Ph
H
N
O
S
N
O
N
OPh
O
O
OMe
19c
^{13}C NMR, 151 MHz, 298 K, DMSO-d_6
ppm

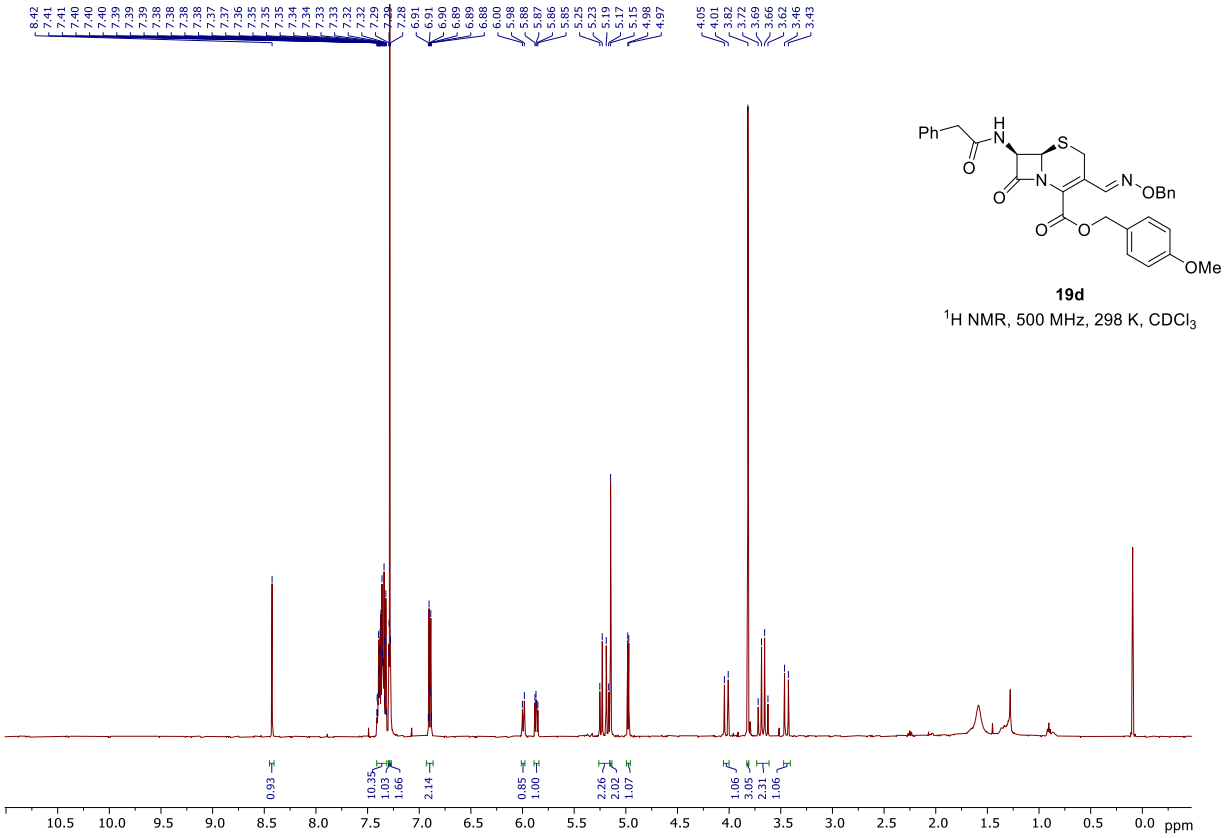

19d

^{1}H NMR, 500 MHz, 298 K, $CDCl_3$

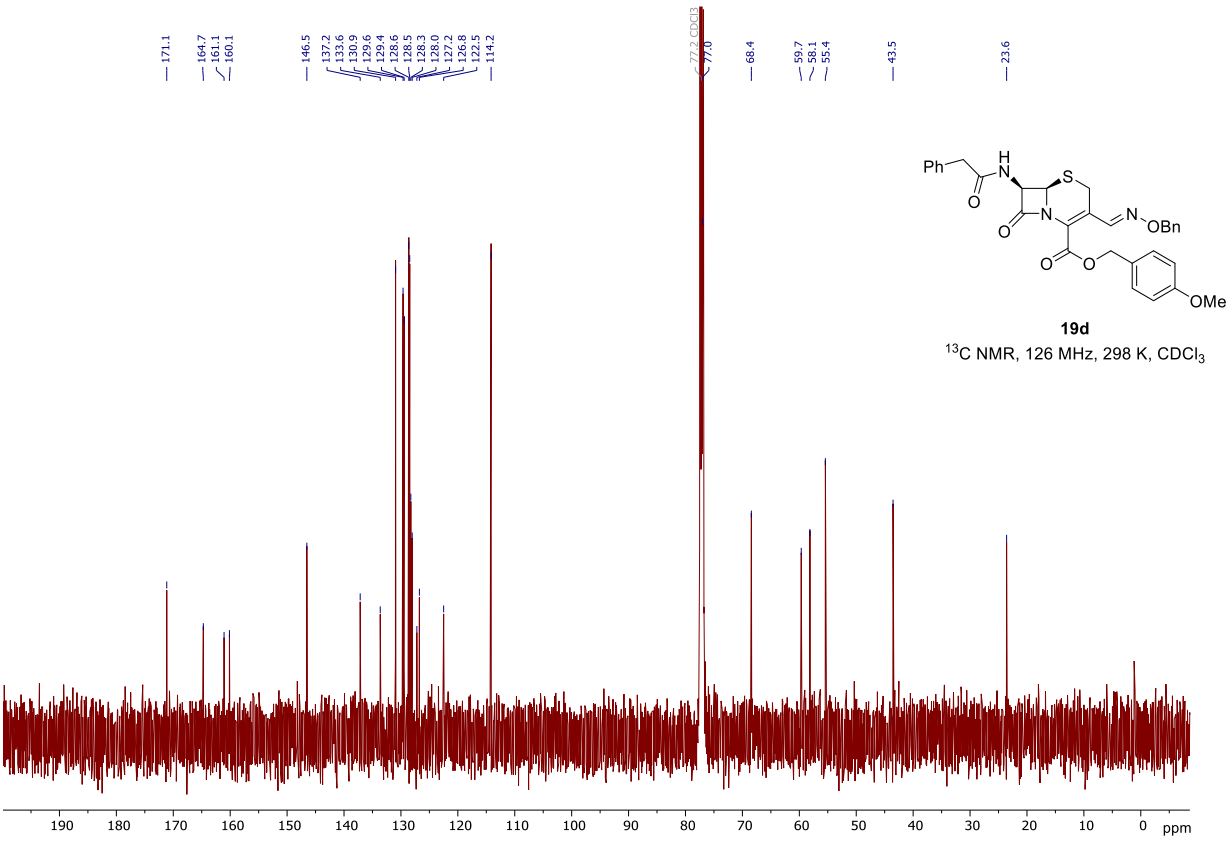

19d

^{13}C NMR, 126 MHz, 298 K, $CDCl_3$

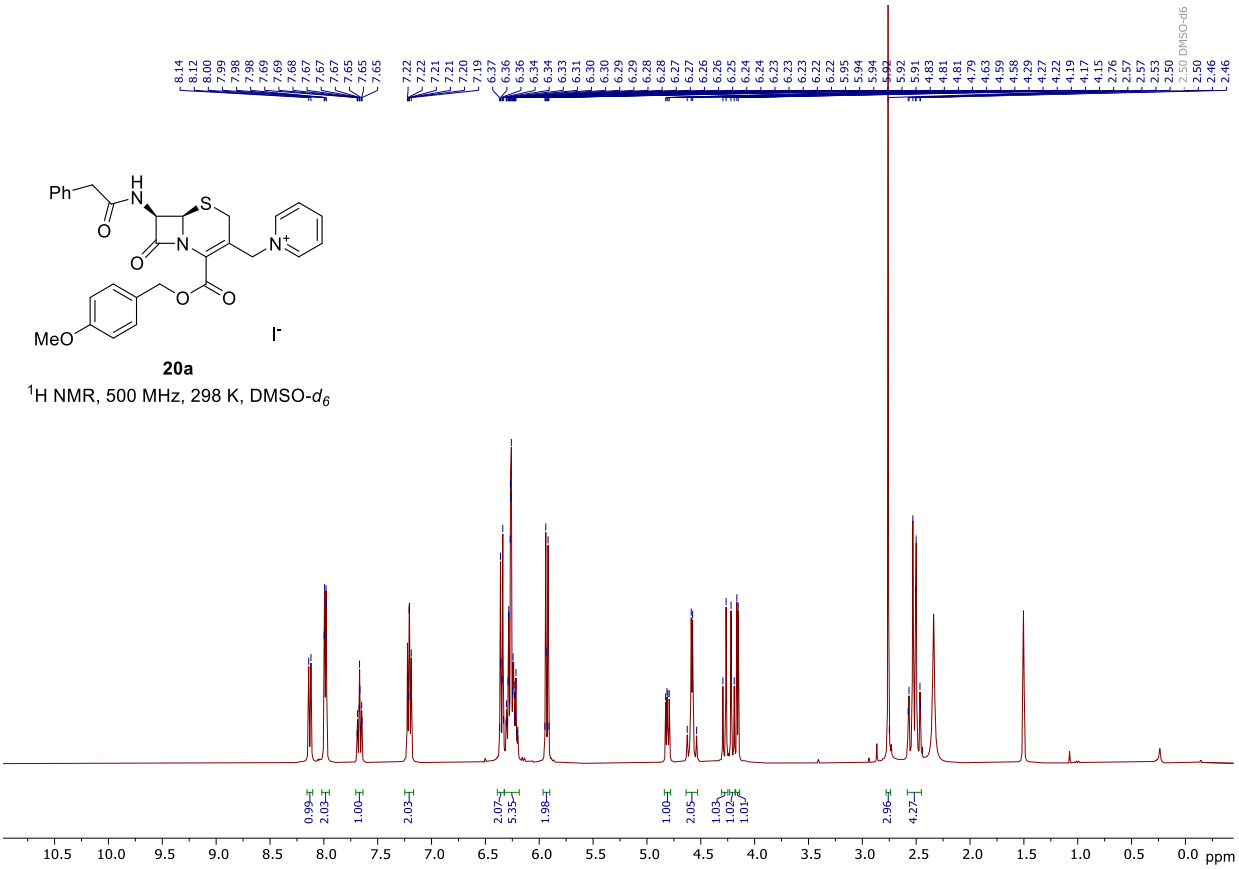

20a

^{1}H NMR, 500 MHz, 298 K, DMSO-d_6



20a

^{13}C NMR, 126 MHz, 298 K, DMSO-d_6

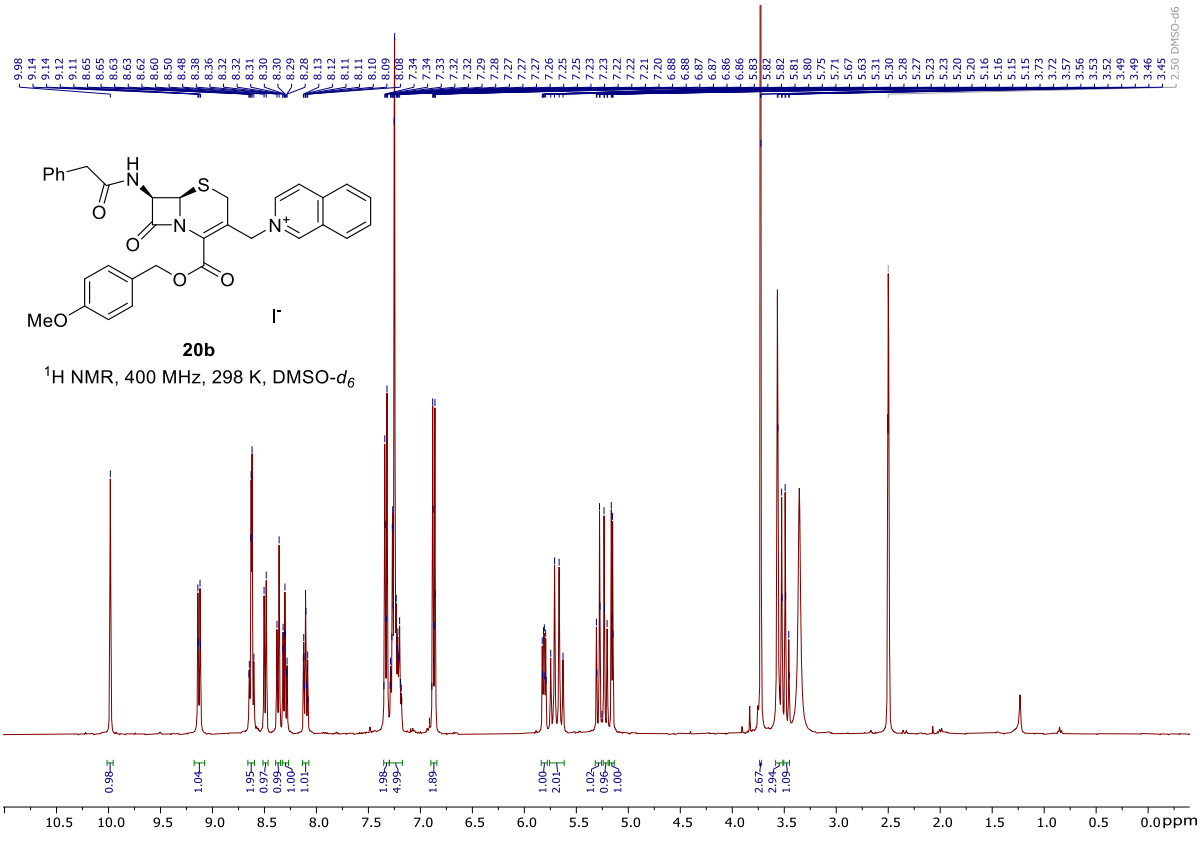

20b

^{1}H NMR, 400 MHz, 298 K, DMSO-d_6

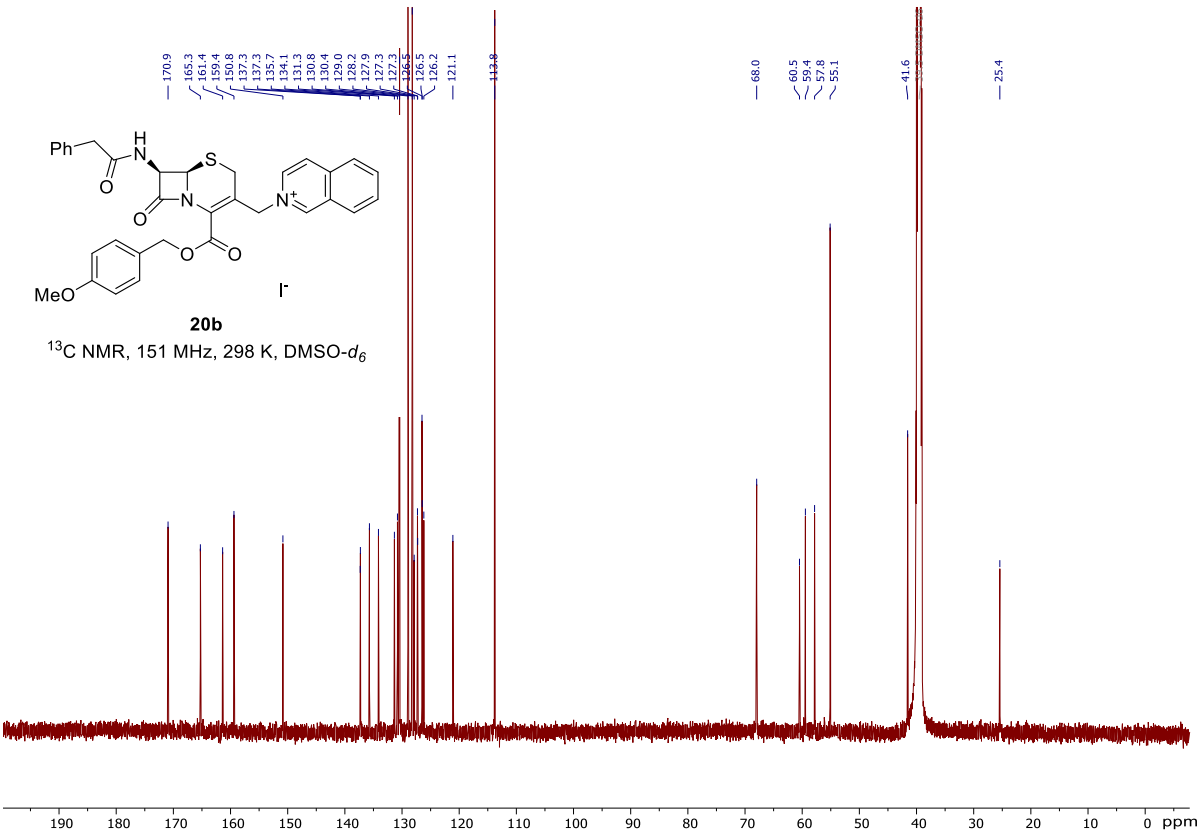

20b

^{13}C NMR, 151 MHz, 298 K, DMSO-d_6

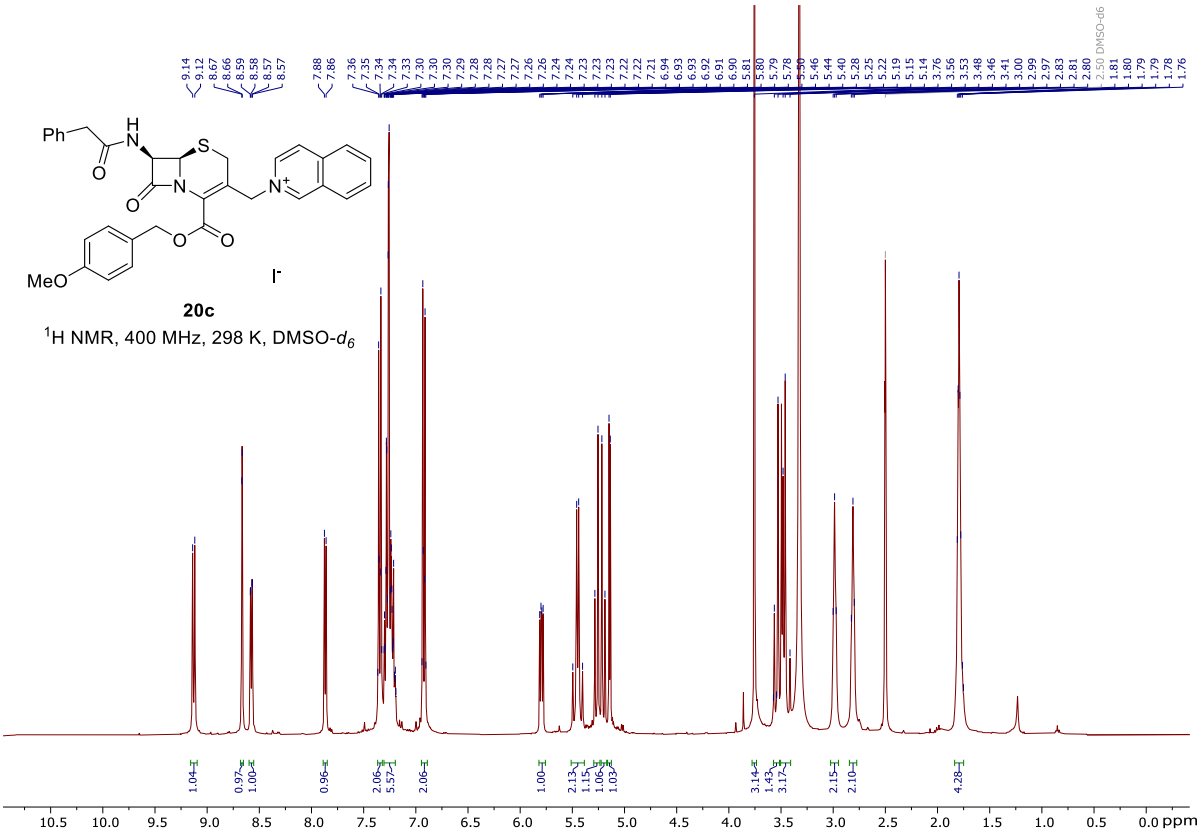
Ph
H
N
S
O
N
O
N+
O
O
MeO
I-
20c
1H NMR, 400 MHz, 298 K, DMSO-d6
DMSO-d6
10.5 10.0 9.5 9.0 8.5 8.0 7.5 7.0 6.5 6.0 5.5 5.0 4.5 4.0 3.5 3.0 2.5 2.0 1.5 1.0 0.5 0.0 ppm

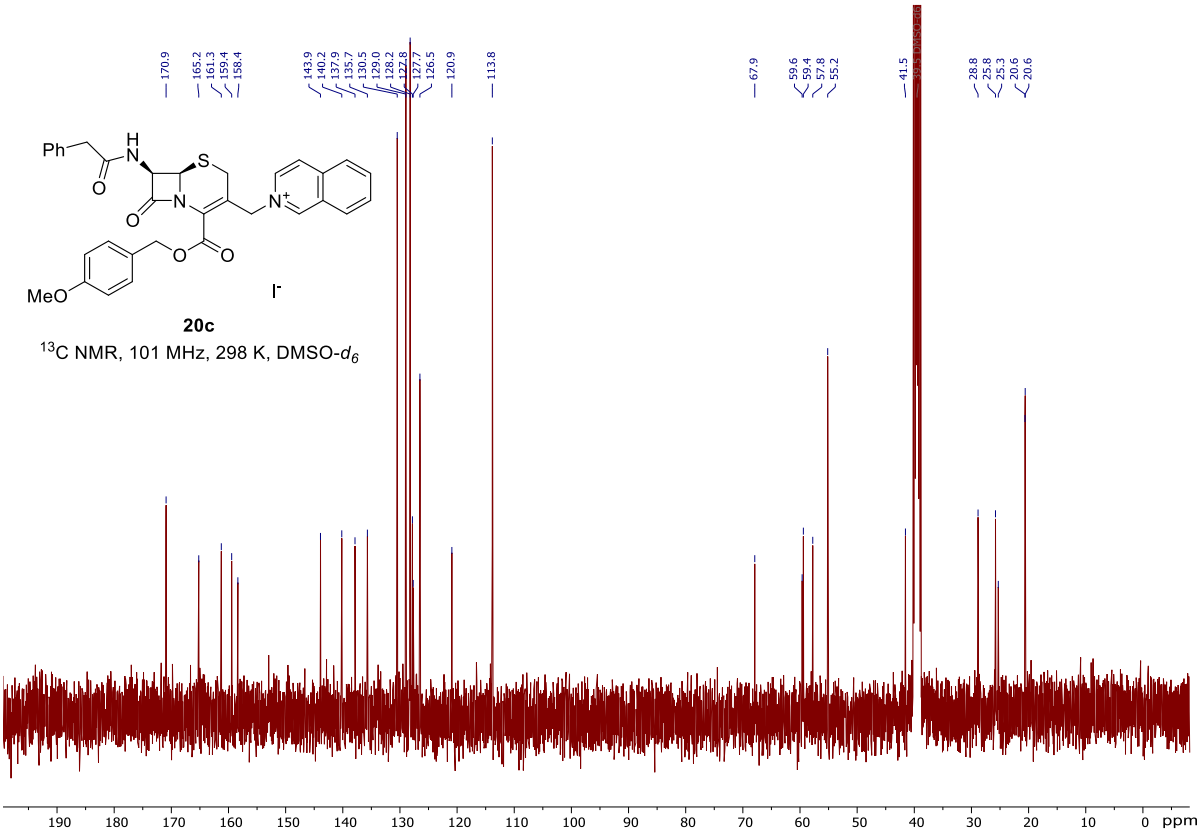
Ph
H
N
S
O
N
O
N+
O
O
MeO
I-
20c
13C NMR, 101 MHz, 298 K, DMSO-d6
190 180 170 160 150 140 130 120 110 100 90 80 70 60 50 40 30 20 10 0 ppm

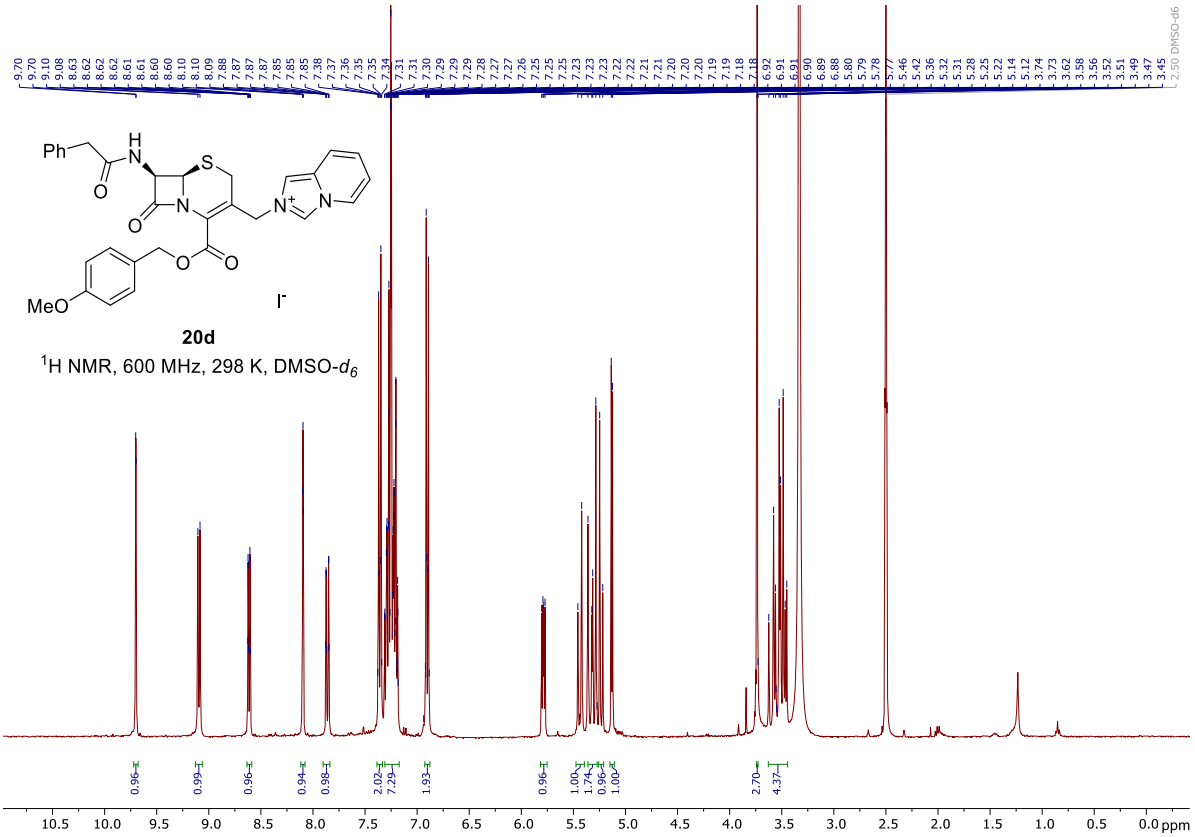

20d

^{1}H NMR, 600 MHz, 298 K, DMSO-d_6

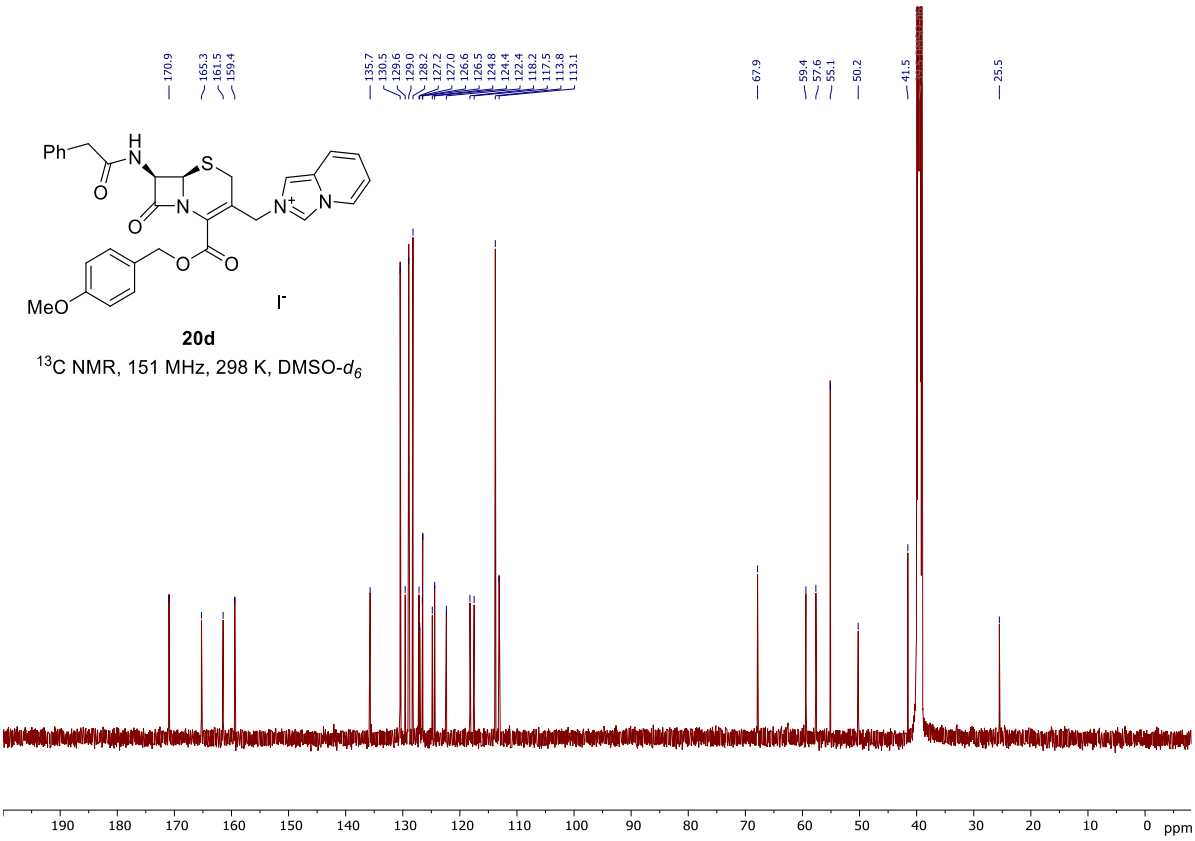

20d

^{13}C NMR, 151 MHz, 298 K, DMSO-d_6

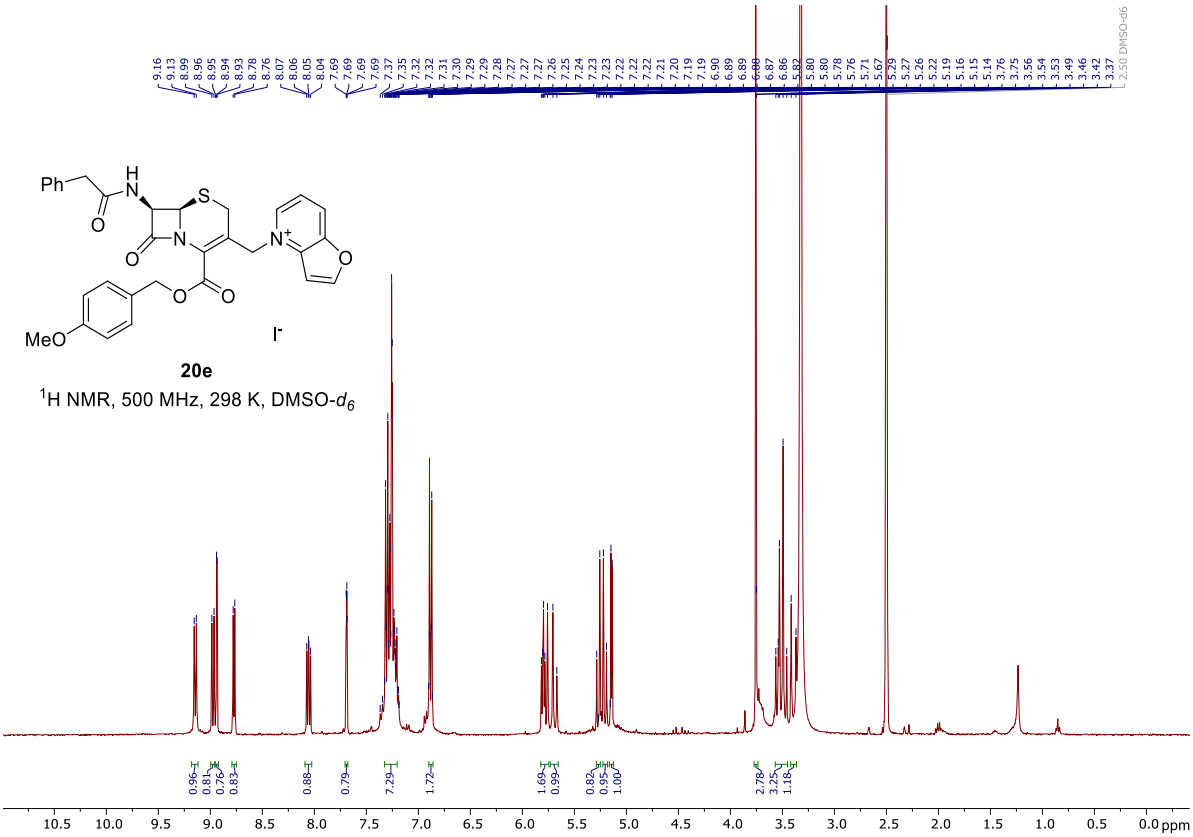

20e

^{1}H NMR, 500 MHz, 298 K, DMSO-d_6

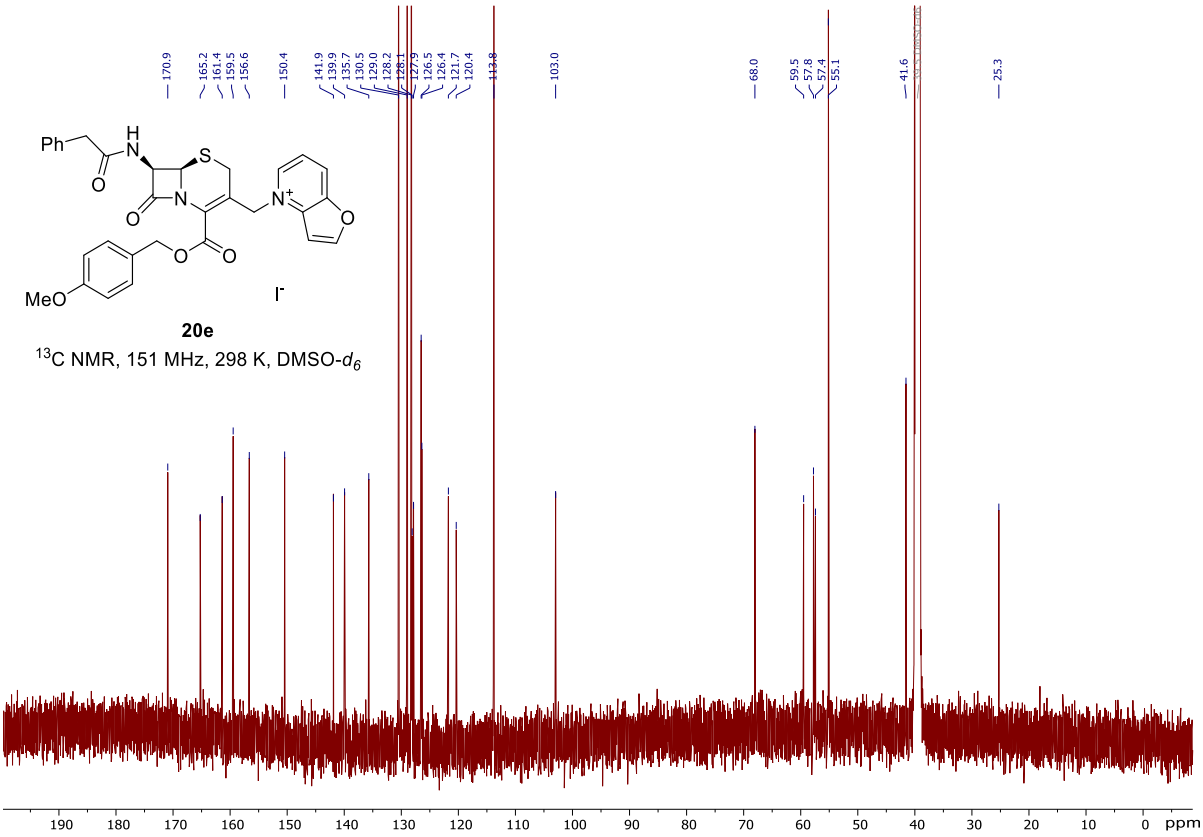

20e

^{13}C NMR, 151 MHz, 298 K, DMSO-d_6

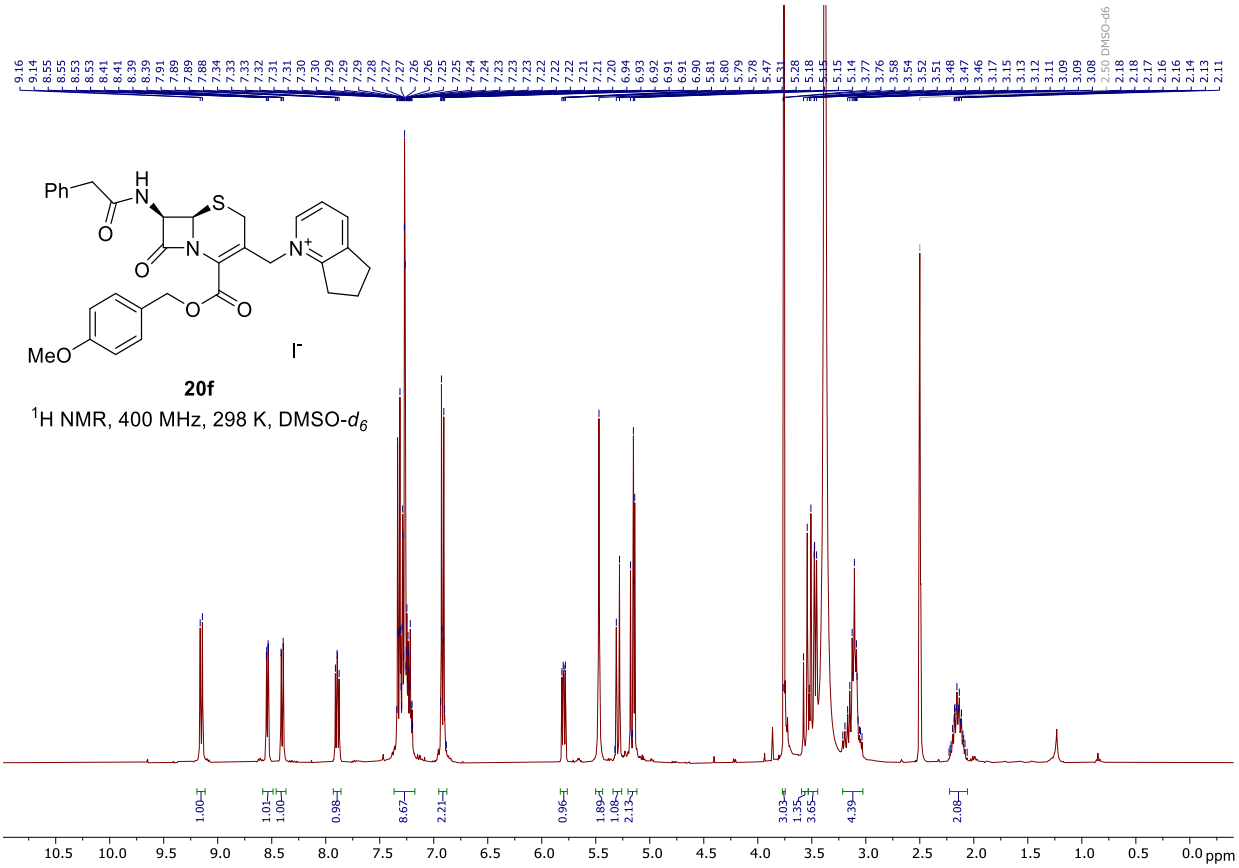
Ph
H
N
S
O
N
O
N+
O
O
MeO
I-
20f
1H NMR, 400 MHz, 298 K, DMSO-d6
DMSO-d6
1.00
1.01
1.00
0.98
8.67
2.21
0.96
1.89
1.08
2.13
3.03
1.35
3.65
4.39
2.08
ppm

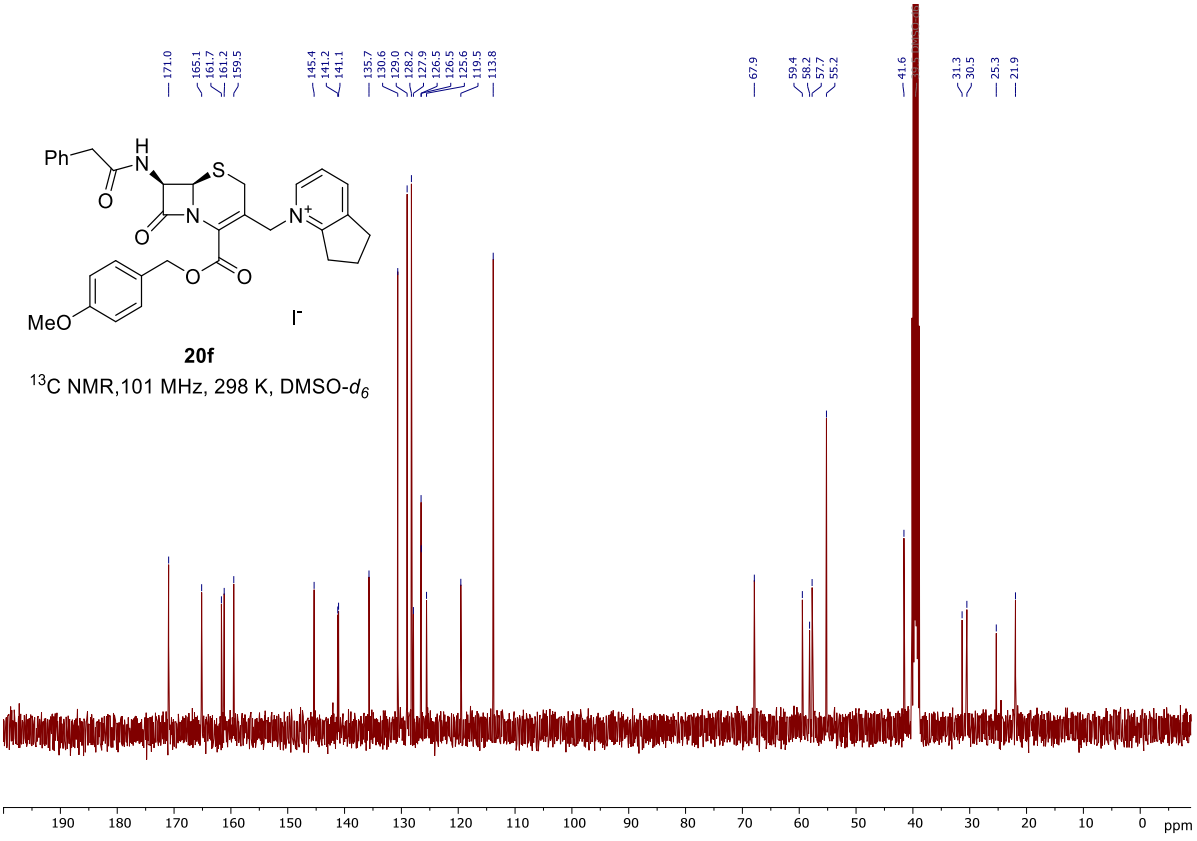
Ph
H
N
S
O
N
O
N+
O
O
MeO
I-
20f
13C NMR,101 MHz, 298 K, DMSO-d6
171.0
165.1
161.7
161.2
159.5
145.4
141.2
141.1
135.7
130.6
129.0
128.2
127.9
126.5
126.5
125.6
119.5
113.8
67.9
59.4
58.2
57.7
55.2
41.6
31.3
30.5
25.3
21.9
ppm

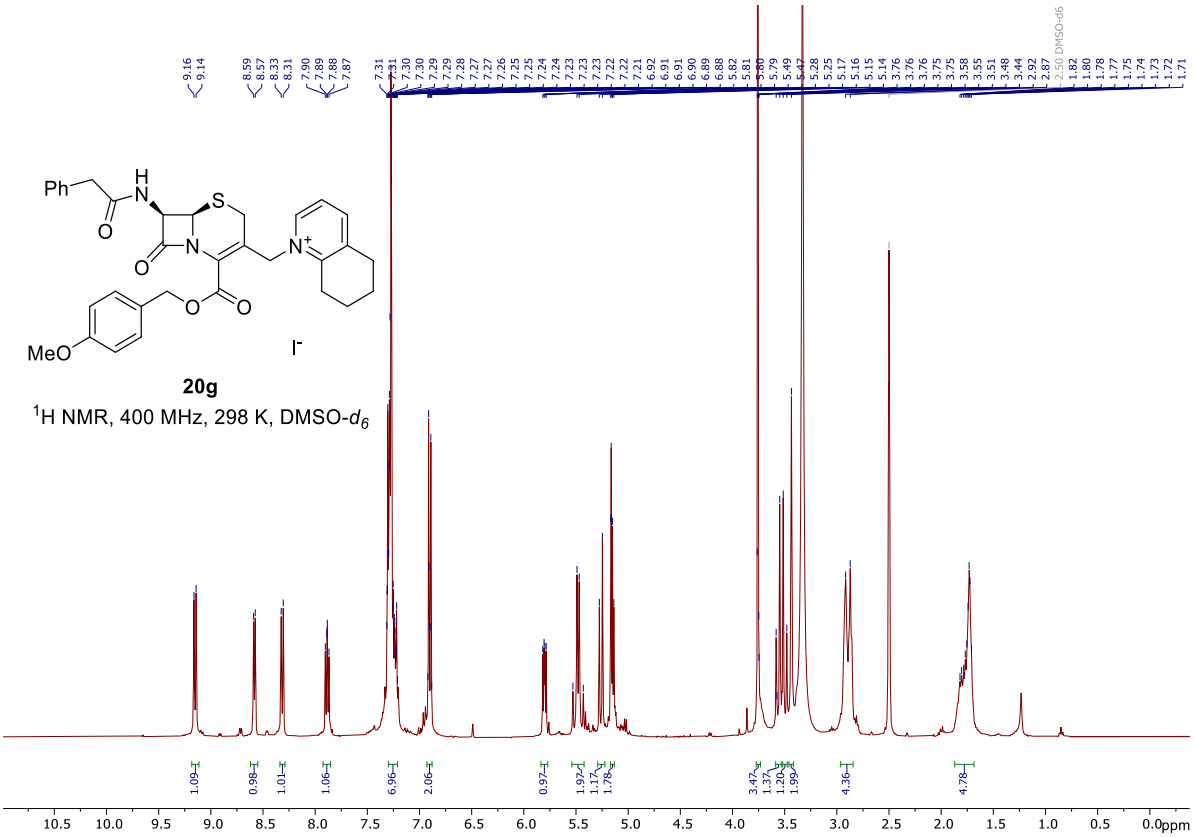

20g

^{1}H NMR, 400 MHz, 298 K, DMSO-d_6

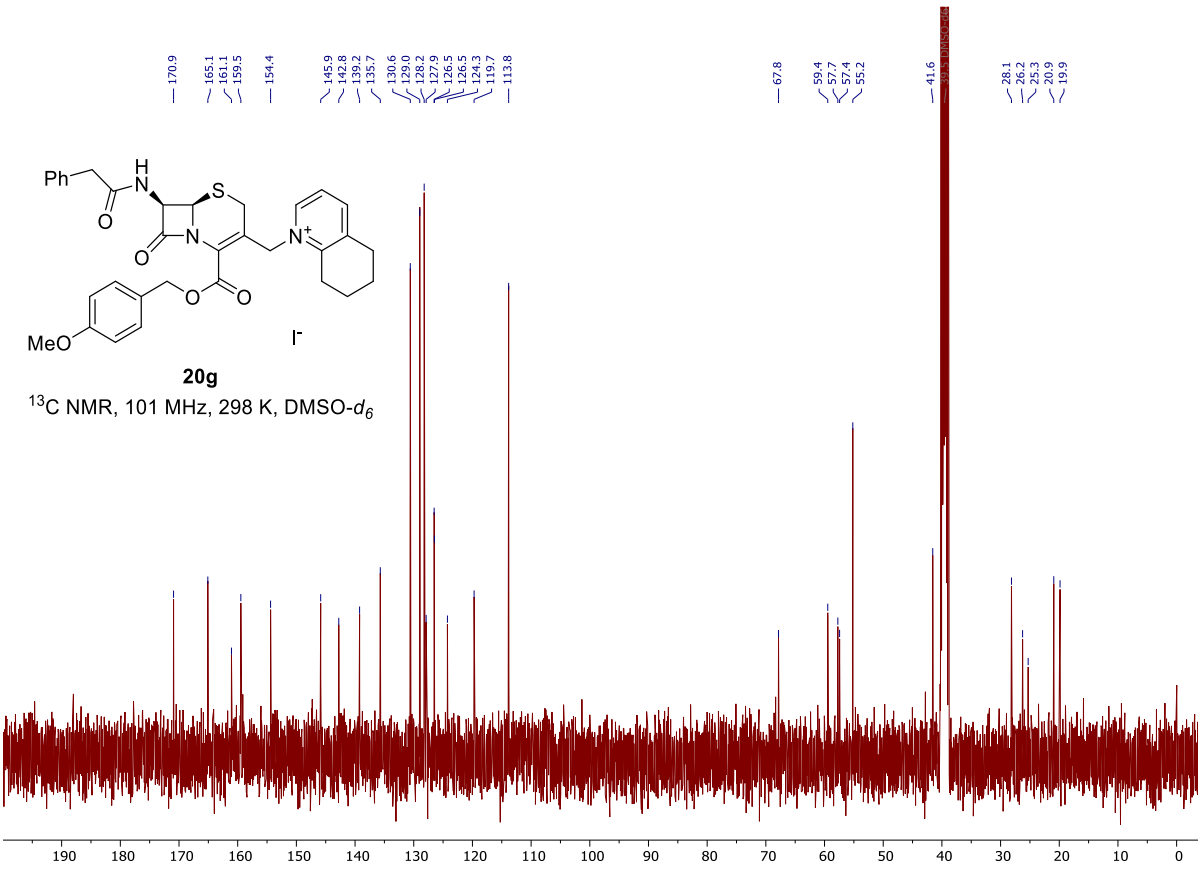

20g

^{13}C NMR, 101 MHz, 298 K, DMSO-d_6

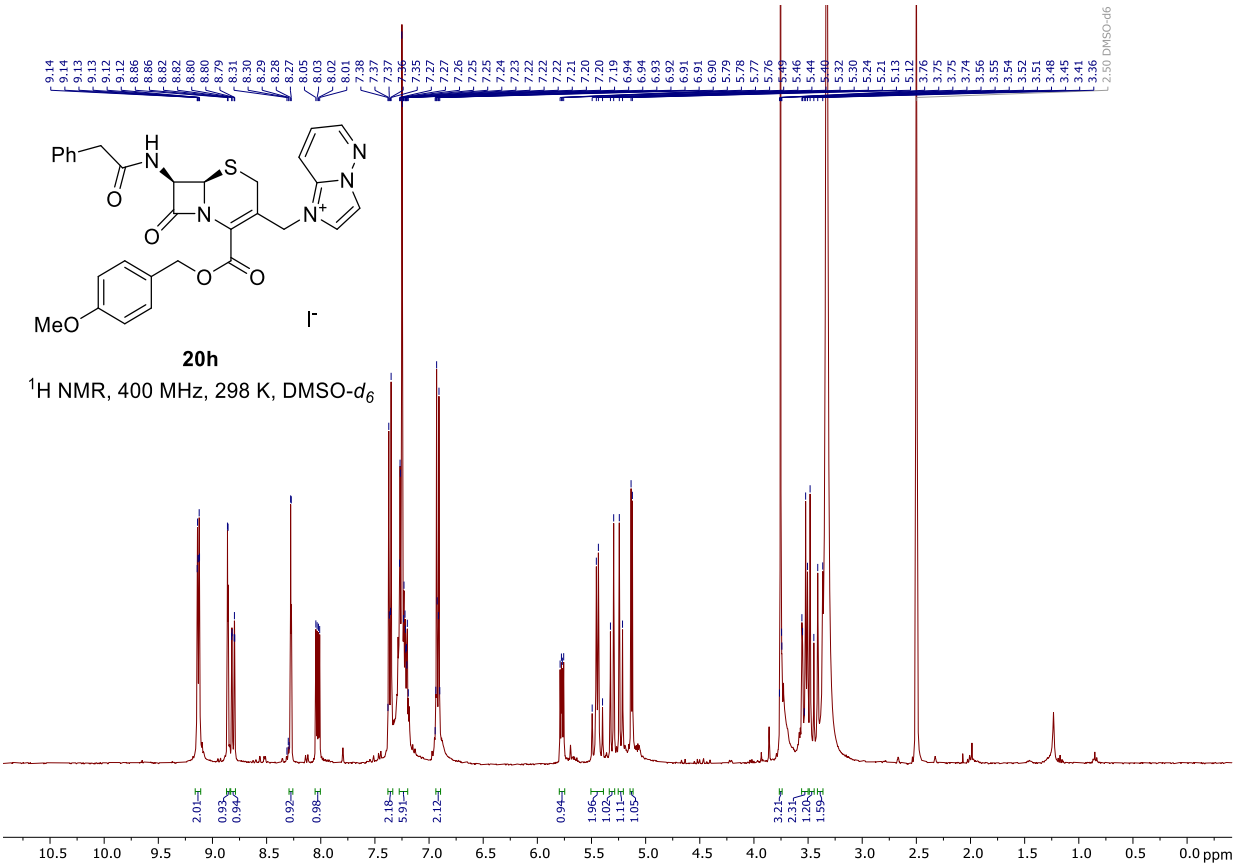
Ph
H
N
O
S
N
O
N
N
N+
O
O
MeO
I-
20h
1H NMR, 400 MHz, 298 K, DMSO-d6
2.50 DMSO-d6
ppm

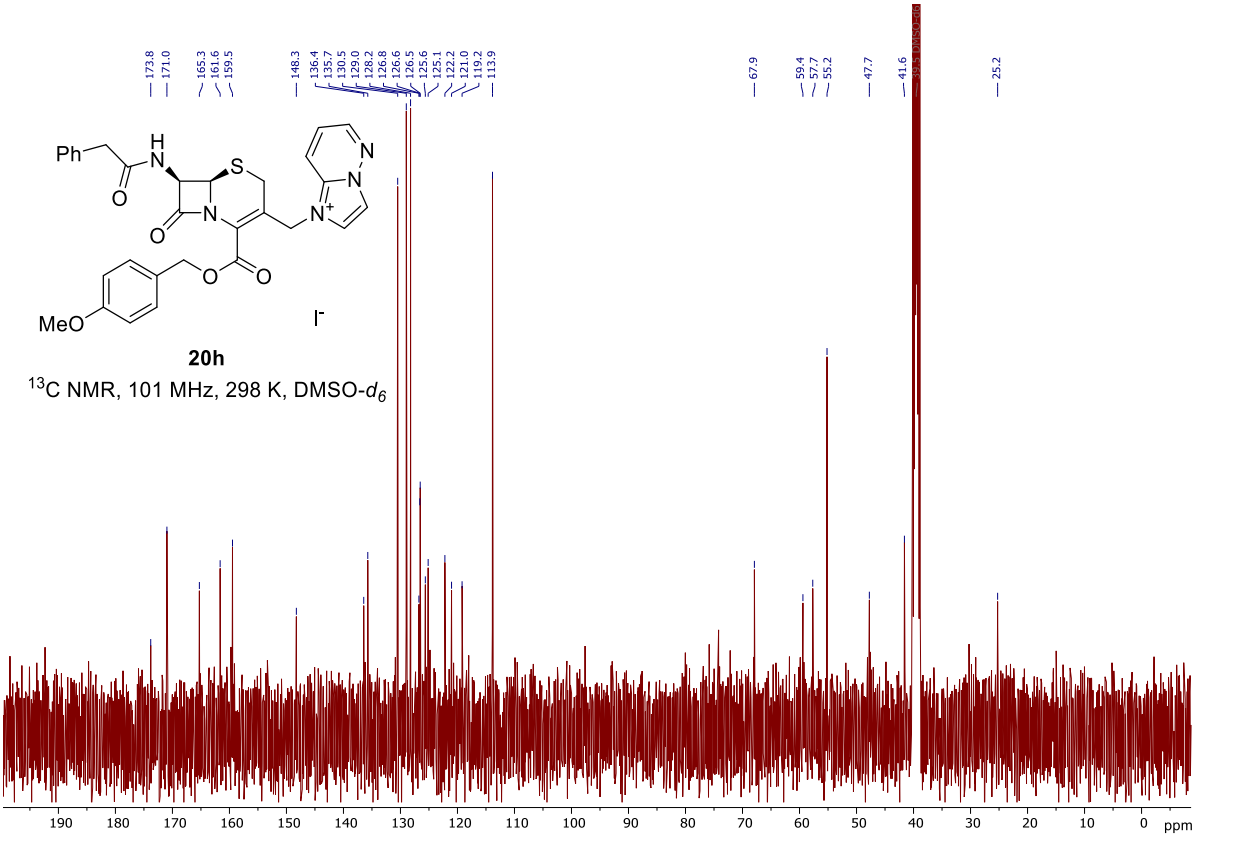
Ph
H
N
O
S
N
O
N
N
N+
O
O
MeO
I-
20h
13C NMR, 101 MHz, 298 K, DMSO-d6
39.5 DMSO-d6
ppm

8.3 Appendix to Chapter IV (Manuscript III)

8.3.1 General synthesis information

Ampicillin, sulbactam, avibactam, durlobactam, captopril, as well as all the reagents employed in synthesis were obtained from commercial sources (Sigma-Aldrich, Inc.; Flurochem Ltd.; Manchester Organics; Tokyo Chemical Industry Ltd.; Ambeed Inc.; MedChemExpress LLC; AstaTech Inc.; AK Scientific Inc.; Apollo Scientific Ltd.; Key Organics Ltd.; Aurum Pharmatech LLC; Biosynth Ltd.) and were used without further purification. The synthesis of **7a-d** and **8a-d** is described in **Appendix 8.1**.

Anhydrous solvents (Sigma-Aldrich, Inc.) were kept under an atmosphere of argon. HPLC grade solvents (Sigma-Aldrich Inc.) were used for reaction work-ups, extractions, and purifications. Flash column chromatography was performed using an automated Biotage Isolera One purification machine equipped with Biotage®Sfär flash chromatography cartridges. ^{1}H and ^{13}C NMR spectra were recorded using Bruker AVANCE AVIIIHD 400, 500 and 600 MHz machines. Chemical shifts for protons are reported in parts per million (ppm) downfield from tetramethylsilane and are referenced to residual protium in the NMR solvent (*i.e.*, $CDCl_3$: δ = 7.26 ppm; DMSO-d_6: δ = 2.50 ppm). For ^{13}C NMR, chemical shifts are reported in the scale relative to the NMR solvent (*i.e.*, $CDCl_3$: δ = 77.2 ppm; DMSO-d_6: δ = 39.5 ppm). NMR data are reported in the following manner: chemical shift, multiplicity, coupling constant (J, Hz; to nearest 0.1 Hz), and integration.

Infrared (IR) spectroscopy was performed using a Bruker Tensor-27 Fourier transform infrared (FT-IR) spectrometer. High-resolution mass spectrometry (HRMS) was performed using either electro-spray ionization (ESI) mass spectrometry (MS) in the positive or negative ionization modes employing a Thermo Scientific Exactive mass spectrometer (ThermoFisher Scientific), or

atmospheric pressure chemical ionization (APCI) in the positive mode using an Agilent 7200 Accurate mass spectrometer; data are presented as a mass-to-charge ratio (m/z). Optical rotation ($[\alpha]_D^{25}$) measurements were performed using a Bellingham + Stanley (ADP450) polarimeter.

8.3.2 General synthesis procedures

General Procedure A

A variation of a reported procedure was followed.[1] To a solution of commercially sourced (+)-6-aminopenicillanic acid (**6-APA**; 1 equiv.) in acetone (0.1 M) was added Et_3N (1.1 equiv.) at 0 °C. After stirring for 30 min at 0 °C, a solution of an alkyl bromide (1.1 equiv.) in acetone (0.1 M) was added dropwise to the reaction mixture; the mixture was stirred for 4 h at 0 °C. The reaction mixture was poured into Et_2O; the formed precipitate was removed by filtration. The filtrate was sequentially washed with saturated aqueous $NaHCO_3$ solution and brine, then dried over Na_2SO_4 and filtered. The organic solution was cooled to 0 °C, then a solution of *p*-toluenesulfonic acid monohydrate (1.1 equiv.) in acetone (0.05 M) was added. The resulting precipitate was collected by filtration and dried *in vacuo.*

General procedure B

To a stirred solution of a penam in anhydrous EtOAc (1 equiv.; 0.02-0.4 M) was added Pd/C (10 wt. %, 0.55-0.75 equiv.). $Ar_{(g)}$ was bubbled through the reaction mixture for 10 min, then $H_{2(g)}$ was bubbled through the solution for 10 min. The reaction mixture was stirred under $H_{2(g)}$ for 4 h at room temperature, before degassing with $Ar_{(g)}$. The mixture was filtered through a pad of Celite® Hyflo Supercel; the filtrate was then concentrated *in vacuo* and purified by reverse-phase flash

column chromatography. The fractions containing the purified product were collected and lyophilised to afford the desired product.

General procedure C

To a stirred solution of a penam in CH_2Cl_2 (1 equiv.; 0.16 M) was added an ice-cold aqueous solution of $NaNO_2$ (2.6 equiv.; 0.9 M), followed by addition of *p*-toluenesulfonic acid monohydrate (0.3 equiv.). The reaction mixture was stirred for 20 min at 0 °C, then the organic layer was separated, and the aqueous phase was extracted with CH_2Cl_2. The combined extracts were sequentially washed with saturated aqueous $NaHCO_3$, H_2O, then dried over Na_2SO_4, filtered, and concentrated *in vacuo* at 30 °C to give crude 4-nitrobenzyl (2*S*,5*R*)-6-diazo-3,3-dimethyl-7-oxo-4-thia-1-azabicyclo[3.2.0]heptane-2-carboxylate. The crude residue was dissolved in anhydrous CH_2Cl_2 (0.2 M), to which an anhydrous alcohol (40-120 equiv.) and *p*-toluenesulfonic acid monohydrate (0.1 equiv.) were added sequentially. The mixture was stirred at 0 °C for 5 min, then at 20 °C for 1-18 h, before being diluted with CH_2Cl_2. The mixture was washed with saturated aqueous $NaHCO_3$ solution and H_2O. The organic layer was dried over Na_2SO_4, filtered, concentrated *in vacuo*, and purified by flash column chromatography.

8.3.3 Experimental procedures and compounds characterisations

(2*S*,5*R*,6*R*)-2-((Benzyloxy)carbonyl)-3,3-dimethyl-7-oxo-4-thia-1-azabicyclo[3.2.0]heptan-6-aminium 4-methylbenzenesulfonate (**5**)

General procedure A was applied using **6-APA** (5 g, 23 mmol, 1 equiv.)

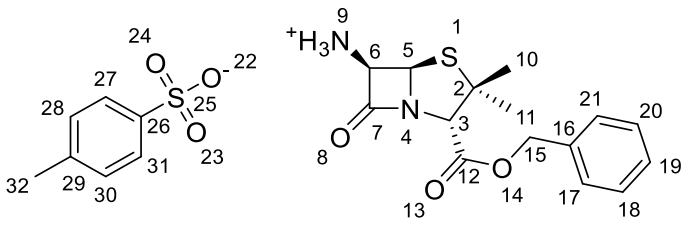

and benzyl bromide (3 mL, 25 mmol, 1.1 equiv.), yielding after the work-up product **5** (7 g, 63%).

White solid; m.p.: 149 °C (decomposition); ^{1}H NMR (400 MHz, 298 K, DMSO-*d*$_6$): δ = 8.89 (s, 2H, *N9H*$_2$), 7.52 – 7.46 (m, 2H, *C27H*, *C31H*), 7.45 – 7.33 (m, 5H, *C17H*, *C18H*, *C19H*, *C20H*, *C21H*), 7.15 – 7.08 (m, 2H, *C28H*, *C30H*), 5.53 (d, *J* = 4.3 Hz, 1H, *C6H*), 5.22 (m, 2H, *C15H*$_2$), 5.12 (d, *J* = 4.3 Hz, 1H, *C5H*), 4.57 (s, 1H, *C3H*), 2.29 (s, 3H, *C32H*$_3$), 1.61 (s, 3H, *C10H*$_3$), 1.39 ppm (s, 3H, *C10H*$_3$); ^{13}C NMR (101 MHz, 298 K, DMSO-*d*$_6$): δ = 168.6, 167.0, 145.5, 137.7, 135.1, 128.7, 128.6, 128.5, 128.1, 125.5, 69.8, 67.1, 65.2, 64.1, 57.1, 30.8, 26.6, 20.8 ppm; ; IR (film): ṽ = 1783, 1735, 1537, 1461, 1385, 1319, 1181, 1123, 1034 cm^{-1}; HRMS (ESI): m/z calculated for $C_{15}H_{18}N_2O_3SNa$ $[M+Na\text{-}(4\text{-}Me)C_6H_4SO_3H]^+$: 329.0930; found: 329.0932; $[\alpha]_D^{25}$ = +116 (c = 0.004 g/mL, acetone).

(2*S*,5*R*,6*R*)-3,3-Dimethyl-2-(((4-nitrobenzyl)oxy)carbonyl)-7-oxo-4-thia-1-azabicyclo[3.2.0]heptan-6-aminium 4-methylbenzenesulfonate (**6**)

General Procedure A was applied using **6-APA** (10 g, 46 mmol, 1 equiv.) and 4-nitrobenzyl bromide (11 g, 50 mmol, 1.1 equiv.), yielding after the work-up product **6** (10.6 g, 44%).

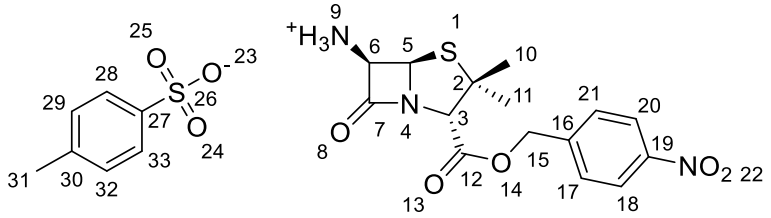

White solid; m.p.: 142 °C (decomposition); ^{1}H NMR (400 MHz, 298 K, DMSO-*d*$_6$): δ = 8.88 (s, 2H, *N9H*$_2$), 8.30 – 8.22 (m, 2H, *C18H*, *C20H*), 7.74 – 7.67 (m, 2H, *C17H*, *C21H*), 7.51 – 7.44 (m, 2H, *C28H*, *C33H*), 7.13 – 7.09 (d, *J* = 8.0 Hz, 2H, *C29H*, *C32H*), 5.55 (d, *J* = 4.3 Hz, 1H, *C6H*), 5.37 (m, 2H, *C15H*$_2$), 5.13 (d, *J* = 4.3 Hz, 1H, *C5H*), 4.66 (s, 1H, *C3H*), 2.29 (s, 3H, *C31H*$_3$), 1.63 (s, 3H, *C10H*$_3$), 1.43 ppm (s, 3H, *C11H*$_3$); ^{13}C NMR (101 MHz, 298 K, DMSO-*d*$_6$): δ = 168.6,

166.9, 147.4, 145.5, 142.7, 137.7, 129.3, 128.1, 125.5, 123.7, 69.7, 65.8, 65.2, 64.2, 57.3, 30.9, 26.7, 20.8 ppm; IR (film): $\tilde{\nu}$ = 1782, 1749, 1607, 1519, 1457, 1348, 1200, 1181, 1150, 1125, 1036, 1011 cm^{-1}; HRMS (ESI): m/z calculated for $C_{15}H_{18}N_3O_5S$ $[M+H-(4\text{-}Me)C_6H_4SO_3H]^+$: 352.0962; found: 352.0951; $[\alpha]_D^{25}$ = +106 (c = 0.006 g/mL, acetone).

(2*S*,5*R*,6*S*)-6-Methoxy-3,3-dimethyl-7-oxo-4-thia-1-azabicyclo[3.2.0]heptane-2-carboxylic acid 4,4-dioxide (**9a**)

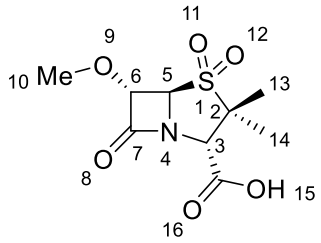

General Procedure B was used using **8a** (117 mg, 0.331 mmol, 1 equiv.) and 10 wt. % Pd/C (207 mg, 0.59 equiv.). After work-up, the product **9a** was obtained (60 mg, 69%), being sufficiently pure for testing.

Amorphous solid; ^{1}H NMR (500 MHz, 298 K, DMSO-*d*$_6$): δ = 5.40 (d, *J* = 1.3 Hz, 1H, *C6H*), 5.00 (d, *J* = 1.3 Hz, 1H, *C5H*), 4.36 (s, 1H, *C3H*), 3.46 (s, 3H, *C10H*$_3$), 1.46 (s, 3H, *C13H*$_3$), 1.38 ppm (s, 3H, *C14H*$_3$); ^{13}C NMR (126 MHz, 298 K, DMSO-*d*$_6$): δ = 169.0, 167.8, 83.4, 65.7, 62.7, 62.3, 57.5, 19.4, 17.6 ppm; IR (film): $\tilde{\nu}$ = 1791, 1464, 1319, 1219, 1157, 1116, 1021 cm^{-1}; HRMS (ESI): m/z calculated for $C_9H_{13}NO_6SNa$ $[M+Na]^+$: 286.0356; found: 286.0340; $[\alpha]_D^{25}$ = +16 (c = 0.001 g/mL, $CHCl_3$).

(2*S*,5*R*,6*S*)-6-Ethoxy-3,3-dimethyl-7-oxo-4-thia-1-azabicyclo[3.2.0]heptane-2-carboxylic acid 4,4-dioxide (**9b**)

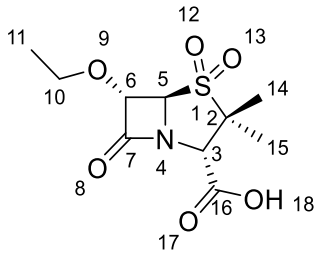

General Procedure B was applied using **8b** (116 mg, 0.316 mmol, 1 equiv.) and 10 wt. % Pd/C (250 mg, 0.77 equiv.). Purification by reverse phase flash column chromatography (6 g Sfär C18 D;

100%$_{v/v}$ aqueous formic acid solution (0.1%) in H_2O (6 CV), followed by a linear gradient (12 CV): 0%$_{v/v}$ → 100%$_{v/v}$ aqueous formic acid solution (0.1%) in CH_3CN) afforded the desired product **9b** (27 mg, 31%).

Amorphous solid; ^{1}H NMR (600 MHz, 298 K, DMSO-*d*$_6$): δ = 5.38 (d, *J* = 1.3 Hz, 1H, *C6H*), 5.03 (d, *J* = 1.3 Hz, 1H, *C5H*), 4.43 (s, 1H, *C3H*), 3.75 (m, 1H, *C10H*), 3.64 (m, 1H, *C10H*), 1.46 (s, 3H, *C14H*$_3$), 1.38 (s, 3H, *C15H*$_3$), 1.19 ppm (t, *J* = 7.0 Hz, 3H, *C11H*$_3$); ^{13}C NMR (151 MHz, 298 K, DMSO-*d*$_6$): δ = 169.2, 167.9, 82.2, 66.4, 66.2, 62.7, 62.0, 19.3, 17.5, 14.8 ppm; IR (film): $\tilde{\nu}$ = 1794, 1465, 1397, 1375, 1319, 1198, 1157, 1117, 1090, 1036 cm^{-1}; HRMS (ESI): m/z calculated for $C_{10}H_{14}NO_6S$ [M-H]$^-$: 276.0547; found: 276.0546; $[\alpha]_D^{25}$ = +221 (c = 0.002 g/mL, $CHCl_3$).

(2*S*,5*R*,6*S*)-6-(*iso*-Propoxy)-3,3-dimethyl-7-oxo-4-thia-1-azabicyclo[3.2.0]heptane-2-carboxylic acid 4,4-dioxide (**9c**)

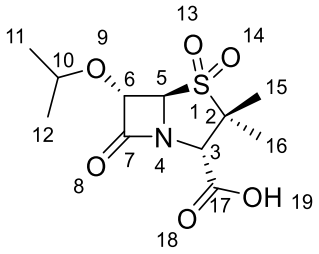

General Procedure B was applied using **8c** (139 mg, 0.364 mmol, 1 equiv.) and 10 wt. % Pd/C (250 mg, 0.65 equiv.). Purification by reverse phase flash column chromatography (6 g Sfär C18 D; 100%$_{v/v}$ aqueous formic acid solution (0.1%) in H_2O (6 CV), followed by a linear gradient (12 CV): 0%$_{v/v}$ → 100%$_{v/v}$ aqueous formic acid solution (0.1%) in CH_3CN) afforded the desired product **9c** (51 mg, 48%).

Amorphous solid; ^{1}H NMR (600 MHz, 298 K, DMSO-*d*$_6$): δ = 5.26 (d, *J* = 1.3 Hz, 1H, *C6H*), 5.00 (d, *J* = 1.2 Hz, 1H, *C5H*), 4.41 (s, 1H, *C3H*), 3.92 (m, 1H, *C10H*), 1.46 (s, 3H, *C15H*$_3$), 1.38 (s, 3H, *C16H*$_3$), 1.18 (d, *J* = 6.1 Hz, 3H, *C11H*$_3$), 1.16 ppm (d, *J* = 6.1 Hz, 3H, *C12H*$_3$); ^{13}C NMR (151 MHz, 298 K, DMSO-*d*$_6$): δ = 169.5, 167.9, 80.9, 73.9, 67.7, 62.7, 62.0, 40.4, 40.1, 22.1, 21.7, 19.3, 17.5 ppm. IR (film): $\tilde{\nu}$ = 1795, 1465, 1375, 1317, 1194, 1157, 1116, 1091, 1013 cm^{-1};

HRMS (ESI): m/z calculated for $C_{11}H_{17}NO_6SNa$ $[M+Na]^+$: 314.0669; found: 314.0660; $[\alpha]_D^{25}$ = +114 (c = 0.006 g/mL, $CHCl_3$).

(2*S*,5*R*,6*S*)-6-(*tert*-Butoxy)-3,3-dimethyl-7-oxo-4-thia-1-azabicyclo[3.2.0]heptane-2-carboxylic acid 4,4-dioxide (**9d**)

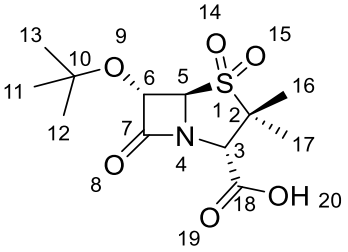

General procedure B was applied using **12d** (116 mg, 0.293 mmol, 1 equiv.) and 10 wt. % Pd/C (200 mg, 0.65 equiv.). Purification by reverse phase flash column chromatography (6 g Sfär C18 D; 100%$_{v/v}$ aqueous formic acid solution (0.1%) in H_2O (6 CV), followed by a linear gradient (12 CV): 0%$_{v/v}$ → 100%$_{v/v}$ aqueous formic acid solution (0.1%) in CH_3CN) afforded the desired product **9d** (40 mg, 45%).

Amorphous solid ; ^{1}H NMR (600 MHz, 298 K, DMSO-*d*$_6$): δ = 5.22 (d, *J* = 1.2 Hz, 1H, *C6H*), 4.98 (d, *J* = 1.3 Hz, 1H, *C5H*), 4.43 (s, 1H, *C3H*), 1.46 (s, 3H, *C16H*$_3$), 1.38 (s, 3H, *C17H*$_3$), 1.23 ppm (s, 9H, *C11H*$_3$, *C12H*$_3$, *C13H*$_3$); ^{13}C NMR (151 MHz, 298 K, DMSO-*d*$_6$): δ =169.8, 167.9, 76.8, 76.2, 68.5, 62.8, 62.0, 27.0, 19.3, 17.6 ppm; IR (film): $\tilde{\nu}$ = 1793, 1319, 1262, 1218, 1175, 1114, 1017 cm^{-1}; HRMS (ESI): m/z calculated for $C_{12}H_{19}NO_6SNa$ $[M+Na]^+$: 328.0825; found: 328.0819; $[\alpha]_D^{25}$ = +145 (c = 0.001 g/mL, $CHCl_3$).

4-Nitrobenzyl (2*S*,5*R*,6*S*)-6-methoxy-3,3-dimethyl-7-oxo-4-thia-1-azabicyclo[3.2.0]heptane-2-carboxylate (**10a**)

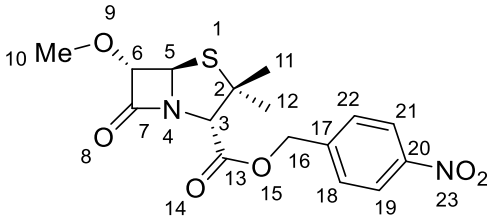

General Procedure C was applied using **6** (1.75 g, 3.34 mmol) and MeOH (15 mL). Purification by flash column chromatography (25 g Sfär, 100%$_{v/v}$

cyclohexane (2 CV), followed by a linear gradient (20 CV): 0%$_{v/v}$ →20%$_{v/v}$ ethyl acetate in cyclohexane) yielded the desired product **10a** (357 mg, 0.97 mmol, 29%).

Oil; ^{1}H NMR (400 MHz, 298 K, $CDCl_3$): δ = 8.29 – 8.21 (m, 2H, *C19H*, *C21H*), 7.59 – 7.53 (m, 2H, *C18H*, *C22H*), 5.32 and 5.24 (ABq, *J* = 13.1 Hz, 2H, *C16H$_2$*), 5.29 (d, *J* = 1.5 Hz, 1H, *C6H*), 4.59 (d, *J* = 1.5 Hz, 1H, *C5H*), 4.55 (s, 1H, *C3H*), 3.54 (s, 3H, *C10H$_3$*), 1.57 (s, 3H, *C11H$_3$*), 1.41 ppm (s, 3H, *C12H$_3$*); ^{13}C NMR (101 MHz, 298 K, $CDCl_3$): δ = 169.6, 167.2, 148.2, 142.0, 129.0, 124.1, 92.7, 69.1, 68.7, 65.9, 64.4, 58.1, 33.9, 25.8 ppm; IR (film): $\tilde{\nu}$ = 1776, 1748, 1607, 1522, 1457, 1372, 1347, 1301, 1261, 1203, 1181, 1157, 1122, 1090, 1012 cm^{-1}; HRMS (ESI): m/z calculated for $C_{16}H_{19}N_2O_6S$ $[M+H]^+$: 367.0958; found: 367.0965; $[\alpha]_D^{25}$ = +83 (c = 0.042 g/mL, $CHCl_3$).

4-Nitrobenzyl (2*S*,5*R*,6*S*)-6-ethoxy-3,3-dimethyl-7-oxo-4-thia-1-azabicyclo[3.2.0]heptane-2-carboxylate (**10b**)

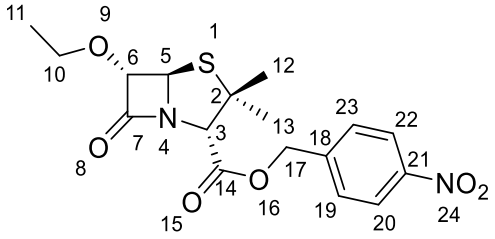

General procedure C was applied using **6** (1.75 g, 3.34 mmol) and EtOH (15 mL). Purification by flash column chromatography (25 g Sfär, 100%$_{v/v}$ cyclohexane (2 CV), followed by a linear gradient (20 CV): 0%$_{v/v}$ →20%$_{v/v}$ ethyl acetate in cyclohexane) yielded the desired product **10b** (340 mg, 0.89 mmol, 27%).

Oil; ^{1}H NMR (500 MHz, 298 K, $CDCl_3$): δ = 8.28 – 8.22 (d, *J* = 8.4 Hz, 2H, *C20H*, *C22H*), 7.55 (d, *J* = 8.4 Hz, 2H, *C19H*, *C23H*), 5.32 and 5.24 (ABq, *J* = 13.1 Hz, 2H, *C17H$_2$*), 5.27 (d, *J* = 1.5 Hz, 1H, *C6H*), 4.62 (d, *J* = 1.5 Hz, 1H, *C5H*), 4.55 (s, 1H, *C3H*), 3.72 (m, 2H, *C10H$_2$*), 1.57 (s, 3H, *C12H$_3$*), 1.40 (s, 3H, *C13H$_3$*), 1.26 ppm (t, *J* = 7.0 Hz, 3H, *C11H$_3$*); ^{13}C NMR (126 MHz, 298 K, $CDCl_3$): δ = 169.9, 167.2, 148.1, 142.0, 129.0, 124.1, 91.5, 69.4, 69.1, 66.8, 65.9, 64.3, 33.9,

25.8, 15.3 ppm; IR (film): $\tilde{\nu}$ = 1777, 1749, 1607, 1523, 1455, 1372, 1347, 1298, 1260, 1203, 1182, 1156, 1127, 1091, 1029 cm^{-1}; HRMS (ESI): m/z calculated for $C_{17}H_{20}N_2O_6SNa$ $[M+Na]^+$: 403.0934; found: 403.0932; $[\alpha]_D^{25}$ = +115 (c = 0.021 g/mL, $CHCl_3$).

4-Nitrobenzyl (2*S*,5*R*,6*S*)-6-(*iso*-propoxy)-3,3-dimethyl-7-oxo-4-thia-1-azabicyclo[3.2.0]heptane-2-carboxylate (**10c**)

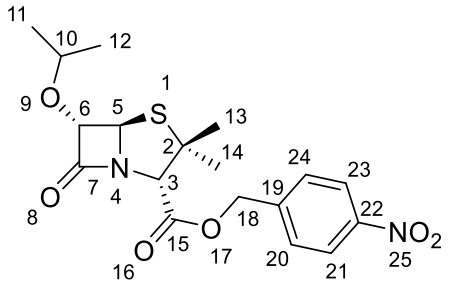

General procedure C was applied using **6** (1.75 g, 3.34 mmol) and EtOH (15 mL). Purification by flash column chromatography (25 g Sfär, 100%$_{v/v}$ cyclohexane (2 CV), followed by a linear gradient (20 CV): 0%$_{v/v}$ →20%$_{v/v}$ ethyl acetate in cyclohexane) yielded the desired product **10c** (220 mg, 0.56 mmol, 17%).

Oil; ^{1}H NMR (500 MHz, 298 K, $CDCl_3$): δ = 8.28 – 8.22 (d, *J* = 8.3 Hz, 2H, *C21H*, *C23H*), 7.55 (d, *J* = 8.3 Hz, 2H, *C20H*, *C24H*), 5.32 (d, *J* = 13.2 Hz, 1H, *C18H*), 5.23 (m, 2H, *C6H*, *C18H*), 4.61 (s, 1H, *C5H*), 4.55 (s, 1H, *C3H*), 3.85 (m, 1H, *C10H*), 1.57 (s, 3H, *$C13H_3$*), 1.40 (s, 3H, *$C14H_3$*), 1.26 (d, *J* = 6.1 Hz, 3H, *$C11H_3$*), 1.21 ppm (d, *J* = 6.1 Hz, 3H, *$C12H_3$*). ^{13}C NMR (126 MHz, $CDCl_3$) δ 170.3, 167.2, 148.1, 142.0, 129.0, 124.1, 90.4, 74.2, 70.7, 69.1, 65.9, 64.2, 33.9, 25.8, 22.64, 22.58 ppm; IR (film): $\tilde{\nu}$ = 1776, 1751, 1670, 1653, 1608, 1558, 1524, 1456, 1374, 1347, 1303, 1261, 1215, 1180, 1155, 1120, 1091, 1016 cm^{-1}; HRMS (ESI): m/z calculated for $C_{18}H_{22}N_2O_6SNa$ $[M+Na]^+$: 417.1091; found: 417.1086; $[\alpha]_D^{25}$ = +94 (c = 0.012 g/mL, $CHCl_3$).

4-Nitrobenzyl (2*S*,5*R*,6*S*)-6-(*tert*-butoxy)-3,3-dimethyl-7-oxo-4-thia-1-azabicyclo[3.2.0]heptane-2-carboxylate (**10d**)

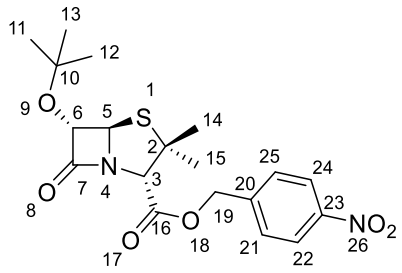

General procedure C was applied using **6** (1.75 g, 3.34 mmol) and EtOH (15 mL). Purification by flash column chromatography (25 g Sfär, 100%$_{v/v}$ cyclohexane (2 CV), followed by a linear gradient (20 CV): 0%$_{v/v}$ →20%$_{v/v}$ ethyl acetate in cyclohexane) yielded the desired product **10d** (120 mg, 0.29 mmol, 9%).

Oil; ^{1}H NMR (500 MHz, 298 K, DMSO-*d*$_6$): δ = 8.30 – 8.23 (m, 2H, *C22H*, *C24H*), 7.71 (m, 2H, *C21H*, *C25H*), 5.39 – 5.30 (m, 2H, *C19H*$_2$), 5.14 (d, *J* = 1.4 Hz, 1H, *C6H*), 4.79 (d, *J* = 1.4 Hz, 1H, *C5H*), 4.70 (s, 1H, *C3H*), 1.53 (s, 3H, *C14H*$_3$), 1.37 (s, 3H, *C15H*$_3$), 1.19 ppm (s, 9H, *C11H*$_3$, *C12H*$_3$, *C13H*$_3$); ^{13}C NMR (126 MHz, 298 K, DMSO-*d*$_6$): δ = 170.2, 167.0, 147.3, 142.9, 129.2, 123.6, 84.6, 76.0, 70.9, 68.4, 65.5, 63.9, 32.6, 27.5, 25.3 ppm; IR (film): ṽ = 1779, 1752, 1608, 1524, 1458, 1347, 1300, 1262, 1178, 1118, 1017 cm^{-1}; HRMS (ESI): m/z calculated for $C_{19}H_{25}N_2O_6S$ $[M+H]^+$: 409.1428; found: 409.1421.

(2*S*,5*R*,6*S*)-6-Methoxy-3,3-dimethyl-7-oxo-4-thia-1-azabicyclo[3.2.0]heptane-2-carboxylic acid (**11a**)

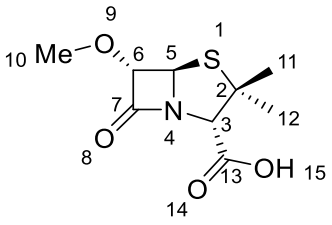

General procedure B was applied using **10a** (200 mg, 0.546 mmol, 1.0 equiv.) and 10 wt. % Pd/C (370 mg, 0.65 equiv.). Purification by reverse phase flash column chromatography (12 g Sfär C18 D; 100%$_{v/v}$ aqueous formic acid solution (0.1%) in H_2O (6 CV), followed by a linear gradient (12 CV): 0%$_{v/v}$ → 100%$_{v/v}$ aqueous formic acid solution (0.1%) in CH_3CN) afforded the desired product **11a** (34 mg, 27%).

Amorphous solid; ^{1}H NMR (500 MHz, 298 K, DMSO-*d*$_6$): δ = 5.29 (d, *J* = 1.2 Hz, 1H, *C6H*), 4.67 (d, *J* = 1.2 Hz, 1H, *C5H*), 4.39 (s, 1H, *C3H*), 3.42 (s, 3H, *C10H*$_3$), 1.50 (s, 3H, *C11H*$_3$), 1.45 ppm (s, 3H, *C12H*$_3$); ^{13}C NMR (126 MHz, 298 K, DMSO-*d*$_6$): δ = 169.1, 168.6, 91.0, 68.7, 67.5, 63.7, 57.1, 32.5, 25.5 ppm; IR (film): $\tilde{\nu}$ = 1765, 1495, 1393, 1373, 1327, 1223, 1157, 1126, 1092, 1025, 1012 cm^{-1}; HRMS (ESI): m/z calculated for $C_9H_{13}NO_4SNa$ $[M+Na]^+$: 254.0458; found: 254.0460; $[\alpha]_D^{25}$ = +212 (c = 0.004 g/mL, $CHCl_3$).

(2*S*,5*R*,6*S*)-6-Ethoxy-3,3-dimethyl-7-oxo-4-thia-1-azabicyclo[3.2.0]heptane-2-carboxylic acid (**11b**)

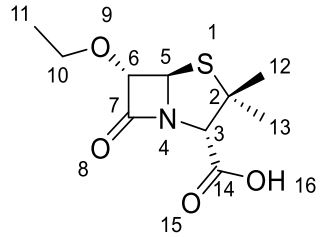

General procedure B was applied using **10b** (200 mg, 0.526 mmol, 1.0 equiv.) and 10 wt. % Pd/C (356 mg, 0.65 equiv.). Purification by reverse phase flash column chromatography (12 g Sfär C18 D; 100%$_{v/v}$ aqueous formic acid solution (0.1%) in H_2O (6 CV), followed by a linear gradient (12 CV): 0%$_{v/v}$ → 100%$_{v/v}$ aqueous formic acid solution (0.1%) in CH_3CN) afforded the desired product **11b** (25 mg, 19%).

Amorphous solid; ^{1}H NMR (500 MHz, 298 K, DMSO-*d*$_6$): δ = 5.24 (d, *J* = 1.3 Hz, 1H, *C6H*), 4.70 (d, *J* = 1.3 Hz, 1H, *C5H*), 4.39 (s, 1H, *C3H*), 3.64 (m, 2H, *C10H*$_3$), 1.50 (s, 3H, *C12H*$_3$), 1.45 (s, 3H, *C13H*$_3$), 1.15 ppm (t, *J* = 7.0 Hz, 3H, *C11H*$_3$); ^{13}C NMR (126 MHz, 298 K, DMSO-*d*$_6$): δ = 169.3, 168.6, 89.8, 68.6, 68.3, 65.5, 63.7, 32.5, 25.5, 15.0 ppm; IR (film): $\tilde{\nu}$ = 1754, 1649, 1507, 1457, 1393, 1372, 1298, 1212, 1158, 1129, 1093 cm^{-1}; HRMS (ESI): m/z calculated for $C_{10}H_{15}NO_4SNa$ $[M+Na]^+$: 268.0614; found: 268.0616; $[\alpha]_D^{25}$ = +152 (c = 0.016 g/mL, $CHCl_3$).

(2*S*,5*R*,6*S*)-6-(*iso*-Propoxy)-3,3-dimethyl-7-oxo-4-thia-1-azabicyclo[3.2.0]heptane-2-carboxylic acid (**11c**)

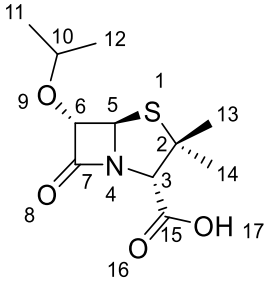

General procedure B was applied using **10c** (202 mg, 0.51 mmol, 1.0 equiv.) and 10 wt. % Pd/C (347 mg, 0.65 equiv.). Purification by reverse phase flash column chromatography (12 g Sfär C18 D; 100%$_{v/v}$ aqueous formic acid solution (0.1%) in H_2O (6 CV), followed by a linear gradient (12 CV): 0%$_{v/v}$ → 100%$_{v/v}$ aqueous formic acid solution (0.1%) in CH_3CN) afforded the desired product **11c** (65 mg, 49%).

Amorphous solid; ^{1}H NMR (500 MHz, 298 K, DMSO-*d*$_6$): δ = 5.14 (s, 1H, *C6H*), 4.71 (s, 1H, *C5H*), 4.39 (s, 1H, *C3H*), 3.84 (m, 1H, *C10H*), 1.50 (s, 3H, *C13H*$_3$), 1.45 (s, 3H, *C14H*$_3$), 1.15 (d, *J* = 6.1 Hz, 3H, *C11H*$_3$), 1.12 ppm (d, *J* = 6.1 Hz, 3H, *C12H*$_3$); ^{13}C NMR (126 MHz, 298 K, DMSO-*d*$_6$): δ = 169.6, 168.7, 88.6, 72.9, 69.6, 68.7, 63.7, 32.6, 25.5, 22.3, 22.1 ppm; IR (film): $\tilde{\nu}$ = 1750, 1508, 1460, 1373, 1313, 1208, 1120, 1002 cm^{-1}; HRMS (ESI): m/z calculated for $C_{11}H_{18}NO_4S$ $[M+H]^+$: 260.0951; found: 260.0950; $[\alpha]_D^{25}$ = +72 (c = 0.043 g/mL, $CHCl_3$).

(2*S*,5*R*,6*S*)-6-(*tert*-Butoxy)-3,3-dimethyl-7-oxo-4-thia-1-azabicyclo[3.2.0]heptane-2-carboxylic acid (**11d**)

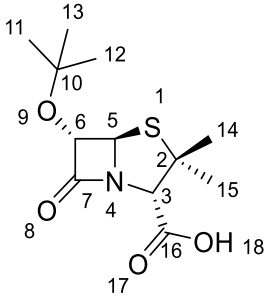

General procedure B was applied using **10d** (100 mg, 0.24 mmol, 1.0 equiv.) and 10 wt. % Pd/C (173 mg, 0.65 equiv.). Purification by reverse phase flash column chromatography (12 g Sfär C18 D; 100%$_{v/v}$ aqueous formic acid solution (0.1%) in H_2O (6 CV), followed by a linear gradient (12 CV): 0%$_{v/v}$ → 100%$_{v/v}$ aqueous formic acid solution (0.1%) in CH_3CN) afforded the desired product **11d** (39 mg, 59%).

Amorphous solid; ^{1}H NMR (500 MHz, 298 K, DMSO-*d*$_6$): δ = 5.09 (d, *J* = 1.3 Hz, 1H, *C6H*), 4.74 (d, *J* = 1.3 Hz, 1H, *C5H*), 4.39 (s, 1H, *C3H*), 1.52 (s, 3H, *C14H*$_3$), 1.45 (s, 3H, *C15H*$_3$), 1.18 ppm (s, 9H, *C11H*$_3$, *C12H*$_3$, *C13H*$_3$); ^{13}C NMR (126 MHz, 298 K, DMSO-*d*$_6$): δ = 170.1, 168.7, 84.4, 75.9, 70.8, 68.7, 63.6, 32.7, 27.5, 25.5 ppm; IR (film): $\tilde{\nu}$ = 1776, 1755, 1461, 1393, 1370, 1333, 1302, 1260, 1235, 1182, 1120, 1094, 1021, 1001 cm^{-1}; HRMS (ESI): m/z calculated for $C_{12}H_{19}NO_4SNa$ $[M+Na]^+$: 296.0927; found: 296.0928; $[\alpha]_D^{25}$ = +77 (c = 0.026 g/mL, $CHCl_3$).

8.3.4 References

1. T. R. Malla, L. Brewitz, D.-G. Muntean, H. Aslam, C. D. Owen, E. Salah, A. Tumber, P. Lukacik, C. Strain-Damerell, H. Mikolajek, M. A. Walsh and C. J. Schofield, Penicillin Derivatives Inhibit the SARS-CoV-2 Main Protease by Reaction with Its Nucleophilic Cysteine, *J. Med. Chem.*, 2022, **65**, 7682–7696.

8.3.5 ^{1}H and ^{13}C NMR spectra of the compounds prepared for this study

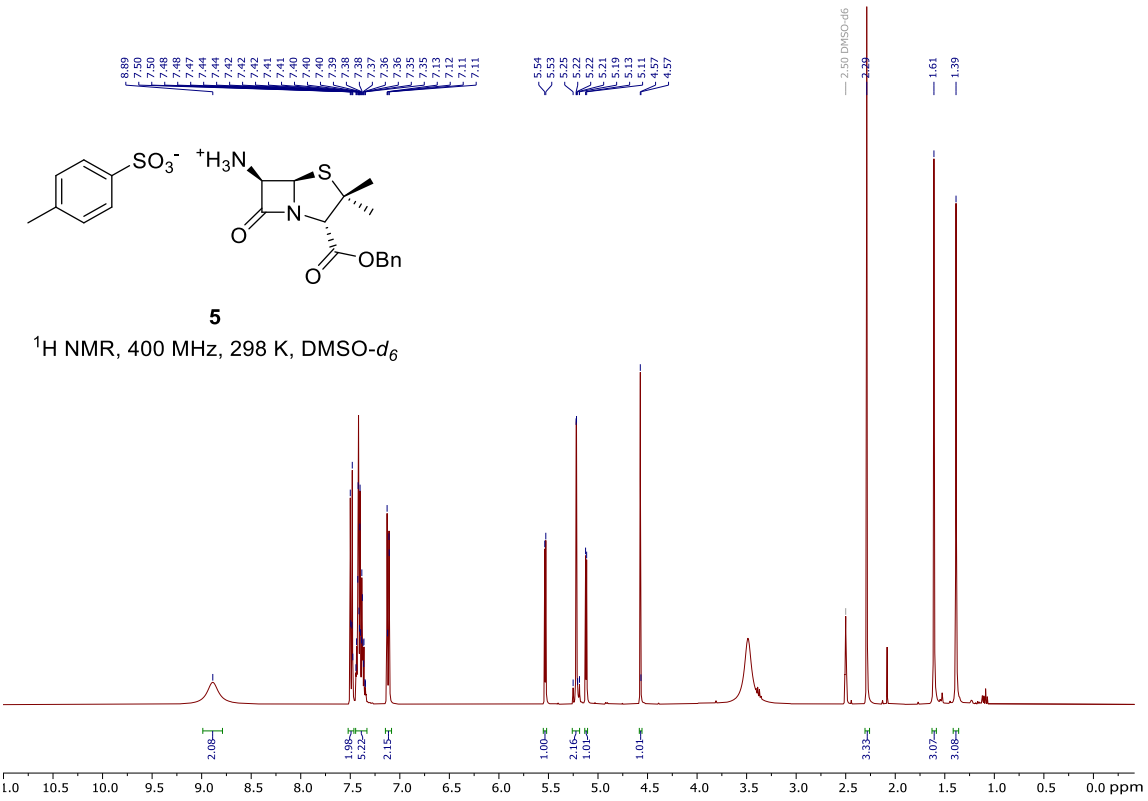

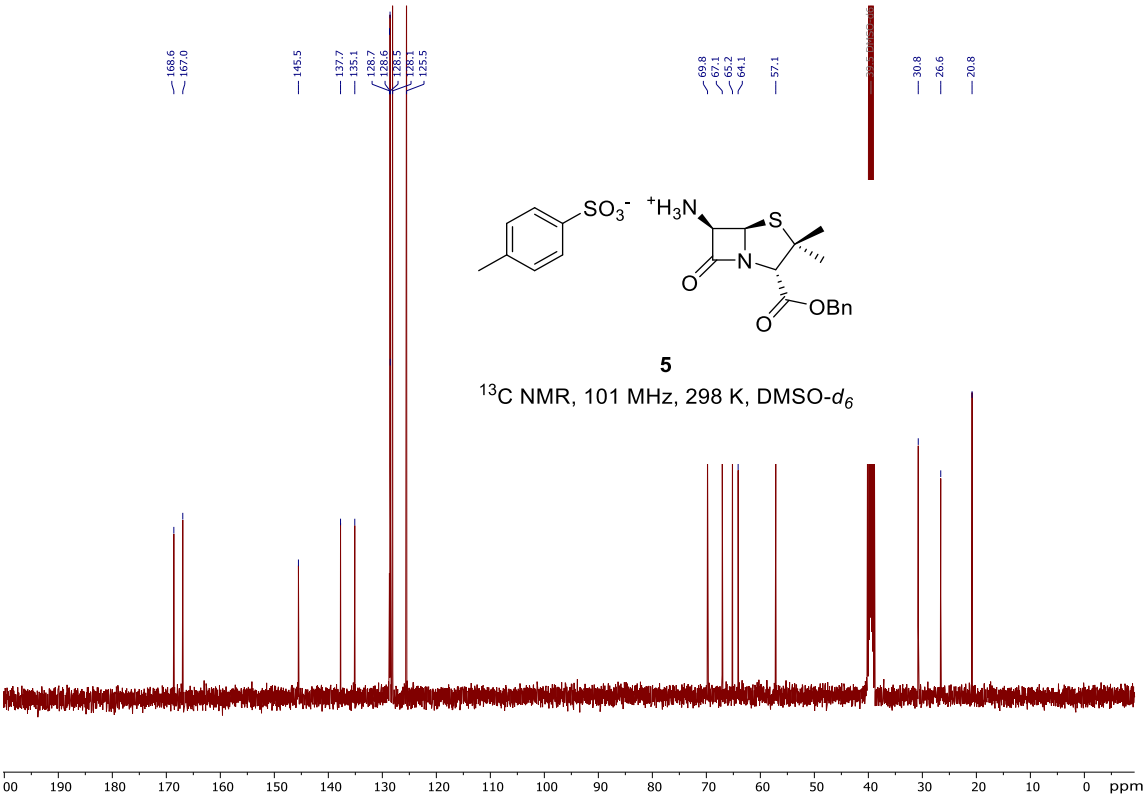

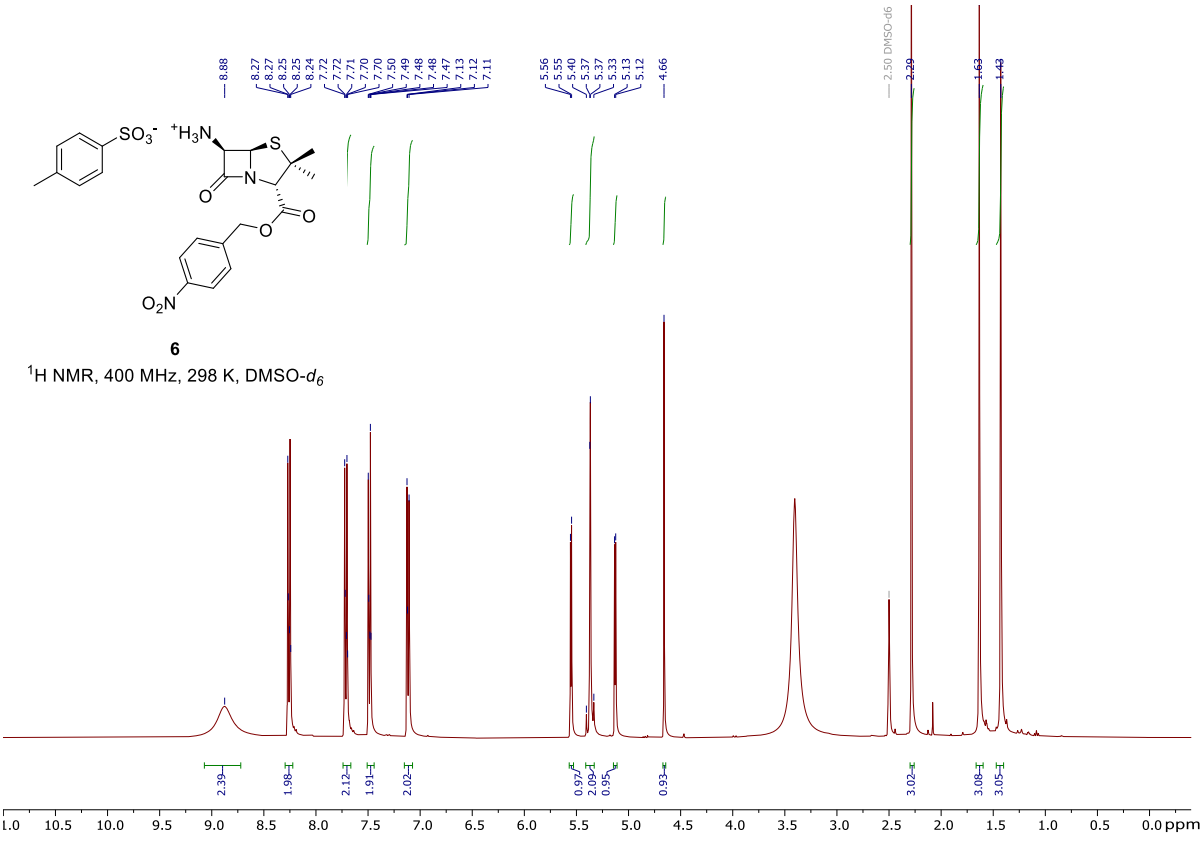

6

^{1}H NMR, 400 MHz, 298 K, DMSO-d_6

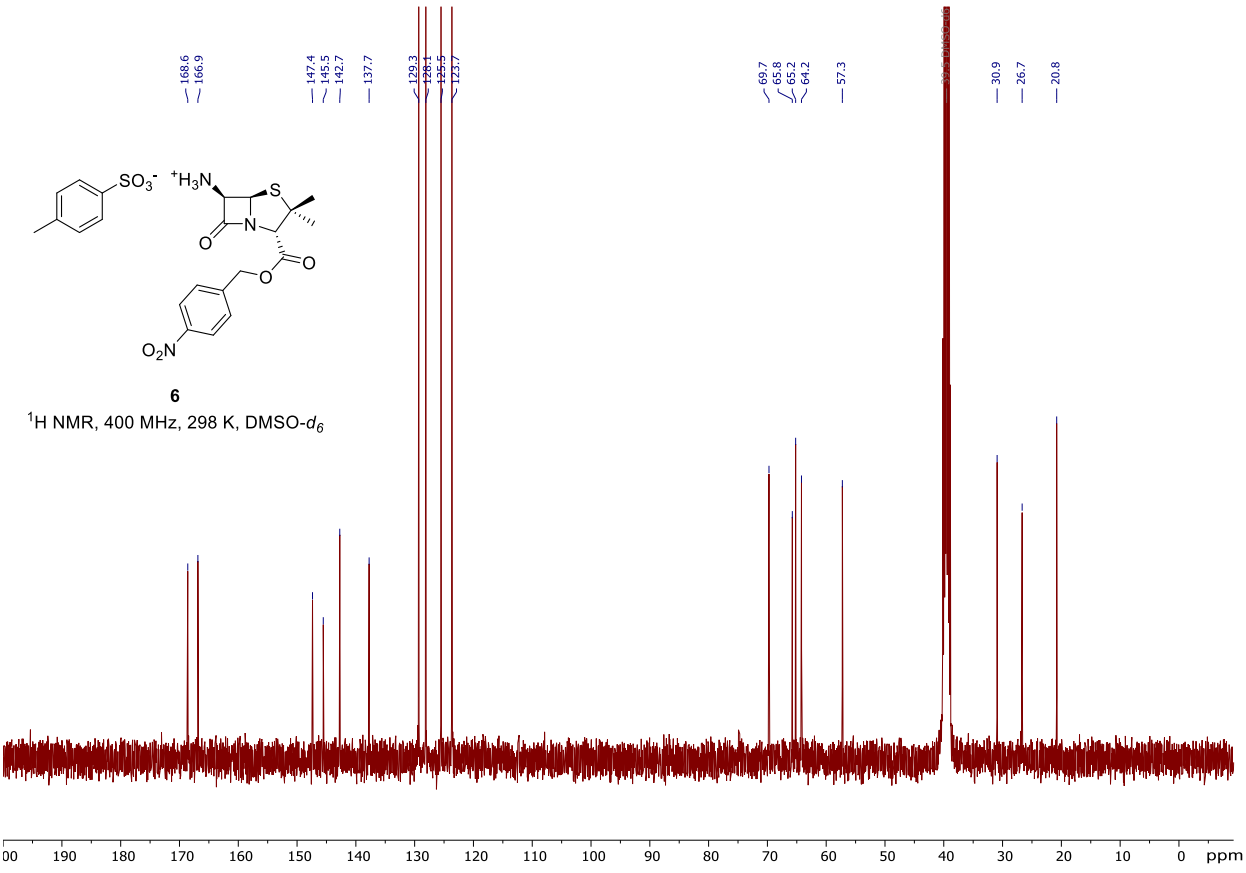

6

^{1}H NMR, 400 MHz, 298 K, DMSO-d_6

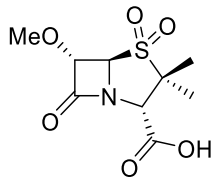

9a

^{1}H NMR, 500 MHz, 298 K, DMSO-d_6

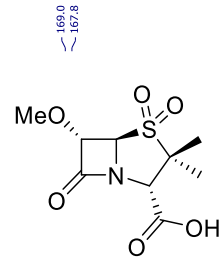

9a

^{13}C NMR, 126 MHz, 298 K, DMSO-d_6

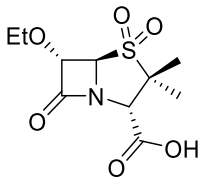

9b

^{1}H NMR, 500 MHz, 298 K, DMSO-d_6

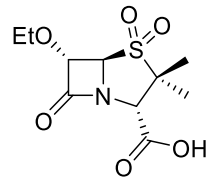

9b

^{13}C NMR, 126 MHz, 298 K, DMSO-d_6

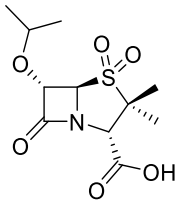

9c

^{1}H NMR, 500 MHz, 298 K, DMSO-d_6

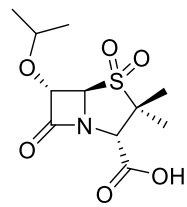

9c

^{13}C NMR, 126 MHz, 298 K, DMSO-d_6

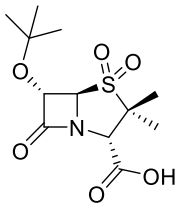

9d

^{1}H NMR, 500 MHz, 298 K, DMSO-d_6

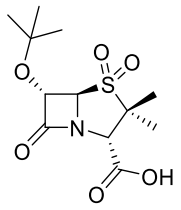

9d

^{13}C NMR, 126 MHz, 298 K, DMSO-d_6

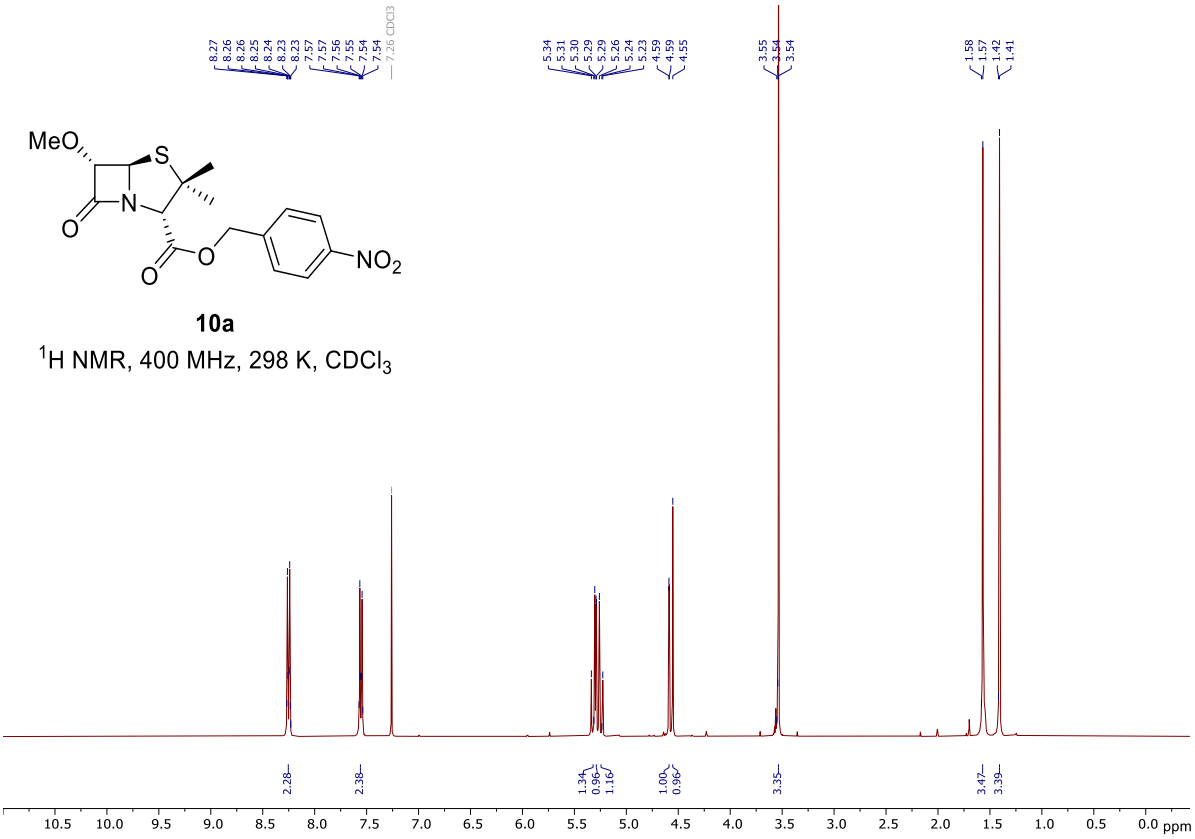

10a

^{1}H NMR, 400 MHz, 298 K, $CDCl_3$

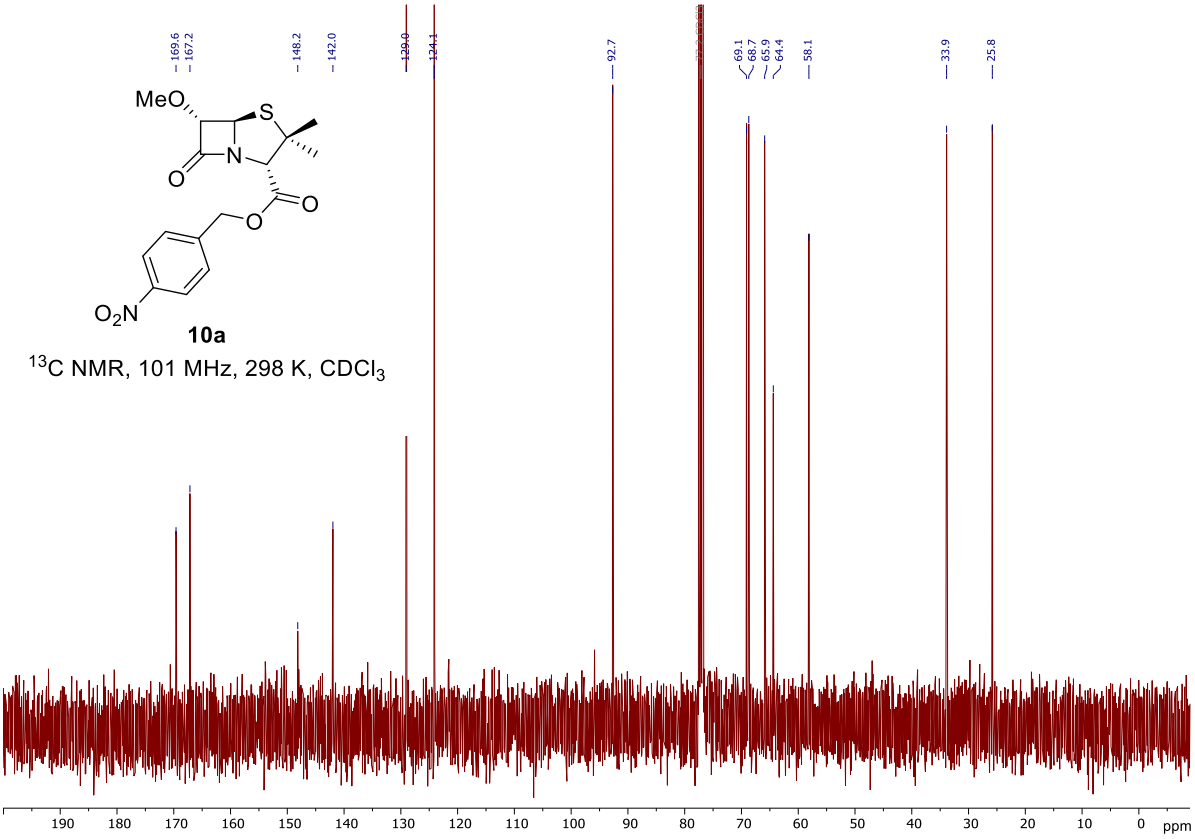

10a

^{13}C NMR, 101 MHz, 298 K, $CDCl_3$

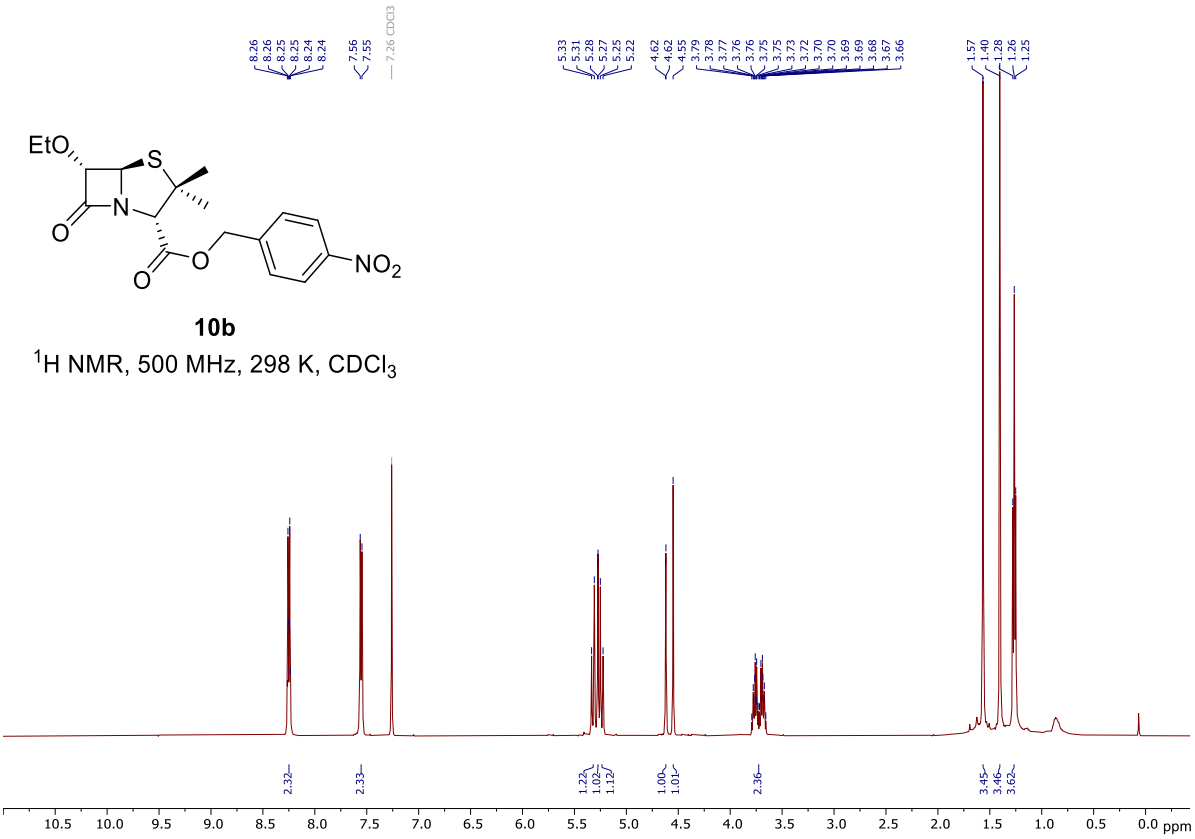

10b

^{1}H NMR, 500 MHz, 298 K, $CDCl_3$

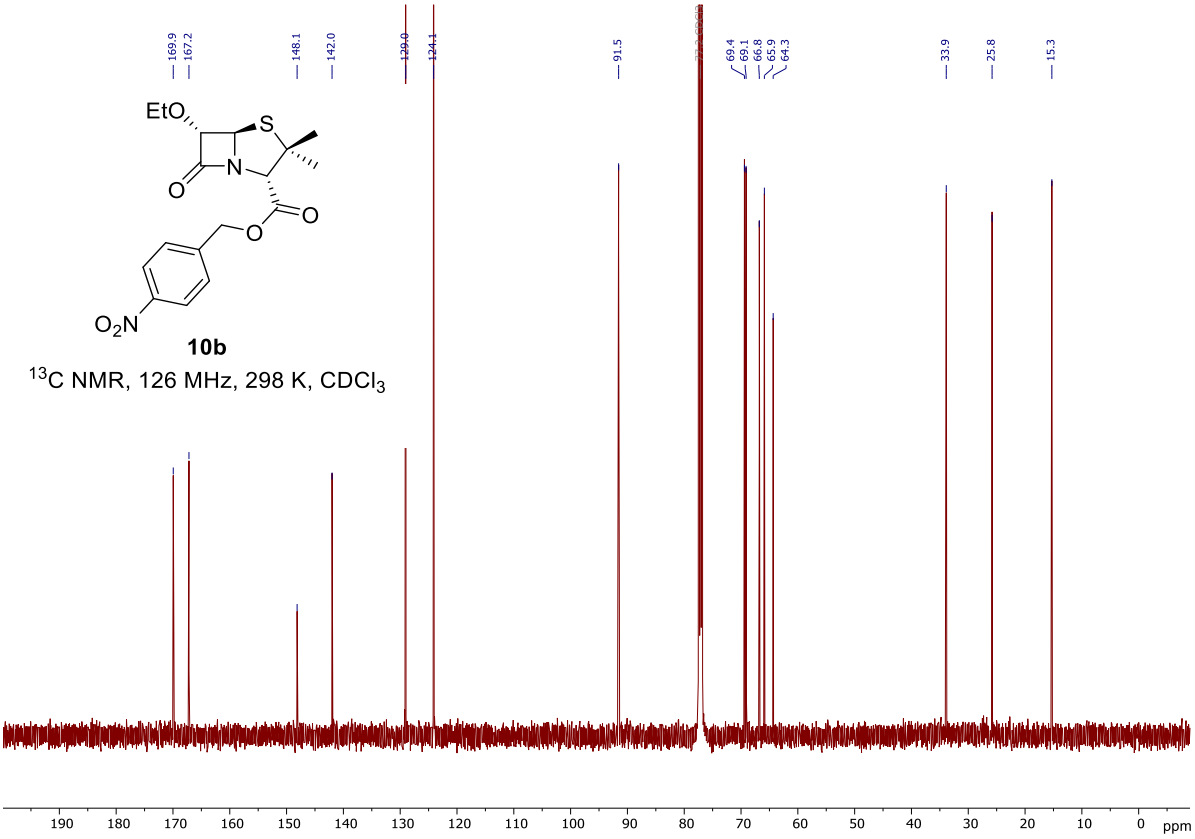

10b

^{13}C NMR, 126 MHz, 298 K, $CDCl_3$

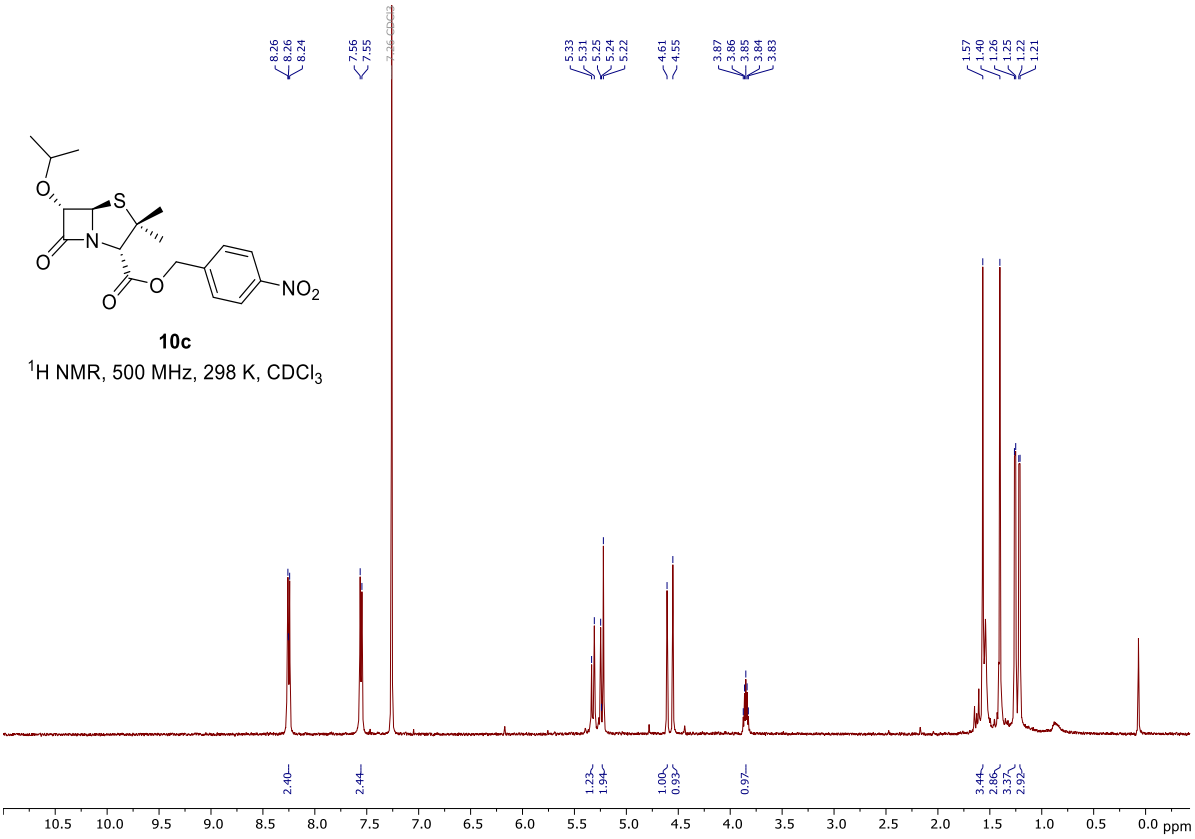

10c

^{1}H NMR, 500 MHz, 298 K, $CDCl_3$

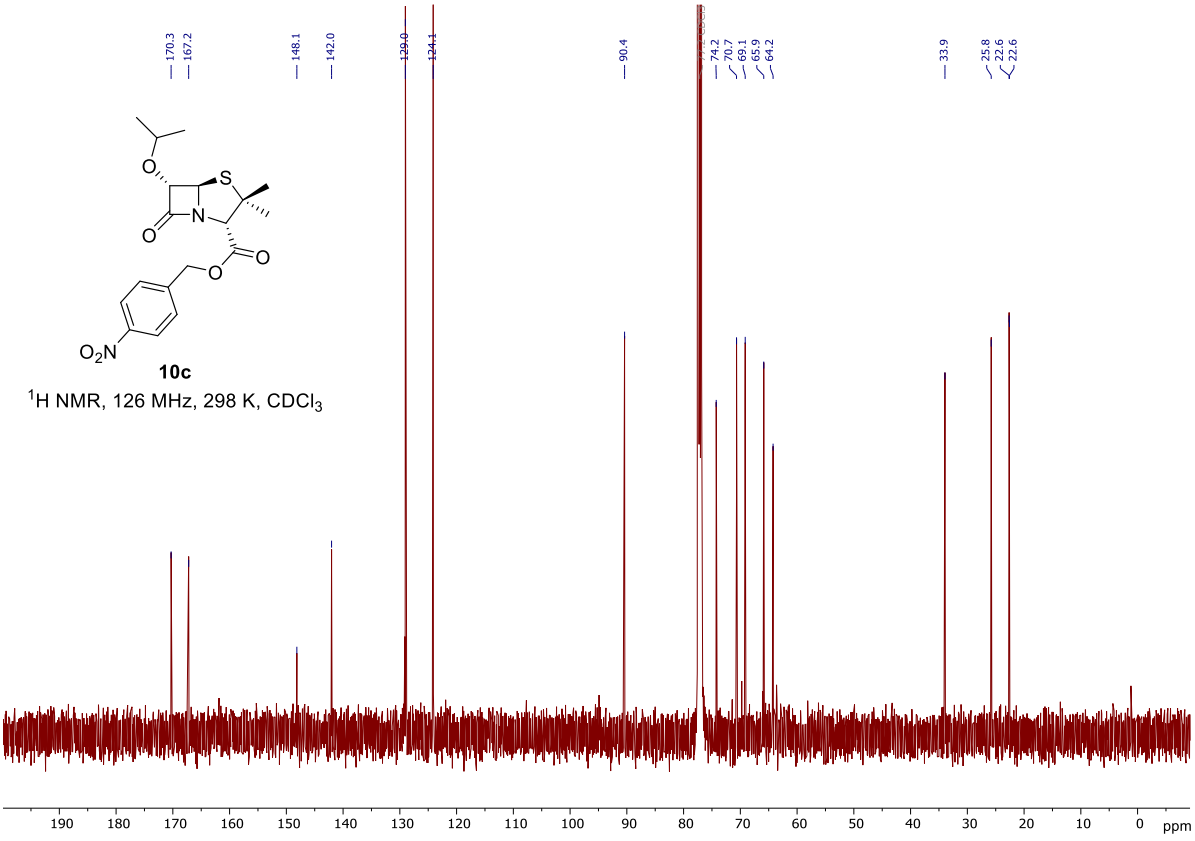

10c

^{1}H NMR, 126 MHz, 298 K, $CDCl_3$

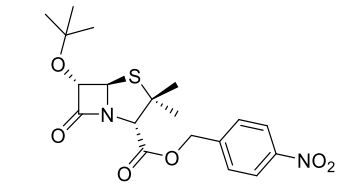

10d

^{1}H NMR, 500 MHz, 298 K, DMSO-d_6

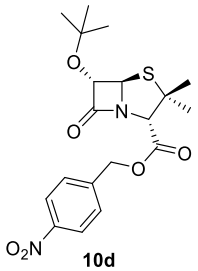

10d

^{13}C NMR, 126 MHz, 298 K, DMSO-d_6

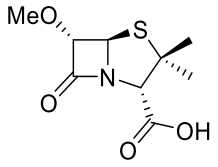

11a

^{1}H NMR, 500 MHz, 298 K, DMSO-d_6

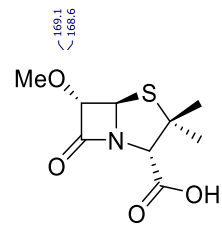

11a

^{13}C NMR, 126 MHz, 298 K, DMSO-d_6

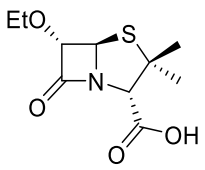

11b

^{1}H NMR, 500 MHz, 298 K, DMSO-d_6

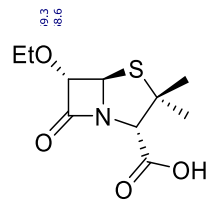

11b

^{13}C NMR, 126 MHz, 298 K, DMSO-d_6

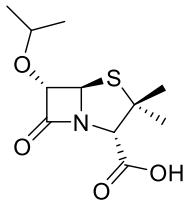

11c

^{1}H NMR, 500 MHz, 298 K, DMSO-d_6

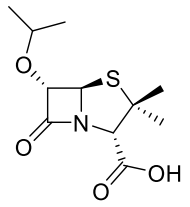

11c

^{13}C NMR, 126 MHz, 298 K, DMSO-d_6

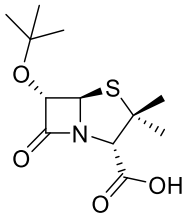

11d

^{1}H NMR, 500 MHz, 298 K, DMSO-d_6

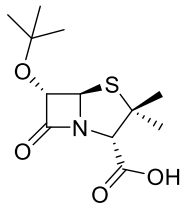

11d

^{13}C NMR, 126 MHz, 298 K, DMSO-d_6

8.4 Appendix to Chapter V (Manuscript IV)

8.4.1 General synthesis information

Penicillin G, **oxacillin**, **cloxacillin**, **dicloxacillin**, **carbenicillin**, **ticarcillin**, **temocillin**, **piperacillin**, **cefoxitin**, and **2**, as well as all the reagents employed in synthesis were obtained from commercial sources (Sigma-Aldrich, Inc.; Flurochem Ltd.; Manchester Organics; Tokyo Chemical Industry Ltd.; Ambeed Inc.; MedChemExpress LLC; AstaTech Inc.; AK Scientific Inc.; Apollo Scientific Ltd.; Key Organics Ltd.; Aurum Pharmatech LLC; Biosynth Ltd.; LGC Standards Ltd.) and were used without further purification. The synthesis of **1a** (**(2*S*,5*R*,6*S*)-6-Methoxy-3,3-dimethyl-7-oxo-6-(2-phenylacetamido)-4-thia-1-azabicyclo[3.2.0]heptane-2-carboxylic acid**) is described in **Appendix section 8.1**.

Anhydrous solvents (Sigma-Aldrich, Inc.) were kept under an atmosphere of argon. HPLC grade solvents (Sigma-Aldrich Inc.) were used for reaction work-ups, extractions, and purifications. Flash column chromatography was performed using an automated Biotage Isolera One purification machine equipped with Biotage®Sfär flash chromatography cartridges. ^{1}H and ^{13}C NMR spectra were recorded using Bruker AVANCE AVIIIHD 400, 500 and 600 MHz machines. Chemical shifts for protons are reported in parts per million (ppm) downfield from tetramethylsilane and are referenced to residual protium in the NMR solvent (*i.e.*, $CDCl_3$: $\delta = 7.26$ ppm; DMSO-d_6: $\delta = 2.50$ ppm). For ^{13}C NMR, chemical shifts are reported in the scale relative to the NMR solvent (*i.e.*, $CDCl_3$: $\delta = 77.2$ ppm; DMSO-d_6: $\delta = 39.5$ ppm). NMR data are reported in the following manner: chemical shift, multiplicity, coupling constant (J, Hz; to nearest 0.1 Hz), and integration.

Infrared (IR) spectroscopy was performed using a Bruker Tensor-27 Fourier transform infrared (FT-IR) spectrometer. High-resolution mass spectrometry (HRMS) was performed using either

electro-spray ionization (ESI) mass spectrometry (MS) in the positive or negative ionization modes employing a Thermo Scientific Exactive mass spectrometer (ThermoFisher Scientific), or atmospheric pressure chemical ionization (APCI) in the positive mode using an Agilent 7200 Accurate mass spectrometer; data are presented as a mass-to-charge ratio (m/z). Optical rotation ($[\alpha]_D^{25}$) measurements were performed using a Bellingham + Stanley (ADP450) polarimeter.

8.4.2 General synthesis procedures

General procedure A

A variation of a reported procedure was followed.[1] To a solution of penam alkali salt (1 equiv.) in *N*,*N*-dimethylformamide/methanol (7:1; 0.17 M) was added dropwise a methanolic solution of 1 LiOMe (1 M; 1.7 equiv.) at -78 °C, followed by freshly prepared ^{t}BuOCl[2] (1.7 equiv.). The reaction mixture was stirred for 15 min at -78 °C, then concentrated H_2SO_4 (0.5 equiv.) was added. The reaction mixture was allowed to warm up to room temperature, before it was diluted with water. The solution was acidified to pH 2 by addition of an aqueous H_2SO_4 solution (1 M). The mixture was extracted with $CHCl_3$, and the combined organic extracts were washed with saturated aqueous LiCl, H_2O, and brine. The organic extracts were dried over Na_2SO_4, concentrated *in vacuo*, and purified by reverse-phase column chromatography. The fractions containing the purified product were collected and lyophilised to afford the desired product.

8.4.3 Experimental procedures and compounds characterisations

(2*S*,5*R*,6*S*)-6-Methoxy-3,3-dimethyl-6-(5-methyl-3-phenylisoxazole-4-carboxamido)-7-oxo-4-thia-1-azabicyclo[3.2.0]heptane-2-carboxylic acid (1b)

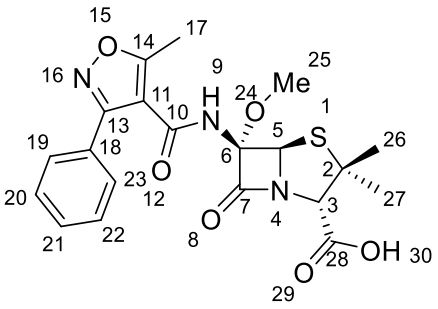

General procedure A was applied using oxacillin sodium (1 g, 2.36 mmol, 1 equiv.). Purification by reverse-phase column chromatography (30 g Sfär C18 D; 100% formic acid solution (0.1% (v/v)) in H_2O (10 CV), followed by a linear gradient (20 CV): 0% → 100% formic acid solution (0.1% (v/v)) in CH_3CN) afforded **1b** (33 mg, 3%).

Amorphous white solid; ^{1}H NMR (500 MHz, 298 K, DMSO-*d*$_6$): δ = 10.05 (s, 1H, *N9H*), 7.73 – 7.66 (m, 2H, *C19H*, *C23H*), 7.55 – 7.46 (m, 3H, *C20H*, *C21H*, *C22H*), 5.45 (s, 1H, *C5H*), 4.38 (s, 1H, *C3H*), 3.41 (s, 3H, *C25H*$_3$), 2.59 (s, 3H, *C17H*$_3$), 1.49 (s, 3H, *C26H*$_3$), 1.45 ppm (s, 3H, *C27H*$_3$); ^{13}C NMR (151 MHz, 298 K, DMSO-*d*$_6$): δ = 170.5, 168.6, 167.1, 162.1, 160.2, 130.1, 128.7, 128.0, 112.1, 95.2, 73.5, 61.6, 53.2, 32.3, 25.8, 12.1 ppm; IR (film): $\tilde{\nu}$ = 1780, 1724, 1676, 1611, 1547, 1513, 1502, 1462, 1443, 1414, 1367, 1306, 1249, 1100 cm^{-1}; HRMS (ESI): m/z calculated for $C_{20}H_{22}N_3O_6S$ $[M+H]^+$: 432.1224; found: 432.1229; $[\alpha]_D^{25}$ = +214 (c = 0.002 g/mL, acetone).

(2*S*,5*R*,6*S*)-6-(3-(2-Chlorophenyl)-5-methylisoxazole-4-carboxamido)-6-methoxy-3,3-dimethyl-7-oxo-4-thia-1-azabicyclo[3.2.0]heptane-2-carboxylic acid (1c)

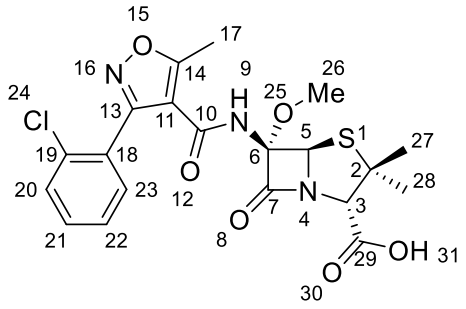

General procedure A was applied using cloxacillin sodium monohydrate (1.18 g, 2.47 mmol, 1 equiv.). Purification by reverse-phase column chromatography (30 g Sfär C18 D; 100% formic acid solution (0.1% (v/v)) in H_2O (10 CV), followed by a linear gradient (20 CV): 0% → 100% formic acid solution (0.1% (v/v)) in CH_3CN) afforded **1c** (145 mg, 12%).

Amorphous white solid; ^{1}H NMR (600 MHz, 298 K, DMSO-*d*$_6$): δ = 9.75 (s, 1H, *N9H*), 7.59 – 7.44 (m, 4H, *C20H*, *C21H*, *C22H*, *C23H*), 5.32 (s, 1H, *C5H*), 4.37 (s, 1H, *C3H*), 3.36 (s, 3H, *C26H*$_3$), 2.64 (s, 3H, *C17H*$_3$), 1.47 (s, 3H, *C27H*$_3$), 1.40 ppm (s, 3H, *C28H*$_3$); ^{13}C NMR (151 MHz, 298 K, DMSO-*d*$_6$) δ 170.2, 168.6, 167.2, 161.1, 160.0, 132.4, 131.7, 131.5, 129.6, 127.5, 127.3, 113.5, 95.3, 73.6, 68.3, 61.5, 53.1, 32.6, 25.7, 12.5 ppm; IR (film): $\tilde{\nu}$ = 1777, 1738, 1679, 1601, 1501, 1442, 1370, 1309, 1205, 1099, 1059 cm^{-1}; HRMS (ESI): m/z calculated for $C_{20}H_{21}ClN_3O_6S$ $[M+H]^+$: 466.0834; found: 466.0844; $[\alpha]_D^{25}$ = +203 (c = 0.004 g/mL, acetone).

(2*S*,5*R*,6*S*)-6-(3-(2,6-Dichlorophenyl)-5-methylisoxazole-4-carboxamido)-6-methoxy-3,3-dimethyl-7-oxo-4-thia-1-azabicyclo[3.2.0]heptane-2-carboxylic acid (1d)

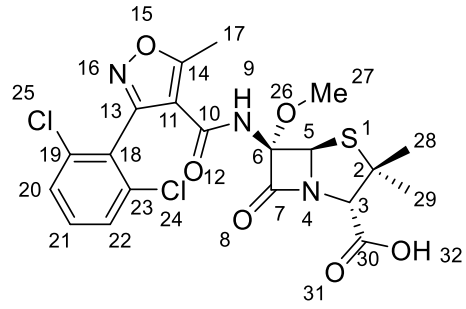

General procedure A was applied using dicloxacillin sodium monohydrate (1.16 g, 2.27 mmol, 1 equiv.). Purification by reverse-phase column chromatography (30 g Sfär C18 D; 100% formic acid solution (0.1% (v/v))

in H_2O (10 CV), followed by a linear gradient (20 CV): 0% → 100% formic acid solution (0.1% (v/v)) in CH_3CN) afforded the **1d** (42 mg, 4%).

Amorphous white solid; ^{1}H NMR (500 MHz, 298 K, DMSO-d_6): δ = 9.79 (s, 1H, *N9H*), 7.64 – 7.51 (m, 3H, *C20H*, *C21H*, *C22H*), 5.29 (s, 1H, *C5H*), 4.39 (s, 1H, *C3H*), 3.37 (s, 3H, *C27H$_3$*), 2.69 (s, 3H, *C17H$_3$*), 1.48 (s, 3H, *C28H$_3$*), 1.39 ppm (s, 3H, *C29H$_3$*); ^{13}C NMR (126 MHz, 298 K, DMSO-d_6): δ = 170.3, 168.6, 167.2, 160.4, 158.1, 134.8, 134.2, 132.3, 128.4, 128.1, 126.9, 113.3, 95.4, 73.5, 68.3, 61.4, 53.0, 32.7, 25.6, 12.8 ppm; IR (film): $\tilde{\nu}$ = 1777, 1682, 1599, 1561, 1493, 1432, 1367, 1303, 1196, 1103 cm^{-1}; HRMS (ESI): m/z calculated for $C_{20}H_{19}Cl_2N_3O_6S$ $[M+H]^+$: 498.0299, found: 498.0288; $[\alpha]_D^{25}$ = +180 (c = 0.003 g/mL, acetone).

(2*S*,5*R*,6*S*)-6-(2-Carboxy-2-phenylacetamido)-6-methoxy-3,3-dimethyl-7-oxo-4-thia-1-azabicyclo[3.2.0]heptane-2-carboxylic acid (1e/1e')

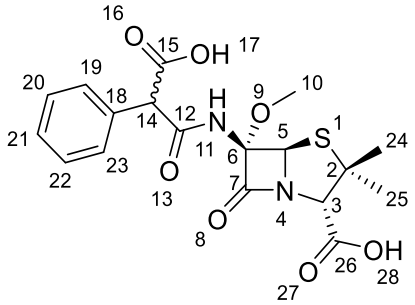

A variation of a reported procedure was followed.[1] **General procedure A** was applied using carbenicillin disodium (1 g, 2.36 mmol, 1 equiv.). Purification by reverse-phase column chromatography (30 g Sfär C18 D; 100% formic acid solution (0.1% (v/v)) in H_2O (10 CV), followed by a linear gradient (20 CV): 0% → 100% formic acid solution (0.1% (v/v)) in CH_3CN) afforded a mixture of *C14* diastereomers **1e** (**(2*S*,5*R*,6*S*)-6-((*S*)-2-carboxy-2-phenylacetamido)-6-methoxy-3,3-dimethyl-7-oxo-4-thia-1-azabicyclo[3.2.0]heptane-2-carboxylic acid**) and **1e'** (**(2S,5R,6S)-6-((R)-2-carboxy-2-phenylacetamido)-6-methoxy-3,3-dimethyl-7-oxo-4-thia-1-azabicyclo[3.2.0]heptane-2-carboxylic acid**) (**d. r.**= 1:1.62; 133 mg, 13.8%).

Amorphous white solid; isomer **1e**: ^{1}H NMR (500 MHz, 298 K, DMSO-d_6): δ = 9.71 (s, 1H, *N11H*), 7.40 – 7.25 (m, 5H, *C19H*, *C20H*, *C21H*, *C22H*, *C23H*), 5.35 (s, 1H, *C5H*), 4.80 (s, 1H,

C14H), 4.32 (s, 1H, *C3H*), 3.09 (s, 3H, *C10H₃*), 1.48 (s, 3H, *C24H₃*), 1.42 (s, 3H, *C25H₃*); Isomer **1e'**: ^{1}H NMR (500 MHz, 298 K, DMSO-*d₆*): δ = 9.74 (s, 1H, *N11H*), 7.40 – 7.25 (m, 5H, *C19H*, *C20H*, *C21H*, *C22H*, *C23H*), 5.30 (s, 1H, *C5H*), 4.80 (s, 1H, *C14H*), 4.25 (s, 1H, *C3H*), 3.42 (s, 3H, *C10H₃*), 1.28 (s, 3H, *C24H₃*), 1.14 (s, 3H, *C25H₃*); ^{13}C NMR (126 MHz, 298 K, DMSO-*d₆*): δ = 169.94, 169.23, 168.70, 168.56, 167.86, 167.77, 167.69, 134.71, 134.13, 129.70, 129.35, 129.23, 128.23, 127.99, 127.70, 127.44, 127.24, 94.53, 94.37, 73.41, 73.29, 68.43, 68.00, 61.22, 60.74, 57.30, 57.14, 52.82, 52.47, 31.59, 31.25, 25.95, 25.52 ppm (^{13}C assignment to individual isomers was not done due to overlapping 2D NMR signals); HRMS (ESI): m/z calculated for $C_{18}H_{20}N_2O_7S$ $[M+H]^+$: 409.1064; found: 409.1064.

(2*S*,5*R*,6*S*)-6-((*R*)-2-(4-ethyl-2,3-dioxopiperazine-1-carboxamido)-2-phenylacetamido)-6-methoxy-3,3-dimethyl-7-oxo-4-thia-1-azabicyclo[3.2.0]heptane-2-carboxylic acid (1f)

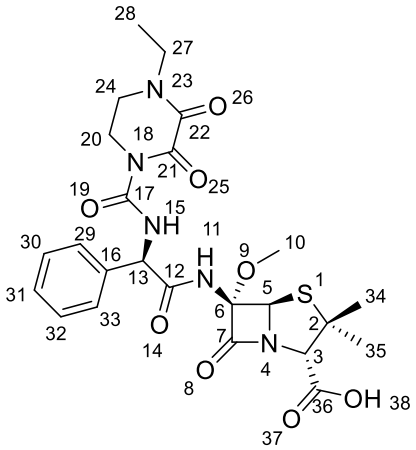

A variation of a reported procedure was followed.[3] **General procedure A** was applied using piperacillin (1.18 g, 2.28 mmol, 1 equiv.). Purification by reverse-phase column chromatography (30 g Sfär C18 D; 100% formic acid solution (0.1% (v/v)) in H_2O (10 CV), followed by a linear gradient (20 CV): 0% → 100% formic acid solution (0.1% (v/v)) in CH_3CN) afforded the **1f** (100 mg, 8%). The analytical data are consistent with those reported.[3]

Amorphous white solid; ^{1}H NMR (400 MHz, 298 K, DMSO-*d₆*): δ = 9.89 (s, 1H, *N11H*), 9.80 (d, *J* = 6.8 Hz, 1H, *N15H*), 7.48 – 7.44 (m, 2H, *C29H*, *C33H*), 7.38 – 7.27 (m, 3H, *C30H*, *C31H*, *C32H*), 5.56 (d, *J* = 6.8 Hz, 1H, *C13H*), 5.29 (s, 1H, *C5H*), 4.20 (s, 1H, *C3H*), 3.89 (m, 2H, *C20H₂*), 3.55 (m, 2H, *C24H2*), 3.39 (m, 5H, *C27H₂*, *C10H₃*), 1.21 (s, 3H, *C34H₃*), 1.08 (t, *J* = 7.2 Hz, 3H,

C28H3), 0.85 ppm (s, 3H, *C35H3*); ^{13}C NMR (126 MHz, 298 K, DMSO-*d6*): δ = 169.1, 168.5, 167.4, 159.6, 155.4, 151.9, 137.2, 128.2, 128.0, 127.8, 94.9, 73.5, 67.9, 60.5, 57.4, 53.1, 42.8, 41.7, 40.3, 32.2, 25.3, 12.0 ppm; IR (film): $\tilde{\nu}$ = 1772, 1715, 1677, 1510, 1458, 1395, 1367, 1326, 1259, 1187, 1097, 1012 cm^{-1}; HRMS (ESI): m/z calculated for $C_{24}H_{28}N_5O_8S$ $[M-H]^-$: 546.1664, found: 546.1668; $[\alpha]_D^{25}$ = -602 (c = 0.002 g/mL, acetone).

8.4.4 References

1. *US Pat.,* US 5750684 A, 1998.
2. M. Benz, T. M. Klapötke, J. Stierstorfer and M. Voggenreiter, Synthesis and Characterization of Binary, Highly Endothermic, and Extremely Sensitive 2,2′-Azobis(5-azidotetrazole), *J. Am. Chem. Soc.*, 2022, **144**, 6143–6147.
3. P. Feyen and W. Schröck, Stereospezifische, einstufige Einführung einer Methoxygruppe an C6 von Penicillinen und C7 von Cephalosporinen, *Angewandte Chemie*, 1981, **93**, 814–815.

8.4.5 ^{1}H and ^{13}C NMR spectra of the compounds prepared for this study

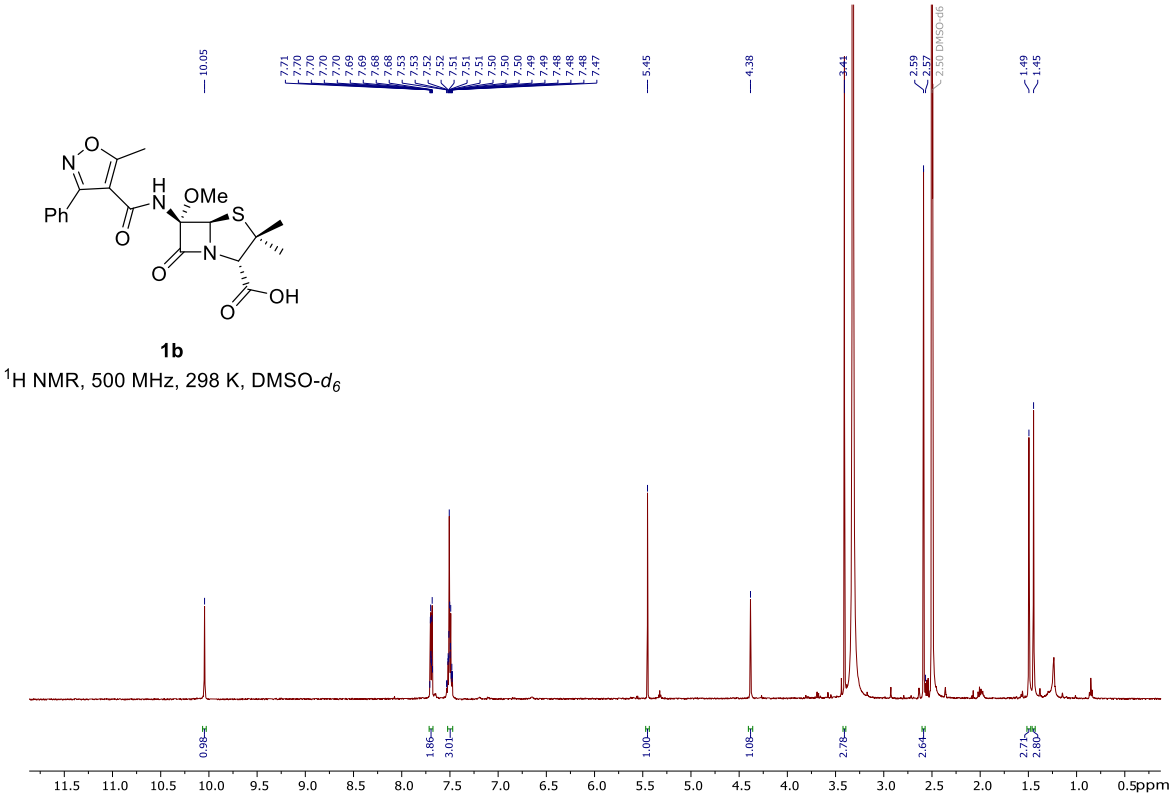

1b

^{1}H NMR, 500 MHz, 298 K, DMSO-d_6

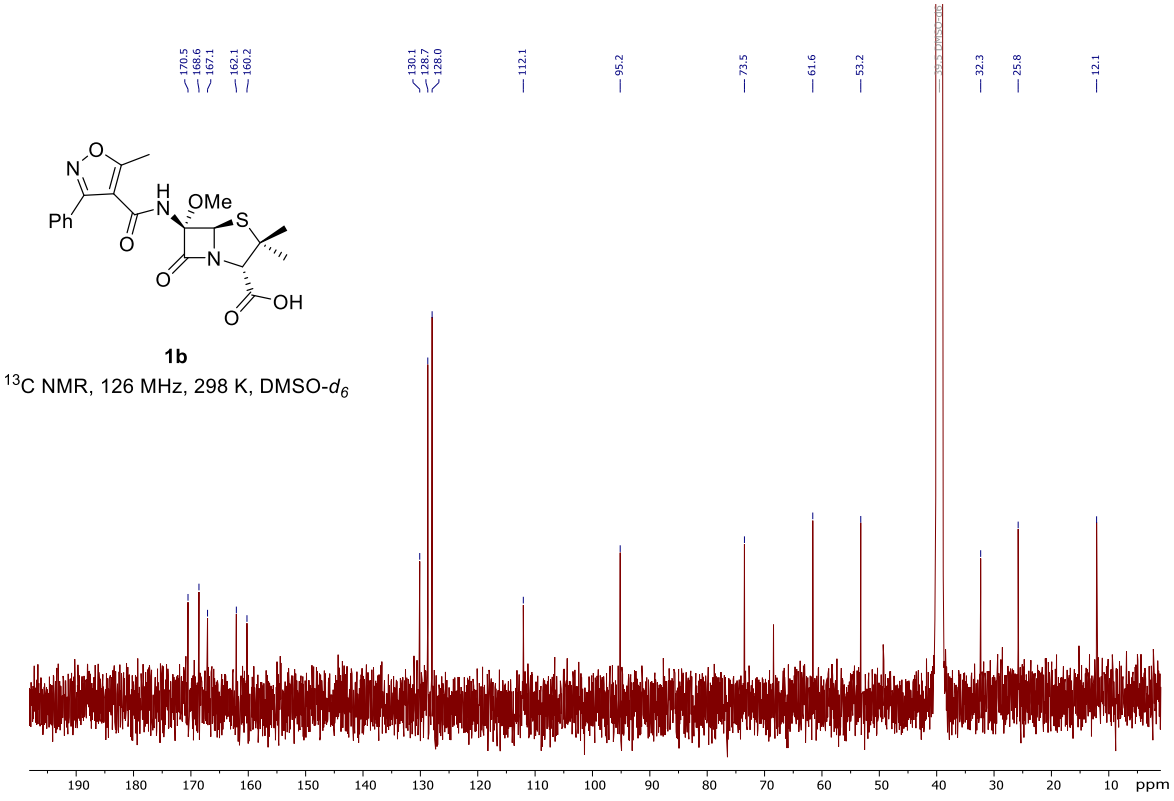

1b

^{13}C NMR, 126 MHz, 298 K, DMSO-d_6

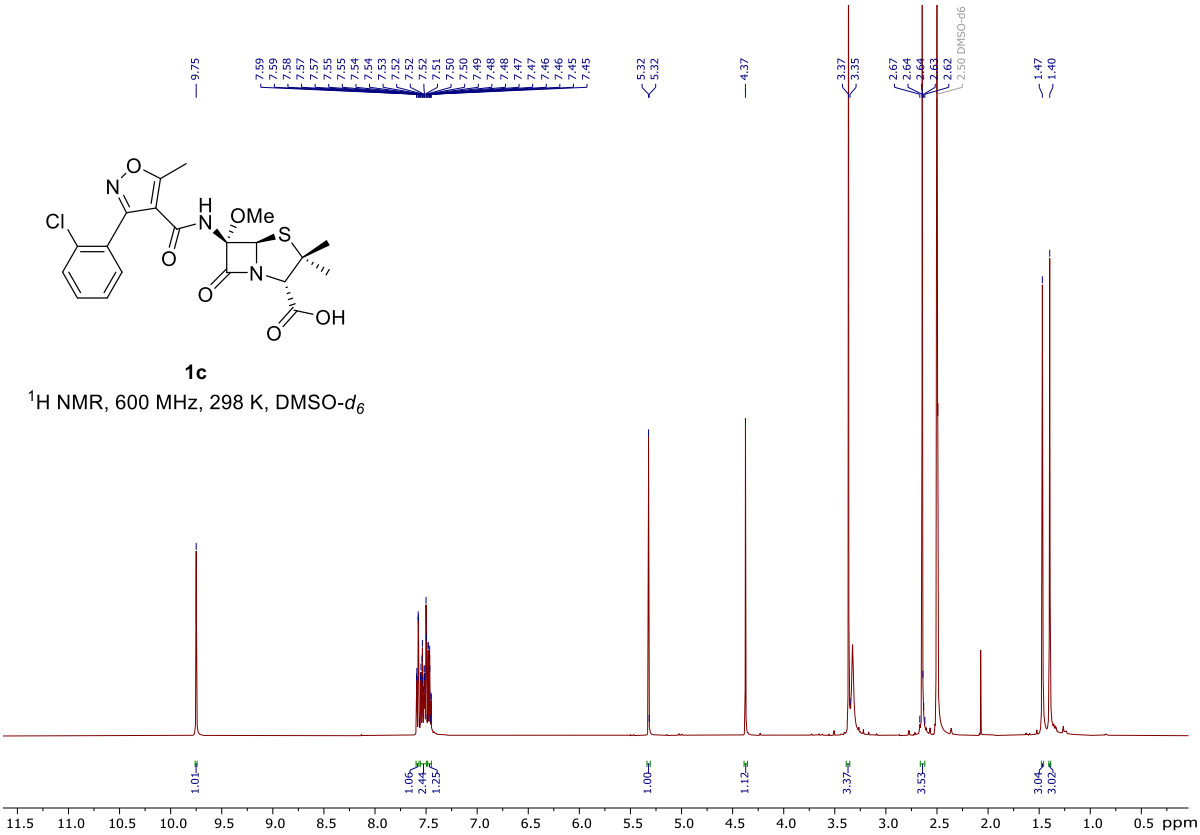

1c

^{1}H NMR, 600 MHz, 298 K, DMSO-d_6

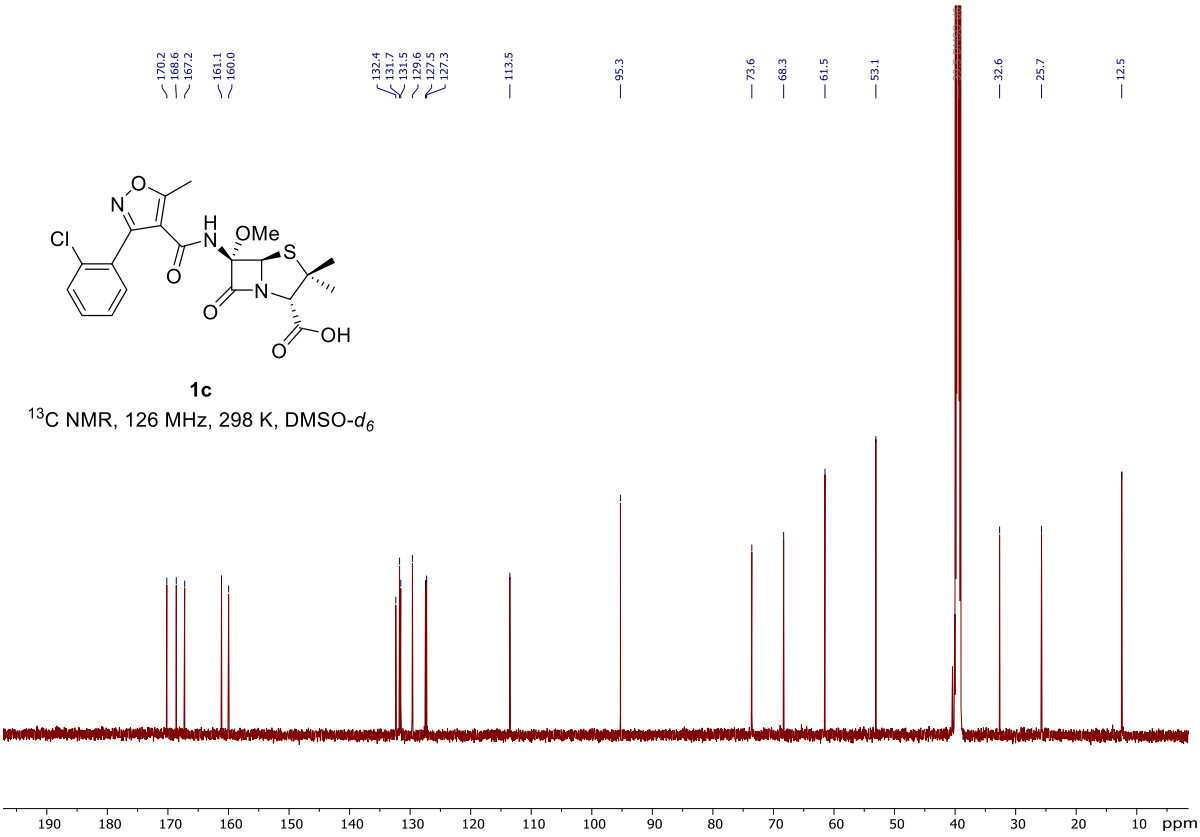

1c

^{13}C NMR, 126 MHz, 298 K, DMSO-d_6

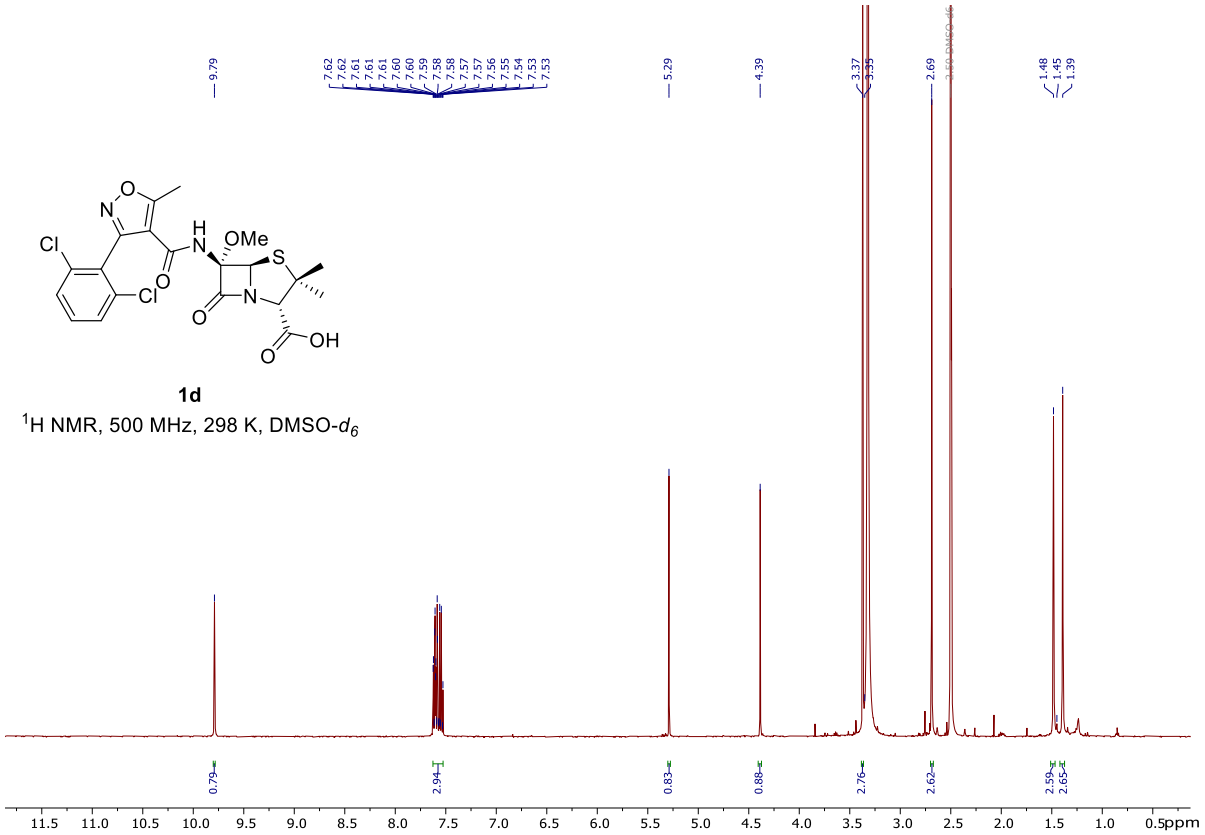

1d

^{1}H NMR, 500 MHz, 298 K, DMSO-d_6

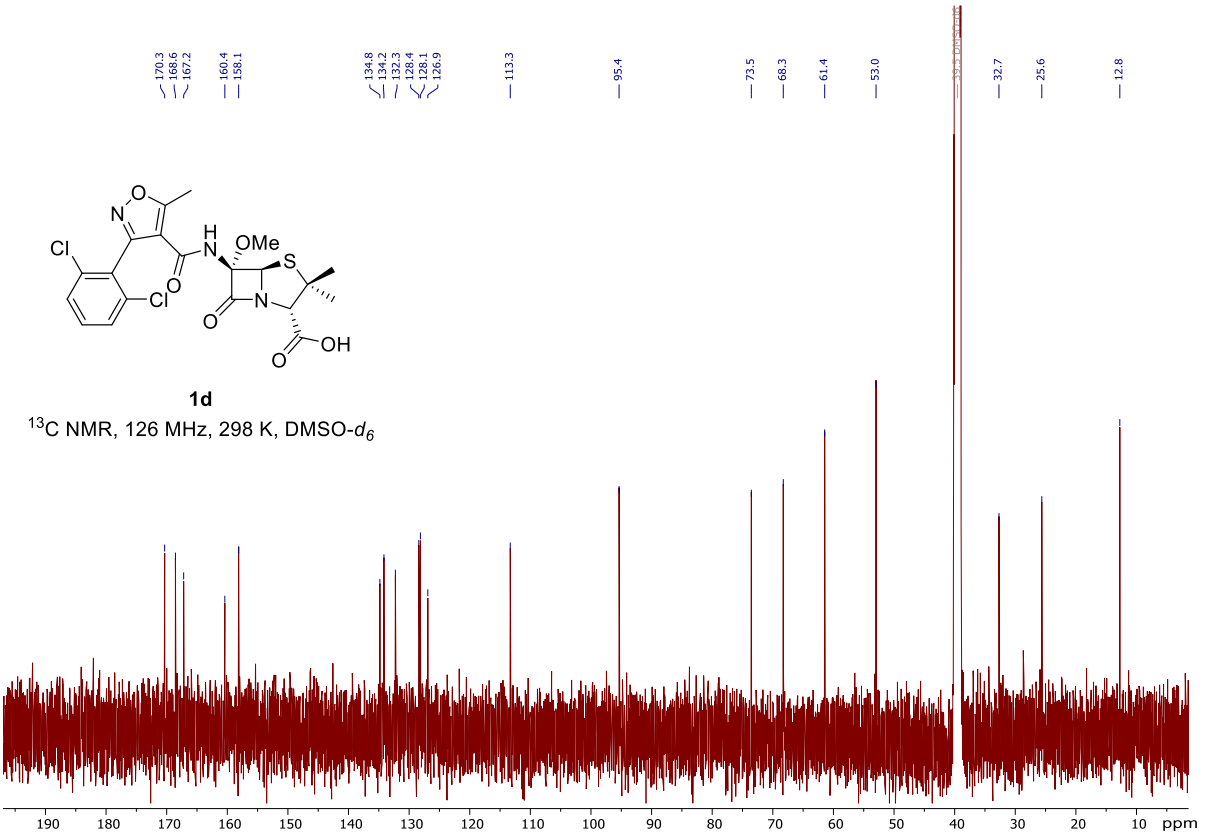

1d

^{13}C NMR, 126 MHz, 298 K, DMSO-d_6

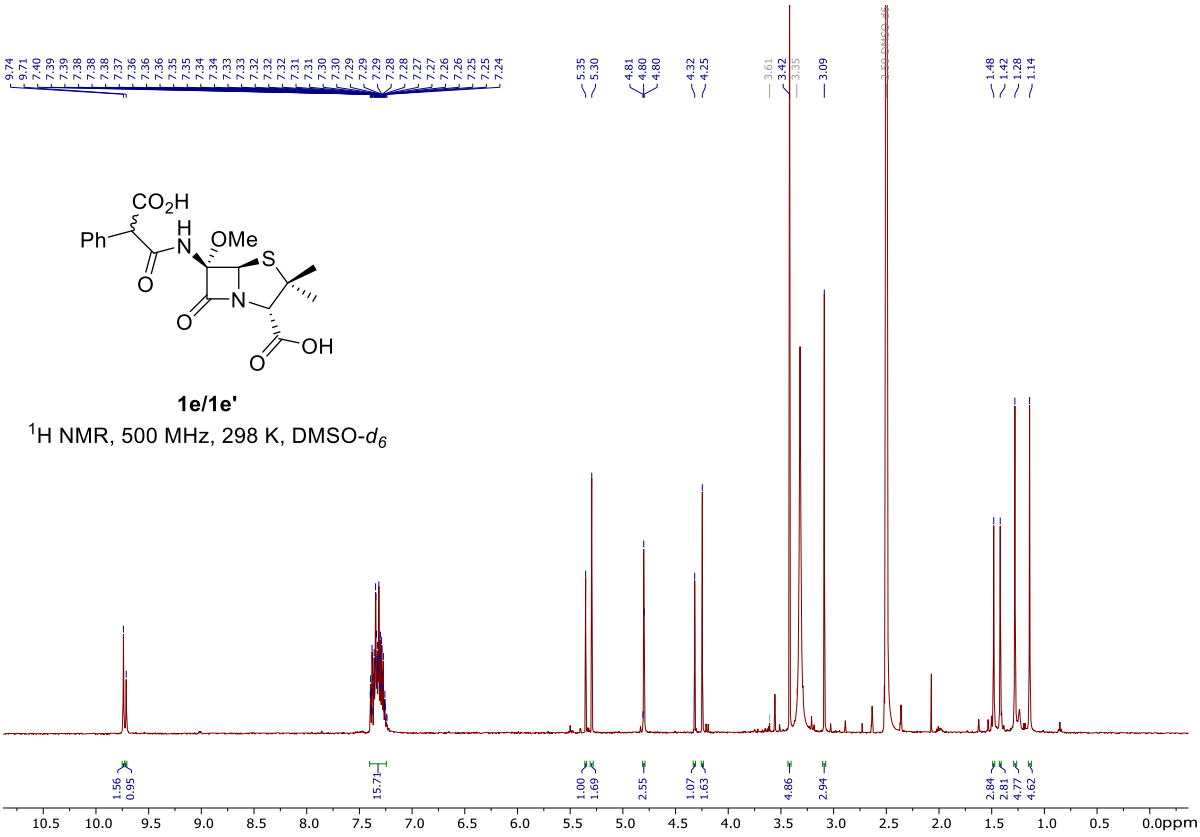

1e/1e'

^{1}H NMR, 500 MHz, 298 K, DMSO-d_6

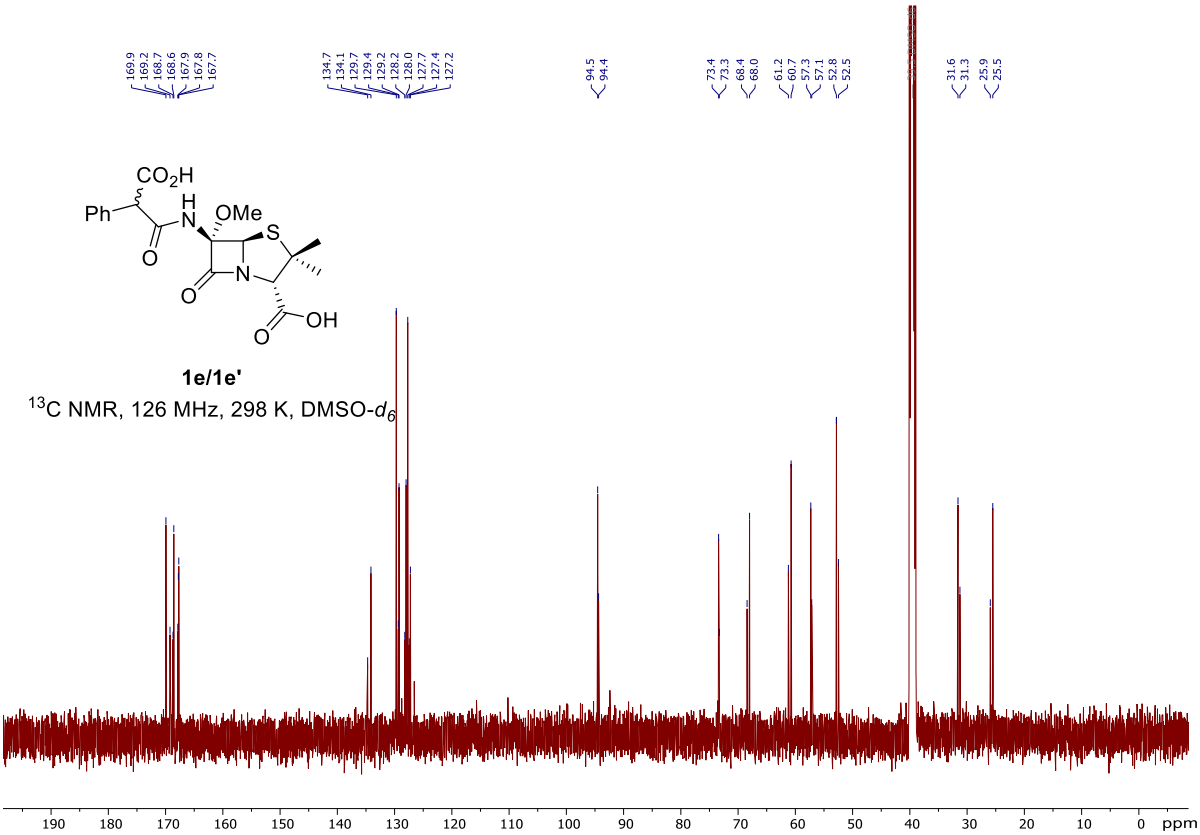

1e/1e'

^{13}C NMR, 126 MHz, 298 K, DMSO-d_6

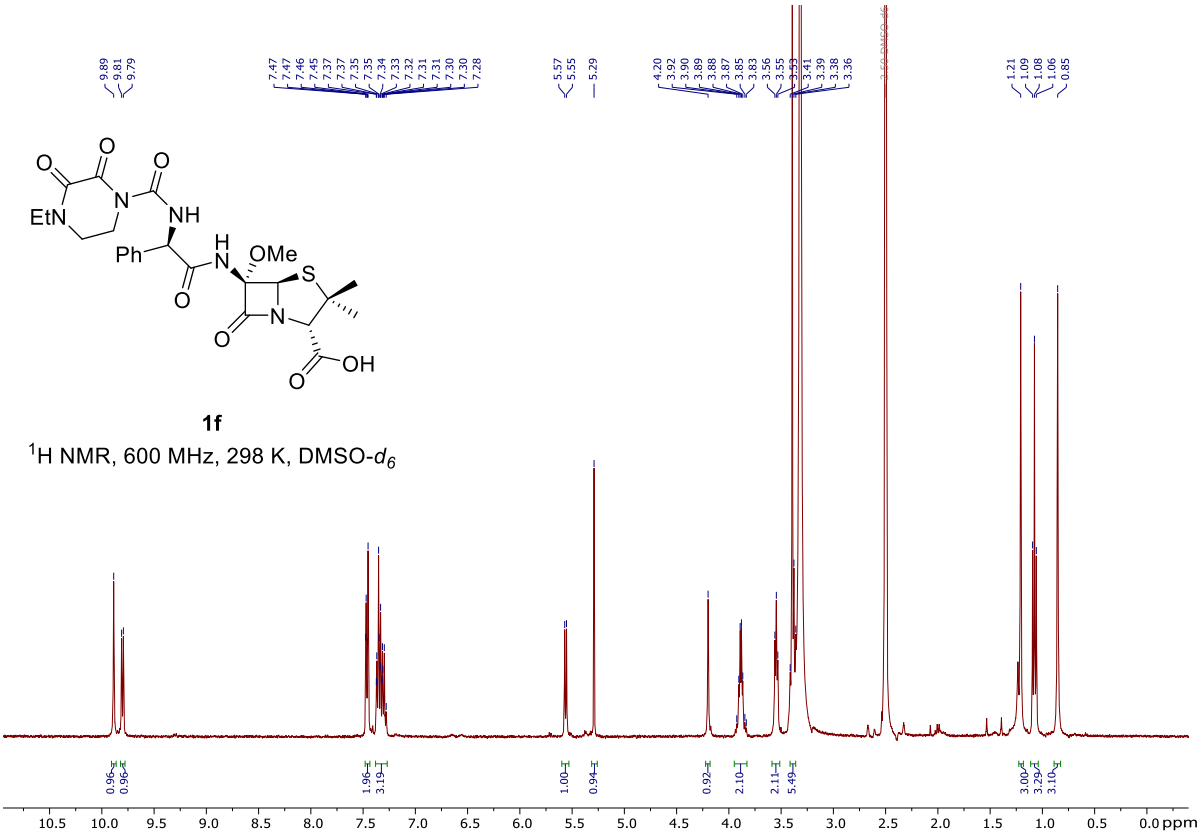

1f

^{1}H NMR, 600 MHz, 298 K, DMSO-d_6

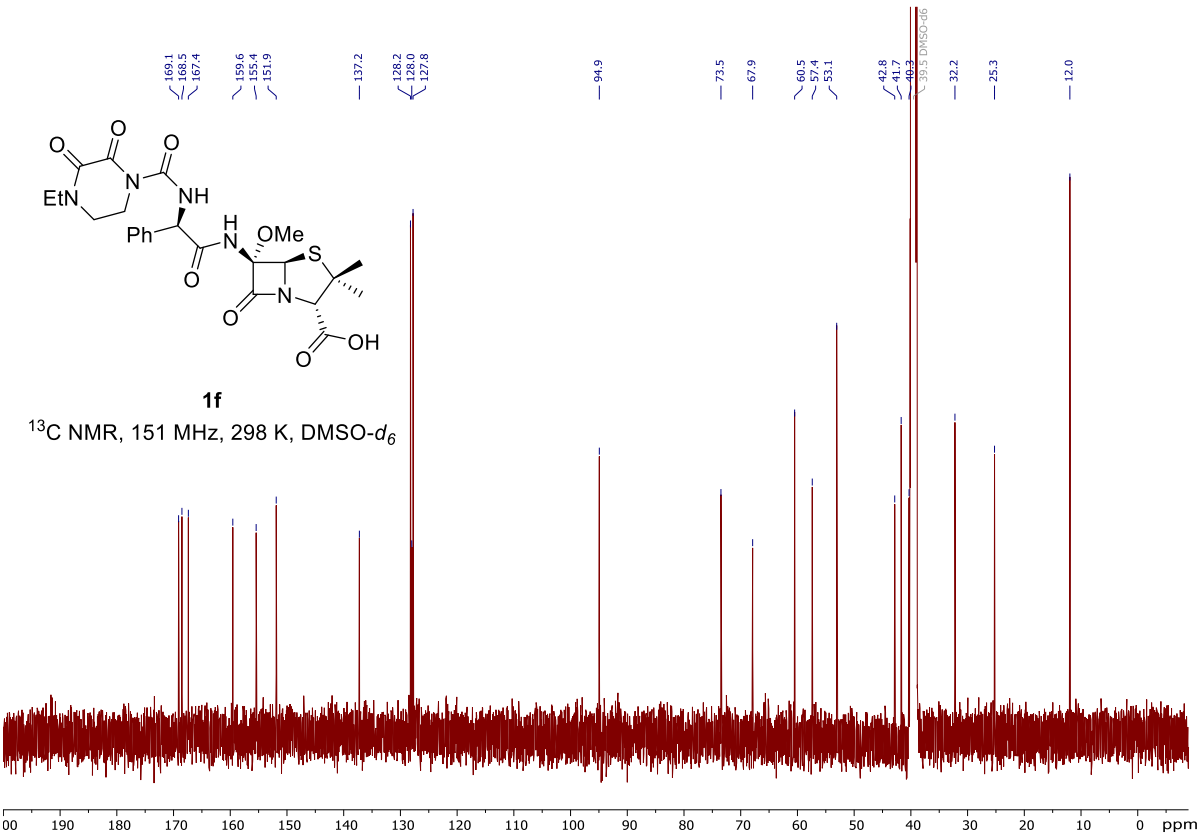

1f

^{13}C NMR, 151 MHz, 298 K, DMSO-d_6

8.5 Appendix to Chapter VI (Manuscript V)

8.5.1 General synthesis information

All reagents were obtained from commercial sources (Sigma-Aldrich, Inc.; Flurochem Ltd.; Manchester Organics; Tokyo Chemical Industry Ltd.) and were used without further purification. Flash column chromatography was performed using an automated Biotage Isolera One purification machine equipped with Biotage®Sfär flash chromatography cartridges. ^{1}H and ^{13}C NMR spectra were recorded using a Bruker AVIII400, AVIII500, and AVIII600. Infrared (IR) spectroscopy was performed using a Bruker Tensor-27 Fourier transform infrared (FT-IR) spectrometer. High-resolution mass spectrometry (HRMS) was performed using either electro-spray ionization (ESI) mass spectrometry (MS) in the positive or negative ionization modes employing a Thermo Scientific Exactive mass spectrometer (ThermoFisher Scientific), or atmospheric pressure chemical ionization (APCI) in the positive mode using an Agilent 7200 Accurate Mass spectrometer; data are presented as a mass-to-charge ratio (m/z). Optical rotation ($[\alpha]_D^{25}$) measurements were performed using a Unipol (Schmidt Haensch) polarimeter.

8.5.2 Experimental procedures and compounds characterisations

Methyl (2*S*,5*R*,6*R*)-3,3-dimethyl-7-oxo-6-(2-phenylacetamido)-4-thia-1-azabicyclo[3.2.0]heptane-2-carboxylate (7-I)

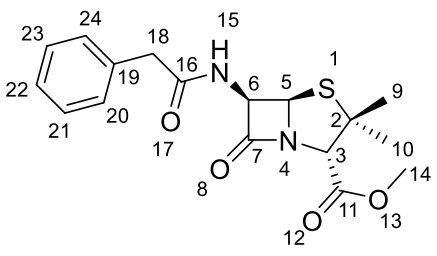

A variation of a reported procedure was followed.[1] MeI (1.9 mL, 30.5 mmol, 1.1 equiv.) was added dropwise under N_2 at room temperature to a solution of commercially sourced **penicillin G potassium salt** (10 g, 26.8 mmol) in *N*,*N*-dimethylformamide (50 mL). After 17 hours, the reaction mixture was poured into ice water, then

extracted with CH_2Cl_2. The combined organic layers were washed with H_2O and brine, dried over Na_2SO_4, filtered, and concentrated *in vacuo*. Purification by column chromatography (100 g Sfär, 100% cyclohexane (2 CV), followed by a linear gradient (18 CV): 0% →45% ethyl acetate in cyclohexane) yielded **7-I** (12.5 g, 94%). The analytical data are consistent with those reported.[1]

Yellow oil; ^{1}H NMR (400 MHz, 298 K, $CDCl_3$): δ = 7.39 – 7.25 (m, 5H, *C20H, C21H, C22H, C23H, C24H*), 5.65 (s, broad, 1H, *N15H*), 5.50 (dd, *J* = 4.3, 0.9 Hz, 1H, *C6H*), 4.37 (s, 1H, *C3H*), 3.75 (s, 3H, *C14H$_3$*), 3.63 (s, 2H, *C18H$_2$*), 1.44 (s, 3H, *C9H$_3$*), 1.43 ppm (s, 3H, *C10H$_3$*); ^{13}C NMR (101 MHz, 298 K, $CDCl_3$): δ = 173.6, 170.4, 168.1, 134.0, 129.7, 129.2, 127.7, 70.4, 68.2, 64.6, 58.9, 52.5, 43.5, 31.9, 26.9 ppm; IR (film) ṽ= 3296,2360, 2341, 1783, 1749, 1662, 1521, 1455, 1299, 1212, 1157, 1130, 1076, 1031 cm^{-1}; HRMS (ESI): m/z calculated for $C_{17}H_{20}N_2O_4S$ $[M+H]^+$: 349.1217, found: 349.1212; $[\alpha]_D^{25}$ = +154 (c = 0.011 g/mL, $CHCl_3$).

Methyl (2*S*,4*S*,5*R*,6*R*)-3,3-dimethyl-7-oxo-6-(2-phenylacetamido)-4-thia-1-azabicyclo[3.2.0]heptane-2-carboxylate 4-oxide (7)

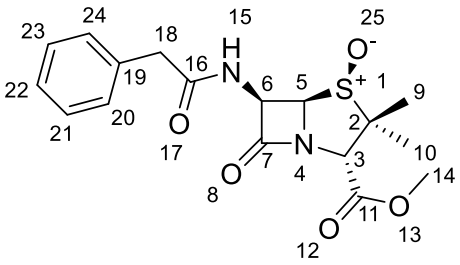

A variation of a reported procedure was followed.[2] To a stirred solution of penam **7-I** (7.26 g, 20.8 mmol, 1 equiv.) in anhydrous CH_2Cl_2 (90 mL), mCPBA (<77% purity; 3.77 g, 21.8 mmol, 1.05 equiv.) was added at 0°C in portions over 30 min. The reaction mixture was further stirred at 0°C for 2 hours, before it was washed with aqueous $Na_2S_2O_5$ solution (10% (w/v)), sat. aqueous $NaHCO_3$ solution, water, and brine. The organic phase was dried over Na_2SO_4, filtered, and concentrated *in vacuo* to give **7** (6.37 g, 84.1%). **7** was directly used in the next step without any further purifications. The analytical data are consistent with those reported.[3]

Yellow oil; ^{1}H NMR (400 MHz, 298 K, $CDCl_3$): δ = 7.37 – 7.25 (m, 5H, *C20H, C21H, C22H, C23H, C24H*), 7.07 (d, *J* = 10.2 Hz, 1H, *N15H*), 6.04 (dd, *J* = 10.3, 4.6 Hz, 1H, *C6H*), 4.98 (d, *J* = 4.6 Hz, 1H, *C5H*), 4.62 (s, 1H, *C3H*), 3.81 (s, 3H, *C14H$_3$*), 3.64 – 3.53 (m, 2H, *C18H$_2$*), 1.68 (s, 3H, *C9H$_3$*), 1.19 ppm (s, 3H, *C10H$_3$*); ^{13}C NMR (101 MHz, 298 K, $CDCl_3$): δ = 173.7, 170.8, 168.4, 133.9, 129.4, 129.1, 127.6, 77.4, 76.9, 75.4, 66.5, 56.5, 53.1, 43.6, 19.5, 18.8 ppm; IR (film) ṽ= 3367, 2955, 2360, 2360, 2341, 1792, 1752, 1680, 1508, 1496, 1455, 1393, 1353, 1286, 1216, 1160, 1132, 1071, 1041 cm^{-1}; HRMS (ESI): m/z calculated for $C_{17}H_{21}N_2O_5S$ $[M+H]^+$: 365.1179, found: 365.1166; $[\alpha]_D^{25}$ = +181 (c= 0.010 g/mL, $CHCl_3$).

Methyl (2*R*)-2-(3-benzyl-7-oxo-4-thia-2,6-diazabicyclo[3.2.0]hept-2-en-6-yl)-3-methylbut-3-enoate (8)

A variation of a reported procedure was followed.[4] A stirred solution of penam **7** (15.3 g, 42.02 mmol, 1 equiv.) and $P(OMe)_3$ (10.8 mL, 92.44 mmol, 2.2 equiv.) in anhydrous benzene (200 mL) was refluxed under N_2 for 24 h. The reaction mixture was filtered through a pad of Celite®, then concentrated *in vacuo*. Purification by column chromatography (100 g Sfär, 100% cyclohexane (2 CV), followed by a linear gradient (32 CV): 0% →45% ethyl acetate in cyclohexane) yielded **8** (10.8 g, 77%). The analytical data are consistent with those reported.[4]

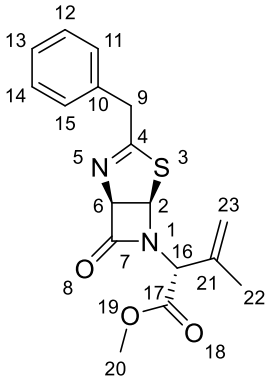

Yellow oil; ^{1}H NMR (400 MHz, 298 K, $CDCl_3$): δ = 7.35 – 7.26 (m, 5H, *C11H, C12H, C13H, C14H, C15H*), 5.96 (dt, *J* = 4.2, 1.0 Hz, 1H, *C2H*), 5.90 (d, *J* = 4.2 Hz, 1H, *C6H*), 5.04 (m, 1H, *C23H*), 4.88 (m, 1H, *C23H*), 4.83 (m, 1H, *C16H*), 3.88 (s, 2H, *C9H$_2$*), 3.74 (s, 3H, *C20H$_3$*), 1.68 ppm (s, 3H, *C22H$_3$*); ^{13}C NMR (101 MHz, 298 K, $CDCl_3$): δ = 173.7, 169.5, 165.5, 137.8, 135.2, 129.3, 128.9, 127.5, 117.3, 92.5, 68.7, 58.7, 52.7, 41.6, 21.6 ppm; IR (film) ṽ= 2360.64, 1769,

1741, 1613, 1495, 1435, 1334, 1248, 1200, 1156, 1078, 1001 cm^{-1}; HRMS (ESI): m/z calculated for $C_{17}H_{18}N_2O_3S$ $[M+H]^+$: 331.1111, found: 331.1109; $[\alpha]_D^{25}$ = -158 (c = 0.012 g/mL, $CHCl_3$).

Methyl 2-((1*R*,5*R*)-3-benzyl-7-oxo-4-thia-2,6-diazabicyclo[3.2.0]hept-2-en-6-yl)-3-methylbut-2-enoate (9)

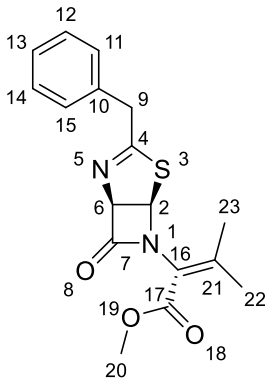

A variation of a reported procedure was followed.[4] To a stirred solution of penam **8** (4.46 g, 13.51 mmol, 1 equiv.) in anhydrous CH_2Cl_2 (30 mL), Et_3N (0.99 mL, 7.12 mmol, 0.52 equiv.) was added under N_2 at room temperature. After 3 hours, the reaction mixture was washed with aqueous NH_4Cl solution (1 M), H_2O, and brine. The organic phase was dried over Na_2SO_4, filtered, and concentrated *in vacuo* to give penam **9** (4.1 g, 91.9%), which was directlyused in the next step without further purification. The analytical data are consistent with those reported.[4]

Yellow oil; ^{1}H NMR (400 MHz, $CDCl_3$) δ 7.34 – 7.26 (m, 5H, *C11H*, *C12H*, *C13H*, *C14H*, *C15H*), 6.01 (dt, *J* = 4.0, 1.0 Hz, 1H, *C2H*), 5.83 (d, *J* = 4.0 Hz, 1H, *C6H*), 3.98 – 3.82 (ABq, 2H, *$C9H_2$*), 3.72 (s, 3H, *$C20H_3$*), 2.18 (s, 3H, *$C22H_3$*), 1.61 (s, 3H, *$C23H_3$*); ^{13}C NMR (101 MHz, $CDCl_3$): δ = 172.5, 163.9, 163.7, 156.3, 135.0, 129.4, 128.9, 127.6, 118.5, 92.8, 77.4, 71.0, 52.1, 41.8, 23.8, 22.0 ppm; IR (film) ṽ= 2928. 2854. 1757, 1724, 1655, 1610, 1439, 1365, 1223, 1172, 1078 cm^{-1}; HRMS (ESI): m/z calculated for $C_{17}H_{18}N_2O_3S$ $[M+K]^+$: 369.0670, found: 369.0672; $[\alpha]_D^{25}$ = +37 (c = 0.013 g/mL, $CHCl_3$).

(1*R*,5*R*)-3-Benzyl-4-thia-2,6-diazabicyclo[3.2.0]hept-2-en-7-one (10)

A variation of a reported procedure was followed.[4] To a solution of penam **9** (3.9 g, 11.8 mmol, 1 equiv.) in aqueous EtOH solution (95% (v/v); 80 mL) cooled to 0°C, a solution of $KMnO_4$ (1.65 g, 10.44 mmol, 0.89 equiv.) and $MgSO_4$ (1.14 g, 9.49 mmol, 0.8 equiv.) in H_2O (65 mL) was added over 80 min. Then, additional $KMnO_4$ was subsequently added (5 x 0.48 g) every 5 min. Following *in vacuo* concentration, ethyl acetate and H_2O were added to the residue. The biphasic mixture was filtered to remove residual MnO_2, then the layers were separated. The aqueous layer was further extracted with ethyl acetate. The combined organic layers were washed with brine, dried over Na_2SO_4, filtered, and concentrated *in vacuo*. The solid residue was washed with cold Et_2O to give penam **10** (1.4 g, 54%). **10** was directly used in the next step without any further purifications. The analytical data are consistent with those reported.[4]

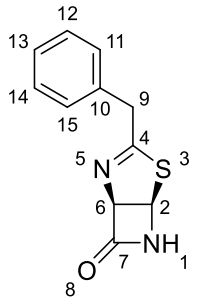

Amorphous yellow-white solid; ^{1}H NMR (400 MHz, 298 K, DMSO-d_6): δ = 8.95 (broad, 1H, *N1H*), 7.37 – 7.23 (m, 5H, *C11H*, *C12H*, *C13H*, *C14H*, *C15H*), 5.96 (m, 1H, *C2H*), 5.58 (d, *J* = 3.9 Hz, 1H, *C6H*), 3.95 – 3.85 (ABq, 2H, *C9H*$_2$); ^{13}C NMR (101 MHz, 298 K, DMSO-d_6): δ = 171.0, 165.3, 135.7, 129.1, 128.5, 127.0, 93.9, 63.6, 40.4 ppm; IR (film) ṽ= 3200, 1741, 1718, 1611, 1596, 1492, 1453, 1438, 1302, 1237, 1188, 1159, 1141, 1077, 1031 cm^{-1}; HRMS (ESI): m/z calculated for $C_{11}H_{10}N_2OS$ $[M+H]^+$: 219.0587, found: 219.0584.

(2*S*,4*R*,5*R*,6*R*)-3,3-Dimethyl-7-oxo-6-(2-phenylacetamido)-4-thia-1-azabicyclo[3.2.0]heptane-2-carboxylic acid 4-oxide (11)

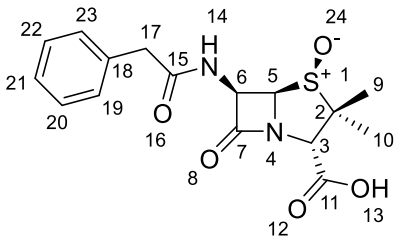

A variation of a reported procedure was followed.[5] To a stirred solution of commercially sourced penicillin G sodium salt (50 g, 0.14 mol, 1 equiv.) in H_2O (667 mL), $NaIO_4$ (33.6 g, 0.15 mol, 1.07 equiv.) was added at room temperature. After for 2 h, upon the addition of a saturated aqueous $NaHSO_3$ solution (100 mL), the colour of the reaction mixture changed from pale yellow, to dark brown, to yellow again. Subsequently, the aqueous phase was extracted with ethyl acetate, and the combined organic layers were dried over Na_2SO_4, filtered, and concentrated *in vacuo* to give penam **11** (45.6 g, 93%). **11** was directly used in the next step without any further purifications. The analytical data are consistent with those reported.[5]

Amorphous yellow foam; ^{1}H NMR (400 MHz, 298 K, $CDCl_3$): δ = 7.37 – 7.23 (m, 6H, *N14H*, *C19H*, *C20H*, *C21H, C22H, C23H*), 6.00 (dd, *J* = 10.1, 4.6 Hz, 1H, *C6H*), 5.01 (d, *J* = 4.6 Hz, 1H, *C5H*), 4.62 (s, 1H, *C3H*), 3.61 (m, 2H, *C17H*$_2$), 1.69 (s, 3H, *C9H*$_3$), 1.25 ppm (s, 3H, *C10H*$_3$); ^{13}C NMR (400 MHz, 298 K, $CDCl_3$): δ = 173.6, 171.9, 170.3, 133.7, 129.4, 129.1, 127.7, 76.7, 75.6, 66.3, 56.4, 43.3, 19.4, 18.7 ppm; IR (film) ṽ= 3369, 2980, 2359, 2341, 1790. 1742, 1675, 1512, 1496, 1455, 1391, 1371, 1279, 1216, 1131, 1072, 1019 cm^{-1}; HRMS (ESI): m/z calculated for $C_{16}H_{19}N_2O_5S$ $[M+Na]^+$: 373.0829, found: 373.0833.

2-((1*R*,5*R*)-3-Benzyl-7-oxo-4-thia-2,6-diazabicyclo[3.2.0]hept-2-en-6-yl)-3-methylbut-2-enoic acid (12)

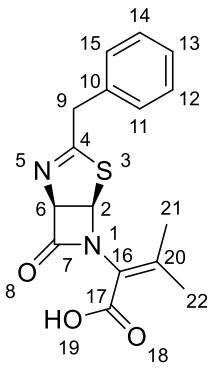

A variation of a reported procedure was followed.[6] A stirred solution of **11** (11.84 g, 33.1 mmol, 1 equiv.), 1,3-bis(trimethylsilyl)urea (11.84 g, 57.9 mmol, 1.74 equiv.), and tributyl phosphite (10.52 mL, 37.2 mmol, 1.12 equiv.) in dry butyl acetate (63 mL) was refluxed for 90 min, before addition of Et_3N (5.26 mL, 37.7 mmol, 1.12 equiv.), after which the reaction mixture was further refluxed for 20 min. Subsequently, after the mixture was cooled to 41 °C, an aqueous H_2SO_4 solution (0.5 M; 149 mL) was added, and the reaction mixture was vigorously stirred at 0 °C for 1 h. The precipitate was collected by filtration, washed with H_2O and butyl acetate, and dried *in vacuo*, yielding penam **12** (4.8 g, 50.2%). **12** was directly used in the next step without any further purifications. The analytical data are consistent with those reported.[6]

Amorphous white solid; ^{1}H NMR (400 MHz, 298 K, $CDCl_3$): δ = 7.33 – 7.26 (m, 5H, *C11H*, *C12H*, *C13H*, *C14H*, *C15H*), 6.00 (dt, *J* = 4.0, 1.0 Hz, 1H, *C2H*), 5.91 (d, *J* = 4.0 Hz, 1H, *C6H*), 3.96 (d, *J* = 14.5 Hz, 1H, *C9H*), 3.84 (dd, *J* = 14.5 Hz, 1H, *C9H*), 2.21 (s, 3H, *C22H*), 1.63 (s, 3H, *C21H*); ^{13}C NMR (101 MHz, 298 K, $CDCl_3$): δ = 172.9, 168.1, 163.8, 159.7, 135.0, 129.4, 128.9, 127.6, 118.2, 92.7, 70.9, 41.7, 24.3, 22.4 ppm; IR (film) ṽ= 2963, 1755, 1702, 1627, 1599, 1496, 1455, 1363, 1249, 1225, 1180, 1137, 1082, 1063, 1033 cm^{-1}; HRMS (ESI): m/z calculated for $C_{16}H_{17}N_2O_3S$ $[M+H]^+$: 317.0954, found: 317.0960; $[\alpha]_D^{25}$ = +30 (c = 0.015 g/mL, $CHCl_3$).

(1*R*,5*R*)-3-Benzyl-6-(hydroxymethyl)-4-thia-2,6-diazabicyclo[3.2.0]hept-2-en-7-one (13)

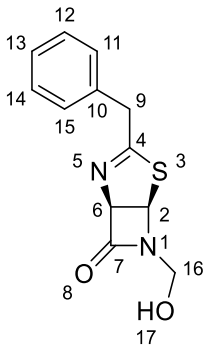

A suspension of penam **10** (3 g, 13.7 mmol), paraformaldehyde (629 mg, 20.9 mmol), and K_2CO_3 (110 mg, 0.79 mmol) in THF (30.27 ml) and H_2O (1.21 mL) was sonicated at room temperature for 8 hours. The reaction mixture was then diluted with ethyl acetate, dried over Na_2SO_4, filtered, and concentrated *in vacuo*. Purification by column chromatography (25 g Sfär, 100% cyclohexane (2 CV), followed by a linear gradient (28 CV): 0% →80% ethyl acetate in cyclohexane) yielded **13** (10.8 g, 77%).

Yellow oil; ^{1}H NMR (400 MHz, 298 K, DMSO-*d*$_6$): δ = 7.42 – 7.16 (m, 5H, *C11H*, *C12H*, *C13H*, *C14H*, *C15H*), 6.12 (t, *J* = 7.1 Hz, 1H, *O17H*), 6.03 – 5.99 (m, 1H, *C2H*), 5.75 (d, *J* = 4.2 Hz, 1H, *C6H*), 4.63 (dd, *J* = 11.4, 7.3 Hz, 1H, *C16H*), 4.35 (dd, *J* = 11.4, 7.0 Hz, 1H, *C16H*), 3.97 – 3.82 ppm (m, 2H, *C9H*); ^{13}C NMR (101 MHz, 298 K, DMSO-*d*$_6$): δ = 171.6, 163.9, 135.6, 129.2, 128.6, 127.1, 92.7, 66.7, 62.4, 40.4 ppm; IR (film) ṽ= 3456, 2920, 1743, 1611, 1597, 1493, 1454, 1373, 1294, 1251, 1157, 1139, 1080, 1051, 1014 cm^{-1}; HRMS (ESI): m/z calculated for $C_{12}H_{12}N_2O_2S$ [M+H]+: 249.0692, found: 249.0690; $[\alpha]_D^{25}$ = -70 (c = 0.018 g/mL, $CHCl_3$).

***N*-((2*R*,3*R*)-1-(Hydroxymethyl)-2-mercapto-4-oxoazetidin-3-yl)-2-phenylacetamide (14)**

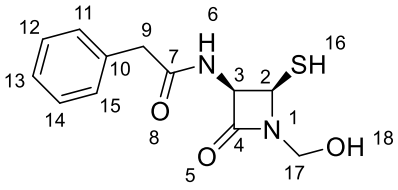

To a stirred solution of penam **13** (0.8 g, 3.22 mmol) in MeOH (15 mL) cooled to 0 °C, an aqueous HCl solution (1 M, 4.4 mL) was added. After 10 min, the reaction mixture was allowed to warm up to room temperature over 20 min. The reaction mixture was poured into H_2O, then extracted with CH_2Cl_2 and EtOAc. The organic phases were dried over Na_2SO_4, filtered, and

concentrated *in vacuo* to give penam **14** (534 mg, 66%). **14** was directly used in the next step without any further purifications.

Amorphous off-white solid; ^{1}H NMR (400 MHz, 298 K, DMSO-d_6): δ = 8.88 (d, *J* = 9.0 Hz, 1H, *N6H*), 7.32 – 7.20 (m, 5H, *C11H*, *C12H*, *C13H*, *C14H*, *C15H*), 6.06 (t, *J* = 6.5 Hz, 1H, *O18H*), 5.28 (dd, *J* = 9.0, 4.8 Hz, 1H, *C3H*), 5.14 (m, 1H, *C2H*), 4.70 (dd, *J* = 11.3, 6.5 Hz, 1H, *C17H*), 4.31 (dd, *J* = 11.3, 7.3 Hz, 1H, *C17H*), 3.53 (s, 2H, *C9H*$_2$), 2.96 ppm (d, *J* = 8.1 Hz, 1H, *S16H*); ^{13}C NMR (126 MHz, 298 K, DMSO-d_6): δ = 170.7, 164.8, 135.7, 129.1, 128.2, 126.5, 61.3, 60.4, 58.0, 42.1 ppm; HRMS (ESI): m/z calculated for $C_{12}H_{14}N_2O_3S$ [M-H]$^-$: 265.0652, found: 265.0661; IR (film) ṽ= 3269, 1742, 1722, 1654, 1546, 1497, 1471, 1453, 1411, 1356, 1313, 1258, 1201, 1129, 1059, 1032 cm^{-1}; $[\alpha]_D^{25}$ = -8 (c = 0.009 g/mL, $CHCl_3$).

Benzyl 2-(((2*R*,3*R*)-1-(hydroxymethyl)-4-oxo-3-(2-phenylacetamido)azetidin-2-yl)thio)acetate (15a)

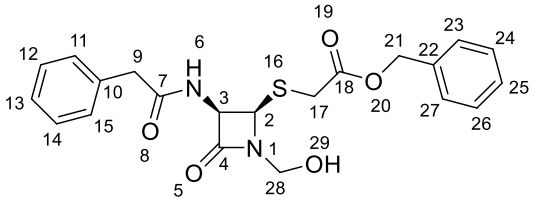

To a stirred solution of penam **14** (200 mg, 0.75 mmol, 1 equiv.) in dry *N*,*N*-dimethylformamides (6 mL) cooled to 0 °C, benzyl 2-bromoacetate (0.11 mL, 0.75 mmol, 1 equiv.) was added. After stirring at 0 °C for 30 min, EtOAc (15 mL) and H_2O (15 mL) were added to the reaction mixture. The organic layer was separated, washed with H_2O and brine, then dried over Na_2SO_4, filtered, and concentrated *in vacuo* to give penam **15a** (310 mg, 96.5%). **15a** was directly used in the next step without any further purifications.

Amorphous white solid; ^{1}H NMR (600 MHz, 298 K, $CDCl_3$) δ 7.40 – 7.27 (m, 10H, *C11H*, *C12H*, *C13H*, *C14H*, *C15H, C23H*, *C24H*, *C25H*, *C26H*, *C27H*), 6.19 (d, *J* = 8.3 Hz, 1H, *N6H*), 5.36 (dd,

J = 8.3, 4.6 Hz, 1H, *C3H*), 5.16 (s, 2H, *C21H₂*), 5.10 (d, *J* = 4.6 Hz, 1H, *C2H*), 4.73 (dd, *J* = 11.7, 8.0 Hz, 1H, *C28H*), 4.57 (dd, *J* = 11.7, 7.6 Hz, 1H, *C28H*), 3.68 – 3.60 (ABq, 2H, *C9H₂*), 3.51 (t, *J* = 7.8 Hz, 1H, *O29H*), 3.28 (s, 2H, *C17H₂*); ^{13}C NMR (151 MHz, 298 K, $CDCl_3$): δ = 171.5, 171.0, 164.8, 135.0, 134.0, 129.7, 129.3, 129.0, 128.9, 128.7, 127.8, 68.1, 66.2, 63.7, 61.3, 43.6, 33.7 ppm; IR (film) ṽ= 3422, 3257, 1761, 1720, 1652, 1534, 1498, 1451, 1406, 1383, 1310, 1297, 1240, 1186, 1107, 1029 cm^{-1}; HRMS (ESI): m/z calculated for $C_{21}H_{22}N_2O_5S$ $[M+Na]^+$: 437.1142, found: 437.1143; $[\alpha]_D^{25}$ = -60 (c = 0.009 g/mL, $CHCl_3$).

Benzyl 2-(((2*R*,3*R*)-1-(hydroxymethyl)-4-oxo-3-(2-phenylacetamido)azetidin-2-yl)thio)propanoate (15b/15b')

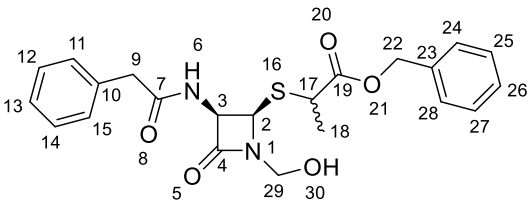

To a solution of (±)-benzyl 2-bromopropanoate (400 mg, 1.65 mmol, 1.1 equiv.) in dry *N*,*N*-dimethylformamides (13 mL) cooled to 0 °C, penam **14** (400 mg, 1.5 mmol, 1 equiv.) and Et_3N (0.21 mL, 1.5 mmol, 1 equiv.) were subsequently added. After stirring for 35 min, EtOAc (30 mL) and H_2O (20 mL) were added to the reaction mixture. The organic layer was then separated, washed with H_2O and brine, dried over Na_2SO_4, filtered, and concentrated *in vacuo*. Purification by column chromatography (10 g Sfär, 100% cyclohexane (2 CV), followed by a linear gradient (25 CV): 0% →90% ethyl acetate in cyclohexane) yielded an inseparable *C17* diastereomeric mixture of penams **15b** and **15b'** (d.r. = 1:1; 376 mg, 58%).

Yellow wax; isomer **15b**: ^{1}H NMR (600 MHz, 298 K, $CDCl_3$): δ = 7.38 – 7.27 (m, 10H, *C11H*, *C12H*, *C13H*, *C14H*, *C15H*, *C24H*, *C25H*, *C26H*, *C27H*, *C28H*), 6.32 (d, *J* = 8.4 Hz, 1H, *N6H*), 5.33 (dd, *J* = 8.4, 4.6 Hz, 1H, *C3H*), 5.17 (m, 2H, *C22H₂*), 5.16 (d, *J* = 4.5 Hz, 1H, *C2H*), 4.63 (d, *J* = 11.7 Hz, 1H, *C29H*), 4.37 (d, *J* = 11.7 Hz, 1H, *C29H*), 3.62 (d, *J* = 2.1 Hz, 2H, *C9H₂*), 3.45 (q,

J = 7.3 Hz, 1H, *C17H*), 1.38 ppm (d, *J* = 7.3 Hz, 3H, *C18H*$_3$); isomer **15b'**: ^{1}H NMR (600 MHz, 298 K, $CDCl_3$): δ = 7.38 – 7.27 (m, 10H, *C11H*, *C12H*, *C13H*, *C14H*, *C15H*, *C24H*, *C25H*, *C26H*, *C27H*, *C28H*), 6.14 (d, *J* = 8.5 Hz, 1H, *N6H*), 5.26 (dd, *J* = 8.5, 4.7 Hz, 1H, *C3H*), 5.24 (d, *J* = 4.7 Hz, 1H, *C2H*), 5.13 (s, 2H, *C22H*$_2$), 4.69 (d, *J* = 11.7 Hz, 1H, *C29H*), 4.46 (d, *J* = 11.7 Hz, 1H, *C29H*), 3.62 (d, *J* = 2.1 Hz, 2H, *C9H*$_2$), 3.56 (q, *J* = 7.2 Hz, 1H, *C17H*), 1.45 ppm (d, *J* = 7.2 Hz, 3H, *C18H*); ^{13}C NMR (151 MHz, 298 K, $CDCl_3$): δ = 173.4, 173.0, 171.5, 171.3, 165.4, 165.1, 135.31, 135.29, 134.1, 134.0, 129.2, 128.9, 128.88, 128.86, 128.8, 128.6, 128.5, 127.7, 67.8, 67.7, 65.3, 63.5, 63.4, 63.1, 61.3, 60.9, 43.5, 42.6, 40.9, 17.4, 17.3 ppm. (^{13}C assignment to individual isomers was not done due to overlapping 2D NMR signals); HRMS (ESI): m/z calculated for $C_{22}H_{24}N_2O_5S$ $[M+Na]^+$: 451.1298, found: 451.1293.

Dibenzyl 2-(((2*R*,3*R*)-1-(hydroxymethyl)-4-oxo-3-(2-phenylacetamido)azetidin-2-yl)thio)malonate (15c)

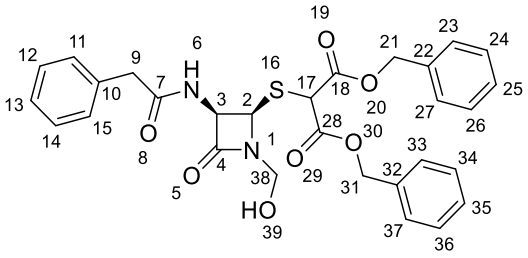

To a stirred solution of penam **14** (50 mg, 0.1875 mmol, 1 equiv.) in dry DMF (10 mL) cooled to 0 °C, dibenzyl 2-(tosyloxy)malonate (85.1 mg, 0.1875 mmol, 1 equiv.) and Et_3N (26.1 μL, 0.1875 mmol, 1 equiv.) were sequentially added to the reaction mixture. After stirring for 1 hour, EtOAc (5 mL) and H_2O (5 mL) were added to the reaction mixture. The layers were separated, and the aqueous phase was further extracted with EtOAc. The combined organic phases were washed with H_2O, and brine, then dried over Na_2SO_4, filtered, and concentrated *in vacuo* to give penam **15c** (68 mg, 66%). After the work-up, the product was used in the next step without any further purifications. (Any attempts to purify the intermediate using flash column chromatography led to substantial product decomposition.)

Colourless oil; ^{1}H NMR (600 MHz, 298 K, $CDCl_3$): δ = 7.36 – 7.24 (m, 15H, *C11H*, *C12H*, *C13H*, *C14H*, *C15H, C23H*, *C24H*, *C25H*, *C26H*, *C27H, C33H*, *C34H*, *C35H*, *C36H*, *C37H*), 6.25 (d, *J* = 8.1 Hz, 1H, *N6H*), 5.29 (d, *J* = 4.7 Hz, 1H, *C2H*), 5.19 (s, 2H, $C21H_2$), 5.18 – 5.13 (m, 2H, $C31H_2$), 4.99 (dd, *J* = 8.1, 4.7 Hz, 1H, *C3H*), 4.70 (d, *J* = 11.7 Hz, 1H, *C38H*), 4.58 (d, *J* = 11.7 Hz, 1H, *C38H*), 4.33 (s, 1H, *C17H*), 3.57 ppm (s, 2H, $C9H_2$); ^{13}C NMR (151 MHz, 298 K, $CDCl_3$): δ = 171.8, 167.0, 166.6, 165.0, 134.8, 134.6, 134.1, 129.8, 129.1, 128.9, 128.81, 128.80, 128.6, 127.6, 68.8, 68.6, 64.2, 63.5, 61.6, 50.2, 43.3 ppm; HRMS (ESI): m/z calculated for $C_{29}H_{29}N_2O_7S$ $[M+H]^+$: 549.1690, found: 549.1666.

Dibenzyl (5*R*,6*R*)-7-oxo-6-(2-phenylacetamido)-4-thia-1-azabicyclo[3.2.0]heptane-3,3-dicarboxylate (19)

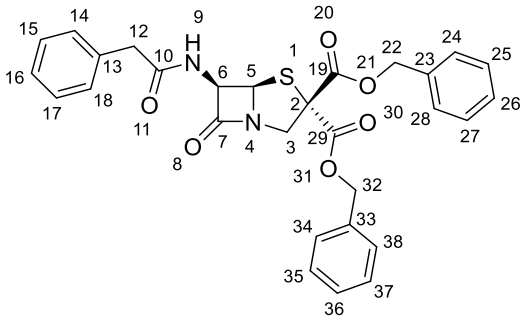

To a stirred solution of penam **15c** (69 mg, 0.126 mmol, 1 equiv.) in tetrahydrofuran (2 mL) cooled to 0°C, tosyl chloride (24 mg, 0.126 mmol, 1 equiv.) and 2,5-lutidine (14.5 μL, 0.126 mmol, 1 equiv.) were sequentially added to the reaction mixture. After stirring for 90 min, the reaction mixture was cooled to -20 ° C, after which 1,8-diazabicyclo[5.4.0]undec-7-ene (18.8 μL, 0.126 mmol, 1 equiv.) was added, and the reaction mixture was further stirred for 30 min. Following the addition of an aqueous HCl solution (1 M; 0.13 mL), the reaction mixture was diluted with EtOAc and H_2O. The organic layer was separated, washed with aqueous HCl solution (1 M), H_2O, and brine, then dried over Na_2SO_4, filtered, and concentrated *in vacuo*. Purification by column chromatography (10 g Sfär, 100% cyclohexane (2 CV), followed by a linear gradient (25 CV): 0% →100% ethyl acetate in cyclohexane) yielded colourless oil fraction (17 mg) containing penam **19** (and other uncharacterised impurities) that

could not be further purified due to apparent product loss/decomposition under chromatographic conditions.

Oil; ^{1}H NMR (600 MHz, $CDCl_3$) δ 7.36 – 7.24 (m, 15H, *C14H*, *C15H*, *C16H*, *C17H*, *C18H*, *C24H*, *C25H*, *C26H*, *C27H*, *C28H*, *C34H*, *C35H*, *C36H*, *C37H*, *C38H*), 6.98 (d, *J* = 9.8 Hz, 1H, *N9H*), 5.75 (dd, *J* = 9.8, 4.0 Hz, 1H, *C6H*), 5.40 (d, *J* = 4.0 Hz, 1H, *C5H*), 5.16 (m, 2H, $C32H_2$), 5.09 (m, 2H, *C22H*), 4.46 (d, *J* = 13.5 Hz, 1H, $C3H_\alpha$), 3.60 – 3.54 (m, 3H, $C22H_2$, $C3H_\beta$); ^{13}C NMR (151 MHz, $CDCl_3$) ^{13}C NMR (151 MHz, $CDCl_3$) δ 173.7, 170.8, 170.0, 168.3, 165.7, 134.5, 134.3, 134.2, 129.7, 129.1, 129.0, 128.9, 128.9, 128.9, 128.8, 128.8, 128.7, 128.4, 128.4, 127.4, 70.4, 69.6, 69.2, 69.1, 68.7, 61.4, 54.2, 43.6, 29.9 ppm; HRMS (ESI): m/z calculated for $C_{29}H_{26}N_2O_6S$ $[M+H]^+$: 531.1584, found: 531.1588.

Benzyl 2-bromoacrylate (**22a**)

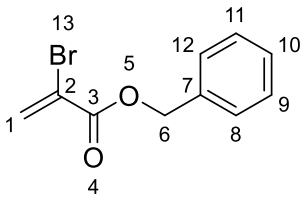

A variation of a reported procedure was followed.[7] To a stirred solution of 2-bromoacrylic acid (5 g, 33.12 mmol, 1 equiv.) in dry DMF (35 mL), K_2CO_3 (4.57 g, 33.12 mmol, 1 equiv.) and benzyl bromide (3.9 mL, 33.12 mmol, 1 equiv.) were added sequentially. After stirring at room temperature under N_2 for 24 hours, the reaction mixture was diluted with ethyl acetate, washed with H_2O, $NaHCO_3$ and brine, then dried over Na_2SO_4, filtered, and concentrated *in vacuo*. The residue was then immediately subjected to vacuum distillation at 136°C, and the fractions were collected in flasks containing small amounts of *p*-benzoquinone (1-2 mg). **22a** was obtained as a colourless oil (4.55 g, 57.2%) that quickly polymerizes at room temperature. The analytical data are consistent with those reported.[7]

Oil; ^{1}H NMR (400 MHz, $CDCl_3$): δ = 7.42 – 7.32 (m, 5H, *C8H*, *C9H*, *C10H*, *C11H*, *C12H*), 7.00 (d, *J* = 1.6 Hz, 1H, *C1H*), 6.30 (d, *J* = 1.6 Hz, 1H, *C1H*), 5.26 ppm (s, 2H, $C6H_2$); ^{13}C NMR (101 MHz, 298 K, $CDCl_3$): δ = 161.9, 135.2, 131.1, 128.8, 128.8, 128.7, 128.4, 121.4, 68.4 ppm; IR (film) ṽ= 2358, 1730, 1607, 1456, 1389, 1259, 1097 cm^{-1}; HRMS (ESI): m/z calculated for $C_{10}H_9BrO_2$ $[M+Na]^+$: 262.9678, found: 262.9678.

Benzyl 3-((1*R*,5*R*)-3-benzyl-7-oxo-4-thia-2,6-diazabicyclo[3.2.0]hept-2-en-6-yl)-2-bromopropanoate (23a/23a')

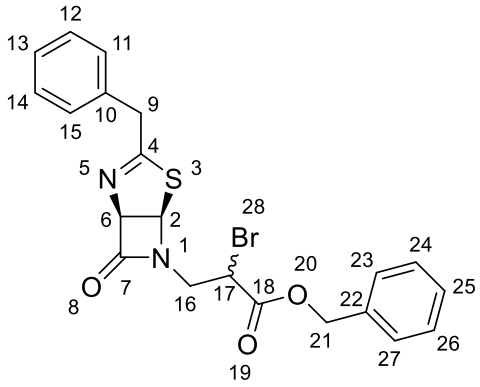

To a solution of **10** (2.01 g, 9.21 mmol, 1 equiv.) in dry acetone (75 mL), K_2CO_3 (2.07 g, 9.21 mmol, 1 equiv.) and **22a** (4.43 g, 18.45 mmol, 1 equiv.) were sequentially added, and the reaction was stirred at room temperature under N_2 for 48 hours. The reaction mixture was filtered through Celite®, then concentrated *in vacuo*. Purification by column chromatography (50 g Sfär, 100% cyclohexane (2 CV), followed by a linear gradient (25 CV): 0% →60% ethyl acetate in cyclohexane) yielded an inseparable *C-17* diastereomeric mixture of penams **23a** and **23a'** (d.r. = 1:0.84; 2.28 g, 54%).

Oil; isomer **23a**: ^{1}H NMR (600 MHz, 298 K, $CDCl_3$): δ = 7.38 – 7.23 (m, 10H, *C11H, C12H, C13H, C14H, C15H, C23H, C24H, C25H, C26H, C27H*), 5.93 (d, *J* = 3.9 Hz, 1H, *C2H*), 5.60 (d, *J* = 3.9 Hz, 1H, *C6H*), 5.17 (m, 2H, $C21H_2$), 4.41 (m, 1H, *C17H*), 3.94 – 3.90 (m, 1H, *C16H*), 3.94 – 3.91 (m, 1H, *C9H*), 3.81 – 3.78 (m, 1H, *C9H*), 3.72 – 3.68 ppm (m, 1H, *C16H*); isomer **23a'**: ^{1}H NMR (600 MHz, 298 K, $CDCl_3$): δ = 7.38 – 7.23 (m, 10H, *C11H, C12H, C13H, C14H, C15H,*

C23H, C24H, C25H, C26H, C27H), 5.81 (d, *J* = 3.9 Hz, 1H, *C2H*), 5.39 (d, *J* = 3.9 Hz, 1H, *C6H*), 5.19 (m, 2H, *C21H*$_2$), 4.43 (m, 1H, *C17H*), 3.93 – 3.91 (m, 1H, *C9H*), 3.87 – 3.84 (m, 1H, *C16H*), 3.79 – 3.77 (m, 1H, *C9H*), 3.72 – 3.68 ppm (m, 1H, *C16H*); ^{13}C NMR (151 MHz, 298 K, $CDCl_3$): δ = 173.1, 173.0, 168.2, 168.0, 165.1, 164.9, 135.0, 134.8, 134.7, 129.4, 129.4, 128.9, 128.9, 128.9, 128.8, 128.7, 128.6, 127.6, 93.5, 93.3, 70.5, 70.2, 68.5, 68.3, 43.3, 43.2, 41.6, 41.5, 40.0 ppm (^{13}C assignment to individual isomers was not done due to overlapping signals); HRMS (ESI): m/z calculated for $C_{21}H_{20}BrN_2O_3S$ $[M+H]^+$: 459.0373, found: 459.0372.

Benzyl (5*R*,6*R*)-7-oxo-6-(2-phenylacetamido)-4-thia-1-azabicyclo[3.2.0]heptane-3-carboxylate (25a/25a')

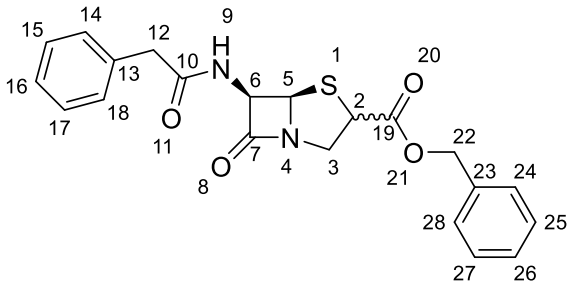

To a stirred solution of **23a/23a'** (330 mg, 0.72 mmol, 1 equiv.) in acetone (3.3 mL) cooled to 0 °C, an aqueous HCl solution (1 M, 1.1 mL) was added. After stirring for 1 at 0 °C, H_2O and EtOAc were added to the reaction mixture. The phases were separated, and the aqueous layer was further extracted with EtOAc. The combined organic layers were washed with brine, then dried over Na_2SO_4, filtered, and concentrated *in vacuo*. The residue was then dissolved in anhydrous tetrahydrofuran (7 mL), to which finely ground K_2CO_3 (99.3 mg, 0.72 mmol, 1 equiv.) was added. The reaction was stirred at room temperature under N_2 for 18 hours. The reaction mixture was filtered through a pad of Celite®, then the filtrate was concentrated *in vacuo* to give an inseparable *C2* mixture of penams **25a** (**benzyl (3R,5R,6R)-7-oxo-6-(2-phenylacetamido)-4-thia-1-azabicyclo[3.2.0]heptane-3-carboxylate**) and **25a'** (**benzyl (3S,5R,6R)-7-oxo-6-(2-phenylacetamido)-4-thia-1-**

azabicyclo[3.2.0]heptane-3-carboxylate) (d.r. = 1.07:1; 259 mg, 90%). **25a/25a'** was directly used in the next step without any further purifications.

Orange waxy foam; isomer **25a**: ^{1}H NMR (600 MHz, 298 K, $CDCl_3$): δ = 7.43 – 7.30 (m, 10H, *C14H*, *C15H*, *C16H*, *C17H*, *C18H*, *C24H*, *C25H*, *C26H, C27H*, *C28H*), 7.00 (d, *J* = 9.7 Hz, 1H, *N9H*), 5.74 (dd, *J* = 9.7, 4.0 Hz, 1H, *C6H*), 5.37 (d, *J* = 4.0 Hz, 1H, *C5H*), 5.20 (s, 2H, $C22H_2$), 4.31 (dd, *J* = 7.5, 5.5 Hz, 1H, *C2H*), 4.15 (dd, *J* = 12.3, 7.5 Hz, 1H, *C3H*), 3.62 – 3.54 (m, 2H, $C12H_2$), 3.37 ppm (dd, *J* = 12.3, 5.5 Hz, 1H, *C3H*); Isomer **25a'**: ^{1}H NMR (600 MHz, 298 K, $CDCl_3$): δ = 7.43 – 7.30 (m, 10H, *C14H*, *C15H*, *C16H*, *C17H*, *C18H*, *C24H*, *C25H*, *C26H, C27H*, *C28H*), 6.26 (d, *J* = 8.9 Hz, 1H, *N9H*), 5.65 (dd, *J* = 8.9, 3.9 Hz, 1H, *C6H*), 5.31 (d, *J* = 3.9 Hz, 1H, *C5H*), 5.13 – 5.05 (m, 2H, $C22H_2$), 4.41 (d, *J* = 13.0 Hz, 1H, *C2H*), 4.11 (d, *J* = 6.6 Hz, 1H, *C3H*), 3.63 (m, 2H, $C12H_2$), 3.11 ppm (dd, *J* = 13.0, 6.6 Hz, 1H, *C3H*); ^{13}C NMR (151 MHz, 298 K, $CDCl_3$): δ = 174.0, 173.9, 173.1, 170.7, 170.6, 170.2, 135.0, 134.7, 134.2, 133.9, 129.7, 129.5, 129.2, 129.0, 128.9, 128.9, 128.8, 128.8, 128.4, 127.7, 127.3, 68.5, 68.5, 67.9, 60.8, 58.6, 53.3, 52.9, 51.6, 49.5, 43.6, 43.4 ppm (^{13}C assignment to individual isomers was not done due to overlapping signals); HRMS (ESI): m/z calculated for $C_{29}H_{29}N_2O_7S$ $[M+Na]^+$: 419.1036, found: 419.1041.

4-Nitrobenzyl 2-bromoacrylate (**22b**)

To a stirred solution of 2-bromoacrylic acid (10 g, 0.066 mol, 1 equiv.) in dry *N*,*N*-dimethylformamide (70 mL), K_2CO_3 (9.1 g, 0.066 mol, 1 equiv.) and 4-nitrobenzyl bromide (14.33 g, 0.066 mol, 1 equiv.) were added sequentially. After stirring at room temperature under N_2 for 24 hours, the reaction mixture

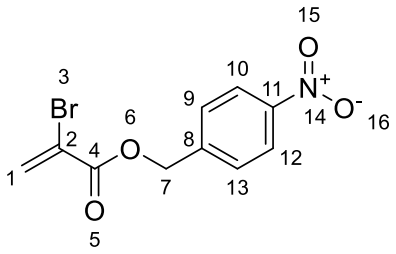

was diluted with ethyl acetate, washed with H_2O, saturated aqueous $NaHCO_3$ solution, and brine, then dried over Na_2SO_4, filtered, and concentrated *in vacuo* to give **22b** (16.2 g, 86%). **22b** was directly used in the next step without any further purifications.

Amorphous off-white solid; ^{1}H NMR (500 MHz, 298 K, $CDCl_3$): δ = 8.27 – 8.22 (m, 2H, *C10H*, *C12H*), 7.59 – 7.54 (m, 2H, *C9H*, *C13H*), 7.04 (d, *J* = 1.7 Hz, 1H, *C1H*), 6.35 (d, *J* = 1.8 Hz, 1H, *C1H*), 5.35 ppm (s, 2H, *C7H*$_2$); ^{13}C NMR (126 MHz, 298 K, $CDCl_3$): δ = 161.7, 148.1, 142.3, 131.9, 128.5, 124.1, 120.6, 66.8 ppm; IR (film) ṽ= 1735, 1656, 1604, 1510m 1496, 1442, 1421, 1394, 1345, 1294, 1261, 1182, 1154, 1098, 1013 cm^{-1}; HRMS (ESI): m/z calculated for $C_{10}H_8BrNO_4Na$ $[M+Na]^+$: 307.9529, found: 307.9546.

4-Nitrobenzyl 3-((1R,5R)-3-benzyl-7-oxo-4-thia-2,6-diazabicyclo[3.2.0]hept-2-en-6-yl)-2-bromopropanoate (23b/23b')

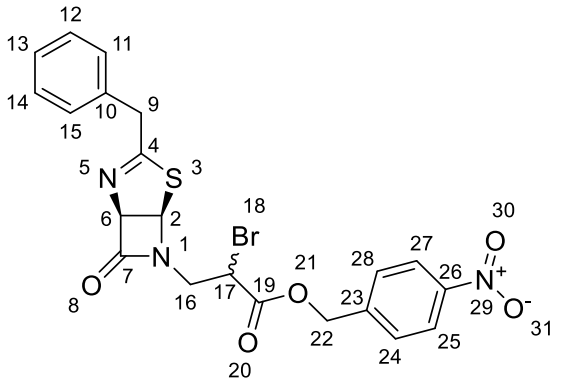

To a solution of **10** (3.35 g, 15.35 mmol, 1 equiv.) in dry acetone (125 mL), K_2CO_3 (3.47 g, 25.11 mmol, 1.63 equiv.) and **22b** (9.62 g, 33.7 mmol, 2.5 equiv.) were sequentially added, and the reaction was stirred at room temperature under N_2 for 72 hours. Removal of excess 4-nitrobenzyl 2-bromoacrylate was required for the next step, but standard column chromatography was found to be inadequate, as prolonged silica exposure led to hydrolysis of the thiazoline ring and product degradation; therefore, dry column vacuum chromatography was employed as the preferred method of purification.[8] The crude product (13 g) was dissolved in a minimum amount of ethyl acetate and loaded onto Merck 60 silica gel (13 g). In a sintered funnel (10 cm diameter) connected

to a separating funnel via a T-joint that can be connected to a vacuum pump, a layer of Merck 60 silica (5 cm depth) was packed under vacuum suction, precautions being taken to firmly press the surface of the silica around the edges. While applying a vacuum, cyclohexane (100 ml) was poured carefully onto the top of the silica column (the surface of the silica gel was protected with the help of a filter paper), then the column was sucked dry. The silica-loaded crude material was then added on the top of the column, then the packing procedure was repeated. The column is then developed by gradient elution using 0-100% EtOAc in cyclohexane (100 mL volumes, 5% increments), the column being allowed to run dry after the addition of each solvent mixture, after which the fractions are collected. Fractions containing the product were collected and concentrated *in vacuo* to give a mixture of inseparable *C-17* diastereomers of penams **23b** and **23b'** (d.r. = 1:1; 5.16 g, 72.6%).

Orange amorphous solid; isomer **23b**: ^{1}H NMR (600 MHz, 298 K, $CDCl_3$): δ = 8.23 (d, *J* = 8.7 Hz, 2H, *C25H*, *C27H*), 7.51 (d, *J* = 8.7 Hz, 2H, *C24H*, *C28H*), 7.33 – 7.22 (m, 5H, *C11H*, *C12H*, *C13H*, *C14H*, *C15H*), 5.98 (d, *J* = 4.0 Hz, 1H, *C2H*), 5.63 (d, *J* = 4.0 Hz, 1H, *C6H*), 5.30 – 5.27 (m, 1H, *C22H*), 5.20 – 5.18 (m, 1H, *C22H*), 4.46 (t, *J* = 6.8 Hz, 1H, *C17H*), 3.95 – 3.91 (m, 2H, *C9H*, *C16H*), 3.83 – 3.90 (m, 1H, *C9H*), 3.73 – 3.69 ppm (m, 1H, *C16H*); isomer **23b'**: ^{1}H NMR (600 MHz, 298 K, $CDCl_3$): δ = 8.23 (d, *J* = 8.7 Hz, 2H, *C25H*, *C27H*), 7.53 (d, *J* = 8.7 Hz, 2H, *C24H*, *C28H*), 7.33 – 7.22 (m, 5H, *C11H*, *C12H*, *C13H*, *C14H*, *C15H*), 5.92 (d, *J* = 4.0, 1H, *C2H*), 5.53 (d, *J* = 3.9 Hz, 1H, *C6H*), 5.32 – 5.28 (m, 1H, *C22H*), 5.24 – 5.20 (m, 1H, *C22H*), 4.51 (dd, *J* = 8.2, 5.4 Hz, 1H), 3.95 – 3.91 (m, 1H, *C9H*), 3.87 – 3.83 (m, 1H, *C16H*), 3.81 – 3.78 (m, 1H, *C9H*), 3.77 – 3.72 ppm (m, 1H, *C16H*); ^{13}C NMR (151 MHz, 298 K, $CDCl_3$): δ = 172.95, 172.78, 167.87, 165.13, 164.97, 148.11, 141.81, 134.94, 134.90, 129.37, 129.34, 128.95, 128.74, 128.68, 127.67, 124.05, 124.01, 123.99, 123.83, 93.61, 93.53, 70.53, 70.23, 66.73, 66.55, 43.44, 43.39,

41.67, 41.63, 40.87, 39.84 ppm (^{13}C assignment to individual isomers was not done due to overlapping 2D NMR signals); HRMS (ESI): m/z calculated for $C_{21}H_{19}N_3O_5S$ $[M+H]^+$: 504.0223, found: 504.0219.

4-Nitrobenzyl (5R,6R)-7-oxo-6-(2-phenylacetamido)-4-thia-1-azabicyclo[3.2.0]heptane-3-carboxylate (25b/25b')

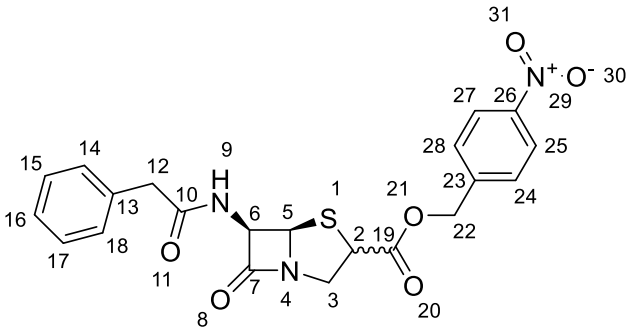

To a stirred solution of **23b/23b'** (4.51 g, 8.96 mmol, 1 equiv.) in anhydrous acetone (40 mL) cooled to 0 °C, an aqueous HCl solution (1 M; 13.6 mL) was added, and the reaction mixture was stirred at 0 °C for 1 h, before being diluted with H_2O (20 mL) and EtOAc (20 mL). The phases were separated, and the aqueous layer was further extracted with EtOAc. The combined organic layers were washed with brine, then dried over Na_2SO_4, filtered, and concentrated *in vacuo.* The residue was then dissolved in anhydrous tetrahydrofuran (80 mL), to which finely ground K_2CO_3 (1.23 g, 8.96 mmol, 1 equiv.) was added. The reaction was stirred at room temperature under N_2 for 18 hours. The reaction mixture was filtered through a pad of Celite®, then the filtrate was concentrated *in vacuo* to give a *C2* mixture of penams **25b** (**4-nitrobenzyl (3R,5R,6R)-7-oxo-6-(2-phenylacetamido)-4-thia-1-azabicyclo[3.2.0]heptane-3-carboxylate**) and **25b'** (**4-nitrobenzyl (3S,5R,6R)-7-oxo-6-(2-phenylacetamido)-4-thia-1-azabicyclo[3.2.0]heptane-3-carboxylate**) (d.r. = 1: 0.8; 3.27 g, 82%). **25b/25b'** was directly used in the next step without any further purifications.

Orange waxy foam; **25b**: ^{1}H NMR (600 MHz, 298 K, $CDCl_3$): δ = 8.25 (d, *J* = 8.7 Hz, 2H, *C25H*, *C27H*), 7.38 – 7.35 (m, 1H, *C16H*), 7.50 (d, *J* = 8.7 Hz, 2H, *C24H*, *C28H*), 7.32 – 7.26 (m, 4H,

C14H, *C15H*, *C17H*, *C18H*), 6.93 (d, *J* = 9.7 Hz, 1H, *N9H*), 5.75 (dd, *J* = 9.7, 4.0 Hz, 1H, *C6H*), 5.38 (d, *J* = 4.0 Hz, 1H, *C5H*), 5.12 (m, 2H, $C22H_2$), 4.38 (d, *J* = 13.1 Hz, 1H, $C3H_\beta$), 4.13 (d, *J* = 6.6 Hz, 1H, *C2H*), 3.63 (m, 2H, $C12H_2$), 3.13 ppm (dd, *J* = 13.1, 6.7Hz, 1H, $C3H_\alpha$); isomer **25b'**: ^{1}H NMR (600 MHz, 298 K, $CDCl_3$): δ = 8.26 (d, *J* = 8.7 Hz, 2H, *C25H*, *C27H*), 7.51 (d, *J* = 8.7 Hz, 2H, *C24H*, *C28H*), 7.38 – 7.35 (m, 1H, *C16H*), 7.32 – 7.26 (m, 4H, *C14H*, *C15H*, *C17H*, *C18H*), 6.05 (d, *J* = 8.8 Hz, 1H, *N9H*), 5.65 (dd, *J* = 8.7, 3.9, 1H, *C6H*), 5.30 (d, *J* = 3.9 Hz, 1H, *C5H*), 5.26 (m, 2H, $C22H_2$), 4.33 (dd, *J* = 7.5, 5.3 Hz, 1H, *C2H*), 4.16 (dd, *J* = 12.3, 7.5 Hz, 1H, $C3H_\beta$), 3.63 (m, 2H, $C12H_2$), 3.38 ppm (dd, *J* = 12.3, 5.3 Hz, 1H, $C3H_\alpha$); ^{13}C NMR (151 MHz, $CDCl_3$) δ 174.16, 173.67, 172.96, 170.69, 170.61, 170.13, 148.26, 148.15, 142.11, 141.72, 134.22, 133.81, 129.80, 129.60, 129.34, 129.09, 128.98, 128.65, 128.61, 127.89, 127.39, 127.15, 124.13, 124.12, 124.08, 123.90, 69.04, 68.65, 66.87, 66.30, 64.18, 60.87, 58.74, 53.09, 52.90, 51.53, 49.37, 43.76, 43.49 ppm (^{13}C assignment to individual isomers was not done due to overlapping 2D NMR signals); HRMS (ESI): m/z calculated for $C_{21}H_{20}N_3O_6S$ $[M+H]^+$: 442.1067, found: 442.1068.

(5*R*,6*R*)-7-Oxo-6-(2-phenylacetamido)-4-thia-1-azabicyclo[3.2.0]heptane-3-carboxylic acid

(26a/26a')

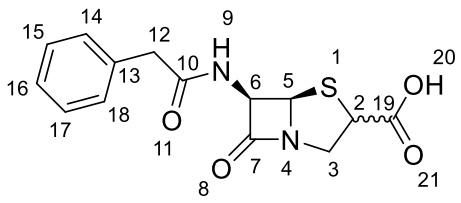

To a stirred solution of **25b/25b'** (100 mg, 0.226 mg, 1 equiv.) in anhydrous tetrahydrofuran (3 mL), 10% wt. Pd/C (89.6 mg, 0.4 equiv.) was added. The solution was degassed with Ar for 5 min, then H_2 was flushed through the solution for 5 min. The reaction was then stirred at room temperature under H_2 for 3 h, before being flushed with N_2, diluted with EtOAc, and filtered through Celite®. The organic phase was diluted with H_2O, cooled to 0°C, and basified to pH 7 using saturated aqueous $NaHCO_3$ solution.

The aqueous layer was separated, and the organic layer was further extracted with H_2O. The combined aqueous layers were diluted with EtOAc and reacidified to pH 2 by addition of aqueous HCl solution (1 M). The organic layer was separated, and the aqueous layer was further extracted with EtOAc. The combined organic fractions were dried over Na_2SO_4, filtered, and concentrated *in vacuo* to give a *C2* mixture of penams **26a** (**(3R,5R,6R)-7-oxo-6-(2-phenylacetamido)-4-thia-1-azabicyclo[3.2.0]heptane-3-carboxylic acid**) and **26a'** (**(3S,5R,6R)-7-oxo-6-(2-phenylacetamido)-4-thia-1-azabicyclo[3.2.0]heptane-3-carboxylic acid**) (d.r. = 0.17:1; 12 mg, 17%).

Amorphous off-white solid; isomer **26a**: ^{1}H NMR (600 MHz, 298 K, DMSO-d_6): δ = 8.90 (d, J = 8.2 Hz, 1H), 7.31 – 7.21 (m, 5H, *C14H*, *C15H*, *C16H*, *C17H*, *C18H*), 5.45 (dd, J = 8.2, 3.8 Hz, 1H, *C6H*), 5.29 (d, J = 3.8 Hz, *C5H*) 4.40 (t, J = 7.0 Hz, 1H, *C2H*), 4.26 (t, J = 7.0 Hz, 1H, $C3H_\beta$), 4.10 (dd, J = 12.3, 7.0 Hz, 1H, $C3H_\alpha$), 3.53 ppm (m, 2H, $C12H_2$); isomer **26a'**: ^{1}H NMR (600 MHz, 298 K, DMSO-d_6): δ = 8.44 (d, J = 8.2 Hz, 1H, *N6H*), 7.31 – 7.21 (m, 5H, *C14H*, *C15H*, *C16H*, *C17H*, *C18H*), 5.44 (dd, J = 8.2, 3.9 Hz, 1H, *C6H*), 5.30 (d, J = 3.9 Hz, 1H, *C5H*), 4.52 (dd, J = 7.6, 3.2 Hz, 1H, *C2H*), 4.18 (dd, J = 12.3, 3.3 Hz, 1H, $C3H_\beta$), 3.55 (m, 2H, $C12H_2$), 3.18 ppm (dd, J = 12.3, 7.5 Hz, 1H, $C3H_\alpha$); ^{13}C NMR (151 MHz, 298 K, DMSO-d_6): δ = 173.13, 172.42, 170.07, 135.83, 135.65, 129.11, 129.04, 128.25, 128.21, 126.52, 126.47, 68.10, 67.70, 59.08, 59.02, 53.97, 52.92, 49.54, 41.79, 41.58 ppm (^{13}C assignment to individual isomers was not done due to overlapping 2D NMR signals); HRMS (ESI): m/z calculated for $C_{14}H_{15}N_2O_4S$ $[M+H]^+$: 307.0747, found: 307.0748.

4-Nitrobenzyl (5*R*,6*R*)-7-oxo-6-(2-phenylacetamido)-4-thia-1-azabicyclo[3.2.0]heptane-3-carboxylate 4,4-dioxide (27/27')

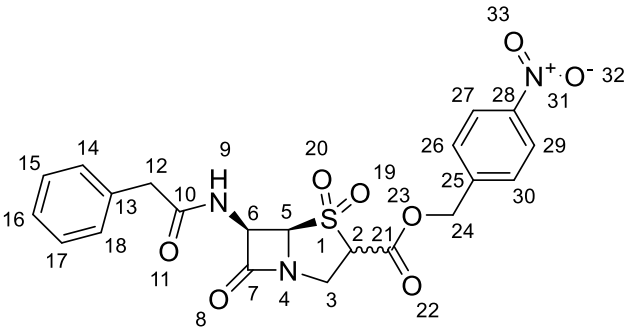

To a stirred solution of **25b**/**25b'** (150 mg, 0.339 mmol, 1 equiv.) in tetrahydrofuran (2 mL) and aqueous AcOH solution (80% (v/v); 2.7 mL) cooled to 0 °C, a solution of $KMnO_4$ (118 mg, 0.746 mmol, 2.2) in H_2O (3 mL) was added dropwise over 5 min. The reaction was stirred at 0 °C for 2 hours, after which an aqueous H_2O_2 (30% (v/v)) solution was added dropwise to quench excess $KMnO_4$. The reaction mixture was diluted with brine and CH_2Cl_2. The phases were separated, and the aqueous layer was further extracted with CH_2Cl_2. The combined organic fractions were washed with brine, saturated aqueous $NaHCO_3$ solution, and brine again. The organic layer was then dried over Na_2SO_4, filtered, and concentrated *in vacuo* to give a *C2* mixture of penams **27** (**4-nitrobenzyl (3R,5R,6R)-7-oxo-6-(2-phenylacetamido)-4-thia-1-azabicyclo[3.2.0]heptane-3-carboxylate 4,4-dioxide**) and **27'** (**4-nitrobenzyl (3S,5R,6R)-7-oxo-6-(2-phenylacetamido)-4-thia-1-azabicyclo[3.2.0]heptane-3-carboxylate 4,4-dioxide**) (d.r. = 1:0.94; 121 mg, 75%).

Amorphous a yellow foam; isomer **27**: ^{1}H NMR (600 MHz, 298 K, DMSO-d_6): δ = 8.62 (d, *J* = 8.3 Hz, 1H, *N9H*), 8.26 – 8.24 (d, *J* = 8.7 Hz, 2H, *C27H*, *C29H*), 7.70 – 7.68 (d, *J* = 8.7 Hz, 2H, *C26H*, *C30H*), 7.30 – 7.21 (m, 5H, *C14H*, *C15H*, *C16H*, *C17H*, *C18H*), 5.81 (dd, *J* = 8.3, 4.1 Hz, 1H, *C6H*), 5.48 – 5.45 (m, 1H, *C24H*), 5.41 – 5.38 (m, 1H, *C24H*), 5.13 (dd, *J* = 9.2, 8.1 Hz, 1H, *C2H*), 5.01 (d, *J* = 4.1 Hz, 1H, *C5H*), 4.25 (dd, *J* = 12.0, 8.1 Hz, 1H, $C3H_\beta$), 3.75 (m, 1H, $C3H_\alpha$), 3.61 – 3.58 (m, 1H, *C12H*), 3.56 – 3.52 ppm (m, 1H, *C12H*); isomer **27'**: ^{1}H NMR (600 MHz, 298 K, DMSO-d_6): δ = 8.73 (d, *J* = 8.1 Hz, 1H, *N9H*), 8.27 – 8.26 (d, *J* = 8.7 Hz, 2H, *C27H*, *C29H*),

7.70 – 7.68 (d, *J* = 8.7 Hz, 2H, *C26H*, *C30H*), 7.30 – 7.21 (m, 5H, *C14H*, *C15H*, *C16H*, *C17H*, *C18H*), 5.63 (dd, *J* = 8.1, 4.4 Hz, 1H, *C6H*), 5. 41 (m, 2H, $C24H_2$), 4.98 (dd, *J* = 8.0, 6.6 Hz, 1H, *C2H*), 4.81 (d, *J* = 4.3 Hz, 1H, *C5H*), 4.40 (dd, *J* = 13.3, 8.0 Hz, 1H, $C3H_\beta$), 3.75 (m, 1H, $C3H_\alpha$), 3.62 – 3.59 (m, 1H, *C12H*), 3.57 – 3.55 [[m (m, 1H, *C12H*); ^{13}C NMR (151 MHz, 298 K, DMSO-d_6): δ = 172.79, 172.71, 171.23, 171.04, 163.86, 162.03, 147.28, 142.78, 142.74, 135.56, 135.35, 129.19, 129.14, 128.72, 128.61, 128.23, 126.55, 126.51, 123.58, 123.56, 69.26, 68.74, 66.40, 66.30, 65.52, 65.11, 59.52, 57.32, 43.99, 42.72, 41.24, 41.21 ppm (^{13}C assignment to individual isomers was not done due to overlapping 2D NMR signals); HRMS (ESI): m/z calculated for $C_{21}H_{19}N_3O_8S$ $[M+Na]^+$: 496.0785, found: 496.0785.

(5*R*,6*R*)-7-Oxo-6-(2-phenylacetamido)-4-thia-1-azabicyclo[3.2.0]heptane-3-carboxylic acid 4,4-dioxide (28/28')

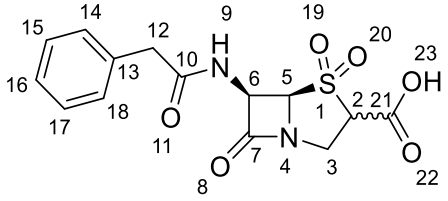

To a stirred solution of **27/27'** (100 mg, 0.211 mmol, 1 equiv.) in anhydrous tetrahydrofuran (3 mL), 10% wt. Pd/C (83.8 mg, 0.4 equiv.) was added. The solution was degassed with Ar for 5 min, then H_2 was flushed through the solution for 5 min. The reaction was then stirred at room temperature under H_2 for 3 hours, before being flushed with N_2, diluted with EtOAc, and filtered through Celite®. The collected organic fraction was diluted with H_2O, cooled to 0 °C, and basified to pH 7 following the addition of saturated aqueous $NaHCO_3$ solution. The aqueous layer was separated, and the organic layer was further extracted with H_2O. The combined aqueous layers were diluted with EtOAc and reacidified to pH 2 by addition of aqueous HCl solution (1 M). The organic layer was separated, and the aqueous layer was further extracted with EtOAc. The combined organic fractions were

dried over Na_2SO_4, filtered, and concentrated *in vacuo* to give an inseparable *C2* mixture of penams **28** (**(3*R*,5*R*,6*R*)-7-oxo-6-(2-phenylacetamido)-4-thia-1-azabicyclo[3.2.0]heptane-3-carboxylic acid 4,4-dioxide**) and **28'** (**(3*S*,5*R*,6*R*)-7-oxo-6-(2-phenylacetamido)-4-thia-1-azabicyclo[3.2.0]heptane-3-carboxylic acid 4,4-dioxide**) (d.r. = 0.76:1; 21 mg, 29%).

Orange wax; isomer **28**: ^{1}H NMR (600 MHz, 298 K, DMSO-d_6) δ 8.56 (d, J = 8.5 Hz, 1H, *N9H*), 7.31 – 7.23 (m, 5H, *C14H*, *C15H*, *C16H*, *C17H*, *C18H*), 5.78 (dd, J = 8.5, 4.1 Hz, 1H, *C6H*), 4.93 (d, J = 4.1 Hz, 1H, *C5H*), 4.89 (t, J = 8.9 Hz, 1H, *C2H*), 4.16 (dd, J = 11.8, 8.5 Hz, 1H, $C3H_\beta$), 3.57 (m, 1H, $C3H_\alpha$), 3.56 ppm (m, 2H, $C12H_2$); isomer **28'**: ^{1}H NMR (600 MHz, 298 K, DMSO-d_6) δ 8.67 (d, J = 8.3 Hz, 1H, *N9H*), 7.31 – 7.23 (m, 5H, *C14H*, *C15H*, *C16H*, *C17H*, *C18H*), 5.65 (dd, J = 8.3, 4.3 Hz, 1H, *C6H*), 4.75 (d, J = 4.4 Hz, 1H, *C5H*), 4.64 (dd, J = 7.9, 6.1 Hz, 1H, *C2H*), 4.31 (dd, J = 13.1, 7.9 Hz, 1H, $C3H_\beta$), 3.65 (m, 1H, $C3H_\alpha$), 3.59 ppm (m, 2H, $C12H_2$); ^{13}C NMR (151 MHz, 298 K, DMSO-d_6) δ 173.05, 172.49, 171.10, 170.97, 165.36, 163.14, 155.27, 135.57, 135.40, 129.55, 129.19, 129.13, 128.87, 128.60, 128.32, 128.25, 128.23, 126.90, 126.54, 68.90, 68.34, 65.75, 65.51, 58.89, 57.02, 44.20, 42.88, 41.28 ppm (^{13}C assignment to individual isomers was not done due to overlapping 2D NMR signals); HRMS (ESI): m/z calculated for $C_{14}H_{14}N_2O_6S$ $[M+Na]^+$: 361.0465, found: 361.0475.

8.5.3 References

1. M. R. Bell, J. A. Carlson and R. Oesterlin, Degradation of penicillin G methyl ester with trifluoroacetic acid, *J. Org. Chem.*, 1972, **37**, 2733–2735.
2. S. Wolfe, J.-B. Ducep and J. D. Greenhorn, A Novel Base-promoted Rearrangement of Penicillin G, *Can. J. Chem.*, 1975, **53**, 3435–3438.
3. D. H. R. Barton, F. Comer, D. G. T. Greig, P. G. Sammes, C. M. Cooper, G. Hewitt and W. G. E. Underwood, Transformations of penicillin. Part I. Preparation and rearrangements of 6β-phenylacetamidopenicillanic sulphoxides, *J. Chem. Soc. C Org.*, 1971, 3540–3550.
4. R. Busson, E. Roets and H. Vanderhaeghe, Circular dichroism of monocyclic .beta.-lactams, *J. Org. Chem.*, 1978, **43**, 4434–4437.
5. J. J. De Koning, H. J. Kooreman, H. S. Tan and J. Verweij, One-step, high yield conversion of penicillin sulfoxides to deacetoxycephalosporins, *J. Org. Chem.*, 1975, **40**, 1346–1347.
6. P. A. M. van der Klein, H. A. Witkamp and E. de Vroom, Reductive rearrangements of silylated penicillin G 1-oxide, *Tetrahedron Lett.*, 1994, **35**, 8691–8692.
7. N. F. Osborne, The chemistry of 4-mercaptoazetidin-2-ones. Part 2. Synthesis of bisnorpenicillins, *J. Chem. Soc., Perkin Trans. 1*, 1980, 150–155.
8. D. S. Pedersen and C. Rosenbohm, Dry Column Vacuum Chromatography, *Synthesis*, 2001, **2001**, 2431–2434.

8.5.4 ^{1}H and ^{13}C NMR spectra of the compounds prepared for this study

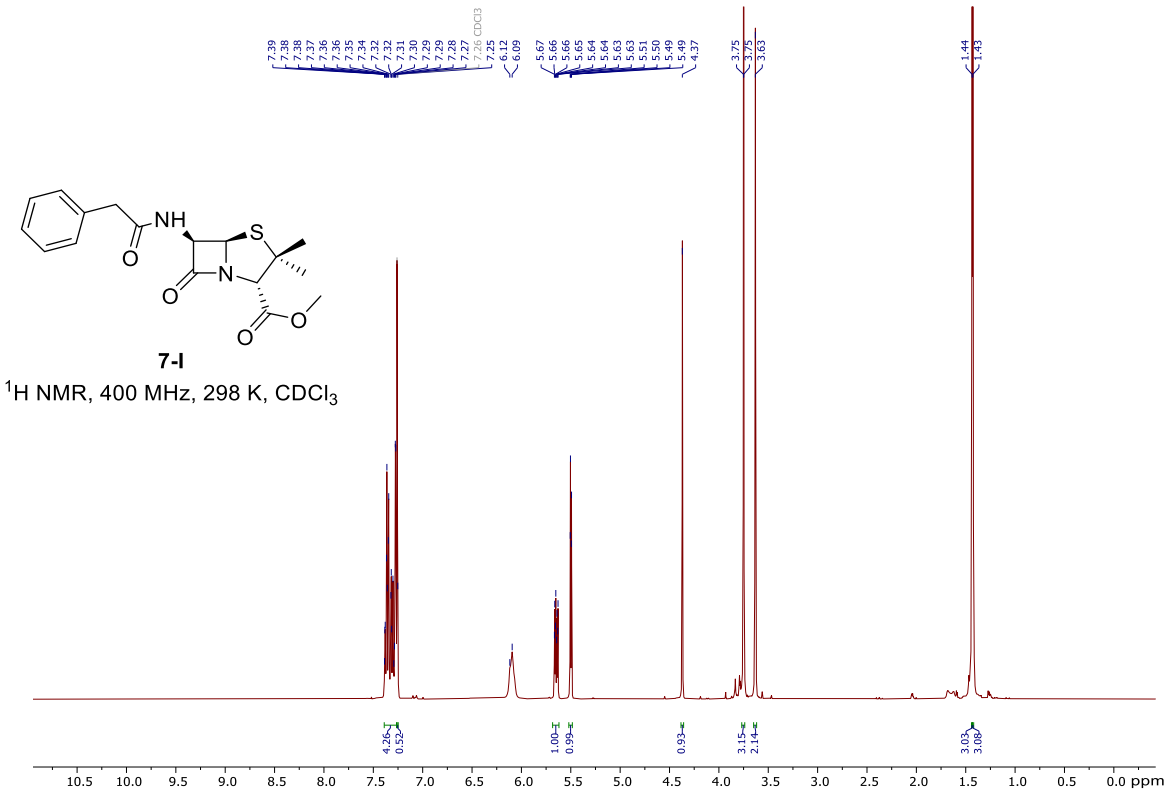

7-I

^{1}H NMR, 400 MHz, 298 K, $CDCl_3$

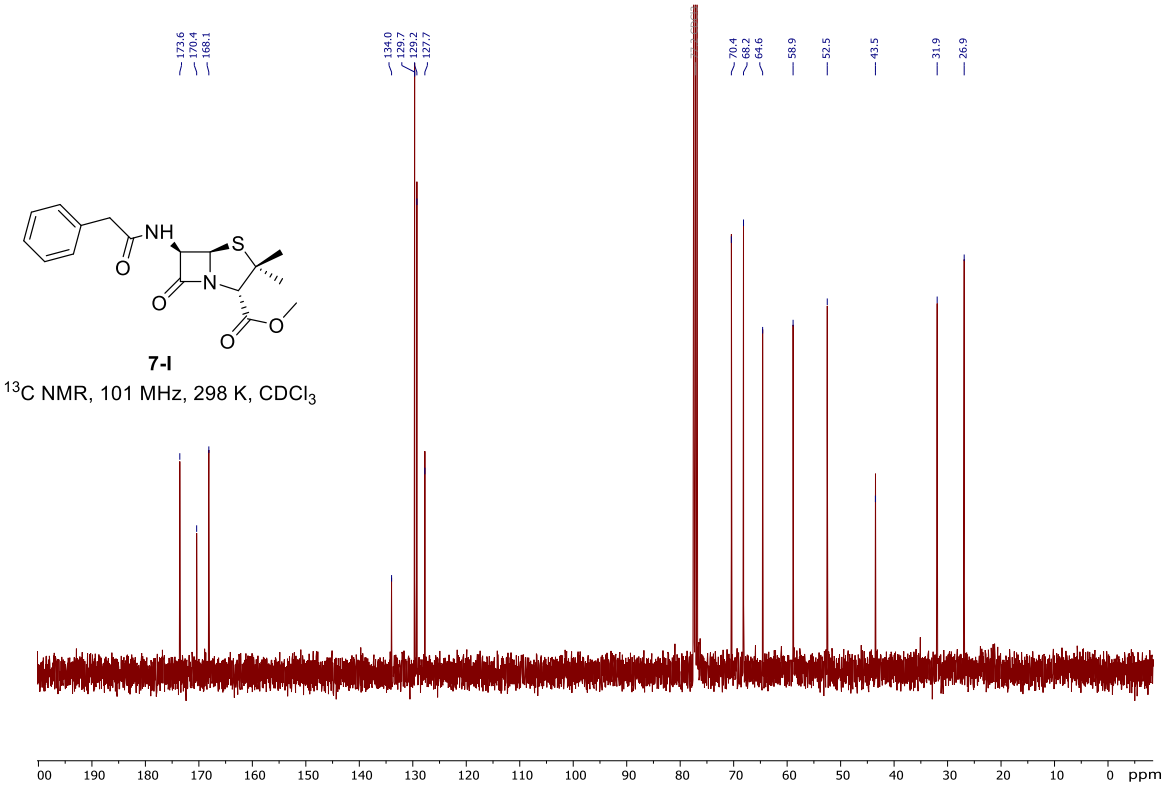

7-I

^{13}C NMR, 101 MHz, 298 K, $CDCl_3$

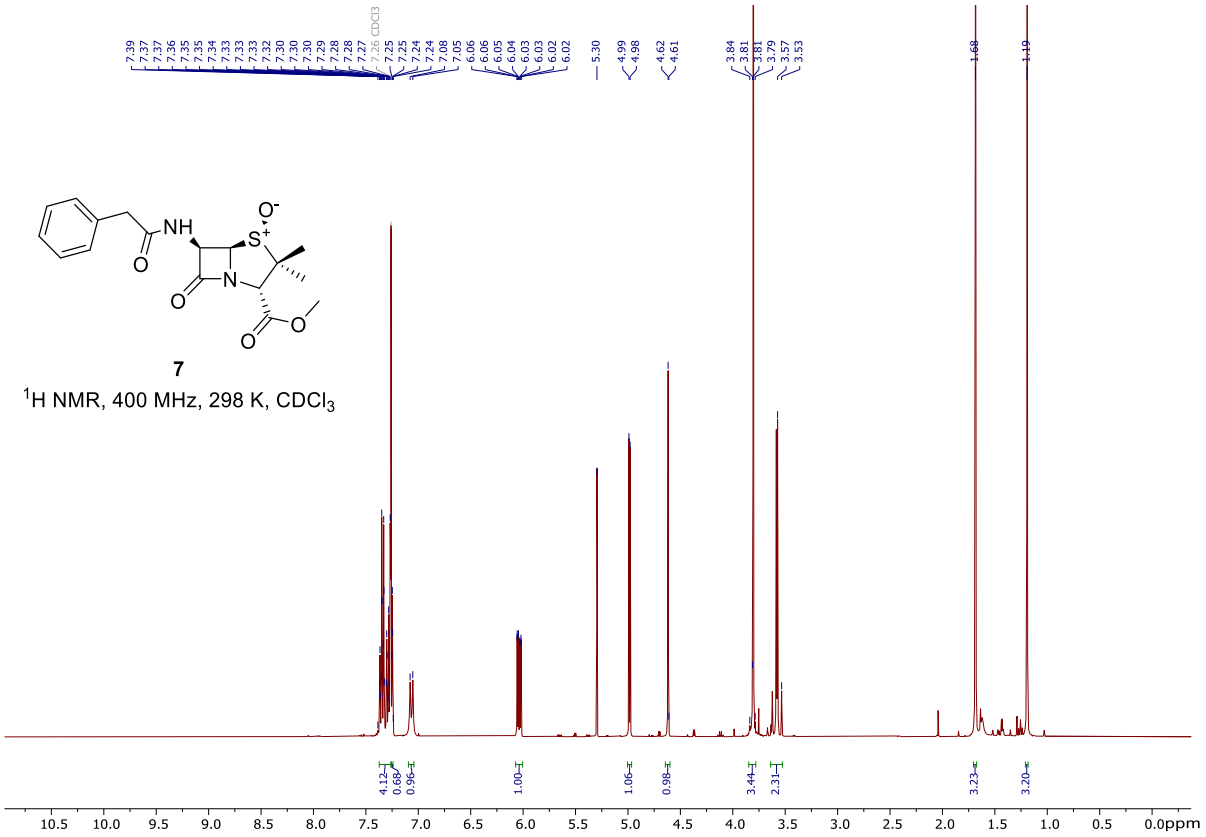

7

^{1}H NMR, 400 MHz, 298 K, $CDCl_3$

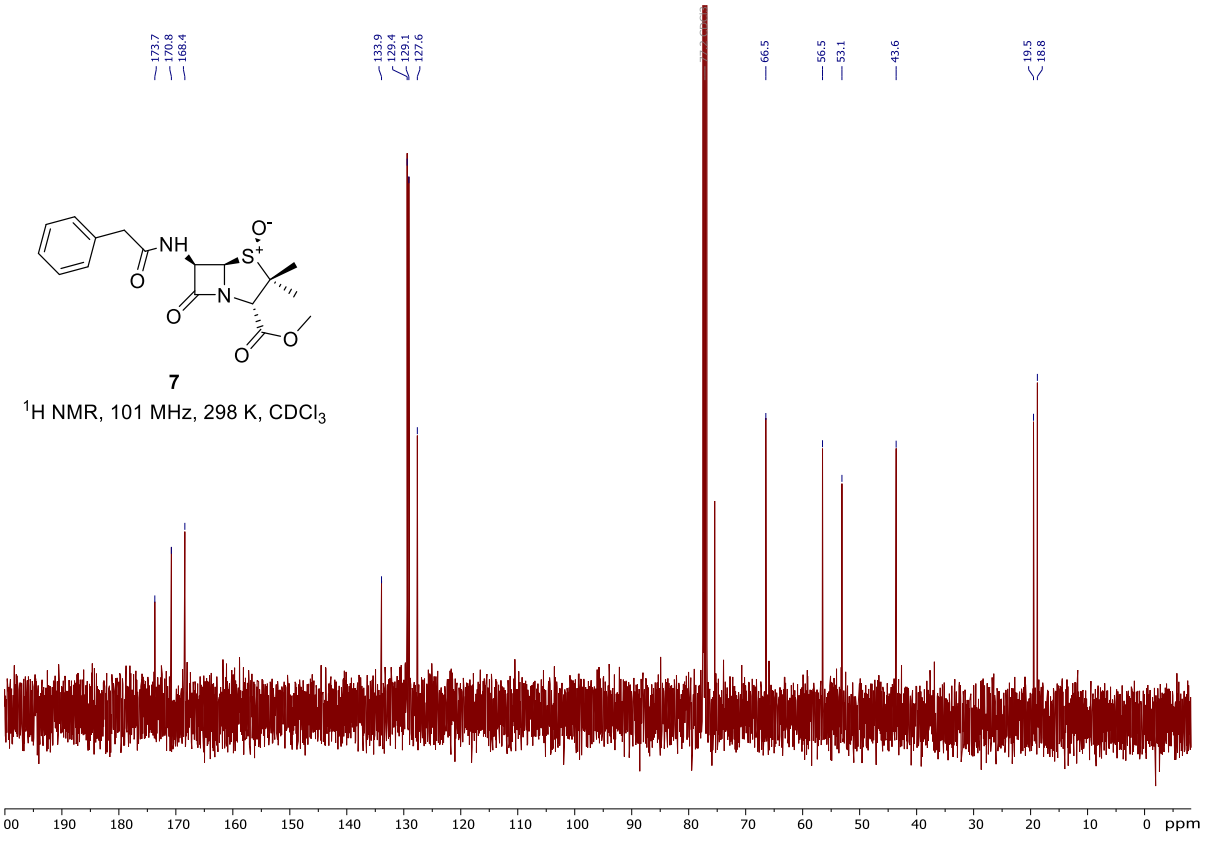

7

^{1}H NMR, 101 MHz, 298 K, $CDCl_3$

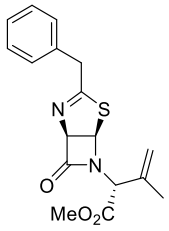

8

^{1}H NMR, 400 MHz, 298 K, $CDCl_3$

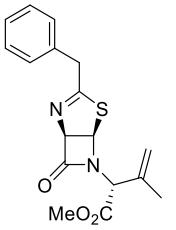

8

^{1}H NMR, 101 MHz, 298 K, $CDCl_3$

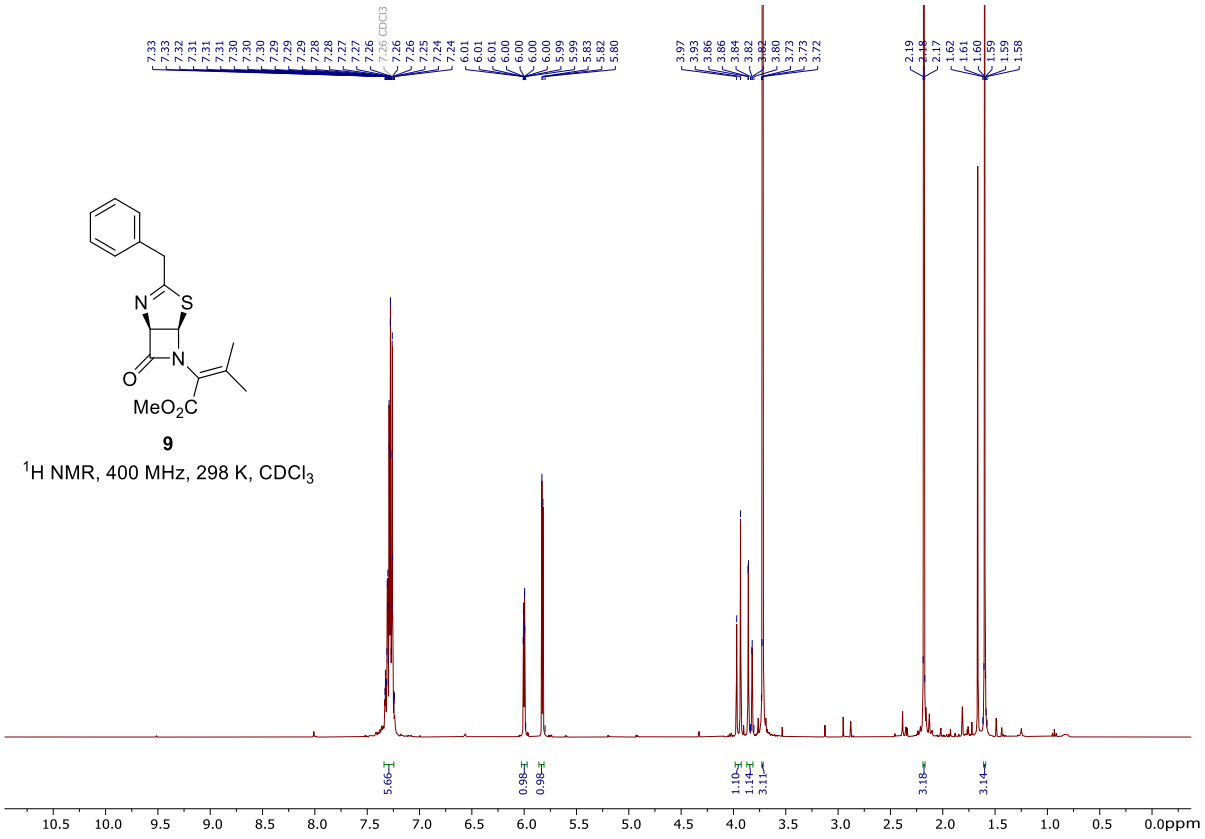

9

^{1}H NMR, 400 MHz, 298 K, $CDCl_3$

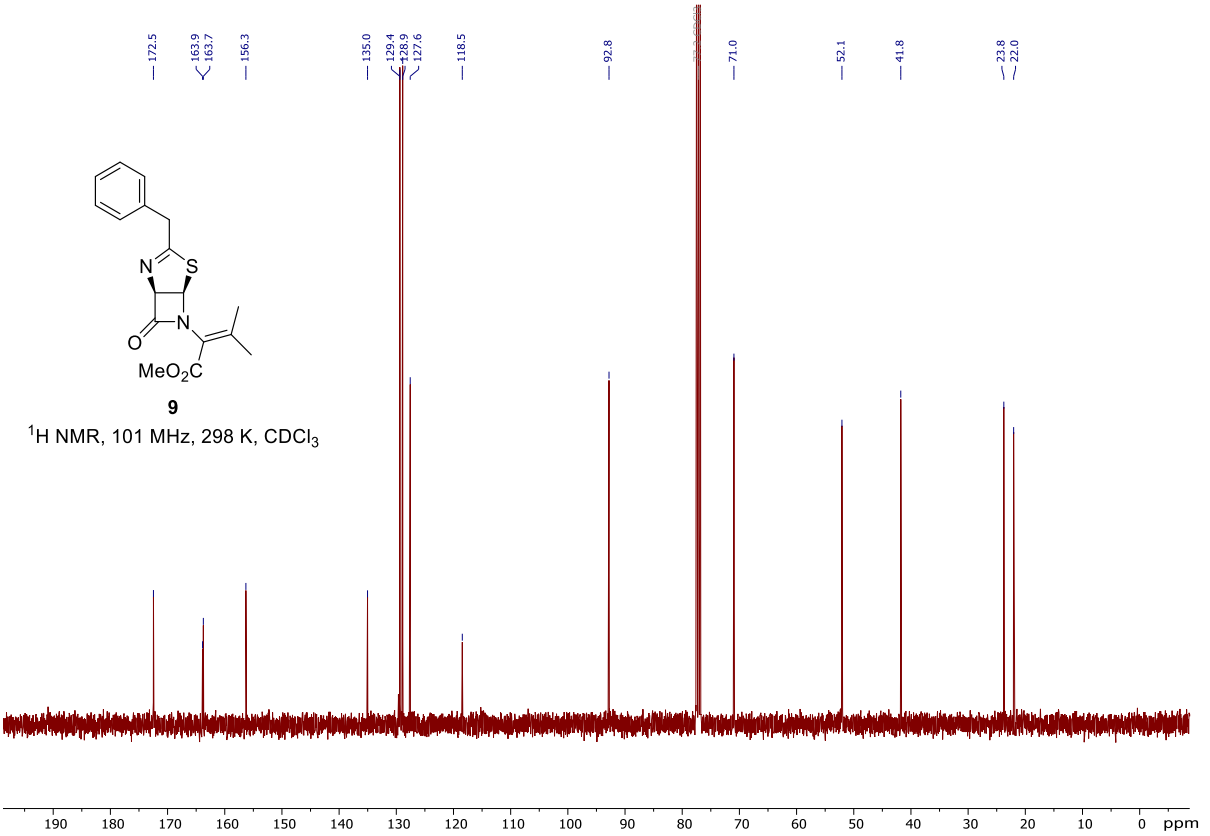

9

^{1}H NMR, 101 MHz, 298 K, $CDCl_3$

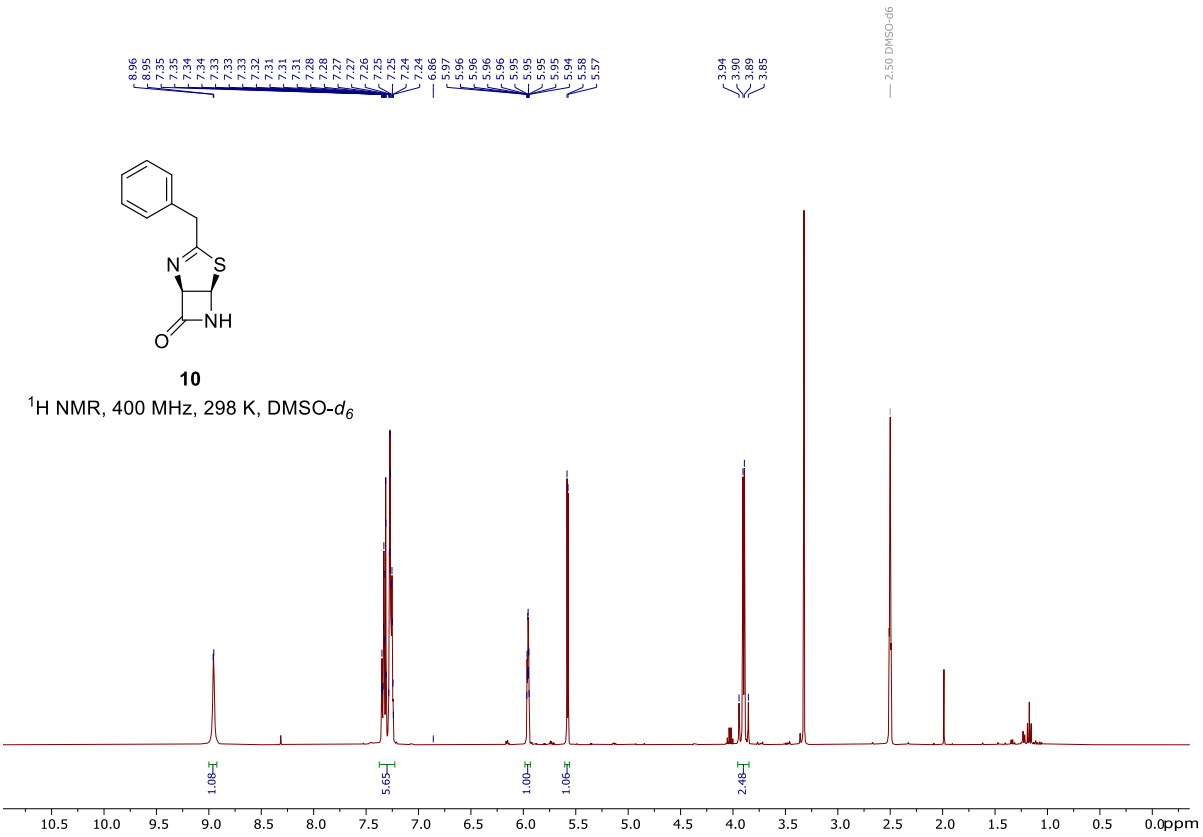

10

^{1}H NMR, 400 MHz, 298 K, DMSO-d_6

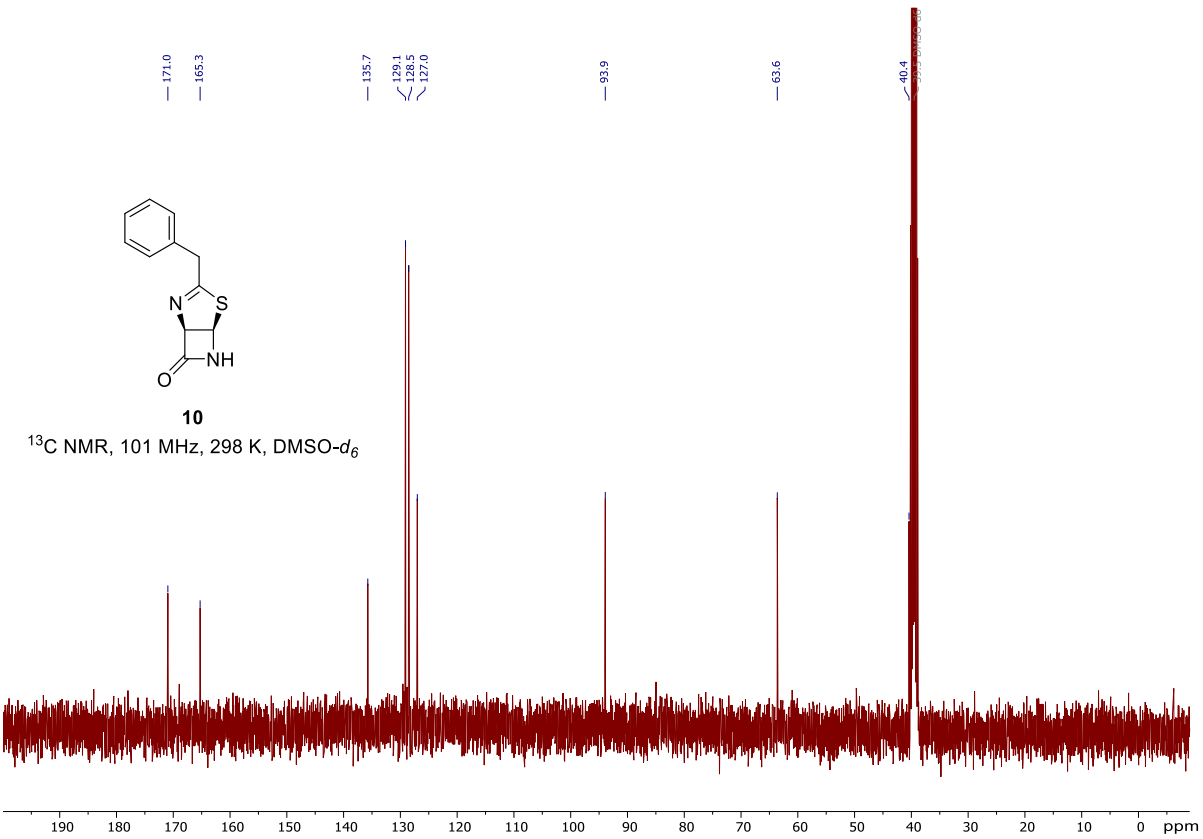

10

^{13}C NMR, 101 MHz, 298 K, DMSO-d_6

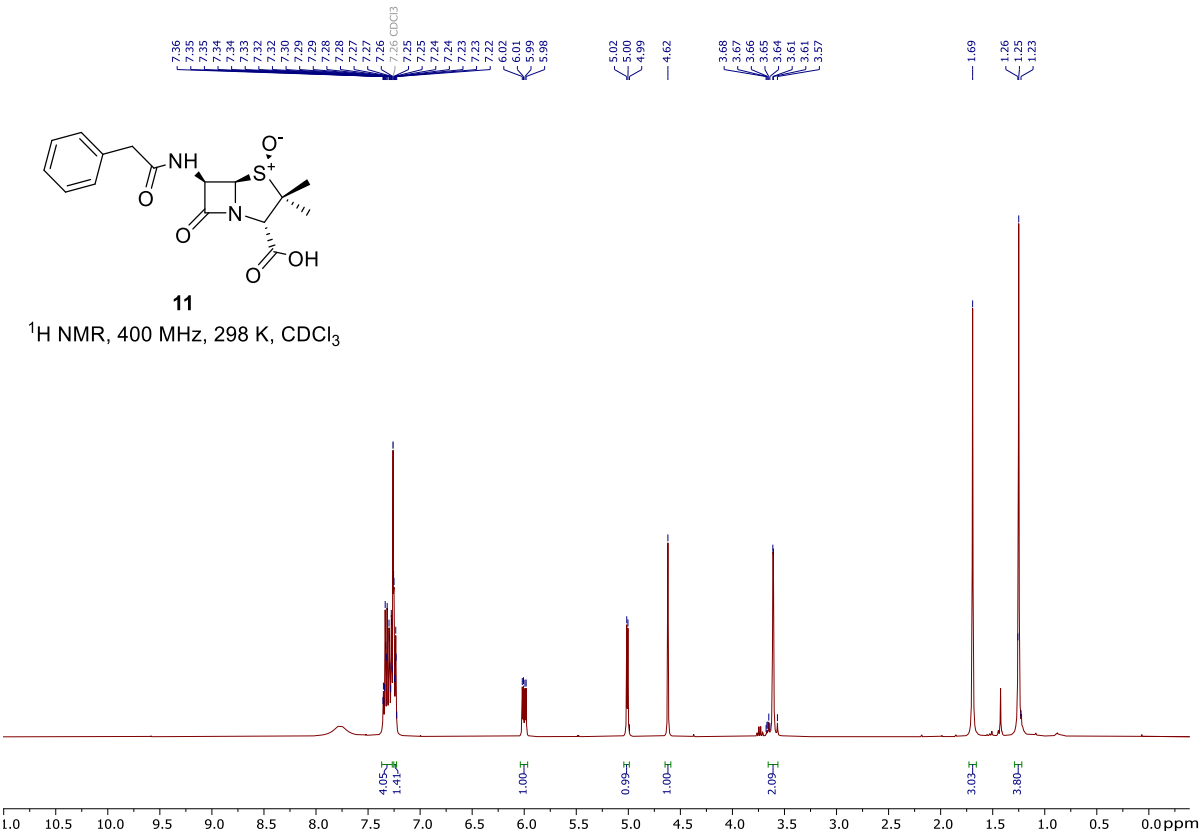

11

^{1}H NMR, 400 MHz, 298 K, $CDCl_3$

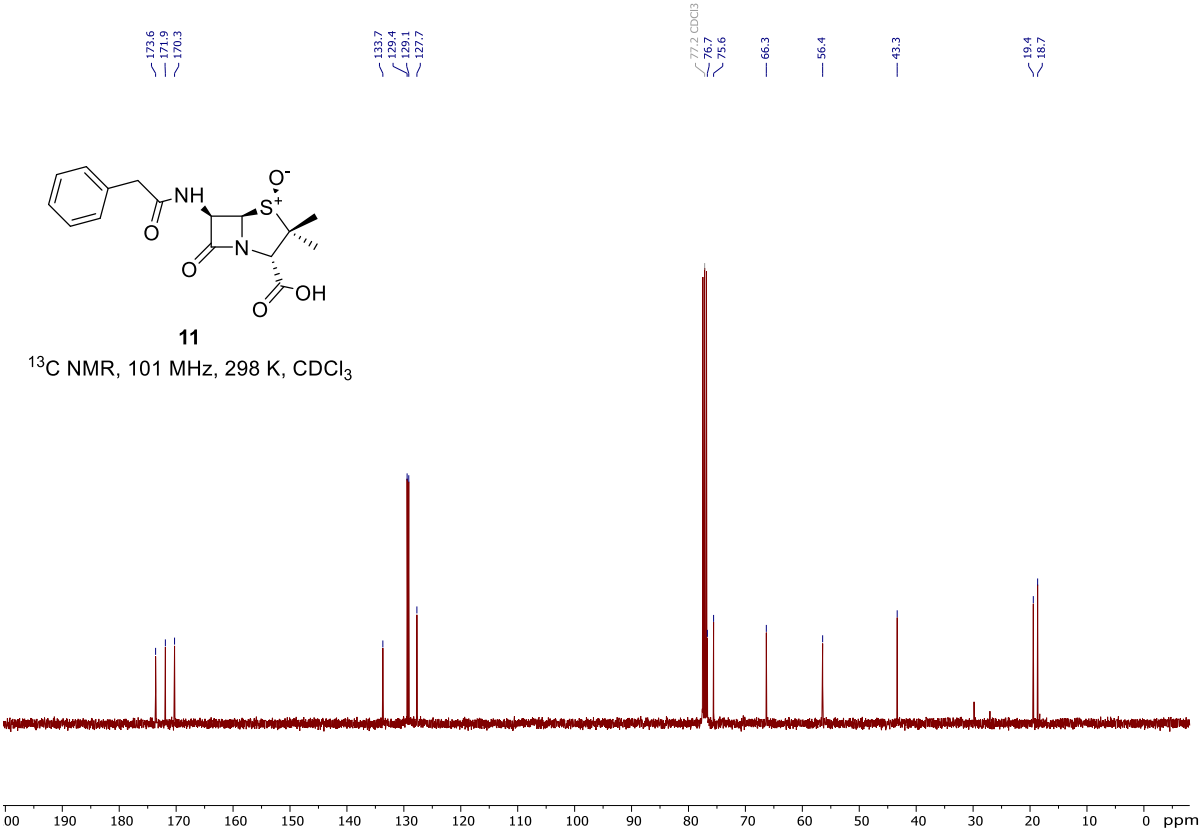

11

^{13}C NMR, 101 MHz, 298 K, $CDCl_3$

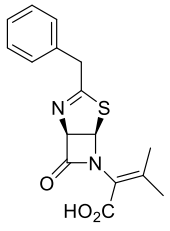

12

^{1}H NMR, 101 MHz, 300 K, $CDCl_3$

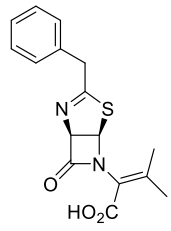

12

^{13}C NMR, 101 MHz, 298 K, $CDCl_3$

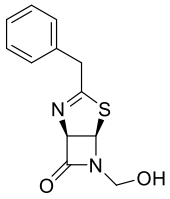

13

^{1}H NMR, 400 MHz, 298 K, DMSO-d_6

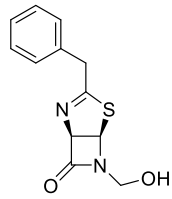

13

^{13}C NMR, 101 MHz, 298 K, DMSO-d_6

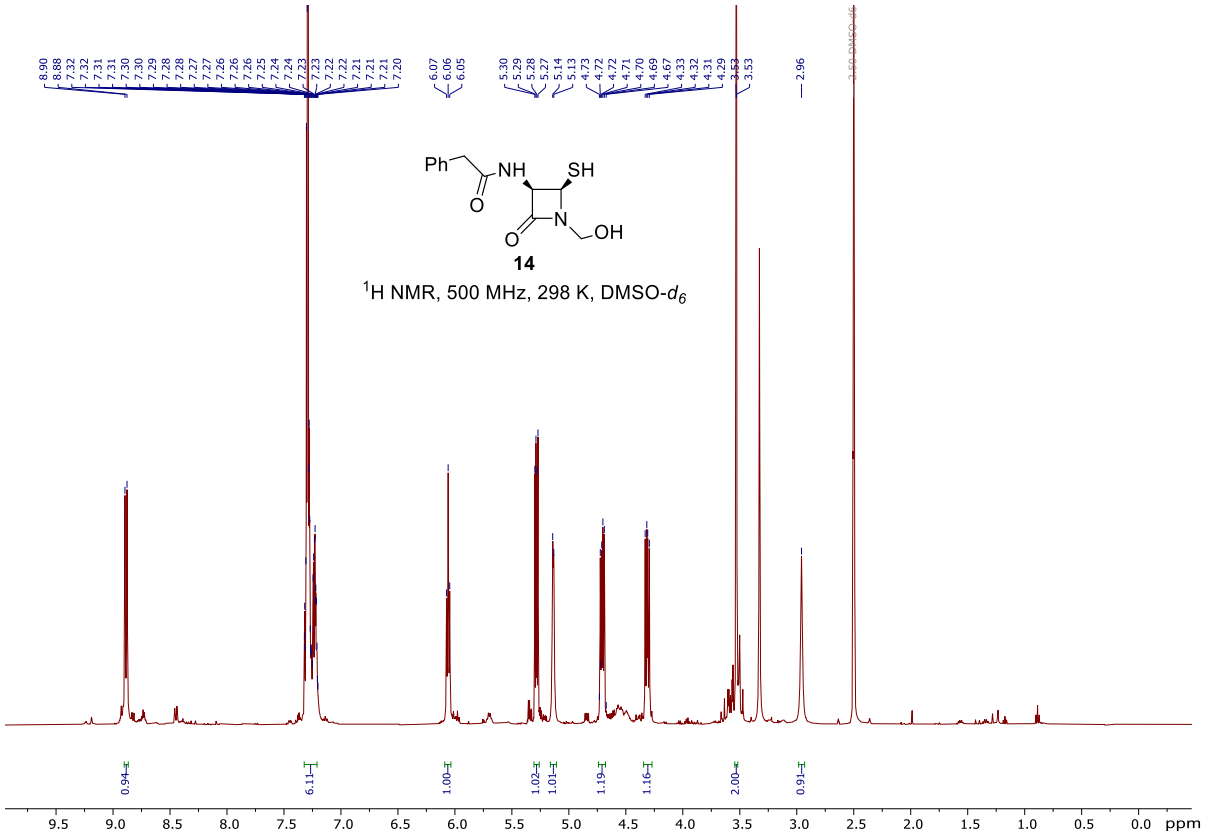

14

^{1}H NMR, 500 MHz, 298 K, DMSO-d_6

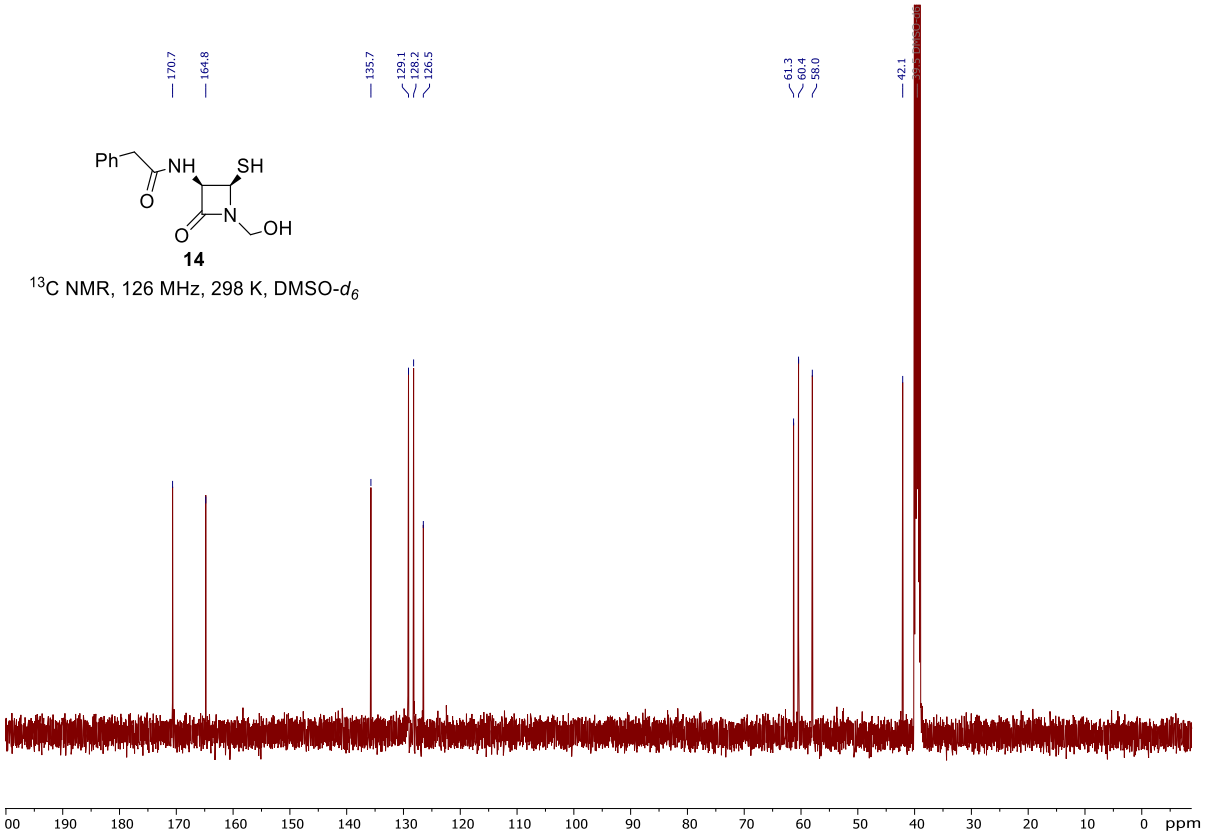

14

^{13}C NMR, 126 MHz, 298 K, DMSO-d_6

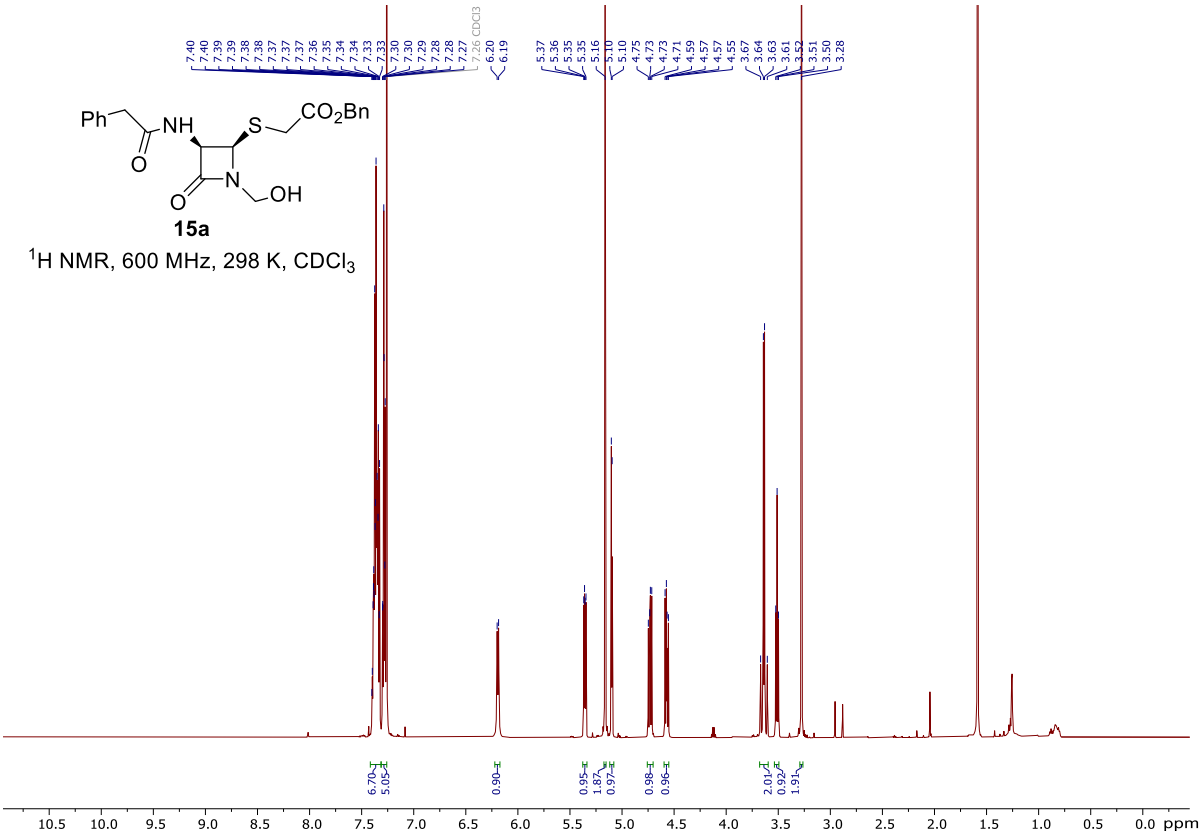

15a

^{1}H NMR, 600 MHz, 298 K, $CDCl_3$

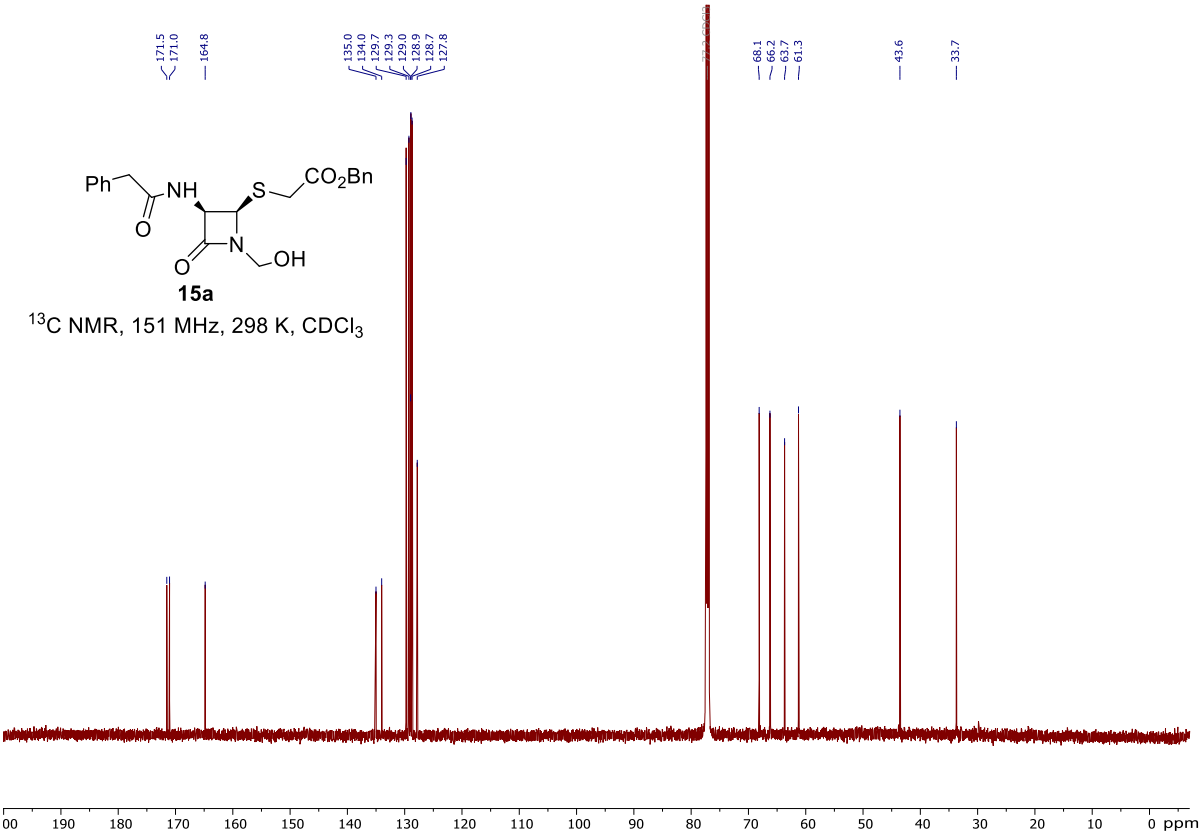

15a

^{13}C NMR, 151 MHz, 298 K, $CDCl_3$

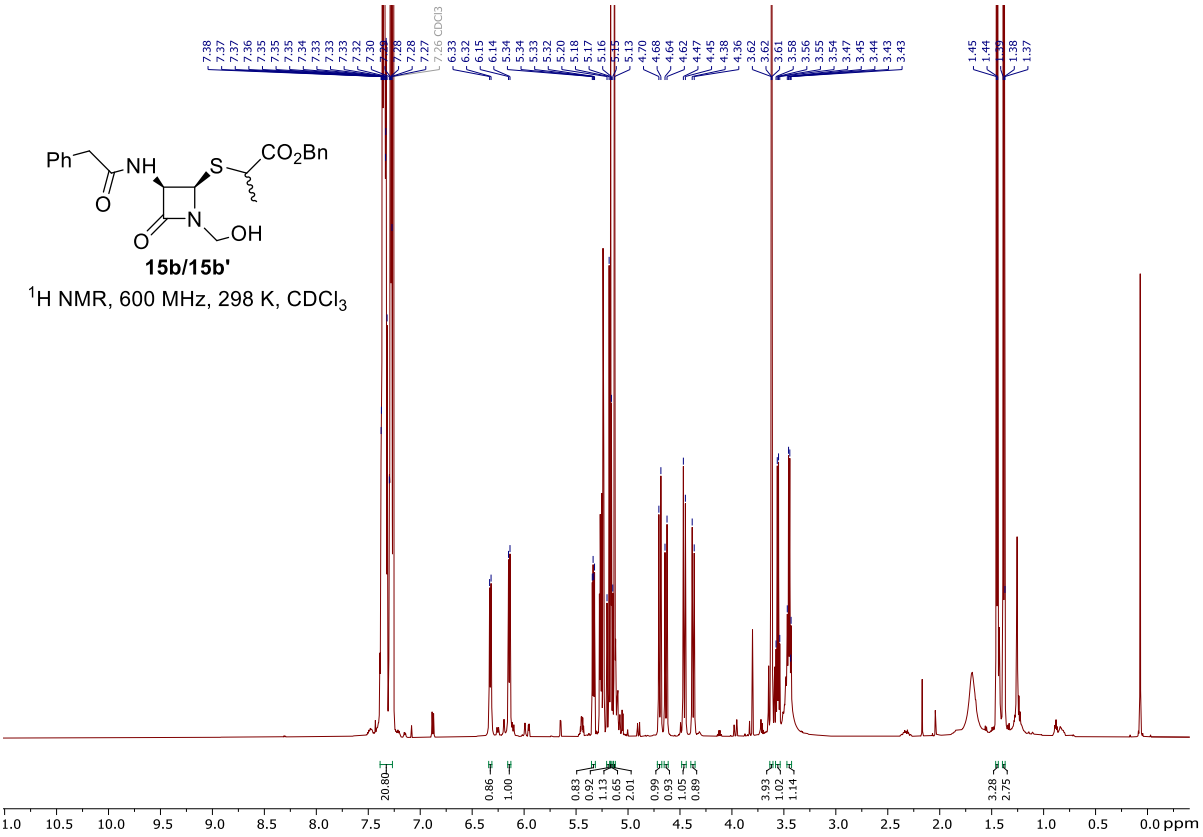

15b/15b'

^{1}H NMR, 600 MHz, 298 K, $CDCl_3$

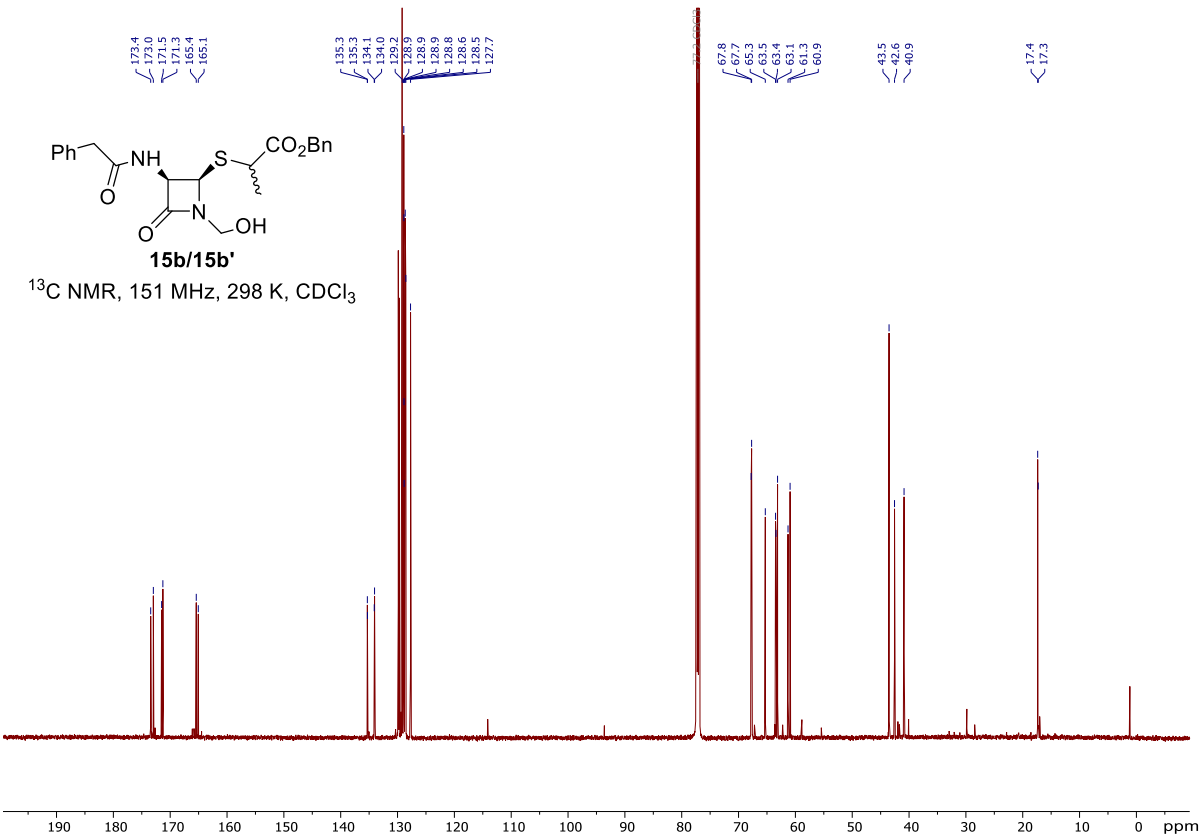

15b/15b'

^{13}C NMR, 151 MHz, 298 K, $CDCl_3$

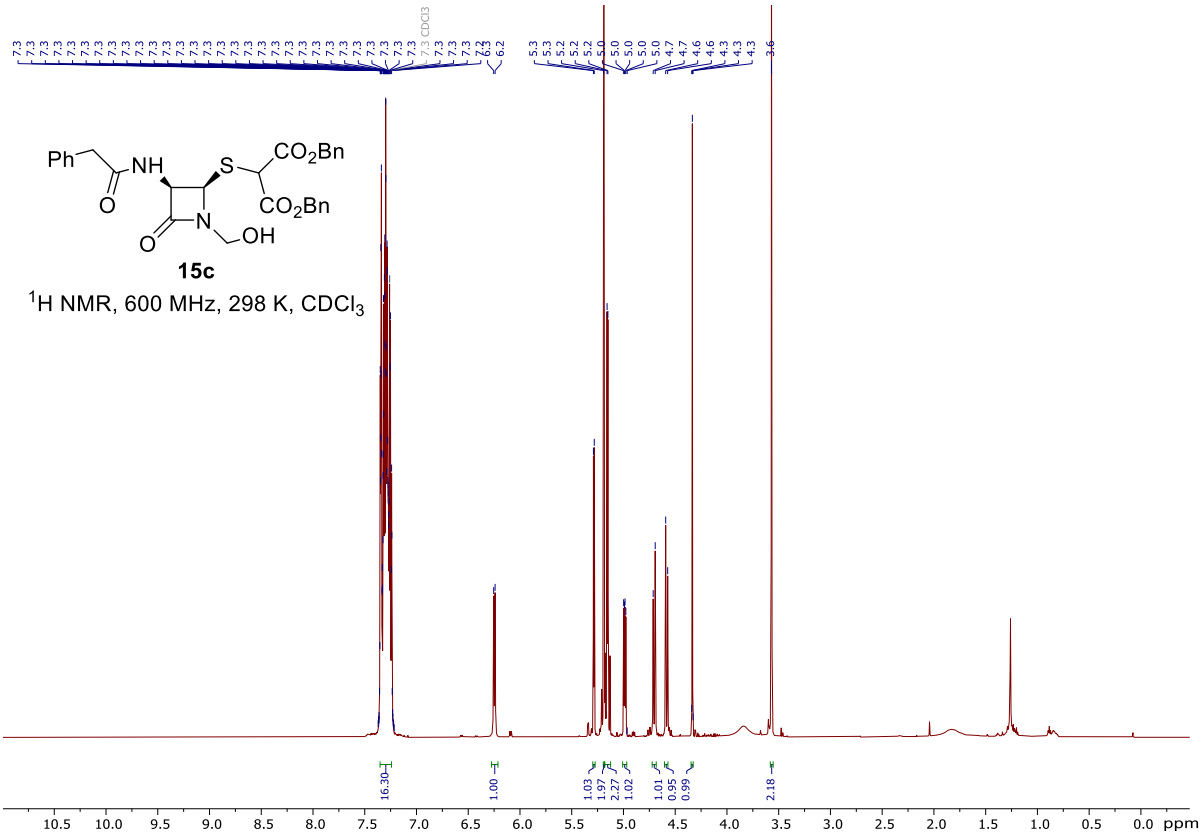

15c

^{1}H NMR, 600 MHz, 298 K, $CDCl_3$

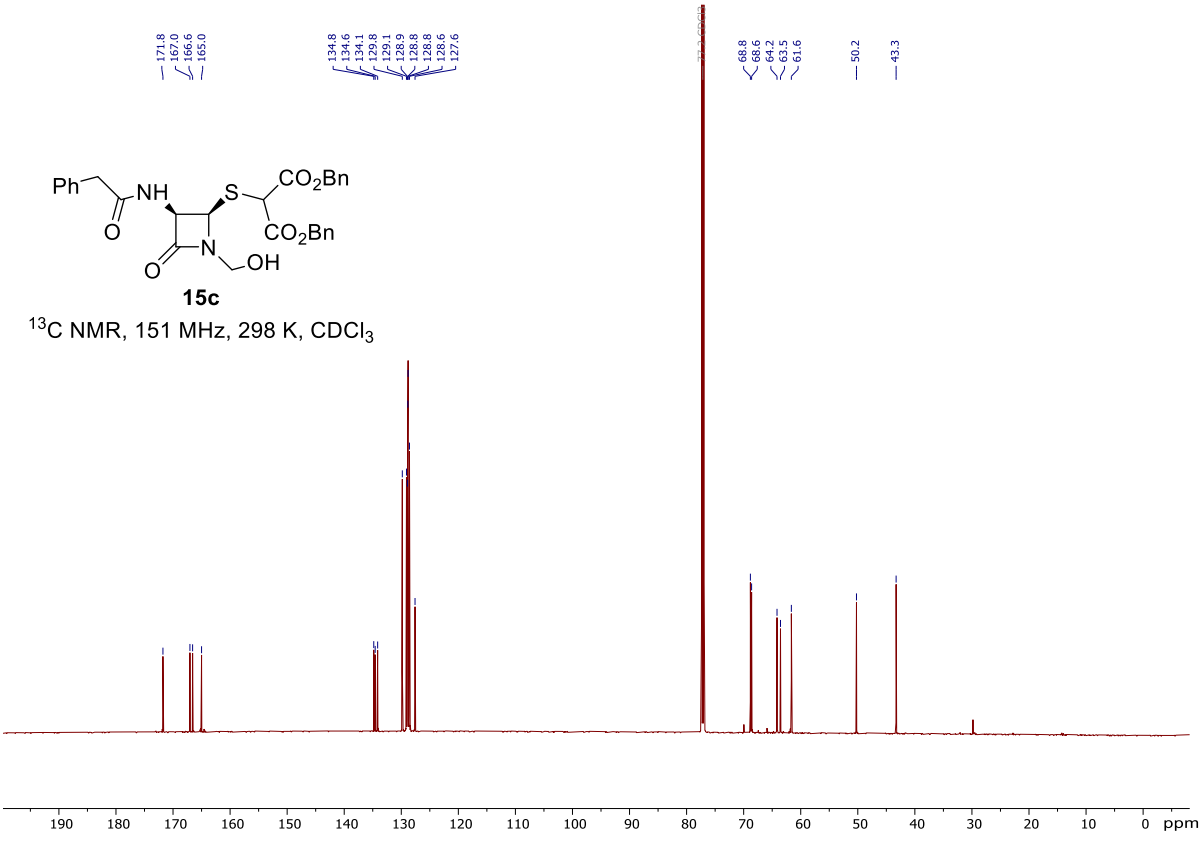

15c

^{13}C NMR, 151 MHz, 298 K, $CDCl_3$

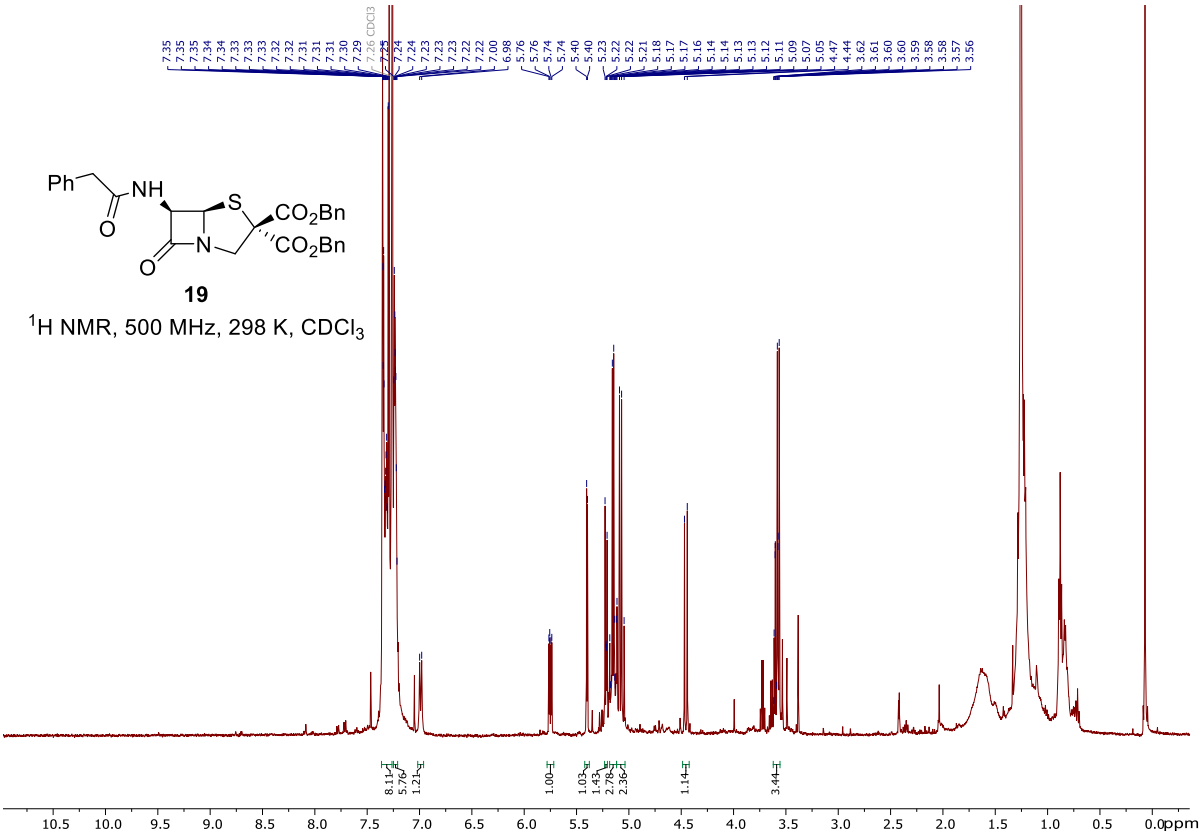

19

^{1}H NMR, 500 MHz, 298 K, $CDCl_3$

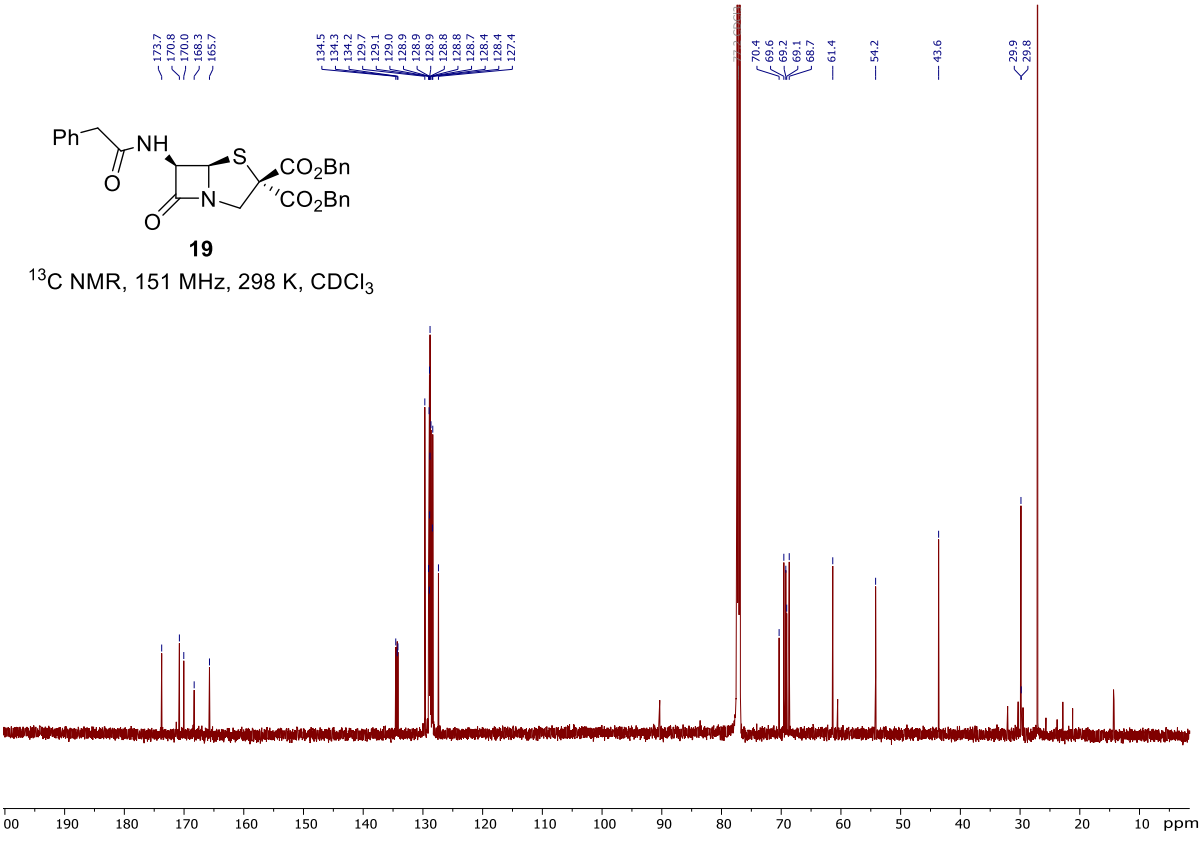

19

^{13}C NMR, 151 MHz, 298 K, $CDCl_3$

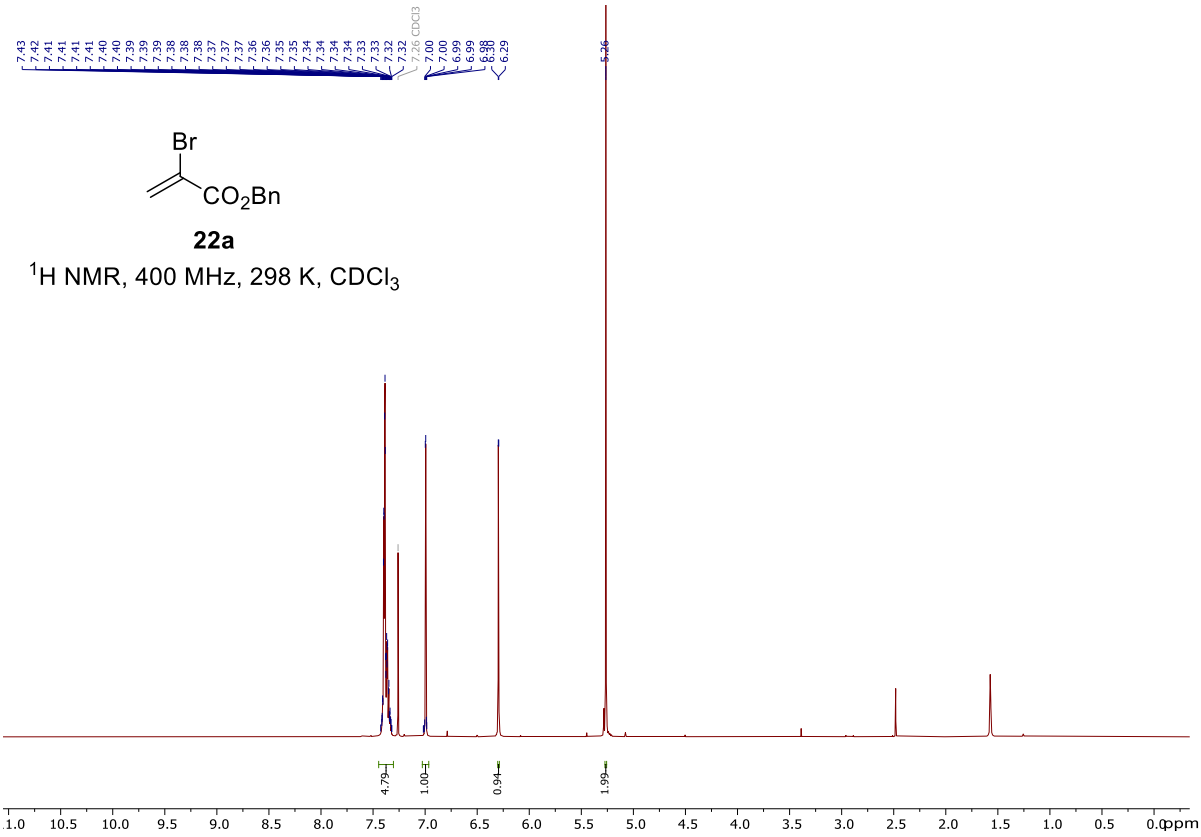

22a

^{1}H NMR, 400 MHz, 298 K, $CDCl_3$

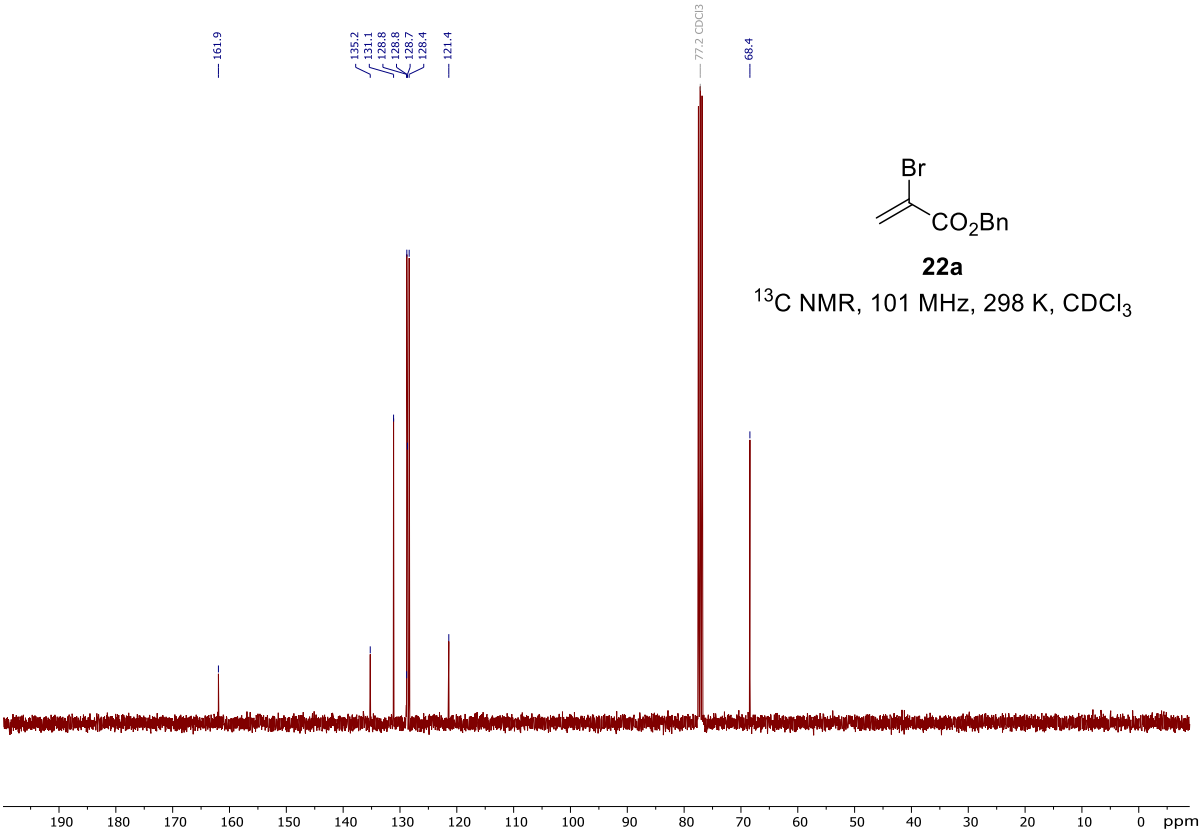

22a

^{13}C NMR, 101 MHz, 298 K, $CDCl_3$

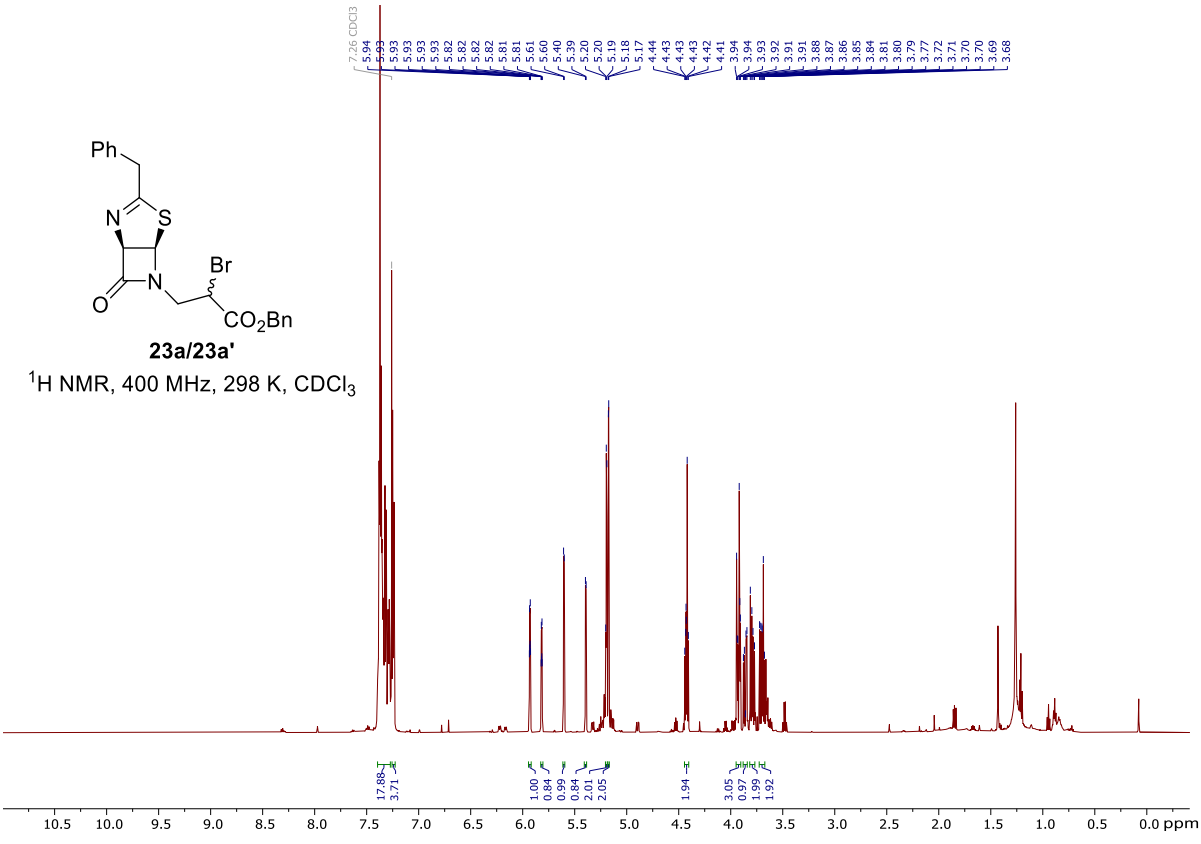

23a/23a'

^{1}H NMR, 400 MHz, 298 K, $CDCl_3$

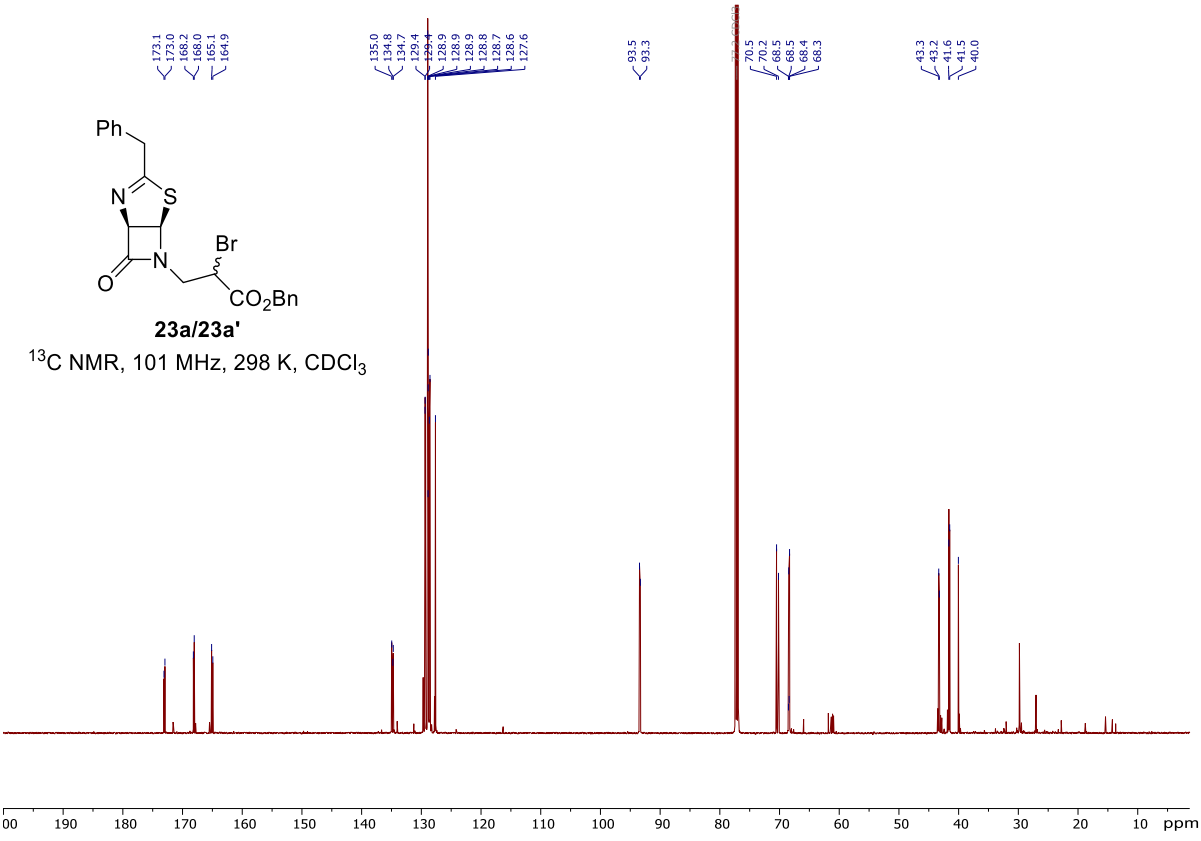

23a/23a'

^{13}C NMR, 101 MHz, 298 K, $CDCl_3$

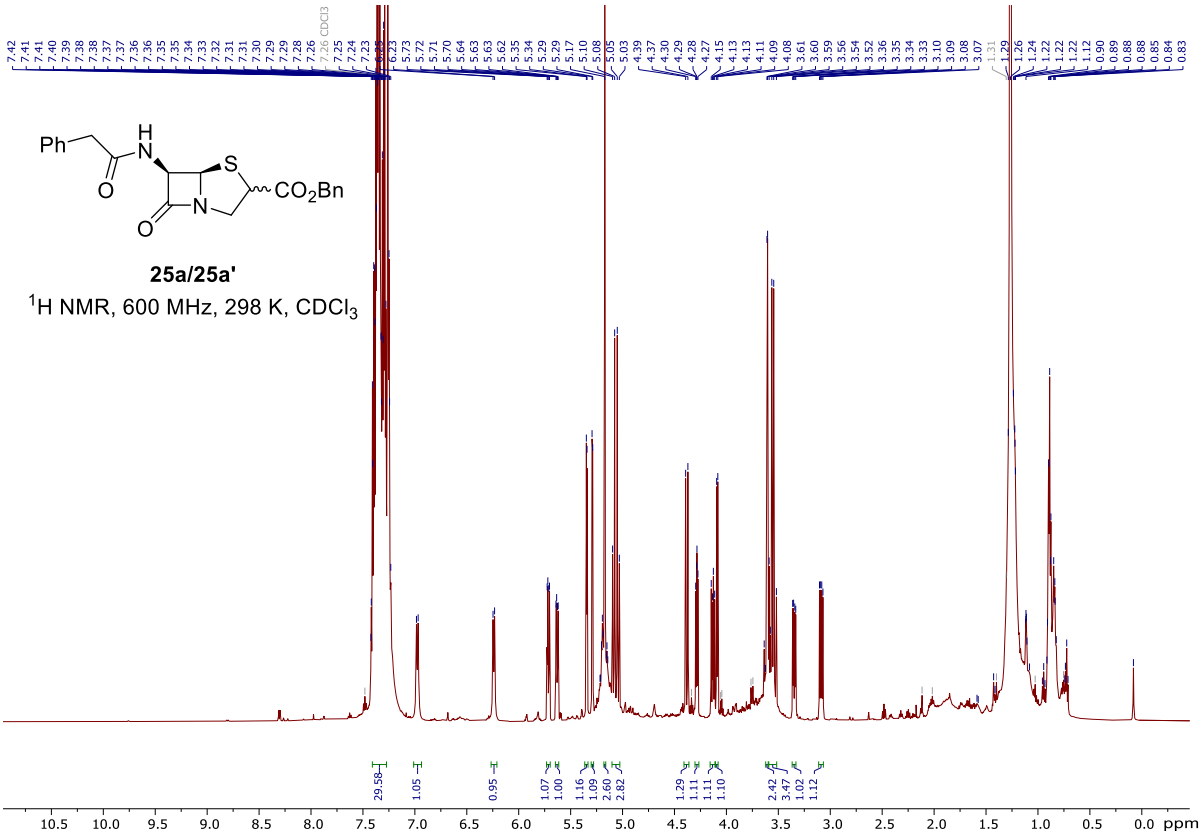

25a/25a'

^{1}H NMR, 600 MHz, 298 K, $CDCl_3$

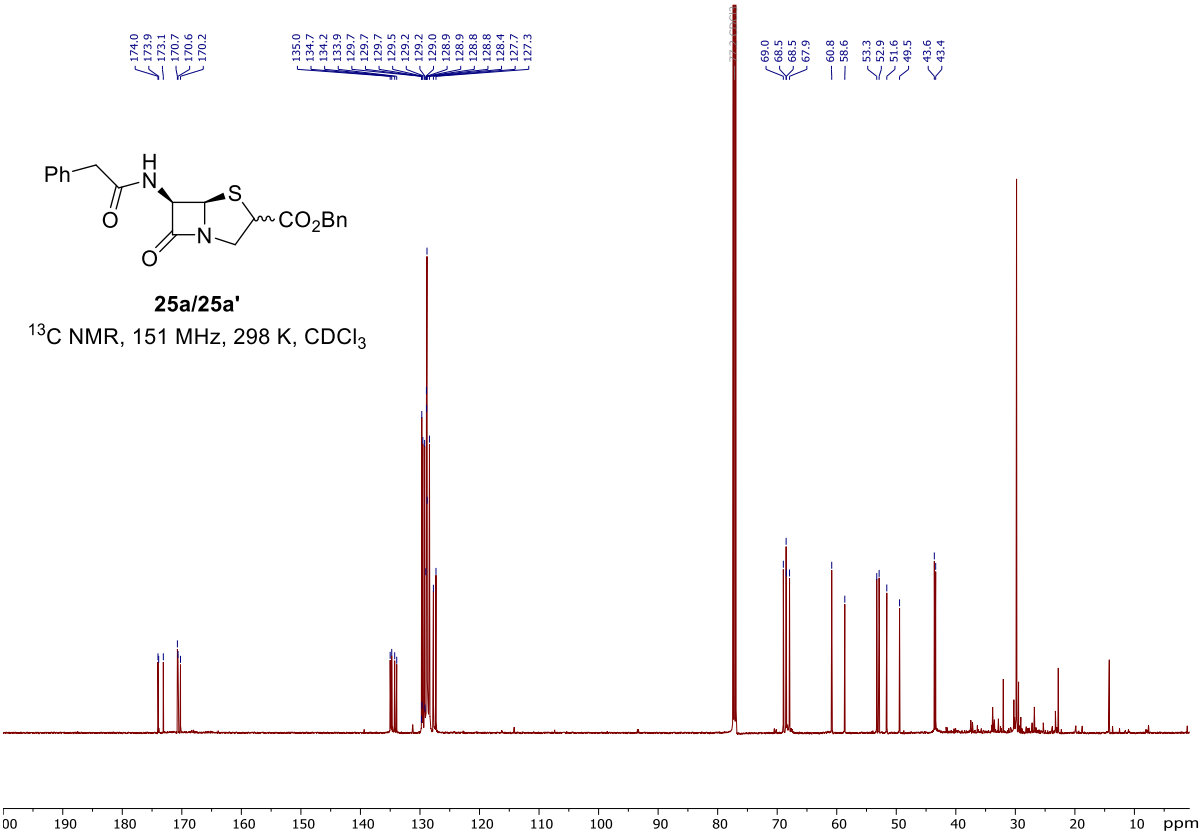

25a/25a'

^{13}C NMR, 151 MHz, 298 K, $CDCl_3$

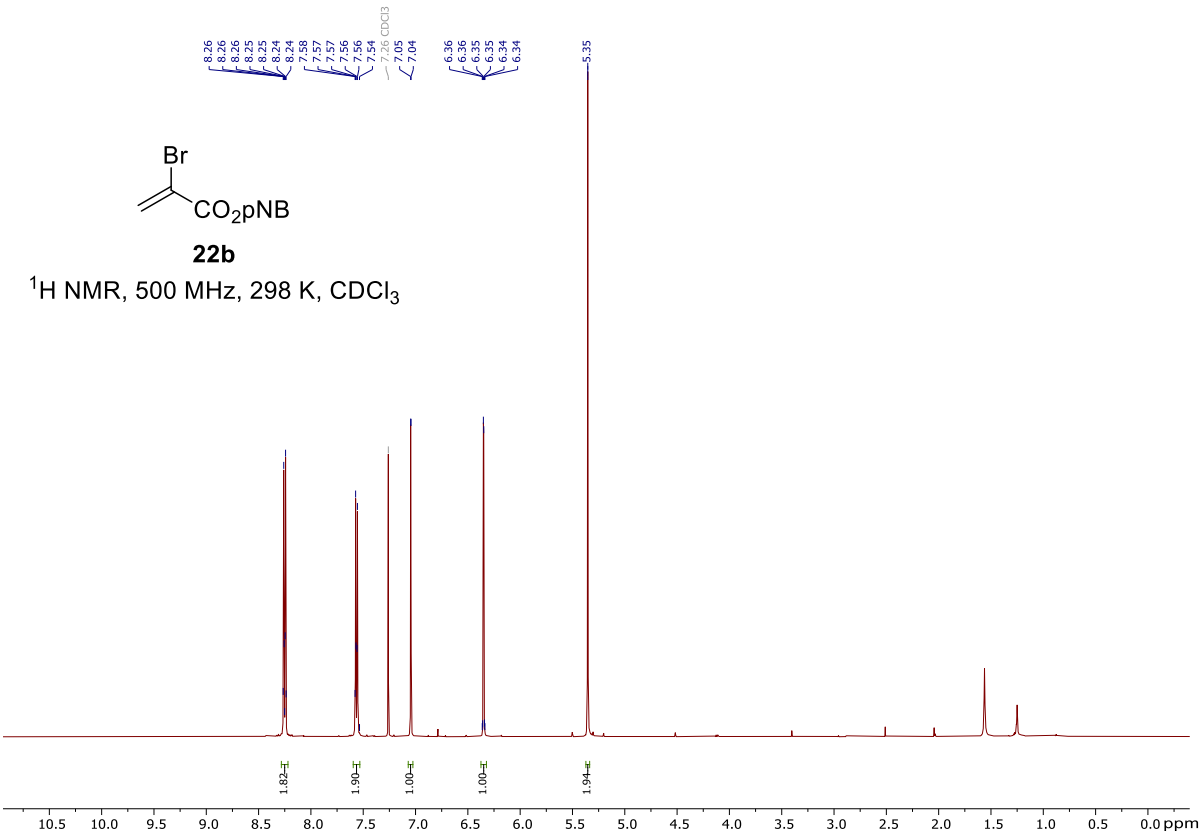
Br
CO2pNB
22b
1H NMR, 500 MHz, 298 K, CDCl3

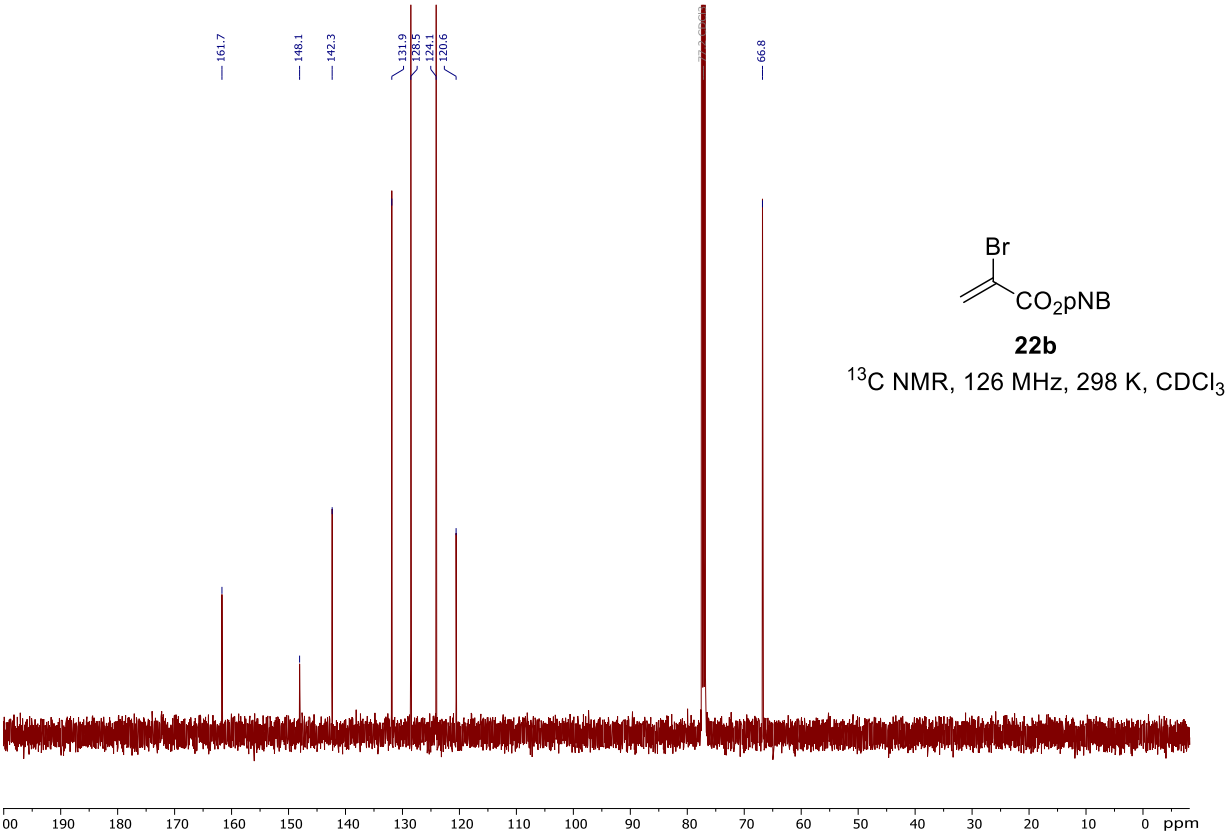
Br
CO2pNB
22b
13C NMR, 126 MHz, 298 K, CDCl3

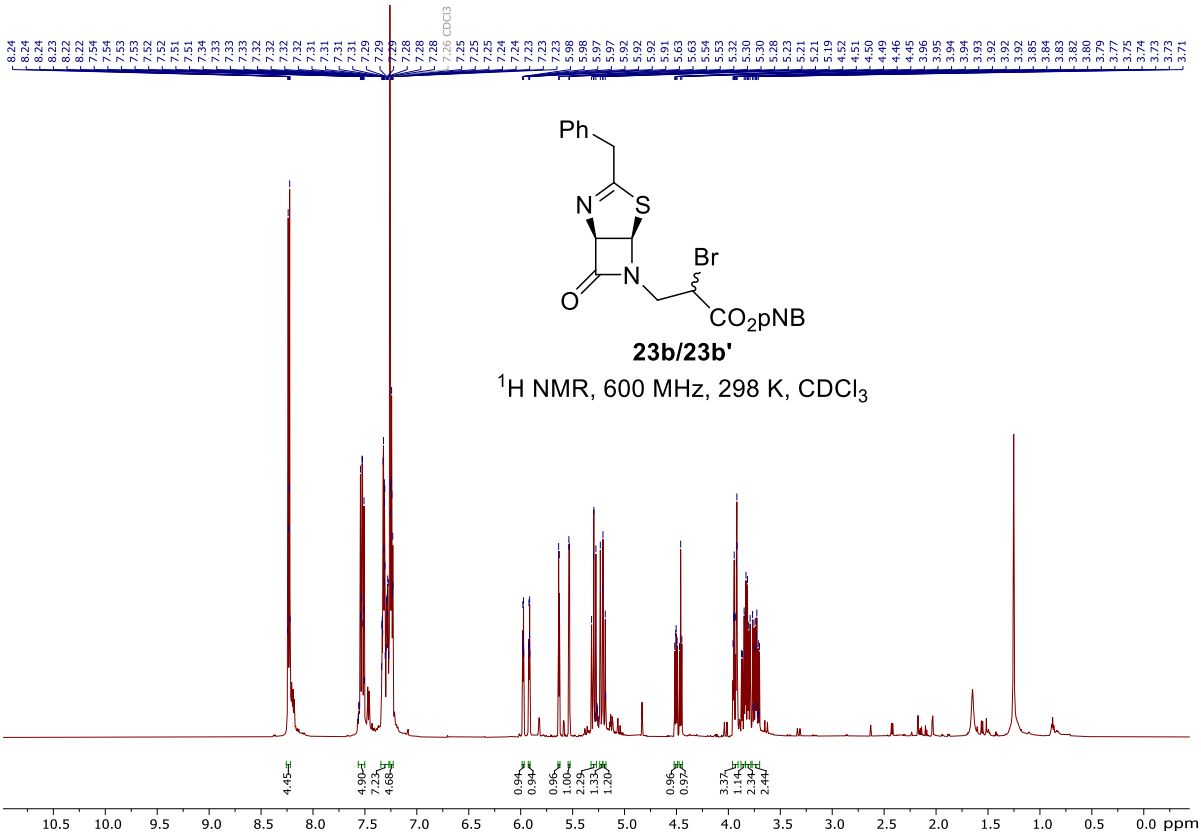

23b/23b'

^{1}H NMR, 600 MHz, 298 K, $CDCl_3$

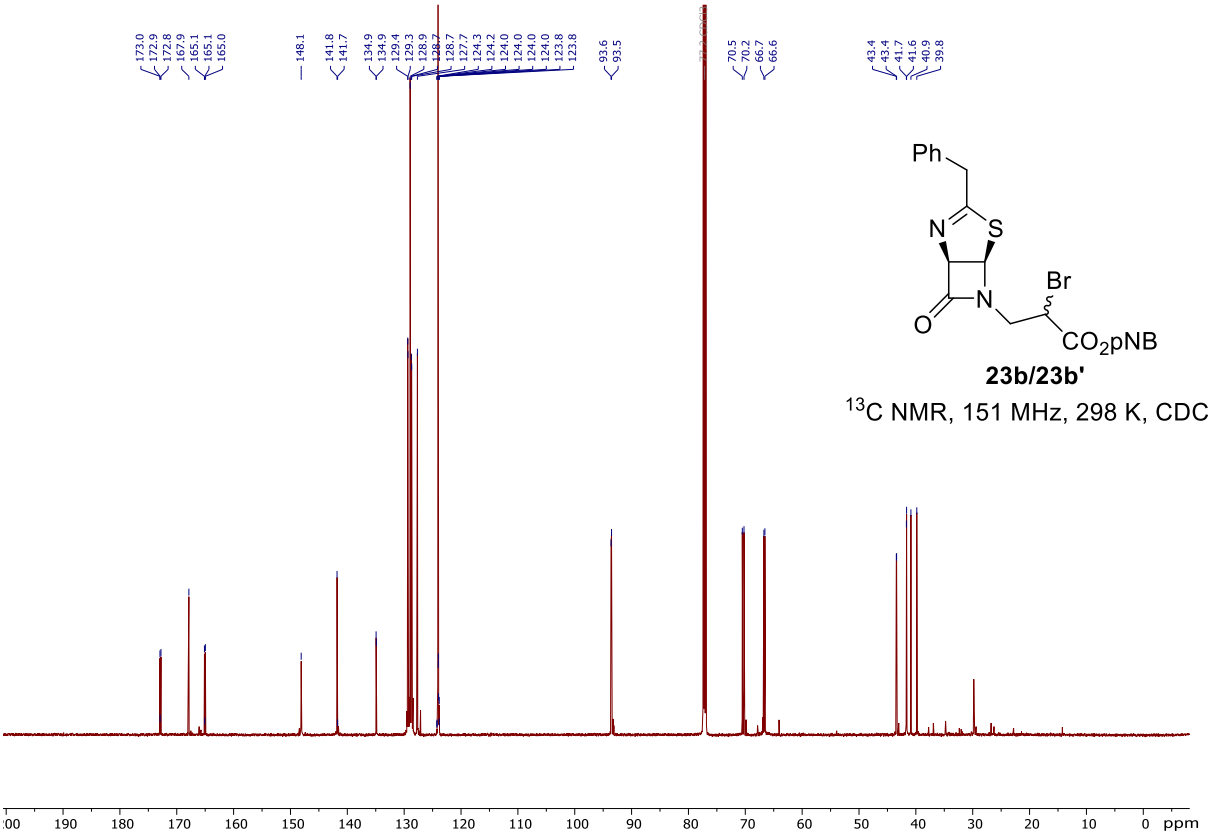

23b/23b'

^{13}C NMR, 151 MHz, 298 K, $CDCl_3$

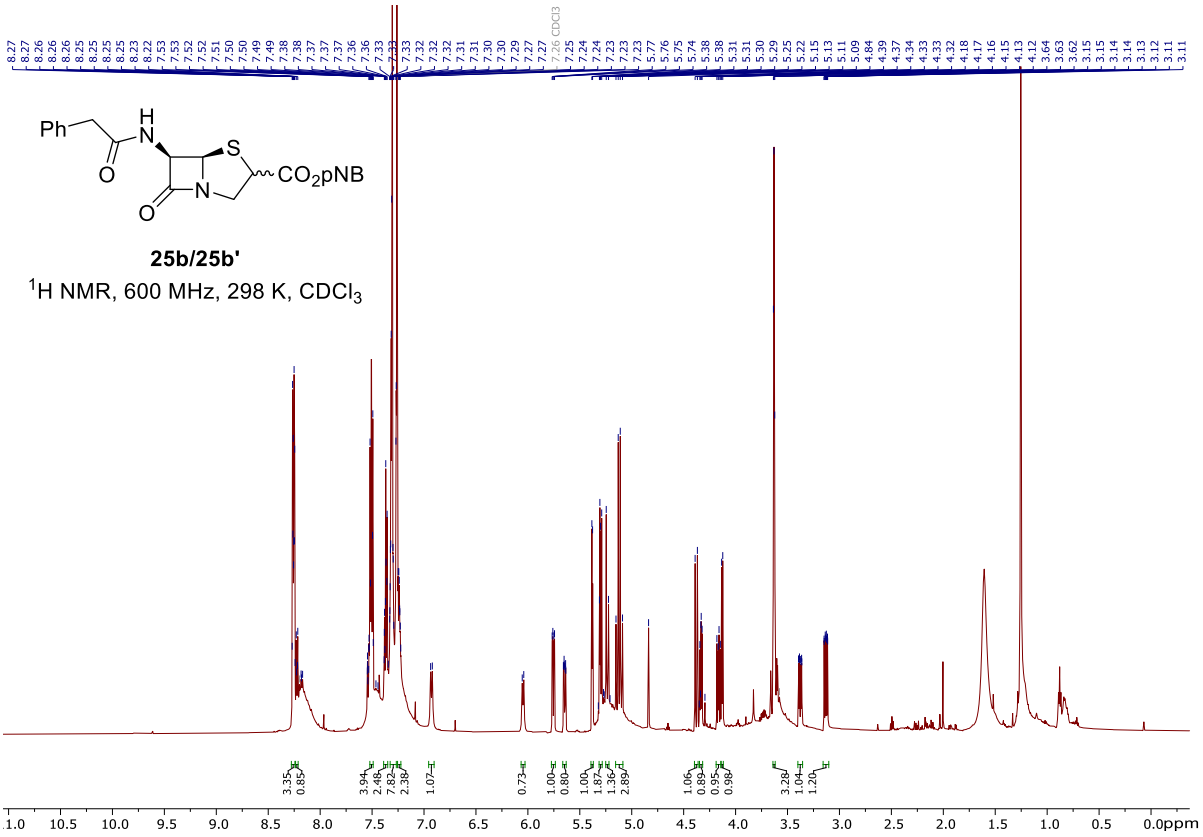

25b/25b'

^{1}H NMR, 600 MHz, 298 K, $CDCl_3$

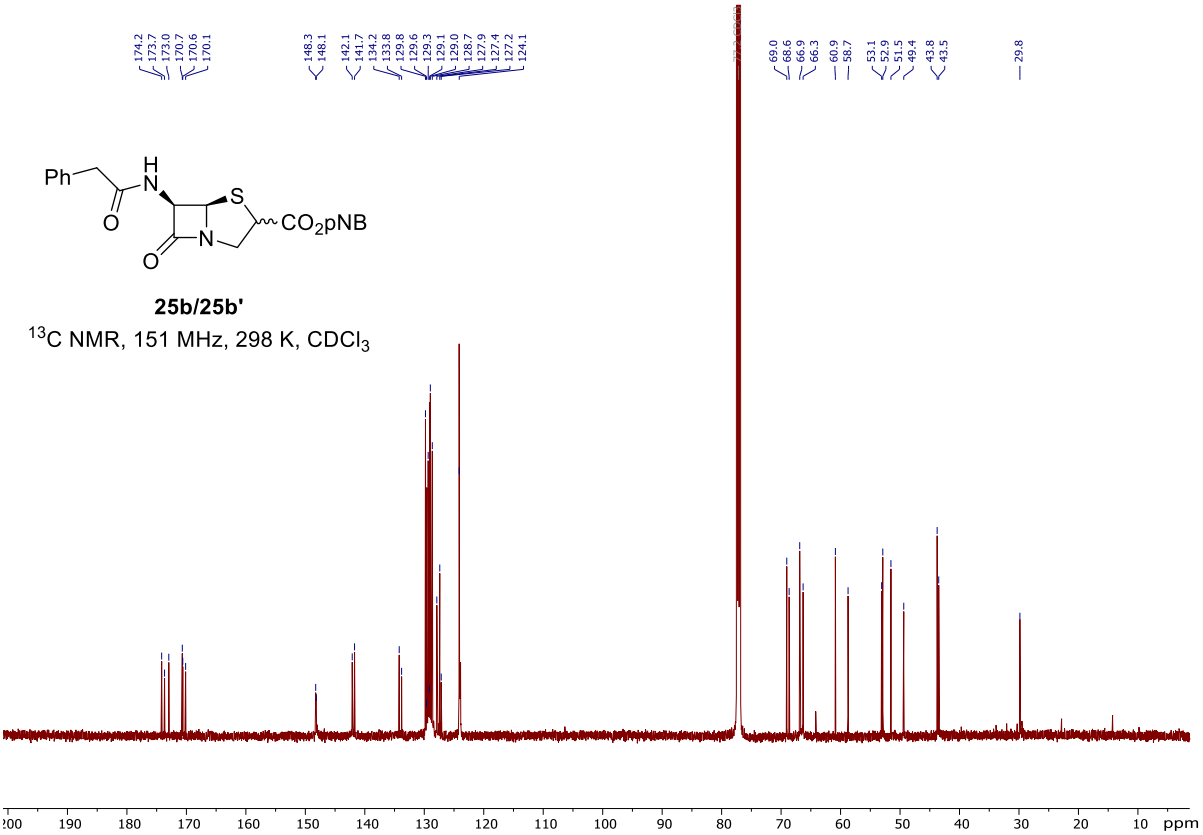

25b/25b'

^{13}C NMR, 151 MHz, 298 K, $CDCl_3$

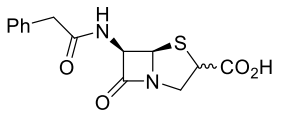

26a/26a'

^{1}H NMR, 600 MHz, 298 K, DMSO-d_6

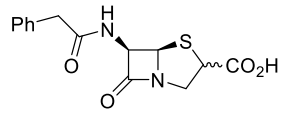

26a/26a'

^{13}C NMR, 151 MHz, 298 K, DMSO-d_6

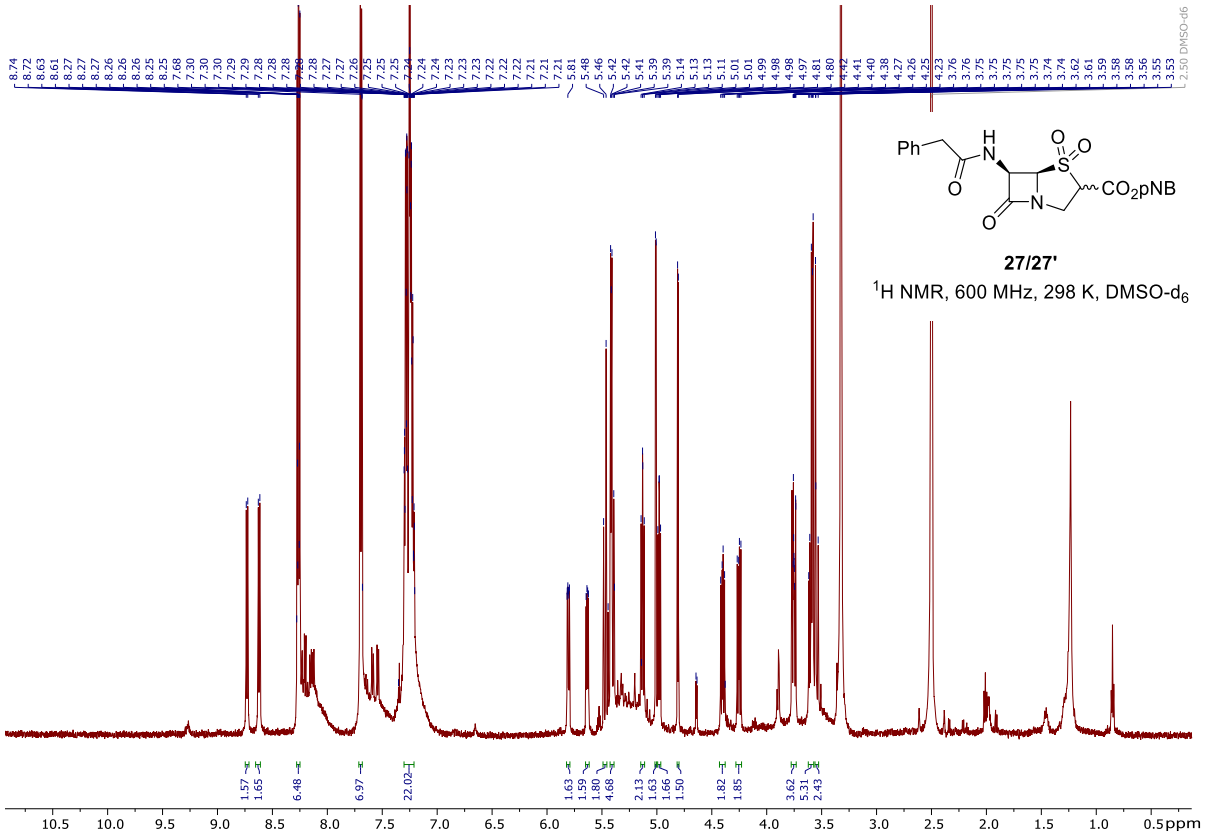

27/27'

^{1}H NMR, 600 MHz, 298 K, DMSO-d_6

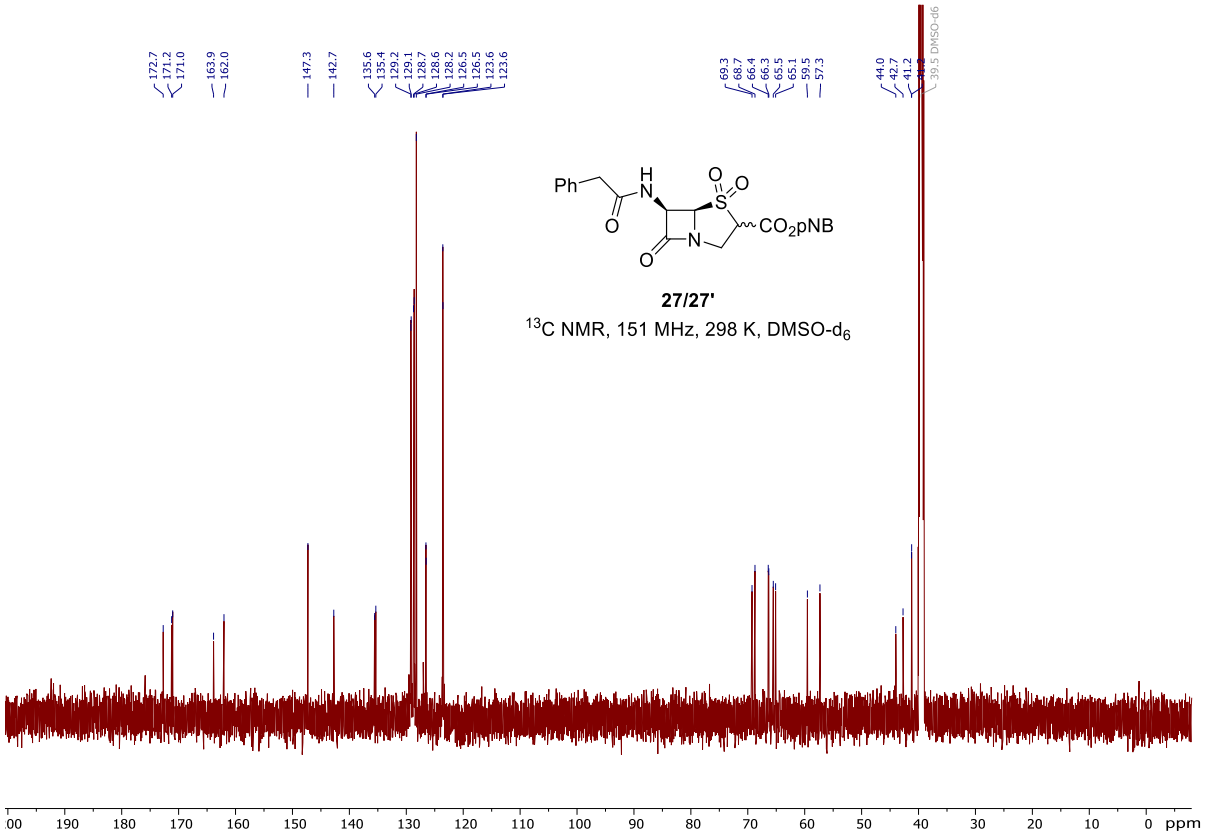

27/27'

^{13}C NMR, 151 MHz, 298 K, DMSO-d_6

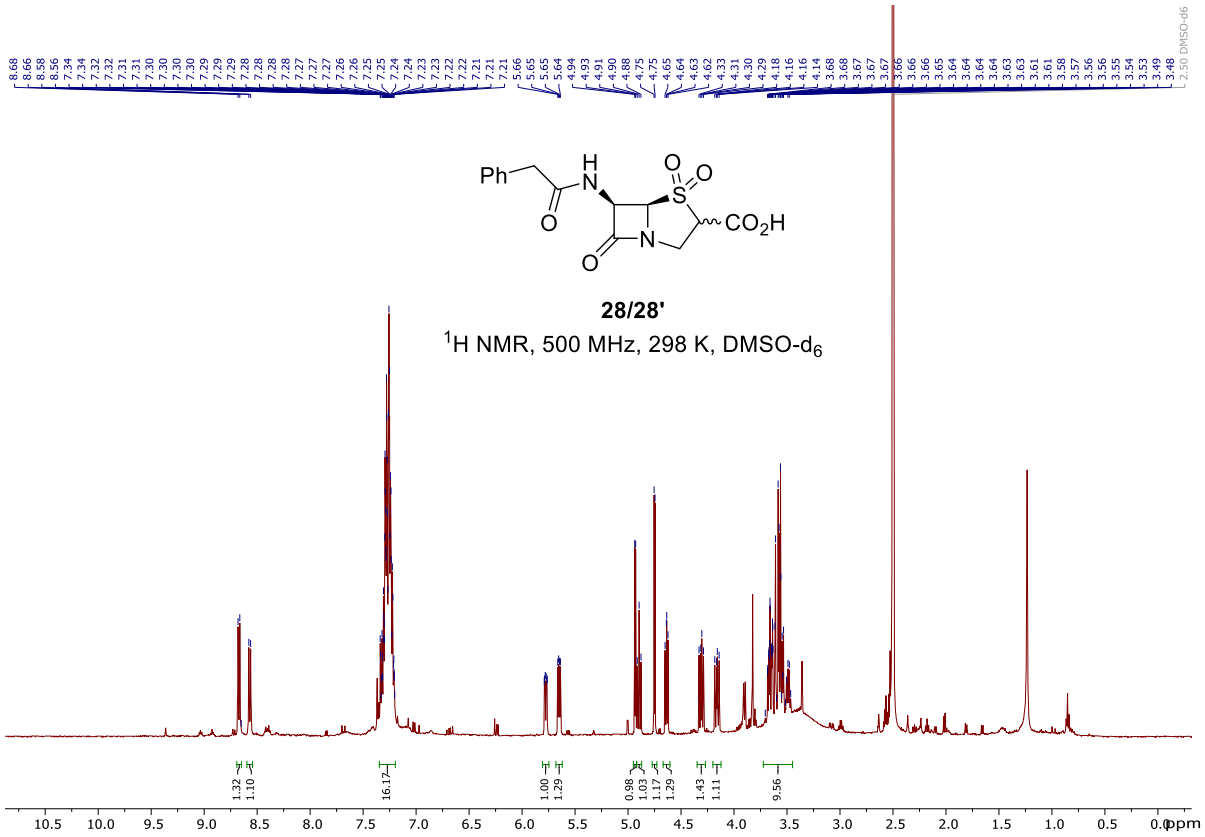
Ph
H
N
O
O
S
O
O
CO2H
N
O
28/28'
1H NMR, 500 MHz, 298 K, DMSO-d6
1.32
1.10
16.17
1.00
1.29
0.98
1.03
1.17
1.29
1.43
1.11
9.56
ppm

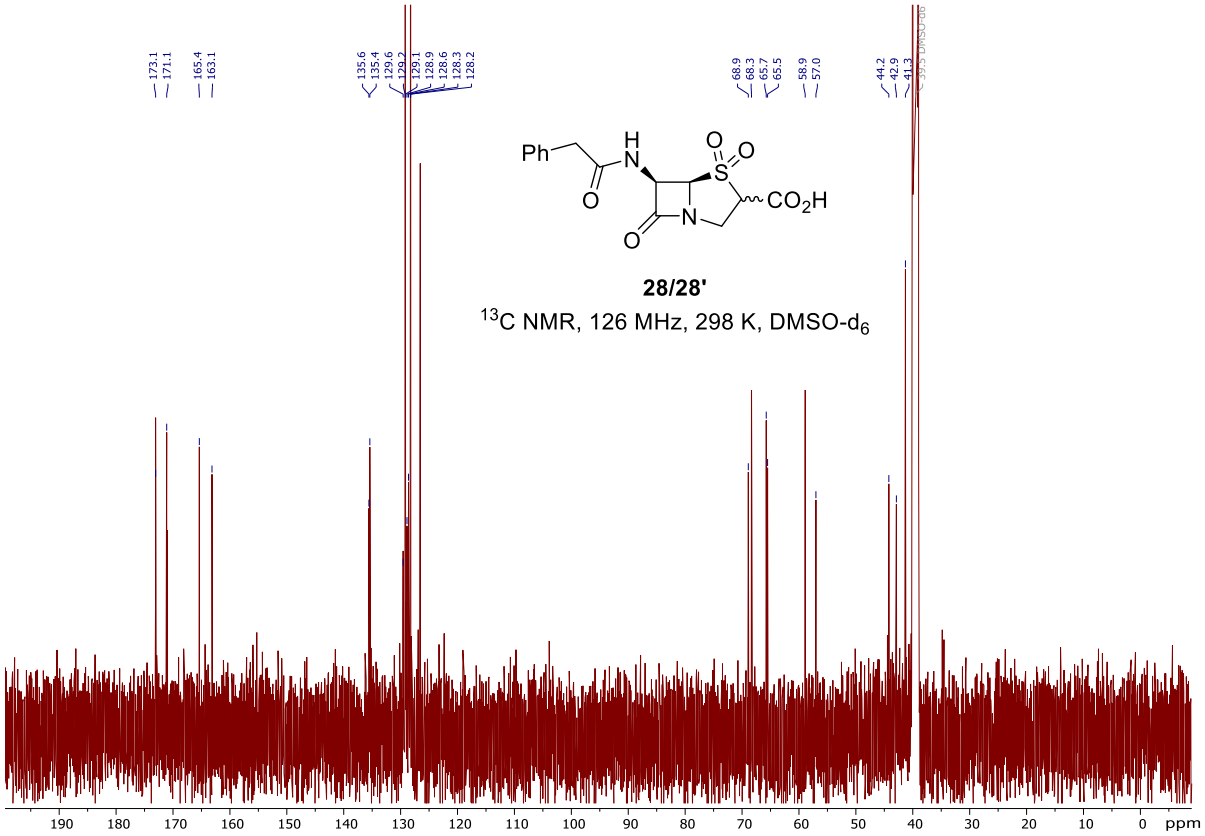
173.1
171.1
165.4
163.1
135.6
135.4
129.6
129.2
129.1
128.9
128.6
128.3
128.2
68.9
68.3
65.7
65.5
58.9
57.0
44.2
42.9
41.3
Ph
H
N
O
O
S
O
O
CO2H
N
O
28/28'
13C NMR, 126 MHz, 298 K, DMSO-d6
ppm